McDONALD INSTITUTE MONOGRAPHS

Temple landscapes

Fragility, change and resilience of Holocene environments in the Maltese Islands

By Charles French, Chris O. Hunt, Reuben Grima, Rowan McLaughlin, Simon Stoddart & Caroline Malone

Volume 1 of Fragility and Sustainability – Studies on Early Malta, the ERC-funded *FRAGSUS Project*

Temple landscapes

McDONALD INSTITUTE MONOGRAPHS

Temple landscapes

Fragility, change and resilience of Holocene environments in the Maltese Islands

By Charles French, Chris O. Hunt, Reuben Grima, Rowan McLaughlin, Simon Stoddart & Caroline Malone

With contributions by
Gianmarco Alberti, Jeremy Bennett, Maarten Blaauw, Petros Chatzimpaloglou, Lisa Coyle McClung, Alan J. Cresswell, Nathaniel Cutajar, Michelle Farrell, Katrin Fenech, Rory P. Flood, Timothy C. Kinnaird, Steve McCarron, Rowan McLaughlin, John Meneely, Anthony Pace, Sean D.F. Pyne-O'Donnell, Paula J. Reimer, Alastair Ruffell, George A. Said-Zammit, David C.W. Sanderson, Patrick J. Schembri, Sean Taylor, David Trump†, Jonathan Turner, Nicholas C. Vella & Nathan Wright

Illustrations by
Gianmarco Alberti, Jeremy Bennett, Sara Boyle, Petros Chatzimpaloglou, Lisa Coyle McClung, Rory P. Flood, Charles French, Chris O. Hunt, Michelle Farrell, Katrin Fenech, Rowan McLaughlin, John Meneely, Anthony Pace, David Redhouse, Alastair Ruffell, George A. Said-Zammit & Simon Stoddart

Volume 1 of Fragility and Sustainability – Studies on Early Malta,
the ERC-funded *FRAGSUS Project*


This project has received funding from the European Research Council (ERC) under the European Union's Seventh Framework Programme (FP7-2007-2013) (Grant agreement No. 323727).

Published by:
McDonald Institute for Archaeological Research
University of Cambridge
Downing Street
Cambridge, UK
CB2 3ER
(0)(1223) 339327
eaj31@cam.ac.uk
www.mcdonald.cam.ac.uk

ISBN: 978-1-902937-99-1

Cover design by Dora Kemp and Ben Plumridge.
Typesetting and layout by Ben Plumridge.

On the cover: *View towards Nadur lighthouse and Ghajnsielem church with the Gozo Channel to Malta beyond, from In-Nuffara (Caroline Malone).*

Edited for the Institute by James Barrett (*Series Editor*).

Contents

Contributors

Dr Gianmarco Alberti
Department of Criminology, Faculty for Social Wellbeing, University of Malta, Msida, Malta
Email: gianmarco.alberti@um.edu.mt

Jeremy Bennett
Department of Archaeology, University of Cambridge, Cambridge, UK
Email: jmb241@cam.ac.uk

Dr Maarten Blaauw
School of Natural and Built Environment, Queen's University, University Road, Belfast, Northern Ireland
Email: marten.blaauw@qub.ac.uk

Dr Petros Chatzimpaloglou
Department of Archaeology, University of Cambridge, Cambridge, UK
Email: pc529@cam.ac.uk

Dr Lisa Coyle McClung
School of Natural and Built Environment, Queen's University, University Road, Belfast, Northern Ireland
Email: l.coylemcclung@qub.ac.uk

Dr Alan J. Cresswell
SUERC, University of Glasgow, East Kilbride, University of Glasgow, Glasgow, Scotland
Email: alan.cresswell@glasgow.ac.uk

Nathaniel Cutajar
Deputy Superintendent of Cultural Heritage, Heritage Malta, Valletta, Malta
Email: nathaniel.cutajar@gov.mt

Dr Michelle Farrell
Centre for Agroecology, Water and Resilience, School of Energy, Construction and Environment, Coventry University, Coventry, UK
Email: ac5086@coventry.ac.uk

Dr Katrin Fenech
Department of Classics & Archaeology, University of Malta, Msida, Malta
Email: katrin.fenech@um.edu.mt

Dr Rory P. Flood
School of Natural and Built Environment, Queen's University, University Road, Belfast, Northern Ireland
Email: r.flood@qub.ac.uk

Prof. Charles French
Department of Archaeology, University of Cambridge, Cambridge, UK
Email: caif2@cam.ac.uk

Dr Reuben Grima
Department of Conservation and Built Heritage, University of Malta, Msida, Malta
Email: reuben.grima@um.edu.mt

Dr Evan A. Hill
School of Natural and Built Environment, Queen's University, University Road, Belfast, Northern Ireland
Email: ehill08@qub.ac.uk

Prof. Chris O. Hunt
Faculty of Science, Liverpool John Moores University, Liverpool, UK
Email: c.o.hunt@ljmu.ac.uk

Dr Timothy C. Kinnaird
School of Earth and Environmental Sciences, University of St Andrews, St. Andrews, Scotland
Email: tk17@st-andrews.ac.uk

Prof. Caroline Malone
School of Natural and Built Environment, Queen's University, University Road, Belfast, BT7 1NN, Northern Ireland
Email: c.malone@qub.ac.uk

Dr Steve McCarron
Department of Geography, National University of Ireland, Maynooth, Ireland
Email: stephen.mccarron@mu.ie

Dr Rowan McLaughlin
School of Natural and Built Environment, Queen's University, University Road, Belfast, Northern Ireland
Email: r.mclaughlin@qub.ac.uk

John Meneely
School of Natural and Built Environment, Queen's University, University Road, Belfast, Northern Ireland
Email: j.meneely@qub.ac.uk

Dr Anthony Pace
UNESCO Cultural Heritage, Valletta, Malta
Email: anthonypace@cantab.net

Dr Sean D.F. Pyne-O'Donnell
Earth Observatory of Singapore, Nanyang Technological University, Singapore
Email: sean.1000@hotmail.co.uk

Prof. Paula J. Reimer
School of Natural and Built Environment, Queen's University, University Road, Belfast, Northern Ireland
Email: p.j.reimer@qub.ac.uk

Dr Alastair Ruffell
School of Natural and Built Environment, Queen's University, University Road, Belfast, Northern Ireland
Email: a.ruffell@qub.ac.uk

George A. Said-Zammit
Department of Examinations, Ministry for Education and Employment, Government of Malta, Malta
Email: george.said-zammit@gov.mt

Prof. David C.W. Sanderson
SUERC, University of Glasgow, East Kilbride, University of Glasgow, Glasgow, Scotland
Email: david.sanderson@glasgow.ac.uk

Prof. Patrick J. Schembri
Department of Biology, University of Malta, Msida, Malta
Email: patrick.j.schembri@um.edu.mt

Dr Simon Stoddart
Department of Archaeology, University of Cambridge, Cambridge, UK
Email: ss16@cam.ac.uk

Dr Sean Taylor
Department of Archaeology, University of Cambridge, Cambridge, UK
Email: st435@cam.ac.uk

Dr David Trump†

Dr Jonathan Turner
Department of Geography, National University of Ireland, University College, Dublin, Ireland
Email: jonathan.turner@ucd.ie

Prof. Nicholas C. Vella
Department of Classics and Archaeology, Faculty of Arts, University of Malta, Msida, Malta
Email: nicholas.vella@um.edu.mt

Dr Nathan Wright
School of Social Science, The University of Queensland, Brisbane, Australia
Email: n.wright@uq.edu.au

Figures

Tables

Preface and dedication

Caroline Malone

The *FRAGSUS Project* emerged as the direct result of an invitation to undertake new archaeological fieldwork in Malta in 1985. Anthony Bonanno of the University of Malta organized a conference on 'The Mother Goddess of the Mediterranean' in which Colin Renfrew was a participant. The discussions that resulted prompted an invitation that made its way to David Trump (Tutor in Continuing Education, Cambridge University), Caroline Malone (then Curator of the Avebury Keiller Museum) and Simon Stoddart (then a post-graduate researcher in Cambridge). We eagerly took up the invitation to devise a new collaborative, scientifically based programme of research on prehistoric Malta.

What resulted was the original Cambridge Gozo Project (1987–94) and the excavations of the Xagħra Brochtorff Circle and the Għajnsielem Road Neolithic house. Both those sites had been found by local antiquarian, Joseph Attard-Tabone, a long-established figure in the island for his work on conservation and site identification.

As this and the two other volumes in this series report, the original Cambridge Gozo Project was the germ of a rich and fruitful academic collaboration that has had international impact, and has influenced successive generations of young archaeologists in Malta and beyond.

As the Principal Investigator of the *FRAGSUS Project*, on behalf of the very extensive *FRAGSUS* team I want to dedicate this the first volume of the series to the enlightened scholars who set up this now 35 year-long collaboration of prehistoric inquiry with our heartfelt thanks for their role in our studies.

We dedicate this volume to:

Joseph Attard Tabone
Professor Anthony Bonanno
Professor Lord Colin Renfrew

and offer our profound thanks for their continuing role in promoting the prehistory of Malta.

Acknowledgements

This volume records research undertaken with funding from the European Research Council under the European Union's Seventh Framework Programme (FP/2007-2013)/ERC Grant Agreement n. 323727 (*FRAGSUS Project*: *Fragility and sustainability in small island environments: adaptation, cultural change and collapse in prehistory* – http://www.qub.ac.uk/sites/FRAGSUS/). All the authors of this volume are indebted to the ERC for its financial support, and to the Principal Investigator of the *FRAGSUS Project*, Prof. Caroline Malone (Queen's University, Belfast, UK), for her central role in devising the project and seeing this research through to publication.

For Chapter 2, we extend warm thanks to the staff of the ^{14}CHRONO centre at QUB, especially Stephen Hoper, Jim McDonald, Michelle Thompson and Ron Reimer, all of whom took a keen interest in the *FRAGSUS Project*. The success of the *FRAGSUS Project* in general and the radiocarbon dating exercise has depended on their work. We thank the Physical Geography Laboratory staff at the School of Geography, University College Dublin, for the use of their ITRAX XRF core scanner. In particular, we would like to thank Dr Steve McCarron, Department of Geography, National University of Ireland, Maynooth and Dr Jonathan Turner, Department of Geography, National University of Ireland, University College, Dublin. We thank Prof. Patrick Schembri for sourcing and collecting the *Acanthocardia* samples from the Natural Museum of Natural History. Sean Pyne O'Donnell thanks Dr Chris Hayward at the Tephrochronology Analytical Unit (TAU), University of Edinburgh, for help and advice during microprobe work. Dr Maxine Anastasi, Department of Classics and Archaeology, University of Malta, helped identify the pottery from the settlement cores. Dr Frank Carroll helped show us the way forward; but sadly is no longer with us. Chris Hunt, Rory Flood, Michell Farrell, Sean Pyne O'Donnell and Mevrick Spiteri were the coring team. They were helped by Vincent Van Walt, who provided technical assistance. Al Ruffell and John Meneely did geophysical evaluation and GRP location of the cores. During fieldwork, Tim Kinnaird and Charles French were assisted by Sean Taylor, Jeremy Bennett and Simon Stoddart. We are grateful to the Superintendence of Cultural Heritage, Malta and Heritage Malta for permission to undertake the analyses and much practical assistance.

For Chapter 5, we would like to thank all at Heritage Malta, the Ġgantija visitor's centre and the University of Malta for their friendly and useful assistance throughout. In particular, we would like to thank George Azzopardi, Daphne Caruana, Josef Caruana, Nathaniel Cutajar, Chris Gemmell, Reuben Grima, Joanne Mallia, Christian Mifsud, Anthony Pace, Ella Samut-Tagliaferro, Mevrick Spiteri, Katya Stroud, Sharon Sultana and Nick Vella. We also thank Tonko Rajkovača of the McBurney Laboratory, Department of Archaeology, University of Cambridge, for making the thin section slides, the Physical Geography Laboratory, Department of Geography, University of Cambridge, and the ALS Global laboratory in Seville, Spain, for processing the multi-element analyses.

For Chapter 6, Reuben Grima wrote the first draft of this contribution, receiving comments and additions from the other authors.

For Chapter 7, Simon Stoddart wrote the first draft of this contribution, receiving comments and additions from the other authors.

For Chapter 9, we thank Sharlo Camilleri for providing us with a copy of the GIS data produced by the MALSIS (MALtese Soil Information System) project. We are grateful to Prof. Saviour Formosa and Prof. Timmy Gambin, both of the University of Malta, who facilitated the donation of LiDAR data, together with computer facilities, as part of the European project ERDF156 *Developing National Environmental Monitoring Infrastructure and Capacity*, from the former Malta

Environment and Planning Authority. A number of individuals were happy to share their recollections of shepherding practices in Malta and Gozo over the last sixty or seventy years; others facilitated the encounters. We are grateful to all of them: Charles Gauci, Grezzju Meilaq, Joseph Micallef, Louis Muscat, Ċettina and Anġlu Vella, Ernest Vella and Renata Zerafa.

Simon Stoddart would like to thank Prof. Martin Jones and Rachel Ballantyne for their advice in constructing Figure 11.4. The editors would like to thank Emma Hannah for compiling the index.

Firstly, the FRAGSUS Project is the result of a very generous research grant from the European Research Council (Advanced Grant no' 323727), without which this and its two partner volumes and the research undertaken could not have taken place. We heartily thank the ERC for its award and the many administrators in Brussels who monitored our use of the grant. The research team also wants to record our indebtedness to the administrators of the grant within our own institutions, since this work required detailed and dedicated attention. In particular we thank Rory Jordan in the Research Support Office, Stephen Hoper and Jim McDonald – CHRONO lab, and Martin Stroud (Queen's University Belfast), Laura Cousens (Cambridge University), Glen Farrugia and Cora Magri (University of Malta), the Curatorial, Finance and Designs & Exhibitions Departments in Heritage Malta and Stephen Borg at the Superintendence of Cultural Heritage. Finally, we thank Fr. Joe Inguanez (Emeritus Head of Department, Department of Sociology, University of Malta) for offering us the *leitmotif* of this volume while a visiting scholar in Magdalene College, Cambridge: '*Mingħajr art u ħamrija, m'hemmx sinjorija*' translating as 'without land and soil, there is no wealth'.

Foreword

Anthony Pace

Sustainability, as applied in archaeological research and heritage management, provides a useful perspective for understanding the past as well as the modern conditions of archaeological sites themselves. As often happens in archaeological thought, the idea of sustainability was borrowed from other areas of concern, particularly from the modern construct of development and its bearing on the environment and resource exploitation. The term sustainability entered common usage as a result of the unstoppable surge in resource exploitation, economic development, demographic growth and the human impacts on the environment that has gripped the World since 1500. Irrespective of scale and technology, most human activity of an economic nature has not spared resources from impacts, transformations or loss irrespective of historical and geographic contexts. Theories of sustainability may provide new narratives on the archaeology of Malta and Gozo, but they are equally important and of central relevance to contemporary issues of cultural heritage conservation and care. Though the archaeological resources of the Maltese islands can throw light on the past, one has to recognize that such resources are limited, finite and non-renewable. The sense of urgency with which these resources have to be identified, listed, studied, archived and valued is akin to that same urgency with which objects of value and all fragile forms of natural and cultural resources require constant stewardship and protection. The idea of sustainability therefore, follows a common thread across millennia.

It is all the more reason why cultural resource management requires particular attention through research, valorization and protection. The *FRAGSUS Project* (Fragility and sustainability in small island environments: adaptation, cultural change and collapse in prehistory) was intended to further explore and enhance existing knowledge on the prehistory of Malta and Gozo. The objective of the project as designed by the participating institutional partners and scholars, was to explore untapped field resources and archived archaeological material from a number of sites and their landscape to answer questions that could be approached with new techniques and methods. The results of the *FRAGSUS Project* will serve to advance our knowledge of certain areas of Maltese prehistory and to better contextualize the archipelago's importance as a model for understanding island archaeology in the central Mediterranean. The work that has been invested in *FRAGSUS* lays the foundation for future research.

Malta and Gozo are among the Mediterranean islands whose prehistoric archaeology has been intensely studied over a number of decades. This factor is important, yet more needs to be done in the field of Maltese archaeology and its valorization. Research is not the preserve of academic specialists. It serves to enhance not only what we know about the Maltese islands, but more importantly, why the archipelago's cultural landscape and its contents deserve care and protection especially at a time of extensive construction development. Strict rules and guidelines established by the Superintendence of Cultural Heritage have meant that during the last two decades more archaeological sites and deposits have been protected in situ or rescue-excavated through a statutory watching regime. This supervision has been applied successfully in a wide range of sites located in urban areas, rural locations and the landscape, as well as at the World Heritage Sites of Valletta, Ġgantija, Ħaġar Qim and Mnajdra and Tarxien. This activity has been instrumental in understanding ancient and historical land use, and the making of the Maltese historic centres and landscape.

Though the cumulative effect of archaeological research is being felt more strongly, new areas of interest still need to be addressed. Most pressing are those areas of landscape studies which often become

peripheral to the attention that is garnered by prominent megalithic monuments. *FRAGSUS* has once again confirmed that there is a great deal of value in studying field systems, terraces and geological settings which, after all, were the material media in which modern Malta and Gozo ultimately developed. There is, therefore, an interplay in the use of the term sustainability, an interplay between what we can learn from the way ancient communities tested and used the very same island landscape which we occupy today, and the manner in which this landscape is treated in contested economic realities. If we are to seek factors of sustainability in the past, we must first protect its relics and study them using the best available methods in our times. On the other hand, the study of the past using the materiality of ancient peoples requires strong research agendas and thoughtful stewardship. The *FRAGSUS Project* has shown us how even small fragile deposits, nursed through protective legislation and guardianship, can yield significant information which the methods of pioneering scholars of Maltese archaeology would not have enabled access to. As already outlined by the Superintendence of Cultural Heritage, a national research agenda for cultural heritage and the humanities is a desideratum. Such a framework, reflected in the institutional partnership of the *FRAGSUS Project*, will bear valuable results that will only advance Malta's interests especially in today's world of instant e-knowledge that was not available on such a global scale a mere two decades ago.

FRAGSUS also underlines the relevance of studying the achievements and predicaments of past societies to understand certain, though not all, aspects of present environmental challenges. The twentieth century saw unprecedented environmental changes as a result of modern political-economic constructs. Admittedly, twentieth century developments cannot be equated with those of antiquity in terms of demography, technology, food production and consumption or the use of natural resources including the uptake of land. However, there are certain aspects, such as climate change, changing sea levels, significant environmental degradation, soil erosion, the exploitation and abandonment of land resources, the building and maintenance of field terraces, the rate and scale of human demographic growth, movement of peoples, access to scarce resources, which to a certain extent reflect impacts that seem to recur in time, irrespectively of scale and historic context.

Anthony Pace
Superintendent of Cultural Heritage (2003–18).

Introduction

Caroline Malone, Simon Stoddart, Chris O. Hunt,
Charles French, Rowan McLaughlin & Reuben Grima

0.1. Introduction

The *FRAGSUS Project* (*Fragility and sustainability in small island environments: adaptation, cultural change and collapse in prehistory*) was devised to explore issues of prehistoric island sustainability set against the background of environmental change and instability. Particular foci were the fragility and sustainability of society and environment in the Maltese Islands (Fig. 0.1), primarily during the Neolithic period of the sixth to third millennia BC. Specifically, the research team aimed to understand and explain the nature of the impact of expanding human populations on a restricted, resource-limited and fragile environment such as the Maltese Islands. Our goal was to advance knowledge of the mechanisms and innovations (cultural, technological and political) that traditional (prehistoric) farming societies developed in order to cope with changing resource availability and environmental unpredictability. We sought to understand how some societies managed population impact and sustained their socio-economic system and culture over long periods of time through examining the evidence preserved in the archaeological and palaeoenvironmental records.

Island studies have long interested archaeologists and ecologists. An island represents a conveniently circumscribed landscape of known size, surrounded by water, and thus remote from larger landmasses and their biological and cultural stimuli. They are sometimes taken as a microcosm of the situation of the human species in a severely circumscribed and overcrowded planet. From the seminal ecological studies of Charles Darwin (Jones 2009) and Alfred Wallace (1892) in the nineteenth century, to the rich theoretical literature on biogeography and equilibrium theory in islands first initiated by MacArthur and Wilson (1963, 1967), an entire sub-discipline of island studies has developed. The studies range from Simberloff's equilibrium theory (1974), the ecology models of Gorman (1979), ecological anthropology (Vayda & Rappaport 1968) to current ideas of evolution and equilibrium (Lomolino *et al*. 2010) and colonization (Cox *et al.* 2016). Generally, the bulk of research has been focused on non-human subjects, with issues of extinctions and conservation foremost, but nevertheless, a number of important theories and models from these island studies are relevant to archaeology.

FRAGSUS has sought to examine the particular impact made by humans on the natural environment and resources available in a prehistoric island context. There have been a number of useful studies on island colonization patterns and case studies of the Mediterranean and the Caribbean in particular, that extract some key ideas from the ecological models and apply them to the anthropic context. Evans (1973a) was amongst the first to present the 'island' as the laboratory case study of an ancient society in the Mediterranean context. Cherry (1981, 1990) further demonstrated the more mathematical outcome of these ideas, and that work has generated a succession of useful, relevant studies some of which specifically focus on Malta (Broodbank 2013; Dawson 2014; Kirch 1986; Kolb 2005; Malone 1997–8; Patton 1996; Rainbird 2007; Renfrew 1973; Stoddart 1997–8, 1999) that have worked to develop both the theory and to show the archaeological relevance of the application of the island ecology models to ancient island issues.

As time has progressed, increasingly detailed complementary information has been added, especially a more detailed and exact chronology. Now with fifty years or so of increasing numbers and resolution of radiocarbon dating estimations, the tempo of island colonization, consolidation and desertion can be more effectively presented and the archaeological record better understood. We can now present an understanding of chronology rather than speculate about when humans arrived on particular islands, and

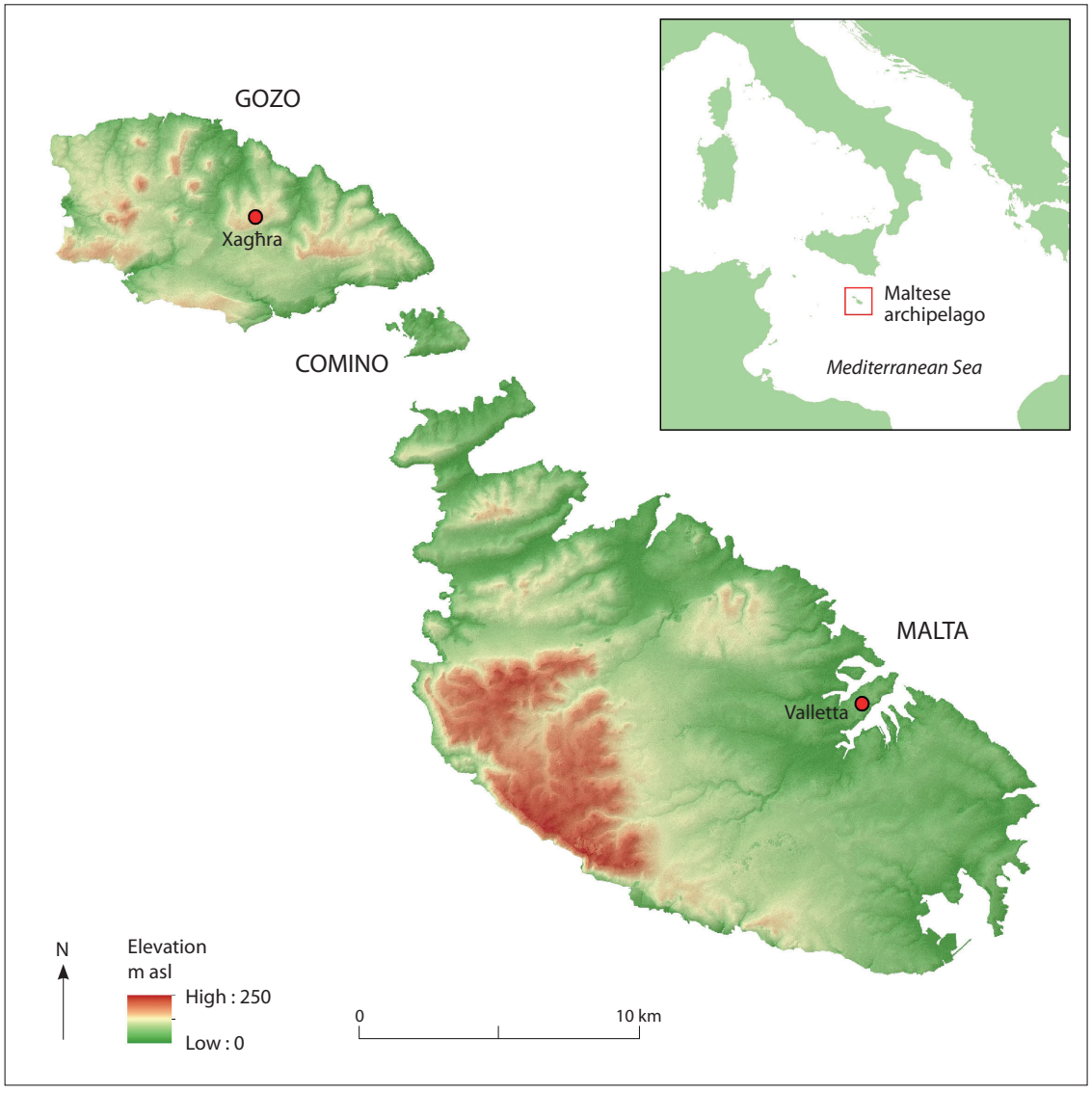

Figure 0.1. *Location map of the Maltese Islands in the southern Mediterranean Sea (J. Bennett).*

when distinctive socio-cultural evidence appeared and disappeared in the sequence of social and environmental evolution. When Cherry (1981, 1990, 2004) was estimating island colonization patterns in the Mediterranean, far fewer uncalibrated radiocarbon dates were available. Whilst he and Patton (1996) identified that the sixth millennium BC witnessed the first major episodes of colonization associated with the spread of farming, there was little chance then to break the key sixth millennium BC into detailed episodes that might trace the dynamics of what was probably an extended and punctuated process. Dawson (2004–6, 2008, 2010, 2014) identified Malta and Gozo as an archipelago likely to have been colonized just once, on the basis of data available, and this was a notion largely supported by Trump (1995–6), although he did speculate about possible breaks in the cultural sequence. Without detailed chronology, the often momentary episodes of cultural activity are impossible to pin down in a time sequence that may cover millennia with little apparent cultural change. Accurate time measurement is fundamental too in controlling and comprehending the relationships between human activity and environmental change and climate fluctuation.

The growing field of palaeoecology, combined with increased knowledge of past climates and catastrophic events, has also added to the need for chronological precision that can correspond with human timescales. Current studies using precise proxies, such as tree-ring dating, demonstrate distinct

events in the past which are clearly signalled by a number of data that demonstrate downturns, climaxes, catastrophes (Baillie 1999) and also, the impact of humans on the natural environment (Butzer 1982; Goudie 1993).

Islands make excellent subjects against which to test these many ideas and technical approaches, especially when a combination of factors are clearly identified, such as:

- a reasonably isolated island of small size (i.e. less than 500 sq. km).
- a distinctive and dated archaeological sequence of human activity and material culture that changes over time.
- potential for extracting suitable environmental data such as pollen, molluscs-invertebrates, soil history, human and faunal remains with the potential to demonstrate dietary and climatic isotopic information.

Such data provide a solid base upon which to explore past human impact on the natural environment, and to identify how humans managed to cope when the resources of the natural world began to fail their needs. *FRAGSUS* was designed to explore and record a long human sequence that could challenge established theories and interpretations, and the outcome is recorded in the three *FRAGSUS* volumes, of which this is the first.

0.2. Background to *FRAGSUS* as an archaeological project

The richness of Maltese prehistoric archaeology has attracted a range of key figures who have explored its unusual qualities. Before the twentieth century, Maltese archaeology was a curiosity noted by travellers and administrators, but the study lacked much coherent scholarship. It was only from the first decade of the twentieth century that the outstanding partnership of Themistocles Zammit (an established scientist and archaeologist) and Thomas Ashby (a stratigraphic excavator whose skills were honed on the Roman monuments of Caerwent in Wales), projected the riches of prehistoric Malta onto the world stage. This followed the detailed published study of the German scholar Albert Mayr (Mayr 1908), who likewise had recognized the extraordinary prehistory of the Maltese Temple culture. The contributions of Ashby to knowledge of sites including Santa Verna, Kordin, Mnajdra and Ħaġar Qim (Ashby *et al*. 1913) and Zammit (1930), independently and more dramatically to the discovery of Tarxien, collectively demonstrated the creativity of the inhabitants of the Maltese Islands from an antiquity that had not previously been accepted. Zammit also developed a powerful understanding of the structure and diversity of the elaborate material culture within the impressive monuments he examined. Above all, he realized the importance of reconstructions *in situ* coupled with rapid publication and dissemination of information in written and museological form. A less well-known figure, until recently, is Luigi Maria Ugolini, who was one of the first scholars to appreciate the socio-cultural significance of these discoveries, stressing their importance over and above the classically inspired wisdom of the time. His work (Ugolini 1934) was amongst the first to interpret the discoveries in terms of the living people who created the monuments. As a synthesis, it is probably fair to state that these pioneers developed a broad understanding of the major monuments, most notably of the so-called temples, together with the underground burial chambers of Ħal Saflieni, but ignored other potential questions (principally those concerned with landscapes, environment and subsistence) that remained under-investigated.

After World War II, two archaeologists, John Evans and David Trump, built on the achievements of these pioneers. John Evans, like many significant figures of his generation, honed his forensic skills at Bletchley Park (the World War II code breaking centre for British Intelligence in Buckinghamshire, England) and applied them to the early Mediterranean through his training in Archaeology and Anthropology at Cambridge. In 1952, he was appointed by a committee led by the Royal University of Malta to systematize the unpublished and outstanding discoveries of the pioneers in a survey of the state of knowledge of the archaeology of the Maltese Islands. He combined this systematization with a series of surgical investigations of key monuments to attempt a chronological resolution to the rich material culture. Evans focused on sites where stratigraphy was clearly preserved by the sealed packed limestone plaster (*torba*) floors, and where uncontrovertible ceramic sequence could be extracted (see Volume 2, Chapter 10). In the tradition of Zammit, he also developed an early synthesis of these results (Evans 1953, 1956, 1959), even if publication of the full dataset took time (Evans 1971), a delay which allowed the inclusion of new and significant information. At the same time, he followed the footsteps of Ugolini by developing an interpretative framework, albeit in a rather different direction and tradition; he both posited the ideas of island archaeology (Evans 1973a, 1977) and considered the role of the priest in some of the monuments that he was synthesizing (Evans 1973b).

David Trump accompanied Evans on his exploratory fieldwork and, following his appointment as Curator of the Museum of Archaeology in Valletta in

1958, developed the subtleties in the prehistoric timetable much further. Most significantly, he excavated the site of Skorba Temple, uncovering new phases in the Maltese sequence and providing the radiocarbon dates to accompany this material (Trump 1961a, 1966). The chronology was no longer relative, but increasingly precise, even if based on remarkably few samples. Trump was also instrumental, with Charles Zammit, the museum director and the son of Themistocles, in displaying these achievements in the newly established National Museum of Archaeology in the centre of Valletta. In fact, David Trump developed a natural, albeit idiosyncratic, talent and strong following in the popularization of the importance of the Maltese Islands in prehistory (Trump 1972, 2002, 2010).

Two further figures (including one of the current authors) helped to steer us to developing the *FRAGSUS Project*. Colin Renfrew (1973) advanced the implications of the new radiocarbon dates largely produced by David Trump, but supplemented by himself, by highlighting the broader setting of calibration, and thus firmly establishing the claim that these monuments were the oldest free-standing stone monuments in the world. At the same time, he took their theoretical understanding further forward by putting forward theories of societies and their territories in an island setting, and how they might have developed over time (Renfrew 1973; Renfrew & Level 1979). Anthony Bonanno, the founding and long-standing head of the Department of Classics and Archaeology at the University of Malta, made his own very real contribution to the debate by synthesizing the available information (Bonanno 1986a) and by jointly proposing an Anglo-Maltese collaboration during a seminal conference that he organized in 1985 (Bonanno 1986b).

The collaboration that followed (1987–95) between the Universities of Malta and Cambridge and the then Museums Department took stock of the current state of knowledge based on Anthony Bonanno's 1986 synthesis. It was clear that study of the Neolithic 'temples', mainly on the island of Malta, had dominated previous research. Questions of death, domestic life, economy, the human and physical landscape had been under-researched. The Cambridge Gozo project under the direction of Anthony Bonanno, Tancred Gouder, David Trump, Caroline Malone and Simon Stoddart sought to investigate these remaining gaps. A single phase Temple Period settlement structure at Għajnsielem on Gozo was investigated in the first 1987 season (Malone *et al.* 1988, 2009a), the Xagħra Brochtorff Circle (sometimes referred to as a hypogeum) over seven field seasons (1987–94), and a field survey was started at the same time in those moments when the great investment of work on the Xagħra Brochtorff Circle permitted (1987–95). The most successful feature of the project was a deeper understanding of death ritual (Malone *et al.* 2009a). Some major strides were made in the survey towards appreciating the principal changes in settlement distribution between the ceramic phases of Għar Dalam to Baħrija in the central part of Gozo through a systematic landscape survey (Malone *et al*. 2009a; Boyle 2013; see Chapters 2 & 7). Some new information was gleaned on domestic life, and several likely settlement sites located, although the excavated Għajnsielem Road structure was largely devoid of informative refuse (Malone *et al*. 1988, 2009a). Very few advances were made in understanding the changes in the physical and natural landscape although several specialist scholars sought to identify means to extract knowledge and data (notably Hunt, Keeley, Canti and Schembri). The most successful work came indirectly from the study of land snails from the Xagħra Brochtorff Circle (Schembri 1995; Schembri *et al*. 2009). The scientific goals of the Cambridge Gozo Project (1987–94) were significant on a number of fronts. In particular, it achieved knowledge of prehistoric funerary ritual and an initial study of the prehistoric population. Inadequate funding meant that the osteological study was preliminary. Nevertheless, that work revolutionized approaches to the bioanthropology of the prehistoric population. It represented only the second discovery of a Temple Period funerary complex (rather than individual tombs) in Malta and the only example of a fully recorded burial assemblage. Chronological progress included a suite of accelerator mass spectrometer (or AMS) radiocarbon dates on human bone, fixing the episodes of burial for the first time, the study of molluscan evidence for environmental reconstruction, the identification of hard stone sources from outside Malta, and preliminary work on diet and the prehistoric exploitation of domestic animals (Malone *et al*. 2009a & b).

This archaeological work between 1986 and 2009 identified a number of directions for future research. There was a specific need for more scientific analysis of the human remains, for better understanding of diet, disease and changing life patterns, more precise AMS radiocarbon dating, and for application of (the then) new and promising aDNA methods on the enormous assemblage of human bones (*c*. 220,000 individual parts). In conjunction with excavated materials, we also suggested that sediment and environmental research might interrogate the question of climatic downturns that might address an overriding question, 'why did the Temple Culture collapse and disappear'? Central to this question is a current concern – the resilience and sustainability of human and natural systems, even though, with the luxury of historical hindsight, it is

evident that almost all cultural system fail eventually, or evolve into new formations. Malta provided an ideal test case to examine how a prehistoric community over time dealt with many constraints of space, resource depletion, and climate change. We hoped that climate and environmental changes in the local environment of Malta might be detectable, with the potential to inform on the archaeological social changes we identify in the human sequence. Rarely is this type of combined approach taken with small-scale prehistoric cultures, but surely an interdisciplinary approach has the potential to tells us far more about our human story and the manner by which humans cope that simply studying cultural materials?

0.3. Environmental research in Malta and the Mediterranean

Research on Quaternary environmental change has its roots amongst the earliest manifestations of the scientific investigations of the world by Classical and Enlightenment authors, many working in the countries around the Mediterranean. In the nineteenth and early twentieth centuries, however, advances were most rapid in the countries of Northern and Alpine Europe, where the very abundant glacial features and deposits had clear analogues in contemporary glaciated landscapes, attesting to the former extent of great ice-sheets. Further, technically straightforward investigations could be, and were, conducted on post-glacial materials such as bog peats and lake muds which contained easily recognisable sub-fossil plant and animal remains. During the earlier twentieth century, Quaternary sciences advanced rapidly in Northern Europe through investigation of previously glaciated landscapes and post-glacial sediments. Consequently, understanding of climate change and the role of humans in landscape change advanced considerably with the development of pollen analysis and a suite of other scientific analytical techniques (i.e. Hunt 2001; Brothwell & Pollard 2005; Sanderson & Murphy 2010; French 2015).

In contrast, investigation of the Quaternary history of the non-glaciated European countries, and particularly those adjacent to the Mediterranean, was initially far less straightforward, since these generally lacked glacial features, bogs and lake basins. The techniques such as pollen analysis, which had been developed for the bogs of northern Europe, were not easily applied to the often highly oxidized deposits available in southern Europe. Thus, although pollen analysis was widely used in northern European countries, its appearance in southern Europe was delayed to the late 1950s. In southern European countries, much early attention was focussed on the relatively abundant and often spectacular archaeology of early humans and particularly on cave deposits, many of which contained archaeological and faunal remains. Consequently, ideas about climate change and human impact on landscapes remained very sketchy and were often extrapolated from models developed north of the Alps (Bowen 1978).

Although several individual researchers, notably Karl Butzer (Butzer 1960; Butzer & Cuerda 1962), Enrico Bonatti (1966) and Thomas van der Hammen *et al*. (1965) had carried out high-quality localized investigations, the first comprehensive attempt to investigate Quaternary environments in the countries of southern Europe and around the Mediterranean was '*Mediterranean Valleys: Geological Changes in Historical Times*' by Claudio Vita-Finzi (1969). This seminal publication provided the impetus for the wide-scale investigation of Quaternary landscapes in many Mediterranean countries, notably the work of Donald Davidson (1971, 1980), John Bintliff (1977) and Tjeerd van Andel (Van Andel & Runnels 1987) in Greece, and a group of English researchers, including David Gilbertson, Chris O. Hunt, Caroline Malone, Simon Stoddart, Antony Brown and Graeme Barker in Italy (Hunt *et al*. 1992; Malone & Stoddart 1994; Barker 1995, 1996; Brown & Ellis 1995; Hunt 1998), Libya (Barker *et al*. 1996), Jordan (Barker *et al*. 2007) and the wider Mediterranean (e.g. papers in Woodward *et al*. 1995). Most of this work dealt with the landscapes and deposits of river valleys, and collectively it demonstrated that landscapes around the Mediterranean were extremely sensitive both to climate change and to human activity. The research confirmed the early observations of Butzer and Cuerda (1962) and Bonatti (1966), of generally arid and cold Pleistocene episodes correlating broadly with episodes of glacial expansion in Northern Europe interspersed with relatively humid temperate phases which coincided with Northern European periods of glacier recession. This and later research identified in the Mediterranean countries a general pattern of aridification after the Early Holocene humid phase, with increasing environmental human impact through grazing and arable agricultural vegetation clearance and consequent soil erosion.

The Cambridge Gozo Project, led in the field by Caroline Malone, Simon Stoddart and David Trump, offered the opportunity to extend landscape research into the Maltese Islands which updated the work of Trechmann (1938) and Pedley *et al*. (1990). Hunt (1997) showed that Trechmann's (1938) synthesis of the Quaternary deposits of Malta had been far in advance of its time, but the supposed interglacial marginal marine deposits identified by Pedley *et al*. (1990) were in fact terrestrial colluvial cold-stage sediments. It was

apparent from this survey that terrestrial evidence for Quaternary landscape change was sparse and discontinuous in the extreme. On the other hand, it also became apparent that the estuaries of the Maltese Islands contained substantial sediment bodies. Reconnaissance coring of a few of these estuarine sediment bodies proved deep sequences of well-preserved, if discontinuous, Holocene sediments of Neolithic and later age containing abundant sedimentary and fossil evidence for past environments (Carroll *et al*. 2012). A key component of the *FRAGSUS Project* was therefore to extend this approach, to generate a continuous landscape and climatic history by systematically exploring the estuarine sediment bodies and their contained sedimentary and biotic evidence.

Shortcomings to all previous work on the prehistory of Malta (and indeed, of much of the southern Mediterranean) have been the lack of coordinated scientific fieldwork and data collection. That coupled with insufficient resources for intensive fieldwork and scientific analysis have resulted in research content simply to identify sites and pottery without background on the 'landscape' and 'monuments'. Too rarely had soil and environment been considered as an integral archaeological component of the record, other than in the general sense of a covering over buried sites. Indeed, never had a soil history been undertaken of Malta that investigated the changing nature of soil over time as it related to the human story. Geographers had undertaken some excellent work in preparation for Independence (Bowen-Jones *et al*. 1961) and observed a much more accessible and visible landscape than is possible today. That work, however, was not aimed at environmental reconstruction and such work was not attempted until the Cambridge Gozo Project from 1987–95. The survey (Boyle 2013; see Chapters 6 & 7) aimed to map the established soil distribution in relation to site location, but the harsh alkaline cave-like environment of the Xagħra Brochtorff Circle funerary site the was such that pollen was not preserved, and by definition it was located some distance from the living sites, where pollen data would be most informative. The environmental questions, nevertheless, remained and one of the team from the original Xagħra work (C.O. Hunt) continued in the quest to obtain suitable environmental material over the two decades before *FRAGSUS* to obtain meaningful pollen samples (Hunt 1997, 2015; Hunt & Schembri 1999; see Chapter 3). The initial history of vegetation change was indicative (Carroll *et al*. 2012; Fenech 2007; Hunt & Schembri 1999), but inconclusive, with substantial gaps in the sequence for Malta at crucial times in later prehistory. Likewise, other environmental work had not investigated animal bone and the settlement and economy of prehistoric Malta at a reliable level. The rise and florescence of the extraordinary Temple Culture could not be explained in socio-economic terms, so prediction of population levels and density in prehistory was speculative. In tandem, it was not possible to measure changes in socio-economic conditions over prehistory without better data and a more extensive chronology. Without a deeper understanding of the environmental or economic base, the Neolithic World Heritage Sites were 'mysterious' and liable to excessive interpretation based more on a fantasy goddess culture than on archaeological facts. Thus there was a solid case for new research which the European Research Council (ERC) assessors generously recognized.

0.4. The development of the *FRAGSUS Project* and its questions

In the years immediately following the 2009 publication of the Xagħra Brochtorff Circle (Malone *et al*. 2009a), while other fieldwork was developed elsewhere in the Mediterranean by the team, the various issues became a discussion point for some of us (especially Malone and Hunt in the Palaeocology Laboratory of Queen's University Belfast, and others in the Universities of Malta and Cambridge, and the newly established bodies of Heritage Malta and the Superintendence of Cultural Heritage), to develop a project that was resolutely designed to solve the many remaining questions, and extend scientifically informative research activity in Malta as well as on the smaller island of Gozo. The precious resources of pollen, soils and sediment thus became central foci for the new project together with investigation of subsistence, food and domestic life in prehistoric times. With the rich resource of the Xagħra Brochtorff Circle population ready for additional scientific analysis to contribute to such studies, the notion of an explicitly interdisciplinary approach was readily embraced by the extended team. It was also realized that the chronology of the Maltese Islands, although established in its broad outlines, was based on too few dating samples, and too much on pottery sequences. If the understanding of the tempo of island life from prehistory to more recent times was to be better established, it was considered vital to invest heavily in cutting edge chronometric techniques that included Optically Stimulated Luminescence (or OSL) as well as Accelerated Mass Spectrometry (or AMS) radiocarbon dating. Without a core of chronological control across all aspects of the research, we realized that the precision needed to understand human and environmental change in general and in the microcosm of Malta in particular would be all but pointless.

FRAGSUS specifically set out to tackle a number of interdisciplinary questions (as presented to the ERC for the grant aid that supported the project). These questions centred around a central query that demanded better understanding of the chronology, environment and its changes and potential for exploitation over several millennia. We were particularly interested to learn whether there had been continuity of cultural activity on the islands over the Neolithic Temple Period and into the Early Bronze Age. Obviously, only a major, very well-funded project could apply the necessary modern levels of interdisciplinary scientific analysis to test the questions, and potentially make an advance in understanding. A period of collaborative discussion in 2011–12 led to the application, headed by Malone, for funding from the European Research Council (ERC). *FRAGSUS* as a project was developed around the five principal questions (see §0.5) and the application of new and well tested approaches which we described as follows:

> *We bring a suite of specialised modern palaeoecological, environmental, landscape, anthropological, archaeological and chronological approaches – practical and analytical – to examine the issues of long-term cultural sustainability in this fragile environment. We will sample sediments, sites, material culture, human remains and landscapes to study interlinked elements which may collectively provide understanding of how a culture developed, was maintained and collapsed. Detailed chronology will be developed using state of the art AMS (Accelerator Mass Spectrometer) radiocarbon, tephra and cultural dating to provide vital control over the data, enabling realistic understanding of cultural and environmental change. We have pilot tested these approaches in previous fieldwork and will apply them to this key case study. As a central focus, eight pollen cores will be drilled, dated and studied for pollen, invertebrate and other fossils proxies to reconstruct the dynamic ancient environment in the context of the human landscape provided by the archaeological evidence of settlement and human remains.*

The application was submitted in April 2012. The multiple project questions were designed to provoke interdisciplinary approaches that employed original fieldwork, fresh data collection, various analyses and a range of new scientific approaches. Some questions were simple, supported by the outcomes of previous study, and they had superficially obvious answers, but mostly, simple questions tackled through new, demanding and precise methodology have invariably opened doors into new theoretical territory. It was the intention of the project to explore and tackle the unknown, to take risks and move the fields of study forward, and the works undertaken very much reflect these aspirations. As the reviewers of the ERC grant application commented, the aspirations were admirable, but although many might not fully succeed, the journey was worthwhile in itself. It was thus that the team set out in May 2013 to start a demanding five-year programme of research into past climate, landscapes, people and their cultures, to explore what enabled or hindered human sustainability in small islands in the past. Our focus was the Maltese Islands, selected partly for our previous knowledge, but also because the size and scale presented opportunities to examine the 'rise and fall' of a distinct civilization. Other parts of the Mediterranean or Aegean might have proven harder to distinguish such distinctiveness, but Malta with its remarkable Temple Culture presented the greatest potential to test our questions. Malta too, was chosen because of the long-standing collaborative relationship extending over decades, and the shared sense of affinity with a remarkable ancient people whose world we had already begun to observe at ever closer quarters since the late 1980s.

The *FRAGSUS Project* attempts to address the many issues identified here in the broader framework of resilience theory within a restricted island community. The concept of resilience may be considered narrowly as the return rate to equilibrium or stasis after a disruptive event, and also infers a capacity to persist and resist change (Folke 2019). In particular, it is a way of understanding the capacity of ecosystems to absorb and retain their current state, and recover to a state of equilibrium following disturbance, as well as how human actions may contribute to coping strategies or a loss of adaptability (Holling 1973; Gunderson 2000; Walker *et al*. 2004; Desjardins *et al*. 2015). It is a dynamic concept focusing on how to evolve and persist with change, with adaptability and preparedness being key (Folke *et al*. 2010). Importantly, social and ecological systems should be envisaged as intertwined (Folke 2006, 2019), and contemporary environmental change may only be fully understood with contributions from archaeological and palaeoenvironmental research over the *longue durée* (van der Leeuw & Redman 2002; Davis 2019).

FRAGSUS necessarily draws on the archaeological work of our predecessors, principally Zammit, Ugolini, Ashby, Evans, Trump and Renfrew, who had in their various ways laid the foundations for this continuing study. The project was born partly from this rich background, coupled with issues arising from

our previous archaeological fieldwork undertaken between 1987 and 1995 (The Cambridge Gozo Project and excavations at the Xagħra Brochtorff Circle), and the complementary studies in environmental change (Carroll *et al.* 2012; Fenech 2007; Hunt & Schembri 1999; Schembri *et al*. 2009). There were many questions that still remained to be addressed, and new studies demanded the investment of modern scientific infrastructure and expensive specialist analyses. *FRAGSUS* could never have been achieved without the availability of substantial funds from the European Research Council, provided through the award of the Advanced Researchers Grant No. 323727. We are very grateful for the support provided and trust that this and its partner volumes provide a suitable acknowledgement.

The original project team comprised comprising nineteen scholars spread between Britain and Malta, and initially from Queen's University Belfast, the University of Cambridge, the University of Malta, Heritage Malta and the Superintendence of Cultural Heritage. Later some colleagues moved to the Universities of Plymouth and Liverpool John Moores, whilst further collaboration with colleagues at University College, Maynooth and University College and Trinity College, Dublin, and SUERC (University of Glasgow) also joined the team. In addition, new research staff attached to the main partner institutions were engaged to undertake specific sub-programmes of specialist work, and over the years a number of post-graduate students also joined the project to undertake PhD and Masters dissertations.

0.5. Archaeological concerns in Maltese prehistory and the *FRAGSUS Project*

The project was devised to tackle the outstanding general questions and issues noted above, through five specific questions that addressed the central question about what occurred at the end of the Maltese Temple Culture. The interlinked questions centred on the fragility and resilience of island life were developed. As so often in such an intensive project, not only have many questions been addressed and partly answered, but also, the answers raise new questions for future researchers to tackle.

A central feature of the project design was to bring multiple techniques together to address the same questions from a variety of angles, thus strengthening the validity of many of the conclusions.

The seven important environmental/socio-cultural questions have been addressed by this project, and are considered in this volume and Volumes 2 (Malone *et al*. in press) and 3 (Stoddart *et al.* in press):

1. What was the impact of human settlement on Malta from Neolithic times onwards, and how rapid was the process of deforestation, erosion and degradation? When did technical mechanisms to manage the environment develop – such as terracing, water and food storage? Were such mechanisms in place before or after the Temple Culture collapsed?

Enormous advances have been made by the interlinking of well dated series of environmental samples taken both from seven new deep cored pollen locations (with a corresponding sevenfold increase in catchment), numerous valley profiles (this volume) and six new AMS dated archaeological stratigraphies (Volume 2). As this and the other *FRAGSUS* monographs will show, a highly complex and fragile turbiditic landscape has been uncovered. Questions about the introduction of terracing, control of water and development of food storage have been less effectively addressed and remain issues to be solved by the next generation of archaeologists.

2. How did a very small island community in prehistoric times manage to sustain dense, complex life over millennia, and what specific social, economic and ritual controls emerged to enable this? Were the monumental temples instrumental in this process of sustaining cultural life?

For the answers to these questions, we necessarily draw on the information provided by Zammit, Evans and Trump, as scholars who investigated the temples when they were better preserved. However, the *FRAGSUS Project* has supplemented this work by the investigation of sequences from four Neolithic temple sites at Ġgantija, Santa Verna, Skorba and Kordin III. In addition, the evidence from the settlement area of Taċ-Ċawla, even if a complex multi-period site, has permitted the elucidation of some of the essential differences between the communal activities of the temples and smaller scale activities of domestic living sites. These results form the basis of Volume 2.

3. What sort of agriculture was used, and what did people eat, especially as the landscape became increasingly degraded and the environment more unpredictable? Were there failures in the food supply?

A two-pronged approach has been successfully delivered, drawing on both the refuse of the living and the remains of the dead. The settlement site of Taċ-Ċawla has delivered an unprecedented series of refuse samples that give a measured development of the food resources (carbonized seed and bone) from the Maltese Islands which can be compared with the evidence from the bodily remains of their near neighbours and contemporaries

interred in the Xagħra Brochtorff Circle. The other sites have also yielded evidence of plant and animal refuse that further indicate evidence for exceptional foods and more routine diets (see Volume 2). Palaeosols, pollen and fungal spore analysis have provided indications of past landscape and land-use changes as well as the intensity of arable agriculture and cereals in the landscape over time (see Chapters 2–5).

4. What was the size and nature of the early Maltese population and what role did demographic connectivity (immigration) play in maintaining island sustainability? What impact did diet, disease and stress have on the population?

By understanding the impact of environmental instability, disease and stress on the early people over the first millennia of occupation, we may be able to assess how they coped, and the mechanisms that may have been in place to control their population and scarce resources. Our insights into the changing demography of the Maltese Islands remain indirect but nevertheless, much better informed than in any previous study. The Cambridge Gozo survey (undertaken in the late 1980s and early 1990s, with summaries presented in Chapters 6 and 7 and in Volume 2, Chapter 1) has given some sense of the relative and changing density of a small sampled part of the landscape. The studies of agricultural development and pastoralism (see Chapters 3, 5, 8 & 9) add to this work, by providing important insight into the potential carrying capacity of the islands. The soil, pollen and molluscan analyses have recorded the impact of these populations on the islands at a date even earlier than the settlement record (see Chapters 3–5). Studies of aDNA, isotopes and the physical anthropology (see Volume 3) have demonstrated different degrees of understanding of the connectivity of humans with the outside world which can be measured against the imported non-organic materials such as stone axes, as well as the local crops, trees, animals and other resources. A deeper understanding of demography remains a substantial challenge, and one that future generations can continue to tackle.

5. Was there social-economic or environmental failure at the end of the Temple Culture in the later third millennium BC*, and what may have caused society and its agricultural economy to change so drastically or possibly collapse? Was there a hiatus between the Temple Culture and later Bronze Age settlers?*

A number of indicators have been combined to investigate the environmental-economic and human situation at the end of the Temple Period, including pollen, molluscan, soil and sedimentary data, human remains and the distribution of radiocarbon dates. Collectively, these do support the evidence for important changes at about 2400–2300 BC, but similar analysis has also detected palaeoenvironmental and demographic changes in the fifth millennium BC, extending over a longer period (see Chapters 3, 6, 7 & 11 & Volumes 2 and 3). The definition and narrowing of these windows of change is one of the exciting results of the current work and stimulating prospects for further analysis by future generations of archaeologists.

6. What, if any, were the effects of long-term climate change on the agricultural resilience and sustainability of the Maltese Islands?

The suite of detailed of complementary pollen, molluscan, soils and sediment data with a robust, newly established chronology has suggested both long-term degradation of the landscape as well as variable imprints of agricultural use and intensification, and valley-by-valley sequences of fill related to catchment responses to human activities, erosion and changing climatic factors over the past 8000 years (see Chapters 2–5). Surprisingly, there has been a substantial degree of resilience in the Maltese landscapes over the longer term.

7. How does the Maltese sequence of palaeoenvironmental and cultural changes compare with the long-term records of environmental change and short-duration extreme events over the last 10,000 years observed elsewhere in the southern Mediterranean region, such as Sicily?

There appears to be a degree of synergy between the Maltese palaeoenvironmental records and other regions of the central and southern Mediterranean basin. Most notably the effects of aridification are evident in the palaeosol and vegetational sequences from the latter part of the Temple period (see Chapters 3–5). But there the detailed, chronological well-defined, studies of the valley deep cores (see Chapter 2) have greatly refined our ability to chart changing human-environment relationships in many parts of Malta and Gozo at a scale of resolution rarely attempted before, both temporally and spatially.

0.6. The research programme: the sites and their selection

The overall project focused on three forms of data collection:

- the environmental material buried in the landscape (this volume).

- the prehistoric sites and their buried deposit and material culture (Volume 2).
- the buried population of the Xagħra Brochtorff Circle and other prehistoric sites (Volume 3).

In addition, the data collected from the intensive landscape survey of Gozo between 1987 and 1995 were also reassessed through GIS and provided important supporting information for the three data groups above (see Chapter 7).

0.7. Investigating the palaeoenvironmental context

The *FRAGSUS Project* enabled an unrivalled opportunity to elucidate the Holocene palaeoenvironmental and archaeological history of the islands of Gozo and Malta. Particular emphasis was placed on the recognition of the impacts of the first Neolithic farmers and Temple Period builders, but also on the investigation of the imprint of human activities on the islands both before and after this unique period, and the impact of climate and environmental change on the human societies and how resilient the islands were to these changes.

Generally, strong monsoonal influence and Hadley circulation in the Early Holocene caused the southeastern and northwestern Mediterranean countries to be relatively humid, while the southwestern and northeastern countries were less humid (Weninger 2006; Magny *et al*. 2009, 2011; Carroll *et al*. 2012; Bini *et al*. 2018). As the Holocene progressed, the monsoonal influence declined and the southeastern and northwestern countries became less humid and the northeastern and southwestern countries became relatively more humid. Punctuating these trends were a series of short periods of climate disruption originating in the North Atlantic. These events at 9.3, 8.2, 6.5 and 4.3 ka BP (7350, 6250, 4550 and 2350 BC) seem to have impacted the countries around the Mediterranean with varying degrees of severity, and some appear to be synchronous with major episodes of societal disruption and population mobility (e.g. Weninger 2006). The trajectory of climate change in neighbouring lowland Sicily does not seem to have been affected severely by these events, although aridification seems to have started *c*. 3050 BC (Noti *et al*. 2009; Tinner *et al*. 2009), but Carroll *et al*. (2012) pointed out the coincidence between the dates associated with the end of the Temple period in Malta and the 4.3 ka BP (2350 BC) event, and demonstrated an interruption in cereal cultivation in the Salina Bay records at this time. Thus, the project aimed to provide new, chronologically robust palaeosol, palaeovegetational and palaeoclimatic data to compare with the archaeological record and with other long-term records of environmental change in the southern Mediterranean region (see Chapters 3–5).

Soil degradation and erosion in the islands of Malta and Gozo are regularly observed as a compelling and prevalent problem today and one that has its origins in earlier prehistoric times (Lang 1960; Blouet 1997; Vella 2003; Fenech 2007; Grima 2008b; Malone *et al*. 2009a). Moreover, these islands appear to share many of the soil characteristics and history of a continual struggle against aridification, dewatering and with the intensification of agriculture associated with the creation of extensive terraced landscapes, just as occurred in many other parts of the Mediterranean area (Brandt & Thornes 1996; Carroll *et al*. 2012; Sadori *et al*. 2013). As a corollary, the development of the typical red Mediterranean soils or *terra rossa* on limestone substrates of this region (Bridges 1978; Lang 1960; Yaalon 1997; Van Andel *et al*. 1990) were also be investigated.

It has always been assumed that the seasonally dry and hot Mediterranean climate made the Maltese landscape quite marginal in agricultural terms (Schembri 1997). As a consequence, it has sometimes been presumed that terracing was adopted extensively from prehistoric times in Malta and Gozo to conserve soils and moisture, and create a better landscape for subsistence based agriculture (Rolé 2007). Like many other parts of the Mediterranean, this landscape is thought to have been prone to deforestation, drought and soil erosion, combined with intensive human activity, and that this has been the case since Neolithic times (Brandt & Thornes 1996; Bevan & Conolly 2013; Grima 2008a & b; Grove & Rackham 2003; Hughes 2011; Djamali *et al*. 2013). This project explored the evidence for the subsistence practices of these early people, and it examined how they managed to develop a sufficiently productive economy to support and sustain temple building in the late fifth to mid-third millennia BC. The latest techniques of dating, geoarchaeology, palaeo-economy, remote sensing, survey and sampling were employed to push the boundaries of knowledge towards understanding this problem. By integrating the archaeological and landscape evidence with environmental reconstruction, chronology and population history, we should be able to connect the disparate bodies of evidence, and to propose models that explain the long-term impact of population and settlement on the Maltese Islands. Moreover, the models should have a wider application to other times and places, given the cyclical nature of human behaviour. This volume begins that process of modelling and integration, and the work continues in Volume 2 by developing the archaeological story and its implications for these islands.

The research reported on here aimed to examine these assumptions and questions and test them using a variety of palaeoenvironmental, geoarchaeological,

chronological, Geographical Information System, archaeological and historical approaches, both on- and off-site (cf. French 2015). This extensive, multi-disciplinary suite of approaches was combined to investigate issues of long-term cultural sustainability in this fragile environment. Multiple investigations of deep valley sediments, buried soils and landscapes, archaeological sites and human remains were all combined in an interlinked study which may collectively provide understanding of how a culture, environment and landscape developed through time. Detailed chronological investigations of off- and on-site locations were developed using state of the art Accelerated Mass Spectrometry (or AMS) radiocarbon, tephra, Optically Stimulated Luminescence (or OSL) and cultural dating techniques to provide vital control over the data, enabling realistic understandings of cultural and environmental changes. As a central focus, a substantial number of deep valley cores was drilled, dated and studied for pollen, invertebrate and other fossil proxies, and along with extensive geoarchaeological survey, sedimentary and buried soil analyses were to reconstruct the dynamic ancient environment through time in the context of the human landscape provided by the archaeological evidence of settlement and human remains (see Chapters 2–5). These combined approaches are still relatively rare, but have provided a stunning battery of new detailed sequence data for the Maltese Islands from which to interrogate and better explain the archaeological record.

0.8. Archaeological investigations

Archaeological sites were chosen to cover the chronological and functional range of human occupation of prehistory in the Maltese Islands to the end of the Temple Culture, with an equal attention to pragmatic issues such as access and ownership. By the end of the project one settlement zone around a probable water hole (Taċ-Ċawla), four temple sites (Ġgantija, Kordin III, Santa Verna and Skorba, the latter two with deep stratigraphies) and a Middle Bronze Age defensive settlement (In-Nuffara) had been investigated (Figs. 0.2 & 0.4). Already collected samples were analysed

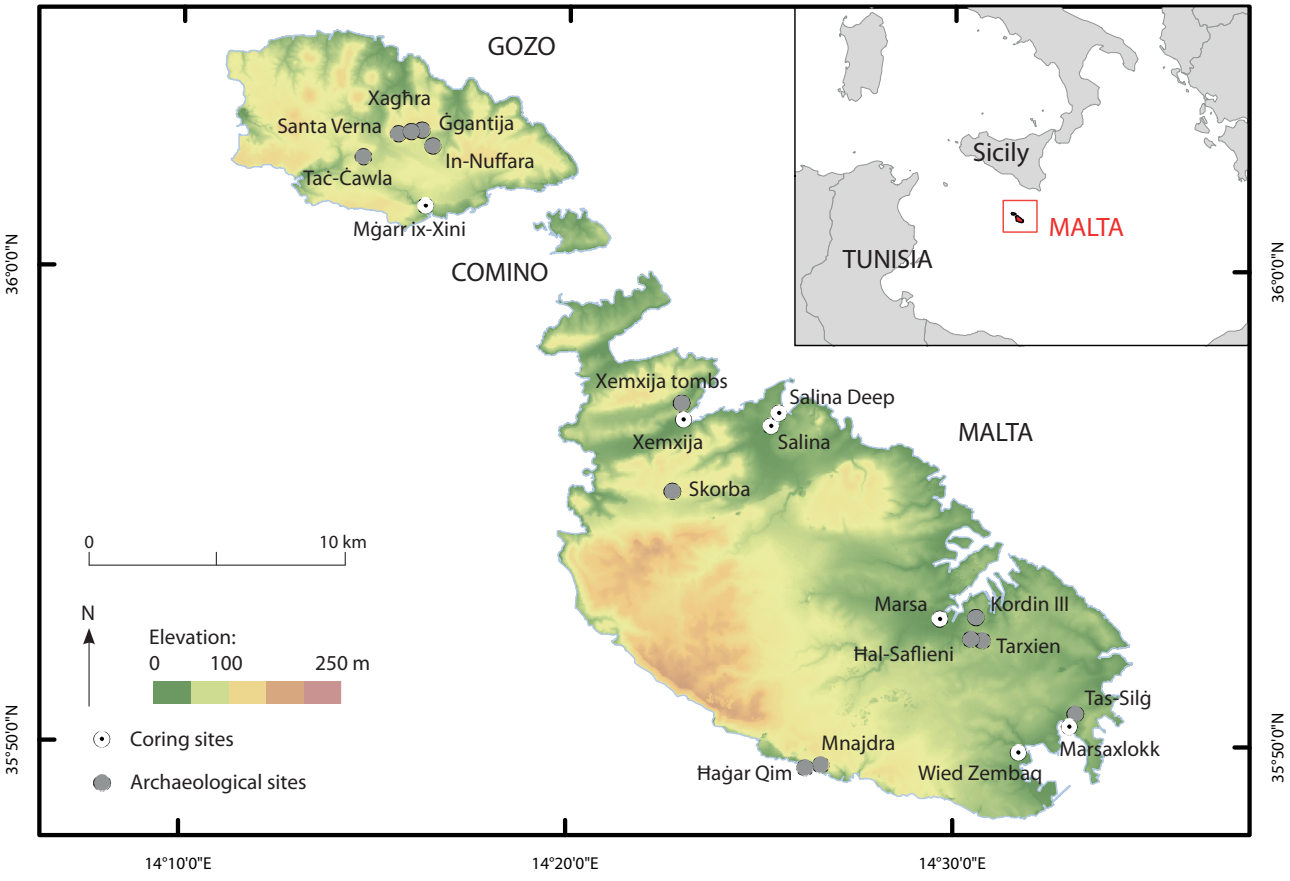

Figure 0.2. *Location of the main Neolithic archaeological and deep coring sites investigated on Malta and Gozo (R. McLaughlin).*

a

b

Figure 0.3 *(above and opposite). Some views of previous excavations on Gozo and Malta. a) Santa Verna, looking east (Ashby(o).XXXVII.91); b & c) Ġgantija, looking southeast (TA[PHP]-XXVII.083, TA[PHP]-XXVIII.011); d) stone circle, Xagħra (TA[PHP]-XXVII.100) (with kind permission from the Ashby Archive, The British School at Rome; all rights reserved).*

c

d

a

b

c

d

e

Figure 0.4. *Some views of recent excavations at Santa Verna (a), Ġgantija (b & c) and Skorba (d) temples, and In-Nuffara (e) (C. French).*

from a further two prehistoric sites (Xagħra Brochtorff Circle and Tarxien) and one medieval site (Mdina) (Fig. 0.3). The sites of Taċ-Ċawla, Santa Verna and Skorba provided the most elaborate and chronologically wide-ranging information, and Taċ-Ċawla, Santa Verna and Kordin III also enabled spatially informative information over the area of a site. The detailed results from this new fieldwork are presented in Volume 2.

The programme of work started with the extensive excavation of Taċ-Ċawla and survey of Ġgantija and Santa Verna (2014), progressed towards the excavation of Ġgantija, Santa Verna and In-Nuffara (spring 2015) and Kordin III (summer 2015), and ended with limited work at Skorba (spring 2016) (Fig. 0.4). The most substantial teams were present at Taċ-Ċawla, Santa Verna and Kordin III. The main personnel at each of these sites was provided by Queen's Belfast, the University of Cambridge and the University of Malta, respectively, together with university student assistance from each university.

The choice of sites for excavation was designed to assess the *FRAGSUS* questions by contributing to understanding of: (i) impact of human settlement on Malta, (ii) social sustainability, (iii) the size and nature of the prehistoric population, and (iv) the social and economic changes at the end of the Temple Period. They were also selected as being representative of particular landscapes that might inform on associated sites. For example, Kordin III, because the site was close to the Tarxien and Ħal Saflieni complex, offered potential insight into the prehistoric landscapes of the now highly urbanized city-scape of Paola.

A number of other sites were considered but were not eventually included in the study on grounds of time, access and certainty of contribution to the *FRAGSUS* questions. However, these continue to be very viable places for study of Malta's past for future generations of archaeologists. Ta' Marżiena (Gozo) (a probable temple site with deep stratigraphy) was laser scanned, but its access would have required negotiation with a private land-owner. The main Bronze Age fortifications of Borġ in-Nadur on Malta were scanned but some work had recently been undertaken and further work was logistically difficult. Xrobb L-Għaġin, a probable temple site on Malta, threatened by cliff collapse, was considered too dangerous to investigate. Għar ta' Għejżu on Gozo was scanned, but had already been badly damaged and contained no deposits. The Xemxija burial chambers were scanned and the skeletal remains recovered by Evans have been considered by Jess Thompson in Volume 3 in a fresh analysis. Għar Dalam was scanned, but the deposits considered too precious for further excavation. The south temple of Ġgantija was scanned but never considered for excavation, except on its margins where the two sondages were recorded (see Chapter 5 & Volume 2). The Xagħra Brochtorff Circle was 3-D scanned, but permission was never received for limited further excavation to assess the eroding condition and conservation needs of the site. The Skorba period site of Ta' Kuljat detected on the original Gozo survey was considered for excavation, but considered logistically too problematic. Many other sites across the now heavily threatened Maltese-Gozitan landscape could have been included, minor temple structures, isolated megaliths, rock cut tombs and exposed sections, but for the present, the six interventions and their associated environmental analysis are the harvest of the *FRAGSUS Project* (see Volume 2).

Part I
The interaction between the natural and cultural landscape – insights into the fifth–second millennia BC

Chapter 1

The geology, soils and present-day environment of Gozo and Malta

Petros Chatzimpaloglou, Patrick J. Schembri, Charles French, Alastair Ruffell & Simon Stoddart

This chapter sets the scene in terms of the geology and present-day climate, vegetation and soils of the Maltese Islands. Geology and faulting has had a huge influence on topography, soils and vegetation, and in turn on the nature of human use and exploitation of the islands. All of these themes are further developed below (and in *FRAGSUS* Volumes 2 and 3), giving time-depth to the sequences of climatic, environmental and landscape changes throughout the Holocene.

1.1. Previous work

The geological formations of Maltese Islands received little attention from scholars before the nineteenth century AD, in common with other parts of Europe. Nonetheless, ancient Greek authors made the first surviving references to fossils found elsewhere in the Mediterranean (e.g. Xenophanes of Colophon, born about 570 BC and Origen, AD 185–254). A number of early advances in the stratigraphic study of geology were made by British scholars such as Smith (1769–1839), following the incorporation of Malta into the British Empire in 1800, when the focus and expertise on geological stratification commenced. Commander Thomas Abel Brimage Spratt made the first comprehensive geological descriptions of the islands, including the identification of chert outcrops (Spratt 1843, 1854). He was followed by John Murray who produced a review of the geology of the islands in 1890 (Murray 1890). His work was focused on oceanic sedimentation, an expertise he gained on the Challenger Expedition (1872–6) and his interpretations demand respect, even if they are not entirely correct. Murray's work stimulated John Henry Cooke, an expatriate teacher of English, to produce a series of detailed and highly considered studies on individual geological features (Cooke 1891, 1893a–c, 1896a–c). They included the only accurate, comprehensive macroscopic investigation of the chert outcrops of the Maltese Islands (Cooke 1983b), which was considered very high-quality research at the time. They presented a high level of detail and largely accurate interpretation in contrast to more generic geological work of the time (Zammit Maempel 1977; Gatt 2006a & b, and references therein).

Research on the geology of the Maltese Islands continued during the twentieth century, when researchers focused on a range of features. A typical example was Hobbs (1914), who interpreted and described many of the faults and structures of the islands. In addition, substantial detailed information on the structure of the islands is contained in the study of water resources by Morris (1952) and Newbery (1968). The recent long-term research of Martyn Pedley is of particular significance as he has observed and published on the full spectrum of Maltese geology (Pedley 1974, 1975, 1978, 1993, 2011; Pedley *et al*. 1976, 1978, 2002). This includes a modern geological map of the Maltese Islands (Pedley 1993) which is still the basis of the present official geological maps published by the Maltese Government (https://continentalshelf.gov.mt/en/Pages/Geological-Map-of-the-Maltese-Islands.aspx). Pedley's work and that of other contemporary workers, laid the foundations for the modern study of the geology, geomorphology and palaeoenvironment of the islands (Pedley & Bennett 1985; Pedley *et al.* 2002; John *et al*. 2003; Magri 2006; Föllmi *et al*. 2008; Gruszczynsk *et al.* 2008; Baldassini & Di Stefano 2015; Galea 2019; Scerri 2019; and references therein). More recently there has been a focus on the now submerged continental shelf around the Maltese Islands associated with pre-Holocene archaeological and palaeoenvironmental investigations around the coasts (Hunt 1997; Micallef *et al*. 2013; Foglini *et al.* 2016; Harff *et al.* 2016; Prampolini *et al*. 2017).

1.2. Geography

Malta is made up of a small group of three principal islands – Malta, Gozo, Comino, and a number of minor

islets and rocks (Fig. 1.1), with a total land surface of 316.75 sq. km. It is characterized by high hills or plateaux (Ta' Dmejrek on Malta is 253 masl and Ta' Dbieġi on Gozo is 187 masl) separated by deeply incised valleys which are characteristically orientated southwest–northeast. Much of the remaining non-urban landscape is dominated by agricultural land with terraced fields on hilly ground to the north of Malta and on Gozo. Although past water bodies have been reported on the surface of the islands, there are today no lakes, rivers or permanent streams, and only some springs and coastal wetland areas.

Malta and Gozo are the largest islands (respectively 245.86 sq. km and 67.1 sq. km), while Comino and Cominotto, which are found in the narrow channel between the main islands, are smaller at 2.8 sq. km and 0.1 sq. km (9.9 ha), respectively. The Maltese Islands lie at the centre of the Mediterranean Sea, with a southeast–northwest orientation, between Sicily and the North African coast (Fig. 1.1). They are far from any mainland, located *c*. 96 km south of Sicily, about 300 km east of Tunis and 290 km north of the Libyan coast (Cassar *et al*. 2008; Schembri, P.J. 2019). In spite of their small size, these islands occupy a very

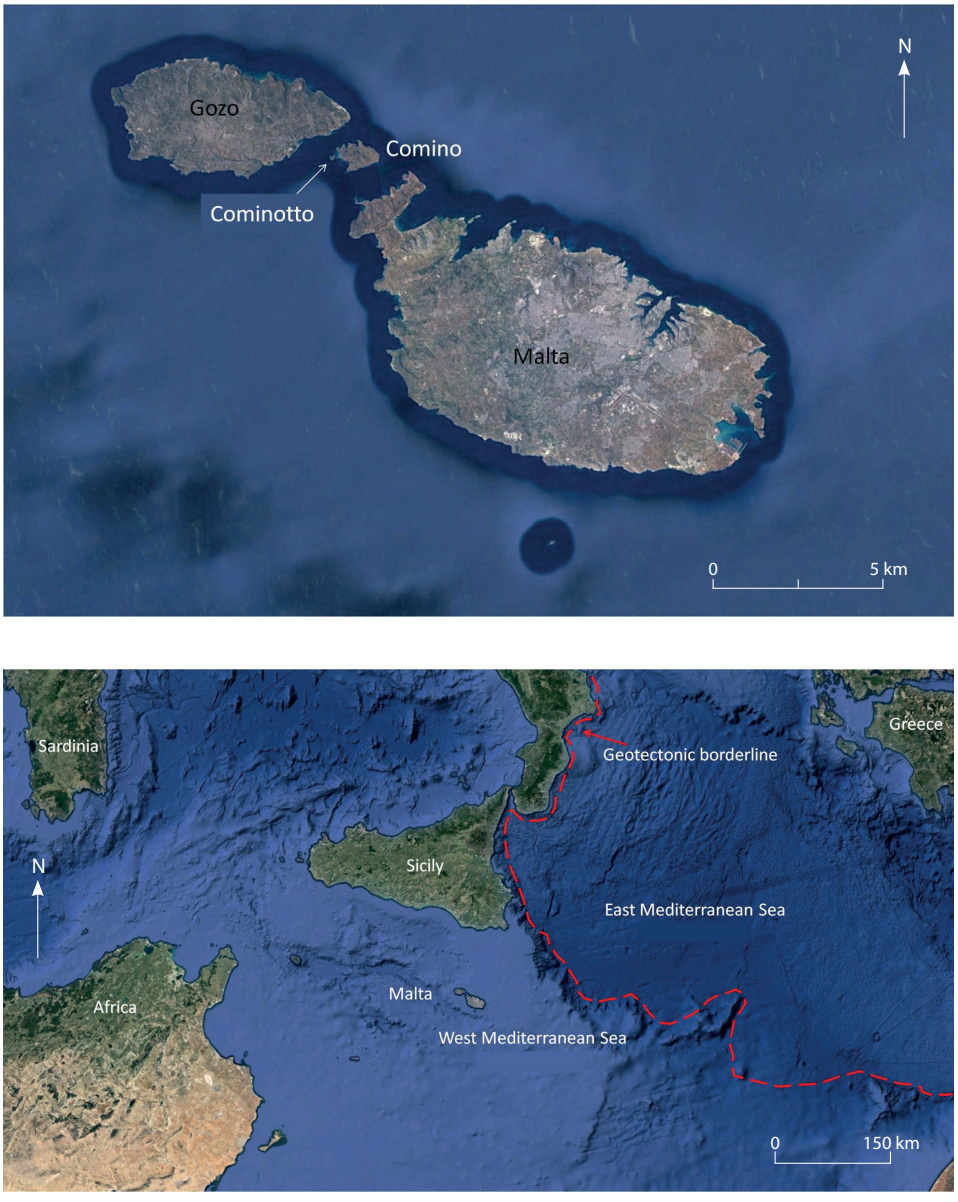

Figure 1.1. *The location of the Maltese Islands in the southern Mediterranean Sea with respect to Sicily and North Africa (P. Chatzimpaloglou).*

significant location within the broader Mediterranean region (Stoddart 1999). Their location in the Sicilian Channel, the main navigational seaway connection between the eastern and western Mediterranean, with the presence of exceptional natural harbours, gave the Maltese Islands an indisputable strategic importance (Blouet 1984; Pedley *et al*. 2002).

1.3. Geology

It is difficult to distinguish when exactly the basin which contains the Maltese Islands began to form. Some authors place this at 150 million years (when Pangea began to break into continents), whilst others suggest 100 million years ago (when Europe split from North America and started moving towards North Africa) (Pedley 1974; Puglisi 2014). Regardless of exactly when this occurred, the progressive approach of the European and African continents transformed the intermediate zone (Tethys seaway) between them, the forerunner of the present day Mediterranean Sea, and created the foundations of the central Mediterranean where the Maltese Islands are located. This, however, was not a simple process, but included a variety of complex movements and caused many stresses to the continents' margins. Moreover, the oceanic crust at the margin of the African continental plate that has subducted beneath the Eurasian plate brought up ocean sediments and slivers of ocean crust to form mountainous coasts or islands, with associated volcanism and orogeny (Pedley 1974; Galea 2007; Puglisi 2014). The African plate is still moving towards the Eurasian plate today. The Maltese Islands have a key position in this environment as they lie in what was originally a shallow sea (depth below 200 m) at the junction of the western and eastern Mediterranean basins (Fig. 1.1). This area called the 'Sicilian-Tunisian Platform,' and also known as the 'Pelagian Block,' represents the foreland margin of the African continental plate and consists of massive marine carbonate deposits (Pedley 1974). Extensional tectonics and the associated uplifting in the central parts of the Pelagian Block as a result of the development of the Pantelleria Rift System in the Late Miocene gave rise to what today are the Maltese Islands to the northeast and the island of Lampedusa to the southwest of the rift (Reuther & Eisbacher 1985; Dart *et al*. 1993; Galea 2007, 2019). This rifting also resulted in deep trenches (grabens) between the Maltese and Lampedusa islands, accounting for the deep water to the east and southeast of Malta in an otherwise shallow sea.

Inevitably, the location of the Maltese Islands in this broader geological environment has shaped the type of rock formations found on them. Maltese rocks are composed almost entirely of shallow to medium-depth marine sedimentary formations, mainly of the Oligo-Miocene age (*c*. 30–5 ma BP) with a variety of scattered freshwater and terrestrial deposits of limited extent and rare brackish and marine deposits of Quaternary age. The Oligo-Miocene marine sediments are most comparable with the mid-Tertiary carbonate limestones occurring in the Ragusa region of Sicily to the north, in the Pelagian Islands and in the Sirte Basin of Libya to the south (Pedley *et al*. 1978; Schembri 1994). There are five main rock formations, which are present in a simple succession with a number of hiatuses (Oil Exploration Directorate 1993; Pedley *et al.* 1976, 2002; Zammit Maempel 1977; Galea 2019; Scerri 2019). These, starting from the bottom, are: a) the Lower Coralline Limestone, b) the Globigerina Limestone, c) the Blue Clay, d) Greensand and e) the Upper Coralline Limestone (Figs. 1.2 & 1.3; Table 1.1). The Lower Coralline Limestone, Globigerina Limestone, and Upper Coralline Limestone are in turn composed of a number of members.

Table 1.1. *Description of the geological formations found on the Maltese Islands.*

Geological time (youngest to oldest)	Formation	Description	Thickness
Miocene	Upper Coralline Limestone	Shallow marine limestone with abundant coral-algal mounds and reefs, commonly altered to micrite and sparite	0.70–175 m; moderate to very high permeability (especially where karstified)
	Greensand	Friable, glauconitic argillaceous sandstone, moderate permeability	0.5–15 m
	Blue Clay	Massive to bedded grey/blue shallow marine/offshore calcareous claystones with occasional to abundant marine fossils. Impermeable or an aquiclude	50–75 m
	Globigerina Limestone	Shallow marine, calcareous mudrocks with abundant fossils, poor permeability, phosphatized hardgrounds	20–227 m
Oligocene	Lower Coralline Limestone	Shallow marine limestones with spheroidal algal structures, abundant echinoid fossils. Well-cemented and permeable	100–140 m

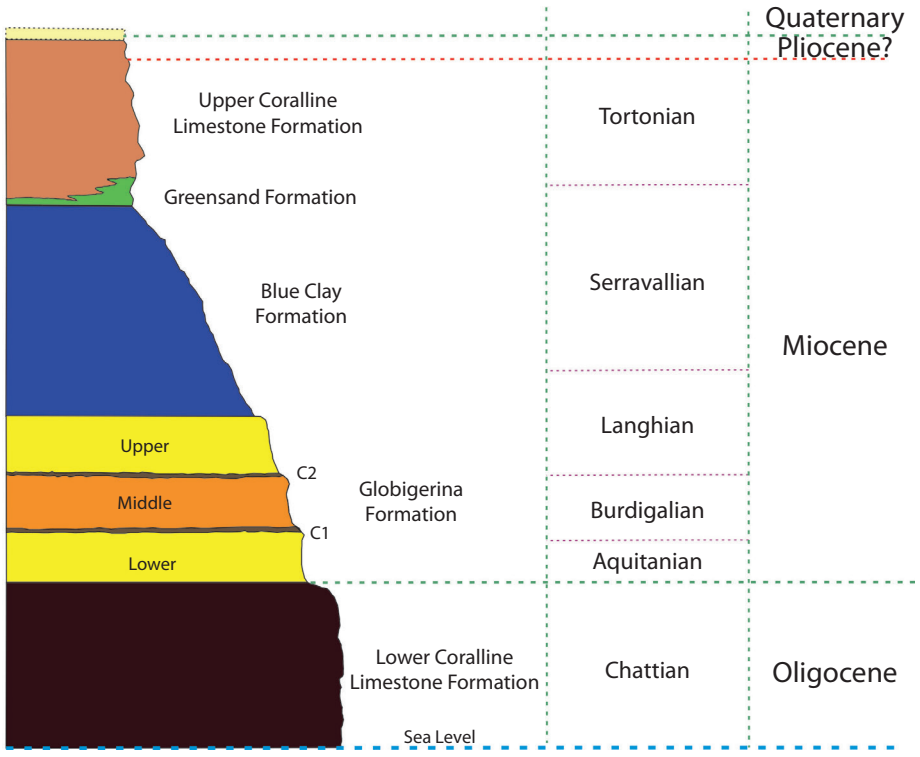

Figure 1.2. *Stratigraphic column of the geological formations reported for the Maltese Islands (P. Chatzimpaloglou).*

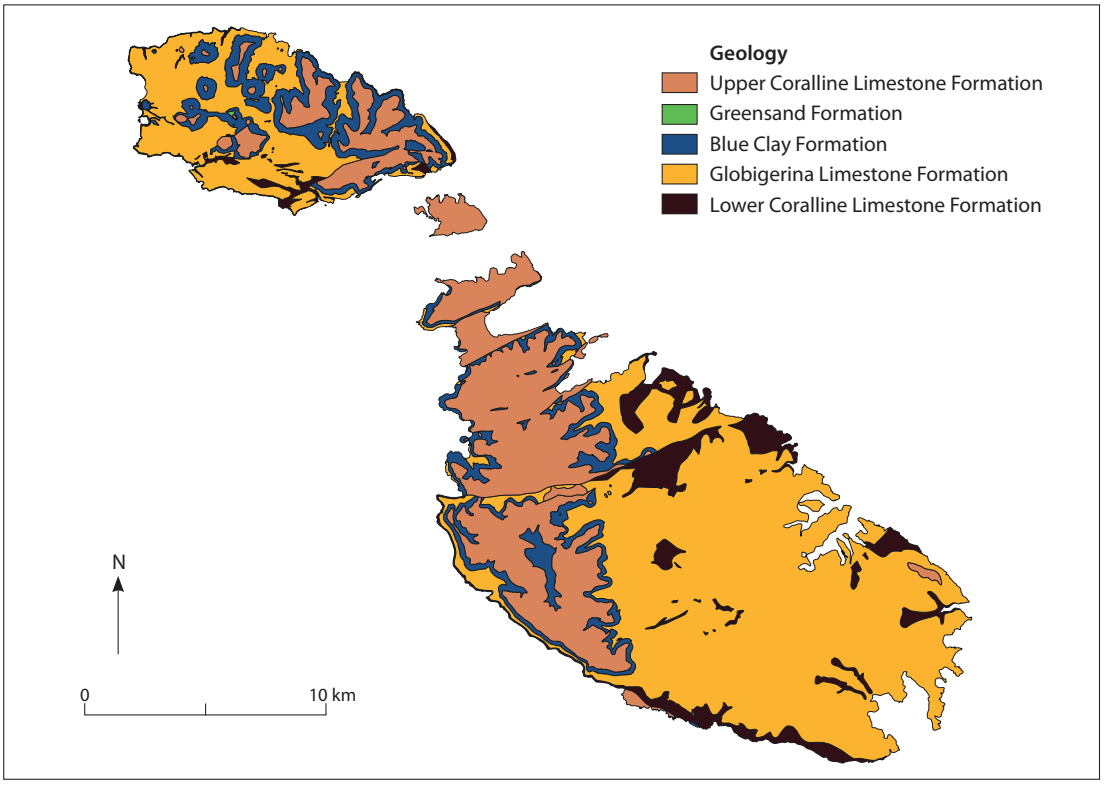

Figure 1.3. *Geological map of the Maltese Islands (P. Chatzimpaloglou, adapted from Pedley 1993).*

Although the geology of the islands appears rather simple with a similar stratigraphy, each formation, and, where present, its members, present different characteristics reflecting their depositional settings (Fig. 1.3). The stratigraphy of Malta is juxtaposed by normal faults, arranged as graben and half-graben. Gozo is structurally less complex with a 'layer-cake' stratigraphy, but has a more varied geology than Malta. The centre of Gozo is dominated by the Upper Coralline Limestone, resting on Blue Clay, where the Globigerina Limestone and Lower Coralline Limestone outcrops in coastal locations and the base of some valleys. Here erosion has occurred low enough in the succession to expose these formations and table-top plateaux or mesas of weathered and eroded Upper Coralline Limestone. Finally, Comino and its satellite islands are composed of only the highest layers of the Upper Coralline Limestone Formation.

1.4. Stratigraphy of the Maltese Islands

1.4.1. Lower Coralline Limestone Formation

The Lower Coralline Limestone is the oldest exposed rock formation on the Maltese Islands. It is a hard, pale grey limestone and contains beds with fossils such as corals and marine calcareous algae. Outcrops of this limestone are mainly restricted to coastal sections along the western coasts of Malta and Gozo (Fig. 1.4). It can be up to 140 m thick, forms sheer cliffs particularly on the southwest coasts of the islands because of the islands' tilt and its base cannot be seen above sea level. When found inland, this formation forms barren grey limestone-platform plateaux on which karstland develops (Schembri 1997), as for example those found in the west of Gozo (Fig. 1.5). The rocks comprising this formation are all indicative of having been laid down in a shallow sea and can be sub-divided into five different facies[1] of limestones (Pedley *et al*. 2002). These facies are: a) the Reef Limestone (Wied Għlaq), b) the fine-grained Shallow Lime Muds (Attard), c) the cross-bedded Lime Sands (Xlendi), d) the Foraminiferal Limestones and e) the 'Scutella Bed' (Il-Mara) (see Gauci 2019 for detail). Felix (1973) suggested that the deposition of the Lower Coralline Limestone had initially been in a shallow gulf-type environment. In addition, succeeding beds provided evidence of increasingly open marine conditions during which algal rhodolites developed. Finally, a shallow marine shoal environment followed and was the dominant environment in all areas except southeastern Malta. In this area, calmer conditions prevailed in a protected deeper water environment (Pedley *et al*. 1976).

1.4.2. Globigerina Limestone Formation

The Globigerina Limestone Formation is a softer, yellowish fine-grained limestone that forms irregular slopes (Fig. 1.6) and is the most extensively exposed formation on these islands (Schembri 1997). It is named after *Globigerina*, a microscopic planktonic foraminifera, which is abundant in this formation. The Globigerina Limestone varies in thickness from some 20 to *c*. 227 m (Fig. 1.2), a characteristic which possibly signifies the onset of the warping of the sea bed and possibly the formation of depressions because of the collapse of the sea bed above underlying caverns (Pedley *et al.* 2002). The lithology and fossils in the rock show that this formation was originally deposited in deeper water between 40 and 150 m below the influence of

Figure 1.4. *Typical coastal outcrops of Lower Coralline Limestone, forming sheer cliffs (P. Chatzimpaloglou).*

Figure 1.5. *Characteristic geomorphological features developed on the Lower Coralline Limestone in western Gozo (Dwerja Point). The picture shows different sub-circular collapsed karstic features (a & b), while the green arrow points to the location of the chert outcrops (image © 2017 Google).*

wave action (Felix 1973). The unexpected occurrence of the planktonic foraminiferans, such as *Globigerina*, in this shallow-water depositional environment may be explained by a drift that brought these organisms into this shallower basin from the surrounding deeper water seas.

The Globigerina Limestone is divided into three members (Upper, Middle and Lower Globigerina Limestone) separated by two main phosphatic conglomerate beds (referred as the Lower Phosphorite Conglomerate Bed C1 and the Upper Phosphorite Conglomerate Bed C2), which do not exceed one metre in thickness (Fig.

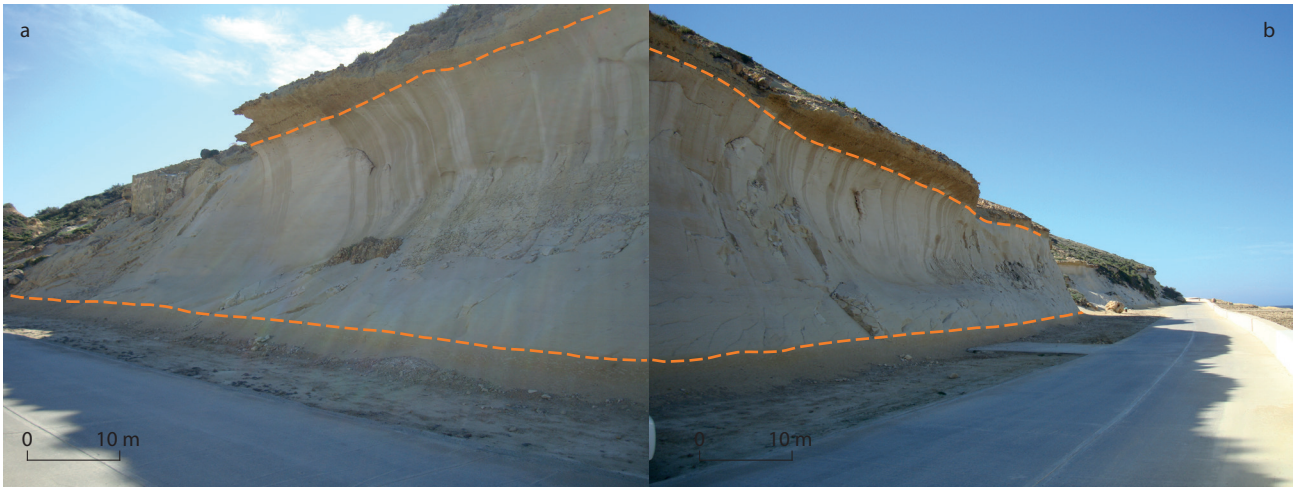

Figure 1.6. *The Middle Globigerina Limestone at the Xwejni coastline. It is one of the biggest outcrops of this unit and the orange lines highlight the two conglomerate layers, which are clearly presented in this location, and signify the transition to the Upper and Lower Globigerina units (P. Chatzimpaloglou).*

1.2); other minor phosphatic layers also occur (Baldassini & Di Stefano 2015). The upper and lower members have a pale yellow colour, while the middle member is pale grey (Fig. 1.6). The latter unit is considered to have been deposited during the time that the central Mediterranean Sea basin reached its deepest level. This could also explain the presence of chert outcrops, which have been found intercalating with the Middle Globigerina Limestone (Fig. 1.7).

The two conglomerate layers show evidence of erosion phases through the incorporation of many pebbles of brown-coloured limestones (Pedley *et al*. 2002). In addition, their presence indicates that the sea basin was influenced by water agitation and that the sea levels had probably fallen during their deposition. The colour of these layers is attributed to the high concentration of francolite (a phosphatic mineral) in the cements. The significant presence of this mineral suggests that the water streaming over the shallow sea bed at the time of deposition was rising from greater depths as an 'up-welling' current which was coming from the depths of the western Mediterranean basin and passing eastwards (Pedley *et al*. 2002). These inputs may also have been supplying material during the deposition of the Middle Globigerina Limestone that contributed to the formation of the chert outcrops.

The fine-grained particles comprising the Upper and Lower Globigerina Limestone members are only lightly cemented and therefore are easily worked as building stone. Indeed, the Lower Globigerina Limestone member, called '*franka*' in Maltese, has proven to be the most suitable building stone available on the islands. This is related to its uniform texture and explains why most of the buildings of the Maltese Islands, until recently, were built from this unit. Its texture, in addition to its extensive exposure on Malta and Gozo, has contributed to the smoothing of the topography of the islands. The thin fine sandy/silt loam soils developed on this formation are intensively cultivated and terraced.

1.4.3. Chert outcrops

The existence of chert outcrops has been long reported (Cooke 1893a), but little is known about their characteristics and the conditions under which they formed. Archaeological research has revealed that these chert

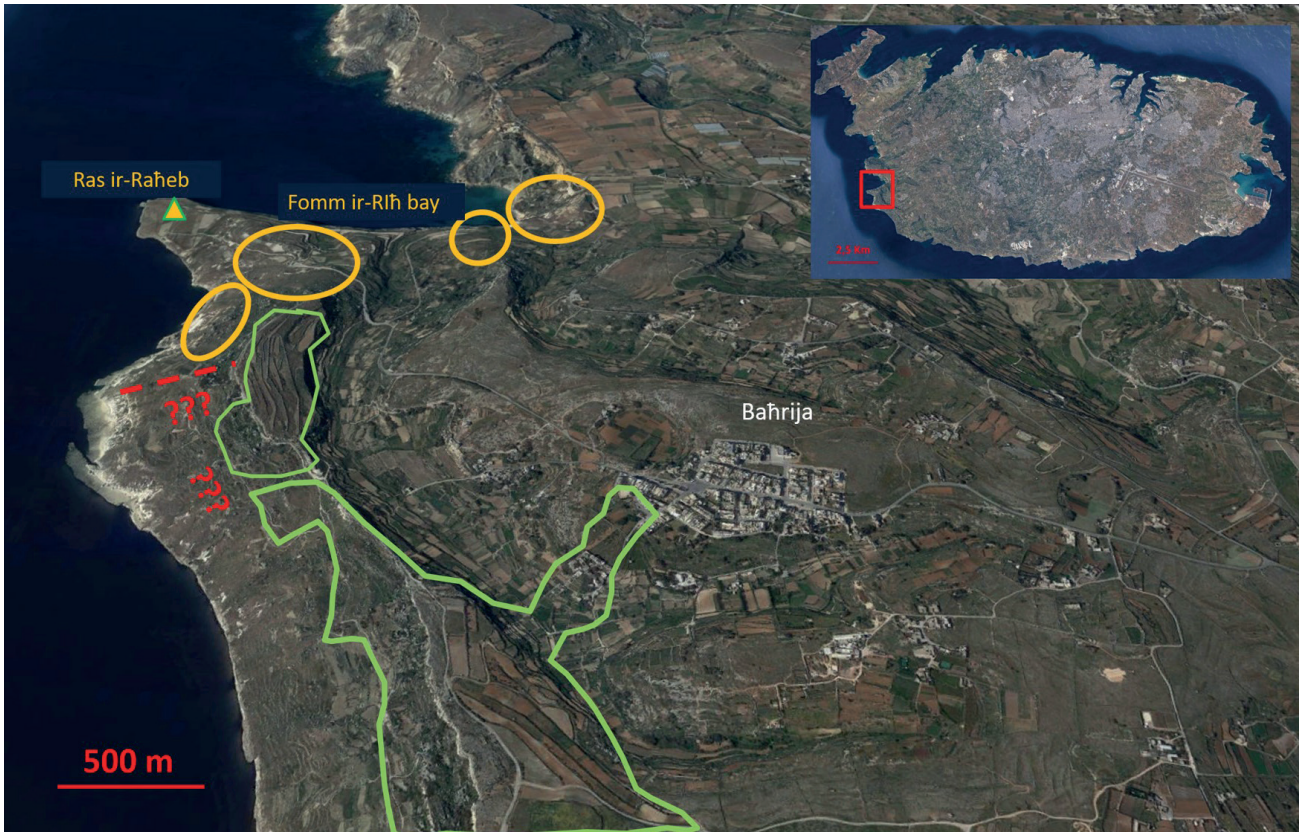

Figure 1.7. *An overview of the area investigated in western Malta. It presents the locations of chert outcrops (yellow lines) and the areas investigated during fieldwork (green lines) (image © 2017 Google).*

Figure 1.8. *The end of the major fault system of Malta (Victoria Lines) at Fomm Ir-Riħ, with chert outcrops to either side (P. Chatzimpaloglou).*

rocks were used by the prehistoric inhabitants (Malone *et al.* 2009a; Vella 2009). The Middle Globigerina Limestone member has extensive exposures in both islands of Malta and Gozo, but not all of them present chert outcrops. Recent fieldwork has revealed that chert outcrops were present only on the western parts of both islands in bedded form (Chatzimpaloglou 2019; Chatzimpaloglou *et al*. 2020).

The main chert outcrops on Malta were located in the Fomm ir-Riħ Bay area at the end of the Great Fault (Fig. 1.8), which is a major tectonic feature of Malta, and are considered more extensive than those on Gozo. The chert outcrops on Gozo were found at Dwejra Point, close to Fungus Rock (Fig. 1.9). The area is characterized by massive karstic features which could have been enhanced by past tectonic activity. The investigation of both exposures showed that nodular chert was present at the top and bottom of the unit, while bedded chert and/or silicified limestone were found in the middle part of the unit (Fig. 1.10). Generally, the outcrops present similar macroscopic characteristics with the bedded outcrops and have a higher concentration of carbonate material than the nodules.

1.4.4. Blue Clay Formation

The Blue Clay Formation is a very soft formation which generally forms either as low or rounded slopes when exposed on the surface or as very steep slopes where it cascades over the underlying Globigerina Limestone (Pedley *et al*. 1976, 2002). The thickness of the formation ranges from 50 to 70 m (at Fomm ir-Riħ Bay) (Fig. 1.11). Although the Blue Clay has macroscopic differences from the Globigerina Limestone, they have very similar characteristics at least to the Upper Globigerina member. The Blue Clay is composed of very fine-grained sediments, with a large proportion of them of foraminiferal origin. This suggests that this formation was deposited in a similar deep-sea depositional setting to the Globigerina Limestone (Pedley *et al*. 2002) and it can be regarded as a continuation of the Upper Globigerina Limestone member sedimentation in which clay material of terrigenous origin became progressively incorporated (Scerri 2019).

Basically, the main factor that distinguishes the Blue Clay Formation from most of the Globigerina Limestone is the presence of clay minerals. This clay content can only have come from a land source, although the possibility that part of the clay fraction originates from volcanic ash of an active volcano should not be excluded (Pedley *et al*. 2002). The quality of clay material mixed with the plankton-derived calcium carbonate detritus prevented the formation from reaching the same level of hardness as the limestones. The Blue Clay is the softest rock formation of the Maltese Islands and produces most of the fertile and water retentive soils found across Gozo and Malta, provided there is the level of plough technology to work these heavier soils. This would have been more

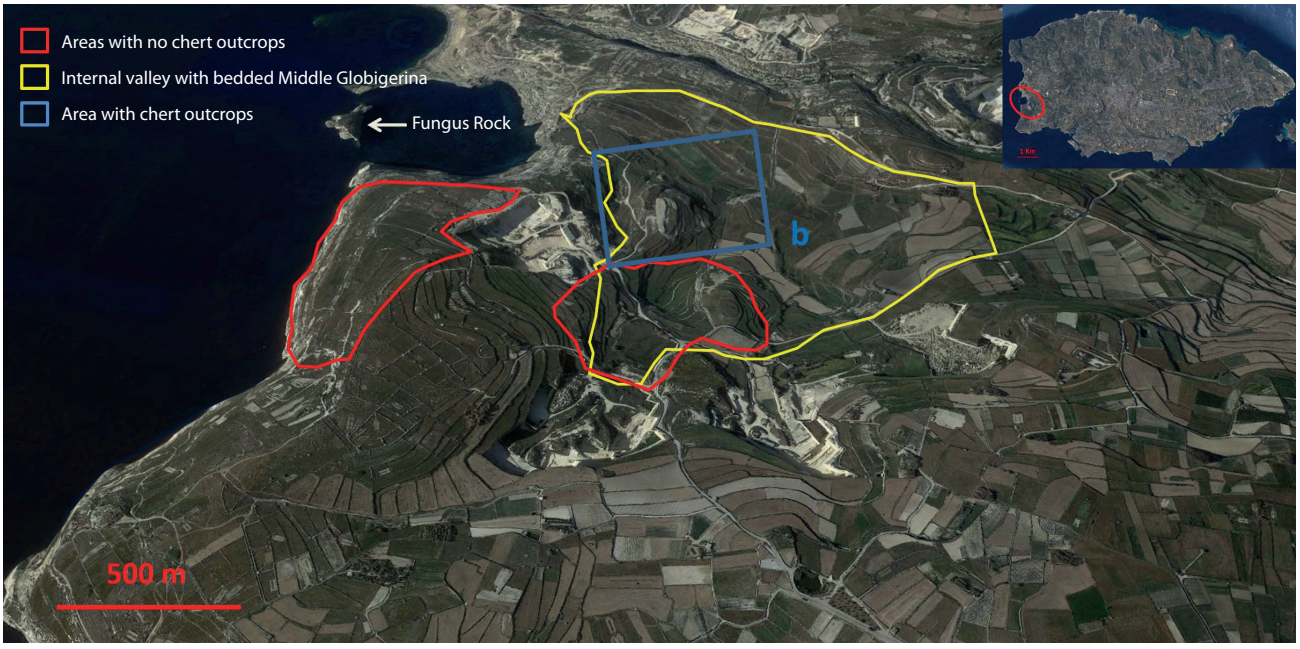

Figure 1.9. *An overview of the western part of Gozo where the chert outcrops are located. The yellow line orientates the internal valley, closer to Fungus Rock, the location of the chert outcrops (blue rectangle), and the areas investigated during fieldwork (red lines) (image © 2017 Google).*

Figure 1.10. *Chert outcrops: bedded chert (a & c), and nodular chert (b & d) (P. Chatzimpaloglou).*

Figure 1.11. *Four characteristic exposures of the Blue Clay formation on Gozo and Malta (P. Chatzimpaloglou).*

likely in Roman and later historical times (Margaritis & Jones 2008). It is also the basis of the perched aquifer as it forms an aquiclude to the porous rocks above. This perched aquifer was practically the only source of freshwater, apart from surface run-off, on the islands up to the British Period because of the springs that originated from it at the level of the Blue Clay-Greensand/Upper Coralline Limestone interface (Cassar *et al.* 2008). The upper parts of the formation show an increase in brown phosphatic sand grains and green grains of the complex mineral glauconite.

1.4.5. Greensand Formation

The Blue Clay transitions into the Greensand Formation with the Upper Coralline Limestone above (Pedley *et al.* 2002). The outcrops of this formation, when they are present, are very thin and only in Gozo do they exceed 11 m (i.e. 11 m at Il-Gelmus). The freshly exposed outcrops, mainly in man-made deep cuts, have a characteristic greenish colour influenced by the presence of glauconite (a complex, silicate based mineral). In contrast, the weathered exposures have an orange-brown colour formed by the oxidation products of this mineral. These Greensand outcrops represent the residue of a long period of submarine erosion and winnowing of sediments, probably related to the uplift of the Maltese area on the north flank of the Pantelleria Rift. Where present, the top part of the formation passes transitionally into the overlying Upper Coralline Limestone Formation. This same upper part of the formation, lying above the Blue Clay, acts as an important point of water seepage and springs in the stratigraphy of the Maltese Islands.

1.4.6. Upper Coralline Limestone Formation

The Upper Coralline Limestone Formation is situated at the top of the stratigraphic sequence of the Maltese Islands. It is a hard, pale grey limestone, similar to the Lower Coralline Limestone Formation. This limestone forms sheer cliffs of varying height and includes a

similar content of fossils such as corals and coralline alga. It can be up to *c*. 170 m thick (Fig. 1.4), although it also forms thin hill cappings and limestone platforms (Schembri 1997). Karstic geomorphological features have been reported on this formation (Fig. 1.4), but not at the same scale as for the Lower Coralline Limestone. The Upper Coralline Limestone is mostly comprised of shallow marine sediments deposited in different marine or intertidal environments and it generally comprises four members (oldest first): Ghajn Melel, Mtarfa, Tal-Pitkal and Ġebel Imbark (Pedley 1978). The Upper Coralline Limestone is the only formation exposed on Comino and Cominoto, while it is fully developed in western Malta and eastern Gozo (Pedley *et al*. 2002).

1.4.7. Quaternary deposits

Although the main marine sedimentation processes ended between the Miocene and Pliocene, there are a variety of post-Miocene Quaternary deposits of limited areal extent scattered throughout the islands (Trechmann 1938; Pedley *et al*. 1976; Hunt 1997; Hunt & Schembri 1999). The best studied of these are the cave and fissure infilling sediments because of their at times abundant fossil vertebrate remains, which provide insights into the climatic conditions and palaeoenvironment at the time of deposition (see Hunt & Schembri 1999 and references therein). Other types of Quaternary deposits include marine highstand deposits, freshwater lake deposits, fluvial conglomerates and alluvial fan deposits, slope deposits, breccias and blown sand (aeolian) deposits.

Initial colonization of the islands by terrestrial biota is thought to have taken place during the Messinian Salinity Crisis when the central Mediterranean was mostly dry land connecting North Africa to Sicily and Europe (Hunt & Schembri 1999; Schembri 2003; Cassar *et al*. 2008). Following the refilling of the Mediterranean during the Zanclean, the Maltese Islands were isolated until the Pleistocene glaciations when they may have become connected to Sicily (but not to North Africa) during lowstands or, if not connected, to have been separated by a channel much narrower than at present because of low sea levels. This facilitated further waves of colonization of the islands by biota able to disperse over the land bridge or across the narrowed channel (Thake 1985a; Hunt & Schembri 1999; Schembri 2003; Cassar *et al.* 2008).

Based on a comparative study of the Maltese fossil Pleistocene fauna recovered from Quaternary deposits with that of the Sicily and the Italian mainland, Hunt and Schembri (1999) have postulated three main waves of colonization of the Maltese Islands by biota: an early influx during a marine regression in the Lower Pleistocene–early Middle Pleistocene (Oxygen Isotope Stage 16: 690,000 years BP), a series of influxes during the marine regressions of the late Middle Pleistocene (between Oxygen Isotope Stage 12: 490,000 years BP and Stage 8: 300,000 years BP), and a final influx during the sea level low-stand of the Last Glacial Maximum (Oxygen Isotope Stage 2: 22,000–17,000 years BP) when sea level fell by 120–130 m and probably connected the Maltese Islands with Sicily via a land bridge. After this the Maltese Islands gradually attained more or less their present configuration and coastline as sea levels rose (Furlani *et al.* 2013).

1.5. Structural and tectonic geology of the Maltese Islands

Tectonics have affected the geography and geomorphology of the Maltese Islands (Galea 2019). The main geological formations essentially lie horizontally, but are displaced at intervals by faults belonging to two main families: a) a series of east–northeast to west–southwest trending faults, and b) the Magħlaq and associated faults which trend northwest to southeast. The first family has been active since the Early Miocene and has resulted in the horst and graben systems most evident north of the Great Fault up to the South Gozo Fault. The second became active in the Late Miocene as a result of development of the Pantelleria Rift System. These faults were responsible for making the western side of Malta higher than the east, forming dramatic seacliffs of the western/northwestern shores (Alexander 1988; Bonson *et al.* 2007; Ruffell *et al*. 2018; Galea 2019). According to Lambeck *et al*. (2011) and Furlani *et al*. (2013, 2018), Malta appears to have remained tectonically stable throughout the Holocene.

The continental shelf around the Maltese Islands was progressively drowned by sea level rise since the Last Glacial Maximum (Furlani *et al.* 2013), such that there are well preserved terrestrial palaeo-landforms present on the present sea floor at depths shallower than *c*. -130 m (Foglini *et al.* 2016; Micallef *et al.* 2013; Prampolini *et al.* 2017). The post-Quaternary tectonics are restricted mainly to regional movements which have resulted in the submergence of archaeological features such as the 'cart-ruts' which enter the sea at St. George's Bay, St. Paul's Bay and Birżebbuġa (Hyde 1955; Furlani *et al.* 2013), and the presence of speleothems (cave mineral deposits, including stalagmites) in marine caves (Rizzo 1932; Furlani *et al.* 2018).

1.6. Geomorphology

The geomorphology of the Maltese Islands has been thoroughly described and discussed by a number

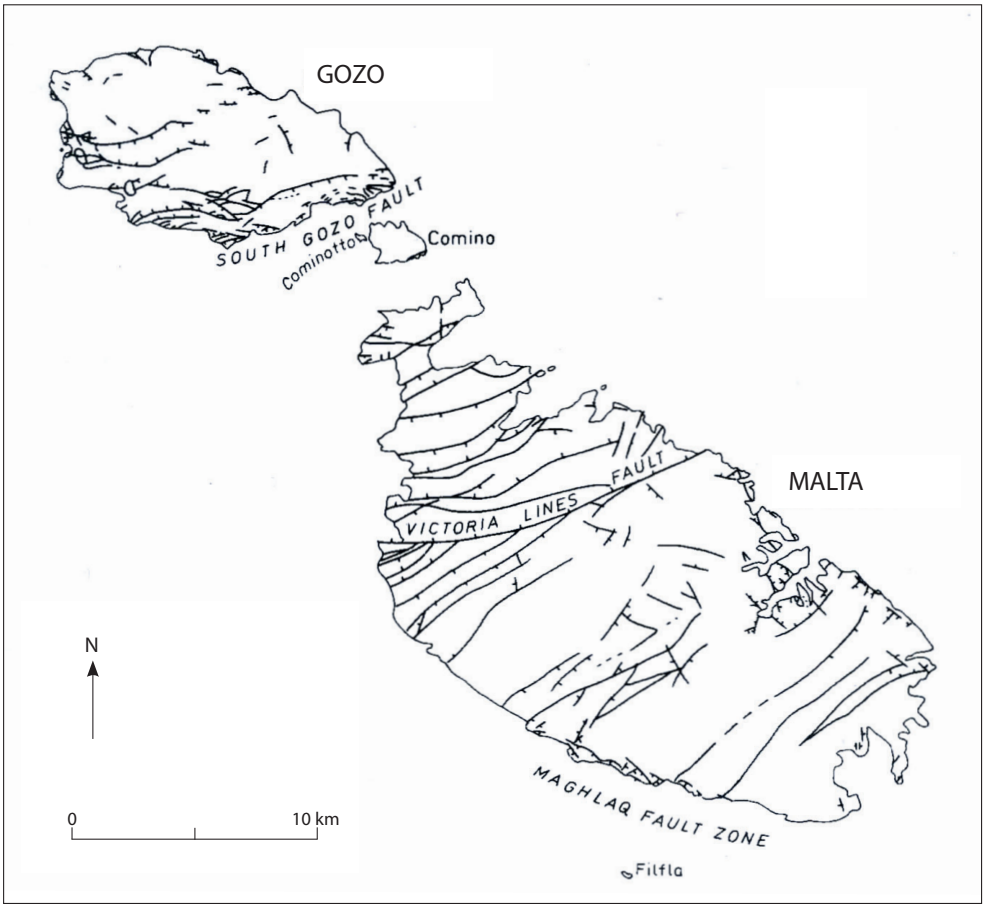

Figure 1.12. *Map of the fault systems, arranged often as northwest–southeast oriented graben, and strike-slip structures (after Gardiner* et al*. 1995; Prampolini* et al*. 2017) (P. Chatzimpaloglou).*

of scholars, including House *et al.* (1961), Vossmerbäumer (1972), Guilcher and Paskoff, (1975), Paskoff and Sanlaville (1978), Ellenberg (1983), Reuther (1984), Alexander (1988), Anderson (1997), Schembri (1993, 1994 & 1997) and Prampolini *et al.* (2017), and, most recently, in a multi-authored volume on the landscapes and landforms of the islands (Gauci & Schembri, 2019). The present account is based on these sources.

As already stressed above, the current geomorphological features of the Maltese Islands have been strongly influenced by the geological and tectonic status of the islands. Both Malta and Gozo are tilted towards the northeast which resulted the Lower Coralline Limestone along the west, southwest and southern coasts of the islands, and formed very steep to vertical cliff faces in most places rising straight from the sea. Along the east and southeast coast of both islands, but especially Malta, the tilt gives generally gently sloping shores, and where valleys open on the coast, drowned valleys form a ria and bay coastline. The Marsamxett and Grand Harbours are the prime examples of this.

On Malta, all five rock formations are only present north of the Great Fault and on the Rabat-Dingli uplands south of it. Elsewhere there are vast exposures of Globigerina Limestone which generally present a large-scale gentle folding which is responsible for the characteristic topography of plains, shallow depressions and low hills; in fact the only high ground in this part of the island is the Naxxar-Għargħur upland. Where the entire geological sequence is present, the Upper Coralline Limestone forms flat limestone-pavement karstic plateaux with steep cliff-like sides bordered by boulder screes at their base (Maltese: *rdum*) made by the slumping of blocks of rock from the cliff edge because of erosion of the underlying soft rock – the Greensand and/or Blue Clay. The eroded Blue Clay cascades down-slope to form taluses that cover the rock underneath (Globigerina Limestone). The Upper Coralline Limestone boulders also travel down-slope riding on the Blue Clay and where this happens on the coast, the result is a boulder-strewn shoreline.

Important and characteristic topographic features of the Maltese Islands are the *rdum* and *widien* (Schembri 1994, 1997). *Rdum* are important since they provide a very rough and dynamic terrain and as such have rarely been cultivated, thus providing refuges for many species of Maltese flora and fauna, which would have otherwise been extirpated from the heavily anthropogenically modified landscape. *Widien* are natural drainage channels formed either by stream erosion during a previous (post-Miocene) much wetter climatic regime, or by tectonism, such as the grabens of northern Malta and southern Gozo, or by a combination of the two processes. Most *widien* are now dry valleys and only carry water along their watercourses during the wet season. A few *widien* drain perennial springs arising from the perched aquifer at the Upper Coralline Limestone–Greensand/Blue Clay interface and have some water flowing in them throughout the year, attaining the character of miniature river valleys. By virtue of the shelter they provide and their water supply, *widien* are one of the richest habitats on the islands and are also extensively cultivated. The submergence of the mouths of some *widien* mainly caused by the tilt of the islands, has led in turn to the formation of wetlands of various types, providing yet another localized, semi-aquatic habitat type in an otherwise arid landscape.

1.7. Soils and landscape

It has reasonably been assumed that the seasonally dry and hot Mediterranean climate made the Maltese landscapes quite marginal for agricultural production especially since there were few natural springs originating from the perched aquifer, and what rain and surface run-off could be collected and stored was slim (Haslam 1969; Schembri 1997; Cassar *et al.* 2008). As a consequence, terracing was adopted extensively in Malta and Gozo to conserve soils and moisture and at the same time to create a more amenable landscape for subsistence based agriculture, although exactly when is a subject of debate (Fenech 2007; Grima 2004, 2008b; Micallef 2019) (see Chapters 5, 8 & 11). Like many other parts of the Mediterranean region, this landscape must have been prone to deforestation, drought and erosion, combined with intensive human activity (Bevan & Conolly 2013; Brandt & Thornes 1996; Hughes 2011; Grove & Rackham 2003), and these factors are the subject of much of this volume to follow. Today, the islands are characterized by highly terraced valleys between flat-topped limestone mesas, generally with substantial towns sprawling across these plateaux. The whole of the southeastern part of Malta, previously mainly agricultural with small scattered villages except for the harbour regions, is now being swallowed up by extensive urban development.

Maltese soils are relatively young and relate directly to the rock formations of islands. Previous studies have highlighted the low contribution of the climate to soil development and the great impact of human activities in their modification, particularly where there is cultivation, as being a valuable and practically non-renewable resource, natural soils have been translocated and mixed together and with various materials since the earliest of times (Lang 1960; Bowen Jones *et al.* 1961; Svarajasingham 1971; Farres, 2019). Possible trajectories of past soil development and change are further discussed in Chapter 5.

Lang's (1960) comprehensive study has laid the foundation for the understanding of Maltese soils and their development. This study identified three main types of soil: Carbonate Raw, Xerorendzinas and Terra soils. Of the four Carbonate Raw series soils, two are formed from Blue Clay parent material (Fiddien and San Lawrenz series), one from weathered Upper Coralline Limestone (Nadur) and one from dune sand (Ramla). These highly calcitic soils conform to an A/C profile, where the upper horizon directly overlies the parent material, and contain a very low level of organic content. The Xerorendizinas, which were divided into three series (San Biaġio, Alcol and Tal-Barrani), are largely formed from Globigerina Limestone parent material and also present an A/C profile. Normally grey, loose and powdery when dry, these soils have a high chalk and gypsum content with limited organic content (yet distinguishably more than the carbonate soils). Lastly, the Terra soils are found as *terra fusca* and *terra rossa*. Both are derived from Upper and Lower Coralline Limestone parent material and present an A/Bw/C profile. The Terra soils are well developed with little organic content (although more than the previous soils) and the notable presence of ferric hydroxide.

Maltese soils have most recently been studied as part of the MALSIS project, a Malta–EU co-funded programme with the objective of setting up a modern Maltese soil information system that includes a soils geo-database (Vella 2000, 2001, 2003). The MALSIS inventory recognizes seven soil groups of the World Reference Base for Soil Resources soil classification system (WRB 2014) that are present in the Maltese Islands. These are:

a) Calcisols (37 per cent), which are soils with a high proportion of translocated calcium carbonate and the most commonly occurring in the islands.
b) Leptosols (15 per cent), which are very shallow calcareous soils with a high gravel content that locally are found on exposed karstic plateaux

and *rdum*, usually associated with low steppic and low garrigue vegetation.

c) Cambisols (7 per cent), which are similar to Leptosols but deeper (>25 cm) and show some horizon development in the form of a subsoil layer (or B horizon), although this is very limited in Maltese cambisols.

d) Vertisols (7 per cent), which are soils with a high content of clay and characterized by deep cracks when dry and occur on the Blue Clay.

e) Luvisols (15 per cent), which are relict soils that formed under a previous wetter climatic regime, most likely during wet periods in the Pleistocene (see Chapter 5). The present climate does not form such soils, but it does modify them through the deposition of secondary calcium carbonate. Locally these soils have a reddish colour because of the presence of iron minerals and when undisturbed develop a surface layer of humus, a thin leached topsoil horizon, and a clayey and mineral rich subsoil. Such soils are found on flat or gently sloping karstland under high garrigue and maquis vegetation.

f) Arenosols, which are porous sandy soils with no or almost no clay content and are usually deep. Locally they develop in a limited number of areas were blown beach sand accumulated inland from the adjacent coast.

g) Regosols (19 per cent), which have been used as a 'bin-group' for soils that do not fit in any of the other local soil types. Such soils consist of broken down but otherwise practically unaltered parent material with no horizon development. Soils formed by mixing other soil types with powdered rock and anthropogenic waste are also classified as regosols.

1.8. Climate and vegetation

The present climate of the Maltese Islands is typically Mediterranean with characteristic mild, wet winters and hot, dry summers with ample sunshine (Chetcuti *et al.* 1992; Schembri 1993, 1994, 1997; Schembri *et al*. 2009; Galdies 2011). The climate is strongly bi-seasonal, particularly in terms of precipitation. Despite an average rainfall of 530 mm, most of it (*c*. 85 per cent) falls during the period from October to March. Precipitation is highly variable from year to year with some years having almost twice the mean annual rainfall and others half. The latter are known as drought years and a continuous run of such (Murray 1890; Blouet 1984) may have caused at least partial abandonment of the islands in the past. There may also have been the abandonment of marginal agricultural land because of a lack of irrigation water and crop failure, since local water resources were, directly or indirectly, entirely dependent on rainfall and the perched aquifer until the British period (Schembri 2003).

The mean monthly air temperature varies from 12 to 26° C, and rarely falls to zero for sufficiently long periods to affect plant growth (Haslam 1969; Chetcuti *et al.* 1992). The arid period extends from approximately the last third of March to the first third of September, with peak aridity reached between June and August and maximum temperatures of up to 43° C (Chetcuti *et al.* 1992). Ground (grass) temperatures may be much higher that the air temperature and values up to 49° C have been measured. Relative humidity is generally high, from 65–80 per cent, with wind prevalent throughout most of the year. This is important as it exposes dry un-vegetated soil to wind-winnowing, rendering already low-quality agricultural soils even more depleted.

The natural vegetation of the islands must be adapted to excess water during the wet season and to drought and heat in the dry season. Plant growth is thus restricted during the dry and hot summers with the main growing seasons being spring and, to a lesser extent, autumn (Haslam 1969; Haslam *et al.* 1977). This is reflected in the landscape which is generally green throughout the wet period, but appears mostly parched and bare of vegetation during the dry period given that many non-phanerophytes (phanerophytes = trees and shrubs) survive the dry season in the form of seeds (annuals) or some form of subterranean perennating organ (Haslam 1969; Schembri 1997).

The terrestrial vegetational assemblages of the Maltese Islands may be grouped into three categories, as follows: a) major communities that are part of the successional sequence towards the climatic climax, b) minor communities which are either specialized to occupy particular habitats or occupy habitats that are rare on the islands, or are relics from a previous ecological regime, now surviving in a few refugia, and c) vegetational assemblages of disturbed habitats, which are those occupying land subject to periodic disturbance, usually as a result of human activities, but also natural disturbances, such as the flooding of dry-valley (*wied*) watercourses following heavy rain (Schembri 1997). The present day vegetational assemblages of the Maltese Islands have been described by Haslam (1969), Lanfranco (1984, 1995), Lanfranco and Schembri (1986), Anderson and Schembri (1989), Schembri (1993, 1997) and Cassar *et al.* (2008).

These combined themes of chronology, climate, soils and vegetation will be developed further by the palaeoenvironmental data presented below in Chapters 2–5.

Notes

1 'Facies' is a term that provides a specific characterization of a group of rocks with distinct similar features. In sedimentary rocks, it embraces major features such as the main composition (e.g. quartz sand, clay or limestone facies), the sedimentary layering (e.g. cross bedded facies, etc.) or the main fossils. These are then related to an interpreted environment in which the sediments were deposited. Consequently, the rock can be referred to as beach-facies, lagoon facies, reef facies, and so on.

Chapter 2

Chronology and stratigraphy of the valley systems

Chris O. Hunt, Michelle Farrell, Katrin Fenech, Charles French, Rowan McLaughlin, Maarten Blaauw, Jeremy Bennett, Rory P. Flood, Sean D. F. Pyne-O'Donnell, Paula J. Reimer, Alastair Ruffell, Alan J. Cresswell, Timothy C. Kinnaird, David Sanderson, Sean Taylor, Caroline Malone, Simon Stoddart & Nicholas C. Vella

2.1. Methods for dating environmental and climate change in the Maltese Islands

Rowan McLaughlin, Maarten Blaauw, Rory P. Flood, Charles French, Chris O. Hunt, Michelle Farrell, Katrin Fenech, Sean D.F. Pyne-O'Donnell, Alan J. Cresswell, David C.W. Sanderson, Timothy C. Kinnaird, Paula J. Reimer & Nicholas C. Vella

Adequate absolute dating is critical to understanding the past, especially where data concerning environmental changes from different sites are being compared, as chronology is often the only reliable way to compare evidence from multiple contexts. The archaeological chronology of Malta is becoming increasingly well resolved and this sets up a challenge – how can we obtain comparable high-resolution chronologies of environmental change in the Maltese Islands? The Maltese landforms pose significant barriers to achieving this goal, as much of the available palaeoenvironmental evidence is limited to cores in alluvial or shallow-marine sediments, which contain materials that have been subject to much re-working through time. In this chapter, we introduce and discuss the various techniques that the *FRAGSUS Project* has brought to bear on this problem, and review the main approaches used.

2.1.1. Data sources for chronology building

2.1.1.1. Background: the cultural sequence of Malta

Rowan McLaughlin

A key aim of the *FRAGSUS Project* has been to establish the parameters that define the relationships between people and their environment in restricted island settings. The human story of Malta and the timing of its unparalleled cultural developments are therefore of great interest, as the focus of our work is on the synchronization of data from palaeoecological and archaeological investigations. Therefore, in parallel with detailed investigation of the palaeoenvironment, the *FRAGSUS Project* conducted archaeological excavations that have re-dated the cultural sequence on the islands. Details of this work are given in detail in Volume 2 and summarized here and in Tables 2.1–2.6.

2.1.1.2. Radiocarbon dating

Rowan McLaughlin, Paula J. Reimer & Maarten Blauuw

Radiocarbon dating provided many of the fundamental data that underpin the chronologies discussed by the *FRAGSUS Project*. Radiocarbon is a well-established technique that estimates the age of once-living things by measuring the quantity of naturally radioactive carbon in a sample (Bronk Ramsey 2008b). Samples suitable for radiocarbon dating include charcoal, seeds, bones and the decayed organic fraction of soil (or humus). For the *FRAGSUS Project*, radiocarbon dating was carried out using accelerator mass spectrometry (AMS) at the ^{14}CHRONO Centre, Queen's University Belfast, using protocols described by Reimer *et al.* (2015). The samples all derived from material either picked out of the sediment cores during their processing for pollen and molluscan analyses described in Chapters 3 and 4, or through sieving 'core catcher' samples – material at the bottom of each core section removed from the profile during extraction of each sediment core segment and bagged separately.

As discussed in detail below, the radiocarbon dates were used to build a chronology (Figs. 2.1 & 2.2) – a time-scale against which other data could be plotted, such as the changing patterns of vegetation revealed in the pollen studies. This was not a simple undertaking, as alluvial sediments in Malta were originally deposited during relatively high-energy rainstorms, causing much recycling of organic material and thus radiocarbon results that may not necessarily truly reflect the date they were buried. In the case of the sediment cores studied by the *FRAGSUS Project*, as described below, this was done using Bayesian age-depth modelling techniques (Blaauw & Christen 2011).

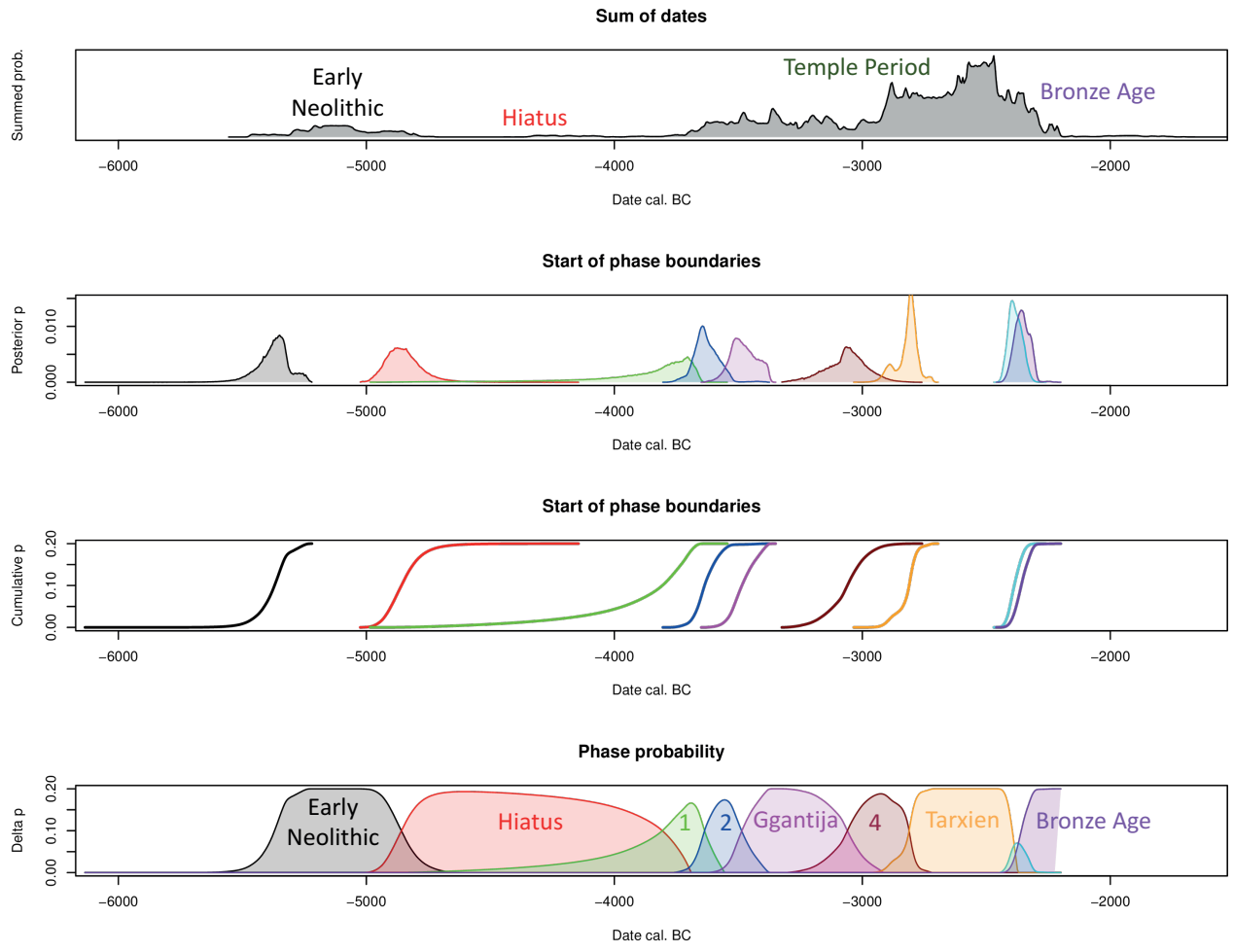

Figure 2.1. *Summary of new radiocarbon dating of Neolithic and Bronze Age sites on Gozo and Malta (R. McLaughlin).*

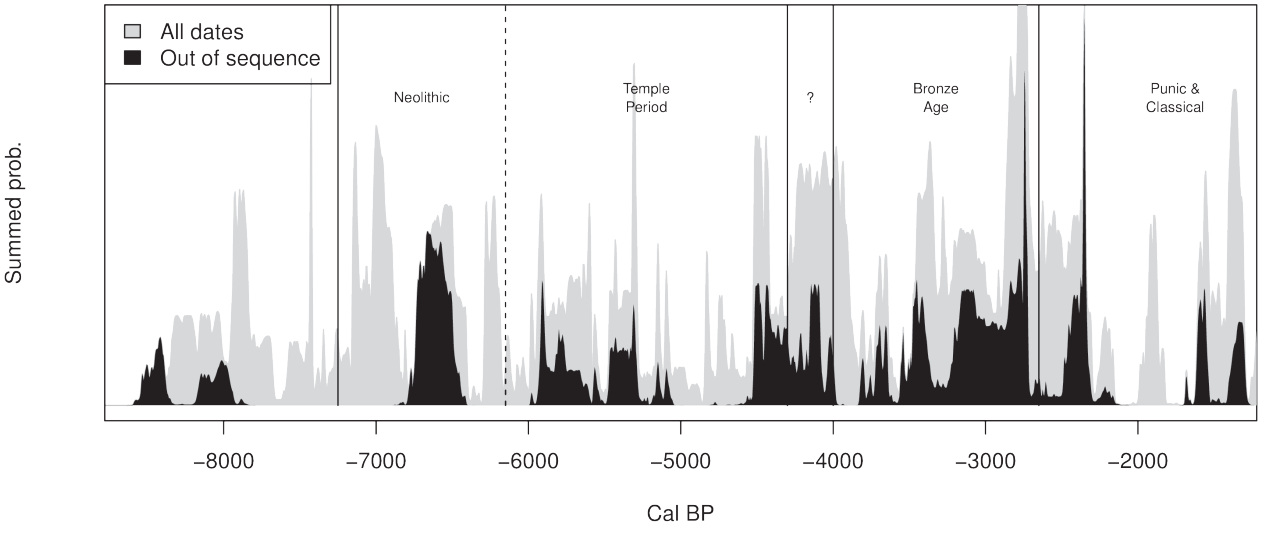

Figure 2.2. *Summed radiocarbon ages for the sediment cores on Gozo and Malta (R. McLaughlin).*

Table 2.1. *The cultural sequence of the Maltese Islands (with all dates calibrated).*

Period & events	From	To	Cultural development
No certain human impact	8000 BC	6000 BC	Impact of major climate events on vegetation
Possible early Neolithic farming: Għar Dalam	6000 BC	5400 BC	Palynological evidence for cereal cultivation and grazing
Early Neolithic: Skorba	5400 BC	4800 BC	Agriculture and permanent settlement, cereal farming, with a peak at 4800 BC, livestock, pottery manufacture; distinctive 'Skorba' material culture
Fifth millennium BC hiatus	4800 BC	3800 BC	Much reduced archaeological evidence, but environmental evidence for agriculture
Temple Period: Żebbuġ phase	3800 BC	3600 BC	'Resettlement' and early megaliths; very high levels of pottery manufacture; burials in rock-cut tombs
Temple Period: Mġarr phase	3600 BC	3400 BC	Change in material culture style
Temple Period: Ġgantija phase	3400 BC	2900 BC	Elaboration of megalithic architecture; change in material culture
Temple Period: Saflieni phase	2900 BC	2850 BC	Elaboration of burial practices
Temple Period: Tarxien phase	2850 BC	2400 BC	Further architectural and ritualistic elaboration; fluorescence of figurative art and other forms of material culture
Thermi ware	2400 BC	2200 BC	An attenuated continuation of Tarxien culture, but with new, imported, pottery forms
Third millennium hiatus	2200 BC	2000 BC	Third millennium hiatus
Earlier Bronze Age (Tarxien Cemetery)	2000 BC	1500 BC	Sudden change in burial practice, megalithic buildings no longer elaborated upon, general reduction in activity, hiatus in cereal agriculture, widespread livestock grazing and eventual agricultural re-intensification
Later Bronze Age	1500 BC	750 BC	Full return of cereal farming; hilltop settlement
Phoenician/Punic	750 BC	218 BC	New cultural and religious developments; viticulture; olive cultivation from the late Punic period; wider trade networks
Roman/Byzantine	218 BC	AD 870	Urban growth; intensive viticulture; internationalization
Arab/Norman	AD 870	AD 1530	Immigration; changing practices of agriculture and irrigation; introduction of the Semitic language; fortifications
Knights	AD 1530	AD 1798	New wave of urban developments; refortification
Modern	AD 1798	present	Growing population density; eventual abandonment of livestock herding; intensive horticulture; industrialization

Radiocarbon dating was also used to investigate directly some aspects of the changing ecology of the islands, following closely the methods of Hill *et al*. (2017). In this exercise, the differences between the carbon ecology of the past and the present were studied by measuring the radiocarbon content of modern snail shells, and comparing the results with snail shells of a known age, removed from an archaeological context at the Taċ-Ċawla settlement using data embedded in the shells of snails removed from an archaeological context of known age and AMS dated.

2.1.1.3. Optically stimulated luminescence (OSL) dating
Alan Cresswell, David C.W. Sanderson & Timothy C. Kinnaird

Luminescence dating estimates the time elapsed since material was heated or exposed to light. In the case of Optically Stimulated Luminescence (OSL) dating, quartz grains are used to estimate the age a sediment was buried. Although the limestone geology of the Maltese Islands is not naturally rich in quartz, windblown fine to very fine quartz sands from the Sahara deliver small quantities of silicates to the island, which are well suited to OSL dating. The *FRAGSUS Project* used OSL dating to provide a temporal framework to underpin investigations into the early Holocene topography of the Ramla and Marsalforn valleys on Gozo, and the excavations at the Neolithic temple sites of Ġgantija on Gozo and Skorba on Malta.

The study reported here uses luminescence techniques to develop chronological frameworks for these investigations. Chronologies have previously been developed based on radiocarbon analysis (Trump 1966; Renfrew 1972) for the temple complex at Skorba with calibrated dates ranging from *c*. 5000 to 3200 BC, however luminescence approaches have not been widely used on Malta and Gozo to date. Luminescence techniques have, however, been widely used in Neolithic contexts in the Mediterranean, and beyond, for establishing robust chronologies. Examples in the Mediterranean region include megalithic tombs at Cabeço dos Pendentes in Portugal (Kinnaird *et al.*

2015), Neolithic monuments in Corsica (Sanderson *et al.* 2014), deltaic sediments associated with cultural activity from the Neolithic onwards on Crete (Zacharias *et al.* 2009), and Neolithic settlements, cemeteries and landscapes in Cyprus (Kinnaird *et al.* 2007, 2013). These techniques have also been used to investigate rates of soil erosion in Greece (Fuchs *et al*. 2004) using material largely devoid of quartz minerals, and river development in Crete (Macklin *et al.* 2010), where quartz minerals are derived from the local sandstone.

The geology of Malta is dominated by limestone (see Chapter 1), resulting in locally derived soils largely devoid of silicate minerals suitable for luminescence dating. However, wind-blown sands from the Sahara are believed to have delivered small quantities of silicates to the islands. The Sahara is the largest source of aeolian dust, accounting for approximately half of the total atmospheric mineral dust burden (Scheuvens *et al.* 2013), with dust from the Sahara deposited in south and central America, the Atlantic Ocean, Europe and the Mediterranean, India and sub-Saharan Africa over the last five million years. In the Western Mediterranean, the dominant source of dust is from the Sahara (Scheuvens *et al.* 2013). Dust emission is a complex relationship between wind and surface conditions. Generally, small particles (<70 μm) experience large inter-particle cohesive forces relative to aerodynamic forces acting on the particles, with aerodynamic forces becoming relatively larger with larger grain size. Thus, larger grains are mobilized first and follow ballistic curves with impacts on the ground mobilizing the smaller particles (Schepanski 2018). Alluvial sediments are very prone to wind erosion, with temporally varying erodibility as the most susceptible particles are removed from the sediment with refreshing of sediments during floods (Schepanski 2018). Thus, dust emission strongly reflects environmental conditions, being largest in dry periods. The transport distance strongly depends on residence time in the atmosphere; fine particles (<70 μm) are kept aloft by atmospheric turbulence for durations of weeks and can be transported thousands of kilometres, with larger particles generally being deposited within a day, although larger particles are occasionally found >1000 km from their source (Schepanski 2018). The typical red Mediterranean soils, or *terra rossa*, on limestone substrates found throughout this region are also common on Malta and Gozo. The silicate minerals in similar soils in Greece have been attributed to aeolian deposition of material blown from North Africa, although larger mineral grains in low-lying regions have been attributed to local beaches (MacLeod 1980; Mizota *et al.* 1988). Yaalon (1997) argues that aeolian dust from the Sahara contributes to all soils in the Mediterranean region, with up to 50 per cent of aeolian material in limestone derived soils. Micromorphological investigations conducted within the *FRAGSUS Project* have already shown the presence of sand-sized silicates within local soils and sediments (French *et al.* 2018) (and see Chapter 5).

Quartz grains from the Sahara are expected to be well suited to OSL dating, with a reputation for being bright (e.g. Bevan *et al.* 2013; Kinnaird *et al.* 2013; Mauz *et al.* 2009; Russell & Armitage 2012), but they may not be abundant. Fuchs *et al.* (2004) have shown that similar soils in Greece without abundant quartz can be accurately dated. The relative abundance of these grains may reflect climatic variations, and in particular changes in aridity in the Sahara which may alter the supply of grains, and prevailing wind directions and strengths affecting the transport of these grains to Malta. Although it is expected that aeolian grains will be bleached in transit, many of the grains in the soils will have been transported to the islands before incorporation in the soils, having been reworked from earlier soils. The aim of the OSL investigations reported here is to provide a temporal framework to underpin investigations into the earlier Holocene topography of the Ramla and Marsalforn valleys, Gozo, and on the excavations at the Neolithic temple sites of Ġgantija on Gozo and Skorba and Tal-Istabal on Malta. The objective of the field campaign was to retrieve samples from existing soil/sediment profiles in Gozo for OSL dating, and to sample the new test excavations at Ġgantija and Skorba for micromorphological analyses with associated physical characterization, radiocarbon and OSL dating.

On Gozo, three profiles were sampled: 1) a terrace/palaeosol sequence on the western edge of the Neolithic temple site of Ġgantija on the Xagħra plateau; 2) an alluvial/hillwash sequence in the lower Ramla valley, which separates the Xagħra plateau from the In-Nuffara plateau to the south; and 3) a terrace/hillwash sequence in the upper Marsalforn valley (Fig. 5.17). From the more extensive geoarchaeological fieldwork of French and Taylor (see Chapter 5), it is known that the plateaux are largely denuded of soil and vegetation (i.e. Holocene strata). The little that remains in terms of (Holocene) hillwash (colluvium) and alluvial deposits is concentrated on the lower slopes and in the lower parts of the topography, such as in the Ramla and Marsalforn valleys. The OSL investigations in the Ramla and Marsalforn valleys were undertaken with the aim of generating a chronology for the sequences of buried palaeosols, hillwash and alluvial deposits preserved there, and thus provide the means to reconstruct the earlier Holocene to recent development of the Gozo valley-scape. At Ġgantija, the objective was to provide a chronology for the buried soil sequence

located just off-site, in test pit 1, to establish the soil catena history for this part of Gozo.

On Malta, two sites were sampled: 1) the archaeological and palaeosol sequence associated with the Neolithic temple site of Skorba; and 2) a terrace/palaeosol sequence located at a development site with Punic-Roman archaeology present at Tal-Istabal, Qormi, on the outskirts of Valletta in Malta. Test excavations in 2016 on the western edge of the Skorba temple/settlement had revealed a 1.5 m deep sequence, within which three curvilinear stone walls of the Neolithic period effectively sealed *c*. 70 cm of soil accumulation. From fieldwork, it is suggested that the lower *c*. 50 cm of this soil was in fact a buried soil, albeit with the upper *c*. 20 cm probably being disturbed (in the past). The objective here was to provide a chronology for the buried soil sequence, and identify any correlations between the soil formation/properties and prehistoric activity at Skorba.

Field and laboratory profile measurements were conducted on 60 samples from seven sequences. All samples were first appraised using the SUERC portable OSL reader, following an interleaved sequence of system dark count (background), infrared stimulated luminescence (IRSL) and OSL, similar to that described by Sanderson and Murphy (2010). This method allows for the calculation of IRSL and OSL net signal intensities, depletion indices and IRSL:OSL ratios, which are then used to generate luminescence-depth profiles. The patterns in these data allow initial inferences and conjectures about trends or discontinuities in field profiles to be made, in combination with other initial observations of the sedimentology, which are used to refine further sampling. Subsequent laboratory profiling measurements confirmed the presence of quartz in prepared sediments with generally bright luminescence signals, and opened the way for Single Aliquot Regenerative (SAR) OSL dating of quartz fractions (Murray & Wintle 2000) from 12 tube samples collected from the five sites. Estimates of the cosmic dose rate were obtained using latitude and altitude specific dose rates for Malta (0.17 ± 0.01 mGy a^{-1}) with corrections for estimated depth of overburden using the method of Prescott and Hutton (1994).

At both the Ġgantija temple and Skorba temple/settlement, profile samples collected from below the modern agricultural soils showed photon counts and apparent doses that increased steadily with depth, indicating that these buried soils accumulated gradually without subsequent disturbance. The OSL equivalent dose measurements showed no significant variation between aliquots, again indicating that the quartz minerals had been zeroed prior to deposition without subsequent disturbance and allowing robust ages to be determined. For both these locations, the OSL dates for the bottom of the sequences indicating the onset of soil accumulation were consistent at 8560±630 BC (Ġgantija) and 8780±710 BC (Skorba). At Ġgantija the top of this buried soil gives a Bronze Age OSL date of 1140±250 BC, whereas the OSL date for the top of the buried soil at Skorba is 7760±560 BC, predating the known Neolithic activity at the site.

In both the Ramla and Marsalforn valleys, OSL investigations were conducted on sequences of buried palaeosols, hillwash and alluvial deposits. For the Marsalforn valley, the profile samples show a slight increase in photon counts and dose with depth, suggesting a gradual build-up of material. However, the OSL samples show evidence of multiple dose components, including high dose residuals, consistent with variations in light exposure during the reworking of soils. The upper sample could not be reliably dated, and the lower two samples generated the same age within uncertainties (1560±240 BC and 1480±340 BC). The Ramla Valley profiles are complex, showing relatively high photon counts in the upper samples decreasing with depth, and no clear trend in the apparent dose estimates. The OSL samples all show evidence of multiple dose components, including both high dose residuals and modern OSL dates in the nineteenth and early twentieth centuries AD.

The investigations reported here, and detailed in Table 2.2 and Appendix 2, are the first applications of luminescence techniques on these sites. Despite the local limestone geology not supplying abundant quantities of silicates to the soils and sediments at these sites, micromorphological studies (see Chapter 5) have already shown the presence of small quantities of silicate minerals. Both field and laboratory profiling measurements had indicated that these minerals carry measurable luminescence signals, with the OSL signals associated with quartz the most promising for dating. Although the quartz yields from the samples collected for OSL dating were limited, the signals from the quartz grains extracted were generally bright, in most cases providing sufficient signal to quantify the ages of the sampled sediments and soils. It is known that dust from the Sahara has been transported across the Mediterranean, and beyond, for approximately five million years (Schepanski 2018) and that this has most probably contributed to the soils on Malta and Gozo. The large signals observed from the quartz grains studied here are similar to those observed from Saharan sand, supporting that source for the silicates measured. This work has demonstrated that even in locations where the local geology is deficient in quartz, OSL measurements can be conducted using aeolian quartz from more distant sources. In locations where this primary aeolian mineral

Table 2.2. *Quartz OSL sediment ages from the Marsalforn (2917–2919) and Ramla (2921–2923) valleys, the Skorba temple/buried soil sequence (2925–2927) and the Tal-Istabal, Qormi, buried soil (2930) (Note: Dates in italics are poorly constrained due to low precision and large dispersion of equivalent doses determined by OSL analysis).*

Sample ID	SUTL no.	Depth /cm	Date	Archaeological significance
Marsalforn valley				
OSL1	2917	175–180	*760±920 BC*	Constrains the final period that the upper incipient soil in hillwash was exposed, phase 2
OSL2	2918	265–270	1560±240 BC	Constrains the final period that the lower incipient soil in hillwash was exposed, phase 1
OSL3	2919	320–330	1480±340 BC	Constrains the onset of hillwash accumulation, phase 1
Ramla valley				
OSL4	2921	15–20	*AD 1880±16*	Provides a temporal constraint on degradation of upper slope
OSL5	2922	62–66	AD 1850±12	Provide temporal constraints on periods of colluviation
OSL6	2923	103–106	*AD 1910±30*	
Ġgantija Temple				
OSL7	2914	78	1140±250 BC	Constrains the final period that the buried soil was exposed
OSL8	2915	92	8560±630 BC	Constrains onset of soil formation
Tal-Istabal, Qormi				
OSL9	2930	295–298	AD 1620±23	Constrains the burial of soil
Skorba Neolithic site				
OSL10	2925	118	7760±560 BC	Constrains the final period that the buried soil was exposed
OSL11	2926	128	8090±590 BC	Constrains the age of the buried land surface
OSL12	2927	145	8780±710 BC	Constrains onset of soil formation

input is preserved this should retain a palaeoclimatic signal combining aridity history in the Saharan source regions and wind patterns that move these minerals across the Mediterranean region.

For most of the samples collected from hillwash and alluvial deposits in valleys, the equivalent doses showed variations of a factor of two to three between aliquots, reflecting inhomogeneous or partial bleaching of the quartz grains in these samples. This suggests that the erosion and sediment transport processes resulting in these deposits did not expose the minerals to sufficient light to remove all the residual signals from burial in earlier sediments. This could be the result of bulk movement of sediment or the rapid erosion, movement and re-burial of the minerals. Although reliable dates were not always quantifiable, the data do provide information about the processes of formation for these deposits.

For the soils directly associated with the Ġgantija and Skorba temple sites the equivalent dose values did not show significant dispersion, suggesting that the quartz grains had been well zeroed prior to burial and that there has not been substantial disturbance since then. This allowed ages to be determined even from the small number of aliquots available. This has demonstrated that OSL dating provides valuable information, and should be applied in any further studies of these, and similar, monuments on Malta and Gozo.

2.1.1.4. Tephrochronology

Sean D.F. Pyne-O'Donnell

Tephrochronology is a technique that identifies layers in sediment cores that contain volcanic glass shards (*cryptotephra*) that derive from eruptions of known date. These layers or isochrons – age-equivalent horizons – can be very useful in matching data from different coring sites and they can greatly aid the interpretation of radiocarbon dates. At face value there is significant potential for this work in the Maltese Islands, given their central position in the Mediterranean, downwind from several active volcanoes. However, the nature of sedimentation on the islands causes severe difficulties, as the *cryptotephra* can be diluted beyond detectible limits by rapid sediment run-off and accumulation. Nonetheless, it was possible to study the tephrochronology of the Xemxija 1 core by extracting sub-samples – 'rangefinders' every 5–7 cm through the core, aside from the upper 1.24 m of overburden and unfavourable brecciated clays present between 6.55 and 7.8 m. *Cryptotephra* were extracted using stepped-centrifuge flotation (Blockley *et al*. 2005), and any rangefinders containing tephra concentrations likely to represent a layer (i.e. greater than background levels) were then examined again at 1 cm resolution to identify the precise stratigraphic position of the peak. Once this was done, individual shards were picked

from peaks by micromanipulator (Lane *et al*. 2014; Pyne-O'Donnell 2004) for WDS-EPMA microprobe geochemical analysis at the Tephra Analytical Unit (TAU), School of Geosciences, University of Edinburgh using a Cameca SX100 electron probe micro-analyser (accelerating voltage of 15 kV and a focused 3 μm beam diameter) (Haywood 2012). Rhyolitic (Lipari, ID 3506), with basaltic (BCR2g) secondary standards were used to test analytical consistency. These geochemical data were then compared to reference data to allow their classification and to identify the source eruptions (*cf*. Albert *et al*. 2012; Civetta *et al*. 1988; Le Bas *et al*. 1986; MacDonald 1974; Peccerillo & Taylor 1976 and references therein). Details of the two tephra horizons identified in the Xemxija 1 sequence are given in Table 2.3.

2.1.2. Pottery finds

Rowan McLaughlin

Human settlement of the Maltese Islands is richly associated with the production and use of pottery, much of which is highly distinctive, and can be dated on the basis of its appearance and study of its fabric, even from quite small fragments (Malone *et al*. 2009a; Malone & Stoddart 2000). A more detailed discussion can be followed in *FRAGSUS* Volume 2. Throughout time, broken pottery was added to field soil with other midden materials to improve fertility. Consequently sediment cores frequently contain small sherds, some of which are identifiable. In cases where this added meaningful information to the chronology, the known age ranges of the pottery types (i.e. the cultural phases in Table 2.1) were included in the age-depth model of the sediment core. Details of pottery sherds used in this way are given in Table 2.3.

2.2. Basin infill ground penetrating radar surveys

Alastair Ruffell, Chris O. Hunt, Jeremy Bennett, Rory P. Flood, Simon Stoddart & Caroline Malone

2.2.1. Rationale

Stratigraphic successions for palaeoenvironmental reconstruction from areas proximal to archaeological sites are required for penecontemporaneous reconstruction of proxy changes (Shackleton *et al*. 1984). For the Maltese Islands, identification of such successions presents a challenge, since the landscape is dominated by rock exposures and thin soils. However, the islands' position on the Libyan Shelf has resulted in late Miocene (~5 mya) uplift, generated by the continued collision of the African Plate to the south, with the Eurasian Plate to the north. This movement is confirmed by dated raised marine deposits (Pedley 2011). Periodically dry river valleys occur throughout the islands, sourced by *widien* in the hinterlands that have provided a sediment source for any accommodation space located downstream or offshore. As a consequence, depressions close to present-day sea level (usually river valleys) comprise flat, fertile plains, underneath which a sediment record may be preserved. Identification of these potential sites can be made by visual observation, but in order to target viable coring locations and extract sediment that may yield useful material for reconstructing past environments, geophysics was used as a basin visualization and prospection tool to aid in the location of the deep core sites for intensive sampling, further described below.

2.2.2. Geophysics for basin fill identification

A range of geophysical techniques can be useful for the imaging of sediment thickness from a few metres to tens of metres in palaeo-valleys. The following were considered for the *FRAGSUS* Maltese Islands surveys:

The gravity/microgravity method relies on a density change between the surrounding country rock and the sediment fill, which is likely in the rock-prone landscape of the Maltese Islands. The method is powerful and requires post-processing of data in order to remove other gravimetric influences (Bouger Anomalies).

Seismic/electroseismic techniques are the standard method of both deep (kilometres) and shallow (tens of metres) imaging of rock and sediment layers and are dependent on density changes in the medium (as with gravity, above). Seismic imaging uses soundwaves as as source, and thus requires a source (commonly percussion such as a hammer shock to the ground (shallow), a mechanical weight-drop, Buffalo Gun/ airgun, small detonation, or vibration).

Ground penetrating radar (or GPR) is similar to the seismic method, but uses radiowaves instead of vibrations as a signal source, and reacts to changes in the electrical makeup of the subsurface (polarization of molecules), termed the dielectric constant (Appendix 1). As such, an energy source is easier to obtain, but this results in less overall depth penetration and only works well in sand, freshwater and rock. Saline and clay-rich subsurface successions are not conducive to GPR surveying.

The Electrical Resistivity Imaging (or Tomography; ERI or ERT) method relies on subsurface changes in chemistry (as opposed to density in the gravity and seismic methods), but uses an electrical charge and its underground impedance (resistivity) or flow (conductivity) to generate an image. The technique works in many environments, but like seismic and gravity, takes time to gather results.

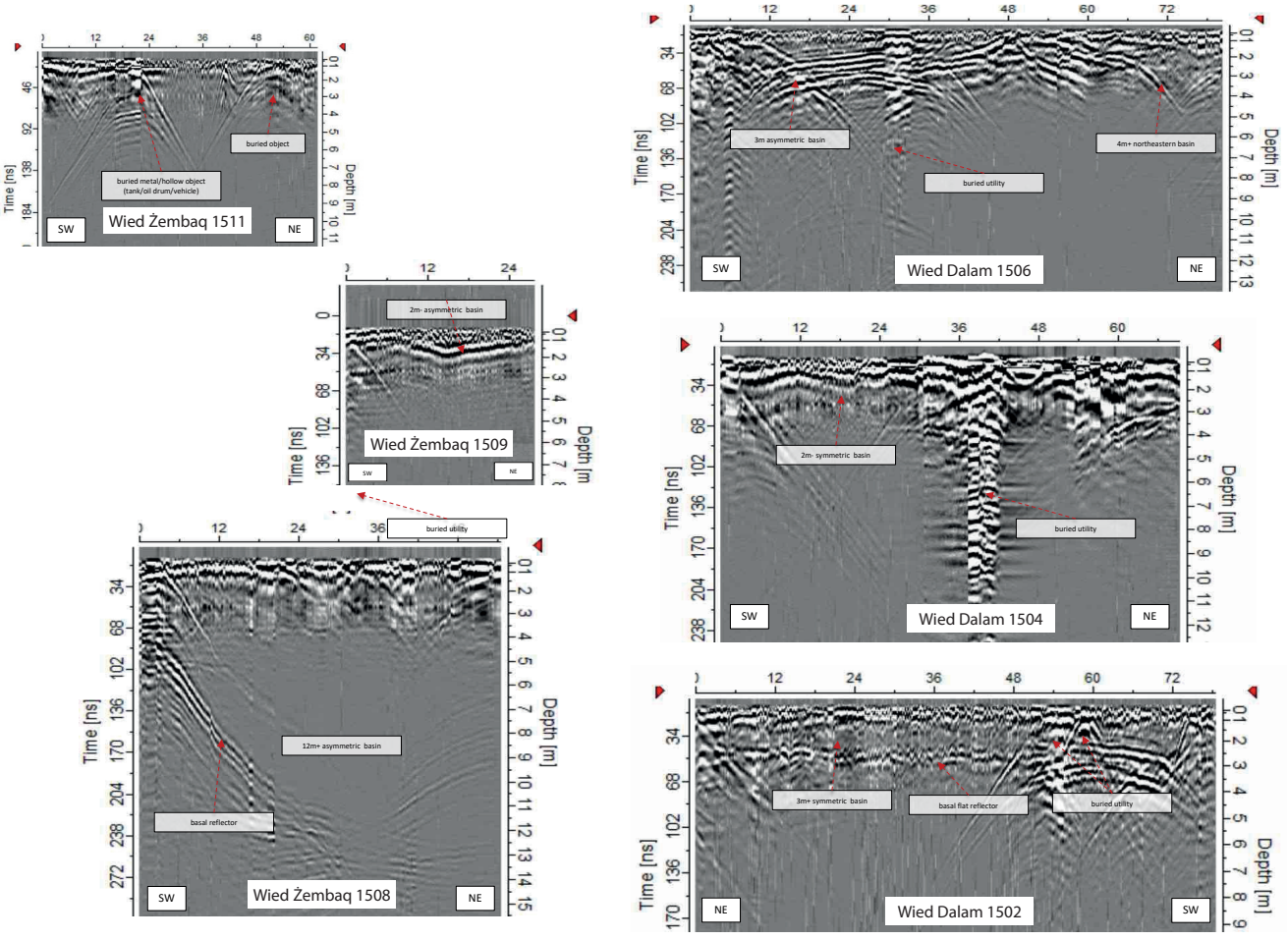

Figure 2.3. *The location of the Birżebbuġa Wied Dalam and Wied Żembaq basins and their GNSS-located GPR lines (A. Ruffell; image © 2020 Google).*

GPR was selected as the most rapid method available for the objective of identifying basin fills on Malta and Gozo. As a result of the limitations detailed above it was chosen as a reconnaissance method for valley fills selected by visual (field and orthophotography) methods, and the proximity of potential coring sites to prehistoric archaeological sites and previous coring/excavation investigations. ERI was also considered, but the success of GPR in identifying the majority of locations allowed coring to proceed without further assessment. The GPR system used was a Mala RAMAC system deploying 100 Mhz, 200 MHz, 250 Mhz antennas.

2.2.3. Valley locations

A. Birżebbuġa. This valley system includes a number of marine inlets, extending inland as plains: Wied Dalam, Wied Żembaq and Marsaxlokk. All three valleys were surveyed, but with poor results (particularly at Marsaxlokk because of the presence of the clay and saline soils). The locations of the Wied Dalam and Wied Żembaq basins and their GNSS-located GPR lines are shown in Figure 2.3. The Wied Dalam valley is underlain in some areas by two palaeo-valleys, of 3 and 4 m depth, and containing significant maritime and maritime-military utilities buried along the length of the valley. The Wied Żembaq valley is partly urbanized around a deep (15 m+) valley that thins to 2–3 m depth upstream (northwest) where fields occur and a coring location would be possible.

B. Marsalforn is a seaside location in the north of Malta and like Birżebbuġa, is urbanized. Likewise, the Marsalforn basin also has a thick sequence of deposits (10 m+) occurring closest to the sea (under the coast road), which thins inland to the west and south to 3–4 m under a flash-flood prone plain.

C. Xemxija. Similarly to the sites described above, the Xemxija valley meets the sea as a broad plain, but unlike the above, is wider and extends for some kilometres inland. The coastal area is urbanized, with extensive agriculture inland. The basin is 4–5 m deep at the coast, and this depth is maintained inland, where windmills have been replaced by mechanical water-pumps, attesting to the thick, permeable nature of the valley fill.

D. Mġarr ix-Xini. On the south coast of Gozo, this valley is of similar dimensions to Wied Żembaq, and to some extent, Wied Dalam, but is narrow and not urbanized. A 2–3 m deep basin occurs at the shore end to the southeast, this divides into two palaeo-valleys upstream to the northwest.

E. Low-lying, flat ground occurs southwest of Valletta Grand Harbour at Marsa, the location of a racecourse (hence it is flat, and likely underlain by significant quantities of sediment). GPR here was unsuccessful, possibly because the basin is too deep for imaging, and also filled with saline water, ingressed from the deep harbour. The soils may also be clay-rich and therefore less suitable for imaging. Thus Marsa, Marsaxlokk and two clay-filled dolines proved to be unsuccessful locations. A shallow, inland palaeovalley fill was also surveyed along Triq il-Mitħna-Triq Ġnien is-Sultan (southeast of Fontana, Gozo).

2.3. The sediment cores

Chris O. Hunt, Michelle Farrell, Rory P. Flood, Katrin Fenech, Rowan McLaughlin, Nicholas C. Vella, Sean Taylor & Charles French

2.3.1. Aims and methods

Investigation of the Holocene sequences addressed several issues:

1) There were suggestions from previous research (Carroll *et al.* 2012) that there were major discontinuities in sedimentation at some of the investigated localities. This is particularly marked at Marsa, where earlier Neolithic sediments are directly overlain by layers relating to the Punic and later periods, and at Salina Bay where Neolithic and Bronze Age sediments are overlain by sediments of likely nineteenth century date (Carroll *et al.* 2012, fig. 11).
2) There were indications from the existing research of spatial patterning of vegetation communities within the middle to late Holocene. For instance, Carroll *et al.* (2012) noted what appeared to be evidence for pine-dominated forest and Neolithic clearance at Marsa, contemporary with very open agricultural landscapes at Salina, while at Burmarrad, contemporary open grazed landscapes with lentisk scrub were reported (Djamali *et al.* 2013; Gambin *et al.* 2016). The number of palynological investigations of mid to late Holocene deposits available at the start of the *FRAGSUS Project* was insufficient to address adequately issues of spatial patterning of environments and vegetation, and hence land-use and human impact: critical for any evaluation of Neolithic sustainability and fragility, but also important for understanding the post-Neolithic development of the Maltese landscape.
3) Previous studies had not located early Holocene deposits which accumulated prior to the first Neolithic colonization, because they lay deeper

in the buried valley network than was reached by previous coring by Carroll *et al*. (2012) and Djamali *et al.* (2013). Therefore, deep boreholes were necessary to reach and sample the Early Holocene sediments.

4) Dating of cored sequences was an issue in previous research (Carroll *et al.* 2012; Djamali *et al*. 2013) with radiocarbon dates often falling out of stratigraphic order. This was likely the result of (1) recycling of old charcoal, and (2) intrusion of modern carbon through the coring process.

5) There has been remarkably little pollen-taphonomic work done in the Central Mediterranean countries. Pollen-vegetation relationships and patterns of pollen dispersal from different vegetation types are therefore unclear. This is a critical issue since some vegetation types, particularly maquis and garrigue, are dominated by insect-pollinated taxa. Further, some pollen assemblages reported by Carroll *et al.* (2012), Djamali *et al.* (2013) and Gambin *et al.* (2016) showed what could be interpreted as taphonomically biased features, such as high percentages of corrosion-resistant taxa such as *Pinus* and Lactuceae. These might result from differential preservation, recycling of pollen from soils, or losses during transport. Alternatively, these assemblages may reflect unbiased pollen assemblages derived from unusual ecologies.

The choice of coring sites was dictated by the prospect of obtaining partial sequences from each site that together would span the Holocene (Fig. 2.4). It was apparent from the earlier studies (e.g. Carroll *et al*. 2012; Djamali *et al*. 2013) that although sedimentation was discontinuous in each of the boreholes drilled by these researchers, the discontinuities occurred at different points in time. In times of sea level stand, sea level controlled sedimentation progrades seaward in wedge-shaped bodies, with increments deposited on the outer face of the wedge, and transport and reworking of fluvial deposits on the top of the sediment body by rivers. When sea level rises, deposition will migrate seaward if the sedimentation rate is greater than the rate of sea level rise, with deposition on the top of the sediment body and on its seaward face. On the other hand, sedimentation will be driven landward if there

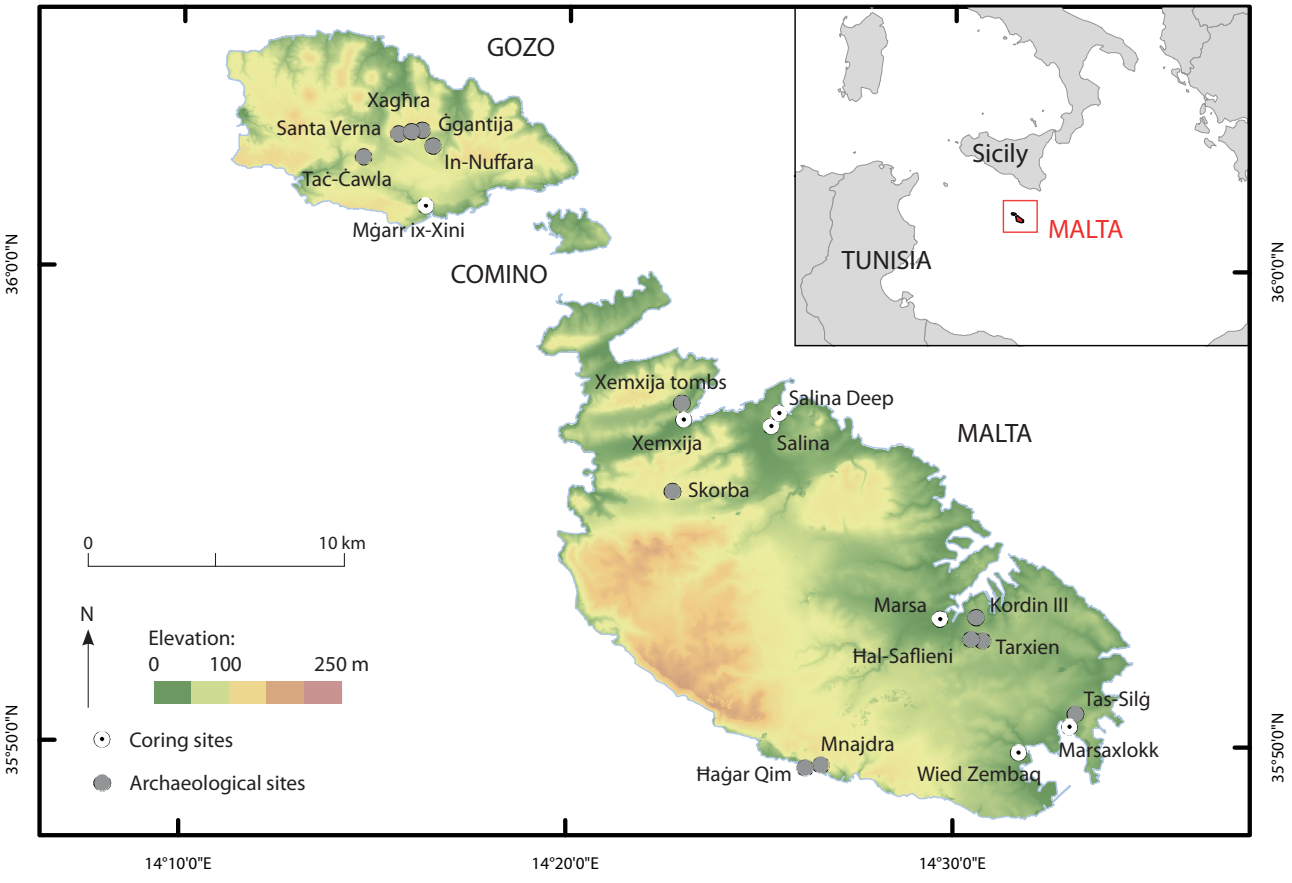

Figure 2.4. *The core locations in Malta and Gozo (R. McLaughlin).*

Table 2.3. *Dating results for positions in the sediment cores. The sites are Bahrija doline (BAH), Marsa Sports Ground (MARSA), Mellieħa Bay (MB), Mġarr ix-Xini (MGX), Marsaxlokk (MX), Salina Bay (SA), Salina Deep Core (SDC), Wied Żembaq (WZ) and Xemxija (XEM). Numbers following site codes denote different sequences recovered from the same site. (Note that tephra horizons are not definitive and pottery identifications are subjective).*

Core	D (cm)	Lab. ID	^{14}C date	±	F^{14}C	±	Calendar range (95%) BC/AD		Material
BAH1	49	UBA-30091	2195	29	.7609	.0028	-360	-180	Charcoal
MARSA2	275	UBA-29443	1487	34	.8310	.0035	430	650	Wood
MARSA2	335	UBA-29452	1510	32	.8287	.0033	430	640	Charcoal
MARSA2	375	UBA-29453	2687	35	.7157	.0031	-900	-800	Charcoal
MARSA2	395	UBA-29454	2686	35	.7158	.0031	-900	-800	Charcoal
MARSA2	435	UBA-29444	2584	28	.7250	.0026	-810	-600	Grape seed
MARSA2	455	UBA-29445	2357	42	.7458	.0039	-730	-360	*Fumaria* seed
MARSA2	475	UBA-29446	2754	41	.7098	.0036	-1000	-820	Seed
MARSA2	487	UBA-30605	7216	75	.4072	.0038	-6230	-5930	Charcoal
MARSA2	495	UBA-29447	3943	69	.6121	.0052	-2620	-2210	Plant macro
MARSA2	495	UBA-29455	3912	40	.6145	.0030	-2550	-2230	Charcoal
MARSA2	513	UBA-30606	2944	40	.6932	.0034	-1260	-1020	Charcoal
MARSA2	590	UBA-29448	2501	50	.7325	.0045	-790	-430	Seed
MARSA2	598	UBA-30607	2587	40	.7246	.0036	-830	-550	Charcoal
MARSA2	617	UBA-30608	2765	25	.7088	.0022	-980	-840	Charcoal
MARSA2	825	UBA-29451		1	1.0367	.0050			Insect
MB1	244	UBA-30092		1	1.0732	.0032			Wood
MGX1	54	UBA-29979		1	1.0138	.0079			Plant macro
MGX1	176	UBA-29980	1230	29	.8580	.0031	690	880	Wood
MGX1	239	UBA-29981	3443	31	.6514	.0025	-1880	-1660	Plant macro
MGX1	302	UBA-29982	2509	30	.7317	.0028	-790	-540	Plant macro
MGX1	365	UBA-29983	2466	30	.7356	.0028	-760	-430	Plant macro
MGX1	365	UBA-29984	2655	34	.7185	.0031	-890	-790	Charcoal
MGX1	428	UBA-29985	2998	35	.6885	.0030	-1380	-1120	Plant macro
MGX1	428	UBA-29986	6905	42	.4233	.0022	-5890	-5720	Wood
MGX1	554	UBA-29987	2991	40	.6891	.0034	-1390	-1060	Plant macro
MGX1	554	UBA-29988	2839	36	.7023	.0031	-1110	-910	Charcoal
MGX1	617	UBA-29989	3124	35	.6778	.0029	-1490	-1290	Plant macro
MGX1	695						-750	-250	Punic-period pot sherd
MGX1	702	UBA-33096	2339	33	.7474	.0031	-510	-360	Plant macro
MX1	86	UBA-29353	1567	29	.8228	.0030	420	560	Charcoal
MX1	186	UBA-29352	2354	33	.7460	.0031	-540	-380	Charcoal
MX1	286	UBA-29351	1444	51	.8355	.0053	440	670	Charcoal
MX1	386	UBA-29346	0	1	1.0397	.0031			Plant macro
MX2	200	UBA-29372	1950	29	.7845	.0028	-20	130	Charcoal
SA1	200	UBA-29031	2403	32	.7415	.0029	-730	-400	Charcoal
SA1	300	UBA-29032	3194	32	.6719	.0026	-1590	-1400	Charcoal
SA1	410	UBA-29033	5038	44	.5341	.0029	-3950	-3710	Charcoal
SA1	520	UBA-29034	4000	29	.6078	.0022	-2570	-2470	Charcoal
SA1	520	UBA-29035	3746	36	.6273	.0028	-2280	-2030	Plant macro
SA1	630	UBA-29036	5775	32	.4873	.0020	-4710	-4540	Charcoal
SA1	630	UBA-29037	4989	72	.5374	.0048	-3940	-3650	Plant macro

Table 2.3 *(cont.).*

Core	D (cm)	Lab. ID	^{14}C date	±	F^{14}C	±	Calendar range (95%) BC/AD		Material
SA1	670	UBA-29038	5862	48	.4820	.0029	-4840	-4600	Charcoal
SA1	770	UBA-27666	4584	41	.5652	.0029	-3500	-3100	Plant macro
SA2	100	UBA-29039	2243	31	.7563	.0029	-390	-200	Plant macro
SA2	400	UBA-29040	3611	39	.6379	.0031	-2120	-1880	Plant macro
SA2	600	UBA-27665	4693	35	.5575	.0024	-3630	-3370	Plant macro
SA2	600	UBA-29045	2344	79	.7469	.0073	-750	-200	Plant macro
SA2	605	UBA-29046	2920	44	.6952	.0038	-1260	-1000	Plant macro
SA2	640	UBA-29047	3241	33	.6680	.0027	-1610	-1440	Plant macro
SA3	150	UBA-29965	1068	33	.8755	.0036	900	1020	Charcoal
SA3	150	UBA-29966	995	26	.8835	.0029	990	1150	Charcoal
SA3	250	UBA-29967	2536	66	.7293	.0060	-810	-430	Charcoal
SA3	350	UBA-29968	3182	61	.6730	.0051	-1610	-1290	Plant macro
SA3	350	UBA-29969	2910	34	.6961	.0030	-1210	-980	Charcoal
SA3	450	UBA-29970	3765	37	.6258	.0029	-2290	-2040	Plant macro
SA3	450	UBA-29971	1678	28	.8115	.0028	260	420	Charcoal
SA3	550	UBA-29972	3768	43	.6256	.0033	-2330	-2030	Plant macro
SA3	650	UBA-29973			1.0026	.0033			Plant macro
SA3	650	UBA-29974	4978	35	.5381	.0023	-3920	-3660	Charcoal
SA3	850	UBA-29975	5657	37	.4945	.0023	-4580	-4370	Plant macro
SA3	850	UBA-29976	9535	61	.3051	.0023	-9170	-8710	Charcoal
SA3	999	UBA-29977	6125	37	.4665	.0021	-5210	-4960	Plant macro
SA3	999	UBA-29978	6131	35	.4662	.0020	-5210	-4960	Charcoal
SA4	102	UBA-30082	864	35	.8980	.0039	1050	1260	Charcoal
SA4	302	UBA-30083	2953	30	.6924	.0026	-1260	-1050	Charcoal
SA4	302	UBA-30084	3469	32	.6493	.0026	-1880	-1690	Plant macro
SA4	402	UBA-30085	3746	37	.6273	.0028	-2280	-2030	Charcoal
SA4	402	UBA-30086	3559	116	.6421	.0092	-2270	-1610	Plant macro
SA4	1002	UBA-30087	6136	43	.4659	.0025	-5210	-4950	Charcoal
SA4	1002	UBA-30088	5709	36	.4913	.0022	-4680	-4460	Plant macro
SA4	1058	UBA-30089	6240	48	.4599	.0027	-5310	-5060	Charcoal
SA4	1058	UBA-30090	6644	39	.4373	.0021	-5630	-5500	Plant macro
SDC	1140	UBA-34970	3793	39	.6236	.0030	-2400	-2050	Charcoal
SDC	1180	UBA-35578	6262	38	.4586	.0021	-5320	-5080	Charcoal
SDC	1210	UBA-34971	6267	48	.4584	.0028	-5340	-5070	Charcoal
SDC	1320						-2850	-2350	Tarxien-period pot sherd
SDC	1360	UBA-35579	8928	47	.3291	.0019	-8250	-7960	Charcoal
SDC	1474	UBA-35580	5378	35	.5120	.0022	-4330	-4070	Charcoal
SDC	1675	UBA-33282	6260	38	.4587	.0022	-5320	-5070	Charcoal
SDC	1785	UBA-35581	6570	35	.4414	.0019	-5610	-5480	Charcoal
SDC	1826	UBA-35583	6515	35	.4444	.0019	-5540	-5380	Charcoal
SDC	1940	UBA-35582	6451	38	.4479	.0021	-5480	-5340	Charcoal
SDC	2068	UBA-35585	6346	43	.4539	.0024	-5460	-5220	Charcoal
SDC	2285	UBA-35586	7145	39	.4109	.0020	-6067	-5821	Charcoal
SDC	2435	UBA-35587	7977	51	.3704	.0023	-7050	-6700	Charcoal

Table 2.3 *(cont.).*

Core	D (cm)	Lab. ID	^{14}C date	±	F^{14}C	±	Calendar range (95%) BC/AD		Material
SDC	2450	UBA-34972	8030	41	.3680	.0019	-7070	-6770	Charcoal
SDC	2500	UBA-34973	7923	39	.3730	.0018	-7030	-6660	Charcoal
SDC	2539	UBA-34974	7019	40	.4174	.0021	-5990	-5810	Charcoal
SDC	2641	UBA-34975	6894	36	.4239	.0019	-5870	-5710	Charcoal
SDC	2670	UBA-35588	7752	52	.3810	.0024	-6660	-6470	Charcoal
SDC	2910	UBA-31707	8957	44	.3279	.0018	-8280	-7970	Charcoal
WZ1	215	UBA-29042	2707	34	.7139	.0030	-910	-800	Charcoal
WZ1	444	UBA-34967	4316	36	.5843	.0026	-3020	-2880	Charcoal
WZ1	450	UBA-29044	7642	61	.3862	.0029	-6600	-6400	Charcoal
WZ1	458	UBA-27667	0	1	1.0141	.0034			Plant macro
WZ1	458	UBA-28262	4707	31	.5566	.0021	-3630	-3370	Plant macro
WZ2	295	UBA-29043	3428	41	.6526	.0033	-1880	-1630	Charcoal
WZ2	495	UBA-28263	4428	43	.5763	.0031	-3330	-2920	Plant macro
WZ2	521.1	UBA-34969	4366	49	.5807	.0036	-3260	-2890	Charcoal
XEM1	147						1190	1270	Monte Pilato tephra horizon
XEM1	157						786	766	Monte Pilato tephra horizon
XEM1	460	UBA-28265	3704	29	.6306	.0023	-2200	-1980	Plant macro
XEM1	501	UBA-31701	4215	29	.5917	.0022	-2900	-2700	Soil humic fraction
XEM1	565	UBA-25211	3063	49	.6830	.0042	-1430	-1130	Plant macro (Poaceae frags)
XEM1	565	UBA-29048	4571	135	.5661	.0094	-3630	-2930	Charcoal
XEM1	656	UBA-31705	5179	37	.5248	.0024	-4050	-3820	Soil humic fraction
XEM1	670	UBA-29041	5357	39	.5133	.0025	-4330	-4050	Charcoal
XEM1	816.5	UBA-31702	7055	41	.4155	.0021	-6010	-5840	Soil humic fraction
XEM1	864.5	UBA-31703	7273	35	.4044	.0018	-6220	-6060	Soil humic fraction
XEM1	886	UBA-31706	7042	41	.4162	.0021	-6000	-5840	Soil humic fraction
XEM1	923	UBA-31704	7045	44	.4160	.0022	-6010	-5840	Soil humic fraction
XEM1	1000	UBA-25001	9353	58	.3122	.0022	-8780	-8460	Charcoal
XEM2	318	UBA-31708	3124	33	.6778	.0028	-1490	-1280	Charcoal
XEM2	413	UBA-31709	4150	51	.5966	.0038	-2880	-2580	Charcoal
XEM2	508	UBA-29349	4873	33	.5452	.0022	-3710	-3540	Charcoal
XEM2	718	UBA-29350	7399	50	.3981	.0025	-6400	-6100	Charcoal
XEM2	823	UBA-29348	7463	39	.3950	.0019	-6420	-6240	Charcoal
XEM2	933	UBA-29347	8334	46	.3543	.0020	-7520	-7200	Charcoal

is insufficient sediment supply to keep pace with the rate of sea level rise. It was thus possible to infer from the geomorphology of the sites and the pattern of discontinuities that careful choice of borehole locations would enable the assembly of a complete stratigraphic sequence from several boreholes, even if there were discontinuities in individual cored sequences. It was decided to establish basin geometries and identify depo-centres using ground penetrating radar and available borehole records, then sample several locations in each of the coastal plains where deep stratigraphies had been located. This strategy was designed to provide the best possible chance of sampling continuously deposited sediments, with multiple cores to cover hiatuses in individual core sites.

Several borehole sites covering as much as possible of the Maltese Archipelago were necessary if regional patterns of land-use were to be identified. In practice, the number of boreholes was limited by logistical and cost implications, and some of those drilled, such as at Marsalforn, transpired to be in very coarse gravelly sediments unsuitable for analysis.

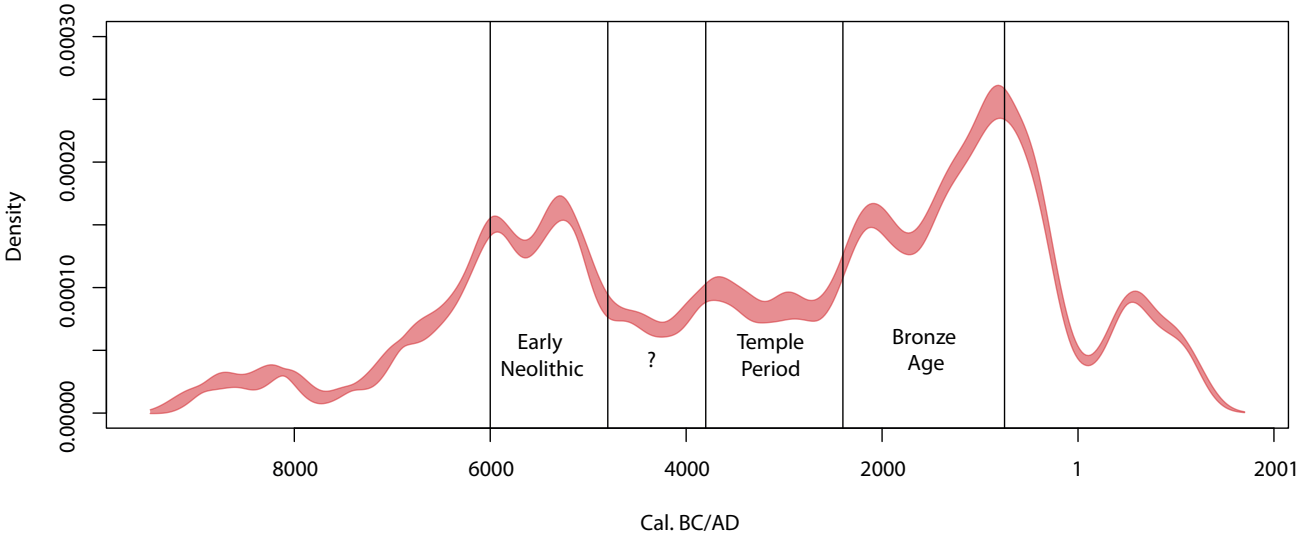

Figure 2.5. *Radiocarbon activity in sediment cores (R. McLaughlin).*

Nevertheless, coverage of the Maltese landscape was more than doubled by the work of the *FRAGSUS Project*. The archaeological sites excavated by the project also contributed samples for palynology, anthracology, plant macro-remains and soil micromorphology.

A particular challenge faced by the *FRAGSUS Project* was the need to reach sediments earlier than those that had been sampled by previous studies, and thereby establish the environments and vegetation present before human colonization of the Maltese Islands. This required extremely deep boreholes, because coastal sedimentation was, and is, controlled by sea level. From a low of about -120 m at *c*. 18,000 BC, sea level rose extremely rapidly in the central Mediterranean. Lambeck *et al*. (2011) suggested sea levels of about -60 m at 10,000 BC, -45 m at 8000 BC, -30 m at 7250 BC, -20 m at 6500 BC and -10 m at 5500 BC, although this might be mitigated locally by crustal levering caused by loading of continental shelves during sea level rise. This suggests that sea level controlled sedimentation might be at or below these depths during the Holocene, and consequently that a slight increment in time would necessitate a considerable increase in the depth of sampling needed. In practice, issues of opportunity, logistics and expense limited the number of very deep boreholes to one, at the Salina salt pans, where geotechnic boreholes indicated that a very deep valley fill was present.

Prospective coring locations were identified from the literature, from maps and aerial photographs, the ground penetrating radar surveys (GPR; see §2.2 above) (Fig. 2.3), and by consultation and discussion with *FRAGSUS Project* team members. Permissions were obtained by the officers of Heritage Malta and the Superintendence of Cultural Heritage, Malta. As there was limited time to drill multiple boreholes, geophysical survey using ground penetrating radar with a 10 m aerial was used to establish the deepest and most complete stratigraphy and thus optimal coring locations. At most prospective localities, the geophysical trace identified the rock-head profile, but at Salina and some coastal locations in south Malta the trace was lost as the result of salt-water intrusion and/or a predominantly clay fill. Core locations were surveyed using differential GPS (dGPS) with full descriptions and granulometry of the cores extracted by the *FRAGSUS Project* in Appendices 3 and 4, with the radiocarbon dating results listed in Table 2.3 (Figs. 2.1, 2.2 & 2.5).

Open-chambered percussion piston augers made by Eijkelkamp were used in very stony deposits. Where possible, paired boreholes were drilled with Eijkelkamp percussion piston order, with cores one metre in length and 5 cm in diameter recovered in rigid plastic liners. A core-catcher was often necessary as the sediments were largely unconsolidated. Core recovery was generally good but hydro-collapse occurred in several core segments in boreholes penetrating the shell gravels at Salina. Cores were stored in the Queen's University Belfast cold store at 4°C prior to splitting and analysis.

The Salina Deep Core was recovered by SolidBase Lts using a shell and auger rig and 8 cm diameter percussion cores 0.5 m in length in groups of three. At this site, the top part of the sequence was in shell gravel which hydro-collapsed and fell from the samplers. Recovery started at *c*. 11 m where silt- and clay-based

sediments began. The recovered sediment sequence was stored in a refrigeration unit at 4°C in Liverpool John Moores University prior to extrusion and analysis.

2.3.2. The core descriptions

2.3.2.1. The Salina Deep Core

The Salina Deep Core was drilled at the edge of an extensive complex of salt pans built by the Knights of St John towards the end of the sixteenth century on marshland at the entrance to the large Burmarrad plain. A fine plan of the complex executed in AD 1742 by the Order's surveyors show the pans as they were extended in AD 1650, with large reservoirs meant to hold seawater before it was channeled into the salt pans (Blouet 1963; National Library of Malta, Treas. B290, f. 23a). The complex was the property of the Grand Master who controlled the use of salt as a condiment and for curing meats (Mercieca 2005). The Burmarrad plain was considered to be good quality land in the first survey carried out by the Order in 1654, given over to the growing of grain, cotton and cumin (Blouet 1963). In 1658, halophytic vegetation that grew at the seaward end is known to have been collected and burnt, with the ash sold as a fertilizer (Blouet 1964). The salt pans are located in an area that was documented as an anchorage in the late fifteenth century and a watch tower stood on the shore at least a century earlier (Dalli 2011). The remains of rock-cut burial complexes of Late Roman date along the east shore, other remains discovered during construction works over the last twenty years, and a large Roman farming estate located on higher ground at San Pawl Milqi to the southwest suggest that the area saw major maritime-oriented activity in Roman times (Marriner *et al*. 2012). This may also be said of an earlier period, when the bay appears to have extended further inland. A Neolithic temple stood on the rocky, eastern edge of the plain at Tal-Qadi while a tomb was cut in the rock in the Żebbuġ phase where the Roman estate was subsequently built (Evans 1971; Cagiano de Azevedo 1969; Grima 2011a).

At Salina, the geotechnical boreholes drilled in preparation for the rehabilitation of the salt pans showed a deep valley fill, as recorded here and in the Burmarrad valley by Carroll *et al*. (2012) and Marriner *et al*. (2012). The Salina valley is highly asymmetric, but close to the northeastern margin of the pans is over *c*. 30 m deep. However the base of the valley fill was not reached. Here, the top part of the Deep Core borehole passed through shell gravel which hydro-collapsed and fell from the samplers, but the same unit was encountered in a nearby borehole (Salina 2 core, see Appendix 2) drilled with a percussion auger by the *FRAGSUS Project*. Recovery of the deep core started at *c*. 11 m where the sequence passed into silt- and clay-based sediments.

The sediments encountered in the Salina Deep Core are shown in Tables 2.4 and A3.1. The borehole was drilled through the trackway at the edge of the salt pans. After passing through *c*. 2.4 m of rubble and masonry, the borehole then passed through *c*. 8.6 m of shallow marine shell gravel, then *c*. 2 m of shallow marine sandy shoal sediments, *c*. 8.0 m of distal pro-deltaic muds, 5.65 m of delta-front and pro-deltaic sediments interbedded with lower energy quiet water sandy muds, 0.35 m of littoral marine muddy gravels, 2.3 m of fluvial gravels, and a *c*. 0.17 m thick silty clay palaeosol, all developed on Globigerina Limestone. AMS radiocarbon dates range from 8280–7970 cal. BC (8957 BP; UBA-31707) at 29.1 m to 4330–4070 cal. BC (5378 BP; UBA-35580) at 14.74 m to 2400–2050 cal. BC (3793 BP; UBA-34970) at 11.4 m below the ground surface (Table 2.3), with an age-depth model suggesting a start to sediment accumulation from at least 7500 cal. BC (Table 2.5).

This sequence can be interpreted as reflecting the development of a terrestrial valley fill and then the drowning of the valley by rising sea levels. The initial valley fill is composed of pedogenically altered muddy hillslope deposits (colluvium) and gravelly alluvium of a multi-channel ephemeral river. It formed during the Late Pleistocene/early Holocene phase of low sea level. The hillslope deposits are consistent with a lightly vegetated and most probably seasonal semi-arid landscape, as are the very poorly sorted fluvial gravels. The carbonate forms and soil development in general are also consistent with strong seasonal aridity.

Littoral gravels record the flooding of the valley by rapidly rising sea level during the Early Holocene. The delta-front and pro-delta deposits overlying these suggest initially deepening water as sea level continued to rise. Very quickly, however, the drowned valley started to infill with the products of soil erosion from the Burmarrad catchment. Soil eroded during high rainfall events was carried seaward by the Burmarrad River and a delta must have developed and then migrated up-valley as sea level rose. Off the delta front, the river water, dense with suspended sediment, will have spread across the sea floor as a series of gravity-driven turbidity currents. The waters in the Salina inlet therefore probably never became very deep, as sedimentation was extremely rapid, but the finely layered sediments comprising most of the pro-deltaic sediments will most probably have been laid down in waters deeper than wave-base. During periods between major floods, the sea bed would have been colonized by marine animals, and bioturbation

will have occurred, leading to massive (structureless) sediments, whereas the turbidity flows will have repeatedly killed benthic animals, thus leading to well laminated sediments undisturbed by burrowing organisms. As sea level rise slowed from *c*. 3000 BC onwards, the sedimentation rate will have exceeded the rate of sea level rise and the waters in the Salina inlet will have shallowed, with the sea coming within wave-base, allowing winnowing to occur during storms. The winnowing will have re-suspended silt and clay, which will have been transported seaward, leaving behind the shelly shoal sands. As the waters of the inlet continued to become shallower, winnowing will have intensified and sand-sized material will have been carried seaward. The shell gravels at the top of the sequence developed in shallow, turbulent waters, with accommodation space and thus sedimentation rate being constrained by the declining rate of sea level rise in the later Holocene. During this time, fine sediments resulting from soil erosion in the Burmarrad catchment will have been carried past the shell-gravel shoals into deeper water.

2.3.2.2. The Salina 4 core

The nearby Salina 4 core was some 11.02 m in depth (Tables 2.4 & A3.2). AMS dates range from 5630–5500 cal. BC (6644 BP; UBA-30090) at 10 m to 1260–1050 cal. BC (2953 BP; UBA-30083) at 3 m and cal. AD 1050–1260 (864 BP; UBA-30082) at 1 m depth (Table 2.3). The basal *c*. 3.5 m is dominated by estuarine sediments of fine sandy silty muds below a *c*. 3 m thick zone of alternating silty clay and fine sandy muds. These sediments are pro-deltaic in origin. The overlying zone between 4.38 and *c*. 3 m depth consists of alternating grey and black silty clays and was slightly shelly sand which hydro-collapsed during extraction. Above this was a metre of olive grey silty clay lagoonal sediments. The upper *c*. 2 m of the core was dominated by yellowish orange and brown silt clays with silty sand lenses between *c*. 0.82–0.58 m down-profile. These appear to be overbank flood deposits accumulating in a back-basin lagoon. This stratigraphy suggests an original estuarine depositional setting close to the mouth of the Burmarrad River. Deposition outpaced sea level rise so the sand unit was deposited, probably rather rapidly, within the wave-base, before the progradation of fluvial overbank deposition across the site. The silt/sand alternation in the top two metres of the core is consistent with vigorous flooding from the Burmarrad River.

2.3.2.3. The Salina 2 core

The core was drilled through the base of the drained Salina saltpans to a depth of 7.9 m before drilling was abandoned in what was probably hydrocollapsing shell gravel, but core recovery, even with the core catcher, started only at 6.54 m. The basal ~5.3 m of the recovered core consists of alternating grey and dark grey-brown very shelly coarse sands/sandy gravels and highly organic sandy silty clays. Some of the sandy silty clays had eroded or burrowed tops, consistent with pauses in deposition of unknown duration and some of the coarser sandy shell-gravel units hydrocollapsed on extraction. These units probably reflect shallow offshore deposition in sandy gravel shoals bearing eel-grass meadows and sheltered, quieter-water inter-shoal environments, respectively, suggesting that the floor of the outer estuary was covered with shifting sandbars. Above 1.27 m in the core, littoral sands alternate with shallow estuarine sediments, suggesting that this part of the estuary had shallowed sufficiently that the sandbars were sometimes emergent.

2.3.2.4. The Xemxija cores

Two cores were taken in a modern pine grove located immediately behind the road that skirts the sandy beach at Pwales, a summer resort that extended along the Pwales Road in the post-World War II period. Documentation shows that the area where the cores were taken formed part of an estate consisting of seven hectares of marshland located behind the foreshore. These were drained in AD 1650 and had been transformed into good quality arable land surrounded by walls and equipped with drainage channels by AD 1658 (Blouet 1964). A plan drawn by the Order's surveyors in AD 1784 shows the extent of the estate (National Library of Malta, Treas. B301, f. 57). The channels can be clearly made out in the western fields as rectilinear anomalies in aerial photographs; some were destroyed when the area was turned into a nature reserve in the early 1990s, as was a large farmhouse that stood in the middle of the estate. The whole area is prone to severe flooding and this happened at least twice in the last century, in 1957 and 1982 (Bowen Jones *et al*. 1961). A small chapel was built further into the valley in AD 1672, where several springs created water gardens. Archaeological remains of note are concentrated not on the plain but higher up on the ridge to the north and consist of a series of Neolithic shaft-and-chamber tombs cut into the rock (Evans 1971), and the remains of an unexplored Neolithic temple at Ta' Żminka (Vella 2002) located on the eastern edge of an olive grove that was planted as part of an afforestation project carried out in 1957. A rock-cut tomb nearby dating to the third century BC (Vella *et al*. 2001), and other caves with evidence of contemporary and later use located along the escarpment overlooking Mistra Bay,

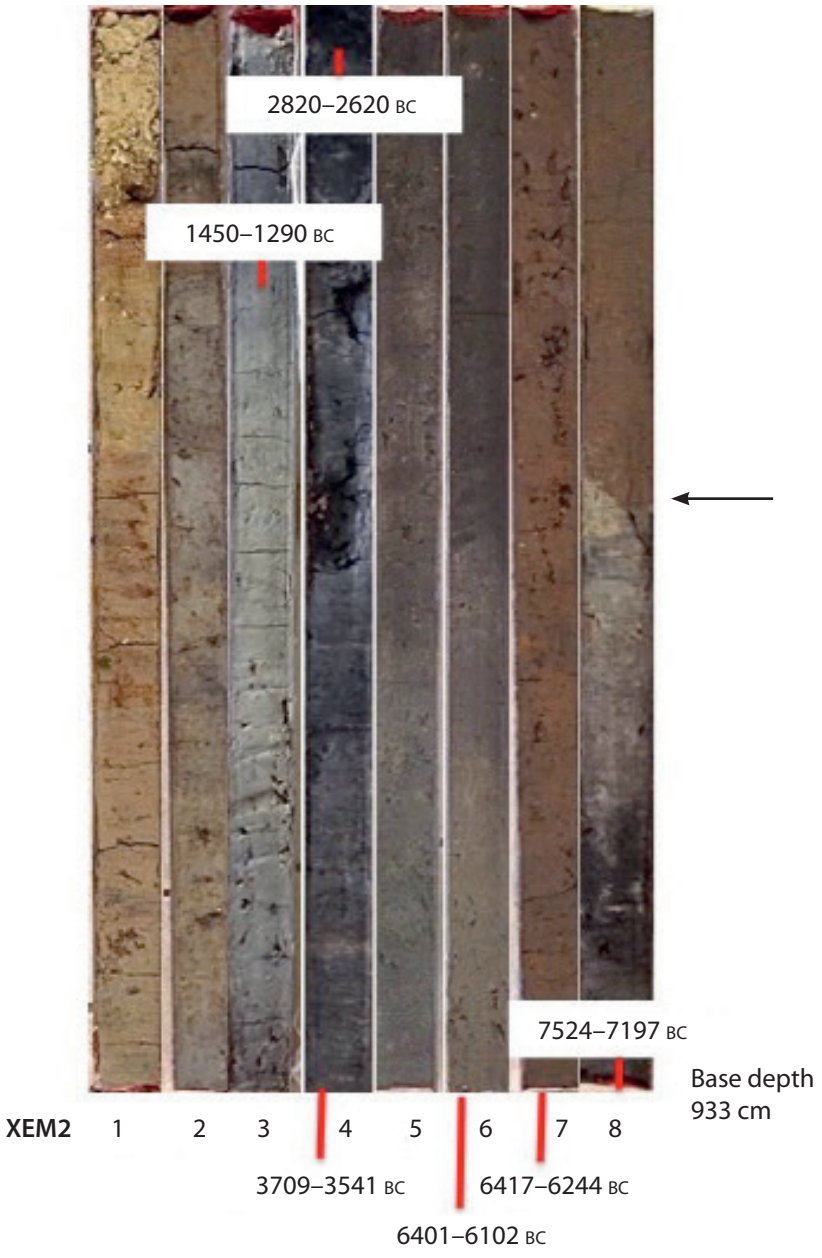

Figure 2.6. *The Xemxija 2 core by depth with the arrow indicating the cumulative palaeosol/mass-flow transition (K. Fenech).*

show that a small community was established here in Late Punic times, possibly exploiting the agricultural potential of an area that saw several attempts at agricultural improvement throughout the Knights and British periods (Hunt & Vella 2004/5).

Two *c*. 10 m deep cores (XEM 1 & 2) were taken, about 2 m apart, with overlapping core segments. They have broadly similar stratigraphy and chronology (Tables 2.4, A3.4 & A3.5). In the basal metre of the 10 m Xemxija 1 core, there is a silty clay loam cumulative soil with some structure and an organic component which began to accumulate from at least 8780–8460 cal. BC (9353 BP; UBA-25001), with sedimentation continuing to more or less the present day (Table 2.3). This basal cumulative soil is very calcitic, indicative of calcareous groundwater and strong seasonal drying, and was most probably an aggrading alluvial soil. Above this, there is a further *c*. 3.4 m of similar mass-flow silty clay material that accumulated in marshy conditions which contains occasional to frequent limestone fragments and pebbles. These deposits may be indicative of greater erosion and exposed limestone substrates in the immediate catchment. Interrupting this aggradation are three layers with finer sediments, weak pedogenic structures and some organic accumulation, suggestive of a slowing of aggradation and

incipient organic A horizon formation at several points up-profile (at 8.15–8.32, 6.7–6.85 and 6.0–6.3 m). These essentially indicate periods of some stabilization of the floodplain surface (see Chapter 5).

There is then a major change in the system with the accumulation of a thick layer of black organic silt mud between *c.* 5.65 and 4.6 m, after about 4330–4050 cal. BC (5357 BP; UBA-29041) and up to at least 2200–1980 cal. BC (3704 BP; UBA-28265) (Tables 2.3 & 2.4). This suggests that there was a lengthy phase of near permanent, shallow standing water, and only minimal input of very fine eroded soil material in this shallow freshwater 'lagoonal' or paludal (marshy) situation, probably behind a bay-bar.

Subsequently, there was a return to fine alluvial calcareous silt accumulation, interrupted by the occasional coarser layer (at 2.5–2.65 m) or incipient palaeosol (at 3.19–3.35 m), (see Chapter 5; Fig. 2.6; Table 2.4; Appendix 3).

2.3.2.5. The Wied Żembaq cores

The low, steep-sided spur or ridge known as Borġ in-Nadur, overlooking the small cove of St. George's Bay in southeast Malta, is defined by two converging deep valleys, the Wied Żembaq to the west and the Wied Dalam to the east. The area has witnessed a long history of human occupation, including a Neolithic temple that was re-used during the Bronze Age when a settlement flourished behind an impressive fortification wall that cut right across the spur and appears to have followed the entire perimeter of the ridge (Tanasi & Vella 2011a & b, 2015). Remains of two dolmens are

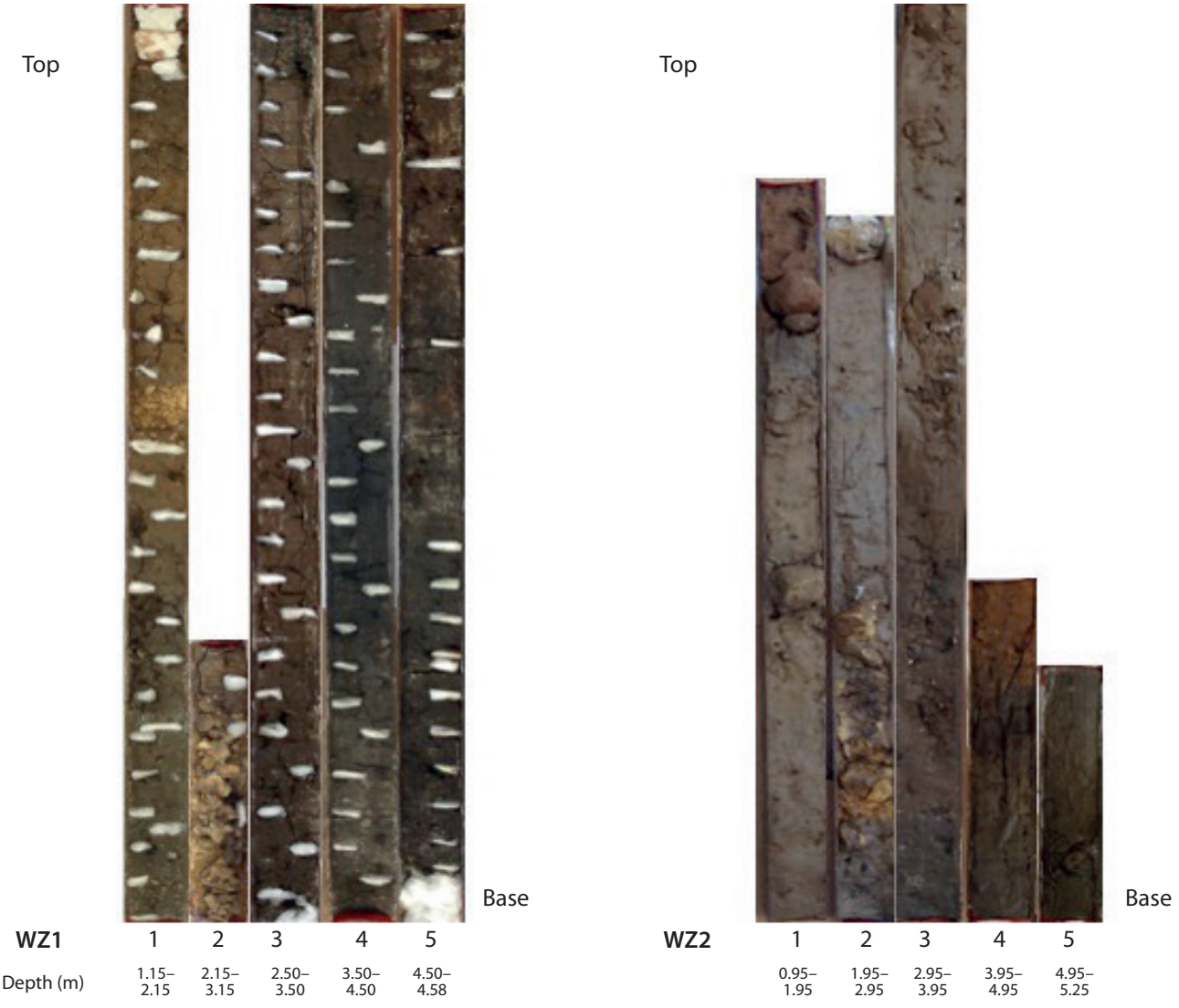

Figure 2.7. *The Wied Żembaq cores 1 (left) and 2 (right) by depth (K. Fenech).*

also known, one near Borġ in-Nadur and the other on the high ground to the west of Wied Żembaq (Evans 1971). On the southern side of the Wied Dalam, on sloping ground at Ta' Kaċċatura, a large Roman villa site with a peristyled courtyard was excavated at the turn of the last century. This contained equipment that was used for extracting olive oil (Anastasi & Vella 2018). A rock-cut burial found on higher ground would appear to be contemporary. Historic records from the mid-seventeenth century identify St George's Bay with marshland, used for retting flax and drained in AD 1736 (Abela 1647; Blouet 1964). Quarrying can be noted along the edges of both valleys where the alluvial plains have been transformed into fields divided by low-lying rubble walls. Some documentary evidence from AD 1750 shows that the valley bottom, right below the Roman villa and extending towards the sea, was planted with trees (National Library of Malta, Treas. B303, f. 128). The fields at Wied Żembaq were probably exploited in a similar manner in the historic period, and they were certainly being worked when the core was taken.

Two cores were taken from the Wied Żembaq (Fig. 2.7; Tables 2.4, A3.6 & A3.7). Core 1 has a basal *c*. 1.8 m of organic silty mud with occasional large limestone blocks, interspersed with layers of less organic silty loam at 4.5–4.8 m and 4.2–4.5 m. The upper part of the core is composed of *c*. 3.64 m of silt loam alluvial material with three layers of sub-angular silty gravel. There are AMS dates of 3630–3370 cal. BC (4707 BP; UBA-28262) at 4.58 m and 910–800 cal. BC (2707 BP; UBA-29042) at 2.15 m (Table 2.3). The core is interpreted as a progression from a basal dark grey to black clay accumulating in shallow standing water from 4.84–5.48 m to stony overbank alluvial sedimentation at 4.51–4.84 m, with occasional inputs of coarse sediment and hillwash from the steep side of the valley, to a shallow water marsh at 3.71–4.51 m, with renewed alluvial activity above.

The Wied Żembaq 2 core profile had significant breaks caused by the loss of material from the core. The basal unit (5.13–4.2 m) consists of an organic silty mud salt marsh deposit with occasional large limestone blocks. This passes up into silt loams with occasional stony layers, then further organic silty mud (4.2–3.85 m), then a shallow, saline lagoon deposit at 3.85–2.96 m. Traces of pedogenesis including blocky peds and strong reddening are visible at 5.28, 4.33, 3.65 and 3.0 m (Table A3.7). There are AMS dates of 3330–2920 cal. BC (4428 BP; UBA-28263) at 4.95 m and 1880–1630 cal. BC at 2.95 m (3428 BP; UBA-29043) (Tables 2.3 & 2.4). Above 2.96 m the core contains brown sandy clay colluvium to 1.15 m below ground surface.

2.3.2.6. The Mġarr ix-Xini core

This core was drilled in the narrow alluvial plain behind the pebbly beach at Mġarr ix-Xini on the southern coast of Gozo. The beach is located at the end of the meandering, deep-sided Wied Ħanżira gorge. Relict phreatic features and cave sediments on the gorge wall suggest that this feature originated as a collapsed cave. A photograph from the early 1930s shows cultivated fields in the area coming right up to the shore, with sufficient space for a watercourse running along the southern edge. A number of hydrological features, including a building housing a water pump built in the 1890s, an aqueduct and a series of dams can be found along the gorge – all attempts to control and harvest water run-off. Early last century, on the Ta' Ċenċ and Sannat uplands to the west, archaeologists discovered several prehistoric sites including the remains of a Neolithic temple at Borġ l-Mramma and at least two dolmens, one at Ix-Xagħra il-Kbira and another at Id-Dura tal-Mara, besides numerous cart-ruts (Evans 1971; Magro Conti & Saliba 2007). Neolithic temple remains were also recorded on the Xewkija side of the valley, where the present parish church stands (Evans 1971; Magri 2009 (1906)). The Mġarr ix-Xini cove was known to have provided a safe haven for small boats throughout history, and a tower was built by the Order of St John at the eastern tip in 1661 to watch over maritime traffic along this stretch of sea. Recent archaeological investigations within the gorge have attempted to understand the function of 17 rock-cut threading pans and vats that are found on the exposed rock surface of the tightly curved meanders and along the bottom of the escarpment. It is thought that some of the features may date to Late Punic or Roman times and would have served to make wine (Pace & Azzopardi 2008; Bonanno 2008) (see Chapter 7). Two hard limestone mills discovered at Tas-Salvatur and Tal-Ħamrija indicated that olive oil was also produced in the vicinity during Roman times (Anastasi & Vella 2018). The remains of a rural shrine from the same period have been found in a restructured cave site at Għar ix-Xiħ, overlooking the cove (Azzopardi 2014).

The basal *c*. 3.9 m of the 7.43 m deep Mġarr ix-Xini core is dominated by fining-upward sequences of poorly sorted gravels, coarse sand and sandy muds, with a silt horizon at 5.84–5.72 m and fine sandy silty clays between 6.17–5.82 m (Fig. 2.8; Tables 2.4 & A3.8). AMS dates range from 1490–1290 cal. BC (3124 BP; UBA-29989) at 7.17 m to cal. AD 690–880 (1230 BP; UBA-29980) at 1.76 m depth (Tables 2.3 & 2.4). The sequence above becomes marked by a calcitic sandy mud, which may be an incipient palaeosol at 3.55–3.3 m, then gravelly sands at 3.09 m overlain by a lens of massive pure clay to 3.06 m. Above was 2.98 m

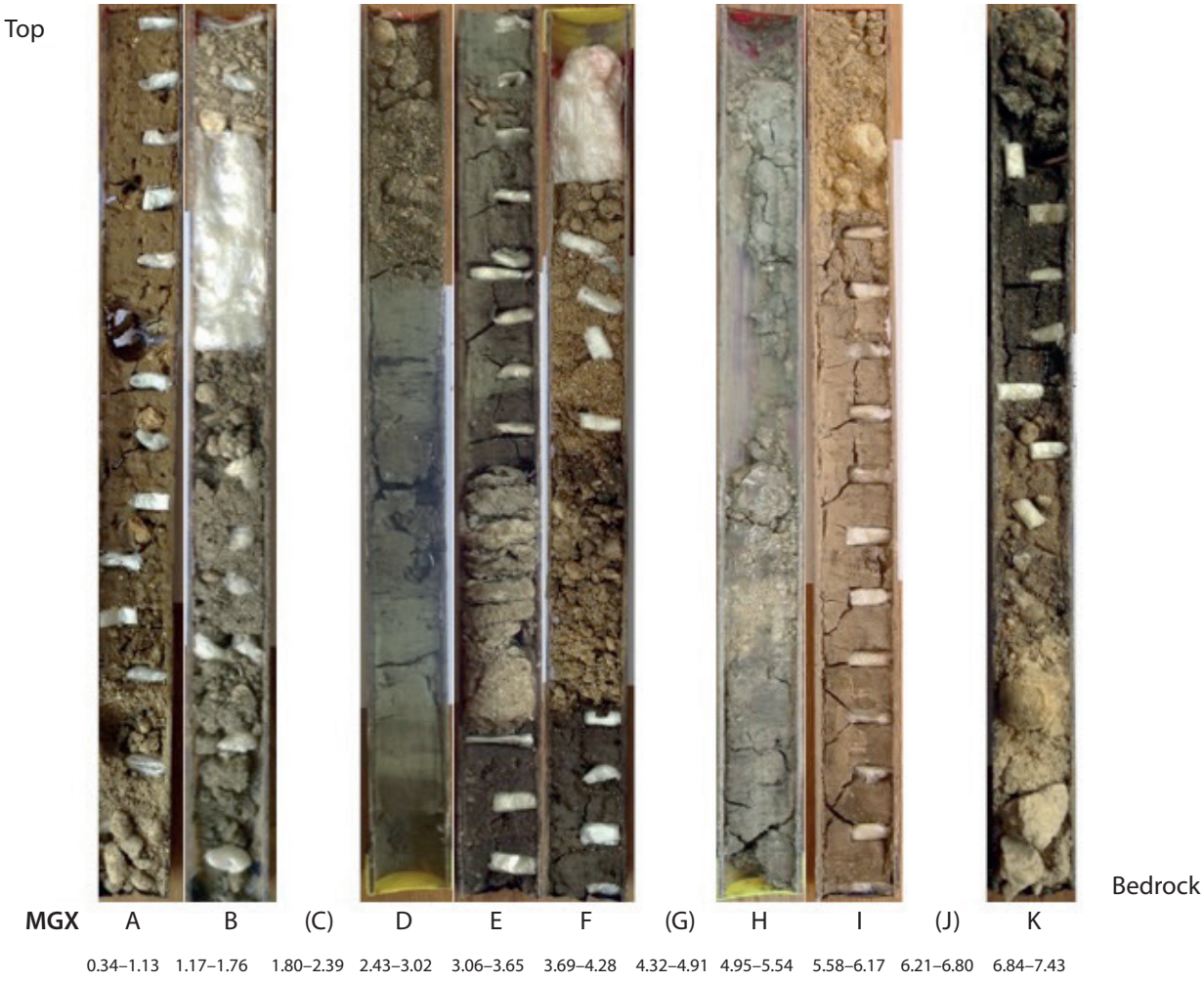

Figure 2.8. *The Mġarr ix-Xini core by depth (K. Fenech).*

of a finer unit of clayey silts interspersed with grey fine sandy silt and coarse clastic shelly sands indicative of a shallow marine environment. This shallow marine setting experienced occasional energetic storm run-off that introduced coarse sediment, which would have been carried across the sea bed to the core site by turbidity currents. Shifting of the river-mouth and the sub-marine thalweg of the turbidity currents will have controlled the coarseness of the sediments. As the coast prograded it is likely that the turbidity currents carried the coarse clastic sediments past the core site and further out to sea, so the site became dominated by shallow marine sedimentation. Coastal progradation was slow, only advancing across the core site within the last thousand years.

2.3.2.7. The Marsaxlokk 1 core

Two cores were attempted and one core was taken from an area adjacent to a salt marshland known as Il-Ballut ta' Marsaxlokk, a designated nature reserve, located on the edge of the fishing village. Fishponds, of unknown antiquity, existed here until they were dredged to make way for a quay in the 1950s. It is hypothesized that the small inner harbour, known as Il-Magħluq, could have existed in some shape or form in antiquity possibly providing shelter for the seacraft that would have used this area in connection with activities that took place at the site of Tas-Silġ, less than a kilometre away up the hill in the direction of Żejtun (Bonanno 2011). Tas-Silġ flourished in Late Neolithic times as a sanctuary that was adapted, transformed and extended in successive historic periods as an extra-urban maritime sanctuary in Punic and Roman times and subsequently as a church with a baptismal font (Cazzella & Recchia 2012; Bonanno & Vella 2015).

The base of core 1 has *c.* 1 m of reddish brown calcitic, stony, silty clay loam (3.46–2.92 m) with a well-developed small, sub-angular blocky structure,

and its groundmass is dominated by a slightly calcitic, silty clay with moderate to strong amorphous sesquioxide reddening (Fig. 2.9; Tables 2.4 & A3.9). This unit is probably a *terra rossa*-type palaeosol. Its upper surface is truncated and overlain by a layer of fine beach gravel and coarse sand deposits and then *c*. 2.86 m of calcitic fine sandy/silt loam. This deposit was receiving terrestrial clastic material in the form of coarse sand/fine gravel, with lenses at 1.92–1.86 m and 1.65–1.55 m, and an organic silt mud layer of likely paludal origin at 1.7–1.65 m. This layer is probably overbank alluvium, or more likely, given the location, hillwash. Two AMS radiocarbon dates more or less overlap in the first half of the first millennium AD (1567 BP; UBA-29353; and 1444 BP; UBA-29351) and a third date is 540–380 cal. BC (2354 BP; UBA-29352) (Table 2.3), suggesting that these deposits are mixed and have probably accumulated over a relatively recent and short time.

2.3.2.8. The Marsa 2 core

Marsa is the largest alluvial plain in Malta, characterized by high ground that rises to the north, south and west. Tributary valleys, especially Wied is-Sewda and Wied il-Kbir, drain into the area now occupied by the Marsa Sports Ground, a complex that was used for the recreation of British servicemen since the 1860s and more recently for a variety of sports including horse-racing, athletics and cricket. Two cores were taken near the eastern entrance to the complex before new building works commenced, which were part of a redevelopment of the site in 2002 (Fenech 2007;

Figure 2.9. *The Marsaxlokk cores 1 (left) and part of 2 (right) by depth (K. Fenech).*

Carroll *et al*. 2012). Despite the absence of Neolithic structures in the plain, human activity there could be ascertained through the presence of several pottery sherds found in the scattered sediments, the earliest dating back to the Ġgantija phase, *c*. 3450–3200 BC. Two inlets join the floodplain to the sea at the head of Grand Harbour. The first of these, Marsa iz-Zgħira (or *Marsetta*, present-day Menqa), lies to the north of the promontory called Jesuits Hill, where, in 1768, Roman warehouses were discovered with clear evidence for use well into Medieval times, together with the remains of a quay uncovered in 1993 (Bruno & Cutajar 2002). The second is Marsa il-Kbira (or *Marsa Grande*, present-day Marsa Creek) to the south of Jesuits Hill and northwards of a limestone knoll or islet (*Isolotto*, *il-Gzira*) where Albert Town developed in the late nineteenth century. Archaeological remains have been recorded in the immediate environs, including tombs and remains of warehouses (Gambin 2008; Bonanno 2011). The Marsa plain and immediate environs are known to have been an important source of revenue for state coffers in Late Medieval times (Bresc 1975). Sedimentation in the inlets led to attempts to drain the marshland, certainly by AD 1650, to create new agricultural land with drainage channels excavated to ensure that storm water ended up in the sea, of a sufficient depth to allow small boats to proceed to the plain in the direction of the Late Medieval chapel located at Ta' Ċeppuna (Blouet 1963, 85).

The Marsa 2 core was extracted at a level of 1.18 m above mean sea level and had a total depth of 9.40 m (Tables 2.4 & A3.10). The bedrock was at 9.25 m. Dense coarse strong-brown to reddish yellow sandy muddy gravel extended from 9.25 m to 6.40 m with a large boulder between 7.00–6.75 m. These sediments are interpreted as a delta-top or delta front facies. From 6.40 m, the sediments were no longer oxic but were dark grey and waterlogged. From 6.20 m, gravel and sand increased relative to fines, and between 5.90–5.20 m the sediments were too sandy to be recovered. It is likely that these are proximal pro-deltaic sediments. Datable organic remains were very scarce and the earliest radiocarbon date at 5.98 m was 980–840 cal. BC (2765 BP; UBA-30608), in the Phoenician era (Table 2.3). The sediments between 5.20–3.90 m were alternating silt/clay and sand layers and are dark grey. These are most probably distal pro-delta sediments. From 3.90 to 1.95 m the sediments are pale grey with the silt/clay content increasing, probably because the water body was bypassed by gravity currents at this time. A radiocarbon date at 2.70 m gave a Late Roman period date of cal. AD 430–650 (1487 BP; UBA-29443) (Table 2.3). An event shortly after that time resulted in the deposition of a boulder between 2.55–2.20 m in the core. From 1.95 m upwards, the sand content increases and the sediments are very light grey, most probably deposited in a shallowing water body. Another boulder between 1.70 m and 1.20 m was overlain by light brown silty sediments, which are most probably delta-top overbank deposits. Above 0.95 m, the area appears no longer to have been waterlogged as a result of further overbank deposition. While penetrating the groundwater table, sediments between 0.8 and 0.3 m could not be retained by the corer. The uppermost 0.3 m of the core was predominantly light brown silts of fluvial overbank and slopewash origin, in agreement with the present day terrestrial conditions at the coring site.

2.3.2.9. The Mellieħa Bay core

Marshland at Mellieħa Bay lies behind a bay-bar of what were low dunes at the back of the sandy beach, although the dunes are now mostly covered by the main road. The core was taken by the entrance to the Nature Reserve on the landward side of the present road. The marshland lies to the north of a low limestone ridge which bisects the plain. The marsh was used for the collection of salt in the early sixteenth century (Mercieca 2005). By AD 1658 the marshland had been drained and equipped with channels, and vegetation that could be burnt and used as fertilizer was collected (Blouet 1964). No archaeological remains have been recorded in the immediate vicinity, but Neolithic megalithic remains were recorded on the southern rocky shore of the bay at Għajn Żejtuna (Evans 1971) and an undated burial was discovered a few years ago in the grounds of the Mellieħa Bay Hotel. A photograph of the pottery contents of a Phoenician tomb from the end of the eighth century BC is labelled 'Mellieħa' and would suggest that Levantine seafarers operated in this area at this early date (Vella 2005). A wreck from the first–third centuries AD excavated around the rocks in the middle of the bay in 1967 would suggest that Mellieħa was frequented in Roman times (Frost 1969). The higher karst ground to the west has been known to be used for rough grazing since the seventeenth century and was certainly used for this purpose in the twentieth century. The slopes to the north, below the ridge of Il-Qammieġħ and L-Aħrax, were improved considerably in the course of the seventeenth and eighteenth centuries, certainly in the later nineteenth century, when the area, which is now equipped with terraces and a service road, was given over by the British administration on long-term agricultural leases (Blouet 1963; National Library of Malta, Treas. B303, f.145A).

The undated (date failure) 5.36 m deep core has a basal unit of grey, organic-rich silty sandy clay containing eel grass fibres and occasional shell (Tables 2.4 & A3.11). This is an offshore sediment deposited

Table 2.4. *Summary stratigraphic descriptions of the sequences in the deep core profiles.*

Core and depth (m)	Stratigraphic description	Age
Salina Deep Core:		
0–2.4	Rubble and masonry	
2.4–11	Marine shell gravel	
11–13	Sandy marine shoal	at 11.4 m: 2400–2050 cal. BC
13–21	Distal deltaic muds	at 14.74 m: 4330–4070 cal. BC
21–26.65	Delta-front and proximal pro-deltaic sandy muds, interbedded with quiet water laminated sediments	
26.65–27	Marine sediments, probably sub-littoral or upper delta-front muddy gravels	
27–28.5	Fluvial gravels with pedogenic features	
28.5–29.3	Fluvial gravels	at 29.1 m: 8280–7970 cal. BC
29.3–29.47	Palaeosol of silty clay with occasional rootlets and fine charcoal	
29.47+	Globigerina Limestone bedrock	
Salina 2:		
0-1.27	Alternating littoral sands and shallow estuarine sandy silty clays	
1.27-6.54	Alternating organic silty sandy clays and coarse to very coarse very shelly sands	
Salina 4:		
0–0.58	Missing	
0.58–2	Alternating brown and yellowish orange silty clays: overbank flood deposits	
2–4.1	Alternating grey/black silty clays with slightly shelly sand which hydro-collapsed during extraction	at 3 m: 1260–1050 cal. BC
4.1–11.02	Alternating pro-deltaic sandy muds, sands, silty clay and shelly gravel	at 10 m: 5630–5500 cal. BC
Xemxija 1:		
0–4.53	Greyish brown/grey clayey silts and silty clays: overbank flood deposits, with incipient palaeosol at 3.19–3.35 m	
4.53–5.67	Shallow freshwater lagoonal or paludal marsh deposits of shelly organic silty clays and fibrous peat	at 4.6 m: 2200–1980 cal. BC
5.67–6.03	Mud flow deposits of silty clay and clay aggregates	
6.03–6.38	Dark greyish yellow silty clay with weak soil development	
6.38–6.68	Mud flow deposits of silty clay and clay aggregates	
6.68–9.09	Alluvial deposits of alternating brown/grey silty clays, interrupted by two phases of weak pedogenesis at 6.7–6.85 and 8.15–8.32 m	at 6.7 m: 4330–4050 cal. BC
9.09–9.93	Palaeosol of dark brownish grey very fine sandy silty clay with fine limestone gravel down-profile	
9.93–10	Breccia of silty clay soil aggregates and fine limestone gravel	at 10 m: 8780–8460 cal. BC
Xemxija 2:		
1.17–1.36	Made ground and modern topsoil	
1.36–6.12	Orangey brown over grey alluvial silty clays	at 3.18 m: 1490–1280 cal. BC
6.12–7.17	Organic silty clays: marsh and alluvial deposits	
7.17–8.91	Alternating mixed deposits of greyish brown silty clay, clay aggregates with fine limestone, charcoal, shell and wood fragments	at 7. 18 m: 6400–6100 cal. BC
8.91–8.99	Dark olive brown clay distal mud-flow deposit	
8.99–9.33	Breccia of clay aggregates	at 9.33 m: 7520–7200 cal. BC
Wied Żembaq 1:		
1.16–3.49	Alluvial sandy clays and clays	at 2.15 m: 913–806 cal. BC
3.49–3.64	Yellowish brown silty clay with limestone fragments: probable mud-flow deposit	

Table 2.4 *(cont.).*

Core and depth (m)	Stratigraphic description	Age
3.64–3.71	Brown fine sandy clay with possible incipient soil formation	
3.71–4.51	Dark grey humic clay laid down in marsh/shallow standing water	
4.51–4.84	Stony alluvial clay	at 4.58 m: 3630–3370 cal. BC
4.84–5.23	Dark grey to black clay laid down in shallow standing water	
5.23	Stone	
Wied Żembaq 2:		
1.15–1.35	Alluvial brownish red clay	
1.35–5.07	Alluvial brown to dark grey fine sandy clay occasionally with fine limestone fragments	at 2.95 m: 1880–1630 cal. BC at 4.95 m: 3330–2920 cal. BC
5.07–5.13	Dark bluish grey sandy clay to clay	
Mġarr ix-Xini:		
0.54–2.43	Grey sandy silts and shelly sands: shallow marine sediments	at 1.76 m: AD 690–880
2.43–3.06	Grey clayey silts	
3.06–3.65	Laminated grey clay and sandy muds	
3.78–4.95	Alternating laminae of fine to coarse gravel with silt and silt/sandy muds	
4.95–5.72	Yellow/grey gravelly sandy muds	
5.72–6.21	Brownish black sandy silts	
6.45–6.8	Yellow sandy muds and gravels	
6.8–6.93	Muddy breccia	
6.93–7.12	Grey clay	
7.12–7.21	Coarse and fine sands	at 7.17 m: 1490–1290 cal. BC
7.21–7.43	Massive coarse and fine gravel	
Marsaxlokk 1:		
0.12–0.5	Calcitic fine sandy/silt loam topsoil	
0.5–2.92	Alluvial sandy/silts to silty clay loams interrupted by three lenses of fine gravel and coarse sand	at 0.86 m: cal. AD 420–560 at 1.86 m: 540–380 cal. BC at 2.86 m: cal. AD 440–670
2.92–3.86	Reddish brown calcitic silty clay loam: *in situ terra rossa* soil	
Marsa 2:		
0–1.2	Pale brown silt, probably eroded soil material as the topsoil	
1.2–1.7	Large boulder	
1.95–3.9	Pale grey sandy/silty clay	at 2.7 m: cal. AD 430–650
3.9–5.2	Laminated dark grey silty clay and sands	
5.2–6.4	Sands and gravels	at 5.98 m: 980–840 cal. BC
6.75–7.0	Boulder	
7.0–9.05	Yellowish brown coarse gravels with sand and silt interbeds	
9.05+	Limestone bedrock	
Mellieħa Bay:		
0.44–1.19	Mixed sand, clay and organic mud	(no dating for this core)
1.19–2.0	Fine-medium sands with hints of bedding	
2.0–5.14	Glauconitic coarse to medium sands, slowly fining upwards	
5.14–5.36	Humic sandy/silty clay with eel grass fragments	

below the wave-base. At 5.15 m this passes into glauconitic medium to coarse sands which generally fine upwards. These accumulated within the wave-base. The sands become slightly finer and exhibit hints of bedding 1.6–1.48 m below ground surface. These sediments are shallow marine lagoonal sediments, most probably deposited in *Posidonia* meadows. The upper 1.48 m exhibits alternating thin horizons of silty

clay, coarse-medium sand and black organic mud. These sediments relate to beach, dune, dune slack and marshland environments.

2.3.3. Magnetic susceptibility and XRF analyses of the cores

Charles French & Rory Flood

A selection of sediment cores was subject to digital core scanning for resistivity and magnetic susceptibility analyses as well as XRF (X-ray fluorescence spectrometry) multi-element analyses. These were undertaken at the Physical Geography Laboratory at University College Dublin and the Geography Department, NUI Maynooth, using an ITRAX XRF core scanner and a GEOTEK Multi-Sensor core logger. Example resistivity and magnetic susceptibility graphs for Xemxija cores 1 and 2 (Figs. 2.10 & 2.11) and multi-element graphs of results for the Xemxija 1 core as well as the Marsaxlokk and Wied Żembaq 1 cores are presented here (Figs. 2.4 & 2.12–2.14).

In both Xemxija cores, there is a remarkable high to low transition in magnetic susceptibility (MS) values that occurs at the level at which the palaeosol begins to become buried by alluvial deposits at a depth of *c*. 8/9 m below ground surface at some time before *c.* 4330–4050 cal. BC (Tables 2.3 & 2.4; Figs. 2.10 & 2.11). This remarkable step-change in high to much lower values may well reflect the change from a relatively stable, albeit probably slowly aggrading (with hillwash) buried soil of the earlier Holocene to a lengthy, later erosive phase above (see Chapter 5). Moreover, the relative troughs and peaks of MS values within the palaeosol itself, could well indicate several (at least four) phases of stable ground surfaces interspersed with phases of colluvial addition to this buried soil profile. For the remainder of the magnetic susceptibility curve upwards, especially in the Xemxija 1 core, the values remain lowish and constant, corroborating the absence of standstill phases in this valley fill sequence, except perhaps at *c*. 4.6 m or 2200–1980 cal. BC where paludal marsh deposits are overlain by renewed alluvial accumulation.

Most element values remain relatively constant throughout the whole depth of the cores (Figs. 2.12 & 2.13). There are, however, a number of exceptions to these trends in some elements. For example in Xemxija core 1, calcium (Ca) begins to increase and fluctuates in values from a depth of *c*. 6.5 m, and especially upwards from *c*. 4.6 m. This coincides with the continuing deposition of alluvial deposits (Table 2.4), and suggests greater disturbance, soil surface exposure and evapo-transpiration leading to the formation of secondary calcium carbonate in the soil/sediment complex as the seasonally alluviated profile dries out repeatedly (Durand *et al*. 2010). Phosphorus (P) is consistently moderately enhanced until the upper *c*. 4 m of the profile. This could reflect a reasonably steady input of plant material into the palaeosol and eroded/redeposited soil material (or alluvium) in the lower part of this core (Cook & Heizer 1965, 12ff; Holliday & Gartner 2007; Karkanas & Goldberg 2010; Linderholm & Lundberg 1994; Middleton & Price 1996; Wilson *et al*. 2005, 2009), a feature which distinctly lessens in the upper *c*. 4 m of the profile.

Potassium (K) in Xemxija core 1 shows distinctive decreases in values between 7.5 and 8 m, and at *c*. 6.5, 5.3–5, 3.9, 3.1, 2.5 and 1.5–1 m below ground surface. These phases more or less equate with phases of sediment influx associated with overbank flood deposits (Table 2.4), and could suggest variable inputs of plant nutrients (Fageria & Baligar 2005). Iron (Fe) is relatively more variable between *c*. 8.8 and 7 m, and is possibly indicative of the opening-up and disruption of the palaeosol. Sulphur (S) exhibits a larger range of more consistent peaks at *c*. 6.5–5 m, which could relate to slight changes in pH (or reduced alkalinity) related to organic inputs (Boreham *et al.* 2011). Arsenic (As), selenium (Se) and bromide (Br) all exhibit a distinctive peak at *c*. 5.25–5 m. Many elements decline or remain low but steady towards the top of the core, but strontium (Sr) becomes much more pronounced between *c*. 2.25–1.5 m, as do tin (Sn) and antimony (Sb) to a lesser extent. These increases may reflect modern soil pollutants (Declercq *et al*. 2019; Wilson *et al.* 2005, 2009).

In the Wied Żembaq 1 core (Fig. 2.13; Table 2.4), aluminium (Al), silica (Si), magnesium (Mg) and phosphours (P) remain constant throughout. These elements, along with iron (Fe) and potassium (K) which exhibit considerable variation, suggest a set of macro- and micro-nutrients inputs, plant matter and ash, reasonably advantageous to agriculture, into the valley system, possibly through phases of soil erosion from the wider valley catchment (Fageria & Baligar 2005). Calcium (Ca) increases between *c*. 5–4 m and markedly above *c*. 3 m, which again possibly suggests increasing evapo-transpiration and aridity (Durand *et al.* 2010). Strontium (Sr), tin (Sn) and antimony (Sb) increase sharply above 1.5 m, as at Xemxija 1, possibly relating to more recent pollution in the valley system (Declercq *et al*. 2019; Wilson *et al.* 2005, 2009).

In the Marsaxlokk 1 core, there is a much greater range of data and irregularities exhibited (Fig. 2.14; Table 2.4). There appears to be a major step-change just above *c*. 3 m in the plots for iron (Fe), potassium (K), managanese (Mn), rubidium (Rb), titanium (Ti), zirconium (Zr) and yttrium (Y). This could suggest a shift towards drier conditions, less input of eroded soil materials and less groundwater in the valley sediments.

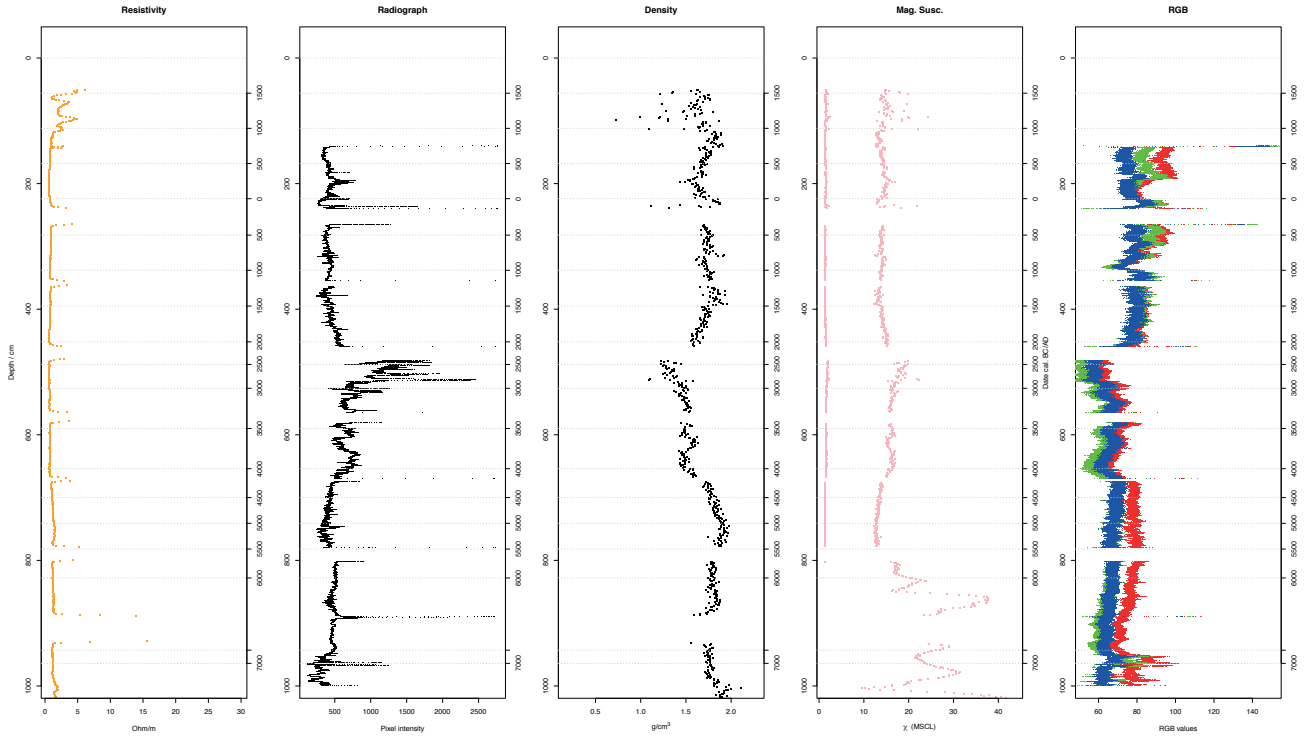

Figure 2.10. *The resistivity and magnetic susceptibility graphs for Xemxija 1 core (R. Flood).*

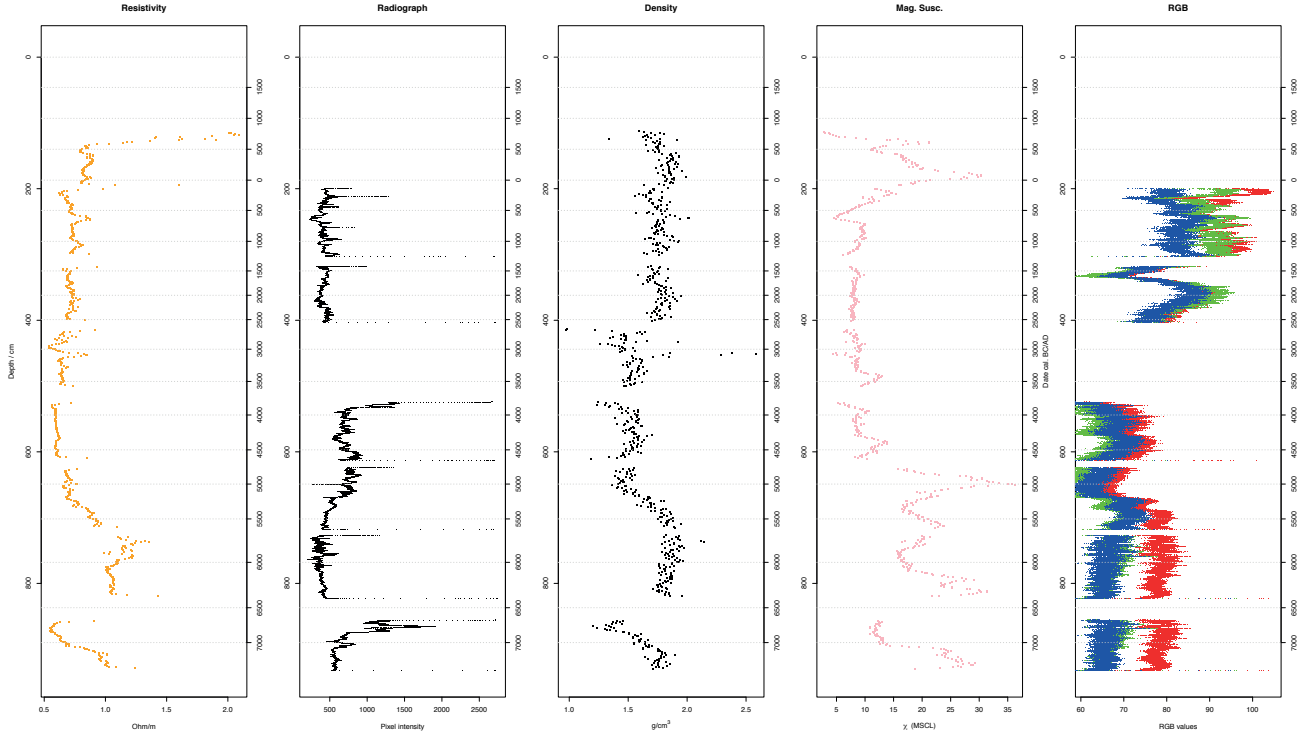

Figure 2.11. *The resistivity and magnetic susceptibility graphs for Xemxija 2 core (R. Flood).*

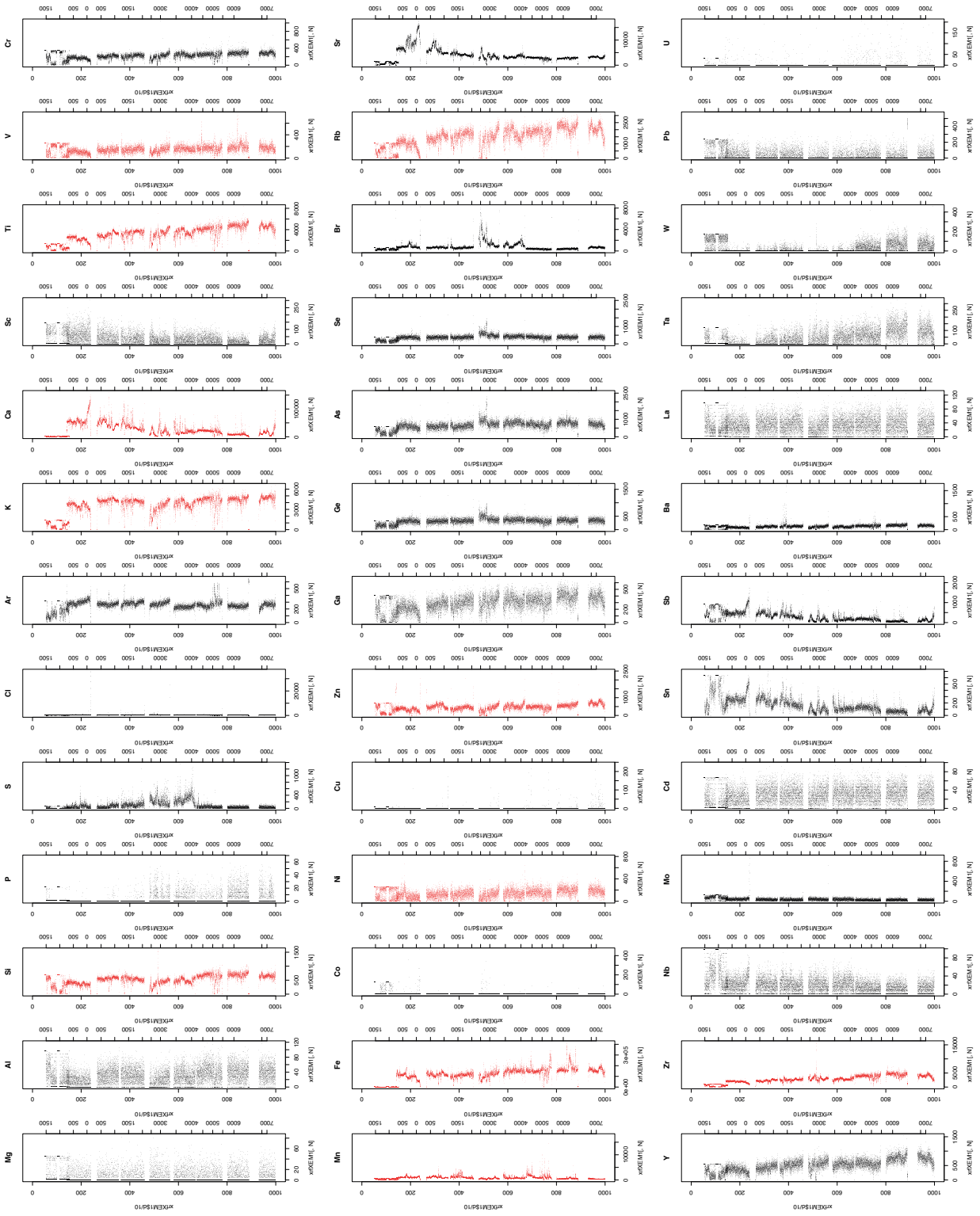

Figure 2.12. *The multi-element data plots for Xemxija 1 core (data from R. Flood, Steve McCarron & Jonathan Turner).*

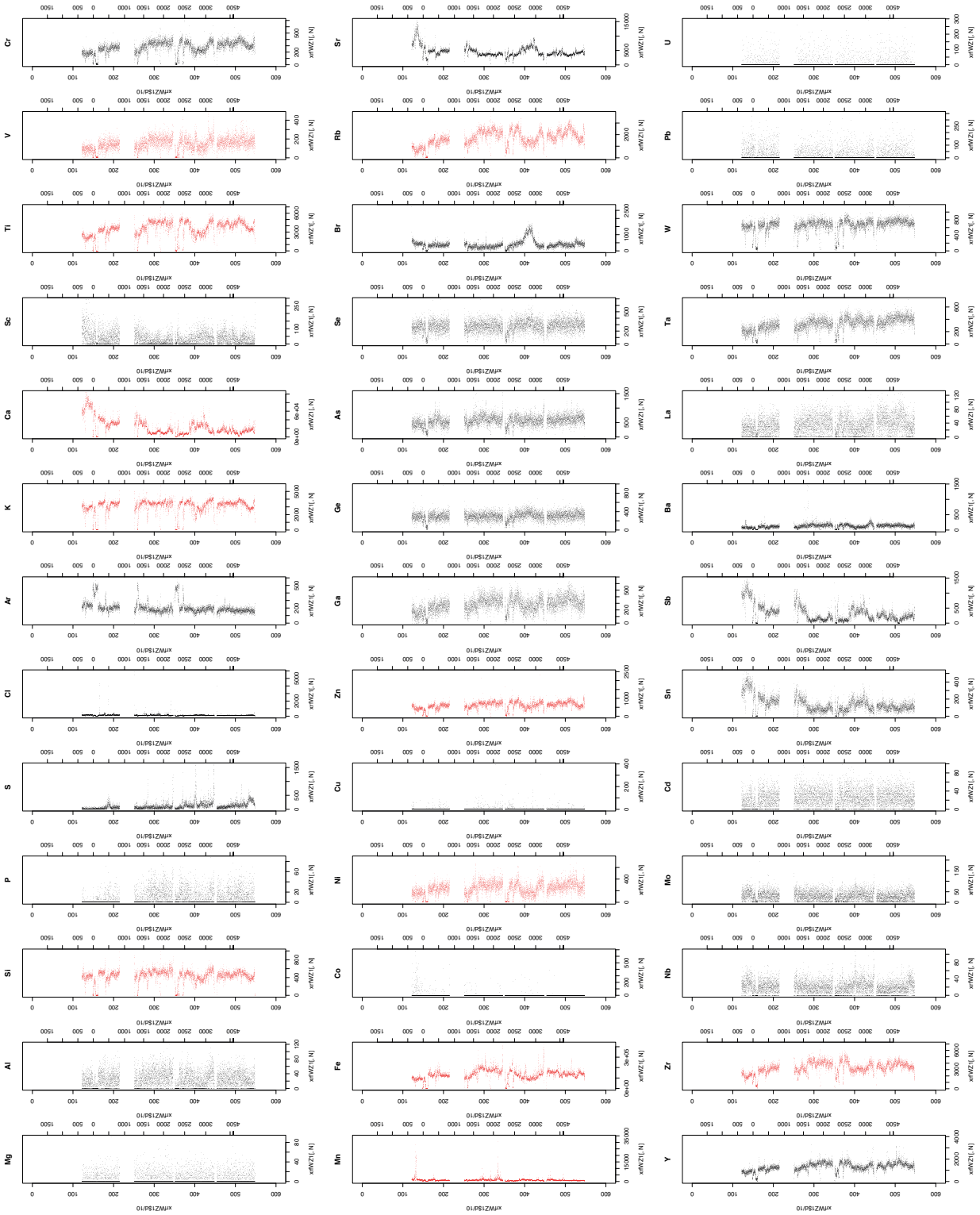

Figure 2.13. *The multi-element data plots for Wed Żembaq 1 core (data from R. Flood, Steve McCarron & Jonathan Turner).*

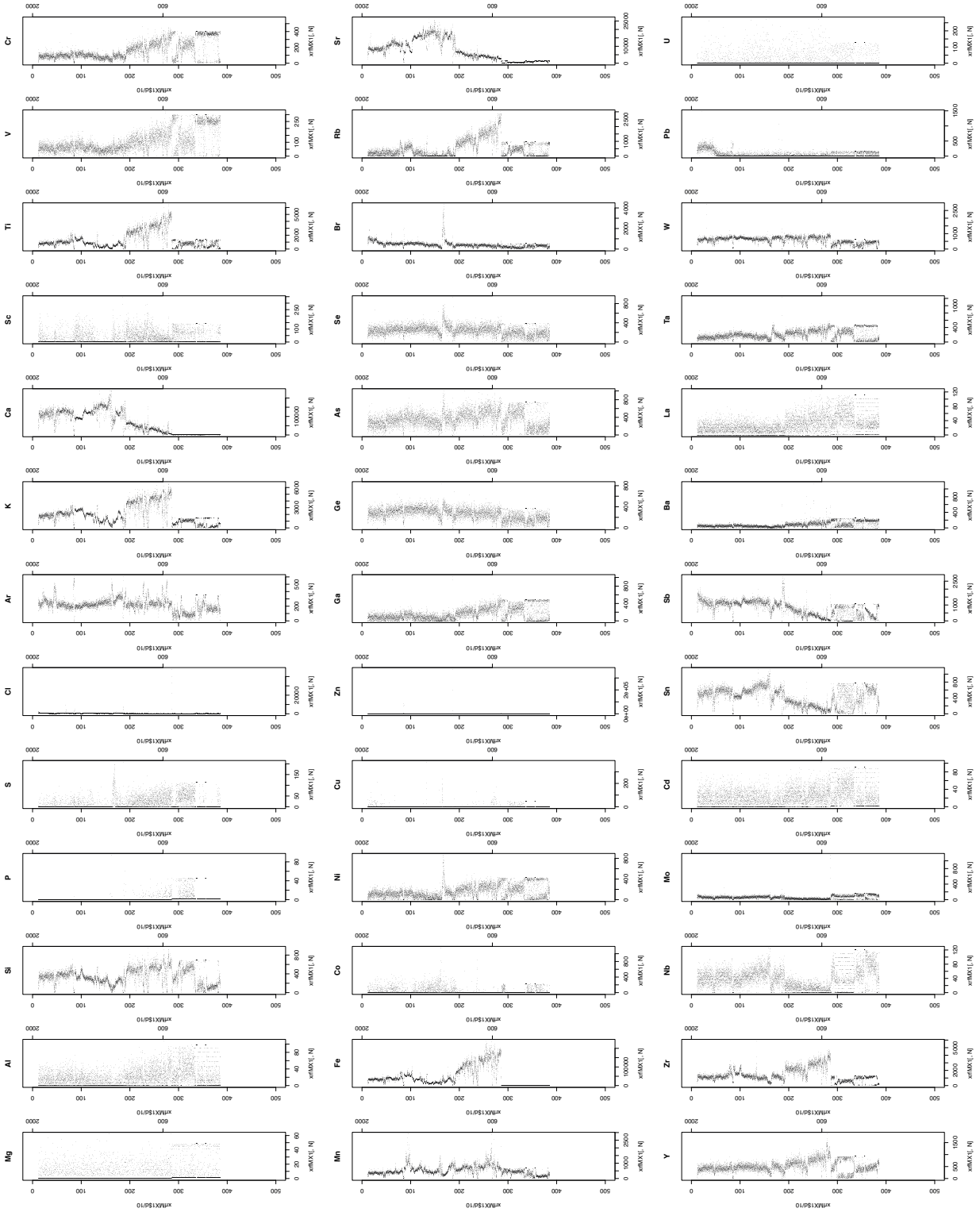

Figure 2.14. *The multi-element data plots for Marsaxlokk 1 core (data from R. Flood, Steve McCarron & Jonathan Turner).*

2.4. Age-depth models

Maarten Blauuw & Rowan McLaughlin

The chronology of each core was established using the data presented in Table 2.3, and then an age-depth model constructed as a statistical description of the relationship between time and the depth of burial of the sediment, and hence the age of the material enveloped within it (Table 2.5). Such models are calculated by first obtaining dates (usually but not necessarily radiocarbon dates) from multiple depths in the sediment profile, then extrapolating between these depths so that the age of any depth in the profile can be inferred. All but the simplest age-depth models are calculated using computers and numerous methods have been developed, including linear interpolation between the dated levels, or fitting a parametric model – a mathematical description of a changing sedimentation rate – to the data points (e.g. Blaauw 2010). More sophisticated approaches deploy various Bayesian methodologies that aim to build realistic chronologies and appropriately sized confidence intervals. This can be done through constraining the data with prior information about the gaps between the dated levels (Bronk Ramsey 2008a) or by modelling the sediment accumulation process itself (Blaauw & Christen 2011). In these cases, the shape of the age-depth curve is deduced through the analysis of millions of 'random walks' or random samples of the data, and is quite computationally intensive, even for the relatively fast computers available at the time of writing.

The age-depth models provide a 'best guess' point estimate for the age of any depth in sediment cores, and an associated confidence interval. For detailed study of certain palaeoecological events, the posterior probability distribution of the age for any given depth can also be extracted and analysed further. The *FRAGSUS Project* used *Bchron* (Parnell *et al*. 2008) and (primarily) *Bacon* (Blaauw & Christen 2011) to derive the age-depth models, using the data given in this chapter. Plots of the summed radiocarbon ages for the main sediment cores (Mġarr ix-Xini, Xemxija, Salina and Wied Żembaq) are given in Figure 2.2.

2.4.1. Accumulation rates

One advantage of the approach to sediment chronology advocated by Blaauw and Christen (2011) is that the sediment accumulation rate is modelled explicitly, and therefore robust estimates of it can be obtained, together with its uncertainty, and plotted as a function of time. This was done for each sediment core so that any synchronous changes in accumulation rate could be identified. Here, however, the confidence intervals of these estimates were quite large, although some useful general observations can be made. In the majority of the cores, the accumulation rate did not appear to change significantly from the confidence intervals of the modelled accumulation rates.

The mean sediment accumulation rate is a function of many factors including the underlying geology, topography, hypsometry, connectivity of drainage channels, catchment size, vegetation cover, soil properties and, in coastal locations, sea level (Table 2.5). None of these factors can be correlated with the mean accumulation rate and all change with time, so steady accumulation rates cannot be seen as evidence for stasis, but rather that the sedimentation within each catchment is driven by a set of variables whose evolving relationship leads to a relative stability when taking a long-term view. An exception to this is the Salina catchment, which according to the Salina Deep Core, experienced a slower accumulation of sediment at the coring site from around 4000 cal. BC, probably largely as a result of rising sea levels (see §3.6). The timing of this is interesting, as it roughly coincides with the start of the 'Temple Period' in Malta, and the intense phase of cultural activity that led to the construction and use of megalithic sites. Frustratingly this moment in time is represented by sediments near the top of the portion of the Salina Deep Core that was suitable for analysis, and at the bottom of the 10 m cores (Salina 3 & 4) retrieved from further inland.

Table 2.5. *Mean sediment accumulation rates per area versus time for the deep cores.*

Core	Period	Mean acc. rate (yr/cm)	Area (sq. km)	Hypometric index
Marsa 2	2000 BC–present	4.6	47.9	.41
Marsaxlokk	AD 100–present	9.5	0.6	.43
Mġarr ix-Xini	500 BC–present	3.6	4.5	.63
Salina 3 and 4	5000 BC–present	7	39.6	.45
Salina Deep Core	7500–4000 BC	2.5	39.6	.45
Salina Deep Core	4000 BC–present	4.3	39.6	.45
Wied Żembaq 1 and 2	3500 BC–present	11.1	11.0	.55
Xemxija 1 and 2	8000 BC–present	10.9	7.2	.41

Therefore, it has not been possible to refine the dating of this transition, as suitable samples for dating and modelling do not exist.

It must be stressed that the pictures provided by short-term and long-term sediment accumulations are radically different. In the cores, there is evidence for discontinuities and short phases of rapid sedimentation, as discussed below.

2.5. A local marine reservoir offset for Malta

Paula J. Reimer

Radiocarbon ages of organisms that lived in the ocean have an older apparent age than contemporaneous terrestrial organisms because of the long residence time of carbon in the ocean (Mangerud & Gulliksen 1975). This apparent age, or reservoir age R, is around 400 years on average throughout most of the Holocene, but age also depends on regional and local conditions such as upwelling of older carbon or input of freshwater from rivers. In order to convert radiocarbon ages to calendar year equivalents and to correct for this difference for marine organisms or humans and animals who consumed these, we need to estimate the local or regional offset, ΔR, from the global marine calibration curve (Stuiver *et al*. 1998). ΔR is usually evaluated by measuring known age corals or mollusc shells which grew prior to the increase in radiocarbon (^{14}C) in the atmosphere because of nuclear weapons testing ('bomb' carbon) or accessing 'pre-bomb' values from the Marine Radiocarbon Reservoir Correction Database (Reimer & Reimer 2001; www.calib.org). There are currently no published measurements from 'pre-bomb' mollusc shells near Malta, since the closest results came from the north of Sicily. It was therefore necessary to determine ΔR from marine mollusc shells collected near Malta in order to be able to properly calibrate radiocarbon ages from marine samples for the *FRAGSUS Project*.

Two specimens of the filter-feeding cockle *Acanthocardia paucicostata* (both valves present) were obtained from the National Museum of Natural History, Malta, in order to evaluate ΔR for the region. These were originally collected live in the period 1914–19 (no exact date) by a well-known local naturalist, Giuseppe Despott, whose collection is held in the Museum. Both specimens come from the same locality, which is the area of the harbours in Valletta, very likely the Grand Harbour.

The shells were pre-treated with 1 per cent HCl to remove approximately 25 per cent of the mass, hydrolysed to CO_2 using phosphoric acid (H_3PO_4) and converted to graphite using the hydrogen reduction method (Vogel *et al.* 1984). The $^{14}C/^{12}C$ ratio of the graphite was measured using accelerator mass spectrometry (AMS). The $^{14}C/^{12}C$ ratio was background corrected, normalized to the HOXII standard (SRM 4990C; National Institute of Standards and Technology) and corrected for isotopic fractionation using the AMS-measured $\delta^{13}C$ which accounts for both natural and machine fractionation. The ^{14}C age and one standard deviation were calculated using the Libby half-life (5568 years) following the conventions of Stuiver and Polach (1977). The ΔR values were calculated from the difference in the measured radiocarbon age of the shells and the radiocarbon age of the marine calibration curve, Marine13 (Reimer *et al*. 2013) using the programme *deltar* (Reimer & Reimer 2017) (Table 2.6).

Table 2.6. *Radiocarbon measurements and ΔR values from early twentieth century ('pre-bomb') marine shells from Malta.*

Lab number	Museum ID	^{14}C date yrs BP	ΔR ^{14}C yrs
UBA-31424	MNH/CON 01326	406±24	-42±24
UBA-31425	MNH/CON 01326	593±24	144±24

There is a statistically significant difference in the radiocarbon ages and ΔR values for these two samples so the values cannot be averaged. Therefore we calculate a weighted mean ΔR and used the square root of the variance to determine the uncertainty which yields a ΔR for Malta of 51±93 ^{14}C years.

A single measurement from Sicily of *Cerastoderma corrugatum* collected in 1900 (Siani *et al*. 2000) provides a comparison value of 71±50 ^{14}C years when calculated with the Marine13 calibration curve (Reimer *et al*. 2013). This value is in agreement with the mean ΔR for the two Malta shells.

The difference in the ΔR values for the two Maltese samples is possibly a consequence of proximity to freshwater input into the harbour. Freshwater from regions of ancient limestone such as Malta can increase ΔR because the dissolved carbonate contains no radiocarbon. Without further analyses on a number of additional samples, any marine radiocarbon samples from Malta will therefore have rather large calibrated age ranges. To improve the ΔR value for Malta, more known age, 'pre-bomb' samples, preferably from locations without freshwater input, would need to be analysed.

2.6. Major soil erosion phases

Rory P. Flood, Rowan McLaughlin & Michelle Farrell

2.6.1. Introduction

Although erosion is an important part of the sedimentation process that leads to the accumulation of deposits suitable for palaeoenvironmental study, severe erosion is problematic in that parts of the sequence can be removed entirely, creating an 'hiatus',

and the upstream mixing of bulk materials may lead to much recycling of older carbon. As a result of these processes, the radiocarbon samples from Maltese sequences were, on occasion, unintentionally procured from materials much older than the sediments in which they were buried. The timing of these episodes of erosion is nonetheless important, and indeed pertinent to the *FRAGSUS Project*'s attempts to understand better the role that environmental changes had in shaping social progress and vice-versa. Two methods were used to estimate the timing of erosion events; statistical analysis of errant 'old' dates from the sediment cores, and new OSL dates obtained from valley fills (see §2.1.1.3). As discussed below and in Chapter 5, soil erosion is an important factor in the evolution of Mediterranean landscapes generally, and in Malta and Gozo especially. Many direct indicators of erosion are present in the cores, such as the sedimentology (see §2.3.2) or the presence of certain biota, especially root fungal symbionts and burrowing snails which were transported from areas of eroding soils into aquatic deposition sites (see Chapter 4).

Soil erosion leading to the thinning of soil on hillslopes and thickening in valley bottoms, and associated changes in soil properties, is generally considered to be the primary vector in Mediterranean landscape evolution during the Holocene (Judson 1963; Vita-Finzi 1969; Hughes & Thirgood, 1982; Bintliff 1992; Butzer 2005; Dusar *et al*. 2011). Mediterranean environments have high rainfall intensities, alternating between wet and dry periods but with low average annual precipitation, and inherently fragile, slowly developing soils, low in nutrients and organic matter (García-Ruiz & Lana-Renault 2011; García-Ruiz *et al*. 2013). Coupled with a predominance of steep slopes and a long history of deforestation, natural fires, and cultivation in extreme topographic situations, these factors have led to extensive soil loss (Wainwright & Thornes 2004; García-Ruiz *et al*. 2013; Dotterweich *et al*. 2013). Geomorphological, pedological, palaeoecological, and geoarchaeological studies have detected significant soil erosion events dating from the Bronze Age and later throughout Mediterranean Europe (Dotterweich 2008), for example in Greece (Van Andel *et al.* 1998; Lespez 2003; Fuchs *et al.* 2004; Bintliff 2005), Cyprus (Fall *et al.* 2012), Turkey (Brückner *et al*. 2005), Italy (Marchetti 2002; Eppes *et al.* 2008; Piccarreta *et al*. 2011, 2012; Pelle *et al*. 2013), southwestern France (Bertran 2004) and Spain (Cerdá 2008; García-Ruiz 2010).

The Maltese Islands contain rich archaeological evidence for the presence of successive human societies, who were present by at least *c*. 5400 cal. BC, with a Neolithic fluorescence occurring around 3400–3000 cal. BC involving the construction of megalithic 'temples' and elaborate funerary hypogea (Evans 1971; Malone *et al*. 2009a; Pace 2000; Zammit 1928a; 1930). Based on palynological data from Burmarrad in northwest Malta (Djamali *et al*. 2013), Salina Bay in northwest Malta, Marsa in southeast Malta and Santa Marija Bay on the island of Comino (Carroll *et al.* 2012), and the archaeological site of Tas-Silġ (Hunt 2015), it appears that the Neolithic and later land-cover of the Maltese Islands largely comprised agriculturally degraded steppe and garrigue communities (see Chapter 3). Little, however, has until recently (see Malone *et al.* in press and this volume) been known about the intensity and extent of prehistoric subsistence agriculture in Malta, beyond the presence of typical 'Neolithic package' cultivars such as wheat, barley and legumes, and domestic livestock (Trump 1966; Renfrew 1972). In particular, it is not clear whether the prehistoric inhabitants of Malta took steps to mitigate the effects of soil erosion. This study investigates this problem in combination with the molluscan and palaeosol data presented in the following Chapters 3–5.

2.6.2. Methods

A combination of methods including AMS dating and sedimentology of the deep cores, hypsometry, and the application of the revised universal soil loss equation (RUSLE) were used in this soil erosion study. Eight sedimentary cores were recovered from four locations on Malta (Marsa, Xemxija, Salina and Wied Żembaq) and one from Gozo (Mġarr ix-Xini) (see §2.3.2) (Fig. 2.4). The Marsa sequence was previously studied by Carroll *et al.* (2012) and Fenech (2007) and all other sequences were investigated as part of this project. Radiocarbon dating of material from the sediment cores and the buried soils associated with the Santa Verna, Ġgantija and Skorba temple sites was performed at the ^{14}CHRONO centre, Queen's University Belfast, using accelerator mass spectrometry (AMS) (Tables 2.3 & 2.7). Previously published radiocarbon dates were also utilized (Carroll *et al*. 2012; Djamali *et al*. 2013; Marriner *et al*. 2012). The dates were calibrated using the IntCal13 and Marine13 calibration curves as appropriate (Reimer *et al*. 2013) and the resulting probability distributions were summed (Williams 2012) for dates that appeared out-of-sequence relative to their order in the core. In this way, the radiocarbon record can be interpreted as a potential indicator of carbon burial rate and erosion intensity (Long *et al.* 2016, 588).

Hypsometry is a measure of the relative proportions of land at different elevations (Strahler 1952). The hypsometric curve represents the relative proportion of land below (or above) a given height and together with the hypsometric index (HI), or elevation/relief ratio, can be used as an indicator of the geomorphic

form of a given catchment and its stage of evolution (Strahler 1952; Lifton & Chase 1992; Chen *et al*. 2003; Willgoose & Hancock 1998). Differences in the shape of the hypsometric curve and hypsometric index (HI) for landforms are considered to be related to the degree of disequilibrium in the balance of erosive and tectonic forces (Strahler 1952; Luo 1998; Weissel *et al*. 1994). Hence HI is often employed to explain erosion and/or sediment dynamics as catchments which are more recently incised possess high HI values, whereas catchments that have evolved into a lower dynamic equilibrium have lower HI values and in turn, smaller sediment yields (Wyatt 1993; Willgoose & Hancock 1998; Haregeweyn *et al*. 2008). The Maltese Islands were delineated in ArcGIS 10.1 from a 1 m resolution digital terrain model derived from airborne LiDAR last return data, with the outline of drainage basins established using standard tools in ArcGIS. Hypsometric and HI analysis for each catchment within which a sediment core was collected was carried out using CalHypso (Pérez-Peña *et al*. 2009).

The revised universal soil loss equation (RUSLE) is a soil erosion model that estimates average long-term soil loss through sheet and rill erosion (Wischmeier & Smith 1978; Renard *et al.* 1997) (Fig. 2.15). It is the product of five factors: R, a measure of rainfall; C, a measure of ground cover; K, a measure of the intrinsic erodibility of the soil; LS, computed from slope length and steepness; and P, derived from management practice (Renard *et al.* 1997; Renschler & Harbor 2002). Although a RUSLE model for Europe has become available recently (Panagos *et al.* 2015c) its 100 m resolution lacks the necessary detail for studying the nature of relatively small Maltese catchments. A separate RUSLE model for Malta has recently been published (Sultana 2015), but in the present study it was considered that the potential for soil erosion in the islands is likely to be highly seasonally variable because of seasonal differences in rainfall (R factor) and ground cover (C factor) (Fig. 2.16) (and see Chapter 8). Therefore, new seasonal models were derived as a product of what follows.

The seasonality in rainfall is a key point when considering its erosive potential. In Malta rain in the summer months is rare, but heavy rainfall can occur during autumn, winter and spring (Mitchell & Dewdney 1961). High resolution rainfall data are not currently available for Malta, so to take account of seasonal variations in rainfall in the RUSLE model, the R-factor estimate of 1672.4 MJ mm/ha/h/yr of Panagos *et al.* (2015a) was used and converted to monthly values using the proportional contribution of monthly rainfall to an annual total of 603 mm (data obtained from www.maltaweather.com, accessed March 2016) (Fig. 2.16).

C-factors were calculated using the Normalized Difference Vegetation Index (NDVI) as an indication of relative biomass (Fig. 2.16). This is calculated from the amounts of visible and near-infrared light reflected by vegetation, and is therefore derivable from multi-spectral remotely sensed images (Tucker 1979). NDVI of 0 is indicative of non-vegetated land, 0–0.3 indicates moderate vegetation cover, and 0.3–1 indicates dense vegetation cover (Carlson & Ripley 1997). Multi-spectral LANDSAT 8 images of Malta were obtained from the United States Geological Service Earth Explorer (earthexplorer.usgs.gov, accessed November 2015), corrected for sun elevation and sensor response to top-of-atmosphere reflectance (Shepherd & Dymond 2003) and masked to exclude urban areas, since these are much more extensive now than in the past. These images were used to calculate rasterized NDVI surfaces for six dates during the years 2014 and 2015. The choice of date was based on the availability of cloud-free imagery for Malta in the LANDSAT 8 archives. Palynological data (see Chapter 3) indicate that the present seasonal and spatial patterns of the Maltese vegetation can be considered as a reasonably close approximation of past land-cover.

To derive the C factor used in this study, the NDVI surface was scaled by the equation given by (Van Der Knijff *et al*. 2000)

$$C = e^{-2\frac{N}{1-N}}$$

where N is the NDVI raster.

Using ArcGIS 10.1, K-factor rasters were derived from the results of MALSIS, the Maltese Soil Information System Project (Vella 2001; Sultana 2015) using Kriging. The LS factor raster was provided by the European Soil Data Centre (Panagos *et al*. 2015b). For the purposes of this analysis, the P-factor was held at 1.0, as the nature and spatial extent of this variable in the past is currently under investigation.

2.6.3. Results

2.6.3.1. Early Neolithic agriculture

The palaeosol investigated beneath the floors of Santa Verna temple is indicative of a stable, well drained and organized, clay-enriched (or Bt) horizon (see Chapter 5). The total organic fraction of this buried soil was measured via loss-on-ignition as 7.1 per cent. The charred plant remains it contained were dominated by domesticated barley, *Hordeum* spp. (n=8), but also included domesticates *Triticum aestivum/durum* (n=2, free threshing wheat), 33 other fragments of domesticated cereals, *Lens culinaris* (n=2, lentil), wild grasses (n=4),

Table 2.7. *Calibrated AMS ^{14}C dates of charred plant remains from Santa Verna palaeosol, Gozo.*

Laboratory code	Radiocarbon date BP	Plant taxon	Calibrated date span (yrs cal. BP/BC, 95% confidence)
UBA-31042	6412±44	*Triticum* cf. *dicoccum*	7424–7270 / 5474–5320
UBA-31043	6181±40	*Hordeum* (cf. hulled straight)	7236–6953 / 5286–5003
UBA-31044	6239±37	Fabaceae	7259–7019 / 5309–5069

wild vetch (n=3) and other unidentifiable fragments. Three AMS radiocarbon dates were obtained from this material to establish a secure time frame for arable cultivation of about 5474–5003 cal. BC (7424–6953 cal. BP; UBA-31042/3/4), and in all likelihood somewhat earlier (Table 2.7). The palaeosol also contained pottery sherds characteristic of the 'Għar Dalam' and 'Skorba' types. These radiocarbon dates therefore also establish a date range for these cultural styles in Malta, refining previous work (Trump 1966; Renfrew 1972). Importantly these dates generally agree with Carroll *et al.*'s (2012) estimate of 5500 cal. BC for the earliest beginnings of agriculture in Malta based on palaeoenvironmental evidence.

2.6.3.2. Sedimentary chronology

Radiocarbon dates from the sediment cores are presented in Table 2.3, showing some samples that are anomalously old relative to their position in the core. Under the premise that these samples were originally enveloped within sediment during episodes of heightened sediment flux in each catchment, the distribution of their radiocarbon ages is thus a proxy for past landscape instability. A comparison of these out of sequence radiocarbon dates with those that appear to be in the correct sequence (Fig. 2.2) indicates that considerable parts of some sediment profiles contain material of mixed ages. The most prominent episode (of recycling of older material?) spans 1500 to 850 cal. BC, which broadly coincides with the Borġ in-Nadur phase of the Maltese Bronze Age.

2.6.3.3. Hypsometry

The hypsometric indices and other physical properties of the drainage basins under study are shown in Table 2.8. The data show that in Malta HI appears to be independent of catchment size, in contrast to the findings of Verstraeten and Poesen (2001) for small intensively cultivated catchments in central Belgium. Instead, at Xemxija, Salina, and Marsa, the HI values are very similar but catchment sizes vary between 7.2 sq. km and 47.9 sq. km (Table 2.7). In the cases of the Mġarr ix-Xini and Wied Żembaq catchments, coupling the HI values of 0.5–0.6 with the associated hypsometric curves demonstrates that both catchments are more susceptible to erosional processes. The data indicate that the Xemxija, Marsa, and Salina catchments are susceptible to fluvial erosion, whereas the Mġarr ix-Xini and Wied Żembaq basins show a greater susceptibility to hillslope processes such as landslides and debris flows (Strahler 1952; Wyatt 1993; Willgoose & Hancock 1998; Verstraeten & Poesen 2001; Haregeweyn *et al*. 2008).

2.6.3.4. Seasonality

Mean NDVI values on a selection of days in 2014–15 are shown for each catchment in Table 2.9. The choice of date was based on the availability of cloud-free imagery for Malta in the Landsat 8 archives.

2.6.3.5. RUSLE model of present-day erosion potential

Resulting RUSLE surfaces for September and March are shown in Figure 2.15 (and see Chapter 8, Fig. 8.2), with R (rainfall-runoff) and C (cover) values being strongly time dependent. The product of R and C models the seasonal signal in soil erosion (Fig. 2.16) which, holding other factors constant, indicates that the potential for soil erosion in Malta from mid-September to mid-December is much higher than at other times of the year.

2.6.4. Discussion

The soils of the Maltese Islands are inherently and easily erodible because of relatively sparse vegetation cover, intensive rainfall during storms, the commonly very fine sand and silt dominated soil fabrics, and a

Table 2.8. *Physical properties of the catchments.*

Catchment	Area / sq. km	Hypsometric Index	Hypsometric interpretation (cf. Willgoose and Hancock, 1998)	Mean LS Factor
Mġarr ix-Xini	4.50	.63	Unstable	1.09
Xemxija	7.23	.41	Fluvial erosion	1.77
Salina	39.66	.45	Fluvial erosion	1.17
Marsa	47.92	.41	Fluvial erosion	.86
Wied Żembaq	11.04	.55	Hillslope processes	.54

Table 2.9. *Normalized Diffuse Vegetation Index (NDVI) for the catchments in 2014–15 and average rainfall data for the weather station at Balzan for the period 1985 to 2012.*

Catchment	NDVI					
	January	March	June	September	November	December
Mġarr ix-Xini	.54	.55	.23	.22	.31	.38
Xemxija	.49	.55	.33	.29	.40	.46
Salina	.47	.57	.31	.25	.40	.48
Marsa	.53	.56	.29	.25	.36	.44
Wied Żembaq	.51	.55	.26	.25	.38	.44
Mean rainfall (mm)	94.7	37	5.4	67.4	108.6	107.7
R-factor (MJ mm (ha hr month)$^{-1}$	263	103	15	187	301	299

relatively large proportion of elevated land. Today, erosion is most likely to occur between September and December each year, and such episodes that have occurred in the recent past have led to the formation of several metres of sediment accumulation on basin floors. For example, a three-day stormy episode in October 1957 led to the removal of 25 mm of topsoil from land surfaces via sheet erosion, walls built across valley floors were swept away, and gullies up to 1.2 m deep were formed, even in very small

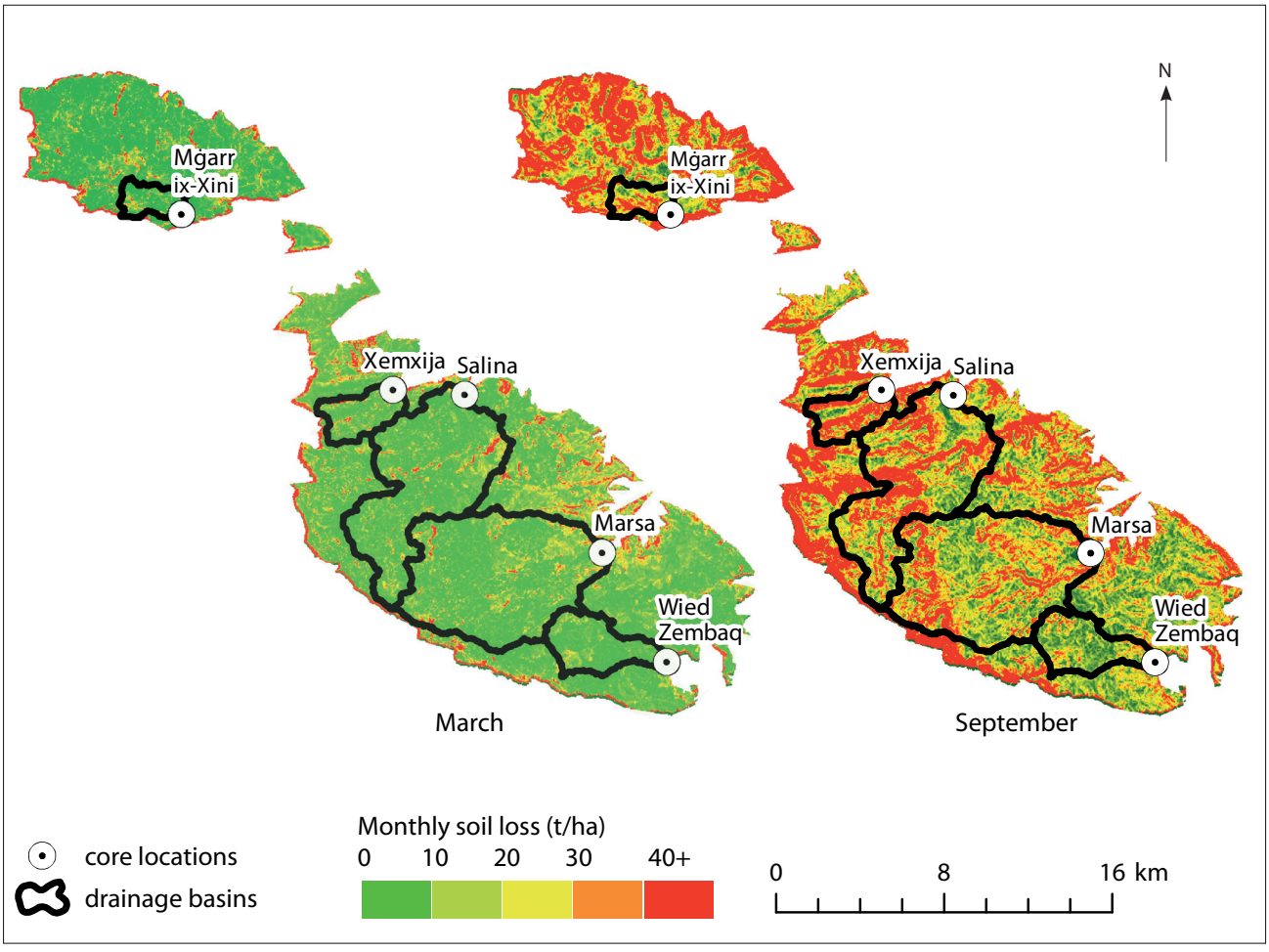

Figure 2.15. *RUSLE models of soil erosion for the Maltese Islands in September and March (R. McLaughlin).*

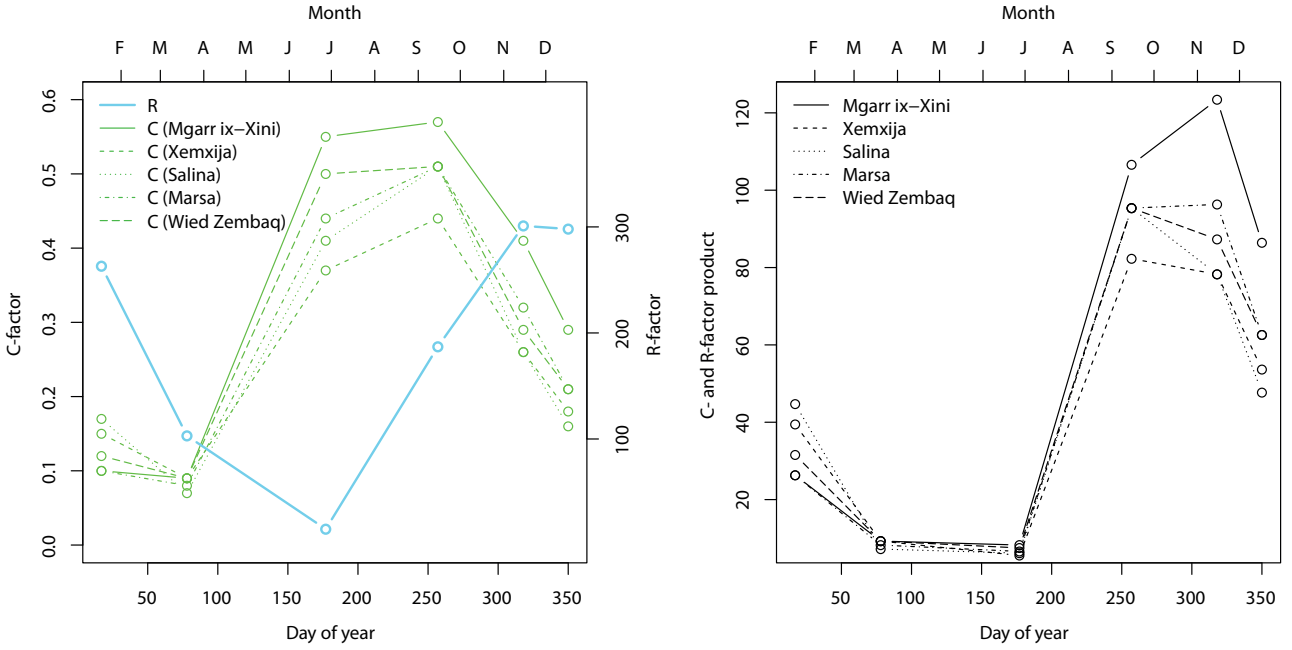

Figure 2.16. *R and C factors and their product (R. McLaughlin).*

catchments (Mitchell & Dewdney 1961). Such events are not atypical, indeed up to 40 per cent of rainfall in Malta occurs during the six wettest days of the year (Mayes 2001). Heavy rainfall is markedly regional, both within any one storm and overall. Some areas seem more susceptible to heavy rainfall than others, with flat land areas draining a large catchment suffering badly from erosion (Mayes 2001; Mitchell & Dewdney 1961).

Although the potential for sudden, catastrophic soil loss is high, the seasonal cadence of Maltese soil erosion events renders them predictable, and agricultural practices and social management can be adapted accordingly (see Chapter 8). Precisely how these management strategies were enacted during prehistoric times is not forthcoming from the archaeological record, although the long sequences of deposits found in the valley floors offer some hints that the strategies changed with time, and occasionally failed altogether.

The inherent fragility and instability of the Maltese landscape implies that agriculture there has always been at risk from soil erosion. The buried soil from Santa Verna indicates that the earliest phases of agriculture were associated with a rich, moist, vegetated soil (see Chapter 5), probably much more resistant to erosion than the soils present in Malta today. Accumulation of sediment in valleys during this time indicates that the steps taken to prevent erosion were limited. During the 'Temple Period' from about 3900 cal. BC, archaeological evidence indicates that cereals were grown and livestock raised, with increasingly elaborate cultural developments taking place at the same time (Fiorentino *et al.* 2012; Evans 1971; Trump 1966; Volume 2). Could this have been possible without a strategy for mitigating the effects of erosion? Although there is no direct archaeological evidence, whether the Temple Period landscape was terraced and whether there was a 'collapse' of the temple civilization at around 2350 cal. BC is a matter for debate. These issues are returned to in Chapters 5, 6 and 11, but what can be said is that there is no evidence of catastrophic destabilization in the valley sedimentary records during the later Neolithic period. However, a period of complete abandonment may be less visible in the sedimentary record because of natural stabilization caused by vegetation regrowth, and the relative lack of organic material in the cored deposits made those core sections difficult to date directly using radiocarbon methods.

The main period of landscape destabilization that is evident in the sediments studied here occurs much later, between *c.* 1550 and 1000 cal. BC during the 'Borġ in-Nadur' period. This time frame saw significant changes in settlement patterns on Malta, compared with previous periods, with the construction of defended settlements on prominent locations (Tanasi & Vella 2015) (see Chapter 7). This time is also one likely date of the 'cart-ruts' – widespread rock-cut tracks leading from hill-tops to valley bottoms. The morphology of these suggest previous soil cover on

hill tops now denuded of soil (Mottershead *et al*. 2010), and one possible explanation for their existence is the act of drawing soil uphill for agricultural purposes, so that food could be grown near the defended settlements, rather than in valley bottoms as is the case today (cf. Evans 1971, 203; Zammit 1928b). This soil management practice differed from soil management practices in the Neolithic and Temple periods for any number of societal reasons, but led to the loss of more soil than before.

It seems that the Phoenician settlement of Malta and Gozo, occurring in the eighth century cal. BC (Vella & Anastasi 2019), heralded a period of relatively greater stability for Maltese sediments which continued into classical times, but erosion was still continuing. Widespread olive and vine cultivation would have been an important factor in this continuing erosion story. It was a risky strategy as these practices typically leave the soil bare and loose and lead to increased soil erosion unless the vines are grown together with an understory of vegetation (Loughran *et al*. 2000; Kosmas *et al.* 1997). Archaeological traces of Phoenician-Punic and Roman olive cultivation and viticulture are widespread in Malta and Gozo (Vella *et al*. 2017; Anastasi & Vella 2018). Similar evidence is present in the environmental record; an increase in *Olea* pollen from *c*. 400 BC into the early Roman period (*c*. cal. AD 20–260) has been observed at Burmarrad (Gambin *et al*. 2016) and in the Marsa cores (see Chapter 3). The risk of disaster could be mitigated by food imports, as Malta was no longer economically self-sufficient during Phoenician-Punic and Roman periods (Bonanno 1990). However, the potential for soil erosion to lead to loss of crops and subsequent economic stress would have been high. Although there is no direct archaeological evidence, the RUSLE model combined with the archaeological and environmental evidence strongly suggest that terracing – or another landscape approach at least as effective as terracing, such as careful management of crop understories, was introduced or reintroduced shortly after *c*. 1000 cal. BC as a means to help control soil erosion.

2.6.5. Conclusions

In this study, it has been demonstrated that the catchments in Malta are a mix of unstable and more mature landforms with the best palaeoenvironmental sequences coming from small catchments with low hypsometric index (HI) values. Thus although there is a high potential for erosion in the Maltese Islands during winter months, the sedimentary history of the islands is punctuated by episodes of stability in the rest of the year. Agriculture was present in Malta from at least *c*. 5400 cal. BC, but varied in intensity throughout prehistory.

Soil erosion management is the key factor that links these issues (and see Chapters 5 & 8). Successive cultural developments took place from at least 5400 cal. BC onwards and the island's sedimentary histories demonstrate how the physical properties of soil and the underlying landforms exist in a system linked to social, economic and cultural factors. This system appears to be at constant risk of failure, leading to widespread soil erosion. Today, in regions isolated from global trade networks (e.g. Haggard *et al.* 2009), or in regions undergoing unchecked agricultural expansion (e.g. Yan *et al.* 2009), the potential of soil erosion to lead to a human cost is high (Bringezu *et al.* 2014). The history of other regions is also relevant in this respect. For example, Boyle *et al*. (2011) have described the 40-fold increase in soil erosion that followed agricultural expansion in early nineteenth century California, demonstrating that USLE-based soil erosion models could predict the phenomenon closely. Similarly, we present these seasonal RUSLE models in the hope that they will be useful in Malta for the on-going evaluation of soil erosion risk, conservation and management. A wider point is to emphasize the prominent role that managing soil erosion had in the day-to-day lives of people in the Mediterranean. From later prehistory onwards, the Mediterranean was the epicentre of many cultural, economic and technological advances, all of which were predicated on sustainable subsistence agriculture. As our Maltese case study illustrates, in such a setting, soil erosion presented an obstacle that could be overcome, but sometimes in concert with other changes in land use, led to a degradation of resources and likely stress.

Chapter 3

The Holocene vegetation history of the Maltese Islands

Michelle Farrell, Chris O. Hunt & Lisa Coyle McClung

3.1. Introduction

Chris O. Hunt

The history of climate and environmental change in the lands around the Mediterranean Sea is dramatic, and our still emerging understanding has changed radically over the last 60 years and is still changing. Pioneering pollen work by Bonatti (1966) first provided evidence that relative to the Holocene (the last 11,500 years) the Late Pleistocene was a time of drought and cold in the region. But for many years alternative viewpoints held currency, especially the work of Vita-Finzi (1969) who held, on the basis of widespread Late Pleistocene gravels, that this had been a period of high precipitation. This view was finally laid to rest only in the 1980s and 1990s by further pollen work on lacustrine deposits (e.g. Bertoldi 1980; Bottema & Woldring 1984; Alessio *et al*. 1986; Follieri *et al*. 1988; Bottema *et al.* 1990), and analysis of the sedimentology and biotic components of Late Pleistocene gravels (e.g. Barker & Hunt 1995).

Vita-Finzi (1969) did, however, pioneer the recognition of the scale and impact of climatic variability within the Holocene in countries bordering the Mediterranean at a time when most researchers thought of the period as extremely stable climatically. Recognition of this climatic variability and its impacts was made more complex because of very strong patterns of human impacts in some Mediterranean countries, which were difficult to disentangle unequivocally from the climatic signal (e.g. Hunt 1998; Grove & Rackham 2003). Only with the rise of isotope-based palaeoclimate studies and high-resolution dating did it become possible to separate the climatic and anthropogenic signals (e.g. Sadori *et al.* 2008).

More recent work has started to show that within the Mediterranean Basin the overall trend and timing of Holocene climate change differs from region to region (Peyron *et al*. 2011). In broad terms, the northeast and southwest of the basin seem to be in phase, with a dry Early Holocene becoming more humid after *c*. 4000 cal. BC, while the northwest and southeast show an opposite trend with a wetter Early Holocene and progressive desiccation after *c*. 4000 cal. BC (Hunt *et al.* 2007). Within this very broad pattern there are considerable regional differences (e.g. Finné *et al.* 2011) and in the central Mediterranean, changes in seasonality are superimposed on these trends (Peyron *et al*. 2011, 2017).

Furthermore, the impact of a series of short, intense aridification phases (some of which seem to relate to events in the North Atlantic (Vellinga & Wood 2002; Wiersma & Renssen 2006) seem to have had dramatically different degrees of severity in different parts of the basin (e.g. Asioli *et al*. 1999; Peyron *et al.* 2011; Jaouadi *et al*. 2016). In some Mediterranean countries, these extreme events had significant landscape impact (e.g. di Rita & Magri 2009; Zielhofer & Faust 2008; Zielhofer *et al.* 2010). Some of these events, at *c*. 6200, 4500, and 2300 BC, disrupted the environmental foundations of human societies, leading to changes in agricultural systems, social organization and migration. The most dramatic of these was the event at *c*. 6200 BC which seems to have triggered dispersal across the Mediterranean of people carrying Neolithic technology from Anatolia (e.g. Zilhão 2001; Weninger *et al.* 2006; Berger & Guilaine 2009; Zeder 2008), although later events also had severe consequences for people in marginal situations and coincide with major technological and societal change (e.g. Carroll *et al.* 2012; Soto-Berelov *et al.* 2015).

The scale and nature of human interference with – and shaping of – landscape and the interrelationships between human activities and climate have also emerged. Patterns of vegetation modification associated with the spread of farming and later waves of extensification and intensification have been widely reported in the northern Mediterranean countries, where agriculturalists cleared landscapes of trees (e.g.

Drescher-Schneider *et al*. 2007; Tinner *et al*. 2009), but are more subtle in the southern and eastern countries which were less heavily vegetated in the early Holocene and where pastoral activity and vegetation management were more significant (Roberts 2002; Asouti *et al.* 2015; Jaouadi *et al*. 2016). Episodes during which agricultural activity expanded and/or intensified are often marked by major valley alluviation phases in the northern Mediterranean countries (Hunt *et al.* 1992; Barker & Hunt 1995; Hunt & Gilbertson 1995; Hunt 1998). The interaction between people and environment emerges particularly from landscape-scale integrated archaeological-palaeoenvironmental surveys and by combining pollen patterns with settlement data (e.g. Malone & Stoddart 1994; Barker 1996; Barker *et al.* 1996; Stoddart *et al.* 2019).

In the Maltese Islands, Pleistocene temperate stages were characterized by fairly dense shrubby or small arboreal vegetation, slope stability and marked palaeosol formation, with calcareous tufa deposits forming around springs. Blown sands accumulated rapidly at the end of temperate stages as sea level fell, exposing the sandy sea bed to wind erosion. Pleistocene cold-stage environments were mostly rather arid, with minimal, very open vegetation. Consequently, high sediment mobility led to deposition of wind-blown loessic silts, thick – often muddy – colluvial slope deposits resulting from wash and mud-flow, and gravelly alluvium of ephemeral rivers (Hunt 1997). The presence of interglacial palaeosols and the absence of interglacial beach sediments in Pleistocene deposits around the coasts of the Maltese archipelago inclined Hunt (1997) to the view that sea level during the current (Holocene) interglacial was relatively higher than during the Last Interglacial, when sea level globally was *c*. 6 m above present day sea levels. Carroll *et al.* (2012) also noted that some Roman portside locations at Marsa were very close to the modern sea level. Both these observations negate the suggestions of Furlani *et al.* (2013) of long-term tectonic stability and instead suggest that generally the Maltese Islands are sinking very slowly relative to modern sea levels, most probably as the result of tectonic factors.

At the beginning of the Holocene, it is likely that the Maltese landscape was rather different from today. Sea levels were much lower – probably about 80 m below present-day sea level (Lambeck *et al.* 2011), so the major islands (Malta, Gozo, Comino and Cominotto) would have been part of one larger landmass. The legacy of Pleistocene slope and aeolian sedimentation was most probably a mantle of silty loessic sediment, which has now been mostly stripped away by erosion. Deep valleys scoured out during the Last Glaciation would have been flooded by the rising sea level in the early Holocene, giving rise to deep inlets. During the mid- to late Holocene these inlets were infilled by sediments eroded from the Maltese landscape, producing coastal plains.

Schembri and Lanfranco (1993) inferred an early Holocene landscape covered by oak-pine sclerophyll woodland on biogeographical grounds. The early Holocene vegetation prior to human colonization was otherwise completely unknown, although evidence for burning and clearance of pine-juniper woodland appears to be present before 3262–2889 cal. BC at Marsa (Carroll *et al.* 2012). Post-colonization prehistoric environments seem to be characterized by open, often steppic landscapes, some lentisk scrub and considerable arable activity and grazing (Evans 1971; Hunt 2001, 2015; Schembri *et al*. 2009; Carroll *et al.* 2012; Marriner *et al.* 2012; Djamali *et al.* 2013; Gambin *et al.* 2016). There is a suggestion of an interruption to cereal cultivation around 2300 cal. BC, probably linked with general regional aridity at this time (Carroll *et al*. 2012). The coastal deposits seem to be marked by discontinuous sedimentation and there are issues with dating as the result of recycling and most probably intrusion of material during the coring process at some sites (Carroll *et al*. 2012; Djamali *et al.* 2013; Gambin *et al*. 2016). Strong taphonomic imprints seem to be present in pollen assemblages from archaeological sites (Hunt 2001, 2015), further complicating the process of reconstructing Holocene vegetation. Charcoal analysis at Skorba provides evidence for trees including carob, hawthorn and ash in the early Neolithic and olive, perhaps cultivated, in the later Neolithic (Trump 1966).

3.2. Palynological methods

Lisa Coyle-McClung, Michelle Farrell & Chris O. Hunt

Cores were sub-sampled for palynology with slices 1 cm thick taken for analysis and bagged in self-seal polythene bags. These were stored at 4° C in cold stores at Queen's University Belfast and Liverpool John Moores University until analysed. Sub-samples of 2.5–5 cm^3 volume were taken from each sample bag.

Samples were prepared for pollen analysis following standard methods (Moore *et al*. 1991), including treatment with 10 per cent hydrochloric acid to remove carbonates, hot 10 per cent potassium hydroxide to disaggregate the sediment before sieving through 120 μm mesh to remove larger mineral and organic material, and 5 per cent sodium pyrophosphate and sieving through 6 μm mesh to remove clay-sized particles. Heavy liquid separation using sodium polytungstate at a specific gravity of 1.95 (Zabenskie & Gajewski 2007) was employed to separate the remaining mineral and organic fractions. The organic residues were stained

using aqueous safranin and mounted on microscope slides in silicone oil.

Slides were counted at a magnification of ×400, with ×1000 magnification and oil immersion used for critical identifications. Pollen and spores were identified using the keys of Moore *et al*. (1991), Reille (1992) and Beug (2004) and the reference collections at Queen's University Belfast and Liverpool John Moores University. Wherever possible, counts of at least 300 pollen grains per sample were made (Benton & Harper 2009, 608). Non-pollen palynomorphs (NPPs) were also identified and recorded during pollen counting.

The sum used to calculate percentages consisted of all terrestrial pollen and spores (TLPS). Percentages of taxa not included within the main sum (i.e. aquatics and NPPs) were calculated using the main sum plus the sum for the taxon group.

Pollen diagrams for the *FRAGSUS* sequences were plotted using Tilia (Grimm 1987) and zoned according to significant changes in the proportions of major taxa. Composite diagrams were compiled for selected taxa from the *FRAGSUS* pollen counts, those of Carroll *et al.* (2012) and Djamali *et al.* (2013), and extracted from Gambin *et al.* (2016) by measuring their pollen diagrams. The data were placed into 20-year bins and calculated and graphed in *Tilia* (Grimm 1987). All pollen diagrams were put into Adobe Illustrator for final preparation.

3.3. Taxonomy and ecological classification

Chris O. Hunt

The Maltese vegetation is in many ways comparable in physiognomy and taxonomy with that of heavily human-impacted landscapes elsewhere in the lowlands of the Mediterranean Basin, although there are differences because of the high rate of endemism in the region and in the Maltese Islands in particular (Schembri 1993). Taxonomic attribution in this study follows Reille (1992, 1995, 1998), Moore *et al.* (1991), Beug (2004) and type collections at Queen's University Belfast and Liverpool John Moores University. The taxonomic level reached is not uniform: in some cases specific identification is possible, but with some taxonomic groupings, in particular the Poaceae and Asteraceae, sub-family or family is the best that could be achieved. This is unfortunate, as members of these large taxonomic groupings have more detailed environmental requirements than can be allocated at higher taxonomic levels, but quite normal in current palynological research. In addition to the pollen and spores, a small number of NPPs were recorded in the pollen diagrams. These include fungal spores and micorrhyzae, some types of green algal spores, dinoflagellate cysts and a few microfossils of uncertain affinity. Identification follows the catalogues of Bas van Geel (i.e. van Geel 1978; van Geel *et al.* 1981, 1989, 2003) and McCarthy *et al*. (2011).

A number of semi-natural habitat-specific plant groupings may be recognized in the Maltese Islands (Table 3.1). Our palynological analyses suggest a more diverse flora existed in the past, but it is likely that similar associations existed, although not present in quite the same locations, or covering the same spatial extent as at present.

Interpretation of pollen diagrams requires attribution of taxa to ecological groupings. Scrutiny of the literature and field experience amongst the *FRAGSUS* environmental team suggests that taxa encountered during pollen counting can be attributed to one or more of the semi-natural plant communities shown in Table 3.1. The attribution of palynologically recognized taxa to plant communities appropriate for the Maltese Islands is shown in Table 3.2.

3.4. Taphonomy

Chris O. Hunt & Michelle Farrell

It has long been recognized that the relationship between pollen-producing vegetation and pollen arriving at depositional settings is far from straightforward, and that further changes to assemblages occur after deposition. Taphonomy (Efremov 1940; Behrensmeyer & Kidwell 1985) is the study of this relationship between life and death assemblages – in the case of pollen and spores it includes the processes of production by the parent plants, dispersal into the environment, transportation by animal vectors, wind and water, deposition and burial by sedimentary processes, post-depositional alteration by decay and diagenetic processes, extraction from sediments and investigation by palynologists (for a recent review see Hunt & Fiacconi 2018). Most pollen taphonomic work has dealt with peat bogs and lakes – fairly simple environments with well-defined taphonomic pathways and generally good pollen preservation, but in the case of the *FRAGSUS Project*, sediments laid down in these environments were not available for study. Therefore, sediments deposited in coastal shallow marine and marginal marine settings were sampled in the *FRAGSUS* boreholes, as previous work (Carroll *et al*. 2012) shows that pollen and other palynomorphs are preserved in these waterlogged deposits. We also sampled soils and redeposited soils associated with archaeological sites where these seemed potentially viable for palynology. Such sites are widely acknowledged to be highly challenging to the palynologist since preservation is frequently poor and subject to

Table 3.1. *Semi-natural plant communities in the Maltese Islands (partly after Schembri 1993).*

Association	Characteristic taxa	Comments	Palynology
Sclerophyll woodland	Pine (*Pinus halepensis*), holm oaks (*Quercus ilex*, *Quercus* spp.), with oleaster (*Olea europaea*) and carob (*Ceratonia siliqua*), and understorey of lentisk (*Pistacia lentiscus*), buckthorn (*Rhamnus lycioides*), hawthorn (*Crataegus* spp.) and a ground flora including polypody fern (*Polypodium* spp.), and ivy (*Hedera* spp.)	Very small stands of probably secondary woodland, strongly impacted by human activity and mostly situated on steep rocky ground. Today there are also more-or-less recent plantations, often characterized by non-native pines	Woodland trees, most notably pines, are mainly wind-pollinated. They produce substantial quantities of pollen and their height enables them to disperse their pollen widely. Pine pollen disperses over immense distances and is highly resistant to decay
Maquis	Oleaster (*Olea europaea*), lentisk (*Pistacia lentiscus*), carob (*Ceratonia siliqua*), buckthorn (*Rhamnus lycioides*), yellow germander (*Teucrium flavum*), white hedgenettle (*Prasium majus*)	Scrub, often characterized by thorny, glaucous or aromatic shrubs. There are fairly extensive areas of maquis in rocky areas on the sides of *widien*, at the foot of inland cliffs and on abandoned farmland. Carob seems to have been a late prehistoric introduction. Today Maltese maquis is often dominated by introduced eucalypts	Many maquis species are insect-pollinated. They produce little pollen which typically is not widely dispersed
Garrigue	Conehead thyme (*Thymus capitatus*), Maltese yellow kidney-vetch (*Anthyllis hermanniae*), tree germander (*Teucrium fruticans*), erica (*Erica multiflora*), Maltese spurge (*Euphorbia melitensis*), squill (*Scilla* spp.) and other geophytes	Low scrub, often characterized by cushion-shaped low bushes and clumps of plants. It is extensive in the Maltese Islands, some natural, but some resulting from degradation of woodland or maquis	Many garrigue plants are insect-pollinated and produce little pollen which is usually not widely dispersed
Steppe	Esparto (*Lygeum spartum*), other grasses (e.g. *Hyparrhenia pubescens, Andropogon distachyos, Brachypodium retusum, Phalaris truncata, Stipa capensis, Aegilops geniculata*), thistles (*Carlina involucrata, Notobasis syriaca, Galactites tomentosa*), plantains (*Plantago* spp.), sandworts and allies (Caryophyllaceae), asphodels (*Asphodelus aestivuus*), and other lilies (e.g. *Urginea maritima*)	Steppe habitats are often dominated by grasses with an admixture of other herbaceous plants and bulbs. In degraded steppes, the proportion of spiky plants such as thistles, unpalatable plants like wormwood, bulbs including asphodels, rosette plants such as plantains, ephemerals such as sandworts and the lettuce group (Lactuceae) tends to rise relative to the grasses	Some steppe plants, such as grasses, are wind-pollinated and produce abundant pollen. Grass pollen is difficult to identify beyond the family level. Pollen of thistles and the lettuce group, although insect-pollinated, are particularly durable so often present in larger proportions in pollen assemblages than their parent plants are in the vegetation. Again, pollen of these taxa cannot often be identified beyond family or sub-family level
Coastal	Grasses (*Elymus farctus, Sporobolus arenarius, Ammophila arenaria*), seakale (*Salsola*), glasswort (*Salicornia*) and other Chenopods (Chenopodiaceae), sea-lavender (*Limonium*-type), thrift (*Armeria*-type), rock samphire (*Crithmum*)	Coastal habitats include saltmarshes, dunes and shallow saline rocky soils adjacent to coasts. Dunes are very rare in the Maltese Islands. They are typically characterized by specialized grasses. Saltmarshes are marked by sea-lavender and some chenopods. The saline coastal soils are characterized by rock samphire and sea-lavender	Coastal grasses and chenopods are not separable palynologically from other members of their families, but very high percentages of chenopod pollen are often associated with saltmarshes. Sea lavender and thrift are indistinguishable palynologically. Apart from the grasses, most coastal taxa are insect pollinated and are low pollen producers.
Rupestral	Caper bush (*Capparis spinosa*), Maltese rock centaury (*Palaeocyanus crassifolius*, the National Plant of Malta) and Maltese cliff orache (*Atriplex lanfrancoi*)	Rock faces and boulder screes have a highly specialized flora and provide important refuges for endemic plants	Most rupestral taxa are insect-pollinated and are low pollen producers. Their pollen is often not widely dispersed
Freshwater	Reeds (*Phragmites australis*), mints (*Mentha*), buttercups (*Ranunculus*), knotgrass (*Persicaria*), poplar (*Populus alba*), willows (*Salix pedicellata, Salix alba*), elm (*Ulmus canescens*), bay (*Laurus nobilis*)	Wetlands are very rare in the Maltese Islands, and perennial wetlands are vanishingly rare. There are few semi-permanently wet valley-floors, characterized by dense stands of reeds with other wetland taxa such as mints, buttercups and knotgrass. There are also a few patches of relict riverine woodland characterized by poplars, willows, elms and bay	Reeds are not distinguishable palynologically from other members of the grass family. Most of the other herbaceous water plants are insect-pollinated. The waterside woodland trees are wind-pollinated and fairly prolific pollen producers, except for the insect-pollinated bay. Poplar pollen is not durable and rarely preserves, while bay pollen is completely non-durable

Table 3.1 *(cont.).*

Association	Characteristic taxa	Comments	Palynology
Disturbed	Ironwort (*Sideritis*), nettles (*Urtica*), figworts (*Scrophularia*), borage (*Borago officinalis*), mustards (Brassicaceae), honeyworts (*Cerinthe*), bindweeds (*Convulvus arvensis*-type), spurges (*Euphorbia*), bedstraws (*Galium*), purslane (*Portulaca oleracea*), corn salad (*Valerianella*)	Disturbed habitats result from human and geomorphic activity (for instance landslides). The disturbed ground species are mostly annuals which mature quickly and disperse seeds prolifically	These species are insect-pollinated and generally low pollen producers
Cultivated	Corn cockle (*Agrostemma githago*), cow wheat (*Melampyrum*), love-in-a-mist (*Nigella*), knotweed (*Polygonum aviculare*), carob (*Ceratonia siliqua*), cereals, barley (*Hordeum*), wheat (*Triticum*), eucalypts (*Eucalyptus*), vines (*Vitis*)	Agricultural weeds such as corn cockle, cow wheat, love-in-a-mist are aliens which arrived with early agricultural plants. Olives only seem to have been domesticated quite late in prehistory	Most, apart from the cereals, are insect-pollinated. All are low pollen producers, but cereal pollen is shed in quantity during threshing

Table 3.2. *Attribution of pollen taxa to plant communities in the Maltese Islands and more widely in the Central Mediterranean. Taxa where the indicated ecology is followed by an asterisk are suggested not to be native to the Maltese Islands during the Holocene because of a combination of (1) absence of macrofossil evidence (2) extremely low or very sporadic pollen counts (3) incompatible ecology. Catholic = not ecologically determinate.*

Pollen taxon	Ecology
Abies	high montane forest*
Betula	montane forest*
Carpinus	montane forest*
Corylus-type	montane forest*
Fagus	montane forest*
Ostrya	montane forest*
Quercus (deciduous type)	montane forest
Tilia	montane forest*
Hedera	woods
Helleborus	woods
Helleborus viridis-type	woods
Ilex aquifolium	woods
Osmunda regalis	woods
Pinus	woods
Polypodium	woods
Pteridium aquilinum	woods
Quercus	woods
Quercus ilex-type	woods
Daphne	maquis
Ephedra	maquis
Erica	maquis
Ericaceae	maquis
Fumana	maquis
Juniperus	maquis
Ligustrum-type	maquis
Olea europaea	maquis
Origanum	maquis
Phillyrea	maquis
Pistacia	maquis
Rhamnus-type	maquis
Rosaceae	maquis
Rosmarinus-type	maquis
Salvia officinalis-type	maquis
Scabiosa	garrigue, maquis, disturbed sites
Centaurium	garrigue
Scilla-type	garrigue
Spergularia media-type	garrigue, rocky places, sand
Tuberaria	garrigue, rocky places
Linum	garrigue, rocky places
Rubiaceae	garrigue, rocky places
Adiantum capillus-veneris	rocky places
Campanula	rocky places
Centranthus ruber-type	rocky places
Gladiolus	rocky places
Linaria-type	rocky places
Sedum-type	rocky places
Theligonum	rocky places
Scrophularia	disturbed, rocky
Borago officinalis	disturbed, rocky, weed of cultivation
Brassicaceae	disturbed, rocky, weed of cultivation
Cerinthe	disturbed, rocky, weed of cultivation
Convolvulus arvensis-type	disturbed, rocky, weed of cultivation

Table 3.2 *(cont.).*

Pollen taxon	Ecology
Euphorbia	disturbed, rocky, weed of cultivation
Galium	disturbed, rocky, weed of cultivation
Portulaca oleracea	disturbed, rocky, weed of cultivation
Valerianella	disturbed, rocky, weed of cultivation
Sideritis	disturbed, weed of cultivation
Urtica	disturbed, weed of cultivation
Agrostemma githago	weed of cultivation
Melampyrum	weed of cultivation
Nigella	weed of cultivation
Polygonum aviculare-type	weed of cultivation
Centaurea cyanus	weed of cultivation
Ceratonia siliqua	cultivated
Cereal-type	cultivated
Eucalyptus	cultivated
Vitis	cultivated
Centaurea	steppe, garrigue, rocky places
Sanguisorba minor-type	steppe, garrigue, rocky places
Acacia	steppe
Ambrosia-type	steppe
Arenaria-type	steppe
Artemisia	steppe
Asphodelus	steppe
Botrychium	steppe
Carduus-type	steppe
Carlina/Onopordum-type	steppe
Hippophae	steppe
Limonium	steppe
Lygeum spartum	steppe
Malva sylvestris-type	steppe
Matricaria-type	steppe
Ophioglossum	steppe
Plantago lanceolata-type	steppe
Plantago major/media-type	steppe
Rumex obtusifolius	steppe
Scabiosa columbaria-type	steppe
Succisa-type	steppe
Allium-type	dry catholic
Caryophyllaceae	dry catholic
Chenopodiaceae	dry catholic
Cirsium-type	dry catholic
Cistus	dry catholic
Dipsacaceae	dry catholic
Helianthemum	dry catholic
Lactuceae	dry catholic
Lathyrus	dry catholic
Polygala	dry catholic
Potentilla-type	dry catholic
Senecio-type	dry catholic
Acanthus	catholic
Apiaceae	catholic
Asteroideae	catholic
Cyperaceae	catholic
Fabaceae	catholic
Gentiana	catholic
Lamiaceae	catholic
Lotus-type	catholic
Poaceae	catholic
Pteropsida (monolete)	catholic
Pteropsida (trilete)	catholic
Ranunculus	catholic
Rubus	catholic
Rumex	catholic
Tamarix	catholic
Trifolium-type	catholic
Valeriana officinalis-type	catholic
Alnus	waterside*
Equisetum	waterside
Filipendula	waterside
Mentha-type	waterside
Littorella-type	waterside
Persicaria maculosa-type	waterside
Ranunculus acris-type	waterside
Sphagnum	waterside
Typha	emergent aquatic
Isoetes	aquatic
Potamogeton	aquatic
Sparganium-type	aquatic

major taphonomic alteration (Edwards *et al.* 2015). It was therefore necessary to understand the taphonomic pathways associated with these depositional environments in the Maltese Islands.

Surface sediment samples were taken in the Mistra Valley on Malta, and from the shallow marine inlet into which it drains, to explore the influence of pedogenic processes and marine sedimentation on

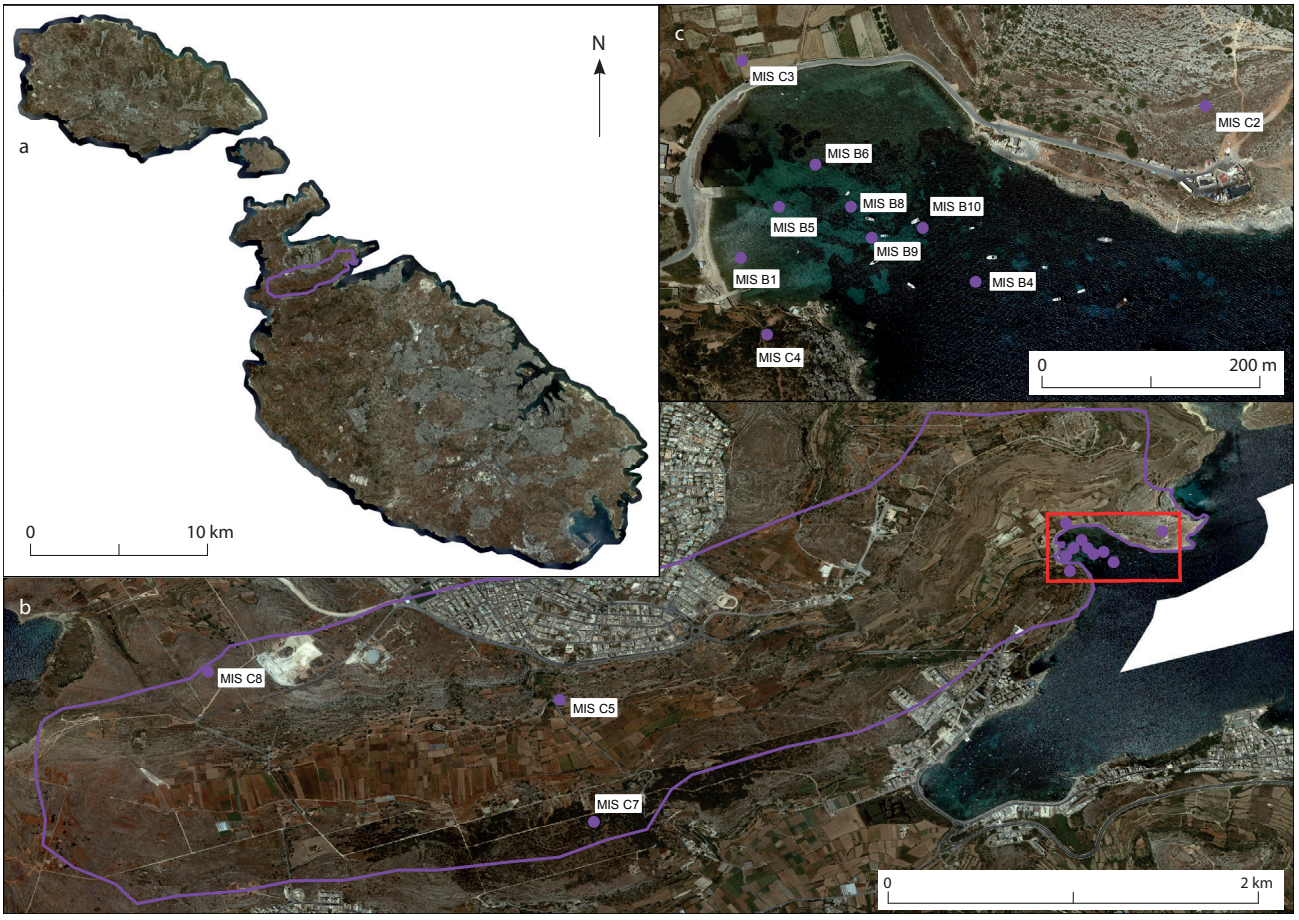

Figure 3.1. *Valley catchments and core locations in the Mistra area of Malta: a) location of the Mistra catchment; b) locations of onshore surface sediment samples from the Mistra catchment; c) locations of the remaining onshore surface sediment samples from the Mistra catchment and offshore surface sediment samples from Mistra Bay (M. Farrell).*

pollen assemblages within a restricted area which is likely to have had relatively uniform pollen rain (Fig. 3.1; Table 3.3). The Mistra Valley was selected because, compared with many other localities in the Maltese Islands, traditional agricultural land-uses are still present and the intensity of anthropogenic alteration of semi-natural vegetation is comparatively low. Stands of planted pines are present in the valley, mostly on higher ground, and although oak woodland is not present within the valley it is present on the slopes of the adjacent Pawles Valley. It therefore offers a reasonable, but not perfect analogue for pre-modern land-uses and the type of depositional environments sampled in this project.

Strong taphonomic biases are most probably seen in all samples (Table 3.3; Fig. 3.2). Comparing these biases is instructive for the interpretation of the *FRAGSUS* core and archaeological site assemblages. The onshore samples were obtained from microbially active, strongly oxidative environments affected by seasonal cyclic wetting and drying and are likely analogues for samples from archaeological sites and buried soils. These environments are not suitable for long-term survival of pollen unless rapid burial occurs. In situations of rapid burial, pollen may survive because bacteria and fungi preferentially scavenge other types of organic material which are less resistant to attack than the sporopollenin from which plants make the resistant exine of pollen and spores (Moore *et al*. 1991). Here well represented taxa are widely acknowledged to be resistant to microbial attack and oxidation, principally *Pinus*, Lactuceae and various Asteraceae such as *Senecio*-type (Havinga 1964, 1967). Nevertheless, some indications of land use and vegetation are also present, for instance the cereal pollen and agricultural weeds like Chenopodiacae in C3, derived from an arable field, maquis plants such as *Olea europaea*, *Phillyrea*, and *Ceratonia siliqua* in samples C5 and C7 where scrub is present, and the extremely high *Pinus* associated with pine scrub woodland in C7. Additionally, Florenzano

Table 3.3. *Characteristics of the taphonomic samples from on-shore and off-shore Mistra Valley, Malta.*

Sample code	Ecology of Location	Major palynological characteristics	Key accessory characteristics
MIS C2	Limestone pavement with low garrigue Dominant species: Poaceae, *Asphodelus* sp., *Psoralea bituminosa*, *Urginea maritima* Also present: *Sedum* sp., *Cirsium* sp., *Galactites tomentosa*, *Fumana* sp., Lotus sp., *Foeniculum vulgare*	*Pinus* 28%, Lactuceae 41%, *Senecio*-type 11%, Poaceae 4%	*Cirsium*-type 3%, *Asphodelus* 2%, Brassicaceae 2%, *Sedum*-type, *Linum*, *Carlina/Onopordum*-type, *Rumex*, Rosaceae, Apiaceae, *Acanthus*, Asteroideae, *Euphorbia*, *Mentha*-type present
MIS C3	Border beween small arable fields close to the sea Dominant species: cultivars (wheat, beans, potatoes), Poaceae, *Borago officinalis*, Brassicaceae Also present: *Calendula arvensis*, *Senecio bicolor*, *Adonis microcarpa*, *Ficus carica*	*Pinus* 15%, Chenopodiaceae 12%, Lactuceae 42%, Poaceae 4%, Brassicaceae 11%, Cereal-type 7%	Caryophyllaceae 2%, *Senecio*-type 2%, Asteroideae 2%, *Sedum*-type, *Linum*, *Cirsium*-type, *Centaurea*, Rumex, Rosaceae, Apiaceae, *Tamarix* present
MIS C4	Coastal maquis Dominant species: *Erica* sp., *Ceratonia siliqua*, *Pistacia lentiscus*, *Prasium majus*, Poaceae, *Foeniculum vulgare*, *Rosa* sp., Asteraceae Also present: *Hedera helix*, *Asphodelus* sp., *Teucrium* sp., *Cirsium* sp., *Galium* sp., *Fumana* sp., *Psoralea bituminosa*	*Pinus* 57%, Ericaceae 5%, *Asphodelus* 11%, Lactuceae 14%	Poaceae 2%, *Ceratonia siliqua* 2%, *Quercus*, *Acacia*, *Carlina/Onopordum*-type, *Cirsium*-type, *Centaurea*, Caryophyllaceae, *Senecio*-type, *Rumex*, Rosaceae, Asteroideae, Poaceae, Brassicaceae, *Tamarix* present
MIS C5	Abandoned agricultural terrace with regenerating scrub Dominant species: Poaceae, *Ceratonia siliqua*, *Eucalyptus* sp., *Foeniculum vulgare*, *Asparagus aphyllus*, *Lotus* sp. Also present: *Cirsium* sp., *Galactites tomentosa*, *Arundo donax*	*Pinus* 40%, Lactuceae 35%, *Senecio*-type 10%, Poaceae 5%	*Cirsium*-type 2%, Brassicaceae 2%, *Linum*, *Carlina/Onopordum*-type, *Centaurea*, *Asphodelus*, Chenopodiaceae, *Helianthemum*, Rosaceae, Apiaceae, Asteroideae, *Euphorbia*, *Ceratonia siliqua*, Cereal-type, *Tamarix* present
MIS C7	Semi-open pine scrub/maquis Dominant species: *Pinus halepensis*, *Olea europaea* Also present: *Acacia*, *Asparagus aphyllus*, Poaceae	*Pinus* 97%	*Olea europaea*, *Phillyrea*, Poaceae, *Eucalyptus* present
MIS C8	Limestone pavement with low garrigue Dominant species: *Thymus capitatus*, Poaceae, *Carlina involucrata*, *Urginea maritima* Also present: *Aster squamatus*, *Atractylis gummifera*, *Euphorbia melitensis*, *Asphodelus aestivus*, *Allium* sp. *Asparagus aphyllus*	*Pinus* 22%, Lactuceae 40%, *Senecio*-type 12%, Poaceae 3%	*Carlina/Onopordum*-type 2%, *Sanguisorba minor*-type 2%, Chenopodiaceae 2%, *Euphorbia* 2%, Ericaceae, *Tuberaria*, *Scilla*-type, *Plantago lanceolata*-type, *Cirsium*-type, *Artemisia*, *Lygeum spartum*, *Asphodelus*, *Helianthemum*, *Allium*-type, *Rumex*, Fabaceae, *Eucalyptus*, *Tamarix* present
MIS B1	Shallow marine. Nearshore, shallow, sandy bottom	*Pinus* 15–30%, Chenopodiaceae 3–11%, Lactuceae 3–20%, Rosaceae 1–7%, Poaceae 5–14%, Brassicaceae 4–12%	*Quercus* 2–5%, *Ostrya* 0–9%, Ericaceae 0–7%, *Sedum*-type 0–9%, *Plantago lanceolata*-type 0–6%, *Carlina/Onopordum*-type 0–4%, *Artemisia* 0–2%, Caryophyllaceae 0–2%, *Helianthemum* 0–3%, *Senecio*-type 0–11%, *Matricatria*-type 0–4%, *Rumex* 0–6%, Asteroideae 0–5%, Cyperaceae 0–3%, *Eucalyptus* 0–4%, *Ceratonia siliqua* 0–4%, Cereal-type 0–5%, *Alnus* 0–2%, *Tamarix* 0–4%, *Mentha*-type 0–1%, *Littorella*-type 0–2%
MIS B4	Shallow marine. Deeper water, eelgrass meadow		
MIS B5	Shallow marine. Shallow, sandy bottom		
MIS B6	Shallow marine. Shallow, sandy bottom on edge of eelgrass meadow		
MIS B8	Shallow marine. Deeper water, eelgrass meadow		
MIS B9	Shallow marine. Deeper water, sandy bottom		
MIS B10	Shallow marine. Deeper water, eelgrass meadow		

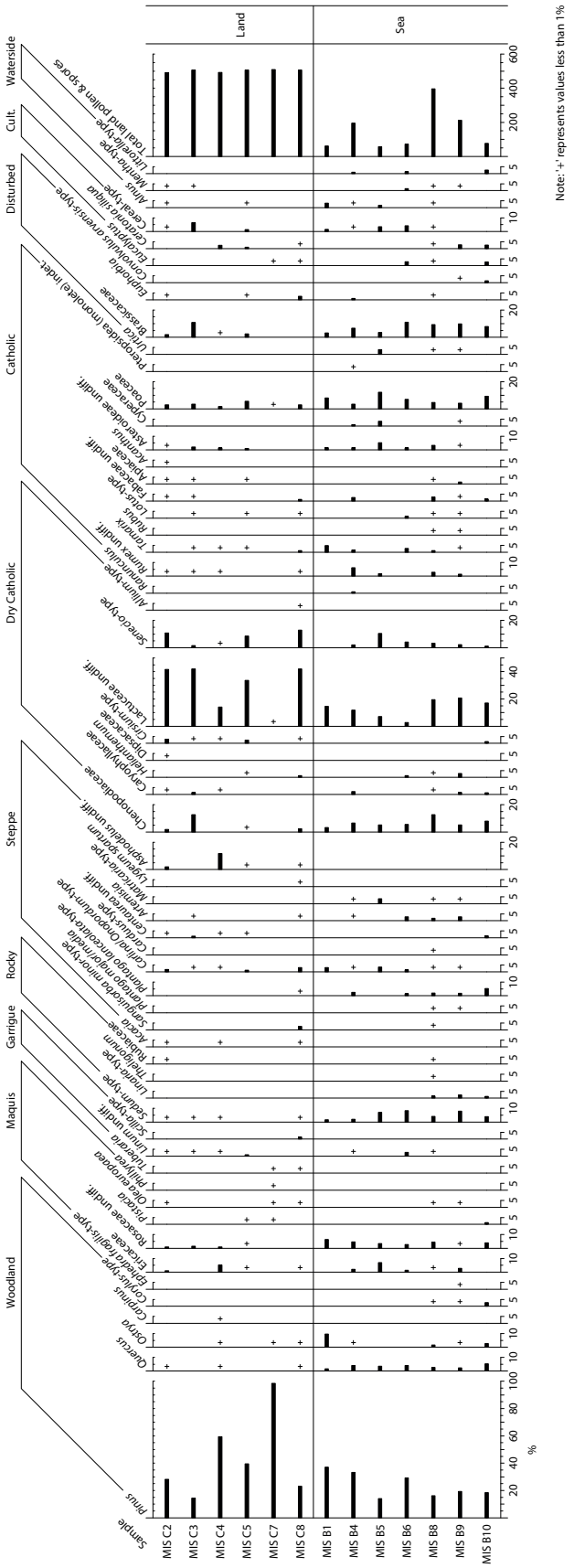

Figure 3.2. *The modern pollen spectra (M. Farrell).*

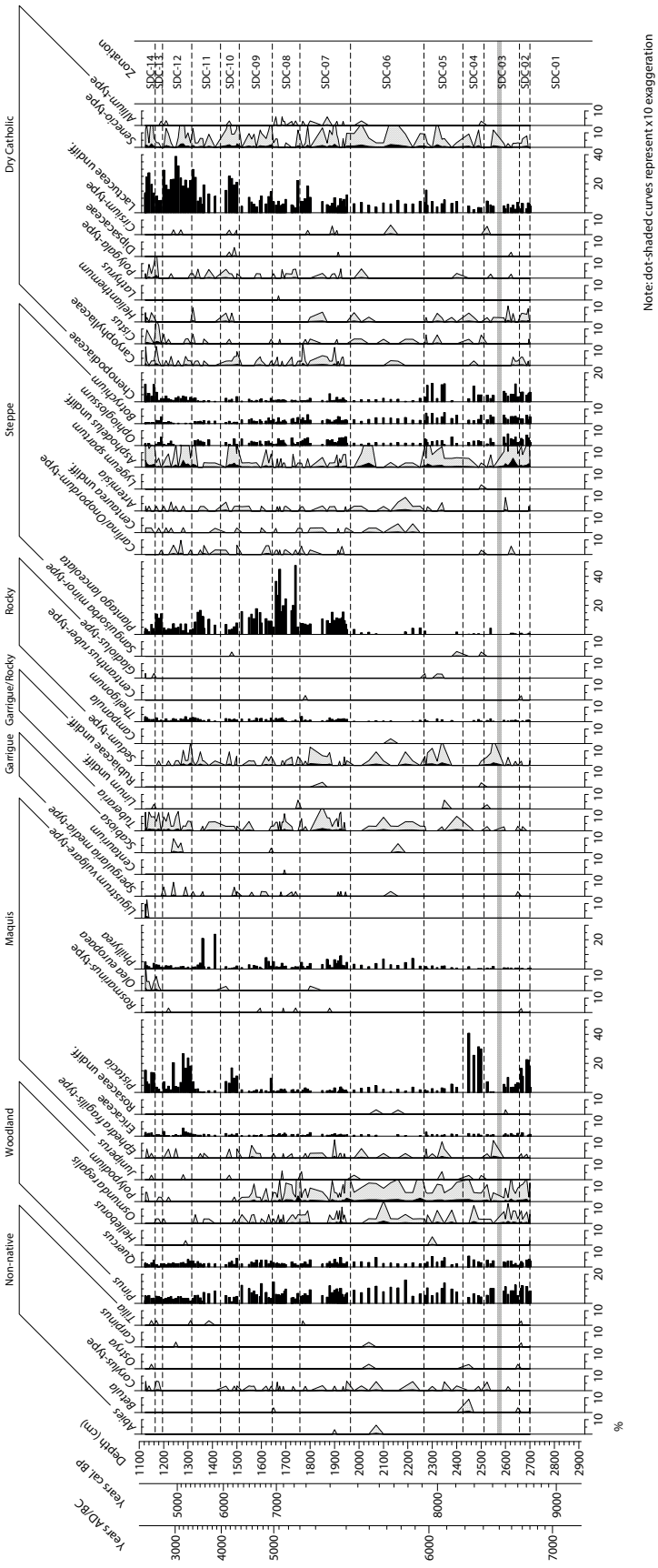

Figure 3.3. *Pollen zonation for the Salina Deep Core (L. Coyle-McClung, C.O. Hunt & M. Farrell).*

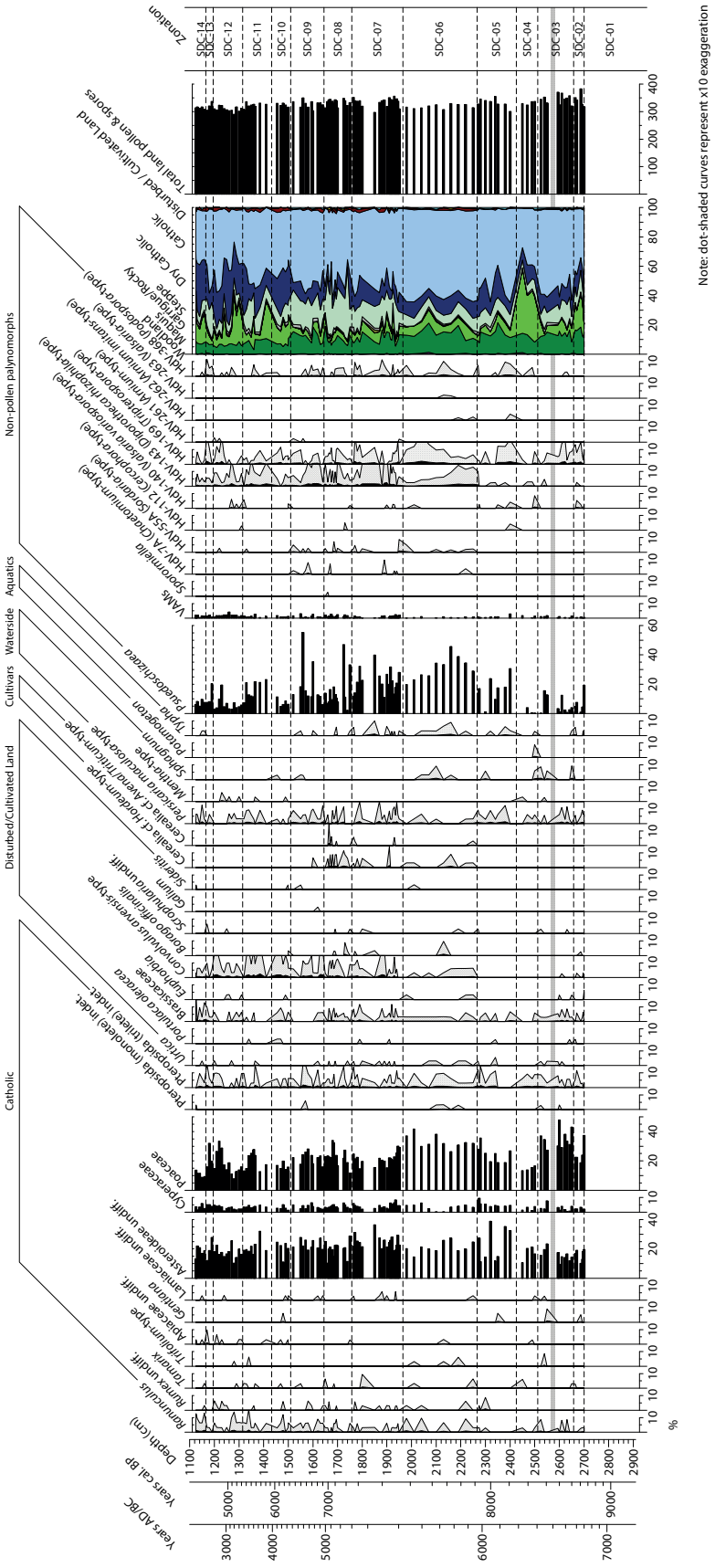

Figure 3.3 *(cont.).*

Table 3.4. *The pollen zonation of the Salina Deep Core with modelled age-depths.*

Zone	Defining taxa	Depth (cm)	Date ranges cal. BC (BP) for zone bases (2σ)	Characteristics	Interpretation
SDC-01	None	3000–2710		Little to no pollen present	Palaeosols and gravels virtually lacking organic matter. A few isolated grains of *Pistacia*, Poaceae, Lactuceae
SDC-02	*Pistacia*-Poaceae-*Pinus*	2710–2660	7042–6553 BC (8992–8503 BP)	*Pinus* increasing (8–10%), low *Quercus* (4%). *Pistacia* rising (5–20%), Ericaceae low (0.5–1%), *Phillyrea* present. Poaceae high but declining (20–40%). Some Asteroideae (8–15%), Lactuceae, *Ophioglossum*, *Botrychium* (2–8%), Chenopodiaceae (4–6%), *Asphodelus*, Cyperaceae (1–3%), *Theligonum*, *Plantago lanceolata*-type. *Persicaria maculosa*-type present. *Pseudoschizaea* decreasing (10–20%). Vesicular arbuscular mycorrhizae (VAMs) and *Tripterospora*-type also present	Lentisk-dominated scrub, dry grassy steppe, some pine-oak woodland, some wetland, soil disturbance declining
SDC-03	Poaceae-*Pistacia*	2660–2510	6858–6419 BC (8808–8369 BP)	*Pinus* fluctuating (5–11%), *Quercus* low (1–4%), *Pistacia* declines (4–10%), *Phillyrea* and Ericaceae present. Poaceae increase (30–48%), Asteroideae (14–20%) and Chenopodiaceae rise (3–12%), some Lactuceae, *Ophioglossum*, *Botrychium* (2–8%), and *Asphodelus* (1–5%). *Theligonum*, *Sedum*-type, *Helianthemum*, Cyperaceae present. *Pseudoschizaea* fluctuates (2–16%), *Tripterospora*-type and VAMs present. A layer at 25.75 m contains no organic material (highlighted in Fig. 3.3)	Dry grassy steppe, with some scrub and a little woodland, some wetland, episodically disturbed soils
SDC-04	*Pistacia*-Poaceae-Asteroideae	2510–2430	6489–6135 BC (8439–8085 BP)	*Pistacia* high and rising (15–40%), *Pinus* low (4–6%), *Quercus* rising (2–7%). *Phillyrea* and Ericaceae present. Poaceae (15–20%), Asteroideae high and declining (10–18%). *Theligonum*, *Ophioglossum*, *Botrychium*, Chenopodiaceae low and declining, *Helianthemum*, Lactuceae and Cyperaceae low (1–3%). Aquatics present, including *Potamogeton*. *Pseudoschizaea* and VAMs present	Steppe partly being replaced by lentisk scrub and with oak woodland expanding slightly, some wetland, soils less disturbed than previously
SDC-05	Poaceae-*Pistacia*-Asteroideae	2430–2265	6350–6037 BC (8300–7987 BP)	Low *Pinus* (6–12%), *Quercus* rising (1–6%). *Pistacia* declines (6–2%), low *Phillyrea* (0.5–2%) and Ericaceae, *Theligonum, Tuberaria, Helianthemum* present. Asteroideae high (15–38%). Poaceae high and rising (15–36%), Lactuceae (6–16%), Cyperaceae (6–8%), Chenopodiaceae (0–12%), *Sedum* (0–2%), *Ophioglossum* (3–8%), *Botrychium* (1–8%) and *Asphodelus* (1–2%) all increase. *Persicaria maculosa*-type present. *Pseudoschizaea* rises significantly (5–30%), other NPPs present include VAMs, *Podospora*-type, *Tripterospora*-type and *Valsaria varispora*-type	Steppe with a little woodland, scrub and wetland, with some eroding soils
SDC-06	Cerealia-Poaceae-*Pinus*-*Phillyrea*	2265–1965	6067–5821 BC (8017–7771 BP)	*Pinus* peaks (6–16%). *Quercus* (2–6%) and *Pistacia* (0.5–5%) both low, *Phillyrea* rises (1–8%). *Ephedra fragilis*-type, Ericaceae, *Tuberaria, Sedum*-type, *Theligonum* and *Asphodelus* are present. *Ophioglossum* (1–2%), *Botrychium* (2–6%) and Chenopodiaceae (0.5–3%) have low peaks in the middle of the zone. Poaceae (28–44%) and Asteroideae (15–22%) are high, and Lactuceae (4–9%) fairly high. The Cerealia-types *Hordeum* and *Avena*/*Triticum* are first recorded and *Plantago lanceolata*-type peaks early in the zone and rises again at the end. *Convolvulus arvensis*-type, *Urtica*, *Sideritis*, *Borago officinalis* and Brassicaceae are present. *Typha* and *Persicaria maculosa*-type are present. *Pseudoschizaea* initially increases from 15–44% before declining to 22%. *Diporotheca rhizophila*-type and *Tripterospora*-type expand slightly, and *Sordaria*-type appears for the first time	Steppe with a little woodland, scrub and wetland. Initiation of cereal cultivation and livestock grazing with some indicators of disturbed ground and significant fungal indicators of disturbed ground and animal dung

Table 3.4 *(cont.).*

Zone	Defining taxa	Depth (cm)	Date ranges cal. BC (BP) for zone bases (2σ)	Characteristics	Interpretation
SDC-07	*Plantago lanceolata* -Cerealia-Poaceae	1965–1755	5625–5419 BC (7575–7369 BP)	*Pinus* declines slightly (2–10%), *Quercus* and *Pistacia* low and rising slightly (2–5%), *Phillyrea* falling after a low peak (1–7%), Ericaceae, *Sedum*-type, *Theligonum* and *Tuberaria* rise slightly (0.5–3%). *Plantago lanceolata*-type increases (5–16%), *Ophioglossum, Botrychium*, Chenopodiaceae (1–5%), Lactuceae (6–12%) and Asteroideae (22–34%) rise slightly while Poaceae decrease (16–30%). Brassicaceae, *Convolvulus arvensis*-type, *Urtica*, *Hordeum*-type and *Avena*/*Triticum*-type are present. *Persicaria maculosa*-type and *Typha* are present. *Pseudoschizaea* high and fluctuating (15–45%). VAMs rise slightly (0.5–2%). *Diporotheca rhizophila*-type, *Tripterospora*-type and *Podospora*-type remain low. *Sordaria*-type and *Valsaria varispora*-type are occasionally present	Steppe with slightly declining minor woodland, with scrub increasing slightly. Strong indications of grazing and the spread of short-grazed grassland, some indications of grazing pressure. Continued cereal cultivation, and strong soil erosion
SDC-08	*Plantago lanceolata*-Poaceae-Cerealia-Asteroideae	1755–1650	5404–5145 BC (7354–7095 BP)	*Pinus* rising (6–14%). *Quercus* (1–4%), *Pistacia* (0.5–2%), *Phillyrea* (0.5–4%), Ericaceae, *Tuberaria, Theligonum* are all low. *Plantago lanceolata*-type rises strongly (15–42%). *Ophioglossum, Botrychium*, Chenopodiaceae and Cyperaceae remain low (1–4%). Lactuceae peak and fall (5–20%). Asteroideae (12–22%) and Poaceae (14–30%) remain high. *Convolvulus arvensis*-type, Brassicaceae, *Borago officinalis* and *Urtica* increase slightly. *Avena*/*Triticum*-type and *Hordeum*-type are present. *Persicaria maculosa*-type and *Typha* are present. *Pseudoschizaea* highly variable (5–45%), VAMs rise slightly (1–3%), *Diporotheca rhizophila*-type, *Podospora*-type and *Tripterospora*-type increase slightly. *Sporormiella*-type makes its only appearance in the profile and *Cercophora*-type, *Valsaria varispora*-type, *Sordaria*-type and *Chaetomium*-type are occasionally present	Steppe with minor scrub and woodland. Further expansion of short-grazed grassland with grazing animals indicated by dung fungi. Some cultivation of wheat and barley and marked phases of soil erosion
SDC-09	*Plantago lanceolata*-Poaceae-*Pinus*-Cerealia-Asteraceae	1650–1510	5202–4759 BC (7152–6709 BP)	*Pinus* (5–15%) and *Quercus* (1–5%) peak in the middle of the zone. *Pistacia* (1–9%) and *Phillyrea* (<1%–6) decline sharply near the base of the zone. Ericaceae, *Theligonum*, *Tuberaria* and *Spergularia media*-type are present. *Plantago lanceolata*-type (7–16%) declines at the beginning of the zone then rises again. *Ophioglossum, Botrychium*, Chenopodiaceae (1–3%) and Cyperaceae (3–6%) remain low. Asteroideae and Poaceae remain significant (20–30%). *Convolvulus arvensis*-type, Brassicaceae, *Galium*, *Sideritis* and *Urtica* are present but sporadic, and cereals are represented by *Hordeum*-type. *Persicaria maculosa*-type and *Typha* are present. *Pseudoschizaea* (6–52%) highly variable but peaks in the middle of the zone. VAMs, *Diporotheca rhizophila*-type and *Tripterospora*-type present consistently. *Podospora*-type, *Sordaria*-type, *Chaetomium*-type and *Arnium*-type occasionally present	Steppe with woodland and a little scrub. There was a slight recovery of woodland, but scrub seems to have been cleared or grazed down. Grazing pressure seems to have remained strong, but cultivation may have waned locally
SDC-10	*Plantago lanceolata*-*Pistacia*-Lactuceae	1510–1435	4566–4177 BC (6516–6127 BP)	*Pinus* and *Quercus* low (2–6%). *Pistacia* peaks (6–18%). *Phillyrea* and Ericaceae are low (0–2%). *Tuberaria, Theligonum, Sedum*-type, *Asphodelus, Ophioglossum, Botrychium, Helianthemum, Polygala*-type and Cyperaceae are all low. *Plantago lanceolata*-type declines then rises (3–12%), Lactuceae peak (12–20%). Asteroideae (12–20%) and Poaceae (16–22%) decline slightly. *Convolvulus arvensis*-type and Brassicaceae are present. *Persicaria maculosa*-type present. *Psuedoschizaea* declines (8–13%). VAMs, *Diporotheca rhizophila*-type and *Tripterospora*-type are present	Degrading steppe with encroaching scrub and a little woodland. Woodland is minor but lentisk scrub expands. Markers of degraded, perhaps rather over-grazed steppe increase but fungal spores often associated with animal dung become less frequent so it is possible that the degradation

Table 3.4 *(cont.).*

Zone	Defining taxa	Depth (cm)	Date ranges cal. BC (BP) for zone bases (2σ)	Characteristics	Interpretation
					of the steppe might be climatic, or livestock were moved elsewhere. Cultivation appears to have ceased locally
SDC-11	Poaceae-*Plantago lanceolata*-*Phillyrea*-*Pistacia*-Lactuceae-Asteroideae	1435–1320	4237–3685 BC (6187–5635 BP)	*Pinus* rises (8–10%), *Quercus* falls slightly (2–4%), *Pistacia* falls (0.5–2%). *Phillyrea* fluctuates (1–23%). *Tuberaria, Theligonum, Asphodelus, Ophioglossum, Botrychium,* Chenopodiaceae low (0–2%). *Plantago lanceolata*-type peaks (5–18%). Lactuceae (7–14%), Asteroideae (18–31%), Poaceae (12–24%) all rise then decline. Brassicaceae, *Convolvulus arvensis*-type and *Persicaria maculosa*-type all present. *Pseudoschizaea* rises, falls and rises again (12–24%) and VAMs, *Diporotheca rhizophila*-type, *Tripterospora*-type and *Podospora*-type are present	Degrading steppe and scrub with a little woodland. Woodland is minor. Lentisk scrub is replaced by *Phillyrea* (false privet). Short-grazed grassland and disturbed ground indicators are present and markers for soil erosion are more prevalent than previously
SDC-12	Poaceae-*Pistacia*-*Plantago lanceolata*-Asteroideae	1320–1195	3823–2979 BC (5773–4929 BP)	*Pistacia* rises, then declines (2–27%). *Quercus* is low and declines gently (1.5–4%). *Pinus* is low (1–5%). Ericaceae, *Asphodelus*, *Plantago lanceolata*-type (1–7%), *Tuberaria,* Chenopodiaceae, Cyperaceae and *Convolvulus arvensis*-type (0.5–2%) are all low. Lactuceae (15–37%), Asteroideae (14–27%) and Poaceae (12–26%) all fluctuate. *Pseudoschizaea* fluctuates (4–16%). VAMs (2–6%) have a low peak and *Diporotheca rhizophila*-type and *Tripterospora*-type are present. *Valsaria varispora*-type is recorded at the beginning of the zone. *Sordaria*-type and *Arnium*-type appear at the end	Degrading steppe and scrub with a little woodland. Woodland is minor, lentisk replaces *Phillyrea* but then wanes. Short-grazed grassland may be replaced by taller vegetation, but there are short phases of degradation and soil erosion
SDC-13	Poaceae-*Pistacia*-Lactuceae-Asteroideae-*Olea*	1195–1165	3047–2355 BC (4997–4305 BP)	*Pinus, Quercus, Pistacia, Phillyrea*, Ericaceae, *Tuberaria, Theligonum, Olea europaea* are all very low (0.5–2%). *Plantago lanceolata*-type peaks, declines then rises again (0.5–16%). *Botrychium*, *Ophioglossum* (0.5–6%), Asteroideae (12–27%) and Poaceae (15–33%) peak then decline. Lactuceae decline (8–9%). Cyperaceae (2–6%), *Convolvulus arvensis*-type and *Persicaria maculosa*-type are present. *Pseudoschizaea* declines (7–19%), while VAMs, *Diporotheca rhizophila*-type, *Tripterospora*-type and *Podospora*-type all rise slightly	Steppe with very little woodland or scrub. A very open landscape characterized by grassy herbaceous vegetation with signs of grazing
SDC-14	*Olea*-*Ligustrum*-Poaceae-*Plantago lanceolata*-*Pistacia*-*Phillyrea*-Lactuceae	1165–1125	2717–2233 BC (4667–4183 BP)	*Pinus* (4–6%), *Quercus* (1–5%), *Pistacia* (6–15%), *Phillyrea* (1–5%), *Olea europaea,* Ericaceae, *Tuberaria, Theligonum, Asphodelus* (1–2%), Chenopodiaceae (5–12%), Lactuceae (15–29%), Asteroideae (12–27%) all rise. *Ligustrum vulgare*-type appears. *Plantago lanceolata*-type (1–5%), Cyperaceae (1–6%) and Poaceae (10–14%) decline. *Convolvulus arvensis*-type and *Persicaria maculosa*-type are present. *Pseudoschizaea* (5–10%), VAMs (1–2%), *Diporotheca rhizophila*-type, *Podospora*-type and *Tripterospora*-type are present	Degraded steppe and with a little scrub and woodland. The rise of scrub taxa and decline in *Plantago* may suggest declining grazing pressure, but the rise in composites and chenopods and decline in grasses might suggest a more arid landscape and/or are a sign of grazing pressure
			Top of sampled interval has an interpolated date of 2464–1979 cal. BC (4414–3929 cal. BP)		

et al. (2015) have argued that over-representation of Cichorieae, members of the Lactuceae tribe, may actually be an indicator of open habitats and grazing activity in Mediterranean landscapes, rather than the result of differential pollen preservation.

The off-shore samples provide an analogue for assemblages from shallow marine layers in the *FRAGSUS* cores. The assemblages are comparatively uniform (Table 3.3), characterized by lower percentages of degradation-resistant taxa (e.g. *Pinus*, Lactuceae and various Asteraceae), than are present in the onshore soil samples. These taxa are, however, still over-represented relative to their occurrence in the catchment vegetation. *Ostrya* and *Corylus*-type, which are not present in the Maltese Islands, reflect long distance dispersal by wind from Sicilian or more distant vegetation to the north. Shoreline taxa such as Chenopodiaceae and Brassicaceae are well-represented. Some anemophilous taxa, such as *Pinus*, *Quercus* and Poaceae, are over-represented relative to their occurrence in the vegetation, while several entomophilous taxa present onshore, principally maquis and garrigue species such as *Pistacia, Olea europaea, Tuberaria* and geophytes such as *Asphodelus*, are either not present or are poorly represented, although the entomophilous Asteraceae and Lactuceae are over-represented.

Although the on-shore and off-shore samples reflect the extant vegetation imperfectly as the result of these taphonomic biases, the overall aspect of that vegetation can be seen. The taphonomic biases are predictable and can therefore be allowed for in the interpretations of the palaeo-ecological sequences that follow in the next sections.

3.5. The pollen results

Michelle Farrell, Lisa Coyle-McClung & Chris O. Hunt

Some 25 deep cores were taken from a wide selection of valley and near-shore environments on Malta and Gozo (see Chapter 2) (Fig. 2.4), but only the Salina Deep Core, Salina 4, Wied Żembaq 1 and Xemxija 1 on Malta were selected and fully analysed for their palynological records, each with an associated AMS radiocarbon chronology (Table 2.3) and age-depth models (Tables 3.4–3.7). In addition, buried soils were sampled and analysed from the Santa Verna and Ġgantija temple sites on Gozo, and the primary fill of a Bronze Age silo at In-Nuffara on Gozo.

3.5.1. The Salina cores

The results of the palynological analysis of the Salina Deep Core are shown in Figure 3.3. A total of fourteen zones, labelled SDC-01 to SDC-14, were identified and are summarized in Table 3.4. This core appears to have a high resolution record spanning the period *c*. 7030–6600 cal. BC (7923 BP; UBA-34973) to 2400–2050 cal. BC (3793 BP; UBA-34970), although the coring technique caused a series of short sampling gaps. The sampled sequence was laid down during a period of rapidly rising sea level (Lambeck *et al.* 2011), so distances from the shoreline (and thus parent vegetation) to the core site will have increased during this interval. This may have impacted slightly on pollen taphonomy, although no strong trends in taphonomic indicators seem to be visible in the record. Of particular note in this core are the events in zone SDC-06 commencing at 6080–5920 cal. BC (7145 BP; UBA-35586) which appear to show the impacts of initial agricultural activity on the Maltese Islands.

The palynological results from the Salina 4 core are shown in Figure 3.4 and Table 3.5. The sampled interval in this core overlaps with the later part of the Salina Deep Core, with dates ranging from before *c*. 5630–5500 cal. BC (6644 BP; UBA-30090) to 1260–1050 cal. BC (2953 BP; UBA-30083) (Table 2.3).

3.5.2. Wied Żembaq

The pollen zonation for the Wied Żembaq 1 core is shown in Figure 3.5 and Table 3.6. The sampled interval runs from before *c*. 3630–3370 cal. BC (4707 BP; UBA-28262) to after 910–800 cal. BC at 2.15 m down-profile (2707 BP; UBA-29042). The Wied Żembaq 2 core, which was not anlaysed for pollen, exhibited a date range from *c*. 3260–2890 cal. BC (4366 BP; UBA-34969) to after 1880–1630 cal. BC at 2.95 m down-profile (3428 BP; UBA29043).

3.5.3. Xemxija

The pollen zonation for the Xemxija 1 core is shown in Figure 3.6 and Table 3.7. The sampled interval here runs from *c*. 8780–8460 cal. BC (9353 BP; UBA-25001) to some time in the twentieth century when natural deposition was terminated by the emplacement of quarried material (made ground) to produce a dry area for scout camping. Age control at the base of this core is, however, problematical and assemblages from the part of the core below 6.6 m show signs of significant taphonomic bias. It is also rather probable that there are major erosive discontinuities in the core, especially below pollen zone XEM-05, dated to *c*. 4330–4050 cal. BC (5357 BP; UBA-29041). Sedimentation above this level seems to have been more continuous, but there are significant taphonomic biases evident in pollen zones XEM-06 and XEM-10 to XEM-13.

3.5.4. In-Nuffara

The results of pollen analysis of the primary fill of a Bronze Age silo at In-Nuffara, Gozo, are shown

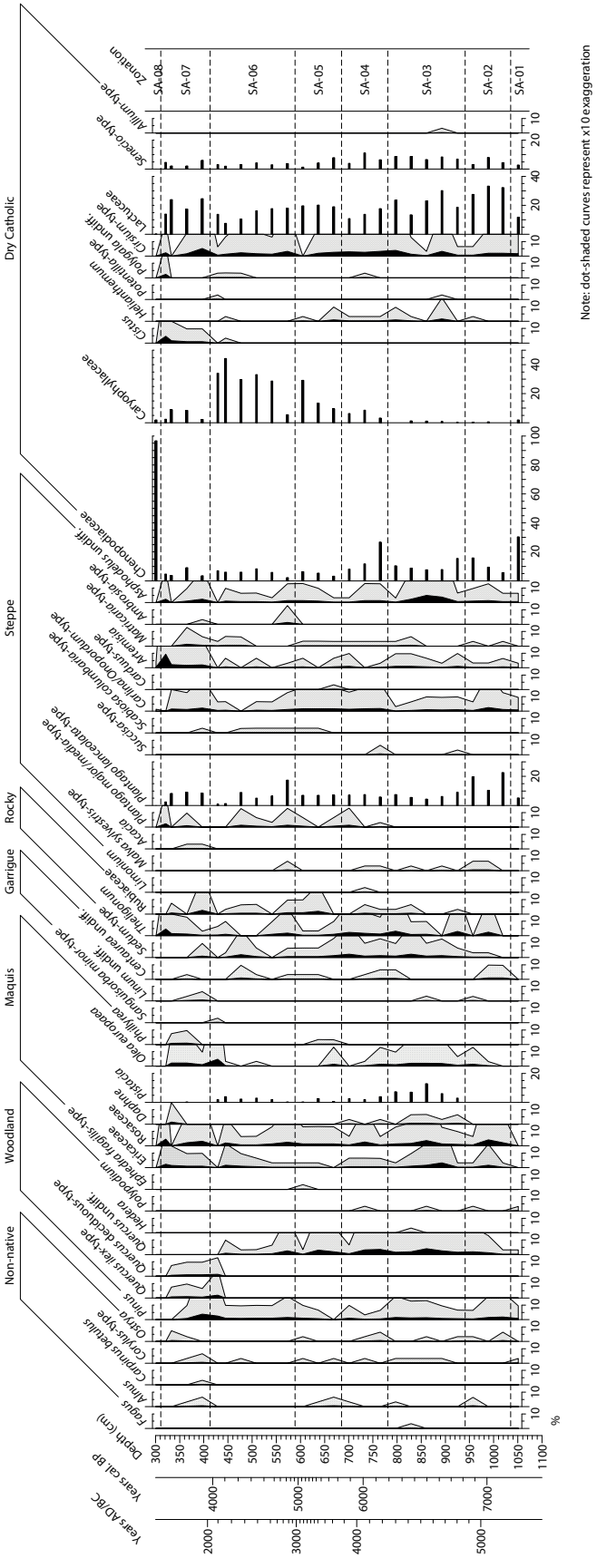

Figure 3.4. *Pollen zonation for the Salina 4 core (M. Farrell).*

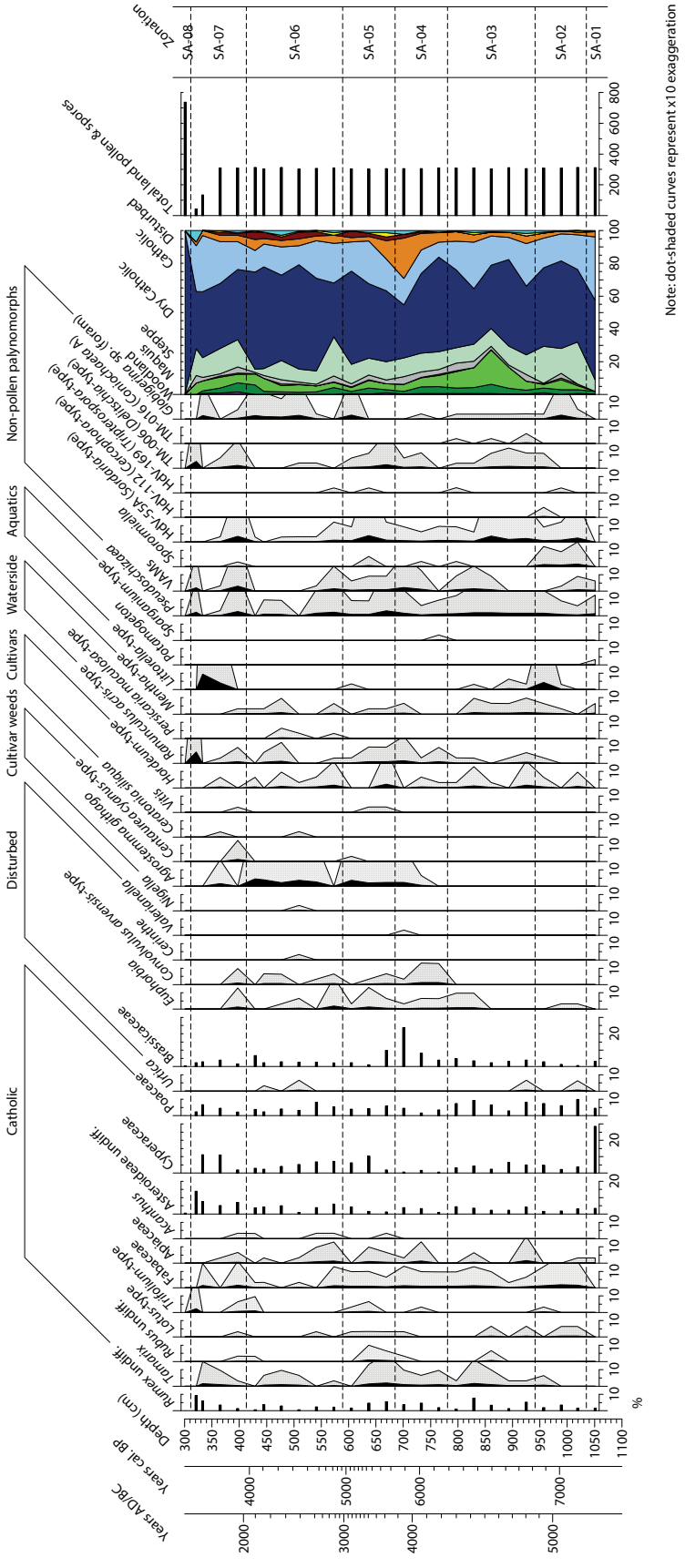

Figure 3.4 *(cont.).*

Table 3.5. *The pollen zonation of the Salina 4 core with modelled age-depths.*

Zone	Defining taxa	Depth (cm)	Date ranges cal. BC (BP) for zone bases (2σ)	Characteristics	Interpretation
SA-01	Chenopodiaceae-Cyperaceae	1055–1040	5608–5238 BC (7558–7188 BP)	High Chenopodiaceae (30%), Cyperaceae (29%). Some Lactuceae (12%), *Senecio*-type (4%), Asteroideae (4%), Poaceae (5%), Brassicaceae (4%). A little *Pinus, Quercus,* Rosaceae, *Matricaria*-type, *Artemisia, Cirsium*-type, *Asphodelus* and *Rumex* (0.5–2%). *Mentha*-type and *Potamogeton* present. *Pseudoschizaea* and VAMs present	An extremely open, rather degraded landscape characterized by ruderals and with coastal vegetation prominent, perhaps with some woodland at a distance. Freshwater wetlands with sedges and slow-moving waters higher in the estuary
SA-02	Lactuceae-*Plantago*-Poaceae	1040–940	5566–5130 BC (7516–7080 BP)	High *Plantago lanceolata*-type (10–24%), Lactuceae (23–36%). Some *Senecio*-type (4–9%), Chenopodiaceae (7–16%), *Rumex* (2–4%), Asteroideae (2–4%), Cyperaceae (3–6%), Poaceae (6–9%), Brassicaceae (1–4%). Low *Pinus, Quercus*, Rosaceae, *Artemisia, Asphodelus, Cirsium*-type, *Lotus*-type, Fabaceae (0.5–2%). *Olea europaea, Centaurea, Theligonum, Malva sylvestris*-type, *Matricaria*-type, *Tamarix, Euphorbia, Hordeum*-type, *Mentha*-type, *Littorella*-type sometimes present. *Sporormiella*-type, *Sordaria*-type, *Pseudoschizaea* present, *Cercophora*-type, *Delitschia*-type, *Tripterospora*-type, VAMs occasionally present	An extremely open landscape. Perhaps some woodland and scrub at a distance. Decline of ruderals suggests the vegetation is less degraded in aspect than SA-01 and there is evidence for cereal cultivation and animal grazing. Declining soil fungi suggest maybe reduced soil erosion
SA-03	Lactuceae-*Pistacia*-Chenopodiaceae	940–780	5063–4670 BC (7013–6620 BP)	High Lactuceae (18–32%), *Pistacia* (2–14%), Chenopodiaceae (10–26%). Some *Plantago lanceolata*-type (4–9%), *Senecio*-type (8–12%), *Rumex* (1–9%), Asteroideae (3–6%), Cyperaceae (2–8%), Poaceae (3–9%), Brassicaceae (2–6%). A little *Pinus, Quercus*, *Daphne*, Ericaceae, *Olea europaea*, Rosaceae, *Sedum*-type, *Theligonum*, *Malva sylvestris*-type, *Carlina/Onopordum*-type, *Artemisia*, *Asphodelus*, *Helianthemum*, *Cirsium*-type, *Tamarix*, Fabaceae, *Hordeum*-type, *Mentha*-type, *Littorella*-type, *Delitschia*-type, *Sordaria*-type, *Pseudoschizaea* are present, *Coniochaeta* Type A, *Sporormiella*-type, *Tripterospora*-type and VAMs are occasionally present	An open, rather degraded landscape with prominent ruderals, encroaching garrigue and scrub, woodland at a distance. Some evidence for cereal cultivation and animal grazing. Some evidence for soil erosion from the soil fungi
SA-04	Brassicaceae-Lactuceae	780–690	4431–4026 BC (6381–5976 BP)	High Brassicaceae (6–24%), Lactuceae (12–20%), Chenopodiaceae (10–30%). Some *Plantago lanceolata*-type (7–8%), Caryophyllaceae (8–10%), *Senecio*-type (4–12%), *Rumex* (2–6%), Asteroideae (1–5%), Poaceae (1–5%). A little *Pinus, Quercus*, *Pistacia*, *Olea europaea*, Rosaceae, *Sedum*-type, *Theligonum*, *Matricaria*-type, *Carlina/Onopordum-type*, *Asphodelus*, *Helianthemum*, *Cirsium*-type, Fabaceae, *Euphorbia*, *Hordeum*-type, *Ranunculus acris*-type, *Convolvulus arvensis*-type. *Delitschia*-type, *Sordaria*-type, *Pseudoschizaea* and VAMs are present, *Sporormiella*-type is occasionally present	An open, fairly degraded landscape with prominent ruderals and with a little scrub and woodland. There is evidence for cereal cultivation and animal grazing and for some soil erosion
SA-05	Lactuceae-Caryophyllaceae-*Plantago*	690–590	4077–3716 BC (6027–5666 BP)	High Lactuceae (21–22%), Caryophyllaceae (10–28%), *Plantago lanceolata*-type (10%). Some Chenopodiaceae (2–8%), *Senecio*-type	An open, rather degraded landscape with prominent ruderals, rising ephemerals, and some scrub and

Table 3.5 *(cont.).*

Zone	Defining taxa	Depth (cm)	Date ranges cal. BC (BP) for zone bases (2σ)	Characteristics	Interpretation
				(2–10%), *Rumex* (2–6%), Asteroideae (1–6%), Cyperaceae (1–12%), Poaceae (1–5%), Brassicaceae (2–11%). A little *Pinus*, *Quercus*, Rosaceae, *Centaurea*, *Sedum*-type, *Theligonum*, Rubiaceae, *Plantago media/major*-type, *Artemisia*, *Asphodelus*, *Cirsium*-type, *Tamarix*, Fabaceae, *Euphorbia*, *Ranunculus acris*-type, *Agrostemma githago*. *Vitis* and *Hordeum*-type are occasionally present. *Delitschia*-type, *Sordaria*-type, *Pseudoschizaea* and VAMs are present, *Sporormiella*-type and *Tripterospora*-type are sometimes present	woodland at a distance. There is some evidence for cereal cultivation, grazing and soil erosion
SA-06	Caryophyllaceae-Lactuceae	590–420	3386–2560 BC (5336–4510 BP)	High Caryophyllaceae (28–45%) and Lactuceae (8–16%). Some *Pistacia* (2–4%), *Plantago lanceolata*-type (1–20%), Chenopodiaceae (8–10%), *Senecio*-type (2–5%), *Rumex* (1–5%), Asteroideae (1–7%), Cyperaceae (2–8%), Poaceae (2–9%), Brassicaceae (2–8%). A little *Pinus*, *Quercus*, *Olea europaea*, Rosaceae, *Carlina/Onopordum*-type, *Asphodelus*, *Cirsium*-type, *Tamarix*, *Agrostemma githago*, *Hordeum*-type, Ericaceae, *Sedum*-type, Rubiaceae, *Matricaria*-type, *Polygala*-type, Fabaceae, Apiaceae, *Urtica* are occasionally present. *Sordaria*-type and *Pseudoschizaea* are present	An open, very degraded, probably rather dry landscape with some scrub and distant woodland. Ruderals and ephemerals prominent. Some evidence for cereal cultivation and a little animal grazing. Soil erosion was present but perhaps a little less prevalent than in earlier zones
SA-07	Lactuceae-Asteroideae	420–315	2220–1885 BC (4170–3805 BP)	High Lactuceae (15–25%), Asteroideae (6–14%). Some *Plantago lanceolata*-type (2–9%), Chenopodiaceae (3–6%), Caryophyllaceae (1–8%), *Senecio*-type (1–4%), *Rumex* (1–9%), Cyperaceae (0–11%), Poaceae (1–7%), Brassicaceae (1–3%). Some Ericaceae, Rosaceae, *Theligonum*, *Artemisia*, *Asphodelus*, *Cistus*, *Cirsium*-type, Fabaceae. *Pinus*, *Quercus*, *Daphne*, *Linum*, *Acacia*, *Plantago media/major*-type, *Agrostemma githago*, *Centaurea cyanus*-type, *Hordeum*-type, *Vitis, Ranunculus acris*-type, *Littorella*-type occasionally present. *Delitschia*-type, *Sporormiella*-type, *Sordaria*-type, *Pseudoschizaea* and VAMs sometimes present	An open, rather degraded landscape with ruderals and ephemerals prominent. Some scrub and garrigue and a little distant woodland. Arable agriculture and animal grazing were present and there were pulses of soil erosion at the bottom and top of the zone
SA-08	Chenopodiaceae	315–300	1326–1064 BC (3276–3014 BP)	Chenopodiaceae dominant (97%). Caryophyllaceae, Asteroideae, Brassicaceae are also present in small amounts	Probably a strong taphonomic imprint. Little can be deduced regarding the landscape, but the Chenopodiaceae include saltmarsh, coastal and exposed open ground taxa, including arable weeds
			Top of sample interval has an interpolated date of 1259–1006 cal. BC (3209–2956 cal. BP)		

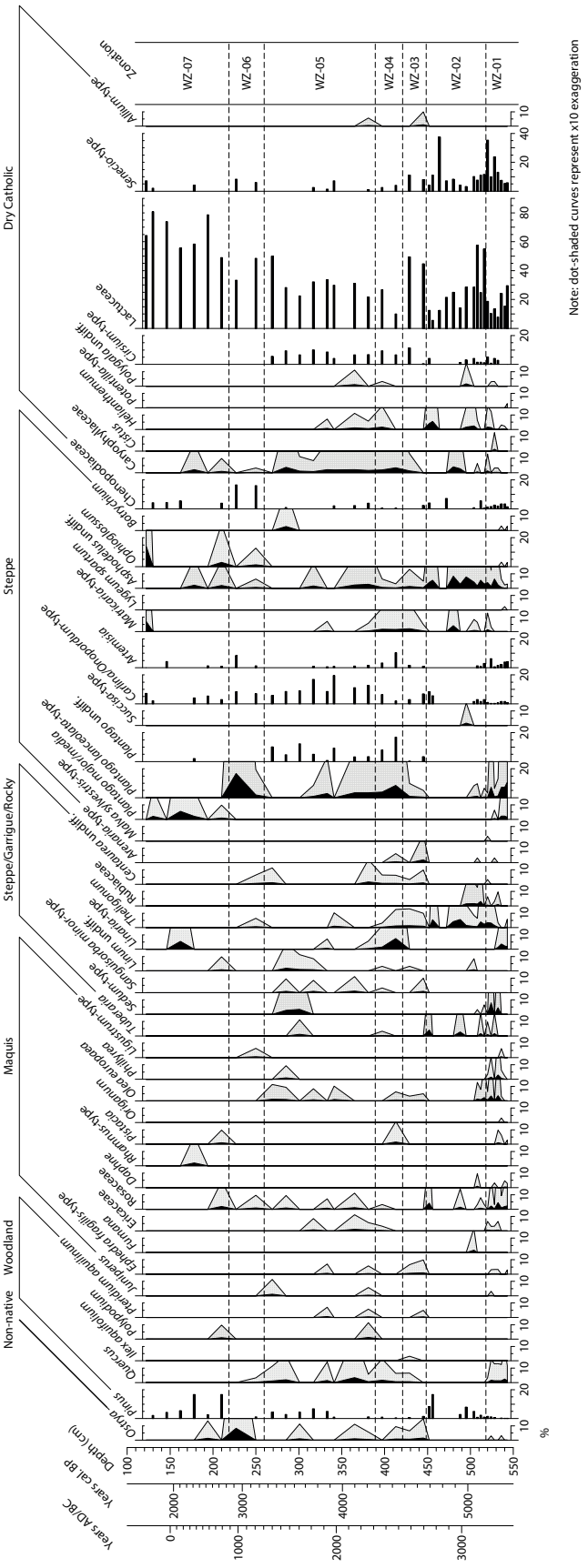

Figure 3.5. *Pollen zonation for the Wied Żembaq 1 core (M. Farrell).*

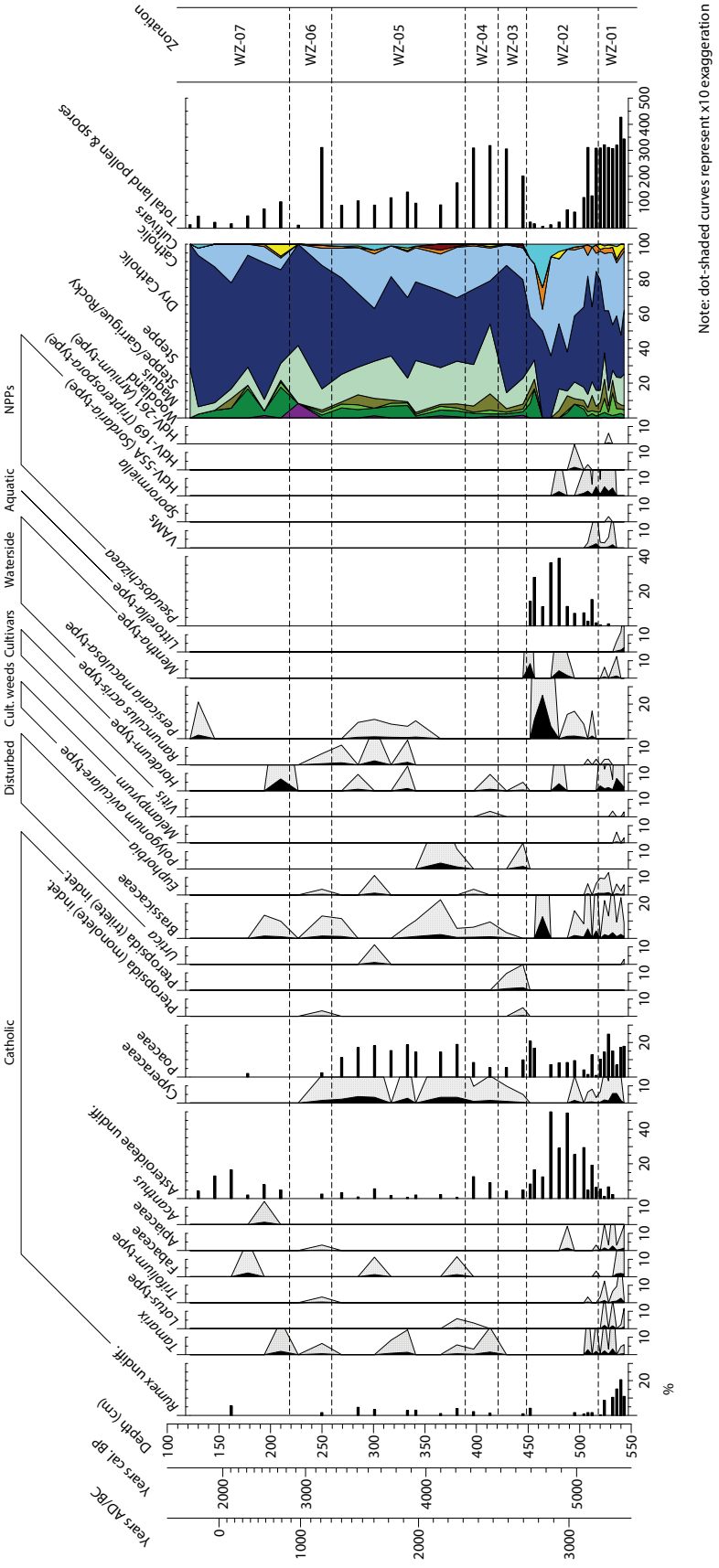

Figure 3.5 *(cont.).*

Table 3.6. *The pollen zonation of the Wied Żembaq 1 core with modelled age-depths.*

Zone	Defining taxa	Depth (cm)	Date ranges cal. BC (BP) for zone bases (2σ)	Characteristics	Interpretation
WZ-01	Lactuceae-Poaceae-*Senecio*-type-*Rumex*	550–520	3587–3352 BC (5537–5302 BP)	High Lactuceae (9–30%), Poaceae (7–25%), *Senecio*-type (5–37%), *Rumex* (10–20%) and *Plantago lanceolata*-type (1–11%). Some *Pinus, Quercus, Olea europaea, Ephedra fragilis*-type, Rosaceae, *Phillyrea, Sedum*-type, *Theligonum, Asphodelus*, Chenopodiaceae, *Helianthemum, Tamarix, Lotus*-type, *Trifolium*-type, Apiaceae, Cyperaceae, Brassicaceae, *Euphorbia, Hordeum*-type, *Mentha*-type and *Littorella*-type (>2%). *Vitis* is occasionally present. *Sordaria*-type, *Arnium*-type, *Sporormiella*-type, VAMs and *Pseudoschizaea* are sometimes present	A predominantly open landscape mosaic with grassland indicators, ruderals and ephemerals, some taxa typical of scrub and garrigue. There are indicators of cereal cultivation and grazing animals
WZ-02	Asteroideae-Lactuceae-*Senecio*-type-Poaceae	520–450	3330–3047 BC (5280–4997 BP)	Some very low counts, particularly in the top half of this zone. Very high Asteroideae (6–49%), high Lactuceae (6–54%), *Senecio*-type (2–38%), Poaceae (4–22%). Some *Pinus* (0–18%), *Theligonum* (0–5%), *Asphodelus* (0–8%), Brassicaceae (0–12%), *Persicaria maculosa*-type (0–23%). *Pseudoschizaea* are very high (2–39%). *Sordaria*-type, *Tripterospora*-type and VAMs are occasionally present	A very open degraded landscape with some intermittent cereal cultivation and animal grazing and very strong soil erosion. It is likely that these assemblages bear a strong taphonomic imprint consistent with erosion and redeposition of material from soil profiles since many common grains in this zone are known to be highly resistant to degradation and preferentially preserved in soils. It may therefore reflect a cluster of significant erosion and sedimentation events
WZ-03	Lactuceae-*Senecio*-type-Poaceae	450–420	2922–2542 BC (4872–4492 BP)	Very high Lactuceae (45–51%) with some *Senecio*-type (8–11%), Poaceae (8–12%), *Cirsium*-type (1–12%) and Asteroideae (5–6%). A little *Ostrya, Quercus, Olea europaea, Ephedra fragilis*-type, *Theligonum, Centaurea, Plantago lanceolata*-type, *Matricaria*-type, *Asphodelus*, Caryophyllaceae, and Cyperaceae. *Ilex aquifolium, Sanguisorba minor*-type, *Arenaria*-type, Chenopodiaceae, Brassicaceae, *Polygonum aviculare*-type and *Hordeum*-type are sometimes present	A very open landscape with a little scrub and woodland at a distance. It is likely, given the high percentage of degradation-resistant grains, that soil erosion continued but this could also reflect a vegetation dominated by ruderals and ephemerals. There are indications of a little cereal cultivation but the lack of dung fungi in this zone makes it difficult to be sure that animals were grazing
WZ-04	Lactuceae-*Plantago*-Asteroideae-Poaceae	420–390	2728–2322 BC (4678–4272 BP)	High Lactuceae (10–28%), *Plantago* spp. (7–18%), Asteroideae (9–12%), Poaceae (6–9%), *Cirsium*-type (7–10%), *Artemisia* (4–10%). Some *Linaria*-type (1–7%), *Carlina/Onopordum*-type (1–5%), *Senecio*-type (2–4%). A little *Ostrya, Pinus, Quercus, Theligonum, Centaurea, Matricaria*-type, *Asphodelus*, Caryophyllaceae, *Tamarix*, Cyperaceae, Brassicaceae. *Pistacia, Olea europaea*, Ericaceae, *Tuberaria, Sanguisorba minor*-type, *Linum, Arenaria*-type, *Helianthemum, Vitis, Hordeum*-type are occasionally present	An open landscape with a little scrub and distant woodland. Soil erosion probably continued but at a reduced rate and parts of the landscape may have started to stabilize. Taxa such as *P. lanceolata* and *Artemisia* are consistent with animal grazing; cereal agriculture and vine cultivation were also present

Table 3.6 *(cont.).*

Zone	Defining taxa	Depth (cm)	Date ranges cal. BC (BP) for zone bases (2σ)	Characteristics	Interpretation
WZ-05	Lactuceae-Poaceae-*Carlina*/*Onopordum*-type-*Plantago*-*Cirsium*-type	390–260	2529–2104 BC (4479–4054 BP)	Lactuceae (25–51%) very high. High Poaceae (15–20%), *Carlina*/*Onopordum*-type (6–20%), *Plantago* spp. (5–16%), *Cirsium*-type (4–10%). Some Asteroideae (1–6%). *Ostrya*, *Pinus*, *Quercus*, *Olea europaea*, Rosaceae, *Sanguisorba minor*-type, *Asphodelus*, Caryophyllaceae, *Helianthemum*, *Senecio*-type, *Rumex*, Cyperaceae, Brassicaceae, *Ranunculus acris*-type and *Persicaria maculosa*-type are often present	A very open steppic landscape with abundant ruderals and ephemerals. Some distant woodland but little scrub. Abundant *Plantago* suggests a great deal of animal grazing. Cereal cultivation was present at times. Areas of wetland were present. High Lactuceae and other degradation-resistant grains suggest continuing soil erosion
WZ-06	Lactuceae-Chenopodiaceae-*Carlina*/*Onopordum*-type	260–220	1501–1120 BC (3451–3070 BP)	Very low count size in uppermost sample of this zone. Very high Lactuceae (33–47%) and high Chenopodiaceae (16–17%). *Carlina*/*Onopordum*-type (9–11%), *Plantago lanceolata*-type (2–18%), *Senecio*-type (7–9%), *Artemisia* (1–8%) are present in all samples	An extremely open, eroding landscape with abundant ruderals and ephemerals. *Plantago* most probably reflects animal grazing. The high Chenopodiaceae most probably represents nearby saltmarsh vegetation in this coastal locality
WZ-07	Lactuceae-*Pinus*-Asteroideae	220–120	1021–819 BC (2971–2769 BP)	Some low counts in this zone, particularly towards the top. Very high Lactuceae (54–81%), high *Pinus* (2–17%) and Asteroideae (2–16%). *Plantago major/media*-type, *Carlina*/*Onopordum*-type, Chenopodiaceae are present in most samples	An extremely degraded steppic landscape with woodland at a distance and marked by strong soil erosion. The vegetation was characterized by ruderals and ephemerals, with nearby saltmarsh. It is possible that the relatively high *Pinus* reflects low local pollen productivity enhancing the regional pollen signal, rather than an expansion of woodland
			Top of sampled interval has an interpolated date of cal. AD 47–763 (1903–1187 cal. BP)		

in Figure 3.7 and Table 3.8. Chronological control is provided by radiocarbon dates on cereal grains recovered from the basal fills, ceramic typology and pollen biostratigraphy. The pollen analyses show significant taphonomic biases but generally suggest extremely open environments.

3.5.5. Santa Verna

Pollen analyses of the buried soil preserved below the floor sequence of the temple structure at Santa Verna, Gozo, exposed by the archaeological investigation, are summarized in Tables 3.9 and 3.11 and Figure 3.8. Pollen counts are very low and the assemblages are very small and probably taphonomically influenced, but the assemblages from the B horizon of the buried soil (contexts SV2/2, 2/3, 5/1, 5/2; see Chapter 5), which most likely dates from the earlier Neolithic, do not show strong evidence that corrosion resistant taxa are present in percentages typical of microbially active, strongly oxidizing environments, as seen in modern soils (Fig. 3.2; Table 3.3). This, along with the very high percentages of spores of liverwort and other lower plants is perhaps consistent with a perennially humid, local sheltered location and deposition in very damp sediments. The *Peridinium* cysts are suggestive of unshaded, mildly eutrophic freshwater. The later assemblage from the buried lower organic (Ah) horizon (context SV2/1) is too small for reliable interpretations to be made.

The combination of very abundant thermally mature (charred) material, plant cell walls and cuticle and fungal hyphae is typical of middens, while the high inertinite in the upper part of Santa Verna 2 (Fig. 3.8) is very typical of seasonally wet biologically active soils.

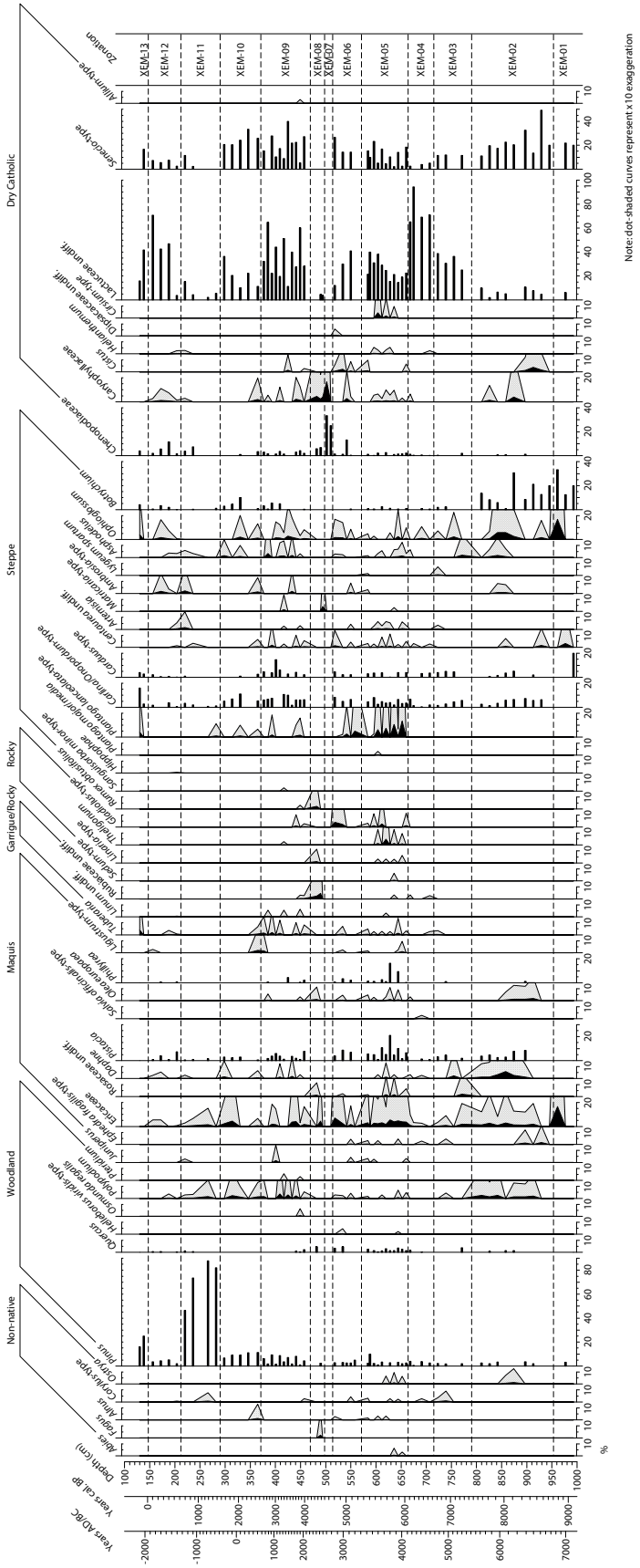

Figure 3.6. *Pollen zonation for the Xemxija 1 core (M. Farrell & L. Coyle-McClung).*

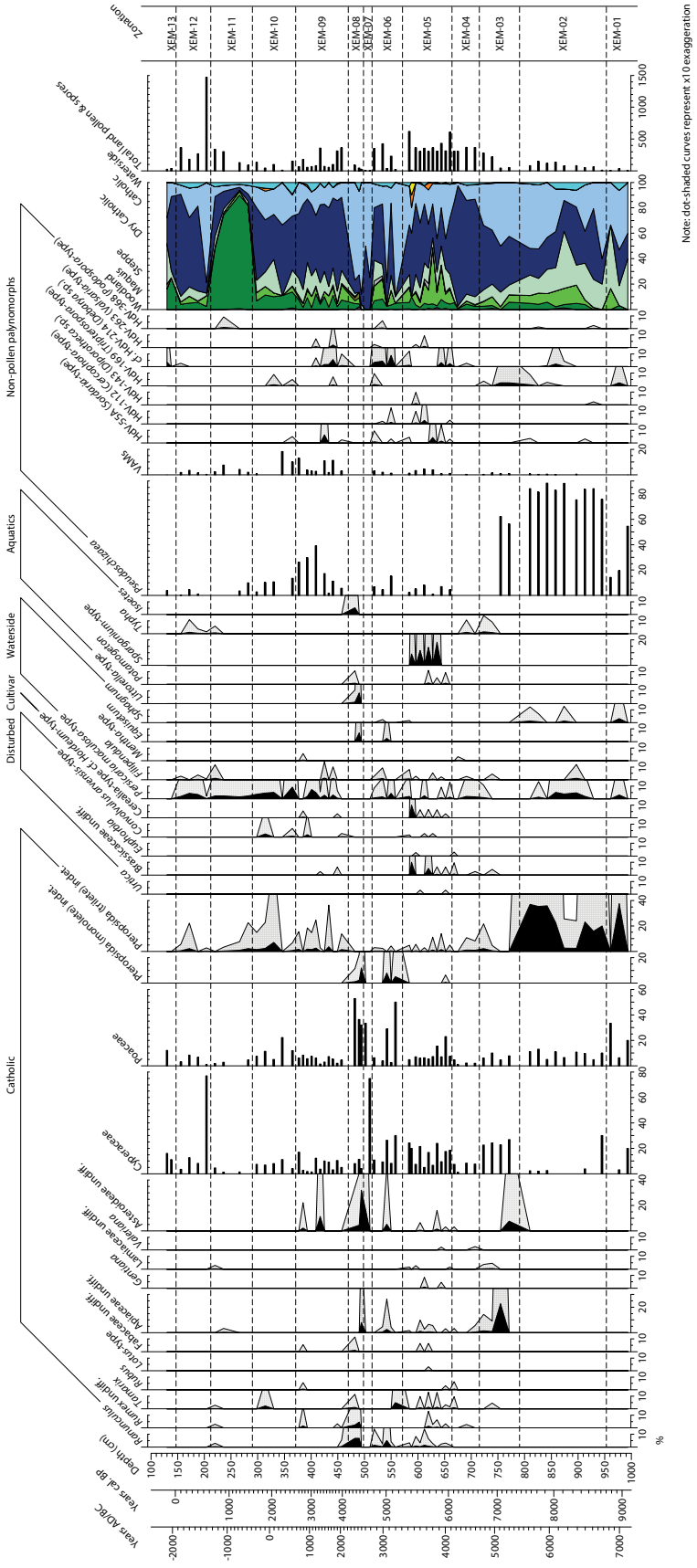

Figure 3.6 *(cont.).*

Table 3.7. *The pollen zonation of the Xemxija 1 core with modelled age-depths.*

Zone	Defining taxa	Depth (cm)	Date ranges cal. BC/AD (BP) for zone bases (2σ)	Characteristics	Interpretation
XEM-01	*Botrychium*-Poaceae	1000–950	7675–6861 BC (9625–8811 BP)	Extremely low pollen counts. High *Botrychium* (11–32%) and Poaceae (6–34%) with sporadic but strong occurrences of Pteropsida (trilete) (0–38%), *Senecio*-type (0–23%), Cyperaceae (0–20%), *Carduus*-type (0–19%), *Ophioglossum* (0–16%), Ericaceae (0–15%), Lactuceae (0–6%) and the occasional presence of *Pinus*, *Persicaria maculosa*-type and *Sphagnum*. *Pseudoschizaea* is common (12–54%) and *Tripterospora*-type is present in one sample	The very limited pollen counts and the high percentages of spores and other degradation-resistant grains constrain confident interpretation but assemblages are consistent with an open, grassy, virtually treeless steppe with ephemerals and ruderals prominent and with some scrub. The high percentages of *Pseudoschizaea* may reflect eroding soils
XEM-02	*Senecio*-type-*Botrychium*-Pteropsida (Trilete)-Poaceae	950–790	7066–6444 BC (9016–8394 BP)	Low pollen counts. High *Senecio*-type (10–48%), Pteropsida (trilete) (2–39%), *Botrychium* (1–30%), Poaceae (6–11%). Some *Pinus, Quercus*, *Olea europaea*, Ericaceae, *Pistacia*, *Daphne*, *Carlina*/*Onopordum*-type, *Asphodelus*, *Ophioglossum*, Lactuceae, *Persicaria maculosa*-type. Very high *Pseudoschizaea* (75–87%), a few VAMs, some *Sordaria*-type, *Tripterospora*-type, *Podospora*-type and *Debarya* sp.	The low pollen counts and considerable proportion of degradation-resistant grains constrain interpretation. Nevertheless, assemblages are consistent with an open grassy steppe with some ruderals and ephemerals, some scrub and distant woodland. Locally, a wetland with standing water is suggested by the green alga *Debarya* and the wetland taxa, while the very high *Pseudoschizaea* is consistent with considerable soil erosion
XEM-03	Lactuceae-Cyperaceae-Poaceae	790–715	5722–5255 BC (7672–7205 BP)	High Lactuceae (22–35%) and Cyperaceae (22–27%), some Poaceae (5–10%), *Carlina*/*Onopordum*-type (1.5–6%), Apiaceae (0–22%), *Senecio*-type (0–12%), *Carduus*-type (0–6%). *Pinus*, *Pistacia*, *Ophioglossum* and *Typha* are often present. *Pseudoschizaea* decline rapidly; VAMs and *Tripterospora*-type are present	Rising pollen counts may point to declining sedimentation rates, but the high proportion of degradation-resistant grains is consistent with continued soil erosion and complex taphonomic pathways. The rise in ephemerals and decline in grassland indicators suggests strong degradation of steppe habitats. Some scrub and wetlands were present
XEM-04	Lactuceae-Poaceae-Cyperaceae	715–660	4923–4439 BC (6873–6389 BP)	Very high Lactuceae (66–94%). Some *Pinus*, Ericaceae, Chenopodiaceae, Cyperaceae, Poaceae. *Persicaria maculosa*-type and *Typha* are occasionally present	The very high Lactuceae most likely reflect a taphonomic bias, most probably reflecting eroding soils, but may also reflect a high incidence of ephemerals and ruderals, given that *Pinus* and other degradation-resistant taxa are not heavily represented. There are hints from the rest of the assemblage of distant woodland, some scrub and wetlands with standing water, but the dominant signal is steppic
XEM-05	Lactuceae-Cyperaceae-Poaceae- *Senecio*-type- *Pistacia*	660–570	4251–3989 BC (6201–5939 BP)	High Lactuceae (15–40%), Cyperaceae (6–25%), Poaceae (4–23%), *Senecio*-type (4–22%), *Pistacia* (4–19%). Some *Pinus* (2–10%), *Quercus* (1–4%), Ericaceae (0–6%), *Carlina*/*Onopordum*-type (2–6%), *Plantago lanceolata*-type (0–14%), Chenopodiaceae (1–3%), Brassicaceae (0–9%), *Hordeum*-type (0–9%), *Sparganium*-type (0–18%).	The assemblages show a less strong taphonomic imprint than those lower in the sequence. Assemblages are consistent with a complex landscape with a mosaic of steppe, garrigue, maquis and local wetlands with perennial pools, and a little distant woodland. Soil erosion continued. There are clear signals for arable agriculture and animal grazing

Table 3.7 *(cont.).*

Zone	Defining taxa	Depth (cm)	Date ranges cal. BC/AD (BP) for zone bases (2σ)	Characteristics	Interpretation
				Olea europaea, Rosaceae, *Phillyrea*, *Tuberaria*, *Theligonum*, *Gladiolus*-type, *Carduus*-type, *Centaurea*, *Artemisia*, *Asphodelus*, *Ophioglossum*, *Botrychium*, Caryophyllaceae, *Cirsium*-type, *Ranunculus*, *Rumex*, Apiaceae, *Tamarix*, Asteroideae and *Potamogeton* are often present in small amounts. *Pseudoschizaea* and VAMs are present. *Sordaria*-type, *Cercophora*-type and *Debarya* sp. are often present	
XEM-06	Poaceae-Cyperaceae-Lactuceae-*Senecio*-type	570–520	3521–3102 BC (5471–5052 BP)	Count sizes very variable. High Poaceae (3–51%), Cyperaceae (11–31%), Lactuceae (0–42%), *Senecio*-type (0–27%). Some *Pinus* (4–5%), *Quercus* (0–5%), *Pistacia* (0–8%), Ericaceae (0–6%), *Phillyrea* (0–4%), *Plantago lanceolata*-type (0–5%), *Carlina*/*Onopordum*-type (0–9%), *Carduus*-type (0–5%), *Centaurea* (0–2%), *Ophioglossum* (0–2%), Chenopodiaceae (0–13%), *Cistus* (0–2%), *Ranunculus* (0–6%), Apiaceae (0–3%), *Persicaria maculosa*-type (0–5%). *Pseudoschizaea*, VAMs, *Sordaria*-type, *Cercophora*-type and *Debarya* sp. are sometimes present	These samples show a variable taphonomic imprint and count sizes are very variable. There are indications of a mosaic of steppe, garrigue, maquis, local wetland with standing water and distant woodland. There are signs of animal grazing
XEM-07	Chenopodiaceae-Cyperaceae-Caryophyllaceae	520–500	3048–2686 BC (4998–4636 BP)	Extremely low pollen counts. High Chenopodiaceae (26–34%), Cyperaceae (12–75%) and Caryophyllaceae (5–17%). Some *Persicaria maculosa*-type and Poaceae (0–35%)	These assemblages have very low pollen counts, but do not show a strong taphonomic imprint. They most probably derived from a very local pollen catchment. The indications are of a wetland environment with standing water and perhaps nearby saltmarsh
XEM-08	Poaceae-Asteroideae-*Ranunculus*	500–470	2824–2503 BC (4774–4453 BP)	Some low pollen counts. Very high Poaceae (34–54%). High Asteroideae (5–31%) and *Ranunculus* (4–8%). Some Ericaceae (0–6%), Rubiaceae (0–4%), Caryophyllaceae (2–5%), Chenopodiaceae (0–8%), *Rumex* (1–5%), Pteropsida (monolete) (1–10%), *Equisetum*, *Littorella*-type, *Potamogeton* and *Isoetes*	Rather small pollen counts constrain interpretation, but there appears to be fairly strong ecological coherence, suggesting that taphonomic alteration was limited. There is a strong successional pattern, suggesting marshland taxa giving way to aquatics in the local environment. It is likely that some of the Poaceae pollen reflects reeds rather than grasses. Away from the wetland was steppe, maquis and perhaps a little distant forest
XEM-09	Lactuceae-*Senecio*-type-*Pinus*- Poaceae-Cyperaceae	470–370	2401–2092 BC (4351–4042 BP)	Some low pollen counts in this zone. High Lactuceae (11–64%) and *Senecio*-type (8–38%). Some Cyperaceae (1–22%), *Pinus* (1–10%), *Carlina*/*Onopordum*-type (0–11%), Poaceae (1–8%). Ericaceae, *Pistacia, Daphne, Tuberaria, Carduus*-type, *Asphodelus, Ophioglossum*, Chenopodiaceae, Caryophyllaceae and *Persicaria maculosa*-type are generally present and *Hordeum*-type is occasionally	The pollen catchment for this zone appears larger than for the previous zones. An open, strongly eroding landscape with rather degraded steppe, scrub and a little distant woodland is indicated, with the site likely a wetland containing shallow pools. There are signs of some grazing animals and occasional cereal cultivation

Table 3.7 *(cont.).*

Zone	Defining taxa	Depth (cm)	Date ranges cal. BC/AD (BP) for zone bases (2σ)	Characteristics	Interpretation
				present. *Pseudoschizaea* and VAMs are common, *Debarya* sp. is often present and *Sordaria*-type, *Tripterospora*-type and *Valsaria*-type are sometimes present	
XEM-10	*Senecio*-type-Lactuceae-Poaceae-Cyperaceae-*Pinus*-	370–290	736–321 BC (2686–2271 BP)	Some very low pollen counts. High *Senecio*-type (20–34%), Lactuceae (10–36%), Poaceae (5–23%), Cyperaceae (5–17%), *Pinus* (7–14%). Ericaceae, *Pistacia, Plantago lanceolata*-type, *Carlina/Onopordum*-type, *Asphodelus, Ophioglossum, Botrychium, Convolvulus arvensis*-type and *Persicaria maculosa*-type are sometimes present. *Pseudoschizaea*, VAMs, *Tripterospora*-type and *Sordaria*-type are occasionally present	Counts are very low and there appears to be a reasonably strong taphonomic imprint in this zone, with high percentages of degradation-resistant grains. Nevertheless, a vegetation mosaic with degraded steppe, some scrub and distant woodland is suggested. The wetland suggested for previous zones appears to have been drier, without permanent pools. There were disturbed soils and some soil erosion took place
XEM-11	*Pinus*-Lactuceae-Poaceae	290–215	AD 141–570 (1809–1380 BP)	Some low pollen counts in the lower half of this zone. Very high *Pinus* (47–86%). Some Lactuceae, Poaceae, Cyperaceae, *Carlina/Onopordum*-type. *Persicaria maculosa*-type is often present. VAMs, some *Pseudoschizaea* and occasional *Podospora*-type are present	The extremely high percentages of *Pinus* pollen are consistent with nearby pine woodland: in this Late Holocene Maltese context, this most likely reflects a pine plantation rather than natural vegetation. Other vegetation was likely a mosaic of degraded steppe with a little scrub with eroding soils. It is likely that the depositional site was seasonally dry
XEM-12	Lactuceae-Cyperaceae	215–150	AD 1092–1509 (858–441 BP)	Very high Lactuceae (5–71%) and Cyperaceae (5–78%). Some Chenopodiaceae (2–12%), Poaceae (3–9%), *Pistacia* (1–9%), *Senecio*-type (2–8%), *Pinus* (2–6%). A little Ericaceae, *Daphne*, *Phillyrea*, *Carlina/Onopordum*-type, *Carduus*-type, *Ambrosia*-type, *Ophioglossum*, *Botrychium*, Caryophyllaceae, *Persicaria maculosa*-type, *Filipendula* and *Typha* in some samples. Some VAMs, *Pseudoschizaea*, and a little *Debarya* sp. in one sample	A very variable taphonomic signal is present in this zone, with a major influx of degradation-resistant Lactuceae grains in the upper part. The assemblages are otherwise consistent with a mosaic landscape with grassy and degraded steppe, scrub and distant woodland. There is evidence for eroding soils and for a local wetland environment with near-permanent pools supporting emergent aquatics by the end of the zone
XEM-13	Lactuceae-*Pinus*-Cyperaceae	150–130	AD 1845–1963 (105–13 BP)	Abundant Lactuceae (16–42%), *Pinus* (15–26%), Cyperaceae (11–16%). Some *Carlina/Onopordum*-type (3–16%) and *Carduus*-type (2–4%). *Tuberaria*, *Plantago lanceolata*-type, *Ophioglossum*, *Botrychium*, Chenopodiaceae, *Senecio*-type and Poaceae are sometimes present. *Pseudoschizaea* and *Debarya* sp. are occasionally present	Counts are extremely low and the proportion of degradation-resistant grains is high, suggesting a marked taphonomic imprint. The high *Pinus* is likely consistent with the presence of pine woodland, most probably a plantation, though further away or less sizeable than that suggested for XEM-11. The other taxa are suggestive of a degraded steppeland, some grassland and some scrub or garrigue. Soils were eroding and shallow pools were present on the deposition site
			Natural sedimentation appears to have ceased during the twentieth century		The uppermost 1.3 m of this core appears to be made ground of twentieth century age.

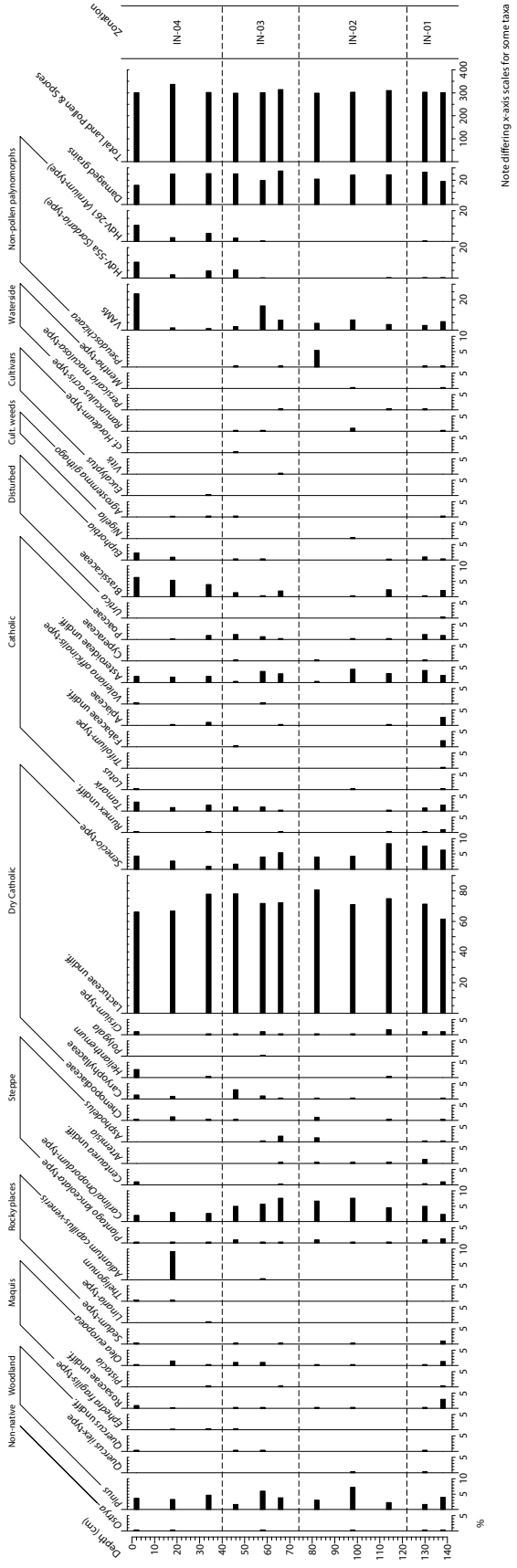

Figure 3.7. *Pollen zonation for the pit fills at In-Nuffara (M. Farrell).*

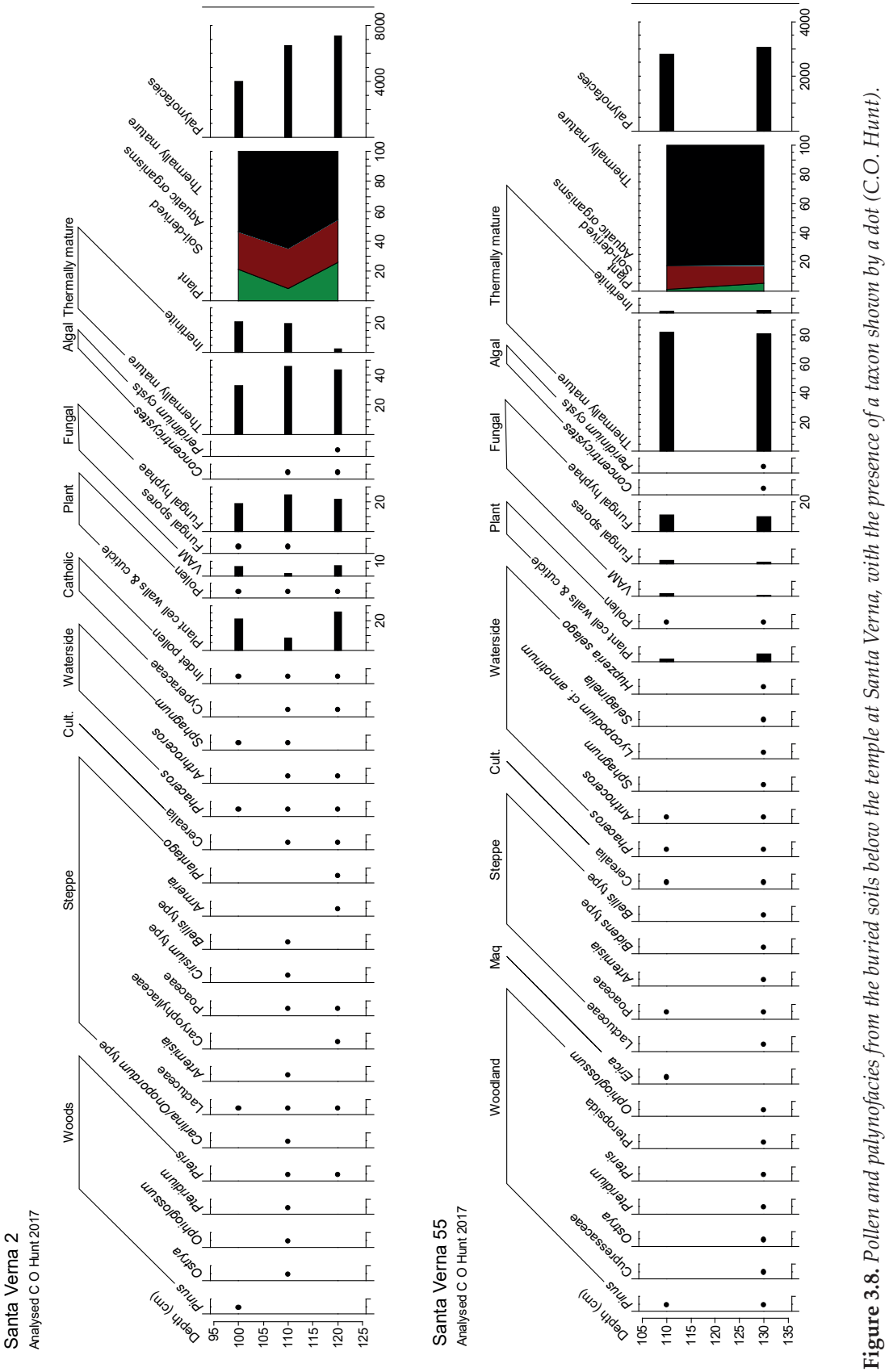

Figure 3.8. *Pollen and palynofacies from the buried soils below the temple at Santa Verna, with the presence of a taxon shown by a dot (C.O. Hunt).*

Table 3.8. *The pollen zonation of the fill of a Bronze Age silo at In-Nuffara, Gozo.*

Zone	Contexts	Defining taxa	Depths (cm)	Period	Characteristics	Interpretation
IN-01	46, 41	Lactuceae-*Senecio*	138–125	Borġ in-Nadur	Dominated by Lactuceae (62–70%). Also present are *Pinus* (2–5%), *Tamarix* (1–3%), *Olea* (1–2%), Rosaceae (0.5–4%), *Rumex* (0.5–1.5%), *Euphorbia* (0.5–1%), *Plantago lanceolata*-type (1–2%), *Carlina/Onopordum*-type (3–6%), *Cirsium*-type (1%), *Centaurea* (0.5%–1), *Senecio*-type (6–8%), Poaceae (1–3%), Asteroideae (2–4%), *Asphodelus* (1%), Brassicaceae (1–2%). VAMs (2–5%) and *Pseudoschizaea* (2%) present in small amounts	Assemblages highly biased taphonomically and showing signs of the recycling of material derived from soil profiles through erosion. Landscape predominantly open steppe, with some scrub. Considerable evidence for grazing and consequent vegetation degradation in the wider landscape
IN-02	41–40	Lactuceae-*Carlina/Onopordum*-type-*Senecio*	125–72	Punic	Dominated by Lactuceae (70–80%. Also present are *Pinus* (3–7%), *Plantago lanceolata*-type (0.5–1%), *Carlina/Onopordum*-type (5–8%), *Senecio*-type (4–9%), Asteroideae (1–4%). VAMs present (4–5%)	Assemblages highly biased, with erosional recycling of material from soil profiles. Landscape mostly very open steppe, probably heavily degraded by grazing
IN-03	39–37	Lactuceae-*Carlina/Onopordum*-type	72–42	Roman–Knights	Dominated by Lactuceae (74–79%). Also present are *Pinus* (2–6%), *Tamarix* (1–2%), Caryophyllaceae (1–3%), *Plantago lanceolata*-type (0.5–1%), *Carlina/Onopordum*-type (6–8%), *Senecio*-type (2–6%), Asteroideae (0.5–4%), Poaceae (0.5–2%), Brassicaceae 1–2%). VAMs present in all samples (2–16%). First appearance of *Hordeum*type and spores of *Arnium*-type and *Sordaria*-type	Assemblages highly biased and with recycling of material from soil profiles. Landscape rather open grassy grazed steppe with some scrub. Minor cereal cultivation. Fungal spores provide evidence for grazing adjacent to the deposition site
IN-04	36–34	Lactuceae-Brassicaceae-*Pinus*	42–0	nineteenth–twentieth centuries AD	Dominated by Lactuceae (71–76%). Also present are *Pinus* (4–5%), *Olea europaea* (1–2%), *Tamarix* (1–2.5%), Chenopodiaceae (0.5–1%), *Plantago lanceolata*-type (0.5%), *Carlina/Onopordum*-type (2–4%), *Senecio*-type (1–5%), Asteroideae (2%), Brassicaceae (4–7%). VAMs (1–38%), *Arnium*-type (2–19%), *Sordaria*-type (2–18%) present. First appearance of *Eucalyptus*	Highly biased assemblages with evidence for recycling of material from soil profiles. Landscape rather open increasingly degraded steppe with some scrub. Possible increase in grazing pressure at top of zone

Table 3.9. *Summary of the pollen analyses of the buried soil below the Santa Verna temple structure.*

Contexts	Defining taxa	Depths (cm)	Period	Characteristics	Interpretation
SV2/2, 2/3, 5/1, 5/2	*Phaceros-Anthroceros*-Lactuceae	110–140	Earlier Neolithic pre-5500 cal. BC (pre-7500 cal. BP)	Woodland taxa 10% (*Pinus*, Cupressaceae, *Ostrya*, *Pteris*, Pteropsida, *Ophioglossum*, *Pteridium aquilinum*), maquis taxa 1% (*Erica*), steppe taxa 15% (*Carlina/Onopordum*-type, Lactuceae, *Artemisia*, Caryophyllaceae, Poaceae, *Cirsium*-type, *Bellis*-type, *Bidens*-type, *Armeria*, *Plantago*), cultivated taxa 9% (cereals), waterside taxa 61% (*Phaceros*, *Anthroceros*, *Sphagnum*, *Lycopodium* cf. *annotinum*, *Selaginella*, *Huperzia selago*, Cyperaceae, 24% *Peridinium* cysts, 8% *Pseudoschizaea*	Very small, highly taphonomically influenced assemblages. An open steppic landscape with some woodland patches, grazed land and cereal cultivation. The abundant waterside plants and *Pseudoschizaea* are consistent with damp, sheltered soils close to water. The planktonic *Peridinium* cysts suggest the presence of mildly eutrophic fresh water
SV2/1	*Pinus*-Lactuceae-*Phaceros-Sphagnum*	100	Early Neolithic 5500–3800 cal. BC (7500–5800 cal. BP)	Presence of *Pinus*, Lactuceae, *Phaceros* and *Sphagnum*	Extremely small assemblage, in which all recorded taxa are known to be degradation-resistant. Suggestive perhaps of the presence of woodland, steppe and damp habitats

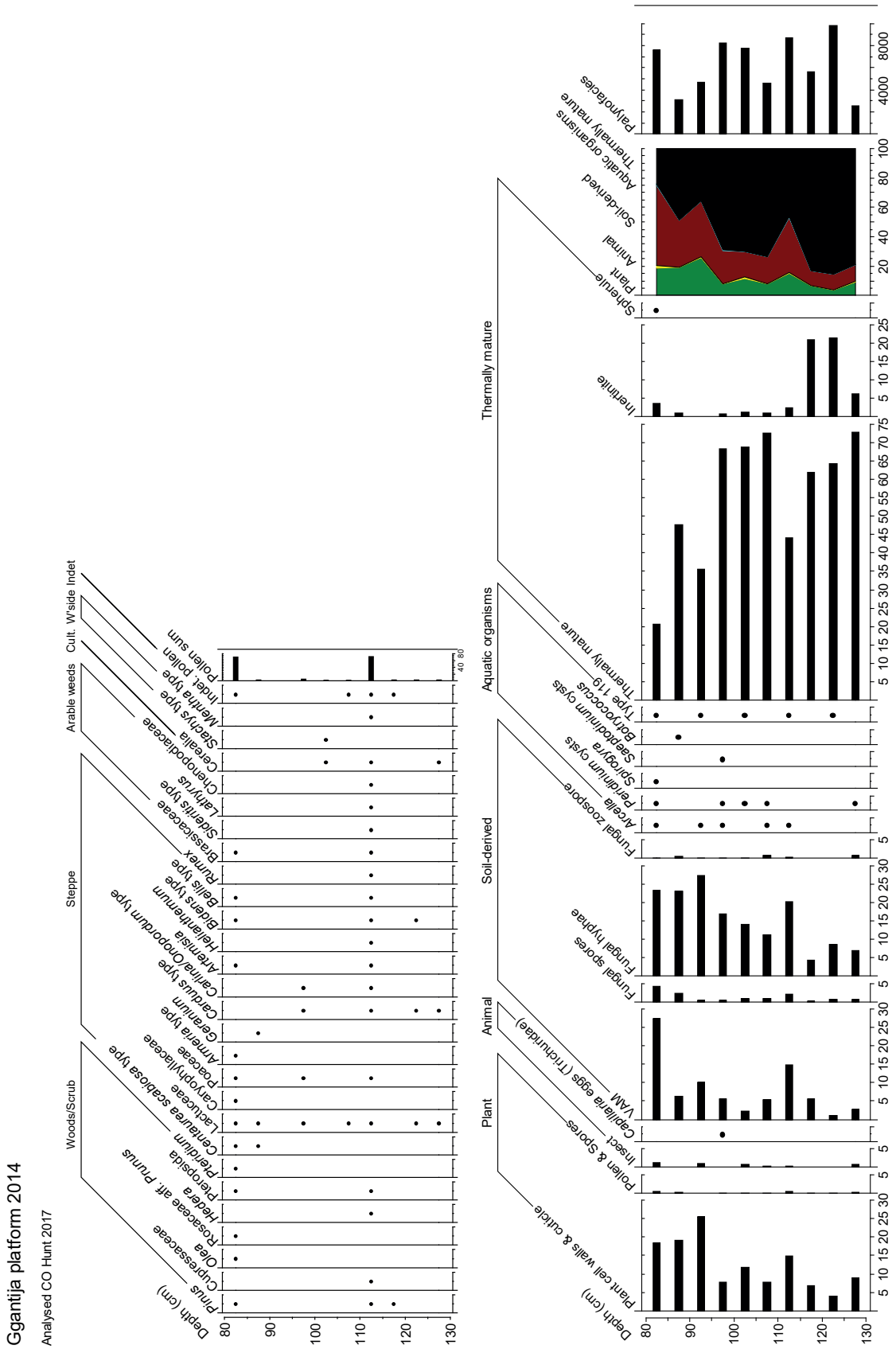

Figure 3.9. *Pollen and palynofacies from Test Pit 1 on the southwestern edge of the Ġgantija platform, with the presence of a taxon shown by a dot (C.O. Hunt).*

Table 3.10. *Summary of the pollen analyses from the buried soil in Ġgantija Test Pit 1.*

Defining taxa	Depths (cm)	Period	Characteristics	Interpretation
Lactuceae-*Hedera-Pinus*	110–130	Tarxien	Woodland/maquis taxa 34% (*Pinus, Quercus*, Cupressaceae, *Hedera*, Pteropsida), steppe taxa 43% (Lactuceae, Poaceae, *Carduus*-type, *Carlina/Onopordum*-type, *Artemisia*, *Helianthemum*, *Bidens*-type, *Bellis*-type, *Rumex*), cereals 5%, agricultural weeds 9% (Brassicaceae, *Sideritis*-type, *Lathyrus*, Chenopodiaceae), waterside taxa 5% (*Tamarix*, *Mentha*-type, *Anthoceros*). Algae 37% (mostly Type 119)	Moderately taphonomically biased assemblages, but suggestive of some woodland (the rather high *Hedera* could have been growing on stonework), open steppe, arable land, damp habitats. Algal assemblage suggestive of rather eutrophic standing water
Lactuceae	85–110	Tarxien	Woodland/maquis taxa 7% (*Pinus, Olea europaea*, Rosaceae aff. *Prunus*, Pteropsida, *Pteridium aquilinum*), steppe taxa 85% (*Centaurea scabiosa*-type, Lactuceae, Caryophyllaceae, Poaceae, *Armeria*-type, *Geranium*, *Carduus*-type, *Carlina/Onopordum*-type, *Artemisia*, *Bidens*-type), cereals 1%, agricultural weeds 1%, waterside taxa 1%. Algae 64% (mostly Type 119 and *Peridinium* sp.)	Strongly taphonomically biased assemblages dominated by Lactuceae. Suggestive of a little woodland/scrub, very open, dry, somewhat degraded steppe, minimal damp habitats and somewhat eutrophic standing water

Table 3.11. *Activity on Temple sites and high cereal pollen in adjacent cores. Pollen data from* FRAGSUS Project*, Carroll* et al. *(2012), Djamali* et al. *(2013) and Gambin* et al. *(2016) and periods of human activity (C. Malone, pers. comm.). Grey shading indicates periods not sampled for palynology in coring or during archaeological excavation. Archaeologically attested or inferred periods of activity on megalithic sites are indicated with an 'a'. Anomalously high cereal pollen values are indicated with an 'h'.*

	Tas-Silġ temple	Tas-Silġ middens	Borġ in-Nadur temple	Wied Żembaq core	Tarxien/Ħal Saflieni temple	Marsa core (Carroll *et al.* 2012)	Buġibba temple	Salina Bay (Carroll *et al.* 2012)	Tal Qadi temple	Burmarrad BM1 and BM2 cores (Djamali *et al.* 2013; Gambin *et al.* 2016)	Xemxija temple	Xemxija core	Ġgantija temple	Ġgantija soils	Santa Verna temple	Santa Verna soils
Later Bronze Age		h	a	h		h										
Tarxien Cemetery					a											
Thermi Ware	a															
Tarxien	a	h			a		?	h					a	h		
Saflieni	a		a		a		?		a				a			
Ġgantija	a		a	h	a	h	?	h	a		a	h	a		a	
Mgarr	?		a		a	h	?	h	?			h	a		a	
Żebbuġ	?				a	h	?	h	?						a	
Earlier Neolithic						h							a		a	h

The algal microfossils suggest that the sites were in receipt of slightly eutrophic standing or slow-moving water or sediments derived therefrom. Representative material is illustrated in Figure 3.10.

3.5.6. Ġgantija

Pollen analyses of the buried soil as exposed in Test Pit 1, located immediately to the southwest of Ġgantija temple are summarized in Tables 3.10 and 3.11 and Figure 3.9. Pollen counts are very low, but peaks in pollen occurrence and the coincident peak in vesicular arbuscular miccorhyzae (VAM) suggests episodes of soil stability around 115 and 85 cm. The combination of very abundant thermally mature (charred) material, plant cell walls and cuticle and fungal hyphae is typical of middens, while the high inertinite in the lower part

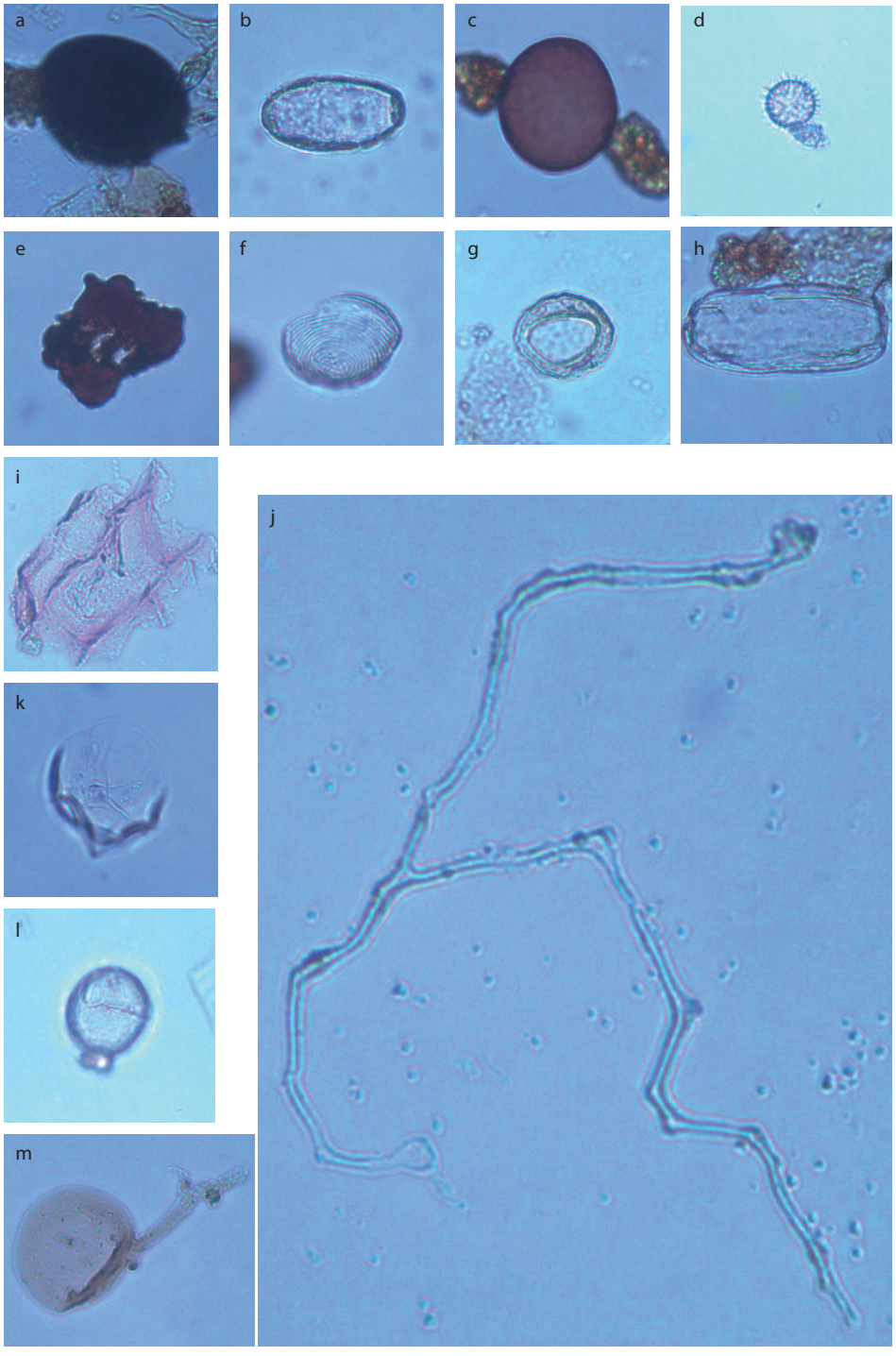

Figure 3.10. *Photomicrographs (×800) of key components of the palynofacies at Santa Verna and Ġgantija: a) Spherule, Ġgantija 80–85 cm; b)* Capillaria *egg, Ġgantija 95–100 cm; c) fungal spore, Santa Verna 2, 105–115 cm; d) fungal zoospore, Ġgantija 95–100 cm; e) thermally mature (charred) material, Santa Verna 2, 105–115 cm; f)* Concentricystes *sp., Santa Verna 2, 105–115 cm; g) Type 119, Ġgantija 80–85 cm; h)* Spirogyra *sp. aplanospore, Ġgantija 80–85 cm; i) plant cuticle, Santa Verna 2, 105–115 cm; j) fungal hypha, Santa Verna 2, 105–115 cm; k)* Saeptodinium *sp. cyst showing large compound archaeopyle, Ġgantija 95–100 cm; l)* Peridinium *sp. cyst showing incipient compound archaeopyle, Santa Verna 55, 120–140 cm; m) vesicular arbuscular miccorhyza, Santa Verna 2, 105–115 cm (C.O. Hunt).*

of the section is very typical of seasonally wet biologically active soils. The nematode *Capillaria* gives rise to a hepatitis-like zoonotic disease causing liver failure in humans, but it can also affect a variety of animal hosts. The algal microfossils suggest that the site was in receipt of fairly eutrophic slow moving or standing water or sediments derived therefrom. Representative material is illustrated in Figure 3.10.

Two phases of sedimentation are evident, both dating to the Tarxien phase. The earlier assemblages (130–110 cm) suggest some soil erosion and a landscape with woodland, open steppe and damp habitats close to water. A rather eutrophic water body nearby is suggested by the algal microfossil assemblage. The later assemblages (110–85 cm) show rather strong soil erosion and a drier landscape with a little woodland, open steppe and less evident damp habitats. The water body had by this time become slightly less eutrophic.

3.6. Synthesis

3.6.1. Pre-agricultural landscapes (pre-5900 cal. BC)

The basal sections of the deeper cores are characterized by extremely sparse pollen assemblages, which show evidence of strong taphonomic bias. The Salina Deep Core has a basal section which predates 7042–6553 cal. BC (8992–8503 cal. BP), consisting of poorly sorted gravels interbedded with incipient palaeosol material, some of which contain pedogenic carbonates. These deposits relate to terrestrial fluvial and colluvial environments, most probably present during the Late Pleistocene and perhaps the Early Holocene, by comparison with similar deposits described by Hunt (1997). The very sparse pollen survival in these deposits may be consistent with dry terrestrial environments supporting steppe and scrub vegetation, as might be expected during interstadial episodes (Hunt 1997), but extremely low numbers of pollen grains and poor pollen preservation caution against reliance on these assemblages.

The basal 3.4 m of the Xemxija 1 core is also rather problematic as the sediments are heavily pedogenically altered. The pollen assemblages contained within are extremely small and appear to have been significantly altered by strongly oxidizing and biologically active terrestrial environments. Indeed, the micromorphological analysis of this core suggests that at least the basal *c*. 1.2 m of sediments are probably eroded soils from the immediate catchment, which are similar to the soils observed beneath several of the Neolithic temple sites and would have undergone some pedogenesis once re-deposited in the base of the valley bottom (see Chapter 5). The abrupt changes in pollen assemblages throughout this core may also suggest that there are sedimentary discontinuities associated with erosion episodes. The latter point may indicate that the modeled ages could be unreliable, but the progressively consistent spread of dates over the last *c*. 8000 years suggests otherwise (see Chapter 2).

Some time after about 8000 cal. BC, shallow marine sedimentation became established at the Salina Deep Core site (Table 2.4). Thereafter, continuing sedimentation was off-set by rising sea level, and it may be suggested that sediment accumulation was essentially continuous. The reducing environment offered by shallow marine sediments led to preservation of sufficient pollen to recognize the biostratigraphy shown in Figure 3.3 and Table 3.4. As with the modern marine samples from the Mistra catchment discussed above, the assemblages show taphonomic biases but these can be accounted for in the interpretation (Table 3.4 and below). These are the oldest reliable data available from which to reconstruct Maltese Holocene vegetation history. Previously the earliest Holocene palynological data from Malta were from the BM1 sequence from Burmarrad, with the oldest sediments there dated to *c*. 5350 cal. BC (7300 cal. BP) (Marriner *et al*. 2012; Djamali *et al*. 2013; Gambin *et al.* 2016).

It is well documented that attempting to disentangle natural climatically forced events from anthropogenic impacts in the palynological record is extremely difficult (e.g. Caló *et al*. 2012; Carroll *et al*. 2012; Djamali *et al*. 2013; Gambin *et al.* 2016; Chapman 2018). Prior to the arrival of farming people in the Maltese Islands, any changes in vegetation would have most likely resulted from environmental processes. The basal pollen zones in the Salina Deep Core (SDC-02 to 05) suggest the cyclic spread of *Pistacia* (lentisk) scrub into steppe landscapes in Salina Deep Core zone SDC-02 at 7042–6553 cal. BC (8992–8503 cal. BP) and zone SDC-04 at 6489–6135 cal. BC (8439–8085 cal. BP). The repeated spread of *Pistacia* was most probably driven by periods of increasing effective humidity within a generally very dry period. *Pistacia* is generally accepted to be under-represented in modern day pollen assemblages (Wright *et al*. 1967; Collins *et al*. 2012; Djamali *et al.* 2013), and the percentages found in these zones indicate dense lentisk-dominated vegetation. Djamali *et al.* (2013) review the edaphic conditions required for *Pistacia* species – an expansion in this taxon may be indicative of high moisture availability either through humidity or increased precipitation (Tinner *et al.* 2009; Carroll *et al.* 2012; Djamali *et al*. 2013; Gambin *et al*. 2016). The very short duration of these episodes seems to have precluded significant expansion of other scrub or woodland taxa, but the substantial decline in *Pseudoschizaea* and vesicular arbuscular mycorrhizae (VAMs) in the Salina Deep Core zones SDC-02 and

SDC-04 also point to the dense vegetation canopy reducing soil erosion. Equivalent chronologically to the second *Pistacia* peak, a humid episode among general aridity is reported in Sicily and in southeastern Spain at *c*. 6450 cal. BC (8400 cal. BP) (e.g. Reed *et al*. 2001; Tinner *et al*. 2009).

Intervening zones in the Salina Deep Core SDC-03 at 6858–6419 cal. BC (8808–8369 cal. BP) and SDC-05 at 6350–6037 cal. BC (8300–7987 cal. BP) show an increase in herbs including grasses, Chenopodiaceae, *Asphodelus* and sporadic occurrences of *Plantago lanceolata*, *Urtica*, Brassicaceae and *Convolvulus arvensis*-type. While some species of *Asphodelus* can be favoured by nutrient-deficient soils resulting from over-grazing, it is also known to colonize rapidly newly exposed ground surfaces following fires (Pantis & Margaris 1988; Abel-Schaad & López-Sáez 2013). Fungal ascospores are also present, with *Podospora*-type (Dietre *et al.* 2012) and *Tripterospora*-type considered to be coprophilous, growing on the dung of large herbivores, while *Diporotheca rhizophila* is associated with nitrogen-rich environments (van Geel *et al*. 2003). Studies of modern palynological assemblages have shown that these ascospores are not dispersed over long distances (Blackford & Innes 2006) and therefore they can be interpreted as indicative of grazing animals close to the deposition site, whether these were naturally present or introduced by people. It has been argued that navigation in the central Mediterranean Sea may have occurred as early as *c*. 8000 cal. BC (9950 cal. BP) (Broodbank 2013) and that temporary exploration and occupation of Malta might have occurred prior to the establishment of permanent settlements (Gambin *et al.* 2016). No archaeological evidence has been identified from this period, however, and whilst the present day mammalian fauna of Malta is relatively impoverished, comprising only around 21 species (Schembri 1993), it is possible that a dwarfed form of red deer was present in the earlier Holocene (Hunt & Schembri 1999). The presence of coprophilous fungal spores could therefore represent either native herbivores or (less likely) wild species introduced by early pioneer settlers. Regression of scrub and woodland was accompanied by rising *Pseudoschizaea* and VAMs, indicating increased erosion in the catchment area (Argant *et al.* 2006; Ejarque *et al*. 2011; Estiarte *et al*. 2008; Gambin *et al.* 2016; van Geel *et al*. 1989). This is likely to have been related to the decline in vegetation cover, as the exposed soil surface would have been more vulnerable to removal via surface run-off.

The expansion of steppe habitats in Salina Deep Core zones SDC-03 and SDC-05 may be consistent with periods of general precipitation decline in Malta. The second of these events (in zone SDC-05) coincides chronologically with the widely reported 8.2 ka BP event which led to cooling in the North Atlantic and aridification in the Mediterranean coastlands (e.g. Barber *et al.* 1999; Weninger *et al.* 2006; Bini *et al*. 2018; Chapman 2018), although the second part of this zone shows a small increase in *Quercus* (oak) pollen, suggesting perhaps the end of climate severity.

3.6.2. First agricultural colonization (5900–5400 cal. BC)

A key point in the Salina Deep Core is at 22.65 m, where pollen zone SDC-06, commencing at 6067–5821 cal. BC (8017–7771 cal. BP), is marked by assemblages containing pollen of cereals. These include both *Avena*/*Triticum* type (oats/wheat) and *Hordeum*-type (barley) and a ruderal flora including *Convolvulus, Borago, Scrophularia* and *Sideritis*, all of which are often associated with arable farming (Fig. 3.3). It is very likely that arable agriculture was established in the vicinity of the present-day Salina salt pans, since cereal pollen is produced in low quantities and is not well-dispersed (Edwards & McIntosh 1988). Pollen of *Plantago lanceolata*-type (ribwort plantain) and *Urtica* (nettle) may indicate grazing. The presence of a range of fungal ascospores, including the coprophilous taxa *Podospora*-type, *Tripterospora*-type, *Sordaria*-type and *Arnium imitans*-type and the nitrophilous *Diporotheca rhizophila*-type is strongly suggestive of the presence of grazing animals locally. The assemblages also show very high incidences of *Pseudoschizaea*, which is of likely fungal origin (Milanesi *et al.* 2006) and associated with damp calcareous soils. Large numbers of this palynomorph deposited in a marine environment are likely to reflect enhanced soil erosion. All these indicators suggest that the base of this zone may reflect the initial colonization of this area by people using cereals and domestic animals, and thus also reflect the beginning of the Neolithic in the Maltese Islands, suggesting that it occurred at 6067–5821 cal. BC (8017–7921 cal. BP). Such an early date was not expected on archaeological grounds, but is broadly consistent with other first Neolithic dates in the central and western Mediterranean (e.g. de Vareilles *et al*. 2020; Zeder 2008; Zilhao 2001), and strengthens the hypothesis for a seaborne Neolithic diaspora from the eastern Mediterranean in response to instability caused by the 8.2 ka BP climate event (i.e. Weninger *et al*. 2006; Zeder 2008).

The vegetation suggested by assemblages in Salina Deep Core zone SDC-06 otherwise comprises a very grassy steppe with some maquis and garrigue and very minor woodland, suggesting a relatively dry seasonal Mediterranean climate. The rise of the drought-resistant but frost-sensitive *Phillyrea* (false privet) might suggest strengthening summer droughts and relatively warm winters at this time.

3.6.3. Early Neolithic (5400–3900 cal. BC)

Plantago lanceolata-type (ribwort plantain, very often associated with grazed pasture) rises strongly in the Salina Deep Core zone SDC-07 at 5625–5419 cal. BC (7575–7369 cal. BP) shortly after the date of the first known archaeological evidence for human activity in the Maltese Islands (Fig. 3.4). Coincident with this, pollen of Lactuceae rises. High percentages of Lactuceae are generally accepted to be indicative of poor pollen preservation as the pollen is relatively resistant to decay (Havinga 1967; Mercuri *et al*. 2006). The pollen assemblages from the Salina Deep Core, however, also contain many other taxa and the condition of the pollen was generally good, so this does not necessarily appear to be a preservation issue. It is possible that this rise reflects the liberation of the resistant Lactuceae pollen grains from the soil, caused by over-grazing of vegetation exposing the soils to erosion. Other taxa resistant to corrosion, oxidation and microbial attack – including *Pinus* and fern spores – do not, however, rise at this time. Alternatively, Florenzano *et al.* (2015) have argued that an abundance of Lactuceae pollen in Mediterranean contexts is related to intensively grazed pasture, and given the abundance of other pastoral indicators, this is a plausible explanation for some of the high percentages seen in the Salina Deep Core and at other sites. Cereal pollen is low in this period, suggesting either low intensity cultivation or cultivation relatively distant from the core site.

In Salina Deep Core pollen zone SDC-08 at 5404–5145 cal. BC (7354–7095 cal. BP) *P. lanceolata*-type rises further and the nitrophilous *Urtica* (nettles), *Rumex* (docks), ruderals including Brassicaceae and *Convolvulus arvensis*-type and rising coprophilous fungal spores (with *Sporormiella*-type now present in addition to those taxa discussed earlier) are consistent with major expansions of pastoral agriculture close to this site. Relatively high *P. lanceolata*-type and Lactuceae are visible in the basal zone of the Salina 4 core (Fig. 3.4), but are not present in the Burmarrad BM1 and BM2 cores (Djamali 2014; Djamali *et al.* 2013; Gambin *et al*. 2016), or at Xemxija (Fig. 3.6) (where, however, pollen preservation is poor in sediments of this age). The signal is probably localized, suggesting that areas of intensive grazing were restricted in size at this time. Cereal pollen shows a short-lived peak in the two *FRAGSUS* Salina cores and at Burmarrad, synchronous with the rise in *P. lanceolata*-type, suggesting that arable farming became more extensive, for a while (Fig. 11.2).

A slight increase in *Theligonum* pollen accompanies other evidence for increased agricultural activity, and the taxon is consistently present throughout the remainder of the Salina Deep Core sequence (Fig. 3.3). *Theligonum* is found in dry, rocky environments and it has been suggested that an increase in this taxon seen in the Burmarrad sequence at *c*. 4650 cal. BC (6600 cal. BP) may reflect the establishment and development of terraces in the landscape (Djamali *et al.* 2013). Climatically, there appears to have been very little change through these events, which thus probably reflect cultural processes and variously successful experiments with agriculture. Broadly contemporary early cereal cultivation in a landscape characterized by steppe with some woodland is also evident on Gozo at this time, in the soils underlying the Santa Verna Temple (Table 3.9). The palynological evidence for early cereal cultivation in Malta is supported by the recovery during *FRAGSUS* excavations at Santa Verna and Skorba of archaeobotanical remains of barley, wheat and lentils dating from *c*. 5400–4900 cal. BC (7350–6850 cal. BP). This period of intensive and extensive arable and pastoral agriculture occurs during the Għar Dalam and Skorba cultural phases.

From about 7000 years ago (5050 cal. BC) there may have been significant changes in effective moisture. It seems highly probable that, at Burmarrad and in other localities where land-use was not intensive in Malta, as in Sicily and southern Spain (Tinner *et al.* 2009; Reed *et al.* 2001), *Pistacia* and other vegetation was responding to an episode of relatively high effective moisture, with widespread major increases in precipitation at this time. The presence of *Pistacia* pollen does seem, however, to have been extremely localized, for instance in the BM1 core it was rising strongly by 5050 cal. BC (7000 cal. BP), while in the nearby BM2 core it was still a relatively minor component of assemblages at that time (Fig. 11.1) (Djamali *et al.* 2013; Gambin *et al.* 2016).

Although high tree pollen is present, a different pattern is visible in the Marsa 1 core, where the basal zone, with an interpolated age of *c*. 5050 to 4850 cal. BC (7000 to 6800 cal. BP) is characterized by pollen suggestive of scrub dominated by *Pinus* (pine) and *Juniperus* or *Tetraclinis* (juniper or sandarac gum), with very little *Pistacia*. There is also pollen indicative of a little steppe and cereal agriculture and there is much microscopic charred wood, suggestive of significant and repeated fire (Carroll *et al.* 2012). Thereafter the landscape at Marsa appears to have become significantly more open and shortly after *c*. 4550 cal. BC (6500 cal. BP) cereal and *P. lanceolata*-type pollen had become more common, suggesting an expansion of arable and pastoral agriculture. This most probably points toward patches of pine-juniper/sandarac gum scrub woodland being cleared. These findings may point to development of a different flora on the dry Globigerina Limestone plateau in southern Malta, in contrast to the lentisk-dominated vegetation associated with the better water-retaining properties and hill-side

springs from the perched Upper Coralline Limestone aquifer associated with the Blue Clay lowlands and muddy colluvial cover of hillsides in northern Malta (Hunt 1997).

Areas of intense arable agriculture and grazing seem to have shifted during the interval between *c*. 5050 and 4550 cal. BC (7000–6500 cal. BP), whether in response to climatic or to socio-cultural factors. In both the Salina Deep and Salina 4 cores, *P. lanceolata*-type and cereals reach minima and peaks of *Pistacia* suggest patches of lentisk scrub around 4550 cal. BC (6500 cal. BP) (Figs. 3.3 & 3.4). The patchiness of vegetation at Salina is indicated by the contrasting record from the Salina Bay core of Carroll *et al*. (2012), which shows an opposite trend, with a maximum of *Plantago* and very little *Pistacia* or other woodland or maquis taxa at the same time. In the Burmarrad BM1 pollen diagram, *P. lanceolata*-type peaks at *c*. 4900 cal. BC (6850 cal. BP), then declines to a minimum at *c*. 4600 cal. BP (6550 cal. BP), while *Pistacia* rises strongly from *c*. 4950 cal. BC (6900 cal. BP), peaking at over 60 per cent at *c*. 4750 cal. BC (6700 cal. BP) before declining to *c*. 45 per cent at *c*. 4550 cal. BC (6500 cal. BP). There are peaks of *Pistacia* and *Phillyrea* around 3850 cal. BC (5800 cal. BP) at Xemxija (Fig. 3.6).

Vitis (vine) appears at *c*. 4750 cal. BC (6700 cal. BP) at Burmarrad (Djamali *et al.* 2013), perhaps reflecting the introduction of grapes. It is also possible, because vines are extremely low producers of pollen, that these were native plants under-represented in the pollen rain (Pagnoux *et al*. 2015). The Burmarrad BM2 pollen diagram (Gambin *et al*. 2016) has an interval with no pollen preservation at this time.

There is evidence for a general decline in agricultural activity around 4550 cal. BC (6500 cal. BP) in many of the Maltese records. Arboreal and scrub pollen expands at several sites, and cereal pollen percentages generally decline apart from at Marsa 1 where they rise sharply (Carroll *et al.* 2012) (Figs. 11.1 & 11.2). The rise in arboreal and scrub pollen might suggest that climatic wetness was rather high at this time. Although this may in part reflect a relaxation of grazing pressure associated with agricultural decline, percentages of tree and shrub pollen are higher at 4550 cal. BC (6500 cal. BP) than during humid episodes before the 8.2 ka BP event when grazing livestock were most likely absent. This suggestion of possible higher effective humidity contrasts with many areas around the Mediterranean (e.g. Magny *et al.* 2011; Sadori *et al.* 2016; Jaouadi *et al.* 2016; Bini *et al*. 2018), which show evidence of climatic disruption and rainfall decline around 4550 cal. BC (6500 cal. BP). It is thus possible to infer that in Malta, the widespread, although not universal decline in agriculture at this time may perhaps reflect social and/or cultural rather than climatic factors. Archaeological excavations by the *FRAGSUS Project* at Skorba and Santa Verna have identified a hiatus in the cultural record between *c.* 4800–3800 cal. BC (6750–5750 cal. BP), which corresponds broadly with the reduced agricultural activity in the palynological record (see Volume 2). The continuation of cereal agriculture at some sites suggests, however, that there might have been some sort of re-organization of the locations preferred by the population and/or changes in social structures and economic activities at this time, rather than a substantial de-population of the islands. This view is supported by the very small number of excavated Neolithic sites.

3.6.4. The later Neolithic Temple period (3900–2350 cal. BC)

After 6000 years ago (4050 cal. BC), Maltese landscapes generally remained extremely open, with cereal cultivation increasing and grazing evident at most core sites. Spores of soil fungi suggest continued soil erosion, while rising values of corrosion-resistant pollen such as Lactuceae and various Asteraceae may suggest that soil erosion was accelerating, perhaps because of agricultural intensification, or expansion of arable activity into more geomorphologically marginal areas. At the same time, the percentages and diversity of pollen of agricultural weed taxa both start to increase, suggesting that farmers may have been losing productivity as weeds proliferated and soils degraded and continued to erode. All of this is consistent with the island being relatively intensively used for agriculture during the later Neolithic (see Chapter 6 and Volume 2).

There are, however, some distinct elements of spatial and chronological patterning. The Salina Deep Core shows three episodes when *Pistacia* (lentisk) scrub regenerated, between *c*. 4450 cal. BC (6400 cal. BP) and 3850 cal. BC (5800 cal. BP), between *c*. 3450 cal. BC (5400 cal. BP) and *c*. 2700 cal. BC (4650 cal. BP) and *c*. 2400 cal. BC (4350 cal. BP) and *c.* 2300 cal. BC (4250 cal. BP) (Fig. 3.3). The second peak in *Pistacia* is also recorded at the Burmarrad BM2 core, where it forms over 60 per cent of the pollen assemblages deposited during the Ġgantija and early Saflieni phases (Fig. 11.1) (Djamali *et al*. 2013; Gambin *et al.* 2016). The first and second peaks seem to be visible at Xemxija, but records further away seem to be out of phase. This therefore suggests the presence of very localized stands of lentisk scrub in an area close to the Burmarrad core sites which was not used heavily for arable agriculture or grazing. It has been hypothesized that *Pistacia* spp. were managed for food, fuel and fodder in the Levant during the pre-pottery Neolithic (Asouti *et al.* 2015) and it is conceivable that something similar occurred

on Malta during the later Neolithic. That management was occurring might be inferred from the Burmarrad BM1 and BM2 diagrams (Djamali *et al.* 2013; Gambin *et al.* 2016), because the expansion of *Pistacia* is not followed by substantive successional expansion of other maquis or woodland taxa for about 2000 years, until after *c*. 3050 cal. BC (5000 cal. BP) when *Pistacia* declines and short-lived peaks of *Olea* and *Quercus* are observed. Substantiating this suggestion further would require intensive investigations of macro-fossil wood and charcoal on Maltese archaeological sites.

During the later Neolithic period, from the Żebbuġ phase (3900–3600 cal. BC) onward, cereal percentages are remarkably high at some sites (Tables 2.1 & 3.11). In the Salina Bay core of Carroll *et al.* (2012), from *c*. 3850–2350 cal. BC (5800 to 4300 cal. BP), there are at times very high values (over 10 per cent) for cereal pollen. This especially occurred during the Ġgantija phase (3450–3200 cal. BC), when there are cereal pollen percentages of the same order at Wied Żembaq and one very high value at Xemxija, and again during the Tarxien phase (2850–2350 cal. BC), when there are very high cereal pollen percentages at Tas-Silġ (Fig. 11.2). There are also some very high values in the segment of the Marsa core assigned to the Żebbuġ to Ġgantija phases (3900–3200 cal. BC), but unfortunately these sediments are followed by a depositional hiatus. The percentages at all these sites are greater than would be expected in a landscape devoted to cereal growing and perhaps reflect threshing on cereal-processing sites rather than cultivation *per se.* Even in the middle of a field of cereals, it is rare for their pollen to form more than 8 per cent of the assemblage (Faegri & Iversen 1975), but threshing releases into the environment abundant cereal pollen, which would otherwise remain trapped within the husks, so sites where threshing occurred are often marked by very high cereal pollen values (e.g. O'Brien *et al*. 2005). This perhaps raises the possibility of cereal processing, or the handling of processed cereals, adjacent to temple sites such as Tas-Silġ, Borġ in-Nadur (close to the Wied Żembaq core site), the Tarxien Ħal Saflieni complex (near the Marsa core sites), Xemxija (adjacent to the Xemxija core site), and Buġibba (close to the Salina core sites). Only the Burmarrad cores, which are not far from the Tal-Qadi temple, do not conform to this pattern, but this area was not cultivated and instead appears to have been covered with dense lentisk scrub. Dispersal of cereal pollen within this environment would likely have been minimal.

The occurrence of pollen of vines in the later Neolithic Żebbuġ phase at Salina 4, and in the Ġgantija and Tarxien phases at Wied Żembaq, and of carob in the Tarxien phase at Salina 4 is possibly of significance (Figs. 3.4 & 11.1; Table 2.1). Both vines and carob have extremely poor dispersal so the very low percentages recovered may indicate that these were actually fairly abundant in the vegetation when first recorded, and absence in the pollen diagrams prior to this cannot be taken as conclusive evidence that they were not present in the Maltese Islands. Indeed, carob charcoal was recovered from the early Neolithic site at Skorba (Metcalfe 1966), suggesting that it was present in Malta from well before the first appearance of the pollen. Carob was thought to be an eastern Mediterranean species domesticated during the Chalcolithic (Ramón-Laca & Mabberley 2004), although recent genetic work suggests populations of wild carob spreading from several glacial refugia such as in Morocco, Iberia, Sicily, Greece and southern Turkey during the early Holocene (Viruel *et al.* 2016). Traditionally, carob pods have been used as animal fodder and famine food in Mediterranean countries (Forbes 1998) and could have been used in Maltese prehistory, wild or domesticated. On the other hand, grape pips first appear at Tas-Silġ in the Early Bronze Age (Fiorentino *et al*. 2012), significantly after the first appearance of the pollen. Nevertheless, the appearance of pollen grains of these species may perhaps indicate rising numbers of the plants and possible widening of the subsistence base during this time.

3.6.5. The late Neolithic–Early Bronze Age transition (2350–2000 cal. BC)

During the Tarxien phase (2850–2350 cal. BC), there is possible evidence for aridification at Ġgantija (Table 3.10), Tas-Silġ (Hunt 2015) and Wied Żembaq (Fig. 3.5), in the form of woodland contraction, steppe vegetation apparently taking on a drier aspect and diminished clear evidence for areas of damp vegetation. Cereal pollen also declines markedly at this time at many sites. Woodland decline occurs during the Tarxien Period at Xemxija, Burmarrad (Gambin *et al.* 2016), Salina 4, Salina Bay (Carroll *et al*. 2012) and in the Salina Deep Core, but trends in other indicators are less clear. Nevertheless, it can be argued that effective precipitation may have declined during the Tarxien Period (cf. Gambin *et al*. 2016), with the corollary that socio-economic systems may have come under increasing stress through declining agricultural productivity and perhaps the drying of some karst water sources.

In the Salina 4 core (Fig. 3.4), Carroll's (2012) Salina Bay core, the Wied Żembaq core (Fig. 3.5) and in the Tas-Silġ middens, there is a short episode around 2350 to 2050 cal. BC (4300 to 4000 cal. BP) during which cereal pollen disappears or becomes very rare and pollen of trees and shrubs increases. The only contrary trend is at Burmarrad BM2 (Gambin *et al*. 2016) where

cereal pollen rises at this time. The behaviour of *P. lanceolata*-type (which may be taken to reflect grazed land) through this episode varies: at Salina 4 it declines markedly and at Wied Żembaq it declines more gently, whereas at Burmarrad BM2 (Gambin *et al.* 2016) and Salina Bay it rises sharply (Carroll *et al.* 2012). This episode is known elsewhere around the Mediterranean as the culmination of a time of climatic stress (e.g. Magny *et al.* 2009, 2011; Jaouadi *et al.* 2016; Ruan *et al.* 2016), but there seems to be no strong climatic evidence from the Maltese pollen records at this point.

When considering all the available records, the decline of cereal pollen at Salina 4 and Salina Bay (Carroll *et al*. 2012), Tas-Silġ and Wied Żembaq and the rising trend of tree and shrub pollen at Salina (Deep Core & Salina 4), Xemxija, and Wied Żembaq close to 2350 cal. BC (4300 cal. BP) may reflect abandonment of agricultural land and regeneration of woody vegetation rather than a climatic signal *per se*. It is worth noting that in Malta during the early Holocene, only times of climatic wetness seem to have supported abundant woody vegetation, so alternatively the rise of woody vegetation at this time may conceivably reflect a rise in effective moisture.

On the other hand, archaeological evidence suggests that there was most probably some form of societal disruption close to 2350 cal. BC (4300 cal. BP), reflected in the apparent abandonment of temple sites and short-lived appearance of the Thermi ware, followed later after *c*. 2000 cal. BC by the Tarxien Cemetery culture (e.g. Malone *et al.* 2009b; Fiorentino *et al.* 2012; Malone & Stoddart 2013) (see Chapters 6 & 7). The pollen evidence suggests that as part of this disruption, cereal cultivation and pastoral activity were abandoned in coastal localities such as Salina, Xemxija and Wied Żembaq. The decline in pollen of woody plants and rise in cereal pollen at Burmarrad counters this trend and would be consistent with relocation of agriculture, and perhaps human populations, toward the interior of the island (see Chapter 7). This may be consistent with an element of population continuity at the end of the Temple Period and into the Bronze Age. The redistribution of agricultural activity and perhaps population away from the coast seems a consistent response to the well-known rise of maritime raiders in the Early Bronze Age (Grima 2007; Wiener 2013) since at this point coastal localities would have become very vulnerable.

3.6.6. The Bronze Age (2000–1000 cal. BC)

After the decline in cereal pollen around the end of the Temple Period (2350 cal. BC), which may reflect partial population decline, by *c*. 2050 cal. BC (4000 cal. BP) there is evidence from the pollen of cereals, agricultural weeds, pasture land taxa and coprophilous fungal spores for widespread cereal cultivation and pastoral agriculture. This coincides with evidence for extensive arable agriculture at this time in the macrofossil record at Tas-Silġ (Fiorentino *et al.* 2012). The number of sites of Later Bronze Age date sampled during this and previous research is rather small and there are marked taphonomic biases to assemblages at Wied Żembaq, Tas-Silġ (Hunt 2015) and Xemxija. Nevertheless, the relatively uniform percentages for tree and shrub pollen are suggestive of there being no major climatic change at this time, while relatively high cereal pollen percentages can be used to infer that cereals were grown and quite probably processed at Tas-Silġ.

3.6.7. Late Bronze Age, Punic and Classical periods (c. 1000 cal. BC to AD 1000)

By the start of the Classical Period, pollen assemblages from Marsa (Carroll *et al*. 2012) are marked by relatively high incidences of Caryophyllaceae, Chenopodiaceae, spiny Asteraceae, *Arabis*, *Spergula*-type, and rather low Poaceae and tree/shrub pollen. This is likely to reflect a highly degraded landscape (Carroll *et al.* 2012). There is ample evidence for eroding soils (e.g. at Xemxija), with relatively high counts for corrosion-resistant taxa, such as *Pinus*, Lactuceae and various Asteraceae, and often very strong representation of soil organisms such as VAMs and *Pseudoschizaea*.

Tree and shrub pollen persisted relatively unchanged from the Late Bronze Age and throughout the Punic period at Xemxija and Marsa (Carroll *et al*. 2012). In contrast, arboreal pollen values are higher at Wied Żembaq and at Tas-Silġ, mostly because of high percentages of *Pinus,* which could be taphonomic or reflecting overall lower pollen productivity locally rather than reflecting changes to the vegetation.

Cereal pollen remains high and rises in the latest Punic period, peaking in the Roman Period at Marsa (Carroll *et al.* 2012). Cereal pollen also appears at In-Nuffara, but declines slightly at Tas-Silġ and disappears at Wied Żembaq (Hunt 2015) at the same time. The long record from Xemxija shows very strong evidence for possible discontinuities and often has very low pollen counts, but nonetheless reflects a degraded steppe landscape adjacent to a drying former marshy area.

It is not possible to separate the pollen of cultivated and wild or feral (descended from cultivated forms) olives, but since *Olea* pollen is recorded prior to the Neolithic at Xemxija, it is almost certainly a native species and therefore likely derives from oleaster (wild olive) for most of the Holocene. Its behaviour prior to the Punic Period is in-phase with the rise and fall

of tree and shrub pollen and out of phase with the pollen of cereals, supporting its likely derivation from oleaster. Only in the later Punic and Roman periods, from *c*. 400 cal. BC (2450 cal. BP) onwards at Burmarrad and Marsa, is *Olea* pollen in phase with cereal pollen, perhaps suggesting that it derives from the cultivation of domesticated olive trees. This corresponds with finds of olive stones at Marsa and Tas-Silġ (Fiorentino *et al.* 2012). Recent investigations have shown that the pollen productivity and dispersal of modern *Olea europaea* are very limited, with pollen percentages in surface samples declining by 60–90 per cent within 100 m of the cultivation site (Florenzano *et al.* 2017). Values of olive pollen as high as 8 per cent at Burmarrad (Gambin *et al*. 2016) and 5 per cent at Marsa (Carroll *et al*. 2012) during the Roman period may therefore reflect extensive olive groves (Anastasi & Vella 2018; Vella *et al*. 2017). Elsewhere in the Mediterranean, such as at Kouremenos in Crete, there is certainly evidence of intensifying olive tree presence from the later Neolithic at about 3600 cal. BC onwards (Langgut *et al.* 2019), coincident with the opening-up of the landscape and intensification of grazing (Stoddart *et al.* 2019), although the early stages of olive tree management may not necessarily imply domestication and cultivation of the tree (Canellas-Bolta *et al.* 2018, 73, & references therein). A recent review of the evidence for olive growing in Puglia, southeast Italy, shows that wild olives have been cultivated there since the early Neolithic, and selective cultivation culminated in the first appearance of the domestic type during the Middle Bronze Age or mid-second millennium BC (Caracuta 2020).

At Xemxija the very high peak of *Pinus* pollen during the period *c*. 150 cal. BC to cal. AD 1150 (1800 to 800 cal. BP) is notable, and can probably be best interpreted as evidence for a Roman period pine plantation that persisted through the Arab period and into Norman times. Supporting evidence for this interpretation may be provided by the observation of al-Idrisi, made around AD 1150, incorporated in a later text by al-Himyari (Brincat 1995) that good timber for ship repair had been available on Malta.

3.6.8. Medieval to modern (post-AD 1000)

All assemblages of Medieval to early Modern age show a very strong taphonomic imprint, being dominated by corrosion-resistant taxa such as Lactuceae. All other evidence points towards very degraded environments, mostly degraded steppe, although most records have poor chronological resolution. Pollen indicative of degraded steppe vegetation is particularly evident in the basal half of the core from Santa Marija Bay on Comino with very low percentages of Poaceae and high percentages of *Centaurea* and *Gladiolus*, taxa which are today associated with degraded steppe environments on the islands (Carroll *et al*. 2012).

Around AD 1600–1650 (assuming constant sedimentation rates), there is a sharp change in the Santa Marija Bay core, with a decline in *Gladiolus* and rise in Poaceae and *Plantago* (Carroll *et al.* 2012). At In-Nuffara, there is a minor increase in Poaceae which is undated, but predates the appearance of the exotic *Eucalyptus* and thus is probably earlier than the British Period (or pre-nineteenth century). At Għajn il-Kbira on Gozo, molluscan assemblages relating to the nineteenth century or earlier are marked by a rise in the grassland species *Truncatellina callicratis* (Hunt & Schembri 2018). These changes were most likely caused by the policy of the Knights, who encouraged the creation of terrace systems (see Chapters 7 & 8) and improvement or manufacture of soils and the development of sheep runs (Blouet 1997), but may also reflect a phase of higher effective humidity during the Little Ice Age (Sadori *et al*. 2016).

Finally, the most recent parts of the In-Nuffara deposit, and the cores from Xemxija, Santa Marija Bay, Salina Bay and Marsa (Carroll *et al.* 2012) all show a strong rise in *Pinus*, consistent with the widespread planting of pines as ornamentals during the British Period. The Australian exotic *Eucalyptus*, was also planted during British times and was present at In-Nuffara and in the Mistra Valley (Hunt & Vella 2004/2005). Maize and cotton were also present in the field-fill in the Mistra Valley (Hunt & Vella 2004/2005). The wider landscape generally remained extremely degraded.

3.7. Conclusions

The work done by the *FRAGSUS Project* has significantly changed our understanding of the sequence and causes of Holocene vegetation change in the Maltese Islands, as well as some aspects of the relationship between the environment and the human population. For the first time, analysis of multiple sediment sequences and archaeological sites has allowed us to differentiate between climatic and anthropogenic signals at times during the Holocene. These entwined issues will be returned to in the concluding Chapter 11.

Chapter 4

Molluscan remains from the valley cores

Katrin Fenech, Chris O. Hunt, Nicholas C. Vella
& Patrick J. Schembri

4.1. Introduction

Molluscs often have quite specific environmental requirements (Evans 1978, 82; Giusti *et al*. 1995; Schembri *et al*. 2018). Many species require only a few square metres of habitat, so they are excellent micro-habitat indicators. Their shells can be dispersed, for instance by running water, but generally, compared with other biotic materials used in palaeoecology (such as pollen grains or seeds), they do not disperse far from their life habitat and therefore provide important indications of local environments. Alkaline sediments, which are very common in the Maltese Islands, will preserve molluscan shells and other calcareous biogenic material over thousands of years. This makes the analysis of molluscan shells potentially a very important tool for the reconstruction of past environments in Malta.

Geologists and archaeologists recognized the value of molluscs as palaeoenvironmental indicators as early the first quarter of the nineteenth century AD (Conybeare 1824; Preece 1998; Evans & O'Connor 2005, 41). Molluscan analysis is still, however, comparatively rare as a palaeoenvironmental tool, and for instance is less commonly used than pollen analysis (e.g. Preece 1998, 158; Fenech 2007).

In the Maltese Islands, the application of the technique has been limited and there has been no comprehensive palaeoenvironmental study using molluscan analysis. Trechmann (1938), Giusti *et al*. (1995) and Hunt (1997) used the sporadic occurrence of land snails in Maltese Quaternary deposits as an indication that these had accumulated in open, exposed conditions. The highly cemented Quaternary deposits precluded anything other than the production of species lists by these authors. Pedley (1980) suggested a brackish depositional environment for the Pleistocene Fiddien Valley Tufa on molluscan evidence. Fenech (2007) and Marriner *et al*. (2012) analysed cores taken in Holocene estuarine deposits at Marsa and Burmarrad, respectively. These studies showed the progress of the Holocene marine transgression and the infilling of the estuaries, and Fenech (2007) also showed the persistence of open, exposed terrestrial environments in the catchment of the Marsa estuary over *c*. 7000 years. At the Neolithic Xagħra Brochtorff Circle (Schembri *et al*. 2009) and the Neolithic and later temple site at Tas-Silġ (Fenech & Schembri 2015), molluscan analysis demonstrated long histories of anthropogenic disturbance and sparse vegetation since the later Neolithic, but a considerable portion of these studies was done on shells recovered by troweling and dry sieving with a large fraction and therefore subject to a form of taphonomic bias caused by the exclusion of most very small taxa. Analysis of a cave fill near Victoria on Gozo, based on assemblages recovered by sieving, identified a phase of spectacular erosion caused by Classical period agricultural practices, followed by a more stable grazed landscape in the Medieval and post-Medieval periods (Hunt & Schembri 2018). Inevitably, the research done before the start of the *FRAGSUS Project* was very partial in coverage. The environmental history of the Maltese Islands was still largely unknown.

To investigate the environment and landscape of the Maltese Islands and the changes they underwent over time, a full molluscan analysis was made of the material extracted from sectioned sediment cores. The shell assemblages found in the *FRAGSUS* cores were controlled by their depositional environment, surrounding habitats and taphonomic factors. They often included molluscs from all four major habitat-groups: marine, brackish water, freshwater and terrestrial. Although it is logical that species would be limited to particular major habitats and that live individuals from other major habitat types would not occur (for example, a freshwater habitat would not be expected to also support live marine and terrestrial species), the result of the analyses of molluscan assemblages from cores is not always easy to relate to the type

of environment when species from different major habitats are admixed. In the present study, it was not always straightforward to determine which snail group is autochthonous (i.e. occurred naturally as live individuals), and which groups are allochthonous (e.g. washed into the coring site from elsewhere by run-off during storm events or by waves during storms or even by tsunamis). Thus for instance, a storm might have overtopped a bay-bar leading to insertion of marine taxa into a non-marine lagoon, but at the same time run-off from heavy rain might have washed land snails into the same deposition site. Additionally, allochthonous recycled material might arrive on a site as sediments and their contained molluscs may have been eroded and redeposited. In some cases, it was possible to discern which species were autochonous and which had been transported to the deposition site from elsewhere.

A further complicating factor is that some deposition sites were at times affected by erosion, for instance scour during fluvial or mud-flow events or by marine storm waves. These erosion events led to non-sequences or hiatuses, sometimes recognizable as very marked and abrupt changes of the molluscan fauna, and by abrupt sediment changes.

Previous studies of non-marine molluscs from various (undated) Quaternary deposits around the Maltese Islands revealed the occurrence of several freshwater or wetland species that are now extinct, indicating the previous occurrence of rare periods characterized by much wetter conditions, at least locally (Hunt & Schembri 1999).[1] On the other hand, several species that occur today, such as the woodland indicator *Lauria cylindracea*, had no palaeontological record (see Trechmann 1938; Thake 1985a & b; Giusti *et al.* 1995; Allen & Eastabrook 2017; Hunt & Schembri 2018). These previous studies form the basis of the research undertaken, together with more recent studies of the ecology of non-marine molluscs in local environmental regimes (Schembri *et al.* 2018) that now allow various species to be more or less reliably assigned to a specific habitat. One of the aims of these ecological studies was to analyse the habitat and micro-habitat distribution of current species and assemblages in order to determine their specificity to different habitat types. On the assumption that the ecology of the species would not have changed significantly in the time spans considered, species and assemblages from archaeological and older contexts might then be used to reconstruct past environments and to study environmental change.

Brackish and freshwater assemblages apart, four present-day terrestrial assemblages were recognized: those from exposed habitats, from sheltered habitats, from habitats dominated by trees or shrubs, and from garrigue. The Maltese low garrigue is also an exposed habitat but quantitatively and to some extent qualitatively, its molluscan assemblages differed from those of other exposed habitats presumably because of its very open nature. However, this study also showed that assemblage composition is determined more by the micro-habitat preferences of the species, especially the spatial and temporal availability of shelter and shade, than by macro-habitat type. Many species were found in more than one macro-habitat, albeit in different relative abundances, very likely because of the extreme mosaic nature of the present day landscape of the Maltese Islands where different habitats may occur within very close proximity to each other, allowing a mixing of molluscan assemblages, especially of the less stenoecious species. The mixing that occurred in the deposits studied here, compounds the problem of the natural 'mixing' of assemblages and therefore only allows broad generalizations to be made about the environment of the catchments of the coring sites.

Stenotopic species (those with narrow environmental tolerances) are most informative about the environments present and we have used these as indications that particular habitats were present at in the catchment of the coring sites. Habitats whose presence was inferred in this way included brackish water (with such species as *Hydrobia* spp. and *Ovatella myosotis*), running freshwater (e.g. *Pseudamnicola* (s.str.) *moussonii*), slower moving water and ponds and lakes (e.g. *Lymnaea truncatula*, *Planorbis* spp., *Gyraulus crista*, *Bulinus truncatus*, *Ancylus fluviatilis*), freshwater wetlands (e.g. *Carychium schlickumi, Oxyloma elegans*, *Vertigo antivertigo*), sheltered habitats (e.g. *Oxychilus draparnaudi*, *Oxychilus hydatinus*, *Vitrea* spp.), wooded habitats (*Lauria cylindracea*), and garrigue (e.g. *Trochoidea spratti* and *Muticaria macrostoma*).

The molluscan analyses undertaken here complement the pollen analyses (see Chapter 3) by providing data about the environment and landscape. The changing compositions of the molluscan assemblages further suggest how climatic and weather events and patterns of human activity affected the depositional environment and the catchments of the respective coring sites. While the resolution of environmental reconstruction provided by analysis of the molluscan assemblages may not be as high as that provided by pollen, given the greater number of plant species involved and the habitat specificity of many plants, molluscan assemblages have the advantage of reflecting local conditions, since the transport of molluscs is usually over much shorter distances than for pollen.

This chapter will describe the core material studied and the methods applied. Results of the analysis are

discussed core by core. An environmental reconstruction based on the molluscs from the early Holocene to the Late Roman period highlights changes in the landscape through time. The molluscan evidence indicates major erosion events and may be used to suggest their causes. Extinct species, taxa that previously had no local fossil record and some useful indicator species are then discussed in the context of the environmental insights they provide.

4.2. Material

Eight sediment cores from six different locations across the Maltese Islands were analysed (Fig. 2.4). With the exception of the Marsa 2 core, these were taken between 2013 and 2015 (see Chapter 3).[2] The Salina Deep Core and Marsa 2 core had been extracted with a mechanical corer by local companies experienced in geological site investigations.[3] The other cores were taken with an Eijkelkamp percussion auger by *FRAGSUS* team members Chris O. Hunt, Sean Pyne O'Donnell, Michelle Farrell and Rory Flood. These were then cut in half lengthwise at NIU Maynooth and subjected to core logging at University College Dublin. One half of each of the cores, in its' plastic tube and wrapped in cling-film was then sent to Malta for the molluscan analyses. Summary and detailed descriptions of the cores are provided in Chapter 2 and Appendix 3**.**

4.3. Methods

The core sections were consecutively divided into segments between 3 and 13 cm in thickness. All segments were weighed and their Munsell soil colour was recorded. Depending on the size of the samples, small sub-samples weighing between 4 and 20 g were taken from every segment and archived for future reference.[4] The material from the segments was then stirred in water. When necessary, sodium hexametaphosphate was added to facilitate the breaking up of aggregated particles. Once disaggregated, the sediment was wet sieved through nested 500 and 63 micron (μm) test sieves and dried. Stones larger than 8 mm diameter were sorted out from the >500 μm fraction. The material in each fraction was then weighed and the silt/clay content calculated. The dried material from the 500 μm sieve was sorted for shells, other organic remains and artefacts such as pottery under a stereomicroscope. The fine sediments retained by the 63 μm sieve were bagged, but not sorted, as they were found to be sterile apart from tiny charcoal fragments. Mollusc percentage abundances were calculated in TILIA (© Grimm 1987), which also generated the diagrams. The molluscan diagrams were subdivided into Mollusc Assemblage Zones (MAZs) by applying stratigraphically constrained cluster analyses to percentage abundance data using CONISS software in TILIA (Grimm 1987). Several deposits contained no molluscan remains. As TILIA does not recognize 0 as a value for percentage calculations, a nominal value of 1 was given to these deposits in a separate category to allow the calculations.

The molluscs were identified to the lowest taxonomic level possible with the help of: a reference collection, Giusti *et al.* (1995) for the non-marine molluscs, Doneddu and Trainito (2005) and other standard identification manuals for the marine species. The vast majority of shells larger than 2 mm were heavily fragmented. Identification was nonetheless mostly possible at least to genus level because of distinctive shell features. Indeterminate fragments of helicid land snails that could not be quantified in terms of actual numbers, were counted as 1. Similarly, the tests of the rock urchin *Paracentrotus lividus* found in several samples, were noted as 1. Although bivalve valves occur naturally in pairs, they usually occurred singly or in uneven pairs in the samples. Each valve was counted as one individual.[5]

All other shells were counted in actual numbers and then grouped according to their macro-habitat: marine, brackish water-associated, freshwater-associated and land snails. The freshwater-associated molluscs and the land snails were further subdivided and grouped according to their more specific habitat requirements (Table 4.1). The presence of the subterranean, burrowing land snail *Cecilioides acicula* was used as an indicator for erosion events when found in subaqueous deposits. Table 4.1 also lists the previously known fossil record of the species found and their current status. The complete dataset of the shells found per sample/depth for all cores is given in Appendix 5.

4.4. Radiocarbon dates and Bayesian age-depth models

As discussed in Chapter 2, a chronology was built with the radiocarbon dates (Tables 2.3 & 2.4) using Bayesian age-depth modelling techniques (Blaauw & Christen 2011). The molluscan data were plotted onto this time-scale to reveal the changing patterns of occurrence through time.

4.5. Results

For core descriptions, logs and precise location, see Chapter 2. As the Marsa 2 core had been taken previously in 2002, see Appendix 3 for soil colours.

Table 4.1. *List of freshwater molluscs and land snails found in the cores, their locally registered habitat requirement, palaeontological record from Quaternary deposits in Malta and Gozo, and current status and conservation in the Maltese Islands (Giusti* et al. *1995; Schembri* et al. *2018; updated by the present authors)*

Species	Habitat	Fossil record	Current status and conservation
Pomatias sulcatus (Draparnaud 1801) The Maltese populations previously assigned to this species are now regarded as belonging to *Tudorella melitense* (Sowerby 1843) (see Pfenninger *et al.* 2010)	Ubiquitous and very eurytopic	Dwejra (Gozo); Wied tal-Baħrija	Common; not threatened
Pseudamnicola (s.str.) *moussonii* (Calcara 1841)	Running freshwater	Wied tal-Baħrija	Patchily distributed because of the restricted distribution of its habitat; locally endangered
Carychium cf. *schlickumi* Strauch 1977	Freshwater wetlands	Wied tal-Baħrija	Present status unknown but at best likely to have a patchy distribution due to the restricted distribution of its habitat; may be extinct
Lymnaea (Galba) truncatula (Müller 1774)	Ponds, lakes, slow-moving water	Wied tal-Baħrija	Widespread in freshwater habitats but such habitats are scarce locally; vulnerable
Planorbis Müller 1774. Two species occur *P. planorbis* (Linnaeus 1758) and *P. moquini* Requien 1848) which are difficult to tell apart on shell characters alone	Ponds, lakes, slow-moving water	*P. planorbis*: Ta' Sarraflu (Gozo) and archaeological deposits Ta' Vnezja; *P. moquini*: Wied tal-Baħrija	*P. planorbis* is probably extinct; *P. moquini* is rare; its habitats have a restricted distribution locally; vulnerable
Gyraulus (Armiger) crista (Linnaeus 1758)	Ponds, lakes, slow-moving water	Wied tal-Baħrija	Extinct
Bulinus (Isidora) cf. *truncatus* (Audouin 1827) complex	Ponds, lakes, slow-moving water	Ta' Sarraflu (Gozo); Wied tal-Baħrija	Extinct
Ancylus fluviatilis Müller 1774	Slow to fast-moving freshwater	Ta' Sarraflu (Gozo); Wied tal-Baħrija	Common; patchily distributed because of the restricted distribution of its habitat
Oxyloma elegans (Risso 1826)	Freshwater wetlands	Wied tal-Baħrija	Extinct
Vertigo cf. *antivertigo* (Draparnaud 1801)	Freshwater wetlands	Wied tal-Baħrija	Extinct
Truncatellina callicratis (Scacchi 1833)	Leaf litter in shady situations but occasionally also in relatively open environments	Għajn il-Kbira (Gozo)	Previously thought to be rare but now regarded as common and quite widespread; not threatened
Granopupa granum (Draparnaud 1801)	Open country and occupies many micro-habitats in this macro-habitat; eurytopic	Wied tal-Baħrija; Għajn il-Kbira and Xagħra Brochtorff Circle (Gozo)	Widespread; not threatened
Lauria cylindracea (Da Costa 1778)	Woodland usually in forest remnants but also in well developed maquis	No fossil record previous to the present study	Rare mainly due to the dearth of woodland habitats in the Maltese Islands; not threatened
Vallonia pulchella (Müller 1774)	Freshwater wetlands	Wied tal-Baħrija	Present status unknown but rare and at best likely to have a patchy distribution due to the restricted distribution of its habitat
Pleurodiscus balmei (Potiez and Michaud 1838)	Leaf litter in shady environments but occasionally also in relatively open environments	Għajn il-Kbira (Gozo)	Common and widespread; not threatened
Chondrula (Mastus) pupa (Linnaeus 1758)	Ubiquitous and eurytopic	Wied tal-Baħrija; Għajn il-Kbira and Xagħra Brochtorff Circle (Gozo)	Common and widespread; not threatened
Vitrea Fitzinger 1833. Three species occur (*V. contracta* (Westerlund 1871), *Vitrea* sp. Giusti, Manganelli and Schembri 1995, and *V. subrimata* (Reinhardt 1871)) but difficult to tell apart without anatomical examination	Leaf litter in shady environments	Wied tal-Baħrija; Għajn il-Kbira and Xagħra Brochtorff Circle (Gozo)	As a group, relatively widespread and common; not threatened

Table 4.1 *(cont.).*

Species	Habitat	Fossil record	Current status and conservation
Oxychilus Fitzinger 1833. Two species occur: *Oxychilus draparnaudi* (Beck 1837) and *Oxychilus* (*Mediterranea*) *hydatinus* (Rossmässler 1838); often difficult to tell apart on shell characters alone, especially if juvenile	Leaf litter in shady situations but *Oxychilus draparnaudi* also in relatively open environments	Wied tal-Baħrija; Xagħra Brochtorff Circle (Gozo)	Both species are common and widespread; not threatened
Cecilioides acicula (Müller 1774)	Burrower	Wied tal-Baħrija; Għajn il-Kbira and Xagħra Brochtorff Circle (Gozo)	Frequent and widespread; not threatened
Ferussacia (s.str.) *folliculus* (Gmelin 1791)	Leaf litter in shady situations but occasionally also in relatively open environments	Għajn il-Kbira and Xagħra Brochtorff Circle (Gozo)	Common and widespread; not threatened
Rumina decollata (Linnaeus 1758)	Open country and occupies many microhabitats in this macro-habitat; eurytopic	Widespread in Quaternary deposits and archaeological sites	Common and widespread; not threatened
Muticaria macrostoma (Cantraine 1835) sensu Giusti *et al*. 1995,	Open country mostly in garrigue habitats	Għajn il-Kbira, Xagħra Brochtorff Circle and Dwejra (Gozo)	Common and widespread; not threatened
Papillifera papillaris (Müller 1774)	Mainly open country but also in sheltered habitats; very eurytopic	Għajn il-Kbira, Xagħra Brochtorff Circle and Ta' Sarraflu (Gozo); Wied tal-Baħrija	Very common and widespread; not threatened
Xerotricha Monterosato 1892. Two species occur: *X. conspurcata* (Draparnaud 1801) and *X. apicina* (Lamarck 1822), which are difficult to tell apart on shell characters alone	Open country but also in some sheltered habitats; somewhat eurytopic	*X. conspurcata*, was found at Għajn il-Kbira and the Xagħra Brochtorff Circle (Gozo); *X. apicina* was found in Wied tal-Baħrija	Both species are common and widespread; not threatened
Trochoidea spratti (Pfeiffer 1846, sensu Giusti *et al*. 1995)	Open country, especially in garrigue, but also in some sheltered habitats; somewhat eurytopic	Ubiquitous in Quaternary deposits and archaeological sites	Common and widespread; not threatened
Cernuella Schlüter 1838. Three species occur: *C. caruanae* (Kobelt 1888), *C.* cf *cisalpina* (Rossmässler 1837) and *C.* cf *virgata* (Da Costa 1778); difficult to differentiate based on shell characters alone if juvenile	*C. caruanae* is ubiquitous and *C.* cf *cisalpina* is more restricted by both are eurytopic	Xagħra Brochtorff Circle (Gozo); Wied tal-Baħrija	*C. caruanae* and *C.* cf *cisalpina* are widespread and abundant and not threatened. *C.* cf *virgata* is very probably extinct
Cochlicella acuta (Müller 1774)	Ubiquitous and very eurytopic	Widespread in Quaternary deposits and archaeological sites	Very widespread and abundant; not threatened
Caracollina lenticula (Michaud 1831)	Ubiquitous and eurytopic	Għajn il-Kbira and Xagħra Brochtorff Circle (Gozo)	Widespread and abundant; not threatened
Theba pisana (Müller 1774)	Ubiquitous and eurytopic	Għajn il-Kbira, Xagħra Brochtorff Circle and Ta' Sarraflu (Gozo)	Widespread and abundant; not threatened
Eobania vermiculata (Müller 1774)	Ubiquitous and eurytopic	Widespread in Quaternary and Holocene deposits	Very common and widespread; not threatened
Cantareus apertus (Born 1778)	Open country normally on leafy vegetation and eurytopic	Għajn il-Kbira and Xagħra Brochtorff Circle (Gozo)	Relatively common and widespread; not threatened
Cantareus aspersus (Müller 1774)	Open country normally on leafy vegetation and eurytopic	Wied tal-Baħrija	Very common and widespread; not threatened
Pisidium Pfeiffer 1821. Two species occur: *P. casertanum* (Poli 1791) and *P. personatum* Malm 1855); difficult to differentiate based on shell characters alone	Slow to fast-moving water but also in ponds, and lakes; in Malta can co-occur in the same habitat	Wied tal-Baħrija	Both are presently very rare due to a highly restricted distribution; endangered

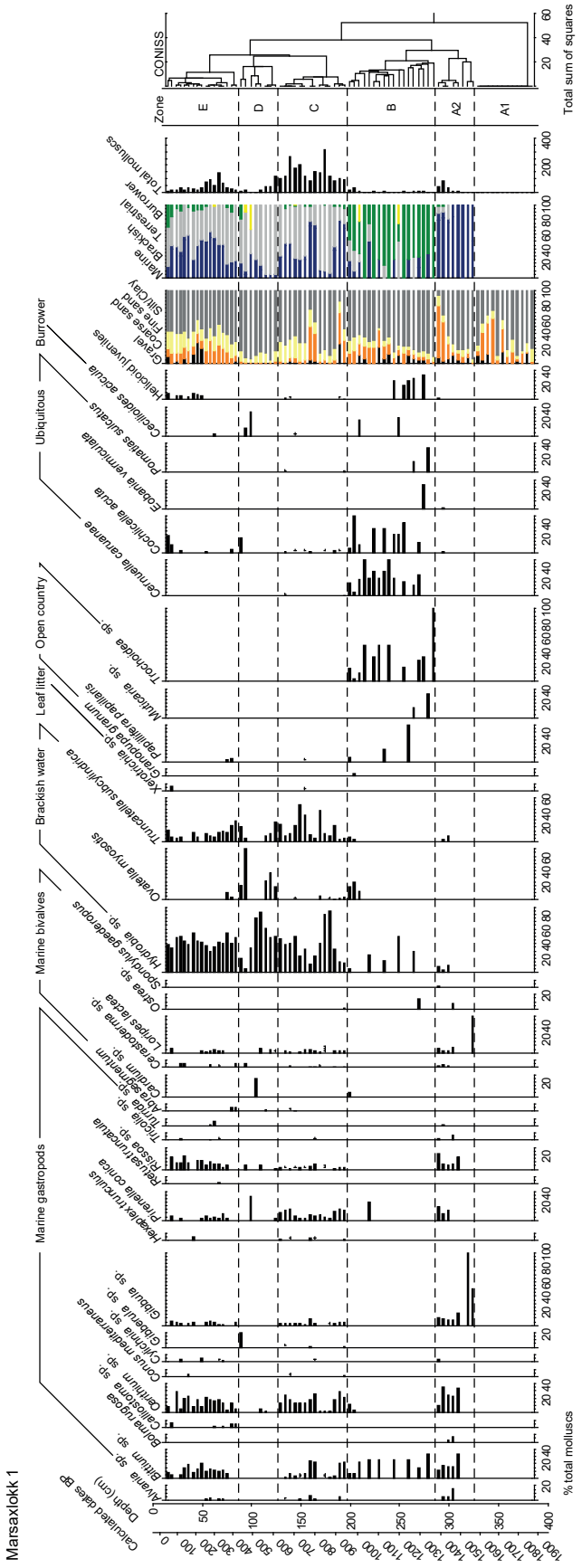

Figure 4.1. *Marsaxlokk 1 molluscan histogram (C.O. Hunt & K. Fenech).*

Table 4.2. *Molluscan zones for the Marsaxlokk 1 core (MX1).*

Zone MX1-	Depth (cm)	Date ranges cal. AD (BP) for the start of each zone (2σ)	Molluscan assemblages	Environment
A1	386–326	n/a	Sterile	Bedrock/bedrock interface
A2	326–286	AD 171–523 (1779–1427 BP)	Total of 195 shells, of which *Cerithium* sp. 26%, *B. reticulatum* 15%, *G. adansonii* 10%, *Hydrobia* sp. 6%, *T. subcylindrica* 3% Few fragments of marine molluscs between 326–306 cm; from 306 cm upwards there was a sharp increase in the variety and abundance of marine species; concurrently, appearance of brackish water/saltmarsh species, which were 20% of total molluscs	Shallow marine environment becoming shallower towards the top, as indicated by the appearance of the shoreline species *Truncatella subcylindrica*
B	286–197	AD 422–678 (1528–1272 BP)	Total of 126 shells, of which *C. acuta* 21%, *C. caruanae* 16%, *O. myosotis* 10%, *B. reticulatum* 9%, *Hydrobia* sp. 6% Assemblages with generally less than 20 shells per sample, containing land snails, brackish water and marine species	Major inwash event into a shallow lagoonal or restricted shallow marine environment; land snails reveal an exposed and open environment with rocks/stones and some scrubby patches; reappearance of *Truncatella subcylindrica* and *Ovatella myosotis* suggest a very marginal shoreline and a possible saltmarsh environment
C	197–127	AD 816–1158 (1134–792 BP)	Total of 2078 molluscs, of which *Hydrobia* sp. 43%, *T. subcylindrica* 19%, *Cerithium* sp. 14%, *O. myosotis* 0.8% and *C. acuta* 0.4% Marine and brackish water species dominated the assemblages; number of molluscs generally exceeded 100 per sample, once reaching more than 300; land snails occurred irregularly in small numbers throughout	Saltmarsh or restricted shoreline to very shallow marine lagoonal sedimentation as indicated by the mudsnail *Hydrobia* sp. and the two shoreline species *T. subcylindrica* and *O. myosotis;* fine layering suggests aquatic deposition mainly of land-derived sediments in quiet waters; continued presence of open ground taxa, particularly *C. acuta* suggests open, exposed terrestrial environments while *Xerotricha conspurcata* may indicate the removal of dense vegetation, either through anthropogenic or natural causes
D	127–86	AD 1146–1486 (804–464 BP)	Total of 274 shells, of which *Hydrobia* sp. 46%, *O. myosotis* 23%, T. *subcylindrica* 15%, *C. acicula* 1%, *C. acuta* 0.3% Predominantly brackish water and shoreline species; marine molluscs occurred in very low numbers throughout; land snails were very rare and only found towards the top of the zone; apart from the lowermost sample, the total number of molluscs found was well below 100	Present day sea level is at 125 cm; very close to the previous zone in terms of environment; again, a restricted shoreline to shallow marine or lagoonal environment as indicated by the mud-snail *Hydrobia* sp. and the shoreline/ saltmarsh species *T. subcylindrica* and *O. myosotis*; hardly any land snails, but the presence of the burrower *Cecilioides acicula* may indicate erosion events that led to the deposition of land derived sediments on the coring site
E	86–14	AD 1357–1663 (593–287 BP)	Total of 729 shells, of which *Hydrobia* sp. 40%, *Cerithium* sp. 15%, *T. subcylindrica* 10%, *C. acuta* 8% and *O. myosotis* 0.5% Mixed assemblages containing mainly marine and brackish water molluscs; land snails were found in most samples, but exceeded 20% of all molluscs only in the uppermost 10 cm	This part also lies above the present day sea level and it is likely that the marine molluscs and the brackish water mud-snail *Hydrobia* sp. were washed on land through wave action; the saltmarsh species *O. myosotis* is no longer found beyond 70 cm, but the shoreline species *T. subcylindrica* occurs throughout; the land snails suggest an open and exposed environment; *X. conspurcata* was only found once close to the top of core, indicating dense vegetation

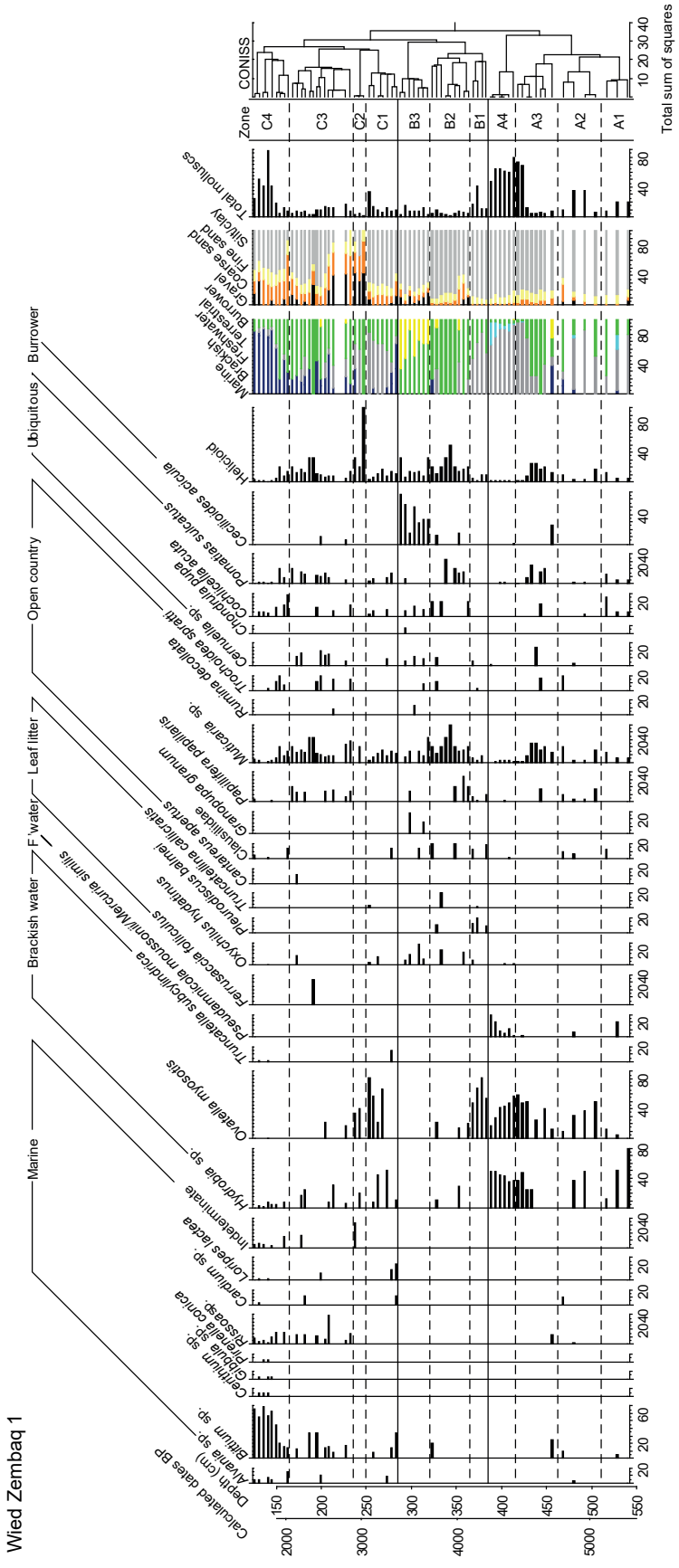

Figure 4.2. *Wied Żembaq 1 molluscan histogram (C.O. Hunt & K. Fenech).*

Table 4.3. *Molluscan zones for the Wied Żembaq 1 core (WŻ1).*

Zone WŻ1-	Depth (cm)	Date ranges cal. BC/AD (BP) for the start of each zone (2σ)	Molluscan assemblages	Environment
A1	548–510	3587–3352 BC (5537–5302 BP)	Total of 48 shells, of which *Hydrobia* sp. (56%), *O. myosotis* (4%), *P. moussonii* (8%), *Muticaria* sp. (6%) Mixed assemblages from the major habitat groups, but less than 20 specimens per sample; freshwater molluscs at 515 cm	Key indicators are *Hydrobia* sp. and *Ovatella myosotis*, suggesting shallowing brackish water, possibly indicating the development of a bay-bar at sea margin to the inlet; presence of freshwater species *Pseudamnicola moussonii* is consistent with inwash from a freshwater stream; very open and erosive terrestrial environments; *Muticaria* sp. are likely derived from the rocky *wied* sides, while *Cochlicella acuta, Pomatias sulcatus* and the helicoids may be associated with very lightly vegetated steppe or garrigue
A2	510–462	3272–2993 BC (5222–4943 BP)	Total of 86 shells, of which *Hydrobia* sp. (35%), *O. myosotis* (33%), *Muticaria* sp. (6%) and *P. moussonii* (2%) Similar to A1, but a sharp rise in the number of brackish water species	Further shallowing of the brackish water and clear transition to salt marsh as indicated by the increased presence of *O. myosotis*; evidence of freshwater stream; increase in karstland species *Papillifera papilaris* and *Muticaria* sp. coupled with a decrease of taxa associated with very lightly vegetated steppe or garrigue may suggest removal of natural vegetation
A3	462–415	2993–2639 BC (4943–4589 BP)	Total of 181 shells, of which *O. myosotis* (48%), *Hydrobia* sp. (35%), *Muticaria* sp. (5%), *C. acicula* (1%) and *P. moussonii* (0.5%) Sudden decrease of brackish water species but increase in land snails; towards the top of this zone, the situation is reversed again; only freshwater snail found	Continuous strong presence of saltmarsh species *O. myosotis*, particularly towards the top of the zone; karstland species like *Muticaria* sp. occur throughout, evidence of a freshwater stream only once (at 423 cm); increase again of species characteristic of lightly vegetated steppe and garrigue like *Cochlicella acuta* and *Pomatias sulcatus*; presence of the burrower *Cecilioides acicula* at the base of this zone may point to an erosion event, perhaps in relation with a storm, as suggested also by the presence of marine taxa
A4	415–385	2698–2284 BC (4648–4234 BP)	Total of 377 shells, of which *Hydrobia* sp. (43%), *O. myosotis* (41%), *P. moussonii* (11%) and *Muticaria* (1%) Sudden increase in freshwater snails, reaching 28% at the top of this zone; dramatic decrease in land snails (now less than 5% throughout); zone is clearly dominated by brackish water species; marine taxa are absent	The freshwater channel may have meandered closer to the coring site or may reflect an increase in precipitation, as indicated by the presence of *P. moussonii*, which requires running, perennial freshwater; very brackish lagoonal to saltmarsh conditions are suggested by an increasing presence of *Hydrobia* sp., while the initial dominance of *O. myosotis* decreases from 60% to 20% at the top of the zone; the very few land snails indicate a landscape similar to the previous zones
B1	385–365	2495–2072 BC (4445–4022 BP)	Total of 80 shells, of which *O. myosotis* (64%), *P. balmei* (14%), *C. acicula* (5%), *Muticaria* sp. and *P. papillaris* (each 4%) Sharp decrease in the number of shells found. No more freshwater snails, but a steady increase in land snails, reaching 50% at the top of this zone; first appearance of leaf litter species; brackish water species consist only of *O. myosotis*; marine molluscs are absent	Saltmarsh conditions indicated by a high number of *O. myosotis* and the sudden absence of *Hydrobia* sp.; breakdown of denser vegetation, washing leaf litter species like *Pleurodiscus balmei* into the channel; open country/karstland species *Muticaria* sp. and *P. papillaris* occur throughout; taxa indicative of light vegetation are rare

Table 4.3 *(cont.).*

Zone WŻ1-	Depth (cm)	Date ranges cal. BC/AD (BP) for the start of each zone (2σ)	Molluscan assemblages	Environment
B2	365–320	2386–1936 BC (4306–3886 BP)	Total of 47 shells, of which *Muticaria* sp. (19%), *O. myosotis* (9%), *O. hydatinus* (4%) and *C. acicula* (4%) Dramatic decrease in the number of shells found; assemblages consisted chiefly of land snails, brackish water species were rarely found; one marine shell occurred at the top of this zone, together with land snails, possibly due to an inwash event	Continuous absence of the fresh water snail *P. moussonii* may point to an aridification of the landscape, due to natural and/or anthropogenic causes; this may have accelerated the breakdown of denser vegetation with more leaf litter species being washed into the channel through increased erosion together with open-country and ubiquitous taxa; the presence of the burrower *C. acicula* suggests severe erosion events; these would have overwhelmed the brackish water taxa at times by the sediment flux
B3	320–285	2014–1644 BC (3964–3594 BP)	Total of 55 shells, of which *C. acicula* (40%), *O. hydatinus* (9%), *Muticaria* sp. (9%), *C. acuta* (5%) Dramatic decrease in the number of shells per sample, rarely exceeding 10; the assemblages consisted exclusively of land snail taxa associated with leaf litter, open country/karstland and lightly vegetated environments	The permanent presence and proportion of the burrower *C. acicula* increased steadily, indicating continuous severe erosion, which included the inwash of stones; the shade species *Oxychilus hydatinus*, which also lives underneath stones, was the only leaf litter species found, indicating a further aridification of the landscape; open country/karstland species, mainly *Muticaria* sp., occurred in low numbers throughout, while species associated with light vegetation such as *C. acuta* were rare
C1	285–250	1714–1371 BC (3664–3321 BP)	Total of 90 shells, of which *O. myosotis* (46%), *Hydrobia* sp. (13%), *Muticaria* sp. (8%) and *O. hydatinus* (2%) Assemblages were dominated by marine and brackish water associated molluscs; land snails occurred throughout, but unlike in the previous zone, the burrower *C. acicula* was absent	Increasing sand may reflect the proximity of the shoreline or may result from higher-energy stream-flows; the coherent molluscan assemblages do not suggest violent inwash events; succession of marine-brackish taxa is indicated by *Cardium* and *Loripes,* which are typically shallow-marine taxa from sheltered locations; these are succeeded by the lagoonal *Hydrobia* sp. and then followed by the salt-marsh *O. myosotis,* pointing to shallowing marginal marine then lagoonal water passing into salt marsh; *Muticaria* sp. suggests inwash from the rocky sides of the *wied* and *C. acuta, P. sulcatus* and the helicoids suggest very lightly vegetated terrestrial habitats
C2	250–235	1403–2033 BC (3353–2983 BP)	Total of 9 shells, *O. myosotis* (33%), *Hydrobia* sp. (11%) and *Muticaria* sp. (11%) Assemblages contained only 1 to 5 molluscs per sample, all heavily fragmented and belonging to marine, brackish water and terrestrial environments	The stony deposits could reflect vigorous flows in the *wied*, but may also be consistent with the approach of the open shoreline with rising sea levels; the continuation of *O. myosotis* and *Hydrobia* sp. points to a marginal lagoon/saltmarsh environment
C3	235–165	1231–907 BC (3181–2857 BP)	Total number of shells: 116, of which *Bittium* sp. (11%), *Rissoa* sp. (9%), *Hydrobia* sp. (8%) and *Muticaria* sp. (15%) Number of molluscs increases irregularly up to 17 shells per sample; most samples contained an admixture of marine, brackish water and land snail species; brackish water species were generally the least common	Coarse sand and stones continue to dominate the lower half of this zone, again reflecting vigorous flows and possibly wave action with continuously rising sea levels, as also indicated by the increase in marine species like *Bittium* and *Rissoa* spp.; *O. myosotis* continues to decline, the persistence of *Hydrobia* sp. is consistent with a lgaoonal environment; leaf litter species were few and only found in the upper part of the zone, probably as a result of inwash events; the other terrestrial species are consistent with open, exposed habitats, with *Muticaria* sp. and *P. papillaris* suggesting inwash from the rocky sides of the *wied* and *T. spratti, Cernuella* sp., *C. acuta* and *P. sulcatus* indicating very lightly vegetated ground

Table 4.3 *(cont.).*

Zone WŻ1-	Depth (cm)	Date ranges cal. BC/AD (BP) for the start of each zone (2σ)	Molluscan assemblages	Environment
C4	165–115	477 BC–AD 124 (2427–1826 BP)	288 shells in total, mainly *Bittium* sp. (56%); *Hydrobia* sp. (5%); *Muticaria* sp. (3%) Increasing dominance of marine molluscs in the mixed assemblages, reaching more than 80% at the top of this zone; brackish water species are rare and generally less than 10%; the remainder are land snails, decreasing from 80% at the base to around 10% at the top	The persistence of *Hydrobia* sp. in this zone points to a lagoonal environment; the marine taxa were all very small and associated with sandy/muddy bottoms and marine algae, possibly washing into the inlet; leaf litter species were reduced to only one specimen in the entire zone (*O. hydatinus*), while the open country species generally persisted throughout, as did species associated with very light vegetation

Table 4.4. *Molluscan zones for the Wied Żembaq 2 core (WŻ2).*

Zone WŻ2-	Depth (cm)	Date ranges cal. BC/AD (BP) for the start of each zone (2σ)	Molluscan assemblages	Environment
A1	521–478	3495–3097 BC (5445–5047 BP)	Total of 212 shells, of which *O. myosotis* (59%), *Hydrobia* sp. (16), *Muticaria* sp. (8%), *P. moussonii* (0.5%) Mixed assemblages, at times from all the major habitat groups; one freshwater mollusc at 503 cm	Key indicators are *Hydrobia* sp. and *Ovatella myosotis*, suggesting shallowing brackish water and development of a saltmarsh; presence of one specimen of the freshwater species *Pseudamnicola moussonii* was inwashed from a freshwater stream; presence of a few leaf litter species indicates dense vegetation in the vicinity. *Muticaria* sp. and the other open country species are likely derived from the rocky *wied* sides, while *Pomatias sulcatus* and the helicoids may be associated with very lightly vegetated steppe or garrigue
A2	478–379	3170–2781 BC (5120–4731 BP)	Total of 192 shells, *O. myosotis* clearly dominating (70%). *Hydrobia* sp. (7%), *Muticaria* sp. (5%), *P. balmei* (2%) Fewer marine molluscs and land snail species than in A1; sharp rise in the saltmarsh species *O. myosotis*	Further shallowing of the brackish water and clear transition to salt marsh as indicated by the sharply increased presence of *O. myosotis*; at the base of this zone, this is coupled with an increase in coarse sand; no more evidence of freshwater stream; decrease in leaf litter taxa and the karstland species *Muticaria* sp. coupled with a decrease of taxa associated with very lightly vegetated steppe or garrigue
B1	379–336	2469–1926 BC (4419–3876 BP)	Total of 54 shells; no clearly dominating species. *Muticaria* sp. (11%), *O. myosotis* (7%), leaf litter species (9%), *C. acicula* (2%) Sharp decrease in the number of shells found; no more marine or freshwater snails, brackish water species occur irregularly in small numbers only	Sharp decrease in brackish water species, coupled with an increase in land snails; beginning of breakdown of denser vegetation, washing leaf litter species like *Pleurodiscus balmei* into the channel; erosion is indicated by *C. acicula*; open country/karstland species *Muticaria* sp. and *P. papillaris* occur throughout, taxa indicative of light vegetation are also present
B2	336–300	2138–1579 BC (4088–3529 BP)	Total of 40 shells, dominated by the land snails *C. acicula* (33%). *O. hydatinus* (10%), *Muticaria* sp. (8%) Further decrease in the number of shells found; assemblages consisted chiefly of land snails, brackish water species were rarely found; only one marine shell occurred at the top of this zone, together with land snails, perhaps due to an inwash event	Significant breakdown of vegetation and stark increase in erosion inwash events indicated by *C. acicula* and the appearance of stones; this may point to aridification of the landscape, which may have accelerated the breakdown of denser vegetation with leaf litter species continuously being washed into the channel through increased erosion together with open country and ubiquitous taxa; the strong presence of the burrower *C. acicula* suggests severe erosion events; like in WŻ1, the sediment flux would have overwhelmed the brackish water taxa at times

Table 4.4 *(cont.).*

Zone WŻ2-	Depth (cm)	Date ranges cal. BC/AD (BP) for the start of each zone (2σ)	Molluscan assemblages	Environment
C1	300–273	1825–1258 BC (3775–3208 BP)	Total of 82 shells; *Bittium reticulatum* (34%), *Rissoa* sp. (8%), *Hydrobia* sp. (12%), *O. myosotis* (5%), *Muticaria* sp. (4%) Assemblages showed a strong component of marine and brackish water associated mollusk; land snails occurred throughout, but unlike in the previous zone, the burrower *C. acicula* only occurred once at the base of this zone	Strong presence of stones and increasing coarse sand may reflect the proximity of the shoreline or may result from higher-energy stream-flows; the molluscan assemblages may perhaps suggest one violent inwash event (at 285 cm) in this initially coherent sequence, where marine taxa (mainly *Bittium* sp.) are succeeded by the lagoonal *Hydrobia* sp.; the land-derived inwash event carried *O. myosotis* and various land snails from open country onto the site; after this event, *Hydrobia* sp. briefly dominate the assemblages, while more land snails like *Muticaria* sp. suggests inwash from the rocky sides of the *wied* and *C. acuta, P. sulcatus* and the helicoids suggest very lightly vegetated terrestrial habitats; marked decrease in diversity and abundance of leaf litter species may point to aridification of the landscape
C2	273–228	1584–944 BC (3534–2894 BP)	Total of 155 shells; *Bittium reticulatum* (30%), *Hydrobia* sp. (8%), *Muticaria* sp. (6%), *C. acicula* (2%) Assemblages contained between 2 and 36 molluscs per sample, increasing towards the top of the zone; all were heavily fragmented and belonged to marine, brackish water and terrestrial environments	Again, the stony deposits could reflect vigorous flows in the *wied*, as indicated by the overwhelming presence of land snails at the base of this zone, including the erosion indicator/burrower *C. acicula*; the following increase in sand may perhaps be consistent with the approach of the shoreline, but land derived erosion continues to wash in open country and ubiquitous land snail species, including *C. acicula*; perhaps as a result of aridification, only one leaf litter species was found in the entire zone; the continuation of *O. myosotis* and *Hydrobia* sp. points to a marginal lagoon/saltmarsh environment, which gradually shows stronger marine influence towards the top of this zone
C3	228–178	1127–375 BC (3077–2325 BP)	Total of 52 shells; *Bittium reticulatum* (33%), *Hydrobia* sp. (10%), *O. myosotis* (21%), *Muticaria* sp. (8%) Number of molluscs varies between 4 and 21 per sample, increasing irregularly to up to 17 shells per sample; most samples contained an admixture of marine, brackish water and land snail species, but one sample contained only land snails (at 193 cm); brackish water species were generally the least common	Coarse sand and stones continue to occur in this zone, again reflecting vigorous flows and possibly wave action with continuously rising sea levels, as also indicated by the increase in marine species like *Bittium* sp. *O. myosotis* features strongly at the base of this zone but then occurs only once again (at 185 cm); the persistence of *Hydrobia* sp. is consistent with a lagoonal environment; leaf litter species were only found once, at the base of the zone, probably as a result of inwash events; the other terrestrial species are consistent with open, exposed habitats, with *Muticaria* sp. and *T. spratti* suggesting inwash from the rocky sides of the *wied*
C4	178–115	566 BC–AD 241 (2516–1709 BP)	Total of 493 shells; *Bittium reticulatum* (44%), *Hydrobia* sp. (9%), *Muticaria* sp. (3%), *T. subcylindrica* (2%) Increasing dominance of marine molluscs in the mixed assemblages, reaching more than 75% from 161 cm upwards; brackish water species are found in low numbers in most samples; the number of land snails varies greatly	Several stony deposits, possibly consistent with the approach of the open shoreline with rising sea levels, as also indicated by the overwhelmingly marine taxa; also here, the persistence of *Hydrobia* sp. in this zone points to a lagoonal environment; the marine taxa are more diverse and numerous than in WŻ1, but also here they were all very small and associated with sandy/muddy bottoms and marine algae, possibly washing into the inlet; leaf litter species were found only once in the entire zone (*O. hydatinus*), while the open country species persisted throughout, as did species associated with very light vegetation. *C. acicula* at the top may be the result of recent burrowing

4.5.1. Marsaxlokk (MX1)[6]

The coring site was located on the northern shore in the inner harbour in Marsaxlokk Bay on a field at a distance of less than 100 m from the sea. The multi-period site of Tas-Silġ, occupied between the Neolithic Temple Period and Late Roman era is located less than 1 km uphill to the north (Bonanno & Vella 2015). The coring site is 1.25 m above present day sea-level. The Marsaxlokk 1 core (MX1) had a total reported depth of 3.86 m and consisted of four core-tubes.

The basal date is likely to be *in situ*, but the dates above and the pottery fragment recovered from the core are most certainly recycled. The Bayesian model is used for the interpretation of the various zones, which show one major inwash event (MX1-C), while the rest of the core shows a fairly steady small-scale sedimentation since the early first millennium AD (Fig. 4.1; Table 4.2).

The land snail assemblages in this core from Marsaxlokk showed a predominantly open country (garrigue and karstland) environment. Only one leaf litter species was present (*Xerotricha* sp.), and it occurred only twice, possibly indicating the past occurrence of shrubs. The majority of land snails belonged to the ubiquitous group, which may reflect a disturbed environment.

The brown sediments which directly overlay the bedrock are indicative of a buried B horizon of a well developed palaeosol (see Chapter 5), in which any land snails have weathered out long ago and only fragments of marine species survived. Given its position below present day sea level and the fact that marine-linked quiet water sedimentation occurred one metre further up, it is possible that there may have been fairly recent tectonic displacement here.

The section shows strong inwash of terrestrial material, but there are also signs for gentle, fairly continuous sedimentation close to a shoreline behind a bay-bar, in some kind of shallow lagoon with a marine connection or in a shallow embayment only slightly connected with the open sea.

4.5.2. Wied Żembaq (WŻ)

Two cores were retrieved at a location close to St George's Bay in Birżebbuġa in a flat area at the mouth of Wied Żembaq. The coring site is 1.05 m above present day sea level and the distance from the present shoreline is around 250 m. Close by, on a hill overlooking the coring location, are the Neolithic remains of Borġ in-Nadur and remnants of a Bronze Age settlement and wall (Tanasi & Vella 2011a & b).

The Wied Żembaq 1 core (WŻ1) extended to a depth of 5.48 m and consisted of five tubes, but bedrock was not reached. The Wied Żembaq 2 core (WŻ2) was taken at a distance of around 5 m from WŻ1 and extended to 5.25 m, also without reaching bedrock. The Bayesian model provides the date frames for both cores, shown in Figure 4.2 and Tables 4.3 and 4.4.

Similarities can be observed between the coring sites WŻ1 and WŻ2, because of their proximity. Differences in the zones in both cores may be because the *thalweg* (i.e. the main channel) is quite narrow and meandering, with the meanders migrating through time. This may have led to a cut-and-fill stratification, where WZ2 would have missed the channel deposits containing *Pseudamnicola moussonii* in Zone A, but received an increased stone inwash in Zone C. Table 4.5 compares and combines the data of both cores.

4.5.2.1. Conclusion: Wied Żembaq

The cores cover a good part of the Temple Period from around 3500 cal. BC and following periods up to cal. AD 115–829 (see Tables 2.3 & 2.4). They revealed several changes in the palaeogeography and palaeoenvironment. It appears that the relative sea level was still rising at Wied Żembaq, possibly because of local tectonics, but it is also possible that what can be seen as marine deepening and shallowing may reflect meandering of the channel and coastal change rather than sea level oscillations.

Molluscs in Zone A, dated from *c*. 3500 to *c*. 2300 cal. BC in WŻ1 and WŻ2 (up to *c*. 2200 cal. BC), indicated that during the Temple Period, the landscape in Wied Żembaq was dry and open, despite the presence of a perennial, running freshwater stream, as indicated by *P. moussonii*. Evidence for this stream occurred only sporadically in zones A1 and A2 of WŻ1 and A1 of WŻ2, but was clearly manifest in A4 of WŻ1, indicating a distinctive humidity event that possibly led to the establishment of shrubs or dense vegetation further upstream. It appears from WŻ1 that the end of this zone (2300±200 cal. BC) may reflect events at the end of the Temple Period. Immediately following the humidity event, a progressive breakdown of the landscape can be observed in both cores (Zone B), where now leaf litter shells (i.e. *Lauria cylindracea*) were washed into the valley as a result of landscape degradation. It is unclear whether this breakdown is a result of anthropogenic pressure or severe aridification or a combination of the two that led to the end of the Temple Period, as evidence for the freshwater stream did not reappear after this date. Erosion events, so strong that even stones and the burrower *Cecilioides acicula* were moved in the mud-flows, progressively accelerated to the end of this zone at about 1543±172 cal. BC (see Table 2.2) in the Bronze Age. Some sort of stabilization can be observed in Zone C in both cores, where however freshwater species remain absent, leaf

Table 4.5. *Integration of molluscan zones from Wied Żembaq cores 1 and 2.*

Date/Period cal. BC/AD (2σ)	Zone	Description	Environment
c. 3500–2300 BC in WŻ1 *c*. 3200–2200 BC in WŻ2 Temple Period to Bronze Age	A	Both cores show broad similarities in the particle size distribution and molluscan assemblages, though WŻ2 has the occurrence of *P. moussonii* only once, towards the base of this zone; sediments datable to the end of the Temple Period were only found in WŻ1	Dry and open landscape, lightly vegetated steppe or garrigue; denser vegetation probably further upstream; shallowing of lagoon and expansion of saltmarsh; presence of a perennial, running freshwater stream
c. 2300–1500 BC in WŻ1 *c*. 2200–1500 BC in WŻ2	B	Strong similarities with regards to molluscan assemblages and particle size distribution	Aridification of the landscape, disappearance of freshwater stream; breakdown of denser vegetation, increase in erosion; sharp decline in saltmarsh species, probably due to high influx of land-derived inwash of eroded sediment
c. 1500 BC–AD 500 in WŻ1 and WŻ2	C	Broad similarity in the molluscan assemblages but differences in the particle size distribution, probably due to a meandering of the channel	Reappearance of saltmarsh environment, which however again progressively declines as lagoonal/marine species increase due to rising sea level; continuous aridification leads to sharp decrease in dense vegetation, open country/ karstland and light vegetation dominate

litter species were scarce and the open country and ubiquitous species persisted throughout, while marine influence grew steadily, marginalizing the saltmarsh.

4.5.3. Mġarr ix-Xini (MĠX)

The coring location was less than 100 m away from the present-day shoreline and in a level area towards the middle of an elongated alluvial plain at the mouth of Wied Mġarr ix-Xini that opens on the south-eastern coast of Gozo. The catchment area for the valley is approximately 4.5 sq. km. There are no Neolithic remains in the immediate vicinity, but rock-cut trenching pans and vats, thought to be late Punic or Roman, have been found close by.[7] The sediment core had a total reported length of 709 cm and extended from 0.34 to 7.43 m depth. It consisted of eleven core-tubes (see description in chapter on cores). The Bayesian model provides the date frame for the core and the molluscan zones are shown in Table 4.6.

4.5.3.1. Conclusion: Mġarr ix-Xini

The earliest sediments retained in this core were datable to the Punic period. Older sediments had not been preserved at this site. Although a large quantity of sediments was washed through fluvial action down the valley of Mġarr ix-Xini, evidence for a perennial freshwater stream was not found. It is possible that, as in Wied Żembaq, there may have been a stream in the more distant past, but run-off was already ephemeral by the time sedimentation started in the Punic period. The light vegetation and karstland of the area is evident from the land snail faunas. Only the very rare occurrences of leaf litter taxa suggest a little denser vegetation at times. Numerous strong storm events caused inwash of land snails and often fragmentary marine molluscs, together with coarse sand and gravel. These alternated with quieter phases characterized by fine-grained sediments and lagoonal faunas. The continuously varied stratigraphy mirrored the changing influences governing the site, with bay-bars forming and breaching repeatedly. Evidence for viticulture was found from the late Punic Period until a severe erosion event, probably around the third/fourth centuries AD, which may perhaps have destroyed the vineyard.

4.5.4. Marsa 2

The floodplain at Marsa, today largely covered by the Marsa Sports Grounds, lies at the base of the largest catchment in the Maltese Islands (43.8 sq. km) and is surrounded by numerous archaeological sites that testify human presence at least from the Ġgantija phase onwards (*c*. 3450–3200 cal. BC) (Fenech 2007). The core had been extracted by a mechanical corer in June 2002, prior to the building of a sports complex on the site at a distance of *c*. 200 m from the present shoreline, and at a spot 1.18 m above mean sea level. As this core was not part of the *FRAGSUS* coring programme, soil colours and additional information are in Appendix 3.[8]

The core had a total length of 9.4 m, which translated into 143 segments of 5 cm, divided in two halves. Problems were encountered when extracting the Marsa 2 core, caused by wet sandy sediments that could not be retained in the core and stones/boulders that caused gaps in the stratification.

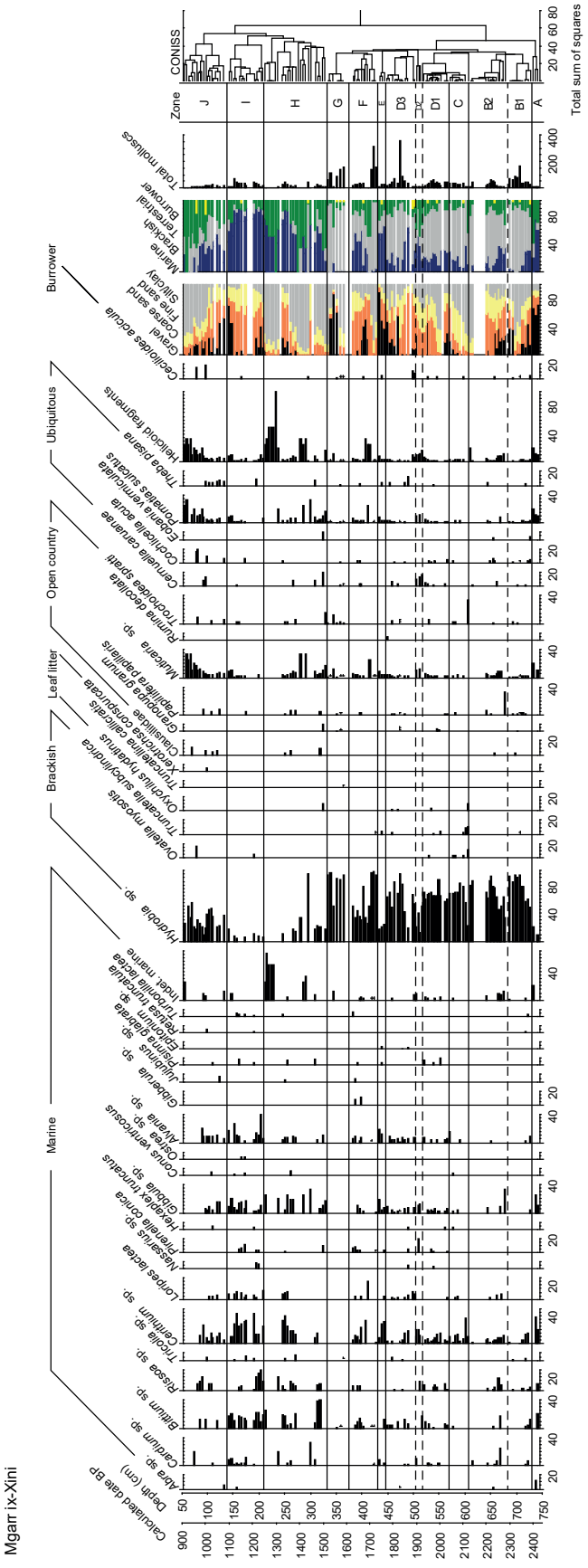

Figure 4.3. *Mgarr ix-Xini molluscan histogram (C.O. Hunt & K. Fenech).*

Table 4.6. *Molluscan zones for the Mġarr ix-Xini 1 core (MĠX1).*

Zone	Depth (cm)	Date ranges cal. BC/AD (BP) for the start of each zone (2σ)	Molluscan assemblages	Environment
A	743–730	no date	Total of 23 shells, of which *Cerithium* sp. (22%), *Gibbula* sp. (14%), *Hydrobia* sp. (9%), *Muticaria* sp. (9%) Cracked bedrock interface with sand and mud, containing molluscs from marine, brackish water/lagoonal and terrestrial environments	Mixed marine environment, dominated by sandy bottoms (*Cerithium* sp.) with hard substrate close by *(Gibbula* sp.); the few land snail fragments washed in were mainly *Muticaria* sp., *P. sulcatus* and a few heliciid fragments, indicating a predominantly open, karstland environment with very little vegetation in the valley
B1	730–683	at 702 cm: 487–236 BC (2437–2186 BP)	Total of 610 shells, of which *Hydrobia* sp. (85%), *Cerithium* sp. (3%), *Muticaria* sp. (1%) General fining up of sediments and increase in the overall number of molluscs, but an inwash with stones again at the top of the zone; land snails are present throughout, marine molluscs decrease while brackish water species increase considerably	Possible formation of a bay-bar may have led to increasingly brackish water conditions; a combination of gravel, land snails and marine molluscs at the base of this zone may point to a flood and storm event, with soil erosion indicated by the presence of the burrower *C. acicula*; the presence of grape seeds of *Vitis vinifera* attests viticultural activity in the vicinity, in a landscape that was predominantly open, with light vegetation and grassland, surrounded by karstland (*Muticaria* sp., *C. acuta, P. sulcatus*)
B2	683–607	448–194 BC (2398–2144 BP)	Total of 340 shells, of which *Hydrobia* sp. (75%), *Cerithium* sp. (4%), *Muticaria* sp. (3%) Stones with coarse sand dominate most of this zone, silt/clay at the top; marine molluscs in varying amounts were present in most samples, as were land snails; brackish water species were the most common	Continuation of brackish water conditions with lagoonal and marine influence; as in the previous zone, there appears to have been another fluvial flood event in combination with a wave-based storm event; the increase in marine diversity and coarse sand compared to the previous zone may be due to stronger wave action; the land snails, chiefly *Muticaria* sp. and *P. sulcatus*, indicate a predominantly open country/karstland with little vegetation and grassland; seeds of *Vitis vinifera* indicate the continuation of viticulture in the vicinity
C	607–568	288–24 BC (2238–1974 BP)	Total of 186 shells, of which *Hydrobia* sp. (72%), *Cerithium* sp. (10%), *O. myosotis* (2%), *Muticaria* sp. (2%) Number of shells decreased, possibly due to rapid sedimentation; silty brownish grey sediments at the base progressively getting lighter in colour and coarsening up to the top of the zone; increase in sand and stones is coupled with an increase in marine molluscs, while the land snail numbers remains relatively steady, but low	Possibly another storm event, where the waves would winnow finer material and once in suspension it would flow out to the sea as a gravity current and be lost to the site, as indicated by the coarsening-upward pattern; strong soil erosion is suggested by the burrower *C. acicula*; seeds of *Vitis vinifera* indicate continuation of viticulture in the vicinity; absence of lagoonal species, but good presence of the infra-littoral sand species *Cerithium* sp. throughout in a brackish water environment dominated by *Hydrobia* sp.; presence of a saltmarsh is indicated by *O. myosotis* and the coastal species *T. subcylindrica*; first appearance of the leaf litter species *O. hydatinus. Muticaria* sp. and *T. spratti* indicate continuation of open country/karstland conditions, grassland is suggested by *C. acuta.*

Table 4.6 *(cont.).*

Zone	Depth (cm)	Date ranges cal. BC/AD (BP) for the start of each zone (2σ)	Molluscan assemblages	Environment
D1	568–518	204 BC–AD 59 (2154–1891 BP)	Total of 440 shells, of which *Hydrobia* sp. (66%), *Cerithium* sp. (6%), *Muticaria* sp. (2%), *C. acicula* (2%) Increase in the number of shells found; sediments were light grey and very sandy, coarsening upwards; stones were found in only one sample, probably as a result of a fluvial inwash event, as indicated by the high number of land snails and the burrower *C. acicula*; one sample at the base of the zone contained no land snails, all other samples had a mixture of marine, brackish water and land snails, with the brackish water species *Hydrobia* sp. dominating the assemblages	Predominantly a brackish water environment with growing lagoonal/marine influence; decreased presence of saltmarsh species *O. myosotis* and coastal *T. subcylindrica*; larger diversity of land snails, indicating a mosaic of dense and light vegetation and persistence of open country/karstland; severe terrestrial erosion is suggested by the burrower *C. acicula*
D2	518–504	98 BC–AD 168 (2048–1782 BP)	Total of 47 shells, of which *Hydrobia* sp. (40%), *Cerithium* sp. (11%), *Muticaria* sp. (4%) In this thin sandy zone, the brackish water *Hydrobia* sp. were a minority, a variety of land snails and marine molluscs dominated, suggesting another storm event	The marine molluscs washed onto the site came from sandy, lagoonal and rocky habitats, suggesting disturbed waters through wave action during a storm; *Hydrobia* sp. were present, but at much lower numbers than in the previous zones; no leaf litter species were found, the land snail assemblages consisted chiefly of the karstland species *Muticaria* sp. and the ubiquitous *C. caruanae* and *P. sulcatus*.
D3	504–447	67 BC–AD 197 (2017–1753 BP)	Total of 740 shells, of which *Hydrobia* sp. (79%), *Cerithium* sp. (3%), *Alvania* sp. (3%), *Muticaria* sp. (1%) Light grey sandy sediments, often with stones; sediments initially fining upwards, indicating quieter times of sediment input but then coarsen upwards again, suggesting an event; amounts of shells per sample greatly varied between 9 and 353 individuals; all assemblages contained marine, brackish water and land snails	Mixed assemblage of marine species from lagoonal, sandy and rocky habitats suggest strong wave-induced movement at the seafloor during windstorms; these storms were likely combined with heavy rainfall as indicated by the presence of land snails throughout, including the occurrence of the burrower *C. acicula*; the land snail spectrum was very similar to zone D1, indicating little change in the environment; brackish water conditions persisted, but there was no longer evidence of a saltmarsh
E	447–430	AD 59–318 (1891–1632 BP)	Total of 60 shells, of which *Hydrobia* sp. (22%), *Cerithium* sp. (27%), *Gibbula* sp. (5%), *Muticaria* sp. (5%), *C. acicula* (2%) Mixed assemblages in all samples, very high stone and sand content	Due to the high stone and sand content, the mud snail *Hydrobia* sp. was no longer dominant; the stone influx may be due to a fluvial inwash event, as indicated by the presence of land snails, notably the karstland *Muticaria* sp. and the ubiquitous *P. sulcatus*, the latter being associated with soils, as is the burrower *C. acicula*; as before, the inwash event may have been in combination with a severe storm, which through wave action would have washed the proportionally high number of marine mollsucs, mainly associated with sand and rocky bottoms onto the site; continuation of viticultural activity close by

Table 4.6 *(cont.).*

Zone	Depth (cm)	Date ranges cal. BC/AD (BP) for the start of each zone (2σ)	Molluscan assemblages	Environment
F	430–375	AD 96–356 (1854–1594 BP)	Total of 782 shells, of which *Hydrobia* sp. (86%), *Cerithium* sp. (2%), *Muticaria* sp. (1%) Mixed assemblages throughout, but the base of this zone shows a strong dominance of the brackish water mudsnail *Hydrobia* sp.; a sudden increase of sand and stones is accompanied by a strong increase in marine and land snails	Initially the zone shows a fairly quiet brackish water environment with only very few marine molluscs and land snails being washed in, with *Hydrobia* sp. reaching more than 300 individuals in one sample (at 423 cm); the situation changes soon afterwards with a sudden influx of stones, coarse and fine sand, fining up to the end of this zone, but with silt/clay remaining reduced to around 10% only; during this episode, sand- and rock-associated marine molluscs are washed in, but the overall number of molluscs per sample decreases dramatically; the land snails contained no leaf litter-associated species and again reflect open country/karstland and lightly vegetated surroundings
G	375–333	AD 218–474 (1732–1476 BP)	Total of 569 shells, of which *Hydrobia* sp. (92%), *T. spratti* (2%), *Muticaria* sp. (1%), *C. acicula* (0.5%) Assemblages consisted chiefly of the brackish water *Hydrobia* sp. with little to no marine molluscan influx; initially, also the land snails were rare, but with the sudden inwash of stones and coarse sand, possibly during a predominantly fluvial event, their numbers increased	Possibly due to a heightened bay-bar, the marine influence is very little in this zone, which is characterized initially by brackish water sandy muds; *Hydrobia* sp. reaches the highest percentages in the core, indicating a fully blown brackish water environment; there was inwash of an array of land snails, predominantly open country/karstland species; grape seeds suggest that viticulture was still practised at this time; a storm event led to the inwash of limestone pebbles accompanied by open country/karstland species, and heavily fragmented marine molluscs
H	333–210	AD 313–566 (1637–1384 BP)	Total of 289 shells, of which *Hydrobia* sp. (22%), *Cerithium* sp. (15%), *B. reticulatum* (12%), *Muticaria* sp. (4%) Despite the length of this zone, the number of molluscs found was comparatively low, indicating dilution during rapid sedimentation; the molluscan assemblages are mixed, with a very strong marine and terrestrial input, considerably diminishing the brackish water influence, except at 296 cm, where for the last time a clear brackish water environment was detected	The land snails show that the terrestrial environment was highly open and exposed, throughout; there is no further evidence of viticulture being practised in the area; at the base of this zone, there is an increase in coarse and fine sand; this is coupled with an increase in marine shells and decrease in land snails, indicating strong marine influence; it is suggested that the severe event at the end of zone G may have led to the breakdown of the bay-bar, dramatically diminishing the brackish water body and increasing marine influence in the bay; the subsequent silt/clay unit was associated with a rise in *Hydrobia* sp. suggesting re-establishment of the brackish lagoon; coarsening sediments, which become predominantly stony, are then associated with a sharp decline in *Hydrobia* sp. and rise in marine molluscs; the final sediments in the zone are silt/clays, but contain mostly unidentifiable fragments of land and marine shells, while brackish water species are no longer present

Table 4.6 *(cont.).*

Zone	Depth (cm)	Date ranges cal. BC/ AD (BP) for the start of each zone (2σ)	Molluscan assemblages	Environment
I	210–138	AD 598–818 (1352–1132 BP)	Total of 391 shells, of which *Cerithium* sp. (28%), *B. reticulatum* (13%), *Hydrobia* sp. (5%), *Muticaria* sp. (2%) The sediments consisted mainly of marine sands, at times with stones and throughout with very little silt/clay; this was reflected in the molluscan assemblages, which were dominated by an array of marine molluscs from all kinds of substrates, with sand dominating	Predominantly a sandy marine environment, where the influx of stones and silt/clay appears to be mainly land-derived through fluvial events, as indicated by the presence of land snails; the occurrence of *O. myosotis* points to a saltmarsh in the vicinity of the severely diminished brackish water body as indicated by the low numbers of *Hydrobia* sp. found; land snails occurred in low numbers in all samples, once also including the burrower *C. acicula*, indicating land-derived erosion
J	138–50	AD 753–982 (1197–968 BP)	Total of 217 shells, of which *Hydrobia* sp. (32%), *Cerithium* sp. (8%), *Alvania* sp. 5%, *Muticaria* sp. (7%) Most of the molluscan assemblages contained marine, brackish water and land snail species, in low numbers; the number of marine molluscs decrease as the presence of land snails increases; the silting-up of the bay is also indicated by the increase in silt/clay and changing sediment colour to light brown	The last zone shows the silting up of the bay and turning it from marine to terrestrial through increased land-derived erosion; marine wave action plays a diminishing role, brackish-water shells also occur, but in very low numbers; here *C. acicula* may be intrusive as a burrower; the land snails continue to attest the open country/karstland of the previous zones; leaf litter is scarce, there is very light vegetation and grassland as suggested by e.g. *T. pisana* and *C. acuta*

As there was a lack of suitable material for dating in the lower three metres of the core, the first date obtained was at 6.17 m, placing that part of the core into the end of the Late Bronze Age. The Bayesian model was adopted to calculate the age against the depth of the core from this date onwards. With the help of the CONISS analysis, the core could be sub-divided into five major zones (Fig. 2.4; Table 2.7).

4.5.4.1. Conclusion: Marsa

Despite the 9.4 m length of the core, the sediments that presumably belonged to prehistory could not be securely dated and hardly contained any land snails. As such, it is difficult to draw any conclusions about the prehistoric environment other than 'open and lightly vegetated'.

The area of the coring site was formerly subjected to numerous high-energy events, which included land-derived flooding, during which vast amounts of sediments that often contained stones were carried into the harbour. An unknown amount of these deposited sediments may have then been subjected to further erosion. Wave-action during windstorm events also could have led to the removal and redeposition of marine sediments at the coring site.

Nonetheless, the eventful stratigraphy also showed that in the past there was an array of freshwater bodies in the vicinity: a perennial running freshwater stream, slow moving water/ponds and associated wetlands at least since the end of the Late Bronze Age onwards, until the harbour silted up. During the era of the Knights of St John, the area was described as a swamp, and the water of the freshwater stream was collected in a reservoir (Abela 1647).

The terrestrial environment throughout appeared to be predominantly open, with some light vegetation. Evidence for dense vegetation/scrub was found from the end of the Late Bronze Age onwards, but could have, like the freshwater environments, existed before as these shells were found in the same levels. The noted reduction of the freshwater environments in Zone D also had an impact on the leaf litter snails and it is possible that this may have been because of progressive aridification. The lack of vegetation cover may have led to more intense erosion, which then eventually led to the silting up of the harbour, gradually turning it eventually into a terrestrial environment.

4.5.5. Salina Deep Core

The coring site lies at the end of the Burmarrad Plain, a large alluvial plain at the base of the second largest catchment in Malta, with an area of 34.8 sq. km. Numerous archaeological remains, including two Neolithic temples in the vicinity, date back to the Temple

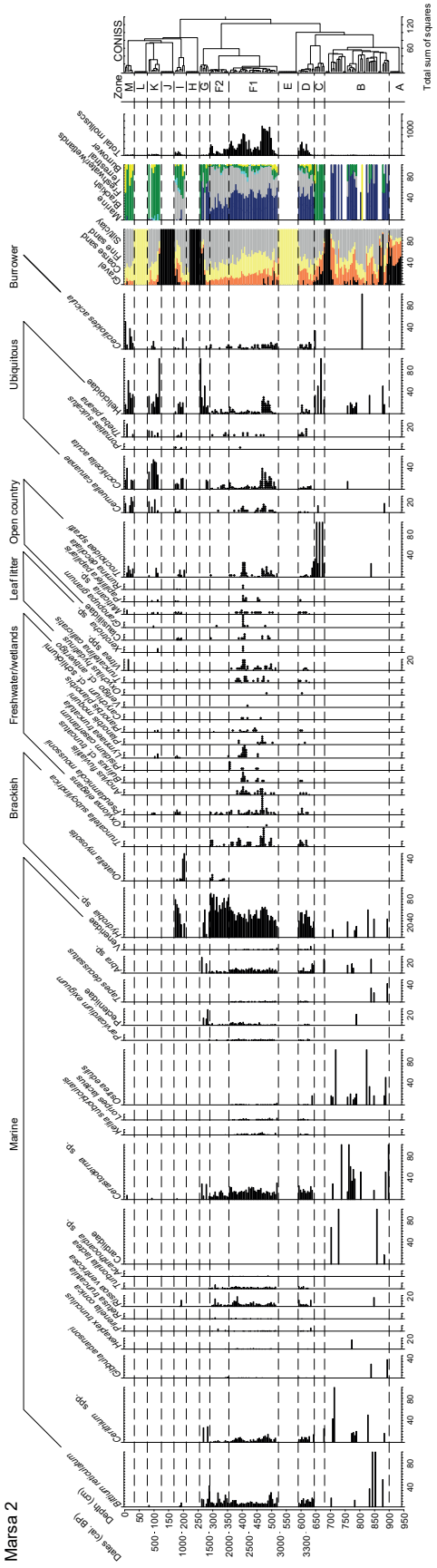

Figure 4.4. *Marsa 2 molluscan histogram (C.O. Hunt & K. Fenech).*

Table 4.7. *Molluscan zones for the Marsa 2 core (MC2).*

Zone MC2-	Depth (cm)	Date ranges cal. BC/ AD (BP) for the start of each zone (2σ)	Molluscan assemblages	Environment
A	943–900	no date	Bedrock and sterile sediments at the base	
B	900–680	no date	Total of 97 shells, of which *Cerastoderma* sp. 24%, *Ostrea* sp. 13%, *Cerithium* sp. 11%, *Hydrobia* sp. 9% and *C. acicula* 2% Despite the length of the zone, only a few molluscs were found, most of them heavily fragmented; the molluscan assemblages were predominantly marine, but often mixed with a few brackish water and land snails	A marine environment is clearly suggested by the number and variety of marine molluscs found, indicating fluctuations between lagoonal (e.g. *Cerastoderma* sp.), marine (e.g. *B. reticulatum* and *Cerithium* sp.) and brackish water conditions (*Hydrobia* sp.); the predominantly sandy/gravelly sediments are likely gravity-flow deposits spreading out across the bottom of the harbour from floods in the catchment; the deposited sediments which included stones and boulders, at times also contained land snail fragments, while many samples were completely sterile, indicating rapid deposition, especially at the top of the zone; severe land-derived erosion is also indicated by the burrower *C. acicula*; the few land snails point to open country with light vegetation (*T. spratti* and *C. acuta*)
C	680–645	no date	Total of 22 shells, of which *T. spratti* 45%, *Cerithium* sp. 5%, *C. acicula* 5% Mainly land snail assemblages with only a few marine molluscs; high stone and coarse sand content, fining upwards	A sudden mass of land derived sediments and molluscs at the beginning of this zone suggest very strong erosion of open country soils into the harbour basin
D	645–590	at 617 cm: 1521–876 BC (3471–2826 BP)	Total of 2122 shells, of which *Hydrobia* sp. 41%, *Cerastoderma* sp. 15%, *B. reticulatum* 10%, *P. moussonii* 0.7 %, *T. spratti* 2%, *C. acicula* 2% The molluscan assemblages at the base consisted of a few land snails only, but gradually get mixed with marine, brackish water and freshwater molluscs, dramatically increasing the total number of shells per sample; only a few stones found, but sand increased to around 50%	Lagoonal and brackish water biota dominate again and increase strongly in number in muddy sandy sediment; severe soil erosion, however, continues as evidenced by the burrower *C. acicula*; an array of freshwater molluscs was also washed onto the site, indicating perennial running water (*P. moussonii)* as well as slow moving water, ponds (e.g. *Lymnaea* sp.), and wetlands (e.g. *C. schlickumi*) in the vicinity; the presence of dense vegetation is suggested by the leaf litter snails (e.g. *Vitrea* sp.)
E	590–523	1407–765 BC (3357–2715 BP)	The zone was missing due to wet sandy sediments	Likely rapid deposition of sandy sediments, possibly due to a very severe storm event
F1	523–355	1164–593 BC (3114–2543 BP)	Total of 15019 shells, of which *Hydrobia* sp. 43%, *Cerastoderma* sp. 14%, *B. reticulatum* 9%, *P. moussonii* 1%, *C. acuta* 2%, *C. acicula* 1% Molluscan assemblages are predominantly marine, with a very strong brackish water signature; freshwater molluscs and land snails occur throughout, the total number of shells per sample vary significantly throughout; some stones occurred towards the base, but the sandy muddy sediments broadly portray a fining upwards trend	The brackish water snail *Hydrobia* sp. was the most common species found, but marine and lagoonal influence remained noticeable; Strong soil erosion continued throughout this zone, as the burrower *C. acicula* was present throughout; the floodwaters also carried freshwater molluscs out of perennial freshwater bodies into the harbor; a stream, slow moving freshwater bodies, ponds and associated wetlands are indicated; the leaf litter snails suggest dense vegetation/scrub, while open country species were also washed in; the grassland species *C. acuta* was proportionally most common in the lower third of the zone but they occurred throughout alongside other Helicioids, indicating light vegetation

Table 4.7 *(cont.).*

Zone MC2-	Depth (cm)	Date ranges cal. BC/AD (BP) for the start of each zone (2σ)	Molluscan assemblages	Environment
F2	355–290	292 BC–AD 215 (2242–1735 BP)	Total of 2105 shells, of which *Hydrobia* sp. 67%, *Cerastoderma* sp. 6%, *B. reticulatum* 12%, *P. moussonii* 0.04 %, *C. acuta* 2% Mixed molluscan assemblages throughout, predominantly brackish water, with waning marine influence; land snails occurred in all samples, the freshwater snail diversity was greatly diminished and the total number of shells per sample was lower than in the previous zone; the sediments were mainly silty clays that contained less sand than before, with the coarse sand content fining upwards	Dramatic change in the environment; mainly brackish water, as suggested by *Hydrobia* sp., with a saltmarsh close by (*O. myosotis*); marine and lagoonal influences appear less pronounced than in the previous zone; freshwater bodies and wetlands seem to have significantly diminished: only the perennial running freshwater *P. moussonii* was found in small numbers intermittently; a slow moving water/pond is only once suggested by *P. planorbis*; the reduction of the freshwater bodies may be due to anthropogenic interventions in the swampy plain or due to aridification; erosion continued to occur, but leaf litter species were no longer found, and even open country species were rare; the few ubiquitous species indicate light vegetation/ grassland
G	290–255	AD 268–575 (1682–1375 BP)	Total of 120 shells, of which *Hydrobia* sp. 32 %, *Bittium reticulatum* 27%, *C. acuta* 3% and *C. acicula* 2% This zone marks the beginning of another event, coarsening up to a boulder in the next zone; the number of shells strongly decreased progressively, the uppermost sample of this zone only contained one shell; concurrently, the stone content increased dramatically	Predominantly marine environment with a strong brackish water influence, as suggested by the diminished number of *Hydrobia* sp.; no freshwater or wetland shells were found in this zone; the very few land snails are indicative of grassland (*C. acuta*) and light vegetation (Helicioid fragments); the erosion indicator *C. acicula* was found at the base of the zone, which, coupled with the increase in the stone content, marked yet another severe erosion event
H	255–210	AD 490–775 (1460–1175 BP)	No shell content; this unit consists of a boulder	The boulder probably reflects a storm
I	210–168	AD 701–1047 (1249–903 BP)	Total of 449 shells, of which *Hydrobia* sp. 53%, *P. moussonii* 5%, *C. acuta* 8%, *T. spratti* 4% The assemblages were mixed, although marine molluscs occur only once; brackish water species generally dominated, land snails were found in all samples, freshwater shell occurred occasionally; the sediments were coarsening up towards the top of the zone	A saltmarsh seems to have occurred briefly at the base of this zone, indicated by *O. myosotis*; brackish water environments then became established; a running perennial freshwater stream and slow moving water are indicated nearby; dense vegetation is suggested once by *Vitrea* sp.: the other land snails indicate open country/garrigue (e.g. *T. spratti*), light vegetation and grassland is suggested by the ubiquitous species and *C. acuta;* the presence of the burrower *C. acicula* in these waterlain deposits points to severe soil erosion
J	168–125	AD 917–1266 (1033–684 BP)	No shell content; this unit consists of a boulder	The boulder probably reflects a storm
K	125–77	AD 1148–1496 (802–454 BP)	Total of 203 shells, of which *C. acuta* 42%, *C. caruanae* 10%, *T. spratti* 4%, *P. moussonii* 2%, *Lymnaea* sp. 2% The assemblages above the second stone contained no marine or brackish water species; a few freshwater molluscs were interspersed with the land snails	The former brackish water environment has now turned into a terrestrial one – the assemblages contained only land snails and a few freshwater snails; apart from this change, the shells found indicate similar terrestrial and freshwater environments as in zone I; dense vegetation in the vicinity is suggested by the presence of *Xerotricha* sp. *C. acicula,* formerly an indicator of erosion, may now be authochtonous; there is no evidence for a saltmarsh
L	77–33	AD 1427–1717 (523–233 BP)	The sediments were wet and sandy and could not be retrieved by the corer	Continuation of silting up of the former harbour

Table 4.7 *(cont.).*

Zone MC2-	Depth (cm)	Date ranges cal. BC/ AD (BP) for the start of each zone (2σ)	Molluscan assemblages	Environment
M	33–0	AD 1699–1901 (251–49 BP)	Total of 70 shells, of which *C. acuta* 17%, *C. caruanae* 16% *T. spratti* 10%, *Vitrea* spp. 1% The assemblages exclusively contained land snails; the sediments contained a small stone only once, and generally showed a stable sand/silt/clay content	The zone shows a terrestrial environment, which no longer had a notable freshwater influence, possibly as a result to anthropogenic action as the swamps had been drained and the freshwater source diverted to a reservoir (Abela 1674); the land snails point to similar environments as before, with dense vegetation in the vicinity (*Vitrea* spp.), open country (*T. spratti*), grassland (*C. acuta*) and light vegetation (*C. caruanae*); the presence of the burrower *C. acicula* may here be intrusive and not the result of erosion events

Period (Evans 1971). The Salina Deep Core (SDC) was extracted in January 2014 from beside the sea water channel (Is-Sukkursu) by the Salina salt pans using a mechanical corer. The core reached an overall depth of 28.5 m, but as a result of loss of material in the first 11 m while coring, caused by hydro-collapse of wet and sandy sediments, only material from 11 m downwards could be analysed (see Chapter 2). The segments of core studied varied in length between 3 and 13 cm. Freshwater and land snails were identified and counted (Fig. 4.5; Table 4.8). Marine and brackish water species were also identified and counted, but as their species diversity and abundance was disproportionately larger than the non-marine molluscan assemblages, they were plotted separately (Fig. 4.6; Table 4.8).

The Bayesian model provides the date range for this core from about 8000 to 2000 cal. BC (see Table 2.2). With the help of the CONISS analysis, the non-marine molluscs in the core could be sub-divided into twelve zones.

4.5.5.1. Conclusion: Salina Deep Core

A high sedimentation rate affected the area since at least *c*. 6000 cal. BC. In the space of 1500 years alone, nearly 12 m of sediments filled the sea water channel (Is-Sukkursu), although the actual sedimentation is likely to have occurred through severe storm episodes rather than at a steady pace, as indicated by the presence of the burrowing snail *C. acicula*. From earliest prehistoric times to at least 2000 cal. BC, there was ample perennial freshwater in the plain, forming slow moving water bodies and perhaps ponds, with associated wetland vegetation (Fig. 4.6; Table 4.9), as is indicated by the aquatic freshwater taxa. The availability of freshwater may have encouraged dense vegetation, allowing the leaf litter snail species to form a prominent group in this analysis, but open country/karstland species also occurred throughout.

The marine taxa present in the lowest parts of the core are in terrestrial sediments of probable Late Pleistocene age. These assemblages are thus very likely to be recycled. The CONISS clustering groups some of these with the basal assemblages of the Holocene marine transgression. This is perhaps suggestive that the marine environments in which these molluscs lived during previous temperate phases were very similar to those during the initial stages of the Holocene transgression, with turbid, turbulent waters, perhaps of slightly abnormal salinity.

As the marine transgression continued, the Salina Inlet rapidly achieved normal marine salinities. Two mildly eutrophic phases, marked by fairly restricted faunas with high *Corbula gibba*, are apparent early in the transgression, during the base of zone C and during zone E. *C. gibba* is able to flourish in oxygen-poor waters and is thus regarded as a marker for eutrophication. In the deep sea, for instance in the Adriatic (e.g. Siani *et al.* 2000) the S1 Sapropel (a layer highly organic mud formed as a result of widespread eutrophication) is contemporary with the second and more marked of these phases of eutrophication, thus suggesting that Malta was affected by an event of regional significance. These events in the Salina borehole are contemporary with pollen diagram phases marked by high *Pistacia* scrub and interpreted as indicative of periods of higher rainfall at about 6700–6600, 6300–6200, 4300–4100 and 3400–2800 cal. BC (see Fig. 3.3). It is tentatively suggested that leaching during these phases led to nutrient enrichment and thus eutrophication in the confined waters of the Salina Inlet and more widely throughout the central Mediterranean.

A further phase marked by low diversity and high *C. gibba* and suggestive of eutrophication is present in zone H, at 22 m. This coincides with the first appearance of cereal pollen and coprophilous fungal spores. It can therefore be suggested that eutrophication

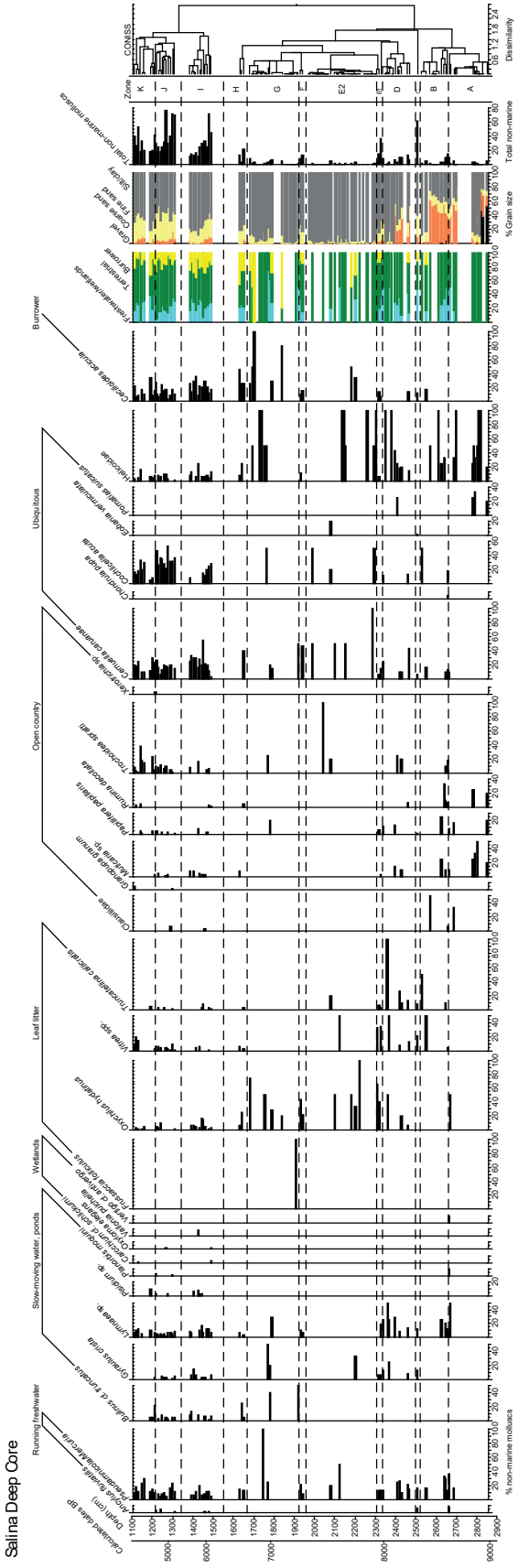

Figure 4.5. *Salina Deep Core molluscan histogram (C.O. Hunt & K. Fenech).*

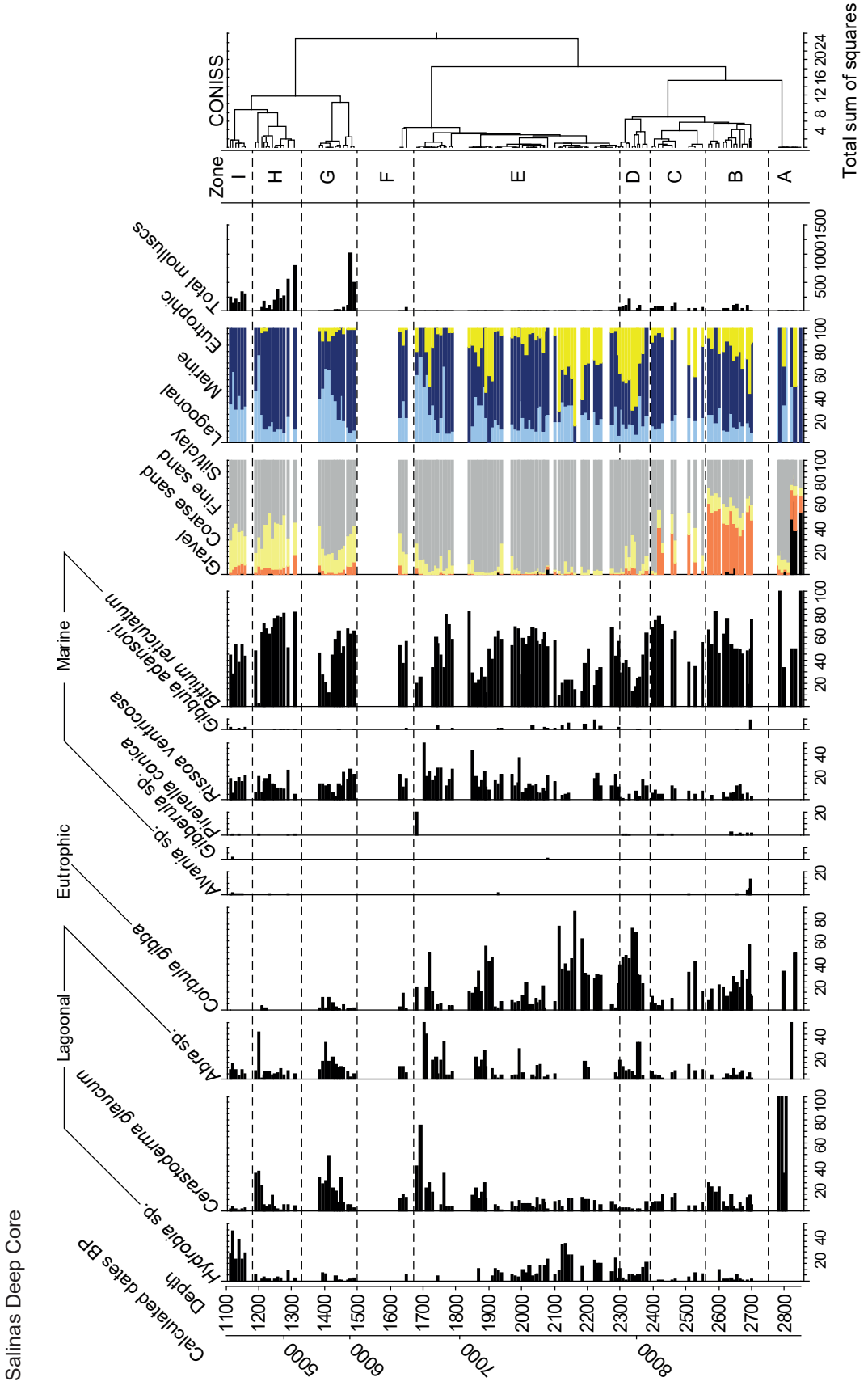

Figure 4.6. *Marine molluscan histogram for the Salina Deep Core (C.O. Hunt & K. Fenech).*

Table 4.8. *The non-marine molluscan zones for the Salina Deep Core.*

Zone	Depth (cm)	Date ranges cal. BC/AD (BP) for the start of each zone (2σ)	Molluscan assemblages	Environment
A	2850–2680	7737–6811 BC (9687–8761 BP)	Among 2183 marine and brackish water molluscs, a total of 39 freshwater and land snails, of which *P. moussonii* 15%, *Muticaria* sp. 15%, *P. sulcatus* 9%, *Lymnaea* sp. 6%, *O. hydatinus* 3% Assemblages consisted of only land snail fragments at the base of the zone; freshwater shells were found from 2690 cm onwards, together with land snails; the sediments at the base were initially very stony, then predominantly silty/clayey and then very sandy at the top of the zone	Basal part possibly belongs to the Late Pleistocene and includes recycled marine and possibly non-marine molluscs; marine Holocene starting at around 2696 cm; predominantly an open country/ karstland environment (*Muticaria* sp.) with very light vegetation (Helicioidae); Evidence of running freshwater stream (*P. moussonii*) and shortly after of shallow pond (*Lymnaea* sp.) and associated wetlands from *c.* 9000 BP onwards; concurrently, appearance of denser vegetation/scrub (*O. hydatinus*)
B	2680–2518	6925–6494 BC (8875–8444 BP)	Among 6267 marine and brackish water molluscs, a total of 44 freshwater and land snails, of which *P. moussonii* 16%, *Lymnaea* sp. 11%, *Vitrea* spp. 9%, *T. spratti* 9%, *C. acuta* 9% and *C. acicula* 2% Several samples devoid of land- and freshwater shells, especially in samples that contained more than 70% of sand, indicating marine events, particularly in the upper half of the zone	Presence of running freshwater stream (*P. moussonii*) and shallow pool with poor conditions (*Lymnaea* sp.), as well as grassland (*C. acuta*), open country/ karstland and garrigue (*T. spratti*) particularly in the lower part of the zone; no evidence for wetlands throughout; the upper part suggests a breakdown of the dense vegetation, where leaf litter species (*Vitrea* sp.) were also washed onto the site; severe soil erosion is suggested by *C. acicula* in the upper part of the zone
C	2518–2500	6502–6146 BC (8452–8096 BP)	Among 664 marine and brackish water molluscs, a total of 63 freshwater and land snails, of which *Vitrea* sp. 22%, *P. moussonii* 16%, *Lymnaea* sp. 13%, *C. acicula* 13% and *C. caruanae* 6% Sharp increase in the number of shells found; silty/clayey sediment was mixed with substantial amount of fine sand	Strong erosion washed in a large number of shells, indicating a fast running freshwater stream (*P. moussonii* and *A. fluviatis*), slow moving water/pond rich in vegetation (*Lymnaea* sp. and *G. crista*), dense vegetation (*Vitrea* sp.), as well as open country and patches of light vegetation (*C. caruanae*), but again, and hereafter, no evidence for wetlands
D	2500–2335	6468–6114 BC (8418–8064 BP)	Among a total of 7963 marine and brackish water molluscs, 70 freshwater and land snails, of which *P. moussonii* 14%, *Lymnaea* sp. 13%, *T. callicratis* 10%, *C. caruanae* 10%, *T. spratti* 4% and *C. acicula* 4% Decrease in the number of shells found; silty sediments are initially mixed with a lot of sand, but towards the top of the zone predominantly silty/clayey	Strong land-derived erosion at the base of the zone; persistence of freshwater bodies but at the top of the zone no more evidence for running freshwater stream, possibly as a result of aridification; increase in the percentage of leaf litter snails, possibly as a result of breakdown of dense vegetation; open country (*T. spratti*) and patches of grassland with light vegetation in the vicinity
E1	2335–2305	6187–6926 BC (8137–7876 BP)	Among a total of 4448 marine and brackish water aolluscs, 52 freshwater and land snails, of which *Vitrea* spp. 25%, *P. moussonii* 13%, *Lymnaea* sp. 13%, *O. hydatinus* 11%, *C. caruanae* 11% and *C. acicula* 10% Marked increase in the number of shells; sediments contained notably more sand than at the end of the previous zone	Severe soil erosion (*C. acicula*), resurgence of freshwater stream (*P. moussonii*) and continuation of vegetated slow-moving water/pond (*Lymnaea* sp. and *G. crista*); environment similar to the previous zone

Table 4.8 *(cont.).*

Zone	Depth (cm)	Date ranges cal. BC/AD (BP) for the start of each zone (2σ)	Molluscan assemblages	Environment
E2	2305–1955	6123–5891 BC (8073–7841 BP)	Among 2992 marine and brackish water molluscs, a total of 30 freshwater and land snails, of which *O. hydatinus* 20%, *C. caruanae* 14%, *C. acuta* 10%, *P. moussonii* 7% and *C. acicula* 7% Sharp decrease in the number of molluscs, with many samples containing no shells; sediments were very clayey with little fine sand	Massive land-derived erosion (*C. acicula*), liberating leaf litter taxa as well as open country and taxa associated with light vegetation; paucity of shells found is likely to be due to the very rapid sedimentation
F	1955–1925	5609–5142 BC (7559–7362 BP)	Among 162 marine and brackish water molluscs, a total of 22 freshwater and land snails, of which *O. hydatinus* 32%, *C. caruanae* 27%, *P. moussonii* 14%, *C. acicula* 14% and *Lymnaea* sp. 9% Short zone, where the land-derived inwash contained an increase in fine sand and shells	Highest proportion on non-marine shells possibly due to another severe land-derived erosion event (*C. acicula*), this time accompanied by an increase in fine sand after perhaps a brief respite which could have allowed the environment and snail populations to recover; environment appears to be similar to the previous zone, with a running freshwater stream (*P. moussonii*), a pond (*Lymnaea* sp.), some dense vegetation (*O. hydatinus*) and light vegetation (*C. caruanae*)
G	1925–1670	5583–5380 BC (7533–7330 BP)	Among 650 marine and brackish water molluscs, a total of 43 freshwater and land snails, of which *C. acicula* 28%, *P. moussonii* 25%, *O. hydatinus* 23%, *B.* cf. *truncatus* 7%, *T. spratti* 2% and *C. acuta* 2% Relatively fewer shells found, with some samples containing no non-marine shells at all; amount of fine sand varied, but sediments were predominantly very silty/clayey	Massive erosion (*C. acicula*), now possibly as a result of early agriculture, which would have led to a breakdown of the vegetation, allowing leaf litter and other taxa to be liberated and carried into the inlet; fewer taxa would have arrived once the stores in the soil had been exhausted; as in Zone E2, intermittent evidence of permanent freshwater bodies (*P. moussonii, G. crista*); appearance of *B.* cf. *truncatus*, indicative of transient, patchily distributed ponds, possibly as a result of the ongoing erosion
H	1670–1550	5256–4909 BC (7206–6859 BP)	Among 790 marine and brackish water molluscs, a total of 40 freshwater and land snails, of which *C. acicula* 33%, *C. caruanae* 23%, *P. moussonii* 7%, *Lymnaea* sp. 3% and *Vitrea* spp. 3% Short zone, with a general increase in the number of shells; predominantly silty/clayey sediments with an increase in sand compared with the previous zone	Even more massive erosion (*C. acicula*), possibly fluctuating hydrology levels (*P. moussoni* and *Lymnaea* sp. once replaced by *B.* cf. *truncatus*); more leaf litter species released, perhaps due to a renewed breakdown of the vegetation
I	1550–1330	4805–4306 BC (6755–6256 BP)	Among 20845 marine and brackish water molluscs, a total of 316 freshwater and land snails, of which *C. acicula* 19%, *C. caruanae* 19%, *C. acuta* 14%, *P. moussonii* 8% and *Lymnaea* sp. 8% Increase in the number of shells, possibly due to intermittent periods of stabilizing environmental/climatic conditions, although erosion still continued unabated; samples initially contained up to 50% of sand, fining upwards to around 25%	Continuous erosion with marine and terrestrial inwash events (*C. acicula*), increase in erosion of grassland (*C. acuta*), open country/karstland and areas with dense and light vegetation (*O. hydatinus* and *C. caruanae*); presence of fast running freshwater (*P. moussonii* and *A. fluviatis*), ponds rich in vegetation (*Lymnaea* sp. and *G. crista*) and reappearance of wetlands

Table 4.8 *(cont.).*

Zone	Depth (cm)	Date ranges cal. BC/AD (BP) for the start of each zone (2σ)	Molluscan assemblages	Environment
J	1330–1213	3866–3038 BC (5816–4988 BP)	Among 33124 marine and brackish water molluscs, a total of 443 freshwater and land snails, of which *C. acuta* 32%, *C. acicula* 14%, *P. moussonii* 10%, *Lymnaea* sp. 6% and *Vitrea* spp. 5% Increase in the amount of non-marine molluscs, reaching a maximum of 78 shells per sample; sediments are silty/clayey with a high sand content (up to 50%)	Evidence of massive erosion and terrestrial inwash throughout (*C. acicula*), mainly eroding areas of grassland (*C. acuta*) and very light vegetation (*C. caruanae*); continuous presence of freshwater bodies, as in the previous zone, but no wetland species were found; leaf litter shells were still washed in, as were open country/karstland species, with a notable increase of the garrigue species *T. spratti*
K	1213–1100	3198–2435 BC (5148–4385 BP)	Among 19107 marine and brackish water molluscs, a total of 277 freshwater and land snails, of which *C. acuta* 16%, *C. acicula* 14%, *P. moussonii* 14%, *T. spratti* 10%, *Lymnaea* sp. 7%, and *Vitrea* spp. 5% Number of shells found comparatively similar to the variations in the previous zone; the sediments also contained a similar amount of sand, first increasing (coarsening up) and then decreasing (fining up)	Continuous evidence of strong terrestrial inwash and erosion (*C. acicula*); running freshwater stream still present (*P. moussonii*), but may have been reduced in size and flow strength as *A. fluviatis* is no longer found; disappearance of *B.* cf. *truncatus, G. crista, P. moquini* and *Pisidium* sp. may point to severe aridification and an impoverished pond environment, in which only *Lymnaea* sp. survived; the land snails found are very similar to the previous zone and as such show little change

Table 4.9. *Molluscan zones for the Salina Deep Core (SDC).*

Zone	Depth (cm)	Date ranges cal. BC (BP) for the start of each zone (2σ)	Molluscan assemblages	Environment
A	2850–2805	unknown	2183 marine and brackish water molluscs; very small, sometimes mono-specific, assemblages; taxa include *Cerastoderma glaucum, Abra* sp., *Corbula gibba, Bittium reticulatum*	Basal part of core is terrestrial, possibly of Late Pleistocene age, including recycled marine taxa
B	2805–2700	unknown	Very small assemblages dominated by Cardiidae, *C. glaucum, Acanthocardia* sp., *C gibba, B. reticulatum*	Basal part of zone is terrestrial, possibly of Late Pleistocene age, including recycled marine taxa; highest part is base of Holocene marine sequence, with a low-diversity assemblage characteristic of rather confined, turbid, turbulent environments of possibly slightly abnormal salinity; *B. reticulatum* suggests presence of marine vegetation
C	2700–2565	7008–6533 BC (8958–8483 BP)	Larger, higher-diversity assemblages, dominated by *B. reticulatum, C gibba, Cerastoderma* spp. and with lesser *Abra* sp. *Nassarius* sp, *Acanthocardium* sp., *Rissoa* sp. *Ostrea edulis, Cerithium* sp. *Kellia* spp. and *Hydrobia* spp.	Assemblages are consistent with a mosaic of environments including fine sand, gravel, rock, marine vegetation and normal marine salinities, with an input from brackish waters; high *C. gibba* in the basal part of the zone may suggest modest eutrophication
D	2565–2375	6601–6211 BC (8551–8161 BP)	Assemblages dominated by *B. reticulatum, C. gibba, Cerastoderma* spp. and with lesser *Parvicardium exigens*, *Abra* sp., *Acanthocardia* sp., *Rissoa* sp. and *Kellia* sp.	Assemblages suggest marine waters with a mosaic of substrates, including fine sand, gravel, rock, marine vegetation
E	2375–2300	6263–5971 BC (8213–7921 BP)	Fairly sizeable assemblages of moderate diversity, dominated by *C. gibba, Abra* sp., *B. reticulatum*, with lesser *Parvicardium* sp, *Retusa truncatula, Acanthocardia* sp., *Kellia* sp. *Hydrobia* sp.	Assemblages suggest quite turbid, eutrophic marine waters with limited marine plants and a waning connection to brackish waters

Table 4.9 *(cont.).*

Zone	Depth (cm)	Date ranges cal. BC (BP) for the start of each zone (2σ)	Molluscan assemblages	Environment
F	2300–2208	6115–5883 BC (8065–7833 BP)	Small, relatively low-diversity assemblages dominated by *B. reticulatum*, with some *Rissoa* sp., *C. gibba* and *Hydrobia* sp.	Assemblages are suggestive of marine waters with abundant marine plants and rocky and gravelly bottoms, and a connection to brackish, perhaps lagoonal waters
G	2208–2190	5990–5716 BC (7940–7666 BP)	Small, low-diversity assemblages dominated by *B. reticulatum* and *C. gibba*, with some Cardiidae and *Abra* sp.	The assemblages are suggestive of fairly eutrophic marine waters with muddy and gravelly bottoms and abundant marine vegetation
H	2190–2110	5964–5684 BC (7914–7634 BP)	Small assemblages with low but rising diversity, dominated by *C. gibba*, with some *B. reticulatum*, *Hydrobia* spp., Cardiidae and *Acanthocardium* sp.	These assemblages are consistent with a rather eutrophic marine to brackish environment, with predominantly gravelly bottoms and some marine vegetation
I	2110–1915		Small assemblages with high diversity, dominated by *B. reticulatum*, with some *Cerastoderma* spp., *Loripes lacteum, Parvicardium exiguum, Abra* sp., *C. gibba, Rissoa* spp., *Cerithium* spp. and *Hydrobia* spp.	Assemblages are suggestive of normal marine waters with a slight connection to brackish waters; there was abundant marine vegetation and a mixture of muddy, gravelly and rocky bottoms
J	1915–1700		Small assemblages of moderate diversity, dominated by *B. reticulatum*, with significant 1700–1670 *Rissoa* sp., *C. gibba,* Abra sp., and some *Cerastoderma* spp., *L. lacteum, P. exiguum, Acanthocardia* sp. and *Turbonilla lactea*	Assemblages are suggestive of normal marine waters, possibly slightly eutrophic at the bottom and top of the zone where *C. gibba* peaks; there is evidence for muddy, gravelly and rocky bottoms and abundant marine vegetation
K	1700–1670		Small and rather variable assemblages of low diversity, with Cardiidae, *Cerastoderma* sp. Pectenidae, *Abra* sp., *Acanthocardia* sp. and *B. reticulatum*	Assemblages are consistent with normal marine waters, sandy and gravelly bottoms and some marine vegetation; Pectenidae might suggest relatively clear waters
L	1670–1330		Variably sized assemblages, large in the middle of the zone, of fairly high diversity, dominated by *B. reticulatum* and with significant *Cerastoderma* spp., *Abra* sp. and *Rissoa* spp. There are some *L. lacteum, P. exiguum, C. gibba, Kellia* spp., and *Hydrobia* spp.	Assemblages are consistent with normal to slightly eutrophic marine waters, with a minor connection to brackish environments; there is evidence for sandy, gravelly and rocky bottoms and abundant marine vegetation
M	1330–1210		Large assemblages of moderate diversity, heavily dominated by *B. reticulatum*, with some *Cerastoderma* spp., *L. lacteum, P. exiguum, Abra* sp., *Rissoa* spp., *Cerithium* spp., *T. lactea* and *Hydrobia* spp.	Assemblages are suggestive of marine waters of normal salinity, with a minor connection with brackish environments; there was very abundant marine vegetation and sandy and rocky bottoms
N	1210–1180		Small, low diversity, very variable assemblages with high *Cerastoderma* spp., *Abra* sp., *B. reticulatum* and *Rissoa* spp.	The low diversity and prevalence of *Cerastoderma*, which has oligohaline tolerances, may suggest marine waters of slightly abnormal salinity, perhaps consistent with development of a saline lagoon behind a bay-bar; taxa are consistent with sedimentary bottoms, with some rocky places and variable marine vegetation
O	1180–1100		Large assemblages of high diversity, with high *B. reticulatum* and *Hydrobia* spp. with some *L. loripes, P. exiguum, Abra* sp. and *Rissoa* spp.	The assemblages are suggestive of marine waters of normal salinity, with a strong connection to brackish waters; taxa are consistent with abundant marine vegetation and sandy and rocky bottoms

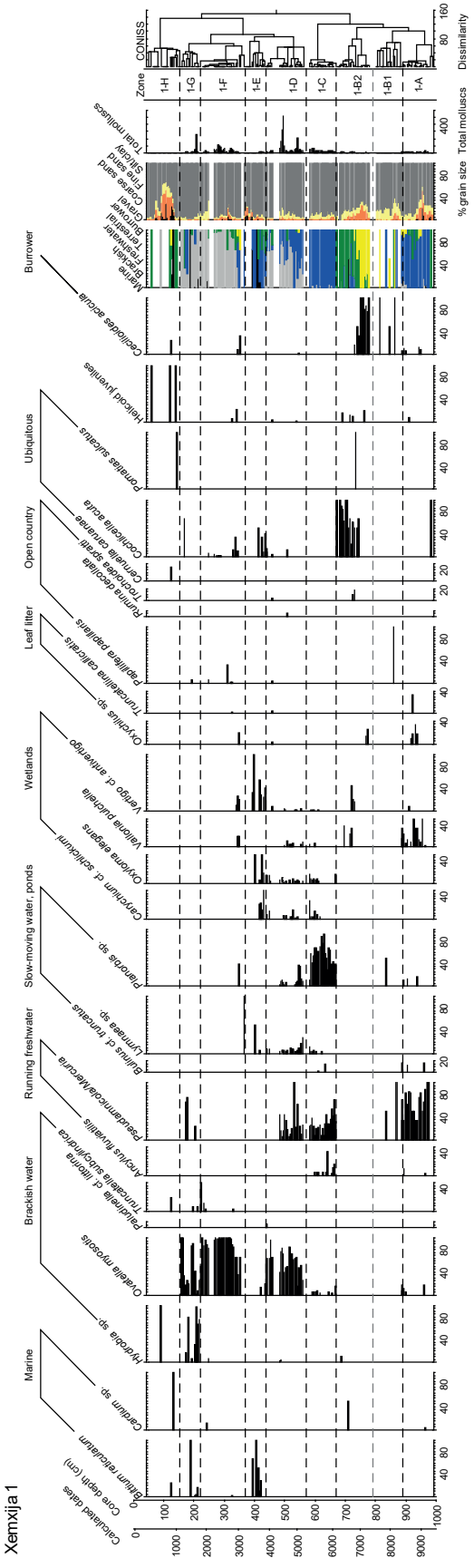

Figure 4.7. *Xemxija 1 molluscan histogram (C.O. Hunt & K. Fenech).*

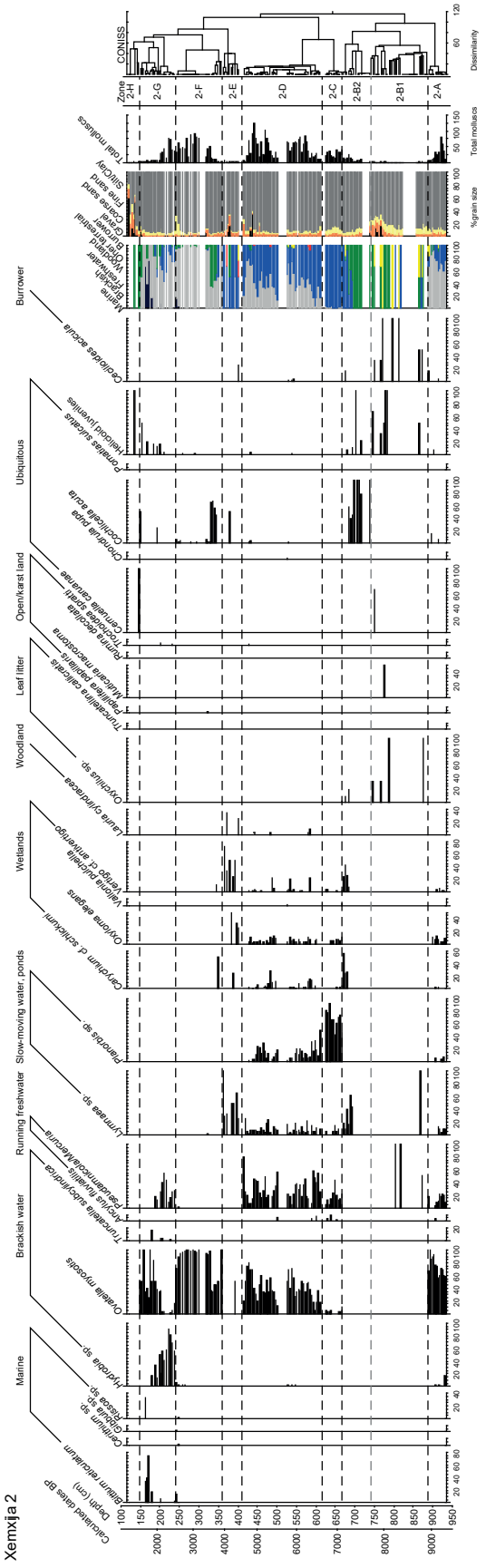

Figure 4.8. *Base of Xemxija 2 molluscan histogram (C.O. Hunt & K. Fenech).*

Table 4.10. *Molluscan zones for the Xemxija 1 core (XEM1).*

Zone	Depth cm	Date ranges cal. BC/AD (BP) for the start of each zone (2σ)	Molluscan assemblages	Environment
1-A	990–888	7568–6779 BC (9518–8729 BP)	Total of 168 molluscs, of which *P. moussonii* 80%, *V. pulchella* 11%, *C. acicula* 3%, *Oxychilus* sp. 2%, *Cardium* sp. 0.6% The lowermost sample was sterile, the maximum number of shells found in a sample was 27; assemblages consisted predominantly of freshwater species, with a few land snails periodically washed in; one marine shell fragment only; influx of stones and coarse sand in the lower half of the zone, which then fines up and becomes predominantly silty/clayey	It is likely that these sediments accumulated by colluviation and alluvial processes behind a coastal barrier; running freshwater (*P. moussonii*), slow moving waters or ponds (*Planorbis* sp.), damp grassy (*V. pulchella*) and dense vegetation (*Oxychilus* sp.) were present; soil erosion events in the catchment are indicated by *C. acicula* and the presence of stones and coarse sand; *O. myosotis* points to saltmarsh and *Cardium* sp. to marine waters nearby; these are rare enough to suggest emplacement on the deposition site by wave-action during storms
1-B1	888–790	6391–6014 BC (8341–7964 BP)	Total of 15 molluscs, of which *C. acicula* 47%, *P. moussonii* 33%, *P. papillaris* 7%, *Planorbis* sp. 7% Only very few molluscs were found in this zone, many samples were sterile; a few small mudballs were found at the base of this zone, indicating rapid sediment influx, the remainder was predominantly silt/clay with small amounts of fine sand	Dramatic environmental change, possibly due to intense aridification, perhaps as a result of the 8.2 ka BP event; the sediments are colluvial in origin, probably accumulating behind a coastal barrier; extreme reduction of the freshwater bodies is suggested by the reduction in aquatic taxa; open karstland is indicated by *P. papillaris*; severe erosion onto the site and hostile conditions may have led to the paucity of molluscan remains
1-B2	790–670	5720–5252 BC (7670–7202 BP)	Total of 105 molluscs, of which *C. acuta* 50%, *C. acicula* 25%, *V. pulchella* 8%, *Oxychilus* sp. 2%, *Cardium* sp. 1%, *Hydrobia* sp. 1% Predominantly land snail assemblages, no subaqueous freshwater species; inwash of one marine mollusc and one brackish water mollusc; after an initial increase, the presence of small mud balls decreases; the top part consists mainly of silt/clay with small amounts of fine sand	Erosion within the catchment seems to have diminished during this zone; in the lower part of the zone a few leaf litter snails (*Oxychilus* sp.) may indicate the former presence of scrub but these and overlying assemblages are rich in the erosion indicator *Ceciliodes acicula*, suggesting the breakdown of vegetation and a phase of soil erosion; higher in the zone the open country *T. spratti* peaks and *Cochlicella acuta* becomes important, perhaps consistent with some garrigue, light grassland or dunes; *Vallonia pulchella* and *Vertigo* cf. *antivertigo* are present in the upper part of the zone; they were which were probably associated with marsh and reeds; the occasional marine taxa were probably thrown into the site by wave action
1-C	670–570	4324–4062 BC (6274–6012 BP)	Total of 564 molluscs, of which *Planorbis* sp. 62%, *P. moussonii* 28%, *C.* cf. *schlickumi* 4%, *O. myosotis* 3%, *A. fluviatilis* (2%) The molluscan assemblages consisted exclusively of different freshwater associated or tolerant species; the sediments were predominantly silt/clay with little fine sand throughout and coarse sand only in the lower half of the zone	Dramatic environmental change and expansion of freshwater bodies, probably behind a coastal barrier and perhaps reflecting increased precipitation; moving water species *P. moussonii, A. fluviatilis*, suggest a rapid perennial freshwater stream; this fed a freshwater lagoon, indicated by *Planorbis* sp., *Bulinus* cf. *truncatus* and *Lymnaea* sp. Encroaching wetlands are suggested by rising *C.* cf. *schlickumi, O. elegans, V. pulchella* and *V. cf. antivertigo* Seaward, *O. myosotis* indicates upper saltmarsh, presumably part of the low coastal barrier

Table 4.10 *(cont.).*

Zone	Depth cm	Date ranges cal. BC/AD (BP) for the start of each zone (2σ)	Molluscan assemblages	Environment
1-D	570–480	3512–3094 BC (5462–5044 BP)	Total of 1791 molluscs, of which *O. myosotis* 63%, *P. moussonii* 22%, *Planorbis* sp. 8%, *C.* cf. *schlickumi* 1% Molluscan assemblages consist of brackish water, freshwater and at times a few land snails; one sample contained solely freshwater shells; the number of shells found varied greatly, the highest number being 508 shells, and one sample containing no shells; variations in the particle size distribution were also noted, with the irregular increases in coarse sand and small stones	Rising *O. myosotis* points to encroaching saltmarsh; freshwater species decline in percentage and diversity, suggesting diminishing input from freshwater streams, declining water quality and the gradual disappearance of freshwater lagoons; the last freshwater species left is *Lymnaea* sp., which is tolerant of poor habitats; wetland taxa decline, then recover, suggesting that fringing reedbeds diminished, then expanded; the very few land snails indicate the presence of light grassland (*C. acuta, T. callicratis*) and scrub (*R. decollata*); leaf litter species were found only at the top of this zone, in association with *C. acicula,* possibly as a result of the breakdown of dense vegetation and soil erosion due to aridification or human activity
1-E	440–366	1953–1574 BC (3903–3524 BP)	Total of 87 molluscs, of which *O. myosotis* 23%, *V.* cf. *antivertigo* 23%, *C.* cf. *schlickumi* 17% *O. elegans* 13%, *C. acuta* 10%, *Bittium reticulatum* 9%, *Lymnaea* sp. 2% Dramatic decrease in the number of shells found, with several sterile samples; the assemblages were often mixed with marine species; freshwater snails were rare, but wetland and land snail species were frequent; the sediments reflect severe erosion in the catchment, with at least three events marked by an influx of stones and coarse sand	Swampy marshland is indicated by *V.* cf. *antivertigo* and *C.* cf. *schlickumi*, but the former freshwater bodies were reduced to shallow pools (*Lymnaea* sp.) and the freshwater stream appears to have vanished, possibly as a result of continued aridification; *C. acuta* denotes the presence of dry grassland or dunes; the saltmarsh (*O. myosotis*) was still present initially, but reduced or more distant; the small marine species *Bittium reticulatum* is usually associated with seaweed and may have been blown or washed into the site with aquatic vegetation by storm waves overtopping a coastal barrier; storms are also indicated by the increase in coarse sand and stones
1-F	366–220	1279–556 BC (3229–2506 BP)	Total of 842 molluscs, of which *O. myosotis* 95%, *C. acuta* 2%, *V.* cf. *antivertigo* 0.6%, *C. acicula* 0.2% Assemblages were strongly dominated by brackish water species, freshwater shells were found only at the base of this zone and again at the top; land snails occurred intermittently in low numbers; the distribution of coarse sediments indicates at least two inwash events	Soil erosion and inwash of eroded materials from nearby slopes is suggested by *C. acicula* at the beginning of this zone; this event may have led to the infilling of the previous shallow pools and marshland; this may have resulted in the extension of the saltmarsh, as indicated by the dramatic increase in *O. myosotis*; the few land snails suggest that a little dense vegetation, indicated by taxa indicative of leaf litter, may have been present at the base of the zone; but higher in the zone there is evidence only for grassland or dunes (*C. acuta*) and open karstland (*P. pappilaris*)

Table 4.10 *(cont.).*

Zone	Depth cm	Date ranges cal. BC/AD (BP) for the start of each zone (2σ)	Molluscan assemblages	Environment
1-G	218–155	AD 52–510 (1898–1440 BP)	Total of 375 molluscs, of which *Hydrobia* sp. 75%, *O. myosotis* 15%, *P. moussonii* 6%, *Bittium reticulatum* 2% Molluscs from all major habitat groups were found in this zone, of which land snails were the rarest; the number of shells per sample varied between 1 and 253 specimens	The sudden appearance of the brackish water/lagoonal *Hydrobia* sp. in large numbers may indicate the formation of a brackish lagoon behind the coastal barrier; the proximity of the coast is also suggested by *T. subcylindrica,* while saltmarsh (*O. myosotis*) persisted; running freshwater directly entering the lagoon is indicated by *P. moussonii*; again, open country/karstland and grassland was present
1-H	158–48	AD 737–830 (1213–1120 BP)	Total of 10 molluscs, of which *Hydrobia* sp. 10%, *T. subcylindrica* 10%, *Bittium reticulatum* 10%, *C. acicula* 10% Dramatic reduction in the number of molluscs found, with many sterile samples; shells from all major habitats were present; the sediments showed a dramatic increase in stones and coarse sand, first coarsening up and then fining up	The site had completely dried up; the freshwater stream was no longer detected; this is perhaps because of anthropogenic water management (the stream is today caught in a reservoir); as a result, wetland species were also absent and the saltmarsh disappeared; infrequent inwash events from the sea led to the deposition of a few marine/lagoonal shells; the very few land snails suggest light vegetation (*e.g. C. caruanae*), while the burrower *C. acicula* may either be intrusive or may have been part of soil erosion and inwash, as suggested by the deposition of coarse sand and stones

Table 4.11. *Molluscan zones for the Xemxija 2 core (XEM2).*

Zone	Depth cm	Date ranges cal. BC/AD (BP) for the start of each zone (2σ)	Molluscan assemblages	Environment
2-A	933–890	7526–7221 BC (9476–9171 BP)	Total of 353 molluscs, of which *O. myosotis* 71%, *P. moussonii* 14%, *Lymnaea* sp. 4%, *C. acuta* 0.5%, *C. acicula* 0.5% All samples contained shells, their numbers varied between five and 81; the assemblages consisted mainly of brackish water associated species, often mixed with freshwater/wetland snails; land snails periodically appeared in the upper half of the zone in low numbers; the sediments were silty/clayey with small amounts of fine and coarse sand throughout	Saltmarsh environment, as indicated by *O. myosotis*, probably behind a coastal barrier, with nearby running freshwater (*P. moussonii*), slow moving water/ponds (*Lymnea* sp. and *Planorbis* sp.) and vegetated wetlands (*O. elegans*); sparse land snails indicate grassland (*C. acuta*); the presence of the burrower *C. acicula* may be intrusive, as the particle size distribution would not necessarily point to input of sediment resulting from severe erosion
2-B1	890–740	7197–6787 BC (9147–8737 BP)	Total of 25 molluscs, of which *C. acicula* 28%, *Oxychilus* sp. 16%, *P. moussonii* 12%, *Muticaria* sp. 4% As in Xemxija 1, only a few molluscs were found, with many sterile samples, indicating rapid sedimentation; the sudden change in sediment colour from light grey to reddish brown suggests an event, but the calculated date for this event would be several hundred years before the similar change in Xem1; initially, the samples contained a relatively stable amount of fine sand	Dramatic change in the environment. The saltmarsh disappeared, but running freshwater (*P. moussonii*) and slow moving water/pond (*Lymnae* sp.) were still present, probably behind a coastal barrier, in the lower half of this zone; the upper half of the zone is characterized by an absence of freshwater-associated snails; in fact, the last occurrence of *P. moussoni* falls into the date range of the 8.2 ka BP event, suggesting that the freshwater species may have vanished as a result of the abrupt aridification that led to the

Table 4.11 *(cont.).*

Zone	Depth cm	Date ranges cal. BC/AD (BP) for the start of each zone (2σ)	Molluscan assemblages	Environment
			(around 20%), but there was a sudden increase of coarse sand and stones at 765 cm, peaking at 750 cm and then gradually fining upwards	drying up of the water bodies; light vegetation suggested by *C. caruanae* and some leaf litter by *Oxychilus* sp.; the presence of the burrower *C. acicula* may perhaps be autochtonous and not necessarily the result of heavy erosion
2-B2	740–670	6054–5437 BC (8004–7437 BP)	Total of 120 molluscs, of which *C. acuta* 40%, *Lymnaea* sp. 22%, *C.* cf. *schlickumi* 13%, *Oxychilus* sp. 5%, *C. acicula* 2% Increase in the number of shells per sample, ranging between three and 26; assemblages contained mainly land snails, with freshwater snails re-appearing in the upper part of the zone; the amount of sand gradually decreased from 25% to 5%	A slow recovery of the freshwater bodies behind the coastal barrier is indicated by the reappearance of *Lymnaea* sp., a freshwater snail tolerant of poor conditions and thus a pioneer species; wetlands soon became re-established (*C.* cf. *schlickumi*), as did denser vegetation (*Oxychilus* sp.), while light grassland persisted, as suggested by common *C. acuta* and the Helicioid juveniles; with the slow re-establishing of a freshwater body, the number of shells also increased, indicating a slowing down of the previous rapid sedimentation
2-C	670–615	5500–4877 BC (7450–6827 BP)	Total of 307 molluscs, of which *Planorbis* sp. 39%, *P. moussonii* 15%, *C.* cf. *schlickumi* 4%, *O. myosotis* 3% Between 14 and 41 shells per sample; the assemblages consisted only of freshwater associated shells and intermittently a few brackish water molluscs; the sediments were silty/clay with sand, sand increasing from 5% to 15% and then fining up towards the end of the zone; tncrease in sand appears to be linked to increased running freshwater (*P. moussonii*)	Freshwater bodies were now fully re-established behind the coastal barrier; shallow standing or slowly moving water is suggested by *Planorbis* sp., fed by a steady running freshwater stream (*P. moussonii* and *A. fluviatilis*); expansion of the water body pushed back the wetland margins; *O. elegans* indicates plant growth in the pond or at the water edge; slow return of the saltmarsh (*O. myosotis*) in the vicinity
2-D	615–415	4974–4381 BC (6924–6331 BP)	Total of 1877 molluscs, of which *O. myosotis* 45%, *P. moussonii* 28%, *Planorbis* sp. 11%, *C.* cf. *schlickumi* 3%, *Lauria cylindracea* 0.2% Marked variations but general increase in the number of shells per sample; strong but fluctuating presence of brackish water species among freshwater associated snails; land snails were few and irregularly found, among which first appearance of the woodland indicator *L. cylindracea*; generally the sediments had a silt/clay content above 90% in all but four samples, indicating fairly stable conditions between periodical inwash events	Fluctuations in the freshwater bodies coupled with increases or decreases in the saltmarsh as evidenced by *O. myosotis*; presence of woodland is indicated by *L. cylindracea* shortly after 4400 BC, while the grassland is also found (*C. acuta*) intermittently; major rainstorms occurred around 4000 BC, which led to the inwash of the brackish water *Hydrobia* sp. from the nearby sea and *C. acicula* from the hinterland, after which the saltmarsh was again diminished through increased flowing freshwater (*P. moussonii*); this fluvial event also left its mark at the same depth in Xem1; there appear to have been strong weather induced fluctuations in the running freshwater flow, which often affected the population of *Planorbis* sp., which do not tolerate intensive water movements; this species disappears at the top of the zone after a major fluvial inwash

Table 4.11 *(cont.).*

Zone	Depth cm	Date ranges cal. BC/AD (BP) for the start of each zone (2σ)	Molluscan assemblages	Environment
2-E	410–360	2837–2470 BC (4787–4420 BP)	Total of 30 molluscs, of which *Lymnaea* sp. 33%, *V.* cf. *antivertigo* 33%, *O. elegans* 10, *C. acuta* 6%, *L. cylindracea* 6% Dramatic decrease in the number of shells found, one sample was sterile; assemblages consisted of mainly freshwater/wetland molluscs, with brackish water species occurring only once, and land snails only in two samples; the sediments had an increased content of coarse sand, stones occurred in the middle of the zone; together with the very low amount of molluscs found, his indicates very rapid sedimentation	The date suggests that this zone describes the beginning of the end of the Temple Period and it is marked by a dramatic change in the environment; there is no more evidence for running freshwater, indicating that stream either dried up or the water output was dramatically reduced, possibly due to severe aridification; the only freshwater snail found is *Lymnea* sp., indicative for poor conditions in the now very shallow freshwater pool, which, however, sustained some vegetation and the wetland surrounding it (*O. elegans*); severe erosion and subsequent inwash events of sediments is suggested by *C. acicula* in the beginning of the zone; inwash events occurred throughout and the continuous presence of coarse sand and at one point also stones may have contributed to the shallowing of the freshwater pond. Some woodland still existed (*L. cylindracea*) as did grassland (*C. acuta*); evidence for the previously extensive saltmarsh occurred only once (*O. myosotis*), possibly indicating that the inwash events were of terrestrial origin, as no marine or subaqueous brackish water species (*Hydrobia* sp.) were found
2-F	360–240	2231–1715 BC (4181–3665 BP)	Total of 870 molluscs, of which *O. myosotis* 93%, *C. acuta* 4%, *P. moussonii* 1%, *P. papillaris* 1%, *Hydrobia* sp. 0.6% The assemblages consisted predominantly of brackish water species, freshwater/wetland species were rare, land snails occurred in small numbers intermittently; marine shells were found at the top of the zone; the sediments were silty/clayey, sand generally occurred in lower amounts than in the previous zone; one event in the middle of the zone had small stones washed in, another at the top had a notable influx of fine sand	Dramatic change of the environment, the pond and wetlands silted up and got replaced with grassland a saltmarsh (*C. acuta* and *O. myosotis*), the latter expanding rapidly, though patches of grassland persisted throughout; the woodland indicator was no longer found, and apart from the grassland species *C. acuta*, the only other land snail identified was the open country species *P. papillaris*; while the pond resurfaced once briefly (*Lymnaea* sp.), the running freshwater stream remained elusive, indicating a continuation of the previous aridification; a strong sea storm at the top of the zone may have led to the breakdown of a bay-bar and led to an influx of a few marine shells, *Hydrobia* sp. and fine sand; this event was also found in Xemxija 1 at the same depth
2-G	240–147	873–245 BC (2823–2195 BP)	Total of 398 molluscs, of which *Hydrobia* sp. 59%, *P. moussonii* 22%, *O. myosotis* 12%, *Bittium reticulatum* 4%, *C. acuta* 0.7% The zone contained molluscs from all major habitat categories in differing mixes; brackish water associated species were the most common ones, *P. moussonii* was the only freshwater	Continuation of seaward inwash onto the site with a sharp increase in the brackish water mud snail *Hydrobia* sp., which replaced the saltmarsh indicator *O. myosotis*; the marine inwash events may have been in conjunction with strong rainfall, as the running freshwater species *P. moussonii* reappears, but it no longer formed ponds or wetlands; with the

Table 4.11 *(cont.).*

Zone	Depth cm	Date ranges cal. BC/AD (BP) for the start of each zone (2σ)	Molluscan assemblages	Environment
			associated snail found, wetland species were absent; land snails occurred intermittently, as did marine molluscs; the sediments were predominantly silty/clayey throughout without notable changes in the low sand content	waning and subsequent disappearance of the freshwater stream, the saltmarsh extended again (*O. myosotis*) and the brackish water body in the nearby sea vanished (*Hydrobia* sp.), leading to the inwash of marine species (*B. reticulatum*); the very few land snails found are indicative of grassland (*C. acuta*) with light vegetation and open country/garrigue (*T. spratti*)
2-H	147–103	AD 74–777 (1876–1173 BP)	Total of 5 molluscs of which *C. acuta* 40%, the remainder indeterminate Heliciid fragments Dramatic reduction in the number of molluscs found, with many sterile samples, particularly at the top of the zone; as in Xem1, the sediments received a strong increase in stones and coarse sand, coarsening up	The site had now completely dried up, there is no longer evidence for a saltmarsh, freshwater or marine influence; the very few land snails are indicative of grassland and light vegetation

Table 4.12. *Correlation and integration of molluscan data from Xemxija 1 (XEM1) and Xemxija 2 (XEM2).*

Date cal. BC/AD (BP) (2σ)	XEM1	XEM2
7550–6250 BC (9500–8200 BP) Pre-Neolithic Period	Zones 1-A, base of 1-B1 Key taxa: *P. moussonii*, *Planorbis* sp., *V. pulchella*, *O. hydatinus* Freshwater bodies and wetland, leaf litter	Zones 2-A, up to middle of 2-B1 Key taxa: *O. myosotis, P. moussonii*, *O. elegans*, *C. acuta* Saltmarsh with freshwater bodies and wetland, grassland
6250–4150 BC (8200–6100 BP) Early Neolithic Period	Zones part of 1-B1, 1-B2 Key taxa: *P. moussonii, Planorbis* sp., *P. papillaris, C. acuta, C. acicula* Aridification leading to drying up of freshwater bodies, establishment of grassland	Zones part of 2-A, 2-B2, 2-C Key taxa: *P. moussonii, Lymnaea* sp., *Planorbis* sp., *C. acuta* Aridification and disappearance of saltmarsh, followed by appearance of grassland, superseded by shallow freshwater pools fed by a stream and surrounding wetlands and reappearance of the saltmarsh
4050–2350 BC (6100–4400 BP) Temple Period	Zones 1-C and most of 1-D Key taxa: *P. moussonii, Planorbis* sp., *O. myosotis* Variety of freshwater bodies and associated wetlands; from *c.* 3250 BC onwards, strong fluctuations of precipitation led to decreases in the freshwater water bodies and extension of saltmarsh	Zone 2-D Key taxa: *O. myosotis*, *P. moussonii*, *Planorbis* sp., *L. cylindracea* Continuous fluctuations between saltmarsh and freshwater bodies, due to variations in precipitation; appearance of woodland *c.* 4050 BC
2350–1950 BC (4400–3900 BP) End of Temple Period, Early Bronze Age (Tarxien Cemetery Phase).	Zone top of 1-D Key taxa: *O. myosotis*, *Lymnaea* sp., *O. elegans* Disappearance of running freshwater stream, persistence of saltmarsh and poor quality shallow freshwater pool and vegetated wetland	Zone 2-E Key taxa: *Lymnaea* sp., *V.* cf. *antivertigo, L. cylindracea, C. acicula* Severe erosion events, and as in XEM1, disappearance of freshwater stream but persistence of poor quality shallow freshwater pool and vegetated wetland; saltmarsh diminished, but woodland still occurred

Table 4.12 *(cont.).*

Date cal. BC/AD (BP) (2σ)	XEM1	XEM2
1950–650 BC (3900–2600 BP) Bronze Age to Phoenician/early Punic	Zones 1-E and half of 1-F Key taxa: *B. reticulatum*, *O. myosotis*, *Lymnaea* sp., *C. acuta* Breaking down of bay-bar, sudden marine influence, presence of small shallow freshwater pool with associated vegetated wetlands, which disappear after 1150 BC; after that, extension of saltmarsh, surrounding landscape is open country and lightly vegetated grassland/steppe	Zone F Key taxa: *O. myosotis*, *C. acuta* Expansion of saltmarsh and disappearance of freshwater/wetlands after 1750 BC; no more evidence for woodland; presence of grassland and open country/garrigue
650 BC–AD 850 (2600–1100 BP) Early Punic to Arab Period	Zones: upper half of 1-F and 1-G Key taxa: *O. myosotis, P. moussonii, Hydrobia* sp., *C. acuta* At first strong presence of saltmarsh, but the eventual breaking down of bay-bar led to the inwash of sediments with *Hydrobia* sp. and *B. reticulatumi,* severely diminishing the saltmarsh; brief reappearance of freshwater stream around AD 650, without formation of pools or wetland; presence of grassland and open country/garrigue	Zones: 2-G and 2-H Key taxa: *O. myosotisi,* Hydrobia *sp., P. moussonii, B. reticulatum*, *C. acuta* As in XEM1, marine inwash of sediments with *Hydrobia* sp. and *B. reticulatumi,* severely diminishing the saltmarsh, but with a stronger signature than in XEM1; reappearance of running freshwater until around 150 BC, but no formation of wetland or pools; after 150 BC, reappearance of saltmarsh with marine influence; presence of grassland and light vegetation
AD 850–1450 (1100–500 BP) Arab Period to pre-Knights Period	Zone H Key taxa: *B. reticulatum, Hydrobia* sp., *C. caruanae* Occasional marine influence, fast sedimentation and disappearance of saltmarsh; presence of light vegetation	no data

in this case was caused by agricultural erosion of nutrient-rich topsoil and inwash into the Salina inlet. Further eutrophication events are suggested by high *C. gibba* at the base and top of zone I and in the middle of zone L. All of these coincide with a sudden significant expansion of *Plantago lanceolata* and expansion of some coprophilous fungal spores in the pollen diagram, interpreted as reflecting a major expansion of livestock grazing and disturbance through agricultural activities. The second event also coincides with a rise in cereal pollen, suggesting an intensification of arable activity. In all of these cases, it is plausible to regard the eutrophication of the Salina Inlet as reflecting rises in the input of nutrients resulting from agricultural activity.

4.5.6. Xemxija 1 and 2

The extraction site of these cores, taken less than 1 m apart, was situated at the end of Pwales Valley outside the Simar Nature Reserve and at a distance of less than 100 m from the sea at Xemxija Bay. Geographically, the area is a graben described as a low-lying, flat bottomed basin (Bowen-Jones *et al.* 1961, 34). The flattish floor of the graben is flanked by steep slopes, with substantial gravelly alluvial fans debouching from tributary valleys. The basin has a catchment of around 7 sq. km. Archaeological remains near the location include a number of Neolithic tombs and the remains of a temple (Evans 1971). The valley has been a prime area for agriculture to this day (National Statistics Office 2016).

A CONISS analysis was performed with both cores in the TILIA graphs, and both could thus be linked and sub-divided into seven different molluscan assemblage zones (MAZs), discussed below. The links, however, are at times only broadly linear with respect to the measured depth in both cores, which may be a result of the different energy environments of the water flow and cut-and-fill stratification (Figs. 4.7 & 4.8; Tables 4.10–4.12). Bayesian models provide the date frame for the cores, with WZ2 covering the last *c*. 7675 years (see Chapter 3, Table 3.6).

4.5.6.1. Conclusion: Xemxija

Of all the cores analysed, the two from Xemxija were the only ones which showed a semi-continuous sequence from the early Holocene. The cores revealed varied freshwater environments that were susceptible to

prolonged droughts and increased rainfall periods during prehistory and beyond until the area was covered in made ground, probably fairly late during the British Period. The combination of a relatively small catchment area with a relatively low-energy environment provided a rare insight into the past environment and climates of the Maltese Islands. Prolonged droughts appear to have left their mark at around 6200 cal. BC and after 2500 cal. BC, shortly after which several freshwater species were no longer found and are now extinct. These may very well coincide with the droughts associated with the 8.2 ka and 4.2 ka BP events. Severe fire events were largely absent from these cores and human impact may be difficult to detect through the molluscan analysis. It is perhaps possible that the presence during the fifth millennium BC (between *c*. 6.15 and 3.6 m in the core) of *Lauria cylindracea,* for which there was no previous fossil record, may have been the result of importing soil around tree saplings for planting at Xemxija. It is perhaps more likely, however, that the species was able to flourish in the wetland vegetation surrounding the freshwater bodies in the valley floor.

4.6. Interpretative discussion

4.6.1. Erosion – evidence of major events from the cores

Erosion is fundamentally a natural process, though often driven and modulated by human activities. The majority of the studied sediments had accumulated following erosion of soils or exposed older deposits within the catchments, transported to the deposition sites by running water. In ephemerally active regimes, typical of semi-arid, seasonal environments such as those characterizing much of the Maltese Holocene, material may be repeatedly eroded and re-deposited as it moves through the catchment. This storage and re-mobilization of sediments and their contained biogenic materials led to some radiocarbon ages not being in stratigraphic order in the cores.[9] Major erosion events could be recognized in the cores through sudden changes in the sediment colour, coarsening of texture and the appearance of large clasts and in the composition of the mollusc assemblages. In particular, *Cecilioides acicula,* which buries itself in the soil at depths varying between 20 cm and 2 m, possibly provides some indication for erosion events (see Chapters 2 & 5), especially when it was found in waterlain sediments at the coring sites. This suggests that significant quantities of soil may have been displaced by erosion over the studied interval.

4.6.1.1. Mġarr ix-Xini

The sediments of the core retrieved from the alluvial plain in Mġarr ix-Xini reflected the high energy environment and interplay of the natural forces in several ways. Sudden soil colour changes in the sediments pointed to at least 15 major events and marine sediments alternated several times with terrestrial deposits. These were always accompanied by dramatic changes in the sediment textures. The particle size analysis (Appendix 4) showed that, on numerous occasions, stones were incorporated in the sediment suggesting highly energetic flows. The molluscan assemblages contained throughout an admixture of shells belonging to three major habitat groups: terrestrial, brackish water-associated and marine snails in widely varying amounts. The possible erosion indicator *C. acicula* occurred irregularly throughout, but only in the upper 60 cm of the core (depth from surface down to 1.2 m) was it likely to have been part of the natural assemblage and to have lived in the sediments.

The lowermost dated deposit may be attributed to the Punic period (510–360 cal. BC; UBA-33096). It is probable that earlier valley fill sediments had been removed, presumably by running water and it is probable that further erosion (by running water or the sea) affected the accumulating sediments on several occasions between that time and the present day.

4.6.1.2. Marsaxlokk

Although the core was only 3.86 m long, there were ten distinctive changes in the sediment colour during this interval, from at least cal. AD 435–670 (at 2.86 m; 1444 BP; UBA-29351). A terrestrial soil was overlain by marine sands, then alluvial/colluvial derived silts, followed by a distinctive layer of decomposed plant material that was overlain by coarse marine sand containing a piece of Punic pottery. Further marine silts passed into alternating terrigenous and marine silts, and terrestrial, possibly colluvial, silts. Most of the samples contained marine gastropods and bivalves, while brackish water shells were prominent and terrestrial species occurred throughout. The total number of molluscs varied greatly. The irregular presence of *C. acicula* may suggest that several severe erosion events occurred.

4.6.1.3. Wied Żembaq

In the Wied Żembaq 1 core over the last 3.5 millennia BC, changes in the soil colours were less marked than in the other cores. Nonetheless, the presence of horizons of limestone pebbles at *c*. 3.5–3.62 m and 2.17–3.15 m suggest an episodically very energetic depositional environment and erosion within the catchment. Most samples contained molluscs belonging to at least three major habitat groups, but several samples had only land snails, albeit in low numbers. There are several horizons marked by the erosion

indicator *C. acicula* and molluscs from several habitat groups, notably near 4.44 m, and between 2.85 and 3.35 m. Marine influence increased considerably in the top metre of studied material.

4.6.1.4. The Marsa 2 core

Fifteen major changes in sediment colour could be observed in the Marsa 2 core, probably from the Neolithic Ġgantija phase onwards. Very strong marine influence could be detected from 9 m upwards in the molluscan assemblages. There is a sharp change from brownish oxidized sediments of largely terrestrial/eroded soil origin to dark grey reduced marine sediments. The lack of dateable material in the lower part of the core is an indication of very rapid deposition. The particle size distribution, characterized by coarse sands and gravel, suggests highly energetic depositional regimes. Major events deposited quantities of gravel on three occasions. Rapid deposition was also indicated by thick layers of hydro-collapsing fine sands that could not be retained by the corer, at 5.25–5.95 m, and towards the top of the core close to the groundwater table. The molluscan assemblages varied, but usually contained at least three major habitat categories (marine, brackish water and land snails), also often freshwater molluscs. The possible erosion indicator *C. acicula* was particularly frequent above 6.5 m. The extent of recycling in this energetic but episodically active environment is brought into sharp relief by the finding of two conjoining potsherds more than one metre apart in the core and by the stratigraphically disordered radiocarbon dates, with insecure dates evident until the Late Bronze Age, a feature remarked on also in the neighbouring Marsa 1 core by Carroll *et al.* (2012). Towards the top of the core, marine molluscs become rare. In the upper 50 cm of the core the presence of *C. acicula* may be autochthonous, given that this was now a terrestrial environment.

4.6.1.5. Salina Deep Core

The roughly 17 m of marine sediments from the Salina Deep Core displayed a large number of sedimentary events, probably from close to the beginning of the Holocene. The sediment colours were dark reddish brown in the basal terrestrial sediments, but the overlying marine sediments are light brown/grey to dark grey/brown, reflecting post-depositional sediment reduction in the presence of organic matter. The sediment textures range from clayey stony silt diamicts to sands, silts and clayey silts. It is likely that most of the sampled marine sequence resulted from the deposition of turbidites (sub-marine mass flows). Typically, this type of sedimentation in shallow waters is caused by very turbid or hypercritical fluvial flows entering a marine basin. Sedimentation was very rapid, in response to enormous sediment flux from the large, steep catchment, but also because accommodation space was created by the very rapid rate of sea level rise during the early Holocene. The relatively offshore nature of sedimentation was indicated by the generally low counts for terrestrial molluscs, particularly between 22.5 and 18.5 m. This interval contained very few marine molluscs, but the possible erosion indicator *C. acicula* was often present in the core. The sherds of Tarxien Phase pottery found near the top of the sampled sequence again point to the energetic nature of the environment and the likelihood of sediment storage and recycling within the catchment.

4.6.1.6. Xemxija

Owing to the basin structure of Pwales Valley, where the influence of the nearby sea was limited and the depositional environment was generally not very energetic, the vast majority of the sediments accumulated because of material arriving from the catchment during precipitation events sufficiently powerful to cause run-off. Both the Xemxija cores are thought to span much of the Holocene period, and certainly the last *c.* 7500 years.

That part of Xemxija 1 below 6.7 m is marked by rather mixed mollusc assemblages, including the possible erosion indicator *C. acicula* and the intermittent occurrence of freshwater snails. These are consistent with several severe events. The presence of small mud balls between 7.8 and 6.7 m indicates torrential rains and high stream flow velocities (Wigand & McCallum 2017). Quieter, more organic-rich sedimentation then occurred. Sedimentation became more energetic between 5.65 and 5.01 m and then intensified further. Some of these events saw a considerable influx of marine molluscs. Mud balls were prominent between 4.4 and 3.5 m, again indicating torrential rains and high stream flow velocities. The occurrence of wind-blown quartz sand in this part of the core suggests the proximity of a dune system.

Xemxija 2 closely mirrored the events found in Xemxija 1 and provided additional information. Often high *C. acicula* and frequent mud balls between 8.08 and 7.18 m indicate episodic torrential rainfall, high streamflow and strong soil erosion. This may possibly coincide with the 8.2 ka BP event.[10] Quieter sedimentation then occurred, but between 4.13 and 3.18 m the number of shells decreased dramatically. The possible erosion indicator *C. acicula* was found at 4.01 m, and again, the massive presence of gravel-sized mud balls up to 2.78 m indicated episodic torrential rainfalls with high stream flow velocities. Wind-blown very fine quartz was abundant throughout.

In both cores, from 1.5 m depth upwards, there was a notable influx of stones and coarse sand and the deposits were often devoid of any mollusc remains. The light brown colour of the sediments indicates severe terrestrial soil erosion.

4.7. Environmental reconstruction based on non-marine molluscs

The following reconstruction is based on the dated results from all the cores, depending on their date ranges and suitability. As the non-marine assemblages in the cores were predominantly death assemblages from within the catchment areas, the emerging picture is of a general nature.

4.7.1. Early Holocene (c. 8000–6000 cal. BC)

The base part of the cores from Xemxija and the Salina Deep Core contained material that was radiocarbon dated to *c*. 8000–6000 cal. BC (see Chapter 2). The molluscan assemblages suggest the presence of perennial streams, slow moving water bodies and ponds, which today no longer exist in these areas. Both sites also had areas of saline marshland as evidenced by the presence of *Ovatella myosotis*. The margins of the freshwater bodies, the extent of which are unknown, had relatively lush plant growth, which provided the leaf litter/damp habitat for different species. Open country/karstland was also in the vicinity. The prevalence of ubiquitous snail species points to a disturbed and, possibly at times, harsh environment. The molluscan evidence from Xemxija suggests a shallowing and subsequent drying up of the water bodies towards the end of the seventh millennium BC, which may very well have been associated with the global 8.2 ka BP event that led to severe aridification through prolonged droughts. This was followed by massive mud-flows containing barely any plant material, which may suggest that the local environment was quite barren at the end of the Early Holocene.

4.7.2. Mid-Holocene (c. 6000–3900 cal. BC)

The period appears to have continued to be marked by environmental instability and prolonged droughts, during which the freshwater bodies at Xemxija were still absent. The signature is different in the Salina Deep Core owing to different energy environments, where very high sedimentation rates could be observed at the coring site and non-marine molluscs, including freshwater/wetland associated species, occurred irregularly throughout. The saline marshland species *O. myosotis* was no longer found at Xemxija and Salina. Of the land snails, ubiquitous species prevailed in both sites, where Xemxija had a decrease in leaf litter snails but this was not mirrored at Salina. Open country/karstland snails were irregularly present in small numbers at both sites.

4.7.3. Temple Period (c. 3900–2400 cal. BC)

This period was marked by a decisive change in the environment at Xemxija, where there was now a full-blown freshwater environment that was host to a large variety of freshwater/wetland snail species and which indicated the presence of perennial running, slow-moving and ponded freshwaters. The presence of the marginal saline marshland species *O. myosotis* was occasionally found again until 3630–2930 cal. BC, increased substantially after this point in both cores, perhaps indicating an increase in the extent of the saline marshland habitat. The land snails found after this date showed the existence of woodland habitats at Xemxija.

From the Salina Deep Core, the upper part, from 14.74–11.4 m, has also been dated to the Temple Period. No clear picture or trend emerged. The molluscan assemblages contained predominantly ubiquitous snails, followed by open country/karstland species and leaf litter species. The freshwater/wetland-associated molluscs showed a wide diversity and abundance, indicating a continuous presence of perennial running freshwater, slow-moving water and ponds in the Burmarrad Plain. Despite this, the saline marshland species *O. myosotis* was not found in the samples.

The lowermost deposits of the Wied Żembaq cores can be attributed to the Temple Period, from around 3600 cal. BC onwards. The general picture from this site is that during the Temple Period, there was a perennial freshwater stream in the valley, as evidenced by the freshwater snails *Pseudamnicola moussonii/Mercuria similis*. This probably created a saline marshland at the mouth of the valley, which provided the habitat for *O. myosotis*. The land snails here were predominantly open country/karstland species, followed by ubiquitous species. Leaf litter-associated snails were generally in a minority, despite the presence of a freshwater stream.

4.7.4. Early to later Bronze Age (2400–c. 750 cal. BC)

The Bronze Age period saw a dramatic decrease in freshwater-associated snails at Xemxija, possibly associated with the 4.2 ka BP event.[11] Most notable was the sudden absence of the running freshwater species *P. moussonii/M. similis* in both cores. The absence or dramatic reduction of freshwater input may have led to a situation where several species vanished and possibly became locally extinct from several sites, particularly after *c*. 1500 cal. BC. Ubiquitous land snails dominated, most prominently the light grassland/dune species *Cochlicella acuta*, while leaf litter species and open country/karstland species occurred only occasionally.

The leaf litter woodland indicator *Lauria cylindracea* was no longer found from around 1800 cal. BC onwards.

Other cores with segments dated to the Bronze Age included Wied Żembaq and Mġarr ix-Xini and Marsa 2, all of which contained relatively high-energy sediments. At the former site, the snails associated with running freshwater vanished during this period. The stream may not have disappeared completely, as leaf litter species and the brackish water/saline marshland species *O. myosotis* occurred in good numbers, although the latter occurred rather irregularly. Open country/karstland species increased, as did the ubiquitous species. At Mġarr ix-Xini, leaf litter species were generally very sparse, the analyses were dominated by open country/karstland species and ubiquitous snails throughout. As deposits belonging to the Temple Period were not found, it is not possible to comment on any changes. In Marsa 2, the non-marine molluscan assemblages in the deposits that were dated to this period showed the presence of running freshwater, slow-moving/standing waters and wetlands. The land snails indicated habitats for leaf litter species. Open country/karstland species also occurred. Again, the most prominent snail group was the ubiquitous species.

4.7.5. Latest Bronze Age/early Phoenician period to Late Roman/Byzantine period (c. 750 cal. BC–cal. AD 650)

There are no radiocarbon dates for the sediments covering this section in the Xemxija cores, but the calculated ranges in Xemxija 2 at 2.57 m showed a decrease in the saline marshland, increasing influence from the nearby sea, and a reappearance of the perennial freshwater stream at about 750 cal. BC as indicated by *P. moussonii/M. similis*. The same signature was found in Xemxija 1 slightly further up at 2.1 m, but the calculated age range is several hundred years younger and there is no overlap. Nonetheless, the reappearance of this snail still fell into the period. *P. moussonii/M. similis* were the only freshwater snails found in this section. Land snails were generally very scarce in both cores from Xemxija, and among the few found, ubiquitous species dominated. No leaf litter species were recovered, whilst open country species were very scarce.

At Wied Żembaq, the brackish water saline marshland species *O. myosotis* was now very scarce, possibly indicating that the freshwater input into the valley was even more limited now than it was before. The amount of leaf litter species also decreased, while open country/karstland species and ubiquitous snails prevailed.

At Mġarr ix-Xini, the radiocarbon chronology is also insecure, but the picture is similar to that of the previous period. The presence of several grape pips of *Vitis vinifera*, dated to the Punic period, show that vines had meanwhile been imported and grew successfully on Gozo (see Chapters 3 & 7).

In the Marsa 2 core, initially deposits dated to the start of that period still contained quite abundant and diverse freshwater snails, but by the end of the period, only *P. moussonii/M. similis* indicated the presence of a freshwater stream. The rare occurrence of *Planorbis* sp. pointed to a slow-moving/stagnant water body in the plain. Ubiquitous snails were dominant, followed by open country/karstland species and a few leaf litter snails.

The situation at Marsaxlokk, a core with a less secure radiocarbon chronology but covering the period in question, revealed an absence of perennial freshwater at the coring site. Ubiquitous snails predominated in the assemblages, followed by open country/karstland species. Leaf litter species were only found on two occasions. The presence of the coastal marshland species *O. myosotis* would indicate that some seasonal freshwater influence occurred.

4.8. Concluding remarks

Full molluscan analyses of snails belonging to all major habitat groups rarely feature in the Mediterranean literature. The results obtained through the *FRAGSUS Project* provide valuable insights into the past environment, landscape and climate that the study of only one singular habitat group could not have achieved on its own. The numbers of snails found varied greatly in the cores, but while they may not have reached statistically viable numbers in many of the samples, the marked variations themselves tell a story of episodes of severe erosion and environmental recovery when placed in context with the sediments in which they were found. The presence of specific indicator species helped to provide insight as to what environments were present in the catchment at any given time.

Although the cores, widely distributed in the Maltese Islands, did not cover the same time intervals, together they covered the different periods of Malta's prehistory and history, allowing a more or less continuous picture to emerge. Few of the deposits dating to the early Holocene, prior to the arrival of the first settlers, contained leaf litter species that would support the notion of a previously forested or densely vegetated environment, at least within the catchments of the coring sites. When the first settlers arrived, possibly around 6000 cal. BC, the non-marine molluscs showed a predominantly open landscape and freshwater habitats in Salina and Xemxija, but the people probably faced an environment that had recently recovered from a prolonged drought, during

which rare torrential rainfall caused severe erosion, possibly as a result of the 8.2 ka BP event.

The rise of the Neolithic and flowering of the Temple Culture occurred during a relatively humid climatic period: freshwater was abundant at Xemxija, Salina and, on a smaller scale, at Wied Żembaq and leaf-litter species which suggest dense vegetation in favoured sites, although much of the landscape was lightly vegetated. Once agriculture started, it is not clear whether the frequently occurring soil erosion episodes resulted from vegetation removal or modification by cultivation and landscape disturbance caused by people and their livestock, or from natural processes relating to the removal of vegetation by drought. It is likely that all these processes were involved, as they are today. Towards the end of the Temple Period, the species diversity and abundance of the non-marine molluscs became severely reduced, especially leaf litter and freshwater taxa. This is suggestive of desiccation and/or land degradation. Furthermore, the presence of marine molluscs at Xemxija indicated the breaching or overtopping of the bay-bar during storms.

The Bronze Age seems to have been initially characterized by rather dry climates and very little dense vegetation, for instance at Wied Żembaq. By about 2000 cal. BC increasing freshwater and leaf-litter taxa seem to indicate a rise in effective moisture, an environment which may have persisted with some fluctuations until the Roman Period, when the assemblages in the cores at Xemxija and Marsa are consistent with the drying of freshwater bodies and decreases in dense vegetation, most probably the result of increasing climatic aridity that seems to have persisted to the present day.

4.9. Notes on selected species

The analyses above were based on several indicator species, which have specific habitat requirements. Among these, some species are today extinct, whilst others had no previous palaeontological record in the Maltese Islands suggesting that some might be recent introductions (compare Table 4.1, after Giusti *et al.* 1995).

4.9.1. Extinct species:

Gyraulus (Armiger) crista (Linnaeus 1758)
This freshwater species occurs in perennial shallow waters of a wide variety of habitat types including ponds, lakes and coastal lagoons with abundant aquatic vegetation (Heino & Muotka 2005; Zettler & Daunys 2007; Zealand & Jeffries 2009). It tolerates freshwater to water with low salinity (Seddon *et al.* 2014) and can resist periods of partial drying (Giusti *et al.* 1995).

While only one juvenile specimen had been found by Giusti *et al.* (1995) in the Quaternary deposit of Wied tal-Baħrija, 36 specimens were found in the Salina Deep Core in association with other extinct species. As the samples in this core did not contain material post *c*. 2500 cal. BC, it is unknown when this species became extinct. Sub-fossils of this species have recently been found together with *Oxyloma elegans*, in an undated Holocene deposit at Salini (Cilia & Mifsud 2012).

Bulinus (Isidora) cf. *truncatus* (Audouin 1827) complex
Specimens of this freshwater species have been found in Xemxija 1, Marsa 2 and in the Salina Deep Core. This species is indicative of a variety of perennial flowing and standing water bodies, where it lives on the banks among vegetation and on stony beaches (Giusti *et al.* 1995; IUCN 2017). Extinct today from the Maltese Islands, it was found in deposits pre-dating the end of the Temple Period in Xemxija 1 and in the upper half of the Salina Deep Core. In the Marsa 2 core it was last found in deposits dated to the Late Bronze Age/ Early Phoenician Period.

This species is an intermediate host for the schistosomiasis (bilharzia) parasite, and the disease has been traced back to Neolithic times in Chad and in Egypt, where it is likened with the Aaa disease (King & Bertsch 2015). It is possible that locally, *Bulinus truncatus* were also an intermediate host for the parasites causing the disease (trematode worms of the genus *Schistosoma*), which then could have negatively affected the local human and animal populations. Untreated, infection with the parasites is deadly in *c*. 60 per cent of cases.

Oxyloma elegans (Risso 1826)
A freshwater-wetland species associated with areas bordering a perennial stream, where it lives on permanently wet ground, but also on plants in the water (Giusti *et al*. 1995; IUCN 2017). Extinct today from the Maltese Islands, it was found in good numbers in Xemxija 2 from the lowermost deposits onwards (*c*. 7000 cal. BC) with interruptions up until shortly after the end of the Temple Period. In Xemxija 1 it was found between the early Temple Period (from *c*. 4000 cal. BC) and deposits dated to the Bronze Age at around 1500 cal. BC. In the Salina Deep Core and in Marsa 2, it only occurred once, in a storm deposit dated to the Tarxien (late Neolithic) phase, while in Marsa 2 the storm deposit cannot be dated more closely than before the end of the Late Bronze Age/early Phoenician period.

Vertigo cf. *antivertigo* (Draparnaud 1801)
This now locally extinct hygrophile species lives among decomposing plant material and under flood debris in swampy meadows, and river and lake margins that

may be flooded occasionally, but never seasonally dry up (Giusti *et al.* 1995; Welter-Schultes 2012). Although its presence in Malta was based on specimens from a Quaternary deposit at Wied il-Baħrija where it occurred in association with *Oxyloma elegans* (Giusti *et al.* 1995), its occurrence preceded and outlived the latter species in both Xemxija cores by several hundred years. In the Salina Deep Core it was found only once, in a deposit dated to *c*. 6000 cal. BC. In Marsa 2, one specimen was found in a Late Bronze Age/early Phoenician deposit.

4.9.2. Species with no previous fossil record:

Lauria cylindracea (Da Costa 1778)
This is the only woodland 'indicator species' in the Maltese Islands, where today it occurs in remnants of forest and in maquis communities under leaf litter. With no palaeontological record, its introduction date to the Maltese Islands was unknown (Giusti *et al.* 1995). *Lauria cylindracea* was found in small numbers in the Xemxija 2 core. The deposits are not closely dated, but it would appear that the species may have been introduced to the area around 4000 cal. BC, possibly in conjunction with olive tree saplings that were planted there, as indicated by the pollen from Xemxija 1 (see Chapter 3). As the olive is not native to Malta, it must have been imported, when the roots would have been covered with soil and leaf litter that could have contained this tiny snail species. The species occurred last in Xemxija 2 core deposits that were not closely dated, but may possibly be from around 2000 cal. BC, at a time when in the same core *Vertigo* cf. *antivertigo* became extinct and other freshwater/wetland snail species disappeared.

4.9.3. Other indicator species:

Truncatellina callicratis (Scacchi 1833)
The species is associated with very dry, calcareous grassy sites, open rocky hillsides, and above all, leaf litter, where, in the Maltese Islands the evidence suggests, it is mainly found (Giusti *et al.* 1995). It has not been reported from the Quaternary deposits of the Maltese Islands, but a few shells were found in the archaeological excavations at the Xagħra Brochtorff Circle in Gozo, dated to the Temple Period (Schembri *et al.* 2009). Its presence was noted in all coring sites except Marsaxlokk and its earliest occurrence could be noted in Xemxija 1 and the Salina Deep Core, in both instances in deposits dated to *c*. 5900 cal. BC.

Ferussacia (s.str.) *folliculus* (Gmelin 1791)
Another leaf litter species, characteristic of damp habitats. It withstands long periods of dryness dormant under stones, wood or litter (Giusti *et al.* 1995). Although today common and widespread in the Maltese Islands, it had no previous fossil record. Two sites revealed its occurrence since prehistory – Wied Żembaq (*c.* 800 cal. BC) and, much earlier, the Salina Deep Core (*c*. 5300 cal. BC).

Pseudamnicola (s.str.) *moussonii* (Calcara 1841) and *Mercuria* cf. *similis* (Draparnaud 1805)
These were the most widespread and commonly occurring freshwater species. They were present in all cores except in Mġarr ix-Xini (Gozo) and in Marsaxlokk. Unless they were the only freshwater species present (as in Wied Żembaq), they appeared as pioneer species before any other freshwater snails and persisted longer, even when others had long vanished (e.g. Xemxija and Marsa). Both species are indicative of a perennial running freshwater stream and their shells look very similar, a secure distinction cannot be made on the basis of the shell alone. *Mercuria* cf. *similis* (Draparnaud, 1805) has no secure fossil record and is thus believed to be a relatively recent introduction to the Maltese Islands (Giusti *et al.* 1995). Although they are placed in different genera, both belong to the same family (Hydrobidae), share the same habitat and were thus listed in the graphs as *Pseudamnicola/Mercuria*.

Ovatella (Myosotella) myosotis Draparnaud 1801
A more terrestrial than aquatic species, it is always found close to beaches without strong wave movement. This brackish water species tolerates environments with low salinities and lives on the shores of pools in saline marshlands and valley mouths that reach the coast, where it is found amongst algae, under stones or wood and on muddy substrata (Giusti *et al.* 1995; Welter-Schultes 2012). As such, it is a good indicator of an environment with a steady freshwater influence close to the sea.

Cecilioides acicula (Müller 1774)
This widespread subterranean species has been regularly found in archaeological deposits in the Maltese Islands, often in very high numbers (e.g. Fenech & Schembri 2015), where it may be intrusive. This burrowing species lives among plant roots and deeply embedded stones, usually at depths of 20 to 40 cm below the soil, but depending on the substrata, it has been found at depths of two metres and more (Giusti *et al.* 1995; Boddington *et al*. 1987). This species occurred prominently in all cores investigated, which had been taken in alluvial plains and where sediments accumulated only by erosion processes. The presence of this burrower among other surface-dwelling snails in the samples suggests a tolerance and association with

severe erosion events that de-stabilized substantial amounts of soils of which this species was part. Where material was available for dating, these invariably resulted in radiocarbon age inversions, underlining the massiveness of these events.

Notes

1 For example, *Oxyloma elegans*, *Bulinus truncatus*, etc.

2 Two cores were extracted from Marsa in June 2002. Of these, the Marsa 1 core formed part of separate PhD projects by Frank Carroll (Queen's University Belfast) and by Katrin Fenech (University of Malta). For the *FRAGSUS Project*, Fenech's half of the unprocessed Marsa 2 core was subjected to similar investigations to those made for the Marsa 1 core. The aim was to get fresh data from Malta's largest water catchment, to compare and contrast the findings with Core 1 and, through radiocarbon and other dating, to put the results in a chronological context.

3 The Marsa 2 core was extracted by A.N. Terracore Ltd., whereas Salina Deep Core was extracted by SolidBase Ltd.

4 All sub-samples and residues are being kept at the Department of Classics and Archaeology, University of Malta.

5 After Ridout-Sharpe 1998, 338.

6 Another core, MX2, was extracted at less than a metre distance from the coring site of MX1. It was one metre long and extended from 1–2 m in depth. The contents of MX2 were analysed, the molluscan assemblages resembled the ones of MX1 and reflected the energy-driven changes in the depositional environment. The molluscan spreadsheet for MX2 is provided in Appendix 5.

7 These are thought to be associated with the production of wine and work by the Superintendence of Cultural Heritage has shown that production could have started in Punic times (see also Jaccarini & Cauchi 1999 for the Mġarr ix-Xini Regional Park Project; Bonanno 2008; Pace & Azzopardi 2008).

8 The mechanical retrieval of the cores from Marsa was sponsored by Ms Linda Eneix through the OTS Foundation in 2002.

9 Radiocarbon age inversions have been detected in similar coring locations in other countries, where they were found to be a consequence of re-deposition of old sediments (see Stanley & Hait 2000; Angulo *et al*. 2008).

10 The 8.2 ka BP event denotes a global abrupt cold event that resulted in an aridity crisis, which interrupted the humid Early Holocene. Evidence of this event, which lasted several hundred years, was found in the Mediterranean in Spain (Gonzales-Samperiz *et al*. 2009), North Africa (Benito *et al*. 2015), Sicily (Tinner & Lotter 2001), France (Magny *et al*. 2009) and the eastern Mediterranean (Pross *et al*. 2009).

11 In Xemxija 1, the deposits attributed to the Bronze Age span from 465 to *c*. 326 cm, and in Xemxija 2 from *c*. 390 to *c*. 265 cm. The upper limits of these ranges were assigned according to the sedimentation rates calculated by Rowan McLaughlin.

Chapter 5

The geoarchaeology of past landscape sequences on Gozo and Malta

Charles French & Sean Taylor

5.1. Introduction

Geoarchaeological survey, test excavations and sampling on Gozo and Malta concentrated on the sites and landscapes associated with the Neolithic temple period of the fourth and third millennia BC. Targeted investigations were carried out at two Neolithic temple sites of Ġgantija and Santa Verna on the Xagħra plateau and the associated Ramla and Marsalforn valleys on Gozo. Sequences were also recovered from the excavations of the Neolithic Taċ-Ċawla settlement site in the modern town of Rabat and the later Bronze Age mesa-top site of In-Nuffara. On Malta, geoarchaeological work focused on the temple site of Skorba, and the nearby valley coring site of Xemxija, as well as the deep valley core sites of Wied Żembaq, Marsaxlokk and Salina (Figs. 2.4 & 5.1).

In the context of the on-site investigations, test excavations at the Santa Verna, Ġgantija and Skorba temple sites and at the Taċ-Ċawla settlement site all revealed old land surfaces beneath mixed soil and cultural deposits. For the off-site geoarchaeological work, some 200 hand-augered boreholes were made during the 2014/15/16 field seasons. Most boreholes were in the Santa Verna to Ġgantija areas on the margins of the modern town of Xagħra, across the intervening Ramla valley to In-Nuffara and down-valley to the sea, and also in the Marsalforn valley from Rabat northwards to the sea (Fig. 5.1). The areas around the Ta' Marżiena and Skorba temple sites were also investigated briefly for comparison using the hand auger, but no sample test pits were excavated. This geoarchaeological programme has provided sufficient soil/sediment sequence data to address several sets of aims as set out below, and in combination with the analysis of the deep valley cores (see Chapters 2 & 3), it is now possible to suggest a model for Holocene landscape development.

It has always been assumed that the seasonally dry and hot Mediterranean climate made the Gozitan and Maltese landscapes quite 'marginal' in agricultural terms (Grima 2008a; Schembri 1997). As a consequence, it has also been presumed that terracing was adopted extensively from the Bronze Age onwards on both islands to conserve soils and moisture, and also to create a more suitable landscape for subsistence based agriculture (Grima 2004). Like many other parts of the southern Mediterranean, this landscape is prone to deforestation, drought and erosion combined with intensive human activity, and that this has been the case since Neolithic times (Bevan & Conolly 2013; Brandt & Thornes 1996; Hughes 2011; Grove & Rackham 2003). The *FRAGSUS Project* aimed to examine these assumptions and test them with a suite of archaeological science approaches that would shed new light on the nature and impact of Neolithic farming and on the degree of fragility of this island landscape.

Within the overall project, the main objectives of the geoarchaeological work were to:

1) investigate the deposit and soil catena sequence of the Xagħra plateau and its associated Ramla and Marsalforn valleys for the Holocene;
2) identify floors, floor deposits, old land surfaces and palaeosols associated with the Neolithic monuments, concentrating on the Santa Verna, Ġgantija and Skorba temple sites, as well as the Taċ-Ċawla settlement site;
3) create a model for the Holocene land-use sequence for Gozo and Malta, focusing on the impact of Neolithic agriculture and later landscape terracing, and
4) establish if there is any correlation between observed soil properties and prehistoric activities and/or longer-term climate change.

The results of the geoarchaeological analyses are discussed below, with the borehole logs and field

Table 5.1. *Micromorphology and small bulk sample sites and numbers.*

Site, profile and context	Micromorphology sample numbers	Small bulk sample numbers	Description
Ġgantija:			
Test Pit 1	28: terrace soil; 27 and 26: lower terrace/buried A; 25, 24, 23: buried B	16 and 17: terrace and buried A 18–22: buried soil	Terrace soil over *in situ* reddish brown palaeosol developed on Upper Coralline Limestone
WC Trench 1	Archaeological horizons: (top) 13, context 1016; 12, context 1015; 6, 7 and 11: contexts 1040, 1042 and 1004; Buried soil: 10, 9 and 8, context 1019 (base)	1–4: Archaeological horizons; 6–10: Buried soil	Later Neolithic stone structure collapse over *in situ* midden and soil aggradation over a reddish brown palaeosol developed on Upper Coralline Limestone
Xagħra town:			
Quarry; new house site 2; house site 3	5 and 6; 9 and 11; 12 and 13	4; 10; 15	*In situ* buried *terra rossa* soils on Upper Coralline Limestone beneath nineteenth century town houses
Santa Verna:			
Temple internal excavations	Buried soils: Ashby Pr2: 2/1–2/3; Cut 55 Pr3: 3/1–3/2; Tr E Pr4: 4/1–4/4 Pit fill in Cut 55: 3/3 and 3/4	 1–3; 1 and 2; 1–4; 3 and 4	*In situ* brown to reddish-brown palaeosols on Upper Coralline Limestone beneath Neolithic temple floors
Trench B (outside temple to north)	Buried soil: Tr B Pr 1: 1/1–1/4	1: Terrace soil 2–4: Buried soil	*In situ* terrace soil over buried *terra rossa* soil on Upper Coralline Limestone
Transects & test pits in vicinity: L	L; Test Pit 5; BH54	3 spot samples	Possible of buried soils
Taċ-Ċawla:	9, 14, 139, 261, 301	-	Possible buried soils
In-Nuffara:	2 silos: 17 and 40, 503 and 509	-	Basal fills of Bronze Age storage silos
Marsalforn valley, Pr 626	Colluvial soil sequence: 626/1–626/3	626/1–626/3	Colluvial/soil valley fill sequence on Globigerina Limestone
Ramla valley, Pr 627	Alluvial aggradation sequence: 627/1–627/3	627/1–627/3	Alluvial aggradation valley fill sequence on Globigerina Limestone
Skorba:			
Section 1, Trench A	11, 20, 24, 28	11, 20, 24, 28	Cumulative buried soil
Section 2, Trench A	23, 26 (x2), 3–5, 75, 78	23, 26 (x2), 3–5	Cumulative buried soil; with 26 as plaster floor
Dwerja:	616	616	Possible buried soil under terraces
Deep cores:			
Xemxija 1	1–25	1–25	Spot samples through core sediments
Wied Żembaq 1	26–38	26–38	Spot samples through core sediments
Marsalokk 1	39–47	39–47	Spot samples through core sediments
Salina 21B	3 spot sub-samples	-	Spot samples of ? eroded soil at base (27.83–28.12 m)

profile descriptions (after FAO & ISRIC 1990) found in Appendix 6, the thin section descriptions in Appendices 7 and 8, the sample list in Table 5.1, the summary dating of the analysed profiles in Table 5.2, and the optically stimulated luminescence (OSL) dating report in Appendix 2. Note that the comprehensive radiocarbon dating study is discussed in this volume (see Chapter 2), and the site-based geoarchaeological and micromorphological studies at Santa Verna, Ġgantija, Skorba, In-Nuffara and Taċ-Ċawla are reported on separately in the *FRAGSUS* excavation Volume 2.

Table 5.2. *Summary of available dating (archaeological, radiocarbon and OSL) for the sites investigated in Gozo (after R. McLaughlin, pers. comm. and Cresswell* et al. *2017) (Note: OSL dates in italics are poorly constrained due to low precision and large dispersion of equivalent doses as determined by OSL analysis).*

Site and context	cal. BP date	cal. BC date (2σ)	Laboratory number	Quartz OSL sediment ages (years/ka)	BC/AD date	SUTL number
Santa Verna:						
Early Neolithic phase	6412±44; 6239±37; 6181±40; 6151±33	5500–5320; 5300–5070; 5290–5000;	UBA-31042; UBA-31044; UBA-31043; UBA-31048			
Temple build	4645±87; 4908±37	3790–3630	UBA-33706; UBA-31041			
Xagħra Brochtorff Circle:		*c*. 3650–3200	(see Malone *et al*. 2009)			
Ġgantija:						
Temple build		3510–3080				
Tarxien period		2840–2380				
Pre-temple midden soil in WC Trench, context 1021	3962±50	2580–2300	UBA-33707			
Base of terrace deposits/ top of old land surface in TP1, 68–72 cm				3.16±0.25	1140±250 BC	2914
Lower horizon of buried soil in TP1, 92–96 cm		*c*. 2900–2350	presence of common Tarxien pottery	10.79±0.68	8560±630 BC	2915
Skorba:						
Base of buried soil				10.80±0.71	8780±710 BC	2927
Old land surface of buried soil				10.11±0.59	8090±590 BC	2926
Amended buried A horizon above				9.78±0.56	7760±560 BC	2925
Early Neolithic phase	6158±51; 6005±51	*c*. 5200–5000; 5000–4800	UBA-33710; UBA-33708			
Ramla valley Pr 66:						
Base of valley hillwash, 103–106 cm				0.10±0.03	*1910±30 AD*	2923
Mid-point in fill sequence, 62–66 cm				0.17±0.01	1850±12 AD	2922
Top of valley hillwash, 15–20 cm				0.14±0.02	*1880±16 AD*	2921
Marsalforn valley Pr 110:						
Base of valley hillwash fill, 320–325 cm				3.50±0.34	1480±340 BC	2919
Lower incipient soil horizon at mid-point of lower valley fill, 265–270 cm				3.58±0.24	1560±240 BC	2918
Top of upper incipient soil horizon at mid-point of valley fill, 175–180 cm				2.78±0.92	*760±920 BC*	2917
Xemxija 2 core, Malta: base at -9.9 m	8334±46	*c*. 7500–7200	UBA-29347			

5.2. Methodology and sample locations

The bulk of the geoarchaeological work involved using hand-augered boreholes at both systematic and judgemental intervals across the landscape to assess the valley deposit sequences and check for the presence/absence of buried soils and former agricultural terrace soils, and to note the geological substrates present from high mesa plateau to valley bottom positions. Auger-hole positions were recorded with a hand-held Garmin GPS and measured descriptive profile records kept (Appendix 6).

Given the archaeological interest and efforts concentrated on the Neolithic temple sites of Santa Verna and Ġgantija and Santa Verna and the Taċ-Ċawla Neolithic settlement site, all on the Xagħra plateau, and the Bronze Age use of the In-Nuffara plateau to the south, it was also essential to investigate the intervening Ramla valley and the sediment/soil sequences between Xagħra and the sea. In addition, the Marsalforn valley to the west of Xagħra, running from Rabat town northwards to the sea, was also investigated. These valley systems were investigated using a series of hand-auger borehole transects undertaken by the authors (Fig. 5.1). Some

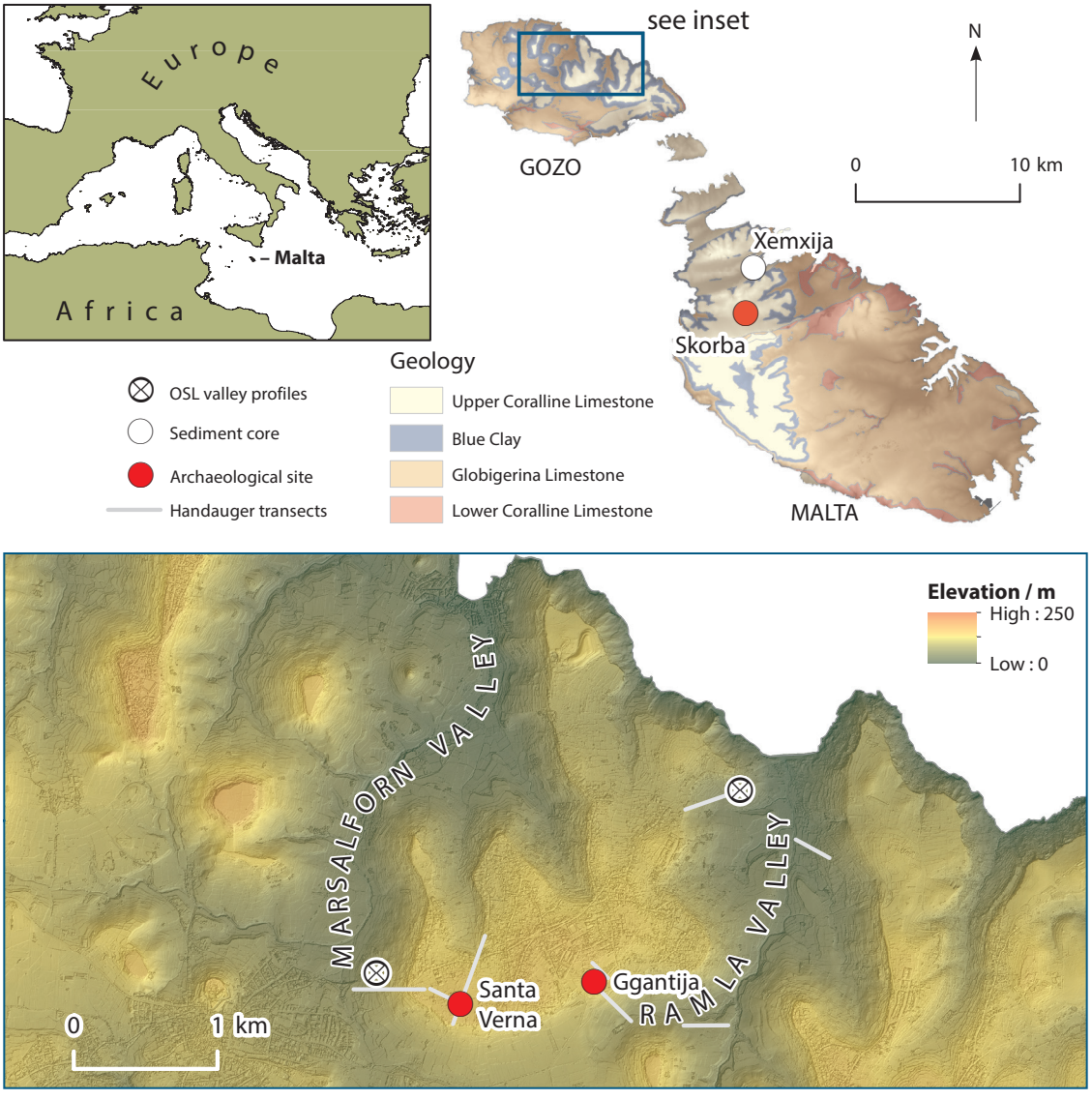

Figure 5.1. *Location map of the test excavation/sample sites and geoarchaeological survey areas on Gozo and Malta, with the geology and elevations, based on LiDAR last return data (December 2012), supplied by the former Malta Environment and Planning Authority, with world coastlines plotted using public domain data from www.naturalearthdata.com, and geology plotted after Lang (1960) (R. McLaughlin).*

150 boreholes were made and recorded (Appendix 6), and a further 50 boreholes were made elsewhere in the island. In addition, five test pits and one excavation area were recorded and sampled at Ġgantija temple, as well as the excavation trenches at the Santa Verna and Skorba temple sites and In-Nuffara storage pit excavations (Appendix 6). Five profiles, one at Ġgantija temple, two at Skorba temple, and one each in the valley bottoms of Ramla and Marsalforn were sampled extensively for OSL profiling and dating by Dr T. Kinnaird (SUERC, University of Glasgow) with an outlier Punic-Roman site of Tal-Istabal, Qormi, on the outskirts of Valletta also sampled with one OSL determination (see Chapter 2; Appendix 2).

This geoarchaeological survey and test excavations exposed buried soil and erosion profiles especially suitable for soil micromorphological block and small bulk sampling (Table 5.1). In total, 70 soil blocks (and 44 complementary small bulk soil samples) from 12 key soil profiles from the archaeological sites and valley profiles, and a further 50 small soil blocks (and a similar number of small bulk samples) from the valley deep cores were prepared for thin section analysis (Table 5.1) (after Murphy 1986; Courty *et al.* 1989) and described using the accepted terminology of Bullock *et al*. (1985), Stoops (2003) and Stoops *et al*. (2010) (Apps. 7 & 8). In addition, a suite of basic physical parameters (pH, loss-on-ignition and magnetic susceptibility) (Table 5.3) and multi-element ICP-AES analyses (Table 5.4) were carried out a series of small bulk samples (44 from soil profiles and 50 from the deep cores) taken in conjunction with the micromorphological block samples (Avery & Bascomb 1974; Clark 1996, 99ff; French 2015; Holliday & Gartner 2007; Oonk *et al.* 2009; Tite & Mullins 1971; Wilson *et al*. 2005, 2008, 2009). pH measurements were determined using a 10 g to 25 ml ratio of <2 mm air-dried soil to distilled water with a Hanna HI8314 pH metre. Determining loss-on-ignition followed the protocol of the Department of Geography, University of Cambridge, to record the percentages of calcium and carbon in the soil (www.geog.cam.ac.uk/facilities/laboratories/techniques/psd.html). For loss-on-ignition (*ibid*.), weighed sub-samples were heated to 105° C for six hours to measure water content, then heated to 400° C for six hours to measure carbohydrate content, then to 480° C for six hours to measure total organic matter content, and finally heated to 950° C for six hours to measure CO_2 content lost from $CaCO_3$ within the sediment (Bengtsson & Ennell 1986). The calcium carbonate content can then be calculated by stoichiometry (Boreham *et al.* 2011). A Malvern Mastersizer was used for the particle size analysis (Table 5.3) using the same Geography facilities at Cambridge. For magnetic susceptibility measurements, a Bartington MS2B metre was used, giving mass specific calculations of magnetic susceptibility for weighed, 10 cm^3 sub-samples (English Heritage 2007, 27). Multi-element analyses using the 35-element aqua regis ICP-AES method were conducted at the ALS Global Laboratory in Seville (www.alsglobal.com), and the elements exhibiting greater than trace amounts and/or are generally considered to be enhanced by human activities (cf. Wilson *et al*. 2008; Fleisher & Sulas 2015) are tabulated in Table 5.4.

5.3. Results

5.3.1. Santa Verna and its environs

Santa Verna is situated on the southwestern side of Xagħra town and the Upper Coralline Limestone plateau overlooking a small valley running south–north, the Wied Ġnien Imrik (Fig. 5.1). The hand-auger survey on the Upper Coralline Limestone plateau around the temple (13 boreholes) revealed less than 50 cm of reddish brown, fine sandy silt loam topsoil to the north of the temple, present in small-holder arable fields (Appendix 6, Transect L). To the south, this was even thinner with increasingly extensive patches of bare rock with open scrub pasture, mainly used for bird hunting today. East of the temple and dipping into the Wied Ġnien Imrik valley, the soil profiles in the auger survey deepened quickly to as much as 100 cm with some B horizon survival consisting of a well-structured, reddish brown silt loam to silty clay loam, before thinning again eastwards to *c*. 10–45 cm of modern ploughsoil, where the area was all used for small-holder arable fields.

The 2015 excavations on the southern edge of the temple surprisingly discovered *in situ* buried soils beneath a series of temple floors and deposits (Fig. 5.2). New radiocarbon dates indicate that this is the earliest monument present on the Xagħra plateau where temple construction began in the early fourth millennium BC (*c*. 3800–3700 cal. BC; 4945±87 BP, 4905±37 BP; UBA-33706, UBA-3141), well prior to the construction of Ġgantija temple just to the east (see Chapter 2). This was particularly well exemplified in Trench E, as well as in the 2015 excavations on the southern edge of the temple where *in situ* buried soils were discovered beneath a series of temple collapse and midden deposits, and in the re-excavated sondages of Ashby and Trump (Figs. 5.3 & 5.4). The base of the Ashby 1911 Sondage revealed a well preserved, *c*. 45 cm thick, palaeosol which comprised of a *c*. 15 cm thick organic A (Ah) silt loam horizon over a reddish brown silt loam B horizon of about 30 cm in thickness. A similar occurrence was also revealed in the Trump Sondage about 3 m to the north and in the trial trench which was cut some 30 m to the northeast

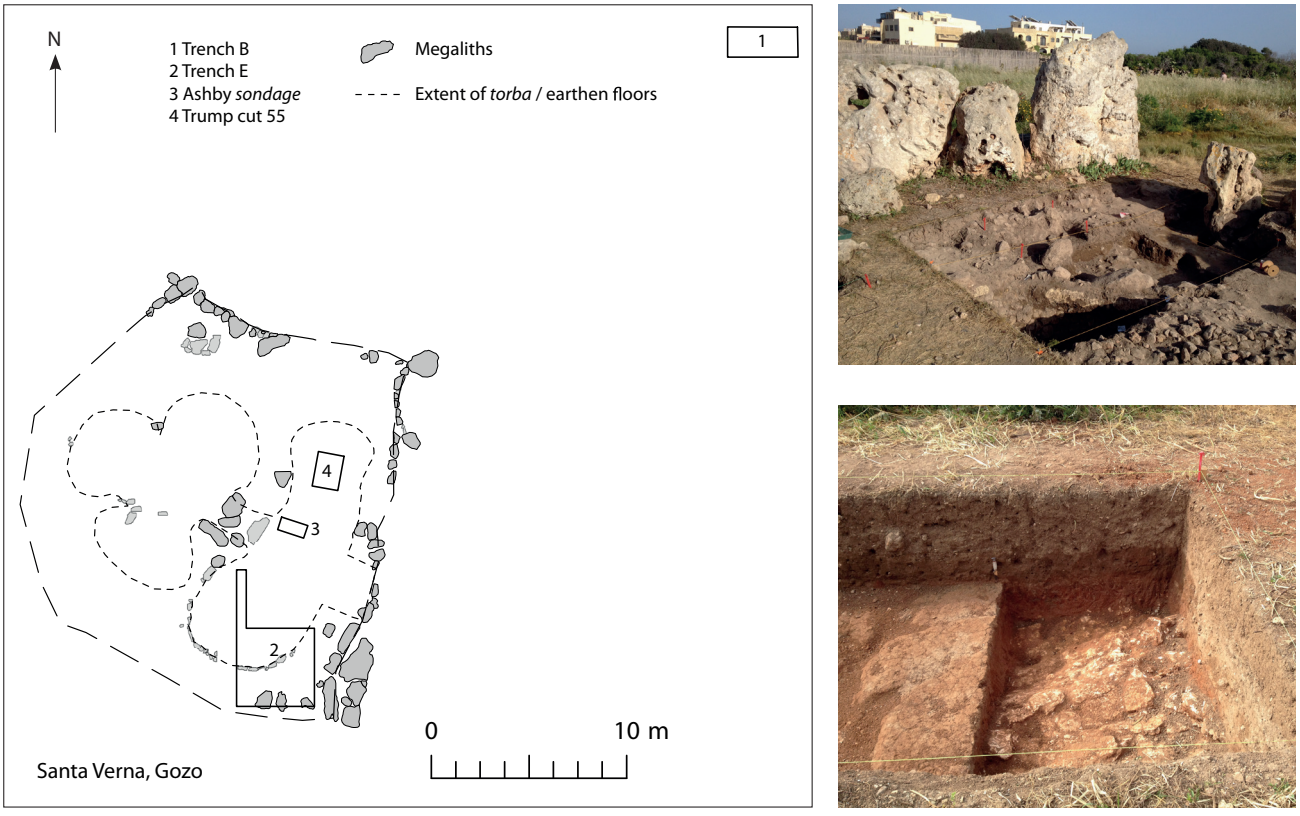

Figure 5.2. *Plan of Santa Verna temple and the locations of the test trenches (R. McLaughlin) (left) with a view of upstanding temple megaliths behind Trench E (upper right) and the* terra rossa *soil below terrace deposits in Trench B outside the temple (lower right) (C. French).*

of the temple site. All three buried soil profiles were sampled for soil micromorphological analysis and physical characterization. Thick (*c*. 30–100 cm) stone rubble deposits were observed directly above these intact buried soils, and these were either interrupted by thin *torba* or earthen floors (Figs. 5.2 & 5.3) (and see Volume 2, Chapter 4).

In July, 2014, the soil sequences around Santa Verna Temple were investigated, especially those to the north of the temple remains where field walking had led to the recovery of a polished stone axe and Żebbuġ, Red Skorba and Għar Dalam pottery of the Neolithic period (see Volume 2). The reason for the interest in these soils was to understand whether there is a correlation between soil properties and prehistoric settlement/activity. A reasonable thickness of soil coverage in this area meant that these fields are presently cultivated. The soils are characterized by reddish brown silt and silty clay loams, and are in places at least 1 m deep. The archaeological material together with the nature of the soils make this a potentially important part of the landscape for geoarchaeological investigation. To the south, closer to the edge of the Upper Coralline Limestone plateau, the soils were characterized as Leptosols, i.e. they were either very thin or non-existent, often with large irregular patches of bare Coralline bedrock exposed. Thus severe rain, wind and agricultural erosion has taken place here, demonstrating the fragility of the soil system on these mesa plateau areas on Gozo.

5.3.1.1. Physical and elemental characterization

At Santa Verna, pH values from the buried soils are very alkaline (ranging from 8.5–8.92) and the magnetic susceptibility values were generally low, except for the lower fill of the pit in Trump Cut 55 (sample 3/4) (Table 5.3). This probably also reflects the amount of organic and fire-related settlement debris contained within this fill deposit (Allen & Macphail 1987; Tite & Mullins 1971). The total organic matter content is a reasonable *c*. 4.1–6.5 per cent in the buried soils, better than the modern topsoil at *c*. 3.4 per cent (Table 5.3). There is a strong calcium carbonate component throughout, ranging from *c*. 8–64 per cent (Table 5.3), but this is generally lower than the values observed in the Ġgantija soil sequence, especially in the base of

the buried soil. The particle size analysis results indicate that the buried soils tend to be dominated by the silt fraction (*c*. 46–76 per cent), a potential loessic or wind-blown component, but with a strong but variable quartz sand component (*c*. 10–52 per cent), with the clay fraction ranging between *c*. 5 and 15 per cent (Table 5.3). The higher clay component in the buried soils as compared to those at Ġgantija is reflected in the well organized clay fraction observed in thin section in the basal horizon of the buried soil (see §5.3.1.2).

In the multi-element analysis, the upper parts of the soil profiles and the *torba* floors at Santa Verna were notably all moderately to highly enhanced with phosphorus and strontium values (Table 5.4). Phosphorus values varied from 1200 to >10000 ppm, with the Trench E profile and pit fill very enhanced throughout (i.e. 4510 ppm in the pit base to 9250 ppm in the upper *torba* floor), with relatively enhanced strontium varying between 195–406 ppm. These elements suggest that the upper horizon of the soils and the *torba* floors were receiving substantial amounts of midden-type, organic settlement-derived, waste material prior to burial (Entwistle *et al*. 1998; Wilson *et al*. 2008) (and see Volume 2). Although calcium values were often of a similar range to those at Ġgantija, the range of values in the pre-temple buried soils (Profiles 2 and 3) was much less (ranging from 1.4–8.4 per cent with higher/lower values in the upper and lower samples), a factor which is also reflected in the micromorphological results below.

5.3.1.2. Soil micromorphology

From the borehole transect and Trench B to the north-northeast of Santa Verna temple, there was a well preserved buried soil of variable thicknesses present beneath *c*. 40 cm of gravelly fine sandy silt

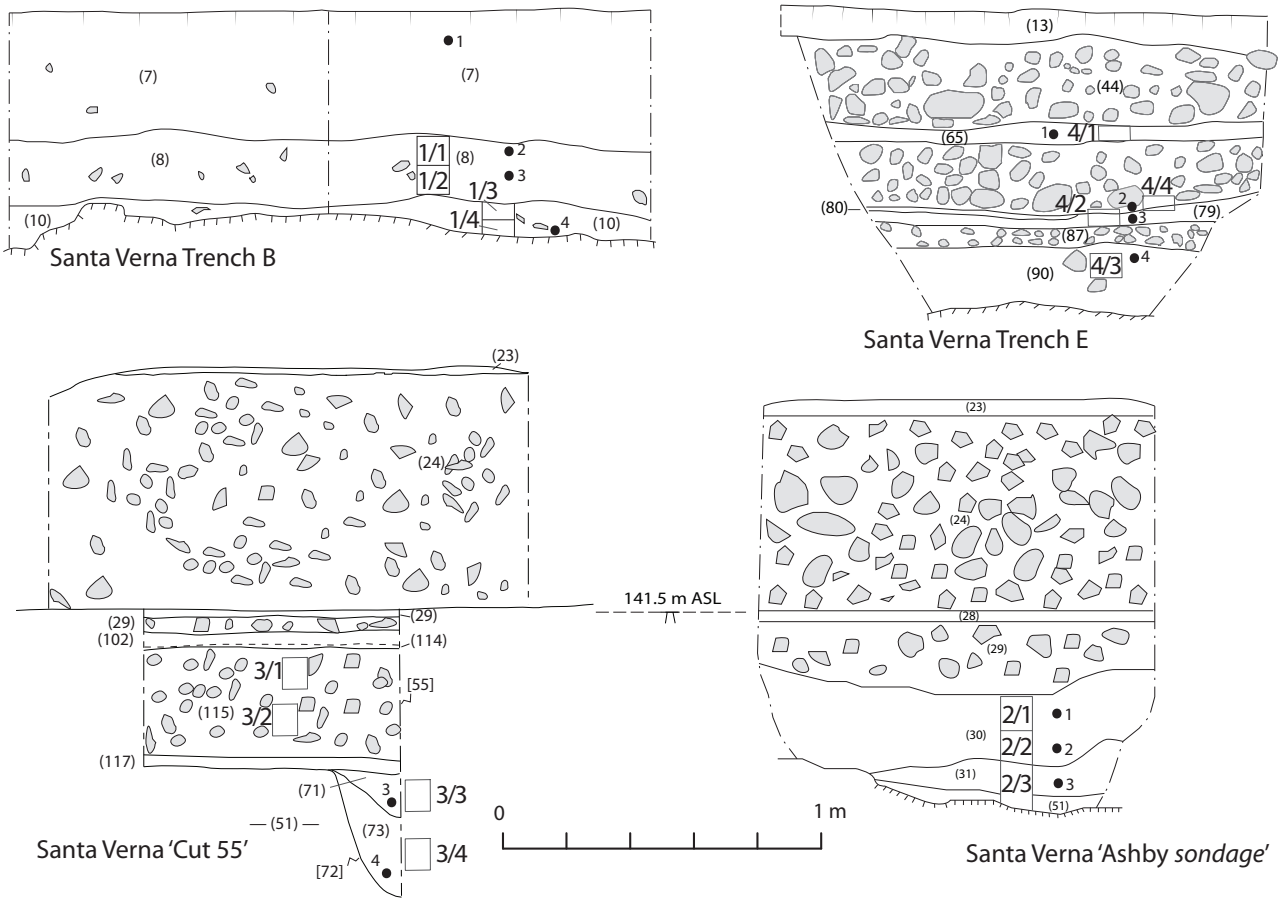

Figure 5.3. *Santa Verna excavation trench profiles all with sample locations marked: upper left: the off-site Trench B buried red soil below terrace deposits; lower left: the Trump Cut 55 profile with pit fill and associated buried soil; upper right: Trench E profile showing a series of thin earthen floors with limestone rubble inbetween and buried soil below; lower right: the Ashby Sondage profile with the buried soil at its base (Note: open boxes = micromorphology block samples; back circles = small bulk samples) (R. McLaughlin).*

Table 5.3. *pH, magnetic susceptibility, loss-on-ignition (% organic matter) and % sand/silt/clay particle size analysis results for Ġgantija, Santa Verna, Xagħra town, Marsalforn valley and Ramla valley profiles, Gozo.*

Site, sample and depths (cm)	pH	MS SI/g x10^{-8}	% total organic matter	% Ca CO3	% sand	% silt	% clay
Ġgantija TP1:							
Modern topsoil: 16, 16–20 cm	7.79	1.77	3.42	72.1	82.24	17.62	0.14
Terrace soil: 17, 70–80 cm	7.91	1.46	5.0	49.25	8.51	82.36	9.13
Buried soil: 18, 80–90 cm	8.0	1.46	5.3	45.26	21.55	71.65	6.8
Buried soil: 19, 90–100 cm	8.06	1.52	4.82	41.42	49.47	45.09	5.44
Buried soil: 20, 100–110 cm	8.16	1.69	4.74	51.65	77.98	21.58	0.44
Buried soil: 21, 110–120 cm	8.2	1.83	4.55	54.26	30.39	60.92	8.69
Buried soil: 22, 120–130 cm	8.19	1.82	4.67	33.83	12.37	73.42	14.21
Ġgantija WC Trench:							
Arch horizons: 12, 1015	8.65	1.04	2.15	77.69	38.74	56.06	5.2
Arch horizons: 13, 1016	8.55	568.6	3.225	70.25	66.73	32.86	0.41
Arch horizons: 6, 1004	8.44	1.085	3.07	70.2	12.24	76.5	11.26
Arch horizons: 7, 1004	8.74	516.4	2.45	72.63	4.9	80.11	14.99
Transition: 11, 1004/1019	8.05	66.4	3.16	67.16	65.21	34.14	0.65
Buried soil: 10, 1019	8.48	62.3	3.5	59.68	62.06	37.44	0.5
Buried soil: 9, 1019	9.05	1.02	4.5	47.26	77.98	21.58	0.44
Buried soil: 8, 1019	9.15	1.97	5.1	41.2	82.25	17.6	0.15
Xagħra town buried soils:			(no sample material left)				
Quarry: 4	7.62	2.56	-	-	-	-	-
Site 3: S16	7.59	3.22	-	-	-	-	-
Site 2: S10	7.37	1.78	-	-	-	-	-
Santa Verna buried soils:							
Tr B 1/1, 10–20 cm	8.72	3.65	5.38	51.26	47.47	47.49	5.04
Tr B 1/2, 50–58 cm	8.84	3.72	4.1	49.35	26.31	69.56	4.13
Tr B 1/3, 60–70 cm	8.7	5.68	5.44	14.58	25.4	66.6	8.0
Tr B 1/4, 80–90 cm	8.5	4.54	6.5	10.14	38.47	55.98	
Ashby 2/1, 95–105 cm	8.36	4.18	4.4	25.15	23.33	71.45	5.22
Ashby 2/2, 105–115 cm	8.5	3.97	5.52	7.68	52.32	46.64	1.04
Ashby 2/3, 115–125 cm	8.6	2.65	5.45	8.17	40.04	54.84	5.12
Trump Cut 55 3/1, 100–110 cm	8.68	2.6	4.92	25.3	32.93	60.33	6.74
Trump Cut 55 3/2, 120–130 cm	8.86	2.6	5.5	15.76	17.02	73.67	9.31
Trump Cut 55 3/3, pit fill: 110–120 cm	8.72	2.62	4.5	42.27	23.97	66.95	9.08
Trump Cut 55 3/4, pit fill: 150–160 cm	8.7	2.6	6.7	31.26	21.18	68.51	10.31
Tr E 4/1, 40–43 cm	8.92	3.01	4.53	48.71	25.09	65.01	9.9
Tr E 4/2, 69–74 cm	8.84	3.02	3.89	64.16	9.71	75.7	14.59
Tr E 4/3, 83–93 cm	8.68	2.8	4.65	36.12	24.81	66.86	8.33
Marsalforn, Pr 626:							
626/1	8.23	136.2	1.97	77.6	28.68	62.33	8.99
626/2	8.36	147.0	2.24	75.02	18.22	64.67	17.11
626/3	8.13	242.72	1.66	79.71	34.57	58.46	6.97
Ramla valley, Pr 627:							
627/1	8.16	117.08	6.3	64.16	17.92	71.28	10.8
627/2	8.07	72.71	3.15	54.95	10.52	79.17	10.31
627/3	8.0	138.21	3.18	56.0	36.4	59.97	3.63

Table 5.4. *Selected multi-element results for Ġgantija, Santa Verna and Xagħra town buried soils, and the Marsalforn and Ramla valley profiles, Gozo.*

Site, sample and depths (cm)	Ba ppm	Ca %	Cu ppm	Fe %	K %	Mg %	Mn %	Na %	P ppm	Pb ppm	Sr ppm	Zn ppm
Ġgantija TP1:												
Modern topsoil: 16–20 cm	30	17	40	2.48	0.45	0.79	0.03	0.04	4610	41	193	110
Terrace soil: 70–80 cm	30	18	36	2.32	0.43	0.74	0.03	0.04	4820	10	198	97
Buried soil: 80–90 cm	30	18.6	33	2.17	0.49	0.78	0.02	0.06	8200	5	255	126
Buried soil: 90–100 cm	30	16.8	32	2.14	0.52	0.71	0.02	0.08	>10000	5	271	148
Buried soil: 100–110 cm	20	15.5	35	2.42	0.61	0.76	0.03	0.09	>10000	6	261	157
Buried soil: 110–120 cm	30	14.8	37	2.48	0.63	0.69	0.03	0.07	9970	10	235	143
Buried soil: 120–130 cm	30	14.2	40	2.65	0.66	0.69	0.03	0.06	8570	8	219	132
Ġgantija WC Trench:							ppm:					
Arch horizons: 12, 1015	40	>25	27	1.25	0.3	1.07	122	0.07	5770	3	322	71
Arch horizons: 13, 1016	40	>25	38	1.47	0.37	0.94	142	0.07	5010	3	292	75
Arch horizons: 6, 1004	40	>25	33	1.83	0.47	1.33	207	0.13	>10000	3	380	185
Arch horizons: 7, 1004	60	22.4	41	2.44	0.64	1.03	378	0.13	9600	11	355	164
Transition: 11, 1004/1019	50	>25	32	1.65	0.87	1.06	160	0.07	8830	4	293	86
Buried soil: 10, 1019	30	21.3	40	2.3	0.73	0.9	221	0.07	7520	9	281	100
Buried soil: 9, 1019	50	18.5	43	2.66	0.59	.85	243	0.08	6940	10	260	108
Buried soil: 8, 1019	30	14.7	46	3.1	0.4	0.89	309	0.08	6720	13	238	120
Xagħra town buried soils:												
Quarry S4	<10	1.66	73	4.59	0.78	0.5	350	0.03	350	25	37	75
Site 3: S16	<10	0.87	79	4.95	0.85	0.53	260	0.03	260	21	36	68
Site 2: S10	<10	1.56	72	4.54	0.74	0.48	330	0.05	330	23	34	63
Santa Verna buried soils:												
Tr B 1/1, 10–20 cm	100	17.6	40	2.61	0.5	1.1	346	0.06	7010	20	222	132
Tr B 1/2, 50–58 cm	80	18.9	26	2.43	0.61	1.18	272	0.06	5380	9	229	86
Tr B 1/3, 60–70 cm	90	1.67	21	4.46	1.16	0.96	381	0.05	480	22	58	75
Tr B 1/4, 80–90 cm	90	3.87	22	4.16	1.03	1.01	392	0.04	1200	18	76	80
Ashby 2/1, 95–105 cm	80	6.18	28	3.51	1.03	1.0	476	0.08	2800	16	122	86
Ashby 2/2, 105–115 cm	80	1.43	26	4.19	1.16	0.89	553	0.06	910	20	57	77
Ashby 2/3, 115–125 cm	80	1.54	26	4.23	1.2	0.88	450	0.06	900	20	53	78
Trump Cut 55 3/1, 100–110 cm	90	13.3	69	2.57	0.9	1.33	482	0.24	>10000	9	301	261
Trump Cut 55 3/2, 120–130 cm	90	8.4	31	3.41	1.04	1.08	464	0.11	3270	16	155	88
Trump Cut 55 3/3, pit fill: 110–120 cm	90	2.41	28	4.04	1.08	0.94	541	0.08	970	19	57	80
Trump Cut 55 3/4, pit fill: 150–160 cm	100	17.4	53	2.22	0.88	1.17	357	0.28	>10000	6	328	178
Tr E 4/1, 40–43 cm	70	18.5	40	2.43	0.75	1.41	307	0.12	9250	9	327	133
Tr E 4/2, 69–74 cm	70	20.7	42	2.03	0.7	2.81	280	0.17	8400	8	361	131
Tr E 4/3, 83–93 cm	70	14.8	34	2.98	1.05	1.24	368	0.09	6850	12	195	115
Marsalforn valley:												
626/1	40	19.4	15	2.61	0.58	0.84	198	0.08	2020	12	527	55
626/2	40	19.4	12	2.58	0.55	0.8	193	0.08	1960	11	506	53
626/3	30	19.6	13	2.61	0.54	0.71	224	0.1	1930	12	494	52
Ramla valley:												
627/1	20	>25	17	1.38	0.31	0.56	168	0.08	2240	26	693	48
627/2	30	>25	10	1.72	0.33	0.52	173	0.09	2300	14	667	41
627/3	30	23.6	11	1.84	0.41	0.6	179	0.11	1930	10	703	47

Figure 5.4. *The red-brown buried soil profiles in Trench E (left), the Ashby (centre) and Trump (right) Sondages within the Santa Verna temple site (C. French).*

loam ploughsoil (Figs. 5.2–5.5; Table 5.5). In all other directions surrounding the temple, the auger survey revealed that the land surface is either severely denuded with large areas of bare exposed areas of Upper Coralline Limestone bedrock present and/or supports only a single horizon, thin (<15 cm thick), turf/organic micritic, fine sandy silt loam topsoil which is often a strong reddish brown in colour.

This buried soil revealed in Trench B exhibited three horizons in thin section. The uppermost horizon (sample 1/1 and the upper *c*. 4 cm of sample 1/2) was a pellety to aggregated, gravelly silty clay, strongly reddened with amorphous sesquioxides (Figs. 5.5a & b). There is a dust of very fine organic matter/charcoal as well as about 10–20 per cent micro-sparite (or silt-sized calcium carbonate), and common sesquioxide nodules throughout the groundmass. The middle horizon (lower part of sample 1/2) was completely dominated by micro-sparitic calcium carbonate with *c*. 30 per cent as small aggregates of the same reddish brown silty clay fabric present in sample 1/1 above (Fig. 5.5c). There was a similar dust of very fine organic matter/charcoal throughout. The lowermost horizon (samples 1/3 & 1/4) was indicative of very different soil formation conditions. It is composed of a weak to moderately developed, small blocky, silty clay with very abundant, moderately birefringent, pure to dusty clay in speckles and striae throughout the groundmass (Fig. 5.5d).

This observed sequence suggests that the upper horizon of the buried soil is the lower A horizon of a very disturbed soil that has been subject to much physical mixing, oxidation and rubification processes (Fedoroff 1997; Kooistra & Pulleman 2010), as well as considerable evapo-transpiration leading to the abundant secondary formation of micro-sparitic calcium carbonate (Durand *et al*. 2010). This importantly implies that it was an open and de-vegetated soil prior to burial. Moreover, this soil has undergone severe physical and soil faunal mixing leading to considerable aeration and oxidation with the concomitant formation of abundant secondary calcium carbonate. In particular, the middle horizon is essentially acting as a depleted, calcified and replaced, upper B or eluvial Eb horizon. The basal, organized clay-dominated lower soil horizon is indicative of a clay-enriched agric (or argillic) or the Bt horizon of a well developed Orthic Luvisol (or brown Mediterranean soil) (Bridges 1978, 69; Fedoroff 1997; WRB 2014; Yaalon 1997). It is characterized first by the weathering of the limestone substrate and then by clay illuviation down-profile creating a clay enriched lower Bt or argillic horizon. Also, there is a considerable component of aeolian dust, contributing to the ubiquitously high silt and very fine sand component of these soils, a feature that is widespread across the Mediterranean region (Muhs *et al*. 2010; Yaalon & Ganor 1973). There are also a few discontinuous linings of the voids with micro-sparite (Fig. 5.5e), indicating secondary calcification processes in this soil. The whole profile, and especially the lowermost horizon, is also becoming very reddened or rubified. This process involves iron compounds which are produced from the weathering of minerals including iron oxides and hydroxides precipitating as poorly crystalline ferrihydrites or haematite, which then coat the silt/sand grains and clays (Lindbo *et al*.

2010; Yaalon 1997). This strong reddening or rubification of the palaeosol probably occurred hand-in-hand with the process of clay illuviation (Fedoroff, 1997; Yaalon, 1997) and rapid bio-degradation of organic material, as well as increasing calcification with time. These latter processes are probably associated with the removal and disturbance of the vegetative cover and alternating periods of wetting/eluviation/leaching and long summer droughts (Bridges 1978, 33; Duchaufour 1982; Catt 1990; Clark 1996, 100; Goldberg & Macphail 2006, 70; Gvirtzman & Wieder 2001; Lelong & Souchier 1982; Lindbo *et al.* 2010; Stoops and Marcelino 2010; Yaalon 1997).

The sesquioxide nodules in the upper horizon of this soil (Fig. 5.5b) have probably formed through cheluviation as organo-metallic compounds associated with humic material from the root complex combining with strong iron staining (and aluminium, magnesium and silica) and moving down-profile through eluviation under weakly acidic and/or redoximorphic conditions (Wilson & Righi 2010). The bio-degradational processes may be caused by a number of factors such as cool and humid climatic conditions, seasonal sub-surface groundwater, acid producing vegetation, quartz-rich and base cation depleted parent materials, or a combination of two or more of these factors (Wilson & Righi 2010). Although one would not expect some of these conditions necessarily to exist here on the limestone bedrock, nonetheless the pollen analysis of the Santa Verna (and Ġgantija) palaeosol suggests a damp, scrubby steppe habitat of pine, juniper, *Erica* and ferns, as well as the presence of aquatic organisms and particularly phytoplankton in the buried soil points to the presence of standing water bodies and an acidic flora in the immediate vicinity (see Chapter 2). These conditions may well have been conducive to creating these sesquioxide nodules in the former lower A horizon of the Santa Verna palaeosol.

In the main excavations within the temple, a series of samples was taken from the possible *torba* floor sequences within the temple complex in Trench E (Profile 4), the Ashby Sondage (Profile 2) and Trump Cut 55 (Profile 3), all of which seal an *in situ* buried soil ranging in thickness from *c*. 15–60 cm (Fig. 5.4). These sequences will be more fully described in the excavation volume (Vol. 2), with the evidence from the buried soils concentrated on here.

In Trench E (Profile 4) just inside the main surviving arc of upright megaliths (Fig. 5.3), there was a series of at least two earthen/plaster 'floors' (samples 4/1 & 4/2) (Fig. 5.5h & i) interrupted by stone rubble deposits, all situated on a possible buried soil (sample 4/3). The buried soil (sample 4/3) beneath was composed of a pellety to small aggregated, reddish brown silty clay loam with common, birefringent, pure to dusty clay striations throughout the groundmass, as well as common very fine organic/charred punctuations and common sesquioxide nodules (Fig. 5.5f) and rare

Figure 5.5 *(overleaf). Santa Verna soil photomicrographs (C. French): a) Photomicrograph of the buried reddish brown, calcitic fine sandy clay loam soil in BH115 (frame width = 4.5 mm; cross polarized light); b) Photomicrograph of pellety, micritc silty clay with sesquioxide nodules, Trench B, sample 1/1 (frame width = 4.5 mm; cross polarized light); c) Photomicrograph of mixed fabric of micritic calcium carbonate with aggregates of reddish brown silty clay fabric, Trench B, sample 1/2 (frame width = 4.5 mm; cross polarized light); d) Photomicrograph of pure clay (centre area) to fine dusty clay (to either side), Trench B, sample 1/4 (frame width = 2.25 mm; plane polarized light); e) Photomicrograph of striated clay-dusty clay groundmass with micritic calcium carbonate void linings, Trench B, sample 1/3 (frame width = 4.5 mm; cross polarized light); f) Photomicrograph of fine humic/charcoal dust with a burnt bone fragment in the basal soil, Trench E, sample 4/3 (frame width = 4.5 mm; plane polarized light); g) Photomicrograph of possible 'floor' composed an even mix of very fine limestone gravel and calcitic silt with abundant very fine organic punctuations and occasional bone fragments, Trench E, sample 4/4 (frame width = 4.5 mm; cross polarized light); h) Photomicrograph of a* torba *floor composed of a dense, brown silty clay with bone inclusions, Trench E, sample 4/1 (frame width = 2.25 mm; cross polarized light); i) Photomicrograph of a possible 'floor' or 'mortar' composed of a fine gravel size limestone, Trench E, upper part of sample 4/2 (frame width = 4.5 mm; cross polarized light); j) Photomicrograph of a mixture of silty clay with 25 per cent fine limestone gravel with a few included sub-rounded aggregates of birefringent clay and common very fine organic punctuations,* torba *floor context 28 (frame width = 4.5 mm; cross polarized light); k) Photomicrograph of similar mixed fabric of micritic calcium carbonate with aggregates of reddish brown silty clay fabric, Ashby Sondage, sample 2/1 (frame width = 4.5 mm; cross polarized light); l) Photomicrograph of striated silty clay fabric, Ashby Sondage, sample 2/3 (frame width = 2.25 mm; cross polarized light); m) Photomicrograph of micritic sandy silty clay with included bone and organic fragments, sample 78* torba *floor (frame width = 4.5 mm; cross polarized light); n) Photomicrograph of the strongly reddened silty clay buried soil, Trump Cut 55, sample 3/2 (frame width = 4.5 mm; cross polarized light); o) Photomicrograph of finely laminar silt and organic dust in pit fill, Trump Cut 55, sample 3/3 (frame width = 4.5 mm; plane polarized light).*

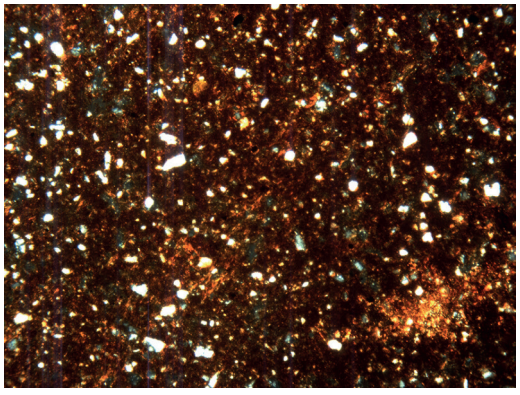

a

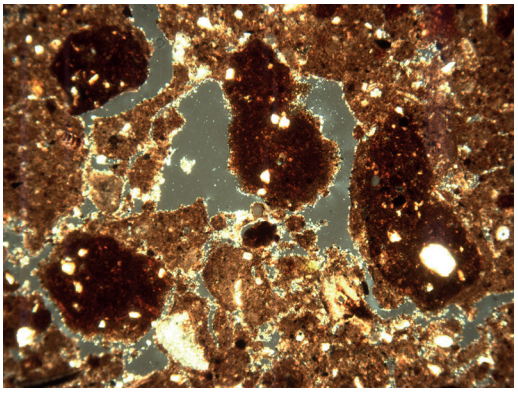

b

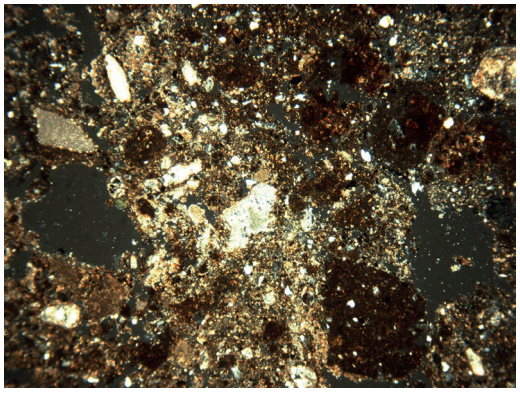

c

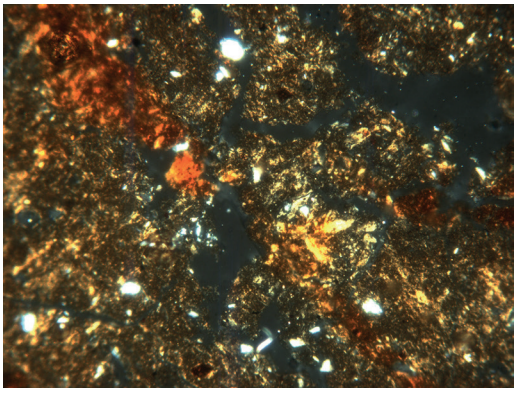

d

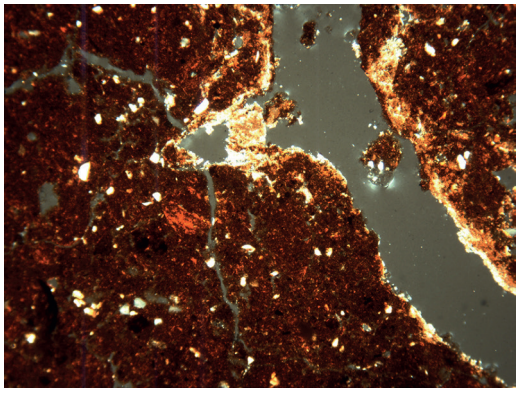

e

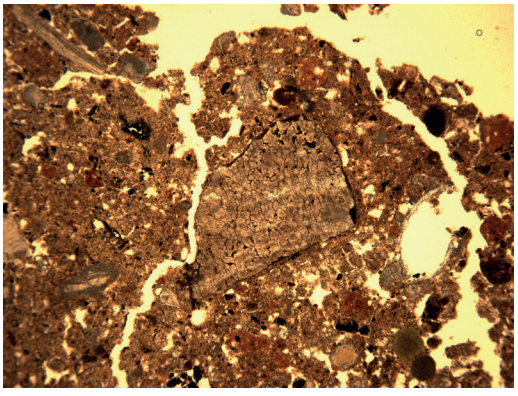

f

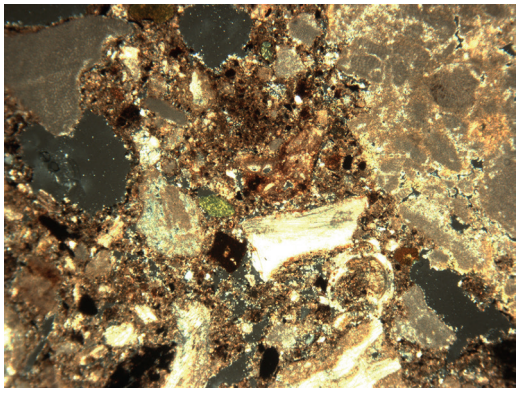

g

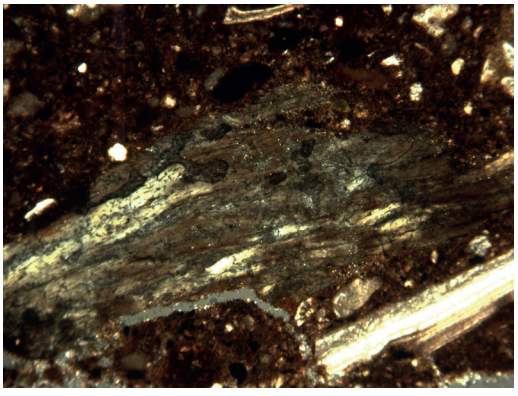

h

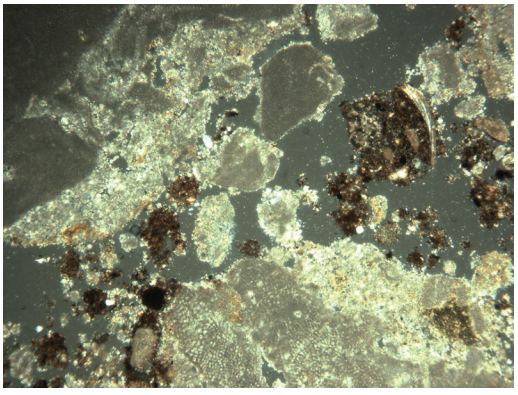

i

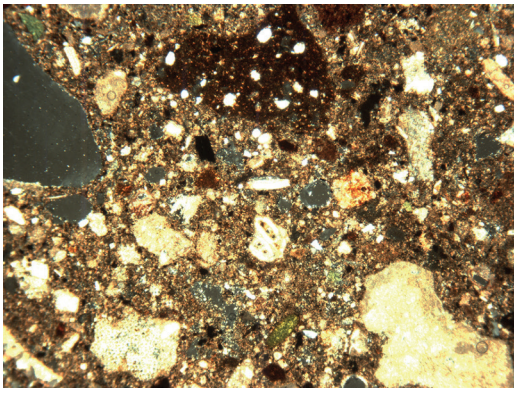

j

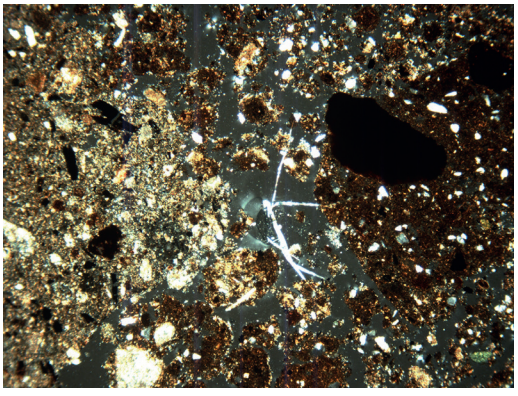

k

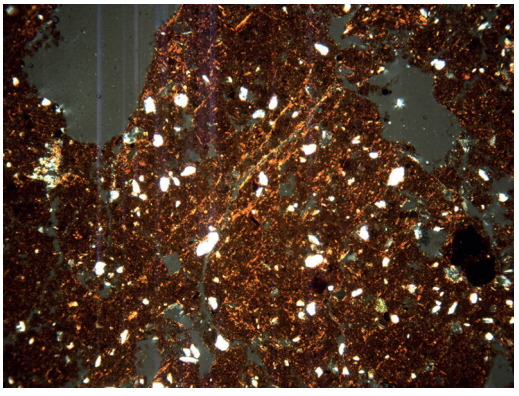

l

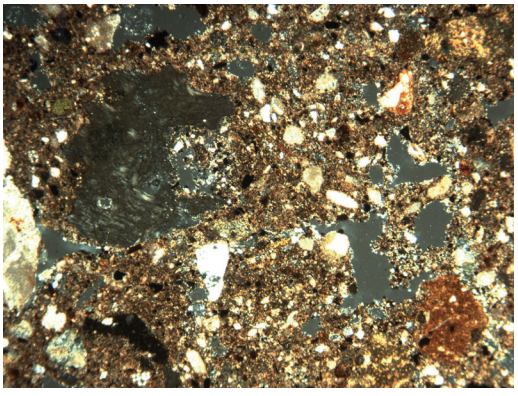

m

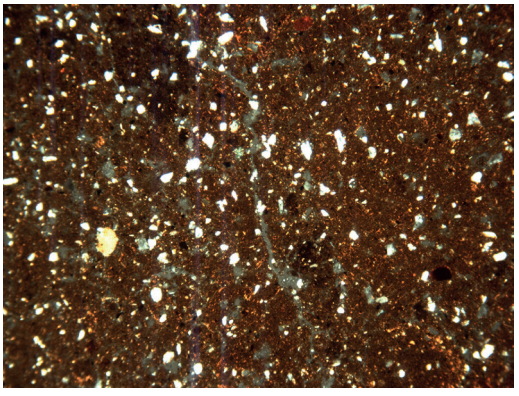

n

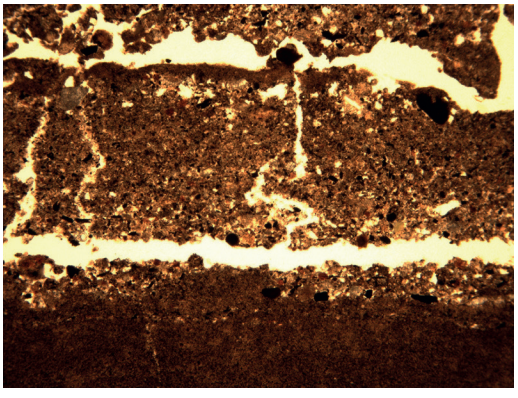

o

occurrences of very small burnt bone fragments. This points to a very disturbed and bioturbated, reddened and clay enriched Bt horizon soil, essentially similar in structure and fabric to that observed outside the temple in Trench B. No upper, organic Ah horizon was present, probably suggesting truncation associated with the act of temple construction.

Five metres to the north in the adjacent Ashby Sondage (Profile 2) (Fig. 5.4), also beneath a *torba* floor (contexts 27 & 28) (Figs. 5.5j & m) and limestone rubble (context 29) sequence, there was a *c*. 45 cm thick *in situ* buried soil. The upper *c*. 15 cm of this soil (sample 2/1; context 30) was a heterogeneous, pellety mixture of mainly micro-sparitic calcium carbonate with abundant fine to very fine charcoal fragments and fine aggregates of orangey brown silty clay, with an occasional pot and bone fragment present (Figs. 5.5g & k). Samples 2/2 (context 51) and 2/3 below over the next 20 cm were predominantly comprised of a striated, birefringent silty clay with strong amorphous sesquioxide reddening and only minor (<5 per cent) micro-sparitic calcium carbonate present (Figs. 5.5h & l). These samples also exhibited an irregular small blocky structure defined by fine channels, and they contained a fine organic/charcoal dust throughout. These features suggest that the buried soil represents a mixed, disturbed, lower A horizon over a relatively undisturbed clay-enriched and organized argillic B (or Bt) horizon. It has not suffered severe disruption, mixing and calcification as in the other profiles at Santa Verna.

In the adjacent Trump Cut 55 (Profile 3) (Fig. 5.3), there was a well preserved buried soil (samples 3/1 & 3/2) about 55 cm thick present beneath a hard-packed earthen floor. In contrast to the soil present in the Ashby Sondage (Profile 2), this buried soil exhibited a blocky to columnar blocky with a micro-aggregated microstructure, but exhibited a similar silty clay fabric strongly reddened with iron oxides and hydroxides with a dust of organic matter and very fine charcoal throughout (Fig. 5.5n). This soil became denser and more clay enriched with depth, exhibiting a well-developed striated to reticulate and birefringent, pure to dusty clay groundmass, just as in the base of the buried soil in Trench B (Fig. 5.5e) and in the Ashby Sondage (Fig. 5.5l). Although these reddened clays could simply be relict in origin (Davidson 1980; Fedoroff 1997) and the result of the long-term weathering of the limestone bedrock material (Catt 1990), the well organized, reticulate, gold to reddish-yellow, pure to dusty clay aspect of the groundmass is more indicative of an illuvial clay-enriched or argillic Bt horizon developed in the base of an *in situ* buried soil (Bullock & Murphy, 1979; Fedoroff 1968, 1997; Kuhn *et al*. 2010). This luvisolic soil is the most well-developed of all the buried soil profiles observed in pre-Neolithic contexts at Santa Verna and Ġgantija.

It is clear that Profiles 2 and 3 have not suffered as severe disruption, mixing and calcification as the other buried soils encountered here and at nearby Ġgantija (see §5.3.2). Significantly, this soil is indicative of an earlier, well-developed and less disturbed soil type, more akin to a brown luvisolic Mediterranean soil associated with more moist and well vegetated conditions (Bridges 1978, 68–9; WRB 2014). Nonetheless, this soil is just beginning to be disturbed and opened-up, as shown by the minor but increasing secondary calcium carbonate formation and the fine organic and micro-charcoal dust throughout its fabric. This soil type change from a well structured and clay enriched agric brown soil (or Orthic Luvisol) to a calcitic reddish brown to red Mediterranean soil (Calcic Luvisol) (Bridges 1978, 68–9; WRB 2014) would appear to be beginning just prior to the construction of the temple at Santa Verna (from *c*. 3800 cal. BC), a process that was interrupted by this soil being sealed by the sequence of temple floors above.

The adjacent upper pit fill in Trump Cut 55 (sample 3) was of similar structure and composition to the buried soil in Trench E/sample 4/3, with a 6–7 cm thick horizon of alternating thick/thin, fine calcitic silt crusts (Fig. 5.5o), generally fining upwards. This suggests soil infilling of the pit, interrupted by a phase of intermittent in-washings of finely sorted soil material in an open and bare earth environment adjacent into the open pit, subject to episodic rain-splash.

5.3.2. Ġgantija temple and its environs

The upper part of the Xagħra plateau comprises three natural terrace steps in the Upper Coralline Limestone over a rising slope height of about 30 m. Ġgantija temple is located on the middle of these three terraces, adjacent to a probable former fault line with a freshwater spring (Ruffell *et al*. 2018). Nearby Santa Verna is located on the uppermost part of the same mesa plateau about a kilometre to the west (Figs. 5.1 & 5.6). Ġgantija temple is dated from about 3510–3080 cal. BC and through the Tarxien period between *c*. 2840 and 2380 cal. BC (see Chapter 2 & Volume 2, Chapter 5).

Augering survey around the southern fringe of the site (below the retaining viewing platform wall) mainly produced thin soils with no sign of the presence of deep agricultural terrace soils or any buried soil being present (Appendix 6). Nonetheless, in the small walled triangular field of the southwestern corner of the Ġgantija platform and in the olive grove to the northeast of the temple results from hand augering suggested the presence of a well preserved buried soil,

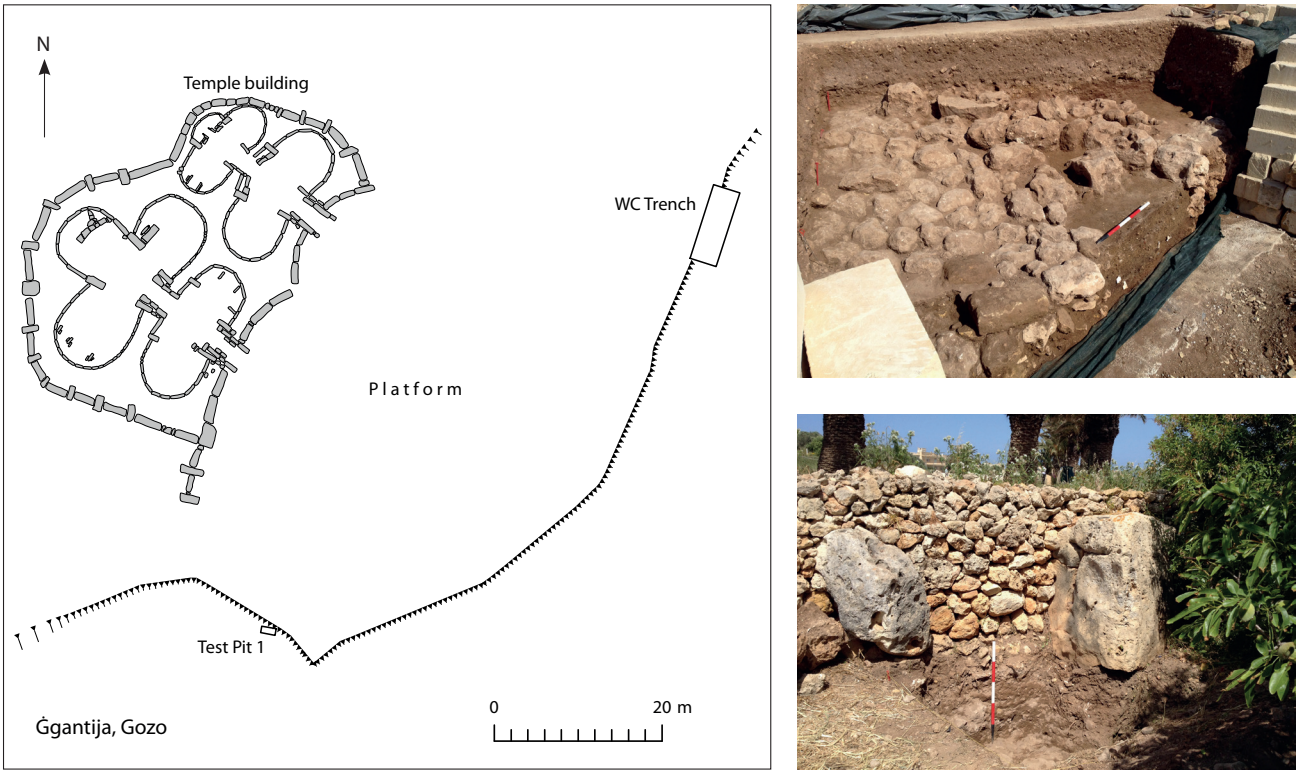

Figure 5.6. *Plan of Ġgantija temple and locations of Test Pit 1 and the WC Trench excavations (R. McLaughlin) (left), with as-dug views of the WC Trench (upper right) and TP1 (lower right) (C. French).*

which was consequently followed up by a resistivity survey and targeted test pitting by hand and machine (TP 1–5) (Appendix 6; see Volume 2).

Immediately to the east of Ġgantija temple there was a small olive grove, established in 1961 (resident farmer, pers. comm.). The greyish brown, silty clay loam modern soil was imported from the adjacent Ramla valley at the same time and dumped over an area of terraced fields in 1961 and again in 1982. Upon augering and test pitting, in places there was survival of a thin reddish brown silty clay loam soil, with a few artefacts within it which were suggestive of temple period Neolithic activity just to the east of Ġgantija temple, beneath about 75–155 cm of made ground. Two spot samples (35 & 41) were taken for micromorphological analysis from the surviving old land surface. The old ground surface/buried soil surviving in Test Pit 5 (sample 35) was a bioturbated, calcitic, sandy clay loam, and that in BH54 (sample 41) was a fine stoney calcitic silt. These appear to indicate a lower B horizon and weathered B/C sequence, essentially similar to that observed in the base of WC Trench 1 (see §5.3.2.2).

On the other side of the paved lane to the south of the olive grove field, four test pits (TP 2–5; *c*. 2.5 x 3 m) were cut by machine in advance of planting palm trees. In each case, there was *c*. 75–155 cm of made ground over a variable but thin thickness (<20 cm) of reddish brown, fine sandy silt loam soil. This buried B horizon soil which and had developed on the weathered surface of the Upper Coralline Limestone bedrock was similar to that found beneath the made ground in the olive grove immediately to the north, but with no sign of architecture or artefacts of any period.

In the small triangular field immediately to the west of the Ġgantija temple platform, augering revealed the presence of a buried soil about 50–70 cm in thickness beneath the modern ground surface. A small test pit (TP 1; *c*. 2.5 x 1.85 m) was hand-excavated immediately in front of the platform wall and two large limestone slabs which appear to be part of the temple complex, now incorporated in the platform wall (Figs. 5.6 & 5.7). First, the test pit revealed several large, sub-rectangular limestone blocks just at and below the ploughsoil surface, which may be part of temple collapse and/or modifications. Beneath, there was *c*. 80 cm of heavily rooted greyish brown silt loam with a mixture of limestone gravel pebbles and abundant artefacts. This horizon is indicative of an agricultural soil but which contains artefactual material contemporary with the late Neolithic use

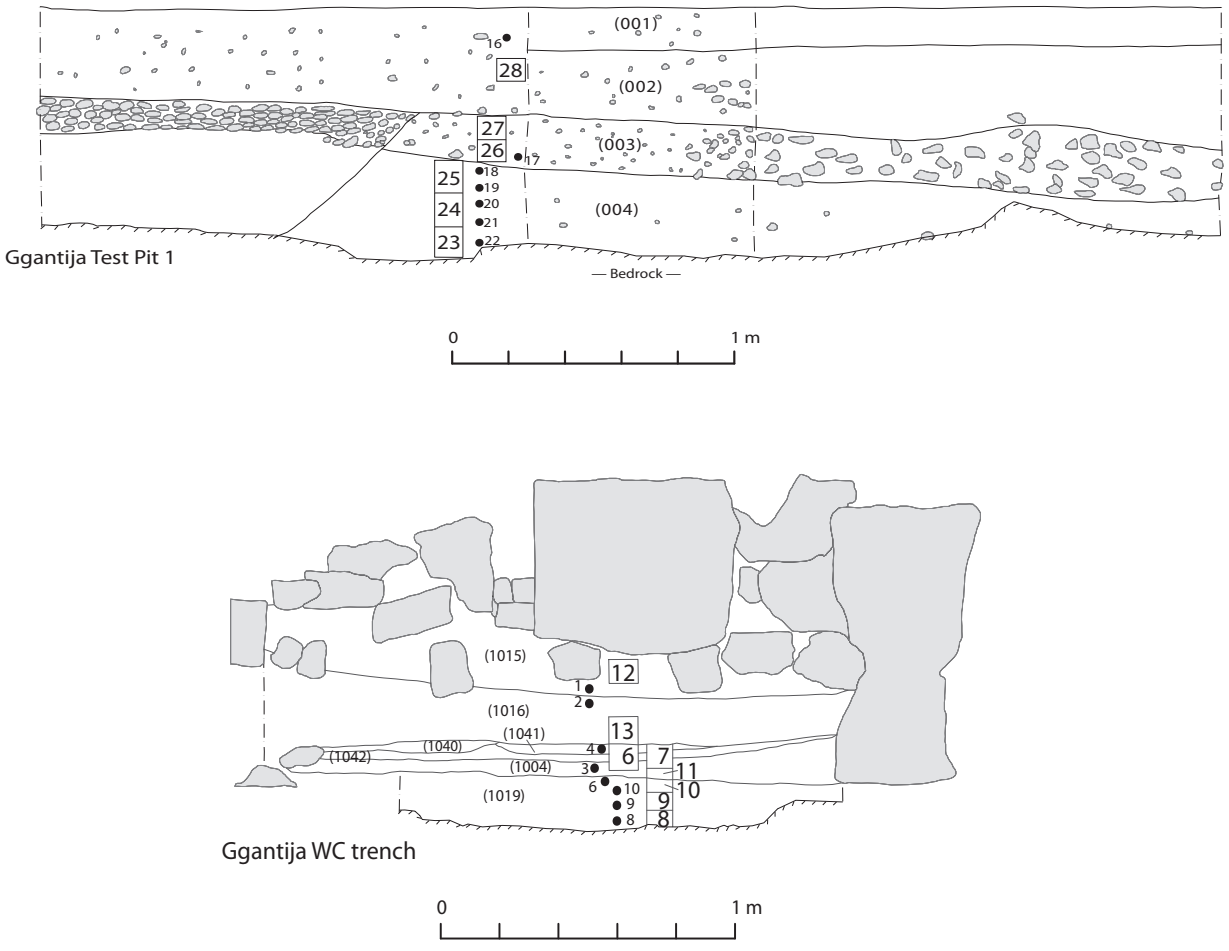

Figure 5.7. *Section profiles of Ġgantija Test Pit 1 on the southwest side of Ġgantija temple (above), and the east–west section of the Ġgantija WC Trench on the southeast side of the temple (below) (Note: open boxes = micromorphology block samples; black circles = small bulk samples) (R. McLaughlin).*

of the temple (see Volume 2, Chapter 5). Then there was a distinctive contact with an *in situ* buried soil profile from *c*. 80–130 cm in depth. Abundant artefacts, primarily Tarxien period pottery sherds (of the later Neolithic) with some bone and lithics continued to be present down-profile to the base of this soil. Their abundance certainly suggests considerable use of this area immediately outside the temple during the Neolithic, perhaps even occupation in the vicinity.

The buried soil comprised three horizons: an upper dark brown silt loam (at 80–90 cm), a brown silt (90–120 cm), a dark reddish brown fine sandy/silt loam (120–125/130 cm), all developed on the weathered Upper Coralline Limestone bedrock (at 125/130+ cm) (Fig. 5.7). Furthermore, at the 80 cm level, there was one large rectilinear block at the horizon boundary in one corner of the test pit, and a cut feature infilled with brown silt loam soil and abundant limestone rubble in the other corner. This suggests that there was an old land surface at 80 cm down-profile associated with a *c*. 45–50 cm thick buried soil. This profile was sampled for micromorphological, geochemical, phytolith and pollen analyses, as well as OSL profiling and dating.

In the WC Trench 1 (beneath the 1970s shop and WC building demolished in 2014), in a similar position to TP1 but on the eastern side of the present-day visitors viewing terrace there was a similar but more complicated sequence was located (Figs. 5.6 & 5.7). Beneath terrace soil make-up, stone-wall collapse and perhaps the construction of a stepped stone entranceway to the temple, there was a well preserved sequence of midden-like deposits overlying an intact and complete buried soil sequence. The abundant artefact recovery suggests that the material is indicative of the whole breadth of the Neolithic, not just the later Neolithic Temple Period itself (see Volume 2, Chapter 5). The

buried soil was of *c*. 35–45 cm in thickness and consists of a lower, brown silty clay loam B horizon with an *in situ* humic silt loam A horizon above. The mixing of the artefact assemblage throughout the profile, albeit with much lesser quantities recovered in the lower half of the profile, suggests that this area has undergone considerable soil faunal mixing and modification in the past. Above this soil there were a series of discontinuous lenses of calcitic ash, fine pea-grit gravel and humified/charcoal rich 'soot' over a thickness of about 10 cm (contexts 1004 & 1041) which are suggestive of a series of thin dumps or accumulations of overlying settlement-derived debris. These in turn were overlain by two major phases of silt loam soil accumulation (contexts 1016 & 1015) which contain very large quantities of later Neolithic Tarxien pottery and bone. These are also suggestive of intensive human settlement activity in the near vicinity, as well as soil surface modification. A wide area of large, collapsed and broken stone blocks then sealed this soil/midden sequence from further disturbance, which could be related to later Neolithic and subsequent modifications of the temple site. This important sequence was thoroughly sampled from a soil and palaeoenvironmental perspective.

5.3.2.1. Physical and elemental characterization

pH values from both test trenches at Ġgantija were all alkaline (ranging from 7.3 to 8.2) and most of the multi-element values were low and/or unremarkable (Tables 5.3 & 5.4). Nonetheless, phosphorus (P) was very enhanced in every horizon, especially in the buried soil in Test Pit 1, as were the calcium (Ca) and strontium values (Sr) (Table 5.4). Phosphorus values in Test Pit 1 ranged from 2200 ppm at the base of the soil to >10,000 ppm in the upper 20 cm of this soil. Strontium values were also relatively enhanced ranging from *c*. 172–380 ppm (Table 5.4). The enhancement of these two elements suggests large additions of organic material and household refuse to the soil (Entwistle *et al.* 1998; Holliday & Gartner 2007; Wilson *et al*. 2008), coincident with the substantial quantities of fragmentary animal bone and Tarxien-period pottery recovered during the excavation. Similarly in the WC Trench, the buried soil and especially the multiple horizons of accumulating soil and archaeological debris above gave very high P values, ranging from 5010 to >10000 ppm along with enhanced strontium values (*c*. 238–322 ppm) (Table 5.4). Likewise the magnetic susceptibility values were either very enhanced or low (Table 5.3), especially in the horizons dominated by archaeological material that had built-up on the buried soil. This suite of high values probably reflects the amount of organic and fire-related settlement debris contained within these deposits (Allen & Macphail 1987; Clark 1996, 109ff; Fassbinder 2016, 502). Calcium and calcium carbonate values were also very high (Tables 5.3 & 5.4), which complements the enhanced phosphorus and strontium values to indicate the strong influence of midden-type refuse and hearth rake-out (Entwistle *et al.* 1998), but may equally reflect weathering and solution from the overlying limestone blocks of the collapsed temple structure above and the large amounts of secondary calcium carbonate observed in the micromorphological analysis of the buried soils at Ġgantija.

5.3.2.2. Soil micromorphology of Test Pit 1 at Ġgantija

In Test Pit 1 on the southern side of Ġgantija temple, there were two soil horizons evident in the buried soil. The basal two-thirds of the buried soil (samples 23 & 24) is a calcitic, fine sandy/silty clay loam with a weakly developed blocky structure and a pellety to small aggregated micro-structure (Fig. 5.8a). Few to common, small sub-rounded aggregates of organized silty clay indicative of Bt horizon or agric material are commonly mixed with the crumb-like soil material. Fine organic matter, charcoal and shell are commonly present throughout, as are minor occurrences of bone fragments (Fig. 5.8b). There is a generally moderate impregnation with amorphous sesquioxides throughout the dusty or silty clay groundmass, as well as common aggregates of strongly amorphous sesquioxide stained clay. There are few if any illuvial clay or dusty clay coatings in the voids or of the grains and/or clay striae in the groundmass, rather dusty clay is only present as the groundmass. In addition, there are some partial to complete infills of the voids with micro-sparitic to amorphous calcium carbonate and very fine organic matter punctuations (Fig. 5.8c), which is becoming increasingly prevalent towards the upper part of the buried soil (Fig. 5.8d).

The upper one-third of the buried soil in samples 25 and 26 is becoming more dominated by micro-sparitic calcium carbonate, humic brown staining, fragments of bone, organic matter and fine charcoal, as well as fine aggregates of herbivore dung (Fig. 5.8e) and red clay soil (Fig. 5.8f). In particular, sample 26 is a very dark brown, humic and amorphous sesquioxide stained, very fine sandy clay loam soil with common interconnected vughs between an aggregated structure (Fig. 5.8g).

The *c*. 80 cm of terrace soil above (samples 27 and 28) is a pellety to aggregated sandy loam with minor micro-sparite and <20 per cent dusty clay in the groundmass, with minor amounts of fine charcoal, bone and shell fragments, and weak to moderate staining with amorphous sesquioxides. It becomes increasingly humic and dark brown stained up-profile (Fig. 5.8h).

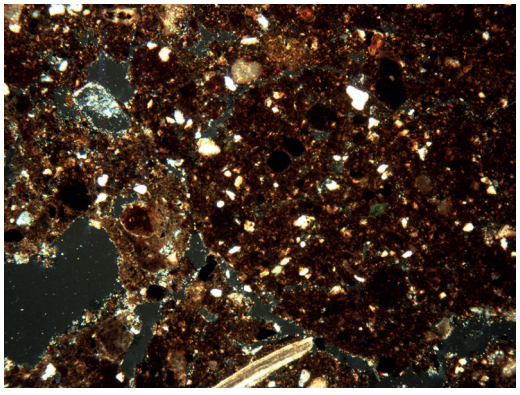

a

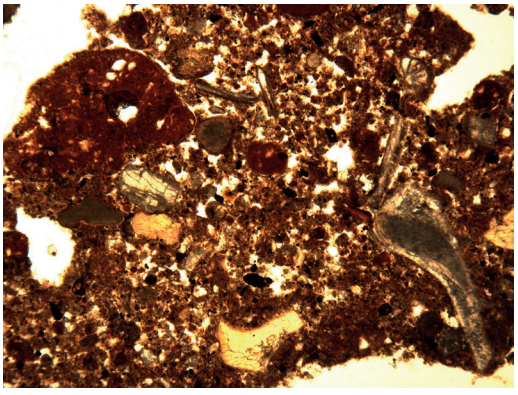

b

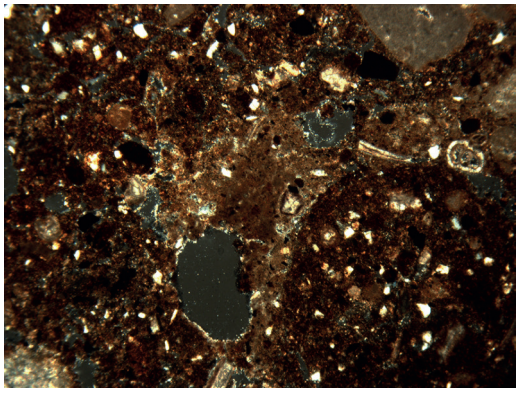

c

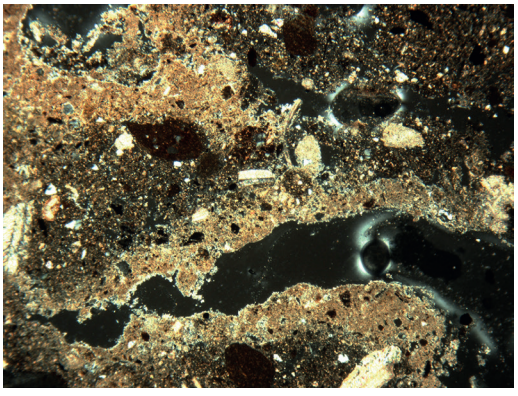

d

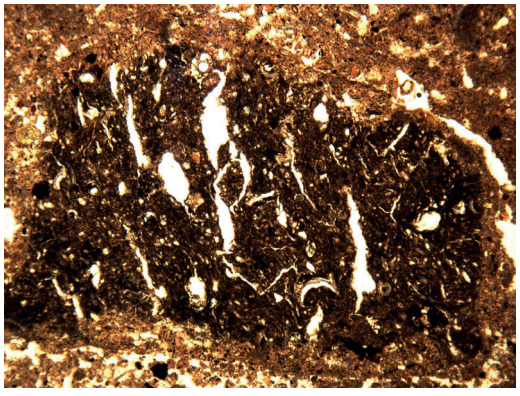

e

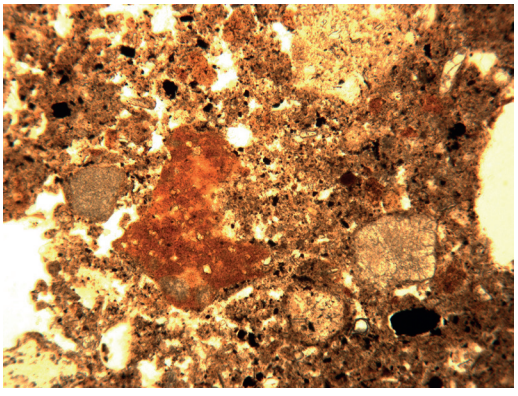

f

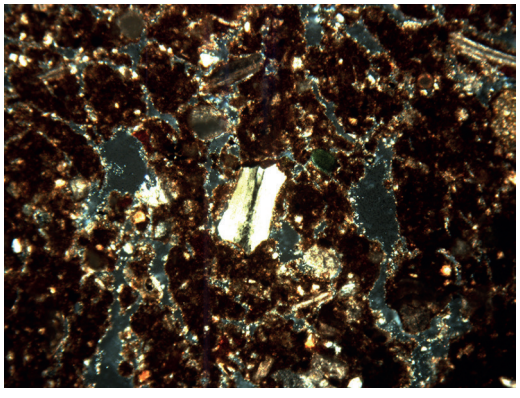

g

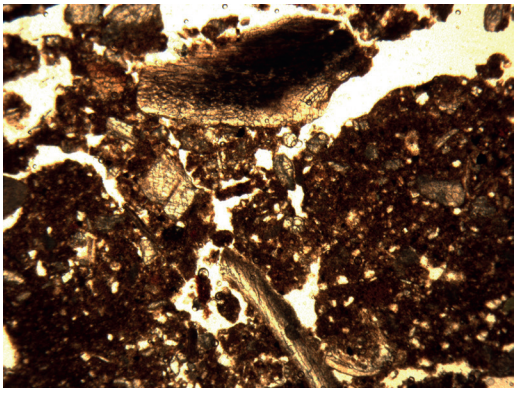

h

In summary, both the terrace soil and the palaeosol beneath are essentially of the same soil material. The terrace make-up is more humic and aggregated, containing few to common fine organic additions such as bone and charcoal. The buried soil beneath is essentially a variation on the same theme. It is marked by very dark brown humic aggregates in its upper organic Ah horizon, and then the B horizon below is more of a mixture of this humic fine sandy clay loam with the addition of much secondary calcium carbonate throughout the groundmass, and especially lining and filling in the voids as a secondary process. There is a slight increase in dusty or silty clay content with depth, and an associated better small blocky ped structure. Thus, it appears that there is a complete Ah/B horizon of a brown earth or cambisol type of palaeosol present (after Bridges 1978, 58), although it is not well developed. It has undergone some pedogenesis, but little in the way of silt and clay illuviation, and then has become disturbed and opened up with the associated secondary formation of calcium carbonate and iron oxides and hydroxides, as well as the incorporation through soil mixing processes by the soil fauna of fine anthropogenic debris (mainly fine charcoal and bone fragments). Significantly soil aggregates indicative of both organic A and argillic Bt horizon material are intimately mixed in the B horizon. This suggests that allochthonous agric or Bt horizon material was contributing to the soil profile, most probably from the erosion of disturbed and truncated soils upslope on the Upper Coralline Limestone plateau. There is also some definite evidence for sedimentation in the form of horizontally orientated planar voids, defining a stacked sequence of micro-facies. This process must have proceeded relatively quickly, which is even more surprising as the soil was biologically active.

Thus this soil has changed from being a relatively stable and structured soil to one that is opened up, disturbed and receiving both eroded soil and midden-derived materials such that its development was interrupted. Consequently, there was up-building and over-thickening of the soil profile, and at the same time it became increasingly affected by drying out and evapo-transpiration. The ubiquitous fine to coarse artefact inclusions are indicative of considerable soil mixing processes at work, that suggest that the anthropogenic inputs to this soil were deliberate, adding organic status and friability to this soil, effectively creating an 'amended soil' suitable for agricultural use (Simpson 1998; Simpson *et al.* 2006).

The terrace soil material above is essentially similar to the organic A horizon of the buried soil below, but more organic-rich and also contains abundant Neolithic artefactual material of the temple period (see Volume 2, Chapter 5) and limestone rubble. This could just be a rubbish heap just outside the temple, but it may well suggest the deliberate inclusion of midden derived settlement waste to create an 'enhanced' and thickened soil, in effect creating the first recognizable agricultural soil adjacent to the southwestern part of Ġgantija temple.

Figure 5.8 *(opposite). Ġgantija TP 1 photomicrographs (C. French): a) Photomicrograph of the calcitic, fine sandy clay loam with a weakly developed blocky structure and a pellety to small aggregated micro-structure, sample 23 (frame width = 4.5 mm; cross polarized light); b) Photomicrograph of the fine bone fragments, sample 28 (frame width = 4.5 mm; plane polarized light); c) Photomicrograph of the partial to complete infills of the voids with micritic to amorphous calcium carbonate and very fine organic matter punctuations, sample 23 (frame width = 4.5 mm; cross polarized light); d) Photomicrograph of the partial to complete infills/linings of the voids with micritic calcium carbonate, sample 25 (frame width = 4.5 mm; cross polarized light); e) Photomicrograph of an aggregate of herbivore dung, sample 25 (frame width = 4.5 mm; plane polarized light); f) Photomicrograph of a fine aggregate of red clay soil in the sandy clay loam with frequent organic punctuations, sample 25 (frame width = 4.5 mm; plane polarized light); g) Photomicrograph of the aggregated, very dark brown, humic and amorphous sesquioxide stained very fine sandy clay loam soil with common interconnected vughs, sample 26 (frame width = 4.5 mm; cross polarized light); h) Photomicrograph of the aggregated, humic sandy clay loam, sample 28 (frame width = 4.5 mm; plane polarized light).*

5.3.2.3. Soil micromorphology of the Ġgantija WC Trench 1

The buried soil (samples 3/3, 3/6, 3/7 & 3/8) at the base of the WC Trench 1 profile (Fig. 5.7) is a pellety to finely aggregated, calcitic, fine sandy loam (Figs. 5.9a & b) with an even mix of fine gravel-sized limestone pebbles (<1.5 cm). The groundmass is dominated by interconnected vughs and non-birefringent dusty clay, with moderate staining with amorphous sesquioxides. There is also a common presence of very fine organic/charcoal punctuations throughout. It is suggested that this is a very bioturbated, formerly quite organic but poorly developed B horizon. Moving up-profile, this soil becomes more organic with increasing amounts of very fine anthropogenic debris (Fig. 5.9c), with the upper surface in sample 3/6 indicative of an organic Ah horizon (Fig. 5.9d). Immediately above the apparent upper contact of the buried soil there

was a *c*. 4 cm thick horizon of calcitic fine sand, then *c*. 6 cm of a calcitic sandy loam soil, with *c*. 4.5 cm of calcitic fine sand above (Fig. 5.7), then a fine limestone gravelly horizon *c*. 4 cm thick. All of these horizons contained abundant later Neolithic Tarxien pottery sherds and animal bone fragments. This alternating soil/fine gravel repeated sequence is suggestive of a cumulative stop/start soil build-up interrupted by

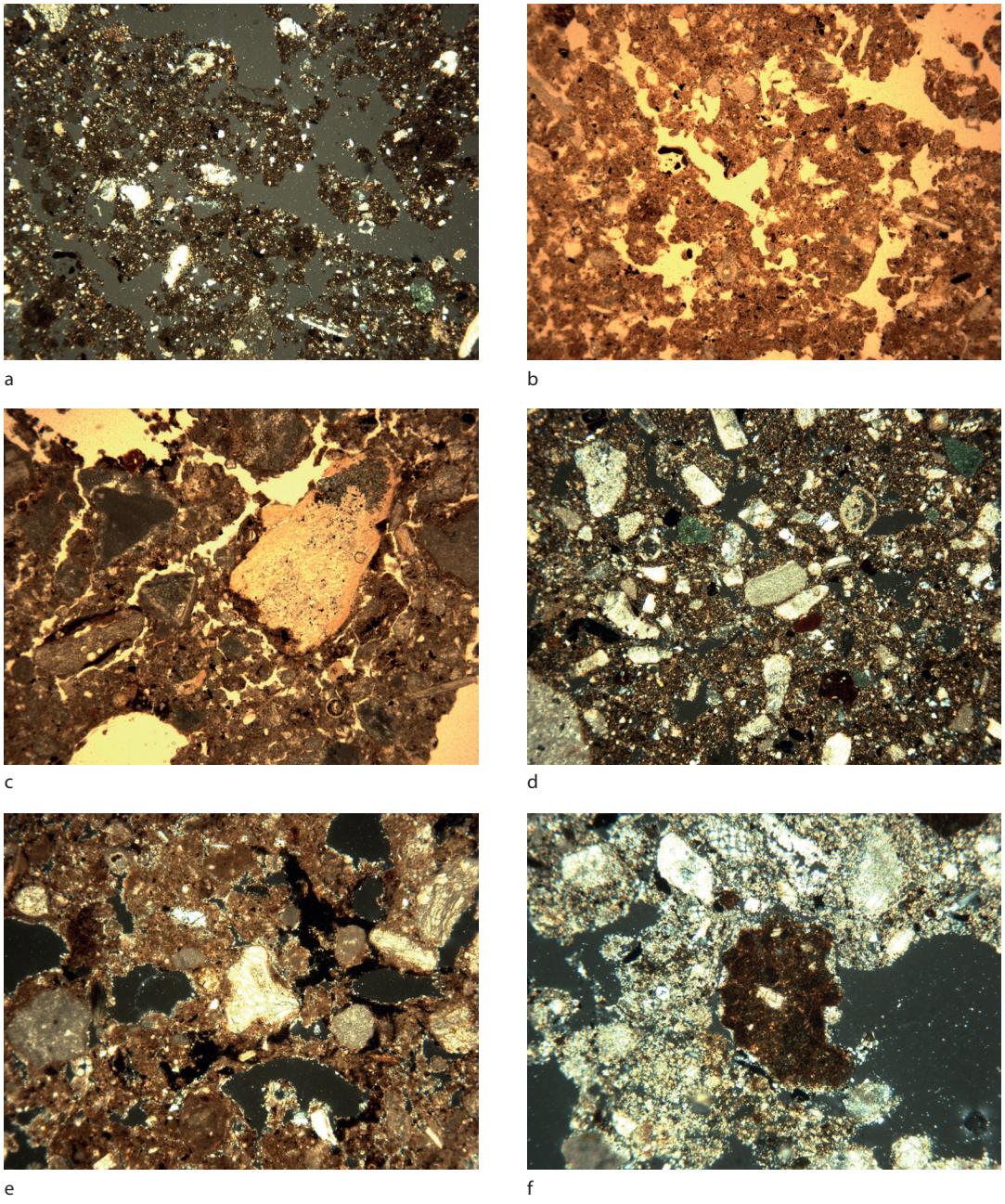

Figure 5.9. *Ġgantija WC Trench 1 photomicrographs (C. French): a) Photomicrograph of the aggregated calcitic sandy loam soil, sample 3/8 (frame width = 4.5 mm; cross polarized light); b) Photomicrograph of the aggregated, humic calcitic sandy loam soil, sample 3/8 (frame width = 4.5 mm; plane polarized light); c) Photomicrograph of fine anthropogenic debris, sample 3/3 (frame width = 4.5 mm; plane polarized light); d) Photomicrograph of the humic calcitic sandy loam Ah horizon, sample 3/6 (frame width = 4.5 mm; cross polarized light); e) Photomicrograph of soil/midden calcitic sandy loam, sample 3/10 (frame width = 4.5 mm; cross polarized light); f) Photomicrograph of reddish brown silty clay soil aggregates in fine calcitic plaster, sample 3/1/2 (frame width = 4.5 mm; cross polarized light).*

Table 5.5. *Summary of the main soil micromorphological observations for the Santa Verna, Ġgantija and Xagħra town buried soil profile*

Site and context	Micromorphology	Interpretation
Santa Verna:		
Buried palaeosol inside temple	*c*. 30–60 cm thick buried soil below earthen temple floor; pre-3800 cal. BC;	Truncated earlier Neolithic palaeosol;
	Small sub-angular blocky, reddish brown silty clay with pellety micro-structure; common dusty clay striae in groundmass; minor very fine charcoal/organic dust and few sesquioxide nodules;	Well structured clay-enriched Bw horizon;
	Over sub-angular blocky, reddish brown silty clay, with pellety micro-structure; very abundant, moderately birefringent, pure to dusty clay in speckles and striae throughout the groundmass;	Well structured, clay-enriched, argillic Bwt soil horizon of brown Mediterranean soil (orthic luvisol);
	Developed on Upper Coralline Limestone	Weathered bedrock C
Buried palaeosol outside temple	*c*. 40 cm thick buried soil below *c*. 60 cm thick terrace soil; undated;	Undated pre-terrace palaeosol;
	Pellety to aggregated, reddish brown, silty clay with fine limestone gravel; very strongly reddened with amorphous sesquioxides; common sesquioxide nodules; common very fine organic dust/micro-charcoal and micrite;	Lower A horizon of a red Mediterranean (chromic luvisol or *terra rossa*) buried soil, with strong rubification and common micritic calcium carbonate formation throughout, all completely mixed by the soil fauna;
	Over heterogeneous mix of 30% aggregates of above silty clay fabric with 70% micro-sparitic calcium carbonate;	Disturbed mix of lower A/eluvial and micritic Eb horizon material, with severe secondary calcification and physical/soil faunal mixing throughout;
	Over moderately to well developed small blocky, orangey brown silty clay; with very abundant, moderately birefringent, pure to dusty clay in speckles and striae throughout the groundmass; few discontinuous linings of voids with micrite;	Argillic Bt horizon of transitional brown to red Mediterranean soil, with slight indications of drying out and secondary calcification in the voids;
	Developed on Upper Coralline Limestone	Weathered bedrock C
Ġgantija:		
Terrace soil over buried palaeosol in Test Pit 1	60–70 cm thick terrace soil over a buried soil; from *c*. 8770±680 to 1140±250 cal. BC; with abundant Tarxien period pottery in the buried and terrace soils	Holocene palaeosol buried by post-late second millennium BC terrace soil;
	Vughy, pellety, dark brown to reddish brown, humic fine sandy clay loam with common fine limestone fragments; weak calcium carbonate and amorphous sesquioxide formation, minor shell, bone and charcoal fragments; abundant Tarxien pottery sherds;	Bioturbated, humic soil with minor included fine anthropogenic components and late Neolithic pottery comprising terrace soil;
	Over aggregated, vughy, dark brown, very humic, fine sandy clay loam; moderate amorphous sesquioxide formation, minor micrite, minor shell, bone and charcoal fragments, and abundant Tarxien pottery sherds;	Organic Ah horizon of buried soil with included fine anthropogenic components and late Neolithic pottery;
	Over finely aggregated, golden brown, calcitic, fine sandy clay loam; few to common anthropogenic components of shell, bone, dung and charcoal;	Bioturbated, calcitic Bca horizon with included fine anthropogenic components;
	Over weakly blocky structured, golden brown, calcitic, fine sandy clay loam; common partial void infills with amorphous to micritic calcium carbonate, and few to common anthropogenic components of shell, bone and charcoal;	Weakly structured, calcitic and clay-enriched Bcaw horizon with increasing secondary calcitic infills and included fine anthropogenic components;
	Developed on Upper Coralline Limestone	Weathered bedrock C

Table 5.5 *(cont.).*

Site and context	Micromorphology	Interpretation
Archaeological strata over buried palaeosol in WC Trench 1	Coralline Limestone blocks of broken stone temple structure;	Collapsed former structure of Neolithic temple period;
	Over at least 5 superimposed horizons (*c*. 65–70 cm thick) of pellety to fine aggregated, calcitic, coarse to fine sand; with up to 40% fine limestone gravel; few fine bone, charcoal and humified organic matter fragments; abundant Tarxien pottery sherds;	Midden-like soil accumulations with abundant late Neolithic pottery;
	Over *c*. 40 cm thick palaeosol; pre-*c*. 2400 cal. BC; small to columnar blocky, calcitic fine to coarse sand; up to 20% moderate staining with humic matter and amorphous sesquioxides; rare fine bone fragments and rare silty clay soil aggregate;	Late Neolithic, weathered former lower A horizon of palaeosol, but missing the organic upper Ah, with some included fine anthropogenic debris;
	Over fine stoney, pellety, reddish brown organic sand; common fine charcoal, shell and organic punctuations, and minor bone fragments; moderate amorphous sesquioxide impregnation throughout;	Bioturbated lower A horizon with some rubefaction and fine anthropogenic debris included;
	Over fine stoney, pellety, vughy, sandy/silty clay loam; minor micrite; 10–15% micro-charcoal and organic punctuations; moderate amorphous sesquioxide impregnation throughout; rare silty clay soil aggregate;	Bioturbated, organic, poorly developed Bw horizon with moderate rubefaction;
	Developed on Upper Coralline Limestone	Weathered bedrock C
Xagħra town:		
Buried palaeosol, House site 2 and quarry	20–35 cm thick; undated, sealed below nineteenth century house basement and street level;	
	Well developed sub-angular blocky reddish brown fine sandy clay loam; with common, moderately birefringent, pure to dusty clay in speckles and striae throughout the groundmass;	Buried, well structured argillic Bt of chromic luvisol (or *terra rossa*) palaeosol;
	Over undulating Upper Coralline Limestone	Weathered bedrock C
Buried palaeosol, House site 3	50–80 cm thick; undated, sealed below nineteenth century house basement;	
	Sub-angular blocky, dark brown fine sandy clay loam with even mix of limestone fragments; with very abundant, moderately birefringent, pure to dusty clay in speckles and striae throughout the groundmass;	Buried, well developed, argillic Bt horizon of chromic luvisol (or *terra rossa*) palaeosol;
	Over sub-angular blocky, dark reddish brown, calcitic, fine sandy clay loam with minor charcoal and bone fragments;	A well developed clay/micrite enriched Bcat horizon of chromic luvisol;
	Developed on undulating Upper Coralline Limestone	Weathered bedrock C

thin, coarse, weathered surfaces. It is suggestive of an open, accumulating soil surface associated with the large upright Coralline stones immediately to the east of this sample sequence. This could in fact be an early terrace construction built in front of the temple.

The two thick overlying contexts, 1016 and 1015 (Fig. 5.7), also beneath the fallen Coralline stones, are both calcitic sandy loams with a weakly developed small blocky structure and up to 20 per cent fine limestone gravel, 10–20 per cent organic punctuations and minor anthropogenic inclusions of bone and charcoal (Fig. 5.9e). There is the occasional silty clay soil aggregate present (Fig. 5.9f). These contexts contained abundant artefactual remains, mainly pottery and bone of the later temple period (see Volume 2) and the occasional 'plaster' fragment. This 'plaster' is an homogeneous, silt-sized calcium carbonate material with minor vughs and fine channels present (Fig. 5.9f).

Thus the buried soil in the WC Trench is a very bioturbated, organic Ah over a poorly developed

weathered, moderately rubified B (or Bw) horizon, and is very similar to that observed in Test Pit 1 at Ġgantija. The ubiquitous silt and very fine quartz sand components suggest that these horizons contain a considerable wind-blown component (Muhs *et al*. 2010; Yaalon & Ganor 1973), probably from fine, dry unconsolidated soil surfaces in the vicinity. Both soil horizons been much affected by soil mixing processes, additions of fine humic and settlement-derived waste material as corroborated by the palynofacies analysis (see Chapter 3), and the formation of secondary calcium carbonate throughout. This is primarily a result of biorturbation by the soil fauna, and the exposure/drying and weathering of the fine limestone gravel content in this soil. Much of this limestone content could be related to the weathering of the adjacent large uprights of the monument adjacent, as well foot traffic/trample on the entrance route into the temple itself.

Subsequently the buried Ah horizon has been deliberately built up in several episodes of deposition through the addition of a similar soil material containing abundant pottery, bone and organic matter. As was evident in the TP1 sequence, the multiple overlying horizons present above the buried soil in the WC Trench could be indicative of a rubbish dump, but equally could suggest the deliberate thickening and enhancement of the underlying soil with settlement-related refuse. This could be seen as an early form of soil amendment and perhaps even an early form of terracing. All indications are that this occurred within the later Neolithic period of the mid- to later third millennium BC, and not just here but also at the Santa Verna and Skorba temple sites (see §5.3.1.2 and §5.3.3.2).

5.3.3. Skorba and its immediate environs

The test excavations in April 2016 exposed buried soil profiles suitable for soil micromorphological block and small bulk sampling, as well as OSL profiling and tube sampling (Figs. 5.1 & 5.10; Tables 5.6 & 5.7; see Chapter 2). New radiocarbon dating places the construction of the temple in the early fourth millennium BC (see Volume 2, Chapter 7) and thus the soil profiles sampled

a b

Figure 5.10. *Section profiles of Trench A at Skorba showing the locations of the micromorphological and OSL samples: a) section 1, profile A–B; b) section 2, profile D–E (Note: open boxes = micromorphology block samples; white circles = small bulk samples) (D. Redhouse).*

Table 5.6. *pH, magnetic susceptibility and selected multi-element results for the palaeosols in section 1, Trench A, Skorba.*

Sample	pH	MS SI/g x10^{-8}	Ba ppm	Ca %	Cu ppm	Fe %	K %	Mg %	Mn ppm	Na %	P ppm	Pb ppm	Sr ppm	Zn ppm
Trench A:														
11	8.15	1.99	50	<2	51	1.55	0.5	0.67	335	0.35	7570	8	319	146
20	8.36	1.78	30	<2	47	1.78	0.59	0.6	371	0.34	6960	11	288	136
24	8.32	1.91	40	2	47	1.93	0.64	0.57	387	0.33	6820	11	267	131
28	8.27	2.27	40	<2	40	2.05	0.67	0.57	400	0.34	6750	9	243	127
75	8.44	1.7	50	<2	57	1.75	0.6	0.74	419	0.37	8370	7	323	172
78	8.63	1.59	30	<2	39	1.64	0.53	0.58	344	0.31	6680	10	270	125

Table 5.7. *Loss-on-ignition organic/carbon/calcium carbonate frequencies and particle size analysis results for the palaeosols in section 1, Trench A, Skorba.*

Sample	% organic	% carbon	% CaCO3	% clay	% silt	% sand
Trench A:						
11	4.88	1.14	48.14	0.34	30.9	68.76
20	4.99	1.23	42.71	0.42	32.32	67.26
24	5.05	1.34	39.19	0.31	26.63	73.06
28	5.76	1.35	35.84	0.33	29.24	70.43
75	4.34	0.92	47.54	0.31	34.07	65.62
78	3.92	0.76	55.55	0.3	30.48	69.22

are indicative of the early to mid-Holocene period. In addition, a hand-augered transect from the site down-slope into the valley to the south revealed a consistently present reddish brown silty clay loam with common limestone pebbles of *c*. 40–55 cm in thickness on wide shallow, natural terraces on the Upper Coralline Limestone.

Section 1 (A–D) in Trench A (Fig. 5.10) was characterized by an upper 80 cm of pale greyish brown calcareous fine sandy/silt loam with varying admixtures of limestone rubble. This overlies *c*. 20 cm (at 80–100 cm) of a dark greyish brown fine sandy/silt loam, which in turn overlies a further *c*. 50 cm of dark brown fine sandy loam, a probable *in situ* buried soil. The whole profile was cut through by two superimposed limestone walls.

Section 2 (D–E), also in Trench A (Fig. 5.10), was characterized by an upper 80 cm of rubbly sandy silt loam (contexts 10, 12 and 23), and as in Section 1 was probably disturbed and/or re-deposited. Beneath this was a *c*. 3–6 cm thick (at *c*. 75–78/82 cm), *in situ* floor horizon (context 26) composed of a pale brown, calcitic loamy sand material with occasional lenses of pale grey calcitic plaster visible in it. This context overlies three horizons of brown, fine sandy loam (at *c*. 78/82–122 cm), with the lowermost horizon (*c*. 10–12 cm thick) being an undisturbed buried soil with a slightly greater clay content and the two horizons above probably being disturbed buried soil material.

5.3.3.1. Physical and multi-element analyses

The deposit sequence in Trench A is all highly alkaline with relatively low magnetic susceptibility values (Table 5.6). The phosphorus (P) values are all very enhanced, especially in the plaster spot sample, the floor level sample/context 26, and the horizon context/sample 75 below. Each of these contains high amounts of wood ash and humified organic matter as seen in the micromorphological analyses; unusually the presence of ash is not also corroborated by high barium (Ba) values in these cases. Nonetheless, these features indicate the high amounts of organic waste which has been incorporated in the soil, presumably from the deposition and incorporation of settlement-derived midden material (Entwistle *et al.* 1998; Wilson *et al*. 2008). The relatively enhanced strontium (Sr) values also corroborate this. The remainder of the soil profiles are also very enhanced with phosphorus, and the high amounts of humified organic matter, very fine charcoal and fine anthropogenic debris as seen to be included in the thin sections of these contexts (see below) appears to corroborate these high values. The loss-on-ignition

values for total organic and carbon are quite consistent around 5 per cent and just over 1 per cent, respectively, throughout the whole profile (Table 5.7).

The particle size analysis is characterized by the near absence of clay, considerable silt (26–34 per cent) and a predominance of sand (65–73 per cent) (Table 5.7), the majority of which is very fine to fine sand in size range. These results are corroborated to some extent by the soil micromorphological analysis (below), but consistently under-represents the amount of clay actually present, and mistakes much of the silt component as micritic (or silt-sized) calcium carbonate.

5.3.3.2. Soil micromorphology

The basal horizon of Section 1 (A–D; sample 28) has a micritic fine sandy loam fabric with variable amounts of fine to coarse limestone pebble inclusions (Fig. 5.11a). It is quite well organized with a humic brown, fine fabric of micro-sparitic dusty clay well mixed with *c*. 10 per cent very fine quartz sand. There were few to occasional very fine charcoal and bone fragments, and a minor fabric of a calcitic fine sandy clay loam included as small aggregates. The fabric of the horizon (context 24) above was similar, but it exhibited a pellety to small aggregated microstructure throughout (Fig. 5.11b). In horizon context 20 above, the fabric was a massive, dense, brown, micro-sparitic, very fine sandy clay loam with common included micro-charcoal (Fig. 5.11c). Immediately above in the base of horizon 11, a similar soil exhibited a well, developed small sub-angular blocky ped structure with a pellety micro-structure and strong humic staining (Fig. 5.11d).

In the field, this sequence was thought to be an aggrading soil on an *in situ* soil, all beneath disturbed/

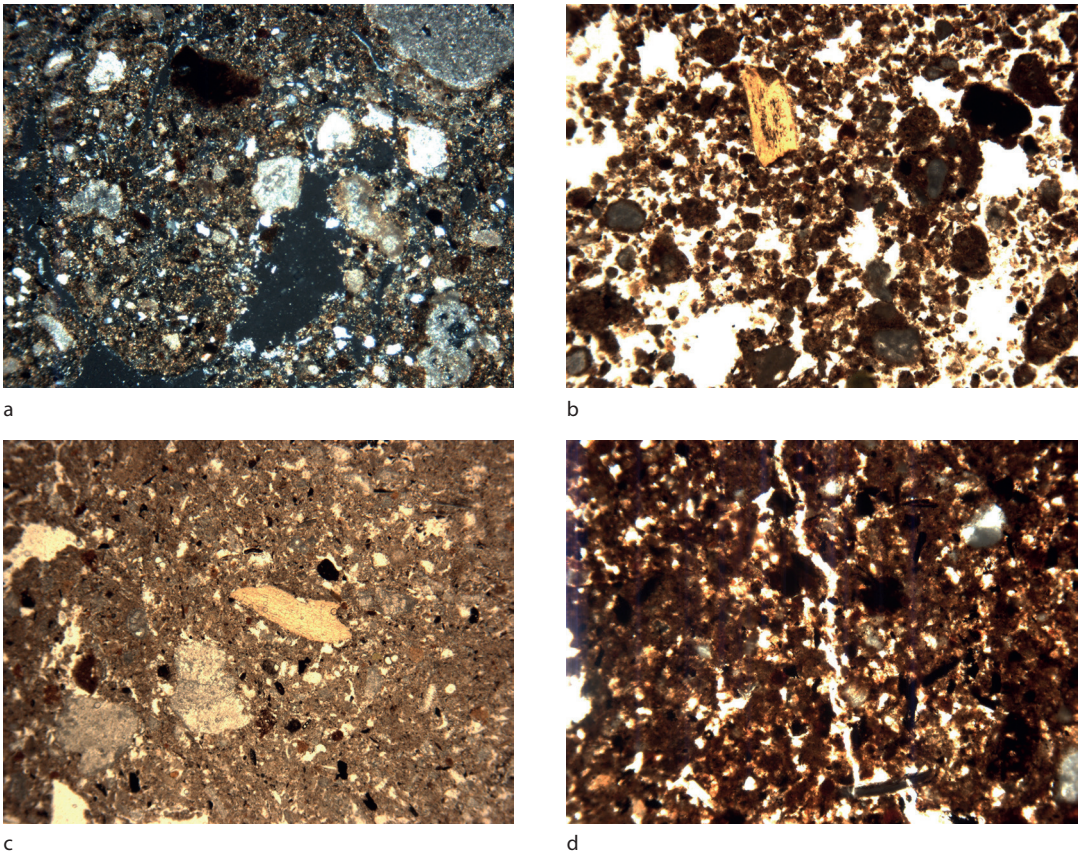

Figure 5.11. *Skorba Trench A, section 1, photomicrographs (C. French): a) Photomicrograph of the loosely aggregated, micritic, fine sandy clay loam fabric, sample 28, section D–E, Trench A (frame width = 4.5 mm; cross polarized light); b) Photomicrograph of the pellety, humic, fine sandy clay loam fabric, sample 24, section D–E, Trench A (frame width = 4.5 mm; plane polarized light); c) Photomicrograph of the massive, micritic fine sandy clay loam fabric with common included micro-charcoal, sample 20, section 1, Trench A (frame width = 4.5 mm; plane polarized light); d) Photomicrograph of the humic, aggregated, fine sandy clay loam fabric within larger peds defined by fine channels, sample 20, section 1, Trench A (frame width = 4.5 mm; plane polarized light).*

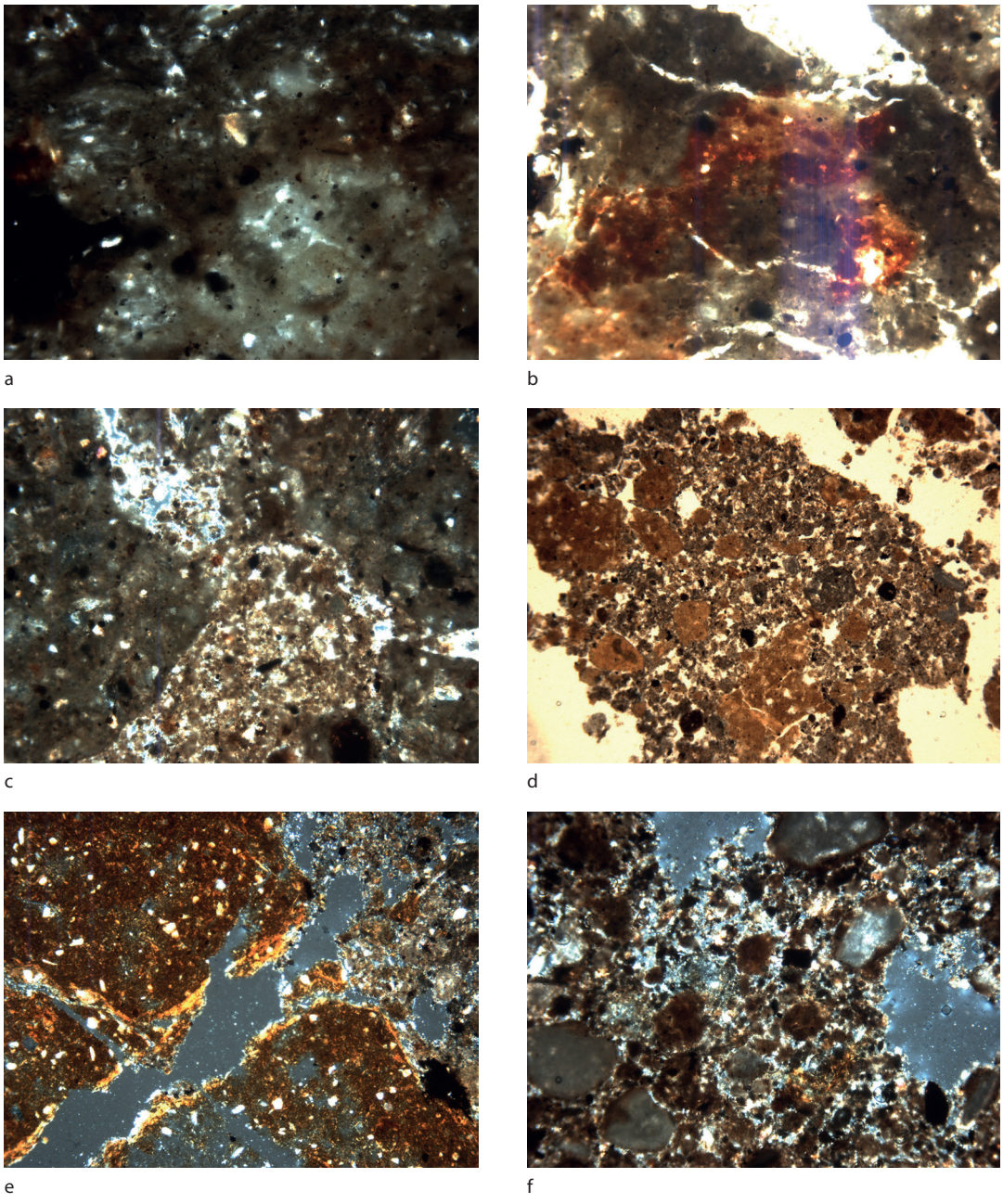

Figure 5.12. *Skorba Trench A, section 2, photomicrographs (C. French): a) Photomicrograph of the calcareous 'slurry' of ash and silty clay soil material with abundant micro-charcoal, sample 26, section 2, Trench A (frame width = 4.5 mm; plane polarized light); b) Photomicrograph of the burnt zones in/on the ash, sample 26, section 2, Trench A (frame width = 4.5 mm; cross polarized light); c) Photomicrograph of calcitic, charcoal-rich, 'slurry', sample 75, section 2, Trench A (frame width = 4.5 mm; plane polarized light); d) Photomicrograph of the pellety, micritic fine sandy/silty clay loam fabric, sample 78, section 2, Trench A (frame width = 4.5 mm; cross polarized light); e) Photomicrograph of the birefringent coatings on the silty clay aggregates, sample 75, section 2, Trench A (frame width = 4.5 mm; cross polarized light); f) Photomicrograph of the micritic plaster and soil aggregates in a plaster fragment, plaster spot sample 1, Trench A (frame width = 4.5 mm; cross polarized light).*

dumped archaeological material. In thin section, the whole sequence from *c*. 80–150 cm has been transformed by a number of processes. Each horizon has undergone varying degrees of soil faunal mixing, and the humification and removal of most of its organic content. This has led to variable porosities and openness of the fabric, and intensive comminution of the organic components and bioturbation of the whole fabric. In conjunction with this and the drying out of the profile, there had been the considerable formation of secondary calcium carbonate as silt-sized micro-sparite throughout the whole profile. At the transition from the lower to upper half of the sequence at *c*. 70–80 cm, the same soil material exhibited a small blocky ped structure. This was unexpected, but it could suggest that this represented a period of stability as an undisturbed soil surface during the life of the immediately adjacent Neolithic site, protected by later soil and stone rubble fall.

Section 2 (D–E) was characterized by a similar accumulation of rubbly soil material on an *in situ* surface (Fig. 5.10). This surface (context 26) is composed of a dense 'slurry' of amorphous calcium carbonate with common micro-charcoal punctuations (Fig. 5.12a), irregular zones of humified organic matter and wood ash aggregates, and a few burnt zones (Fig. 5.12b). The spot sample of a 'plaster' fragment from the same context location was essentially a similar dense 'slurry' of calcium carbonate with fine gravel-size/coarse sand-sized limestone and very fine charcoal inclusions (Fig. 5.12c). Sample 75 below is composed of three different fabrics, present either as aggregates and/or as a 'slurry' – a micro-sparitic fine quartz sand (*c*. 40–60 per cent), a golden brown dusty clay (*c*. 20–30 per cent) and 10–20 per cent calcitic ash aggregates, with up to 20 per cent interconnected vughy pore space and common micro-charcoal throughout (Fig. 5.12d). The dusty/silty clay aggregates generally exhibit weak birefringence, but occasionally have birefringent surface coatings (Fig. 5.12e). Sample 78 below is a pellety, calcitic, fine sandy clay loam as seen in the base of section 1/sample 28 (Fig. 5.12f), but which exhibits a weakly to moderately well developed columnar blocky ped structure. The channels defining the peds often exhibit discontinuous soil infills of the same fabric.

Context 26 is an *in situ* calcareous floor deposit. The predominantly dense, amorphous calcium carbonate material was spread on the underlying soil surface wet, and quickly dried. In addition, the horizon below (in sample 75) appears to comprise broken-up fine aggregates of calcitic flooring material evenly mixed with humic silty clay soil aggregates and wood ash. This could result from weathering and collapse of adjacent wall and floor surfaces, or could perhaps be from the dumping of floor sweepings. These two horizons are found above a thick, calcitic soil horizon, essentially similar to that observed in section 1 (see above), but exhibiting some ped structure.

5.3.3.3. Interpretative discussion

The buried soil profiles in Trench A at Skorba comprise a *c*. 40–50 cm thick A horizon over a *c*. 15–30 cm thick *in situ* B horizon (Table 5.8). The soil fabrics are generally aggregated to small blocky structured, calcitic fine sandy clay loams, with the A horizon typified by humified organic matter, calcitic ash and very high phosphorus values. There are few to common fine anthropogenic debris throughout the profile, including very fine charcoal, humified organic matter, calcitic ash, pottery and bone fragments. The whole profile appears to have been disturbed in the past, and once much more organic as indicated by the vughy/interconnected vegetal voids present. The bulk of the silt component was comprised of micro-sparitic calcium carbonate throughout, indicative of severe seasonal drying out of the profile (Durand *et al*. 2010). The B horizon is also calcitic, but it exhibits abundant illuvial silty clay striae which are suggestive of a once more well developed and clay enriched argillic B horizon (Kuhn *et al.* 2010), as also observed in the pre-temple buried soil at Santa Verna. There is little sign of the secondary formation of amorphous sesquioxides leading to soil reddening.

In the field, this sequence was thought to be an aggrading soil over an *in situ* soil, all beneath disturbed/dumped archaeological material. The soil micromorphological analysis has confirmed this. Also, the high phosphorus values and common fine anthropogenic debris components suggest that this is an amended soil, with the A horizon built up through the addition of settlement derived midden-type debris as a cumulative soil, perhaps even a form of early managed terrace soil formation.

In many respects, this soil profile is a better developed version of what has already been observed in the WC Trench 1 on the southeast side of Ġgantija temple on Gozo where there were at least two horizons of soil with abundant included midden debris. The soil profile has been a well developed clay enriched soil but it was already open and becoming desiccated with very strong calcification and secondary formation of micro-sparitic calcium carbonate prior to the period of temple collapse above. The OSL and radiocarbon chronology would suggest that this process has already occurred by the early fourth millennium BC, and similarly implies major human impact on the surrounding landscape during the middle-later Neolithic period leading to similar associated soil changes and degradation effects as

Table 5.8. *Summary of the main soil micromorphological observations of the buried soils in sections 1 and 2, Trench A, Skorba.*

Sample	Main features	Additional features	Interpretation
Profile A-D: Section 1			
11	Well developed small sub-angular blocky, micritic fine sandy clay loam	5% limestone pebbles; common fine charcoal; rare shell, bone & plant fragments	Pre-temple stable, lower A1 soil horizon, once more organic sandy clay loam, with fine anthropogenic inclusions; affected by evapo-transpiration and secondary formation of calcium carbonate
20	Massive, micritic, humic, fine sandy clay loam fabric	10% limestone pebbles; common charcoal fragments & organic punctuations, and few shell, bone & plant fragments; moderate humic & amorphous sesquioxide staining	Affected by evapo-transpiration and secondary formation of calcium carbonate; possible aggrading/amended soil (A2) with well mixed, fine anthropogenic inclusions
24	Pellety, micritic, fine sandy clay loam fabric	10% limestone pebbles; few charcoal, shell, bone & plant fragments; some birefringence in dusty clay	Once more organic sandy clay loam, bioturbated, affected by evapo-transpiration and secondary formation of calcium carbonate; possible aggrading/amended soil (A3) with well mixed, fine anthropogenic inclusions
28	Loosely aggregated, micritic, fine sandy clay loam fabric	10% limestone pebbles; few charcoal fragments & organic punctuations; rare dusty clay aggregate	Disturbed *in situ* micritic B3ca soil horizon; once more organic sandy clay loam, bioturbated, affected by evapo-transpiration and secondary formation of calcium carbonate
Profile D-E: Section 2			
75	Even mix of aggregates of micritic fine sand, silty clay and ash	20% open vughy; common micro-charcoal; few birefingent surface coatings of the silty clay aggregates	Dumped, mixed deposit of an heterogeneous mix of micritic soil, silty clay soil and ash; amended A soil horizon
78	Micritic, pellety to loosely aggregated, fine sandy/ silty clay loam fabric	Discontinuous channel fills with fine fabric; few charcoal fragments	*In situ* micritic Bca soil horizon; affected by evapo-transpiration and secondary formation of calcium carbonate

have also been observed at Santa Verna and Ġgantija over a similar time span.

5.3.4. Taċ-Ċawla settlement site

The main micromorphological study was carried out by McAdams (2015) and is reported on in detail in *FRAGSUS* Volume 2, Chapter 3. This work and the investigation of settlement-related deposit sequences in the Horton Trench at Taċ-Ċawla (samples 47, 48, 52–54, 151 and 159) are not included here, but the present report instead concentrates on the description and micromorphological study of several possible buried soil contexts encountered (Tables 5.1 & 5.9). It should be pointed out that none of these buried soil contexts exhibited anything like the thicknesses observed at the Santa Verna, Skorba and Ġgantija temple sites. Samples 9, 14, 139 and 261 in the Horton Trench, and 301 in the deep karstic feature were examined in thin section, some or all of which may be the very base of the surviving buried soil beneath this Neolithic settlement site.

Sample 9 is very fine sandy clay loam with strong reddening with amorphous sesquioxides. The dusty clay component varies from stipple speckled to short striae with moderate to strong birefringence, and the groundmass contains minor fine charcoal fragments (Fig. 5.13c). Sample 14 exhibits a similar fabric, but also has a weakly developed sub-angular blocky ped structure. Both of these samples are indicative of clay enriched lower B (or Bt) horizon material with strong secondary impregnation with amorphous sesquioxides, making it a Bst horizon.

In contrast, sample 301 is a much more poorly preserved and thin soil. It is a reddish brown, humic silty clay about 5 cm thick over limestone pebbles with common organic/charcoal punctuations and strong reddening with amorphous sesquioxides (Fig. 5.13b). The soil in sample 261 was even more poorly preserved. It exhibited a largely micro-sparitic calcium carbonate dominated secondary fabric with minor very fine quartz and dusty clay, but which contained common charcoal fragments and a few sub-rounded aggregates of herbivore dung (Fig. 5.13a).

Sample 139 is a calcitic, fine sandy clay loam with invasive micro-sparitic calcium carbonate in the voids (Fig. 5.13d). It does not appear to be an *in situ* soil, but its similarity to the buried soils on site may suggest that it is either re-deposited local soil material and/or represents some soil development subsequent to the Neolithic occupation.

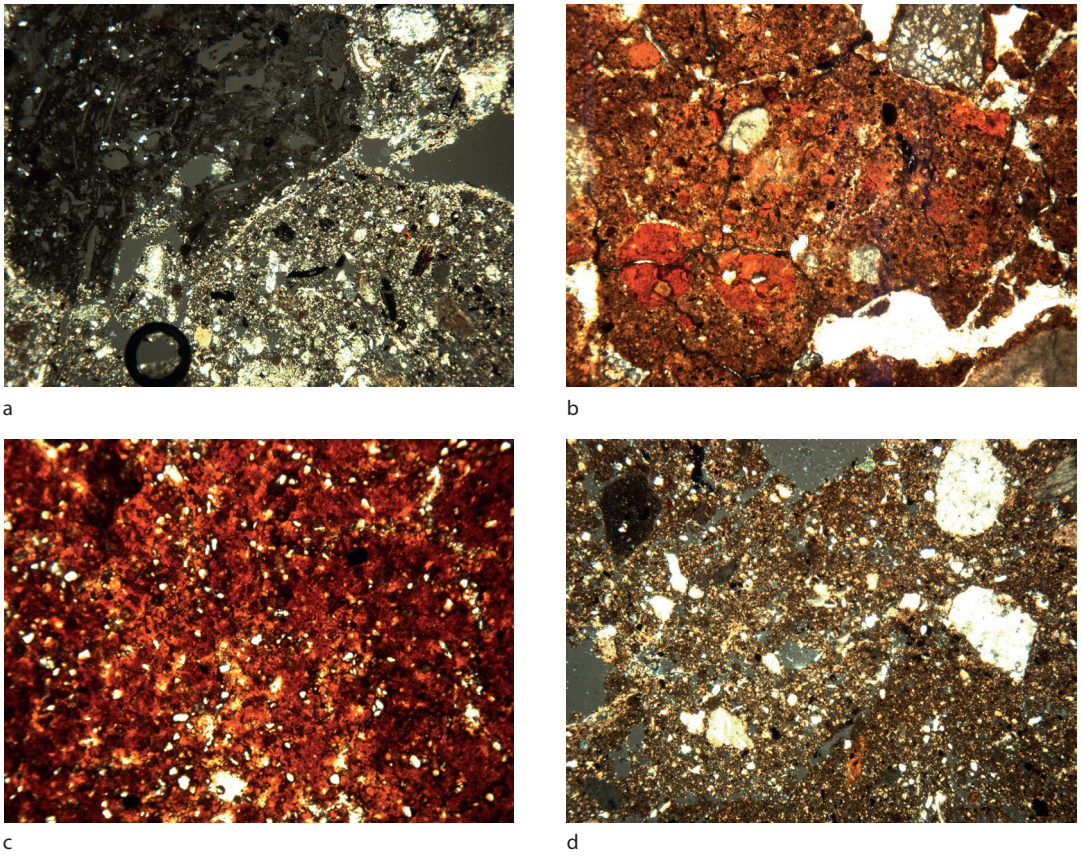

Figure 5.13. *Taċ-Ċawla soil photomicrographs (C. French): a) Photomicrograph of micritic calcium carbonate secondary fabric with common charcoal fragments and an aggregate of herbivore dung, sample 261 (frame width = 4.5 mm; cross polarized light); b) Photomicrograph of the 'dirty' silty clay fabric with included clay aggregates, sample 301 (frame width = 4.5 mm; plane polarized light); c) Photomicrograph of the stipple speckled to short striae dusty clay fabric, sample 9 (frame width = 4.5 mm; plane polarized light); d) Photomicrograph of the 'dirty' micritic silty clay fabric with very fine charcoal included (frame width = 4.5 mm; cross polarized light).*

Table 5.9. *Summary of the main soil micromorphological observations of the possible buried soils at Taċ-Ċawla.*

Context	Sample number	Main fabric	Features & inclusions	Interpretation
? buried soil	9	Reddish brown, very fine sandy clay loam	Dusty clays are stipple speckled to short striae; strong reddening with amorphous sesquioxides	Basal clay and iron enriched Bst horizon of an *in situ* buried soil on Coralline limestone
? buried soil	14	As above, with blocky ped structure	As above	As above
dark soil deposit below 58, with 137-8	139	Fine stoney, aggregated, micritic fine sandy clay loam	Frequent partial infills & linings of voids with calcium carbonate, & minor charcoal fragments	Brown sandy clay loam with abundant secondary calcium carbonate associated with strong evapo-transpiration; redeposited soil or post-occupation soil development?
? buried soil	261/1	Predominantly micritic dusty clay	Few dung aggregates; few to common fine charcoal fragments	Weathered calcitic Bc horizon with incorporated fine charcoal & dung
? buried soil	301	Reddish brown, humic silty clay over limestone pebbles	Organic dust and micro-charcoal in groundmass	Thin Ah horizon over weathered B/C of limestone

5.3.5. Xagħra town

As many houses were under construction in Xagħra town and deep basement areas were being excavated into the top of the Upper Coralline Limestone plateau (or mesa), there was the opportunistic chance of observing some relatively well preserved buried soil profiles in the town. In three instances, there were thick (*c.* 50–80 cm), strongly reddened and structurally well-developed soils observed, all developed on the limestone bedrock and also in vertical weathering fissures into this bedrock (Fig. 5.14; Table 5.10).

These palaeosols exhibited two distinct horizons, both in the field and in thin section: a lower, deep purplish red, silty clay loam, and an upper orangey red, fine calcitic, silty clay loam. In the lower horizon, strongly amorphous sesquioxide impregnated dusty clay predominates, with only about 15 per cent very fine quartz sand present in addition. The clay component is speckled to striated, weakly reticulate striated in places, with moderate to strong birefringence (Figs. 5.15a–c) and has a considerable very fine organic/charcoal component present throughout, well worked into the groundmass. The upper horizon is more vughy, contains a greater very fine to fine quartz sand component and minor micro-sparitic content, and exhibits some very fine organic/charcoal punctuations (Fig. 5.15d).

These strongly reddened soils are characterized by a well-developed blocky ped structure, organized illuvial clays and silty clays with depth, a great degree of reddening with secondary iron oxides and hydroxides (rubification), and lesser amounts of included limestone pebbles and fragments with depth. Although these soils were becoming slightly more organic and vughy up-profile, no *in situ* organic Ah horizons were observed in any location; these have probably been truncated and removed by house building in the last century and more recently. Nonetheless, there is a very fine to fine included organic component throughout these soils, which is suggestive of the long-term incorporation of organic material, especially carbonized and fine humified organic material.

Although these palaeosols are undated, they have been sealed by buildings above for at least a century. They appear to be characteristic red Mediterranean soils (*terra rossa* or Chromic Luvisols) (Bridges 1978, 68; WRB 2014). They feature an A/B1/B2/C set of horizons,

Table 5.10. *Field descriptions and micromorphological observations for the quarry and construction site profiles in Xagħra town.*

Context	Sample no.	Field descriptions and depths	Micromorphology	Interpretation
Stone quarry	5		Well developed sub-angular blocky, reddish orange fine sandy clay loam; very strong amorphous sesquioxide impregnation of all groundmass	Well developed Bst horizon of a buried soil
House 1 (N 36 03.058/E 014 16.601)	None	0–15 cm: brown silt loam with tree rooting 15–25 cm: red silt loam 25–80 cm: pale reddish brown calcareous silt loam with common limestone pebbles; terrace soil 80–85 cm: pockets of reddish brown silt loam; buried Bw of palaeosol 85+ cm: undulating Upper Coralline Limestone bedrock		0–15 cm: modern topsoil 15–25 cm: redeposited soil ? 25–80 cm: buried Bwt of *terra rossa* palaeosol
House 2 (N 36 03.004/E 014 16.549)	9	0–15 cm: modern concrete yard surface 15–25 cm: reddish brown silt loam	As below	As below
House 2	11	25–35 cm: reddish brown silt loam 35+ cm: undulating Upper Coralline Limestone bedrock	Compact/dense, dark red, fine sandy clay loam	Well developed clay-enriched Bt horizon of a buried soil
House 3 (N 36 03.004/ E 014 16.549)	12 upper	0–50/80 cm: dark brown silt loam with even mix of limestone fragments (<3 cm)	50–60 cm: fine stoney, small sub-angular blocky, reddish brown fine sandy clay loam	Well developed clay-enriched Bt horizon of a buried soil
House 3	12 lower	Red silt loam	60–70 cm: dark reddish brown, calcitic, fine sandy clay loam; minor charcoal and bone fragments	Well developed clay/micrite enriched Bct horizon of a buried soil
House 3	14	As above 100+ cm: undulating Upper Coralline Limestone bedrock	As above	As above

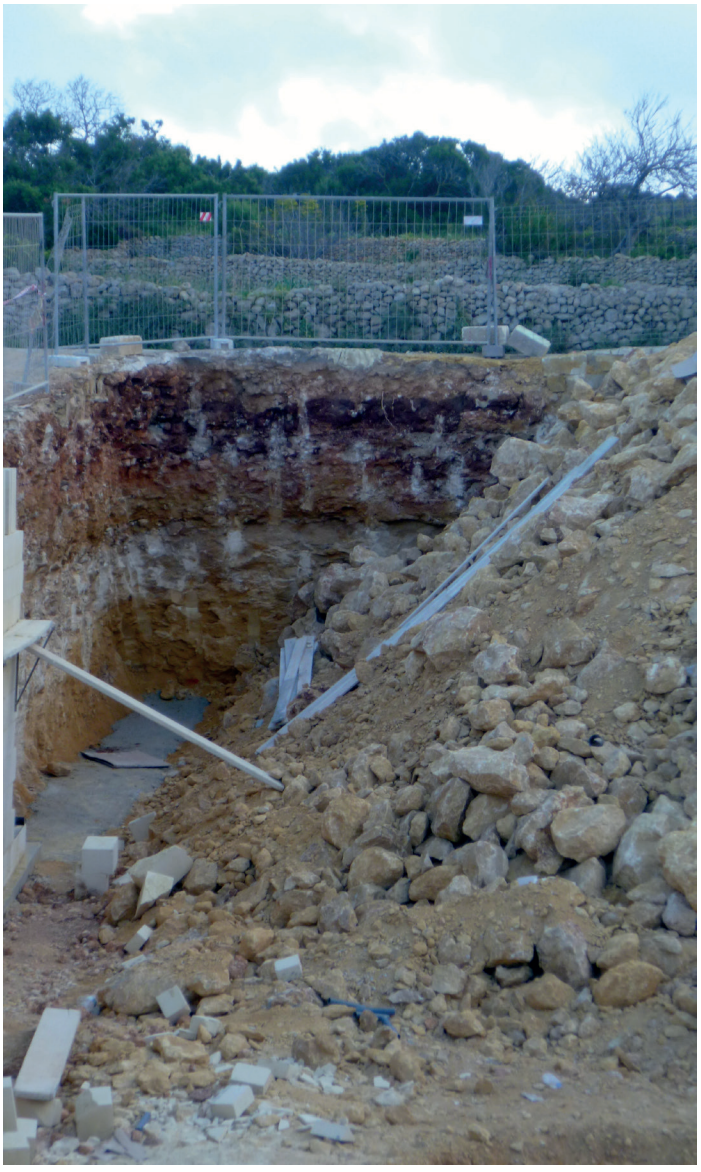

Figure 5.14 *(above). A typical* terra rossa *soil sequence in Xagħra town at construction site 2 (C. French).*

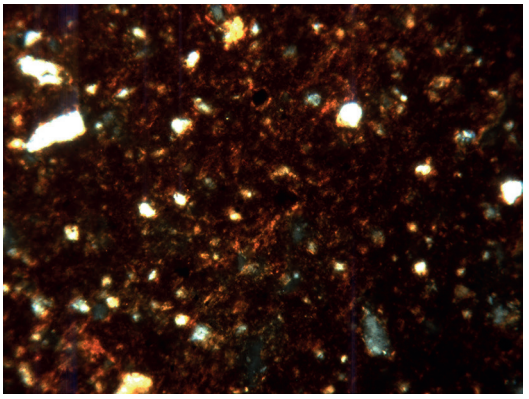

a

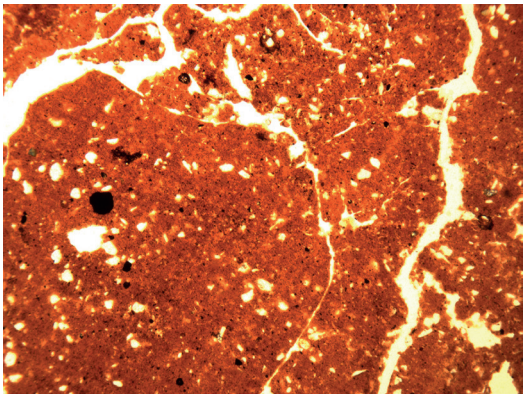

b

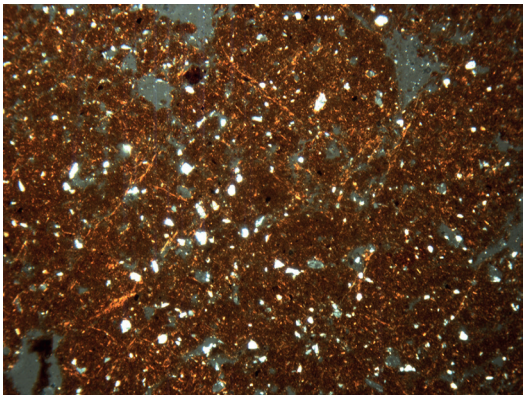

c

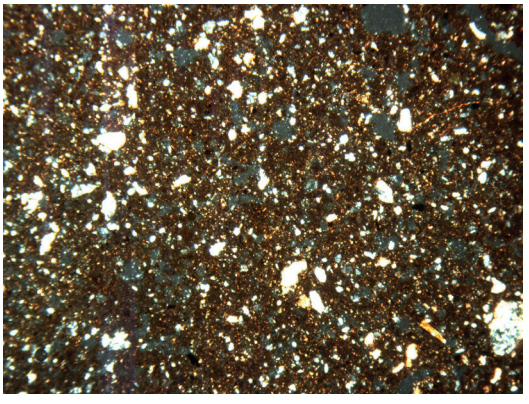

d

Figure 5.15 *(right). Xagħra soil photomicrographs (C. French): a) Photomicrograph of the reticulate striated clay in the lower horizon, sample 5, abandoned quarry (frame width = 4.5 mm; cross polarized light); b) Photomicrograph of the blocky silty clay groundmass with very fine included organic matter punctuations in the lower horizon, sample 5, abandoned quarry (frame width = 4.5 mm; cross polarized light); c) Photomicrograph of the striated fine sandy clay loam in the upper horizon, sample 12, construction site 3 (frame width = 4.5 mm; cross polarized light); d) Photomicrograph of the organic, striated silty clay loam in the upper horizon, sample 11, construction site 2 (frame width = 4.5 mm; cross polarized light).*

with strong weathering, clay eluviation and illuviation, and abundant secondary iron oxide/hydroxide formation, probably predominantly haematite (Fe_2O_3) (Duchaufour 1982; Lelong & Souchier 1982), much of which could be related to the long-term weathering of the limestone bedrock beneath (Catt 1990). There is also the illuvial deposition of pure clay and/or sometimes calcium carbonate in the lower agric horizon (B2 or Bt). Although these soils may be of much greater antiquity than the Holocene (Catt 1990; Kemp 1986; Yaalon 1997), the environmental factors which are thought to be important for the development of this soil type include strong seasonal variation with rainfall during the winter and spring months (<650 mm) and xeric conditions during the summers (Bridges 1978, 68; Yaalon 1997), conditions which still prevail today in the Maltese Islands.

5.3.6. Ta' Marżiena

Transect H comprised nine hand-augered boreholes in a north–south aligned transect from Ta' Marżiena temple across the shallow valley between the towns of Sannat and Munxar. Both within and immediately around the temple, there is only very shallow soil cover of <10 cm. Once off the low Upper Coralline Limestone promontory on which the temple site is located, the soil profile thickens southwards to *c*. 75–80 cm and becomes a grey silty clay throughout. This thick silty clay ploughsoil may well have colluvial additions to it. About 20 m north of the main road in the valley bottom in borehole 73, there was a reddish to strong brown silty clay loam buried soil present that was up to 40 cm thick. Although no soil samples were taken for analysis, this is probably indicative of *in situ* buried Bt horizon material, which points to soil formation and landscape stability here earlier in the Holocene, as is also evident in the palaeosols present at Santa Verna and Ġgantija.

5.3.7. In-Nuffara

Test excavations of two later Bronze Age (*c*. 1000 cal. BC) storage pits cut into the Upper Coralline Limestone bedrock on the In-Nuffara plateau revealed a number of primary/lower secondary fills composed of what appeared to be soil-like material (Table 5.11). Given the otherwise severe denudation of the topsoil over this plateau, this was the only opportunity to investigate the soil material that had been associated with the construction of these pits in the later Bronze Age, and they were accordingly sampled for micromorphological analysis. Four soil blocks (samples 17, 40, 503, 509) from four pits were prepared for thin section analysis (Appendix 7).

5.3.7.1. Thin section descriptions

Samples 17 and 40 were essentially similar to each other, as were samples 503 and 509. Samples 17 and 40 were both calcitic, fine limestone-rubble rich, silty clay primary deposits (Fig. 5.16a). Sample 17 exhibited at least four horizons of the same material, suggesting pulses of fine erosion into the pit cavity. These pit fills were all finely aggregated, and they contained only minor small fragments of anthropogenic material such as pottery, bone, fired clay and very fine charcoal (Fig. 5.16b). These deposits were also stained brown, suggesting a strong humic content, and occasionally exhibited zones of finely sorted micro-laminar silt crusts (Fig. 5.16c) as a result of fine soil material washing into the pit cavities.

In contrast samples 503 and 509 were fine sandy clay loam material which exhibited a weakly developed blocky ped structure and weakly birefringent dusty clay predominant throughout the groundmass. Again, fine anthropogenic inclusions of pottery, bone, fired clay and charcoal are present, but on a very low scale.

5.3.7.2. Interpretative discussion

The deposits in samples 503/509 are likely to have been soil material that had fallen into the pit, and thus could be representative of the mid-Holocene soil cover of the In-Nuffara plateau. This is suggested by its well structured aspect and the predominance of silty clay illuvial material integral to the fine groundmass. These features may well suggest a period when the plateau was still well vegetated and not yet disrupted by significant human activities (Aguliar *et al*. 1983; Bullock & Murphy 1979; Kuhn *et al*. 2010) from the Bronze Age onwards (see Volume 2, Chapter 8). This is also corroborated by the fact that there is little or no micritic calcium carbonate present in this soil material.

Table 5.11. *Sample contexts and micromorphological observations for two silo fills at In-Nuffara.*

Sample number	Silo	Context	Micromorphology
17	1, context 22	Lower secondary fill	Four horizons of porous, finely aggregated, micritic, brown humic silty clay primary deposits with a common fine limestone-rubble component, and a minor, fine anthropogenic content of pottery, bone, fired clay and very fine charcoal fragments
40	2, contexts 41/42	Upper primary fill	Pellety to finely aggregated, brown humic silty clay with occasional zones of finely sorted micro-laminar silt crusts

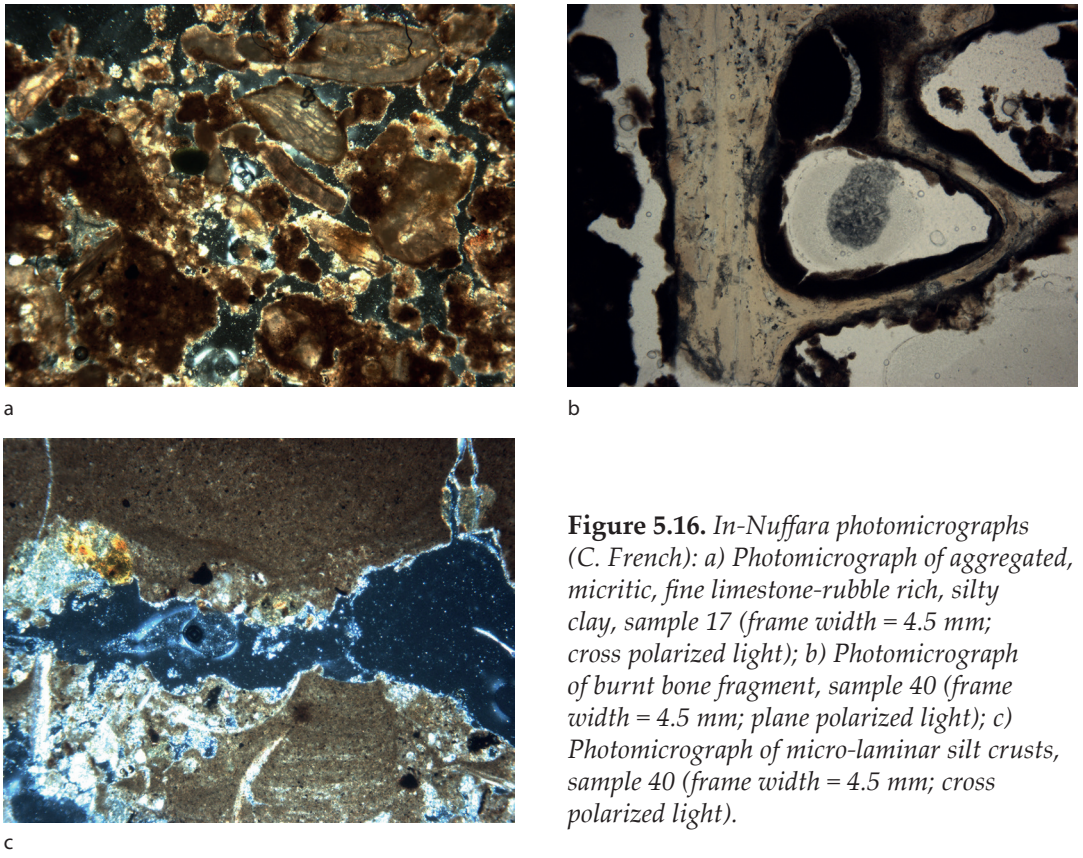

a b c

Figure 5.16. *In-Nuffara photomicrographs (C. French): a) Photomicrograph of aggregated, micritic, fine limestone-rubble rich, silty clay, sample 17 (frame width = 4.5 mm; cross polarized light); b) Photomicrograph of burnt bone fragment, sample 40 (frame width = 4.5 mm; plane polarized light); c) Photomicrograph of micro-laminar silt crusts, sample 40 (frame width = 4.5 mm; cross polarized light).*

By contrast the humic silty clay in samples 17 and 40 exhibits the ubiquitous secondary formation of secondary micro-sparitic calcium carbonate, a feature most probably related to the opening-up of the landscape, soil drying and evapotranspiration (Durand *et al*. 2010). In many respects this secondary soil material is more similar to the later Neolithic calcitic buried soils observed across the Ramla valley at the Ġgantija temple site (see §5.3.2.2).

5.3.8. The Ramla valley

The upper part and mid/lower slopes of the Ramla valley are dominated by grey silty clay loam soils developed on the Blue Clay geology. These are essentially single horizon ploughsoils, often in part saturated and gleyed below a depth of *c*. 50–60 cm. As the valley opens out and shallows towards the sea to the north, flat lower plateau tongues of land emerge of Globigerina Limestone. These have a very characteristic calcitic, fine sandy/silt loam soil developed on them, almost like a loessic silt loam soil, generally <50–60 cm in thickness.

In the central area of the valley towards the sea, a modern drainage canal cut revealed up to *c*. 3 m of hillwash and alluvial deposits that had aggraded across the valley bottom. This cut profile is typified by a series of alternating thin horizons of calcitic silt loam and coarse sand/pebble horizons, with the whole profile generally fining upwards, over a depth of *c*. 1.4 m (i.e. BH66/Pr 627, *c*. 200 m inland from Ramla Bay) (Figs. 5.1 & 5.17). The profile was developed on the weathered Globigerina Limestone bedrock, and the upper 1 m of the profile above was disturbed by recent agricultural activities and water pipes.

A series of 11 small bulk samples were taken from the finer silt loam horizons and three tubes taken for OSL dating at 15, 62 and 103 cm down-profile (see Chapter 2 & Appendix 2). The latter sample loci were also sampled for micromorphological analysis. Initial field impressions indicated aggradation over time with at least two clear breaks, suggesting palaeo-surfaces of some kind at *c*. 46 cm and 115 cm, potentially indicative of changes in erosion processes from alternating fast/slow to a much slower aggradational dynamic (Fig. 5.17). The profiles indicate the parts of the sedimentary sequence which are likely to have been re-deposited without the luminescence signals being re-set at deposition; note, the step-like shifts in signal intensities at 46 cm and 115 cm are to be noted. The most promising targets for dating were the horizons immediately beneath these units. Moreover, the ratio of net signal intensities between the upper (those not affected by

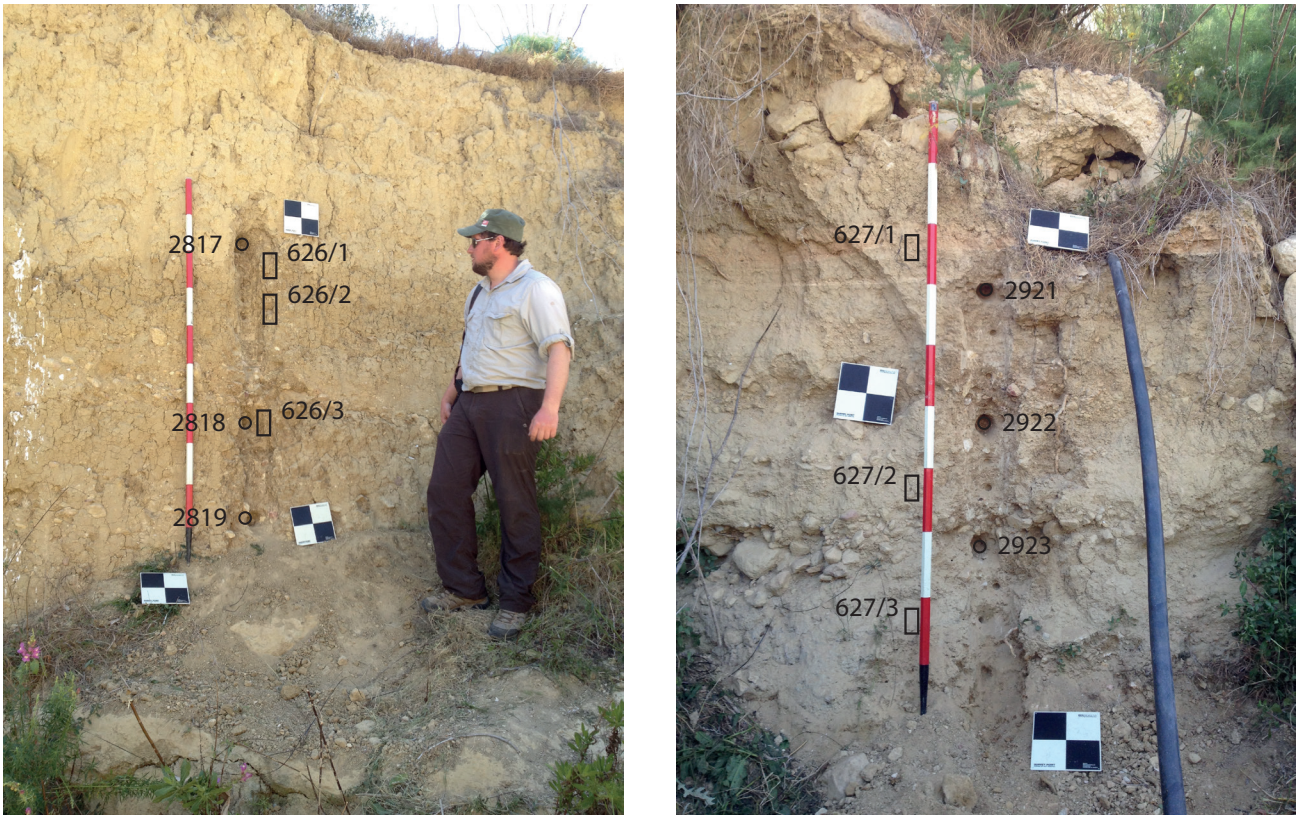

a b

Figure 5.17. *The Marsalforn (Pr 626) (a) and Ramla (Pr 627) (b) valley fill sequences, with the micromorphology samples and OSL profiling/dating loci marked (scale = 2 m) (C. French).*

recent soil turnover) and lower units, implies that the temporal range represented by these units was relatively short. In fact, the OSL dates obtained indicate that this variable flow valley deposition took place in the mid-nineteenth to early twentieth centuries AD.

The multi-element results of the three spot samples taken from the alluvial fills in the Ramla valley profile reveal a similar story of elemental enhancement to that described for the Marsalforn valley (Table 5.4). The fill deposits were all alkaline but with quite low magnetic susceptibility enhancement (Table 5.4), high calcium carbonate (*c*. 55–64 per cent) and silt component (*c*. 60–79 per cent) (Table 5.4), and moderately enhanced phosphorus values (Table 5.4). This may reflect activities in the immediate catchment, but it is harder to ascribe to *in situ* rather than derived evidence of human activity.

The soil micromorphological analysis of three levels in the Ramla sequence revealed at least four pale grey, calcareous 'soil' horizons alternating with fine to coarse pebbly horizons (Table 5.12). The physical and soil micromorphological analyses of these grey 'soil' horizons (at 4–13, 13–15, 26–28 & 60–90 cm) indicated that they are composed of relatively organic, very calcitic, fine sandy/silty clay loam soil (Table 5.12) with greater/lesser amounts of included very fine limestone gravel (Fig. 5.18a). They exhibit evident bioturbation and some weak secondary ped formation. There were minor amounts of silt and clay, very fine charcoal and organic matter fragments present, and the occasional silt or silty clay crust (Fig. 5.18c). There was also the very occasional void infill or aggregate of a very fine sandy clay loam with a reticulate striated dusty (or silty) clay component reminiscent of argillic (or Bt) horizon material (Fig. 5.18d), incorporated in this profile. The lowermost horizon (627/3; 100–140 cm) is a dense but aggregated, calcitic, shelly sand with indications of fine laminations (Fig. 5.18b) is situated directly on the Globigerina Limestone bedrock. The laminar aspect of this profile suggests the stop/start aspect of its accumulation, with the coarse limestone rubble units (at least three) indicative of episodic phases of alluvial fan type of deposition, and the finer units inbetween indicative of fine soil erosion from the catchment and overbank deposition in the valley bottom (Goldberg & Macphail 2006, 77ff).

5.3.9. The Marsalforn valley

An erosion cut in a lane in the central area of the Marsalforn valley near Ta'Mena (BH110/Pr 626) in Wied ir-Riggu exhibited a *c*. 3.7 m thick colluvial sequence of deposits of grey, calcitic, fine sandy/silt loam (Figs. 5.1 & 5.17). This hillwash-dominated sequence was interrupted by two phases of incipient soil formation, more weakly developed at *c*. 2.70–2.85 m and better developed at *c*. 1.75–2.10 m down-profile. Between these two soils and below the lower soil, the hillwash was of a more gravelly in character, with the whole sequence developed on the Globigerina Limestone bedrock.

This profile was cut back and sampled for OSL profiling and dating (see Chapter 2 & Appendix 2). A series of 10 small bulk samples were taken for OSL profiling from 1.75–3.25 m, and three OSL tube samples at 1.75, 2.65 and 3.2 m down-profile. Initial field impressions were that there was an age-related gradual accumulation of hillwash-type sediment throughout the profile (Fig. 17). This is corroborated by the OSL dates obtained which indicate deposition from the earlier to mid-second millennium BC and well into the earlier first millennium BC (Table 2.2).

The three samples taken from the upper (1.75–2.10 m) and lower (2.70–3.10 m) incipient soils within the colluvial profile at the Marsalforn valley profile 626 (Fig. 5.17) were all very alkaline with a low total organic content (*c*. 1.6–2.2 per cent) and very high calcium component (Table 5.4) as well as relatively enhanced phosphorus and strontium values (Table 5.4). The high calcium content is corroborated by the silt-sized micro-sparitic calcium carbonate so dominant in the thin sections of the same contexts, and the moderately enhanced phosphorus and strontium components would indicate the receipt of midden-type refuse

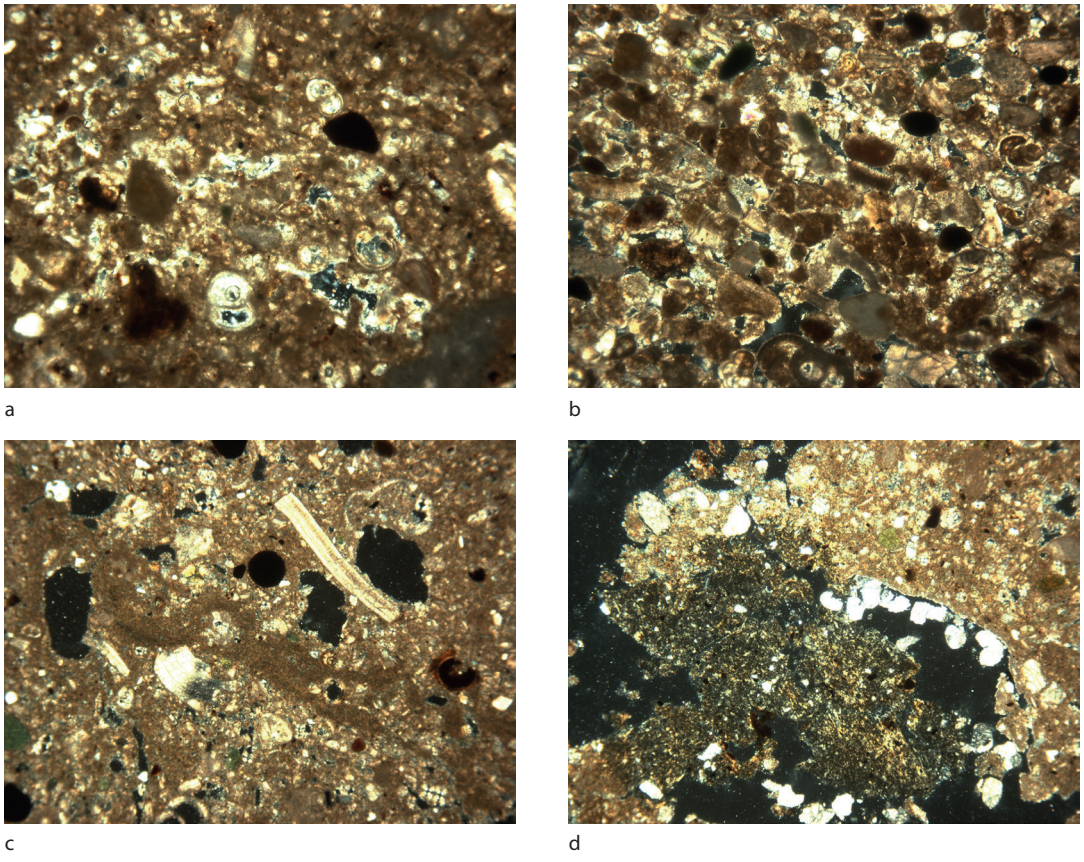

Figure 5.18. *Ramla and Marsalforn valley profiles soil photomicrographs (C. French): a) Photomicrograph of dense calcitic, shelly sand with included fine charcoal, Marsalforn Pr 627, sample 1 (frame width = 4.5 mm; cross polarized light); b) Photomicrograph of dense but aggregated, calcitic, shelly sand with indications of fine laminations, Marsalforn Pr 627, sample 3 (frame width = 4.5 mm; cross polarized light); c) Photomicrograph of calcitic, shelly sand with fine silt crust, Ramla Pr 626, sample 3 (frame width = 4.5 mm; cross polarized light); d) Photomicrograph of silty clay aggregate in the calcitic, shelly sand, Ramla Pr 626, sample 1 (frame width = 4.5 mm; cross polarized light).*

Table 5.12. *Summary of the main micromorphological observations from the Ramla and Marsalforn valley fill profiles.*

Profile and sample number	Micromorphology	Features and inclusions	Interpretation
Marsalforn Pr 626:			
626/1	Calcitic fine sandy loam with weakly developed sub-angular blocky ped structure	Common fine limestone gravel and shell fragments; rare silty clay soil aggregate	Weathered and hillwash eroded micritic soil and fine limestone gravel derived from Coralline Limestone bedrock up-valley/ upslope; with secondary ped formation; similar calcitic fabric to late Neolithic altered soil at Ġgantija
626/2	Calcitic fine sandy loam with well developed sub-angular blocky to columnar ped structure	Occasional fine limestone gravel and shell fragments	As above
626/3	Calcitic fine sandy loam with weakly developed sub-angular blocky to columnar ped structure	Few fine limestone gravel and shell fragments; occasional silt or silty clay crust or lens	Weathered and eroded micritic soil derived from Coralline bedrock up-valley/upslope; occasional surface exposure and rapid wetting/ drying events; with secondary ped formation
Ramla Pr 627:			
627/1	Calcitic fine sandy loam with well developed sub-angular blocky ped structure	Common fine limestone gravel and shell fragments; rare bone and plant fragments	Weathered/eroded micritic soil with secondary ped formation; stabilized alluvial valley fill
627/2	Calcitic fine sandy loam with well developed sub-angular blocky ped structure	Up to 50% fine limestone gravel, occasionally oriented horizontal; abundant shell fragments and rare bone fragment	Weathered/eroded micritic soil material with bioturbation and some weak secondary ped formation; stabilized alluvial valley fill
627/3	Aggregated micritic sandy loam with fine limestone gravel over dense, shelly, micritic fine sandy loam	Occasional laminar aspect; few fine limestone gravel in upper half, and shell fragments throughout	Weathered/eroded micritic soil material with/without bioturbation; episodic alluvial valley fill

and hearth rake-out material (Entwistle *et al.* 1998), as does the moderately enhanced magnetic susceptibility values, especially in the basal colluvial soil horizon. These features could be seen as an attempt to increase the fertility of these soil surfaces in the past, which is also reflected in the fine included anthropogenic debris visible in thin section.

Soil micromorphological analysis of three samples taken from the upper (1.75–2.10 m) and lower (2.70–3.10 m) incipient soils within this colluvial profile revealed highly calcitic, shell-rich, fine sandy loams with the sand-size component being almost entirely composed of fine, sub-rounded Coralline Limestone material (Table 5.12; Fig. 5.18c). There were minor amounts of silt and clay, very fine charcoal and organic matter fragments present, the occasional silt or silty clay crust (Fig. 5.18c), and the very occasional void infill or aggregate of a very fine sandy clay loam with a reticulate striated dusty clay component reminiscent of argillic (or Bt) horizon material (Fig. 5.18d), most probably eroded and incorporated in this colluvial profile. Nonetheless, each of these incipient soil levels exhibited a sub-angular to columnar blocky ped structure of greater and lesser expression, respectively, which implies some longer-term stability of these horizons in the profile. There is a general absence of anthropogenic inclusions, even very fine charcoal.

5.3.10. Micromorphological analyses of possible soil materials in the Xemxija 1, Wied Żembaq 1, Marsaxlokk and Salina Deep (SDC) cores

Recording and sampling of the intact sediment cores from Malta were undertaken in the laboratory in Queen's University Belfast by the authors, not in the field. Cores from Xemxija 1, Wied Żembaq 1, Marsaxlokk and the base of Salina Deep Core (21B) on Malta (Fig. 3.1) were selected from the larger assemblage of available cores as they appeared to contain possible buried soils and/or sequences of alluvial/colluvial sediments derived from eroded soils which could relate to prehistoric land-use and erosion in each associated valley catchment. In combination with the radiocarbon chronology, pollen and molluscan evidence from the same cores (see Chapters 2–4), these datasets should provide reliable data on the nature of landscape exploitation and land-use practices in each valley. In turn, these sequences should be comparable to the detailed molluscan and palynological studies from

several places on the islands and the geoarchaeological investigations carried out in the Ramla and Marsalforn valleys of Gozo (see §5.3.8 & 5.3.9).

Small 2 x 2 cm size cubes of sediment were taken judgementally from the cores for micromorphological analysis (after Bullock *et al*. 1985; Courty *et al*. 1989; Goldberg & Macphail 2006; Murphy 1986; Stoops 2003; Stoops *et al*. 2010) (Tables 5.13–5.17; Appendix 8). Twenty-five small blocks from Xemxija 1, thirteen blocks from Wied Żembaq 1, nine blocks from Marsaxlokk and three spot samples from the base of the Salina Deep Core (21B) were selected for micromorphological analysis.

5.3.10.1. The Xemxija 1 core

This core appears to be primarily composed of an upper *c*. 4.5 m of fine eroded soil as overbank alluvial deposition over *c*. 2 m of highly organic (black) silt mud, over overbank alluvial deposition in the form of *c*. 3.4 m of silt loam soil material, all developed on a *c*. 1.1 m thickness of aggrading eroded soil material at its base (Appendix 8; Table 5.13). The micromorphology of the core deposits is described in more detail below, as are the interpretative implications, from the base to the top.

Samples 25 to 18 in the basal *c*. 1 m of this 9.9 m Xemxija 1 core profile can be grouped together as they broadly share similar properties. This soil/sediment is a silty clay loam with some structure and organic component (Figs. 5.20a & b) which began to accumulate from at least 8780–8452 cal. BC (9353 BP; UBA-25001). Sample 25 (9.75–9.77 m) is characterized by humified plant tissue, very fine channels, and fine horizontally orientated bedding planes, but without pedogenic indicators of soil maturity with the exception of evidence for gleying. Sample 24 (9.65–9.67 m) is slightly more porous with slightly increased gleyic properties and associated humified plant tissue and hypo-coatings. Sparitic and micro-sparitic calcium carbonate and iron hydroxide pedofeatures suggest that oxidation and reduction phases had intensified. This trend increases in sample 23 (9.45–9.47 m) and the sediment/soil becomes more biologically active with abundant soil faunal excrements associated with root tissues. Sample 22 (9.25–9.27 m) shows similarities but is more intensely gleyed with horizontally bedded planes and abundant channels from about 6010–5840 cal. BC (7045 BP; UBA-31704). Sample 21 (9.13–9.15 m) is less gleyed with an increase in chambers and channels,

Table 5.13. *Main characteristics of the Upper and Lower Coralline Limestone, Globigerina Limestone, Blue Clay and Greensand (after Bianco 1993; Pedley* et al*. 1976, 2002).*

Geological source	Geological characteristics (youngest to oldest)	Mineral inclusions
Upper Coralline Limestone	Shallow marine limestone with abundant coral-algal mounds and reefs, commonly altered to micrite and sparite; hard but porous, crystalline, brittle and pale grey limestone; resistant to erosion but freshwater slowly dissolves the limestone and forms fissures; easily worked; the lower division is characterized by micrites and bio-sparites, with diverse included fauna and flora; the upper division is coarser, bio-clastic and oolitic limestones, rich in coralline algae	Carbonate clasts, silt-sized calcite, feldspar, dolomite, glauconite, apatite and haematite
Greensand	Bioclastic, friable, glauconitic argillaceous sandstone, deposited under shallow marine conditions; moderate permeability; poorly cemented; with iron oxides from weathering	Fine quartz sand and sand-size glauconite; cemented by silica, lime, clay and iron oxides
Blue Clay	Massive to bedded grey/blue shallow marine/offshore calcareous claystones with occasional to abundant marine fossils and planktonic calcium carbonate detritus; very soft; impermeable to water flow	Mainly fine grained carbonates and clay minerals; rich in alumina and very fine quartz silt and lime-rich fossil fragments; upper parts have increased glauconite and brown phosphatic sand grains
Globigerina Limestone	Shallow marine, calcareous mudrocks with abundant fossils, poor permeability, divided into three beds with two thin, harder phosphatic conglomerate beds characterized by francolite; the lower and middle Globigerina is pale yellow to pale grey, fine-grained limestone, bedded, and with globigerinid biomicrites; phosphorite pebbles in upper main conglomerate bed above; high percentage of planktonic foraminifera above indicative of deposition in shallow water in Upper Globigerina	Yellow to pale grey biomicrites, phosphatic pebbles and foraminifera; chert outcrops intercalate with Middle Globigerina Limestone
Lower Coralline Limestone	Shallow marine limestones with spheroidal algal structures and abundant echinoid fossils; well-cemented and permeable; hard and resistant; forms sea cliffs; yellow biomicrites rich in benthonic foraminifera with bedded, pale grey, Coralline Limestone above	Yellow bio-micrites; foraminifera

and sample 20 (8.68–8.7 m) returns to being more gleyed. Samples 19 (8.33–8.35 m) and 18 (8.23–8.26 m) are characterized by a significant increase in organic matter with large pseudomorphs and channels infilled with fine calcitic material and gypsum crystals. Sample 18 becomes more organic with much of the plant tissues horizontally bedded, but with iron-hydroxide hypo-coatings.

The humic components and several phases with hints of some soil structure and micro-lamination in samples 25–18 suggest that there have been repeated episodes of surface vegetation and stabilization, with greater/lesser effects of gleying. On balance, this appears to be slowly accumulating eroded soil material that has been affected by of calcium carbonate rich groundwater and strong seasonal drying.

Importantly, samples 25–18 appear to have a parent material that is very similar to the Blue Clay/Greensand geological substrates regularly found beneath the Upper Coralline Limestone in valley exposures across the Maltese Islands (Table 5.13; Figs. 5.19a & b). The assemblage of fine calcitic material is similar to that found in undisturbed deposits of Blue Clay from mid-upper-valley locations (Fig. 5.19a). The fine fossiliferous limestone material and gypsum could also be derived from the Globigerina Limestone outcrops in the base of many valleys, but there is an absence of foraminifera which would be more indicative of this substrate (Figs. 5.19d–f). In particular in sample 20 (8.68–8.70 m), there is the first occurrence of the mineral glauconite and very fine quartz sand (Fig. 5.19g) which suggests that soil material was being derived from the intersection of the Blue Clay and the Greensand through erosion. Considered together, this evidence strongly suggests that this material is coming from soils developed on several different lithologies and therefore spatially different loci within the Xemxija valley landscape. On the Globigerina Limestone today, the soils today are fertile, very fine sand, silt, alumina and calcium carbonate dominated or Leptic Calcisols (or xero-rendzinas) (*cf*. Lang 1960), but in the past may have been more of a Luvic Calcisol (or calcitic argillic soils). On the Blue Clay in the past, the soils would almost certainly have been classified as a Humic Leptosol (or rendzina soil type) (cf. Lang 1960). The soils on the Greensand zones up-slope would have had a lighter and well drained texture because of their higher sand content and consequently would have been easier to cultivate, and may also have been in response to the negative consequences of soil change and erosion of the soils which had developed on the Globigerina Limestone and Blue Clay. Secondly, glauconite is a source of potassium (Loveland & Findlay 1982), as is the Globigerina Limestone (Rehfeld & Janssen 1995), an important soil nutrient which would have resulted in increased yields when compared with the initial interaction of earlier Neolithic people with a variety of 'fragile' soils.

Above this first zone of eroded soil accumulation, there is a further *c*. 3.2 m accumulation of a fine, calcitic silt soil material (Fig. 5.20c) which contains occasional to frequent limestone fragments and pebbles, which is also indicative of overbank alluvial accumulation coincident with greater erosion and exposed limestone substrate surfaces in the immediate catchment. Interrupting this fine/coarse aggradation are at least three phases of a slowing in the aggradational dynamic with some organic accumulation and weak pedogenesis suggestive of incipient organic A horizon formation at 8.15–8.32, 6.7–6.85 and 6.0–6.3 m (Fig. 5.20d). These latter deposits essentially indicate a period of relative stabilization of the floodplain surface.

Figure 5.19 *(opposite). Photomicrographs of the Blue Clay and Greensand geological substrates from the Ramla valley (S. Taylor and C. French): a) Photomicrograph of the fine carbonate material impregnated with sesquioxides, well sorted very fine quartz and a few gypsum crystals in the Blue Clay, Ramla valley background sample (frame width = 1.25 mm; cross polarized light); b) Photomicrograph of the glauconite and carbonates in the Upper Coralline Limestone, Ramla Bay background sample (frame width = 4.5 mm; cross polarized light); c) Photomicrograph of the fine quartz sand, fine carbonate material and glauconite aggregates as opaque rounded sand, some of which are stained with iron oxides, in the Greensand, Ramla valley background sample (frame width = 1.25 mm; cross polarized light); d) Photomicrograph of the fossils and fine calcitic material of the Globigerina Limestone, background sample from Fungus Rock, Gozo (frame width = 4.5 mm; cross polarized light); e) Photomicrograph of the fine fossiliferous limestone material, Xemxija sample 23 (9.45–9.47 m) (frame width = 2.25 mm; cross polarized light); f) Photomicrograph of lenticular gypsum, Xemxija sample 23 (9.45–9.47 m) (frame width = 2.25 mm; cross polarized light); g) Photomicrograph of well sorted, very fine quartz and glauconite within a highly calcitic, massive structured groundmass, Xemxija sample 20 (8.68–8.7 m) (frame width = 1.25 mm; plane polarized light); h) Photomicrograph of mixed organic topsoil aggregates, silty clay aggregates, calcite, fine quartz, limestone clasts and glauconite, Xemxija sample 5 (3.02–3.04 m) (frame width = 4.5 mm; cross polarized light).*

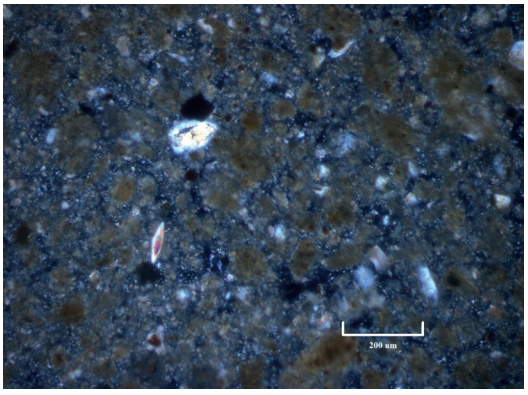

a

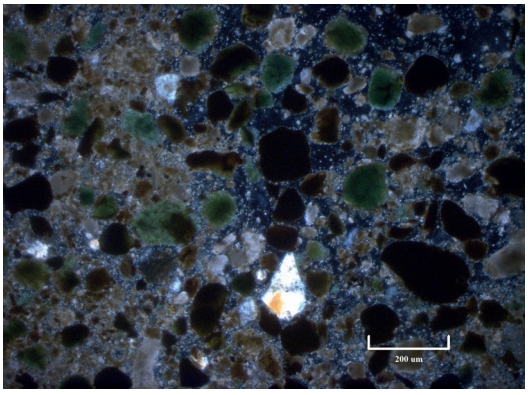

b

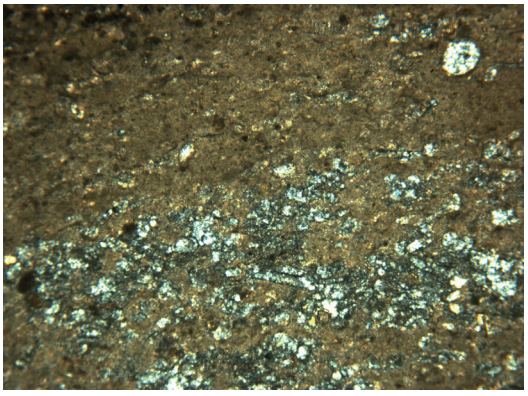

c

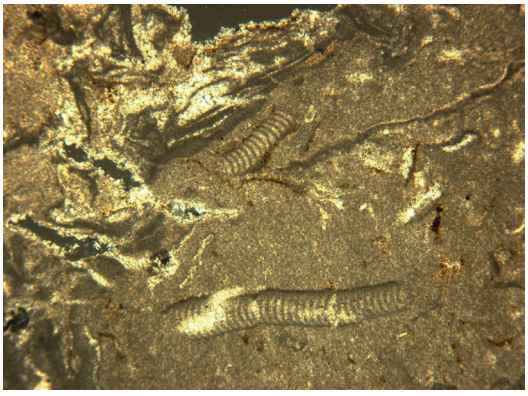

d

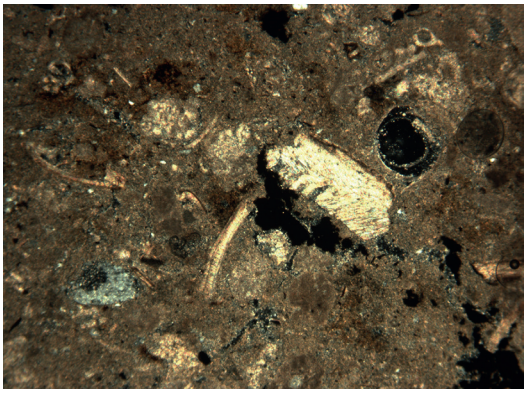

e

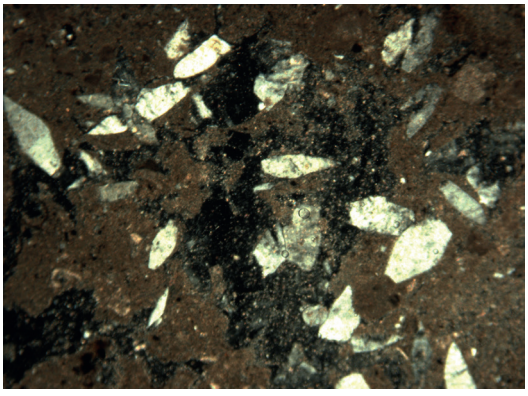

f

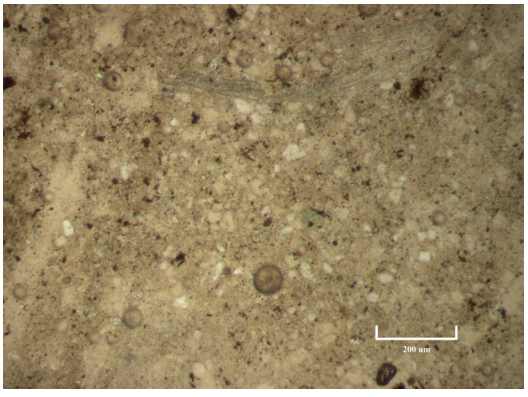

g

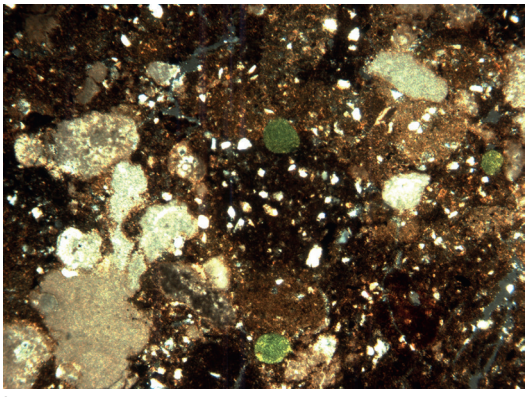

h

Table 5.14. *The summary micromorphological descriptions and suggested interpretations for the Xemxija 1 core.*

Sample number	Depth (cm)	C-14 dates cal. BC (2σ)	Micromorphology	Interpretation
1	199–201		Fine gravelly, micritic sandy clay loam, with few to common very fine organic/ charcoal punctuations	Eroded soil material?; very similar to the Ġgantija buried soil fabric; affected by evapo-transpiration and secondary micrite formation
2	220–223		Sub-angular blocky, fine gravelly, micritic sandy clay loam	As above, but slightly coarser substrate material included; highly alkaline; subject to wetting and drying
3	250–253		Mix of fine gravel, sand-size limestone and crumb structured minor micritic silty clay	As above, but coarser substrate material included
4	273–275		Very fine sandy clay loam with 10% very fine limestone gravel	Hillwash type material probably derived from the soils of the Upper Coralline Limestone plateau
5	302–304		Mix of very fine sandy clay loam and 25–50% very fine limestone gravel	Hillwash type material probably derived from the soils of the Upper Coralline Limestone plateau
	318	1290–450 BC		
6	335–339		Finely aggregated very fine sandy clay loam with up to 50% amorphous sesquioxide staining	Possible eroded topsoil, bioturbated and humified, derived from the soils of the Upper Coralline Limestone plateau
7	403–405		Micro-laminar very fine quartz and silt, strongly reddened with amorphous sesquioxides	Episodically aggrading fine alluvial sediments
	460	2198–1985 BC		
	460–543		Black organic silt mud to highly humified peat	Shallow, freshwater marsh
8	495–497		Horizontally bedded very fine quartz sand and silt with greater/lesser zones of amorphous sesquioxides and strong humic staining, but with <10% of striated clay soil fabric similar to sample 1; few limestone clasts and minor glauconite	Brief period of mixed, disturbed, eroded soil, probably derived from the Upper Coralline Limestone plateau, deposited in a moist marshy environment
	508	3709–3541 BC		
9	515–517		Very dark brown humic fine sandy/silty clay loam; striated b-fabric with rare to few dusty clay coatings with strong birefringence; 60% amorphous sesquioxide staining	Eroded soil derived from Luvisols of Upper Coralline Limestone plateau, deposited in a moist marshy environment
10	545–547		Very fine sandy/silt with strong sesquioxide staining of clay and calcitic groundmass; very fine organics and impregnated with calcite; strong sesquioxide staining; very fine quartz silt and glauconite from the Blue Clay, carbonate clasts may have come from the plateau areas	Fine organic and calcitic alluvial sediments, strongly humified; material derived from both the Blue Clay and Upper Coralline Limestone
11	578–580		Very fine sandy/silt with strong sesquioxide staining of clay and calcitic groundmass; very fine organics and impregnated with calcite; moderate sesquioxide staining; very fine quartz silt and glaucophane from the Blue Clay, carbonate clasts may have come from the plateau areas	Fine, organic and calcitic alluvial sediments, moderately humified; material derived from both the Blue Clay and Upper Coralline Limestone
12	610–612		Heterogeneous mix of shelly micritic very fine sand/silt and 10% charred plant matter	Fine alluvial sediments with shells and included fine charred matter
13	645–647	4050–3940 BC	Very fine sandy/silt loam with >50% strong sesquioxide staining and 10–15% charred plant remains and few gypsum crystals	Alternating wet/dry fine alluvial sediments with fine charred matter incorporated, and very strong humifying conditions

Table 5.14 *(cont.).*

Sample number	Depth (cm)	C-14 dates cal. BC (2σ)	Micromorphology	Interpretation
	670	4326–4053 BC		
14	685–687		Micritic very fine sandy/silt loam with >50% strongly amorphous sesquioxide staining	Alternating wet/dry fine alluvial sediments with fine charred matter incorporated, and strong wet/dry humifying conditions
	718	6401–6102 BC		
15	725–727		Micritic very fine to fine sandy clay loam with abundant organic matter and root tissues; *c.* 50% strong amorphous sesquioxide staining; gypsum crystals and calcium carbonate nodules	Fine alluvial sediments with fine charred matter incorporated, and strong wet/dry humifying conditions, possibly marshy; with sediment derived from Blue Clay/Greensand transition
16	772–774		Very humic, shelly, micritic silt with very strong amorphous sesquioxide staining	Lithological discontinuity; fine alluvial sediments with humic and fine charred matter incorporated; and strong wet/dry humifying conditions; first freshwater shells
17	785–787		Dark reddish brown, micritic, very fine sandy silt with strong amorphous sesquioxide staining throughout; presence of fine quartz silt, silt, glauconite and gypsum	Fine alluvial sediments with strong wet/dry humifying conditions; probably derived from upper Blue Clay/Greensand zone of valley
18	823–826	6417–6244 BC	Yellowish brown, micritic, very fine sandy silt with common strong amorphous sesquioxide replaced organic matter fragments; horizontally bedded plant tissues; large pseudomorphs; infilled channels; fine calcitic material and gypsum iron-hydroxide hypo-coatings	Rooted and bedded, fine alluvial sediments with strong wet/dry humifying conditions
19	833–835		Pale yellowish brown, micritic, very fine sandy silt; common organic matter with large pseudomorphs and infilled channels; fine calcitic material and gypsum	Fine alluvial sediments, with strong humifying and drying conditions
20	868–870		Yellowish brown/grey, micritic, very fine sandy silt with small, very weakly developed sub-angular blocky peds (<1 cm) with 10% organic punctuations; strong amorphous sesquioxide staining of groundmass; first appearance of glauconite and fine quartz sand of Greensand origin	Stabilized fine alluvial sediments with some pedogenesis and strong gleying; probably derived from upper Blue Clay/Greensand zone of valley
21	913–915		A more porous and less gleyed version of sample 20	Stabilized fine alluvial sediments with some pedogenesis with some gleying
22	925–927		Weak sub-angular blocky, pale brown, micritic silty clay, with abundant channels and bedding planes; strong amorphous sesquioxide staining of groundmass	Cumulative, stabilized fine alluvial soil with some pedogenesis and strong gleying
	933	7524–7197 BC		
23	945–947		As below with minor charcoal and amorphous sesquioxide replaced organic matter, root tissues and excrements	As below
24	965–967		As below	As below
25	975–977		Dense, homogeneous, pale golden brown, micritic silty clay with vertical fine channels and horizontal bedding planes, minor organic punctuations, humified plant tissue, and sesquioxide nodules and 20% amorphous sesquioxide staining of groundmass; quartz silt and fine calcite of Blue Clay origin	Alluvial silty clay soil; probably derived from upper Blue Clay zone of valley; with evidence of alternating groundwater and secondary calcification
	990			Base of valley fill

Sample 17 (7.85–7.87 m) is significantly different from the previous samples although there is some continuity in processes. There is a continued input of fine quartz silt, glauconite and gypsum, but there is a significant increase in concentration of silt and there is abundant fine humified organic matter. This suggests that the soil environment was becoming saturated but also aerobic, with a mineral assemblage is derived from the Greensand/Blue Clay boundary as below.

A major change in the system followed as shown by the accumulation of a thick zone of black humic mud between 5.65 and 4.05 m, after about 4326–4053 cal. BC (5357 BP; UBA-29041) and up to at least 2198–1985 cal. BC (3704 BP; UBA-28265). Sample 16 (7.72–7.74 m) marks a lithological discontinuity with the previous samples. It is entirely organic without the quartz silts and other mineral assemblage that is typical of all the samples encountered in the lower stratigraphy of the core. The groundmass is composed almost completely of humified organic matter giving the horizon its strong brown pigmentation, with a high component of molluscan shells.

Sample 16 (7.72–7.74 m) marks a major change in the environment with shallow freshwater conditions

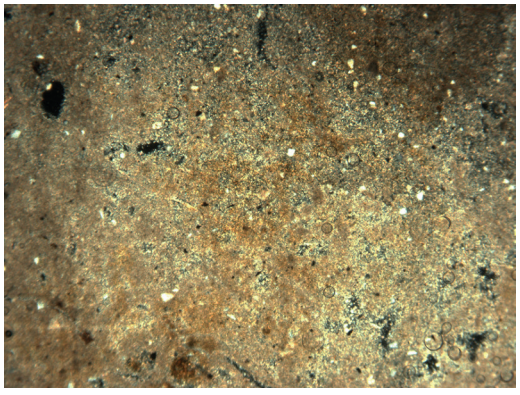
a

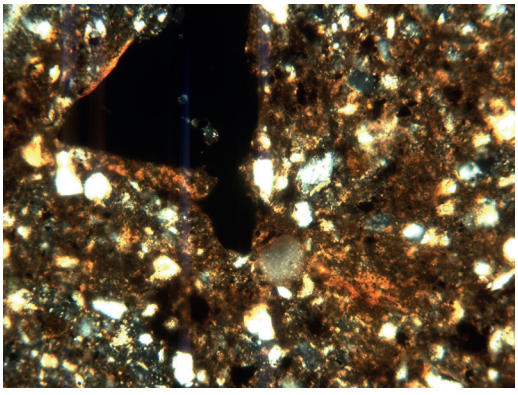
b

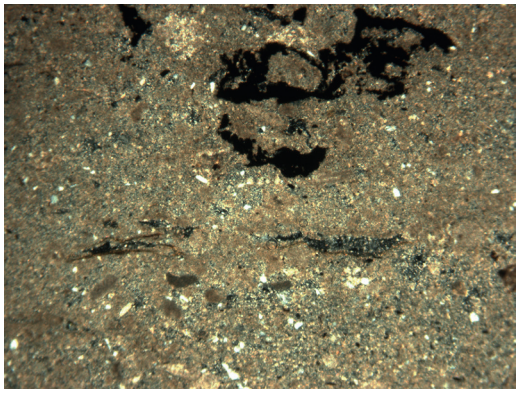
c

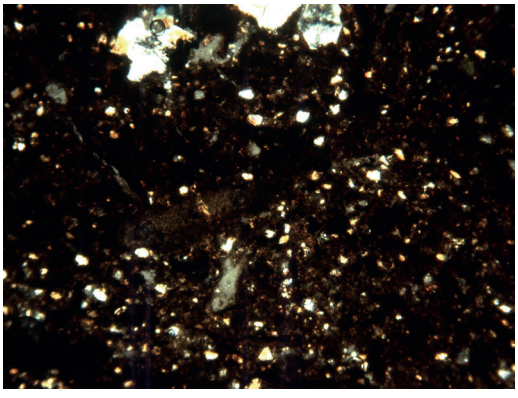
d

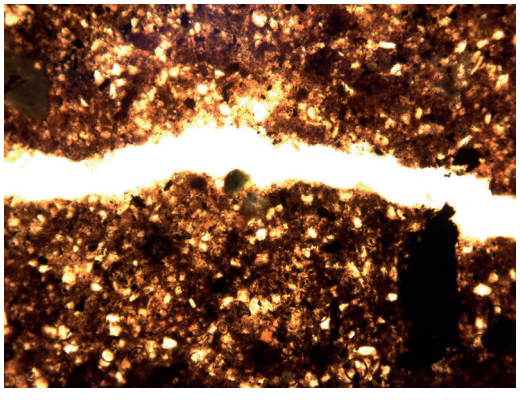
e

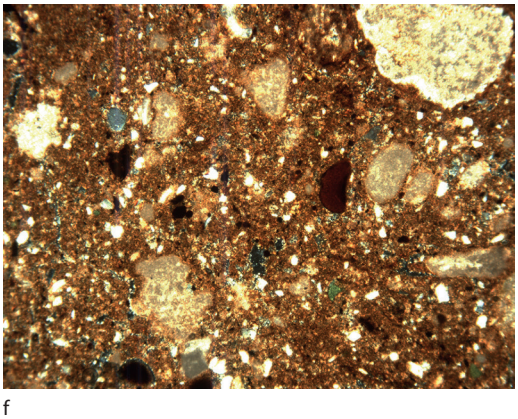
f

established with very little material coming into the system from soils within the valley catena. Perhaps this marks the initiation of a shallow freshwater marsh or lagoonal environment caused by sediment deposition along-shore, or perhaps an oxbow cut-off channel. This is corroborated by the molluscan data which suggest a continuing freshwater availability throughout the Neolithic, and then a major change towards the end of the Neolithic with a major erosion event (see Chapter 4). The cause of this change is unclear, but the environment was becoming significantly moister. If this were associated with increased precipitation, one would have expected greater sediment run-off, but this was not the case. Instead, there appears to have been greater stabilization of soils in the system and a greater availability of freshwater, perhaps from springs emanating from the geology (see Chapters 1 & 2) (Ruffell *et al*. 2018). Significantly this change appears to have coincided with the beginning of the Temple Period in the early fourth millennium BC. People were perhaps, for some unknown reason, interacting with soils differently for some unknown reason and this seems to correlate with the more patchy cereal cultivation observed in the pollen record at this time (see Chapter 3).

Subsequently, there was a return to fine alluvial silt accumulation, often subject to alternating wetting and drying conditions and the secondary formation of amorphous sesquioxides throughout the fabric (Fig. 5.20e). This phase of aggradation is interrupted by a period of relative stabilization at 3.19–3.35 m, a major coarser erosion phase (at 2.5–2.65 m) from *c*. 1300–450 cal. BC (3124 BP; UBA-31708), and then the uppermost *c*. 1.2 m accumulation of a calcitic silty clay as overbank alluvium (Fig. 5.20f).

Figure 5.20 *(opposite). Xemxija 1 deep valley core photomicrographs (C. French): a) Photomicrograph of the micritic silty clay at the base of the profile, Xemxija 1 core, 9.75 m (4.5 mm frame width; cross polarized light); b) Photomicrograph of the illuvial dusty (silty) clays in the voids and groundmass, Xemxija 1 core, 9.75 m (2.25 mm frame width; cross polarized light); c) Photomicrograph of micritic very fine sand/silt, Xemxija 1 core, 9.45 m (4.5 mm frame width; cross polarized light); d) Photomicrograph of humic fine sand/silt, Xemxija 1 core, 7.85 m (4.5 mm frame width; cross polarized light); e) Photomicrograph of amorphous sesquioxide reddened, fine sandy/silty clay alluvial fabric, Xemxija 1 core, 5.15 m (4.5 mm frame width; plane polarized light); f) Photomicrograph of the micritic, coarse to very fine sandy silty clay alluvium, Xemxija 1 core, 1.99 m (4.5 mm frame width; cross polarized light).*

Samples 15–12 can be grouped together. Sample 15 (7.25–7.27 m) contains abundant organic matter and root tissues within a highly calcitic sediment with large crystals of gypsum. The latter may have probably formed *in situ* through rapid drying although some of this will have come from the Blue Clay. There are large nodules of calcium carbonate that were pedogenically formed indicating not only the calcareous nature of this soil, but that sufficient drying was taking place during the year. The sediment has a relatively high porosity with inter-connecting chambers, dense clusters of faunal excrements, excremental infillings, organic punctuations and fragments of molluscs that all indicate severe bioturbation. Samples 14–12 (6.85–6.87, 6.45–6.47 & 6.10–6.12 m) are very similar with the addition of horizontally bedded organic plant tissue.

The molluscan assemblage at the same level in the core (see Chapter 4) indicates moist environmental conditions. Nonetheless it is still a dynamic environment with the presence of silt-sized quartz suggesting a re-establishment of sedimentation derived from the Blue Clay geology upslope. Radiocarbon dating of 4050–3940 cal. BC from sample 13 (5179 BP; UBA-31705) and a date of 4326–4053 cal. BC (5357 BP; UBA-29041) between samples 13 and 14 at 6.7 m suggest that this occurred just before the start of the Temple Period.

Samples 11–8 can be broadly grouped together. Samples 11 (5.78–5.8 m) and 10 (5.45–5.47 m) are a fine sandy/silt that is dominated by very fine organics and impregnated with calcite. The micromass of a brown speckled Fe-impregnated clay and calcitic crystallitic b-fabric suggest that the major component was topsoil material, although highly transformed through the process of transport and deposition. The planar microstructure and horizontal orientation of voids shows that this had been emplaced relatively rapidly, although plant tissue fragments associated with excremental fabrics within many of the voids indicate a biologically active cumulic soil. Significantly, the mineral composition of these samples suggests that there were several potential sources of the eroded soils and a significant transformation in terms of the sediment source. For the first time in the core relatively large and heterogeneous rounded carbonate rock fragments can be observed within the groundmass. The very fine quartz silt and glauconite (Fig. 5.19g) indicate a sediment source of the Blue Clay/Greensand transition, and the carbonate clasts may have come from the Upper Coralline Limestone bedrock (Fig. 5.19b) just above which is forming the plateau areas. Considered together, this evidence suggests that there was greater activity across more extensive parts of the landscape.

Sample 9 (5.15–5.17 m) is very dark in colour and is composed predominantly of fine organic material

with a high proportion of silt and sands. The groundmass is heterogeneous with a diverse fabric including aggregates of topsoil and subsoil material, and abundant fine amorphous fines exhibiting very strongly striated b-fabrics have been preserved in the weakly crystallitic b-fabric of the groundmass. These must be remnant aggregates of former topsoils and argic horizons that have been transported as sediment down-valley. These features suggest that these eroded soils had once developed on the Upper Coralline Limestone bedrock plateau under moister conditions were Luvisols, as was also concluded for the Santa Verna and Ġgantija palaeosols described above (see §5.3.2.2 & 5.3.3.3). Superimposed on this fabric are moderately impregnated, orthic, dendritic, iron-hydroxide nodules, also indicating a moist environment during their deposition. This remarkable evidence suggests that the evolution of the soil system on Malta occurred just before 3709–3541 cal. BC (4873 BP; UBA-29349) during the beginning of the Temple Period.

Sample 8 (4.95–4.97 m) is characterized by horizontally bedded very well sorted quartz silt in an organic amorphous groundmass with a high proportion of pedogenic clay in the form of striated b-fabrics, a high organic component, a small amount of glauconite, and very few carbonate clasts, larger limestone rock fragments and subsoil aggregates. The organic nature of these indicates that the soils had been forming in a relatively moist environment and elements of the whole soil profile were being eroded and deposited in the valley. Significantly the glauconite and silt components could also have been derived from the Upper Coralline Limestone plateau as could the wind sorted silt loess.

The micromorphological analysis indicates that a relatively organic rich topsoil had formed. Perhaps there had been an improvement of the soils of the plateau and this section of the core shows that people were exploiting them for arable agriculture. This was occurring just before approximately 2198–1985 cal. BC (3704 BP; UBA-28265) towards the beginning of the Bronze Age. Therefore, this is interpreted as the first stage of erosion of the rejuvenated soils of the Upper Coralline Limestone, and the interpretation is corroborated by the enriched A horizons observed in several late Temple–early Bronze Age contexts (see §5.3.2.2 & 5.3.3.3) causing the down-slope movement of organic-rich topsoil which accumulated at the base of the valley. Subsequent erosion led to the deposition of much coarser material as revealed higher in the core.

Samples 7–4 can be grouped together. Sample 7 (4.03–4.05 m) is a micro-laminar very fine quartz sand and silt, strongly reddened with amorphous sesquioxides. Sample 6 (3.35–3.37 m) is a finely aggregated, very fine sandy clay loam with up to 50 per cent amorphous sesquioxide staining. The fine organic amorphous organic component of the micromass contains abundant silicate clay mixed in with small aggregates of humic topsoil and subsoil (Fig. 5.19h). There is little evidence for fine laminations although there are some horizontal planes suggesting sedimentation. Sample 5 (3.02–3.04 m) has a mineral component that is heterogeneous with a significant increase in carbonate clasts and clay-rich subsoil aggregates derived from the Luvisols on the plateau, and dark topsoil aggregates. The mineral assemblage is all typical of the Upper Coralline Limestone so we can be very confident as to the provenance of this sediment. Sample 4 (2.73–2.75 m) is very like sample 6 with generally fine material and the same silt component, small subsoil aggregates and the presence of silicate clay.

These features indicate that the rate of erosion had greatly increased. Soils have lost part of their upper profile as well as striated b-fabrics of the B horizon and subsoil material, all of which had developed on the Upper Coralline Limestone. These plateau soils were now being seriously eroded, probably as a result of arable agriculture. The amount of regolith and the heterogeneous nature of the fabric suggest that ploughing had been responsible for the initial dislodgement of the soil before its subsequent erosion. The one radiocarbon date from this approximate depth in the core of 1290–450 cal. BC (3124 BP; UBA-31708) suggests that this period of greater disruption in the landscape occurred in later prehistoric times, a feature which is seen repeatedly in many of the valley deep cores (see Chapter 2).

In sample 3 (2.5–2.53 m) there is a significant change with a much greater component of abraded rock clasts of up to 1 cm and subsoil aggregates containing illuvial clay and an increase in silt-sized calcium carbonate and fine charcoal fragments. These features indicate that drier calcitic soils had developed, as observed at several Temple Period sites (see §5.3.2.2 & 5.3.3.3), probably associated with a change in the soil water balance through cultivation, generally greater anthropogenic disturbance, and relatively higher energies to move this material. It is clear that the plateau soils are becoming extensively degraded, most probably though tillage.

Sample 2 (2.2–2.23 m) is similar to sample 3 with the primary difference that the mineral assemblage is slightly coarser. It exhibits a massive microstructure with associated low porosity of void planes, and all the rock fragments, whether it be glauconite or limestone, are very well rounded and moderately sorted. This is colluvial sediment, either derived from the greater erosion of the regolith and higher energy bringing

material into the valley or from erosion of the immediate upland down to the bedrock (Alberts *et al*. 1980; Mucher *et al*. 1972, 2010).

Significantly there is abundant silt-sized angular quartz present in sample 2. It is probably derived either from the weathering of the Coralline Limestone bedrock or drawn from a significant aeolian component of the soils which were emplaced upon these rocks (Hunt 1997). However, a proportion of this material could also derive from the Greensand as there is also a large quantity of glauconite, although this too also can be derived from the weathered limestone (Felix 1973). Haematite has been inherited from the subsoils of the plateau where it had formed *in situ* as a result of soil forming processes (Lindbo *et al*. 2010; Yaalon 1997). There are several other pedofeatures which indicate soil processes which had been in operation. For example, the amorphous iron-impregnative nodules indicate wetting and drying caused by a fluctuating groundwater table (Lindbo *et al*. 2010). The system is highly alkaline with dissolution and re-precipitation of calcium carbonate (Durand *et al*. 2010). As a consequence, the entire groundmass is calcitic. The stipple speckled fabric indicates clay, derived from the former soils of the plateau, although not to the same degree, perhaps indicating that some fine particles have been removed from the system altogether.

Sample 1 (1.99–2.10 m) is a fine gravelly, calcitic sandy clay loam with a low porosity, rich in clay, some silt, a few rounded grains of glauconite, and occasional limpid clay adhering to the gravel fraction (Fig. 5.20f). Redox features indicate the effects of a fluctuating groundwater table (Lindbo *et al*. 2010). It is clear that this deposit is derived from soil material that had formed on the Upper Coralline Limestone plateau (Lang 1960) as well as from the Greensand geological strata immediately above the Blue Clay (Pedley 1976), with an almost certain aeolian material which was incorporated into the soils and then subsequently moved down the valley as colluvial fill.

5.3.10.2. Wied Żembaq

The Wied Żembaq 1 core profile (samples 26–38) is dominated by the aggradation of *c*. 5.6 m of coarse to fine alluvial material from about 3331–2920 cal. BC (4428 BP; UBA-28263; at 4.95 m) until some time after 913–806 cal. BC (2707 BP; UBA-29042; at 2.15 m), associated with pollen evidence of cereal crops, disturbance and grazing land (see Chapter 3; Appendix 8; Fig. 5.21a). This alluvial material is developed on what looks like cumulative eroded soil material. In at least two phases (at 3.8–4.2 and 4.8–5.6 m), this alluvial dynamic changes to one of shallow standing water and the accumulation of organic remains, with minimal alluvial input (Fig. 5.21b). At 3.5–3.62 m, there is a phase of severe hillwash erosion leading to the accumulation of bedrock derived fine gravel-size limestone material in the core. In the other fine alluvial phases, which constitute the bulk of the stratigraphic record here, there are often indications of fine episodic variations in the aggradation of fine material and intermittent drying out of the deposits accompanied by the formation of secondary amorphous sesquioxides (Fig. 5.21c). There are also strong hints of interruptions in the erosive sequence with incipient soil formation at depths of *c*. 3.0, 3.65, 4.33 and 5.28 m, with some sub-angular blocky ped formation, illuvial silty clays (Fig. 5.21d) and moderate to strong reddening with amorphous sesquioxides, all suggestive of some relatively short-lived phases of gleying and pedogenesis. These 'quieter' episodes may equate with periods when pastoralism became more predominant within the associated valley catchment (see Chapter 3).

At the base of the core in sample 38 (5.28–5.3 m), there is a reddish brown, calcitic, coarse-very fine sandy/silty clay with a great amount of quartz silt, minor very fine charcoal and a heterogeneous assemblage of mainly rounded carbonate rocks that have been rolled and abraded. There is evidence for excrements, crumbs and granules which are characteristic of topsoil or Ah aggregates as well as chambers and channels, often containing highly humified organic matter. This had been a relatively moist environment because there is a good preservation of tissue and other organics although highly humified as well as minor fine charcoal. The entire fine fabric is impregnated with calcite indicating the precipitation of carbonate rich soil water. The presence of iron nodules also suggests a fluctuating groundwater table. This sample/horizon is indicative of an aggrading, cumulic topsoil with characteristic biological activity formed on limestone parent material. The size and shape of this soil material represents loessic material that had been incorporated into the soils on the valley slopes, but was easily erodible. The included glauconite and carbonate clasts indicate that the parent material derived from the Upper Coralline Limestone geology.

Sample 37 (4.96–4.98 m) is very similar to sample 38 below, although there are some differences. It is more porous with a higher prevalence of better preserved plant tissues but these are still highly humified. There is a high proportion of silt and smaller carbonate clasts, with the mineral component fining-upwards. There are iron-hydroxide nodules suggesting a fluctuating water table. It almost certainly represents an aggrading, organic and biologically active topsoil but with slightly lower energies for the erosional processes up-profile.

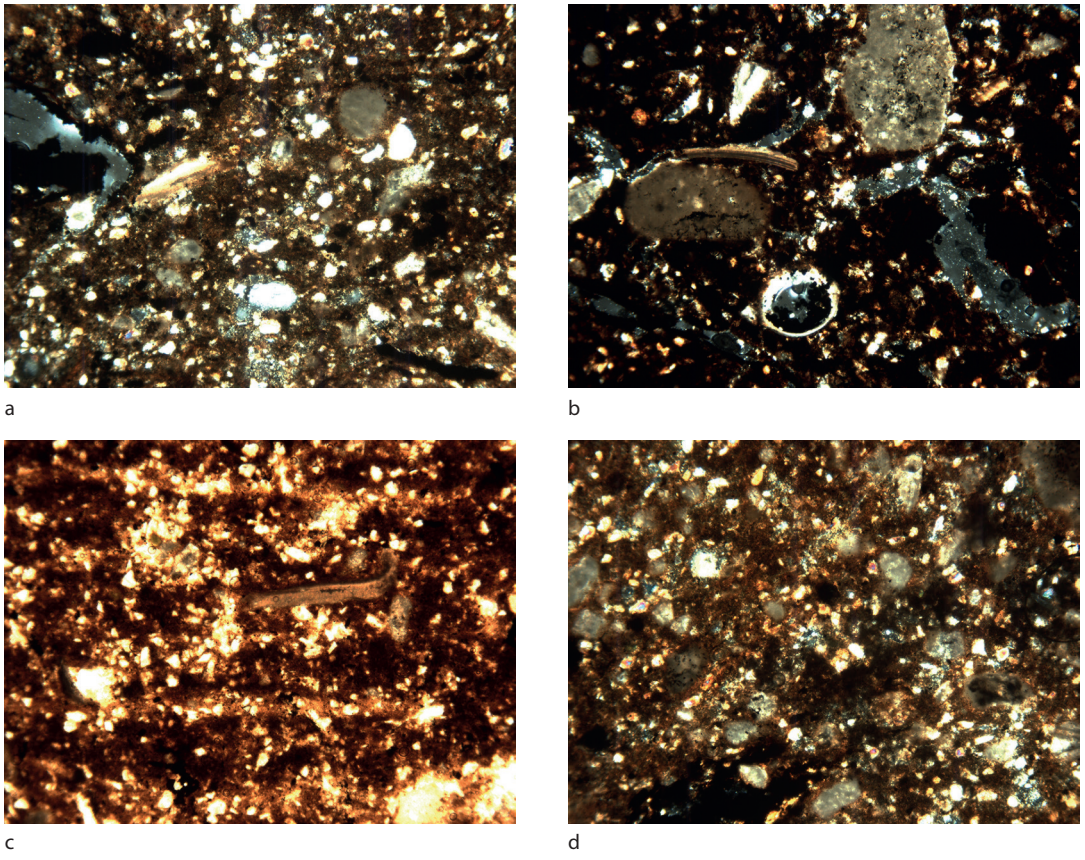

Figure 5.21. *Wied Żembaq 1 deep valley core photomicrographs (C. French): a) Photomicrograph of coarse to fine sandy clay loam at the base of the profile, Wied Żembaq 1 core, 4.96 m (4.5 mm frame width; cross polarized light); b) Photomicrograph of organic accumulation, Wied Żembaq 1 core, 4.6 m (4.5 mm frame width; plane polarized light); c) Photomicrograph of episodic, micro-laminar, fine/very fine alluvial deposition, Wied Żembaq 1 core, 3.0 m (4.5 mm frame width; cross polarized light); d) Photomicrograph of illuvial dusty clay, sesquioxide formation and humic accumulation in incipient soil horizons within the alluvium, Wied Żembaq 1 core, 4.33 m (4.5 mm frame width; cross polarized light).*

Sample 36 (4.6–4.61 m) is also a highly organic soil with a slightly reduced input of carbonate rock clasts and quartz silt, but there is great humification of organics and excrements associated with a very biologically active soil, and the first formation of neo-formed gypsum. There is also common calcium carbonate in the calcitic fabrics of the groundmass and in the precipitated calcite crystals in many of the voids. This is probably an incipient histic soil horizon where there is the growth and humification of organics and a high groundwater table. The gypsum is formed through a chemical reaction between calcium carbonate and sulphur compounds in the organic component (Poch *et al*. 2010), which suggests a very moist environment combined with high rates of evaporation.

The upper surface of this cumulative soil profile appears to have developed just before 3631–3373 cal. BC (4707 BP; UBA-28262; at 4.58 m). Significantly this evidence strongly suggests that soils developed on the Upper Coralline Limestone are being eroded during this period in a manner that is consistent with evidence from the Xemxija core, all during the Neolithic Temple period.

Sample 35 (4.33–4.35 m) is similar to the previous samples of this core. It is composed of a golden/reddish brown, coarse-very fine sandy/silty clay with a large input of now humified organic material, with horizontally orientated bedding planes and a small blocky ped structure. There is a strong quartz silt component, again indicative of a loessic component. Re-precipitated calcium carbonate is common, and there are many included carbonate clasts. The presence of gypsum indicates not only a moist environment but also evaporation of soil water and the reaction of sulphides with calcium carbonate (Poch *et al*. 2010).

Sample 34 (4.1–4.12 m) is almost exclusively organic with some very fine quartz silt and a small component of carbonate rock clasts. This sample represents

Table 5.15. *The summary micromorphological descriptions and suggested interpretations for the Wied Żembaq 1 core.*

Sample number	Depth (cm)	C-14 dates cal. BC (2σ)	Micromorphology	Interpretation
26	7–9		Excremental to aggregated, porous, brown/humic, highly micritic, coarse-very fine sandy/silty clay with minor very fine charcoal	Modern alluvial topsoil, subject to strong humification and drying
27	45–7		As above	As above
28	80–2		Golden brown, micritic, coarse-very fine sandy/silty clay with illuvial silty clay infills, carbonate clasts and limestone gravel, iron hydroxide coatings and nodules, fine charcoal and bone fragments	Base of modern alluvium (as above) with periods of standing/drying water conditions
29	215–7	913–806 BC	Fine gravelly, reddish brown, micritic, coarse-very fine sandy/silty clay with minor very fine charcoal	As above, but greater energy/erosive input of coarse to fine material; possibly greater input from Upper Coralline Limestone plateau
30	253–5		Fine gravelly, golden/reddish brown, micritic, coarse-very fine sandy/silty clay with illuvial silty clay in voids, humified organic matter, gleyic features and carbonate nodules	Eroded soil material of slightly higher energy with high evapotranspiration
31	300–302		Small blocky to aggregated, golden/reddish brown, micritic, very fine sandy/silty clay, with illuvial silty clay infills and weakly laminar micro-structure	Fine, episodic stop/start eroded mix of topsoil and subsoil material; derived from the Upper Coralline Limestone plateau
32	365–7		As below with some horizontal bedding and gleying	As below; biologically active cumulic soil
33	396–8		Golden brown, micritic, coarse-very fine sandy/silty clay with illuvial silty clay infills, glauconite and carbonate clasts, plant tissues and excremental fabric	Sandy/silty clay aggrading alluvium with periods of standing/drying water conditions; derived from the Upper Coralline Limestone plateau
34	410–2		Humified and amorphous sesquioxide replaced organic matter with minor very fine quartz silt and carbonate clasts	Shallow standing water and organic, humified peat-like accumulation
35	433–5		Small blocky and finely bedded golden/reddish brown, coarse-very fine sandy/silty clay with common humified organics and very fine quartz silt	Coarse-fine alluvial aggradation with loessic additions, subject to some pedogenesis and becoming an alluvial soil
	458	3631–3373 BC		
36	460–1		Porous, very humified and amorphous sesquioxide replaced organic matter with coarse-fine limestone/quartz, micrite and gypsum	Histic organic horizon at the top of the cumulic soil with high groundwater and evapotranspiration
37	496–8		As below with greater humic matter, plant tissues and carbonate clasts	Aggrading alluvium forming a cumulic A horizon soil with periods of standing/drying water conditions, but greater energy/erosive input of coarse to fine material
38	528–30		Reddish brown, micritic, coarse-very fine sandy/silty clay with rounded carbonate gravel and glauconite, humified plant tissue and minor very fine charcoal	Aggrading coarse to fine alluvium forming a cumulic A horizon soil subject to a fluctuating groundwater table; derived from the Upper Coralline Limestone plateau

a very wet, calcareous environment where there is the growth of peat, which is amorphous because of frequent oxidation and seasonal hydrological variation.

Sample 33 (3.96–3.98 m) is quite different to the previous samples. It is quite porous with less organic pigmentation than the other samples below, but it is biologically active as seen in the amount of plant tissue and excremental fabrics within the voids. There is abundant micro-sparite calcium carbonate, plus quartz silt, glauconite and carbonate clasts, indicative of an origin from the Upper Coralline Limestone.

Sample 32 (3.65–3.67 m) is similar to sample 33 in terms of the aggregates and crumbs, silt and carbonate clasts component, but it is exhibiting some

horizontal orientation and gleying. This soil material is a biologically active, cumulic topsoil with some evidence for sedimentation and slightly gleyic properties suggesting that there was a fluctuating groundwater table in the valley hydrology.

Sample 31 (3.0–3.02 m) it is very similar to sample 32. It is composed of topsoil aggregates, crumbs and granules with humified root tissues and organic punctuations, and strong amorphous iron-humic compounds because of recycling of organic matter. There are rounded clasts, although less than the previous samples, micro-sparitic calcium carbonate, and the same quartz silt component which suggests that this material is derived from the Upper Coralline Limestone exposures up-valley. The main difference between this and the previous two samples is the presence of a significant component of illuvial silicate clay within the soil aggregates which have formed from luvisolic subsoil parent material. Perhaps this is indicative of subsoil material being eroded and transforming into topsoil aggregates with superimposed humic compounds.

Sample 30 (2.53–2.55 m) is somewhat different from the previous samples as it is significantly more calcareous with heterogeneous rock clasts. There are abundant shell and plant tissue fragments with chambers and channels, calcium carbonate nodules throughout the groundmass, illuvial silty clay void infills, and gleyic pedofeatures. Thus this biologically active material has high evapo-transpiration despite a fluctuating groundwater table, all deposited in a slightly higher energy sedimentary environment.

Sample 29 (2.15–2.17 m) exhibits much coarser carbonate rock clasts and limestone gravel in a heterogeneous mix with a calcitic sandy/silty clay and minor included fine charcoal and bone fragments. Again, there are iron-hydroxide coatings and nodules indicating a fluctuating groundwater table. Perhaps this heterogeneous horizon indicates that regolic subsoils developed on the Coralline Limestone geology were coming into the sedimentary system through the intensification of human interaction with soils on the limestone plateau up-valley, as observed in the Xemxija core during the latter part of the Bronze Age. A radiocarbon date of 913–806 cal. BC (2707 BP; UBA-29042) for this level lends corroboration to this suggestion.

Samples 28–26 (80–82, 45–47 & 7–9 cm) can be grouped together because of their similar properties. These samples all exhibit a slightly different structure to the previous samples with a porous crumb and excremental structure with channels containing humified tissues. The brown fine material indicates humification and brunification of organic matter. The entire system is highly calcareous and shows that calcification is a dominant soil process through the evaporation of calcium rich soil water. These features suggest that this is well developed topsoil horizon with surface vegetation formed in relatively stable conditions.

5.3.10.3. Marsaxlokk

A series of 29 small blocks were taken from this core for thin section analysis to characterize its deposits and examine the stratigraphy for evidence of eroded soil material (Appendix 8).

The basal sample 47 (3.65–3.67 m) is a very pale yellow calcitic silty clay with slight indications of gleying (Fig. 5.22c). It is 100 per cent carbonate material with no porosity and a massive microstructure. It probably represents an *in situ* weathered geological formation of the Blue Clay.

Sample 46 (3.2–3.22 m) contrasts with the previous sample. This is a dark reddish brown fine sandy/silty clay with a well developed angular blocky microstructure and a high proportion of silicate clay (Fig. 5.22a). Micro-sparitic calcium carbonate pervades the fine fabric and coats channels, and there is strong staining with amorphous sesquioxides consequent on a high and fluctuating groundwater table. This fabric represents is a luvisolic (or *terra rossa*) soil which has taken time to develop in a stable environment, coincident with clay illuviation which has moved down the soil profile. It has developed through the chemical weathering of minerals, either already present in the parent material or as an aeolian component. There are some carbonate fragments showing that there is material coming from a limestone environment and very fine quartz silt. It forms a lithological and pedogenic discontinuity with the previous sample.

Sample 45 (2.96–2.99 m) is very similar to sample 46 below. It has a very well developed angular blocky microstructure with a high porosity with very large planes separating the peds. It has a silt component, abundant micro-sparitic calcium carbonate throughout, and some small carbonate clasts. The defining feature of this one is the evidence for intense calcium carbonate presence in the peds and in smaller aggregates. Fragments of the ped clasts can be seen within carbonate nodules. This shows that the entire system was moving from a de-carbonated soil environment to one dominated by calcium carbonate. There are dense infillings of sparitic and micro-sparitic calcium carbonate and hypo-coatings. All of the peds are decalcified and exhibit illuvial silty clay. These soils formed in relatively humid environments. There is repeated transpiration and re-calcification in this soil either because of changes in climate and/or vegetation complex.

Sample 44 (2.55–2.57 m) is very similar to sample 45. The main difference is that peds are larger and more well developed, and there is a greater abundance of larger carbonate rock fragments indicating an input of eroded soil material from a limestone area. It is slightly browner suggesting some organic pigmentation through humification. Although this sample is still highly calcareous, there are striated b-fabrics indicative of luvisolic properties. Sample 43 (2.15–2.17 m) is similar to sample 44, except that there is little quartz silt, perhaps indicating that the availability of loessic deposits on the valley sides in the catchment is declining. There are impregnative redox gleyic features suggesting a perched groundwater table (Lindbo *et al.* 2010).

Sample 42 (1.70–1.72 m) is very different to the previous samples and represents a lithological and pedogenic discontinuity. This is a highly calcitic and organic sediment with the organic material displaying horizontal bedding (Fig. 5.22d).

Sample 41 (1.10–1.12 m) exhibits a massive microstructure, calcareous very fine quartz silt and gleyic properties with iron-stained fines. It contains very few minerals except the characteristic very fine quartz typical of the Blue Clay geology, as does sample 42 below. This thin section shows little soil development and probably reflects a very unstable sedimentary environment.

Sample 40 (62–66 cm) is formed from a heterogeneous mixture of different parent materials, namely from carbonate rock clasts and subsoil aggregates (Fig. 5.22b). These show strongly striated fabrics indicating illuvial clay with calcitic infillings. There are channels with remains of plant tissues, and it has been a biologically active. Iron nodules are present suggesting that there has been a fluctuating groundwater table. This material probably represents hillwash erosion from diverse and spatially extensive parts of the landscape.

Sample 39 (5–6 cm) is a brown pigmented, porous soil with a crumb and granular microstructure and plant tissue fragments and excrements in the voids which suggests that it was a biologically active topsoil. The entire fine fabric is highly calcitic and there are also redox pedofeatures suggesting a fluctuating

Table 5.16. *The summary micromorphological descriptions and suggested interpretations for the Marsaxlokk 1 core.*

Sample number	Depth (cm)	C-14 dates cal. AD (2σ)	Micromorphology	Interpretation
39	5–6		Finely aggregated, vughy, brown calcitic silt with limestone clasts	Eroded, bioturbated, xeric, calcitic silt topsoil and subsoil derived from the Upper Coralline Limestone
40	62–6		Mix of dense, pale grey weathered limestone and calcium carbonate with illuvial silty clay, iron nodules and plant tissues	Hillwash derived material from a variety of sources in the catchment
	86	AD 419–556		
41	110–2		Massive, pale grey weathered limestone and calcitic silt with minor gleying	Eroded, weathered calcitic material associated with bare surfaces upslope
	155–165		Lens of fine gravel and coarse sand	High energy erosive event
42	165–172		Micro-laminar humified and amorphous sesquioxide replaced plant remains	Repeated fine accumulations of humified plant remains under alternating wet-dry, marshy conditions
	186–192		Lens of fine gravel and coarse sand	High energy erosive event
43	215–7		Well developed sub-angular blocky structured, reddish brown, coarse to very fine sandy/silty clay loam	Aggrading alluvial soil, derived from erosion of luvisols/*terra rossa* soils of the Upper Coralline Limestone area in catchment
44	255–7		Well developed sub-angular blocky structured, reddish brown, calcitic, coarse to very fine sandy/silty clay loam	As above
	286	AD 435–670		
45	296–9		Well developed sub-angular blocky structured, reddish brown, coarse to very fine sandy/ silty clay loam with carbonate clasts and fine limestone gravel; at 286–292 cm lens of fine gravel/coarse sand	As above; with high energy erosive event interrupting soil formation at 286–292 cm
46	320–2		As above	As above
47	365–7		Dense amorphous calcium carbonate	Weathered B/C horizon of Blue Clay

groundwater table. There are poorly sorted fossils and limestone clasts which suggests that the parent material is carbonate rock of the Upper Coralline Limestone.

Thus, this core has a different character than the Xemxija and Wied Żembaq cores. It also aggraded much later in historic times, from at least cal. AD 435–670 (at 2.86 m; 1444 BP; UBA-29351). In this case, there is a well developed, *c*. 40 cm thick, reddish brown, sandy/silty clay loam, *terra rossa*-like soil at its base. It exhibits a well developed small, sub-angular blocky structure, and its groundmass is dominated by a weakly calcitic, silty clay with moderate to strong amorphous sesquioxide reddening. Above this soil, there was an episode of fine gravel and coarse sand deposition at 2.86–2.92 m, and again at 1.55–1.65 m. These latter deposits are both suggestive of relatively high energy erosive events, associated with bare rock surfaces in the catchment. There is a brief paludal, organic silt mud phase at 1.65–1.7 m, followed by the accumulation of massive calcitic fine quartz silt, possibly derived from the Blue Clay mid-slopes, and then a mixed material of calcitic silt, humic matter and illuvial clay suggestive of a variety of erosional influences from different parts of the valley hinterland.

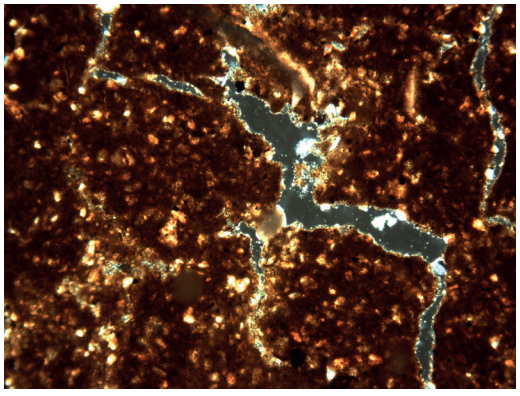

a

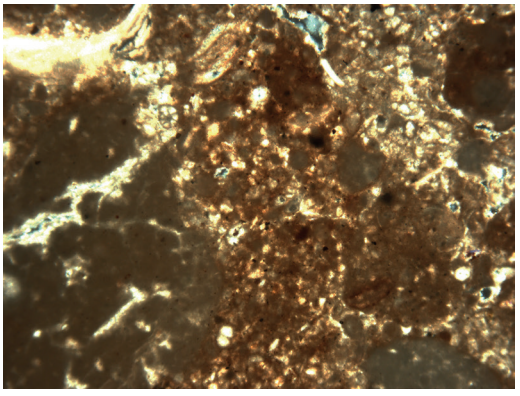

b

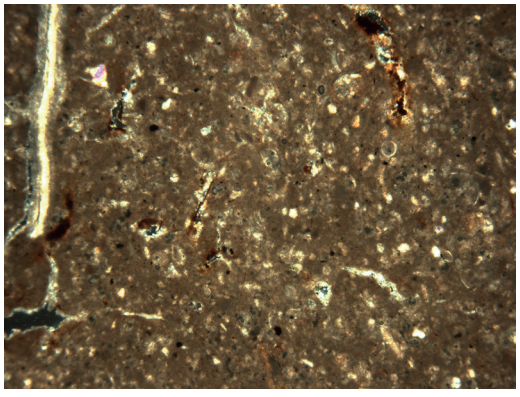

c

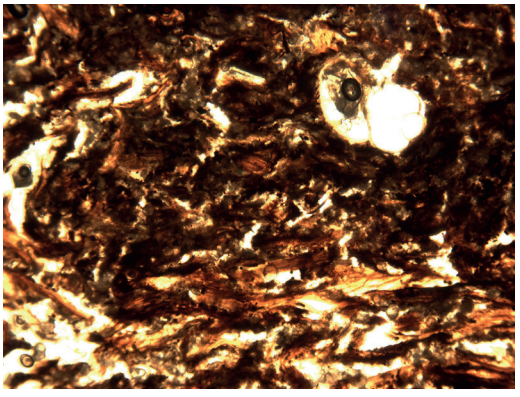

d

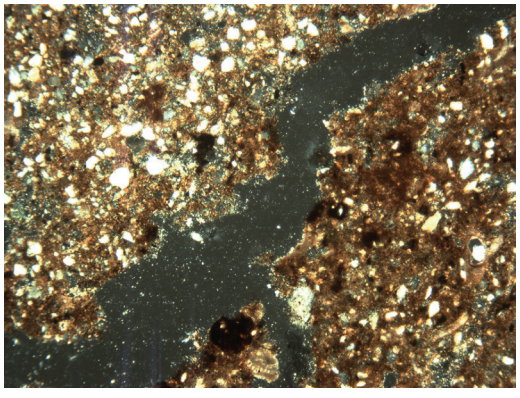

e

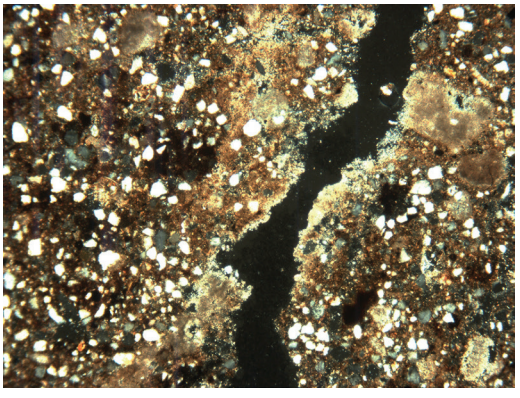

f

Table 5.17. *The summary micromorphological descriptions and suggested interpretations for the basal zone of the Salina Deep Core.*

Sample number	Depth (m)	Micromorphology	Interpretation
1	27.83–27.88	Well developed, small, sub-angular blocky, calcitic fine sandy clay loam over basal lens of fine limestone gravel	Eroded soil that has been stable for a period of time over eroded hillwash material
2	27.91–27.96	Massive, calcitic fine sandy clay loam with all voids filled with micro-sparite/amorphous calcium carbonate and 30% amorphous humic/sesquioxide staining	As below with considerable secondary influence of calcareous groundwater and wetting/drying
3	28.04–28.12	Massive, calcitic fine sandy clay loam with micritic/amorphous calcium carbonate linings of channels and iron hypo-coatings of channels, with glauconite and small limestone rock fragments	Eroded calcitic soil and subsoil, derived from the Upper Coralline Limestone

5.3.10.4. The base of Salina Deep Core

Although the Salina Deep Core (SDC) was not examined by the authors in person, it was recorded and sampled by C.O. Hunt who provided three sub-samples of the possible soil material contained in the base of core (21B) at a depth of 28.04–27.95 m (Appendix 8). Above this basal zone of soil there was a continual accumulation of eroded material from *c*. 6000 cal. BC to the present with the first signs of cereal cultivation occurring from about 5500–5000 cal. BC (UBA-30087/30088) (see Chapter 2).

The basal sample is a massive very fine sandy clay loam fabric (Fig. 5.22e) which exhibits sedimentation in the form of very large planes. There is a calcitic fine component of amorphous pigmented sesquioxide surrounding very well sorted quartz silt. Channels, which are almost all filled with micro-sparitic/amorphous calcium carbonate suggest that there is some residual vegetation growing on a land surface with which this soil is associated. Redox has been intense as there are many iron hypo-coatings of channels and there is evidence for the re-precipitation of calcium carbonate indicating a calcareous soil environment. There is glauconite and small carbonate rock fragments suggesting that this material is being eroded from the Upper Coralline Limestone bedrock upslope in the valley.

The sample above is very similar although slightly more alkaline. There is some clay in the system with weakly striations superimposed on a calcitic b-fabric. This suggests that there is considerable drying and the formation of secondary calcium carbonate (Fig. 5.22f), with illuvial clay either formed *in situ* or eroded from soils in the catchment which had formed argic horizons.

The upper sample is also very similar with calcareous fine material and very fine quartz silt exhibiting a well developed sub-angular blocky microstructure comprising at least 50 per cent of the thin section with a heterogeneous mix of a wide size range of rounded to sub-angular rock clasts. The quartz shows some sedimentary properties in terms of horizontal orientation. It is suggested that this material was also derived from the Upper Coralline Limestone geology, in addition to contributions from aeolian silt, fine calcareous material and rock clasts. Subsequent soil formation developed the ped structure and gleyic soil properties through a fluctuating groundwater table.

5.3.10.5. Interpretative discussion

In three of the four cores there were good indications that buried soils and/or eroded buried soil material were present at the base of the valley core profiles. In particular at Xemxija, Wied Żembaq and Marsaxlokk, there are thick accumulations of eroded soils from their valley catchments, incrementally aggrading at different times but from as early as the seventh millennium BC at Xemxija, the mid-fourth millennium BC at Wied Żembaq and the mid-first millennium AD

Figure 5.22 *(opposite). Marsaxlokk and Salina Deep Core photomicrographs (C. French): a) Photomicrograph of the sub-angular blocky, reddish brown, micritic, fine sandy clay loam, Marsaxlokk core, 2.96 m (4.5 mm frame width; cross polarized light); b) Photomicrograph of mixed fine limestone gravel and calcitic very fine sandy/silt, Marsaxlokk core, 2.15 m (4.5 mm frame width; cross polarized light); c) Photomicrograph of dense, calcitic very fine sandy/silt, Marsaxlokk core, 1.1 m (4.5 mm frame width; cross polarized light); d) Photomicrograph of laminar amorphous sesquioxide replaced and humified organic remains, Marsaxlokk core, 1.70 m (4.5 mm frame width; plane polarized light); e) Photomicrograph of calcitic fine sandy clay loam, Salina Deep Core 21B, 27.83–27.88 m (4.5 mm frame width; cross polarized light); f) Photomicrograph of calcitic channel linings, Salina Deep Core 21B, 28.08–28.12 m (4.5 mm frame width; cross polarized light).*

at Marsaxlokk. These deposits also exhibit gleying features, indicative of alternating and variable more moist/dry conditions of deposition (Lindbo *et al*. 2010). Significantly at Xemxija, this early Holocene eroded soil material is aggrading through repeated alluvial additions of the same material, which is probably initially derived from the Blue Clay and Greensand geologies exposed up-slope in the valley.

Over this same period, the seventh to early fourth millennia BC, particularly at Xemxija but also at Salina and Wied Żembaq, there are a number of indications of repeated tree pollen minima at the interpolated dates of *c*. 6600, 6150, 5900, 5850, 5450, 4750, 4800, 4550 and 3900 cal. BC (see Chapters 3 & 11). Perhaps significantly, these are coincident with the occurrence of gypsum at Xemxija in the mid-seventh millennium BC (Table 5.14) and with two early Holocene aridification events, including the wider mid-seventh millennium BC event across the western Mediterranean and the 8.2 ka BP event (Weninger *et al*. 2006; Bini *et al*. 2018), and again at 4050–3940 cal. BC, just prior to the beginning of temple construction. This may possibly reflect periods of enhanced seasonality in a fairly dry environment, rather than overall drought, and after these two early events, increased land-use pressure at the very least.

Subsequently from about the later fifth millennium BC, eroded soil material and limestone clasts derived from the Upper Coralline Limestone plateau in the associated Pwales valley become the main source of soil material on the move in the erosion complex. This, combined with the changes in the nature of the buried soils associated with the Neolithic temple sites (see §5.3.2.2 & 5.3.3.3), points to sustained disruption of the soils in the valleys from early prehistoric times. At Xemxija during the earlier Neolithic period in the fifth millennium BC, there are inputs into the valley that indicate several landscape zones from the upper slopes of the catchment being utilized and becoming prone to erosion. At Wied Żembaq in the mid-fourth millennium BC, there is clearly the erosion of soil from the clay-rich red soils developed on the Upper Coralline Limestone plateau, also corroborating the buried soil story of disruption and change associated with the temple sites examined in this study. A remnant of these same transformed xeric *terra rossa* soils (or Luvisols) occurs in the valley base at the Marsaxlokk core site much later at about the mid-first millennium AD. All of these soil derived deposits are showing signs of strong evapo-transpiration and the secondary formation of silt-sized calcium carbonate, testifying to both the effects of aridification, poor vegetative cover and agricultural activities (Duarand *et al.* 2010; Jongerius 1993; Kooistra & Pulleman 2010). Subsequently in historic to more recent times, there is the suggestion of irregular and mixed pulses of eroded soil material derived from all the geological substrates in the valley system, which reflects increasing disruption in the landscape associated with agricultural activities and probably also terrace construction (see Chapters 7 & 8).

At several of the core sites, there is at least one main phase of humic silt mud accumulation, pointing to a major change in the depositionary environment and therefore the nature of human activity in each valley and potentially also slight differences in the wider climatic regime. The very fine and relatively minor minerogenic components of these phases of organic accumulation under shallow standing water conditions, point to a wider stability in the landscape, and greater catching of soil surface run-off water in the valley bottoms. Nonetheless, the humification of these humic silts points to strong seasonal drying. At Xemxija, the onset of these paludal, shallow freshwater, conditions at the mouth of the valley occurred from *c*. 4326–4053 cal. BC at a depth of 5.7 m, ceasing some two millennia later by *c*. 2198–1985 cal. BC at a depth of 4.6 m. This period of water run-off capture appears to bracket the whole Neolithic Temple Period and into the Early Bronze Age (see Chapters 2 & 4). In the Wied Żembaq core, the thickness of similar deposits is much reduced with two episodes of *c*. 40 cm of accumulation, which both probably occurred within the fourth millennium BC. These observations point to variation in periodicity, time-line and duration of periods of landscape stability and disruption occurring in each valley catchment. Indeed, the Xemxija core location may be quite different than the others, since it is captured behind a near-shore dune system on an uplifted part of the northern coastline of Malta (C.O. Hunt, pers. comm.), and this may explain its lengthy time-depth and apparent uniqueness as a potentially wet refugium resource.

In each core, the enormous volume of eroded soils from each valley catchment that has been on the move and accumulating in the valley bottoms is significant, certainly in earlier prehistoric (pre-*c*. 4000 cal. BC), later prehistoric (post-*c*. 2000 cal. BC), historic times (from the mid-first millennium BC), and more recent times in the last 100–150 years. These hillwash derived, alluvial accumulations range from at least 2.5–9 m to as much as 25 m in thickness. They are typified by the reddish brown silty clay loams and calcitic fine sandy/silty loams of Marsaxlokk and Xemxija/Salina, respectively. These re-deposited soils then remain stable for sufficient periods of time to form and exhibit a good soil structure, which suggests relatively lengthy periods of landscape stability punctuated by episodes of alluvial deposition with an almost continual slight input of fine wind-blown material. This

major landscape transformation process can only be directly associated with de-vegetation and physical disruption of the watershed valleys, and the associated Upper Coralline Limestone upper slopes and plateaux where present. The combined effects of soil disturbance through agricultural use, xerification and periodic rainfall events made the earlier-mid-Holocene highly soils mobile when they were either de-vegetated and/or with bare soil surfaces after any crop harvest. How much the investment in time, labour and energy of making the terrace systems that cover this landscape today served to halt or slow this twin process of soil erosion and alluviation remains as yet unanswered, but, at face value, does not appear to have been overtly successful until relatively recent times.

5.4. The Holocene landscapes of Gozo and Malta

The flat-topped limestone mesas of Gozo that are not occupied by towns and villages today are highly denuded of soil and vegetation. These 'garrigue' areas are characterized by shallow eroded remnants of earlier soils called Luvisols or shallow A/C type Leptosols (WRB 2014) with large areas of exposed bedrock and sparse scrub and grass vegetation (Fig. 5.23). Springs tend to emanate from just below the mesa plateau zone, often at the Upper Coralline–Greensand/Blue Clay boundary, leading to lateral flush wet zones immediately down-slope. These are often occupied by modern cisterns and small reservoirs built by present day farmers to enhance water capture. Down the variable degrees of slope into the valleys below, it is common to see extensive exposed areas of grey silty clay on Blue Clay geology across the mid-upper slopes, situated between the Upper Coralline and Globigerina Limestones, such as occurs in the Ramla valley. Thin and variable Greensand exposures often emerge at the transition boundary between the upper part of the Blue Clay and the base of the Upper Coralline Limestone formations, usually about two-thirds of the way up-slope towards the mesa plateaux. Springs often emerge at these geological boundaries. These transitional Upper Coralline/Greensand and Blue Clay valley slope areas are commonly used for arable cereal crops today as they are relatively moisture and nutrient retentive, even if the Blue Clays in particular are 'heavy' soils that require a plough. In many valleys such as the lower Ramla and Wied il-Kibr, the limestone bedrock (of both Upper Coralline and Globigerina) outcrops in a series of low steps or inset plateaux which are all farmed today, usually with wheat, barley or vine crops (Fig. 5.24). The valley bottoms have a varied

Figure 5.23. *Scrub woodland on an abandoned terrace system and garrigue plateau land on the north coast of Gozo (C. French).*

geomorphology, but are often narrow and meandering, often scoured out and incised into the limestone bedrock through water action, and/or infilled with thick combinations of eroded coarse to fine hillwash material derived from the soils and geology upslope, with inset low plateaux areas in the lower parts of the valleys, often composed of Globigerina Limestone.

In general, hillwash accumulation on the lower Blue Clay slopes is relatively thin and variable, whereas there may be up to *c*. 10–12 m of aggraded hillwash-derived material captured in the base of the valleys dominated by limestone bedrock, especially towards the sea. Several of the deep cores contain a distinctive captured record of soil erosion from the different geological and slope components of the valley systems (see Chapter 2 and §5.3.8 & 5.3.9). As best expressed in the Xemxija core in northeastern Malta, fine soil erosion and aggradation had begun by at least *c*. 7000 cal. BC with indications represented from its mineral suite and size classes that this material was at least initially derived from the upper slopes of the valley inland at the Blue Clay/Greensand geological transition. Within the Neolithic period of temple building in the fourth millennium BC this initial trend gave way to eroded red silty clay soil material derived from the Upper Coralline Limestone plateaux and other upper slopes areas of the valley.

Moving into post-Neolithic times, the erosion sequences commonly become dominated by more massive silt-sized calcitic sediments associated with the erosion and aggradation of dry, de-vegetated and degraded soils, interrupted by occasional influxes of coarse gravelly material indicative of more major erosive events. These fine/coarse calcitic sediments are commonly found aggrading in great thicknesses in valley bottoms towards the sea in most of the deep cores investigated such as Xemxija, Wied Żembaq, Marsaxlokk and Salina (see Chapter 2). In the upper Marsalforn valley this material was on the move from the mid-second millennium BC with a basal phase of relative stability dated to *c*. 1560–1480 BC and a middle zone of lengthier stability and soil formation dated to before *c*. 760 BC. In the lower Ramla valley, soil erosion accumulating in the lower valley bottom was much more recent (mid-nineteenth–early twentieth century AD) with relatively short phases of temporary soil stability and soil formation, interrupted by phases of renewed soil run-off and re-deposition. In contrast, the lower slope erosion profiles on the Blue Clay and Globigerina Limestone geologies in the Ramla valley are rarely deeper than *c*. 70–80 cm, and tend to be characterized by A/C type soil profiles (or Leptosols) with or silty clay or fine sandy silt soils, respectively, which have been completely homogenized by recent ploughing activity. There is considerable modern down-cutting by flash-flood streams generated from thunderstorm events, often cutting into the bedrock by 1–1.5 m such as occurs in the Wied ta'Xħajma valley of the upper Ramla valley to the east of the In-Nuffara plateau. In many cases, land-owners have attempted to prevent further valley incision by building sets of walls at different heights and times to contain soil erosion at the base of the valley slopes, but in each case the flood event flows have continued episodically to down-cut into the Globigerina Limestone bedrock below.

In the geoarchaeological survey of the Ramla and Marsalforn valleys, very few pre-hillwash erosion buried soils were in evidence. Indeed, the best preserved earlier Holocene soils were found directly associated with the Neolithic temple sites investigated and on several modern construction sites on the Xagħra mesa. These soils were characterized by a two-horizon, well developed sub-angular to columnar blocky structured, strong red to purplish red, silty clay loam soil. This typical Luvisol or red Mediterranean soil type was probably formed under a wetter pedo-climatic regime leading to clay illuviation down-profile during the earlier Holocene, which subsequently became subject to long-term drying out and predominant secondary iron formation (Gvirtzman & Wieder 2001). It is the very eroded and transformed version of this type of soil which is now commonly found on the mesas and around their margins, such as around the margins of the Xagħra plateau.

A completely different 'brown to red' Mediterranean soil was revealed at Santa Verna beneath the earthen *torba* floors within the temple and in Test Trench B just outside the temple to the northeast (Figs. 3 & 10). In each case, these soils were thicker (*c*. 50–60 cm) and exhibited much better development characteristics than in the buried soils found elsewhere on the Xagħra plateau and at Ġgantija temple. Two horizons are visible, a lower more reddish brown to purply brown horizon and a slightly browner but still reddish brown upper horizon, which is indicative of both B and A horizon survival. The pellety crumb structure of the upper horizon is indicative of the base of a mollic or mull horizon of a brown earth type of soil (Gerasimova & Lebedeva-Verba 2010, 354; Goldberg & Macphail 2006, 65). In addition, the upper parts of all the profiles analysed contained significantly enhanced phosphorus values. Both inside and outside the Santa Verna and Ġgantija monuments, the transition from this lower A horizon to the B horizon is marked by a very mixed fabric of pellety/aggregated silty clay and varying admixtures of micritic calcium carbonate, which can more or less predominate. This is essentially acting as a depleted and oxidized, calcium

carbonate dominated eluvial Eb horizon. Below this, and especially in the Ashby and Trump Sondages within the interior of the temple, there is *c*. 20–40 cm of a clay-enriched B horizon present. This is primarily composed of a silty clay with greater/lesser degrees of striation with pure to slightly dusty clays evident, and a well developed, small blocky to columnar ped structure. This is indicative of a stable, well drained and organized, illuvial, clay enriched or argillic (or Bt) horizon (Bullock & Murphy 1979; Fedoroff 1968; Kuhn *et al*. 2010, 233ff). This type of argillic brown earth soil no longer appears to exist in present day Malta and Gozo, and its presence in a pre-early fourth millennium BC buried context at Santa Verna on the Upper Coralline Limestone of the Xagħra plateau is therefore of great significance. Importantly also, this same type of soil material was present in a very thick cumulative exposure (up to 1.1 m) in the base of the Xemxija 1 core in northern Malta, dated from about 8780–8452 cal. BC (UBA-25001) at its base to 6000–5840 cal. BC (UBA-31706) at its upper surface (see Chapter 2).

This type of palaeosol or red-brown Mediterranean soil (or Orthic Luvisol) was probably formed under a well vegetated and moister pedo-climatic regime in the earlier Holocene (Fedoroff 1997; Yaalon 1997). OSL dating of this primary soil at Ġgantija and Skorba suggests that this soil had begun to form by at least the ninth millennium BC (see Chapter 2). It is characterized first by the weathering of the limestone substrate and then by clay illuviation down-profile creating a clay enriched lower Bt or agric horizon (Verhaye & Stoops 1973). In all the buried soil profiles there is also a considerable component of aeolian dust, contributing to the ubiquitously high silt component of these soils, a feature that is widespread across the Mediterranean region (Yaalon & Ganor 1973). Strong reddening or rubification of the Xagħra palaeosols probably occurred hand-in-hand with the process of clay illuviation (Fedoroff 1997; Yaalon 1997) and rapid bio-degradation of organic material, as well as increasing calcification with time. These latter processes are probably associated with the removal and disturbance of the vegetative cover and a marked, lengthy dry season (Goldberg & Macphail 2006, 70; Gvirtzman & Wieder 2001; Yaalon 1997). It is the very eroded, disturbed and highly weathered thin base of this type of soil which is now commonly found on and around the margins of the limestone plateaux of Gozo, such as at Xagħra.

Nonetheless, this buried soil does not exhibit or preserve an upper organic litter horizon (Ah/l). The surviving A horizon and upper part of the B horizon has been disturbed and mixed throughout, largely by the soil fauna, and considerably affected by the secondary formation of calcium carbonate and iron oxides/hydroxides. This soil mixing aspect is more evident and to a much greater depth in the profiles at Ġgantija and Skorba than at Santa Verna. These soils may also have been disturbed by physical mixing as there is often a mix of fine crumbs and small irregular blocky peds of soil in the same soil horizon, and probably also truncated by subsequent human activities associated with constructing the temples. In addition, the strong reddening or rubification (or ferrallitization) with iron oxide depletion hypo-coatings (Bridges 1978, 33; Gerasimova & Lebedeva-Verba 2010, 357), and indeed the ubiquitous formation of common micro-sparitic calcium carbonate, especially in the upper half of the profiles, suggests that this soil became open and largely devegetated, and subject to evapo-transpiration and oxidation processes (Lindbo *et al*. 2010). At Santa Verna and Skorba, this occurred just before burial by monument construction in the earlier fourth millennium BC. Nonetheless, the very high phosphorus values and fine included anthropogenic debris do suggest that there has been some kind of management of these soils in the past, undoubtedly associated with manuring and probably also the deliberate re-deposition of settlement derived refuse.

The buried soils discovered to either side of the viewing terrace on the southern side of Ġgantija temple revealed another variation in the soil story on the Xagħra plateau. On the western side beneath the late Neolithic temple blocks and a thick agricultural soil in Test Pit 1, there is a complete Ah/Bwt/C horizon brown loam soil (or Luvisol) developed on the Upper Coralline Limestone bedrock (Fig. 5.7). This soil must have formed under moister, organic, nutrient-rich conditions, unlike the present day pedo-climatic regime of dry Mediterranean with seasonal rains and a marked and lengthy dry season (Fedoroff 1997; Yaalon 1997). Nonetheless, it is exhibiting signs of fines (of silt and clay) depletion and secondary calcification and amorphous iron formation, and therefore marking a change in soil formation conditions to one that is more disturbed and xeric. Before burial by the terrace soil above, this soil has therefore become subject to evapo-transpiration and the formation of secondary calcium carbonate and to a lesser extent amorphous sesquioxides. This suggests that it had been an earlier Holocene soil similar to that which was observed beneath the nearby Santa Verna temple. It has also seen some anthropogenic influence and disturbance in terms of opening-up its vegetated surface and greater humification and transpiration processes. But at the same time, there appears to have also been some management in terms of organic input and the incorporation of later Neolithic pottery, bone, charcoal and

humic material to amend or enhance the fertility and stability of this soil. These suggestions are corroborated by the palynofacies analyses of the buried soils at both Santa Verna and Ġgantija which point to highly biologically active soils that were enriched with organic and charred material, most probably derived from settlement activity nearby (see Volume 2). Standing water bodies were probably also present nearby during the later Neolithic at Ġgantija (Ruffell *et al*. 2018), and in the very early Neolithic phase at Santa Verna, and the micro-plankton observed in the buried soils at both sites suggest the 'slubbing-out' of organic mud from the base of these pools of water and its addition to these soils as well as molluscan evidence from several deep valley cores such as Xemxija on Malta during the Temple period for marshy and standing water areas (see Chapters 3 & 4).

On the southeastern side of Ġgantija in the WC Trench there is a well preserved variant of this same soil profile. Here the buried soil is buried by thick mixed soil-midden deposits with plentiful included Neolithic artefactual material with a radiocarbon date suggestive of burial by *c*. 2580–2300 cal. BC (UBA-33707). The soil itself has a similar Ah/Bwt/C profile to that observed in TP1, although it is just beginning to show signs of reddening with depth and calcification through drying effects. Thus both these Ġgantija profiles appear to be a 'half-way' soil-type in development terms between a brown and a red Mediterranean soil, with the Ġgantija soil formation sequence more altered as a result of a longer period of continuing human use and disturbance, in contrast to the Santa Verna palaeosol which was buried about 1000–1300 years earlier. A similar sequence of formation events was also evident in the buried soil profiles at Skorba, although it was occurring much earlier in the early fourth millennium BC as at Santa Verna.

The variable expression of mixing, oxidation and secondary calcium carbonate and amorphous iron forming processes imply that the original thick and well developed soils at Santa Verna are on the cusp of major pedogenic change from a brown to red Mediterranean soil. This change is best seen in its early onset form at Santa Verna in the Ashby and Trump sondages, and is much more advanced in both the Skorba and Ġgantija buried soil profiles. This transitional process of soil change is no doubt associated and aggravated by the human use of this part of the Xagħra plateau, in terms of clearance and temple construction, and undoubtedly also associated settlement and agricultural activities. Significantly, this major soil change may also be reflective of a wider change in the moisture and vegetational

Figure 5.24. *Terracing within land parcels (defined by modern sinuous lanes) on the Blue Clay slopes of the Ramla valley with Xagħra in the background on the Upper Coralline Limestone plateau, probably established by the Order of St John in the sixteenth century* AD *(C. French).*

regime, from a moister and well vegetated landscape to one with a low but periodic rainfall, poor moisture retention and general aridification or xeric processes, which are all at work by the time of temple construction from about 3800 cal. BC onwards and through the first half of the third millennium BC. Nonetheless, there are clear signs of management of these soils in this same time frame through the addition of settlement derived midden debris in an attempt to enhance these soils, most probably for arable agricultural use.

In the valley bottom about 500 m to the south of Ta Marżiena, there was a well preserved reddish brown silty clay loam preserved beneath about 90 cm of silty clay loam, possibly of colluvial origin derived from the silty clay shallow slopes to the north. The presence of a buried soil here as well as on the mesa top at Xagħra and Santa Verna strongly suggests a once greater ubiquity of red/brown Mediterranean soils in this landscape, based on the observation of other capture zones of eroded earlier Holocene soils in the Xemxija and Wied Żembaq cores for example.

One notable land-use feature was observed in the Ramla valley between Ġgantija and In-Nuffara, especially on the southeast-facing slope of the valley. Large rectilinear parcels of land, probably dating from the knights of the Order of St John 'colonization' of this area from the sixteenth century AD (see Chapters 9 & 10), occupy the exposed Blue Clay geology valley slopes (Fig. 5.24) (Alberti *et al*. 2018). This is notable in that this geology now supports thick, homogeneous, silty clay vertisols with a groundwater table close to the surface in many places, making these soils both moisture retentive as gleys but at the same time relatively intractable in terms of ease of ploughing until the arrival of machinery. This could imply that these clay valley slope zones were the last to be cleared and taken into private ownership as it was relatively hard land to farm (but not nutrient poor), requiring either metal-tipped ploughs and/or animal-drawn or mechanized ploughs.

5.5. A model of landscape development

On the basis of the geoarchaeological survey and the buried soil analyses, it is now possible to propose the following model of landscape soil development and land-use for the central area of Gozo around Xagħra as well as in the north/northeastern part of Malta around Skorba during the Holocene.

The thick purplish red, columnar to sub-angular blocky ped silty clay soil with distinct clay-enrichment that is observed deeply set into fissures in the Upper Coralline Limestone on the Xagħra town mesa conforms to classic *terra rossa* of the soil classification systems (Bridges 1978, 69). These soils may have their origins to be in the last interglacial period (van Andel 1998; Catt 1990), but are generally understood to be the climax soil type present for this parent material in a strongly seasonal, semi-arid Mediterranean landscape (Bridges 1978; Duchaufour 1982; Durn 2003; Lang 1960; Yaalon 1997). The geoarchaeological and micromorphological study presented here strongly supports this to be the case with well developed brown luvisolic soils developed by the early Neolithic or the seventh–fifth millennia BC on the Upper Coralline Limestone geology on Gozo and Malta. These soils slowly but surely degraded to become thin red, calcitic soils through the combined effects of human intervention and xerification during the Neolithic and later prehistoric periods.

This earlier Holocene brown Mediterranean soil was thick (up to *c*. 80 cm), had a higher percentage of soil organic matter, was well structured (blocky or columnar) and multi-horizonal (Ah/Eb/Bwt/C) loam, with evidence of clay illuviation in a clay-enriched Bt or argillic horizon towards its base. It was undoubtedly associated with a moister climate with higher annual precipitation which supported an increased biomass, a sparse, scrubby woodland vegetation, all leading to good stability and reasonable moisture retention. The palynological and molluscan studies of the *FRAGSUS Project* appear to corroborate this theme of relatively sparse, scrubby woodland cover for much of Gozo/Malta in earlier Neolithic times with a greater availability of freshwater in many of the valley systems (see Chapters 3 & 4). This soil type appears to have been largely confined to the upper third of the valley slopes and on the mesa plateaux, and directly associated with the Upper Coralline Limestone geology. It is suggested that this soil was just beginning to become transformed by the time that the Santa Verna temple was being built in the early fourth millennium BC, and indeed the buried soil at Santa Verna exhibited characteristics that indicate that it was buried right at the cusp of change. This same trajectory of change was slightly further developed at Skorba by the same period of the early fourth millennium BC. In contrast, the buried soils present at Ġgantija temple indicate that this soil had become fully transformed to a calcitic, poorly structured soil by the middle of the third millennium BC. But at both Skorba and Ġgantija, the soils were already being amended and improved though the deliberate addition of settlement-derived organic waste during the Temple period, and subsequently at Ġgantija became subject to terrace soil aggradation by the mid-/later second millennium BC.

In some valleys, there are very early signs of landscape disruption and soil erosion taking place from

the Blue Clay/Greensand boundary zone of the upper valley slopes from the early Neolithic if not before. By the time of the main development of the Neolithic Temple Period, this erosion signature was shifting to the erosion of the well developed soils derived from the Upper Coralline Limestone. Moreover, there is a much greater influence of freshwater in the valley bottoms at the same time, suggesting that there may have been contemporary greater rainfall and greater spring activity in the valley landscapes during the same period. These features are best expressed in the Xemxija core and associated valley system as well as at Wied Żembaq on Malta.

In contrast to Xemxija and Wied Żembaq, the slopes of the Ramla and Marsalforn valleys on Gozo were initially quite stable, possibly associated with scrub woodland on the Blue Clay geology and vertisol exposures in the middle-lower slope zones. Streams/rivers in the valley bottoms were quite small, meandering and relatively stable. The upper-middle parts of the valleys appear to have suffered from hillwash erosion and aggradation such as observed at Marsalforn where there was significant erosion off the Coralline Limestone upper slopes throughout much of the second and first millennia BC. In contrast, the lower clay slopes of the Ramla valley appear not to have been subject to any significant colluvial aggradation through hillwash and slope processes, whereas there are several metres of relatively recent/last century coarse/fine colluvial aggradational fills in the valley bottom towards the sea, occasionally interrupted by variable lengths of relative stability and incipient soil formation. These more aggressive erosional features appear to be a much later feature of the last couple of centuries, and are undoubtedly associated with agricultural activities on the upper and lower slopes, in spite of terracing. In contrast, in several places within the lower Ramla valley for example, there are very fine silt-rich (or loessic) soils on low upstanding mesa exposures of Globigerina Limestone at about *c*. 5–20 m above the valley floor. These naturally very fertile silt soils are where modern vineyards are situated which would have provided a long-term nutrient-rich resource for arable farming in the past as well. The evident variation in soil and erosion histories from valley to valley suggests that there is no one synchronous sequence of erosion across the Maltese Islands in prehistoric times, rather multiple variations in time, space and characteristics, dependent on the human–landscape interactions in each valley system.

The one consistent feature which is absolutely clear is that the well structured, clay-enriched brown soil-type observed repeatedly on several of the limestone mesa plateaux was probably the climax Holocene soil type for the Gozo and Malta islands by the early Neolithic period/sixth millennium BC, as previously hypothesized for many parts of the Mediterranean region (Bridges 1978; Lang 1960; van Andel 1998). Through a combination of human activities associated with clearance and agriculture, it is very clear that soil type change had begun during the Neolithic period. Soils on the mesa plateaux became characterized by a reddish brown, secondary amorphous iron oxide and calcium carbonate dominated, fine sandy/silt loam soil, as seen today in the fields outside the temple areas at Ġgantija, Ta Marżiena, Santa Verna and Skorba. This soil type change was occurring in the fourth and third millennia BC just before and during the Temple Period. Importantly, the continuing human exploitation of these soils, combined with drier climatic conditions from at least 2300 cal. BC and certainly from the second millennium BC onwards (Carroll *et al*. 2012; Magny *et al*. 2011; Sadori *et al*. 2013) (see Chapters 2 & 3) led to significant secondary soil formation and erosion processes taking precedence. Initially this was marked by clay and iron movement via the soil water system and their redeposition down-profile, but then increasingly the formation of silt-sized calcium carbonate associated with xerification. In combination, these now organic depleted and poorly structured soils became thin, single horizon, highly iron impregnated and calcium carbonate dominated, xeric red or pale grey soils (Aguilar *et al*. 1983). As an associated consequence, these thin and poorly structured soils also became very prone to erosion especially without well vegetated ground cover (Butzer 1982; Kwaad & Mucher 1979).

This model of soil change is the most probable scenario, and there is excellent corroborative soil evidence at both Santa Verna and Ġgantija on the western part of the Xagħra plateau, and at Skorba in northern Malta. At Santa Verna, the buried soil found beneath the *torba* floors is a dark brownish red reflecting the down-profile illuvial movement of clay creating a stable and well structured, clay enriched soil that soon becomes dominated by the secondary formation of iron oxides. This is the type of soil change trajectory that occurs when a well vegetated, moist, humic brown soil becomes subject to some disturbance and oxidation. This soil appears to be a precursor soil to the calcitic reddish brown soils observed at Skorba and Ġgantija, but not necessarily for the off-site, Xagħra red soils. In many respects, it appears that the soil development catenas between Santa Verna and Ġgantija, and also at Skorba, are tracing the beginnings of soil change associated with use and disruption of this landscape that began to occur just before the main construction of these temples in the early fourth millennium BC.

The slightly different development trajectories of the buried soils present at each Neolithic site investigated could be associated with the building chronologies of these temple sites. From the comprehensive new set of AMS radiocarbon dates made available by the *FRAGSUS Project*, the Santa Verna and Skorba temples began construction much earlier at about 3800 cal. BC as opposed to *c*. 3400–2500 cal. BC at recently excavated areas of what may be the later phases of Ġgantija (see Chapter 2 & Volume 2, Chapters 4, 5 & 7). This apparent time-depth differential and lengthier exposure may explain the greater xeric qualities of the Ġgantija profiles versus the better developed earlier buried soil profiles present at Santa Verna and Skorba for example, and indeed the unknown longer potential exposure of the Xagħra house construction site profiles and the Taċ-Ċawla settlement site in Rabat.

The observed soil formation sequence at these temple/mesa plateaux sites suggests that the single horizon, dry, red calcitic soils with thin organic A horizons (or Leptosols) were becoming the norm on the Upper Coralline Limestone geology of the mesa plateaux areas of Gozo and Malta from at least beginning of the fourth millennium BC, and were very well established by the third millennium BC. Associated and subsequent over-use for arable and grazing land, de-vegetation and disruption of the landscape led to gradual and continuing denudation and depletion, coincident with the widespread soil erosion and the establishment of an impoverished garrigue flora, thus creating the landscape we see today.

Later prehistoric and early historic agriculture in combination with the dry Mediterranean climate kept these thin xeric soils ubiquitously present on most of the higher/upper parts of the Gozo/Malta landscape, ostensibly associated with the Upper Coralline Limestone. These red soils probably thinned with time and became less moisture retentive, more iron- and calcite-rich, and less fertile, unless subject to continual amendment with household waste and domestic livestock manure, and/or a mixed pasture, fruit tree and arable use. At Ġgantija for example, there does appear to have been a concerted attempt at amending and enhancing the fertility and thickness of the later Neolithic topsoil with domestic refuse. Nonetheless from at least the Neolithic period (or fourth–third millennium BC), soil erosion has also been a factor in causing slope erosion and valley infill processes in many parts of Malta/Gozo (see Chapter 2) as well as Europe more broadly (*cf*. Bevan & Conolly 2013; Brandt & Thornes 1996; Grove & Rackham 2003; Hughes 2011; Imeson *et al*. 1980; Kwaad & Mucher 1979; Thornes 2007). Stratigraphic records recovered from a number of valley sites in Malta in the *FRAGSUS Project* (see Chapter 2) and through earlier palynological work on Malta (Carroll *et al*. 2012) and similar intensive studies in this volume (see Chapter 3) suggest continuing disruption of the landscape associated with agricultural exploitation from at least the sixth millennium BC, and especially from *c*. 2300 cal. BC with increasing aridification. In addition, recent palynological work on Malta suggests coincident disruption of the landscape as marked by a gradual decline in the scrub and tree vegetation (and see Chapter 3), which became more pronounced from *c*. 4000 cal. BC onwards and especially from *c*. 2300 cal. BC, and perhaps even the relative 'abandonment' of arable agriculture in the late third millennium BC with an associated greater emphasis on pastoral activities (Carroll *et al.* 2012; Djamali *et al.* 2013). Together these evident signals of deterioration in the landscape could have prompted the development and onset of terrace construction, especially on the Coralline Limestone upper slopes, in an effort to slow landscape degradation, but secure archaeological evidence remains far from convincing (and see Chapter 11).

The human exploitation of these transitional brown to red soils during the Late Neolithic period was followed by drier climatic conditions probably from the late third millennium BC onwards, a consistent feature also observed across much of the Mediterranean area (Carroll *et al.* 2012; Magny *et al.* 2011; Morris 2002; Sadori *et al*. 2013), and in the palynological and molluscan studies conducted in this project (see Chapters 2–4). It is the xeric moisture regime of strong seasonal winter/summer rainfall contrasting with winter rainfall in excess of evapo-transpiration versus a lengthy period of the drying out of the root zone in the soil over the summer months which defines the climatic constraints on soil formation in Malta and elsewhere in the Mediterranean region (Yaalon 1997). In combination with human use of the mesa plateaux and the coincident removal of vegetation, there were the associated processes of soil moisture loss, de-stabilization and humic and fines depletion. Consequently, a number of significant secondary soil processes then took precedence, predominantly the bio-degradation of the humic components and the common formation of silt-sized calcium carbonate, as well as clay and iron movement and their re-deposition down-profile leading to finer and denser soil fabrics and strong soil reddening. These combined processes resulted in the development of thin, organic depleted, highly iron oxide impregnated xeric soils which were becoming increasingly dominated by secondary calcium carbonate formation (Aguilar *et al*. 1983). These secondary processes changed the earlier Holocene soil type and moisture-vegetation balance once and for all.

From the evidence gleaned in the geoarchaeological survey, valley slope hillwash deposits range from slight to substantial. For example, earlier Neolithic soil erosion is evident in the deep Xemxija core from the seventh millennia BC and at Wied Żembaq in the mid-fourth millennium BC, but much of the valley fill in the Marsalforn valley is of later prehistoric age (mid-second to first millennium BC), and in the Ramla valley of the late nineteenth–early twentieth century AD. Moreover, most of the deep valley cores show a major step increase in erosion from after about 2000 cal. BC (see Chapter 2). Thus it is suggested that exploitation of the wider landscape became more and more extensive during later prehistoric times, with greater and lesser phases of major intensity, a feature corroborated by the deep valley core stratigraphic records and palynological analyses (see Chapters 2 & 3).

In the Marsalforn valley, thick hillwash accumulations of highly calcitic, rubbly, fine sandy and silty soils have continued for some time, undoubtedly associated with arable agricultural activities upslope. This was taking place long after the major soil and climatic changes in the mid-/later Neolithic, from at least the mid-second millennium BC and throughout much of the first millennium BC (Table 12). The already calcitic/xeric soils that are on the move down-slope as overland flow imply substantial and severe disruption on the hill-slopes above, and strongly suggest the physical disruption of bare soils. This could well have been associated with the construction of terrace systems in this valley. In many respects, the Marsalforn sequence is probably more typical of the island, where the original soils are either long gone through down-slope erosion, and/or so deeply buried and present only as remnants such that it is extremely difficult to discover and recover them.

In contrast, the largely silty clay loam dominated Ramla valley slope soils appear to have remained relatively stable at the time that the soils on the Upper Coralline Limestone geology were being transformed during the Neolithic and later prehistoric times. In addition, the intractability of these clay and silt dominated vertisols developed on the Blue Clay geology valley slopes (Vella 2003) meant that they were best avoided for arable agriculture until the arrival of metal-shod, mouldboard ploughs, at least from Roman times onwards (Margaritis & Jones 2008). Despite some indications of initial erosion from the Blue Clay/Greensand zone of the upper valley slopes in some valley sequences, it is suggested that the Blue Clay slope areas would have probably largely remained as scrub woodland and/or grassland for grazing for most of prehistoric times. There are also numerous springs emanating from the upper and lower contacts of the clay with the limestone geology which would have provided natural water sources and wet areas for reed and sedge growth (as they still do today), all suitable as roofing/building materials for example. There are also hints of Roman period settlement activity towards the base of slope down-valley, such as at Ramla Bay (Ashby 1915), which was undoubtedly utilizing similar landscape features.

Finally, there were many landscape modifications occurring from the later medieval period (mid-sixteenth century AD) onwards (Blouet 1997; Carroll *et al*. 2012; Wettinger 2011). Certainly the Ramla valley slopes become systematically exploited in the sixteenth century AD crusader Order of St John period and again in the mid-nineteenth century AD (Alberti *et al*. 2018; Blouet 1997) with two sets of superimposed systems of field boundaries and sinuous property boundaries located up/down the slopes (Fig. 24) (see Chapters 8–10). This combined extensification and intensification of landscape development may well have been associated with pressure on land to enable more sustainable arable agriculture to support the island population (see Chapters 7 & 8), but was also related to the use of better plough machinery and importantly the presence of reliable water sources from the natural spring lines in each valley.

There has been significant exploitation of the valley slopes and Blue Clay geology areas over the last five centuries or so (Grima 2008a), and as seen in the *Cabreo* maps of AD 1861 (Alberti *et al*. 2018). This agricultural expansion has undoubtedly led to increased down-slope erosion off the clay slopes and mixed accumulations of limestone rubble, sand and silty clay materials as hillwash in the valley bottoms such as in the lower Ramla, and confirmed by later nineteenth to early twentieth centuries AD OSL dates (Table 2.6). Nonetheless, there is some degree of balance and resilience in this landscape imposed through the widespread remodelling of the landscape with terrace systems. Today, this apparent landscape stability is interrupted by intense individual thunderstorm events which remove any easily erodible soils out to sea and contribute to continuing incision into the bedrock basement of the valleys by 1.5 m or more.

Since the 1960s, there has been continuing transformation of the Gozitan and Maltese landscapes with widespread clearance and uptake of arable land in the valleys and slope areas and expanding town-scapes on the limestone plateaux (Vella 2003). There has been soil removal and re-deposition as deliberate amendment of the thin red soils around the mesa margins using silty clay soil taken from the mid-/upper slope area on Blue Clay geology. For example, this occurred in the fields on the eastern side of Ġgantija temple in 1961 and again in 1985. At the same time, many of

the mesa plateaux areas have become more and more occupied by urban development, especially since the 1980s, perhaps as a corollary of the poor state of soil development on these plateaux.

Today, the landscape is extensively terraced and farmed for arable cash crops, olives and vines. In contrast, pastoral use for sheep/goat has largely recently disappeared, a casualty of EU marketing regulations. The natural springs at the upper Blue Clay/Greensand–Upper Coralline Limestone contacts survive, and the landscape is also relatively stable, although heavy rainfall events still lead to surface water and soil run-off to the sea that can be severe.

5.6. Conclusions

Geoarchaeological fieldwork on the island Gozo focused on the Ramla and Marsalforn valleys and the associated Neolithic archaeological sites at Ġgantija and Santa Verna, the Taċ-Ċawla settlement site, Ta' Marżiena temple and the Skorba temple as well as a number of deep valley sites such as Xemxija and Wied Żembaq on Malta. This study has suggested a new model of soil development for the early to mid-Holocene which especially shows the impact of Neolithic and later historic period communities on the soil/landscape system. It is suggested that a well developed, thick, moist, vegetated and clay-enriched brown soil or Luvisol had developed on several of the limestone plateaux areas of the Maltese Islands in the earlier Holocene. Similar brown argillic soils were probably once more widespread in the Maltese Islands and indeed the wider Mediterranean region (cf. Yaalon 1997). This soil type exhibited signs of disturbance from at least the earlier Neolithic period at some notable locations on both Gozo and Malta, but then witnessed the beginnings of major soil changes associated with both aridifying and de-vegetation trends trend from at least the beginning of the fourth millennium BC. This trend intensified throughout the third millennium BC and the later prehistoric periods, with soil erosion and its re-deposition being major factors in modifying the plateaux and valley landscapes, especially taking place from the mid-second millennium BC. These transformations set the scene for the subsequent palaeoenvironmental record characterized by thin, dry, calcitic soils and open xeric landscapes from the late third millennium BC onwards. Of course, these soil development trajectories need not have occurred everywhere on the Maltese Islands in the same manner, nor over the same time frames. Although there are repeated signs of fine soil erosion from the Blue Clay, Greensand and Upper Coralline Limestone geologies as exposed in most of the valleys on Malta from at least the beginning of the seventh millennium BC, it was probably not until post-mid-sixteenth century AD times that the Blue Clay, or silty clay vertisol, valley slope landscapes began to be exploited for agriculture in any intensive and extensive way, and especially during the second half of the nineteenth century AD, leading to later erosional aggradation in the lower valleys such as the Ramla in northern Gozo.

Chapter 6

Cultural landscapes in the changing environments from 6000 to 2000 BC

Reuben Grima, Simon Stoddart, Chris O. Hunt, Charles French, Rowan McLaughlin & Caroline Malone

6.1. Introduction

The highly fragmented landscape of the Maltese archipelago presents a range of different environments which evolved along different trajectories and presented different constraints and opportunities to its prehistoric inhabitants. It is remarkable how such a small surface area could show such variation and how each phase of the Neolithic responded to that variation. The *FRAGSUS Project* has yielded a wealth of new data and insights on a number of sites and landscapes across the archipelago and the opportunity is also taken to publish relevant elements of the survey undertaken in the Cambridge Gozo Project undertaken between 1987 and 1995, whose data were analysed by Sara Boyle (Figs. 6.1 & 6.2) in her doctoral dissertation (Boyle 2013; 2014). The picture that is emerging is one of different sites following life-histories that were often divergent (Volume 2). Comparison of these diverging stories allows some broad generalizations to be put forward about the way the inhabitants appropriated, exploited and ordered the landscape. However, given the diversity of life history, we can envisage that the next generation of scholars will uncover further diversity, perhaps even filling what currently appear to be clear gaps during the fifth millennium BC in the total life histories of the islands. Drawing on the rich detail of environmental and archaeological evidence revealed by the project, this chapter will tentatively outline some of the cultural responses to the changing environment that can be made out so far, after a brief analysis of the formal surface surveys undertaken in the Maltese Islands.

6.2. A short history of survey of a fragmented island landscape

Islands offer enormous opportunities for surface survey, and a number of notable Mediterranean examples now exist which have taken up this important challenge (Renfrew & Wagstaff 1982; Cherry 1990, 2004; Bevan & Connolly 2004, 2013). The idea of an island laboratory may have been critiqued (Rainbird 1999), but the small island does offer opportunities for an intensity and degree of coverage that is more problematic in larger landscapes. This was the motivation for the Cambridge Gozo survey of the late 1980s and early 1990s, even if ultimately thwarted by the unanticipated enormity of the Xagħra Brochtorff Circle and its consumption of the then meagre resources. The same problem faced the team when the Xagħra Brochtorff Circle was published in 2009 and only the briefest of outlines of the surface survey were given (Malone *et al*. 2009a, 41–2). Gozo was chosen as the sample area because of its greater preservation of cultural remains, a situation that was apparent even in the early twentieth century when Ashby chose Santa Verna as one of his excavation areas. This reasoning was the same that motivated the choice of sites for excavation in the 1980s on an island that had been relatively little explored and certainly never systematically excavated, even if investigated by a number of illustrious scholars of Maltese archaeology such as Ashby and Zammit. The clarity of its geology also permitted an easily articulated sampling programme (Figs. 1.3, 6.1 & 6.2). This programme started with an intensive study of the Xagħra plateau, later partly complemented by a much less complete study of the Ghajnsielem plateau, that was to be linked by transects cross-cutting the geological framework of the island. These transects were never completed, because of the absorption of resources in the completion of the Xagħra Brochtorff Circle excavation, but nevertheless a useful coverage was achieved, more than has been systematically undertaken in the Maltese Islands before or since. The aim was principally to investigate the distinctive prehistory of the island while also collecting the easily recognized Punic and Roman material, together with medieval and modern ceramics, and recording

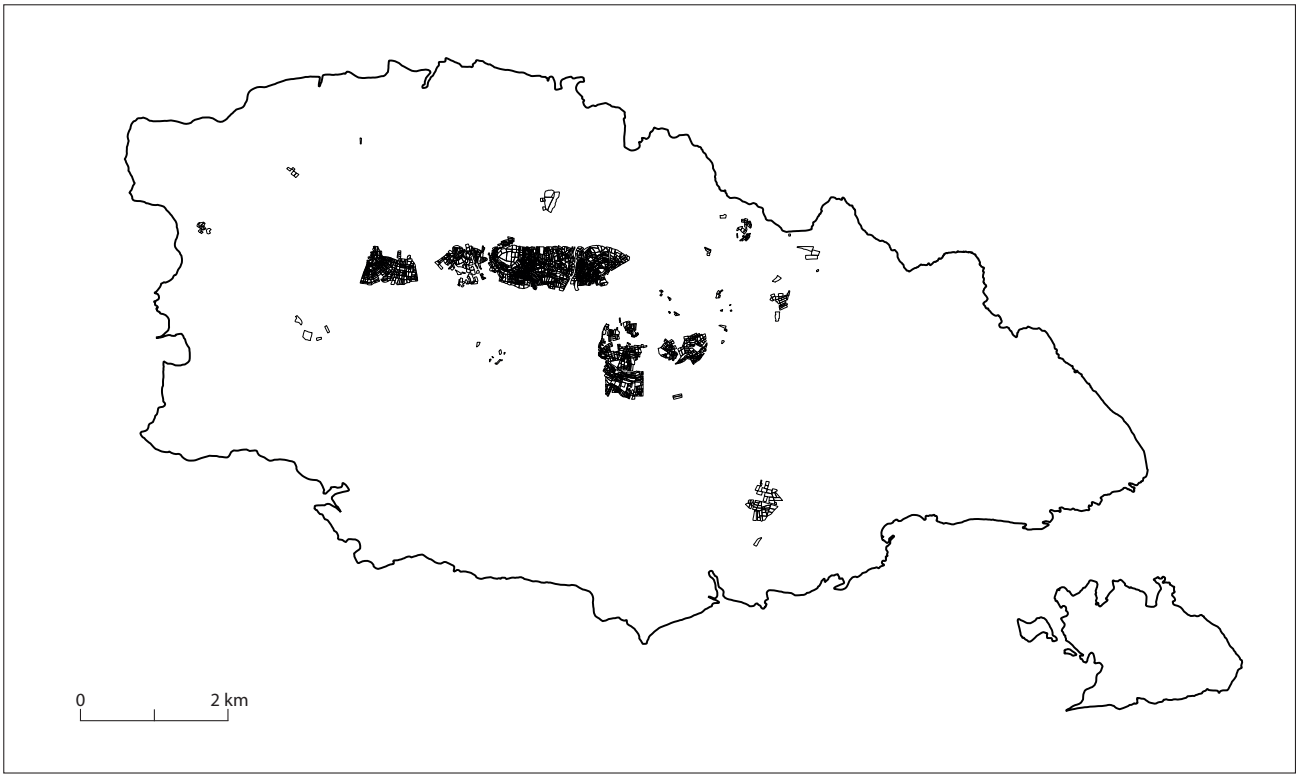

Figure 6.1. *The location of the Cambridge Gozo Project survey areas (R. McLaughlin).*

standing remains, water systems and evidence for shooting of birds, also from the modern period. The period of the survey from 1987–95 coincided with a generally fairly relaxed attitude by local farmers, tenants and owners, who normally permitted access to their fields. Such an attitude no longer exists, with more intensive crops, great land value and general suspicion of people walking over a farmland which is now usually encased in high wire fences.

The survey was designed from experience in the Ager Lunensis (Delano Smith *et al*. 1986), Punta Stilo (Hodder & Malone 1984) and the Gubbio valley surveys (Malone & Stoddart 1994), adapted to the distinctive terrace landscape of Gozo. From the very first (Stoddart n.d.) the aim was to record density of human land use (that is scatters of cultural material) as well as 'sites'. The idea was to produce a density map of weight of material per unit area (usually a terrace) and also a fragmentation index per unit area (weight/number of fragments). It was always intended that these maps would be used to interpret the cultural use of the landscape and the effect of geomorphological factors. Surveyors were instructed to collect all portable cultural material, 'except for rubbish that would be a danger to health'. Notes were made on the form of both collected and uncollected material on specially designed sheets, including a consistent policy to recover gun cartridge cases as well as other distinctive modern material. One of the young surveyors was something of an expert in clay pigeon shooting and started a simple typology of gun cartridge cases according to their use. The principal aim though, was to recover prehistoric material because it addressed the focal aims of the Cambridge Gozo project and was unusually distinctive, allowing a level of phasing even from small sherds that is unusual in the prehistoric Mediterranean (Malone & Stoddart 2000). Previous experience had shown that later material was more easily recovered (di Gennaro & Stoddart 1982) even if Medieval and modern material at that stage had not been catalogued for the Maltese Islands. The surveyors were, therefore, instructed to give equal weight to all periods.

The sampling units within the plateaux and transects were determined by the cultural patterns of the landscape, namely the terraced field. Each terraced field had a paper recording form allocated to it even if nothing was found. A new area number was also selected when there was a change in land use or if the field was larger than normal (this decision was left to the team leader, but a rough guide was the size of the interior of the Xagħra Brochtorff Circle (diameter of

45 m), so that the surveyors had a rapid visual guide to the sampling unit on the basis of where they otherwise spent much of their time. The field sampling unit was usually very much smaller, reflecting the fragmented nature of the landscape.

The survey benefitted from the high standard of topographic maps from the islands. A photocopy was taken into the field, where the direction of travel on each numbered terrace was recorded, with additional details on the back of the survey form. A master copy was held in the finds hut. Labelling of finds bags included the Area (usually terrace) number, the date, initials and visit number. The pottery was weighed and sorted by David Trump and a Small Finds Register kept for distinctive or complete objects, in the same pattern as the Xagħra Brochtorff excavation. A small group of project members, notably Duncan Brown, specialized in maintaining the survey standards and leading teams.

The pre-numbered survey forms provided the central register of information connected to the finds, and ultimately the database, indexed on the site number. A new form was filled in for each visit. Where necessary an area was subdivided (e.g. 1.01, 1.02 ….). The forms provided information on the four figure 1:2500 map number, the eight figure grid reference, the local Maltese toponym, estimated dates (for later verification), the density of finds, linkages to other areas, the amount of material collected, any small finds (flint, obsidian, coins, etc.), time spent in each area, time of day, density of coverage (generally 3 m apart), the phase of activity (transect, revisit, informant, etc.), ground cover, ground (especially level of washing) and weather conditions, as well as the merit of a return visit. Details of the topographic and geological location were recorded but later enhanced using GIS methodologies.

The same aims were shared by the Mġarr ix-Xini valley survey on the southeastern quarter of the island of Gozo, directed by Anthony Pace and George Azzopardi. Although this has yet to be published, we do know from the hypsometric study of its catchment and the pollen core taken at the interface of this valley with the sea (see Chapters 2 & 3), that it is one of the locations in Gozo which has the most intensive and destructive erosional run-off. For this reason, it is no surprise that the information kindly provided by Anthony Pace shows this valley largely to have material from the first millennium BC onwards (see Chapter 7). The aim of the (North West) Malta survey project (Docter *et al*. 2012) on the immediately adjoining land on the mainland of Malta was focused on the Phoenician and Punic period and the field survey made a relatively small contribution to the prehistoric period through some struck stone and one piece of Tarxien pottery relating to the period in this chapter. However, a desktop documentation of the same area nevertheless recorded 222 sites dated to the prehistoric period on a total of 308 data sheets, demonstrating the ubiquity of prehistoric activity on this part of the island. Nevertheless, for these reasons, the Cambridge Gozo Project survey remains the main source of information on the prehistoric landscapes covered by this chapter and Chapter 7 that is not otherwise available in archives held in Malta's National Museum of Archaeology and at the Superintendence of Cultural Heritage, recovered largely by rescue work.

A number of trends in settlement choices were identified through the GIS study undertaken by Sara Boyle (2013): namely that hotspots of occupation tended to be reoccupied on many occasions through prehistory, that the location of choice for settlement tend to be the east and south facing slopes of the landscapes, away from the cold northwesterly prevailing winds, and also at the geological interface between limestone and clay, where springs tended to emerge. The lighter and better drained soils of the plateau tops were also preferred over the heavy clay slopes that only came into active use in the second millennium BC. Furthermore, a scatter of 228 struck stone fragments were recovered across the landscape showing land use beyond the habitational hotspots (190 chert, 32 obsidian and 6 other materials).

6.3. Fragmented landscapes

The different topographic regions of the archipelago, described in Chapter 1, played an important role in shaping the evolution of different local environments, and the changing constraints and opportunities that they presented for human exploitation (Grima & Farrugia 2019). The main island of Malta may be divided into three main regions: the parallel ridges and valleys to the northwest, the Rabat-Dingli uplands to the west, and the central plain, made up largely of gently rolling and low-lying terrain stretching from the centre of the island to the east and southeast coast. The surface geology of the first two is predominantly Upper Coralline Limestone, while that of the third is mainly Globigerina Limestone. The topography of Gozo, on the other hand, is distinctly different. Flat-topped hills capped in Upper Coralline Limestone form mesas that rise dramatically across much of the island, while the lower ground, where the surface geology is predominantly Globigerina Limestone, is more gently contoured. This varied surface geology has largely determined the different soils that formed in different parts of the archipelago (see Chapters 1

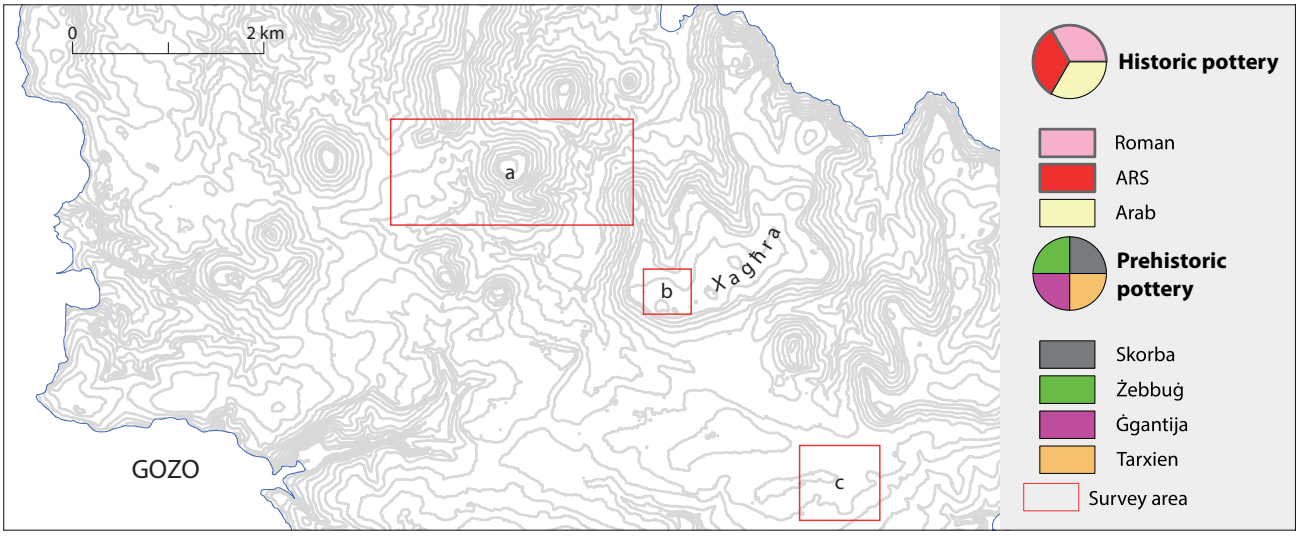
0
2 km
a
b
Xagħra
c
GOZO
Historic pottery
Roman
ARS
Arab
Prehistoric pottery
Skorba
Żebbuġ
Ġgantija
Tarxien
Survey area

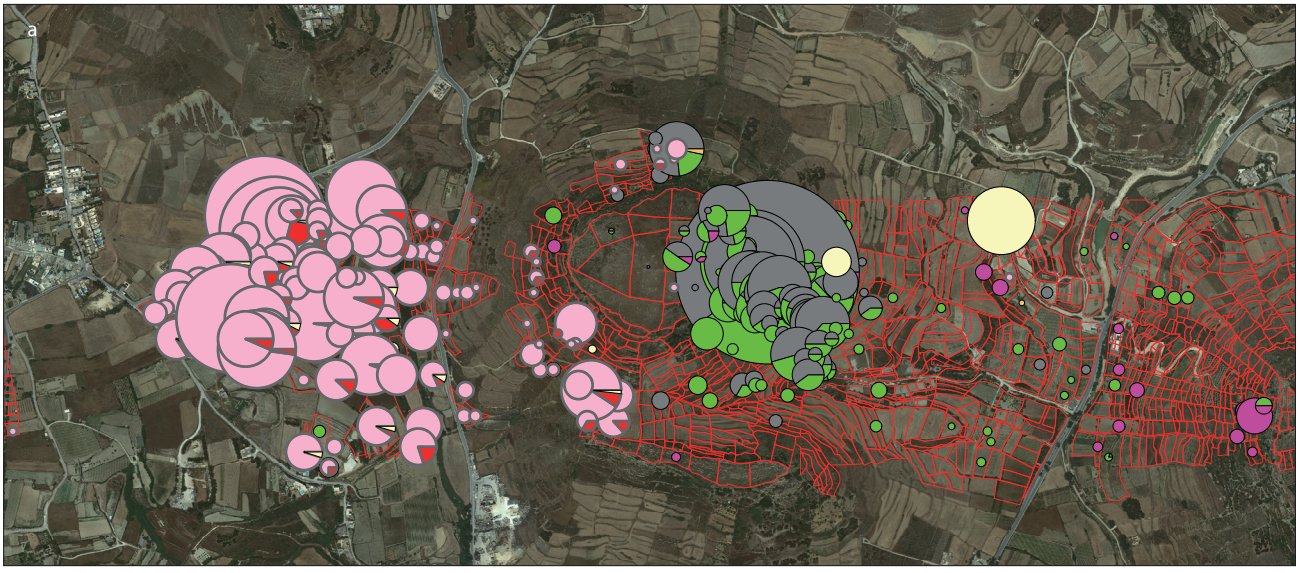
a

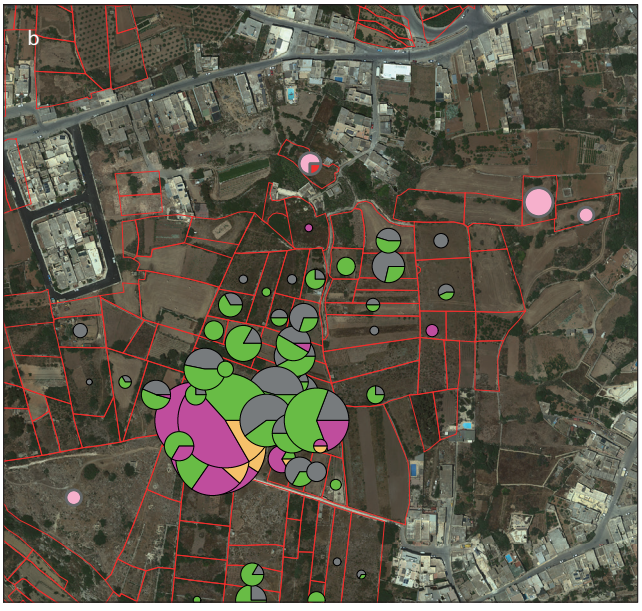
b


c

& 5). The slope and topography had influenced the different rates of loss of soil cover in different areas (see Chapters 2, 5 & 8). The more low-lying areas have been more susceptible to change as a result of coastal erosion and sedimentation, compounded by rising sea levels and changes in coastal lagoons (see Chapter 4). Each of these factors played a part in how successive generations of inhabitants perceived and organized their island world.

One of the most significant results of the geoarchaeological work conducted during the course of the *FRAGSUS Project* has been to establish that during the Neolithic, well-developed soils were present on the Upper Coralline Limestone mesas on Gozo, such as the Xagħra plateau (see Chapter 5). The low-lying Globigerina Limestone landscape that stretches across much of the southern half of the island might also have been ideal for earlier prehistoric agriculture as it presented a light, fine loessic-silt-like soil that would have been easily tillable in the past. However, it would have been less moisture retentive and prone to wind-blow and run-off erosion by rain-splash, so it may have been a challenge to maintain as resilient and productive arable land in the past. These areas have also been more heavily disturbed by modern activity, making geoarchaeological investigation more difficult. Nevertheless, results obtained from south of Ta' Marżiena have also detected the possible traces of relict well-developed reddish-brown buried soils comparable to the ones identified on the Xagħra plateau, suggesting that such soils were probably once more widely present in the surrounding landscape (see Chapter 5).

6.4. The Neolithic appropriation of the landscape

A crucially important result that has emerged from the *FRAGSUS Project* is the apparent decline in human activity during much of the fifth millennium BC. The intensive dating programme undertaken during the project has had far-reaching implications for the way the history of early human settlement of the archipelago is understood. Prior to the project, the general consensus was that the islands witnessed an unbroken human presence from the end of the sixth millennium BC through to the end of the Temple Period around the mid-third millennium BC. The apparent absence of datable archaeological evidence for human activity for the greater part of the fifth millennium BC may suggest a decline in the human population. The lacuna even raises the question of whether the islands were practically depopulated, before receiving a fresh influx of inhabitants after the end of the fifth millennium BC. Equally there was never a time when signatures of arable agriculture and pastoral activities disappeared from the palynological record, nor indeed a cessation in soil erosion in the deep core records, which together suggest that there were still people active in the landscape and practising subsistence agriculture (see Chapters 2, 3 & 5). However, as already indicated above, the investigation of new stratified sites and a new life history of the early inhabitants could easily have a substantial effect on our future understanding of the overall pattern of occupation. Nevertheless, some of the broad characteristics of the island environments in which these successive stages of human settlement took place in Malta have become clearer in light of the *FRAGSUS Project*. Some of the possible effects that the changing environments may have had on the cultural appropriation of the landscape are outlined below.

Figure 6.2 *(opposite). Fieldwalking survey data from around a) Ta' Kuljat, b) Santa Verna, and c) Għajnsielem on Gozo from the Cambridge Gozo survey and the* FRAGSUS Project *(R. McLaughlin).*

6.5. A world in flux (5800–4800 cal. BC)

The first clearly attested human presence on the archipelago in the sixth millennium BC was a time of rapid change in the physical landscape. During this period, the sea level rose by nearly a metre every century (Benjamin *et al*. 2017, 42). The impact on different parts of the archipelago varied according to the local topography and the effects would have been more detectable on the northeastern flanks of the islands where there is now a drowned landscape (Prampolini *et al*. 2019) and lagoons persisted over a long and variable period of time (see especially Chapter 4). Marine incursions deep inland were witnessed in the Marsa valley (Carroll *et al*. 2012, 33) and the Burmarrad valley (Marriner *et al*. 2012, 11). Much of St Paul's Bay was submerged at this time, but it appears that the inner end of the bay at Xemxija, which is dry land today, was not inundated (see Chapter 3). Further north, the Sikka l-Bajda reef was completely submerged (Foglini *et al*. 2016). Within Mellieħa Bay, the wave-cut Quaternary deposits which are still visible along the northern shore of the bay, standing to a height over two metres above sea level (Pedley *et al*. 2002), probably started eroding into the sea at a similar time. Similar wave-cut deposits survive along the northern coast facing Comino, which could only have started eroding into the sea as the inundation of the channel between Malta and Comino progressed. The same is true of the Quaternary deposits along the modern shoreline of the Ħamrija Bank on the south

coast of Malta (Pedley *et al*. 2002). The loss of land to marine transgression and erosion between the early sixth and the early fifth millennia BC was unrelenting and dramatic, and its effects palpable to each generation of inhabitants, who must have wondered how far and how long it would continue. The relationship to the sea level rise might have been particularly focused on the lagoons located at the foot of significant access points to some temple locations, notably near Borġ in-Nadur, Buġibba, Għajn Żejtuna and Xemxija, since these would have continued to witness visible change more readily than other parts of the island landscape. Moreover, in the presence of considerable infant mortality recorded at least over the following two millennia within the Xagħra Brochtorff Circle (Stoddart *et al*. 2009), the populations of prehistoric Malta must have been affected by both the loss of island space and, at times, the loss of people to occupy that space (Stoddart 2015; Thompson *et al*. 2020).

During the millennia preceding the earliest recorded presence of humans on Malta, the sea level had risen at even faster rates (Benjamin *et al*. 2017). The land-bridge between Malta and Sicily was submerged between 14,000 and 13,000 BC, and between 11,000 and 8000 BC, the extent of the archipelago was reduced to about half its size (Foglini *et al*. 2016). An inevitable consequence of this dramatic loss of land was that the archipelago became a constricted refuge for wild animal species migrating away from the inundated areas. It is reasonable to surmise that the varied wild flora and fauna and the absence of large predators would have been part of the initial attraction of the archipelago for the settlers who appear to be established there by early in the sixth millennium BC.

Evidence of agricultural activity has been documented by *FRAGSUS* from around 5900 BC (see Chapter 3). Even as the terrain was being improved for agricultural purposes, indigenous wild animals would have represented a very temporary and rapidly diminishing resource. Bird trapping might have been one seasonal source of food together with molluscs from the shoreline. As the islands continued to shrink in size during the first millennium of agricultural activity, wild animal species that could be hunted for food were probably driven rapidly to extinction. Marine food that might have been exploited appears not to have been extensively used, perhaps as taboos relating to food changed as farming became established. A future research aim would be to discover dated archaeological deposits that can address these issues.

The Cambridge Gozo survey provides a useful indication of the micro-changes in human occupation over this period (Boyle 2013; Fig. 6.3). In the very first occupation phase (identified by Għar Dalam style pottery), eleven locations are known on Gozo, of which five can be defined as hot spots and three locations within the survey area were more densely occupied than elsewhere in the landscape: the future 'temple' areas of Ġgantija and Santa Verna, and the eastern flank of Ta' Kuljat. From the survey evidence, over the course of the next phase (Grey Skorba and Red Skorba ceramics), occupation became focused around the spring on the eastern flank of Ta' Kuljat, and settlement was maintained at Santa Verna, these sites perhaps offering an indication of the retrenchment of human occupation into zones centred on crucial perennial springs. In contrast, there was little evidence for contemporary activity at Ġgantija, in spite of its water supplies. More broadly, during the Skorba phases, there were nine locations on Gozo of which five were hotspots, suggesting more concentrated, consolidated activity.

6.6. The fifth millennium BC hiatus (4800 to 3800 cal. BC)

The hiatus in archaeological evidence in the fifth millennium BC between the periods marked by Red Skorba and Żebbuġ ceramic styles was largely unsuspected before the application of high-resolution dating by the *FRAGSUS Project*. At face value, this might be a phase when the Maltese landscape was abandoned by people. There is, however, what seems to be evidence for human activity in the landscape from the pollen analyses, which show the continuation of cereal pollen and indicators of grazing throughout the fifth millennium BC. The pollen analysis is probably also indicative of increasing effective moisture levels from the beginning of the fifth millennium BC, which is consistent with rising lake levels and expanding forest in Sicily at this time (see Chapter 3; Carroll *et al*. 2012). While domesticated livestock, if abandoned by their keepers, might be expected to continue living in the Maltese Islands, domesticated cereals are dependent on people for their propagation and would be unlikely to continue as a significant component of the vegetation without human intervention.

Whether this agricultural activity was the signature of full-fledged occupation of the Maltese Islands, or the actions of groups coming from Sicily, perhaps seasonally, to sow, harvest and tend animals is uncertain, currently. If people remained resident in the landscape, it is possible that they abandoned ceramic manufacture (or adopted the making of non-durable low-fired or non-distinctive ceramics) and constructed flimsy dwellings that left no trace, or that they relocated all habitation to now-submerged coastal localities and/or currently heavily built-up locations where archaeological evidence has been lost. This hiatus is certainly

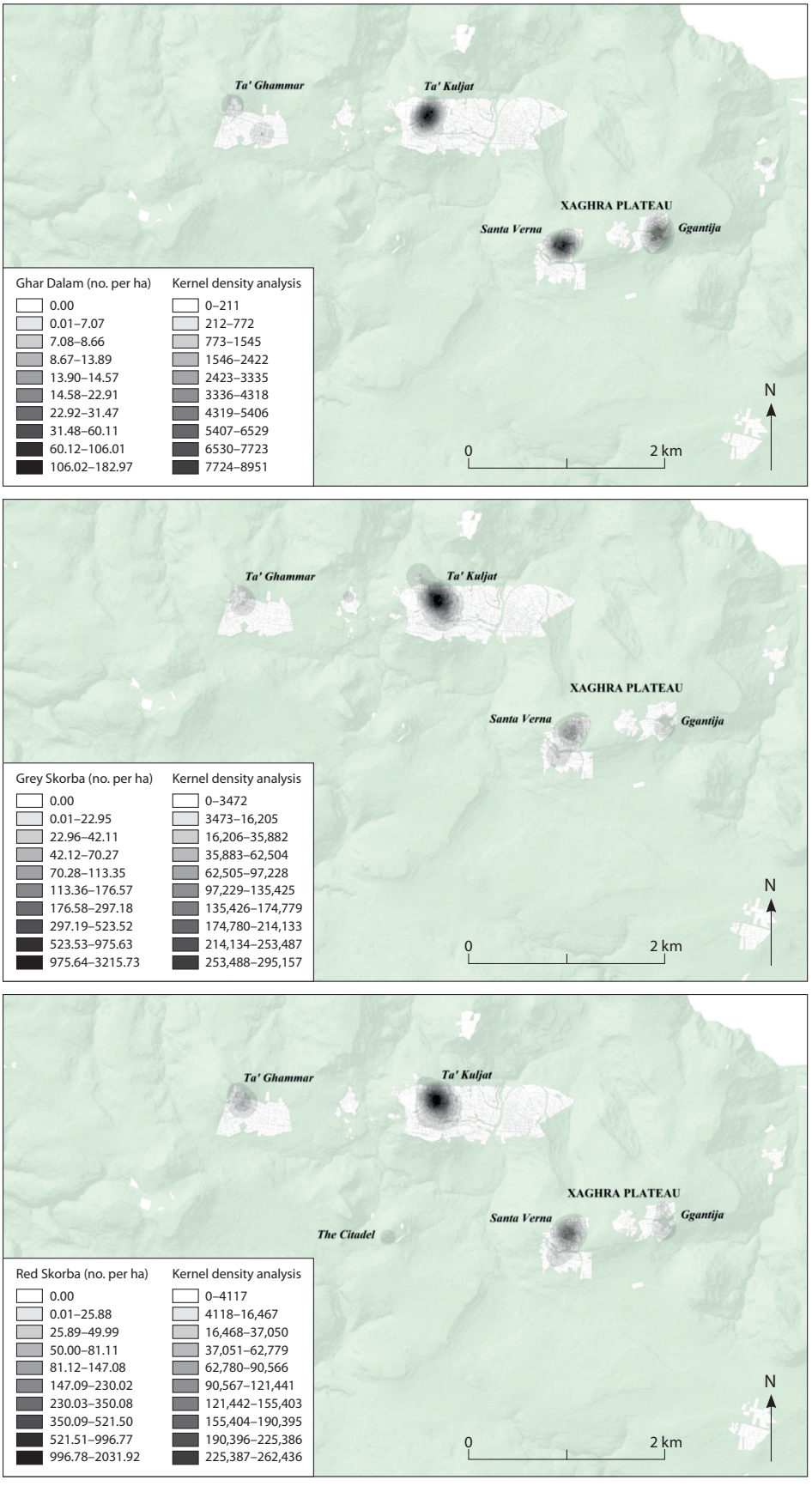

Figure 6.3. *The first cycle of Neolithic occupation as recorded by the Cambridge Gozo survey using kernel density analysis for the Għar Dalam, Red Skorba and Grey Skorba phases (S. Boyle).*

something for future research to explore more fully in the Maltese Islands.

The beginning and end of this archaeological hiatus coincides with evidence of gypsum deposits in our cores at Xemxija and Wied Żembaq suggesting extremely strong seasonality and possible pollen evidence from the Salina Deep Core for short episodes of low precipitation. In a marginal environment, the effects of factors which may appear to have a limited impact are often multiplied, because they may help push a population across the critical threshold between subsistence and starvation. It is conceivable that seasonal water stress contributed to the destabilization of some communities and precipitated a reorganization and relocation of human activity, with abandonment of established settlements. There could even have been a strategic withdrawal, as seen earlier in prehistoric Cyprus (Guilaine *et al*. 2011, ch. 52; Dawson 2014, 185ff) at the start of the hiatus, and possibly the incoming of people from Sicily at the start of the Żebbuġ phase. Meanwhile, the rate of sea level rise fell off from around a metre a century to around a metre every millennium (Benjamin *et al*. 2017, 42).

6.7. Reappropriating the landscape: the 'Temple Culture'

The resurgence of evidence of human activity that has been attested by the *FRAGSUS* dating programme occurs at the earliest from 3910/3640 cal. BC (see Chapter 2, and Volume 2, Chapters 2, 4 and 7)) and coincides with significant changes in the material culture repertoire. The Żebbuġ ceramic phase (3800–3600 cal. BC) has long been considered to be a new departure from the preceding Ghar Dalam/Grey Skorba and Red Skorba ceramic styles (ending by 4980/4690 cal. BC) (Trump 1966) since it shows many more similarities to the succession of ceramic styles that follow it, through the period of megalithic construction generally known as the 'Temple Period'. The Żebbuġ phase has, in fact, often been considered the first phase of the Temple Period (*c*. 3800–3600 cal. BC). The possibility of a hiatus in ceramic production during the fifth millennium BC has also shed light on the innovative forms and patterns seen in the ceramic sequence at around the same time (see Volume 2, Chapter 10). The innovations in decorative technique, pottery forms, fabric and temper that appear with the Żebbuġ phase appear consistent with the suggestion of a fresh influx of inhabitants with a close relationship to Sicily. The importance of this new cycle of inscription on the landscape was much emphasized in 1990 (Bonanno *et al*. 1990, 199, table 1), a generation before the evidence of a possible hiatus in the chronology began to emerge. In that paper, it was pointed out on the basis of Evans' data that the Żebbuġ phase was crucial to a new stage in the islands' 'ideological' development. Later, in 2004, David Trump reiterated that observation on the basis of the ceramic style:

> *While Red Skorba shows remarkable advances on Grey, these were not followed up. The second cycle opens with Żebbuġ phase pottery, its antecedents firmly back in Sicily, showing no local continuity. Whatever that may mean in terms of Maltese history is quite uncertain in the present state of knowledge* (Trump 2004, 254).

The revised chronological framework goes a long way to answer precisely the questions that Bonanno, Gouder, Malone, Stoddart and Trump had variously posed over the last quarter century. It also helps explain the emergence of another cultural phenomenon, which is perhaps the most remarkable material expression of the Neolithic in Malta, the monumental megalithic temples. Since David Trump's excavations at Skorba more than half a century ago (Trump 1961a & b, 1966), the appearance of megalithic monuments had popularly been attributed to the Ġgantija phase ('the earliest temple'), although some scholars had argued for earlier antecedents in the Żebbuġ (Trump 1966, 49; Evans, 1971, 34; Bonanno *et al*. 1990). Following recalibration of radiocarbon dates, the phase was shown to span from 3700–3500 cal. BC. The general understanding, until new dating offered the present picture, was that following a millennium and a half of human settlement of the archipelago, megalithic monuments appeared across the archipelago in a short space of time in the Ġgantija phase. Since megalithic monuments were often built on sites which had already been nodes of human activity for several centuries, and in some cases stretching back to the earliest known human habitation of the islands during the Għar Dalam phase, the triggers that gave rise to this sudden investment in monument-building had remained elusive.

The new chronology that has emerged through *FRAGSUS* has cast light on the dating problem of the earliest temple building, a problem that has challenged scholars until now. The more refined dating made possible by the re-excavation of Santa Verna in particular has pushed back the date for the earliest phases of the megalithic monument firmly to the Żebbuġ phase, and dated it to around 3700 cal. BC (see Chapters 2 & 12, and Volume 2 Chapter 2). This revised chronology for the onset of megalithic monument building has far-reaching implications. Prior to this revision, no elegant or compelling explanation has been forthcoming for the apparent temporal separation

between the start of a distinct cultural sequence suggested by the ceramic evidence and rock cut tomb building from the Żebbuġ phase, while placing the emergence of megalithic monument building only from the Ġgantija phase (*c*. 3400 cal. BC) onwards. The revised chronology appears to resolve this difficulty with a parsimonious explanation, which may also have far-reaching implications for the cultural reappropriation of the landscape that started by the mid fourth millennium BC, and the role of megalithic monuments in this process, as discussed below.

A close association between the environmental and cultural evidence is now confirmed by the revised chronological sequence. This shows that firstly, the arrival of new groups or renewed intensification of human activity on the archipelago was accompanied by renewed social organization, which had not been suspected previously. Second, the new cultural sequence represented by the Żebbug phase ceramic repertoire, which was always suspected to be related to Sicilian groups, can now be shown to be contemporary with them. Third, the extraordinary emergence of megalithic monument building, which traditionally was thought to have started at the onset of the Ġgantija phase, and had little association with contemporary developments on Sicily, now dates to the very beginning of this landscape cycle. The close temporal association emerging between these three crucial processes in the *FRAGSUS* evidence is of major significance. In light of the new chronological framework, the three processes are different aspects of a single cultural phenomenon. The emergence of a new ceramic tradition and the adoption of monument-building were inseparable from the repopulation and intensive reoccupation and exploitation of the landscape. In this light, the building of monuments was arguably a process of 'altering the land' (cf. Bradley 1993) to possess and control the landscape.

The distribution of Żebbuġ phase sites in the landscape is instructive here. The comparison between what is known of the distribution and the intensity of cultural activity before and after the apparent hiatus of the fifth millennium BC is particularly revealing. This comparison is made possible by the evidence gathered from a series of sondages that John Evans and David Trump excavated on megalithic monumental sites during the 1950s and 1960s (and a feature of the Bonanno *et al*. (1990) analysis), the fieldwalking data from the 1987–1995 Cambridge Gozo Survey, and the results of the site excavation and fieldwalking surveys undertaken during the *FRAGSUS Project* (see Chapter 7 & Volume 2). Some considerable emphasis was given to the power of this new ideological cycle starting in the Żebbug in earlier research (Bonanno *et al*. 1990, 199 & table 1), but the detection of the possible fifth millennium BC hiatus gives much greater emphasis to its importance.

The new interpretation is supported by the trends visible from the Cambridge Gozo survey (Fig. 6.4). In the first part of this cycle (Żebbug) the concentrations of activity returned to Santa Verna and Ġgantija, the two future 'temple' sites. During this phase there were 11 locations on Gozo of which five were 'hotspots' discovered on the survey. The distribution of sites was statistically more clustered that in the previous cycle (Boyle 2013). This developed into an oscillation of the relative importance of these sites over the following 1500 years. In the next part of the cycle (the elusive Mġarr), Santa Verna declined in importance, although it recovered its role in the Ġgantija phase, only to lose its importance once again in the final Tarxien phase (Fig. 6.5). During the Ġgantija phase there were 15 locations on Gozo of which five were survey 'hotspots'. Sites tended to have an easterly aspect, perhaps to enhance their agricultural potential. More generally there was continuity into the Tarxien phase, allowing for some contraction into 12 locations on Gozo. These transitions are borne out by the available excavation evidence (see Volume 2), since this suggests that the Santa Verna site was sidelined during Tarxien phase and many of the paraphernalia transported either to the Xagħra Brochtorff Circle or to the Ġgantija 'temple,' where activity was concentrated until the end of the Temple Period. A similar tendency may also be observed in the data from the intensive fieldwalking survey conducted around Santa Verna and Ġgantija (2014) during the *FRAGSUS Project* (see Volume 2).

The evidence from excavations and sondages undertaken on a number of megalithic sites by Ashby *et al*. (1913), Evans (1971) and Trump (1966) (cf. Bonanno *et al*. 1990, 199, table 1) have been corroborated by the intensive re-excavation work conducted during the *FRAGSUS Project*, which has also provided more refined dating than was previously possible. Both at Santa Verna and at Skorba, the sixth to early fifth millennia BC ceramic phases of Għar Dalam, Grey Skorba and Red Skorba are well represented. In both sites, activity on the same site appears to resume in the Żebbuġ phase. A background scatter of Għar Dalam and Skorba ware was also detected in the *FRAGSUS* excavations at Ġgantija, Taċ-Ċawla and at Kordin III (see Volume 2, Chapters 3, 4, 5, 6 & 7). These sites also showed a well-attested Temple Period presence from the Żebbuġ phase onwards.

Turning to other sites where no excavations were undertaken as part of the *FRAGSUS Project*, we may refer to the results of earlier work. At Ta' Ħaġrat, the earliest pottery recorded is from the Għar Dalam phase

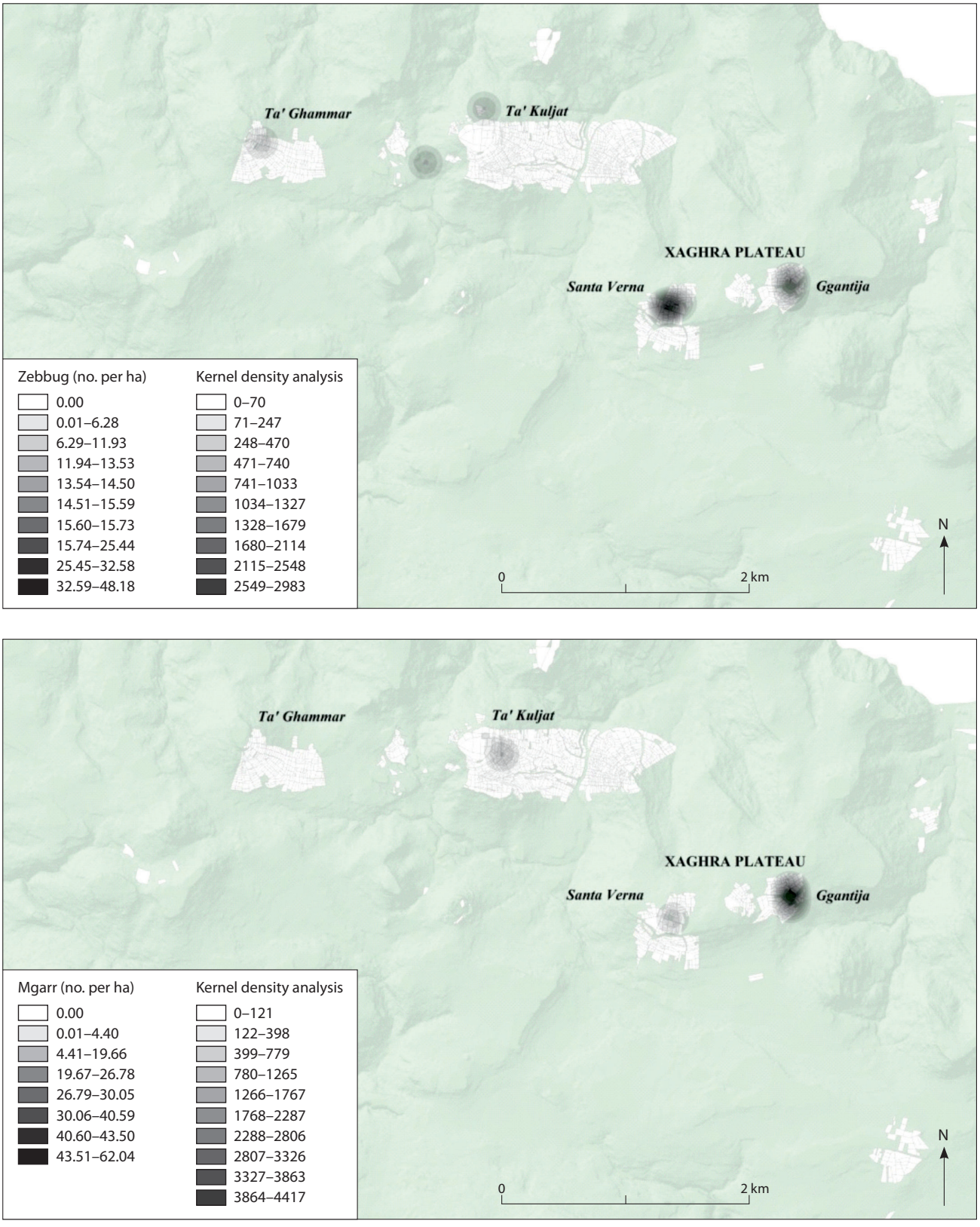

Figure 6.4. *The first half of the second cycle of Neolithic occupation as recorded by the Cambridge Gozo survey using kernel density analysis implemented for the Żebbuġ and Mġarr phases (S. Boyle).*

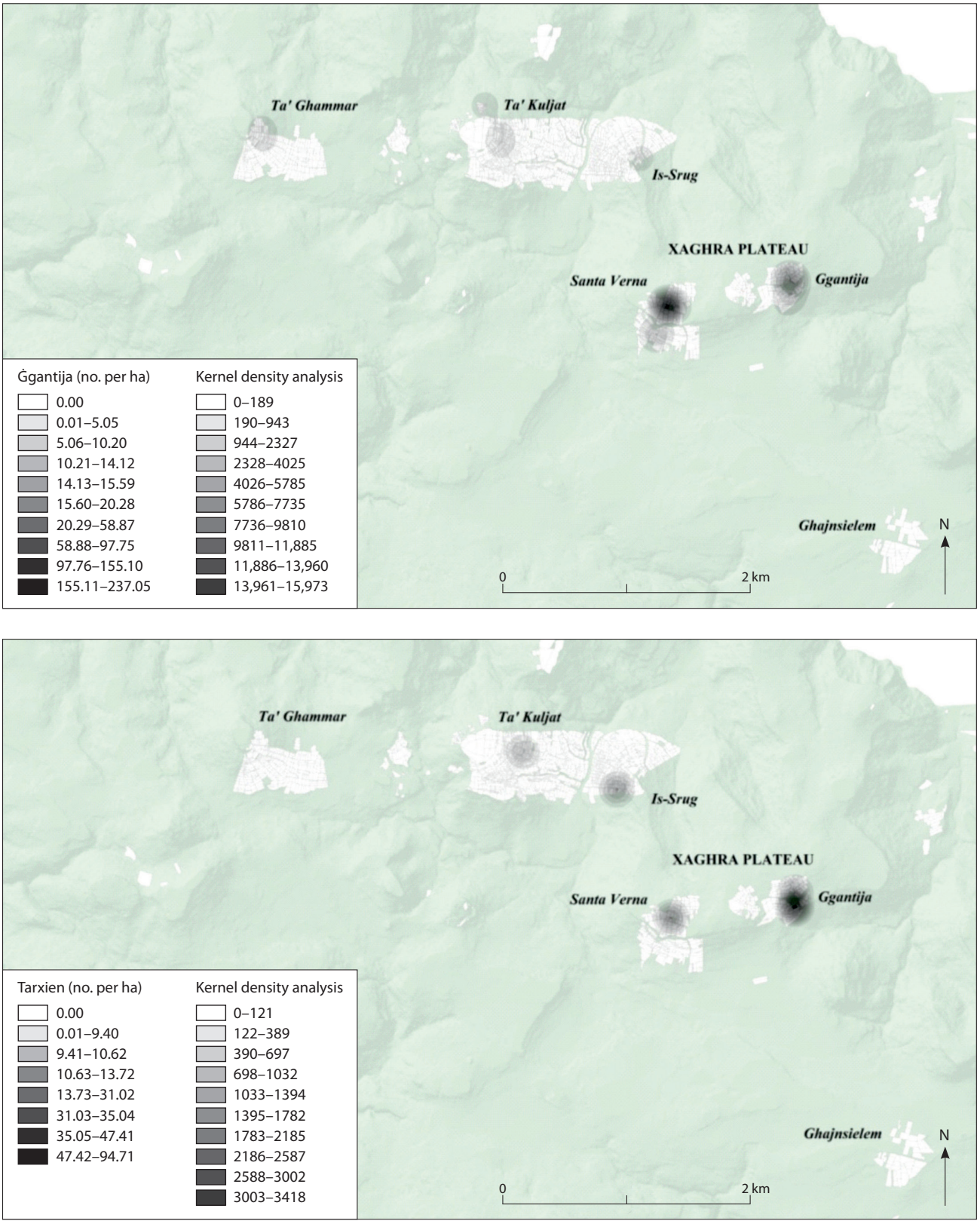

Figure 6.5. *The second half of the second cycle of Neolithic occupation as recorded by the Cambridge Gozo survey using kernel density analysis for the Ġgantija and Tarxien phases (S. Boyle).*

(Evans 1971, 33), but detection of later phases was difficult. The sondages cut by Evans at Tarxien yielded no evidence earlier than the Żebbuġ phase (Evans 1971, 135). At Ħaġar Qim, the earliest pottery detected in a series of sondages below the floors only stretched back to the Mġarr phase (Evans 1971, 88). The earliest pottery recorded from Mnajdra was, once again, from the Żebbuġ phase (Evans 1971, 101). At the Buġibba temple, the four trenches cut by Evans in 1954 failed to detect any pottery earlier than the Tarxien phase (Evans 1971, 111). Nonetheless, the palynological data from the Salina Deep Core (see Chapter 3) certainly suggests that people were in the vicinity and practising agriculture from the earlier Neolithic even if there are no sites or artefacts to indicate this presence, and the high frequency of charcoal in Maltese sediments dating to around 6000 cal. BC also indicates clearance around that time. In the case of the Tal-Qadi site, the dating evidence available is admittedly more tenuous, as it is presently limited to the pottery held in storage from the 1927 excavations, which includes a single sherd from the Żebbuġ phase, but no earlier material (Evans 1971, 43). In recent decades, extensive investigations have been undertaken by the Italian Archaeological Mission on the prehistoric deposits associated with the megalithic monument at Tas-Silġ. Notwithstanding careful excavation to bedrock at a number of points, the earliest material that was detected was from the Tarxien phase (Cazzella & Recchia 2012, 18).

The evidence that has just been reviewed is admittedly uneven, and the results may appear sporadic. Site locations seem to fall into two main groups: sites that had longevity of successive occupation back to the earlier Neolithic, and sites which in the later Temple Period were occupied for the first time. It could be argued this pattern may be better understood in the light of the geoarchaeological and palaeoenvironmental results presented in this volume by the *FRAGSUS* team. The relationship between the evolution of monumental activity and the wider environment may in turn shed light on how the cultural appropriation of the landscape continued to unfold during the Temple Period.

Of the sites that have been assessed and for which there is dating evidence, it seems that they fall into two major groups. One group represents megalithic monuments that were built on sites already in use before the apparent hiatus in human activity during the fifth millennium BC. A second group includes megalithic complexes that were built on sites that only started being used after the fifth millennium BC from the Żebbuġ phase or later. This observation may sound like a tautology; 'some sites are in use much earlier, while others are not'. What makes this observation more interesting is the topographical and geological context in which they occur. The sites where earlier Neolithic activity has been detected are located on the Upper Coralline Limestone, in close proximity to the freshwater springs that emerge from the perched aquifer above the underlying clay (Ruffell *et al*. 2018). Santa Verna, Ġgantija, Ta' Ħaġrat and Skorba all share this characteristic. The one exception is Kordin III, which has yielded early Neolithic evidence, yet is located away from the Upper Coralline Limestone outcrops, along the margins of the open rolling Globigerina Limestone landscape of southeast Malta. The remaining monumental sites (which to date have not yielded pre-Żebbuġ material are located on or around the margins of the open Globigerina Limestone landscape that characterizes eastern and southern Malta. Tas-Silġ, Tarxien, Ħaġar Qim, Mnajdra, Buġibba and Tal-Qadi all share this common factor. It should be emphasized that this is an argument from silence, and that new evidence from future work may significantly alter the patterns noted here. With these limitations in mind, it is nevertheless useful to consider the possible implications.

This broad correlation between the history of use of these sites and their landscape setting appears to be significant. An earlier attempt has been made to suggest a model for how megalithic monuments in different parts of the landscape developed over time (Grima 2007, 2008b). In that contribution, it was noted that megalithic monuments associated with the ridges and valleys in northern Malta emerged during the earlier period of megalithic monument construction in the Ġgantija phase, but generally did not register much further growth during the Tarxien phase. On the other hand, the megalithic buildings on the Globigerina Limestone landscape in south and east Malta continued to register significant growth through the Tarxien Temple Period, resulting in the most extensive megalithic complexes in the archipelago. The complexes – Tas-Silġ, Borġ in-Nadur, Ħaġar Qim, Mnajdra, Tarxien and the Ħal Safleni Hypogeum are all on the margins of the plateau and most are associated with springs or wells or are close to valleys where there would have been at least intermittent fresh water. The Tarxien phase was a time of declining effective moisture and the light well-drained soils on the Globigerina Limestone would have been the first to become drought-prone and unable to support arable farming. It is conceivable that the growth of these sites in the Tarxien phase was a response to the increasing difficulty faced by farming communities.

The new evidence that has been captured by *FRAGSUS* with fresh fieldwork has shed new light on the questions of continuity, growth and constraint, and allows a better-informed explanatory model to be

proposed. On the basis of the megalithic monuments where tenable chronological and stratigraphic evidence is available, it appears that the life-histories of those examples that were built on the Upper Coralline Limestone mesas of Gozo and the ridges of northern Malta share two important characteristics. The first is that, in most cases, they stand on sites that were already in use as sustainable if modest foci during the earlier Neolithic settlement of the archipelago. The second is that the same megalithic complexes generally appear to register less growth in the later Temple Period, an episode of often extravagant building, expansion and cultural expression. An extra detail of the *FRAGSUS* research from the Xagħra plateau of Gozo is that the long-standing site of Santa Verna does not appear to continue into the Tarxien period, when activity and expansion was transferred to the adjacent Xagħra Brochtorff Circle and Ġgantija (see Volume 2), one of the largest temples. The palynological analyses at Santa Verna show a drying trend, with the disappearance of algae in the latest samples, so it can be hypothesized that the site was not retained because water on the site failed. Ġgantija in the Tarxien period also presents evidence for manuring in its immediate vicinity, which could be related to the reliable spring water emerging beneath the temple complex (Ruffell *et al*. 2018) (see Chapters 3 & 5). The low-intensity scatters of Żebbuġ- and Ġgantija-phase potsherds evident in the Cambridge Gozo survey (Figs. 6.1, 6.2), which may be the result of manuring, are not replicated by spreads of Tarxien-phase material, suggesting retrenchment of arable farming into small irrigated enclaves in the last phase of the Temple Period.

At least for Gozo, the cultural landscape appears to have focused on these trustworthy 'club houses' as arid landscape conditions made subsistence increasingly difficult (Barratt *et al*. 2020). These pressures were perhaps more evident in most of the megalithic complexes located around the Globigerina Limestone landscape of south and east Malta, which more often than not appear to trace their origins to no earlier than the Żebbuġ phase, but then appear to have continued to be enlarged and elaborated into the final Tarxien phase of the Temple Period. This distinct pattern could be related to the different landscape environments in which they are located. We could suggest that the different life-histories of these two groups of monuments are tied to the changing constraints and opportunities that these environments presented, and which may be tied to a reliable water supply.

During the sixth millennium BC the Neolithic settlement of the archipelago appears to have taken full advantage of the abundant freshwater springs around the Upper Coralline Limestone mesas on Gozo and ridges on northwest Malta. The geoarchaeological results have also given firm indications that the brown argillic soils on these Upper Coralline Limestone environments were already well-developed during the early Neolithic settlement of the archipelago (see Chapter 5). The same geoarchaeological work has shown that during the earlier Neolithic, soil erosion from the upper parts of the valley slopes is already evident in, for example, the Xemxija valley, and that by the time of the construction of the early megalithic monuments in the fourth millennium BC, over-exploitation had impoverished these soils through erosion and depletion. The geoarchaeological investigation has also identified the relicts of possible well developed buried soils on the Globigerina Limestone landscape, for example to the south of Ta' Marżiena on Gozo, and in the cores from Wied Żembaq and Marsaxlokk on Malta (see Chapter 5). The general indications from the dating evidence that has been captured for these buried soils are that the soils on the Upper Coralline Limestone and at the upper slope transition zone between the Blue Clay/Greensand and Upper Coralline Limestone were already being exploited from at least the sixth millennium BC, and especially so in the fourth and third millennia BC. Unfortunately, there is an absence of good soil/sediment evidence to suggest that the fine silt soils on the Globigerina Limestone were being intensively exploited at similar periods, but these areas would have been ideal for early agricultural exploitation. Rather, there is later evidence in the second millennium BC for all areas being utilized for agriculture except the Blue Clay geological exposures in many of the valleys. This could reflect that while human presence was probably ubiquitous across the archipelago throughout the different periods of Neolithic settlement, the exploitation of different areas by different communities may have followed various trajectories of intensification.

There appears then, from these data, to be a convergence between the palaeoenvironmental and cultural evidence under discussion. Drawing together the different strands that have been considered, the new *FRAGSUS* evidence implies a broad picture of renewed intensification of activity on the archipelago at the start of the Żebbuġ phase focused on the Upper Coralline Limestone landscapes of the plateaux. Also, that the upper third of the valley slopes that had been more intensively occupied during the earlier Neolithic settlement appear to have been intensively reoccupied in the Żebbuġ. Subsequently, activity seems to have become more concentrated by the Tarxien phase in the early third millennium BC, with some areas becoming less intensively used and some temple sites disused.

6.8. Transition and decline

The end of the Temple Period in Malta has, to date, been viewed as a social and economic collapse or failure (Trump 1976), leading to drastic changes in culture and even a hiatus in settlement by many, but not for all scholars (e.g. Bonanno *et al*. 1990; Grima 2008a; Malone & Stoddart 2013). The evidence for the collapse was never as strong as some may have hoped; the idea ultimately stemmed from Zammit's excavations at Tarxien and the identification of an apparently sterile layer lying between the Tarxien and Tarxien Cemetery phases (Zammit 1930). However, a gradual transition between the phases has been noted at a number of other archaeological sites, most notably the platform façade of the Ġgantija temples, where Evans (1971, 180) found occasional Tarxien Cemetery sherds under structural features, and in a footnote to his report states:

> *This poses something of a problem, since it seems to imply that pottery of the Tarxien Cemetery type must have been imported into Gozo, or that the people of the Tarxien Cemetery culture must have been present in the island before the end of the Tarxien phase.*

It should be noted that new dating at three sites (Xagħra Brochtorff Circle, Taċ-Ċawla and Tas-Silġ) all confirm a chronological distinction between the Thermi pottery and Tarxien Cemetery. Previously the materials were conflated as one post-Temple episode. Now Thermi is associated with the final Tarxien phase, whilst the Cemetery material is quite separate and later. Previous excavations at Ħal Saflieni, Buġibba, Mnajdra, Kordin III and Tal-Qadi (Evans 1971) have all yielded sherds identified broadly as Tarxien Cemetery but have not yet been reassessed. From the new dates, it seems clear there was a gap of some centuries between Thermi (*c*. 2400–2200 cal. BC) and Tarxien Cemetery (after 2000 cal. BC). This gap implies that sites were often occupied in the TX/Thermi, and again in the TXC, but there is little suggestion of continuity of occupation, given the centuries long gap. At Skorba, ruins of the West Temple were occupied during the Tarxien Cemetery phase by people Trump (1966, 7), perhaps unhelpfully, named 'squatters'. The megalithic building was altered to accommodate a domestic function; but no radiocarbon evidence was ever sought to date when this occurred. Instead the original radiocarbon dates of *c*. 1600 cal. BC for the Tarxien Cemetery phase were obtained from a cache of charred *Vicia faba* (horse beans) found at Tarxien itself, and now re-dated through *FRAGSUS* to *c*. 1800 cal. BC. At the Xagħra Brochtorff Circle, the main Tarxien Cemetery activity areas were spatially and temporally distinct from the burial activity, and located above the collapsed and abandoned burial caves. This Early Bronze Age activity dated to around 1900–1800 cal. BC (Malone *et al*. 2009a, 341ff) associated with a small number of distinctive Tarxien Cemetery sherds, cups and figurine fragments, was part of apparently domestic occupation. Earlier in the sequence, however, Thermi-grey ware style almond rim sherds were associated with both the final burial deposits at Xagħra, probably around 2350–2400 cal. BC (the end of the Neolithic-Copper Age) and also found scattered in the superficial domestic levels of the Tarxien Cemetery occupation. The Thermi-style grey wares were likely made from local clay employing grog (see Malone *et al*. 2009, 239) and appear to be a local production. Until now, both these style categories have been seen as a signal of disturbance or intrusion rather than the distinction of different material cultures that may have been present in Malta in the final centuries of the third and early years of the second millennium BC. Additional evidence is now attested from Taċ-Ċawla (see Volume 2, Chapter 3, and Tas-Silġ (Cazzella & Recchia 2012, 2013, 2015; Recchia & Cazzella 2011; Recchia 2004–5) which can expand on the detail and dating of this elusive period. As mentioned above, there has been a consensus view that the end of the Tarxien phase was a social and economic collapse, and this led to a likely break in the cultural sequence, though it has been widely acknowledged that definitive evidence for this has been lacking (Azzopardi 2014; Pace & Azzopardi 2008; Malone *et al*. 2009a). A new scenario might argue that new ceramics (Thermi-grey wares of the Cetina complex) were introduced into the still functioning Tarxien Culture, perhaps with new populations, in the period 2400–2200 cal. BC and the two distinct cultural identities coexisted with a level of continuity at several sites. Meanwhile, burial activity at Xagħra evidently slowed and stopped at this very period. The current dating does reveal a period of between two and four centuries between the Thermi-style ceramics episode and the establishment of the Tarxien Cemetery phase with its distinctive pottery and cremation burial traditions. The AMS dates achieved for this appear for this next phase to be securely dated to the early second millennium BC. It is certainly not proven that Thermi Grey wares and Tarxien Cemetery pottery occurred contemporaneously together at any securely dated site.

Evidence from the *FRAGSUS Project* excavations of the Taċ-Ċawla settlement (see Volume 2, Chapter 3) provides detail of the dating relationship for Thermi. At this site, which contained a domestic structure and midden deposits associated with occupation at

a seasonal water source, Thermi pottery occurred in contexts dating to as early as *c*. 2400 until *c*. 2200 cal. BC. The sherds appeared mainly in a pit dug into the upper levels of the stratigraphic profile of plastered floors of a Tarxien period house, distinct and separate from Tarxien pottery. Importantly, no distinctive Tarxien Cemetery pottery was identified on the site (see Volume 2, Chapter 10). Elsewhere Tarxien Cemetery material has been noted in various temple sites (e.g. Ġgantija) but always in levels dissociated from secure Tarxien deposits.

In terms of the landscape context, occupation of settlements such as Taċ-Ċawla and the megalithic sites signals the enduring importance of freshwater sources during the opening centuries of the Bronze Age. At a human level, the landscape was probably not significantly reorganized from the Temple Period patterns. It is possible that the intensity of activity was somewhat less than in previous centuries, as the overall quantity of Tarxien Cemetery pottery from sites is typically much less than that of the Tarxien Period. The quantity may reflect a short duration of use over three to five centuries at most, or a small population. In contrast, Tarxien style was sustained from *c*. 2800–2400 cal. BC with an apparently dense and dynamic population.

The current evidence from the *FRAGSUS* study does clarify these questions of time and space a little. The environmental story suggests drying conditions towards the end of the third millennium BC, a reduction in cereal pollen indicative of reduced arable activity, and a slight and short-lived regrowth of scrub in a few localities. These factors together could suggest that there was a marked reduction in intensive occupation of the Maltese islands, tallying neatly with the cultural changes seen in ceramics, settlement and burial practices.

The *FRAGSUS Project*'s palynological work (see Chapter 3) was undertaken in tandem with an extensive programme of radiocarbon dating and Bayesian age-depth modelling, which has allowed the ages of such events to be estimated more robustly and with more precision than before. This development, and the greater number of sediment cores now available for study, have demonstrated that cereal agriculture continued at a low level at a few sites throughout the period, similar to the rather insubstantial archaeological evidence. Generally, the overall area of cultivation in established coastal sites was probably significantly lower than in earlier periods, but there was some relocation of activity inland, suggested by a rise of cereal pollen in the Burmarrad 2 core from *c*. 2400 BC (Gambin *et al*. 2016).

Reduced activity in the later part of the Tarxien phase is also apparent from the temporal distribution of radiocarbon dates at Taċ-Ċawla, the various temple sites excavated by the *FRAGSUS Project*, and at the Xagħra Brochtorff Circle (see Volume 2). These data suggest a steady reduction in activity spanning *c*. 2500–2100 cal. BC occurring at similar rates in different contexts, as would be expected if the underlying population was steadily reducing.

The evidence from the Cambridge Gozo survey, in as much as sherds can be assessed from surface material (and without the current understanding of Thermi wares and their third millennium BC date), appears both to support and to qualify the interpretations of the transition to the Early Bronze Age Tarxien Cemetery phase (Fig. 7.1). On the one hand, there is evident reoccupation in the period around Santa Verna with greater intensity than in earlier phases, whilst at Ġgantija, there was a decline in intensity. The landscape appears to fill out with the eastern flank of Ta' Kuljat reoccupied, whilst a new occupation started on Ta' Għammar further west. These distributions seem to suggest a level of expansion in settlement and landscape exploitation. Indeed, there appear to have been as many as 16 Early Bronze Age sites on Gozo of which eight were hotspots and these were statistically clustered (Boyle 2013). These observations might argue against a complete socio-economic collapse at the end of the Temple Period, although environmental change nonetheless strongly influenced the events of this era. The well-known 4.2 ka BP climate event, which is the culmination of a long trend of aridification in the central Mediterranean from about 2500 cal. BC (Sadori *et al*. 2013) must have impacted upon Malta too, and may partly explain the apparent lack of continuity between Tarxien-Thermi and the Tarxien Cemetery phases at some sites. Importantly, climatic fluctuation was not directly responsible for the end of the Temple Period. That 'end' had already begun a protracted cultural transformation as effective moisture and agriculture started to decline more than two centuries before, but it likely contributed to the reduced activity levels, and constrained the abilities of the islanders to reverse the pattern of on-going decline. This situation, where climatic and ecosystem trends interacted with cultural development, but did not dominate them completely, is a recurring feature of the settlement history of the Maltese Islands, and speaks for the resilience of those prehistoric populations.

6.9. Conclusion

The more detailed picture of the changing landscape that has emerged from the *FRAGSUS Project* has revealed a complex mosaic of different environmental constraints and opportunities, unfolding at different

scales and following different time frames. The more complex understanding that this emerging picture is permitting is also shedding new light on cultural processes that were at least in part a response to these changing environmental conditions. Cultural phenomena such as the emergence of megalithism in the early fourth millennium BC have been considered in this new light, which has allowed a more parsimonious, satisfactory and perhaps simpler explanation than hitherto available. The emerging evidence is allowing periods of cultural intensification to be considered against the changing environmental context. The apparent dearth of evidence of cultural activity during much of the fifth millennium BC is challenging but cannot be explained by less favourable environmental conditions, while the fourth millennium BC 'boom in megalithism' may now be reconsidered with the apparent renewed intensification of human activity in the landscape after the preceding lull. The diverging life-histories of different megalithic monuments across the landscape can be better explained against the emerging backdrop of a changing environment. The transition to the Early Bronze Age has also been reconsidered in light of the *FRAGSUS Project*, as one of complex cultural transformation rather than abandonment and recolonization, in which environmental change, though not necessarily the prime causal factor, was nevertheless a significant catalyst.

Part II
The interaction between the natural and cultural landscape – insights from the second millennium BC to the present: continuing the story

Chapter 7

Cultural landscapes from 2000 BC onwards

Simon Stoddart, Anthony Pace, Nathaniel Cutajar, Nicholas C. Vella, Rowan McLaughlin, Caroline Malone, John Meneely & David Trump†

7.1. An historiographical introduction to the Neolithic–Bronze Age transition into the Middle Bronze Age

The transition from the Neolithic to the Bronze Age has always been a focus of considerable debate (Bonanno 1993a & b; Stoddart 1999, 141) (see Volume 2, Chapter 10), ever since the transition was recognized, most prominently by Zammit in Tarxien temple. Early debate dwelt on substantial changes in material culture and rites of death, and emphasized the abandonment silts of the Tarxien temple detected by Zammit (1930, 45–7; Evans 1971, 149–51). These data, interpreted in a cultural historical framework, suggested that not only was there radical change in the population, but a substantial period of abandonment (Trump 1961a & b, 303; Evans 1971, 224). As more stratigraphies began to be investigated at Skorba, Xagħra Brochtorff Circle and Tas-Silġ in the second half of the twentieth century, distinct relationships between the two succeeding societies were suggested, as outlined in the previous Chapter 6. What is becoming clearer is that the so-called Bronze Age transition emerged in the final centuries of the third millennium BC, evolved, albeit in punctuated and uneven steps through to its demise at the start of the first millennium BC and lasted a remarkable 1200 years or so. It remains a complex and still poorly understood episode of distinctive ceramics, monuments and landscapes that deserves better understanding and chronological refinement, through fresh problem oriented fieldwork similar to the *FRAGSUS Project*.

One approach has been to detect transitional modes and combinations of material culture in the major monuments that have been excavated. Both Evans (1971, 180 & 1984, 496) and Trump (1976–7) began to suggest the presence of intermediate forms of pottery or layers which contained material of both phases. This approach has particularly been developed by Italian scholars working at Tas-Silġ (Cazzella & Recchia 2012, 28–32; Copat *et al*. 2013, 49–51) who have interpreted many forms of ceramic continuity between the two phases. Cazzella and Recchia (2015) have taken this further by identifying a distinct Thermi ceramic phase between the Late Neolithic Tarxien and the Early Bronze Age Tarxien Cemetery. This has allowed them to identify distinct contexts, such as a hollow altar at Tarxien and even the depiction of boats on an upright Globigerina Limestone slab at Tarxien, as belonging to this intermediate phase that they have identified (Cazzella & Recchia 2015, 144). As described in the previous chapter and in Volume 2, the results of the *FRAGSUS Project* broadly agree with this interpretation, but stress that Thermi ware is found in the latest Tarxien layers and thus is the final stage of Temple use, not the beginning of the Bronze Age.

Another approach has been to investigate the transition in the realm of the living (that is settlements) rather than of death and ritual. One major break-through here has been the Gozo survey, the first systematic survey to record the ceramic transition from the end of the Neolithic into the Early Bronze Age, as imprinted on the rural landscape rather than on a few selected monuments. A complementary break-through has been the activity of the Superintendence in response to the enormous development activity over the last thirty years. This work is complementary since it has been most intensive in its effect on the long standing and continuing urban centres of the island, most notably the citadels of Gozo and Mdina and their surrounds on their respective islands of Gozo and Malta. The combination of these two vital activities has given us a solid understanding of the changing processes of centralization and dispersal which became critical at the onset of the early second millennium BC and continued into later periods.

The study of the physical landscape had been dominated by the investigation of 'cart-ruts.' These

features in the landscape have fascinated scholars from a very early period of research (Fenton 1918) and have often been dated to the Bronze Age, although deeply intractable in terms both date and explanation. The probable *longue durée* process of creation (apparently repeated abrasion of the rock along pairs of lines) is one reason why a simple date is difficult. Their creation, which has been placed as early as the Neolithic by Zammit (1928; 1930), has the highest academic consensus in the Bronze Age (Magro Conti & Saliba 2007), but many others place them as late as the Roman and medieval periods (e.g. Fenton 1918). Causation may also be made more complex by this long stretch of time over which they were probably created, since equifinality may be an important factor. However, the regular pairing of the ruts does make wheeled transport the most likely cause. Some suggestions, such as lazy bed field systems (Sagona 2004), drawn from the ethnography of distant, temperate Europe, seem deeply improbable. The study of the physical landscape has been developed in a different way by the *FRAGSUS Project* as already discussed in the previous two chapters. Subsequent ubiquitous soil erosion from at least the early Neolithic period as clearly demonstrated in the *FRAGSUS* results described in Chapters 2, 5 and 8, coupled with long-term arable cropping in Chapter 3, is the more probable cause of the deepening and exposure of the ruts (cf. Mottershead *et al*. 2010; 2017).

A related issue is that of the development of terraces on the Maltese islands (Bennett 2020) (see Chapter 8). In spite of their much greater importance for life and heritage on Maltese islands than cart ruts, their chronology has received very much less attention. A number of Neolithic temples set within terraced forecourts show that the technological capacity was present by the second cycle of agricultural intensification on the Maltese Islands. When constructed they could even have been conceived as enclosures for the horticulture around the clubhouse temples (Barratt *et al*. 2020). However, this 'terrace' construction appears to have been very limited, even if the presence of *Theligonum* (Djamali *et al.* 2013) has been considered as a proxy for terrace construction at this early date (see Chapter 3). It is more probable that terraces were first systematically constructed during the Bronze Age, but there is so far no direct evidence of their construction during this phase. The mid-first millennium BC has a much stronger case since this is when the landscape was substantially tamed for tree crops (as discussed below). Dating remains a severe problem, since the discovery of datable pottery is a rare occurrence, but the use of OSL dating practised by the *FRAGSUS Project* (see Chapters 4 & 8) is clearly the way forward, since the sediments within the terraces can be directly dated by this technique. However, so far the dates so far achieved from this technique have only corroborated the dates provided by the *Cabreo* land tenure documents (Alberti *et al.* 2018) (see Chapter 9).

A further theme of great importance is the degree of connectivity. Early work was focused on distinctive artefacts such as bossed bone plaques and copper axes. More recent work has investigated the discovery of Maltese pottery outside the islands (Bernabo Brea 1966; Tusa 1983, 307; Raneri *et al.* 2015). It has now been established that imported Maltese pottery has been found at eleven sites on Sicily and Sicilian pottery, imitated Maltese pottery at two Sicilian sites (Ognina and Matrensa) and Sicilian material on three sites in Malta during the Middle Bronze Age (In-Nuffara, Borġ in-Nadur and Tas-Silġ). The connectivity also extended beyond pottery to the very uses of the pottery itself since the same 'Maltese ritual vessel set, composed of a two-handled bowl, an open-mouthed jug, and a pedestalled basin, existed and was used in religious and funerary rituals in Malta and in Sicily' (Tanasi & Vella 2015; Tanasi 2011a, 304 & 2013, 13). All this evidence shows that the maritime landscape had become traversable in a way not achieved in earlier periods. Tanasi (2008) has interpreted Malta as a small Sicily lost in the Mediterranean, but nevertheless connected to Mycenae though small ports of trade such as Borġ in-Nadur. The presence of fish in some deposits (Tanasi 2013) also suggests a greater exploitation of this part of the landscape compared with preceding periods.

The most recent approach has been the direct application of absolute chronology. In this respect, the *FRAGSUS Project* has had a major impact, even though the main focus of the project was on the preceding period. The current consensus by the project team is of a more gradual transition from the Neolithic as has also been covered in the previous chapter, notably with an important effect of dating levels with Thermi pottery, whilst still allowing for a gap before the early Bronze Age.

All these elements build up into a range of explanations of the change that took place between the two social organizations, represented by the Late Neolithic and Early Bronze Age. Earlier explanations were more cataclysmic. Later explanations have been more ideological (Bonanno 1993a; Bonanno *et al*. 1990) and gradualistic. Though seemingly marking a clear departure from long established customs such as collective inhumation, or the construction of extensive megalithic buildings, the Early Maltese Bronze Age still reflected a preoccupation with megaliths, which was, in fact, deeply rooted. Besides the re-utilization of older megalithic centres (Zammit 1930; Azzopardi 2007, 9–17) the smaller and less conspicuous 'dolmen'

made an appearance at this time in several locations across the archipelago (Pace 1995, 57). The evidence is accumulating that the intentionality of the change was as much internally as externally driven. The original discovery of the Bronze Age cremation cemetery within the Tarxien temple was originally interpreted by Zammit as separated by a period of abandonment and silting. This same deposit can be reinterpreted as a deliberate preparatory surface for the insertion of the cremation burials in a limited area of the temple, a performative act (Evans 1971, 149; Bonanno 1993b, 37). The same level of intentionality can be detected in the closure of activity at the Xagħra Brochtorff Circle. A medium-sized standing skirted figure was deliberately smashed (Malone *et al.* 2009a, 283–98) while smaller significant liturgical artefacts were deliberately inverted in the final deposit within the heart of the ritual monument in the period 2450–2350 BC. Similar arguments have been applied to the large standing skirted statue found at Tas-Silġ which may have been deliberately slighted at the moment of transition and transformation of the site (Vella 1999). In the subsequent Bronze Age, in the early centuries of the second millennium BC, significant intact ceramic containers were placed around the edges of the depression formed by the collapsed main cave structure at the Xagħra Brochtorff Circle. The depressions were then in-filled with artefact-rich domestic deposits, an action which might be interpreted as deliberate manuring of the site with rich agricultural materials. Judging from diagnostic ceramic fragments examined by John Evans (Evans 1971) many of the other major monuments of the Neolithic, such as Skorba and Borġ in-Nadur, appear also to have attracted attention and were occupied leaving rich domestic deposits and structures.

7.2. Bronze Age settlements in the landscape

The study of the full Bronze Age (Borġ in-Nadur and Baħrija phases) has been dominated by the study of a few defended sites and indeed this observation endures. However, as in central Italy where the same process occurred, we have to be very careful that the sampling strategy has not reinforced the evidence. The most important pair of these defended sites are Borġ in-Nadur and Baħrija themselves. The first was first explored by Murray (1923–9), more recently by Trump (2002) and extensively restudied by Tanasi and Vella (2011a & b, 2015). The second was first studied by Peet (1910), more recently by Trump (2010) and surveyed by Maria Elena Zammit (2006). During the *FRAGSUS Project*, a pair of late Bronze Age silos were excavated on another defended site of In-Nuffara on Gozo and are reported in Volume 2, once again building on the work of David Trump and Joseph Attard Tabone (Trump 1962). A digital surface survey was also undertaken in 2014 of the entire hilltop, giving a broader spatial setting to the occupation of the mesa in the Bronze Age, by recording visible silos and other emerging floors. This work is covered in the companion Volume 2.

Complementing this focus on individual sites, the 1987–95 Cambridge Gozo survey provides the first detailed evidence of the cyclicity these developments in the course of the Bronze Age (Fig. 7.1), as well as a preliminary check on the influence of targeted research on the collection of evidence. As already indicated in the previous chapter, settlement occupation expanded from the 'temple' areas of the Xagħra plateau during the Tarxien Cemetery period to include other mesa tops (Ta' Kuljat and Ta' Għammar). During the Borġ in-Nadur phase, settlement distribution (measured by pottery density) expanded considerably to include spreads beyond the immediate defended areas, suggesting that Borġ in-Nadur settlement had a demographic expansion which led to the expansion of occupation to the undefended flanks of some mesas, notably Ta' Kuljat. It is likewise notable that the Xagħra Brochtorff Circle, Santa Verna and Ġgantija were also intensively occupied at this time. Finally, though the citadel of Gozo seems to have been used during the Tarxien Late Neolithic phase, it was then re-occupied during the Borġ in-Nadur phase, as was the area below in the square near St. George (as shown by David Trump). During Borġ in-Nadur 29 domestic sites were found on Gozo, including 18 hotspots found during the survey (Boyle 2013). The Cambridge Gozo survey has, therefore, registered a pattern more complex than that detected by the targeted research of earlier generations. The final Baħrija phase of the Bronze entailed a considerable retraction of settlement into just two locations: Ta' Għammar and the Citadel which became the focal point of settlement activity from this moment onwards on Gozo.

In parallel to the Cambridge Gozo survey, the Superintendence of Cultural Heritage has been engaged in (largely) urban rescue excavation over the course of the last twenty-five years. This has uncovered a similar pattern for the Borġ in-Nadur period. On Malta (Fig. 7.2a), the defended position of Mdina (2005, 2008) was encircled by other Middle Bronze Age deposits found at Mtarfa (1995), Ta'Sawra (Rabat) (2012), Triq San Pawl (Rabat) (2012), Doni Street (Rabat) (2012) and Għeriexem (Rabat) (2013). On Gozo (Fig. 7.2b), further evidence of the intensity of occupation of the citadel was uncovered in the form of distinctive rock-cut silos. This evidence, particularly that from Mdina, has thus revolutionized our understanding of the Middle Bronze Age occupation of the islands, revealing a process of nucleation

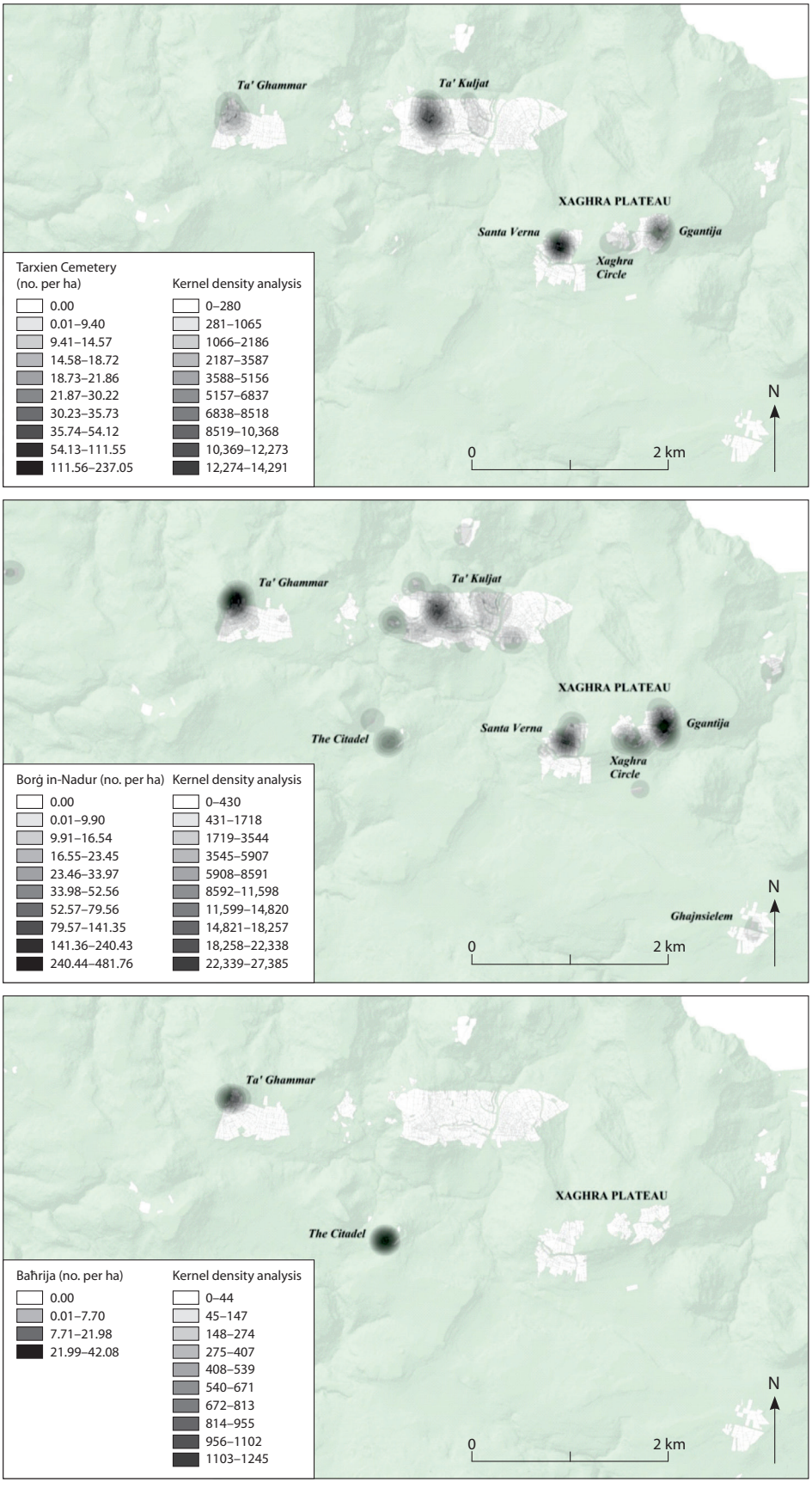

Figure 7.1. *Kernel density analysis of the Tarxien Cemetery, Borġ in-Nadur and Bahrija periods for the areas covered by the Cambridge Gozo survey (S. Boyle).*

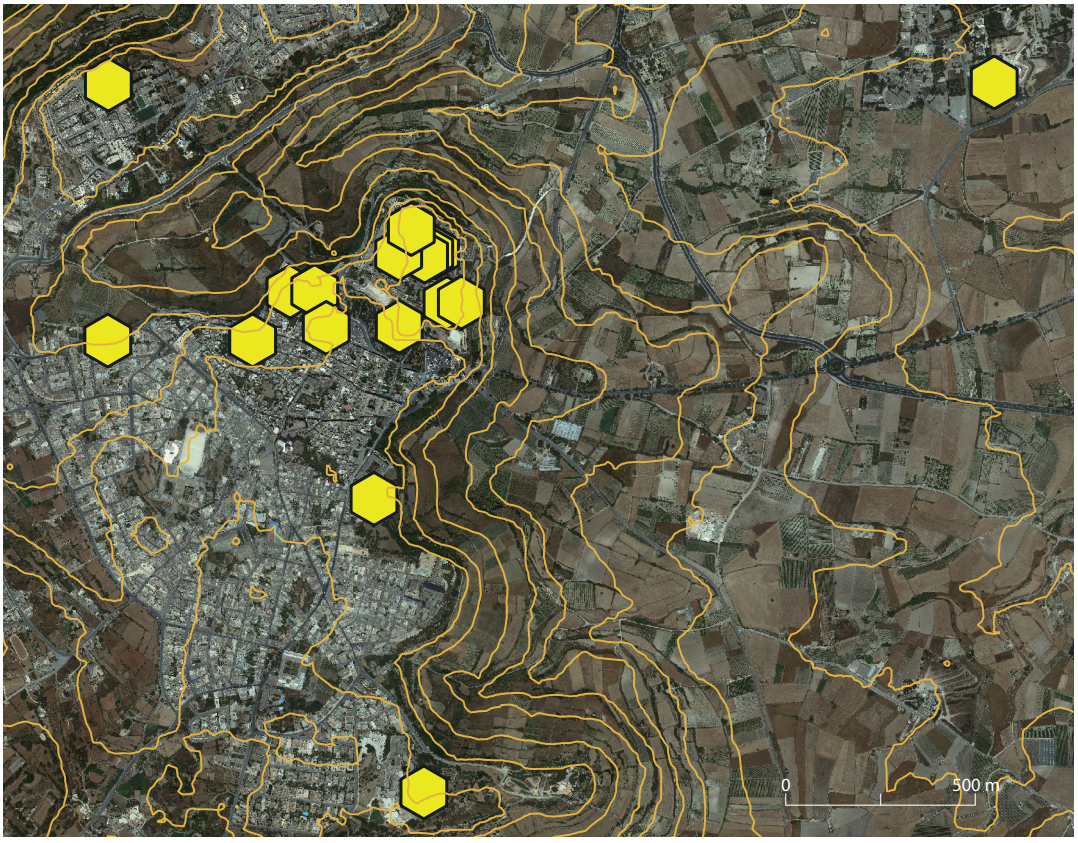

Figure 7.2a *(above). The evidence for Bronze Age settlement in the Mdina area on Malta (data from records from the Superintendence archives) (R. McLaughlin).*

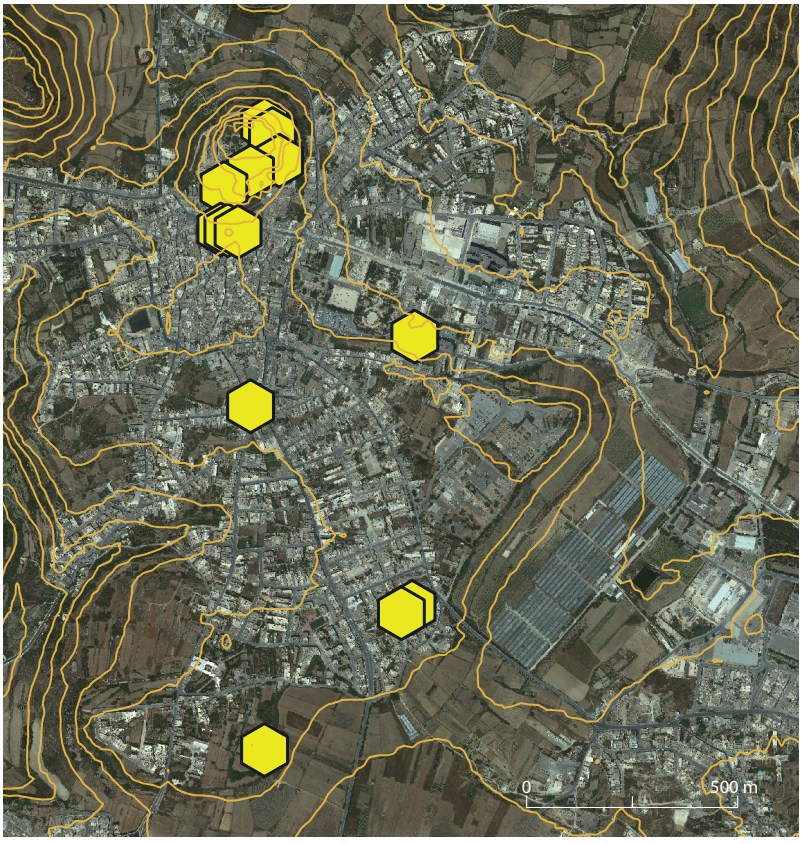

Figure 7.2b *(left). The evidence for Bronze Age settlement in the Rabat (Gozo) area (data from records from Superintendence archives) (R. McLaughlin).*

that started in the Early Bronze Age and intensified in the Final Bronze Age, serving as a precursor of the Phoenician and Punic urban centre.

A further dimension of Bronze Age activity is that of the funerary landscape. In the Early Bronze Age, dolmens seem to have been placed along the 'margins of major topographic features such as on Ta' Ċenċ on Gozo, including deep side wadis, plateaus and plains' (Tanasi & Vella 2011a, 414), but these relatively fragile monuments, currently some 17 in number (Evans 1956; Sciberras 1999; Pásztor & Roslund 1997) have never been effectively surveyed and are often too poorly preserved to determine their orientation (Fig. 7.3). Another dimension of the funerary landscape, probably of the Middle Bronze Age is occupation within caves around the Maltese Islands. The cave of Għar Mirdum, a discovery by speleologists, has been ably contextualized by Tanasi (2014), within the limits of the recorded evidence, and substantially dated to the Borġ in-Nadur phase. It is located within 2.5 km of the defended Bronze Age site of Wardija ta' San Gorġ on the Dingli cliffs and appears to have had many functions ranging from burial (two inhumations) to associated ritual. The finds included substantial quantities of pottery, animal bone, some fish bone and egg shell, a bone tool, a bone handle, quartz blades, pebbles, one imported basalt quern, one local Globigerina Limestone grindstone and hammer. Significantly, there was also a faience bead and bronze material, including a dagger blade, an ingot fragment and two rivets. Notably some of these elements point to the new levels of connectivity within the Maltese Islands of exotic material or in terms of shared decorative styles (such as the multiple circlets on the bone handle that echo similar patterns in Sicily and the eastern Mediterranean).

We can also make inferences of the character of Bronze Age economy from the changes in material culture. The presence of textile in the cave of Għar Mirdum, also seen in the Tarxien Cemetery itself and supported by finds of spindle whorls, loom weights and 'anchors' from elsewhere (Evans 1971, 151; Zammit 1930, 72–3), suggests a new strategy of the land use, unless the wool was itself imported. There is also evidence for buffering against fluctuations in resource availability from the local landscape, seen both in the increasing size of ceramic containers in settlements (Barratt *et al.* 2018) and the increasing provision of what are probably storage silos in the many of Bronze Age settlement sites.

7.3. The Bronze Age Phoenician transition and the Phoenician/Punic landscape

The transition into history, brought about by contact with the Phoenician world has also been the subject of some debate, not least about the complex palimpsest of their identity (Vella 2014). A major problem is the lack of definitive publication of stratigraphy that crosses the boundary between the latest Bronze Age and the earliest Phoenician, even though target sites exist in a number of places: such as Borġ in-Nadur (Trump 1961, 253–62), and Tas-Silġ (Cazzella & Recchia 2008,

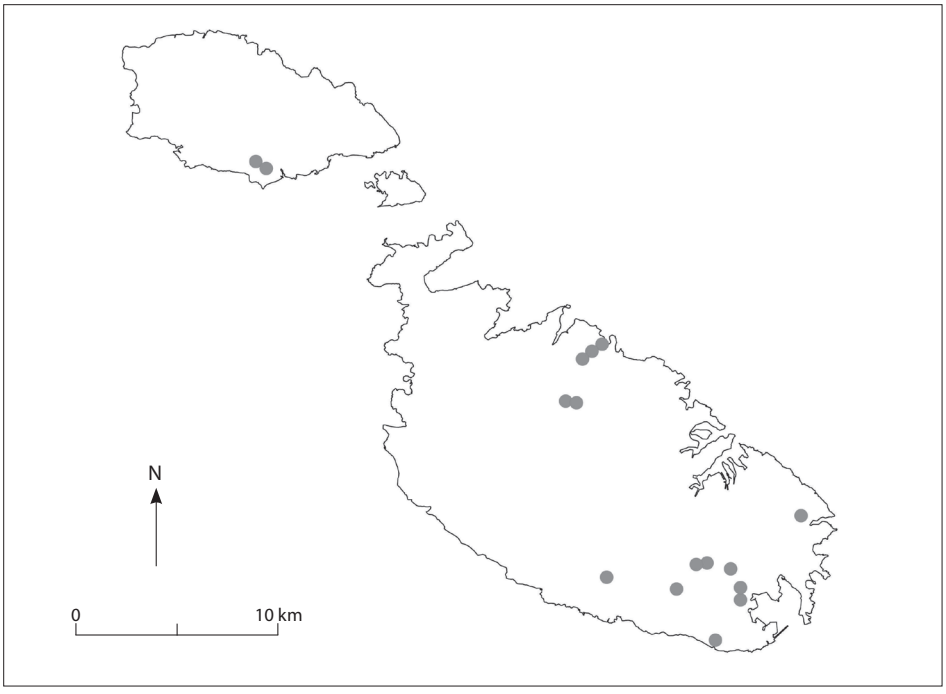

Figure 7.3. *Distribution of Early Bronze Age dolmen on the Maltese Islands, drawing on data taken from Pásztor & Roslund (1997) (S. Stoddart).*

2012; Recchia & Cazzella 2011), Mdina (Buhagiar 2000) and Mtarfa (Ward-Perkins 1938–9, 1942). At least some Phoenician specialists of Malta (Sagona 2015, 180) are now of the opinion that there is sufficient evidence to show the co-existence of Late Bronze Age occupation with the Phoenicians, countering the argument for a hiatus that has been sometimes made (Brusasco 1993; Gómez Bellard 1995, 452; Bonanno 1993a, 236–8). Nevertheless, the fact remains that what is still needed is a convincing settlement stratigraphy (Stoddart 1999, 142) and independent absolute dating to settle the question.

The arrival of the Phoenicians was dependent on a new level of navigational skills and reliability of ships (Broodbank 2013). The dating of permanent settlement in the western Mediterranean by Phoenicians is a matter of some controversy, particularly when comparing textual and archaeological sources (Mederos Martin 2005). In Malta, this is illustrated by the discovery of a fragment of a thirteenth century BC cuneiform inscription on crescent-shaped brown and white agate material at Tas-Silġ (Cazzella *et al*. 2011, 2012) which was found in a much later context. It is the most westerly example of cuneiform in an ancient level, but given the Hellenistic date of the floor in which it was found, it is very difficult to establish the timing, meaning and mode of transport. On this basis, the arrival of the Phoenicians could have been as early as 1100 BC, if emphasis is given to textual evidence or as late as 800 BC if greater weight is given to archaeological evidence without the application of any absolute dating. One clear indication is the recent discovery of what appears to be a Phoenician shipwreck off Gozo dating to 700 BC (Azzopardi 2013; Gambin & Sourisseau 2015; Sourisseau 2015; Gambin 2015; Renzulli *et al.* 2019). From this period onwards, we are dealing with the cultural seascape as well as a cultural landscape of Malta (Vella 1998; Vella & Anastasi 2018; Azzopardi 2013). This point is not only shown by shipwrecks and ceramic imports, but also by feasting from the sea, illustrated by the offerings at Tas-Silġ, the principal sanctuary on the island at least from the Punic period (De Grossi Mazzorin & Battafarano 2012; Fenech & Schembri 2015; Corrado *et al*. 2004).

The main evidence for Phoenician occupation of the islands is largely funerary and the settlement distribution is substantially an inference from their location (Said Zammit 1997; Sagona 2002). The most sophisticated analysis was first undertaken by Said Zammit (1997, 65–9). This work demonstrated the early nucleated concentration of Phoenician settlement in the central citadel areas of the island (Mdina/Rabat, Malta and Rabat, Gozo) in direct continuity with the preceding Bronze Age phases. Said Zammit was able to show from the dated tomb groups which were then available, a first spread of settlement towards another probable nucleation in the Paola/Marsa Grand Harbour area during the full Punic period (post-600 BC) and an increasing density of presumably rural settlement towards the southeast of the main island including around Żurrieq and Marsaxlokk (Said Zammit 1997, 43). Said Zammit estimates that the nucleations of Rabat (Malta), Grand Harbour (Malta) and Rabat (Gozo) could have been as large as 50, 35 and 8.5 ha, respectively. Sagona (2005, 223ff) has analysed the available excavation data and distinguishes (residential) Mdina (*c*. 35 ha) from (sacred) Rabat totalling 45 ha. Said Zammit also suggested that the distribution of undated tombs showed a much denser rural landscape, a point that was later picked up by Sagona (2002, 681) once some more of the provenanced tomb groups had been investigated.

A further feature of the Punic landscape is the presence of ritual landmarks visible to mariners approaching the islands, a nodal network common to the Phoenician and Punic world (Vella 1998). On the Maltese Islands (Sagona 2002, 273–7; Vella & Anastasi 2019), the western extremities of both the major islands are marked by such structures: Rar ir-Raħeb on western Malta and Ras il-Wardija (Cagiano de Azevado *et al*. 1964–73, 177–80) on Gozo. In addition, eastern Malta is dominated by the upper ground around Tas-Silġ (Cagiano de Azevado *et al*. 1964–73), the site of the major sanctuary built on Neolithic 'temple' and of sufficient wealth to be considered worth plundering by Verres, the notorious governor of Sicily in Roman times. This site was set slightly inland but easily visible from the west above the harbour of Marsaxlokk. Sagona also mentions a series of 'sacred wells' and stele which were clearly less visible from the sea and generally inland at locations such as Rabat (Malta), Paola and Kordin (Sagona 2002, 275).

By the time of the Punic period (after the sixth century BC), their Levantine cities had been incorporated within the empires of the Middle East, and the Punic cities of the west developed strategies of more independent local intensification, which included territorial expansion (seen more prominently in nearby Carthage) and rural intensification (De Grossi Mazzorin & Battafarano 2012; Fiorentino *et al*. 2012: Locatelli 2005–2006). Malta appears to provide a small-scale example of this general process. What is clear is that the Maltese Islands had entered a new geo-political context (Stoddart 1999, 142–3) which had immense implications for the carrying capacity of the islands. The islands were no longer necessarily dependent substantially on their own subsistence resources but part of a wider network, that could, for the first time have comprised appreciable external investment of human and other capital. Debates on population levels depend on how

this is interpreted. Said Zammit (1997, 41) attempted to arrive at population numbers by looking at the carrying capacity of cultivable land arriving at a peak figure of just below 18,000. These figures assume (as he himself realized) many factors including relative self-sufficiency. He also realized that only a small proportion of the dead (1800) had been recovered in the tombs he had studied, but perhaps did not stress enough that trends in the buried population were likely to have followed social as much as demographic factors. The main debate is, therefore, about the degree of external input by the wider Phoenician and Punic world, and in this regard Moscati (1993) largely considers Malta to be relatively insignificant, whereas Sagona is more positive (Sagona 2002, 278–80), although she has been reluctant to hazard any quantification of what this means in practice. The question of demography is addressed in more detail in the next chapter (8), and will be considered in the third volume in the *FRAGSUS* series (Stoddart *et al.* in press), but some the broad estimates for pre-modern figures range from 4000 (Blouet 2004) to 11,000 (Renfrew 1973, 169).

There is gradually more detailed evidence of the occupation of the landscape, from which a more evidence based picture can be reconstructed. The earliest evidence is from the pollen (olive), macrobotany (grape) (Fiorentino *et al*. 2012) and inverted stratigraphy in the pollen cores (see Chapters 2, 3, 5 & 11). The stratigraphy could indicate the opening-up of the landscape in response to the implementation of new tree crops to produce what might be for the first time described as the tamed Mediterranean landscape of today. Further direct evidence for oil and vine production comes either from presses or from vine pits where these can be successfully dated. One sophisticated study of this type has been undertaken in the Mġarr ix-Xini valley on Gozo (Fig. 7.4) by Anthony Pace and George Azzopardi respectively on behalf of the Superintendence of Cultural Heritage and the Sannat and Xewkija Local Councils, where some fifteen presses have been discovered along the sides of the valley. This project included the excavation of two terraces in which wine presses had been cut. The oldest of these terraces, at Tal-Knisja, on the Xewkija side of the valley, was dated to the sixth century BC on account of drinking cups that were found wedged in rock crevices adjacent to a wine press. These cups dated the underlying preparatory field layers, while the surface soil had not experienced deep ploughing for over two millennia. The other excavation, at Tal-Loġġa, less than a kilometre upstream from Tal-Knisja, showed signs of long use. The ancient retaining wall of the wine press terrace had been modified during the ninth century AD (Pace & Azzopardi 2008). The sixth century BC date of the Tal-Knisja terrace and its structure, suggest that by the Punic period, the several tracts of the Maltese landscape may have already been extensively modified by the systematic construction of

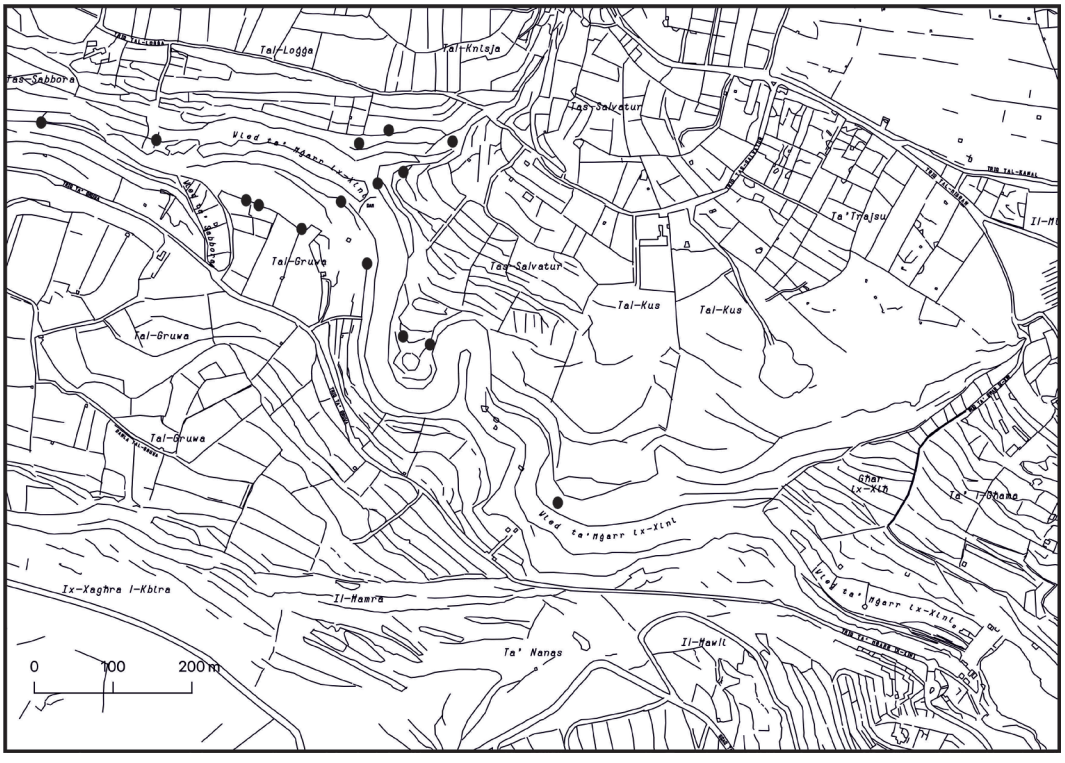

Figure 7.4. *Distribution of presses discovered in the Mġarr ix-Xini valley during the survey (S. Stoddart after A. Pace).*

Figure 7.5. *The cultural heritage record of the Punic tower in Żurrieq through the centuries: a) photograph by Thomas Ashby,* c. *1910 (© British School at Rome); b) scan by John Meneely; c) watercolour by Jean Houël, late 1770s (Hermitage Museum, St. Petersburg); d) scan by John Meneely with post-processing to reveal some internal details set on the plan by Jean Houël.*

terraces and field systems. Field construction remained a central feature of Maltese agriculture through Classical and Late Antiquity, the Middle Ages and modern times. The excavation at Tac-Ċawla just south of Rabat on Gozo uncovered lines of probable vine pits and trenches cut into the prehistoric levels which are more convincingly of Roman date, but such practices may have started earlier to maximize return. As for rural farmsteads, it is also highly probable that many of the later Roman farmsteads had their foundation during this period (Vella *et al*. 2017). The clearest direct spatial evidence for Phoenican/Punic material has been found by the North West Malta survey project (Docter *et al*. 2012) which showed a fairly comprehensive light scatter across the landscape with a tendency for higher concentrations to cluster on the terraces just below the garrigue escarpments. The surveyors suggest that there may have been a coastal site to the north in the Buġibba area, which would match Phoenician/Punic settlement organization in other areas of the Mediterranean. Even more accurate datable evidence of this has been provided (on stylistic grounds) by the Żurrieq tower structure in the back garden of the present-day parish priest's house, a tantalizing survival of a more prosperous rural structure, first planned and drawn by Houël, and now integrated with a 3D digital scan of the relevant part of the surviving structure during the *FRAGSUS Project* (Fig. 7.5). Sagona (2005, 239ff) also dates six round towers in the Maltese islands to the Punic period.

7.4. Entering the Roman world

We can give a significant date (218 BC) to the entry of Malta into the Roman political system, but this political event had relatively little effect on the landscape processes of the islands. The three nucleated centres (Mdina, Rabat (Gozo) and Paola/Marsa) and the surrounding rural landscape had been established during the preceding Punic phase. Similarly, the population levels of the islands probably remained in the region of the 18,000 suggested by Said Zammit (1997) (although see Chapter 8 for a counter argument). The dating evidence of both urban and rural structures is, however, better for the Roman period (Bonanno 1977, 1992), in part because of the now well dated products of connectivity, mainly pottery (Bruno 2009). In urban Rabat (Malta), we now have evidence of rich *domus* (Ashby 1915, 34–42) and in the countryside some 22 farmsteads (Bonanno 1977, 75), most of which were engaged in agricultural production, especially olive oil production (Anastasi & Vella 2018), but some of which might be classified as villas, such as the villa on the beach of Ramla on Gozo (Bonanno 2018).

The current urban evidence for the Roman period has been summarized by Anastasi (2019, 3–31) showing the future promise of recent rescue work, particularly in conjunction with building development on the Maltese islands. The examples she has so far studied reveal a range of activities: quarry activity from Bulebel, pottery wasters indicating kilns from Foreman Street, Rabat (Gozo) and a sequence of urban stratigraphy dating from the second century BC until the fourth century AD of street fronts and cisterns from the Melita Esplanade in Rabat Malta. These show, as might be expected, strong interaction from across the Mediterranean including Pantelleria, North Africa, Greece and Sicily. In some urban deposits in Rabat as much as 90 per cent of urban ceramic material was imported. In the earliest phases, wine was imported but olive oil seems to have been largely of local production served with food off locally produced pottery. By the second century AD food was increasingly served off imported pottery.

Detailed survey evidence comes from three sources, the Cambridge Gozo survey, the Mġarr ix-Xini survey and the North West Malta survey. The analysis of the material from the prehistory focused Cambridge Gozo survey was less sensitized to the distinction between Punic and Roman, but it does appear that the greatest concentration of Roman occupation was in two locations, one on the Għajnsielem plateau and the other on the Ta' Għammar plateau and its slopes. Both of these concentrations had a reasonable proportion of African Red Slip pottery suggesting that occupation continued into the full imperial period. In the Mġarr ix-Xini survey, there appears to have been a decline in Roman activity compared with the relative intensity during the Punic period. The North West Malta survey (Docter *et al*. 2012) has the greatest detail since the classical world was the principal focus of the project. This work convincingly shows an increased intensity of occupation in the same areas initiated during the Phoenician/Punic period, namely on the terraces immediately below the escarpments, focused on three principal concentrations, in association with rock-cut tombs. This latter association strengthens the inference of Said Zammit (1997) that farmsteads were closely related to tombs. Some records of structures of two of these (Ġebel Għawzara and San Pawl Milqi) were pre-existent and from the equipment recorded seem to be closely related to oil production (Locatelli 2008). The combination of Locatelli's analysis and the evidence of the survey suggests small estates of 10 to 14 hectares were engaged in oil production, and dependent on a readily available spring or a large cistern. A more recent survey of the evidence suggests that olive oil production was a particular feature of the Roman landscape of Malta (Anastasi & Vella 2018). One concentration found in the survey seems to intensify in the later Antique period and (see §7.6) further intensify in the Medieval period, providing an intriguing link into the next phases.

7.5. Arab

Historical sources suggest that islands entered the Arab world in about AD 870, but both historical and archaeological evidence are relatively scanty of information on the cultural landscape. It is highly probable that many of the surviving water systems date back to this time (Jones & Hunt 1994; Buhagiar 2016), but that may be as much expectation as dated reality. Whatever the age of these systems, the recent work of Buhagiar (2016) highlights the crucial importance of access to water for the cultural landscape of Malta. In earlier prehistory, access to a reliable spring was an important factor in settlement location (Grima 2004; Ruffell *et al*. 2018). Once nucleation took place on an increasing scale, starting in the Bronze Age, locating deeper water supplies and ultimately their storage became increasingly important.

Much can be retro-projected back from the medieval world of the twelfth century, because of the continuing Islamic presence in later periods (Bresc 1991, 51), but there is the danger that this becomes an Islamic trope of resistance to the advancing Christianity of the Norman world, emphasizing an Utopian egalitiarianism, without slavery (Bresc 1991, 49).

Another historical trope is that the islands were largely abandoned with a population as low as 5000, allowing a regeneration of woodland coverage in the islands (Brincat 1995).

The historiographic tropes of insular abandonment and re-afforestation are being incrementally contradicted by a growing body of archaeological evidence. Published ceramic sequences from Mdina indicate that by the ninth century the town had been heavily refortified and received a steady flow of imported amphorae and fine wares, mostly from Byzantine areas adjoining the Ionian Sea, but also, to a lesser extent, from Muslim areas. A rural deposit from Ħal Far (SE Malta) similarly seems to document an early stage in the introduction of characteristic North African hand-made casserole types alongside Ionian or Adriatic amphorae – an event probably dated to the tenth century (Bruno & Cutajar 2018; Cutajar 2018). Pollen analyses also suggest that the cultivation of cereals was never interrupted by an event of depopulation, nor does it support the idea that the island was re-afforested (Carroll *et al*. 2012). The evidence suggests that Malta was rapidly and systematically amalgamated into the prevailing Islamic cultural and economic world-system at the latest by the early eleventh century.

The three systematic surveys from the Maltese Islands were uniformly weak in retrieving evidence for this period because of the lack of dated pottery series. The Cambridge Gozo survey data also require more study, but the initial work suggests the presence of one large settlement concentration west of the northern extension of the Xagħra plateau and a smaller presence further west. These results are enough to give confidence that an Arab landscape can one day be recovered.

7.6. Medieval

The Medieval landscape also remains largely unstudied and the archaeology unpublished (see Chapter 10). The historical source of Al-Himyari mentions pines (although most of Malta did not have them except at Xemxija *c*. AD 400–1000 (C.O. Hunt, pers. comm.)), junipers and olive trees, harbours, deforestation and the abundance of fish and honey (Brincat 1995; Fiorini 1993a, 176) (see Chapter 3). Idrisi from the twelfth century rather stresses pasture, flocks, fruits and honey (Luttrell 1975, 32). It is very difficult to quantify these claims unless we turn to the pollen cores, but here our study concentrates on earlier periods. Population levels have been estimated to be about 10,000 for the early fifteenth century (Blouet 1984, 38; Wettinger 1969; Brincat 1991, 97) with some fluctuations in times of raiding and probably disease. By the early modern period of the sixteenth century, it has been estimated that population levels had doubled to 20,000 and deforestation was once again almost complete (Blouet 1984, 39; Brincat 1991, 97) (see Chapter 8).

The human occupation of the landscape by about AD 1400 appears to have been substantially dispersed (Blouet 1984; Fiorini 1993a & b; Stoddart 1999) (see Chapter 10) apart from significant nucleations in *castrum maris*, Birgu and Rabat on Malta. The greater insecurity for the smaller island of Gozo may have led to more nucleation, particularly in Rabat at the centre of the island. Blouet (1984) suggests that increased insecurity and cotton production in the course of the fifteenth century, prior to the arrival of the Knights, led to greater nucleation. The Cambridge Gozo survey recovered material of this period, but apart from the obvious evidence near the citadel of Gozo, the data require further study. The North West Malta survey (Docter *et al*. 2012) clearly shows the foundation of the local medieval village of Bidnija, emerging from late Antique origins. The Mġarr ix-Xini survey shows a gentle increase in occupation during the Medieval period. The *FRAGSUS* Santa Verna excavations give some indication that there was an extra mural chapel, with the burials originally found by Ashby, which gave its name to the megalithic structure.

7.7. The Knights and the entry into the modern period

The choice of Malta by the Knights in AD 1530 created a completely different environment for human and financial capital in the islands (Stoddart 1999) and much of the detail of these changes are covered in Chapter 10. The revenues of the Order of Knights from across Europe could be placed in the islands, enabling new infrastructure particularly connected to defence and shipping, requiring new levels of manpower and opportunities for new communities. The population consequently rose from about 17,000 in AD 1530 to about 43,000 in AD 1617 (Mallia-Millanes 1992, 4–5) or even higher by some estimates (Brincat 1991, 97). At the same time, the islands became more urbanized as measured by nucleation. Greater political and financial opportunities existed in the nucleated centres and the proportion of the population in nucleated centres increased from 5 per cent before the arrival of the Knights to 54 per cent in the AD 1760s (Mallia-Millanes 1993, 15), just before the toppling of the Knights by Napoleon. The major nucleation, in response to the priorities of connectivity and fortification, was placed around the Grand Harbour. War, famine and plague caused some fluctuations, but generally the resilience

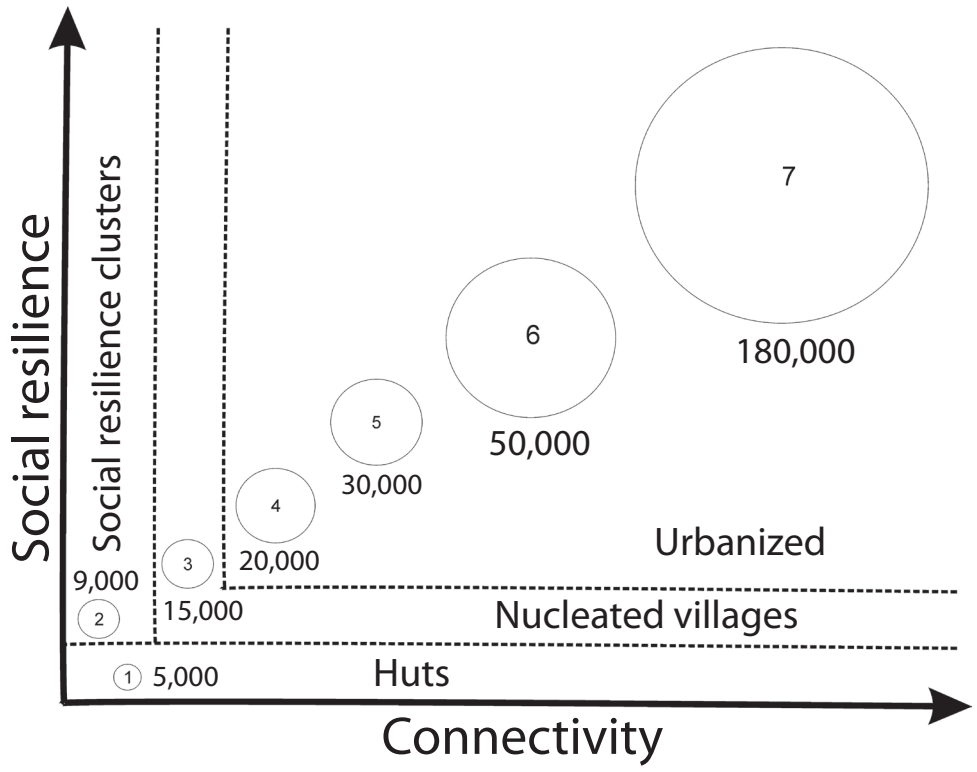

Figure 7.6. *The changing patterns of social resilience, connectivity and population (within circles) over the course of the centuries in the Maltese Islands (Chronology of numbered circles: 1) Sixth millennium* BC*; 2) Fourth millennium* BC*; 3) Second millennium* BC*; 4) First millennium* BC*; 5)* AD *1550; 6)* AD *1700; 7)* AD *1900) (S. Stoddart).*

of the islands was increased because of their connectivity and the implementation of more integrated political structures.

These trends also created demands on the rural landscape. The incoming Knights set up legal structures and investigative procedures, preserved in the *cabrei* records to understand and, to a certain extent, maximize the resilience of production from the landscape. Like many such initiatives the intent was more powerful than the outcome (see Chapters 8 & 9), but the increase in terrace construction almost certainly intensified in this modern period.

The incorporation of the islands into the British Empire intensified these trends. The effect was most readily seen in the increase in population levels from about 100,000 in AD 1800 to about 200,000 one hundred years later. The population increase was tempered by emigration (Brincat 1991, 97) at various times since the enlarged economic and political network gave rise to external opportunities in various parts of the British political and economic system. Very substantial immigration also took place immediately after World War II, often to other parts of the British Commonwealth such as Canada and Australia. The Durham geographers (Bowen-Jones *et al*. 1961) substantially misunderstood the economic opportunities offered by Independence, concentrating their analysis on a continued agricultural intensification. In fact, the continued population increase of the Maltese Islands to 400,000 inhabitants today has been supported by new levels of connectivity and political integration within wider structures including the European Union, that rapidly included the Schengen Area and the Euro currency. Human and financial capital have been the central foci of current trends. These have included banking, gambling, uncertain sources of money and inward investment, education, tourists and tax exiles. Such influxes of money have led to increased values of buildings and land which today lie at the heart of Maltese identity. '*Mingħajr art u ħamrija, m'hemmx sinjorija*' translates as 'without land and soil, there is no wealth' (Joe Inguanez pers. comm.). As the *FRAGSUS Project* has shown, this is a land that has been continuously under pressure, but where human capital has been increased in capacity by a sequence of different strategies and devices of social resilience in interplay with changing levels of connectivity (Fig. 7.6).

Chapter 8

The intensification of the agricultural landscape of the Maltese Archipelago

Jeremy Bennett

In this harsh environment man created the land on which he could live.

Bowen-Jones, Dewdney & Fisher (1961, 350)

8.1. Introduction

Bowen-Jones *et al*. (1961) in *Malta: Background for Development* furnish the reader with a prophetic edict which carries the threat of environmental catastrophe unless there is continual human investment.

> *Everything one sees in Malta* [the Maltese Archipelago], *other than major topographical features, is man-made and man-maintained in existence. For this reason, there is an unstable equilibrium that eternally threatens to collapse* (1961, 349).

This book provides an unparalleled geographic assessment of the Maltese agricultural economy, in the years prior to independence, and still serves as a compendium of knowledge and terminology nearly sixty years later. The authors' opening gambit recognizes the swell in national identity and the resulting desire to exert more control over the nation's socio-economic direction. However, their opening tonality also expresses an awareness of the influence of development and its potential threat moving into the future, thus directing the authors to the formation of a study that facilitated a greater understanding of the interplay between socio-economics and the landscapes of the Maltese Islands.

Reflecting upon their edict, a modern reader could be forgiven for agreeing with this assertion. A cursory overview of the islands reveals a marginal, alkaline environment with thin and heavily worked soils, overlain by rampant development and inhabited by 1505 people per sq. km (National Statistics Office 2019). However, at a deeper level, the environmentally deterministic and modernist view of Bowen-Jones *et al*. (1961) should be eschewed. Writing in the 1950s, these authors continued by stating 'the collapse foreseen is an increasing reality, the unstable equilibrium no longer being maintained.' Yet, in 2020, 'the collapse' has not arrived. What the authors failed to predict was that the future of the islands lay in connectivity: tourism, financial services, light skilled industry and casinos. A deeper historical perspective would have noted a critical threshold at the beginning of the first millennium BC when external investment first became crucial, adding external input to the island system, and reducing direct dependence on the land. At a more theoretical level, what the authors failed to consider was the delicate equilibrium of fragility and sustainability – the core themes of the *FRAGSUS Project*. Where Bowen-Jones *et al.* (1961) lacked a chronological framework, this project has re-asserted the importance of understanding human, rather than simply physical environments, through the full length of time. This leads to a greater comprehension of how humans live in, adapt and manage their environment, forging dynamic landscapes that have deep-seated histories.

A landscape represents an idea greater than the sum total of its constituent parts. Indeed, a concept such as the Maltese (or Gozitan) landscape contains within itself a nested hierarchy of landscape units, which are responses to lower and higher order processes. Although the spatial elements of landscapes are usually in flux, it is the palimpsest-like nature of landscapes through time that should be recognized as the key to understanding the inter-connected relationships between humans and their environments. This can be viewed as the central philosophical difference between Bowen-Jones *et al*. (1961) and the present project.

The *FRAGSUS Project* has focused on the successful reinvestigation and development of the complexities of the prehistoric Maltese Archipelago. However, in recognition of how landscapes develop

through time, elements of the project stretched beyond the prehistoric world to include the classical, medieval and early modern periods. Building on the temporal nature of landscapes, an *Annales* school framework could be adopted to aid the observation of how people have managed the agrarian environment through time, especially in association with the establishment of the Anthropocene epoch. *FRAGSUS* offers detail on three major agricultural phases available for study – prehistory (encompassing the early Neolithic through to the end of the Temple Period and into the Bronze Age), the 1800s (via Alberti *et al*.'s quantitative analysis in Chapter 9) and the contemporary Maltese landscape (see Chapter 10). This chapter will therefore provide a union between these strands of the *FRAGSUS Project* by providing a synthesis of the population change and the linked agricultural intensification within the region. This will link together a synthesis of the *longue durée* of the Maltese landscapes, applying a *quellenkritik* to various phases of evidence. In doing so, the central lines of inquiry will focus on what the available agricultural resource is on the islands and how people have successfully intensified the use of the landscape to balance environmental fragility with population sustainability. This study forms part of a larger doctoral project (Bennett 2020), and many of its implications are further wrapped into the discussion in the concluding Chapter 11.

8.2. The *Annales* School and the Anthropocene

Braudel (1966), the historian, introduced the concept of structuring the understanding of human activity through time, through the medium of three scales of history and change: événements, *conjonctures* and *longue durée*. Bintliff (1992) provides a valuable archaeological application of these concepts, describing this paradigm as a series of interdependent wavelengths, which is a useful analogy especially when considering the nature of how waves combine. The shortest of these wavelengths is the history of events or événements, which can be described as the staccato record of activities on the shortest timescale. This is framed by the more structuralist account of medium- and long-term markers of time – *conjonctures* and *longue durée* respectively, each of increasing duration and of apparently lower frequency to the observer. Knapp describes the *Annales* direction as having a 'fundamental ambivalence' and the propensity to 'adapt and grow with the demands of an always-shifting method and theory' (Knapp 1992, 16). In sum, it enables the understanding of how long-term processes relate to shorter term events. The increasing acceptance of the Anthropocene as a distinct geological epoch (Waters *et al.* 2016) raises the implication that intensely applied événements can impinge on *longue durée* geological scales.

Goudie and Viles (2016) adopt an approach which blends the often conflicting accounts of various scholars, demonstrating the entwined nature of human activities and geomorphology; avoiding the application of the term 'golden spike', which is common in the Anthropocene literature. Their synthesis negates the marking of the Anthropocene as événement and accounts for the ebb and flow of human activities through time, beginning with the *Palaeoanthropocene* (*c*. 5050 BC–AD 1750), followed by the *Industrial Era* (AD 1750–1945), the *Great Acceleration* (AD 1945–2000) and culminating in the proposed era of *Earth Systems Stewardship* (AD 2000 onwards). Although the authors openly concur with the escalating pulse of change from the Industrial Era onwards, their timeline is designed to account for the 'many examples of the potent impact of humans in previous millennia' (Goudie & Viles 2016, 13). The rationale accords with the *time-transgressive* synthesis, called for by Brown *et al*. (2013) and Butzer (1996, 2015), which promotes a less alarmist response to the changing world. In particular, Butzer stresses the need for a non-anthropocentric view as 'the dynamic menu of ongoing changes … are by no means ready to be synthesised' (2015, 1540). This agrees with the commonly held view that geological epochs can only be viewed at a distance, from a suitable perspective. Caution must therefore be taken, as the study of the Anthropocene is a complex affair which must account for the 'natural' process of the Holocene and the subsequent layering of human activity (Butzer 2015, 1541). Bauer and Bhan (2018) recognize the tendency for earth systems scientists to observe the Anthropocene in terms of broad geophysical effects, therefore masking the nuanced impact of regional human activities. Human impacts with such locational specificity could necessitate the use of different terminologies, such as *Anthropoeurocene*, that reflect the prominence of particular regions in particular periods (Edgeworth *et al*. 2016); the net effect of human activity is generated from 'place-based actors through a number of differentiated activities that have long been documented by both archaeologists and cultural anthropologists alike' (Bauer & Bhan 2018, 13). However, it should also be noted that significant disparities exist when considering the variation in anthropic effects worldwide (Malm & Hornborg 2014); influenced by long-term social, political and economic factors. Understandably, many islands lie at the least impactful end of this scale, as they are attenuated by their geomorphological size. Despite this, an island such as Malta is by no means devoid of the evidence of the Anthropocene. Where the earth systems approach to the Anthropocene may overlook

the specificity of human activities, it serves to remind us of a core commonality shared by humanity. Gibson and Venkateswar (2015) dwell on this unifying nature of *Anthropos* and build upon the idea that the concept of Anthropocene is not yet fact, instead existing as a product of thought. To take this a step further, I would propose that thought – human cognition – is central to the Anthropocene's physical origin as opposed to its conceptual origin. The epoch's genesis is rooted in the net effect of human cognitive traits which value species needs over environmental stability. The Goudie and Viles (2016) approach, perhaps inadvertently, encapsulates the interplay between the *longue durée* and *conjonctures* by emphasizing the role of long and medium term factors with the onset of the Anthropocene. Laparidou *et al*. (2015), emphasize that humans have always had a role in modifying their environments, 'as we employ flexible and novel solutions for the survival and well-being of our societies'. Captured within this is the sense of événements, or the history of events, since niche construction (Smith 2011) can be viewed as a short-term series of events, as well as a longer-term paradigm of human activity. In short, the three temporal categories of the Annales School of thought bleed together, as time progresses. Niche construction can be an event and a cultural pattern; cultural patterns can be viewed geographically and demographically; geography and demography are influenced by the permanence of societies and other natural factors – all of which can influence the creation of one's niche. This cyclicality is a potential antithesis for Butzer's (2015) need for analysis of the Anthropocene at a distance. In summary, the *longue durée* of the Anthropocene involves the creation of a complex feedback loop, where early human activities remain layered in the environment and act as an influence for subsequent people.

8.3. The Maltese Archipelago and the *longue durée* of the Anthropocene

While keeping these thoughts in mind, we can turn to the islands of Malta. At present, visitors to the islands are met with a rich palimpsest of overlapping cultural history which has been carved into, and layered above, the natural limestone. Explicitly, much of the islands' history is visible as built heritage, yet an almost intangible time-depth can be seen within the implicit traditions of the rural world. Neolithic monuments, flanked by terraced slopes, are surrounded by buildings of the nineteenth and twentieth centuries. Each of these features is representative of short-term traditions which are intertwined through time as people act in relation to elements of the past that remain present in their contemporary landscapes.

The central resource is, in essence, the islands themselves – with limestone the primary building material used across time. It is rare to encounter a structure that is not comprised of limestone blocks, especially those which are quarried from the Globigerina Limestone strata. This encapsulates the *longue durée* of the Anthropocene, at least locally, as the layers of human development are constructed using materials which were initially deposited during the Miocene Epoch (*c*. 5.3 mya – 23 mya). Perhaps ironically, the voids left from this resource extraction have become refilled with the less dense waste of human activity. This has continued to such an extent that new landforms have been generated by the deposition of this anthropic layer, as can be seen at the Magħtab landfill. Fittingly, this site is now undergoing environmental management, including a landscaping programme which has constructed a striking set of terraces on this anthropic landform (Fig. 8.1). In many ways, Magħtab is a microcosm for the Anthropocene within the Maltese Archipelago, with its anachronistic terraces carved to disguise the artificial nature of the location, appearing to mimic the local landscape. Yet, this approach is likely to be ignorant of the ancient and essentially human origin of terracing practices. This is indicative of an engrained *mentalité* where current landscape traits are perceived as the norm, irrespective of what the true natural state may have been.

Focusing on the issue of terracing, there are many similar *longue durée* traits worth considering. Primarily, the archipelago's topography is dominated by the construction of terraces across all geological zones, through time. Thompson (2006) conveys how the shifting practices in wall construction evidence the gradual change in the cultural makeup of the islands, yet the walls still display a commonality that is millennia old. While the scientific analyses of the terraces may alter the understanding of some terracing practices, particularly where the geological variability is concerned, Thompson's anthropological study still provides value in the form of the engagement with lived experiences. 'The contrasting modes of wall, ancient and modern, are reflections of the values supported by the people of the times… No wall is created strictly favouring one ideal set of values over another. Rather, each wall is a complex of these contrasting values and their designs' (Thompson 2006, 34). Thus, the terraces are as much a cultural palimpsest as the wider landscape is. On a superficial level, they are the anthropic reshaping of the environment, with the creation of each terrace wall as an événement which involves a juxtaposed set of *longue durée* processes (quarried geology and subsequent soil erosion). Equally so, on a deeper level, these walls also represent their own palimpsest of fluctuating *mentalités*.

Figure 8.1. *An oblique aerial image of the northern slopes of the Magħtab land-fill site, depicting landscaping efforts including 'artificial' terracing (image © 2020 CNES / Airbus).*

The blurring of *mentalité* and *conjoncture* can be seen within the system of land tenure in the islands, as demonstrated by Bugeja (2018) who outlines the division between established landlords/church land and peasant landowners. The entrenched stagnation of ownership made it difficult for less economically viable farmers to acquire the land in which they worked. However, the availability of long-term perpetual leasing, *emphyteusis*, 'elevated the tenant into a position of *quasi*-ownership' (Bugeja 2018, 26). While this form of lease represented balance between the landlord and the tenant, the short-term leasing that was available represented greater gains for the landlord, especially considering the fluctuating value of the land based on its perceived quality. More developed private land would usually be subject to higher taxation, which would be reflected in the leasing costs. In contrast, long-term leasing was commonly found with Government and Church land, which came with lower taxation and 'very often characterised by feudal practices' (Bugeja 2018, 26). Although the annual rent, *qbiela*, relieved the farmer from tithe, they were obliged to repair field walls and to not sub-let land. Where extensive repairs were required, it was not uncommon for the landowner to intervene, assumedly as a matter of responsibility for maintaining an element of control. Where farmers invested in improving the land, at their own expense, it was common for landlords to increase the rent after the end of tenancies. Accordingly, tenant farmers were disinclined to move on from land they had heavily invested in, especially since no system of compensation existed to account for their improvements. Where landowners 'were largely characterised by a strong sense of elitism' (Bugeja 2018, 27), it is understandable that tenant farmers would opt for long-term leasing in order to regain a sense of control over their destinies.

From the 1850s, there was a considerable effort to encourage the expansion of agricultural practices to the barren, *xagħra* lands (Bugeja 2018). This served to increase governmental revenue and thus offset the cost of repairs elsewhere. Although this land was rarely productive, competitions were held to reward the most successful farmers, and the prizes became a valuable income source. In the period surrounding World War II, when the need for agricultural productivity was heightened, farmers enjoyed legislative changes that

promoted their positive input, protecting them from excessive rent increase and harsh changes in lease conditions. Equally so, the landowner retained the right to reassess tenancy if the farmer was not operating the land adequately. Finally, in the post-war period, the accumulation of wealth and the rise of pensions resulted in the redevelopment of the land tenure system. With farmers retiring earlier and sub-letting their land, the overall amount of cultivated land increased while freeholding was in decline.

In essence the rise of the tenant-farmer class, as described by Bugeja (2018), is an artefact of long-standing tenancy practices. Although aspects of these practices have transformed through time, the process still maintained the architecture of the medieval traditions. This reflects the process of 'Agricultural Involution' (Geertz 1963), as increasing complexity can be found within a seemingly static system. Tied to these practices, the personal experience of the farmer, as presented by Thompson (2006), is effectively encoded in the walls they build and repair; they are indicative of the *conjonctures* that exist. Ultimately, these *conjonctures*, such as the expansion of land in the post-war era, are physically embedded in the *longue durée* as altered and abandoned land, now subject to unimpeded ecological processes. These 'Anthroscapes' ultimately reflect how short and medium term histories can directly influence the flow of the *longue durée*, therefore reinforcing how, at least in Malta, the Anthropocene has been present for a considerable period of time.

During the early twenty-first century, continual population growth and rampant development have placed renewed pressure on the landscapes of the archipelago. The traditional and historical rural locations are increasingly threatened by the advance of urban areas. A variety of public interest groups, utilizing social media, have formed to raise awareness of the risk to the local heritage. When observing much of this development, it is noticeable that many sites remain abandoned. Not wishing to comment further on the specific causes of this, all that remains to be said is that modern development and expansionism are mimicking the drive to incorporate new land, as described above. Ultimately, both cases involve the inscribing of the Anthropocene, with the cyclical nature of the expansion beyond need perhaps forming part of a medium-term *mentalité*.

8.4. Intensification

The concept of intensification is fundamental to the understanding of a number of *longue durée* environments. In this instance, the term specifically refers to the aspects of human activity which drive increased productivity from managed landscapes. Although this discussion refers to agricultural intensification, it is prudent to remain cognizant of the subsequent forms of intensification that are facilitated by increased agricultural output. Boserup's (1965) model is a fitting point of departure. A basic interpretation suggests that population increase is supported by an advancing technological framework available to that population, with the carrying capacity of the land constantly improved by greater investment of labour and/or the investment in infrastructure. Boserup (1975) pursued this further by emphasizing the importance of the ratio between people and land as the central factor in determining productivity within the context of a rural socio-economic system. Morrison (1994) stresses that archaeologists should exercise caution when using Boserup's (1965) model as a means of understanding intensification, since the approach acts more like a typology of societies rather than a mode of analysis. Morrison notes that Boserup's model cannot account for the myriad of strategies employed by societies through time and space. The restriction of Boserup's model is its linearity and lack of clarity on the specific nature of what intensification involves; instead, research should focus on 'delineating the actual paths of intensification' (Morrison 1994, 145). A more cautious approach should be adopted, especially considering the risk of dichotomous interpretations of intensification/disintensification, with emergent complexity serving as a broad concept that encompasses the intersection between population and production – specifically, the genesis of a complex and self-organizing system comprised of a variety of actors (Marcus & Stanish 2006). Further to this, Miller (2006) stresses the nuances of intensification, noting the concepts of *extensification* and Fuller's (2001) *diversification* as alternate routes to producing an end result similar to Boserupian intensification.

In effect, there is an element of Annales school thinking that needs to be considered here – that production and intensification strategies are part of the cyclical process discussed earlier. Boserup (1975) could be interpreted as observing the concept of production as a string of événements, framed by the *conjonctures* of investment methods. The central caveats to draw from Boserup are that investment in pre-mechanized societies is often seen with an increase of labour using pre-existing tools and methods; productivity can be achieved through greater use of status quo techniques. Interestingly, it is worth drawing comparison with Geertz (1963), where the process of 'Agricultural Involution' was defined. In this instance, agriculture develops into a system of increasing complexity, with ever increasing land divisions dominating the outward appearance of the agricultural system. Comparison between both

models suggests that each population continues to a point of maximal indigenous carrying capacity, from which new management strategies must be employed. Boserup (1975) posits the greater investment of labour/technology, followed by economic migrations, while Geertz (1963) observes increasingly complex social management. Crucially, only Geertz (1963) is referring to an island context. Boserup's consideration of economic migration is attenuated by an island setting. Despite this, a fitting proxy would be the factors surrounding the socio-political setting of an island and how these influence the agrarian world. Boserup (1975) suggests that a population has little incentive to produce surplus beyond subsistence, unless external factors provide enough influence to generate a need. This is a vital idea to consider in the framework of the complex history of the Maltese archipelago.

8.5. Population

Dwelling on population as the motivator behind increased production, we must observe the complex demography of Malta through time. Undoubtedly, the complexity of demography is deeply interrelated to the growth of population and social networks. During the Neolithic and Temple Periods, these networks were primarily local-regional/Malta-Sicily, as evidenced by ceramic styles (Malone 1985; Bonanno 1986a) (see Chapter 6) and chert procurement for lithic tools (Chatzimpaloglou *et al*. 2020). Moving through the Bronze and Phoenician periods, the islands enter a wider maritime network (Stoddart 1999) (see Chapter 7), where the archipelago's natural harbours served to increase the external perception of the archipelago's value. These periods represent the islands on the cusp of broad connectivity with the wider Mediterranean, something which would be achieved from the Punic period onwards. Later historical records provide insight to the islands' relationship to the political powers of Sicily and the interplay between the needs of the inhabitants and the structure of wider regional politics. Thus, the phasing of population can be divided into two categories, sub-carrying capacity and post-carrying capacity. Since the islands have finite resources, it is logical to observe the periods that are drawing on insular means of production as distinct from those which rely on the outside world. Not surprisingly, the latter periods involve a marked shift in Malta's inclusion within the extra-regional political world.

8.5.1. Sub-carrying capacity periods

Understandably, the measurement of population in this period carries the most uncertainty, regardless of chronology and technology. There have been attempts by Renfrew (1973; Renfrew & Level 1979) to estimate the Temple Period population, and from several authors to relate this to death rates from the cultural patterns of burials (Bocquet-Appel 2002; Stoddart & Malone 2015; Thompson *et al.* 2020). From the perspective of this discussion, a prehistoric population estimate could act as an initial representation of the carrying capacity, assuming limited trade and population mobility. Renfrew's estimates for the archipelago reached *c*. 11,000 individuals, based on territories defined by the positions of pairs of megalithic sites and the population required to build such structures. Perhaps more reasonably, Clark (2004) estimated a population of 1407 for the Late Neolithic of Gozo, based on 60 per cent land utilization and 2 ha of land per person. If we extrapolate this to include Malta, the total number becomes 8787. Grima (2008b) presents a systematic analyses of estimated carrying capacity based on areas of low slope (<5 per cent gradient) and a minimum of 1.5 ha per person, which reveals pockets of low lying land totalling 7071 ha and supporting 4713 individuals. Usefully, the Clark (2004) and Grima (2008b) estimations do not exceed records of the medieval population which was not reliant on imports as a means of sustenance. During the fourteenth century, Malta exported grain to Sicily, although this is likely to have been an uncommon practice (Aloisio 2007). During the fifteenth century, the islands suffered from grain shortages every 2–3 years (Wettinger 1982) which drove increased demand of Sicilian grain imports (Aloisio 2007). Referring to Table 8.1, below, the population is likely to have been between 8000 and 10,000 individuals during this century. In contrast, Sagona (2015) presents a brief analysis of the potential carrying capacity of land with recorded archaeological field scars, although this is an unconvincing interpretation which is reliant on poorly applied, northern latitude, ethnography. In brief, the suggested land utilization, based on Gregg (1988), is 0.62 ha to 0.73 ha per person and therefore would suggest a considerable difference in carrying capacity in comparison with the Clark extrapolation.

Table 8.1. *Carrying capacity estimates for the Neolithic/Temple Period of the Maltese Archipelago. Figures are based on areas of low slope and calculations of low soil loss, with figures from Grima (2008b) provided for comparison. The figures classed as RUSLE 0–10 t/ha/yr represent a conservative estimate of population based on areas of stable soils. The RUSLE 0–25 t/ha/yr is an expanded area which includes slightly less stable soils as well as those which fall within the RUSLE 0–10 t/ha/yr.*

	RUSLE 0–10 t/ha/yr	**RUSLE 0–25 t/ha/yr**	**Grima (2008b)**
Area (ha)	3843.81	13997.61	7071
Population (1.5 ha/person)	2562.54	9931.74	4713

Although this may initially conjure the idea of populations ranging towards the Renfrew computation, it is worth considering the highly undefined nature of the prehistoric agricultural environment. *FRAGSUS* has highlighted the potential role of the hilltop plateaux for early agriculture, and emphasized the relative inaccessibility of the clay slopes (see Chapter 5). It is entirely possible that the prehistoric agrarian world, envisaged by each of these models, was far more restricted in reality, and was a landscape of fragmented tamed pockets (see Chapter 6). Finally, while observing the physical remains of the Temple Period, Malone *et al*. (2009a) caution that the current record only offers a limited synthesis of prehistoric populations, with isolated sites providing an uncertain cross-section of ancient communities.

The use of RUSLE (Revised universal soil loss equation) provides a direct measure of soil stability and erosion (Wischmeier & Smith 1978) (Fig. 8.2; Table 8.1; see Chapter 2), whereas the Grima (2008b) model was based on the presumption of soil stability from low lying areas. These new estimations help extrapolate

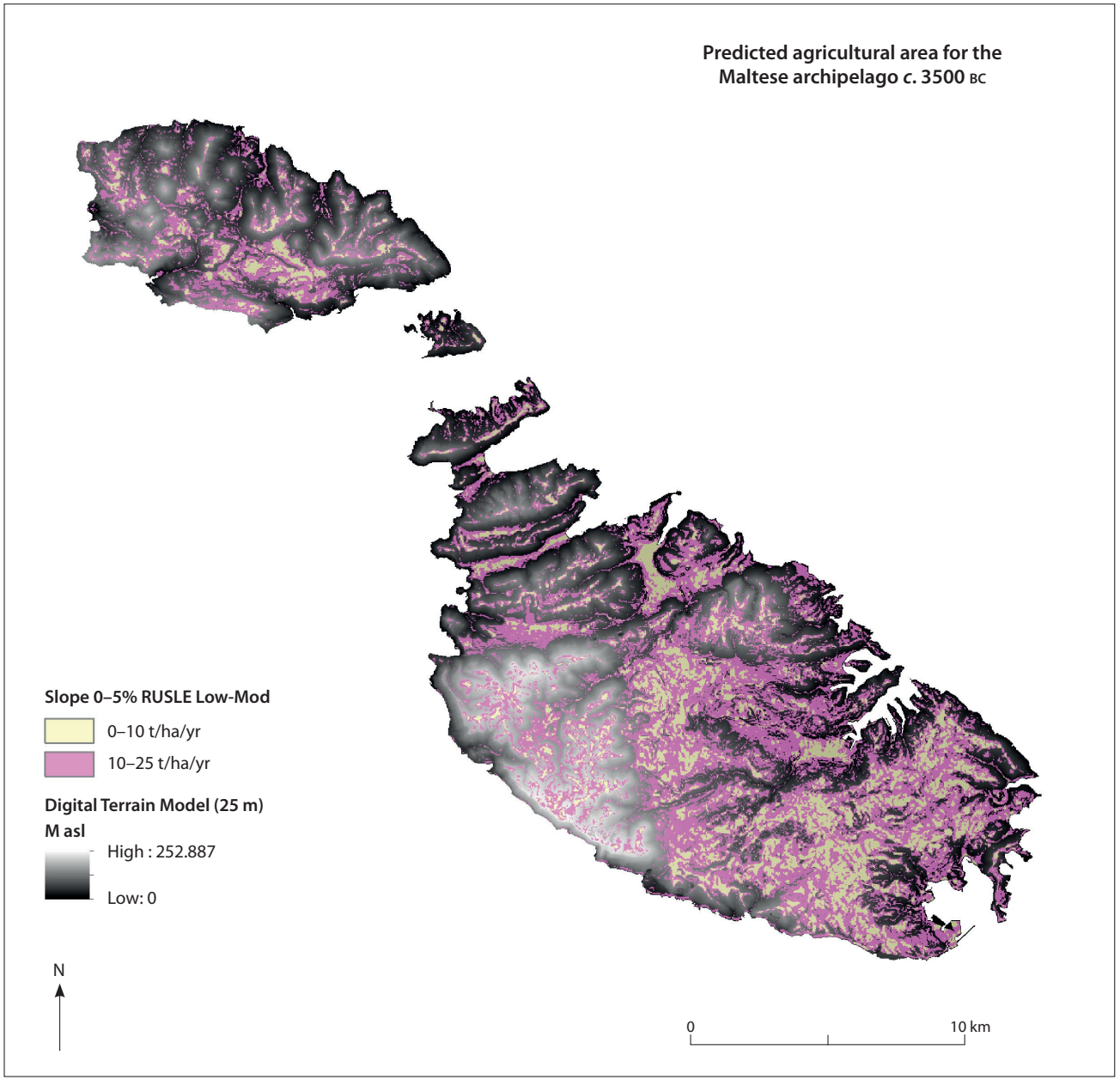

Figure 8.2. *RUSLE estimates of areas of low and moderate erosion for Gozo and Malta (J.M. Bennett).*

some of the recent environmental findings discussed in this volume and enrich the understanding of the lived experience of these islands during prehistory. Importantly, Grima's (2008b) approach should be recognized as meritorious as it sets the agenda for quantifying the past landscapes of the archipelago. Undoubtedly, future data and refinement of this GIS investigation will further delineate the parameters of early population in these islands.

Moving forward in time, the Bronze Age has had comparatively less research on population structure. Recchia and Fiorentino (2015) suggest that the Maltese archipelago was still within carrying capacity at the end of the Temple period, with the Early Bronze Age population co-habiting with the indigenous in a manner that suggests the islands could support a subsistence based economy. The evidence from the Cambridge Gozo survey (see Chapter 7) suggests an expansion of domestic territory, with site clustering similar to what was seen during the Early Neolithic, and an intensity of activity at re-used sites from earlier periods which is interpreted as a 'recommencement of a cycle of domestic activity that was played out of the earlier Neolithic and Temple Period phases' (Boyle 2013, 287). Boyle also indicates the value of focal locations as loci of trade and communication, given their position on the best routes to natural harbours. However, this perhaps contradicts the assertion that the Bronze Age was marked by a socio-ideological transformation, rather than a significant demographic change. Adding to this, a marked hiatus in cereal agriculture occurred in tandem with an increase in livestock grazing indicated by the palynological data (see Chapter 3). This could be indicative of a net reduction in human activity on the islands. It could be speculated that this reduction is tied to a form of Boserupian economic migration where a proportion of the population left the archipelago because of their inability to intensify production effectively.

Progressing through the Late Bronze Age/Borġ in-Nadur phase, the accumulated data suggest a return to greater levels of productivity along with the establishment of defended hilltop settlements (see Chapter 7). The climatic fluctuations between arid and humid periods is reflected in the variation between adopted cereals, which is indicative of local strategies to support population. The crucial difference that Recchia and Fiorentino (2015) highlight is the advantage of wider cultural contacts, which perhaps enabled the used of climate adapted crops more readily than would be found with a less connected island community. This reflects the fact that the Maltese Islands were beginning to enter the increasingly complex Mediterranean classical world which was already urbanized in the east (Malone & Stoddart 2009, 379). Phoenician activity in the archipelago is well documented, however the generation of a population estimate remains difficult because of the nature of contact and colonization. The account from Herodotus (Book IV, 196) tells of a building of trust through indirect trade at new locations. The Maltese Islands, with poor natural resources other than rock and crops, would appear to have little to offer Phoenician colonizers (Bowen-Jones *et al*. 1961; Blouet 1963; Vella & Anastasi 2019). However, such an assertion ignores the value of the archipelago's sheltered harbours and strategic position between the North African littoral and the Near Eastern heartland of Phoenicia (Recchia & Fiorentino 2015). Considering this, there is an accepted model (Bondì 2014; Sagona 2015) of overlap between the Phoenician traders and the indigenous population, which ultimately gave way to a more permanent form of Phoenician settlement, a feature which is highly evident from the rock-cut burial tombs (Said-Zammit 1997; Sagona 2002). At this stage, the issue of carrying capacity becomes a little more tenuous since the presence of a trade network would suggest that the operation of supply and demand may have existed within the Phoenician period. The subsequent population development, and the transition of Phoenician (trading outposts) to Punic (hinterland management) (Vella 2014), brought the Maltese archipelago into the period of post-carrying capacity populations, or post-insular reliance, where the islands were reliant on external contact as a means of supporting local production capabilities.

8.5.2. Post-carrying capacity periods

Said-Zammit (1997) has produced a population estimate for the Punic period of the archipelago, with the estimate representing the population just prior to entry into the Roman world. Based on 100 per cent utilization of cultivable land (equalling 18,960 people on 60 per cent of the total land area), Said-Zammit proposes that the total population was in the region of 17,555 individuals with population incrementally rising to this level. However, caution must be taken with the concept of complete land utilization as geological factors render areas inaccessible to agricultural practices. Although technological innovation would improve accessibility, a significant area of land will always remain unavailable e.g. littoral and steep gradient locations. This is echoed by Alberti *et al*. (2018) in a logistical regression analysis of nineteenth century land quality assessment. Although this will be discussed in more detail in Chapter 9, the central theme to consider is that the later historic landscape contained locations which spanned the gamut of agricultural viability. Notably, this includes areas of exceptionally poor agricultural viability, despite near contemporary technology. By

Table 8.2. *Summary of population changes in the Maltese Archipelago (after Bowen-Jones* et al. *1961 and Cassar 2002).*

Year (AD)	Population	Source	Comments by Bowen-Jones *et al.* (1961)	Comments by Cassar (2002)
991	21000	Emir Yusef al Futah	Excessive in comparison with Giliberto's report	
1240	5600	Giliberto Abbate		
1241	2199			Potentially the number of hearths as opposed to total population
1400	10000	Bosio	Population did not exceed this number	
1419	8335			Established figure for Malta
1480s	9829			Established figure for Malta
1528	17000	Commisioners of the Order of the Knights of St. John	Number includes 5000 Knights	
1530	25000	Chev. L. de Boisgelin, Bosio and Fra Joannus Quintinus	Multiple suggestions of local population at 20,000 (plus 5000 Knights)	
1535	22000			
1565	31000	Order of the Knights of St. John	22,000 (plus 9000 Knights) pre-Great Seige	
1565	23000	Following casualties according to Zabarella and Bosio	20,000 (plus 3000 Knights)	
1582	20000	Grand Inquisitor Visconti (Malta only)		
1590	32290	Knight de Quadra, for the Viceroy of Sicily		
1632	52900 (51750)	Enumeration under Grand Master de Pawla	48,450 (plus 4450 Knights)	Cassar presents 51,750 excluding 5000 Knights
1736/40	66364			
1741	111000	Enumeration under Grand Master de Despuiz	Conflicts with Ciantar's assessment	
1760	66800	G. A. Ciantar. 1772. *Malta Illustrata*. (Malta only, excluding members of the Order of Knights)	Excluding members of the Order of Knights	
1798	114000 (98000)	Boisgelin	Unreliable as Gozo estimate is 24,000; this conflicts with 1842 population of 14,000 as there is no known population migration to Gozo	Cassar presents 98,000
1807	115154	*Almanaco di Malta* 1807	Based on Parish registers; 93,000 'native Catholic' and 22,100 'other inhabitants and domesticated strangers'	
1813	110803	Burril, W. H. 1813. *Report on the Plague in Malta*		
1828	115945	*Historie de Malte* 1840	Little difference in comparison with the 1807 account; the plague may have limited population growth, however the enumeration process must be questioned	
1837	119878	Watson, S. B. 1838. *The Cholera at Malta in 1837*	Over-estimation is also a likely to be at fault here	
1842	113864	The First Census of the Maltese Islands		
1871	200000			
1931	245640			
1948	304991			
1990	355910			

applying this new understanding to the landscapes from the classical period onwards, it is obvious that 100 per cent utilization of the environment is simply not possible. Returning to Said-Zammit's (1997) work, it is straightforward to re-scale this estimate according to a reduction in available land. For example, at 60 per cent utilization of cultivable land (including the additional support of trade) the population would have been around 10,200. Although this is only speculation, it serves as a reminder that a more detailed analysis of the environment must take place – one which incorporates the pedological and spatial investigations of the *FRAGSUS Project*.

In her study of the Roman Imperial and the Byzantine periods, Bruno (2009) states that there is no concrete way to determine the population size. She suggests that the recorded military garrison of 2000 (all male and of military age) is consistent with what would be expected for a significant population size. However, this overlooks the role of the garrison, perhaps suggesting that it served to defend/exert control over the local population, when in fact a frontier garrison may have had other strategic purposes and whose numbers should not be used as an indicator of local demography.

With the appearance of historical records, there is a more reliable basis for understanding the output and requirements of the Maltese Islands. Bowen-Jones *et al*. (1961, 133) provide a useful summary of the population record during the historic period which is adapted in Table 8.2, incorporating their comments and those of Cassar (2002). The first official census on the islands took place *c*. AD 1241, under the jurisdiction of the Norman King Frederick II. Across both islands the local governor, Gilberto Abbate, recorded 1891 families, which equates to *c*. 7267 individuals (Bruno 2009). However, comparing this figure with Table 8.2 reveals discrepancies. This emphasizes the need for caution when scrutinizing these early population records, using them as a guide to the general trajectory rather than as absolute fact, at least until the later Medieval period.

Although Bowen-Jones *et al*. (1961) scrutinized the validity of each of these estimates, their overview presents a much clearer idea of how the population has accumulated within the archipelago. At this juncture, the concept of Boserup (1975) and intensified production meets a complex socio-political structure where the nature of external events and external investment influenced activities taking place within the Maltese Islands. To chart this, the following section will consider the environment within which agriculture takes place, and which frames the adaptations driven by either internal or external influences.

8.6. The agrarian archipelago

To develop a synthesis of the development of intensification within the Maltese archipelago, it is essential to comment on the nature of the agricultural environment through time. This section will observe the geological and pedological constraints which provide the context within which technological and population changes occur.

8.6.1. The agricultural substrate

Lang's (1960) study has acted as the foundation for the understanding of Maltese soils and their development with three main types of soil identified: Carbonate Raw, Xerorendzinas and Terra soils. In more recent years, *MALSIS – A MALtese Soil Information System (TCY00/MT/036)*, has developed an inventory of soil for the Maltese Archipelago (Vella 2000, 2001, 2003). This has progressed from Lang's considerable work to a quantitative survey which is aligned with the FAO World Reference Base (WRB 2014) of soils. Specifically, this has reclassified the soils identified by Lang (1960) and added some more niche soils that were not previously acknowledged. Calcisols are noted as the most dominant and likely correlate with Lang's Carbonate Raw soils. Linked by the Blue Clay parent material, Vertisols are another reclassification of the carbonate raw soils, defined by deep clayey fissures during the dry summer months. Luvisols correspond to the Terra soils, which are essentially relict soils with subsequent $CaC0_3$ concentrations which are indicative of the present climatic conditions. Utilizing the WRB (2014) and working with archaeological considerations, French and Taylor (Chapter 5) have presented an extensive re-analysis of the soils and palaeosols across the Maltese Archipelago which emphasizes a shift away from developed argillic brown soils (or Luvisols) as the result of anthropic factors, leaving an environment characterized by thin xeric soils and vertisol slopes. Thus, to manage this delicate situation, soils must be constrained by agricultural terraces and improved through the use of natural and artificial fertilizers.

8.6.2. The development of agricultural technology

Sustaining the agricultural environment requires the careful management of a variety of different factors. In the case of the Maltese Archipelago, soil conservation is the key to maintaining any level of agricultural viability. Given the restricted limestone environment, as described by Chatzimpaloglou *et al*. (Chapter 1), the variety of soils available is relatively limited. This is exacerbated by the difficulties of geology, with the predominance of Blue Clay slopes, especially in Gozo. Sagona (2015) reports ethnographic accounts of 1830s

soil production which tell of thin and friable soils, which have good agricultural return. However, where the landscape is denuded of soil, these accounts include the practices involved with the regeneration of a viable substrate. Generally, this relies on the breakdown of the soft limestone (usually the Globigerina), sometimes aided by manual interaction. Through weathering, and improvements such as manuring and crop rotation, the land can be 'amended' to something more viable and productive. Bugeja (2011) describes the practices of surface preparation, such as depicted in Jean Houël's late eighteenth century drawing of Borġ in-Nadur. Typically, these involved the clearance of barren rocky areas, with the levelling of protruding stone and the infilling of negative space in the bedrock. Such preparation echoes the medieval 'Red Soil Law,' latterly incorporated within the Fertile Soils (Preservation) Act of 1973, which required anyone who is erecting a building to gather and preserve the red soil present at the building site. Thus the legislative structure of the archipelago preserves an entrenched practice of bedrock preparation and redistribution of soil used to encourage better agricultural productivity.

Folk practices and accounts of pre-mechanized farming (Halstead 2014) are invaluable to the interpretation of agrarian practices through time. Observed practices provide a reference tool for how ancient landscapes may have been utilized, with varying states of technological development. The folk accounts reported by Sagona (2015) are the first 'technological' step in managing the landscape. Awareness of soil performance and the methods required for improvement were advances made during the prehistoric phases. French and Taylor (Chapter 5) describe pockets of developed Pleistocene soils which would have been readily available to prehistoric agriculturalists. Despite this likelihood, evidence from a number of 'Temple' sites suggests that much work was already taking place to improve the productivity of the soil prior to the construction of the 'Temple' buildings (see Chapter 5). Notably, soils at Ġgantija show significant levels of enrichment with settlement-derived organic waste, contained within what could only be described as a rudimentary terrace, based on the spatial setting of the soils. The related strata appear to underlie elements of the megalithic structure and represent an intentional accumulation of soil to form a viable agricultural topsoil. It could be postulated that this may be one of the earliest forms of agricultural terrace in the Mediterranean and beyond; however, further investigation would be required to confirm the veracity of this interpretation.

As Chapters 2 and 5 have revealed, the continual degradation of soils within the archipelago has led to the adoption of agricultural terracing in the traditional sense. This technology acts as an effective control mechanism for eroding soils. By physically altering the gradient of the hillslope, and creating additional surface roughness, soil can be captured and built into flat surfaces. Terracing is also advantageous as it maximizes water retention within fields – which is vital in semi-arid locations. Labour investment therefore surrounds the construction and maintenance of terraces. On limestone bedrock, Pace (2004) has demonstrated the intentional 'cutting' of the bedrock surface, prior to the creation of a terrace structure, dating to *c*. 800 BC (see Chapter 7). Although relating to a much later landscape, that practice can also be seen at the site of Tal-Istabal, Qormi, in Malta where the *FRAGSUS Project* used Optically Stimulated Luminescence dating in relation to the exposed archaeological landscape (see Chapters 2 & 5; Appendix 2). Fundamentally, this practice is not dissimilar to the soil preparation techniques described by Sagona (2015) as the limestone cut during the formation process could be crushed and used as for soil formation, if not used in wall construction. Borg (1915) reflects that fields had reached a peak of development as a result of the division of land into terraces. Ploughing was meticulous and reliant on the use of non-mechanized techniques, including the 'Maltese plough.' This device balanced the need for a strong steel ploughshare with the practicalities of maintaining a shallow depth of furrow which avoided exposing the bedrock. Borg also describes the use of the hoe, especially as a spade is not effective in the stony and stiff soils. The challenges, overcome by traditional practices and steel tools, were likely an even greater problem for ancient agriculturalists. The creation and development of soil is one achievement while the seasonal process of working the soil is another. Accounts such as those of Borg (1915) and Halstead (2014) suggest that scratch agriculture, using simple tools, may have been very long established, perhaps since the prehistoric period.

Establishing a date for the onset of agricultural terracing is difficult in practice, as soil stratigraphy and chronology pose a significant challenge to overcome. A combination of thin soils and regular ploughing ensures that cultural material has lost its stratigraphic security. As material slowly erodes into terraces, there is a small chance of dateable material entering the fill. However, to utilize this, the material would need to be found in an intact deposit, or perhaps in the lower parts to the wall. Any secure dateable material relating to the formation of the terrace may provide a *terminus post quem*, while subsequent additions during the use of the terrace would represent a *terminus ante quem*. However, finding distinction between these would

be exceptionally challenging when considering the stratigraphic nature of terraces. One potential way to overcome this problem is by using Optically Stimulated Luminescence (OSL) dating, which allows the acquisition of absolute dates from the soil itself (see Chapter 2; Appendix 2). Although the uncertainties of soil accumulation would still apply to this technique, the use of relative accumulation profiling (Sanderson & Murphy 2010) would enable a controlled observation of this effect alongside the use of direct OSL dating. This could be achieved in two ways. Firstly, an attempt could be made to date individual terraces (Davidovich *et al*. 2012), which could be an arduous and expensive process that provides dates with very specific spatial dates. A second, novel method, is to consider terracing's effect on erosion into the valley basins. By searching for deep valley deposits, the use of OSL profiling could be used to date terracing relatively through the proxy of valley stratigraphy (see Chapter 2). Logically, the onset of terrace construction would constrain the amount of soil eroding into the valleys. By profiling a deep valley section, it is possible that the pre- and post-terrace erosion deposits could be identified and dated. In 2016, the *FRAGSUS Project* tested this method at a number of sites, as discussed in Chapters 2 and 5. Dates obtained from the Ramla Valley, Gozo and the site of Tal-Istabal, Malta, show much promise for the technique. In the lower Ramla Valley, AD 1880±16 is the date after which the degradation of the upper slope was constrained (Appendix 2). At the latter site, AD 1620±23 has been noted as the start of soil accumulation. Further samples were taken in the Marsalforn Valley, and suggest colluvial accumulation from at least 1560±240 BC and throughout later prehistoric times, but do not directly constrain the fixing of the period of terrace construction (see Chapter 5).

The two sites dated above represent the use of Globigerina Limestone and Blue Clay geological zones for terracing. Tal-Istabal, represents a continuation of the hard geology terrace construction methods, utilizing the easily worked limestone to prepare a flat bedrock surface upon which a terrace can be constructed. Interestingly, this site also contained a deep channel for water flow from a cistern and an interconnected wheel well. As such, this weight of archaeological evidence is indicative of the Knights period for production intensification – and this is further corroborated by the OSL date. Similarly, in the Ramla Valley, colonization and field demarcation in the mid-sixteenth century AD associated with the Knights of St John suggests that the Blue Clay slopes were not intensified through terracing until at least this period and well into the late nineteenth century. This is likely because of the difficulty encountered when working with the soils on these slopes, as the plough horizon is no more than a restructuring of the parent material – a stiff, moisture retentive argillic layer. The intensification of these slopes is therefore an artefact of a drive to increase productivity during the Knights of St John and the British periods, when a significant level of investment could be made to alter this landscape.

8.7. Discussion: balancing fragility and sustainability

The Maltese archipelago can be viewed as an allegory for the Anthropocene world. The analyses of the changing environment have shown that the influence of human actions can have consequences that remain for the *longue durée*. The flourish of agricultural activity in the later Neolithic caused resounding effects to the stability of soils on the islands. Through clearance of scrub and heavily worked soils, the processes of erosion and soil loss began. Quickly, people adapted by working to improve soils using uncomplicated enriching techniques in an attempt to sustain the viability of soil. However, the need to expand agricultural zones also arose, and is possibly visibly indicated by cart ruts (Pace 2004) which have become inscribed into the bedrock. Although much uncertainty exists regarding the function(s) of the cart-ruts (Hughes 1999; Magro Conti & Saliba 2007), a common interpretation is one of short-range commodity and communication routes, likely utilizing wheeled vehicles as indicated through geomorphological investigations (Mottershead *et al*. 2017). While the haulage may well have varied in composition, its perceived existence is indicative of more intensified landscape from the Bronze Age onwards, especially considering the ruts as markers of vectorized movement towards upland areas. Equally so, the process of terracing has been occurring throughout the historic period, and probably stretches back in some form to the Late Bronze Age.

In summary, these threads of intensification would suggest a trajectory of growth throughout the prehistoric period that would have necessitated a greater output from the land. Although soil exhaustion may only be a marker of the most commonly used land, it is likely that a continually increasing population associated with the rise of the Temple Period culture was the true driving force behind the need to intensify the prehistoric landscape. It could therefore be postulated that the notable cultural change between the Temple Period and the Bronze Age was partly influenced by the degrading agricultural landscape. Through time, the population may have dropped through lower birth rates and out-migration, although

the *FRAGSUS* study has confirmed that a complete abandonment did not occur (see Chapters 6 & 11, and Volumes 2 & 3). As such, sustainability gives way to fragility. From the later Bronze Age onwards, the influx of new technologies and external interests in the archipelago allowed the population to adapt the agricultural environment once more. The adoption of agricultural terracing helped to preserve the fragile *status quo*, and is still extant in the modern era. Terraced 'anthroscapes' are an almost indelible mark on the landscape, one which states the general discontent with the natural processes of erosion. As such, they mark human intentionality to change the environment, rather than change occurring as a by-product. Crucially, in the Maltese archipelago, terracing is indicative of the *longue durée* effects of early farming practices. However, in the twenty-first century, the Maltese Islands have managed to preserve a modest level of sustainability. Nonetheless the reliance on the land for subsistence rapidly diminished through the late twentieth century, allowing the expansion of local produce and market gardening enabled by the permanence of knowledge within folk agrarian practices. In addition to development pressures growing hand-in-hand with an increasing population, the possible abandonment of marginal coastal zone agricultural land, particularly since the mid-twentieth century (Grima 2008a), may have also had an important role to play. Together these factors could lead to a catastrophe not unlike that predicted by Bowen Jones *et al.* (1961). However, continuing rampant development may lead to a much greater anthropic erasure of the agrarian landscape, well before any widespread environmental collapse takes place.

Chapter 9

Locating potential pastoral foraging routes in Malta through the use of a Geographic Information System

Gianmarco Alberti, Reuben Grima & Nicholas C. Vella

9.1. Introduction

The study presented in this chapter aims to complement the earlier GIS study of nineteenth century AD land-use of the islands of Gozo and Malta by Alberti *et al.* (2018) by adding another dimension to the reconstruction of the human exploitation of the landscape, and thus provide a better understanding of the agricultural potential and productivity of the Maltese landscape. It locates potential pastoral foraging routes across the landscape with the aid of a Geographic Information System. While the method and procedures used to accomplish this goal are detailed in the following section, the availability of a model of agricultural productivity of the land on the one hand, and a repertoire of evidence directly and indirectly related to pastoral movements across the island (such as the location of the garrigue areas, public spaces and farmhouses with animal pens) provided sufficient grounds to undertake this research. This approach was meant both to enrich the interpretation of evidence dating to earlier/pre-modern periods and to suggest a range of archaeological and anthropological questions as well as new avenues of inquiry driven by the results of analyses of a better documented (however recent) period.

Modelling of the agricultural quality in Malta on the basis of the data provided by mid-1800s cadastral maps (*cabrei*) showed that the Maltese landscape is a complex patchwork as far as its suitability for human economic exploitation is concerned (Alberti *et al*. 2018). The analysis made it evident that there is a wide variability in land quality, even over small distances, because of a complex interplay between different natural and cultural factors, resulting in a fragmented and variable landscape. The modelled agricultural suitability also showed that a considerably large part of Malta is unlikely to have been optimal for agriculture during the early modern period. This holds true for the thin-soiled and scrub-covered karstland (or garrigue areas; in Maltese: *moxa* and *xagħri*) which features as a relatively large part of the Maltese landscape, such as the flat-topped Upper Coralline Limestone plateaus in the west-central part of the island. It has been observed that farmhouses with animal pens, as well as public spaces or wasteland, are located at the very fringe of (and/or amongst) these uncultivated areas. It has also been stressed that this apparently unproductive landscape has been turned into an important part of the agrarian economy. Importantly, the uncultivated areas provided (and to an extent still provide) grazing grounds for sheep and goats, quarried stone for construction, brushwood for fuel, as well as herbs, greens, wild game and flowering plants for bee pasture (Blouet 1963; Forbes 1996; Lang 1961; Rolé 2007; Wettinger 1982).

9.2. Methods

9.2.1. Data sources

The research presented here is based on three strands of evidence which are each linked to pastoral activities and foraging excursion networks. These are the location of farmhouses with animal folds, and the garrigue and wasteland areas of the islands. In combination with archival, ethnographic and oral evidence, these traits provided the building blocks of the GIS used in this analysis of pastoral foraging routes.

The location of farmhouses in which the presence of animal-folds or 'stables' is documented has been derived from the sample of *Cabreo* maps used for the modelling of agricultural quality (Alberti *et al.* 2018). Within the sample, 29 stables were identified for inclusion in this analysis. No sites in the central-eastern part of Malta were included because the modification of the landscape, caused by the dense urbanization of this sector of the island, has made it impossible to locate any set of ground control points to be used in the process of geo-referencing the cadastral maps.

The location and extent of the garrigue areas have been recorded as a GIS shapefile layer consisting of 52 polygons. This data layer is part of a larger dataset about the Maltese natural and man-made landscape produced by the MALSIS (MALtese Soil Information System) project (Vella 2001), which was made available to us by the former Ministry of Sustainable Development, the Environment and Climate Change. In this dataset, garrigue zones have a minimum and maximum area of 2.18 and 530.2 hectares, respectively, with a median value of 18.74. Their average elevation (m asl) goes from nearly 0 to 242.4 m, with a median value of 87.65 m. The average slope goes from 0 to 64.72 degrees, with a median value of 13.17. They correspond to portions of the karstic Upper Coralline Limestone plateaus, which, as noted, are generally not suitable for agriculture due to a host of factors including the virtual absence of soil, the high exposure to the winds and the lack of water (Rolé 2007). Both literature and ethnographic sources indicate that these areas have been used for different activities, among which goats and sheep grazing (Lang 1961; Rolé 2007).

The third element useful to the aim of this research is the location and extent of areas that were recorded and described in the British period as 'public spaces' or waste land. These data were derived from early 1900s survey sheets (Alberti *et al.* 2018), and was subsequently fed into the GIS through manual digitization. A total of 217 polygons were employed. Public spaces feature a minimum and maximum area of 0.02 and 17.83 hectares respectively, with a median value of 0.32. Their average elevation goes from 0.33 to 248.22, with a median value of 98.77. Their average slope goes from 0.72 to 31.22, with a median value of 5.71.

These spaces proved to be variable in shape and location. They may open-up along the roads or tracks flanked by rubble walls, actually consisting of an enlargement in the area taken up by the road itself. These are zones that are often overgrown and ideal for roadside grazing. In some cases, the spaces are located at the junction between roads or tracks, probably providing flocks travelling in different directions with manoeuvring space in order not to get in the way of one another. Public spaces can be thought of as important nodes along the routes used for the movement of herds across the landscape. In the GIS dataset, more than half of the public spaces or 60 per cent (n=131) intersect a road, with the remainder placed at a certain distance from them. In comparatively fewer instances (86 cases), public spaces do not have an apparent connection with the road network; rather, they correspond to portions of the karstic Upper Coralline Limestone plateaux.

The distances between the public or waste land spaces and the 1895 road network were analysed using the survey map drawn and compiled by Captain E.M. Woodward, Leicestershire Regiment 28 D.A.A.G. A total of 69 per cent (150) of the public spaces were found to lie at a distance between 0 and 10 m from the nearest road, regardless of the road type. The remaining cases are spread over different distance classes (defined at 10 m intervals), each comprising a decreasing amount of cases. Only one public space lies between 310 and 320 m from the nearest road. If we take the road type into account, about half of the public spaces have a minor road in their close proximity (51 per cent, corresponding to 111 cases), while the remainder breaks down between secondary roads (24 per cent, 52), footpaths (13 per cent, 28), and main roads (12 per cent, 26). These figures do not take into account the actual distance to the nearest road type. The latter is admittedly difficult to summarize with a single representative value (e.g. mean or median) because of the very right-skewed distribution. However, if we consider the proportion of cases whose distance to the nearest road type is between 0 and 10 m, it turns out that public spaces tend to be comparatively closer to footpaths (75 per cent, 21 out of 28), minor roads (74 per cent, 82 out of 111) and secondary roads (69 per cent, 36 out of 52) than to main roads (42 per cent, 11 out of 26).

9.2.2. Foraging routes and least-cost paths calculation

The location of stables, garrigue areas and public spaces provides the foundation for attempting to locate potential foraging routes. To accomplish that, a GIS-based calculation of least-cost paths (LCPs) was used. This is a widely applied approach in the study of how human behaviour relates and engages with movement across the landscape (Conolly & Lake 2006; Herzog 2014; Van Leusen 2002; Wheatley & Gillings 2002). LCP analysis is generally adopted in the study of land accessibility and land-use patterns (Wheatley & Gillings 2002), when the relation between humans and the landscape, such as for instance, for the acquisition of raw materials (Tripcevich 2007) which must be grounded in an understanding of how human movement is differentially affected by the landscape (Conolly & Lake 2006, 214). Once the influence of external factors (either environmental or cultural, or both) on the movement of humans through the landscape is framed in terms of cost, then an analysis which can take into account the cost of movement, instead of simple straight-line distances between locations, may provide a more complex, more realistic and less misleading picture of human spatial behaviours and decisions (Gorenflo & Gale 1990, 243).

GIS-aided estimation of least-cost paths has been used in a variety of contexts and for a wide array of

purposes including, but not limited to (and see also: Herzog 2014; Verhagen *et al.* 2011), the study of prehistoric travel corridors (Bell *et al.* 2002; Kantner 2004; Teeter 2012; Whitley & Hicks 2003), human movement and land accessibility (Contreras 2011; Murrieta-Flores 2012; Richards-Rissetto & Landau 2014), prediction of archaeological sites location (Rogers *et al.* 2014), maritime pathways (Alberti 2017; Indruszewski & Barton 2006; Newhard *et al.* 2014), Roman aqueducts (Orengo & Miró 2011) and roads (Verhagen & Jeneson 2012).

In this study, the cost of movement is conceptualized in terms of walking time. This was appropriate as both literature and ethnographic accounts frame foraging excursions in terms of time spent to move from the starting location to the target grazing areas (Arnon *et al.* 2011; Endre Nyerges 1980; Schlecht *et al.* 2006, 2009). Since livestock trails have turned out to follow least-effort routes trying to minimize the impedance provided by the terrain's slope (Arnon *et al.* 2011; Ganskopp *et al.* 2000; Stavi *et al.* 2008), and since slope is a significant factor, albeit not the only influential one (see also symbolic costs, type of terrain, energy expenditure, weather condition, clothing, loads carried, gender, age, fitness, body characteristics, headwinds, field of view (Aldenderfer 1998, 11; Kondo & Seino 2009; Pingel 2010; Wheatley & Gillings 2002, 141)), affecting the speed of movement in rugged terrains (Bell *et al.* 2002; Bicho *et al.* 2017; Kondo & Seino 2009; Murrieta-Flores 2014) (Fig. 9.1a), it was decided to implement a re-scaled version of the widely used (Herzog 2014, 2016) Tobler's hiking function (Tobler 1993), whose modification to fit animal walking speed is described shortly. This is a useful and more accessible tool for estimating the influence of terrain slope on the timing of movement (Aldenderfer 1998, 11; Kantner 2004; Richards-Rissetto & Landau 2014).

Grounded in empirical data, the function predicts the walking speed as dependent on slope according to the following formula: v= 6*exp[-3.5*abs(s+0.05)], where *v* is the walking speed in km/h and *s* is the slope measured as rise over run. The maximum predicted walking speed of about 6 km/h is reached on a gentle (-2.86 degrees) downhill slope (Conolly & Lake 2006, 218). Beyond that threshold, the walking speed exponentially decreases because during downhill walks the muscular energy of the legs is spent in braking. Remarkably, while the function has been devised on the basis of mid-1950s empirical data, recent GPS-aided studies have confirmed the function's broad validity (Kondo & Seino 2009; Zolt & Dombay 2012). Tobler's function cannot be directly used in its form (expressing km per hour), but has to be solved for time (Pingel 2010, 138); in other words, it is the reciprocal of the function (hours per km) that has to be implemented in GIS.

As noted above, Tobler's function has been re-scaled to fit an animal's walking speed during foraging excursions. The distribution of the latter, as empirical data show, turns out to be right-skewed and to vary along a continuum. It ranges from very low speed values (corresponding to grazing while walking) to comparatively higher values (up to about 4.0 km/h) corresponding to directional travel toward feeding stations (Arnon *et al.* 2011). In an attempt to find a balance between different figures (Arnon *et al.* 2011; Endre Nyerges 1980; Schlecht *et al.* 2009, 2006), it was decided (but see below) to consider 1.5 km/h as the average flock speed (Endre Nyerges 1980, 468). It roughly corresponds to the average speed recorded in other studies (Arnon *et al.* 2011; Schlecht *et al.* 2009). The above figure is considered the typical speed of flocks during excursions in which grazing takes place while walking (Fig. 9.1b), which in most situations can be

Figure 9.1. *a) Sheep being led to their fold in Pwales down a track; notice the quite steep slope which is bound to negatively affect the walking time; b) Sheep grazing along a track on the Bajda Ridge in Xemxija, Malta. The pasture is located in fallow fields in Miżieb ir-Riħ. Notice that sheep are grazing while walking (estimated average speed derived from literature: about 1.5 km/h) (N. Vella, 9 January 2005) (G. Alberti).*

considered a typical form of grazing (Arnon *et al.* 2011). Tobler's (1993) hiking function has been rescaled by a factor of 0.25 to represent the walking pace of a flock instead of humans. The mentioned factor corresponds to the ratio between the flock average speed (1.5) and the maximum human walking speed (about 6.0) on a favourable slope (-2.86 degrees).

Paths following least costly routes have been calculated using ArcGIS 10.1's Path Distance tool (ESRI 2017d), which locates the minimum cumulative travel cost when moving on a raster from a source location to destination locations. Remarkably, it allows anisotropic cost estimation (Conolly & Lake 2006, 215–21; Wheatley & Gillings 2002, 138ff) that includes the calculations of slope-dependent costs such as those based on Tobler's (1993) function. The reciprocal of the latter, expressed in metres (representing the time in hours to traverse 1 m), has been fed into the tool as a customized vertical factor table, following the procedure first used by Tripcevich (2007) in the context of archaeological research. The table stores the time (in hours) it takes to cross 1 m for each slope value, the latter ranging from -90 to +90 degrees. While a slope raster derived from a digital terrain model (DTM) and expressing the slope in absolute values (i.e. not distinguishing between down and up slopes) is fed into the tool as a cost surface. In this case, the tool internally calculates whether each slope value is either negative or positive when moving from one cell to another (ESRI 2017c), and associates each signed slope value with its corresponding time value (in the mentioned vertical factor table). Once the time it takes to traverse 1 m at each signed slope value is determined, it is finally multiplied by the actual surface distance (ESRI 2017c & d; Etherington 2016; Rogers *et al.* 2014, 263). Eventually, the tool calculates the accumulated time it takes when moving from the source raster cell to the next neighbouring cell, producing a cumulative cost-distance raster. The tool also returns a backlink raster, which indicates, for each cell, which neighbouring cell one has to move to in order to reach the source location along a least costly path (ESRI 2017d).

Two rasters were fed into the Path Distance tool. The first was a LiDAR-derived DTM with a cell size of 10 m. The resolution used has been deemed suitable for the research questions at hand given the spatial extent of the analysis. The relatively coarse cell size has been considered a good compromise in an attempt to find a balance between accuracy in the representation of the terrain's elevation and the need to reduce the distortions caused by the human-made structures retained in the DTM (e.g. Verhagen & Jeneson 2012). This is particularly evident in the southern sector of the island, where the runway of Malta international airport is located. Apart from that, the DTM provides a more generalized picture of the terrain, in which some characteristic features of the landscape, such as terrace walls, have been smoothed out to a certain extent.

The slope raster fed into the Path Distance tool as a cost surface was derived from the DTM referred to earlier. The slope raster has been preliminarily modified in order to gauge the influence of our model of agricultural suitability on the LCP calculation. Literature and ethnographic evidence indicate that during their grazing journeys shepherds tend to avoid cultivated fields (Bevan *et al*. 2013). On this informed assumption, it was decided to factor agricultural quality into the LCP analysis. This was achieved by applying weights (e.g. Rogers *et al.* 2014, 264; White 2015, 410) to the slope, deriving them from the raster representing the fitted probability of optimal agricultural quality (Alberti *et al.* 2018). A higher slope value has been assigned to those parts of the landscape for which the estimated probability for optimal agricultural quality is larger than 0.60, rendering those areas costlier to traverse.

We decided to calculate two series of LCPs. The first uses garrigue areas as both the source and the destination of movement, in order to estimate the path network between them. The rationale behind this rests on the fact that, as noted, these areas are indicated by literature and ethnographic sources as being preferentially used for grazing. Since the calculation of LCP needs both a source (i.e. the starting location) and destination locations (i.e. places where the movement actually ends), and since there is no substantive reason to prefer any given location over another as a destination within each garrigue area, it was decided to draw a set of random points within the garrigue polygons, with a minimum inter-point distance of 20 m. In total 139 points were eventually generated. Each point has been used as a destination in the LCP calculation from each garrigue area.

A second series of LCPs was calculated using the stables as source locations and the mentioned random points as targets. The aim of this second series of LCPs was to estimate the least costly paths along which foraging journeys may have taken place. Since both ethnographic data and literature indicate that time is an important constraining factor for foraging journeys, and since (in spite of a considerable variability across species and season) 10 hours can be considered an average duration of grazing day (Schlecht *et al.* 2006), the present calculation of LCPs has been first limited to five hours, and increased to six and eventually to seven for the reasons described later while reporting the results. The rationale for using a time limit is to locate which target location can be reached along a least

costly path from each stable, while also leaving enough time for the return journey to the stables. Finally, it should also be noted that the calculation of these two LCP networks allows the relationship between public spaces and potential pastoral routes to be examined. This is useful to explore the hypothesis, informed by the existing literature and ethnographic evidence, that the public spaces may be nodes along foraging paths.

9.3. Results

9.3.1. Garrigue to garrigue least-cost paths

Figure 9.2a shows the network of LCPs connecting each garrigue area to each random point within them. Dashed lines have been used to represent the paths; when they show up as a continuous black line, it means that two or more paths are actually overlapping (see §9.3.2). Overall, the image represents the potential routes along which a foraging journey may take place. As expected, these paths (139 in total) minimize the traversed slope. The minimum and maximum average slope is 1.28 and 15.77 degrees, respectively. The median average value is 5.19 degrees, with 90 per cent of the cases having an average slope equal to or smaller than 9.76 degrees, and just the top 10 per cent of the cases exhibit an average slope between 9.76 and 15.78 degrees.

As a result of the described weighting scheme, the LCPs also tend to avoid areas with a high probability for optimal agricultural quality. The median average probability of the terrain they traverse is 0.05, with a minimum and maximum equal to 0 and 0.51, respectively. In 90 per cent of the cases it is equal to or smaller than 0.23. The effect of the adopted weighting scheme can be visually appreciated from Figure 9.2b. It is apparent how LCPs tend to avoid the bottom of valleys since these feature the highest probability for optimal agricultural quality. This holds particularly true for the central sector of the island, and for two 'pockets' in the north-central area, in the Mosta and Naxxar neighbourhood.

As touched upon earlier, the estimated LCPs show some degree of overlap, which can be better appreciated (e.g. Bevan & Conolly 2013) in Figure

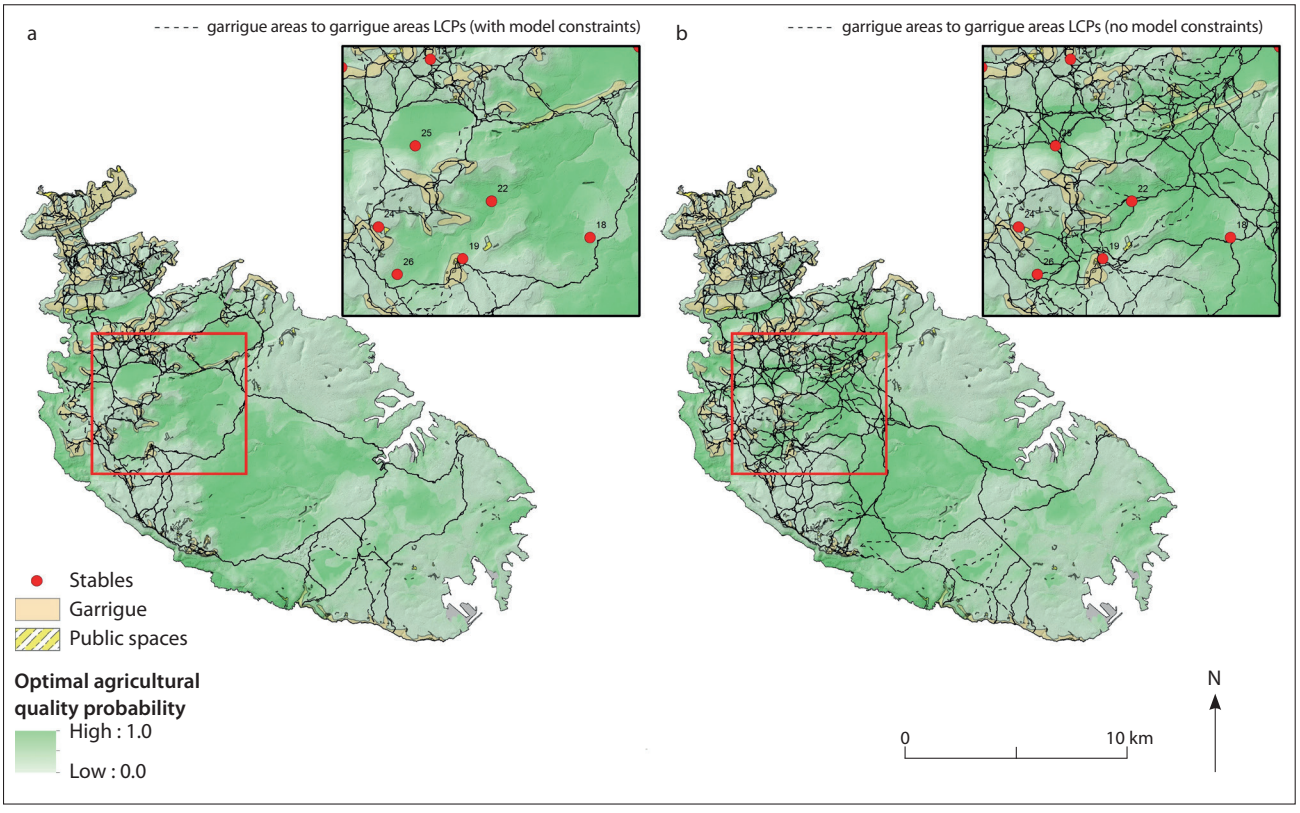

Figure 9.2. *Least-cost paths (LCPs), connecting garrigue areas, representing potential foraging routes across the Maltese landscape (the latter is given a colour that represents the probability of optimal agricultural quality, according to the* Cabreo *model): a) LCPs with the model used as a constraint (LCPs tend to avoid more fertile areas); b) no model constraint (see also Fig. 9.3) (G. Alberti).*

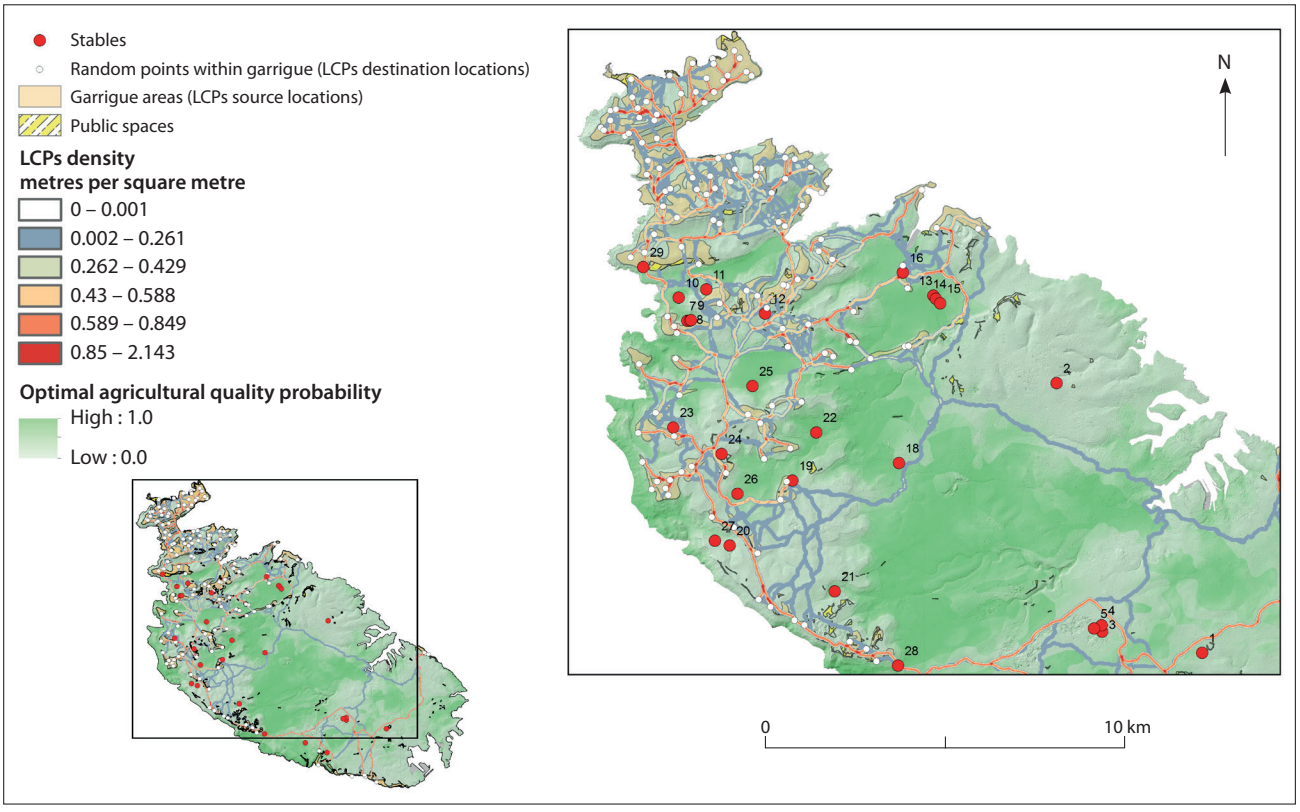

Figure 9.3. *Density of LCPs connecting garrigue areas to random points within the garrigue areas themselves. Density (metres per square metre) calculated as the sum of the length of each path's segment falling within a 50 m search radius centred on each raster cell, divided by the area enclosed by the search radius (G. Alberti).*

9.3. It represents the density of LCPs (in metres per square metre) calculated as the sum of the length of each path's segment falling within a given search radius centred on each raster cell, divided by the area enclosed by the search radius (ESRI 2017b). A search radius of 50 m has been used, and to break the density values down into five classes. Jenks' classification algorithm (Jenks 1967; Smith 1986) has been employed for its ability to maximize groupings inherent in the data (ESRI 2017a). This is apparent in the extent to which among all the areas traversed by the estimated LCPs, some are actually characterized by a comparatively higher density of paths. This holds true for the northernmost sector of the island, the north-central part, and the westernmost part along the western coast of Malta.

The analysis indicates that public spaces tend to lie close to the estimated LCPs. The median planar distance of public spaces to the nearest LCP turns out to be 89 m, which becomes 39 m if we consider a 50 m buffer around each side of the LCP. Remarkably, the first quartile of the distribution is equal to 0, meaning that one quarter of the cases (out of a total of 217) has a minimum distance equal to 0. In other words, the LCPs either cross the public spaces or touch their boundary. Overall, 53 per cent (116) of the public spaces lie between 0 and 100 m away from the nearest LCP, while just 20 per cent (43) lie between 100 and 300 m away. Cumulatively, 73 per cent (159) lie within a distance of 300 m. It is worth noting that only 27 (12 per cent) public spaces feature a distance equal to or larger than 1 km to the nearest LCP. Remarkably, these more distant public spaces are mainly located at the fringe of the densest urbanized area of the island (see Fig. 9.4, where the Jenks' method has been used). They could possibly have been related, spatially and functionally, to garrigue areas cancelled out by modern urbanization.

The tendency for public spaces to be close to the estimated LCPs can be statistically assessed by means of a randomized procedure (O'Sullivan & Unwin 2010; Wheatley & Gillings 2002) whereby the distance from each public space's centroid to the nearest LCP is first computed and averaged. The significance of the observed average minimum distance is assessed by comparing it against a distribution of

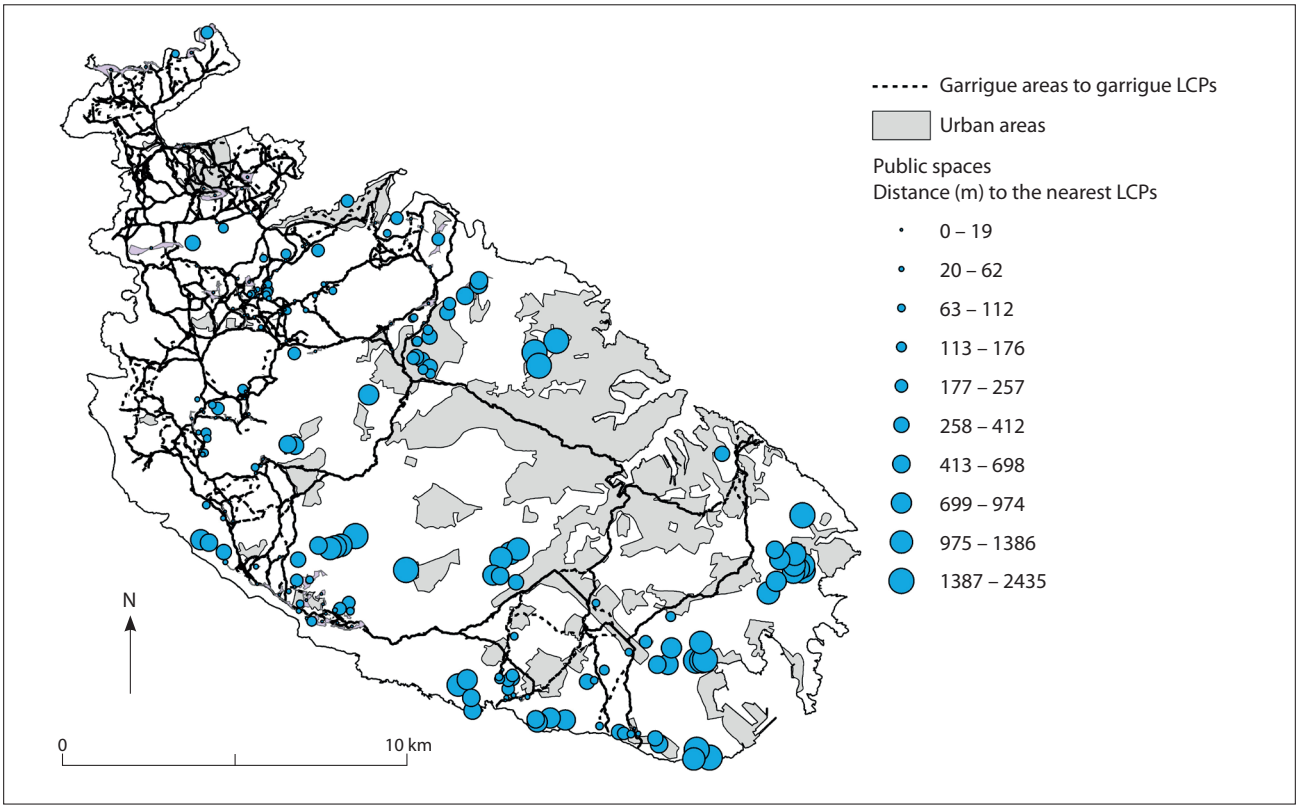

Figure 9.4. *Location of 'public spaces', with size proportional to the distance to the nearest garrigue-to-garrigue LCP. The classification of the distance value is based on Jenks' natural break method for its ability to maximize groupings inherent in the data. Extent of the modern urbanized area is also shown (G. Alberti).*

average minimum distances calculated across 199 sets of random points drawn within a study window (Rosenberg & Anderson 2011). A p-value can be empirically worked out; it reflects the proportion of cases in which simulated average distances proved equal or smaller than the observed average distance (Baddeley *et al.* 2016, 384–7). The study window is the extent of Malta excluding the urbanized areas and those zones that the LCPs are intentionally avoiding (modelled probability of optimal agricultural quality larger than 0.60; see §9.3.1). The analysis indicates that the observed average minimum distance is 380 m, while the average of the randomized minimum distances is 510 m. The tendency for public spaces to lie close to the estimated LCPs is significant (p: <0.05).

9.3.2. Stables to garrigues least-cost paths

Figures 9.5–9.7 show the LCPs connecting stables to the random points within the garrigue areas. Two symbologies refer to the two legs of the journey, one from the start location to the destination (outbound), the other in the opposite direction (inbound). As stated above, the LCP have been calculated with a time limit of five hours for the outbound journey, devised on the basis of literature. Additional calculations have been nonetheless performed increasing the limit to six and, eventually, seven hours. The reason for this was to maximize the number of target locations that could be reached. In fact, while just 35 per cent and 40 per cent (out of 139 cases) could be reached with time intervals of five and six hours respectively, 50 per cent (69) of the destinations can be reached once seven hours are considered. It must be noted that for ten stables (2, 6, 10, 13–15, 17, 22, 25, 27) the analysis resulted in no LCP being estimated. In one instance (2; see Fig. 9.6b), this was because the nearest target location is beyond the 7-hour limit. Nine stables (6, 10, 13–15, 17, 22, 25, 27) cannot be connected to any destination because they are surrounded by land featuring a probability for optimal agriculture above 0.6, resulting in an extremely limited area than can be traversed within seven hours.

Overall, the time spent in median to reach the destinations is 3.51 hours. One quarter of the destinations can be reached within 2.47 (1st quartile) hours, and three quarters within 5.39 (3rd quartile).

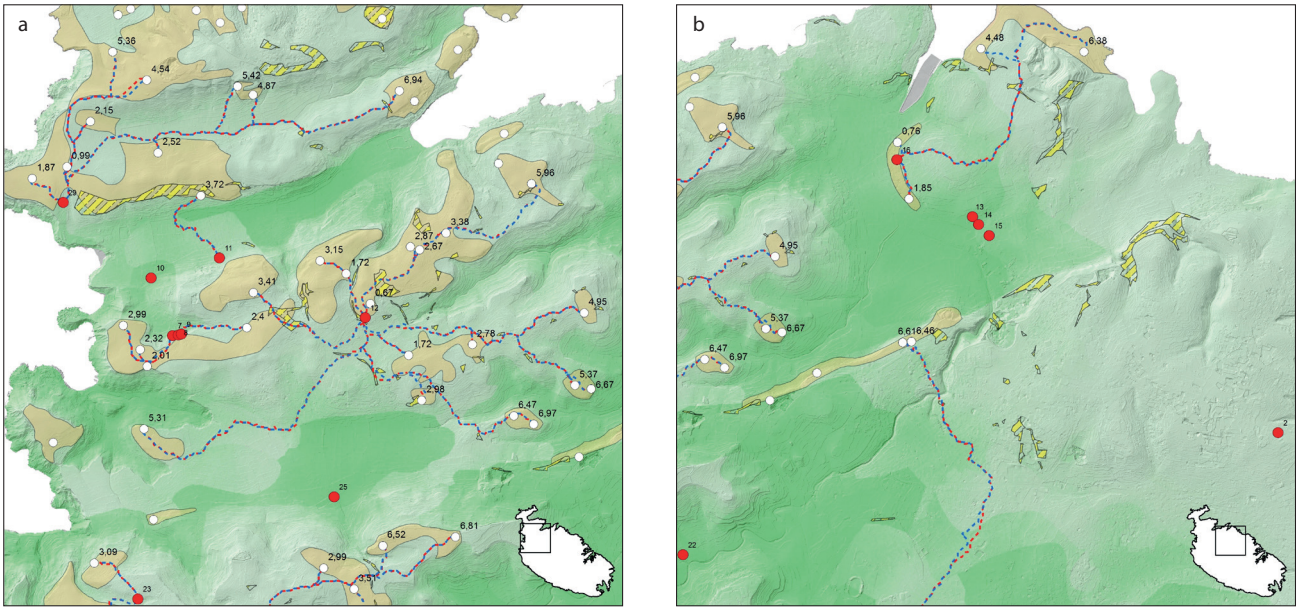

Figure 9.5. *LCPs connecting farmhouses hosting animal pens (hereafter 'stables') to randomly generated points within garrigue areas in northwestern (a) and northeastern (b) Malta. Dashed blue and red lines represent the outbound and inbound journey respectively (for legend and scale bar, see Fig. 9.7) (G. Alberti).*

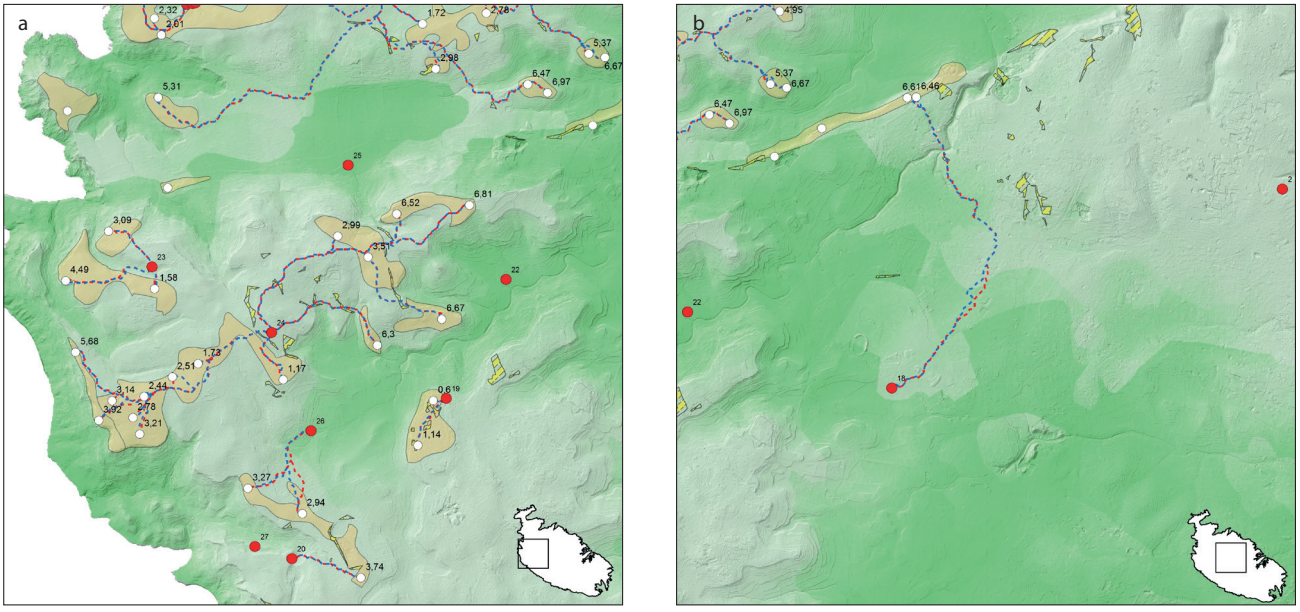

Figure 9.6. *As for Figure 9.5, but representing west-central and east-central Malta (for legend and scale bar, see Fig. 9.7) (G. Alberti).*

If we break down the data by a two-hour interval, 17 per cent (12) of the locations can be reached with a journey between zero and two hours, 39 per cent (27) between two and four hours, 25 per cent (17) between four and six hours, and 19 per cent (13) between six and seven hours. Cumulatively, 56 per cent of the location can be reached within a four-hour journey, 81 per cent within six hours, with the remaining 19 per cent reachable within seven hours. The outbound excursions reach a median planar distance of 996 m

from the starting locations. In the middle 50 per cent of the cases, the distance is between 625.40 m (1st quartile) and 1708.83 m (3rd quartile). In only the top 10 per cent of cases is the distance covered between 2161.71 and 3761.52 m, with just two cases scoring a distance between 2500 and 3000 m, and just one case between 3500 and 4000 m.

As touched upon above while considering the overall LCPs, the weighting scheme used allows the addition of complexity to the estimated paths as well. Considering for instance stable number 11 in northern Malta (Fig. 9.5a), it is interesting to note that the LCP, while traversing quite a flat area featuring a relatively low probability for optimal agricultural quality, makes a westward detour to bypass a zone featuring a higher probability. The same holds true for the LCPs from stable number 18 (Fig. 9.6b), which follow an eastward-bent path that traverses a low-probability portion of the land.

The analysis shows that the time spent to return to the stables is in median 3.47 hours, with the 1st and 3rd quartile equal to 2.46 and 5.38, respectively. There is no remarkable difference in the duration of the outbound and inbound journeys, as their median difference of 0.013 hours indicates. The maximum absolute difference is equal to 0.153 hours, corresponding to the time differential between the LCPs connecting stable number 24 to a destination lying west of it and that can be reached in 5.68 hours (Fig. 9.6a). The journey in the opposite direction would last 5.84 hours. Considering the two legs of the estimated LCPs, the analysis indicates that a typical grazing journey would last 6.99 hours (median), with 50 per cent of the journeys competed between 4.94 (1st quartile) and 10.77 (3rd quartile) hours. The lower 10 per cent (7 cases) of the journeys can be performed within 3.18 hours, and the top 10 per cent can be completed in a time-span between 13.03 and 13.90 hours.

As for the distance between stables-to-garrigues LCPs and centroids of public spaces, the observed average minimum distance is of 908.90 m is considerably smaller the randomized average minimum distance of 1347 m (across 199 simulations; using the same analytical windows mentioned earlier), with an associated significant p-value (p: <0.05). About 15 per cent of the public spaces (32) lie at a distance between 1000 and 2500 m, and a small group (about 10 per cent, corresponding to 20 public spaces) lies between 3000 and 5000 m. If the location of all these cases is considered (Fig. 9.8), it can be noted that they tend to lie in the eastern part of the island, in the very sector which is opposite to the zone (namely, the northwestern and western) toward which the location data of the stables is 'structurally' skewed as mentioned earlier. If these cases are excluded, the remaining 165 instances indicate that public spaces are in median 188.27 m distant to the nearest LCP connecting each stable to the destination points within a 7-hour walk; 12 per cent (20) are at a distance of 0 m, meaning that LCPs actually cross the spaces or touches the public spaces' boundary. Some 25 per cent (41) are within 47 m distance, while 75 per cent (124)

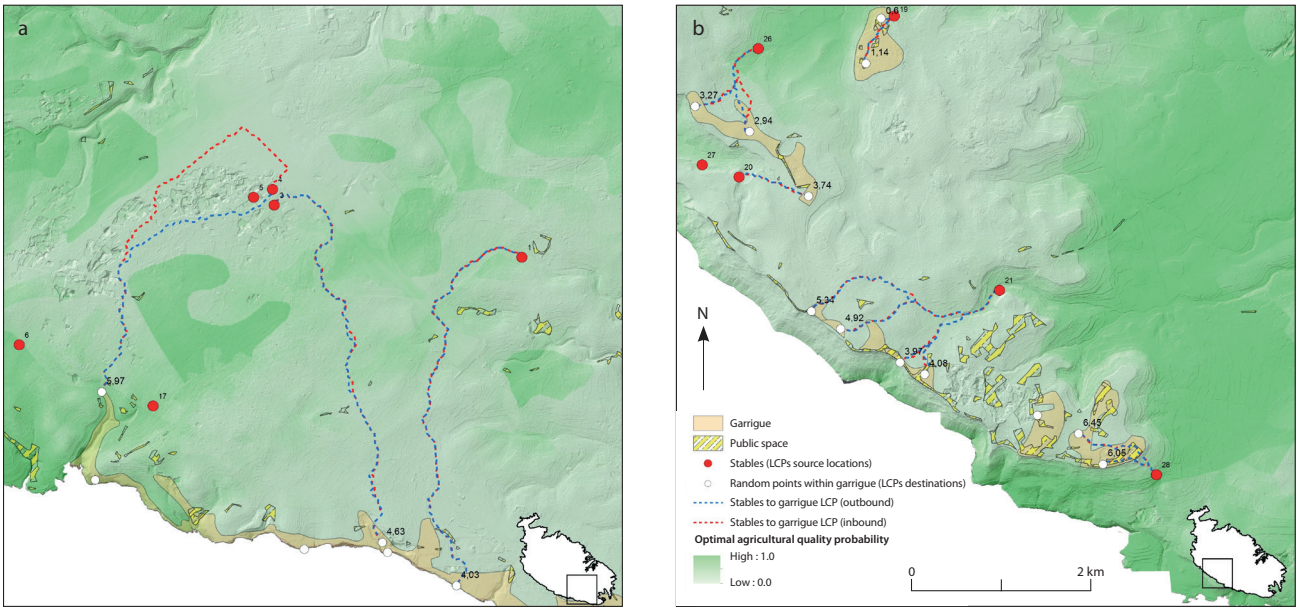

Figure 9.7. *As for Figure 9.5, but representing southern and southwestern Malta (G. Alberti).*

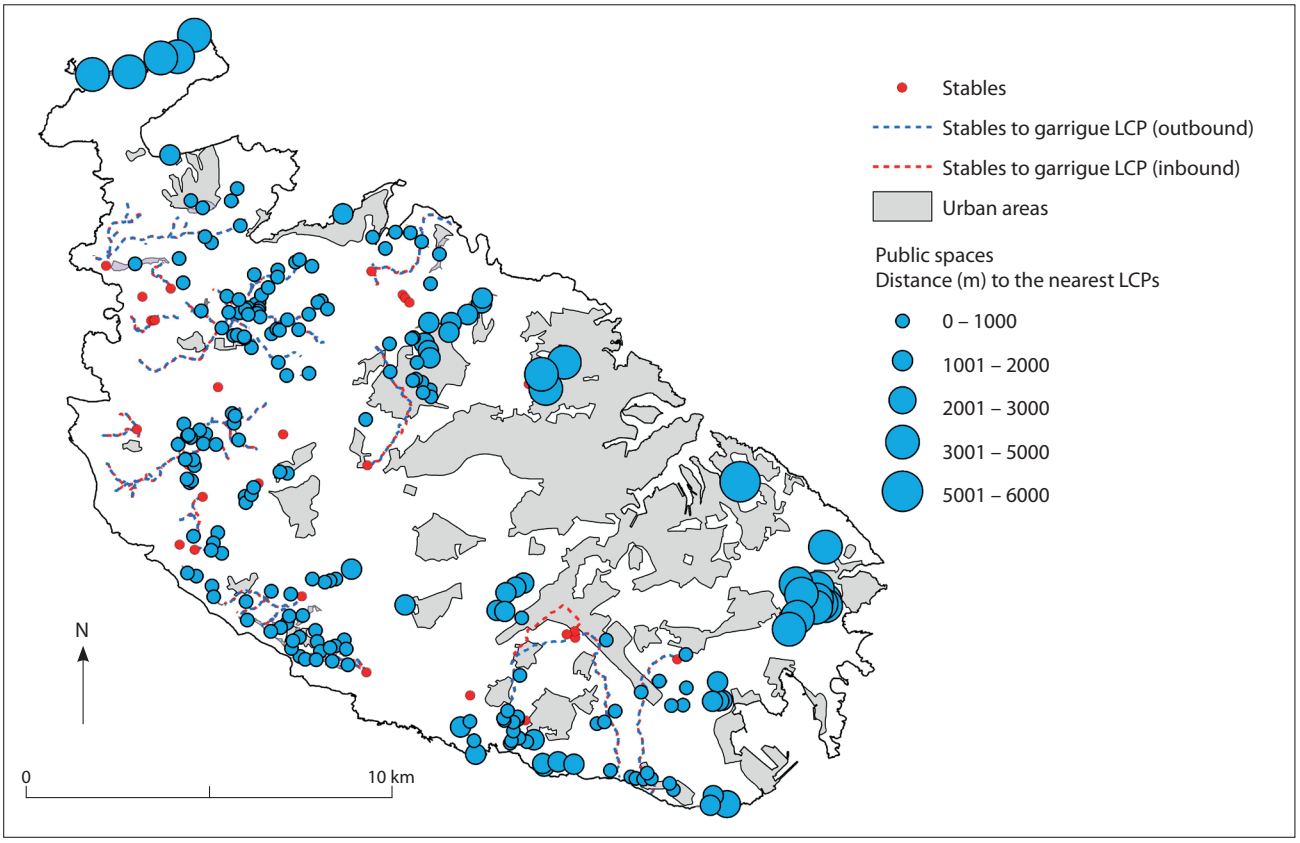

Figure 9.8. *Location of 'public spaces', with size proportional to the distance to the nearest outbound journey (stables to garrigue areas). Distance values classified using the Jenks' natural breaks method as in Figure 9.3. Inbound and outbound journeys, and the extent of modern urbanized area, are also shown (G. Alberti).*

lie within 447.44 m. Overall, these figures indicate that the estimated LCPs and public spaces tend to be close in space.

9.4. Discussion

The analysis reveals some interesting features of the Maltese rural landscape in relatively recent historical periods. These findings nicely dovetail with the previous study of the agricultural productivity in Malta in the mid-1800s (Alberti *et al.* 2018). While the latter has generally brought to the fore the interplay between good agricultural land and sectors of the landscape less suitable for agriculture but potentially exploitable for other economic activities, the research pursued in the present work allows the further characterization of the way in which the parts of the Maltese landscape less suited for agriculture have been exploited for complementary, yet equally important, purposes such as herding and grazing.

Employing as constraining factors the modelled agricultural quality and the documented tendency of grazing routes to avoid good agricultural areas, this study has proposed a model of likely grazing itineraries that features a complex network of paths connecting those garrigue areas used by shepherds as grazing areas. Informed by the parameters selected on the basis of the literature, the network minimizes the traversed slope and tries to avoid the bottom of valleys, the latter corresponding to areas of good agricultural quality. This network can be thought of as representing plausible routes connecting areas of foraging exploitation.

The analysis has also attempted to gauge how (if any) the so-called public spaces or wasteland areas relate to that network.[1] Interestingly, those areas were found to be spatially related to the foraging route network. Even though from an analytical standpoint, a complicating factor is represented by the different preservation of public spaces between the eastern and western sectors of study area, the fact that the majority of the public spaces lie within a 300 m distance from the estimated foraging paths is taken here as evidence hinting to a functional connection between the two.

It has been noted above that, in our GIS-based foraging routes estimation, some farmhouses could not be connected with any destination location within the garrigue areas since the farmhouses are surrounded by land featuring a very high agricultural quality. In this respect, it must be noted that the possibility to move flocks in areas of densely cultivated fields was assured by the existence of walled paths (droveways). Interesting examples still survive in a quite densely urbanized area between the modern towns of Mosta and Naxxar, in central-eastern Malta (Fig. 9.9). In the locality called Tal-Wei, for example, four walled paths converge in a public space (0.33 ha). From a functional point of view, the paths would have allowed flocks to move across the landscape without traversing cultivated fields, unless some sort of agreement had been previously established between shepherds and farmers to allow grazing on their fields following a harvest or in those, particularly in Gozo, where self-seeded *sulla* (*Hedysarum coronarium*) grows in abundance, as we know from the literature and local informants (Bowen-Jones *et al.* 1961, 199, 227).[2] The public space would have also provided manoeuvring space for flocks moving towards different destinations. It turns out that a segment of the GIS-based estimated foraging route connecting the garrigue areas is just 147 m away

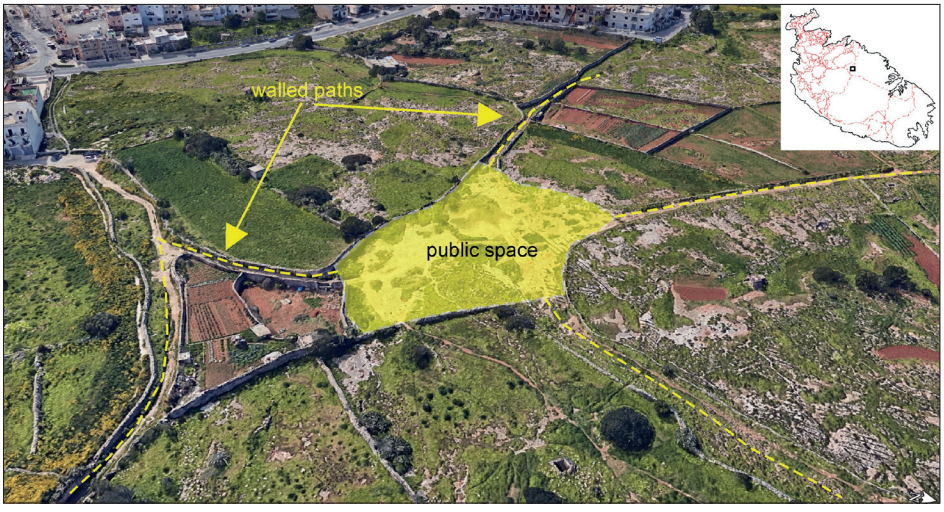

a

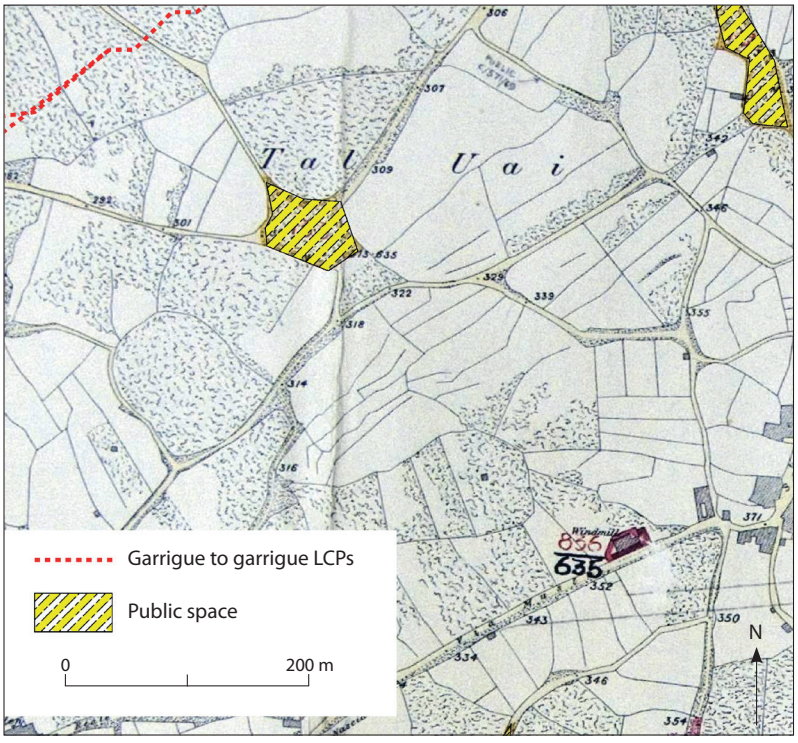

b

Figure 9.9. *a) Public space at Tal-Wei, between the modern town of Mosta and Naxxar; the extent of the public space and the layout of the walled paths leading to the space are highlighted; b) Tal-Wei public space as represented in 1940s survey sheets. The red line represents a segment of the GIS-estimated foraging route passing about 100 m away from the public space (G. Alberti).*

from the mentioned public space. Bearing in mind that in a highly dense urbanized zone, like the one under discussion, the estimation of the foraging route is likely to have been affected by the noise retained in the DTM purged from modern construction, the Tal-Wei case represents an interesting instance in which, from a postdictive standpoint (Armstrong *et al.* 2016; Patacchini & Nicatore 2016), GIS-based estimates show a reasonable degree of plausibility in relation to actual evidence on the ground.

If the estimated LCPs can be taken as representing potential corridors for movement of flocks across the landscape, another strand of evidence turns out to dovetail with the GIS-based estimations. The evidence relates to the location and spatial distribution of villages bearing the Maltese prefix *raħal* (often contracted to ħal), a number of which have been associated with minor settlements, hamlets or more generally 'villages' that disappeared during the Medieval period (Wettinger 1975). The Arabic meaning of the word *rahl*, which survives in Spain and Sicily, is that of a stopping place after a day's journey. It must be acknowledged that the etymology and the process of linguistic and semantic adaptation along the transmission from Arabic to local languages (such as Spanish, Sicilian and Maltese) is extremely intricate and not without uncertainties. It has been argued, however, that the prefix can be etymologically connected to traveller's way-stations or huts used by itinerant shepherds in southern Spain (Glick 1995) and in Sicily (Dalli 2016, 373) and by extension, to locales associated to livestock breeding or animal husbandry, such as farmsteads, animal folds or estates (Dalli 2016). The Maltese *merħla* (herd, normally of sheep and/or goats) and its plural *mriehel* or *merħliet* share the common root *r-ħ-l* with *raħal* seemingly confirming the pastoral connotation (Fiorini 1993, 118).

Building on the available documentation of the distribution of those toponyms, this study has made a considerable effort to improve their positioning beyond the six-figure reference given by Wettinger (1975, 190, 205 & fig. 12) by looking at all minor localities associated with individual ħal toponyms (recorded in Wettinger 2000) and locating these on the series of six-inch to one mile maps of Malta produced in the early 1900s. Some uncertainties do remain as for the exact location and the original extent of these villages. In any case, the above procedure allowed the building of a database featuring 69 locations. These are shown in Figure 9.10, where they have been given a 500 m radius buffer representing the hypothetical, and admittedly subjective, extent of each village. The colour of the buffers reflects the division of the distance to the nearest garrigue-to-garrigue LCPs into four classes using the Jenks' (1967) natural breaks method cited earlier. In spite of positional uncertainties, it can be appreciated that the villages seem to lie not far from the network of LCPs. As a matter of fact, 58 per cent (40 out of 69) of the buffers are at a distance of zero metres from the LCPs, meaning that the latter are tangential to, or intersect, the buffer; 10 (*c*. 15 per cent) are at a distance between 41 and 295 m, with fewer and fewer instances falling within increasing distance classes. All in all, it seems that the location of the *raħal* toponyms tends to be close to the estimated pastoral foraging routes. Another characteristic that deserves further study is that several of these toponyms, such as Ħal Mann, Ħal Millieri, or Ħax-Xluq, coincide with nodes where several minor roads and tracks converge, linking them to the network of walled droveways.

Other evidence turns out to be interesting from a postdictive standpoint. East of Rabat, the estimated LCPs pass in the vicinity of the Tal-Merħliet road (minimum distance *c*. 120 m), whose name (meaning 'of the herds') is actually related to sheep and flocks (Fig. 9.10). West of Rabat, an area called Tal-Merħla turns out to be surrounded by the estimated LCPs, with the nearest estimated foraging route being about 100 m distant. Further west, another Tal-Merħla place-name and a Tal-Merħla road are close to the estimated LPCs, with the former 250 m distant from the nearest foraging route, and the latter actually intersecting part of the LCP. West of Qrendi, the LCPs pass near a church dedicated to San Nikola Tal-Merħliet (minimum distance *c*. 515 m) that, in turn, falls within the territory of the lost village of Raħal Niklusi (Wettinger 1975, 374). In the eastern sector of Malta, the estimated LCPs leading to the garrigue areas lying in the same zone cross an area named after St Rocco (distance to the nearest LCP: 51 m). The latter is traditionally considered to be protector of herds, especially against infectious diseases (Mandarini 1860, 338–9). Moving to the south, two place-names featuring a connection to the same saint lie at 243 m (Misraħ Santu Rokku) and 600 m (Ta' Santu Rokku) away from the nearest LCP. Finally, immediately east of Salina Bay (north-eastern Malta), the estimated LCPs cross an area named Il-Merħla.

Besides the general foraging route network connecting the grazing areas, the analysis sought to locate likely paths connecting individual farmhouses to garrigue areas within an animal walking-time limit of seven hours. The latter has been devised whilst taking into consideration both literature and analytical constrains. While the actual routes located by the analysis are interesting in their own right from a purely cartographic perspective, the estimated journey duration proves even more interesting once compared

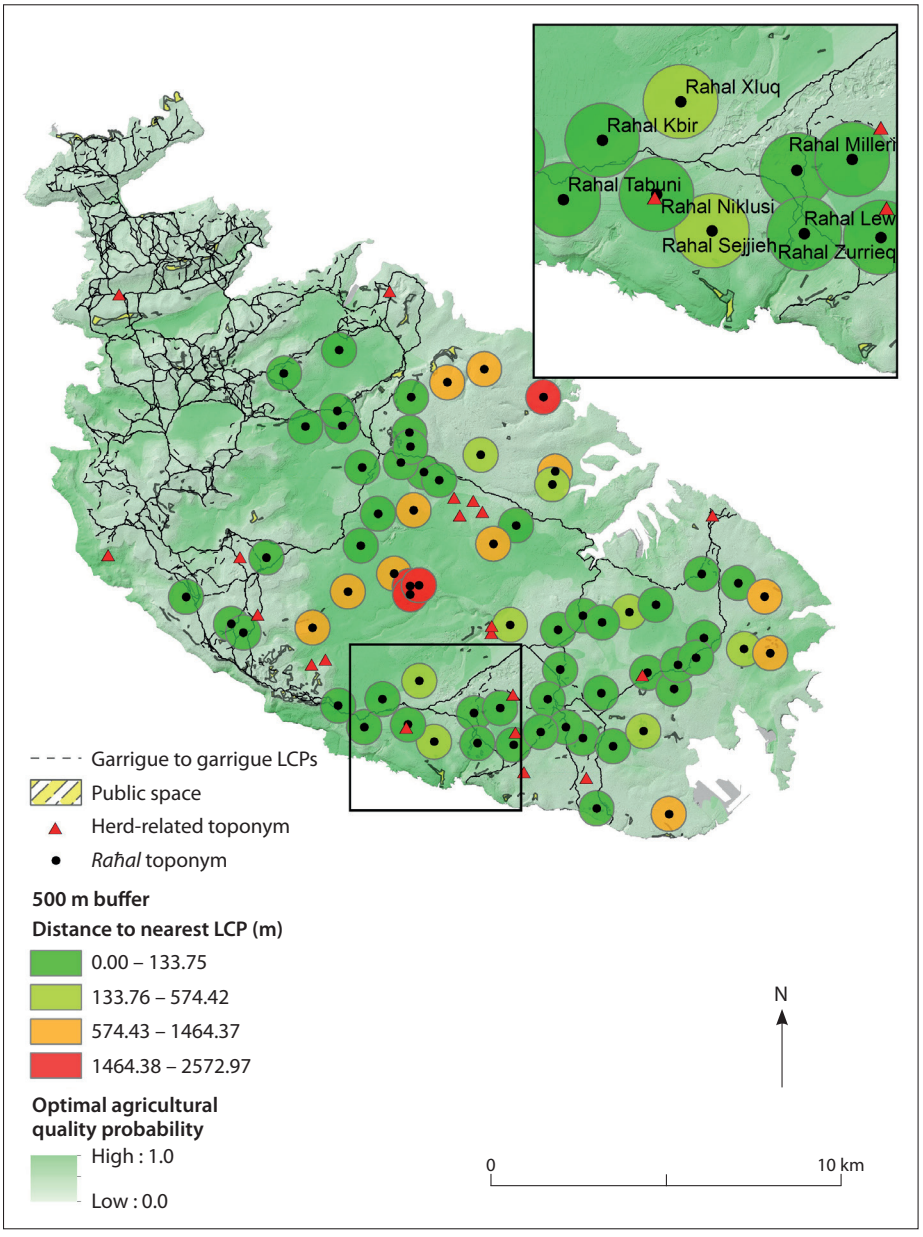

Figure 9.10. *Approximate location of the (mostly disappeared)* raħal *toponyms. Circles represent 500 m buffer to account for locational uncertainty. Buffers are given colours reflecting the distance to the nearest GIS-estimated foraging route. Red triangles represent the location of herd-related toponyms (G. Alberti).*

with empirical and ethnographical data. Considering that 50 per cent of the estimated foraging excursion (outbound plus inbound) in Malta fall between 4.94 and 10.77 hours (see §9.3.2), it turns out that these figures are comparable with empirical GPS-derived data gathered in other cultural and geographical contexts. In the Negev (Israel), for instance, the average journey has a duration of 5.5 hours, with a minimum of 4.3 recorded in May and a maximum of 7.7 recorded in March (Arnon *et al.* 2011, 137–8). In northern Oman, foraging excursions last about 9 hours on average (Schlecht *et al.* 2009, 358), while in western Niger it varies across seasons between 7.6 and 10.4 hours (Schlecht *et al.* 2006, 230).

The plausibility of the GIS-based estimates is strengthened by ethnographic data derived from interviews with local shepherds conducted by one of us (NCV) between 2016 and 2018. These relate to practices that go back to the period between the 1950s and 1970s when the informants were young and used to tend flocks with their father or other relatives. One of the informants was the owner of a farmhouse located in western Malta, in the Għar il-Kbir area (Fig. 9.11). The shepherd reported that the main grazing area for his flock consisted of the garrigue zones lying immediately southwest and northwest of the farmhouse, along the escarpment of the Dingli Cliffs and at Il-Bosk, respectively. He also provided information about the duration

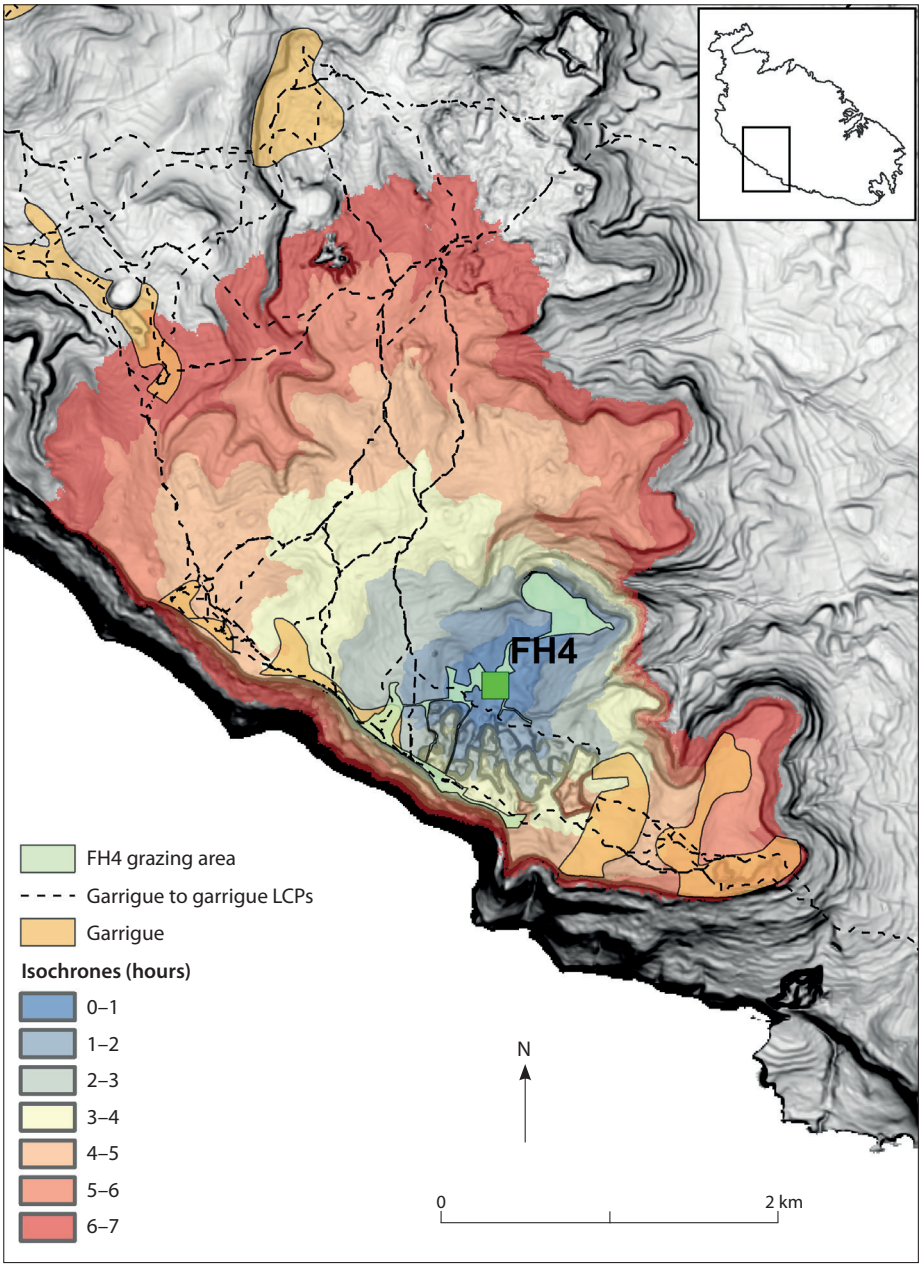

Figure 9.11. *Isochrones around farmhouse 4 representing the space that can be covered at 1-hour intervals considering animal walking speed (grazing while walking; averaging 1.5 km/h on a favourable slope) (G. Alberti).*

of the foraging excursions, which used to be done between 6:00 and 8:30 am in summer (June–October), and between 9 am and 2 pm in winter (November–May). Even though these figures feature seasonal variability, they prove consistent with the estimates deriving from our analysis. The shorter summer duration fits in lower 10 per cent of the estimated journeys, which, as seen, can be performed within 3.18 hours. The longer winter excursions fall between the 1st quartile (4.94) and the median (6.99) of the estimated durations.

The duration of the excursions reported by the informants turns out to be also consistent with the accumulated (animal) walking time surface calculated moving from the farmhouse outwards (Fig. 9.11). The grazing area immediately surrounding the farmhouse at Misraħ Għar il-Kbir lies well within the one-hour walking time buffer. The larger garrigue zones south-west of the farmhouse, lying between the Maddalena Chapel and Ta' Żuta, is reachable within four hours, while the foraging area lying to the northeast at Il-Bosk can be reached within a maximum walk of two hours. In these settings, it is possible to complete the whole journey (outbound and inbound) well within the limits of the time windows reported by the informant, especially during the most time-constrained summer excursions.

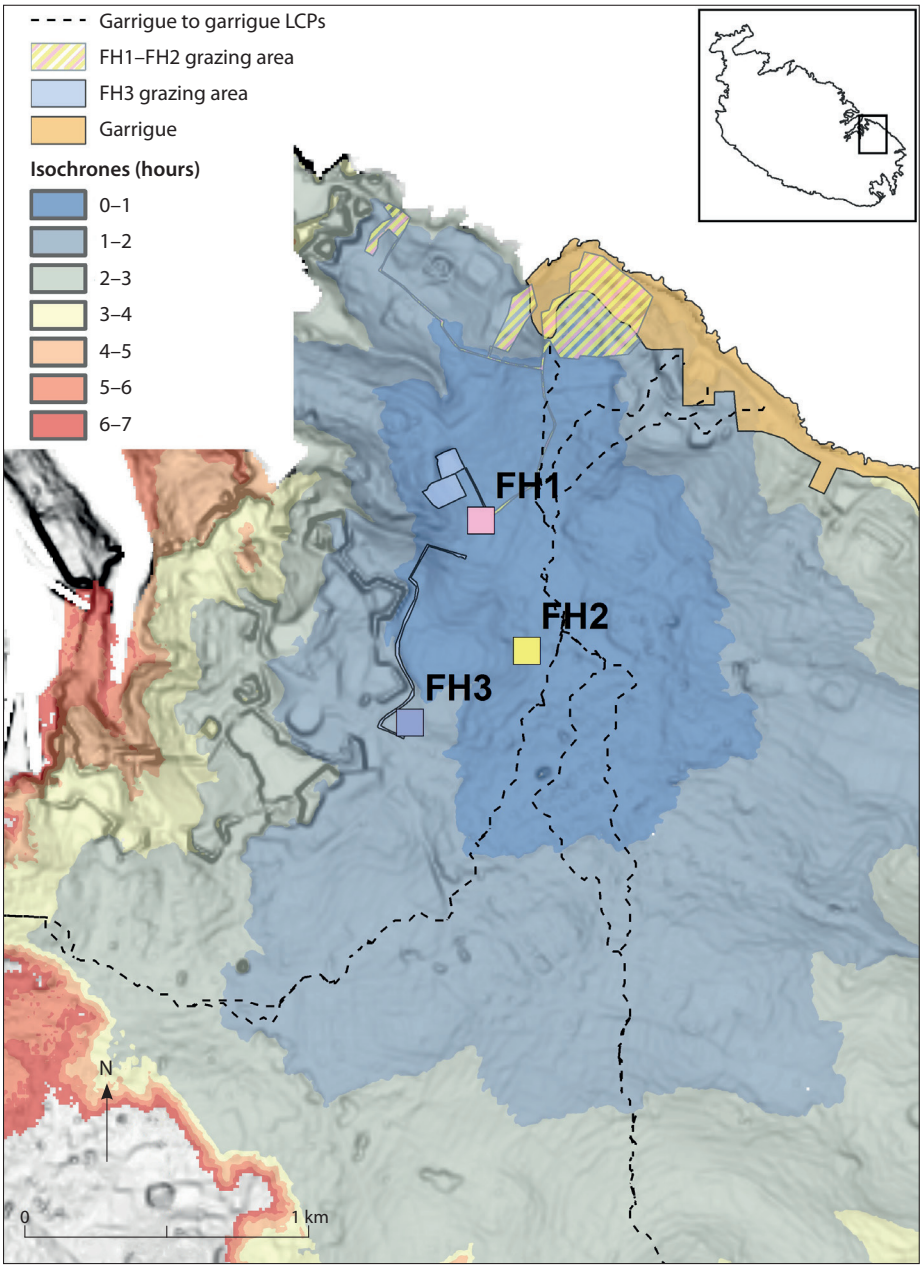

Figure 9.12. *Isochrones around farmhouse 2 representing the space that can be covered at 1-hour intervals considering animal walking speed (grazing while walking) (G. Alberti).*

A similar picture emerges from the ethnographic data relative to three farmhouses located in southeastern Malta, immediately east of Kalkara (Fig. 9.12). One person whose father was a shepherd who kept a flock of about 50 sheep/goats in farmhouse 1 at Il-Wileġ recalled how just like the shepherd from farmhouse 2 (located at the intersection of country roads near Santa Domenica) he used to take the herd to two garrigue areas lying to the north between Rinella and San Rokku, overlooking Il-Kalanka tal-Patrijiet. The farmer from farmhouse 3 (located at Tal-Fata) used to take a herd of cows to two smaller rocky areas, immediately northeast of farmhouse 1. Besides further confirming the use of garrigue areas as grazing land, and besides indicating that the choice of the grazing area is not always dictated by geographic proximity, these cases prove consistent with the GIS-based estimates. The grazing areas used by the herds kept in farmhouses 1 and 2 can be reached in a walking time between one and two hours from both locations, with just the northeasternmost fringe of the larger garrigue area lying outside the two-hour limit. The same holds true for farmhouse 3, whose grazing area lies in the middle of the two-hour walking time buffer. They prove therefore suitable, time-wise, for grazing excursions similar to those reported by the owner of the farmhouse in western Malta.

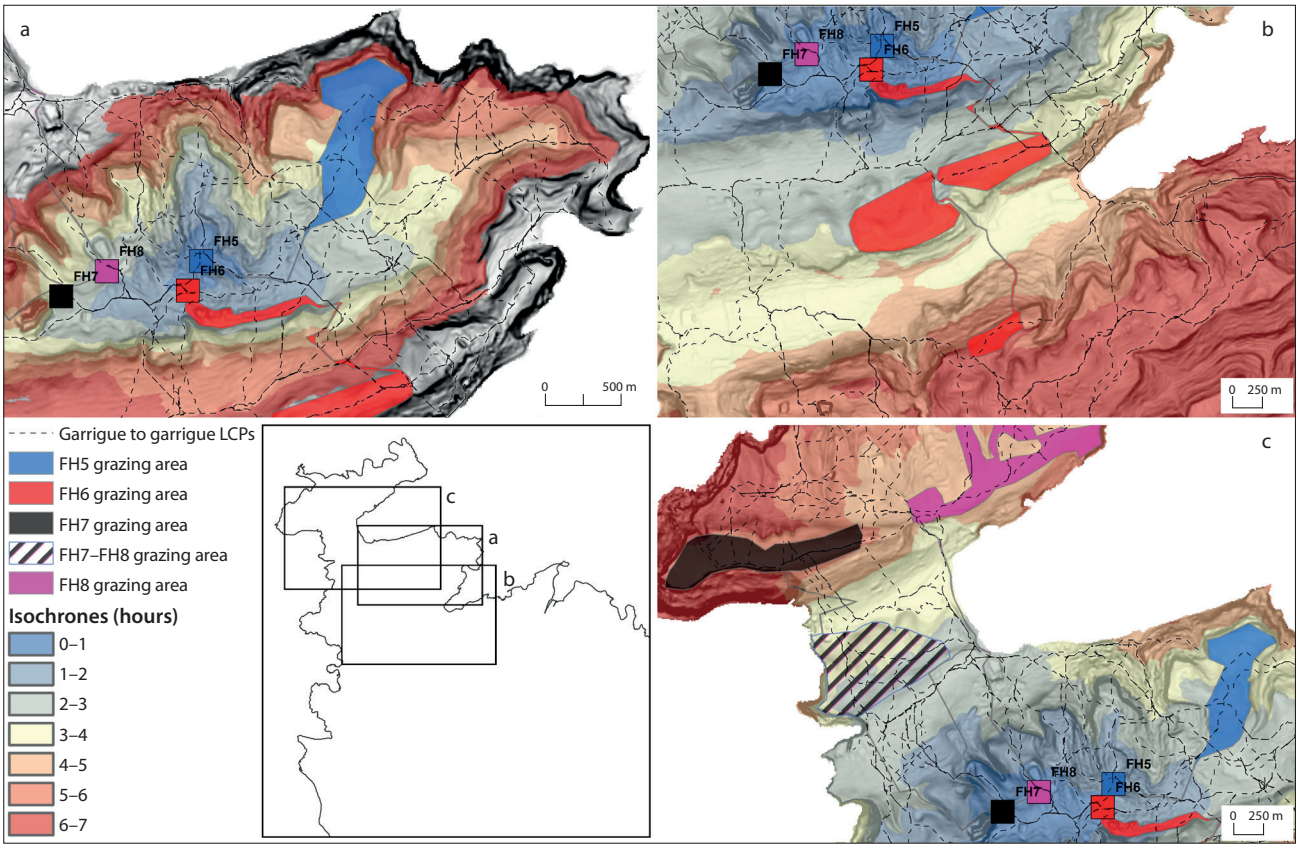

Figure 9.13. *a) Isochrones around farmhouse 5 representing the space that can be covered at 1-hour intervals considering animal walking speed (grazing while walking); b) Isochrones around farmhouse 6; unlike Figs. 9.11, 9.12, 9.13a, animal walking speed during directional travels is considered (averaging 3.6 km/h on a favourable slope); c) Isochrones (considering directional travel's speed) around farmhouse 7 (G. Alberti).*

Data derived from interviews of shepherds in northern Malta present a slightly different picture. One out of four informants (farmhouse 5) used to take flocks to a garrigue area that lies not too far (both time- and distance-wise) to the northwest (Fig. 9.13a). About half of the garrigue area can be reached within four hours, with only the northernmost sector requiring six hours to reach. Considering the animal average walking speed while grazing, the garrigue areas used by the other three informants lie at a larger time distance. Yet, if we keep in mind that both literature (Arnon *et al.* 2011; Schlecht *et al.* 2006, 2009) and ethnography indicate that shepherds may opt for faster directional long-distance travels (featuring an average speed of about 3.6 km/h) (Arnon *et al.* 2011, 140), the data regarding those three cases prove not too different from farmhouse 5 and, all in all, consistent with our GIS-based estimates. The large grazing area south of farmhouse 6 at Mellieħa (Fig. 9.13B), in the areas of Ix-Xagħra tal-Ħawlija and Ix-Xagħra tal-Għansar/ Xagħra tad-Dar il-Bajda, can be reached within three and four hours of fast directional walk down walled droveways, while the smaller one further south at Il-Qala (near San Martin) can be reached within six hours, again along walled tracks. The owner of the sheep/goat fold (Maltese: ċikken) marked as farmhouse 7 reported the use of a grazing area lying to the north at Il-Biskra (Fig. 9.13c).[3] It can be reached within three and four hours along a track and a minor road, while the other one in use further north at Id-Dahar is reachable within six hours along minor roads. The shepherd from another sheep/goat fold (ċikken) marked as farmhouse 8 (Fig. 9.13c) reports the use of the grazing area at Il-Biskra common to the preceding farmhouse, which can be reached within a 4-hour walk. The same farmhouse uses another grazing area further north at L-Aħrax (Fig. 9.13c), whose southern half (namely, the one for which the evidence of its use as pasture is more certain) can be reached within five hours.

It is worth noting that the reported duration of the foraging excursions in this area turns out to be generally longer compared with the evidence from

southern Malta, with a time inflation that is reasonably related to the larger distances to be covered between the farmhouses and the garrigue areas. The excursions span from about eight hours in winter (8 am to 4 pm) to about 13 hours overall during summer (4–9 am, 4–12 pm). In spite of larger distances to be covered, the very possibility to opt for a faster directional route, using a road network that is related to post-AD 1850s agricultural improvement in the area, enables the shepherds to meet the time limits imposed by the season during which the excursions take place.[4] In these settings, the estimated walking time buffers prove compatible with the reported durations. Garrigue areas reachable within three, four, five, or even six (in the most extreme case) hours of directional travel turn out to be suitable for excursions whose duration may last from a minimum of five to a maximum of eight hours. The reported durations are also compatible with the duration of the foraging excursions estimated from our sample of farmhouse locations. Foraging excursions lasting five and eight hours fall within the middle 50 per cent of the distribution of the estimated journeys, which ranges between 4.94 and 10.77 hours.

9.5. Conclusions

The present study has drawn together and presented archival, archaeological, ethnographic and oral evidence of traditional pastoral foraging routes and practices in a small Mediterranean island setting. Informed by ethnographic work elsewhere, and by earlier work on the highly variable affordances presented by the early modern landscape, least-cost path modelling and post-dictive evaluations have been developed to elucidate the spatial-temporal dynamics that dictated pastoral routes and practices in Malta. Using GIS-based weighted cost-surface analysis, the successive iterations of the argument have examined the relationship between farmsteads where herds were penned, the public open spaces where garrigue was available, and the network of droveways that connected them together, and which may trace their origins at least as far back as the late Medieval period. It has been demonstrated that their distribution and inter-relationships is consistent with strategies to optimize the exploitation, through pastoral foraging, of land that was less optimal for agriculture. The portrait that emerges is one of intensive exploitation of the landscape through a mixture of strategies, each adapted to the highly variable affordances presented by different environments. It has also been demonstrated that the relationship between these different strategies, most notably between crop cultivation and pastoralism, was very carefully managed and regulated. The network of droveways that controlled and facilitated the movement of flocks across the landscape was integral to the sustainable co-existence of these activities, and an essential component of subsistence strategies in a fragile and frugal small island environment.

Notes

1 A comprehensive diachronic study of Malta's 'public spaces' or commons has still to be undertaken. In the Late Middle Ages, public spaces often consisted of precious grazing grounds for sheep and goats, unhindered access to which was considered a right to be upheld (Wettinger 1982). In the early modern period this practice continued, as it most certainly did in the British period, but the granting of parcels of rocky ground (xagħri) for cultivation by reclamation from the late sixteenth century onwards (Blouet 1967; Chircop 1993, 30–2) must have reduced the area for rough grazing considerably and probably made the need of walled paths/tracks or droveways for safe passage of flocks from one grazing ground to another more acutely felt. The process of enclosure through the erection of rubble walls and fields connected by paths, tracks that can act as droveways recalls the situation in the limestone uplands of south-east Sicily, a process which got underway in the mid-nineteenth century (see Giorgianni 1990). The analogy warrants further study.

2 Grazing on stubble following the harvest or in fallow fields was confirmed by the informant of farmhouse 1 from Kalkara who recalled descending with his father into the terraced fields in the valley between Rinella battery and the area taken up by the industrial estate of Kalkara (now Smartcity). Informants from Qala (Gozo) confirmed the existence of the same practice. Unless the fields belonged to the shepherd, the rights to allow animals to graze was obtained from the owner, often against payment, a practice which has a deeper ancestry (see Catania 2015, 120–4).

3 A ċikken consisted of an open-air enclosure built in rubble where animals pertaining to small owners of sheep and goats were bred. The surface was rocky and slanting to ensure easy removal of animal liquid waste. Cane and reeds were used to roof certain areas of the enclosure to provide animals with shelter from the summer sun. No formal lodging quarters for the shepherd existed. The Mellieħa examples are here denoted farmhouses 5, 7 and 8.

4 The rectilinear pattern of roads and tracks is related to the project of agricultural improvement in this part of Malta undertaken in the British period and the local agricultural society in the second half of the nineteenth century (Società Economica Agraria) (see Hunt & Vella 2004/5, 63 & note 18).

Chapter 10

Settlement evolution in Malta from the Late Middle Ages to the early twentieth century and its impact on domestic space

George A. Said-Zammit

This study analyses settlement development in the Maltese Islands between the late Medieval period and the early twentieth century and the impact this had on the evolution of native houses. It examines the main causes which led to the rise, development or desertion of villages and hamlets through time and how different political, economic and social situations have influenced the way people (natives and foreigners) lived within their abodes and settlements. For the purposes of this study the houses referred to in this chapter range from simple rural dwellings, including cave-dwellings, to more elaborate *palazzi* which usually dominate the town or village centres.

10.1. The Medieval Period (AD 870–1530)

The earliest historical evidence that refers to local settlements is Al-Himyari's account, which narrates how the Arabs conquered and depopulated the Maltese Islands, razed a fortress to the ground and built a *madina* in the early eleventh century. Al-Himyari gives no further information about other settlements. That this Islamic *madina* is synonymous with the medieval town of Mdina is confirmed by its toponym (the Arabic term *madina* means a town) and by the archaeological evidence (Dalli 2006, 44).

A planimetric analysis of present-day Mdina suggests that this still retains some of its Islamic urban past, particularly its narrow and maze-like streets. This reminds us of the North African *madinas* like Mahdia and Sousse in Tunisia (Buhagiar 1991, 16). On the basis of other North African *madinas*, and considering Malta's typically hot and arid climate, especially in summer, it can be assumed that its streets were purposely planned to ensure favourable climatic conditions. They were probably also intended to prevent easy movement and ensure privacy (De Lucca 1995, 34ff).

Another common characteristic of these *madinas* is their defensive walls. Although no Muslim phase buildings have survived, Mdina's particular streetscape leads us to deduce that it probably resembled a typical Arab fortified citadel. A long winding spine road possibly led to the town's main public buildings, for example the Friday mosque.

Just outside the Mdina walls, Rabat developed into a thriving suburb occupied by a community of artisans, labourers and peasants. Apparently Rabat emulated Mdina's streetscape, since its centre also consists of a network of narrow, winding streets and *culs-de-sac*.

Another urban settlement developed in central Gozo where the medieval Castello stands today. The Citadel's streetscape resembles that of Mdina, implying that this possibly followed similar Islamic town planning concepts. Its strategically central position, like Mdina, made it an ideal place from where any potential enemy incursion could be detected. Outside its walls a small suburb, also known as Rabat, soon developed (Dalli 2006, 310).

In the heart of the Grand Harbour a maritime settlement, Birgu, developed close to the thirteenth century *Castrum Maris*. There is no historical evidence when this castle, which was the only defensive system in this harbour at the time and served as a shelter for the nearby Birgu, was built, however indications show that it could have already existed since the twelfth century.

Outside the urban and suburban settlements, the rest of the native community settled in rural hamlets to cultivate the land and rear their animals. The earliest documented references to open settlements date back to the late fourteenth century, although there are archaeological indications that certain rural areas could have already been settled even before (Wettinger 1975). However, the available archaeological and historical data are certainly not enough to determine the possible type, layout and extent of any rural settlements that could have existed locally in early Medieval Malta. Apart from the open villages, there were also cave-dwellings spread in different areas.

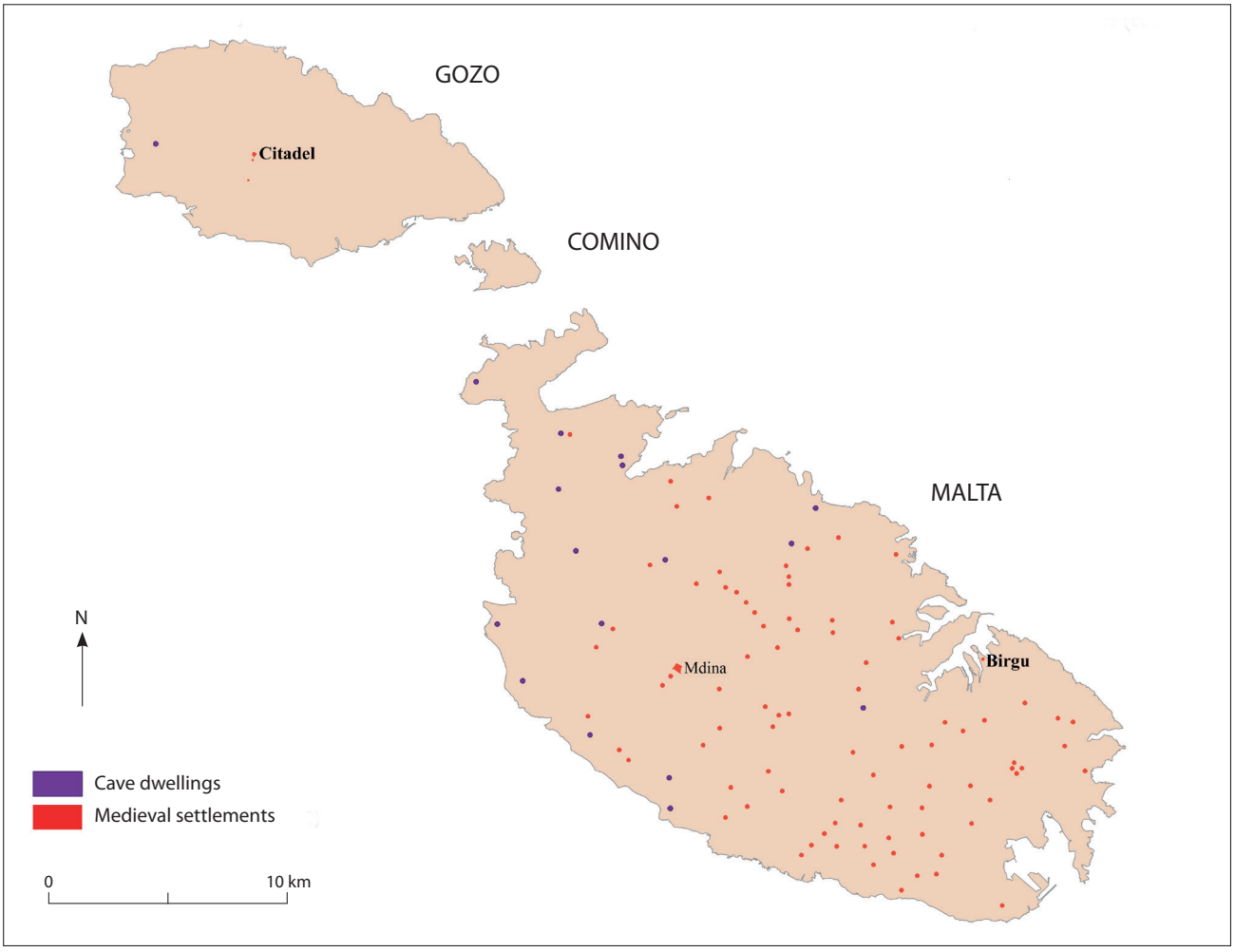

Figure 10.1. *The likely distribution of built-up and cave-dwellings in the second half of the fourteenth century (G.A. Said-Zammit).*

Figure 10.1 shows the likely distribution of built-up and cave-dwellings in the second half of the fourteenth century; the list is much longer, but several of these settlements could not be located on this map since the available records do not provide any clear indication regarding their location. Here one can observe a centrally located urban centre in Malta, another one in Gozo, with the rural settlements scattered in different areas. Birgu was the only maritime urban centre, hence Malta's only point of contact with the outside world. For many centuries Gozo's population remained concentrated in the Castello and its suburb, because this island was often exposed to sudden enemy attacks. This possibly also meant that, as happened in Malta, many of Gozo's urban peasants cultivated their lands or reared their animals close to these settlements, where they had the shortest distance possible (based on a normal walking distance of 5 km per hour) (see Chapter 9). Those who had to walk over longer distances to reach their fields possibly constituted a smaller group as this was seemingly less practical. In Malta the situation appears to have been different since there was a dispersion of settlements, which meant that the peasants probably tried to establish their settlements where the land was suitable for farming and grazing and where they could reach their lands in the shortest time possible (Fiorini 1993, 143).

A number of settlements had disappeared by AD 1419, particularly those located close to the coast or the harbours (Wettinger 1975, 192). Blouet (1978, 374) contends that, apart from the perennial problem of sudden enemy attacks on the island, another reason which led to settlement desertion was the shift from a subsistence based economy to one dominated by the cultivation of cash crops. This phenomenon became

more evident by the first half of the fifteenth century when there seems to have been an attempt for less settlement dispersion, as Figure 10.2 demonstrates. For example, by AD 1420 no record of open villages is registered in northern Malta, while those located in the Grand Harbour area, except for Birgu, had likewise disappeared. Western and southeastern Malta experienced a similar situation, although it was comparatively more evident in the latter. There could have been three main reasons why fewer settlements were abandoned in western Malta:

a) the land is suitable for agriculture and there are many springs of perennial water;
b) its southern shoreline is marked by cliff systems that hinders easy access to the enemy;
c) Mdina was within easy walking distance from all parts of this district.

Southeastern Malta, with its flat plain and sheltered harbours and inlets, was potentially more prone to enemy attacks. Hence, this could have been one of the reasons why here several hamlets were also deserted. In Gozo, the population remained concentrated only in the Citadel and its suburb.

The historical evidence shows that while certain hamlets were abandoned, others became more populated and eventually achieved parish status. This meant that by the first half of the fifteenth century there was already a certain degree of hierarchical organization of settlements, at least on a parochial basis, since parishes usually had a number of minor hamlets under their care (Blouet 1993, 42).

Figure 10.3 shows the distribution of settlements just before AD 1530. Here we observe a further shift towards more nucleation. While between AD 1420 and 1530 more villages and hamlets continued to

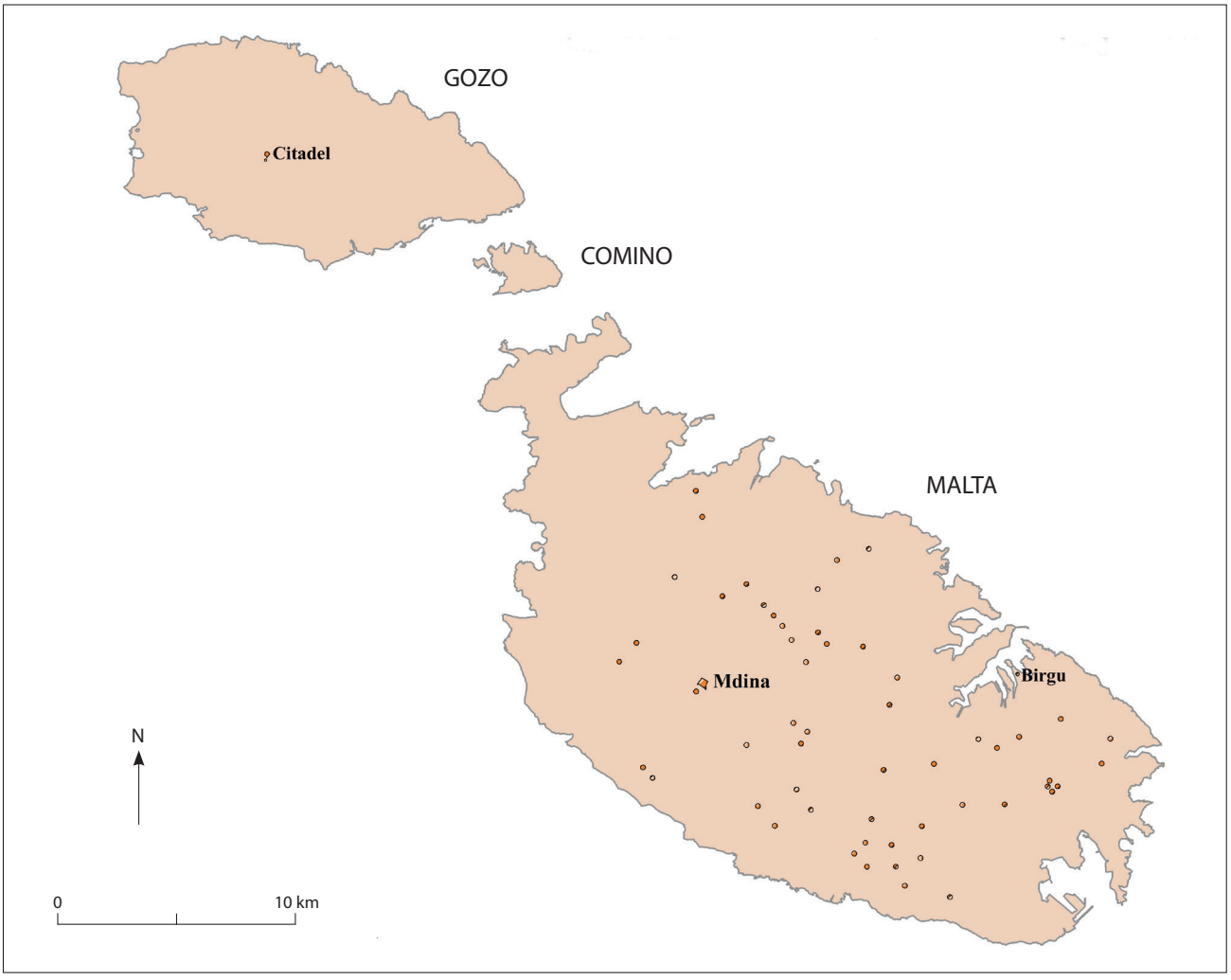

Figure 10.2. *The lower frequency of settlement distribution by* c. AD *1420 (G.A. Said-Zammit).*

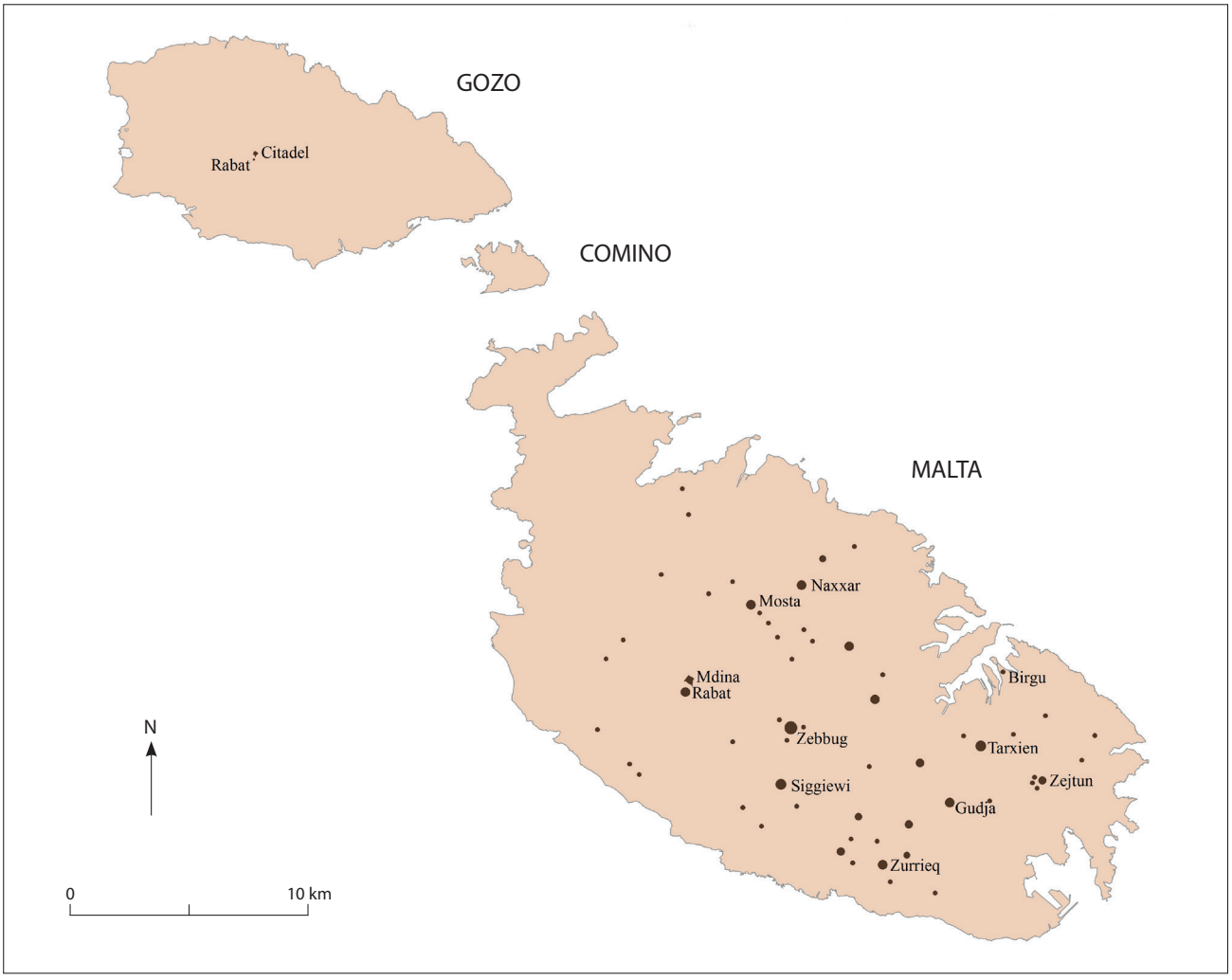

Figure 10.3. *The distribution of settlements just before* AD *1530 (G.A. Said-Zammit).*

be deserted, particularly those in coastal or harbour areas, others situated more inland increased in terms of population size. This map also indicates that some of the major settlements that prospered during the fifteenth and early sixteenth centuries developed to an extent that some of the hamlets nearby eventually were incorporated into the territorial limits of the major villages to form a single settlement. Mdina and the *Castrum Maris* and the shelter they provided may have been one of the reasons that permitted the inland settlements to flourish. In Gozo the Citadel and its suburb remained the only built-up settlement on that island.

The desertion of a number of hamlets and the concomitant expansion of inland settlements, with their development into proto-industrial centres, coincided with the general rise in population that these islands experienced from the early fifteenth century onwards. Apart from episodes of enemy attacks, this pattern also seems to suggest the gradual transmigration of the peasant population from the hamlets to the proto-industrial inland settlements, similar to what occurred in contemporary Europe (Epstein 2002).

10.1.1. Medieval houses

The economic development that occurred locally during this period, together with the external political influences from different parts of Europe, namely the Arabs, the Normans and the Spanish, led to the rise of a rigidly segmented medieval society ranging from the nobility and the Church at the top to the peasantry, the destitute and the slaves at the bottom. This affected not only where the local inhabitants lived, but also the kind of dwellings they possessed (Said-Zammit 2016, 22ff).

The earliest historical records, datable to the second half of the fifteenth century, consistently refer

to houses with a central courtyard, giving the impression that this was the most common house layout in the urban and rural settlements (Said-Zammit 2016). Notarial contracts refer to single-floor and two-storey urban and rural houses. The fact that in these records the former occur more frequently than the latter suggests that single-storey dwellings were more common and two-storey ones were possibly a later development. This observation concurs with Aalen's (1984) model for Greece, and that, in Malta, two-storey houses presumably evolved from single-storey dwellings. This is further proved by the presence of certain late medieval *palazzi*; Falson Palace in Mdina and Stagno Palace in Qormi, for instance, both show that originally these were single-storey houses with their upper floors as a later addition (Fig. 10.4).

Elite urban houses are referred to as *hospicium domorum* (a townhouse), while rural or urban poor dwellings are generally described as *domus* (a house) or *casalinum* (a small house) (Said-Zammit 2016). Certain records also refer to the *cortile domorum*, a house which formed part of a group of tenements with a shared central courtyard and a common entrance. The notarial records sometimes also refer to particular rooms of the house, for example the kitchen or the millroom. The cistern, usually located in the courtyard, seems to have been a staple feature in townhouses, farmhouses as well as in lower class urban and rural dwellings. Access to these houses from the outside was reached either through a door or an arched passageway (*siqifa*) which led to the central courtyard. It was also noted that these records do not refer to the specific use of the upper floor rooms, indicating that these could have been multi-functional spaces.

The façades of these houses, except for the Mdina *palazzi*, generally lacked any architectural decoration, while apertures were kept to a minimum (Said-Zammit 2016). The perimeter walls of the central courtyard were usually high for security reasons and to ensure privacy. Thus, the façades were usually simple, austere and asymmetical.

10.1.2. Giren and hovels

Although the courtyard house is mentioned in a number of records and its layout occurred in the urban and rural context, Quintin (1536, B2) refers to another type

Figure 10.4. *The late medieval Falson Palace in Mdina (G.A. Said-Zammit).*

of rural dwelling, which was probably smaller in size and simpler in form. He describes these dwellings as '*Africana magalia*' (African hovels). The author provides no further details and such an ambiguous description can lead to various interpretations. For instance, it is possible that this is simply a generic statement, intended as a broad reference to the rural farmhouses he noted in different hamlets, which were more or less of the same kind. However, this description could indicate that Quintin (1536) saw something far less elaborate than the mature farmhouse (*razzett*). For example, he could have been referring to the native *girna* (corbelled stone hut), which commonly occurs in northwestern and western Malta.

The *giren* have a roughly circular plan, with their diameter and height varying from one structure to the other. The *girna* generally has a single entrance and a small window to permit light and air circulation. *Giren* occur as single units or in clusters and often include features like tie-loops, sheds, mangers and recesses. Clusters of *giren* were usually surrounded by a dry wall precinct (Fig. 10.5).

These native corbelled hovels are usually associated with the storage of crops or with the sheltering of animals. However, it is possible that these could have also been places of human habitation. Such hypothesis is based on the following evidence:

a) a number of *giren* are substantially high so that a person can easily stand in an upright position;
b) lamp-holes are another indication that certain *giren* were used for human habitation when it was dark;
c) some *giren* are characterized by recesses which were probably utilized for the storage of personal items;
d) certain *giren* were complemented by a rock-cut water cistern;
e) there is historical evidence that until the twentieth century some *giren* still served as a place of permanent human habitation (Fsadni 1992).

Figure 10.5. *A* girna *integral with and surrounded by dry stone walling (G.A. Said-Zammit).*

Figure 10.6. *A hovel dwelling with a flight of rock-cut steps (G.A. Said-Zammit).*

The fact that *giren* clusters are characterized by features which are typically found in the farmhouse and associated with human or animal habitation, has led scholars to believe that these could have been dwellings where animals and humans lived within the same complex (Buhagiar 1991; Vella 2010). Scholars also contend that these could have possibly been the most primitive exemplars of the proto-*razzett* which eventually, presumably in late medieval times, paved the way for the evolution of the single-storey farmhouse (Jaccarini 2002, 6). However, our evidence does not exclude the possibility that during this period these *giren* and the earliest single-storey farmhouses could have existed concomitantly.

None of the native *giren* were ever discovered within an archaeological context, therefore it is difficult to determine their precise age. Although there seems to have been a strong tradition of *giren* building during the nineteenth century (Vella 2010), the evidence suggests that this could have been a much more primitive structure, possibly dating back to late medieval times. A sixteenth century notarial contract refers to a certain tenement called Corna hiren, in the limits of Għarb, Gozo (*Acts* Ferdinando Ciappara 9-vi-1578, R185/4 f. 577v). An etymological analysis of this place-name led Zammit to suggest that this could have been a corruption of the toponym *il-girna ta' Ħerrin* (literally meaning the *girna* of Herrin) (M. Zammit, pers. comm.). This hypothesis casts new light on the corbelled stone hut:

a) *giren* were already in existence in the sixteenth century, which suggests that these could have possibly been late medieval structures, and
b) they were also present in certain parts of Gozo.

Therefore, on the basis of this hypothesis, it is possible that the *giren* could have been synonymous with the 'African' huts mentioned by Quintin (1536).

That simple hovels existed in late medieval times is confirmed by several toponyms which include the words *gorboġ*, *għarix* and *newwiela*, all of which mean a hut or a hovel (Vella 2010, 214ff). These names could have been an alternative to the term *girna* or they could have simply referred to a different type of structure. For instance, these place-names and/or Quintin's description could have been a reference to a particular type of

rectangular dry rubble huts, examples of which have survived in certain localities like Baħrija and Mellieħa. The layout and building techniques of these structures suggest a late medieval date. The Baħrija example, characterized by a masonry exterior and a rock-cut interior, consists of two contiguous spaces, one of which was possibly the animals' quarters and the other served for human habitation, the latter being evidenced by the presence of certain features like lampholes and rock-cut recesses. Access to this particular dwelling was through a flight of rock-cut steps (Fig. 10.6).

10.1.3. Cave-dwellings

Cave-dwellings were also common, particularly in northern and western Malta (Buhagiar 2002, 2012). Elaborate cave-dwellings were usually divided into a number of compartments, usually separated by dry stone walls. Occasionally they were also preceded by an open-air terrace which, apart from serving as a common space, provided access to the different compartments of the complex (Saliba *et al*. 2002).

10.1.4. Architectural development

The present evidence allows us to formulate a hypothetical reconstruction of the main phases of architectural development in late medieval Malta. From our investigations the following observations have emerged:

a) troglodytism was a common phenomenon;
b) in the open villages the central courtyard farmhouse seems to have been the most elaborate type of rural dwelling. Farmhouses were single- or two-storey buildings. Single-storey dwellings were seemingly less complex than two-storey houses. There were also *giren* and hovels, the latter being masonry built or hybrid (partly rock-cut and partly built);
c) in the urban settlements, the central courtyard house layout is documented since the late thirteenth century. Some of them consisted of a single storey, while others were two-storey. The evidence shows that the latter were presumably chronologically later than the former. Poorer dwellings, also with a central courtyard, were usually small, consisted of a single floor and generally characterized by poor quality masonry.

The evidence presented above suggests that, while in the medieval urban settlements the courtyard house was the basic house type, in the countryside the peasants lived in three categories of dwellings: the central courtyard farmhouse, cave-dwellings or hovels. On the basis of the present data it is not possible to ascertain whether these types of houses existed concomitantly or in a chronological sequence, as certain scholars suggest (Jaccarini 2002). However, indications show that, at some point in time, these three types of dwellings existed concurrently, with the *giren*, hovels and farmhouses, therefore being the earliest examples of dwellings in the open settlements.

When there was in Malta a shift from dispersion to nucleation of settlements from the fifteenth century onwards, many hamlets were abandoned. Their inhabitants settled in inland villages, which eventually grew in population. At the same time the amount of hovels and troglodyte dwellings apparently dwindled, while the number of central courtyard *rziezet* or village houses increased, as the late medieval notarial records tend to suggest.

On the basis of Aalen's hypothesis, one can assume that the native two-storey farmhouses evolved from the simpler one-storey *razzett* and were an emulation of late medieval urban dwellings. If the native two-storey *razzett* is an emulation of the late medieval *palazzi*, this major step forward in the architectural development of the farmhouse could possibly have occurred during the late fifteenth or early sixteenth centuries. The historical evidence suggesting such date for the development of this rural dwelling stems from the fact that a number of late medieval houses in Mdina had their second floor added in the fifteenth century. It was also from the late fifteenth/early sixteenth centuries onwards that two-storey farmhouses start featuring more in the local notarial records.

Incidentally, this development occurred at a time when these islands still experienced the effects of defeudalization, which brought about the liberalization of the land market and more peasants, at least the wealthier ones, had more access for land possession (Said-Zammit 2016, 27ff). It was also a time when there was a shift in the local economy from subsistence to one based more on cash-cropping. Therefore, this demonstrates that the social and economic changes of this period had an indelible effect on the type of houses that developed in Malta's rural areas, which possibly suggests that by the late medieval period the local peasants were living in houses which reflected their social and economic background, as happened in other parts of medieval Europe (Catling 2013). Those living in the cave houses, *giren* and hovels were possibly the poorer un-landed peasants, while those dwelling in the farmhouses enjoyed a better standard of living (these were possibly the free landed peasants). Those living in two-storey *rziezet* could have been the wealthiest and represented a community of late medieval rural elite.

In the urban centres, the inhabitants lived in central courtyard houses. The poorest inhabitants generally lived in small dwellings or occupied tenements

with a common central courtyard. Even the elite who lived in *palazzi* or sumptuous dwellings had buildings with a central courtyard. Therefore, the central courtyard appears to have been one of the most basic features of the local late medieval urban houses. The addition of a second floor to a number of urban houses from the fifteenth century onwards suggests a shift towards more comfortable and spacious dwellings.

Despite the limited archaeological evidence, coupled with incomplete population and parish records for medieval Malta, the surviving structures of this period still reflect the different social classes, from the elite at the top who generally lived in the town centres, to the lower urban classes that lived in smaller dwellings in the periphery of the towns, and then to the peasantry who lived in the villages and hamlets in farmhouses, hovels or cave-dwellings.

10.2. The Knights' Period (AD 1530–1798)

This period comprises two main phases of settlement evolution: the phase between AD 1530 and 1565 (characterized by the reluctance of the Knights of St. John to occupy these islands permanently) and the phase between AD 1566 and 1798 (a time of political and economic stability, with Malta becoming the Order's permanent seat).

10.2.1. The phase AD 1530–1565

Although Charles V of Spain donated the Maltese Islands to the Order of St. John in perpetuity, the Knights still considered the possibility of reconquering Rhodes, which they had lost in AD 1523. Their main concern about Malta and Gozo was the poor state of their fortifications. If these islands were perhaps to become their permanent home, the existing defensive systems had to be heavily restored, while new ones had to be built.

During this period there was also a shift of political power from Mdina to Birgu. The former was located away from the harbour, and therefore could not meet the Order's naval and administrative needs. The establishment of the Order in Birgu, sheltered as it was by the *Castrum Maris*, led this urban settlement to experience a change in its townscape and a sudden rise in population, to become the most important administrative and commercial centre on the island.

The fortifications that the Knights built during this phase because of the increasing threat of an Ottoman invasion had considerable influence on local settlement development. For instance, the Order's decision to settle in Birgu in AD 1530 generated more employment opportunities, a sense of security and more building activity. In addition, behind the walls of Fort St. Michael a new settlement, Senglea, was established after AD 1541. This was the first settlement built by the Knights and which did not follow the traditional streetscape and morphology of the existing local settlements. It was instead characterized by a rectilinear street plan imitating that of other contemporary military European towns (Hughes 1993).

Mdina continued to dominate the villages of western Malta and offer shelter to their inhabitants in times of peril. The northern district remained largely uninhabited. At a time when an Ottoman invasion on the islands seemed imminent, especially in AD 1564 and 1565, Malta experienced the gradual abandonment of several villages.

The Gozo Castello remained the only fortified settlement on that island. Gozo was almost completely depopulated in AD 1551, after it had been raided by a Turkish armada (Blouet 1993, 52).

Thus the pattern that emerges during this phase is characterized by the increasing importance of Birgu and by the decline of Mdina's political control. Birgu's importance was reinforced by the establishment of Senglea. The years close to the Great Siege were marked by the further abandonment of several rural settlements, whose inhabitants sought protection in or immediately near the fortified towns.

10.2.2. The phase AD 1565–1798

This phase witnessed the consolidation of the Knights' occupation of these islands. During this time, when enemy attacks became more sporadic, Malta and Gozo prospered both demographically and economically (Blouet 1993, 102ff). Moreover, the Order financed the building of new defensive systems in different parts of these islands.

In AD 1566 the Order embarked on the building of a new fortified city, Valletta. It was built on Sciberras peninsula between the Grand Harbour and Marsamxett Harbour. By the late sixteenth and early seventeenth centuries Valletta came to symbolize the Order's seat of power and the grandeur of local Baroque architecture (Hughes 1986).

Valletta was built on a strictly rectilinear street plan modelled on other contemporary Renaissance military European towns (Pollak 1991). Its roads are characterized by an uninterrupted straight line of vision, with the buildings and houses being spread across different *insulae*. Although building regulations were strict, as happened elsewhere in contemporary European cities (Polak 1991, 18–25), the sharp rise in population, particularly during this phase, led to a higher demand in accommodation. The area originally earmarked for the galley port and arsenal, a project eventually abandoned, soon developed into

the Manderaggio, a slum area occupied by the poorest inhabitants (Borg 2003, 31ff). Other slum areas developed along the outskirts of Valletta, however these did not affect the original streetscape of its central quarters.

When the demographic situation in Valletta and the Three Cities was no longer sustainable the Order tried to mitigate the situation by encouraging lower class families to settle in other areas of these islands, including Gozo after this remained largely depopulated after AD 1551.

In terms of settlement evolution, the building of Valletta certainly left an indelible mark which affected the Grand Harbour area until the first half of the twentieth century. Valletta and the various employment opportunities it generated led to an intensive urbanization process in the Harbour district, particularly in the areas close to Valletta and Birgu.

During this phase the major rural medieval settlements in Malta, some of which were temporarily depopulated just before the Great Siege, were repopulated and gradually prospered again, albeit all at their own pace. From the late sixteenth century, and particularly during the seventeenth century, thirteen settlements became parishes, indicating that they had a sizeable population and some kind of organizational control over the minor settlements nearby (Blouet 1993, 74ff). These villages are dominated by massive Baroque parish churches, which emulated their urban counterparts. The village parish church was usually situated in an open square (*pjazza*) almost in the centre of the village. Nonetheless the network of labyrinthine roads surrounding the parish church and the side alleys remained one of the major characteristics of the early modern village.

Figure 10.7 shows the distribution of local settlements just after AD 1798. It demonstrates that by this time various hamlets had disappeared or were else incorporated into the territorial limits of the nearby major settlements. Many of these hamlets were deserted probably because of economic reasons, where they had become 'too small to support a tavern, a store, a carpenter or a stone mason' (Blouet 1993, 81). This shift from dispersion to more nucleation of rural settlements, together with the simultaneous migration from the countryside to the urban maritime centres brought about three important phenomena in the settlement evolution:

a) the desertion of hamlets that were no longer economically sustainable;
b) the expansion of the major villages in locations where the surrounding land allowed horizontal spread;
c) the expansion of the maritime urban centres at a relatively fast rate. However, these settlements could not expand horizontally because they were fortified. Consequently, to accommodate more families, houses had to be small in size or partitioned into smaller units, or else consisted of multi-storey dwellings built on narrow plots.

Although the Order built new defence systems in different parts of Malta, most of the inhabitants apparently remained reluctant to occupy the island's coastal areas, except for the Grand Harbour area. The hierarchical organization of settlements that emerged in the previous periods persisted also during this phase. In fact, Figure 10.7 shows a similar pattern, with the addition of Valletta, Floriana and the new towns around Birgu. One can also note that the major rural settlements are all located inland, almost towards the centre of the island.

This map also shows that the coastal areas of southeast Malta remained relatively void of any human habitation, except for the tiny village of Marsaxlokk. It also indicates that from the seventeenth century onwards more hamlets in this area continued to be deserted or to be absorbed by the major villages located inland. One can also observe the almost complete absence of built-up settlements in the northernmost part of the island. In western Malta, the main medieval settlements survived too, but a number of hamlets continued to be deserted.

Although cave-dwellings also declined, historical records indicate that troglodytism still survived in several localities (Buhagiar 2002). Therefore, this demonstrates a change in local land-use during this period, with the settlements becoming less dispersed either because the inhabitants of the rural hamlets went to live in the established larger villages or else migrated to the harbour towns, which both provided more employment opportunities. This transmigration of natives to the maritime towns or to the larger villages led to the desertion of a number of hamlets, and presumably also affected the amount of land that was cultivated locally, and while certain rural areas were no longer cultivated (e.g. in northwestern Malta), others became more extensively cultivated (i.e. in western and central Malta).

This period also witnessed the rise and development of various rural settlements in Gozo, many of which eventually became parishes. The sumptuous parish churches that dominate the centre of the main villages of this island show a similar trend towards a better standard of living among the rural community.

10.2.3. Early modern houses

The context of political and economic development of this period undoubtedly had a direct influence on the

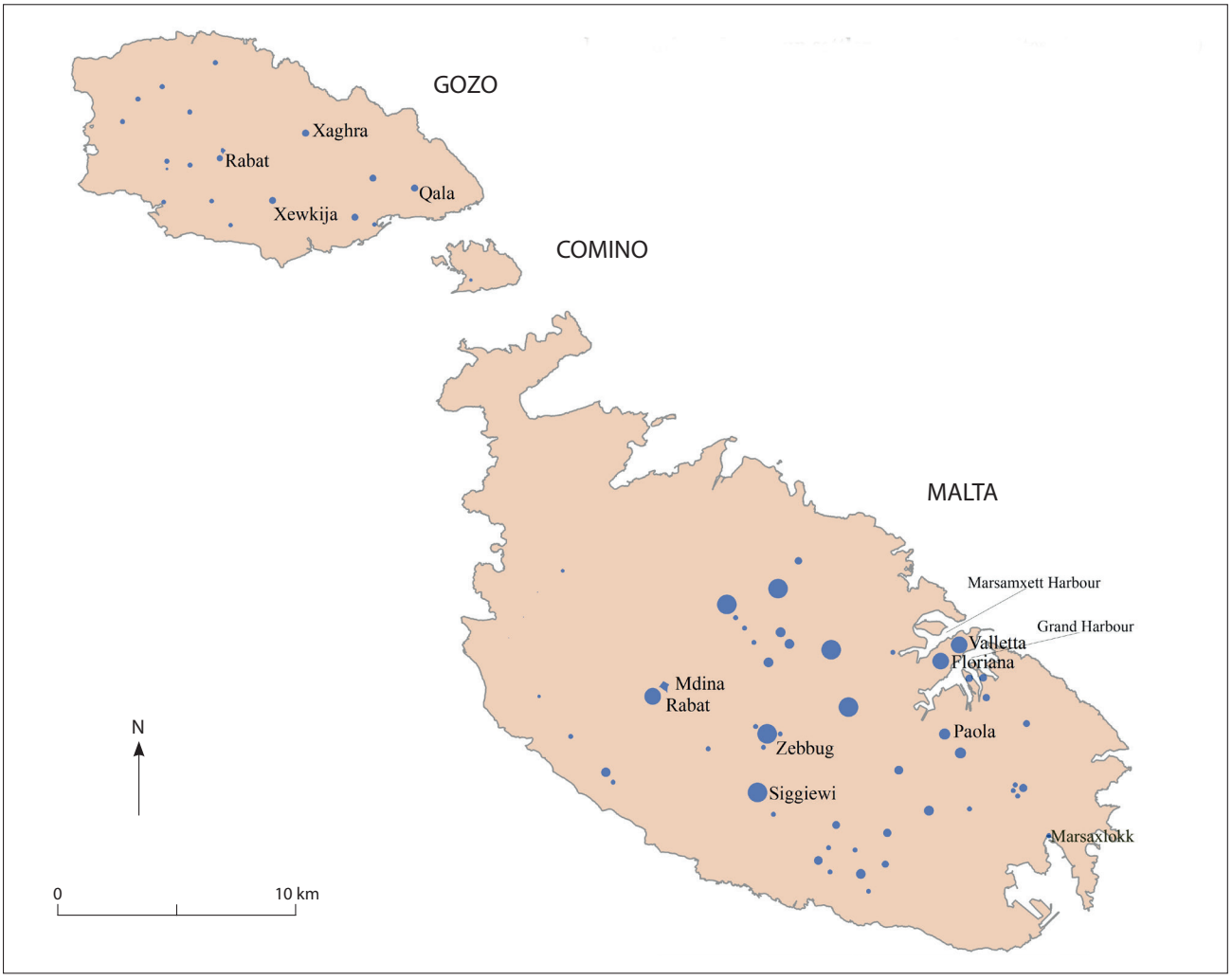

Figure 10.7. *The hierarchical organization of settlements continued, with the addition of Valletta, Floriana and the new towns around Birgu (G.A. Said-Zammit).*

type of dwellings which the local inhabitants occupied in the towns and villages. During this period the evolution of the Maltese houses was not only restricted to the urban centres, but extended to all parts of the islands. This period is characterized by Baroque art and architecture, a style which was popular in the main settlements and in the major villages. With the expansion of the villages from the early seventeenth century onwards, the main dwellings of the village which were occupied by prominent residents or those which served as a country residence of certain noble families, often emulated the Baroque idiom to mirror their urban counterparts.

During this time, both the local architect and local stonemason improved their knowledge and skills. The stonemasons who were involved in the fortification projects or in the building of the Valletta *palazzi* deployed their knowledge and skills to build sumptuous churches and houses that were of a better building quality, even in the villages. This has been particularly observed during the house surveys, which showed a tendency towards improved construction techniques from AD 1650 onwards in the urban and rural settlements.

The townhouse (or townhouse style) façade became more symmetrical, which generated more aesthetic beauty, and was generally dominated at its centre by an open stone or closed timber balcony (Fig. 10.8). Thus, contrary to the medieval *palazzo*, seventeenth and eighteenth century elite houses were characterized by more elaborate and extroverted façades, sometimes also with more than one door that led to the interior. Their façades were often embellished by architectural details, such as reliefs,

Figure 10.8. *An example of a seventeenth century townhouse with open and closed timber balconies (G.A. Said-Zammit).*

columns and coat-of-arms. The use of glass windows and wooden louvered shutters also became commoner.

The courtyard house layout survived and continued to develop through the influence of Baroque art. Examples of early modern courtyard houses can be found in the urban centres, in Gozo, and in a number of villages. Another house layout which became quite popular was the terraced house, its basic plan essentially consisting of a set of rooms with a courtyard at the back (Tonna 1985).

Depending on the area of the building plot and the house layout the ground floor rooms were normally reserved for the kitchen, the *gabinetto* (water closet) and for storage, while those of the *piano nobile* were the occupants' living quarters.

A number of townhouses were extensive enough to include a small mezzanine, which was generally used as living quarters for the domestic staff or else was rented to third parties. The mezzanine, which was usually situated in between the ground floor and the first floor of the house, generally consisted of some rooms characterized by a low ceiling and a window to the outside. Access to the mezzanine was usually through a separate entrance situated near the main door of the house or else via the house through a separate internal doorway.

Within the domestic spaces, the elite dwellings usually had a series of interconnecting spaces. Rooms had the tendency to have more than one access point, so that it was easy to cross from one room to the other in the swiftest time possible. Sometimes, houses had a linear plan layout, thus consisting of a string of rooms (*enfilade*) which gave access to each other forming a straight line. This new concept shows that the courtyard of many elite houses no longer served as a hub which provided access to the other rooms through their separate entrance. This development in domestic space direction and organization reflects the changes that occurred in the configuration of Baroque townhouses and *palazzi* across Europe (Grundmann & Fürst 1998). It also shows the harmonization of the local architect's knowledge and technical skills with what was happening elsewhere on the Continent in architectural planning.

Another important development concerned the staircase. Whereas previously the staircase had been placed in the courtyard, or outside the house, in many early modern townhouses this was relocated to the inside. Hence, access to the upper floor was through a covered staircase. The shift from an open staircase in the courtyard to a covered staircase in a central position of the house is also the result of foreign architectural Baroque influences (Lemerle & Pauwels 2008). A number of *palazzi* and townhouses also had a secondary staircase usually at the rear of the dwelling's spatial network, which connected together all the house floors from the ground floor to the roof. While the grand staircase was usually reserved for the owners, the secondary one was apparently used by the domestic staff, given its particular location near the kitchen and other spaces which, in such houses, were usually associated with domestic servants. The grand staircase was seemingly a symbol of social status, which separated the occupants from their servants (Said-Zammit 2016, 102ff).

The shift from houses with multi-functional domestic spaces to more complex dwellings with additional internal divisions to permit specialized functions, evidently visible in the townhouses and *palazzi*, mirrors the social and economic changes that occurred in early modern Malta and Europe (Johnson 1996). The social change that the market economy of this period generated, especially among the elite and the upper middle class, was reflected in the type of dwellings that they occupied. Their houses were elaborate and elegant in style and internally more complex, with the presence of several private spaces

to separate the owners from the servants as well as to enjoy a lifestyle typical of the urban elite and upper middle class.

10.2.4. Lower class dwellings

The urban centres, despite the strict building regulations, became a place where many lower class families settled in quest of more employment opportunities and a better standard of living. However, with their limited financial resources to acquire comfortable dwellings, poor families had no other option but to live in small dwellings or in cellars (Cassar 2000, 131ff). These houses generally had a limited space and lacked proper ventilation and lighting, particularly when they did not even have a backyard to allow air circulation. They lacked adequate hygienic standards and were often the cause of various health problems and contagious diseases (Mahoney 1996). They were certainly places offering little space and lacking amenities, where the family enjoyed little privacy and where all domestic activities had to be conducted in a restricted space.

This shows that the urban settlements included a combination of different social classes: the elite (the Order, the nobility and the Church), the upper middle class (members of different professions and entrepreneurs), the lower middle class (craftsmen, small business owners and clerical workers), and the lower class (labourers, servants and the destitute).

In the villages and hamlets, the situation was different. In the centre of the major villages a group of rural elite (e.g. the parish priest and the village doctor) lived in houses which often emulated the urban *palazzi*, however on a smaller scale. Many peasant families, with limited disposable income and with a lack of aspiration to change their dwellings according to fashion, continued living in small vernacular houses, often outside the village core which, contrary to the early modern townhouses and *palazzi*, remained similar in style and general layout to those of the late medieval period.

The farmhouses of this period were usually two-storey buildings. The ground floor rooms were generally intended for animal sheltering and storage, while the *għorfa* was the family's living quarters. Others consisted of a single floor, where animals and humans lived together at the same level. A number of rural dwellings also had an underground cellar. On

Figure 10.9. *An example of a two-storey* razzett *belonging to a wealthier peasant family (G.A. Said-Zammit).*

the basis of Aalen's model, it is possible to infer that the single-storey farmhouses possibly belonged to the poorer peasants, while the two-storey *rziezet* belonged to a wealthier group of peasant families (Fig. 10.9). The two-storey farmhouses had become widespread in the Maltese Islands, which demonstrates that a large section of the native peasant community were by now living in dwellings which vertically separated animals from humans.

10.2.5. Cave-dwellings and hovels

Although the number of cave-dwellings had diminished by this period, certain others were still inhabited (Zammit Ciantar 2002). Dry rubble hovels and *giren* experienced a similar fate, with many of them being converted into animal shelter or storage and others ending up completely neglected. This decline in the number of cave-dwellings and hovels demonstrates that rural peasants sought better accommodation and also an improved standard of living either because their economic opportunities increased and/or because their landlords sponsored better housing.

10.2.6. The houses: a reflection of social and economic change

The particular economy that developed during this period, based primarily on different harbour and commercial activities, generated a long phase of urbanization in the Grand Harbour area, with the establishment of new settlements and the expansion of existing ones. By the eighteenth century, about half of the local population was living in one of these urban centres. Houses were acquired according to a person's level of material wealth and social status. The size, the building quality, the architectural style and the dwelling's location were all crucial indicators of class and material wealth.

Outside the urban centres, the villages continued to expand, showing a general trend towards an improved standard of living. The village centre was usually the area where the rural elite lived; it was also here where some of the urban elite established their second residence. The evidence shows that more primitive dwellings declined, while the number of peasant families occupying two-storey farmhouses increased. The emulation of the urban *palazzi* and aspects of town life by the rural elite from the late seventeenth century onwards suggests that, in the proto-urban settlements, village and town life began to merge into each other, narrowing down the cultural barrier that existed between the rural elite and the peasants since late medieval times.

The distinction between the elite houses and lower class dwellings is evident in their exterior and internal organization. While the former were characterized by elaborate Baroque façades, the latter generally adhered to the vernacular idiom, thus having a simpler and an asymmetrical exterior. Regarding the interior, the elite houses became more complex with the addition of separating walls to create spaces with specialized functions. Lower class dwellings had limited domestic space, suggesting that rooms were multifunctional. Apart from class separation, the interior of the elite houses also permitted more individual privacy and gender segregation. For example, it was normal in these dwellings for men and women to sleep in separate bedrooms. In lower class dwellings, however, there was little room for privacy and gender segregation.

10.3. The British Period (AD 1800–1900)

This period constitutes Malta's last phase of foreign colonization. The island's occupation by the British to become a crucial fortress in the Mediterranean, with all the political, economic and social changes that this brought about in the nineteenth century, certainly had a significant impact on local settlement evolution. This phase saw the expansion of already existing settlements and the establishment of new ones in different areas. The main reasons for this settlement development are:

a) a general demographic rise in the Maltese islands;
b) the building of new fortifications in addition to the already existing defensive systems;
c) the prosperous economic activity of the Grand Harbour area;
d) land reclamation incentives for agricultural purposes;
e) an improved road network.

Figure 10.10 shows the distribution of built-up settlements in about AD 1900. The main settlements of northern Malta were the already established in Naxxar and Mosta. However, land reclamation incentives for agricultural purposes led to the re-emergence of Mellieħa, an area with a parish status since the fourteenth century, but which had subsequently been abandoned. A new maritime village, St. Paul's Bay, developed in one of the harbour areas of this district. Some hamlets survived, given their proximity to agriculturally fertile lands. Settlement development in this region, particularly its northernmost part, suggests that this had by now become a safe place for habitation.

The main settlements of western Malta were Rabat, Żebbuġ and Siġġiewi, which remained largely rural. There were some hamlets which were inhabited by different farming communities, for example Mtaħleb and Is-Santi. Towards the eastern part of this district

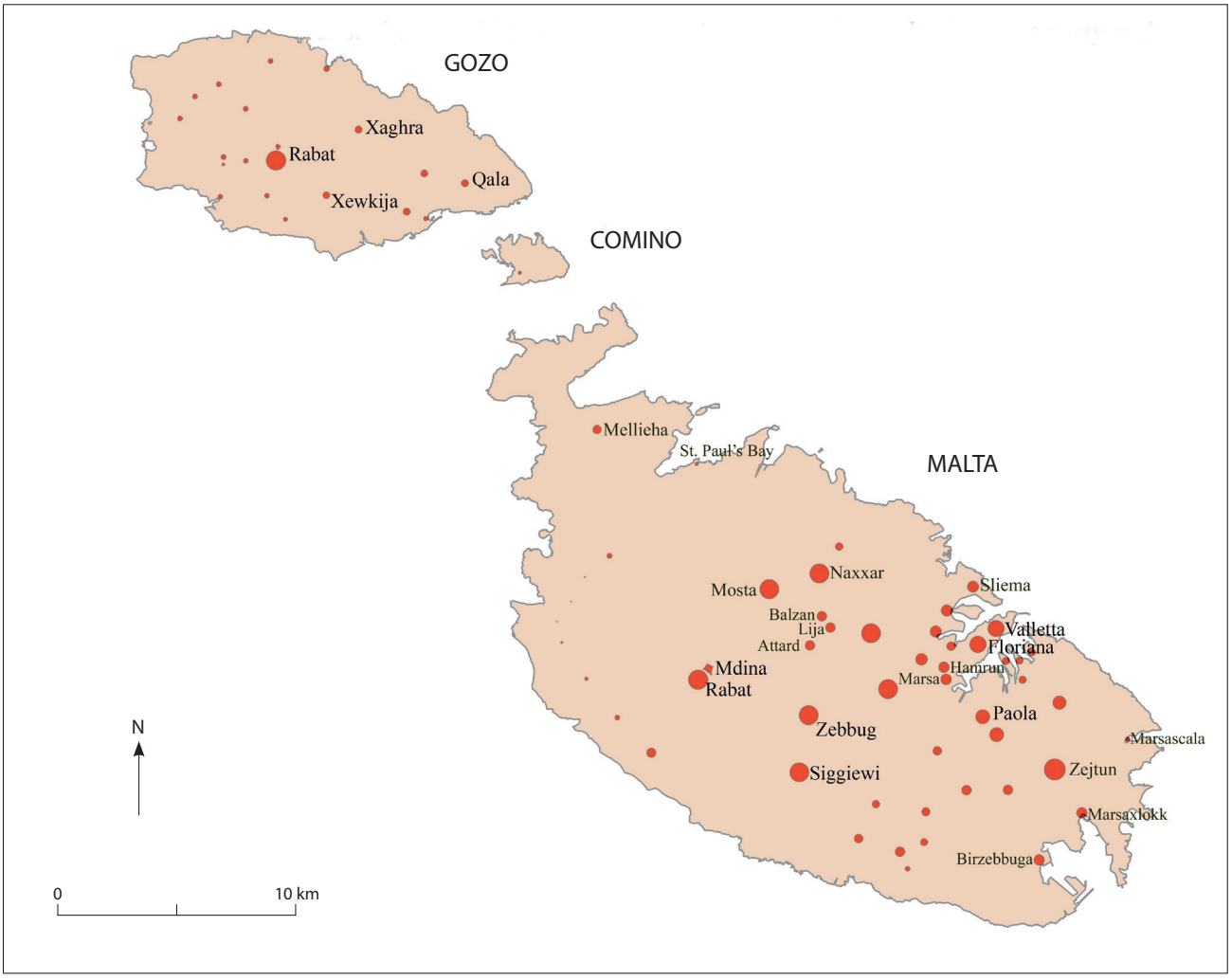

Figure 10.10. *The distribution of built-up settlements in about* AD *1900 (G.A. Said-Zammit).*

the nearby settlements of Attard, Lija and Balzan continued to prosper.

The major development that took place in terms of settlement evolution was in the Marsamxett Harbour district. While the existing settlements continued to expand in terms of population size, several new ones were established too. In the area surrounding Marsamxett Harbour, four new settlements were established, including Sliema, Marsa and Ħamrun, located towards the south of Valletta and Floriana, grew into larger towns to respond to the increasing number of working class families (Tonna 1985, 38).

On the outskirts of the Three Cities a new settlement, Kalkara, developed on the northeastern part of the Grand Harbour. The settlements of this region were the ones that grew rapidly in terms of population size, so much that some of them were eventually divided into more than one parish.

The settlements of southeastern Malta, except for Żejtun, were relatively smaller than those of the other districts. Three other villages (Marsaxlokk, Birżebbuġa and Marsascala) developed in two harbour areas. South-eastern Malta remained an area generally characterized by a low population density.

In Gozo, the settlement pattern remained similar to that of the late eighteenth century. However, one can note the emergence of some coastal settlements in different parts of the island. The small settlement on Comino, which already existed in the previous period, survived until the second half of the twentieth century.

10.3.1. The houses of the British Period

The island's particular political situation and its economic development during the nineteenth century led to the emergence of a new social set-up, comprising different levels which ranged from the Anglophile

elite, the nobility and the Church at the top, a strong middle class, to the lower urban class and the peasantry at the bottom (Cassar 1988). This period also had an indelible effect on the development of the Maltese house. The Knights had left behind them an island fortress, with various defensive systems spread in various localities. The *palazzi* and houses which had been previously occupied by the Order became vacant, and were gradually converted into offices or private dwellings in the British period.

The Baroque idiom remained entrenched in local architecture for many more decades, reminiscences of which survived until practically the early twentieth century. Baroque-style houses continued to be built in the centre of the major villages, where the rural elite normally lived. The persistence of Baroque architecture hampered, in a way, the development of other architectural styles which were already popular in Europe, for example the Neo-Classical and Neo-Gothic styles (Hooker 1994). In fact, these styles were adapted locally from the second half of the nineteenth century onwards and remained popular until the early twentieth century.

The re-utilization of houses by the British meant that certain structural alterations were needed to meet the specific needs of their new occupants. The Victorian age, marked by the effects of the Industrial Revolution, affected the British living in Malta as well as the local community, particularly the Anglophile elite (Frendo 1988, 190). The progress which the Victorian era brought with it generated a major change in Maltese society and how people lived.

As part of its task to improve sanitation and health conditions in the islands, in the second half of the nineteenth century the government issued strict housing regulations which affected the layout of local dwellings. For instance, these encouraged the end of the courtyard house in favour of the terraced house, which had already been quite popular in the previous period (Tonna 1985). The terraced house, consisting of a room at the front, a staircase at the core, another room at the back with an appendage to the kitchen and sanitary facilities, and with a courtyard at the back, remained the standard type of house layout which persisted till well into the twentieth century (De Lucca 1988). This house layout became common in the settlements which were established during this period and in the various new residential areas that developed in the periphery of the agro-towns (Tonna 1985, 38).

10.3.2. The effect of the Victorian Age

The Victorian era had a great influence on the family. It was a time when the mother was considered the ideal housewife and the husband was deemed the dominant and rational *paterfamilias* (Löfgren 2004). The gender segregation and the contrasting roles of both husband and wife influenced the way elite houses were built and their spaces organized. Such segregation led to the development of gender-related spaces within the same house. For example, in a typical nineteenth century elite house the gentleman's area consisted of a study, a smoking or a billiard room and a library; the lady's area included the drawing room, the boudoir and her private bedroom (De Lucca 1988, 321). Whilst after dinner, men would assemble in the smoking room or else remained in the dining room to socialize, women went into the drawing room. The latter had to observe the highest etiquette and decorum in the drawing room, but the boudoir allowed them more flexibility since here they could talk in private, away from the formality of the drawing room (Horn 1997). This mentality, therefore, created a segregation of spaces within the house layout itself.

To ensure a high degree of domestic privacy, interconnecting doorways of Knights' Period houses were usually blocked so that rooms had only a single access point. As in the previous period, however, the ground floor rooms of the elite house remained associated with the domestic staff (the kitchen, stores, etc.), hence there was a clear sense of class segregation between the domestic staff and the house owners (Löfgren 2004, 145).

So far, this section has been concerned with the townhouses, where the elite and upper middle class families lived. These houses were usually situated in the town centres, however from the late nineteenth century onwards there was a tendency among the well-off to settle in villas that were situated in new and quiet residential areas outside the urban centres, similar to what occurred in South Italy and Sicily (Sabelberg 1983, 1986). Consequently, several palaces and townhouses in Valletta left unoccupied by the well-off were gradually converted into common dwellings. However, in the main town of Gozo the situation was different. While the urban centres of Malta experienced a phase of pauperization of the elite dwellings, from AD 1850 onwards Gozo's main town, Victoria, saw the building of a number of houses of Neo-Classical, *Art Nouveau* and *Art Deco* inspiration along its main street, a development which persisted until the early twentieth century (Fig. 10.11). Gozo's traditional economy and lifestyle were perhaps two of the main reasons which, during this period, encouraged the island's elite to continue living and building their houses along Victoria's central street.

The elite and the upper middle class lived in five types of houses, namely:

Figure 10.11.
An example of a Neo-Classical house (G.A. Said-Zammit).

a) Knights' Period *palazzi* and townhouses, with their interior being left in the original state;
b) Knights' Period *palazzi* and townhouses, with their interior being converted to suit the needs of a typical Victorian lifestyle;
c) the houses of Neo-Classical, Neo-Gothic, *Art Nouveau* or *Art Deco* inspiration that were built in the town centres, for example in Victoria, Gozo;
d) the houses of Neo-Classical, *Art Nouveau* or *Art Deco* style which were built outside the towns and agro-towns in new residential areas;
e) the houses located in the agro-town centres, occupied by the rural elite. Several of these belonged to the previous period, while others were built during the nineteenth century, often emulating Baroque-style houses.

10.3.3. Urban lower class dwellings

The urban lower classes, which formed the overwhelming majority of the urban community, lived in smaller houses or cellars. Statistical records show that in about AD 1850 approximately 12 per cent of the Valletta residents were living in houses which often lacked ventilation, air circulation and lighting (Cassar 1988, 93). These overcrowded dwellings permitted neither individual privacy nor a decent quality of life. They often lacked a proper sewage system and a drinking water supply, and therefore contagious diseases here spread like wildfire. With the elite movement to the urban suburbs, various townhouses of the previous period, particularly in Valletta, were partitioned into smaller units to accommodate more low-income families.

10.3.4. Peasant houses, cave-dwellings and hovels

The peasants continued to live in the same type of dwellings as in the previous period. The available evidence has revealed that during this period the farmhouse retained the same layout and features, thus consisting of a central courtyard surrounded by a number of rooms. It also shows that many cave settlements in Malta and Gozo continued to be abandoned, while others were still inhabited by isolated farming communities (Buhagiar 2002, 2012). There are also indications that a small number of rural families still lived in dry rubble hovels or *giren* (Fsadni 1992). This further decline in the number of cave-dwellings and hovels suggests that more peasant families, particularly those with a higher disposable income, sought better accommodation in the villages. Many landless

peasants and farm labourers migrated to the harbour regions in quest of more employment opportunities.

10.4. Conclusions

This study has explored settlement evolution in the Maltese Islands. Our analysis has demonstrated that from a dispersed settlement distribution in the early Medieval period, the economic and social changes that occurred from the fourteenth century onwards led to more nucleation of settlements, with a general tendency to occupy inland areas. By the late medieval period a number of villages were deserted, while others were absorbed by the major settlements. The three urban centres of habitation were Mdina, Birgu and the Gozo Castello.

In the Knights' Period the Grand Harbour area became a commercial hub, while the seat of government was transferred from Mdina to Birgu, and later on to Valletta. The urban demographic expansion of this period, which persisted in the British period, led to the development of new urban settlements and to the extension of existing ones. The main villages of Malta prospered in terms of size and population and became proto-industrial settlements, while the number of hamlets and cave-dwellings further declined. Additionally, the re-population of Gozo from the late sixteenth century onwards led to the establishment of various new settlements.

In the nineteenth century, government incentives and the presence of the British military encouraged settlement in those areas which had been deserted for a long time. This phase of settlement evolution was, in fact, characterized by the spread of new villages, including coastal ones, some of which later grew into towns.

The evidence of houses for medieval Malta has demonstrated that the sumptuous urban dwellings consisted of single-storey buildings; however, by the late Middle Ages a number of them developed into two-storey houses. In the outskirts of the urban centres of habitation the urban poor lived in smaller dwellings, which certainly lacked the architectural elegance of the elite counterparts. Our investigations have shown that the urban poor dwellings were also originally single-storey buildings, but by the late Medieval period a number of them were converted into two-storey dwellings.

In the villages and hamlets the medieval peasants lived in three types of dwellings: the single-storey farmhouses with a central courtyard, the hovels (possibly including the *giren*), and the cave-dwellings. The available evidence does not indicate whether these three types of dwellings developed in different phases or else concomitantly. However it seems that, at some point in time during this period, the peasants were living in one of these three types of dwellings. By the late Middle Ages, possibly in emulation of the two-storey *palazzi*, a number of farmhouses were converted into two-storey dwellings.

In the early modern period new house types emerged. Elite houses were generally characterized by elaborate and extroverted façades. The interior of these houses usually had a series of interconnecting spaces to facilitate movement from one part of the building to the other. On the contrary, many urban poor families ended up living in sub-standard houses, consisting mainly of single-room dwellings or cellars, where living conditions were awful.

From about AD 1650 onwards the centre of the major villages became associated with the rural elite who, like their urban counterparts, lived in elegant houses which emulated the urban *palazzi*. The lower class peasants occupied smaller introverted dwellings which, together with the farmhouses, were characterized by asymmetrical façades and a central courtyard, like those of the medieval period. The number of native peasants living in cave-dwellings or hovels declined, which demonstrates a shift towards a better standard of living among the peasant community.

In the nineteenth century while a number of elite houses in the established urban centres (Mdina and Valletta) adhered to the Baroque idiom, many others, which were built in new urban areas, were inspired by Neo-Gothic, Neo-Classical, *Art Nouveau* and *Art Deco* architecture. There is also evidence that while certain elite seventeenth and eighteenth century houses in Valletta retained a Baroque exterior, they underwent internal structural alterations to resemble Victorian mansions, in which privacy, class and gender segregation were crucial. Comparable to the previous period, the urban poor continued living in small dwellings or cellars, in which sanitary conditions were inadequate. The village centre remained synonymous with the rural elite. Outside the village core the peasants occupied one- or two-storey vernacular dwellings. A few others lived in cave dwellings or in hovels, particularly in northern and western Malta and in certain parts of Gozo.

An important aspect that emerged from this analysis concerns the changes that occurred within the Maltese dwellings during the period under review. While the wealthy houses changed externally and internally through time to suit fashion, changes in the rural and urban poor dwellings were generally minimal and sporadic. With their limited disposable income and with a lack of aspiration to change their dwellings according to fashion, the peasants and the urban poor continued living in small vernacular houses.

Chapter 11

Conclusions

Charles French, Chris O. Hunt, Michelle Farrell, Katrin Fenech, Rowan McLaughlin, Reuben Grima, Nicholas C. Vella, Patrick J. Schembri, Simon Stoddart & Caroline Malone

There is now a large degree of synergy exhibited by the various classes of palaeoenvironmental data investigated through the *FRAGSUS Project* on Malta and Gozo and the direct inter-linkages and associations of aspects of the environment with human activities during the last 8000 years. The geological setting and well dated palynological, molluscan and soil/sediment data present a background picture of vegetational and landscape change throughout the Holocene, with some very specific data on trajectories of clearance, erosion and farming activities in various valleys of the Maltese landscape. Nested within this broader framework, there is an immense amount of more specific data on the development of and changes in palaeosols, the frequencies and types of soil erosion and formation of valley fill sequences, as well as the dynamics of near-shore, valley and plateaux landscapes through prehistoric and historic times in both Malta and Gozo. Within these, there is an exceptional amount of data concerning the impacts of the first farming communities and the resilience of these island landscapes during the Neolithic period between the seventh and third millennia BC. The following summative interpretational sections attempt to draw out the main themes and trajectories of landscape change that have occurred during the Holocene in the Maltese archipelago.

11.1. The palynological record

Chris O. Hunt & Michelle Farrell

The intensive palynological and molluscan analyses of a number of deep core sites at Salina, Marsa, Xemxija, and Wied Żembaq, along with new pollen and soil micromorphological evidence from Neolithic palaeosols at the Santa Verna, Ġgantija and Skorba temple sites, and complementary existing palynological data from Salina Bay, Marsa and Santa Marija (Carroll *et al.* 2012), Burmarrad (Djamali *et al.* 2013; Gambin *et al.* 2016) and Tas-Silġ (Hunt 2015) have provided well dated and detailed sequences of vegetational and landscape change throughout the last 9000 years of the Holocene (Table 11.1; Figs. 11.1 & 11.2). Not only do the analyses of the cores provide evidence for vegetation and landscape change from before the Neolithic period, but they reflect both anthropogenic impacts from land-use and climatic changes in the same records. In combination with the molluscan and palaeosol records, we now have unparalleled detail on the nature of human impacts over the *longue durée* on the Maltese Islands.

11.1.1. Climate

The climate of Malta has been affected by significant regional climate events, notably the 8.2 ka BP desiccation. In contrast, later events and their impacts are more muted in comparsion with their magnitude and effects elsewhere in the Mediterranean Basin. The 6.5 ka BP event hardly registers in the palynological record and the 4.3 ka BP event is equivocal in its signal, possibly suggesting a short period of lower effective moisture. Against a generally rather arid earlier Holocene, short phases of relatively high effective moisture occurred at approximately 6650–6550 cal. BC (8600–8500 cal. BP), 6350–6200 cal. BC (8300–8150 cal. BP) and 5650–5500 cal. BC (7600–7450 cal. BP). The episode at 6350–6200 cal. BC (8300–8150 cal. BP) is a regional event, widely visible in palaeoenvironmental records from the arid western and central Mediterranean lowlands (e.g. Reed *et al*. 2001; Tinner & Lotter 2001; Tinner *et al.* 2009), but the other two are more localized. This episode is followed by a very dry period coincident chronologically with the 8.2 ka BP event (Alley *et al*. 1997). This is a short episode of significant aridity that appears to have occurred at many localities in the central Mediterranean (Tinner *et al.* 2009; Sadori *et al*. 2013, 2016; Magny *et al*. 2009, 2011; Jaouadi *et al.* 2016).

Around 4970 cal. BC (6920 cal. BP) there is a profound reorganization of moisture regimes in the Maltese Islands and more widely in the arid western

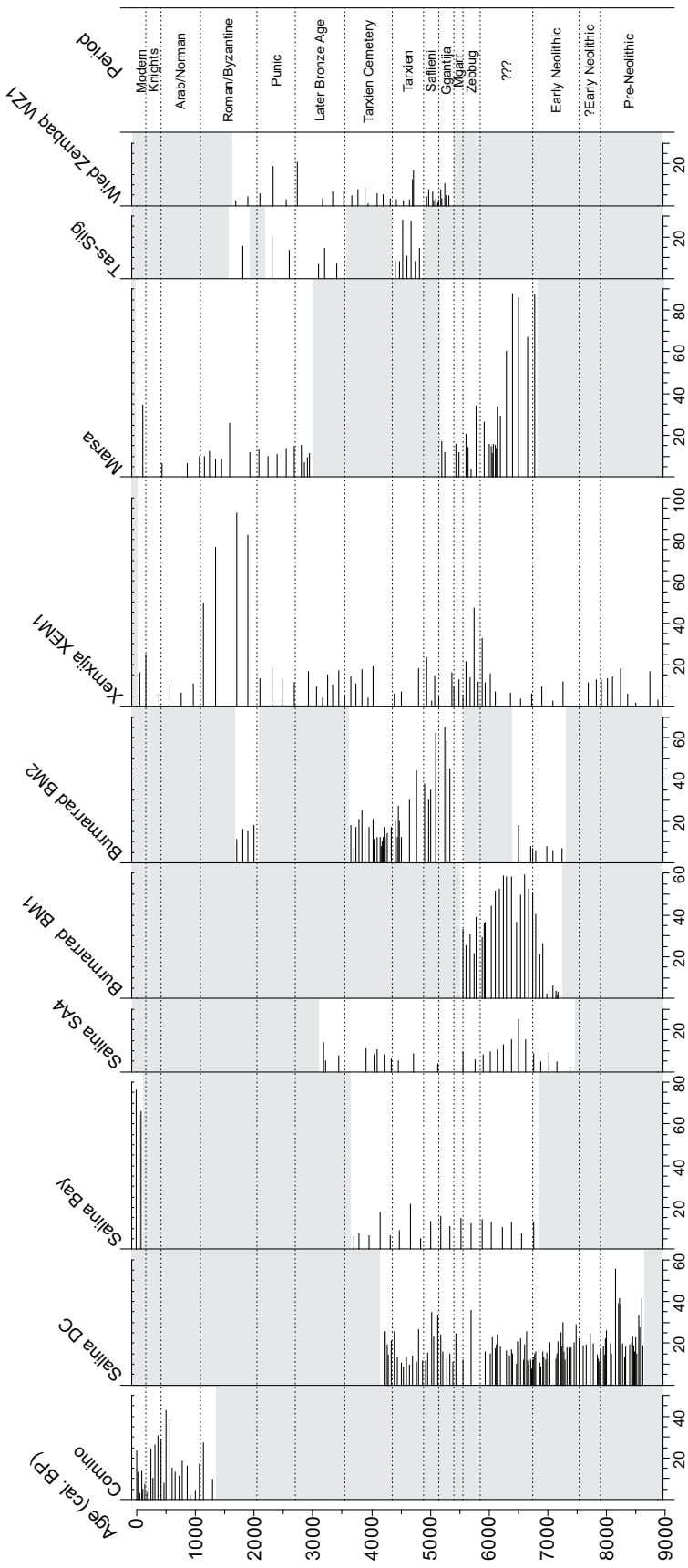

Figure 11.1. *Summary of tree and shrub pollen frequencies at 10 sample sites (C.O. Hunt).*

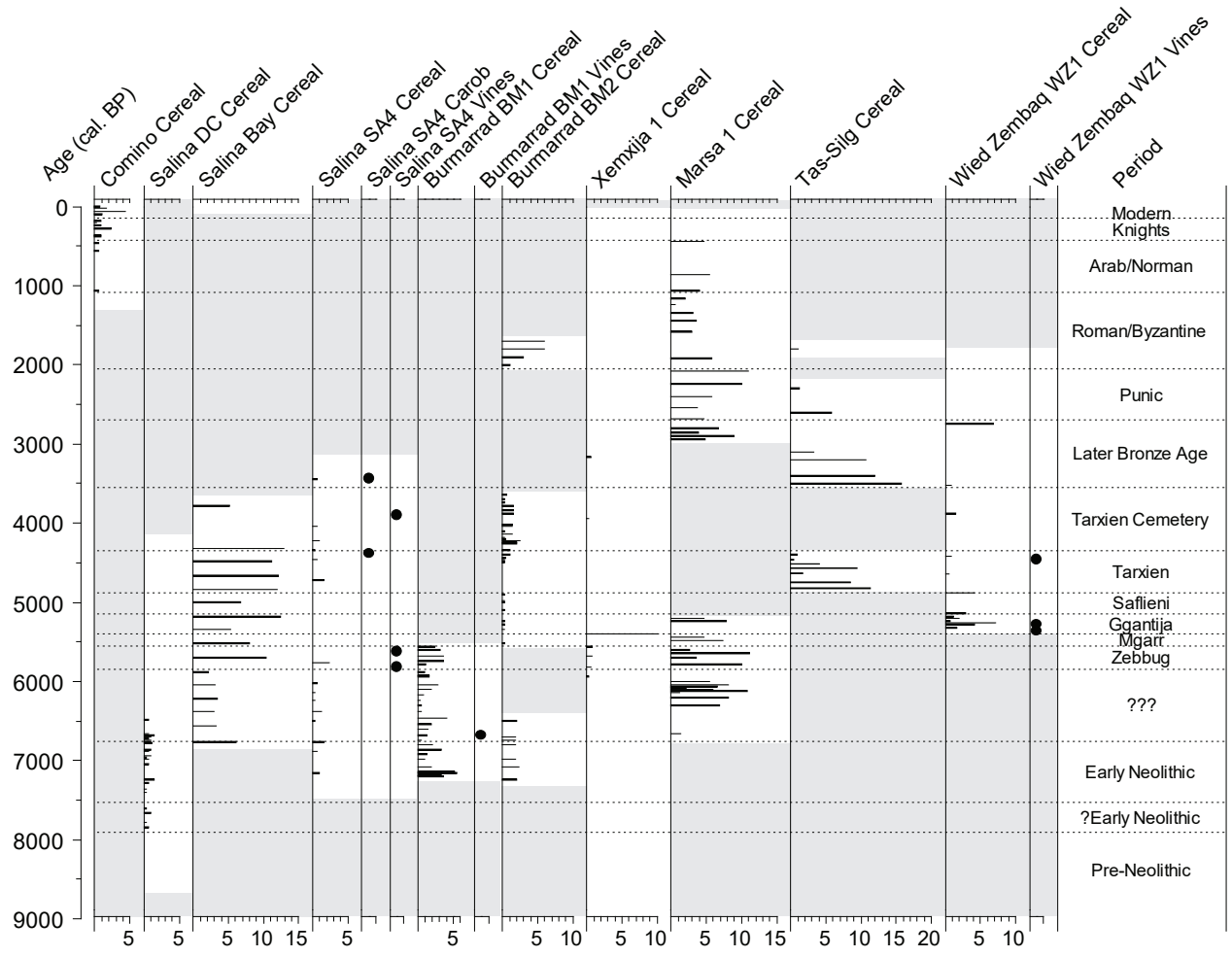

Figure 11.2. *Summary of cereal pollen frequencies at 14 sample sites (C.O. Hunt).*

and central Mediterranean coastal regions, caused by weakening African monsoonal circulation and thus greater regional incursions of moisture-bearing Atlantic air masses (Tinner *et al.* 2009; Bini *et al*. 2018). In the Maltese Islands, this is manifested by the growth of dense scrub in low-lying areas where intensive agriculture was not practised, most notably at Burmarrad (Djamali *et al*. 2013), but also at Marsa (Carroll *et al.* 2012) (Fig. 11.1). The effective humidity remained relatively high in the Maltese Islands until approximately 3050 cal. BC (5000 cal. BP), when more generally arid conditions began to prevail. Within this period of generally higher effective humidity, there seem to have been periods of especially high moisture at 4750–4250 cal. BC (6700–6200 cal. BP) and 3450–3050 cal. BC (5400–5000 cal. BP).

Following the onset of more arid conditions *c*. 3050 cal. BC (5000 cal. BP), there was a further short humid episode at 2850–2650 cal. BC (4800–4600 cal. BP). The next major climatic event in the Mediterranean around 2350–2250 cal. BC (4300–4200 cal. BP) (e.g. Sadori *et al*. 2013; Jaouadi *et al*. 2016; Ruan *et al*. 2016; Bini *et al*. 2018) is marked in the Salina Deep Core by rising *Pistacia* (lentisk scrub), but this is not a general trend and it is not clear whether this marks a relaxation of agricultural pressure at this one site (cereal pollen falls at this point in nearly all cores, but elsewhere tree and shrub pollen percentages do not rise) or a climatic response to rising humidity. There is, however, no convincing evidence for aridification in the available pollen records from Malta, but there is evidence for a gradual trend of aridification over the *c*. 400 years before, with generally falling tree pollen curves (Fig. 11.1). Thereafter, there is no strong evidence for periods of enhanced effective humidity, other than the possibility of a minor episode much later in the Little Ice Age. It must be remarked, however, that the later Holocene in the Maltese Islands was characterized by

Table 11.1. *Summary of environmental and vegetation change in the Maltese Islands over the* longue durée.

Chronology cal. BC/AD	Years BP	Environmental history
7500–5900 BC	9450–7850	The Maltese Islands were covered by grassy steppe with patches of scrub and a few trees, mostly oaks and pines. At times 6650–6550 cal. BC (8600–8500 cal. BP) and 6350–6200 cal. BC (8300–8150 cal. BP) the climate was wetter than at present, causing lentisk scrub and Mediterranean woodland to spread, but around 6550 and again at 6200 cal. BC the climate became much drier, each time for about 200 years, causing the scrub and woodland to die back. Sea level was rising rapidly and so the Maltese landmass was shrinking.
5900–5400 BC	7850–7350	People arrived with grazing animals around 5900 cal. BC, burnt much of the natural vegetation around their settlements (scrub at Burmarrad and open pine-juniper scrub woodland at Marsa) and started small garden-like cereal plots to grow barley and some wheat. Early cultivation caused soil degradation and erosion, so people shifted their cultivation plots every few years. Cultivation, grazing, burning and drought caused severe soil erosion, particularly around Marsa, the Burmarrad Plain and Xemxija. The uncultivated land was still predominantly grassy steppe. Sea level continued to rise.
5400–5200 BC	7350–7150	Grazing intensified and at this point the grassland started to degrade, with ruderals (weeds) beginning to replace steppic vegetation. Cereal use became generally more intensive and intense soil erosion continued, probably because of grazing pressure. It became a little drier. Sea level rise slowed.
5200–4800 BC	7150–6750	Olives appear in the pollen record, and barley cultivation expanded. The grazed land continued to degrade. The climate became substantially wetter allowing scrub and woodland to spread where human impact was still low, for instance around the large alluvial plains at Xemxija and Burmarrad.
4800–3900 BC	6750–5750	Sea level rise slowed. Humidity was generally relatively high but there was a pattern of environmental instability probably caused by human impact, as scrub at Burmarrad and Mediterranean woodland at Marsa declined, with evidence for substantial burning at Marsa. *Vitis* appears at Burmarrad at the beginning of this period. Woodland seems to have expanded at Xemxija. There were low levels of cereal cultivation, except at Marsa where cereal cultivation became prominent.
3900–2350 BC	5750–4250	Substantial but patchy cultivation of wheat, barley, perhaps some olives and grapes, the latter appearing at Salina and a little later at Wied Żembaq. The exception seems to have been in the Burmarrad lowland where woodland remained prominent. Grazing pressure caused the gradual replacement of grassy scrub by a ruderal flora. Woodland came and went in the landscape, at Xemxija, Salina, Wied Żembaq and Tas-Silġ, perhaps suggestive of some sort of rotational land use at these sites. Sea level rise slowed further.
2350–2000 BC	4250–3950	Humidity declined, with severe droughts, especially at the start of the period. Cereal cultivation ended except at Burmarrad, where it seems to have started. Grazing may have continued and ruderal vegetation flourished.
2000–1000 BC	3950–2950	Patchy cultivation of cereals, vines and possibly olives. Grazed areas had very degraded vegetation. Humidity remained fairly low and it is likely that droughts remained common.
1000 BC–AD 100	2950–1850	Widespread cultivation of cereals, vines and olives with very degraded grazed lands and much soil erosion. Humidity probably remained relatively low.
AD 100–400	1850–1550	Very widespread cultivation of vines, olives and cereals with grazed lands dominated by ruderal flora. Intense soil erosion. Humidity probably remained fairly low. During this period a pine plantation was established at Xemxija.
AD 400–1550	1550–400	Very degraded landscape with some cereals and olives. The pine plantation at Xemxija was cut down around cal. AD 800–900. Humidity was probably very low and irregular with marked declines around cal. AD 1100, 1300 and 1500.
AD 1550–1800	400–150	Gozo had grassy landscapes with widespread sheep-runs. Cereal cultivation became more important on Malta and Comino with terracing under the Knights, and cotton became an important cash crop. Humidity may have increased somewhat, but declined towards the end of the period.
AD 1800–present	150–present	Cereal cultivation became more important. Pines and eucalyptus were introduced in the late nineteenth century. Non-cultivated landscapes were highly degraded. Humidity may have recovered somewhat.

extremely resilient anthropogenically degraded vegetation under severe pressure that may have suppressed any marked response to climate change.

11.1.2. Farming and anthropogenic impacts on vegetation
From the extensive data gathered by the *FRAGSUS Project*, there is no convincing evidence for human impact on vegetation in the pollen record prior to the first traces of cultivation provided by pollen of wheat and barley, and coprophilous fungal spores providing evidence for livestock grazing, which occur at *c*. 6067–5971 cal. BC (8017–7921 cal. BP). The initiation of farming likely followed the arrival of people using Neolithic technology, relating to the well known Neolithic diaspora into the western Mediterranean (Ammerman & Cavalli-Sforza 1984; Malone 1997–8, 2003, 2015; Whittle 1996; Zilhão 2001). As such, this date is slightly later than the first Neolithic dates in southeast Italy, but is earlier than those for all known Neolithic sites further west (Zeder 2008). Thus, it is possible that the Maltese Islands were a key staging post in this diaspora. As yet, no archaeological evidence in Malta or Gozo corroborates these findings, but if the first settlements were coastal, they must now lie beneath some 20 m of sediment and water.

After the first appearance of cereal pollen in the Salina Deep Core about 7950 years ago, it is represented virtually continuously in at least one pollen diagram until the present day (Fig. 11.2). It is clear, however, that during the earlier Neolithic there were cyclic changes in the cereal curves, with generally low cereal pollen percentages, which suggests more or less small-scale, shifting arable activity. Initial cereal cultivation, visible only in the Salina Deep Core, was of both barley and wheat, but wheat cultivation seems to have been generally less widespread and is less frequently recorded in the Early Neolithic than barley. This may reflect the ability of barley to cope well with seasonal aridity, in what must have been a relatively dry landscape, at least seasonally. Falling biodiversity of crop plants following first farming occurred widely in the western Mediterranean (de Vareilles *et al.* 2020) as agriculturalists adapted to localized conditions.

Around 5550 cal. BC (7500 cal. BP), grazing became more intensive. It intensified further and peaked around 5350–5050 cal. BC (7300–7000 cal. BP), as did cereal cultivation, suggesting that this episode may have been a time of relatively high population engaged in both arable and pastoral farming that began the opening-up of the Maltese and Gozitan landscapes. There may have been active localized clearance of vegetation to facilitate farming. Recent corroboration of this type of impact has been found in a deep core from Marsa by Marriner *et al*. (2019), which shows repeated fire episodes associated with rapid run-off observed in the charcoal and geochemical records between 5650 and 5400 cal. BC (7600 and 7350 cal. BP). Evidence also comes from Burmarrad where rapid sedimentation rates between 5550 and 5350 cal. BC (7500 and 7300 cal. BP) correspond with human-modified vegetational change from forest stands to mixed shrub-grassland (Djamali *et al.* 2013).

Around 5050 cal. BC (7000 cal. BP), a strong rise in *Pistacia* at Burmarrad, with values staying remarkably high until around 2250 cal. BC (4500 cal. BP) (Djamali *et al.* 2013; Gambin *et al.* 2016), may suggest the appearance of a patch of dense lentisk (*Pistacia*) scrub. The expected successional development, with expansion of olive and then oak, did not start for another 2000 years. It is possible that the lentisk patch was a managed resource rather than natural vegetation which would have provided animal fodder, oily fruit/seeds and firewood, all resources likely to have been in relatively short supply in this early agricultural system.

There appears to be a relatively long hiatus in the archaeological record between *c*. 4800 and 3800 cal. BC (6750 and 5750 cal. BP). In contrast, the pollen record shows that after a brief decline in cereal pollen, further peaks of cereals are evident at Salina and Burmarrad close to 4800 cal. BC (6750 cal. BP). At Salina (Carroll *et al*. 2012), this period was followed by continuous high frequencies of cereals and there was a significant peak of cereals at Marsa around 4350–4150 cal. BC (6300–6100 cal. BP). Grazing indicators also remained high at these sites throughout. It is likely, therefore, that there was some sort of population continuity through the apparent archaeological hiatus, and it is hoped that this will be corroborated by further archaeological research. Nonetheless to date, no dated archaeological sites have any representative stratigraphy or artefacts relating to this apparent millennium-long hiatus.

The Later Neolithic (or Temple Period) is marked by very high cereal percentages, notably in the Żebbuġ, Ġgantija and especially the early Tarxien phases of the early to mid-third millennium BC. At Salina Bay the high cereal percentages persist into the end of the Tarxien phase in the mid-third millennium BC (Carroll *et al.* 2012). It is likely that arable agriculture was widely practised and intensive, but diminishing at several locations during the Tarxien phase, possibly in response to aridification and related environmental degradation. The very high percentages of cereal pollen at or close to major archaeological sites may reflect handling or threshing of cereals adjacent to temple sites.

The end of the Neolithic at about 2400 cal. BC (4350 cal. BP), coincident with general abandonment of the temple sites, is marked by a hiatus in cereal cultivation at all sites except at Burmarrad, where cultivation

seems to have continued (Gambin *et al.* 2016). Cereal production at this site alone parallels the continued use of cereals at Tas-Silġ through the Early Bronze Age (Fiorentino *et al*. 2012). Grazing and animal husbandry continued at some sites, but may have ended at others as shown by the faunal remains in post-Temple Period cultural levels at Taċ-Ċawla (see Volume 2, Chapter 3). It is possible that along with profound cultural change at this time, populations contracted into the higher land of the Globigerina Limestone plateau on Malta, perhaps in response to coastal raiders (cf. Wiener 2013).

Later in the Early Bronze Age, cereal cultivation seems to have resumed at coastal localities, and this continued into the nineteenth century AD at Marsa (Carroll *et al.* 2012). Evidence from other sites is patchy, partly because assemblages were affected by strong taphonomic biases. Olive groves were important at Marsa in the Punic and Roman periods and at Burmarrad in the Roman Period, and there seems to have been a pine plantation at Xemxija in Roman to early medieval times. These tree crops may not have been completely for consumption on Malta as there was an olive oil trade in the Mediterranean from late Punic times. This expanded in the first and second centuries AD to satisfy demand from Imperial Rome, and Rome was also a voracious market for grain, wine, timber and many other products (Hohlfelder 2008; Margaritis & Jones 2008).

During Medieval times, the Maltese landscape seems to have been extremely degraded, although some cereal cultivation continued. After the mid-sixteenth century, the Knights of St John seem to have started the regeneration of the Maltese landscape through the encouragement of terracing and exploitation of new parts of many valley systems, such as the Ramla valley on Gozo. Crops such as cotton were adopted and grazed grassland seems to have become widespread. Finally, the British and modern periods saw the widespread planting of ornamental trees, especially pines and eucalypts.

11.2. The molluscan record

Katrin Fenech, Chris O. Hunt, Nicholas C. Vella & Patrick J. Schembri

The detailed molluscan analyses of the long cores taken through many of the deep valley sedimentation sequences have provided extensive sets of quite specific palaeoenvironmental data for the Holocene, which augment both the palynological and soil/sediment analytical results. These are summarized in Table 11.2.

From the analysis, four major themes consistently present themselves. The first, is the initial influence of freshwater in the lower reaches of several valleys, just inland from the sea, which continues from at least 4800 cal. BC (6750 cal. BP) into the fourth and third millennia BC of the Neolithic Temple Period. There is evidence of perennial freshwater streams and shallow, marshy areas, with slow to stagnant freshwater and accumulations of abundant leaf litter. These habitats often exhibit considerable variation in spatial extent and frequency of occurrence through time, no doubt reflecting seasonal changes in rainfall and possibly even longer-term climatic trends in terms of greater or lesser rainfall, together with geomorphic changes caused by sedimentation and sea level rise. This is particularly evident in the Xemxija and Wied Żembaq cores. It is certainly possibly that the climate was wetter than today, since this evidence falls within the Holocene Climatic Optimum, evidence for which is also found in nearby Sicily (Carroll *et al*. 2012; Sadori *et al*. 2013). However, by the first millennium BC and certainly by the end of the Roman period, freshwater habitats were in strong decline, and rarely recovered thereafter. Exceptions include the Pwales valley where today a spring is caught in a reservoir.

Second, there were a number of near-shore lagoonal environments with brackish water especially at Salina, Wied Żembaq and Mġarr ix-Xini. These environments persisted from the Temple Period of the later Neolithic and through into the Roman period. These environments would have supported important wild food sources (e.g. fish, fowl, molluscs and shellfish) and would have supplied various kinds of household construction materials (e.g. reeds, grasses, withies). Stable isotope studies suggest these additional food sources were not prominent in the Neolithic diet, although some mollusc shells and bones of fish and fowl occur in archaeological sites of the period.

The third characteristic was the general openness of the landscape, with little sign of densely vegetated environments from the early Holocene onwards. Very few woodland molluscan species were recovered from the cores, and the only definitive occurrence was of *Lauria cylindracea* in the Xemxija 2 core at depths which equate to about 4300–2000 cal. BC. This indicator species had disappeared by *c*. 1800 cal. BC. Before and after that time there are suggestions of leaf litter habitats occasionally being present, but there is very rarely evidence to suggest anything other than ubiquitous open karstland over the *longue durée*.

Fourth is the evidence for continuing landscape degradation from at least the seventh millennium BC onwards. This evidence complements and corroborates the considerable aggradations of eroded soil material observed in most valley systems. Soil erosion was already occurring by the 8.2 ka BP aridification event, and was observed in the base of the Xemxija

Table 11.2. *Summary of events revealed by the molluscan data in the deep cores.*

Chronology cal. BC/AD	Location	Landscape/sediments/erosion	Local vegetation
8000–6000 BC	Xemxija and Salina	Saline marshland, perennial streams, slow moving water and ponds	Open country with quite lush vegetation on margins; open country/ karstland in vicinity
6000–3900 BC	Xemxija and Salina	Receding freshwater bodies; marsh disappearing; landscape instability and droughts; high sedimentation rates	Decrease in leaf litter; open country with grassland, karstland
from 5900 BC	All cores, especially Xemxija, Wied Żembaq and Salina	Soil erosion and aggradation in lower parts of valleys	Open country with sparse vegetation, karstland
3900–2400 BC	Xemxija	Perennial running freshwater stream; slow to stagnant water and pond;	Expansion of saline marshland after *c*. 2930 cal. BC; low leaf litter;
	Salina	Running freshwater and ponds; several episodes of severe erosion and storm events;	Breakdown of vegetative cover associated with agriculture;
	Wied Żembaq	Stream in valley, with saline marsh at valley mouth	Open country/karstland in vicinity
2400–750 BC	Xemxija	Decrease in freshwater habitats, especially of running water;	Light grassland, open country/ karstland; leaf litter occasionally; no woodland snails present past 1800 cal. BC;
	Wied Żembaq	Stream/running water ceases; brackish/ saline marsh continues;	Open country/karstland increases
	Wied Żembaq, Marsa 2 and Mġarr ix-Xini	High energy sedimentation	
750 BC–AD 650	Xemxija	Brief reappearance of freshwater stream; decrease in saline marsh with increased marine influence;	Open country/land species scarce;
	Wied Żembaq	Freshwater input becoming more limited;	Mainly open country/karstland;
	Mġarr ix-Xini	Similar to previous period;	Mainly open country/karstland, with grapevines in Punic period;
	Marsa 2	Declining freshwater with slow/stagnant water;	Scrub and open exposed habitats;
	Marsaxlokk	No freshwater, except possibly seasonally	Mainly open country/karstland
from 750 BC	Wied Żembaq	Freshwater input becoming more limited	Mainly open country/karstland
from AD 800	Xemxija	Erosion and aggradation of pale brown stony soils	Sparsely vegetated open country/ karstland

cores. Nonetheless, the erosion and deposition of soil from the Pwales valley catchment appears to have begun relatively slowly and episodically. Fine eroded soil material associated with a gradual trajectory of degradation that intensified over time is especially evident from the first millennium BC onwards. This sedimentation process probably continued to be driven by prehistoric farming activities in the higher parts of the Maltese landscapes from the sixth millennium BC, a suggestion corroborated by both the palynological and soil micromorphological data. Certainly, molluscan diversity and abundance began to decrease from the end of the Neolithic period, evidence which strongly suggests the increasing and coincident influence of drying and soil and land degradation. The aggradation sequences are occasionally punctuated by evidence of more significant erosion events, related to either storm events from the sea, and/or severe rainfall erosion events generating eroded soil and limestone breccia valley fills from inland.

11.3. The soil/sediment record
Charles French

Geoarchaeological fieldwork and laboratory analyses focusing on the Neolithic temple sites located on the Xagħra plateau and the associated Marsalforn and Ramla valleys on Gozo and the Skorba and Xemxija/Salina/Pwales valley areas of northeastern Malta have suggested a new model of soil development for the early to mid-Holocene (Table 11.3; Fig. 11.3). Well developed, thick, moist and vegetated clay-enriched (or argillic) brown soils (or Orthic Luvisols) with a considerable wind-blown silt component had developed on the Upper Coralline Limestone plateaux and hill-top shoulder areas of the islands from at least the ninth–sixth millennia BC. Similar soils with a greater sand component had probably developed on the Greensand exposures just below the plateaux, and with a greater silt component on the Globigerina Limestone areas, often in the lower parts of the valley systems. There is corroborative evidence for this formerly slightly moister and more vegetated landscape associated with good soil development observed in the palynological and molluscan data, and in particular, the evidence of scrubby open woodland and shallow, slow-moving freshwater streams and marshy areas at several valley locations such as Xemxija in the lower Pwales valley, Wied Żembaq and Ġgantija and the Ramla valley. In contrast, the soils on the intervening Blue Clay geological exposures on the valley slopes were thin and poorly developed organic A horizons over thick, slowly weathered silt and clay-rich subsoils (or Leptosols), but were either just below or associated with springs, many of which are still viable today such as in the Ramla valley immediately south of Ġgantija temple.

The palaeosol records revealed that the reasonably well developed, clay-enriched, brown soils in the upper parts of the valley and mesa plateau landscapes subsequently underwent major soil changes during the mid-Holocene, especially during the Neolithic and Bronze Age periods. The micromorphological analyses clearly showed the combined effects of the impact of Neolithic farming communities on the soil/landscape system from at least the sixth millennium BC, and particularly during the fourth–third millennia BC Temple Period, and subsequently with the increasingly very dry climatic regime. The thick, well structured brown and clay enriched soils (Orthic Luvisols) gradually changed to either red Mediterranean soils (Chromic Luvisols) and/or very thin red calcitic A horizon versions of these soils on the limestone bedrock (or Leptosols), equating with Lang's (1960) 'terra soils' and 'xero-rendzinas,' respectively.

Despite the naturally low base status of these transformed soils, associated with rapid bio-degradation of the near surface organic matter, a degree of agricultural productivity may well have been maintained though the enhancement of the soil's organic content by the deliberate incorporation of household derived organic and artefactual waste. This significant soil management feature appears to have begun in the mid-third millennium BC, certainly at Ġgantija and probably also but slightly earlier at Santa Verna and Skorba. It is possible that deliberate soil enhancement would have improved soil fertility and stability, and as a soil conservation measure, this action may well have underpinned the viability of later Neolithic agricultural society in the Maltese Islands. But whether this soil management was actually the beginning of constructed terraces is much harder to say with any certainty. Moreover, the resilience and agricultural productivity of the wider landscape continued to be evidenced in the palynological record throughout Neolithic and later prehistoric times in terms of the continuing utilization of arable and pastoral landscapes, despite coincident and on-going landscape degradation. This utilization suggests that the landscape's inherent resilience was well understood by the farming population of these islands, but despite that understanding, it remained continually susceptible to soil loss through alternating periods of de-vegetation and aridification, punctuated by high rainfall events. Certainly the substantial thicknesses of valley fills across the islands that accumulated over the last *c*. 9000 years revealed in the coring programme testifies to continuing physical disruption and erosion of most of the valley catchments.

Of course, this new model of soil change in Neolithic times in Gozo and Northern Malta need not have been the soil development trajectory everywhere on the Maltese Islands. Soil changes would have undoubtedly varied locally, dependent upon geology, vegetation, moisture and erosion regimes, human activities and time. Clearly geoarchaeological investigations of each valley/plateau system in Malta and Gozo are desirable, in association with an enhanced programme of OSL and radiocarbon dating to establish reliable chronologies of landscape change. Nonetheless, from what has already been achieved by the *FRAGSUS Project*, there is a strong degree of corroboration between several classes of evidence and events observed in the palynological, molluscan, soil, stratigraphical and chronological records across the islands. Moreover, these confluences of data clearly suggest that seminal models of the setting of monuments now need to be reassessed. It is no longer justifiable to rely on modern soil-type distribution as a guide to the nature of past landscapes.

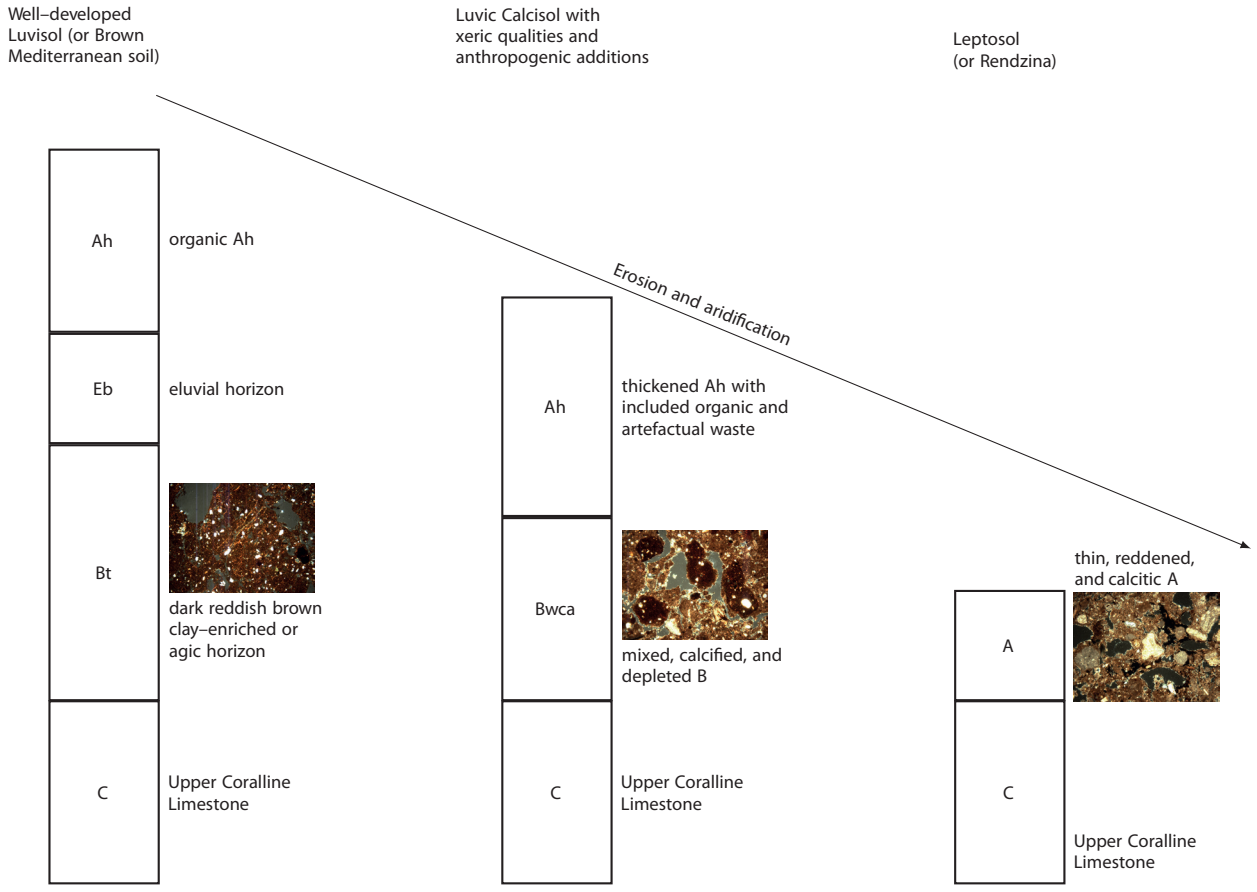

Figure 11.3. *Schematic profiles of possible trajectories of soil development in the major geological zones of Malta and Gozo (C. French).*

With time, the system of prehistoric soil improvement came under inevitable strain. A combination of de-vegetation, sustained human use and a wider coincident aridifying trend led to the formation of either dry, organic-poor, red Mediterranean *terra rossa* soils and/or thin, organic-poor, calcitic soils associated with open xeric landscapes. This coincident set of processes was in-train from at least the early fourth millennium BC onwards, and was well advanced a millennium later, probably making successful arable farming both more intensive but riskier in many parts of the landscape. More specifically, arable farming would have become very difficult to sustain on the Upper Coralline Limestone plateaux, a conclusion that is corroborated by the shrinking evidence for cereal cultivation and an increase in poor pastoral land in the wider palynological record from the third millennium BC onwards.

The aggradation of fine eroded soil was well underway in many of the valleys from the mid-Holocene or the sixth millennium BC. In the base of the Xemxija cores, there is strong evidence for the erosion and aggradation of silt-sized soil-derived material both from just before and during the early Neolithic (seventh to fifth millennia BC). The beginning of this erosional trend could have been triggered at Xemxija by the 8.2 ka BP climatic drought event, but the on-going input of fine eroded soil into the valley bottoms from higher up the valley slopes suggests the continuing destabilizing impact of early and later Neolithic farmers.

More frequently, limestone-rich hillwash accumulations in valley bottoms appear to be a later prehistoric, historic and modern feature of the valley landscapes. In the basal third of the Xemxija 1 core for example, initial erosion appears to have been derived from disruption of the upper parts of the Blue Clay slopes at the transition to the Greensand geology, but subsequently becomes dominated from the Temple Period in the fourth millennium BC by erosion of clay-enriched and carbonate dominated soils derived from the Upper Coralline Limestone plateau. In post-Neolithic times, severe soil erosion and accumulation down-slope

Table 11.3. *Major phases of soil, vegetation and landscape development and change during the Holocene.*

Chronology and location	Vegetation and landscape	Soil and erosion features	Human impact
Earlier Holocene, ninth–seventh millennia BC	Variable to open cover of coniferous scrub and deciduous woodland with lentisk and grassy steppe	Incipient to well developed, moist, humic and stable brown soils with fine silt and clay illuviation and argillic lower Bt horizon formation on Upper Coralline Limestone; thick vertisols in many valleys	Minimal knowledge of earliest Holocene
Early Neolithic, seventh–sixth millennia BC	Open scrub woodland with wild fires; first signs of grasses and herbs increasing and some regression of scrub; perennial streams and marshy areas in lower parts of some valleys	Stable, moist well developed, clay enriched brown soils on Upper Coralline Limestone; first signs of soil erosion of upper valley slopes and aggradation in some valley bottoms	First signs of soil erosion and incremental alluvial aggradation in many valleys from the seventh–sixth millennia BC relating to early clearance and human agricultural interference; e.g. Xemxija and Salina cores
Middle Neolithic, fifth millennium BC	Open, mixed deciduous scrub and grassy steppe; first small wheat/barley plots and grazing animals	Stable, vegetated, well developed, moist, humic, brown soils; continuing signs of soil erosion & aggradation in valley bottoms	Continuing soil erosion moving material from the upper valley slopes and limestone plateaux into valley bottoms
Neolithic Temple Period; from the early fourth millennium BC	Open, deciduous scrub with limited cereal cultivation and more intensive grazing and development of ruderal vegetation	Red-brown soils showing further signs of clearance and drying out with thinning, fines depletion, calcification and rubification, thus becoming transitional reddish brown soils	Upper Coralline Limestone plateaux becoming extensively utilized for settlement, temples, burial and farming; continuing soil thinning and erosion; some marshy areas in lower valley locations
Later Neolithic Temple Period; early–mid-third millennium BC	Scrubby to open with mixed agricultural use with cereals, poosibly olives and vines; turning to dry ruderal dominated garrigue in places with soil erosion; marshy areas in lower valleys drying out and receding	Reddish brown soils becoming more strongly calcified and reddened with secondary iron oxides; in places with signs of amendment of the A horizon with settlement derived organic midden waste material	Continuing extensive utilization; some managed arable fields along upper, southern edge of Upper Coralline Limestone plateaux and poor grazing land on plateaux and valley slopes; continuing soil erosion from the plateaux areas into the valley bottoms
From the Bronze Age; second millennium BC onwards	Ostensibly open, mix of arable cultivation of cereals, vines and olives and ruderal dominated pasture land, with developing garrigue on plateau	Extensive development of thin, dry, depleted, mixed, calcitic red soils on the Upper Coralline Limestone plateaux	Poor grazing and arable land on the Upper Coralline Limestone plateaux; intensifying soil erosion from the plateaux and slope areas into the valley bottoms, especially during 1550–1000 cal. BC
Ramla and Marsalforn valleys throughout prehistoric times	Valley slopes with scrubby woodland and natural springs/ marshy areas	Thick, moisture retentive, silty clay vertisol-like soils in the Blue Clay Ramla valley and fine sandy/silty clay loam hillwash soils in Marsalforn valley	Minimal human impact; possible use of Blue Clay valleys for some pannage for livestock and use of springs and natural raw materials
Marsalforn valley from at least mid-second millennium BC	Clearance, cultivation of vines, olives and cereals and hillwash accumulating in valley bottom; lower valleys now dry	Calcitic silty clay soils with thin A horizons on slopes, prone to overland flow when bare	Extensive utilization and erosion; stop/start hillwash associated with arable use and/ or construction of terraces; but no absolute data on when terracing starts
Ramla valley from medieval times	Scrubby open slopes	Thick, moisture retentive silty clay vertisol-like soils with thin A horizons	Pasture and limited arable use?; use of springs and natural raw materials?
Ramla valley from fifteenth–sixteenth centuries AD	Clearance and field enclosure of grassy landscape; first definite terracing with cereal cultivation becoming more important	Clearance, terracing and stone wall construction leading to reworking, thinning/thickening of soils; prone to summer drying out and some hillwash effects	Establishment of first lanes and terraced field systems by Knights of the Order of St John; general disruption, surface drying and hillwash effects
Plateaux and valleys from the nineteenth century AD	Mix of olive, vines, fruit and cereal cultivation and grazing with some urban development on plateaux	Thin, single horizon, depleted, *terra rossa* and rendzina-like soils on Upper Coralline Limestone; thick to thin, silty clay vertisol-like soils on terraced valley slopes	Extensive mixed agricultural economy with ubiquitous terracing and new urban development on the Xagħra plateau
Plateaux and valleys from the twentieth–twenty-first centuries AD	Mix of olive, vines, fruit and cereal cultivation and grazing, with increasing urban development on plateaux	As above	Urban and garrigue expansion on plateaux; extensive mixed agriculture on valley slopes and bottoms

was well underway by the mid- to late second millennium BC, for example in the Marsalforn valley on Gozo. This evidence equates with strong evidence for a period of maximum erosion from *c*. 1350–550 cal. BC, as observed in several deep valley cores such as Salina, Xemxija and Wied Żembaq in Malta. This landscape trajectory is supported up by the application of the revised universal soil loss equation to these same sediment cores, which also suggests that there was a major phase of destabilization and valley sedimentation occurring between *c*. 1550 and 1000 cal. BC. Although there is no absolute proof, this evident widespread disruption of the landscape might well signify the beginnings of extensive terraced field construction on the upper limestone slopes of the valleys.

From the sixteenth century AD the Blue Clay valley slope landscapes were intensively exploitated for arable agriculture, which led to later erosion and aggradation in the lower valleys, such as the Ramla valley of Gozo in the late nineteenth–early twentieth centuries. Nonetheless, the terrace systems established extensively across the islands in the British period by the late nineteenth century gave a substantial degree of stability to most of the valley slope landscapes, though they have not prevented continuing incision and down-cutting in the base of many valleys, a process which is still continuing today.

11.4. Discontinuities in Maltese prehistory and the influence of climate

Chris O. Hunt

There is a complicated relationship between climate and human activity which can be extremely difficult to grasp, because it is contingent on so many factors, because thresholds are so variable and because it is quite often very difficult to establish the magnitude of change, both in climate and in human response. Humans and their societies are extremely resilient and sometimes seem able to cope with significant climate and environmental change. At other times and in other places, what seem to be quite small environmental fluctuations seem to have led to (or at least coincided with) significant changes in human activity. Within the Holocene, our understanding of climate change is still evolving, but it is becoming clear that this was not a uniform period climatically.

Climate is the result of the aggregation of long sequences of weather events and many factors contribute to it. There is a tendency to reduce these to figures such as annual averages of rainfall or temperature, but there is much more texture to climate which can become hidden in these apparently simple figures, with things like the degree of seasonality, or the prevalence of extreme low or high temperature or rainfall events extremely significant in the lives of plants, and thus of the animals and humans dependent on them, if not to the animals and people themselves.

In the context of prehistoric Malta, our ability to resolve climatic variables is limited because we are dealing with the limiting factors of the techniques available to us. With the pollen evidence, it is difficult to discern temperature and rainfall changes because we are dealing with an extremely resilient, drought-tolerant flora, most of which is far from its climatic limits, and in particular because of the strong anthropogenic influence on vegetation since first colonization. Further, the concept of 'effective moisture' reflects the fact that plants respond not to rainfall totals *per se*, but to a complex interplay between rainfall, atmospheric temperature and humidity and the distribution of these variables through the year. The response of plants also varies depending on their growth habit. While herbaceous annual plants may respond fairly immediately to rainfall and effective moisture variation – in extreme cases not germinating at all or not flowering in major droughts – longer-lived perennials and especially trees may be able to 'ride out' several years of climatic stress because well-developed root systems may be able to access groundwater not available to shallow-rooted annuals.

Nevertheless, the main evidence for climatic change discussed in this volume is from the pollen analysis. It can be extremely difficult to separate stochastic variation in pollen statistics from the imprint of environmental events (Blaauw *et al.* 2010) and therefore replication of results from different sites is needed to separate signal from random noise. The interpretation of climatic data in the *FRAGSUS Project* has therefore relied on replication of signal between the project results and/or those of Carroll *et al.* (2012), Djamali *et al*. (2013), Hunt (2015) and Gambin *et al.* (2016). In locations where cereal cultivation and grazing were not greatly in evidence, we can interpret as a climatic signal the rise of tree and shrub pollen around 5000 cal. BC, and its persistence at high levels and eventual decline between 3000 and 2500 cal. BC. This is evidence for an increase and then decrease of effective moisture and we can rely on it because it is replicated in two or more cores. Minor fluctuations in percentages of tree and shrub pollen in our cores may similarly reflect minor variations in effective moisture, but correlation of these between our records is highly problematical because of the inherent uncertainties embedded in the dating models for individual sites.

Similarly, the Maltese terrestrial molluscan fauna is extremely well-adapted to the very variable climate of the Maltese Islands: most has been in place through

many glacial/interglacial cycles and the animals can compensate for variations in climate by adjusting their distributions at the microscale in the landscape. Congruent points may be made about soils and sediments as climatic indicators – events lasting only a few months or years are unlikely to have left much impact on soils which evolved to prevailing conditions over many hundreds or thousands of years. The sediments record depositional facies, but again the Maltese Islands lie far from the climatic limits of most of the processes that dominated the Maltese Holocene.

One exception amongst the sedimentary evidence is the rare occurrence of gypsum in our cores (see Chapter 5). Although other geochemical routes such as the oxidation of pyrite in a calcareous environment can also lead to gypsum formation, most gypsum forms in recently deposited sediments in near-coastal situations as a response to extremely strong evaporation of sea-water in strongly seasonal environments (Poch *et al.* 2010). This happens today in *sabkhas* (coastal wetlands) on the shores of the Persian Gulf and in places along the North African littoral (Gunatilaka 2012). As such it is a signal for evaporative regimes stronger than present and thus extreme seasonality. Moreover, it can only have happened with sea-water incursion into the margins of the fresh groundwater lens of the Maltese lower aquifer, which could only be possible because of insufficient recharge by rainfall, before the era of groundwater abstraction by pumping. Layers in the cores containing gypsum are thus a signal for periods of low rainfall and extreme summer drought. These are indicated in Table 11.4, along with known contemporary events.

It can be seen in Table 11.4 that there is approximate coincidence between gypsum formation in our cores and major aridification events in the earlier Holocene. The later tree pollen minima in the Salina Deep Core may reflect other episodes of general aridity, although human activity in the landscape makes this less certain. There is also a coincidence between the formation of gypsum and these tree-pollen minima and several key moments in Maltese prehistory. It could therefore be suggested that climatic perturbations and particularly episodes of high seasonality present conditions placing societies under stress. These may be times where old ways of doing things and perceiving the world seemed unsuccessful, allowing new thinking and behaviours to become more easily established than at other times.

11.5. Environmental metastability and the *longue durée*

Chris O. Hunt

The *longue durée* in the Maltese Islands presents a picture of subtle, almost imperceptible change, which only really becomes apparent when comparing environmental and vegetation patterns over the millennia (Braudel 1966; Lee 2012, 2; Mathias 2015, 5) (Table 11.1). The vegetation of the rural environment of 30 years ago or of the landscape before settlement would be recognisable to a prehistoric Maltese farmer, although he or she might notice that the proportions of different plant species will have changed a little over this immense period of time. This change is because of the inherent resilience of the Maltese flora and the ability of many species to recover following impacts of natural hazards or human intervention, either because of their ability to disperse rapidly through seed or vegetatively, or for seed to remain viable in the soil over long periods until conditions again became suitable for growth. This resilience means that the basic configuration of vegetation has survived many *evènements* during the last 9000 years, including notable natural events such

Table 11.4. *Occurrence of gypsum in* FRAGSUS *cores and contemporary events (tree pollen mimima are those in the Salina Deep Core, which is most probably the least taphonomically impacted of our cores).*

Approximate date cal. BC	Depth (m)		Event
	Xemxija 1	Wied Żembaq 1	
6600	9.45–9.47 m		Tree pollen minimum and strong aridification across the western Mediterranean
6150	8.68–8.70		Tree pollen minimum and regional 8.2 ka BP aridity event
5900	8.33–8.35		Tree pollen minimum
5850	8.23–8.26		Tree pollen minimum
5450	7.85–7.87		Tree pollen minimum. Start of Għar Dalam phase
4800	7.25–7.27		Tree pollen minimum. Start of Maltese archaeological hiatus
4750		4.60–4.61	
4550		4.33–4.35	tree pollen minimum
3900	6.45–6.47		Tree pollen minimum. Start of Żebbuġ phase

as storms, tsunamis, floods, severe and long-lived droughts, and anthropogenic activities including vegetation clearance for agriculture and construction and the impacts of grazing animals. Similarly resilient, metastable vegetation is prevalent in semi-arid landscapes throughout the wider Mediterranean basin, from Jordan and Turkey in the east to Iberia and Morocco in the west (Bini *et al*. 2018; Magny *et al*. 2011; Peyron *et al*. 2017; Zanchetta *et al*. 2011; Zielhofer *et al*. 2010, 2017a & b), and the trends apparent in Table 11.1 are broadly duplicated during the Holocene across this immense area.

The Maltese (and wider Mediterranean) vegetation has its dynamic stability because of its history. For much of the Tertiary, the lands around the Mediterranean and much of North Africa supported humid forests (of which the last remnants are the Infra- and Thermo-Mediterranean woodlands, best represented in southwest Morocco). The climatic shocks of the Messinian Salinity Crisis, some six million years ago, when the Mediterranean became isolated from the Atlantic and repeatedly dried up, catalysed the development of dryland floras (Dansgaard *et al*. 1993; Pedley 1974; Puglisi 2014). The adaptability and resilience of these dryland floras was developed during the long sequence of late Pliocene and Pleistocene glacial episodes, which were marked in the Mediterranean by very rapid and unstable climate change and very considerable aridity.

One of the reasons for the stability of the human systems of the Maltese Islands over the *longue durée* has to be that the underpinning environmental systems were and are resilient. The aquifers were always present, so water was assured except possibly in the longest and hardest of droughts. It is symptomatic that freshwater molluscs were present at Xemxija through the period of declining rainfall which coincided with the last phases of the Temple Culture. Equally, the Maltese vegetation had resilient, dynamic stability and could recover from over-grazing, over-cultivation and the effects of natural hazards. Vegetation in other biomes, such as tropical rainforest or temperate deciduous forest does not have that resilience to the same degree. Degradation of less resilient vegetation would have had catastrophic consequences for people dependent on it. The changing climate did, however, have significant impacts on Maltese prehistory. The first farmers seem to have arrived shortly after the nadir of the 8.2 ka BP event. In contrast, this event in the eastern Mediterranean seems to have destabilized farming societies, sending a wave of emigrants into the western Mediterranean, including some who apparently reached Malta (Ammerman & Cavalli-Sforza 1984; Bini *et al*. 2018; Malone 2015; Whittle 1996). Life was probably a struggle for these first immigrants, whose population remained below the level of archaeological visibility for several hundred years. The only traces that we have found that reflect this early human presence are the pollen of their cereals and spores of the fungi associated with the dung of their domesticated animals.

The rise in population which culminated in the Maltese population becoming archaeologically visible during the Għar Dalam cultural phase (5400–4800 cal. BC) seems to have coincided with the start of a period of sharply rising rainfall. This may have allowed the expansion of settlement and cultivation of what were previously rather drought-prone and thus difficult soils. This climatically humid phase seems to have persisted through much of the Maltese Neolithic, including all but the latest phase of the Temple Period. It is noteworthy that there is evidence for land clearance by fire and substantial cereal cultivation during a second phase where the population seems to have effectively been archaeologically invisible, between *c*. 4800 and 3800 BC.

The Temple Period of Malta (3900–2350 cal. BC) seems to have been a time of relatively high rainfall. This seems to have allowed rainfed agriculture to flourish and cereal pollen percentages are generally high except at Burmarrad, where greater tree pollen percentages might point to an area of woodland maintained to provide timber for uses such as boat-building, construction and fuel. Prehistoric people largely depended on wood or dung for fuel, and dung would have been important for maintaining soil fertility when populations were dense and agriculture intensive. The persistence of this area of woodland further points to strong and effective social control mechanisms through a period of over 1000 years. The cereal and arboreal pollen at the other sites seems to have fluctuated during the Temple Period, perhaps consistent with some sort of long-fallow rotation.

Only in the Tarxien phase of the later part of the Temple Period (2850–2350 cal. BC) did the climate start to become more arid. The trend was not constant: there may have been an initial period of aridity, a second more humid phase and then further increased aridity. The association between locations with water and the temple sites no doubt started long before the Tarxien phase, but in a drying landscape decreasing rainfall would have made those temples such as Ġgantija that were associated with, and perhaps even controlled, persistent springs of particular significance (Ruffell *et al*. 2018).

At the end of the Tarxien phase (*c*. 2400 cal. BC) cereal cultivation seems to have ceased at most coastal locations. Only at Burmarrad did cereal pollen rise in the Tarxien Cemetery phase (2000–1500 cal. BC), perhaps because this was an inland location less vulnerable

to raiding, or perhaps because drainage into this large alluvial basin would have enabled agriculture to be maintained when it was too arid elsewhere. Tree pollen increases slightly at several sites, but whether this reflects the cessation of human activity and a decrease in grazing pressure, or whether it is a response to rising rainfall, is presently unclear.

From that point to the present day, Malta's climate seems to have been largely semi-arid, with intermittent droughts. There seem to have been shifts in the emphasis of farming, with cereals of importance in the Later Bronze Age and Punic periods, and olive cultivation beginning in the late Punic period but with increased significance in the Roman period. By Classical times, soils were extremely degraded, with the sediments of this period in the Victoria Caves being derived from unweathered bedrock. The Roman period also saw the establishment of a pine plantation at Xemxija, perhaps providing suitable timber for ship building. The plantation at Xemxija seems to have been cut down about 1000 years ago. There is little detailed evidence in our cores for later periods, but what there is points to the continuation of cultivation and grazing in a highly degraded landscape.

The continuity of the *longue durée* contrasts with rapid, catastrophic change in the modern landscape, which is currently being over-run by introduced eucalypts, wattles and the Cape violet (which have no local natural competitors and thus flourish unchecked) and by construction. It is ironic that the Maltese vegetation, which for 9000 years has survived almost unchanged despite everything that the environment, people and their animals could do to it, has perhaps changed more during the lifetime of the *FRAGSUS Project* which was set up to study the resilience of this island environment.

11.6. Implications for the human story of the Maltese Islands

Charles French, Chris O. Hunt, Caroline Malone, Katrin Fenech, Michelle Farrell, Rowan McLaughlin, Reuben Grima, Patrick J. Schembri & Simon Stoddart

Environmental studies for understanding archaeological cultures in the Maltese landscape commenced with the 1987–95 Cambridge Gozo Project, which attempted to identify preserved deposits that might illuminate a much-neglected area of archaeological study in Malta. The main achievements of that work were the analyses of molluscan remains that described the local prehistoric environment (e.g. Hunt & Schembri 1999; Schembri *et al*. 2009), since the focus on a subterranean burial complex was always unlikely to produce significant organic economic evidence, other than animal bones and molluscs. The landscape survey of the Xagħra environs attempted to classify the surface archaeology in relation to the underlying soil and geology, using the standard maps available. The collected data provided adequate information for a GIS study of human settlement set against the natural landscape (Boyle 2013), showing that settlement choice was closely linked to a range of factors including access to springs, good soils, wind direction, slope direction and gradient. However, without additional new research the interpretation of human activity and the history of the landscape itself was impossible. Thus, one goal of the multi-disciplinary approach of the *FRAGSUS Project* was to establish a much more detailed and accurate understanding of landscape evolution and its role in the development, sustainability and demise of prehistoric cultures on the Maltese Islands.

The *FRAGSUS Project* immediately recognized that once the physical surface of present-day Malta and Gozo was examined, there was an extensive captured palaeoenvironmental and archaeological story preserved in many places, notably where protected by surviving prehistoric monuments (Fig. 11.4). Initially this survival was a surprise, especially given the evident and transformative soil erosion, coupled with extensive agricultural terrace construction and encroaching modern development. The execution of new on- and off-site fieldwork rapidly demonstrated the potential horizons for new data collection and analysis. The huge potential of sedimentary cores for understanding the focus of human activity over time through using erosion as a proxy is significant. Moreover, the substantial depths of burial in the valley systems of Malta suggest that we are probably recovering a very skewed archaeological record.

Despite this new research, there is still little demonstrable archaeological evidence of people in the landscape prior to about 6000 cal. BC, but there are plenty of hints that people were already present and altering the varied Maltese landscapes from that time. Across the wider central Mediterranean area, there is little clear stratigraphic evidence for actual agricultural settlement before *c*. 6000 cal. BC west of southeastern Italy (Natali & Forgi 2018). That evidence is profoundly affected by the absence of stratigraphic control except in the western Sicilian caves of Uzzo and Oriente. In these two caves, there is Impressed Ware from 6200 cal. BC, but it is not clear how much this material was connected to any level of intensive agricultural practice (Lo Vetro & Martini 2016; Tinè & Tusa 2012). Malta, although only separated by *c*. 80 km from Sicily, was far less connected, and required adequate maritime technology to enable a reliable passage to and from the islands from nearby landmasses. It is quite possible that early prospectors visited Malta, as they had done on Cyprus

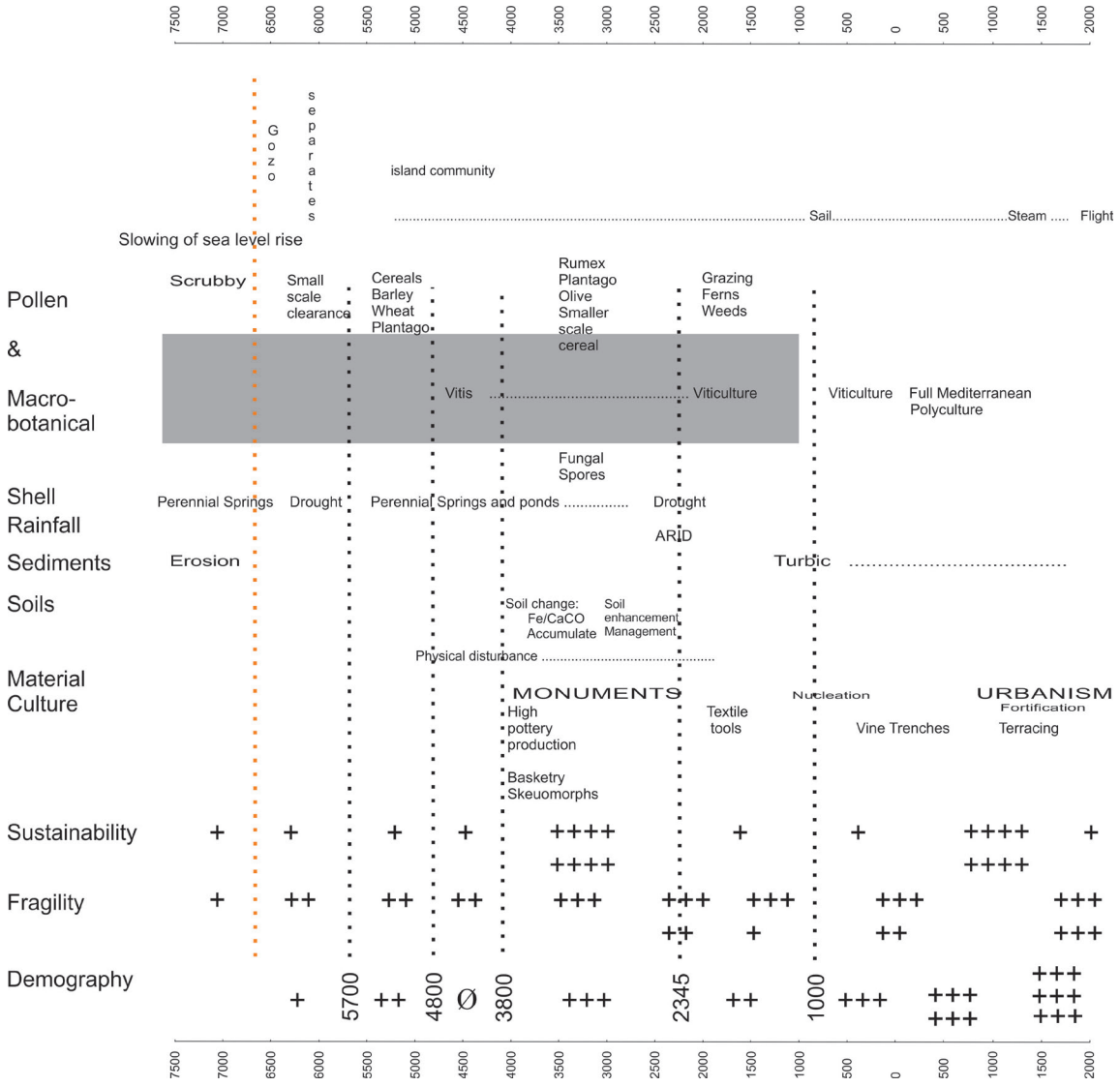

Figure 11.4. *The main elements of a new cultural-environmental story of the Maltese Islands throughout the last 10,000 years (R. McLaughlin and S. Stoddart).*

a millennium earlier (Guilaine *et al*. 2011) to exploit certain resources. That there is still no clear evidence for pre-Neolithic settlement or dated deposits with human activity connected on Malta may be explained by the likely transient nature of such visits, and the superficial remains that resulted. Perhaps periodic visitors lit fires as suggested by charcoal in the lowest parts of the Marsa 1 and Salina Deep cores. At Marsa, two recycled dates of *c*. 23,000–25,000 cal. BP (Carroll *et al*. 2012) might point to such an event, although natural fires are equally probable. Such expeditions clearly did not last long or become permanent. What is relatively clear is that longer term occupation of Malta, after it became an island, required an agricultural input, since the biomass in such a restricted area was unlikely to have been sufficient to sustain a preagricultural population on a long-term basis (Malone 1997–8). In this major respect, occupation of Sicily was very different given its much larger land mass and the recorded evidence from the western caves for a transition from Hunter Gatherer to Agricultural economy. As for the nature of the agents of this transformation of economic life, the preliminary genetic evidence (Ariano *et al*. in press) suggests a closer relationship with modern Sardinian and LBK Neolithic groups than other Mediterranean Neolithic groups, and less affinity with western hunter gatherers, since they could have had very little economic stability on such a small island archipelago.

At about 6000 cal. BC, Malta had a general background vegetation of *Pistacia* scrub woodland

expanding into a steppic landscape on the limestone plateaux, driven by increasing effective humidity within an otherwise relatively dry period. The local environment presented useful resources for early settlers. For example, well-developed brown Mediterranean soils were associated with the scrub woodland landscape, especially on the Upper Coralline Limestone bedrock areas, and rich silt loam soils on the Globigerina Limestone areas. At low altitude, there were freshwater streams and shallow, wet marshy areas in many of the valley bottoms close to the seashore, such as at Salina, Xemxija and Wied Żembaq. This earlier Holocene landscape picture soon began to change. At Salina for example, there were at least two early episodes (6858–6419 and 6350–6037 cal. BC) showing an increase in herbs and grasses as well as a sporadic presence of nettles, ribwort plantain and ruderals and some regression of scrub woodland accompanied by mycorrhizae. This change clearly hints at the presence of some bare and disturbed ground, perhaps associated with grazing fauna, and the beginnings of soil erosion, which is particularly marked in the base of the Xemxija core at the same time. That erosion was also coincident with a more general decline in rainfall in Malta, most probably associated with the wider 8.2 ka BP event leading to an aridification trend in Mediterranean coastal areas.

In the early sixth millennium BC, the first clear signs of agriculture can be observed. These involved arable cultivation with the introduction of wheat and barley, together with a ruderal flora, and ribwort plantain and nettles that indicate grazing. There was still some scrubby woodland, but the landscape became more grass-dominated with some areas of maquis and garrigue, which together suggest a relatively dry seasonal Mediterranean climate. Thus, the collected evidence indicates that there were already agriculturalists in this landscape prior to the 'Earlier Middle' Neolithic (Għar Dalam and Skorba phases), making the first inroads as farmers into a less than fully resilient landscape.

From the middle of the sixth millennium BC, the first solid evidence for human settlement is recorded at Santa Verna, in the buried deposits and land surface beneath the later fourth millennium BC temple levels. Għar Dalam-Stentinello pottery is present amongst the artefacts of that first settlement phase, a type familiar across eastern Sicily and Calabria and off-shore islands in the second phase of Neolithic populations. It is very interesting that Malta appears currently to lack (see Chapter 2 & Volume 2) the first *impressed* phase of pottery which is present in Southern Italy and Sicily (Natali & Forgi 2018) dating to *c*. 6200 BC. The chronology of the current pottery repertoire from Malta compares well with the best dated sites of Capo Alfière in Calabria (Morter 1990) and Curinga (Ammerman 1985), and reflects a trend of settlement and farming over the entire region (Malone 2015). The charred remains of the wheat, barley and pulses grown on Malta and the bones of domesticated sheep, goat, pig and cattle are found in close association with the pottery during this phase of its settlement.

As the sixth millennium progressed into the fifth millennium BC, the trends of expanding settlement and agriculture continued, and especially the expansion of plants indicative of pastoral activities. Cereal cultivation did continue however, probably in fits and starts and at different frequencies, with spatial variations. The corroborative evidence of macro-botanical data of wheat/barley and lentils from the buried soils beneath the Santa Verna and Skorba temples date to about 5400–4900 cal. BC. The varied mosaic of arable and pastoral agriculture could be related to the topography and geology of the islands (see Chapter 6) as much as human endeavour, with the more water retentive Blue Clay geology and Greensand/Upper Coralline Limestone geological contact zone associated with springs and more structured soils, as opposed to the free-draining Globigerina Limestone areas. It is also possible that the Blue Clay valley areas could have been utilized differently compared with the adjacent higher limestone areas, and were instead used for livestock pannage with easy access to springs, as well as natural raw materials such as reeds and withies for house building purposes.

Importantly, there may have been some management of the Upper Coralline Limestone slopes and soils from about 4650 cal. BC. The evidence is slight, but has merit. First, there is a slight increase in *Theligonum* pollen, characteristic of dry rocky environments such as those provided by terrace walls, alongside palynological evidence suggestive of increased agricultural activity. This evidence is seen in the Burmarrad sequence, where it was suggested that similar management may reflect the advent of terrace construction in the landscape (Djamali *et al.* 2013). Although other evidence for this was not identified then by the Bumarrad project, there is now good evidence of soil amendment of topsoils with settlement-derived refuse beneath the Santa Verna and Skorba temples at some point prior to *c*. 3800 cal. BC. Similar amendment was also identified later in the earlier to mid-third millennium BC at Ġgantija. These examples certainly point to early attempts at soil management of arable land on the upper margins of the Upper Coralline Limestone plateaux. There is also evidence, in the form of algae and dinoflagellate cysts, for irrigation at Santa Verna and Ġganitija in association with these very early soil amendments.

From about 4550 cal. BC onwards, there appears to have been a general decline in agricultural activities,

with an apparent reduction in intensive cereal cultivation coupled with a relative expansion in scrub/tree pollen (Figs. 11.1–11.3). This change could be coincident with a period of higher effective rainfall, and there appears to be palynological, molluscan and soil evidence from this project for a period of relatively higher moisture considerably earlier than the beginning of temple construction, specifically between about 4750–4250 cal. BC. This evidence, however, is in contrast to the generally decreasing rainfall trend seen elsewhere around the Mediterranean at this time (e.g. Magny *et al*. 2011; Sadori *et al*. 2008, 2016; Jaouadi *et al*. 2016; Bini *et al*. 2018). At the Skorba and Santa Verna temple sites during this period, there is an apparent hiatus in the archaeological occupation evidence of settlement beneath the later temples, which reveals a very clear gap in the comprehensive radiocarbon dating records now available (see Chapter 2 & Volume 2, Chapter 2).

Nonetheless, the palynological records clearly imply that cereal cultivation continued throughout the mid- to later fifth millennium BC, coupled with on-going soil erosion and aggradation in many of the valley sequences. Although it is tempting to suggest a major depopulation of the islands, we could also consider the changes as indicative of a reorganization of less intensive activities and landscape exploitation. There is what seems to be evidence for human activity in the landscape from the pollen analyses, which show the continuation of cereal pollen and indicators of grazing throughout the fifth millennium BC. While livestock, if abandoned by their keepers, might be expected to continue living in the Maltese Islands, domesticated cereals are dependent on people for their propagation and would be unlikely to continue as a significant component of the vegetation without human intervention. However, evidence of early agricultural settlement elsewhere (i.e. Cyprus especially, but generally across early Neolithic Europe) does indicate that early settlers frequently abandoned their attempts to establish occupation of a new area (see also Shennan 2018). There are a multitude of reasons for this, but a small restricted and relatively isolated island would have presented challenges to communities more familiar with extensive subsistence practices in a larger, connected landmass where migration or seasonal movement was feasible.

From the Middle–Later Neolithic period at about 4000 cal. BC, the Maltese island landscapes became primarily open land used for grazing, probably coupled with intensifying cereal cultivation. This is a period of apparent intensive reoccupation, or at least a growing population and denser settlement. It is also a period during which a strongly Sicilian-related culture became established on Malta (Żebbuġ) and saw the development of aggregations of domestic and more elaborate proto-temple structures. Many, if not all, of the sites that later became major megalithic buildings (temples) had their origins in this period (Bonanno *et al*. 1990) which was also characterized by subterranean rock cut tombs, clustered for the most part in small cemeteries. Evidently locales, territories and identities were important components of settlement and burial for the Żebbuġ communities. It was a period of intensive production, as seen by the enormous quantities of pottery made and fired during the Żebbuġ phase (*c*. 3800–3600 cal. BC), indicative of storage and consumption at a new level when compared to previous periods (see Volume 2, Chapter 10). The firing of the pottery in particular might suggest a significant impact on timber resources, but there is little sign of this seen in the pollen record (Fig. 11.1).

In association with expansion and intensification, soil change was occurring as evidenced by the increasing secondary formation of both silt-sized calcium carbonate and amorphous iron oxides in the later Neolithic palaeosol profiles. As mentioned above, there are also indications of soil amendment at Santa Verna, Ġgantija and Skorba. Nonetheless, in places these changes occurred at slightly different times, represented by short-lived peaks in the pollen record of lentisk scrub regeneration at Salina and Burmarrad, which perhaps indicate shifting patterns of exploitation in the landscape and even some kind of soil and/or land management, possibly even long-fallow crop rotation in different fields. The creation of several megalithic monuments on the Globigerina Limestone lowlands of southeast Malta may also be an indication of demographic shifts related to changing patterns of exploitation. In tandem, the frequencies and biodiversity of agricultural weeds in the pollen assemblages increased, suggesting a proliferation of these taxa. This ruderal flora could indicate dry and patchy open ground, but would have been ideal for pastoral activities, shifting over relatively short distances. Conversely, there may also have been reduced productivity from land left to long periods of fallow, which is at odds with the indications of settlement expansion and the likely demands on increased production. The presence of spores of soil fungi however, suggest continuing soil erosion, with many of the valleys such as Xemxija infilled with eroded soil material, and perhaps this signals an economic system that was already showing signs of stress and instabilty. Furthermore, the fluctuating richness of pottery finds and the sporadic nature of occupation at sites like Taċ-Ċawla and Santa Verna suggest that human activity may have oscillated to some degree throughout the later fourth to third millennia BC (see Volume 2, Chapters 3, 4 & 10).

Towards the end of the Neolithic, from around 2700 cal. BC, there may have been a major shift in emphasis in landscape use, associated with socio-cultural changes which are not fully understood. Many of the smaller temple sites were abandoned (including Santa Verna and Kordin III), whilst others (such as Ġgantija) grew in significance and perhaps in economic influence (see Volume 2, Chapters 4–6). The many interpretations of the role and function of megalithic temples within the later Neolithic society of Malta are varied and lively, but it is highly likely that they played an important economic and social role. The interior spaces of the megalithic structures contained storage and cooking facilities, feasting debris and masses of pottery, grindstones and installations intended to display most likely, food and feast. Therefore, one interpretation is that the structures were used in competitive feasting (Malone 2017; Malone *et al*. 2016; Barratt *et al.* 2020).

There are very high (>10 per cent) cereal pollen frequencies at or very near to several temple sites during the Temple Period (Żebbuġ-Saflieni-Tarxien phases) of *c*. 3800–2400/2200 cal. BC which is compelling evidence for food processing at these sites. The increased cereal pollen may also coincide with two periods of relatively higher effective moisture at about 3450–3050 and 2850–2650 cal. BC. There were also vines evident in the Żebbuġ phase and carob occurred in the Tarxien phase, both plants representing new resources which could suggest a broadening of the subsistence base, as well as an increase in processing activities in close proximity to some of the temple sites in their latest phase of use.

In the last centuries of the third millennium BC, several changes occurred simultaneously at the end of the Temple period. Cereals declined, scrub woodland contracted, the steppe areas appear to have been drier, and the once marshy, lower valley zones were drying out. These changes are complemented by both the archaeological and osteological data from Gozo which suggest changing and more difficult times around 2550–2450 cal. BC (see Volumes 2 & 3). At the same time, there are indications of drought in the molluscan records from the deep cores in Malta (see Chapter 4). In addition, wider regional records from the Mediterranean area indicate that a significant change in hydrological conditions was taking place, with more arid climatic conditions and locally cooler temperatures taking hold between about 2350 and 1850 cal. BC, that were locally and seasonally varied (Bini *et al.* 2018; Di Rita & Magri 2019). Concurrently, in the valley/coastal zones at Salina, Xemxija and Wied Żembaq, there is evidence to demonstrate a decline in both cultivation and pastoral activities, suggesting a shift away from exploitation of the coastal margin zones to a renewed focus on more inland areas. Although it is not possible to identify many new archaeological data during this period, given the paucity of records for the final phases of the Temple Culture and its successor in most investigated sites, the palynological and soil erosion records corroborate the final centuries of the third millennium as a period of distinct land-use change.

During the Early Bronze Age, current evidence suggests that settlement partly continued in the same locations such as Ġgantija and the Xagħra Brochtorff Circle, partly returned to old locations such as Santa Verna, and partly started the trend toward defendable locations such as Ta' Kuljat (see Chapter 7). This settlement shift all occurred after the well-recorded 4.2 ka BP climate event, and there is extensive evidence for widespread cultivation and agricultural activities during the Bronze Age occurring during a time of climatic stability. By contrast, the soil evidence indicates accelerated accumulation in many of the valley bottoms from at least the mid-second millennium BC, such as at Marsalforn, Salina, Xemxija and Skorba. This erosion could indicate that new areas of the landscape in the hinterland valleys were being exploited for the first time, and/or were being more intensively utilized. Interestingly, the freshwater input to valley bottoms such as at Xemxija was now drastically reduced, which could reflect greater uptake of groundwater higher up the catchment associated with increased agricultural activities. Moreover, whilst these features could well be related to the establishment of terraced field systems, they may well be more coincident with the Upper Coralline Limestone areas than anywhere else. Unfortunately, well dated evidence for the extensive development of terracing in later prehistory is not yet available from these islands.

By the Final Bronze Age, settlement tended to be concentrated either on prominent defendable inland hill-tops (In-Nuffara for example) or on defensive coastal promontories (such as Borġ in-Nadur and Baħrija). Such locations frequently had no direct access to agricultural land. The main period of destabilization in the landscape evident in the sediment sequences investigated in this project dates to between *c*. 1550 and 1000 cal. BC. Culturally, this 'Borġ in-Nadur' time frame saw significant changes in settlement patterns on Malta, compared with the previous more stable periods. These changes included the construction of defended settlements in prominent locations (Tanasi & Vella 2015) (see Chapter 7) and probably also the contemporary 'cart-ruts' that led from hill-tops to valley bottoms (Evans 1971, 203; Magro Conti & Saliba 2007). These latter features may have served to draw soil up-hill for agricultural purposes, so that food could be grown near the defended settlements, rather

than in valley bottoms as is the case today. This drastic intervention differed from management practices in the Neolithic and Temple periods and may well have led to the loss of more soil than before. Certainly, the stratigraphic and OSL evidence from the Marsalforn valley in Gozo, for example, indicates severe erosion and substantial accumulations of eroded soil material in valley bottoms from this same period. More geo-archaeological testing of the cultivated valley-scapes of today is required to judge how widespread a phenomenon soil erosion was during the latter half of the second millennium BC across the Maltese Islands, but every indication is that this was extensive.

Evidence for earlier prehistoric terracing is much harder to pin down. Certainly, the earlier Holocene palaeosols under the Santa Verna, Ġgantija and Skorba temple sites all exhibit indications of having received both settlement waste and also some soil build-up. This is most probably indicative of some soil management and conservation practices, but it does not necessarily imply that terraces were being constructed in the later Neolithic over the whole landscape. Djamali *et al*. (2013) have suggested that *Theligonum* (dog cabbage) pollen may be used to infer the establishment of terraces, based on the observation that in Mediterranean France and Corsica terrace walls are intensively colonized by this taxon. In Malta, there are indeed increases in *Theligonum* pollen (to *c*. 5 per cent) at Burmarrad between *c*. 4650 and 2550 cal. BC. There is also a slight increase in *Theligonum* pollen which accompanies other evidence for increased agricultural activity, and it is consistently present from *c*. 5000 cal. BC throughout the Salina Deep Core pollen sequence. However, one indicator of dry rocky ground is probably an unreliable single identifying feature for the advent of terracing. It is much more likely that terracing began in response to the need from the latter part of the second millennium BC to slow soil erosion and conserve soil and limited moisture, but clearly this question requires much more extensive proof from detailed landscape analyses with good chronological control (see Chapter 7).

In addition to this circumstantial *Theligonum* 'indicator species' evidence, there are a number of other palynological, stratigraphic and palaeosol hints that point to human management and exploitation of the landscape, which of course could include terrace construction. Shrubs/scrub and trees decline from about 4000 cal. BC, but especially towards the end of the Temple period from *c*. 2350 cal. BC. This appears to be coincident with pollen evidence for the intensification of agricultural activities, both arable and pastoral. At the same time, the palaeosol record is exhibiting strong hints of increasing aridification, making the soils around several of the Neolithic temples much more calcitic and affected by oxidation and rubification. At this time and slightly later within the late third and into the early to mid-second millennia BC, there are strong hints of human attempts to enhance soil A horizons through the addition of settlement-derived midden material, for example soil aggradation at Ġgantija that may indicate a managed arable field. There is also evidence for substantial hillwash erosion and accumulation in many valleys such as Marsalforn on Gozo and Xemxija on Malta. All of these datasets suggest widespread greater attempts to manage, manipulate and adapt the agricultural landscapes of the Maltese Islands physically, and these may be our best currently available indicators that terracing of some valley slopes had begun.

Soil erosion management and terracing trends appear to continue and intensify over time most probably aggravated by autumn rain storms and minimal vegetative cover during the later Bronze Age, Punic and Roman periods (Mitchell & Dewdney 1961; Mayes 2001). Settlement expanded and it seems to have become more widespread, especially on the plateau areas (see Chapter 7). Cereal cultivation increased in the Punic period, and, by the time of the Roman occupation, intensive landscape management and terrace construction was routinely practised to control serious soil erosion. The same erosion was coincident with domesticated olive and vine cultivation, probably on a widespread and intensive scale (Bouby *et al*. 2013; Caracuta 2020; Carroll *et al*. 2012). Although some trees and shrubs persisted, the landscape mainly supported a ruderal dominated grazing land, which was degraded and continued to be subject to soil erosion during the winter rains. Freshwater stream and pond habitats generally continued to decrease.

From the Roman period onwards, the vegetation and landscape features described persisted, but pine trees increased in some areas and that increase continued into the Medieval period, alongside grassland and pasture. The more intense soil erosion of the Roman period was undoubtedly enhanced by the effects of the introduction and use of the mould-board plough (Margaritis & Jones 2008). That technology turned the soil clods over and thereby increased their exposure to both drying out and rain-splash generated erosion, in turn generating further soil erosion downslope (Jongerius 1983; Kirkby 1969; Lewis 2012). Soil erosion was also exacerbated by the widespread and risky strategy of olive and vine cultivation; risky since traditional management typically left the soil bare and loose. This would have led to increased vulnerability to soil erosion, unless the crops were grown together with an understory of vegetation or multi-cropping was practised (Loughran *et al*. 2000; Kosmas *et al*. 1997;

French 2010). The outcome was the development of open karstland, with poor, patchy vegetation and frequent zones of bare soil predominant across the landscape.

From the fourteenth century AD onwards, there was increasing nucleation of settlements, with a general tendency to occupy inland and upland areas (see Chapters 7 & 10). A combination of subsistence arable farming and livestock grazing was the norm with scattered farmsteads in the wider countryside (Chapter 9). By the late Medieval period, many villages were deserted, and the focus shifted to the few urban centres in defendable positions such as Mdina, Birgu and Gozo Castello. Only in the Knights of St John period from the later sixteenth century did the Grand Harbour area (later Valletta) become the main commercial hub of Malta. The early modern period saw new areas of the landscape being exploited and developed with terracing, such as the Blue Clay geology slopes in the Ramla valley of Gozo. The Knights Period also saw terracing systems installed over almost all parts of the islands. This regime of management was effectively continued in the British Period during the nineteenth century, with cotton introduced alongside cereals forming a very important crop in its own right. Indeed, as seen in the cadastral maps (*cabrei*) which also recorded land-use, a highly developed terraced and enclosed landscape arose as a result of this progressive intensification, which culminated around the end of the nineteenth century. Its traces are still visible today in most valley landscapes on the Maltese Islands.

Another enduring characteristic of the exploitation of the Maltese landscape is the mixed strategies that were developed in response to the very varied constraints and opportunities offered by different parts of the islands, often in close proximity. Like many Mediterranean environments (Horden & Purcell 2000), the Maltese archipelago presents a number of highly fragmented landscapes (see Chapter 6). Agricultural practices and subsistence strategies were and are heavily conditioned by these variable characteristics. Land unsuitable for crop cultivation may provide ideal environments for sheep and goat grazing. Many parts of the coastal areas were probably always too precipitous and inclement to host good arable land, especially on Malta's windy and dry northwestern coastline, likewise the Blue Clay valley slopes, especially in northern Malta and Gozo. Cultivable land irrigated by a source of freshwater allows different crops to be grown compared with land that receives no water other than rainfall, making some zones of the landscape, such as the Greensand/Upper Coralline geological boundary zone on the north side of the Ramla valley and Xagħra plateau, more sought after than others. The response to these constraints was often the long-term development of mixed strategies which were ultimately more resilient against climate and crop failure (McLaughlin *et al*. 2018).

Although Malta is an island landscape, many of its characteristics are shared with those countries of the Mediterranean fringe of southern Europe. It would have been similarly affected by a fast-rising sea level and loss of coastal margin land during the early Holocene, as well as the disappearance of wild animal species, even if it acted as an isolated refugium for a while. The *FRAGSUS Project* has definitively revealed that people were in this landscape as early as *c.* 6000 cal. BC, who were farming and, at least in part, beginning to de-stabilize the landscape. Yet in spite of over a millennium and a half of this palaeoenvironmental evidence of activity, there are few if any known sites until the construction of the first temples from about 3900 cal. BC. Does this mean three cycles of Neolithic colonization? The first cycle before 6000 cal. BC appears to have occupied a part of the landscape that is no longer preserved or too fragile to have been so far detected. The second cycle has been detected at least under later monuments, and its practitioners may have moved around the landscape to maintain their resilience. The third cycle adopted new social strategies embedded in the 'temple' structures, focused on watered horticultural enclaves within the fragmented landscape, and was for fifteen hundred years highly successful. These issues are further discussed from a site based perspective in Volume 2. Within these generalized patterns, there were different regional trajectories in play, since the first temple sites in Gozo and northern Malta underwent modifications throughout the Neolithic through to the mid- to later third millennium BC. In contrast, the temples in south and east Malta appear to have developed slightly later and were apparently abandoned somewhat earlier. Whilst there is no break in later Neolithic Tarxien phase evidence, there was decreased farming activity in the later third millennium BC. Whether this decrease reflects population reduction, or people emigrating from the islands, or just a different, more dispersed form of subsistence farming is still to be established.

The degree of connectivity in the Later Neolithic is still difficult to measure with precision. Much of the material and organic world was locally sourced. Some parts of the material world (e.g. some chert, obsidian and greenstones) were procured in quite modest quantities from outside the islands. Some individuals (or their ancestors) also had histories from outside worlds, as indicated by the emerging genetic history of some individuals from Xagħra. These issues are more

thoroughly explored, and increasingly quantified, (see Volumes 2 & 3). Some connectivity with lands beyond Malta were always sustained, if not always visible in the archaeological record, but the limited technologies of navigation would have provided a substantial brake on movement of materials and people, until it becomes much more widespread from Phoenician, Punic and Roman times onwards. Increasing trade and exchange may well have gone hand-in-hand with a greater resilience of the islands' economy and therefore created the potential for population growth (see Chapter 7). This combined economic development and population growth with a wide social hierarchy became much more evident from the mid-fifteenth century onwards with influences from different parts of Europe, namely the Arabs, the Normans and the Spanish.

Throughout these later periods, the importance of soil and preventing its erosion must have been a constant concern. Indeed the Medieval 'Red Soil Law' was incorporated into the Fertile Soils (Preservation) Act of 1973, where red soil discovered on building sites has to be gathered and saved. As land quality varies with respect to the geology and different zones of each valley landscape over very short distances, this would have favoured an interconnected arable and pastoral economy. Increasing new land ownership from the sixteenth century AD may then have enabled a shift from a more subsistence base to greater cash-cropping and land-use intensification with the development of courtyarded farmsteads and new towns. Despite evidence of some ebb and flow of people and activity in the Medieval period with de-population from time to time (eg. Gozo in AD 1551, Knights period from AD 1565–1798, British period) there was renewed occupation of the islands and the expansionary uptake of land for farming, especially on to the Blue Clay valleys of Gozo.

The work of the *FRAGSUS Project* reveals immense variation in the development and use of the Maltese landscape over very short periods of time. When set within the wider Mediterranean climatic and palaeoenvironmental sequences (cf. Bini *et al.* 2018), the data obtained on Malta and Gozo correspond with regional trends, but there is not necessarily a direct correlation of events in time. Clearly wider regional and sub-regional environmental changes, especially changing rainfall patterns, affected the livelihoods of the prehistoric people of Malta and Gozo. Each valley, however, tells its own slightly different story of agricultural exploitation, erosion and management, reflecting a wider regional picture of fragmented variation. During the lengthy Maltese Neolithic period (over 3000 years in duration), temple construction and land-use can be set against a changing and extensively exploited agricultural landscape. Over centuries, the landscape of the Temple Period suffered vegetational and soil change and erosion, with changing patterns of use and economic productivity governed by a number of factors. These patterns vary according to location, slope by slope, valley by valley, geological substrate by substrate, and potentially inform on the longevity and economic success of the many temple sites, some of which were abandoned earlier in the sequence. Such variation is observed in the Pwales valley at Xemxija in Malta, where there was evident and sustained soil erosion from the earliest Neolithic activity, but at Salina towards the coast the valley landscape remained wet and marshy throughout much of prehistory. On the Xagħra plateau on Gozo, there was sustained human exploitation associated with soil-type change and thinning for at least a millennium and a half through much of the Neolithic period. Although the soils on this plateau were degrading slowly, there appears to have been no severe erosion evident in the associated valleys until about a millennium later from the mid- to later second millennium BC. Thus, there was probably much more understanding by prehistoric people about how to utilize and cope with the inherently unstable landscapes of Malta and harness the resilience in the soil-vegetational system, despite the longer-term aridifying trend, than has been credited hitherto. As the saying goes, *Mingħajr art u ħamrija, m'hemmx sinjorija* (without land and soil, there is no wealth) (Joe Inguanez, pers. comm.).

Today, it is to be hoped that this underlying landscape resilience will continue despite the creeping advance of modern development, industrialized exploitation and settlement pressure. The goals of the *FRAGSUS Project* were designed especially to understand the economic and technological means that sustained an ancient culture in a very small island context. In large part, that goal has been met, and with it, a greater understanding of the much longer time frame within which the Maltese Islands evolved. Undoubtedly, many of the aspirations to expand knowledge and understanding have been achieved, especially insight into the close association of local environment, soil and climatic instability that supported complex social systems in the past, and potentially will continue to do so into the future. An important lesson of balance emerges from this study, one that demonstrates conclusively that when climate fluctuations occur, human over-exploitation of natural resources in fragile environments invariably results in episodes of quite dramatic retrenchment, and even complete collapse. This is repeating story of human civilization in marginal areas, such as Iraq and the

Maya lowlands (Mathews 2005; Webster & Evans 2005), but it is also one repeated in regions of much greater environmental wealth and resilience.

As the companion volumes in this project publication series demonstrate, the human story of survival in early Malta is one of resourcefulness coupled with destructive activities, advanced social structures and the ability to intensify activity in a manner only seen in small island systems in prehistory. The hope has been to see patterns in the past that inform us in the present, and perhaps influence human behaviours in the future, enabling conservation and protection of vulnerable environments, whatever the wider climatic world may act out.

References

Aalen, F.H.A., 1984. Vernacular Buildings in Cephalonia, Ionian Islands, Greece. *Journal of Cultural Geography* 4 (2), 56–72.

Abela, G.F., 1647. *Della descrittione di Malta*. Malta: Paolo Bonacota.

Abel-Schaad, D. & J.A. López-Sáez, 2013. Vegetation changes in relation to fire history and human activities at the Peña Negra mire (Bejar Range, Iberian Central Mountain System, Spain) during the past 4,000 years. *Vegetation History and Archaeobotany* 22, 199–214.

Aguilar, J., J.L. Guardiola, E. Barahona, C. Dorronsoro & F. Santos, 1983. Clay illuviation in calcareous soils, in *Soil Micromorphology*, eds. P. Bullock & C.P. Murphy. Berkhamsted: A.B. Academic, 541–50.

Aitken, M.J., 1983. Dose rate data in SI units. *PACT: Journal of the European Study Group on Physical, Chemical and Mathematical Techniques Applied to Archaeology* 9, 69–76.

Albert, P.G., E.L. Tomlinson., V.C. Smith, A. Di Roberto, A. Todman, M. Rosi, M. Marani, W. Muller & M.A. Menzies, 2012. Marine-continental tephra correlations: Volcanic glass geochemistry from the Marsili Basin and the Aeolian Islands, Southern Tyrrhenian Sea, Italy. *Journal of Volcanology and Geothermal Research* 229 (Supplement C), 74–94.

Alberti, G., 2017. TRANSIT: a GIS toolbox for estimating the duration of ancient sail-powered navigation. *Cartography and Geographic Information Science* 46, 1–19.

Alberti, G., R. Grima & N.C. Vella, 2018. The use of geographical information system and 1860s cadastral data to model agricultural suitability before heavy mechanization. A case study from Malta. *Plos One* 13 (2), 1–28.

Alberts, E.E., W.C. Moldenhauer & G.R. Foster, 1980. Soil aggregates and primary particles transported in rill and interrill flow. *Soil Science Society of America Journal* 44, 590–5.

Aldenderfer, M.S., 1998. *Montane Foragers. Asana and the South-Central Andean Archaic*. Iowa City: University of Iowa Press.

Alessio, A., L. Allegri, F. Bella, G. Calderoni, C. Cortesi, G. Dai Pra, D. De Rita, D. Esu, M. Follieri, S. Improta, D. Magri, B. Narcisi, V. Petrone & L. Sadori, 1986. 14C dating, Geochemical Features, Faunistic and Pollen Analyses of the uppermost 10 m Cores from Valle di Castiglione (Roma, Italy). *Geologica Romana* 25, 287–308.

Allen, M.J. & B. Eastabrook, 2017. (Some thoughts on) using molluscs for landscape reconstruction and ecology in Malta, in *Molluscs in Archaeology: Methods, Approaches and Applications*, ed. M.J. Allen. Oxford: Oxbow Books, 165–78.

Allen, M.J. & R.I. Macphail, 1987. Micromorphology and magnetic susceptibility studies: their combined role in interpreting archaeological soils and sediments, in *Soil Micromorphology*, eds. N. Fedoroff, L.M. Bresson & M-A. Courty. Paris: Association Francaise pour l'Etude du Sol, 669–76.

Alley, R.B., P.A. Mayewski, T. Sowers, M. Stuiver, K.C. Taylor & P.U. Clark, 1997. Holocene climatic instability; A prominent, widespread event 8200 yr ago. *Geology* 25, 483–6.

Alexander, D., 1988. A review of the physical geography of Malta and its significance for tectonic geomorphology. *Quaternary Science Reviews* 7, 41–53.

Aloisio, M.A., 2007. A Test-Case for Regional Market Integration? The Grain Trade between Malta and Sicily in the Late Middle Ages, in *Money, Markets and Trade in Late Medieval Europe: Essays in Honour of John H. A. Munro*, eds. L. Armstrong, I. Elbl, I. & M.M. Elbl. Leiden: Brill, 297–309.

Ammerman, A., 1985. *The Acconia Survey: Neolithic settlement and the Obsidian Trade.* London: Institute of Archaeology.

Ammerman, A.J. & Cavalli-Sforza, L. 1984. *The Neolithic Transition and the Genetics of Population in Europe*. Princeton: Princeton University Press.

Anastasi, M., (ed.) 2019. *Pottery from Roman Malta.* Oxford: Archaeopress.

Anastasi, M. & N.C. Vella, 2018. Olive oil production technology in Roman Malta, in *The Lure of the Antique: Essays on Malta and Mediterranean Archaeology in Honour of Anthony Bonanno*, eds. N.C. Vella, A.J. Frendo & H.C.R. Vella. Leuven: Peeters, 275–300.

Anderson, E.W., 1997. The wied: a representative Mediterranean landform. *GeoJournal* 44, 111–14.

Anderson, E.W. & P.J. Schembri, 1989. *Coastal zone Survey of the Maltese Islands report*. Beltissebh, Malta: Planning Services Division, Works Department.

Angulo, R.J., M.C. De Souza, M.L. Assine, L.C.R. Pessenda & S.T. Disaro, 2008. Chronostratigraphy and radiocarbon age inversion in the Holocene regressive barrier of Paraná, southern Brazil. *Marine Geology* 252 (3), 111–19.

Argant, J., J.A. López-Sàez & P. Bintz 2006. Exploring the ancient occupation of a high altitude site (Lake Lauzon, France): comparison between pollen and non-pollen palynomorphs. *Review of Palaeobotany and Palynology* 141, 151–63.

Ariano, B., R. McLaughlin, R. Power, J. Stock, B. Mercieca-Spiteri, S. Stoddart, C. Malone & D. Bradley, in press. aDNA: Origins, in *Temple People. Bioarchaeology, Resilience and Culture in Prehistoric Malta,* eds. S. Stoddart, R. Power, J. Thompson, B. Mercieca, R., McLaughlin & C. Malone. Cambridge: McDonald Institute for Archaeological Research.

Arnon, A., T. Svoray & E.D. Ungar, 2011. The spatial dimension of pastoral herding: A case study from the northern Negev. *Israel Journal of Ecology & Evolution* 57 (1–2), 129–49.

Armstrong, K., C. Tsigonaki, A. Sarris, A. & N. Coutsinas, 2016. Site Location Modelling and Prediction on Early Byzantine Crete: Methods Employed, Challenges Encountered, in *Keep the Revolution Going. Proceedings of the 43rd Annual Conference on Computer Applications and Quantitative Methods in Archaeology*, eds. S. Campana, R. Scopigno, G. Carpentiero & M. Cirillo. Oxford: Archaeopress, 659–68.

Ashby, T., 1915. Roman Malta. *Journal of Roman Studies* 5, 25–80.

Ashby, T., R.N. Bradley, T.E. Peet & N. Tagliaferro, 1913. Excavations in 1908–11 in various megalithic buildings in Malta and Gozo. *Papers of the British School at Rome* 6, 1–126.

Asioli, A., F. Trincardi, J.J. Lowe & F. Oldfield, 1999. Short-term climate changes during the last glacial-Holocene transition: Comparison between Mediterranean records and the GRIP event stratigraphy. *Journal of Quaternary Science* 14, 373–81.

Asouti, K., C. Kabukcu, C.E. White, I. Kuijt, B. Finlayson & C. Makarewicz, 2015. Early Holocene woodland vegetation and human impacts in the arid zone of the southern Levant. *The Holocene* 25 (10), 1565–80.

Avery, B.W. & C.L. Bascomb (eds.), 1974. *Soil Survey Laboratory Methods*. Harpenden: Soil Survey Technical Monograph No. 6.

Azzopardi, E. 2013. The Shipwrecks of Xlendi Bay, Gozo, Malta. *International Journal of Nautical Archaeology* 42 (2), 286–95.

Azzopardi, G., 2006–7. Cremation burials in Early Bronze Age Malta. *Malta Archaeological Review* 8, 9–17.

Azzopardi, G., 2014. 'Religious Landscapes and Identities of the Maltese Islands in a Mediterranean Context: 700 B.C. – A.D. 500.' Unpublished PhD thesis, University of Durham.

Azzopardi, G. & A. Pace, 2008. 'Economic landscapes of the Maltese Islands during antiquity: a survey of ancient wine presses.' Poster presented at the XVII Congresso Internazionale di Archeologia Classica, Rome.

Baddeley, A., E. Rubak & R. Turner, 2016. *Spatial Point Patterns. Methodology and Applications with R*. Boca Raton: CRC Press.

Baillie, M.G.L., 1999. *Exodus to Arthur: Catastrophic Encounters with Comets.* London: B.T. Batsford.

Baldassini, N. & A. Di Stefano, 2015. New insights on the Oligo–Miocene succession bearing phosphatic layers of the Maltese Archipelago. *Italian Journal of Geosciences* 134 (2), 355–66.

Barber, D.C., A. Dyke, C. Hillaire-Marcel, A.E. Jennings, J.T. Andrews, M.W. Kerwin, G. Bilodeau, R. McNeely, J. Southon, M.D. Morehead & J.-M. Gagnon, 1999. Forcing of the cold event of 8,200 years ago by catastrophic drainage of Laurentide lakes. *Nature* 400, 344–8.

Barker, G., 1995. *A Mediterranean Valley: Landscape Archaeology and Annales History in the Biferno Valley*. London: Leicester University Press.

Barker, G., 1996. *The Biferno Valley: Archaeology as Annales History in a Mediterranean Valley*. Leicester: Leicester University Press.

Barker, G. & C.O. Hunt, 1995. Quaternary valley floor erosion and alluviation in the Biferno valley, Molise, Italy: the role of tectonics, climate, sea level change and human activity, in *Mediterranean Quaternary River Environments*, eds. J.C. Woodward, M.G. Macklin & J. Lewin. Rotterdam: Balkema, 145–57.

Barker, G., D. Gilbertson, B. Jones & D.J. Mattingley (eds.), 1996. *Farming the Desert: The UNESCO Libyan Valleys Survey*. Paris: UNESCO.

Barker, G., D. Gilbertson & D. Mattingly (eds.), 2007. *Archaeology and Desertification: The Wadi Faynan Landscape Survey, Southern Jordan*. (CBRL Levant Series Volume 6.) Oxford: Oxbow Books, 445–64.

Barratt, R., R. McLaughlin, C. Malone & S. Stoddart, 2018. Celebrations in Prehistoric Malta. *World Archaeology* 50 (2), 271–84.

Barratt, R., Malone, C., McLaughlin, R. & Parkinson, E., 2020. Hypogea and the clubhouse: Neolithic Malta's houses of the living and houses of the dead. In Barclay, A., Field, D. & Leary, J. (eds.), *Houses of the Dead*. Oxford: Oxbow, 15–38.

Barrowclough, D.A. & C. Malone (eds.), 2007. *Cult in context: reconsidering ritual in archaeology.* Oxford: Oxbow Books.

Bauer, A.M. & M. Bhan, 2018. *Climate without Nature: A Critical Anthropology of the Anthropocene*. Cambridge: Cambridge University Press.

Behrensmeyer, A.K. & S.M. Kidwell, 1985. Taphonomy's contributions to paleobiology. *Paleobiology* 11, 105–19.

Bell, T., A. Wilson & A. Wickham, 2002. Tracking the Samnites: Landscape and Communications Routes in the Sangro Valley, Italy. *American Journal of Archaeology* 106 (2), 169.

Bengtsson, L. & M. Enell, 1986. Chemical analysis, in *Handbook of Holocene palaeoecology and palaeohydrology*, ed. B.E. Berglund. Chichester: John Wiley, 323–451.

Benito, G., R. Brazdil, J. Herget & M.J. Machado, 2015. Quantitative historical hydrology in Europe. *Hydrology and Earth System Science* 19, 3517–39.

Benjamin, D.J., J.O. Berger & V.E. Johnson, 2018. Redefine statistical significance. *Nature Human Behaviour* 2, 6–10.

Benjamin, J., A. Rovere, A. Fontana, S. Furlani, M. Vacchi, R.H. Inglis, E. Galili, F. Antonioli, D. Sivan, S. Miko, N. Mourtzas, I. Felja, M. Meredith-Williams, B. Goodman-Tchernov, E. Kolaiti, M. Anzidei & R. Gehrels, 2017. Late Quaternary sea-level changes and early human societies in the central and eastern Mediterranean Basin: An interdisciplinary review. *Quaternary International* 449, 29–57.

Benton, M. & D.A.T. Harper, 2009. *Introduction to palaeobiology and the fossil record*. Wiley-Blackwell, Oxon.

Bennett, J.M., 2020. 'Testing Terraces: Managing and Sustaining the Agrarian Environment in the Maltese Archipelago.' Unpublished PhD thesis, Department of Archaeology, University of Cambridge.

Berger, J.-F. & J. Guilaine, 2009. The 8200 cal BP abrupt environmental change and the Neolithic transition: A Mediterranean perspective. *Quaternary International* 200, 31–49.

Bernabò Brea, L., 1966. Abitato Neolitico e insediamento Maltese dell'Eta del Bronzo nell'isola di Ognina (Siracusa) e i rapporti fra la Sicilia e Malta dal XVI al XXIII Sec. a.C. *Kokalos* 12, 40–69.

Bertoldi, R., 1980. Le vicende vegetazionali e climatiche nella sequenza paleobotanica würmiana e post-würmiana di Lagdei (Appennino settentrionale). "L'Ateneo Parmense." *Acta Naturalis* 16, 147–75.

Bertran, P., 2004. Soil erosion in small catchments of the Quercy region (southwestern France) during the Holocene. *The Holocene* 14, 597–606.

Beug, H.-J., 2004. *Leitfaden der Pollenbestimmung für Mitteleuropa und Angrenzende Gebiete*. München: Verlag Dr. Friedrich Pfeil.

Bevan, A. & J. Conolly, 2004. GIS, archaeological survey, and landscape archaeology on the island of Kythera, Greece. *Journal of Field Archaeology* 29 (1–2), 123–38.

Bevan, A. & J. Conolly, 2013. *Mediterranean Islands, Fragile Communities and Persistent Landscapes*. Cambridge: Cambridge University Press.

Bevan, A., J. Conolly, S. Colledge & A. Stellatou, 2013. The long-term ecology of agricultural terraces and enclosed fields from Antikythera, Greece. *Human Ecology* 41, 255–72.

Bicho, N., J. Cascalheira & C. Gonçalves, 2017. Early Upper Paleolithic colonization across Europe: Time and mode of the Gravettian diffusion. *PLOS ONE* 12(5), e0178506.

Bini, M., G. Zanchetta, A. Persoiu, R. Cartier, A. Catala, I. Cacho, J.R. Dean, F. Di Rita, R.N. Drysdale, M. Finne, I. Isola, B. Jalali, F. Lirer, D. Magri, A. Masi, L. Marks, A.M. Mercuri, O. Peyron, L. Sadori, M-A. Sicre, F. Welc, C. Zielhofer & E. Brisset, 2018. The 4.2 ka BP event in the Mediterranean region: an overview. *Climate of the Past Discussions* 15, 1–36.

Bintliff, J., 1977. *Natural Environment and Human Settlement in Greece*. Oxford: British Archaeological Reports, Supplementary Series 28.

Bintliff, J., 1992. Erosion in the Mediterranean lands: a reconsideration of pattern, process and methodology, in *Past and Present Soil Erosion: Archaeological and Geographical Perspectives*, eds. M.G. Bell & J. Boardman. Oxford: Oxbow Books, 125–31.

Bintliff, J., 2005. Human impact, land-use history, and the surface arhaeological record: A case study from Greece. *Geoarchaeology* 20, 135–47.

Blaauw, M., 2010. Methods and code for 'classical' age-modelling of radiocarbon sequences. *Quaternary Geochronology* 5 (5), 512–18.

Blaauw, M. & J.A. Christen, 2011. Flexible paleoclimate age-depth models using an autoregressive gamma process. *Bayesian Analysis* 6 (3), 457–74.

Blaauw, M., K.D. Bennett & J.A. Christen, 2010. Random walk simulations of fossil proxy data. *The Holocene* 20 (4), 645–9.

Blackford, J.J. & J.B. Innes, 2006. Linking current environments and processes to fungal spore assemblages: surface NPM data from woodland environments. *Review of Palaeobotany and Palynology* 141, 179–87.

Blockley, S.P.E., S.D.F. Pyne-O'Donnell, J.J. Lowe, I.P. Matthews, A. Stone, A.M. Pollard, C.S.M. Turney & E.G. Molyneux, 2005. A new and less destructive laboratory procedure for the physical separation of distal glass tephra shards from sediments. *Quaternary Science Reviews* 24 (16), 1952–60.

Blouet, B., 1963. *The Changing Landscape of Malta during the Rule of the Order of St John of Jerusalem 1530–1798*. Hull: University of Hull.

Blouet, B., 1964. The distribution of marshland in Malta during the seventeenth century. *Journal of Maltese Studies* 2, 198–203.

Blouet, B., 1967. Some observations on the distribution of Xagħra place-names in Malta. *Journal of Maltese Studies* 4, 81–4.

Blouet, B., 1978. The impact of armed conflict on the rural settlement pattern of Malta. *Transactions of the Institute of British Geographers* 3 (3), 367–80.

Blouet, B., 1984. *The Story of Malta* (2nd edition). Malta: Progress Press.

Blouet, B., 1993. *The Story of Malta* (5th edition). Malta: Progress Press.

Blouet, B., 1997. *The Story of Malta* (6th edition). Malta: Progress Press.

Boddington, A., A.N. Garland & R.C. Janaway (eds.), 1987. *Death, Decay, and Reconstruction: Approaches to Archaeology and Forensic Science*. Manchester: Manchester University Press.

Bonanno, A., 1977. Distribution of villas and some aspects of the Maltese economy in the Roman period. *Journal of the Faculty of Arts* 6 (4), 73–81.

Bonanno, A., 1986a. A socioeconomic approach to Maltese prehistory, in *The Temple Builders. Malta. Studies of its Heritage and History*. Malta: Mid-Med Bank Ltd. – Interprint Ltd., 17–46.

Bonanno, A. (ed.), 1986b. *Archaeology and Fertility Cult in the Ancient Mediterranean. Papers Presented at the First International Conference on Archaeology of the Ancient Mediterranean. The University of Malta 2–5 September 1985.* Amsterdam: B.R. Grüner Publishing Co.

Bonanno, A., 1990. Malta's role in the Phoenician, Greek and Etruscan trade in the western Mediterranean. *Melita Historica* 10, 209–24.

Bonanno, A., 1992. *Roman Malta. The Archaeological Heritage of the Maltese Islands*. Lugano: World Confederation of Salesian past pupils of Don Bosco.

Bonanno, A., 1993a. The prehistory and protohistory of the Maltese Islands: Current problems and perspectives, in La Prehistòria de les Illes de la Mediterranìa Occidental. *Jornades d'Estudis Històrics Locals* 10, 215–41.

Bonanno, A., 1993b. Tarxien and Tarxien Cemetery. Break or continuity between Temple Period and Bronze Age in Malta?. *Mediterraneo. Revistade Estudos Pluridisciplinares sobre ad Sociedades Mediterranicas* 2, 35–47.

Bonanno, A., 2008. Maltese wine pressing in antiquity. *Melita Historica* 11, 1–18.

Bonanno, A., 2011. The rise of a maritime strategic island: Malta under the Phoenicians and the Romans, in *The Maritime History of Malta: The First Millennia*, eds. C. Cini & J. Borg. Malta: Salesians of Don Bosco and Heritage Malta, 37–71.

Bonanno, A. 2018. Roman Villas in the Maltese Archipelago, in *The Roman Villa in the Mediterranean Basin: Late Republic to Late Antiquity*, eds. A. Marzano & G. P. R. Métraux, Cambridge: Cambridge University Press, 255–65.

Bonanno, A. and N.C. Vella, 2015. *Tas Silġ, Marsaxlokk (Malta) I: Archaeological Excavations Conducted by the University of Malta, 1996–2005*. (Ancient Near East Studies Supplement Series 48). Leuven: Peeters Publishers.

Bonanno, A., T. Gouder, C. Malone & S. Stoddart, 1990. Monuments in an island society. *World Archaeology* 22 (2), 190–205.

Bonatti, E., 1966. North Mediterranean climate during the last Würm glaciation. *Nature* 209, 984–5.

Bondì, S.F., 2014. Phoenicity, punicities, in *The Punic Mediterranean*, eds. J.C. Quinn & N.C. Vella. Cambridge: Cambridge University Press, 58–68.

Bonson, C.G., C. Childs, J.J. Walsh, M.P.J. Schöpfer & V. Carboni, 2007. Geometric and kinematic controls on the internal structure of a large normal fault in massive limestones: The Maghlaq Fault, Malta. *Journal of Structural Geology* 29, 336–54.

Bocquet-Appel, J. P. 2002. Paleoanthropological Traces of a Neolithic Demographic transition. *Current Anthropology* 43 (4), 637–50.

Boreham, S., C. Conneller, N. Milner, B. Taylor, A. Needham, J. Boreham & C.J. Rolfe, 2011. Geochemical indicators of preservation status and site deterioration at Star Carr. *Journal of Archaeological Science* 38, 2833–57.

Borg, A.P., 2003. 'Migration and Mobility in Early Modern Malta. The Harbour City of Valletta as a Case-Study, 1575–1650.' Unpublished MA thesis, University of Malta.

Borg, J., 1915. Agriculture and Horticulture in Malta, in *Malta and Gibraltar Illustrated: Historical and Descriptive, Commercial and Industrial, Facts, Figures and Resources*, ed. A. Macmillan. London: W.H. & L. Collingridge and Malta: Midsea Books, 224–9.

Boserup, E., 1965. *The Conditions of Agricultural Growth.* Chicago: Aldine.

Boserup, E., 1975. The Impact of Population Growth on Agricultural Output. *The Quarterly Journal of Economics* 89 (2), 257–70.

Bottema, S. & H. Woldring, 1984. Late Quaternary vegetation and climate of southwestern Turkey. *Paleohistoria* 26, 123–49.

Bottema, S., G. Entjes-Nieborg & W. Van Zeist (eds.), 1990. *Man's Role in the Shaping of the Eastern Mediterranean Landscape*. Rotterdam: Balkema.

Bøtter-Jensen, L., E. Bulur, G.A.T. Duller & A.S. Murray, 2000. Advances in luminescence instrument systems. *Radiation Measurements* 32 (5), 523–28.

Bouby, L., I. Figueiral, A. Bouchette, N. Rovira, S. Ivorra, T. Lacombe & J.F. Terral, 2013. Bioarchaeological insights into the process of domestication of grapevine (*Vitis vinifera* L.) during Roman times in Southern France. *PLoS One 8* (5), e63195.

Bowen, D.Q., 1978. *Quaternary Geology: A Stratigraphic Framework for Multidisciplinary Work.* London: Pergamon.

Bowen Jones, H., J.C. Dewdney & W.B. Fisher (eds.), 1961. *Malta, a Background for Development.* Durham: Durham University Press.

Boyle, J., A.J. Plater, C. Mayers, S.D. Turner, R.W. Stroud and J.E. Weber, 2011. Land use, soil erosion, and sediment yield at Pinto Lake, California: Comparison of a simplified USLE model with the lake sediment record. *Journal of Paleolimnology* 45 (2), 199–212.

Boyle, S., 2013. 'The Social and Physical Environment of Early Gozo – A Study of Settlement and Change.' Unpublished PhD thesis, Queen's University Belfast.

Boyle, S., 2014. Potty about pots: exploring identity through the prehistoric pottery assemblage, in *Exploring Prehistoric identity in Europe*, eds. V. Ginn, R. Enlander & R. Crozier. Oxford: Oxbow, 85–96.

Braudel, F., 1966. *The Mediterranean and the Mediterranean World in the Age of Philip II*, vol. 1 (2nd edition). London: Penguin Books.

Bresc, H., 1975. The 'Secrezia' and the Royal Patrimony in Malta: 1240–1450, in *Medieval Malta: Studies on Malta before the Knights*, ed. A. Luttrell. London: British School at Rome, 126–62.

Bradley, R., 1993. *Altering the Earth. The Origins of Monuments in Britain and Continental Europe*. Edinburgh: Society of Antiquaries of Scotland.

Brandt, C.J. & J.B. Thornes, 1996. *Mediterranean Desertification and Land-use*. London: John Wiley & Sons Ltd.

Bresc, H., 1991. Sicile, Malte e Monde Musulman, in *Malta. A case study in international cross-currents. Proceedings of the First International Colloquium on the History of the Central Mediterranean held at the University of Malta, 13–17 December 1989*, eds. S. Fiorini & V. Mallia-Milanes. Malta: Salesian Press, 47–79.

Bridges, E.M., 1978. *World Soils* (2nd edition). London: Longman.

Bringezu S., H. Schütz, W. Pengue, M. O´Brien, F. Garcia, R. Sims, R. Howarth, L. Kauppi M. Swilling & J. Herrick, 2014. 'Assessing Global Land Use: Balancing Consumption with Sustainable Supply. A Report of the Working Group on Land and Soils of the International Resource Panel.' New York: United Nations Environment Programme.

Brincat, J.M., 1991. Language and demography in Malta: the social foundations of the symbiosis between semitic

and romance in standard Maltese, in *Malta. A case study in international cross-currents. Proceedings of the first international colloquium on the history of the central Mediterranean held at the university of Malta, 13–17 December 1989*, eds. S. Fiorini and V. Mallia-Milanes. Malta: Salesian Press, 91–110.

Brincat, J.M., 1995. *Malta 870–1054 Al-Himyari's Account and its Linguistic Implications*. Valletta: Said International Ltd.

Bringezu S., H. Schütz, W. Pengue, M. O´Brien, F. Garcia, R. Sims, R. Howarth, L. Kauppi, M. Swilling & J. Herrick (eds.), 2014. *Assessing Global Land Use: Balancing Consumption with Sustainable Supply. A Report of the Working Group on Land and Soils of the International Resource Panel.* New York: United Nations Environment Programme (UNEP).

Broodbank, C., 2013. *The making of the Middle Sea: a history of the Mediterranean from the beginning to the emergence of the Classical world*. London: Thames and Hudson.

Bronk Ramsey, C., 2008a. Deposition models for chronological records. *Quaternary Science Reviews* 27, 42–60.

Bronk Ramsey, C., 2008b. Radiocarbon Dating: Revolutions in Understanding. *Archaeometry* 50 (2), 249–75.

Brothwell, D.R. & Pollard, A.M. (eds.) 2005. *Handbook of Archaeological Sciences*. Chichester: Wiley.

Brown, A., P. Toms, C. Carey & E. Rhodes, 2013. Geomorphology of the Anthropocene: Time-transgressive discontinuities of human-induced alluviation. *Anthropocene* 1, 3–13.

Brückner, H., A. Vött, M. Schriever & M. Handl, 2005. Holocene delta progradation in the eastern Mediterranean – case studies in their historical context. *Méditerranée* 104, 95–106.

Bruno, B., 2009. *Roman and Byzantine Malta: Trade and Economy* (Vol. 15). Valletta: Maltese Social Studies.

Bruno, B. & N. Cutajar, 2002. Archeologia bizantina a Malta: primi risultati e prospettive di indagine, in *Da Pyrgia a Mozia: Studi sull'archeologia del Mediterraneo in memoria di Antonia Ciasca*, eds. M.G. Amadasi Guzzo, M. Liverani & P. Matthiae. Roma: Università di Roma La Sapienza, 109–38.

Bruno, B. & N. Cutajar, 2018. Malta between the ninth and tenth century – two early medieval contexts. *Archeologia Medievale* 45, 111–22.

Brusasco, P., 1993. Dal Levante al Mediterraneo centrale: La prima fase fenicia a Tas-Silg, Malta. *Journal of Mediterranean Studies* 3, 1–29.

Bugeja, A., 2011. Understanding the past: Borġ in-Nadur in antiquarian and early archaeological literature, in *Site, Artefacts and Landscape: Prehistoric Borġ-in-Nadur, Malta (Praehistorica Mediterranea 3)*, eds. D. Tanasi & N.C. Vella. Italy: Polimentrica, 15–44.

Bugeja, J.R., 2018. Land Tenure System in the Late 19th and Early 20th Centuries. *Tesserae* 6, 22–31.

Buhagiar, K., 2002. 'Medieval and early modern cave-settlements and water galleries in North-West Malta South of the Great Fault: a field survey and gazetteer.' Unpublished MA thesis, University of Malta.

Buhagiar, K., 2012. Caves in Context: The Late Medieval Maltese Scenario, in *Caves in Context: The Cultural Significance of Caves and Rockshelters in Europe*, eds. K.A. Bergsvik. & R. Skeates. Oxford: Oxbow, 153–65.

Buhagiar, K. 2016. *Malta and Water (AD 900 to 1900): Irrigating a Semi-Arid Landscape*. Oxford: British Archaeological Reports – Hadrian Books.

Buhagiar, M., 1991. Post-Muslim Malta – A Case Study in Artistic and Architectural Cross-Currents, in *Malta – A Case Study in International Cross-Currents*, eds. S. Fiorini & V. Mallia Milanes. Malta: Malta University Publications, 13–31.

Bullock, P. & C.P. Murphy, 1979. Evolution of a palaeo-argillic brown earth (Paleudalf) from Oxfordshire, England. *Geoderma* 22, 225–52.

Bullock, P., N. Fedoroff, A. Jongerius, G. Stoops & T. Tursina 1985. *Handbook for Soil Thin Section Description*. Wolverhampton: Waine Research.

Burbidge, C.I., D.C.W. Sanderson, R.A. Housley & P. Allsworth Jones, 2007. Survey of Palaeolithic sites by luminescence profiling, a case study from Eastern Europe. *Quaternary Geochronology* 2, 296–302.

Butzer, K.W., 1960. Archaeology and geology in ancient Egypt. *Science* 132, 1617–24.

Butzer, K.W., 1982. *Archaeology as Human Ecology*. Cambridge: Cambridge University Press.

Butzer, K.W., 1996. Ecology in the Long View: Settlement Histories, Agrosystemic Strategies, and Ecological Performance. *Journal of Field Archaeology* 23, 141–50.

Butzer, K.W., 2005. Environmental history in the Mediterranean world: Cross-disciplinary investigation of cause-and-effect for degradation and soil erosion. *Journal of Archaeological Science* 32, 1773–800.

Butzer, K.W., 2015. *Anthropocene* as an evolving paradigm. *The Holocene* 25 (10), 1539–41.

Butzer, K.W. & J. Cuerda, 1962. Coastal stratigraphy of southern Mallorca and its implications for the Pleistocene chronology of the Mediterranean Sea. *Journal of Geology* 70, 398–416.

Cagiano de Azevedo, M., 1969. Lo scavo. In *Missione Archeologica Italiana a Malta: Rapporto preliminare della Campagna 1968*. Roma: Consiglio Nazionale delle Ricerche, 93–5.

Cagiano de Azevado, M., C. Caprino, A. Ciasca, E. Coleiro, A. Davico, G. Garbini & F. Saverio Mallia, 1964–73. *Missione Archeologica Italiana a Malta. Rapporti Preliminari delle Campagne 1963–1970.* Roma: Istituto di Studi del Vicino Oriente, Università di Roma.

Caló, C., P.D. Henne, B. Curry, M. Magny, E. Vescovi, T. La Mantia, S. Pasta, B. Vanniére & W. Tinner, 2012. Spatio-temporal patterns of Holocene environmental change in southern Sicily. *Palaeogeography Paleaoclimatology Palaeoecology* 323–325, 110–22.

Canellas-Bolta, N., S. Riera-Mora, H.A. Orengo, A. Livarda & C. Knappett, C. 2018. Human management and landscape changes at Palaikastro (Eastern Crete) from the late Neolithic to the Early Minoan period. *Quaternary Science Reviews* 183, 59–75.

Caracuta, V., 2020. Olive growing in Puglia (southeastern Italy): a review of the evidence from the Mesolithic to the Middle Ages. *Vegetation History and Archaeobotany* https://doi.org/10.1007/s00334-019-00765-y

Carlson, T.N. & D.A. Ripley, 1997. On the relation between NDVI, fractional vegetation cover, and leaf area index. *Remote Sensing of Environment* 62, 241–52.

Carroll, F.A., 2007. 'The Holocene Environment of the Maltese Islands.' Unpublished PhD, Queen's University Belfast.

Carroll, F.A., C.O. Hunt, P.J. Schembri & A. Bonanno, 2012. Holocene climate change, vegetation history and human impact in the Central Mediterranean: evidence from the Maltese Islands. *Quaternary Science Reviews* 52, 24–40.

Cassar, C., 1988. Everyday Life in Malta in the Nineteenth and Twentieth Centuries, in *The British Colonial Experience, 1800–1964: The Impact on Maltese Society*, ed. V. Mallia Milanes. Malta: Mireva, 91–126.

Cassar, C., 2000. *Society, culture and identity in early modern Malta*. Malta: Mireva.

Cassar, C., 2002. *A Concise History of Malta*. Malta: Mireva.

Cassar, L.F., E. Conrad & P.J. Schembri, 2008. The Maltese archipelago, in M*editerranean Island Landscapes: Natural and Cultural Approaches*, eds. I.N. Vogiatzakis, G. Pungetti and A.M. Mannion. Heidelberg: Springer, 297–322.

Catania, P., 2015. *The People of the North 1546–1610*. Malta: Midsea Books.

Catling, C., 2013. Peasant houses in Midland England. *Current Archaeology* 279, 12–19.

Catt, J.A., 1990. Paleopedology manual. *Quaternary International* 6, 1–95.

Cazzella, A. & G. Recchia, 2008. L'area sacra megalitica di Tas-Silg (Malta): nuovi elementi per lo studio dei modelli architettonici e delle pratiche cultuali. *Scienze dell'Antichità* 13, 689–99.

Cazzella, A. & G. Recchia, 2012. Tas-Silġ: the Late Neolithic megalithic sanctuary and its re-use during the Bronze Age and the Early Iron Age. *Scienze dell'antichità* 18, 15–38.

Cazzella, A. & G. Recchia. 2013. Malta, Sicily, Aeolian Islands and Southern Italy during the Bronze Age: The meaning of a changing relationship in, *Exchange, Interaction, Conflicts and Transformations: Social and Cultural Changes in Europe and the Mediterranean between Bronze and Iron Age,* eds. Alberti. E. & S. Vitri. Oxford: Oxbow, 80–91.

Cazzella, A. & G. Recchia, 2015. The early Bronze Age in the Maltese islands, in *The Late Prehistory of Malta: Essays on Borg in-Nadur and Other Sites*, eds. D. Tanasi and N.C. Vella. Oxford: Archaeopress, 139–59.

Cazzella, A., A. Pace & G. Recchia, 2011. The late second millennium B.C. agate artefact with cuneiform inscription from the Tas-Silg sanctuary in Malta: an archaeological framework. *Scienze dell'Antichità* 17, 599–609.

Cazzella, A., A. Pace & G. Recchia, 2012. Cult and exchange in the Mediterranean: A second millennium BC cuneiform inscription from the sanctuary of Tas-Silġ in Malta. *Le Science Web* (News online: http//en.lswn.it/archaeology/cult-and-exchange-in-the-mediterranean-a-second-millennium-bc-cuneiform-inscription-from-the-sanctuary-of-tas-silg-in-malta/).

Cerdá, A., 2008. *Erosión y Degradación del Suelo Agrícola en España*. Valencia: Universitat de Valencia Estudi General.

Chapman, J., 2018. Climatic and human impact on the environment?: A question of scale. *Quaternary International* 496, 3–13.

Chatzimpaloglou, P., 2019. 'Geological reconnaissance and provenancing of potential Neolithic lithic sources in the Maltese Islands.' Unpublished PhD, Department of Archaeology, University of Cambridge.

Chatzimpaloglou P., C. French, M. Pedley & S. Stoddart, 2020. Connecting chert sources of Sicily with the Neolithic chert artefacts of Malta. *Journal of Archaeological Science: Reports* 29, 102–11.

Chen, Y.C., Q. Sung & K.Y. Cheng, 2003. Along-strike variations of morphotectonic features in the Western Foothills of Taiwan: Tectonic implications based on stream-gradient and hypsometric analysis. *Geomorphology* 56, 109–37.

Cherry, J.F., 1981. Pattern and process in the earliest colonisation of the Mediterranean islands. *Proceedings of the Prehistoric Society* 47, 41–68.

Cherry, J.F., 1990. The first colonisation of the Mediterranean islands: a review of recent research. *Journal of Mediterranean Archaeology* 3 (2), 145–221.

Cherry, J.F., 2004. Mediterranean island pre-history: what's different and what's new?, in *Voyages of Discovery: The Archaeology of Islands*, ed. S.C. Fitzpatrick. Westport: Praeger Publishers, 233–48.

Chetcuti, D., A. Buhagiar, P.J. Schembri & F. Ventura, F. 1992. *The Climate of the Maltese Islands: A Review*. Msida: Malta University Press.

Chircop, J., 1993. *Underdevelopment: The Maltese Experience 1880–1914*. University of Malta.

Cilia, D.P. & C. Mifsud, 2012. Contributions to the malacology of Malta, I: a new location for subfossil *Oxyloma elegans* (Risso, 1826) (Pulmonata: Succineidae) from the Salini Holocene deposits in Malta. *Central Mediterranean Naturalist* 2011 (5), 3–4.

Civetta, L., Y. Cornette, P.Y. Gillot & G. Orsi, G. 1988. The eruptive history of Pantelleria (Sicily channel) in the last 50 ka. *Bulletin of Volcanology* 50, 47–57.

Clark, A., 1996. *Seeing beneath the Soil: Prospecting Methods in Archaeology* (2nd edition). London: Routledge.

Clark, D., 2004. Building Logistics, in *Malta before History: The World's Oldest Free-Standing Stone Architecture*, ed. D. Cilia. Malta: Miranda, 367–77.

Coles, G.M., D.D. Gilbertson, C.O. Hunt & R.D.S. Jenkinson, 1989. Taphonomy and the palynology of cave sediments. *Cave Science* 16 (3), 83–9.

Collins, P.M., B.A.S. Davis & J.O. Kaplan, 2012. The mid-Holocene vegetation of the Mediterranean region and southern Europe, and comparison with the present day. *Journal of Biogeography* 39, 1848–61.

Coneybeare, W.D., 1824. On the discovery of an almost perfect skeleton of a Plesiosaurus. *Transactions of the Geological Society Journal of Science* VII, 203–40.

Conolly, J. & M. Lake, 2006. *Geographic Information Systems in Archaeology*. Cambridge: Cambridge University Press.

Contreras, D.A., 2011. How far to Conchucos? A GIS approach to assessing the implications of exotic materials at Chavín de Huántar, *World Archaeology* 43 (3), 380–97.

Cook, S.F. & R.F. Heizer, 1965. *Studies on the Chemical Analysis of Archaeological Sites*. Berkeley: University of California Press.

Cooke, J.H., 1891. Notes on the 'Pleistocene Beds' of Gozo. *Geological Magazine* 28, 348–55.

Cooke, J.H., 1893a. On the occurrence of concretionary masses of flint and chert in the Maltese limestones. *GeoMagazine* 30, 157–60.

Cooke, J.H., 1893b. The marls and clays of the Maltese Islands. *Quarterly Journal of the Geological Society London* 49, 117–28.

Cooke, J.H., 1893c. On the occurrence of concretionary masses of flint and chert in the Maltese limestones. *GeoMagazine* 30, 157–60.

Cooke, J.H., 1896a. Contributions to the stratigraphy and palaeontology of the Globigerina Limestones of the Maltese Islands. *Quarterly Journal of the Geological Society London* 52, 461–2.

Cooke, J.H., 1896b. Notes on the Globigerina Limestone of the Maltese Islands. *Geological Magazine* 33, 502–11.

Cooke, J.H., 1896c. Notes on the 'Pleistocene Beds' of the Maltese Islands. *Geological Magazine* 32, 201–10.

Copat, V., M. Danesi and C. Ruggini, 2013. Late Neolithic and Bronze age pottery from Tas-Silġ sanctuary: new research perspectives for the Maltese prehistoric sequence. *Scienze dell'Antichità* 18, 39–63.

Corrado, A., A. Bonanno & N.C. Vella 2004. Bones and Bowls: a Preliminary Interpretation of the Faunal Remains from the Punic Levels in Area B, at the Temple of Tas-Silġ, Malta, in *Behaviour Behind Bones: The Zooarchaeology of Ritual, Religion, Status and Identity*, eds. S. Jones O'Day, W. Van Neer & A. Ervynvk, Oxford: Oxbow, 47–53.

Courty, M-A., P. Goldberg & R.I. Macphail, 1989. *Soils and Micromorphology in Archaeology*. Cambridge: Cambridge University Press.

Cox, C.B., P.D. Moore & R.J. Ladle, R.J., 2016. *Biogeography: An Ecological and Evolutionary Approach.* (9th edition) Chichester: Wiley-Blackwell.

Cresswell, A.J., D.C.W. Sanderson, T.C. Kinnaird & C. French, 2017. 'Luminescence analysis and dating of sediments from valley fills and archaeological sites on Gozo and Malta.' Unpublished report, July, 2017. East Kilbride: SUERC.

Cresswell, A.J., Carter, J. & Sanderson, D.C.W. 2018. Dose rate conversion parameters: assessment of nuclear data. *Radiation Measurements* 120, 195–201.

Cutajar, N., 2018. *Core and Periphery – Mdina and Hal Safi in the 9th and 10th centuries,* Valletta, Heritage Malta.

Dalli, C., 2006. *Malta – The Medieval Millennium*. Malta: Midsea Books.

Dalli, C., 2011. The sea in Medieval Maltese History, in *The Maritime History of Malta: The First Millennia*, eds. D. Cini & J. Borg. Malta: Salesians of Don Bosco and Heritage Malta, 73–109.

Dalli, C., 2016. From medieval dar al-Islam to contemporary Malta: rahal toponymy in a wider western Mediterranean context. *Island Studies Journal* 11 (2), 369–80.

Dansgaard, W., S.J. Johnsen, H.B. Clausen, D. Dahl-Jensen, N.S. Gunderstrup, C.U. Hammer, C.S. Hvidberg, J.P. Steffensen, A.E. Sveinbjornsdottir, J. Jouzel & G. Bond, 1993. Evidence for general instability of past climate fron a 250-kyr ice-core record. *Nature* 364, 218–22.

Dart, C.J., D.W.J. Bosence & K.R. McClay, 1993. Stratigraphy and structure of the Maltese graben system. *Journal of the Geological Society* 150, 1153–66.

Davidovich, U., N. Porat, Y. Gadot, Y. Avni & O. Lipschits, 2012. Archaeological investigations and OSL dating of terraces at Ramat Rahel, Israel. *Journal of Field Archaeology* 37 (3), 192–208.

Davidson, D.A., 1971. Geomorphology and prehistoric settlement of the Plain of Drama. *Revue Geomorphology Dynamique* 20, 22–6.

Davidson, D.A., 1980. Erosion in Greece during the first and second millennia BC, in *Timescales in Geomorphology*, eds. R.A. Cullingford, D.A. Davidson & J. Lewin. New York: Wiley and Sons, 143–58.

Davis, D.S., 2019. Studying human responses to environmental change: Trends and trajectories of archaeological research. *Environmental Archaeology* 24 (4) (doi.org/10.1080/14614103.2019.1639338)

Dawson, H., 2004–6. Understanding colonisation. Adaptation strategies in the central Mediterranean islands. *Accordia Papers* 10, 35–60.

Dawson, H., 2008. Unravelling 'mystery' and process from the prehistoric colonization and abandonment of the Mediterranean Islands, in *Comparative Island Archaeologies*, eds. J. Conolly & M. Campbell. (BAR International Series 1829.) Oxford: British Archaeological Reports, 105–33.

Dawson, H., 2010. Question of Life or Death? Seafaring and Abandonment in the Mediterranean and Pacific Islands, in *The Global Origins and Development of Seafaring*, eds. A. Anderson, J.H. Barrett & K.V. Boyle. Cambridge: McDonald Institute, 203–12.

Dawson, H., 2014. *Mediterranean Voyages: The Archaeology of Island Colonisation and Abandonment.* Publications of the Institute of Archaeology, University College London 62. Walnut Creek, CA: Left Coast Press, Inc.

Declercq, Y., R. Samson, A. Castanheiro, S. Spassov, F.M.G. Tack, E. Van De Vijver & P. De Smedt, 2019. Evaluating the potential of topsoil magnetic pollution mapping across different land use classes. *Science of the Total Environment* 685, 345–56.

De Grossi Mazzorin, J. & M. Battafarano 2012. I resti faunistici provenienti dagli scavi di Tas Silġ a Malta: testimonianze di pratiche rituali, in *Atti del 6° Convegno Nazionale di Archeozoologia Centro Visitatori del Parco dell'Orecchiella 1–24 maggio 2009 San Romano in Garfagnana – Lucca*, eds. J. De Grossi Mazzorin, D. Saccà & C. Tozzi, Lecce: Associazione Italiana di Archeozoologia, 357–63.

Delano-Smith, C., N. Mills & B. Ward-Perkins, 1986. Luni and the Ager Lunensis. The Rise and fall of a Roman town and its territory. *Papers of the British School at Rome* 54, 82–146.

De Lucca, D., 1988. British Influence on Maltese Architecture and Fortifications, in Mallia Milanes, V. (ed.) *The British Colonial Experience, 1800–1964: The Impact on Maltese Society*, pp. 313–27. Malta: Mireva.

De Lucca, D., 1995. *Mdina: A History of Its Urban Space and Architecture*. Malta: Said International.

Desjardins, E., G. Barker, Z. Lindo, C. Dielman & A.C. Dussault, 2015. Promoting reslience. *The Quarterly Review of Biology* 90, 147–65.

de Vareilles, A., L. Bouby, A. Jesus, L. Martin, M. Rottoli, M. Vander Linden & F. Antolin, 2020. One sea but many routes to Sail. The early maritime dispersal of Neolithic crops from the Aegean to the Western Mediterranean. *Journal of Archaeological Science: Reports* 29, 102140.

di Gennaro, F. & S.K.F. Stoddart, 1982. A review of the evidence for prehistoric activity in part of South Etruria. *Papers of the British School at Rome* 50, 1–21.

Di Rita, F. and D. Magri, 2009. Holocene drought, deforestation and evergreen vegetation development in the central Mediterranean: A 5500 year record from Lago Alimini Piccolo, Apulia, southeast Italy. *The Holocene* 19, 295–306.

Di Rita, F. & D. Magri, 2019. The 4.2ka event in the vegetation record of the central Mediterranean. *Climate Past* 15, 237–51.

Dietre, B., E. Gauthier & F. Gillet, 2012. Modern pollen rain and fungal spore assemblages from pasture woodlands around Lake Saint-Point (France). *Review of Palaeobotany and Palynology* 186, 69–89.

Djamali, M., 2014. Pollen profile BM1, BurMarrad ria, Malta. *European Pollen Database (EPD), PANGAEA* (https://doi.org/10.1594/PANGAEA.835773).

Djamali, M., B. Gambin, N. Marriner, V. Andieu-Ponel, T. Gambin, E. Gandouin, S. Lanfranco, F. Medail, D. Paron, P. Ponel & C. Morhange, 2013. Vegetation dynamics during the early to mid-Holocene transition in NW Malta, human impact versus climate forcing. *Vegetation History and Archaeobotany* 22, 367–80.

Docter, R.F., N.C. Vella, N. Cutajar, A. Bonanno & A. Pace, 2012. Rural Malta: First Results of the Joint Belgo-Maltese Survey Project. *Babesch. Bulletin Antieke Beschaving* 87, 107–49.

Doneddu, M. & E. Trainito, 2005. *Conchiglie del Mediterraneo: Guida ai Molluschi conchigliati*. Trezzano sul Naviglio: Il Castello.

Dotterweich, M., 2008. The history of soil erosion and fluvial deposits in small catchments of central Europe: Deciphering the long-term interaction between humans and the environment – A review. *Geomorphology* 101, 192–208.

Dotterweich, M., M. Stankoviansky, J. Minár, S. Koco & P. Papco, 2013. Human induced soil erosion and gully system development in the Late Holocene and future perspectives on landscape evolution: The Myjava Hill Land, Slovakia. *Geomorphology* 201, 227–45.

Drescher-Schneider, R., J-L. de Beaulieu, M. Magny, A-V. Walter-Simonnet, G. Bossuet, L. Millet, E. Brugiapaglia & A. Drescher, A. 2007. Vegetation history, climate and human impact over the last 15,000 years at Lago dell'Accesa (Tuscany, Central Italy). *Vegetation History and Archaeobotany* 16, 279–99.

Duchaufour, P., 1982. *Pedology*. London: Allen and Unwin.

Durand, N., H. Curtis Monger & M.G. Canti, 2010. Calcium carbonate features, in*Interpretation of Micromorphological Features of Soils and Regoliths*, eds. G. Stoops, V. Marcelino & F. Mees. Amsterdam: Elsevier, 149–94.

Durn, G., 2003. Terra rossa in the Mediterranean region: parent materials, composition and origin. *Geologia Croatica* 56, 83–100.

Dusar, B., G. Verstraeten, B. Notebaert & J. Bakker, 2011. Holocene environmental change and its impact on sediment dynamics in the eastern mediterranean. *Earth-Science Reviews* 108, 137–57.

Edgeworth, M., C. Waters, J. Zalasiewicz & S. Stoddart, 2016. Second Anthropocene Working Group Meeting. *The European Archaeologist* 47, 27–31.

Edwards, K.J., R.M. Fyfe, C.O. Hunt & E. Schofield, 2015. Moving forwards? Palynology and the human dimension. *Journal of Archaeological Science* 56, 117–32.

Edwards, K.J. & C.J. McIntosh, 1988. Improving the detection of cereal-type pollen grains from *Ulmus* decline and earlier deposits from Scotland. *Pollen et Spores* 3, 179–88.

Efremov, A., 1940. Taphonomy: a new branch of palaeontology. *Pan American Geologist* 74, 81–93.

Ejarque, A., Y. Miras & S. Riera, 2011. Pollen and non-pollen palynomorphs indicators of vegetation and highland grazing activities obtained from modern surface and dung datasets in the eastern Pyrenees. *Review of Palaeobotany and Palynology* 167, 123–39.

Ellenberg, L., 1983. Die kusten von Gozo. *Essener Geograpische Arbeiten* 6, 129–60.

Endre Nyerges, A., 1980. Traditional Pastoralism and Patterns of Range Degradation, in *Browse in Africa. The Current State of Knowledge*, ed. H.N. Le Houerou. Addis Ababa: International Livestock Center for Africa, 465–70.

English Heritage, 2007. *Geoarchaeology: Using Earth Sciences to Understand the Archaeological Record* (2nd edition). Swindon: English Heritage.

Entwistle, J.A., P.W. Abrahams & R.A. Dodgshon, 1998. Multi-element analysis of soils from Scottish historical sites, interpreting land-use history through physical and chemical analysis of soil. *Journal of Archaeological Science* 25, 53–68.

Eppes, M.C., R. Bierma, D. Vinson & F. Pazzaglia, 2008. A soil chronosequence study of the Reno valley, Italy: Insights into the relative role of climate versus anthropogenic forcing on hillslope processes during the mid-Holocene. *Geoderma* 147, 97–107.

Epstein, S.R., 2002. *An Island for Itself: Economic Development and Social Change in Late Medieval Sicily*. Cambridge: Cambridge University Press.

Estiarte, M., J. Peñuelas, C. López-Martínez & R. Pérez-Obiol, 2008. Holocene palaeoenvironment in a former coastal lagoon of the arid south eastern Iberian Peninsula: salinization effects on $\delta^{15}N$. *Vegetation History and Archaeobotany* 17, 667–74.

ESRI, 2017a. *Data Classification Methods*. http://pro.arcgis.com/en/pro-app/help/mapping/symbols-and-styles/data-classification-methods.htm [Accessed 18 Apr 2017].

ESRI, 2017b. *How Line Density works*. http://desktop.arcgis.com/en/arcmap/10.3/tools/spatial-analyst-toolbox/how-line-density-works.htm [Accessed 18 Apr 2017].

ESRI, 2017c. *How the Horizontal and Vertical Factors Affect Path Distance*. http://desktop.arcgis.com/en/arcmap/10.3/

tools/spatial-analyst-toolbox/how-the-horizonal-and-vertical-factors-affect-path-distance.htm [Accessed 11 Apr 2017].

ESRI, 2017d. *Understanding Path Distance Analysis*. http://desktop.arcgis.com/en/arcmap/10.3/tools/spatial-analyst-toolbox/understanding-path-distance-analysis.htm [Accessed 11 Apr 2017].

Etherington, T.R., 2016. Least-Cost Modelling and Landscape Ecology: Concepts, Applications, and Opportunities, *Current Landscape Ecology Reports* 1 (1), 40–53.

Evans, J.D., 1953. The prehistoric culture sequence of the Maltese archipelago. *Proceedings of the Prehistoric Society* 19, 41–94.

Evans, J.D., 1956. The dolmens of Malta and the origins of the Tarxien cemetery culture. *Proceedings of the Prehistoric Society* 22, 85–101.

Evans, J.D., 1959. *Malta. Ancient People and Places.* London: Thames and Hudson.

Evans, J.D., 1971. *The Prehistoric Antiquities of the Maltese Islands: a survey*. London: Athlone Press.

Evans, J.D., 1973a. Islands as laboratories for the study of culture process, in *The Explanation of culture change. Models in Prehistory*, ed. A.C. Renfrew. London: Duckworth, 517–20.

Evans, J.D., 1973b. Priests and people – a note on evidence for social distinctions in prehistoric Malta, in *Estudios Dedicados al Profesor Dr. Luis Pericot* (*Publicaciones Eventuales* 23), ed. J. Maluqer de Motes. Barcelona: Universidad de Barcelona, Instituto de Arqueología y Prehistoria, 215–19.

Evans, J.D., 1977. Island archaeology in the Mediterranean, problems and opportunities. *World Archaeology* 9, 12–26.

Evans, J.D., 1984. Maltese prehistory: A reappraisal, in *The Deya Conference of Prehistory*, eds. W. Waldren, R.W. Chapman, J. Lewthwaite & R.C. Kennard. Oxford: British Archaeological Reports, International Series 229, 489–97.

Evans, J.G., 1978. *An Introduction to Environmental Archaeology.* New York: Cornell University Press.

Evans, J.G. & T. O'Connor, 2005. *Environmental Archaeology, Principles and Methods* (2nd edition). Stroud: Sutton Publishing.

Faegri, K. & K. Iversen, 1975. *A textbook of pollen analysis*. Stockholm: Munksgaard.

Fageria, N.K. & V.C. Baligar, 2005. Nutrient availability, in *Encyclopedia of Soils in the Environment*, ed. D. Hillel. Amsterdam: Elsevier, 63–71.

F.A.O. & I.S.R.I.C., 1990. *Guidelines for Soil Description* (3rd edition revised). Rome: FAO.

Fall, P.L., S.E. Falconer, C.S. Galletti, T. Shirmang, E. Ridder & J. Klinge, 2012. Long-term agrarian landscapes in the Troodos foothills, Cyprus. *Journal of Archaeological Science* 39, 2335–47.

Farres, P., 2019. Paleosoils: Legacies of past landscapes, with a series of contrasting examples from Malta, in *Landscapes and Landforms of the Maltese Islands*, eds. R. Gauci & J.A. Schembri. Cham, Switzerland: Springer Nature, 141–52.

Fassbinder, J.W.E., 2016. Magnetometry for archaeology, in *Encyclopedia of Geoarchaeology*, ed. A.S. Gilbert. Dordrecht: Springer, 499–514.

Fedoroff, N., 1968. Génese et morphologie des sols a horizon b textural en France atlantique. *Science du Sol* 1, 29–65.

Fedoroff, N., 1977. Clay illuviation in Red Mediterranean soils. *Catena* 28, 71–189.

Felix, R., 1973. *Oligo-Miocene Stratigraphy of Malta and G020*. Wageningen: H. Veenman and Zonen, B.V.

Fenech, K., 2007. *Human-induced changes in the environment and landscape of the Maltese Islands from the Neolithic to the 15th century AD as inferred from a scientific study of sediments from Marsa, Malta*. British Archaeological Reports, International Series 1692. Oxford: Archaeopress.

Fenech, K. & P.J. Schembri, 2015. Environmental analyses based on molluscan and other sedimentological remains, in *Tas-Silġ, Marsaxlokk (Malta) I: Archaeological Excavations Conducted by the University of Malta, 1996–2005*, eds. A. Bonanno, A. & N.C. Vella. Leuven: Peeters, 401–96.

Fenton, E.G., 1918. The Maltese Cart Ruts. *Man* 18, 67–72.

Finné, M., K. Holmgren, H.S. Sundqvist, E. Weiberg & M. Lindblom, 2011. Climate in the eastern Mediterranean, and adjacent regions, during the past 6000 years – A review. *Journal of Archaeological Science* 38, 3153–73.

Fiorentino, G., C. Oronzo & G. Colaianni, 2012. Human-Environmental Interaction, in Malta From The Neolithic To The Roman Period: Archaeobotanical Analyses At Tas-Silġ. *Scienze dell'Antichità* 18, 169–84.

Fiorini, S., 1993a. Malta in 1530, in *Hospitaller Malta 1530–1798: Studies on Early Modern Malta and the Order of St. John of Jerusalem*, ed. V. Mallia Milanes. Malta: Mireva, 111–98.

Fiorini, S., 1993b. Demographic growth and urbanisation of the Maltese countryside to 1798, in *Hospitaller Malta, 1530–1798: Studies on Early Modern Malta and the Order of St John of Jerusalem*, ed. V. Mallia-Milanes. Msida, Malta: Mireva, 296–310.

Fleisher, J. & F. Sulas, 2015. Deciphering public spaces in urban contexts: Geophysical survey, multi-element analysis, and artefact distributions at the 15th–16th century AD Swahili settlement of Songa Mnana, Tanzania. *Journal of Archaeological Science* 55, 55–70.

Florenzano, A., M. Marignani, L. Rosati, S. Fascetti & A.M. Mercuri, 2015. Are Cichorieae an indicator of open habitats and pastoralism in current and past vegetation studies? *Plant Biosystems* 149, 154–65.

Florenzano, A., A.M. Mercuri, R. Rinaldi, E. Rattighieri, R. Fornaciari, R. Messora & L. Arru, 2017. The representativeness of *Olea* pollen from olive groves and the late Holocene landscape reconstruction in central Mediterranean. *Frontiers in Earth Science* 5, 1–11.

Foglini, F., M. Prampolini, A. Micallef, L. Angeletti, L. Vanfdelli, A. Deidum & M. Taviani, 2016. Late Quaternary coastal landscape morphology and evolution of the Maltese Islands (Mediterranean Sea) reconstructed from high-resolution seafloor data, in *Geology and Archaeology: Submerged Landscapes of the Continental Shelf*, eds. J. Harff, G. Bailey & F. Luth. London: Geological Society Special Publication 411, 77–95.

Folke, C., 2006. Resilience: The emergence of a perspective for social-ecological system analyses. *Global Environmental Change* 16 (3), 253–67.

Folke, C., 2019. Resilience, in *Oxford Research Encyclopedia of Environmental Science*, ed. H.H. Shugart. Oxford: Oxford University Press, 1–60.

Folke, C., S. Carpenter, B. Walker, M. Scheffer, F.S. Chapin & J. Rockstrom, 2010. Resilience thinking: Integrating resilience, adaptability and transformability. *Ecology and Society* 15 (4), 20–28.

Follieri, M., D. Magri & L. Sadori, 1988. 250,000-year pollen record from the Valle di Castiglione (Roma). *Pollen et Spores* 30, 329–56.

Föllmi, K.B., B. Gertsch, J-P. Renevey, E. De Kaenel & P. Stilles, 2008. Stratigraphy and sedimentology of phosphate-rich sediments in Malta and south-eastern Sicily (latest Oligocene to early Late Miocene). *Sedimentology* 55, 1029–51.

Forbes, H., 1996. The uses of the uncultivated landscape in modern Greece: a pointer to the value of the wilderness in antiquity?, in *Human Landscapes in Classical Antiquity: Environment and Culture*, eds. G. Shipley & J. Salmon. London-New York: Routledge, 68–97.

Forbes, H., 1998. European Agriculture Viewed Bottom-side Upwards: Fodder- and Forage-provision in a Traditional Greek Community. *Environmental Archaeology* 1, 19–34.

French, C., 2010. Sustaining prehistoric agricultural landscapes in southern Spain, highland Yemen and northern New Mexico: the geoarchaeological perspective, in *Perspectives in Landscape Archaeology*, eds. H. Lewis & S. Semple. B.A.R. International Series 2103. Oxford: Archaeopress, 37–44.

French, C., 2015. *A Handbook of Geoarchaeological Approaches to Landscapes and Settlement Sites*. Oxford: Oxbow Books.

French, C., S. Taylor, R. McLaughlin, A. Cresswell, T. Kinnaird, D. Sanderson, S. Stoddart & C. Malone, 2018. A Neolithic palaeo-catena for the Xagħra Upper Coralline Limestone plateau of Gozo, Malta, and its implications for past soil development and land use. *Catena* 171, 337–58.

Frendo, H., 1988. Maltese Colonial Identity: Latin Mediterranean or British Empire?, in *The British Colonial Experience, 1800–1964: The Impact on Maltese Society*, ed. V. Mallia Milanes. Malta: Mireva, 185–214.

Frost, H., 1969. *The Mortar Wreck in Mellieha Bay: Plans and Soundings. A Report on the 1967 Campaign carried out on behalf of the National Museum of Malta*. London: Appetron Press.

Fsadni, M., 1992. *The Girna. The Maltese Corbelled Stone Hut.* Malta: Dominican Publication.

Fuchs, M., Lang, A. & Wagner, G.A. 2004. The history of Holocene soil erosion in the Phlious Basin, NE Peloponnese, Greece, based on optical dating. *The Holocene* 14, 334–45.

Fuller, D.Q., 2001. Harappan seeds and agriculture: some considerations. *Antiquity* 75, 410–14.

Furlani, S., F. Antonioli, S. Biolchi, T. Gambin, R. Gauci, V. Lo Priesti, M. Anzidei, S. Devoto, M. Palombo & A. Sulli, 2013. Holocene sea level change in Malta. *Quaternary International* 288, 146–57.

Furlani, S., F. Antonioli, T. Gambin, S. Biolchi, S. Formosa, V. Lo Priesti, M. Mantovani, M. Anzidei, L. Calcagnile & G. Quarta, G. 2018. Submerged speleothem in Malta indicates tectonic stability throughout the Holocene. *The Holocene* 28 (10), 1588–97.

Galea P., 2007. Seismic history of the Maltese Islands and considerations on seismic risk. *Annals of Geophysics* 50 (6), 725–40.

Galea, P., 2019. Central Mediterranean Tectonics – A Key player in the geomorphology of the Maltese Islands, in *Landscapes and Landforms of the Maltese Islands* (World Geomorphological Landscapes), eds. R. Gauci & J.A. Schembri. Cham, Switzerland: Springer Nature, 19–30.

Galdies, C., 2011. *The climate of Malta: statistics, trends and analysis, 1951–2010*. Valletta: National Statistics Office.

Gambin, T., 2008. Archaeological discoveries at Marsa over the centuries. *Malta Archaeological Review* 7 (2004–2005), 49–54.

Gambin, T. 2015. A Phoenician Shipwreck off Gozo, Malta. *Malta Archaeological Review* 10, 69–71.

Garmbin, T. & J.-C. Sourisseau 2015. Xlendi, Malta. *Homepage of Laboratoire des Sciences de l'Information et des Systèmes, Centre Camille-Jullian, Centre National de la Recherche Scientifique (France)*, http://www.lsis.org/groplan/article/art_Xlendi.html

Gambin, T., V. Andrrieu-Ponel, F. Medail, N. Marriner, O. Peyron, V. Montade, T. Gambin, C. Morhange, D. Belkacem & M. Djamali, 2016. 7300 years of vegetation history and climate for the NW Malta: A Holocene perspective. *Climate of the Past* 12, 273–97.

Ganskopp, D., R. Cruz & D. Johnson, 2000. Least-effort pathways?: a GIS analysis of livestock trails in rugged terrain. *Applied Animal Behaviour Science* 68 (3), 179–90.

García-Ruiz, J.M., 2010. The effects of land uses on soil erosion in Spain: A review. *Catena* 81, 1–11.

García-Ruiz, J.M. & N. Lana-Renault, 2011. Hydrological and erosive consequences of farmland abandonment in Europe, with special reference to the Mediterranean region – A review. *Agriculture, Ecosystems and Environment* 140, 317–38.

García-Ruiz, J.M., E. Nadal-Romero, N. Lana-Renault & S. Begueria, 2013. Erosion in Mediterranean landscapes: Changes and future challenges. *Geomorphology* 198, 20–36.

Gardiner, W., M. Grasso & D. Sedgeley, 1995. Plio-Pleistocene fault movement as evidence for mega-block kinematics within the Hyblean-Malta Plateau, central Mediterranean. *Journal of Geodynamics* 19, 35–51.

Gatt, M., 2006a. *Il-Ġeoloġija u l-paleontoloġija tal-Gżejjer Maltin I*. Sensiela Kullana Kulturali, Nru. 68. Pietà, Malta: Pubblikazzjonijiet Indipendenza.

Gatt, M., 2006b. *Il-Ġeoloġija u l-paleontoloġija tal-Gżejjer Maltin II*. Sensiela Kullana Kulturali, Nru. 69. Pietà, Malta: Pubblikazzjonijiet Indipendenza.

Gauci, R. & J.A. Schembri (eds.), 2019. *Landscapes and Landforms of the Maltese Islands* (World Geomorphological Landscapes.) Cham, Switzerland: Springer Nature.

Gerasimova, M. & M. Lebedeva-Verba, 2010. Topsoils – Mollic, takyric and yermic horizons, in *Interpretation of Micromorphological Features of Soils and Regoliths*, eds. G. Stoops, V. Marcelino and F. Mees. Amsterdam: Elsevier, 351–68.

Geertz, C., 1963. *Agricultural Involution: The Process of Ecological Change in Indonesia*. Los Angeles: University of California Press.

Gibson, H. & S. Venkateswar, 2015. Anthropological Engagement with the Anthropocene: A Critical Review. *Behaviour and Information Technology* 6, 5–27.

Giorgianni, M., 1990. *La Pietra Vissuta. Il Paesaggio Degli Iblei*. Palermo: Sellerio Editore.

Giusti, F., G. Manganelli & P.J. Schembri, 1995. *The Non-marine Molluscs of the Maltese Islands.* Torino: Museo Regionale die Scienze Naturali.

Glick, T.F., 1995. *From Muslim Fortress to Christian Castle*. Manchester: Manchester University Press.

Goldberg, P. & R.I. Macphail, 2006. *Practical and Theoretical Geoarchaeology*. Oxford: Blackwells Scientific.

Gómez Bellard, C., 1995. The first colonization of Ibiza and Formentera (Balearic Islands, Spain): Some more islands out of the stream? *World Archaeology* 26 (3), 442–55.

Gonzales-Samperiz, P., P. Utrilla, C. Mazo, B.L. Valero-Garces, M. Cruz Sopena, M. Morellon, M.S. Lopez, A. Moreno & M. Bea, 2009. Patterns of human occupation during the early Holocene in the Central Ebro Basin (NE Spain) in response to the 8.2 ka climatic event. *Quaternary Research* 71 (2), 121–32.

Gorenflo, L.J. & N. Gale, 1990. Mapping regional settlement in information space. *Journal of Anthropological Archaeology* 9 (3), 240–74.

Gorman, M.L., 1979. *Island Ecology*. (Outline Studies in Ecology.) London: Chapman and Hall.

Goudie, A.S., 1993. *The Human Impact on the Natural Environment*. Hoboken: Wiley-Blackwell.

Goudie, A.S. & H.A. Viles, 2016. *Geomorphology in the Anthropocene*. Cambridge: Cambridge University Press.

Gregg, S.A., 1988. *Foragers and Farmers: Population Interaction and Agricultural Expansion in Prehistoric Europe*.

Grima, R., 2004. The landscape context of megalithic architecture, in *Malta Before History*, ed. D. Cilia. Malta: Miranda, 327–45.

Grima, R., 2007. The Cultural Construction of the Landscape in Late Neolithic Malta, in *Cult in Context*, eds. D. Barrowclough & C. Malone. Oxford: Oxbow Books, 35–40.

Grima, R., 2008a. *The Making of Malta*. Malta: Midsea Books.

Grima, R., 2008b. Landscape, territories, and the life-histories of monuments in Temple Period Malta. *Journal of Mediterranean Archaeology* 21, 35–56.

Grima, R., 2011a. Hercules' unfinished labour: the management of Borġ in-Nadur and its landscape, in *Site, Artefacts and Landscape: Prehistoric Borġ in-Nadur, Malta* (*Praehistorica Mediterranea* 3), eds. D. Tanasi & N.C. Vella. Monza: Polimetrica, 341–72.

Grima, R., 2011b. The prehistoric islandscape, in *The Maritime History of Malta: The First Millennia*, eds. C. Cini & J. Borg. Malta: Salesians of Don Bosco and Heritage Malta, 10–35.

Grima, R. & S. Farrugia, 2019. Landscapes, landforms and monuments in Neolithic Malta, in *Landscapes and Landforms of the Maltese Islands*, eds. R. Gauci and J.A. Schembri. Cham, Switzerland: Springer Nature, 79–90.

Grimm, E.C., 1987. CONISS: a FORTRAN 77 program for stratigraphically constrained cluster analysis by the method of incremental sum of squares. *Computers & Geosciences* 13, 13–35.

Grove, A.T. & O. Rackham, 2003. *The Nature of Mediterranean Europe: An Ecological History*. New Haven: Yale University Press.

Grundmann, S. & U. Fürst, 1998. *The Architecture of Rome: An Architectural History in 400 Presentations*. Stuttgart: Edition Axel Menges.

Gruszczynski, M., J.D. Marshall, R. Goldring, M.L. Coleman, L. Malkowski, E. Gazdzicka, J. Semil & P. Gatt, P. 2008. Hiatal surfaces from the Miocene Globigerina Limestone Formation of Malta: biostratigraphy, sedimentology, trace fossils and early diagenesis. *Palaeogeography, Palaeoclimatology, Palaeoecology* 270 (2–3), 239–51.

Guilaine, J., F. Briois & J-D. Vigne, 2011. *Shillourokambos, un Etablissement Néolithique Précéramique à Chypre. Les fouilles du Secteur 1*. Paris-Athènes: Errance -Ecole française d'Athènes.

Guilcher, A. & R. Paskoff, 1975. Remarques sur la geomorphologie littorale de l'archipel maltais. *Bulletin de l'Association Geographique de France* 427, 225–31.

Gunatilaka, A., 2012. Holocene evolution of Arabian coastal sabkhas: a re-evaluation based on stable-isotope analysis, forty years after Shearman's first view of the sabkha, in *Quaternary Carbonate and Evaporite Sedimentary Facies and their Ancient Analogues: A Tribute to Douglas James Shearman*, eds. C.G. St.C. Kendall, A.S. Alsharhan, I. Jarvis & T. Stevens. *International Association of Sedimentologists Special Publication* 43, 113–32.

Gunderson, L.H., 2000. Resilience in theory and practice. *Annual Review of Ecology and Systematics* 31, 425–39.

Gvirtzman, G. & M. Wieder, 2001. Climate of the last 53,000 years in the eastern Mediterranean, based on soil-sequence stratigraphy in the coastal plain of Israel. *Quaternary Science Reviews* 20, 1827–49.

Haggard, S., M. Noland & A. Sen, 2009. *Famine in North Korea: Markets, Aid, and Reform*: New York: Columbia University Press.

Halstead, P., 2014. *Two Oxen Ahead: Pre-mechanized Farming in the Mediterranean*. Hoboken, New Jersey: John Wiley & Sons.

Haregeweyn, N., J. Poesen, J. Nyssen, G. Govers, G. Verstraeten, J. de Vente, J. Deckers, J. Moeyersons & M. Haile, 2008. Sediment yield variability in Northern Ethiopia: A quantitative analysis of its controlling factors. *Catena* 75, 65–76.

Harff, J., G. Bailey & F. Luth (eds.), 2016. *Geology and Archaeology: Submerged Landscapes of the Continental Shelf*. London: Geological Society Special Publications.

Haslam, S.M., 1969. *Malta's Plant Life*. Malta: Progress Press Co.

Haslam, S. M., Sell, P.D. & Wolseley, P.A. 1977. *A Flora of the Maltese Islands*. Msida: Malta University Press.

Havinga, A.J., 1964. Investigation into the differential corrosion susceptibility of pollen and spores in various soil types. *Pollen et Spores* 6, 621–35.

Havinga, A.J., 1967. Palynology and pollen preservation. *Review of Palaeobotany and Palynology* 2, 81–98.

Haywood, C., 2012. High spatial resolution electron probe microanalysis of tephras and melt inclusions without

beam-induced chemical modification. *The Holocene* 22, 119–25.

Heino, J. & T. Muotka, 2005. Highly nested snail and clam assemblages in boreal lake littorals: roles of isolation, area, and habitat suitability. *Ecoscience* 12, 141–6.

Herzog, I., 2014. A Review of Case Studies in Archaeological Least-cost Analysis. *Archeologia e Calcolatori* 25, 223–39.

Herzog, I., 2016. Potential and Limits of Optimal Path Analysis, in *Computational Approaches to Archaeological Spaces*, eds. A. Bevan & M. Lake. New York: Routledge, 179–211.

Hill, E.A., P.J. Reimer, C.O. Hunt, A.L. Prendergast & G.W. Barker, 2017. Radiocarbon Ecology of the Land Snail *Helix melanostoma* in Northeastern Libya. *Radiocarbon* 9, Special Issue 5, 1–22.

Hobbs, W.H., 1914. The Maltese Islands: a tectonic-topographic study. *Scottish Geographical Magazine* 30, 1–13.

Hodder, I. & C. Malone, 1984. Intensive survey of prehistoric sites in the Stilo region, Calabria. *Proceedings of the Prehistoric Society* 50, 121–50.

Hohlfelder, R.L. (ed.), 2008. 'The maritime world of ancient Rome,' in Proceedings of "The Maritime World of Ancient Rome" Conference held at the American Academy in Rome, 27–29 March 2003. Ann Arbor, Michigan: American Academy in Rome and University of Michigan Press.

Holliday, V.T. & W.G. Gartner, 2007. Methods of soil P analysis in archaeology. *Journal of Archaeological Science* 34, 301–33.

Holling, C.S., 1973. Resilience and stability of ecological systems. *Annual Review of Ecology and Systematics* 4, 1–23.

Hooker, D. (ed.), 1994. *History of Western Art: From Ancient Greece to the Present Day*. London: Barnes and Noble.

Horden, P. & N. Purcell (eds.), 2000. *The Corrupting Sea: A Study of Mediterranean Prehistory*. Oxford: Blackwell Publishers.

Horn, P.P., 1997. *The Victorian Town Child*. Stroud: Sutton Publishing Ltd.

House, M.R., K.C. Dunham & J.C. Wigglesworth, 1961. Geology of the Maltese Islands, in *Background for Development*, eds. H. Bowen-Jones, J.C. Dewdney & B.W. Fisher. Newcastle: University of Durham, 24–33.

Hughes, J.D., 2011. Ancient deforestation revisited. *Journal of History of Biology* 44, 43–57.

Hughes, J.K., 1999. Ancient Tracks of the Maltese Islands. *The Geographical Journal* 165, 62–78.

Hughes, Q., 1986. *The Building of Malta during the Period of the Knights of St. John 1530–1795*. Malta: Progress Press.

Hughes, Q., 1993. The Architectural Development of Hospitaller Malta, in *Hospitaller Malta 1530–1798: Studies on Early Modern Malta and the Order of St. John of Jerusalem*, ed. V. Mallia Milanes. Malta: Mireva, 483–507.

Hughes, J.D. & J. Thirgood, 1982. Deforestation, erosion, and forest management in ancient Greece and Rome. *Forest & Conservation History* 26, 60–75.

Hunt, C.O., 1997. Quaternary deposits in Maltese Islands: A microcosm of environmental change in Mediterranean lands. *Geo-Journal* 41 (2), 101–9.

Hunt, C.O., 1998. The impact of agricultural soil erosion on prehistoric and historic-period valley sedimentation in Central Italy, in *Il Sistema upmo-ambuiente tra passato e presente* 1, eds. A.C. Livadie & F. Ortolani. Bari: Edipuglia, 99–111.

Hunt, C.O., 2001. Palynology. *Mediterranean Archaeology* 13, 111–14.

Hunt, C.O., 2015. Palynology of some archaeological deposits from Tas-Silġ. In *Tas-Silg, Marsaxlokk (Malta) 1: Archaeological Excavations conducted by the University of Malta, 1996–2005*, ed. A. Bonanno. University of Malta, 437–50.

Hunt, C.O. & M. Fiacconi, 2018. Pollen taphonomy of cave sediments: What does the pollen record in caves tell us about external environments and how do we assess its reliability? *Quaternary International* 485, 68–75.

Hunt, C.O. & D. Gilbertson, 1995. Human activity, landscape change and valley alluviation in the Feccia Valley, Tuscany, Italy, in *Mediterranean Quaternary River Environments*, eds. J. Lewin, M.G. Macklin & J.C. Woodward. Rotterdam: Balkema, 167–76.

Hunt, C.O. & P.J. Schembri, 1999. Quaternary environments and biogeography of the Maltese Islands, in *Facets of Maltese Prehistory*, eds. A. Mifsud & C. Savona Ventura. Malta: Prehistoric Society of Malta, 41–75.

Hunt, C.O. & P.J. Schembri, 2018. Historic-period terrestrial environments and soil erosion in the Maltese Islands: evidence from mollusc assemblages from cave-fills at Ghajn il-Kbira, near Victoria, Gozo. *Ancient Near Eastern Studies, Supplement* 4, 67–74.

Hunt, C.O. & N.C. Vella, 2004/2005. A view from the countryside: pollen from a field at Mistra Valley, Malta. *Malta Archaeological Review* 7, 61–69.

Hunt, C.O., D.D. Gilbertson & R.E. Donohue, 1992. Palaeobiological evidence for agricultural soil erosion in the Montagnola Senese, Italy, in *Past and Present Soil Erosion: Archaeological and Geographical Perspectives*, eds. M.G. Bell & J. Boardman. Oxford: Oxbow Monograph 23, 163–74.

Hunt, C.O., D.D. Gilbertson & H.A. El-Rishi, 2007. An 8000-year history of landscape, climate and copper exploitation in the Middle East: the Wadi Faynan and the Wadi Dana National Reserve in southern Jordan. *Journal of Archaeological Science* 34, 1306–38.

Hyde, H.P.T., 1955. *Geology of the Maltese Islands*. Malta: Lux Press.

Imeson, A.C., F.J.P.M. Kwaad & H.J. Mucher, 1980. Hillslope processes and deposits in forested areas in Luxembourg, in *Timescales in Geomorphology*, eds. R.A. Cullingford, D.A. Davidson & J. Lewin. Chichester: John Wiley & Sons, 31–42.

Indruszewski, G. & C.M. Barton, 2006. Simulating sea surfaces for modeling Viking Age seafaring in the Baltic Sea, in *Computer Applications and Quantitative Methods in Archaeology, Proceedings of the 34th Conference*, 616–30.

IUCN, 2017. *The IUCN Red List of Threatened Species. Version 2017-2*. http://www.iucnredlist.org.

Jaccarini, C.J., 2002. *Ir-Razzett. The Maltese Farmhouse*. Malta: Open Library.

Jaccarini, C.J. & M.N. Cauchi, 1999. The enigmatic rock-cut pans of Mġarr ix-Xini. *Melita Historica* XII (4), 419–44.

Jaouadi, S., V. Lebreton, V. Bout-Roumazeilles, G. Siani, R. Lakhdar, R. Boussoffara, L. Dezilieau, N. Kallel, B.

Mannai-Tayech & N. Comborieu-Nebout, 2016. Environmental changes, climate and anthropogenic impact in south-east Tunisia during the last 8 kyr. *Climates of the Past* 12, 1339–59.

Jenks, G.F., 1967. The Data Model Concept in Statistical Mapping. *International Yearbook of Cartography* 7, 186–90.

Johnson, M., 1996. *An Archaeology of Capitalism*. New York: Wiley.

Jolliffe, I.T., 2002. *Principal Component Analysis* (2nd edition). Dordrecht: Springer.

John, C.S., M. Mutti & T. Adatte, 2003. Mixed carbonate-siliciclastic record on the North African margin (Malta) – coupling of weathering processes and mid Miocene climate. *Geological Society of America Bulletin* 115 (2), 217–29.

Jones, A. & C. Hunt, 1994. Walls, wells and water supply: aspects of the cultural landscape of Gozo. *Landscape Issues* 15, 24–9.

Jones, S., 2009. *Darwin's Island: The Galapagos in the Garden of England.* London: Little, Brown.

Jongerius, A., 1983. Micromorphology in agriculture, in *Soil Micromorphology*, eds. P. Bullock & C.P. Murphy. Berkhamsted: A.B. Academic Publishers, 111–38.

Judson, S., 1963. Erosion and deposition of Italian stream valleys during historic time. *Science* 140, 898–9.

Kantner, J., 2004. Geographical Approaches for Reconstructing Past Human Behavior from Prehistoric Roadways, in *Spatially Integrated Social Science*, eds. M.F. Goodchild & D.G. Janelle. Oxford: Oxford University Press, 323–44.

Karkanas, P. & P. Goldberg, 2010. Phosphatic features, in *Interpretation of Micromorphological Features of Soils and Regoliths*, eds. G. Stoops, V. Marcelino & F. Mees. Amsterdam: Elsevier, 521–41.

Kemp, R. 1986. Pre-Flandrian Quaternary soils and pedogenic processes in Britain. In ed. V. Wright *Palaeosols, Their Recognition and Interpretation*. London; Blackwell, 242–62.

Kinnaird, T.C., D.C.W., Sanderson, C. Burbidge & E. Peltenburg, 2007. OSL Dating of Neolithic Kissonerga-Mylouthkia, Cyprus. *Neolithics* 2/07, 51–7.

Kinnaird, T.C., J.E. Dixon, A.H.F. Robertson, E. Peltenburg & D.C.W. Sanderson, 2013. *Mediterranean Archaeology and Archaeometry* 13, 49–62.

Kinnaird, T.C., C.J. Scarre, L. Oosterbeck & D.C.W. Sanderson, 2015. 'OSL dating of remnants of the megalithic site of Cabeço dos Pendentes, Portugal.' Unpublished SUERC Technical Report, University of Glasgow.

King, C.H. & D. Bertsch, 2015. Historical perspective: snail control to prevent schistosomiasis. *PLoS Neglected Tropical Diseases 9* (4), e0003657.

Kirch, P.V., 1986. *Island Societies: Archaeological Approaches to Evolution and Transformation.* Cambridge: Cambridge University Press.

Kirkby, M.J., 1969. Erosion by water on hillslopes, in *Water, Earth and Man*, ed. R.J. Chorley. London: Methuen, 229–38.

Knapp, A.B., 1992. Archaeology and Annales: time, space, and change, in *Archaeology, Annales and Ethnohistory*, ed. A.B. Knapp. (New Directions in Archaeology.) Cambridge: Cambridge University Press, 1–21.

Kolb, M. J., 2005. The genesis of monuments among the Mediterranean islands, in *The Archaeology of Mediterranean Prehistory*, eds. E. Blake & B. Knapp. Oxford: Wiley-Blackwell, 156–79.

Kondo, Y. & Y. Seino, 2009. GPS-aided Walking Experiments and Data-driven Travel Cost Modeling on the Historical Road of Nakasendō-Kisoji (Central Highland Japan), in *Making History Interactive. Computer Applications and Quantitative Methods in Archaeology. Proceedings of the 37th International Conference, Williamsburg, Virginia, USA, March 22–26, 2009*, eds. L. Fische, B. Frischer & S. Wells. (BAR International Series.) Oxford: Archaeopress, 158–65.

Kooistra, M.J. & M.M. Pulleman, 2010. Features related to faunal activity, in *Interpretation of Micromorphological Features of Soils and Regoliths*, eds. G. Stoops, V. Marcelino & F. Mees. Amsterdam: Elsevier, 397–414.

Kosmas, C., N. Danalatos, L.H. Cammeraat, M. Chabart, J. Diamantopoulos, R. Farand, L. Gutierrez, A. Jacob, H. Marques, J. Martinez-Ferenandez, A. Mizara, N. Moustakas, J.M. Nicolau, C. Oliveros, G. Pinna, R. Puddu, J. Puigdefabregas, M. Roxo, A. Simao, G. Stamou, N. Tomasi, D. Usai & A. Vacca, 1997. The effect of land use on runoff and soil erosion rates under Mediterranean conditions. *Catena* 29, 45–59.

Kuhn, P., J. Aguilar & R. Miedema, 2010. Textural features and related horizons, in *Interpretation of Micromorphological Features of Soils and Regoliths*, eds. G. Stoops, V. Marcelino & F. Mees. Amsterdam: Elsevier, 217–50.

Kwaad, F.J.P.M. & H.J. Mucher, 1979. The formation and evolution of colluvium on arable land in Northern Luxembourg. *Geoderma* 22, 173–92.

Lambeck, K., F. Antonioli, M. Anzidei, L. Ferranti, G. Leoni, G. Scicchitano & S. Silenzi, 2011. Sea level change along the Italian coasts during Holocene and prediction for the future. *Quaternary International* 232, 250–7.

Lane, C.S., V.L. Cullen, D. White, C.W.F. Bramham-Law & V.C. Smith, 2014. Cryptotephra as a dating and correlation tool in archaeology. *Journal of Archaeological Science* 42 (Supplement C), 42–50.

Lanfranco, E., 1984. *Guida alle escursioni a Malta; Aprile 1984*. Societa Botanica Italiana sezzione Siciliana.

Lanfranco, E., 1995. The vegetation of the Maltese Islands, in *The non-marine molluscs of the Maltese Islands*, eds. F. Giusti, G. Manganelli & P.J. Schembri. Torino, Italy: Museo Regionale di Scienze Naturali, 27–9.

Lanfranco, E. & P.J. Schembri, 1986. Maltese wetlands and wetland biota. *Potamon* (Malta) 15, 122–5.

Lang, D.M., 1960. *Soils of Malta and Gozo*. Colonial Office, Colonial Research Studies Report No. 29. London: H.M.S.O.

Lang, D.M., 1961. Soils of Malta and Gozo, in *Malta. Background for Development*, eds. H. Bowen-Jones, J. Dewdney & W. Fisher. Durham: Department of Geography, Durham Colleges, 83–98.

Langgut, D., R. Cheddadi, J.S. Carrion, M. Cavanagh, D. Colombaroli, W. Eastwood, R. Greenberg, T. Litt, A.-M. Mercuri, A. Miebach, N. Roberts, H. Woldring & J. Woodbridge, 2019. The origin and spread of olive cultivation in the Mediterranean basin: the fossil

pollen evidence. *Holocene. Special issue. The Changing Face of the Mediterranean: Land Cover, Demography and Environmental Change* 29 (5), 902–22.

Laparidou, S., M.N. Ramsey & A.M. Rosen, 2015. Introduction to the special issue 'The Anthropocene in the Longue Durée'. *The Holocene* 25, 1537–8.

Le Bas, M.J., R.W. Le Maitre, A. Streckeisen & B. Zanettini, 1986. A chemical classification of volcanic rocks based on the total alkali–silica diagram. *Journal of Petrology* 27 (3), 745–50.

Lee, R., 2012. *Fernand Braudel, the Longue Durée, and World Systems Analysis.* Albany: University of New York Press.

Lelong, R. & B. Souchier, 1982. Ecological significance of the weathering complex: relative importance of general and local factors, in *Constituents and Properties of Soils*, eds. M. Bonneau & B. Souchier. London: Academic Press, 82–108.

Lemerle, F. & Y. Pauwels, 2008. *Baroque Architecture: 1600–1750*. Michigan: Random House Incorporated.

Lespez, L., 2003. Geomorphic responses to long-term land use changes in Eastern Macedonia (Greece). *Catena* 51, 181–208.

Lessa, G.C., R.J. Angulo, P.C. Giannini & A.D. Araújo, 2000. Stratigraphy and Holocene evolution of a regressive barrier in south Brazil. *Marine Geology* 165, 87–108.

Lewis, H., 2012. *Investigating Ancient Tillage: An experimental and soil micromorphological study*. B.A.R. International Series S2388. Oxford: Archaeopress.

Lifton, N.A. & G.G. Chase, 1992. Tectonic, climatic and lithologic influences on landscape fractal dimension and hypsometry: implications for landscape evolution in the San Gabriel Mountains, California. *Geomorphology* 5, 77–114.

Lindbo, D.L., M.H. Stolt & M.J. Vepraskas, 2010. Redoximorphic features, in *Interpretation of Micromorphological Features of Soils and Regoliths*, eds. G. Stoops, V. Marcelino & F. Mees. Amsterdam: Elsevier, 129–47.

Linderholm J. & E. Lundberg, 1994. Chemical Characterization of Various Archaeological Soil Samples using Main and Trace Elements determined by Inductively Coupled Plasma Atomic Emission Spectrometry. *Journal of Archaeological Science* 21, 303–14.

Locatelli, D. 2005–2006. Nuove ricerche a San Pawl Milqi: primi risultati. *Rendiconti della Pontificia Accademia Romana di Archeologi* 78, 257–73.

Locatelli, D., 2008. L'oro verde di Malta. Stime sulla produzione olearia nella villa San Pawl Milqi, in *L'Africa Romana: le ricchezze dell'Africa: risorse, produzioni, scambi. Atti del XVII Convegno di studio, Sevilla, 14–17 dicembre 2006*, eds. J. Gonzaléz, P. Ruggieri, C. Vismara, & R. Zucca. Rome: Carocci, 1351–74.

Löfgren, O., 2004. The Sweetness of Home, in *The Anthropology of Space and Place: Locating Culture*, eds. S.M. Low & D. Lawrence-Zuñiga. New York: Wiley, 142–59.

Lomolino, M.V., B.R. Riddle, R.J. Whittaker & J.H. Brown, 2010. *Biogeography* (4th edition) Sunderland, Mass.: Sinauer Associates.

Long, T., C.O. Hunt & D. Taylor, 2016. Radiocarbon anomalies suggest late onset of agricultural intensification in the catchment of the southern part of the Yangtze Delta, China. *Catena* 147, 586–94.

Loughran, R.J., G.L. Elliott, L.T. Maliszewski & B.L. Campbell, 2000. Soil loss and viticulture at Pokolbin, New South Wales, Australia. *IAHS Publications* 261, 141–52.

Loveland, P.J. & D.C. Findlay, 1982. Composition and development of some soils on glauconitic Cretaceous (Upper Greensand) rocks in southern England. *Journal of Soil Science* 33, 279–94.

Lo Vetro, D. & F. Martini, 2016. Mesolithic in Central-Southern Italy: Overview of lithic productions. *Quaternary International* 423, 279–302.

Luo, W., 1998. Hypsometric analysis with a geographic information system. *Computers and Geosciences* 24, 815–21.

Luttrell, A.T., 1975. Approaches to Medieval Malta, in *Medieval Malta: Studies on Malta Before the Knights*, ed. A.T. Luttrell. London: The British School at Rome, 1–70.

MacArthur, R.H. & E.O. Wilson, 1963. An equilibrium theory of insular zoogeography. *Evolution* 17 (4), 373–87.

MacArthur, R.H. & E.O. Wilson, 1967. *The Theory of Island Biogeography.* Princeton, NJ: Princeton University Press.

MacDonald, R., 1974. Nomenclature and petrochemistry of the peralkaline oversaturated extrusive rocks. *Bulletin Volcanologique* 38 (2), 498–516.

MacLeod, D.A., 1980. The origin of the red Mediterranean soils in Epirus, Greece. *Journal of Soil Science* 31, 125–36.

Macklin, M.G., S. Tooth, P.A. Brewer, P.L. Noble & G.A.T. Duller, 2010. Holocene flooding and river development in a Mediterranean steepland catchment: The Anapodaris Gorge, south central Crete, Greece. *Global and Planetary Change* 70, 35–52.

Magny, M., B. Vanniere, G. Zanchetta, E. Fouache, G. Touchais, L. Petrika, C. Coussot, A-V. Walter-Simonnet & F. Arnau, F. 2009. Possible complexity of the climatic event around 4300–3800 cal. BP in the central and western Mediterranean. *The Holocene* 19, 823–33.

Magny, M., B. Vanniere, C. Calo, L. Millet, A. Leroux, O. Peyron, G. Zanchetta, T. La Mantia & W. Tinner, 2011. Holocene hydrological changes in south-western Mediterranean as recorded by lake-level fluctuations at Lago Preola, a coastal lake in southern Sicily, Italy. *Quaternary Science Reviews* 30, 2459–75.

Magri, E., 2009 (1906). *Ruins of a Megalithic Temple at Xeuchia. (Shewkiyah), Gozo, Malta. First Report. Reprinted with Introduction by Josef Mario Briffa SJ.* Valletta: Heritage Malta – Salesians of Don Bosco (Malta).

Magri, O., 2006. A geological and geomorphological review of the Maltese Islands with special reference to the coastal zone. *Territoris* 6, 7–26

Magro Conti, J. & P.C. Saliba (eds.), 2007. *The Significance of Cart-Ruts in Ancient Landscapes*. Malta: Culture 2000 & Midsea Books.

Mahoney, L., 1996. *5000 years of Architecture in Malta.* Malta: Valletta Publications.

Mallia-Milanes, V., 1992. *Venice and Hospitaller Malta, 1530–1798: aspects of a relationship.* Marsa, Malta: PEG.

Mallia-Milanes, V., 1993. *Hospitaller Malta, 1530–1798: Studies on Early Modern Malta and the Order of St John of Jerusalem.* Msida, Malta: Mireva.

Malm, A. & A. Hornborg, 2014. The geology of mankind? A critique of the Anthropocene narrative. *The Anthropocene Review* 1, 62–9.

Malone, C. 1985. Pots, prestige and ritual in neolithic southern Italy. In eds. C. Malone & S. Stoddart, *Papers in Italian Archaeology IV. Vol. ii. Prehistory*. Oxford: British Archaeological Reports, 118–51.

Malone, C.A.T., 1997–8. Processes of Colonisation in the central Mediterranean. *Accordia Research Papers* 7, 37–57.

Malone, C. 2003. The Italian Neolithic: a synthesis of research. *Journal of World Prehistory* 17 (3), 235–312.

Malone, C. 2015. The Neolithic in Mediterranean Europe. In eds. C. Fowler, J. Harding, J. & D. Hofmann, *The Oxford Handbook of Neolithic Europe*. Oxford: Oxford University Press, 175–94.

Malone, C., 2017. Review of Clare Manen, in La transition néolithique en Méditerranée. Actes du colloque. Transitions en Méditerranée, ou comment des chasseurs devinrent agriculteurs. Muséum de Toulouse, 14–15 avril 2011, eds. T. Perrin & J. Guilaine. *Germania* 94, 291–5.

Malone, C. & S. Stoddart (eds.), 1994. *Territory, Time and State: The Archaeological Development of the Gubbio Basin*. Cambridge: Cambridge University Press.

Malone, C. & S. Stoddart, 2000. The current state of prehistoric ceramic studies in Mediterranean survey, in *Extracting Meaning from Ploughsoil Assemblages*, eds. R. Francovich, H. Patterson & G. Barker. Oxford: Oxbow Books, 95–104.

Malone, C. & S. Stoddart, 2009. Conclusions. In C. Malone, S. Stoddart, A. Bonanno & D. Trump (eds.), *Mortuary Customs in Prehistoric Malta. Excavations at the Brochtorff Circle at Xagħra (1987–94)*. Cambridge: McDonald Institute for Archaeological Research, 361–84.

Malone, C. and S. Stoddart, 2013. Ritual failure and the temple collapse of prehistoric Malta, in *Ritual Failure: Archaeological Perspectives*, eds. V.G. Koutrafouri & J. Sanders. Leiden: Sidestone Press, 63–84.

Malone, C.A.T., D.A. Barrowclough & S. Stoddart, 2007. Introduction, in *Cult in Context*, eds. D. Barrowclough & C. Malone. Oxford: Oxbow Books, 1–7.

Malone, C., R. Grima, R. McLaughlin, E. Parkinson, S. Stoddart & N. Vella, In press. *Temple Places: Excavating Cultural Sustainability in Prehistoric Malta*. Volume 2 of Fragility and sustainability – Studies on Early Malta, the ERC-funded Project. Cambridge: McDonald Institute for Archaeological Research.

Malone, C., S. Stoddart & D. Trump, 1988. A house for the temple builders. Recent investigations on Gozo, Malta. *Antiquity* 62, 297–301.

Malone, C., C. Brogan, R. McLaughlin & S. Stoddart, 2016. Small island sustainability in a case study for Malta. *Scienze delle Antichità* 2, 403–16.

Malone, C., S. Stoddart, A. Bonanno & D. Trump (eds.), 2009a. *Mortuary Customs in Prehistoric Malta. Excavations at the Brochtorff Circle at Xagħra (1987–94).* Cambridge: McDonald Institute for Archaeological Research.

Malone, C., R. Grima, J. Magro-Conti, D. Trump, S. Stoddart & H. Hardisty, 2009b. The domestic environment, in *Mortuary Customs in Prehistoric Malta. Excavations at the Brochtorff Circle at Xagħra (1987–94)*, eds. C. Malone, S. Stoddart, A. Bonanno & D. Trump. Cambridge: McDonald Institute for Archaeological Research, 41–56.

Mandarini, E., 1860. *Storia di S. Rocco da Mompellieri e delle sue più celebri pestilenze dal suo tempo sino ai nostri giorni (XIV–XIX)*. Venezia: Lito-tipografia Mozzoni.

Mangerud, J.A.N. & S. Gulliksen, 1975. Apparent radiocarbon ages of recent marine shells from Norway, Spitsbergen, and Arctic Canada. *Quaternary Research* 5 (2), 263–73.

Marchetti, M., 2002. Environmental changes in the central Po Plain (northern Italy) due to fluvial modifications and anthropogenic activities. *Geomorphology* 44, 361–73.

Marcus, J. & C. Stanish, 2006. Introduction, in *Agricultural Strategies*, eds. J. Marcus & C. Stanish. Los Angeles: Cotsen Institute of Archaeology, 1–13.

Margaritis, E. & M.K. Jones, 2008. Greek and Roman Agriculture, in *The Oxford Handbook of Engineering and Technology in the Classical World*, ed. J.P. Oleson. Oxford: Oxford University Press, 158–74.

Marriner, N., T. Gambin, M. Djamali, C. Morhange & M. Spiteri, 2012. Geoarchaeology of the Burmarrad ria and early Holocene human impacts in western Malta. *Palaeogeography, Palaeoclimatology, Palaeoecology* 339, 52–65.

Marriner, N., D. Kaniewski, T. Gambin, B. Gambin, B. Vanniere, C. Morhange, M. Djamali, K. Tachikawa, V. Robin, D. Rius & E. Bard, E. 2019. Fire as a motor of rapid environmental degradation during the earliest peopling of Malta 7500 years ago. *Quaternary Science Reviews* 212, 199–205.

Mathias, G., 2015. *What Could the Longue Durée Mean for the History of Modern Sciences?* Boston: Greenstone.

Matthews, R., 2005. The rise of civilization in southwest Asia, in *The Human Past: A Textbook of World Prehistory*, ed. C. Scarre. London: Thames & Hudson, 432–71.

Mauz, B., N. Elmejdoub, R. Nathan & Y. Jedoui, 2009. Last interglacial coastal environments in the Mediterranean–Saharan transition zone. *Palaeogeography, Palaeoclimatology, Palaeoecology* 279, 137–46.

Mayes, J., 2001. Rainfall variability in the Maltese Islands: changes, causes and consequences. *Geography* 86 (2), 121–30.

Mayr, A., 1908. *The Prehistoric Remains of Malta*. Translated from the German. Malta: Printed for Private Circulation.

McCarthy, F.M.G., K.N. Mertens, M. Ellegaard, K. Sherman, V. Pospelova, S. Ribeiro, S. Blasco & D. Vercauteren, 2011. Resting cysts of freshwater dinoflagellates in southeastern Georgian Bay (Lake Huron) as proxies of cultural eutrophication. *Review of Palaeobotany and Palynology* 166 (1–2), 46–62.

McLaughlin, T.R., S. Stoddart & C. Malone, 2018. Island risks and the resilience of a prehistoric civilization. *World Archaeology* 50 (4), 570–83.

Mederos Martín, A., 2005. La cronologia Fenicia entre el Mediterráneo Oriental y Occidental. *Anejos del Archivo Español de Arqueología* 33, 305–46.

Mejdahl, V., 1979. Thermoluminescence dating: Beta-dose attenuation in quartz grains. *Archaeometry* 21, 61–72.

Mercieca, S., 2005. The production of salt in Malta in Early Modern times, in *La navigation du Savior: Réseau des*

Arsenaux Historiques de la Méditerranée, ed. S. Giannino. University of Malta and UNESCO: Villefranche-sur-Mer: Euromed Heritage, 122–38.

Mercuri, A. M., C.A. Accorsi, M.B. Mazzanti, G. Bosi, A. Cardarelli, D. Labate, M. Marchesini & G.T. Grandi, 2006. Economy and environment of Bronze Age settlements – Terramaras – on the Po Plain (Northern Italy): first results from the archaeobotanical research at the Terramara di Montale. *Vegetation History and Archaeobotany* 16, 43–60.

Metcalfe, C.R., 1996. Report on the botanical determination of charcoal samples, in *Skorba: Excavations Carried Out on Behalf of the National Museum of Malta, 1961–1963*, D.H. Trump. (Reports of the Research Committee of the Society of Antiquaries of London.) London and the National Museum of Malta: The Society of Antiquaries, Appendix V.

Micallef, A., F. Foglini, L. Bas, L. Angeletti, V. Maselli, A. Pasuto & M. Taviani, M. 2013. The submerged paleo-landscape of the Maltese Islands: Morphology evolution and relation to Quaternary environment change. *Marine Geology* 335, 129–47.

Micallef, S., 2019. The terraced character of the Maltese rural landscape: a case study of Buskett Area, in *Landscapes and Landforms of the Maltese Islands*, eds. R. Gauci & J.A. Schembri. (World Geomorphological Landscapes.) Cham, Switzerland: Springer Nature, 153–65.

Middleton, W.D. & D.T. Price, 1996. Identification of activity areas by multi-element characterization of sediments from modern and archaeological house floors using Inductively Coupled Plasma-Atomic Emission spectroscopy. *Journal of Archaeological Science* 23, 673–87.

Milanesi, C., R. Vignani, F. Ciampolini, C. Faleri, L. Cattani, A. Moroni, S. Arrighi, M. Scali, P. Tiberi, E. Sensi, W. Wang & M. Cresti, 2006. Ultrastructure and DNA sequence analysis of single *Concentricystis* cells from Alta Val Tiberina Holocene sediments. *Journal of Archaeological Science* 33, 1081–7.

Miller, H.M-L., 2006. Water Supply, Labor Requirements, and Land Ownership in Indus Floodplain Agricultural Systems, in *Agricultural Strategies*, eds. J. Marcus & C. Stanish. Los Angeles: Cotsen Institute of Archaeology, 92–128.

Mitchell, P. & J. Dewdney, 1961. The Maltese climate and weather, in *Malta, a Background for Development*, eds. H. Bowen-Jones, J.C. Dewdney & W.B. Fisher. Durham: Durham University Press, 48–82.

Mizota, M., M. Kusakabe & M. Noto, 1988. Eolian contribution to soil development on Cretaceous limestones in Greece as evidenced by oxygen isotope composition of quartz. *Geochemical Journal* 22, 41–46.

Mommsen, H., A. Bonanno, K. Chetkuti Bonavita, I. Kakoulli, M. Musumect, C. Sagona, A. Schwedt, N. C. Vella & N. Zacharias 2006. Characterization of Maltese Pottery of the Late Neolithic, Bronze Age and Punic Period by Neutron Activation Analysis, in *Geomaterials in Cultural Heritage*, eds. M. Maggetti & B. Messiga, (Special Publications 257.) London: The Geological Society of London, 81–9.

Moore, P.D., J.A. Webb & M.E. Collinson, 1991. *Pollen analysis* (2nd edition). Oxford: Blackwell Scientific.

Morter, J., 1990. The Excavations at Capo Alfiere, 1987–present, in *The Chora or Croton 1983–89*. (Institute of Classical Archaeology.) Austin: University of Texas at Austin, 16–30.

Morris, M.W., 2002. *Soil Science and Archaeology: Three Test Cases from Minoan Crete*. Philadelphia: The Institute for Aegean Prehistory Academic Press.

Morris, T.O., 1952. *The Water Resources of Malta*. Malta: Government Printing Office.

Morrison, K.D., 1994. The intensification of production: archaeological approaches. *Journal of Archaeological Method and Theory* 1 (2), 111–59.

Moscati, S., 1993. Some reflections on Malta in the Phoenician World. *Journal of Mediterranean Studies* 3 (2), 286–90.

Mottershead, D.N., P. Farres & A. Pearson, 2010. The changing Maltese soil environment: Evidence from the ancient cart tracks at San Pawl Tat-Tarġa, Naxxar. *Geological Society London Special Publications* 331, 219–29.

Mottershead, D., A. Pearson & M. Schaefer, 2017. The cart ruts of Malta: an applied geomorphology approach. *Antiquity* 82, 1065–79.

Mucher, H.J., T. Carballas, F. Guitan Ojea, P.D. Jungerius, S.B. Kroonenberg & M.C. Villar, 1972. Micromorphological analysis of effects of alternating phases of landscape stability and instability on two soil profiles in Galicia, N.W. Spain. *Geoderma* 8, 241–66.

Mucher, H.J., H. van Steijn & F.J.P.M. Kwaad, 2010. Colluvial and mass wasting deposits, in *Interpretation of Micromorphological Features of Soils and Regoliths*, eds. G. Stoops, V. Marcelino & F. Mees. Amsterdam: Elsevier, 37–48.

Muhs, D.R., J. Budahn, A. Avila, G. Skipp, J. Freeman & D. Paterson, 2010. The role of African dust in the formation of Quaternary soils on Mallorca, Spain and the implications for the genesis of Red Mediterranean soils. *Quaternary Science Reviews* 29, 2518–43.

Murphy, C.P., 1986. *Thin Section Preparation of Soils and Sediments*. Berkhamsted: A.B. Academic.

Murray, A.S. & A.G. Wintle, 2000. Luminescence dating of quartz using an improved single-aliquot regenerative-dose protocol. *Radiation Measurements* 32, 57–73.

Murray, J., 1890. The Maltese Islands, with special reference to their geological structure. *Scottish Geographical Magazine* 6, 449–88.

Murray, M.A., 1923–1929. *Excavations in Malta.* London: B. Quaritch.

Murrieta-Flores, P., 2012. Understanding human movement through spatial technologies. The role of natural areas of transit in the Late Prehistory of South-western Iberia. *Trabajos de Prehistoria* 69, 103–22.

Murrieta-Flores, P., 2014. Space and Temporality in Herding Societies. Exploring the Dynamics of Movement during the Iberian Late Prehistory, in *Space and Time in Mediterranean Prehistory*, eds. S. Souvatzi & A. Hadji. New York: Routledge, 196–213.

Natali, E. & V. Forgi, 2018. The beginning of the Neolithic in Southern Italy and Sicily. *Quaternary International* 470, 253–69.

National Statistics Office, 2016. *Agriculture and Fisheries 2014*. Valletta: National Statistics Office.

National Statistics Office, 2019. *Regional Statistics Malta 2019 Edition*. Valletta: National Statistics Office.

Newbery, J., 1968. The perched water table in the Upper Limestone aquifer of Malta. *Journal of the Institution of Engineers (India)* 22, 551–70.

Newhard, J.M.L., N.S. Levine & A.D. Phebus, 2014. The development of integrated terrestrial and marine pathways in the Argo-Saronic region, Greece. *Cartography and Geographic Information Science* 41 (4), 379–90.

Noti, R., J.F.N. van Leeuwen, D. Colombaroli, E. Vescovi, S. Pasta, T. La Mantia & W. Tinner, 2009. Mid- and Late-Holocene vegetation and fire history of Biviere di Gela, a coastal lake in southern Sicily. *Vegetation History and Archaeobotany* 18, 371–87.

O'Brien, C., K. Selby, Z. Ruiz, A. Brown, M. Dinnin, C. Caseldine, P. Langdon & I. Stuijts, 2005. A sediment-based multiproxy palaeoecological approach to the environmental archaeology of lake dwellings (crannogs), central Ireland. *The Holocene* 15 (5), 707–19.

Oil Exploration Directorate, 1993. *Geological Map of the Maltese Islands. Sheet 1 – Malta – Scale 1:25,000*. Malta: Office of the Prime Minister.

Oonk, S., C.P. Slomp & D.J. Huisman, 2009. Geochemistry as an aid in archaeological prospection and site interpretation: current issues and research directions. *Archaeological Prospection* 16, 35–51.

O'Sullivan, D. & D.J. Unwin, 2010. *Geographic Information Analysis* (2nd edition). Hoboken: John Wiley & Sons, Inc.

Orengo, H.A. & C. Miró, 2011. Following Roman waterways from a computer screen: GIS-based approaches to the analysis of Barcino's aqueducts, in *Go Your Own Least Cost Path: Spatial Technology and Archaeological Interpretation; Proceedings of the GIS Session at EAA 2009*, eds. J.W.H. Verhagen, A.G. Posluschny & A. Danielisova. Oxford: Achaeopress, 47–53.

Pace, A., 1995. Malta and the Dawn of the Metal Ages. *Treasures of Malta* 2 (1), 55–9.

Pace, A. (ed.), 2000. *The Ħal Saflieni Hypogeum 4000 BC – 2000 AD*. Malta: National Museum of Archaeology.

Pace, A., 2004. Malta During Prehistory: An Overview, in *Malta: Roots of a Nation; The Development of Malta from an Island People to an Island Nation*, ed. K. Gambin. Malta: Midsea Books Ltd., 25–44.

Pace, A. & G. Azzopardi, 2008. Economic landscapes of the Maltese Islands during antiquity: a survey of ancient wine presses. *Poster Presented at the XVII Congresso Internazionale di Archeologia Classica, Rome*.

Pagnoux, C., L. Bouby, S. Ivorra, C. Petit, C., S.M. Valamoti, T. Pastor & J.F. Terral, 2015. Inferring the agrobiodiversity of *Vitis vinifera* L. (grapevine) in ancient Greece by comparative shape analysis of archaeological and modern seeds. *Vegetation History and Archaeobotany* 24, 75–84.

Panagos, P., C. Ballabio, P. Borrelli, K. Meuseburger, A. Klik, S. Rousseva, M.P. Tadic, S. Michaelides, M. Hrabalikova, P. Olsen, J. Aalto, M. Lakatos, A. Rymszewicz, A. Dumitrescu, S. Begueria & C. Alewell, 2015a. Rainfall erosivity in Europe. *Science of The Total Environment* 511, 801–14.

Panagos, P., P. Borrelli & K. Meusburger, 2015b. A new European slope length and steepness factor (LS-factor) for modeling soil erosion by water. *Geosciences (Switzerland)* 5, 117–26.

Panagos, P., P. Borrelli, J. Poesen, K. Meuseburger, C. Ballabio, E. Lugato, L. Montanarella & C. Alewell, 2015c. The new assessment of soil loss by water erosion in Europe. *Environmental Science & Policy* 54, 438–47.

Pantis, J. & N.S. Margaris, 1988. Can systems dominated by asphodels be considered as semi-deserts? *International Journal of Biometeorology* 32, 87–91.

Parnell, A., J. Haslett, J.R.M. Allen, C.E. Buck & B. Huntley, 2008. A flexible approach to assessing synchroneity of past events using Bayesian reconstructions of sedimentation history. *Quaternary Science Reviews* 27, 1872–85.

Paskoff, R. & P. Sanlaville, 1978. Observations géomorphologiques sur les côtes de l'archipel maltais. *Zeitschrift für Geomorphologie* 22 (3), 310–28.

Pásztor, E. & C. Roslund, 1997. Orientation of Maltese 'dolmens'. *Journal of European Archaeology* 5, 183–9.

Patacchini, A. & G. Nicatore, 2016. Potential paths and historical road network between Italy and Egypt: from predictive to postdictive approach, in *Keep the Revolution Going. Proceedings of the 43rd Annual Conference on Computer Applications and Quantitative Methods in Archaeology*, eds. S. Campana, R. Scopigno, G. Carpentiero & M. Cirillo. Oxford: Archaeopress, 669–81.

Patton, M., 1996. *Islands in Time: Island Sociogeography and Mediterranean Prehistory*. London: Routledge.

Peccerillo, A. & S.R. Taylor, 1976. Geochemistry of eocene calc-alkaline volcanic rocks from the Kastamonu area, Northern Turkey. *Contributions to Mineralogy and Petrology* 58, 63–81.

Pedley, H.M., 1974. Miocene seafloor subsidence and later subaerial solution subsidence structures in the Maltese Islands. *Proceedings of the Geological Association* 85, 533–47.

Pedley, H.M., 1975. 'The Oligo-Miocene Sediments of the Maltese Islands.' Unpublished PhD thesis, University of Hull.

Pedley, H.M., 1978. A new lithostratigraphical and palaeoenvironmental interpretation for the coralline limestone formations (Miocene) of the Maltese Islands. *Overseas Geology and Mineral Resources* 54, 1–17. London: H.M.S.O.

Pedley, H.M., 1980. The occurrence and sedimentology of a Pleistocene travertine in the Fiddien Valley, Malta. Proceedings of the Geologists' Association 91 (3), 195–202.

Pedley, H.M., 1993. *Geological maps of the Maltese Islands. Scale, 1: 25,000, 2 sheets. In Oil Exploration Directorate, 1993. Sheet 1 (Malta); Sheet 2 (Gozo and Comino).* Keyworth: British Geological Survey.

Pedley, H.M., 2011. The Calabrian stage, Pleistocene highstand in Malta: a new marker for unravelling the late Neogene and Quaternary history of the islands. *Journal of the Geolological Society, London* 168, 913–26.

Pedley, H.M. & S.M. Bennett, 1985. Phosphorites, hardgrounds and syndepositional subsidence: a paleoenvironmental model from Miocene of the Maltese Islands. *Sedimentary Geology* 45, 1–34.

Pedley, M., D. Bosence, C. Dart & S. Pratt, 1990. Tectonic and stratigraphic evolution of the Maltese Islands, in *Field*

Guide to the Cainozoic Platform Carbonates of the Maltese Islands, ed. D. Bosence. Nottingham: International Sedimentological Congress, 9–39.

Pedley, H.M., M. Hughes-Clarke & P. Galea, 2002. *Limestone Isles in a Crystal Sea: The Geology of the Maltese Islands*. Malta: PEG Ltd.

Pedley, H.M., M. House & B. Waugh, 1976. The geology of Malta and Gozo. *Proceedings of the Geologists' Association* 87, 325–41.

Pedley, H.M., M.R. House & B. Waugh, 1978. The geology of the Pelagian block: the Maltese Islands, in *The Ocean Basins and Margins: 4B, the Western Mediterranean*, eds. A.E.M Nairn, W.H. Kanes & F.G. Stehli. London: Plenum Press, 417–33.

Pedley, H.M., M.H. Clark & P. Galea, 2002. *Limestone Isles in a Crystal Sea: The Geology of the Maltese Islands*. San Gwann: Publishers Enterprises Group Ltd.

Peet, T.E., 1910. Contributions to the Study of the Prehistoric Period in Malta. *Papers of the British School at Rome* 5 (3), 141–63.

Pelle, T., F. Scarciglia, E. Allevato, G. Di Pasquale, M.F. La Russa, D. Marino, E. Natali, G. Robustelli & V. Tine, 2013. Reconstruction of Holocene environmental changes in two archaeological sites of Calabria (Southern Italy) using an integrated pedological and anthracological approach. *Quaternary International* 288, 206–14.

Pérez-Peña, J., J. Azañón & A. Azor, 2009. CalHypso: An ArcGIS extension to calculate hypsometric curves and their statistical moments. Applications to drainage basin analysis in SE Spain. *Computers & Geosciences* 35, 1214–23.

Peyron, O., S. Goring, I. Dormoy, U. Kotthoff, J. Pross, J-L. de Beaulieu, R. Drescher-Schneider, B. Vanniuere & M. Magny, 2011. Holocene seasonality changes in the central Mediterranean region reconstructed from the pollen sequences of Lake Accesa (Italy) and Tenaghi Philippon (Greece). *The Holocene* 21, 131–46.

Peyron, O., N. Combourieu-Nebout, D. Brayshaw, S. Goring, V. Andrieu-Ponel, S. Desprat, W. Fletcher, B. Gambin, C. Ioakim, S. Joannin, U. Kotthoff, K. Kouli, V. Montade, J. Pross, L. Sadori & M. Magny, 2017. Precipitation changes in the Mediterranean basin during the Holocene from terrestrial and marine pollen records: a model-data comparison. *Climate Past* 13, 249–65.

Piccarreta, M., M. Caldara, D. Capolongo & F. Boenzi, 2011. Holocene geomorphic activity related to climatic change and human impact in Basilicata, Southern Italy. *Geomorphology* 128, 137–47.

Piccarreta, M., D. Capolongo & M.N. Miccoli, 2012. Deep gullies entrenchment in valley fills during the Late Holocene in the Basento basin, Basilicata (southern Italy). *Geomorphologie: Relief, Processus, Environnement* 18 (2), 239–48.

Pingel, T.J., 2010. Modeling Slope as a Contributor to Route Selection in Mountainous Areas, *Cartography and Geographic Information Science* 37 (2), 137–48.

Poch, R.M., O. Artieda, J. Herrero & M. Lebedeva-Verba, 2010. Gypsic features, in *Interpretation of Micromorphological Features of Soils and Regoliths*, eds. G. Stoops, V. Marcelino & F. Mees. Amsterdam: Elsevier, 195–216.

Pollak, M.D., 1991. *Turin 1564–1680: Urban Design, Military Culture and the Creation of the Absolutist Capital*. Chicago: University of Chicago Press.

Prampolini, M., F. Foglini, S. Biolchi, S. Devoto, S. Angelini & M. Soldati, 2017. Geomorphological mapping of terrestrial and marine areas, northern Malta and Comino (central Mediterranean Sea). *Journal of Maps* 13, 457–69.

Preece, R.C., 1998. Mollusca, in *Late Quaternary Environmental Change in North-west Europe. Excavations at Holywell Coombe, South-east England*, eds. R.C. Preece & D. Bridgland. London: Chapman and Hall, 158–212.

Prescott, J.R. & J.T. Hutton, 1994. Cosmic ray contributions to dose rates for luminescence and ESR dating: Large depths and long-term time variations. *Radiation Measurements* 23 (2), 497–500.

Pross, J., U. Kotthoff, U.C. Muller, O. Peyron, I. Dormoy, G. Schmiedl, S. Kalaitzidis & A.M. Smith, 2009. Massive perturbation in terrestrial ecosystems of the Eastern Mediterranean region asociated with the 8.2 ka limatic event. *Geology* 37, 887–90.

Puglisi, D., 2014. Tectonic evolution of the Sicilian Maghrebian Chain inferred from stratigraphic and petrographic evidences of Lower Cretaceous and Oligocene flysch. *Geologica Carpathica* 65, 293–305.

Pyne-O'Donnell, S.D.F., 2004. 'The Factors Affecting the Distribution and Preservation of Microtephra Particles in Lateglacial and Early Holocene Lake Sediments.' Unpublished PhD, University of London.

Quintin, J., 1536. *Insulae Melitae Descriptio*. Lyons: Gryphius.

Rainbird, P., 1999. Islands out of time: a critique of island archaeology. *Journal of Mediterranean Archaeology* 12, 216–34.

Rainbird, P., 2007. *The archaeology of islands.* Cambridge: Cambridge University Press.

Ramón-Laca, L. & D.J. Mabberley, 2004. The ecological status of the carob-tree (*Ceratonia siliqua*, Leguminosae) in the Mediterranean. *Botanical Journal of the Linnean Society* 144, 431–6.

Raneri, S., Barone, G., Mazzoleni, P., Tanasi, D. & C. Emanuele, 2015. Mobility of men versus mobility of goods: Archaeometric characterization of Middle Bronze Age pottery in Malta and Sicily (15th–13th century BC). *Periodico di Mineralogia* 84, 23–44.

Recchia, G., 2004–2005. Il tempio e l'area sacra megalitica di Tas-Silġ: le nuove scoperte dagli scavi nei livelli del III e del II millennio a.C. *Scienze dell'Antichità* 12, 233–62.

Recchia, G. & Cazzella, A. 2011. Maltese prehistoric ceramic sequence and chronology: On-going problems, in *Ceramics of the Phoenician-Punic World: Collected Essays*, ed. C. Sagona. (Ancient Near Eastern Studies Supplement 36). Louvain: Peeters, 373–96.

Recchia, G. & G. Fiorentino, 2015. Archipelagos adjacent to Sicily around 2200 BC: attractive environments or suitable geo-economic locations?, in *2200 BC – A climatic breakdown as a cause for the collapse of the old world?, Proceedings of the 7th Archaeological Conference of Central Germany*, eds. H.H. Meller, H.W. Arz, R. Jung & R. Risch. Halle: Landesmuseums fur Vorgeschichte, 305–20.

Reed, J.M., A.C. Stevenson & S. Juggins, 2001. A multi-proxy record of Holocene climate change in southwestern Spain: The Laguan de Medina, Cadiz. *The Holocene* 11 (6), 707–19.

Rehfeld, U. & A.W. Janssen, 1995. Development of phosphatized hardgrounds in the Miocene Globigerina Limestone of the Maltese archipelago, including a description of the *Gamopleura melitensis* sp. nov. *Facies* 33 (1), 91–106.

Reille, M., 1992. 'Pollen et spores d'Europe et d'Afrique du Nord.' Unpublished report. Laboratoire de Botanique Historique et Palynologie, Universite d'Aix Marseille III.

Reille, M., 1995. 'Pollen et Spores D'Europe et D'Afrique Du nord' (Supplement 1). Unpublished report. Marseilles: Laboratoire de Botanique Historique et Palynologie.

Reille, M., 1998. 'Pollen et spores d'Europe et d'Afrique du nord' (Supplement 2). Unpublished report. Marseilles: Laboratoire de Botanique Historique et Palynologie.

Reimer, P. & R. Reimer, 2001. A marine reservoir correction database and on-line interface. *Radiocarbon* 43 (2A), 2 Part I, 461–3.

Reimer, R.W. & R.J. Reimer, 2017. An online application for ΔR calculation. *Radiocarbon* 59 (5), 1623–7.

Reimer, P.J., H.S. McDonald, J.R. Reimer, S. Svyatko & M. Thompson, 2015. *Laboratory protocols used for AMS radiocarbon dating at the 14CHRONO Centre, The Queen's University, Belfast.* Portsmouth: English Heritage.

Reimer, P.J., E. Bard, A. Bayliss, J.W. Beck, P.G. Blackwell, C. Bronk Ramsey, C.E. Buck, H. Cheng, R.L. Edwards & M. Friedrich, 2013. IntCal13 and Marine13 radiocarbon age calibration curves 0–50,000 years cal BP. *Radiocarbon* 55 (4), 1869–87.

Renard, K.G., G.R. Foster, G.A. Weesies, D.K. McCool & D.C. Yoder, 1997. *Predicting Soil Erosion by Water: A Guide to Conservation Planning with the Revised Universal Soil Loss Equation (RUSLE).* Washington: USDA Handbook 703.

Renfrew, C., 1972. Malta and calibrated radiocarbon chronology. *Antiquity* 46, 141–4.

Renfrew, C., 1973. *Before Civilization: The Radiocarbon Revolution and Prehistoric Europe.* London: Johnathan Cape.

Renfrew, C. & E.V. Level, 1979. Exploring dominance: Predicting polities from centres, in Renfrew, C. & Cooke, K.L. (eds.) *Transformations: Mathematical Approaches to Culture*. New York: Academic Press, 145–68.

Renfrew, A.C. & M. Wagstaff (eds.), 1982. *An island polity. The archaeology of exploitation in Melos.* Cambridge: Cambridge University Press.

Renschler, C.S. & J. Harbor, 2002. Soil erosion assessment tools from point to regional scales – The role of geomorphologists in land management research and implementation. *Geomorphology* 47, 189–209.

Renzulli, l., P. Santi, T. Gambin & P. Bueno Serrano, 2019. Pantelleria Island as a centre of production for the Archaic Phoenician trade in basaltic millstones: New evidence recovered and sampled from a shipwreck off Gozo (Malta) and a terrestrial site at Cádiz (Spain). *Journal of Archaeological Science: Reports* 24, 338–49.

Reuther, C.D., 1984. Tectonics of the Maltese Islands. *Centro (Malta)* 1, 1–16.

Reuther, C.D. & G.H. Eisbacher, 1985. Pantelleria Rift – crustal extension in a convergent intraplate setting. *Geologische Rundschau* 74 (3), 585–97.

Richards-Rissetto, H. & K. Landau, 2014. Movement as a means of social (re)production: using GIS to measure social integration across urban landscapes. *Journal of Archaeological Science* 41, 365–75.

Rizzo, C., 1932. *Geology of the Maltese Islands*. Malta: Government Printing Office.

Roberts, N., 2002. Did prehistoric landscape management retard the post-glacial spread of woodland in Southwest Asia? *Antiquity* 76, 1002–10.

Robb, J., 2007. *The Early Mediterranean Village: Agency, Material Culture and Social Change in Neolithic Italy*. Cambridge: Cambridge University Press.

Rogers, S.R., C. Collet & R. Lugon, 2014. Least cost path analysis for predicting glacial archaeological site potential in central Europe, in *Across Time and Space. Papers from the 41st Computer Applications and Quantitative Methods in Archaeology Conference*, ed. A. Traviglia. Amsterdam: Amsterdam University Press, 261–75.

Rolé, A., 2007. The Terraced Landscapes of the Maltese Islands Malta, in *Europe's Living Landscape. Essays on Exploring Our Identity in the Countryside*, eds. B. Pedroli, A. Van Doom, G. De Blust, M. Paracchini, D. Wescher & F. Bunce. Uitgeverij: KNNV, 405–20.

Rosenberg, M.S. & C.D. Anderson, 2011. PASSaGE: Pattern Analysis, Spatial Statistics and Geographic Exegesis. Version 2. *Methods in Ecology and Evolution* 2 (3), 229–32.

Ruan, J., F. Kherbouche, D. Genty, D. Blamart, H. Cheng, F. Dewilde, S. Hachi, R.L. Edwards, E. Régnier & J-L. Michelot, 2016. Evidence of a prolonged drought ca. 4200 yr BP correlated with prehistoric settlement abandonment from the Gueldaman GLD1 Cave, Northern Algeria. *Climates of the Past* 12, 1–14.

Ruffell, A., C. Hunt, R. Grima, R. McLaughlin, C. Malone, P.J. Schembri, C. French & S. Stoddart, 2018. Water and cosmology in the prehistoric Maltese World: Fault control on the hydrogeology of Ġgantija. *Journal of Archaeological Science. Reports* 20, 183–91.

Russell, N.J. & S.J. Armitage, 2012. A comparison of single-grain and small aliquot dating of fine sand from Cyrenaica, northern Libya. *Quaternary Geochronology* 10, 62–7.

Sabelberg, E., 1983. The persistence of palazzi and intra-urban structures in Tuscany and Sicily. *Journal of Historical Geography* 9 (3), 247–64.

Sabelberg, E., 1986. The 'South-Italian City' – a Cultural-Genetic Type of City. *GeoJournal* 13, 59–66.

Sadori, L., G. Zanchetta & M. Giardini, 2008. Last Glacial to Holocene palaeoenvironmental evolution at Lago di Pergusa (Sicily, Southern Italy) during the Bronze Age: A multi-disciplinary approach. *Quaternary International* 113, 5–17.

Sadori, L., C. Giraudi, A. Masi, M. Magny, E. Ortu, G. Zanchetta & A. Izdebski, 2016. Climate, environment and society in southern Italy during the last 2000 years. A review of the environmental, historical and archaeological evidence. *Quaternary Science Reviews* 136, 173–88.

Sadori, L., E. Ortu, O. Peyron, G. Zanchetta, B. Vanniere, M. Desmet & M. Magny, 2013. The last 7 millennia of vegetation and climate changes at Lago di Pergusa (central Sicily, Italy). *Climate Past* 9, 1969–84.

Sagona C., 2002. *The Archaeology of Punic Malta*. Leuven: Peeters Press.

Sagona C., 2004. Land Use in Prehistoric Malta. A Re-Examination of the Maltese 'Cart Ruts'. *Oxford Journal of Archaeology* 23, 45–60.

Sagona, C., 2015. *The Archaeology of Malta: from the Neolithic through the Roman period*. Cambridge: Cambridge University Press.

Said-Zammit, G.A., 1997. *Population, Land Use and Settlement on Punic Malta. A contextual analysis of the burial evidence*. Oxford: B.A.R. International Series 682.

Said-Zammit, G.A., 2016. *The Development of Domestic Space in the Maltese Islands from the Late Middle Ages to the Second Half of the Twentieth Century*. Oxford: Archaeopress.

Saliba, P.C., J. Magro Conti & C. Borg, 2002. *A Study of Landscape and Irrigation Systems at Is-Simblija limits of Dingli, Malta & Conservation Report.* Malta: Gutenberg.

Sanderson, D.C.W., 1987. *Thermoluminescence dating of vitrified Scottish forts*. Paisley: Paisley College.

Sanderson, D.C.W., 1988. Thick source beta counting (TSBC): A rapid method for measuring beta dose-rates. *International Journal of Radiation Applications and Instrumentation. Part B. Nuclear Tracks and Radiation Measurements* 14, 203–7.

Sanderson, D.C.W. & S. Murphy, 2010. Using simple portable OSL measurements and laboratory characterisation to help understand complex and heterogeneous sediment sequences for luminescence dating. *Quaternary Geochronology* 5, 299–305.

Sanderson, D.C.W., P. Bishop, I. Houston & M. Boonsener, 2001. Luminescence characterisation of quartz-rich cover sands from NE Thailand. *Quaternary Science Reviews* 20, 893–900.

Sanderson, D.C.W., P. Bishop, M.T. Stark & J.Q. Spencer, 2003. Luminescence dating of anthropogenically reset canal sediments from Angkor Borei, Mekong Delta, Cambodia. *Quaternary Science Reviews* 22, 1111–21.

Sanderson, D.C.W., T.C. Kinnaird, F. Leandri & C. Leandri, 2014. 'OSL Dating of Neolithic Monuments at Capu di Lugu, Belvédère-Campomoro, SW Corsica.' Unpublished SUERC Technical Report, University of Glasgow.

Scarre, C. (ed.) 2005. The world transformed: from foragers and farmers to states and empires. In *The Human Past: A Textbook of World Prehistory*. London: Thames & Hudson.

Scerri, S., 2019. Sedimentary evolution and resultant geological landscapes, in *Landscapes and Landforms of the Maltese Islands* (World Geomorphological Landscapes), eds. R. Gauci & J.A. Schembri. Cham, Switzerland: Springer Nature, 31–47.

Schembri, J.A., 2003. *Coastal Land use in the Maltese islands: a Description and Appraisal*, PhD Dissertation, University of Durham [Available at Durham E-Theses Online: http://etheses.dur.ac.uk/4417/]

Schembri, J.A., 2019. The Geographical Context of the Maltese Islands, in *Landscapes and Landforms of the Maltese Islands* (World Geomorphological Landscapes), eds. R. Gauci & J.A. Schembri. Cham, Switzerland: Springer Nature, 9–17.

Schembri, P.J., 1993. Physical geography and ecology of the Maltese Islands: A brief overview, in *Optiones Mediterraneennes: Serie B. Etudes et Recherches* 7, eds. S. Busuttil, F. Lerin & L. Mizzi. Montpellier: Centre International de Hautes Etudes Agronomiques Mediterraneennes, 27–39.

Schembri, P.J., 1994. Malta's natural heritage, in *Malta culture and identity*, eds. H. Frendo and O. Friggeeri. Valletta: Ministry of Youth and the Arts, 105–24.

Schembri, P.J., 1995. Molluscan samples from the Żebbuġ tomb, in Mortuary ritual of 4th millennium BC Malta: the Żebbuġ period chambered tomb from the Brochtorff Circle at Xagħra (Gozo), eds. C. Malone, S. Stoddart, A. Bonanno, T. Gouder & D. Trump. *Proceedings of the Prehistoric Society* 61, 342.

Schembri, P.J., 1997. The Maltese Islands: climate, vegetation and landscape. *GeoJournal* 41, 1–11.

Schembri, P.J., 2003. Current state of knowledge of the Maltese non-marine fauna, in *Malta Environment and Planning Authority. Malta Environment and Planning Authority Annual Report and Accounts 2003*. Malta Environment and Planning Authority. Floriana: Malta, 33–65.

Schembri, P.J. & Lanfranco, E. 1993. Development and the natural environment in the Maltese Islands, in *The development process in small island states*, eds. D.G. Lockhart, D. Drakakis-Smith & P.J. Schembri. London & New York: Routledge, 247–66.

Schembri, P.J., K. Fenech & K. Terribile, 2018. Unlocking the past through the present: exploring the use of present-day land snail assemblages as indicators of past environments in the Maltese Islands, in *The lure of the antique. Essays on Malta and Mediterranean archaeology in honour of Anthony Bonanno*, eds. N.C. Vella, A.J. Frendo & H.C.R. Vella. (Ancient Near Eastern Studies Supplement Series 54.) Leuven, Belgium: Peeters, 75–86.

Schembri, P.J., M. Pedley, C.O. Hunt & S. Stoddart, 2009. The environment of the Maltese Islands, in *Mortuary Customs in Prehistoric Malta. Excavations at the Brochtorff Circle at Xagħra (1987–94)*, eds. C. Malone, S. Stoddart, A. Bonanno & D. Trump. Cambridge: McDonald Institute for Archaeological Research, 17–39.

Schepanski, K., 2018. Transport of Mineral Dust and Its Impact on Climate. *Geosciences* 8 (5), 151–70.

Scheuvens, D., L. Schutz, K. Kandler, M. Ebert & S. Weinbruch, S. 2013. Bulk composition of northern African dust and its source sediments – A compilation. *Earth Science Reviews* 116, 170–90.

Schlecht, E., U. Dickhoefer, E. Gumpertsberger & A. Buerkert, 2009. Grazing itineraries and forage selection of goats in the Al Jabal al Akhdar mountain range of northern Oman. *Journal of Arid Environments* 73 (3), 355–63.

Schlecht, E., P. Hiernaux, I. Kadaouré, C. Hülsebusch & F. Mahler, 2006. A spatio-temporal analysis of forage availability and grazing and excretion behaviour of herded and free grazing cattle, sheep and goats in

Western Niger. *Agriculture, Ecosystems & Environment* 113 (1–4), 226–42.

Sciberras, D., 1999. The Maltese dolmens, in *Facets of Maltese Prehistory*, eds. A. Mifsud & C. Savona Ventura. Malta: Prehistoric Society of Malta, 101–6.

Seddon, M.B., Ü. Kebapçı, M. Lopes-Lima, D.V. Damme & K.G. Smith, 2014. Freshwater mollusks, in *The Status and Distribution of Freshwater Biodiversity in the Eastern Mediterranean,* eds. K.G. Smith, V. Barrios, W.R.T. Darwall & C. Numa. ICUN: Cambridge, UK, Malaga, Spain and Gland, Switzerland: ICUN, 43–56.

Shackleton, J.C., T.H. van Andel & C.N. Runnels, 1984. Coastal Paleogeography of the Central and Western Mediterranean during the last 125,000 Years and its archaeological implications. *Journal of Field Archaeology* 11, 307–14.

Shennan, S., 2018. *The First Farmers of Europe: An Evolutionary Perspective*. Cambridge: Cambridge University Press.

Shepherd, J.D. & J.R. Dymond, 2003. Correcting satellite imagery for the variance of reflectance and illumination with topography. *International Journal of Remote Sensing* 24, 3503–14.

Siani, G., M. Paterne, M. Arnold, E. Bard, B. Métivier, N. Tisnerat & F. Bassinot, 2000. Radiocarbon Reservoir Ages in the Mediterranean Sea and Black Sea. *Radiocarbon* 42 (2), 271–80.

Simberloff, D.S., 1974. Equilibrium theory of island biogeography and ecology. *Annual Review of Ecology and Systematics* 5, 161–82.

Simpson, D.J. & C.O. Hunt, 2009. Scoping the past human environment: a case study of pollen taphonomy at the Haua Fteah, Cyrenaica, Libya. *Archaeological Review from Cambridge* 24, 2, 27–46.

Simpson, I.A., 1998. Early land management at Tofts Ness, Sanday, Orkney: the evidence of thin section micromorphology, in *Life on the Edge: Human Settlement and Marginality*, eds. C.M. Mills & G. Coles. Oxford: Oxbow Monograph 100, 91–8.

Simpson, I.A., E.B. Guttman & A. Shepherd, 2006. Characterising midden in Neolithic settlement construction: an assessment from Skara Bare, Orkney. *Geoarchaeology* 21, 221–35.

Soil Survey Staff, 1999. *Soil Taxonomy*. (U.S. Department of Agriculture, Agriculture Handbook 436.) Washington, D.C.: Department of Agriculture.

Soto-Berelov, M., P.L. Fall, S.E. Falconer & E. Ridder, 2015. Modeling vegetation dynamics in the Southern Levant through the Bronze Age. *Journal of Archaeological Science* 53, 94–109.

Smith, B.D., 2011. General patterns of niche construction and the management of 'wild' plant and animal resources by small-scale pre-industrial societies. *Philosophical Transactions of the Royal Society B: Biological Sciences* 366 (1566), 836–48.

Smith, R.M., 1986. Comparing Traditional Methods for Selecting Class Intervals on Choropleth Maps. *The Professional Geographer* 38, 62–7.

Sourisseau, J.-C. 2015. Xlendi, réflexions sur la cargaison de l'épave. *Homepage of Laboratoire des Sciences de l'Information et des Systèmes, Centre Camille-Jullian, Centre National de la Recherche Scientifique (France)*, http://www.lsis.org/groplan/papers/groplan_livrableXlendiCargaisonOctobre2015.pdf

Spratt, T.A.B., 1843. On the geology of the Maltese Islands. *Proceedings of the Geological Society* 4, 225–9.

Spratt, T.A.B., 1854. *The Geology of Malta and Gozo*. Valletta, Malta: Literary and Scientific Society of Malta.

Stanley, D.J. & A.K. Hait, 2000. Deltas, radiocarbon dating, and measurements of sediment storage and subsidence. *Geology* 28 (4), 295–8.

Stavi, I., E.D. Ungar, H. Lavee & P. Sarah, 2008. Surface microtopography and soil penetration resistance associated with shrub patches in a semiarid rangeland. *Geomorphology* 94 (1–2), 69–78.

Stockmarr, J., 1971. Tablets with spores used in absolute pollen analysis. *Pollen Spores* 13, 614–21.

Stoddart, S. n.d. *Survey Instructions*. Unpublished archive held in the National Museum of Malta.

Stoddart, S., 1997–8. Contrasting political strategies in the islands of the southern central Mediterranean. *Accordia Research Papers* 7, 59–73.

Stoddart, S.K.F., 1999. Long term dynamics of an island community: Malta 5500 BC – 2000 AD, in *Social Dynamics in the Central Mediterranean*, ed. R.H. Tykot. Sheffield: Sheffield Academic Press, 137–47.

Stoddart, S.K.F., 2015. Mediating the Dominion of Death in Prehistoric Malta. In *Death Rituals, Social Order and the Archaeology of Immortality in the Ancient World. 'Death Shall Have No Dominion'*, eds. A.C. Renfrew, M. Boyd & I. Morley. Cambridge: Cambridge University Press, 130–7.

Stoddart, S. & C. Malone, 2015. Prehistoric Maltese Death: Democratic Theatre or Elite Democracy?, eds. Z.L. Devlin & E.-J. Graham, *Death Embodied: Archaeological Approaches to the Treatment of the Corpse*. Oxford: Oxbow, 160–74.

Stoddart, S., G. Barber, C. Duhig, G. Mann, T. O'Connell, L. Lai, D. Redhouse, R.H. Tykot, & C. Malone, 2009. The Human and Animal Remains, in *Mortuary Customs in Prehistoric Malta. Excavations at the Brochtorff Circle at Xagħra (1987–94)*, eds. C. Malone, S. Stoddart, A. Bonanno & D. Trump. Cambridge: McDonald Institute for Archaeological Research, 315–40.

Stoddart, S., J. Woodbridge, A. Palmisano, A.-M. Mercuri, S. Mensing, D. Colombaroli, L. Sadori, D. Magri, F. di Rita, M. Giardini, M. Mariotti Lippi, C. Montanari, C. Bellini, A. Florenzano, P. Torri, A. Bevan, S. Shennan, R. Fyfe & N. Roberts. 2019. Tyrrhenian central Italy: Holocene population and landscape ecology. *Holocene. Special issue* 29 (5), 761–75.

Stoddart, S. R. Power, J. Thompson, B. Mercieca Spiteri, R. McLaughlin & C. Malone (eds.), in press. *Temple People: Bioarchaeology, Resilience and Culture in Prehistoric Malta.* Volume 3 of Fragility and Sustainability – Studies in Early Malta, the ERC-funded FRAGSUS Project. Cambridge: McDonald Institute for Archaeological Research.

Stoops, G., 2003. *Guidelines for analysis and description of soil and regolith thin sections*. Madison, Wisconsin: Soil Science Society of America, Inc.

Stoops, G. & V. Marcelino, 2010. Lateritic and bauxitic materials, in *Interpretation of Micromorphological Features of Soils and Regoliths*, eds. G. Stoops, V. Marcelino & F. Mees. Amsterdam: Elsevier, 329–50.

Stoops, G., V. Marcelino & F. Mees (eds.), 2010. *Interpretation of Micromorphological Features of Soils and Regoliths*. Amsterdam: Elsevier.

Strahler, A.N., 1952. Hypsometric (area-altitude) analysis of erosional topography. *Geological Society of America Bulletin* 63, 1117–42.

Stuiver, M. & H.A. Pollach, 1977. Discussion: Reporting of ^{14}C data. *Radiocarbon* 19 (3), 355–63.

Stuiver, M., G.W. Pearson & T.F. Braziunas, 1986. Radiocarbon age calibration of marine samples back to 9000 cal yr BP. *Radiocarbon* 28, 980–1021.

Stuiver, M., P.J. Reimer, E. Bard, J.W. Beck, G.S. Burr, K.A. Hughen, B. Kromer, G. McCormac, J. van der Plicht & M. Spurk, 1998. INTCAL98 radiocarbon age calibration 24,000–0 cal BP. *Radiocarbon* 40 (3), 1041–83.

Sultana, D., 2015. Numerical Modelling of Soil Erosion Susceptibility in the Maltese Islands using Geographic Information Systems and the Revised Universal Soil Loss Equation (RUSLE). *Xjenza Online – Journal of The Malta Chamber of Scientists* 3, 41–50.

Svarajasingham, S., 1971. *The soils of Malta*. (UNOP/SF Project MAT/5, Water disposal and water supply). Rome: Food and Agriculture Organization of the United Nations.

Tanasi, D., 2008. *La Sicilia e l'arcipelago Maltese nell'età del Bronzo Medio*. (1. ed.) Palermo: Officina di studi medievali.

Tanasi, D., 2010. Bridging the gap, New data on the relationship between Sicily, the Maltese Archipelago and the Aegean in the Middle Bronze Age. *Mare Internum* 2, 111–19.

Tanasi, D., 2013. Prehistoric painted pottery in Malta: a century later. *Malta Archaeological Review* 2008–2009 (9), 5–13.

Tanasi, D., 2014. Lighting up the dark: the role of Għar Mirdum in Maltese Prehistory, in *From Cave to Dolmen. Ritual and symbolic aspects in the prehistory between Sciacca, Sicily and the central Mediterranean*, ed. D. Gulli. Oxford: Archaeopress Archaeology, 287–308.

Tanasi, D. & N.C. Vella, 2011a. Taking Stock, in *Site, Artefacts and Landscape. Prehistoric Borg in-Nadur, Malta*, eds. D. Tanasi & N.C. Vella. (Praehistorica Mediterranea 3). Monza: Polimetrica, 413–7.

Tanasi, D. & Vella, N.C. (eds.) 2011b. *Site, Artefacts and Landscape: Prehistoric Borġ in-Nadur, Malta*. Monza: Polimetrica.

Tanasi, D. & N. C. Vella, 2014. Islands and mobility: exploring Bronze Age connectivity in the south-central Mediterranean, in *The Cambridge Prehistory of the Bronze and Iron Age Mediterranean*, eds. P. Van Dommelen & B. Knapp. Cambridge: Cambridge University Press, 184–201.

Tanasi, D. & N.C. Vella (eds.), 2015. *The Late Prehistory of Malta: Essays on Borġ in-Nadur and other sites*. Oxford: Archaeopress.

Teeter, S.L., 2012. *A GIS Analysis of Archaeological Trails and Site Catchments in the Grand Canyon, Arizona*. Northern Arizona University.

Thake, M.A. 1985a. The biogeography of the Maltese Islands illustrated by the Clausiliidae. *Journal of Biogeography* 12, 269–87.

Thake, M.A., 1985b. Land snails from the Mellieha Quaternary Deposit. *Potamon (Malta)* 14, 93.

Thompson, A., 2006. The Character of a Wall. The changing construction of agricultural walls on the island of Gozo. *OMERTAA Journal of Applied Anthropology* 2007, 31–7.

Thompson, J.E., E. Parkinson, R. McLaughlin, R.P. Barratt, R.K. Power, B. Mercieca-Spiteri, S. Stoddart & C. Malone, 2020. Placing and remembering the dead in late Neolithic Malta: bioarchaeological and spatial analysis of the Xagħra Circle Hypogeum, Gozo. *World Archaeology.* DOI: *10.1080/00438243.2019.1745680.*

Thornes, J.B., 2007. Modelling soil erosion by grazing: Recent developments and new approaches. *Geographical Research* 45 (1), 13–26.

Tinè, V. & S. Tusa, 2012. Il Neolitico in Sicilia. *Dai Ciclopodi Agli Ecisti, Societa e Territorio Nella Sicilia Preistorica e Protostorica. Atti dell'Istituto Italiano di Preistoria e Protostoria. San Cipirello (PA), 16–19 Novembre 2006.* Florence: Istituto Italiano di Preistoria e Protostoria, 49–80.

Tinner, W. & A.F. Lotter, 2001. Central European vegetation response to abrupt climate change at 8.2 ka. *Geology* 29, 551–4.

Tinner, W., J.F.N. van Leeuwen, D. Colombaroli, E. Vescovi, W.O. van der Knaap, P.D. Henne, S. Pasta, S. D'Angelo & T. La Mantia, 2009. Holocene environment and climate changes at Gorgo Basso, a coastal lake in southern Sicily, Italy. *Quaternary Science Reviews* 28, 1498–510.

Tite, M.S. & C. Mullins, 1971. Enhancement of the magnetic susceptibility of soils on archaeological sites. *Archaeometry* 13, 209–19.

Tobler, W., 1993. Three Presentations on Geographical Analysis and Modeling, Technical Report 93–1, *NCGIA Technical Reports* 1, 1–26.

Tonna, S., 1985. 'Origins of Planning on Malta Island and Its Evolution – A Study of Human Settlements.' Unpublished BE & A thesis, University of Malta.

Trechmann, C.T., 1938. Quaternary Conditions in Malta. *The Geological Magazine* 75, 1–26.

Tripcevich, N., 2007. *Quarries, Caravans, and Routes to Complexity. Prehispanic Obsidian in the South-Central Andes*. University of California (Santa Barbara).

Trump, D.H., 1961a. Skorba, Malta and the Mediterranean. *Antiquity* 35, 300–3.

Trump, D.H., 1961b. The later prehistory of Malta. *Proceedings of the Prehistoric Society* 27, 253–62.

Trump D.H., 1962. In-Nuffara, Rabat, Gozo, storage pit. *Report on the Working of the Museum Department for the Year 1960*. Malta: Department of Information, 5.

Trump, D.H., 1966. *Skorba. Excavations carried out on behalf of the National Museum of Malta. 1961–3.* (Research Reports of the Society of Antiquaries of London 22.) London: Society of Antiquaries.

Trump, D.H., 1972. *Malta: an archaeological guide.* London: Faber and Faber.

Trump, D.H., 1995–6. Radiocarbon dates from Malta. *Accordia Research Papers* 6, 173–8.

Trump, D.H., 2002. *Malta: prehistory and temples. (Malta's living heritage).* Malta: Midsea Books.

Trump, D.H., 2010. *Malta. An archaeological Guide.* Valletta: Allied Publications.

Trump, D. H. & D. Cilia, 2008. *Cart-ruts and their Impact on the Maltese Landscape.* Sta. Venera, Malta: Heritage Books.

Tucker, C.J., 1979. Red and Photographic Infrared Linear Combinations for Monitoring Vegetation. *Remote Sensing of the Environment* 8, 127–50.

Tusa, S., 1983. *La Sicilia Nella Preistoria*. Palermo: Sellerio.

Ugolini, L.M., 1934. *Malta. Origini Della Civiltà Mediterranea.* Roma: La Libreria dello Stato.

van Andel, T.H., 1998. Paleosols, red sediments, and the Old Stone Age in Greece. *Geoarchaeology* 13, 361–3.

Van Andel, T.J. & C. Runnels, 1987. *Beyond the Acropolis: A Rural Greek Past*. Stanford: Stanford University Press.

Van Andel, T., E. Zangger & A. Demitrack, 1990. Land use and soil erosion in prehistoric Greece. *Journal of Field Archaeology* 17, 379–96.

Van der Hammen, T., T.A. Wijmstra & W.H. Van der Molen, 1965. Palynological study of a very thick peat section in Greece, and the Würm-Glacial vegetation in the Mediterranean region. *Geologie en Mijnbouw* 44, 37–9.

Van Der Knijff, J.M., R.J.A. Jones & L. Montanarella, 2000. *Soil Erosion Risk Assessment in Europe*. Brussels: European Soil Bureau.

Van der Leeuw, S. & C. Redman, 2002. Placing archaeology at the center of socio-natural studies. *American Antiquity* 67, 597–605.

Van Geel, B., 1978. A palaeoecological study of Holocene peat bog sections in the Netherlands and Germany based on the analyses of pollen, spores, and macro – and microscopic remains of fungi, algae, cormophytes and animals. *Review of Palaeobotany and Palynology* 25, 1–120.

Van Geel, B., S.J.P. Bohncke & H. Dee, 1981. A palaeoecological study of an upper Late Glacial and Holocene sequence from 'De Borchert', The Netherlands. *Review of Palaeobotany and Palynology* 31, 367–448.

Van Geel, B., G.R. Coope & T. van der Hammen, 1989. Palaeoecology and stratigraphy of the lateglacial type section at Usselo (the Netherlands). *Review of Palaeobotany and Palynology* 60, 25–129.

van Geel, B., J. Buurman, O. Brinkkemper, J. Schelvis, A. Aptroot, G. van Reenen & T. Hakbijl, 2003. Environmental reconstruction of a Roman Period settlement site in Uitgeest (The Netherlands), with special reference to coprophilous fungi. *Journal of Archaeological Science* 30, 873–83.

Van Leusen, P.M., 2002. *Pattern to Process: Methodological Investigations into the Formation and Interpretation of Spatial Patterns in Archaeological Landscapes*. University of Groningen.

Vayda, A.P. & R.A. Rappaport, 1968. Ecology, cultural and non-cultural, in *Introduction to Cultural Anthropology*, ed. J.A. Clifton. Boston: Houghton Mifflin, 477–97.

Vayda, A., J.C. Woodward, M.G. Macklin & J. Lewin (eds.), 1995. *Mediterranean Quaternary River Environments*. Rotterdam: Balkema.

Vella, C., 2009. The lithic toolkit of Late Neolithic Ta' Hagrat, Malta. *Origini* 31, 85–103.

Vella, C., 2010. 'The Mediterranean context of the art and architecture of medieval Malta.' Unpublished MA thesis, University of Malta.

Vella, E., 2002. The archaeological legacy, in Catania, J. (ed.) *Mellieħa through the tides of time*. Malta: Mellieħa Local Council, 25–40.

Vella, N.C., 1998. 'Ritual, Landscape, and Territory. Phoenician and Punic Non-Funerary Religious Sites in the Mediterranean: An Analysis of the Archaeological Evidence.' Unpublished PhD, University of Bristol.

Vella, N.C., 1999. 'Trunkess legs of stone': debating ritual continuity at Tas-Silg, Malta, in *Facets of Maltese Prehistory*, eds. A. Mifsud & C. Savona-Ventura. Malta: The Prehistoric Society of Malta, 225–39.

Vella, N.C., 2005. Phoenician and Punic Malta. *Journal of Roman Archaeology* 18, 436–50.

Vella, N. C. 2014. The invention of the Phoenicians: on object definition, decontextualization and display, in *The Punic Mediterranean: Identities and Identification from Phoenician Settlement to Roman Rule*, eds. J.C. Quinn & N.C. Vella. Cambridge: Cambridge University Press, 24–41.

Vella, N. & M. Anastasi 2019. Malta and Gozo, in *The Oxford Handbook of Phoenician and Punic Studies*, eds. C. López-Ruiz & B. R. Doak, Oxford: Oxford University Press, 553–68.

Vella, N.C., A. Borg, B. Borg, N.J. Cardona, K. Chetcuti-Bonavita, A. Corrado, E. De Gaetano, K. Fenech, C. Sagona, J. Zamut-Tagliaferro & I. Vella Gregory, 2001. Report on the excavation of a Punic tomb, Bajda Ridge, Xemxija (Malta). *Malta Archaeological Review* 5, 16–22.

Vella, N. C., A. Bonanno, M. Anastasi, B. Bechtold, R. Farrugia, K. Fenech, D. Mizzi, L. Verdonck & A. R. Zammit. 2017. A view from the countryside: the nature of the Late Punic and Early Roman activity at the Żejtun Villa site, Malta. *Rivista di Studi Fenici* 45, 109–43.

Vella, S.J., 2000. The Status of Soil Mapping in the Maltese Islands, in *The European Soil Information System, Proceedings of a Technical Consultation Rome, Italy*, 2–3 September 1999. (European Soil Bureau European Commission and Food and Agriculture Organisation of the United Nations.) Rome: FAO.

Vella, S.J., 2001. Soil information in the Maltese Islands, in *Soil Resources of Southern and Eastern Mediterranean Countries*, eds. P. Zdruli, P. Steduto, C. Lacirignola & L. Montanarella. Bari: Centre International de Hautes Etudes Agronomiques Mediterranéennes, 171–91.

Vella, S.J., 2003. Soil Survey and Soil Mapping in the Maltese Islands: the 2003 Position, in *Soil Resources of Europe*, eds. R. Jones, B. Houšková, P. Bullock & L. Montanarella. (European Soil Bureau, Research Report No. 9.) Luxembourg: European Office for Official Publications of the European Communities, 235–44.

Vellinga, M. & R.A. Wood, 2002. Global climatic impacts of a collapse of the Atlantic thermohaline circulation. *Climatic Change* 54, 251–67.

Verhagen, J.W.H., A.G. Posluschny & A. Danielisova, 2011. *Go Your Own Least Cost Path. Spatial Technology and Archaeological Interpretation*. Oxford: Archaeopress-British Archaeological Reports.

Verhagen, P. & K. Jeneson, 2012. A Roman Puzzle. Trying to Find the Via Belgica with GIS, in *Thinking Beyond the Tool. Archaeological Computing and the Interpretive Process*, eds. A. Chrysanthi, P. Murrieta-Flores & C. Papadopoulus. Oxford: Archaeopress, 123–30.

Verhaye, W. and G. Stoops, 1974. Micromorphological evidences for the identification of an argillic horizon in terra rossa, in *Soil microscopy: Proceedings of the Fourth International Working Meeting on Soil Micromorphology*, ed. G.K. Rutherford. Kingston: Limestone Press, 817–31.

Verstraeten, G. & J. Poesen, 2001. Factors controlling sediment yield from small intensively cultivated catchments in a temperate humid climate. *Geomorphology* 40, 123–44.

Viruel, J., F. Medail, M. Juin, A. Haguenauer, G.N. Feliner, M. Bou Dagher Kharrat, S. La Malfa, L. Ouahmane, H. Sanguin & A. Baumel, 2016. Mediterranean carob populations, native or naturalized? A continuing riddle. *OPTIMA XV*, June 2016. Montpellier, France. https://hal.archives-ouvertes.fr/hal-01794260

Vita-Finzi, C., 1969. *The Mediterranean Valleys*. Cambridge: Cambridge University Press.

Vogel, J.S., J.R. Southen, D.E. Nelson & T.A Brown, 1984. Performance of catalytically condensed carbon for use in accelerator mass spectrometry. *Nuclear Instruments and Methods* 223 (B5), 289–93.

Vossmerbäumer, H., 1972. Malta, ein Beitrag zur Geologie und Geomorphologie des Zentralmediterranen Raumes. *Wurzburger Geograpische Arbeiten* 38, 1–213.

Wainwright, J. & J.B. Thornes, 2004. *Environmental issues in the Mediterranean: Processes and Perspectives from the Past and Present*. London: Routledge Taylor.

Walker, B., C.S. Holling, S.R. Carpenter & A. Kinzig, 2004. Resilience, adaptability and transformability in social-ecological systems. *Ecology and Society* 9 (2), 5 (http://www.ecologyandsociety.org/vol9/iss2/art5/).

Wallace, A.R., 1892. *Island Life* (2nd and revised edition). London: Macmillan and Co.

Ward-Perkins, J.B., 1938–9. Tombs at Mtarfa. *Annual Report of the National Museum of Archaeology, Malta*, 12.

Ward-Perkins, J.B., 1942. Problems of Maltese Prehistory. *Antiquity* 16 (61), 19–35.

Waters, C.N., J. Zalasiewicz, C. Summerhayes, A.D. Barnosky, C. Poirier, A. Gałuszka, A. Cearreta, M. Edgeworth, E.C. Ellis, M. Ellis, C. Jeandel, R. Leinfelder, J.R. McNeill, D. de B. Richter, W. Steffen, J. Syvitski, D. Vidas, M. Wagreich, M. Williams, A. Zhisheng, J. Grinevald, E. Odada, N. Oreskes & A.P. Wolfe, 2016. The Anthropocene is functionally and stratigraphically distinct from the Holocene. *Science* 8, 351.

Webster, D. & S.T. Evans, 2005. Mesoamerican civilization. In *The Human Past: A Textbook of World Prehistory*, ed. C Scarre. London: Thames & Hudson, 594–639.

Weissel, J.K., L.F. Pratson & A. Malinverno, 1994. The length-scaling properties of topography. *Journal of Geophysical Research: Solid Earth* 99, 13997–14012.

Weninger, B., E. Alram-Stern, E. Bauer, E. Clare, U. Danzeglocke, O. Jöris, C. Kubatzki, G. Rollefson, H. Todorova & T. van Andel, 2006. Climate forcing due to the 8200 cal yr BP event observed at Early Neolithic sites in the eastern Mediterranean. *Quaternary Research* 66, 401–20.

Wettinger, G., 1969. The Militia list of 1419–20: a new starting point for the study of Malta's population. *Melita Historica* 2, 80–106.

Wettinger, G., 1975. The Lost Villages and Hamlets of Malta, in *Medieval Malta, Studies on Malta Before the Knights*, ed. A.T. Luttrell. London: British School at Rome, 181–216.

Wettinger, G., 1982. Agriculture in Malta in the Late Middle Ages, in *Proceedings of History Week*, ed. M. Buhagiar. *Malta: The Historical Society*, 1–48.

Wettinger, G., 2000. *Place-Names of the Maltese Islands*. Malta: PEG.

Wettinger, G., 2011. Malta in the high middle ages. *Melita Historica (Malta)* 15 (4), 367–90.

Wheatley, D.W. & M. Gillings, 2002. *Spatial Technology and Archaeology. The Archaeological Applications of GIS*. London-New York: Taylor & Francis.

White, D.A., 2015. The Basics of Least Cost Analysis for Archaeological Applications, *Advances in Archaeological Practice* 3 (4), 407–14.

Whittle, A., 1996. *Europe in the Neolithic: The Creation of New Worlds*. Cambridge: Cambridge University Press.

Whitley, T.G. & L.M. Hicks, 2003. A GIS approach to Understanding potential prehistoric and historic travel corridors. *Southeastern Archaeology* 22, 77–91.

Wiener, M.H., 2013. 'Minding the Gap': Gaps, Destructions, and Migrations in the Early Bronze Age Aegean. Causes and Consequences. *American Journal of Archaeology* 117 (4), 581–92.

Wiersma, A.P. & H. Renssen, 2006. Model-data comparison for the 8.2 ka BP event: Confirmation of a forcing mechanism by catastrophic drainage of Laurentide Lakes. *Quaternary Science Reviews* 25, 63–88.

Wigand, P. & M. McCallum, 2017. The Varying Impact of Land Use and Climate in Holocene Landscape Dynamics in the Mezzogiorno. *Journal of Mediterranean Studies* 3 (2), 121–50.

Willgoose, C. & G. Hancock, 1998. Revisiting the hypsometric curve as an indicator of form and process in transport-limited catchment. *Earth Surface Processes and Landforms* 23, 611–23.

Williams, A.N., 2012. The use of summed radiocarbon probability distributions in archaeology; a review of methods. *Journal of Archaeological Science* 39, 578–89.

Wilson C.A., D.A. Davidson & M. Cresser, 2005. An evaluation of multielement analysis of historic soil contamination to differentiate space use and former function in and around abandoned farms. *The Holocene* 15 (7), 1094–9.

Wilson, C.A., D.A. Davidson & M. Cresser, 2009. An evaluation of the site specificity of soil elemental signatures for identifying and interpreting former functional areas. *Journal of Archaeological Science* 36, 2327–34.

Wilson, C.A., D.A. Davidson, S. Malcolm & M. Cresser, 2008. Multi-element soil analysis: an assessment of its potential as an aid to archaeological interpretation. *Journal of Archaeological Science* 35, 412–24.

Wilson, M.A. & D. Righi, 2010. Spodic materials, in *Interpretation of Micromorphological Features of Soils and Regoliths*, eds. G. Stoops, V. Marcelino & F. Mees. Amsterdam: Elsevier, 251–73.

Wischmeier, W.H. & D.D. Smith, 1978. *Predicting Rainfall Erosion Losses: A Guide to Conservation Planning*. Agriculture Handbook 537. Washington: USDA.

W.R.B., 2014. *World Reference Base for Soil Resources*. World Soil Resources Report No. 106. Rome: F.A.O.

Wright, H.E. Jr., J.H. McAndrews & W. van Zeist, 1967. Modern pollen rain in western Iran, and its relation to plant geography and Quaternary vegetational history. *Journal of Ecology* 55, 415–43.

www.alsglobal.com>europe>west>spain>andalucia (Seville – Geochemistry)

www.calib.org (CALIB Marine Reservoir Correction CALIBomb IntCal)

www.geog.cam.ac.uk/facilities/laboratories/techniques/psd.html

Wyatt, A.R., 1993. Continental size, eustasy and sediment yield. *Geologische Rundschau* 82, 185–8.

Yaalon, D.H., 1997. Soils in the Mediterranean region: what makes them different? *Catena* 28, 157–69.

Yaalon, D.H. & E. Ganor, 1973. The influence of dust on soils during the Quaternary. *Soil Science* 116, 146–55.

Yan, H., J. Liu, H.Q. Huang, B. Tao & M. Cao, 2009. Assessing the consequence of land use change on agricultural productivity in China. *Global and Planetary Change* 67, 13–19.

Yellin-Dror, A., M. Grasso, Z. Ben-Avraham & G. Tibor, 1997. The subsidence history of the northern Hyblean plateau margin, southeastern Sicily. *Tectonophysics* 282, 277–89.

Zabenskie, S. & K. Gajewski, 2007. Post-glacial climatic change on Boothia Peninsula, Nunavut, Canada. *Quaternary Research* 68, 261–70.

Zacharias, N., Y. Bassiakos, B. Hayden, K. Theodorakopoulou & C.T. Michael, 2009. Luminescence dating of deltaic deposits from eastern Crete, Greece: Geoarchaeological implications. *Geomorphology* 109, 46–53.

Zammit, M.-E., 2006. 'An Archaeological Survey of Baħrija.' Unpublished M.A. thesis, Department of Classics and Archaeology, University of Malta.

Zammit, T. 1928a. *The Neolithic Hypogeum at Ħal-Saflieni. Casal Paula-Malta.* Valletta: Empire Press.

Zammit, T. 1928b. Prehistoric cart-tracks in Malta. *Antiquity* 2 (5), 18–25.

Zammit, T., 1930. *Prehistoric Malta, the Tarxien Temples*. Oxford: Oxford University Press.

Zammit Ciantar, J., 2002. *Life in Għar il-Kbir*. Malta: Dingli Local Council.

Zammit-Maempel, G., 1977. *An outline of Maltese Geology and guide to the geology hall of the National Museum of Natural History, Mdina, Malta*. Malta: Progress Press Co. Ltd.

Zanchetta, G., R. Sulpizio, N. Roberts, R. Cioni, W.J. Eastwood, G. Siani, B. Caron, M. Paterne & R. Santacroce, 2011. Tephrostratigraphy, chronology and climatic events of the Mediterranean basin during the Holocene: An overview. *The Holocene* 21, 33–52.

Zealand, A.M. & M.J. Jeffries, 2009. The distribution of pond snail communities across a landscape: separating out the influence of spatial position from local habitat quality for ponds in south-east Northumberland, UK. *Hydrobiologia* 632, 177–87.

Zeder, M.A., 2008. Domestication and early agriculture in the Mediterranean Basin: Origins, diffusion, and impact. *Proceedings of the National Academy of Sciences, USA* 105 (33), 11597–604.

Zettler, M.L. & D. Daunys, 2007. Long-term macrozoobenthos changes in a shallow boreal lagoon: comparison of a recent biodiversity inventory with historical data. *Limnologica-Ecology and Management of Inland Waters* 37 (2), 170–85.

Zielhofer, C. & D. Faust, 2008. Mid- and Late Holocene fluvial chronology of Tunisia. *Quaternary Science Reviews* 27, 580–8.

Zielhofer, C., J. Bussmann, H. Ibhouten & K. Fenech, 2010. Flood frequencies reveal Holocene rapid climate changes (Lower Moulouya River, northeastern Morocco). *Journal of Quaternary* Science 25, 700–14.

Zielhofer, C., W.J. Fletcher, S. Mischke, M. De Batist, J.F.E. Campbell, S. Joannin, R. Tjallingii, N. El Hamouti, A. Junginger, A. Stele, J. Bussmann, B. Schneider, T. Lauer, K. Spitzer, M. Strupler, T. Brachert & A. Mikdad, 2017a. Atlantic forcing of Western Mediterranean winter rain minima during the last 12,000 years. *Quaternary Science Reviews* 157, 29–51.

Zielhofer, C., H. von Suchodoletz, W.J. Fletcher, B. Schneider, E. Dietze, M. Schegel, K. Schepanski, B. Weninger, S. Mischke & A. Mikdad, 2017b. Millennial-scale fluctuations in Saharan dust supply across the decline of the African Humid Period. *Quaternary Science Reviews* 171, 119–35.

Zilhão, J., 2001. Radiocarbon evidence for a maritime pioneer colonisation at the origins of farming in West Mediterranean Europe. *Proceedings of the National Academy of Sciences, USA* 98, 14180–5.

Zolt, M.S. & S. Dombay, 2012. Determining minimum hiking time using DEM. *Geographica Napocensis* 6 (2), 124–9.

Appendix 1

How ground penetrating radar (GPR) works

Alastair Ruffell

Ground penetrating radar (or GPR) uses the transmission and reflection of radio waves (typically 25 to 2 GHz) in imaging the subsurface. Radar waves, introduced in the ground, may reflect back to surface when they intersect objects or surfaces of varying dielectric permittivity. Thus a GPR system requires a source antenna and receiving antenna (built to measure the same frequency). *Note that the plural of electrical devices is antennas; antennae are exclusively for animals such as insects. The transmitting antenna generates a pulse of radiowaves that the receiver detects at a set time interval: the longer the time interval, (potentially) the deeper the waves will have travelled into the ground (or to a nearby surface object) and back again. When the ground has a slow radarwave velocity, so a buried object may appear deeper than in ground with a fast transmissive velocity. As the antennas pass over discrete objects with different dielectric properties to the surrounding medium (boulders, pipes, coffins, trenches), they may generate hyperbolae, or arc-like reflections, or depressions. Radar waves also travel horizontally from the transmitting antenna, which in open ground simply dissipate with distance. However, in areas with upstanding structures, especially those that have a significant dielectric contrast to their surroundings, interference from such surface objects can create artefacts on the radargram. When such isolated objects (powerlines, telegraph wires, metal poles, trees, windmills/waterpump structures) are passed during a traverse, a series of hyperbolae may be generated that appear like a subsurface object but are simply out-of-plane reflections. Radar antennas are commonly elongate, generating radar waves in a widening arc from their long axis. Thus when moved in parallel to the antenna axis, the radar waves may reflect from a larger subsurface area in front and behind the antenna, (the so-called footprint) than when moved with the antennas at right angles to survey direction. Antennas may be shielded with radio-wave attenuating materials that reduce such out-of-plane interference. Unlike other forms of electromagnetic radiation used in geophysics, radio waves have far higher rates of attenuation, and thus penetration and reflection depths are typically low, but horizontal accuracy is high, coupled with rapid, real-time results, unlike all other geophysical techniques bar metal detectors and magnetometer raw data. The receiving antenna has either electronic or fibre-optic link to a recorder that converts incoming radiowaves to digital format and displays these graphically as wavelets. As the transmitter-receiver array is moved, so these wavelets are stacked horizontally to produce a radargram, a kind of x-ray slice into the Earth, but recorded in the time taken for radar waves to penetrate and reflect, as opposed to real depth. The speed of radiowave propagation is determined by the makeup of the transmitting medium: in this case the speed of light and dielectric permittivity. Magnetic properties can also influence radar wave speed. Changes in dielectric permittivity can cause radar wave reflection, without which GPR profiling would be impossible. Radarwave attenuation, or signal loss is extreme in conductive media such as seawater, clays (especially hydrous) and some leachate. GPR has good depth penetration (tens to hundreds of metres) in ice (with minor fracturing/interstitial water), hard rocks like limestone and granite and clay-poor quartz silts or sands. Vertical resolution *vs.* depth penetration is of major concern when choosing antenna frequency. Low frequencies (15–50 MHz) achieve deep penetration with poor vertical resolution in the received signal, due to the long wavelength. High frequencies (500–1000 MHz) show high resolution with weak penetration (centimetres to metres). Low-frequency antennas are large (a few metres long), high frequency antenna are small (tens of centimetres). Again, this can influence the use of the method, as deeply buried targets in enclosed spaces are virtually impossible to survey.

As with all geophysical methods, some intelligence concerning the likely size and makeup of the target is useful: where unknown or questioned, then a range of antennas should be used, and in very poorly understood locations, with other geophysical and invasive techniques (Blunderbuss Approach). Moisture contents influence radar wave velocity because in homogenous media porosity has a direct relationship to dielectric permittivity. Thus dry sand will allow increased wave propagation: sand with high freshwater content will give improved vertical resolution. A problem with unshielded antenna is the effect of 'out-of-plane' reflections (see above, trees, poles), analysed by surveying the same line with different antenna orientations. It is easy to think of the radar wave as a focused beam (the ray-path at right-angles to the wave) when in fact the radar wave as it travels into the subsurface is more like a bubble, hemispherical at first, expanding and becoming distorted as it travels at different speeds into the ground. Thus lateral to the antenna, on or in the ground surface may be structures that cause reflections at ground level. The effect of these surface features can be diminished by altering the orientation of the antennas, or by shielding the above-ground portion of the antenna, such that the radio wave is only allowed to penetrate the ground. GPR has found it's best uses in imaging glaciers, sand deposits (river, non-saline coastal sands), aquifers (porous nature), archaeological features (moats, buried buildings) and concrete/pavements.

Appendix 2

Luminescence analysis and dating of sediments from archaeological sites and valley fill sequences

Alan J. Cresswell, David C.W. Sanderson, Timothy C. Kinnaird & Charles French

A2.1. Summary

This report describes Optically Stimulated Luminescence (OSL) investigations to provide a temporal framework to underpin investigations into the early Holocene topography of the Ramla and Marsalforn valleys, Gozo, and excavations at the Neolithic temple sites of Ġgantija, Gozo and Skorba, Malta, and the Punic-Roman site of Tal-Istabal, Qormi, on the outskirts of Valletta in Malta. These chronologies are also of benefit in understanding the development and history of these World Heritage Site monuments.

Although the local limestone geology was not expected to generate quartz-rich sediments, micromorphology conducted by the *FRAGSUS* team had shown the presence of sand sized quartz within local soils and sediments. Field and laboratory profile measurements were conducted on 60 samples from seven sequences to provide initial assessments of the brightness of luminescence signals from different silicate fractions, and the stratigraphic relationships between the range of signals measured, to assess the prospects of being able to determine robust age quantifications from these materials, and guide the collection of larger tube samples for OSL dating. Laboratory profiling measurements confirmed the presence of quartz in prepared sediments with generally bright luminescence signals, and opening the way for Single Aliquot Regenerative (SAR) OSL dating of quartz fractions from 12 tube samples collected from five sites, with accompanying field and laboratory dose rate measurements.

At both the Ġgantija Temple (Gozo) and Skorba Temple/settlement (Malta), profile samples collected from below the modern agricultural soils show photon counts and apparent doses that increase steadily with depth, indicating that these buried soils accumulated gradually without subsequent disturbance. The OSL equivalent dose measurements showed no significant variation between aliquots, again indicating that the quartz minerals had been zeroed prior to deposition without subsequent disturbance, allowing robust ages to be determined. For both these locations, the OSL dates for the bottom of the sequences indicating the onset of soil accumulation were consistent at 8560±630 BC (Ġgantija) and 8780±710 BC (Skorba). At Ġgantija the top of this buried soil gives a Bronze Age OSL date of 1140±250 BC, whereas the OSL date for the top of the buried soil at Skorba is 7760±560 BC, predating the known Neolithic activity at the site.

At Ramla and Marsalforn Valleys, OSL investigations were conducted on sequences of buried palaeosols, hillwash and alluvial deposits. For Marsalforn Valley, the profile samples show a slight increase in photon counts and dose with depth, suggesting a gradual build-up of material. However, the OSL samples show evidence of multiple dose components, including high dose residuals, consistent with variations in light exposure during the reworking of soils. The upper sample could not be reliably dated, and the lower two samples generate the same age within uncertainties (1560±240 BC and 1480±340 BC). The Ramla Valley profiles are complex, showing relatively high photon counts in the upper samples decreasing with depth, and no clear trend in the apparent dose estimates. The OSL samples all show evidence of multiple dose components, including both high dose residuals and modern OSL dates in the nineteenth and early twentieth centuries AD.

The investigations reported here are the first applications of luminescence techniques on these sites. The results show that quartz OSL is an applicable approach to investigations of these sites, and that luminescence profiling techniques using field instruments and laboratory methods are highly informative. There is clearly the potential to apply these techniques to establish more detailed chronologies in future work.

A2.2. Introduction

Situated in the Mediterranean, the archipelago of Malta and Gozo lies close to the route of the spread of agricultural practices from the Fertile Crescent along the southern coast of Europe, and later dispersions of Neolithic cultural practices including monumental architecture. Agriculture based on wheat cultivation developed in the Fertile Crescent of the Near East around 9000 BC, and spread along the southern coast of Europe, largely associated with maritime movement, with early farming communities on Crete (*c.* 7000 BC), east-central Greece (*c.* 6500 BC), Dalmatia (*c.* 5700 BC), southern Italy (*c.* 6000 BC) and southern Iberia (*c.* 6000 BC). The first evidence of Holocene human activity on Malta, evidenced by pottery shards and the charred remains of fires and bones, has been dated to approximately 5000 BC (Trump 1966; Renfrew 1972). The emergence of visible social complexity is evidenced in enclosed sites and communal tombs in southeast Spain in the later fourth millennium BC. It has been suggested that the necessity of water control in arid regions lead, in part, to the emergence of such social complexity.

The archipelago of Malta and Gozo has a seasonally dry and hot climate which makes the natural landscape marginal for agriculture, and it has been presumed that from prehistoric times terracing has been extensively adopted to conserve soils and moisture, improving the landscape for agriculture (Sagona 2015). In addition, common to other parts of the Mediterranean, the islands are believed to have been prone to deforestation, drought and soil erosion since Neolithic times (Bevan & Conolly 2013; Brandt and Thornes 1996; Djamali *et al*. 2013; Grima 2008a; Grove & Rackham 2003; Hughes 2011). The research on these islands within the *FRAGSUS Project* aimed to examine these assumptions through a detailed geoarchaeological and micromorphological study of two significant Neolithic palaeosol contexts from beneath the Santa Verna and Ġgantija Neolithic temple sites and the associated Marsalforn and Ramla valleys to either side of the Xagħra plateau on Gozo.

The work reported here uses luminescence techniques to develop chronological frameworks for these investigations. Chronologies have previously been developed based on radiocarbon analysis (Trump 1966; Renfrew 1972) for the temple complex at Skorba with calibrated dates ranging from *c*. 5000 BC to 3200 BC, however luminescence approaches have not to date been widely used on Malta and Gozo. Luminescence techniques have, however, been widely used in Neolithic contexts in the Mediterranean, and beyond, for establishing robust chronologies. Examples in the Mediterranean region include megalithic tombs at Cabeço dos Pendentes in Portugal (Kinnaird *et al*. 2015), Neolithic monuments in Corsica (Sanderson *et al.* 2014), deltaic sediments associated with cultural activity from the Neolithic onwards on Crete (Zacharias *et al.* 2000), and Neolithic settlements, cemeteries and landscapes in Cyprus (Kinnaird *et al.* 2007, 2013). These techniques have also been used to investigate rates of soil erosion in Greece (Fuchs *et al.* 2004) using material largely devoid of quartz minerals, and river development in Crete (Macklin *et al.* 2010) where quartz minerals are derived from local sandstone.

The geology of Malta is dominated by limestone, resulting in locally derived soils largely devoid of silicate minerals suitable for luminescence dating. However, windblown sands from the Sahara are expected to deliver small quantities of silicates to the island. The Sahara is the largest source of aeolian dust, accounting for approximately half of the total atmospheric mineral dust burden (Scheuvens *et al.* 2013), with dust from the Sahara deposited in south and central America, the Atlantic Ocean, Europe and the Mediterranean, India and sub-Saharan Africa over the last 5 million years. In the Western Mediterranean, the dominant source of dust is from Tunisia and northern Algeria with dust generated from dry lakes and alluvial deposits (Scheuvens *et al*. 2013). Dust emission is a complex relationship between wind and surface conditions. Generally, small particles (<70 μm) experience large interparticle cohesive forces relative to aerodynamic forces acting on the particles, with aerodynamic forces becoming relatively larger with larger grain size. Thus, larger grains are mobilized first and follow ballistic curves with impacts on the ground mobilizing the smaller particles (Schepanski 2018). Alluvial sediments are very prone to wind erosion, with temporally varying erodibility as the most susceptible particles are removed from the sediment with refreshing of sediments during floods (Schepanski 2018). Thus, dust emission strongly reflects environmental conditions, being largest in dry periods. The transport distance strongly depends on residence time in the atmosphere; fine particles (<70 μm) are kept aloft by atmospheric turbulence for durations of weeks and can be transported thousands of km, with larger particles generally depositing within a day although larger particles are occasionally found >1000 km from their source (Schepanski 2018). The typical red Mediterranean soils, or *terra rossa*, on limestone substrates found throughout this region are also common on Malta and Gozo. The silicate minerals in similar soils in Greece have been attributed to aeolian deposition of material blown from North Africa (MacLeod 1980; Mizota *et al*. 1988), although larger mineral grains in low lying

regions have been attributed to local beaches (Mizota *et al.* 1988). Yaalon (1997) argues that aeolian dust from the Sahara contributes to all soils in the Mediterranean region, with up to 50 per cent of aeolian material in limestone derived soils. Micromorphological investigations conducted within the *FRAGSUS Project* have already shown the presence of sand sized silicates within local soils and sediments (French *et al.* 2018).

Quartz grains from the Sahara are expected to be well suited to OSL dating, with a reputation for being bright (e.g. Bevan *et al*. 2013; Kinnaird *et al.* 2013; Mauz *et al.* 2009; Russell & Armitage 2012), but may not be abundant. Fuchs *et al*. (2004) have shown that similar soils in Greece without abundant quartz can be accurately dated. The relative abundance of these grains may reflect climatic variations, in particular changes in aridity in the Sahara which may alter the supply of grains and prevailing wind directions and strengths affecting the transport of these grains to Malta. Although it is expected that aeolian grains will be bleached in transit, many of the grains in the soils will have been transported to the islands before incorporation in the soils having been reworked from earlier soils. The aim of the OSL investigations reported here is to provide a temporal framework to underpin investigations into the earlier Holocene topography of the Ramla and Marsalforn valleys, Gozo, and on the excavations at the Neolithic temple sites of Ġgantija, Gozo and Skorba, Malta. The objective of the field campaign was to retrieve samples from existing soil/sediment profiles in Gozo for OSL dating, and to sample the new test excavations at Skorba in Malta for micromorphology, physical characterization and OSL dating.

On Gozo, three sites were visited: the Neolithic temple site of Ġgantija on the Xagħra plateau; the Ramla valley, which separates the Xagħra plateau from the Nuffara plateau to the south; and the Marsalforn valley, a tributary valley of the Ramla. From the more extensive fieldwork of French and Taylor (see Chapter 5), it is known that the plateaus are largely denuded of soil and vegetation (i.e. Holocene strata), the little that remains in terms of (Holocene) hillwash (colluvium) and alluvial deposits is concentrated on the lower slopes and in the lower parts of the topography, such as in the Ramla and Marsalforn valleys. The OSL investigations in the Ramla and Marsalforn valleys were undertaken with the aim of generating a chronology for the sequences of buried palaeosols, hillwash and alluvial deposits preserved there, and thus the means to re-construct the earlier Holocene to Recent development of the Gozo valley-scale with time. At Ġgantija, the objective was to provide a chronology for the buried soil sequence located off-site, in Test Pit 1, to establish the soil catena history for this part of Gozo.

On Malta, two sites were visited: the Neolithic temple site of Skorba and a development site with Punic-Roman archaeology present at Marsa in Valletta. Test excavations in 2016 on the western edge of the Skorba temple/settlement had revealed a 1.5 m deep sequence, within which three curvilinear stone walls of the Neolithic period effectively sealed *c*. 70 cm of soil accumulation. From field excavations, it is suggested that the lower *c*. 50 cm of this soil was in fact a buried soil, albeit with the upper *c.* 20 cm probably being disturbed (in the past) (see Chapter 5). The objective here, was again to provide a chronology for the buried soil sequence, and identify any correlations between the soil formation/properties and prehistoric activity.

A2.3. Methods

A2.3.1. Sampling and field screening measurements

The aim of the April 2016 fieldwork was to retrieve samples from existing soil/sediment profiles in Gozo for OSL dating, and to sample the new test excavations at Skorba in Malta for OSL dating, physical characterization and micromorphology. In addition, a development site with Punic-Roman archaeology present at Marsa in Valletta was also sampled.

All samples were first appraised using the SUERC portable OSL reader, following an interleaved sequence of system dark count (background), infra-red stimulated luminescence (IRSL) and OSL, similar to that described by Sanderson and Murphy (2010). This method allows for the calculation of IRSL and OSL net signal intensities, depletion indices and IRSL:OSL ratios, which are then used to generate luminescence-depth profiles. The patterns in these data allow initial inferences and conjectures about trends or discontinuities in field profiles to be made, in combination with other initial observations of the sedimentology, which are used to refine further sampling. These can be refined and evaluated through further laboratory assessments.

A2.3.2. Laboratory calibrated screening measurements

Having established that there were measureable stratigraphic trends in the luminescence 'field' profiles, it remained to be determined whether these signal progressions are influenced, or indeed controlled, by sensitivity variations. Laboratory profiling provides one means to assess luminescence sensitivity distributions, and the first preliminary assessment of apparent doses.

All profiling samples were wet sieved at 90 and 250 μm. The 90–250 μm fractions were then subjected

to acid treatments of 1M HCl for 10 minutes, 15 per cent HF for 15 minutes and 1M HCl for 10 minutes. The samples were split into two fractions, one for polymineral analysis and one for quartz analysis. The quartz fraction was submitted to further acid treatments of 40 per cent HF for 40 minutes and 1M HCl for 10 minutes.

Luminescence sensitivities (Photon Counts per Gy) and stored doses (Gy) were evaluated from paired aliquots of the polymineral and HF-etched quartz fractions, using Risø DA-15 automatic readers (following procedures established in Burbidge *et al*. 2007; Sanderson *et al*. 2001, 2003). The readout cycles comprised a natural readout, followed by readout cycles for a nominal 1 Gy test dose, a 5 Gy regenerative dose, and a further 1 Gy test dose. For the polymineral samples, a 220°C preheat was followed by 60s OSL measurements using the IR LEDs at 50°C, the blue LEDs at 125°C, and a TL measurement to 500°C. For the quartz samples, a 220°C pre-heat was used with 60s OSL measurements using the blue LEDs.

A2.4. Quartz OSL SAR measurements

A2.4.1. Sample preparation

Water contents
Dating materials and bulk sediment samples were weighed, saturated with water and re-weighed. Following oven drying at 50 °C to constant weight, the actual and saturated water contents were determined as fractions of dry weight. These data were used, together with information on field conditions to determine water contents and an associated water content uncertainty for use in dose rate determination.

HRGS and TSBC sample preparation
Bulk quantities of material, weighing 50–100 g, were removed from each full dating and bulk sediment sample for environmental dose rate determinations. These dried materials were transferred to high-density-polyethylene (HDPE) pots and sealed with epoxy resin for high-resolution gamma spectrometry (HRGS). Each pot was stored for three weeks prior to measurement to allow equilibration of ^{222}Rn daughters. A further 20 g of the dried material was used in thick source beta counting (TSBC; Sanderson 1988).

Quartz mineral preparation
Approximately 5–10 g of material was removed for each tube and processed to obtain sand-sized quartz grains for luminescence measurements. Each sample was wet sieved to obtain the 90–150 and 150–250 μm fractions. The 90–150 μm fractions were treated with 1 M hydrochloric acid (HCl) for 10 minutes, 15 per cent hydrofluoric acid (HF) for 15 minutes, and 1 M HCl for a further 10 minutes. The HF-etched sub-samples were then centrifuged in sodium polytungstate solutions of ~2.58, 2.62, and 2.74 g cm^{-3}, to obtain concentrates of potassium-rich feldspars (<2.58 g cm^{-3}), sodium feldspars (2.58–2.62 g cm^{-3}) and quartz plus plagioclase (2.62–2.74 g cm^{-3}). The selected quartz fraction was then subjected to further HF and HCl washes (40 per cent HF for 40 minutes, followed by 1M HCl for 10 minutes).

All materials were dried at 50° C and transferred to Eppendorf tubes. The 40 per cent HF-etched, 2.62–2.74 g cm^{-3} 'quartz' 90–150 μm fractions were dispensed to 10 mm stainless steel discs for measurement. The purity of which was checked using a Hitachi S-3400N scanning electron microscope (SEM), coupled with an Oxfords Instruments INCA EDX system, to determine approximate elemental concentrations for each sample. 8–32 aliquots were dispensed for each sample, depending on quartz yield.

A2.4.2. Measurements and determinations

Dose rates
Dose rates were measured in the laboratory using HRGS and TSBC. Full sets of laboratory dose rate determinations were made for all samples.

HRGS measurements were performed using a 50 per cent relative efficiency 'n' type hyper-pure Ge detector (EG&G Ortec Gamma-X) operated in a low background lead shield with a copper liner. Gamma ray spectra were recorded over the 30 keV to 3 MeV range from each sample, interleaved with background measurements and measurements from SUERC Shap Granite standard in the same geometries. Sample counts were for 80 ks. The spectra were analysed to determine count rates from the major line emissions from ^{40}K (1461 keV), and from selected nuclides in the U decay series (^{234}Th, ^{226}Ra + ^{235}U, ^{214}Pb, ^{214}Bi and ^{210}Pb) and the Th decay series (^{228}Ac, ^{212}Pb, ^{208}Tl) and their statistical counting uncertainties. Net rates and activity concentrations for each of these nuclides were determined relative to Shap Granite by weighted combination of the individual lines for each nuclide. The internal consistency of nuclide specific estimates for U and Th decay series nuclides was assessed relative to measurement precision, and weighted combinations used to estimate mean activity concentrations (Bq kg^{-1}) and elemental concentrations (per cent K and ppm U, Th) for the parent activity. These data were used to determine infinite matrix dose rates for alpha, beta and gamma radiation.

Beta dose rates were also measured directly using the SUERC TSBC system (Sanderson 1988). Count rates were determined with six replicate 600 s counts on

each sample, bracketed by background measurements and sensitivity determinations using the Shap Granite secondary reference material. Infinite-matrix dose rates were calculated by scaling the net count rates of samples and reference material to the working beta dose rate of the Shap Granite (6.25 ± 0.03 mGy a^{-1}). The estimated errors combine counting statistics, observed variance and the uncertainty on the reference value.

The dose rate measurements were used in combination with the assumed burial water contents, to determine the overall effective dose rates for age estimation. Cosmic dose rates were evaluated by combining latitude and altitude specific dose rates (0.17 ± 0.01 mGy a^{-1}) for the site with corrections for estimated depth of overburden using the method of Prescott and Hutton (1994).

Quartz SAR luminescence measurements

All measurements were conducted using a Risø DA-15 automatic reader equipped with a $^{90}Sr/^{90}Y$ β-source for irradiation, blue LEDs emitting around 470 nm and infrared (laser) diodes emitting around 830 nm for optical stimulation, and a U340 detection filter pack to detect in the region 270–380 nm, while cutting out stimulating light (Bøtter-Jensen *et al*. 2000).

Equivalent dose determinations were made on sets of 8–32 aliquots per sample, using a single aliquot regeneration (SAR) sequence (cf. Murray & Wintle 2000). Using this procedure, the OSL signal levels from each individual disc were calibrated to provide an absorbed dose estimate (the equivalent dose) using an interpolated dose-response curve, constructed by regenerating OSL signals by beta irradiation in the laboratory. Sensitivity changes which may occur as a result of readout, irradiation and preheating (to remove unstable radiation-induced signals) were monitored using small test doses after each regenerative dose. Each measurement was standardized to the test dose response determined immediately after its readout, to compensate for changes in sensitivity during the laboratory measurement sequence. The regenerative doses were chosen to encompass the likely value of the equivalent (natural) dose. A repeat dose point was included to check the ability of the SAR procedure to correct for laboratory-induced sensitivity changes (the 'recycling test'), a zero dose point is included late in the sequence to check for thermally induced charge transfer during the irradiation and preheating cycle (the 'zero cycle'), and an IR response check included to assess the magnitude of non-quartz signals. Regenerative dose response curves were constructed using doses of 0.5, 1, 2.5, 10 and 2.5 Gy, with test doses of 1.5 Gy. The 32 aliquot sets were sub-divided into eight subsets of four aliquots, such that eight preheating regimes were explored (200° to 270° C, in 10° C increments), the small aliquot sets were divided into a small number of sub-sets.

A2.5. Results

A2.5.1. Sampling and preliminary luminescence stratigraphies

Field work was conducted in April 2016, with the collection of seven profiles and 12 OSL dating samples, as summarized in Tables A2.1 and A2.2, with selected photographs of the sampling sites in Figures A2.1 to A2.8. Field gamma spectrometry measurements were also collected for each of the OSL sampling sites, reported in Table A2.4. All samples were first appraised using the SUERC portable OSL reader, to produce IRSL and OSL net signal intensities, depletion indices and IRSL:OSL ratios, and luminescence-depth profiles. The results are shown in Figures A2.9 to A2.13, and presented in the Table A2.1.

A2.5.2. Gozo

Three profiles were sampled on Gozo:

Profile 1: an erosion cut profile in the middle Marsalforn valley, opposite Ta'Manea in Weid ir-Rigu (profile BH110; N 36 03.472/ E 014 14.946) was cut back and sampled for OSL. This profile comprised *c*. 3.7 m of rubbly fine sandy/silt loam which was interrupted by two incipient buried soil horizons at *c*. 1.75–2.10 and 2.70–2.85 m down-profile. Figures A2.1 and A2.2 show photographs of this site. A series of 10 small bulk samples were taken for luminescence profiling from 1.75–3.25 m. Initial field impressions, including the luminescence profiles (Fig. A2.9) showing broadly similar luminescence intensities within and between the soils with the exception of P1/2, were that this represents an age-related gradual accumulation of hillwash-type sediment throughout the profile. Three OSL tube samples at 1.75, 2.65 and 3.2 m down-profile were collected (as indicated in Fig. A2.9), representing the top of the upper buried soil and the top and bottom of the lower soil.

Profile 2: an erosion cut profile in the lower Ramla valley about 200 m inland from Ramla Bay (profile BH 66; N 36 03.442/E 014 17.045) was cut back and sampled for OSL. This profile is comprised of a series of alternating horizons of calcitic silt loam and coarse sand/pebble horizons, with the whole profile generally fining upwards, over a depth of *c*. 1.4 m. The site is shown in Figure A2.3. A series of 11 small bulk samples were taken from the finer silt loam horizons for profiling (Fig. A2.10). These indicate that parts of the sedimentary sequence are likely to have been re-deposited without the luminescence signals being

Table A2.1. *Sample descriptions, contexts and archaeological significance of the profiling samples used for initial screening and laboratory characterization (estimated from local datums).*

	Field no.	SUTL no.	Depth /cm	Field description/ context	Archaeological significance
Ta'Manea, Marsalforn valley, Gozo off-site palaeoenvironmental proxy record; reconstruct earlier Holocene landscape of Gozo					
Profile 1	P1/1	2916A	180	above soil; pale yellowish-grey silty clay loam; hillwash	TAQ for age of buried soil (upper horizon)
	P1/2	2916B	195	buried old land surface/incipient soil in hillwash; pale yellowish brown silty clay loam with columnar ped structure	Buried soil surface 1.75–2.10 m (upper horizon)
	P1/3	2916C	205		
	P1/4	2916D	215	rounded limestone pebbles (<5 cm); erosion event/ temporary stream	TPQ for age of buried soil (upper horizon)
	P1/5	2916E	225	mix of greyish brown fine-medium sand and silt with limestone gravel pebbles	-
	P1/6	2916F	270		TAQ for age of buried soil (lower horizon)
	P1/7	2916G	290	buried old land surface/incipient soil in hillwash; pale yellowish brown fine sandy/silt loam with columnar blocky ped structure	Buried soil surface 2.70–2.85 m (lower horizon)
	P1/8	2916H	300		TPQ for age of buried soil (lower horizon)
	P1/9	2916I	310		-
	P1/10	2916J	320	pale grey silty clay loam with abundant rounded stone pebbles (<10 cm)	-
Ramla valley, Gozo exploited in the sixteenth and nineteenth centuries, with two superimposed systems of field and property boundaries; significance of profile – response to intensification of landscape/arable development on adjacent slopes					
Profile 2	P2/1	2920A	7.5	pale grey calcitic silt loam; calcitic alluvial lens	temporal constraints on degradation of upper slope
	P2/2	2920B	15		
	P2/3	2920C	27.5	fine pebbles (<2 cm); pebbly hillwash lens	fluvial phase
	P2/4	2920D	45	pale grey calcitic silt loam; calcitic alluvial lens	temporal constraints on degradation of upper slope
	P2/5	2920E	60		
	P2/6	2920F	75		
	P2/7	2920G	82.5		
	P2/8	2920H	105	fine sandy/silt loam	
	P2/9	2920I	115		Thin hillwash accumulations – may indicate some degree of balance and resilience in the landscape, or individual events removed most of the eroded soils to the sea
	P2/10	2920J	125		
	P2/11	2920K	140	weathered Globigerina bedrock	
Ġgantija Temple Test Pit 1, Gozo					
Profile 3	P3/1	2913A	10	greyish brown silt loam with common limestone fragments (<5 cm); Ap and terrace soil	-
	P3/2	2913B	18		later prehistoric and historic agricultural activity
	P3/3	2913C	25		
	P3/4	2913D	34	greyish brown silt loam with abundant limestone rubble and abundant Neolithic artefacts (pot, bone, lithics)	
	P3/5	2913E	45		
	P3/6	2913F	54		
	P3/7	2913G	68		Base of agricultural soil
	P3/8	2913H	78	brown silt loam with abundant Neolithic artefacts; *in situ* Ah of palaeosol	'field' profile implies some chronology with depth; beginnings of soil change associated with use and degradation of this landscape prior to construction of temple?
	P3/9	2913I	85	mid-brown silt loam with abundant Neolithic artefacts; buried lower A-B horizon of palaeosol	
	P3/10	2913J	92		Base of buried soil; constrain onset of soil accumulation

Table A2.1 *(cont.).*

	Field no.	SUTL no.	Depth /cm	Field description/ context	Archaeological significance
Skorba Neolithic site (Malta), Trench A, East section profiles 4 (East), 6 and 7 (south) taken on western edge of Skorba temple/settlement; like at Ġgantija, profiles encompass a buried soil associated with the landscape prior to construction of temple; here, sealed by three curvilinear stone walls					
Profile 4	P4/1	2924A	22	modern topsoil and fill of wall robber trench	-
	P4/2	2924B	32		-
	P4/3	2924C	41	dark brown sandy silt loam with occasional limestone rubble (<5 cm)	context [2]; fill of robber trench; re-deposited materials, carry residuals from earlier depositional cycle
	P4/4	2924D	51		
	P4/5	2924E	63	mix of dark brown sandy silt loam and limestone rubble (<15 cm)	context [11]; clear signal-depth progression through contexts 11, 20, 24
	P4/6	2924F	75		
	P4/7	2924G	86	dark greyish brown sandy silt loam; ?aggraded soil?	context [20]; aggraded soil?; later prehistoric and historic agricultural activity (as at Ġgantija?)
	P4/8	2924H	96		
	P4/9	2924I	106	dark brown sandy silt loam; disturbed, possible A horizon of palaeosol	context [24]; possible A horizon to buried soil; beginnings of soil change associated with use and degradation of this landscape prior to construction of temple?
	P4/10	2924J	113		
	P4/11	2924K	121	dark brown sandy silt loam; *in situ* B horizon of palaeosol	context [28]; in situ B horizon to buried soil
	P4/12	2924L	131		
	P4/13	2924M	138		potentially disturbed in prehistory; note inflection in luminescence intensities at *c*. 138 cm depth
	P4/14	2924N	147		
	P4/15	2924O	148		
Marsa, Valletta, Malta a Punic-Roman area of terraces and irrigation features; little in way of soil preservation due to commercial development at site					
Profile 5	P5/1	2929A	283	brown, calcitic, fine sandy/silt loam; ?pre-terrace soil/?palaeosol	TPQ for wall; sixteenth century AD soil accumulation and later terrace build-up?
	P5/2	2929B	287		
	P5/3	2929C	292		
	P5/4	2929D	298		
Skorba Neolithic site (Malta), Trench A, South section					
Profile 6	P6/1	2928A	65	dark brown fine sandy loam	context [23]
	P6/2	2928B	80	dark brown fine sandy loam; ?aggraded soil?	beneath context [26] – a possible Neolithic floor 75–78 cm; there is no clear progression in luminescence signals across the possible Neolithic floor/surface (in the position of this profile); this may indicate that this surface was not exposed for any length of time
	P6/3	2928C	90		
	P6/4	2928D	100	dark brown fine sandy loam with 20–25% small limestone rubble <5 cm); ?disturbed upper part of a palaeosol?	disturbed upper part of buried soil; reset during laying of floor / construction of Skorba complex?
	P6/5	2928E	115	dark brown fine sandy loam; *in situ* palaeosol	in situ buried soil; constrain onset of soil accumulation
	P6/6	2928F	120		
Skorba Neolithic site (Malta), Trump Trench cut in 1961					
Profile 7	P7/1	2931A	103	modern topsoil and fill of wall robber trench	within backfill to Trump's 1961 excavation; compare and contrast signal intensities with profiles 4 and 6
	P7/2	2931B	113		
	P7/3	2931C	123		
	P7/5	2931D	146	dark greyish brown sandy silt loam; ?aggraded soil?	should be equivalent to context [20] – samples P4/7 – 4/8

Table A2.2. *Sample descriptions, contexts and archaeological significance of sediment samples SUTL2914–2930 (†depths estimated relative to the overlying landforms for cosmic attenuation estimation).*

Sample ID	Profile	SUTL no.	Depth /cm	Description	Archaeological significance
OSL1	1	2917	175–180	=P1/1	Constrain final period soil was exposed, phase 2
OSL2	1	2918	265–270	=P1/6	Constrain final period soil was exposed, phase 1
OSL3	1	2919	320–330	= P1/10	Constrain onset of soil accumulation, phase 1
OSL4	2	2921	15–20	=P2/2	Provide a temporal constraint on degradation of upper slope
OSL5	2	2922	62–66	=P2/5	Provide temporal constraints on periods of colluviation
OSL6	2	2923	103–106	=P2/8	
OSL7	3	2914	78	=P3/8; buried soil 'A' horizon	Constrain final period soil was exposed
OSL8	3	2915	92	=P3/10; buried soil 'B' horizon	Constrain onset of soil accumulation
OSL9	5	2930	295–298	=P5/3 – 5/4	Constrain onset of soil accumulation, and date standing wall overlaying soil
OSL10	4	2925	118	=P4/11; [28]; rich-brown silty loam; 5% clay; 15–20% sand	Constrain final period soil was exposed
OSL11	4	2926	128	=P4/13	Provide temporal constraint on age of buried palaeo-surface
OSL12	4	2927	145	=P4/15	Constrain onset of soil accumulation

re-set at deposition; note, the step-like shifts in signal intensities at 46 cm and 115 cm. The most promising targets for dating are the horizons immediately beneath these units. Moreover, the ratio of net signal intensities between the upper (those not affected by recent soil turnover) and lower units, implies that the temporal range represented by these units may be relatively short. Three tube samples were taken for OSL dating at 15, 62 and 103 cm down-profile. The latter sample loci were also sampled for micromorphological analysis. Initial field impressions were not that clear, but the profile exhibited aggradation over time with at least two clear breaks, suggesting palaeo-surfaces of some kind at *c*. 46 cm and 115 cm, potentially indicative of changes in erosion processes from alternating fast/slow to a much slower aggradational dynamic.

Profile 3: Test Pit 1 which was excavated in 2014 on the western edge of the platform south of Ġgantija temple was re-excavated to reveal the complete profile through the agricultural soil build-up over the *in situ* buried soil. This is shown in Figure A2.4. A series of 10 small bulk samples were taken at approximately 10 cm intervals down-profile for luminescence profiling. Initial field impressions were that the agricultural soil had accumulated gradually over time, with a clear stratigraphic break at ~70 cm with the buried soil below, but with the buried soil exhibiting a longer and more stable time-depth. The luminescence profiles

Figure A2.1. *Marsalforn valley, Gozo.*

Figure A2.2. *Marsalforn valley, Gozo.*

Figure A2.3. *Ramla valley, Gozo.*

Figure A2.4. *Ġgantija Test Pit 1, Gozo.*

Figure A2.5. *(above) Skorba Neolithic site; trench A, East section; (left) trench A, South section, arrow shows position of Figure A2.6.*

Figure A2.6. *Skorba, Trench A, South section.*

(Fig. A2.11) show a significant increase in net signal below this horizon increasing with depth. Two tube samples for OSL dating were taken from the base of the agricultural soil (at 68 cm down-profile) and the base of the buried soil (at 92 cm down-profile).

A2.5.3. Skorba

The test excavations on the western edge of the Skorba temple/settlement revealed a 1.5 m deep sequence, within which three curvilinear stone walls of the Neolithic period effectively sealed *c.* 70 cm of soil accumulation. From field observation, it is suggested that the lower *c.* 50 cm of this soil was in fact a buried soil, albeit with the upper *c.* 20 cm probably having been disturbed (in the past). This soil exhibits a very fine sandy/silt dominated texture, which is very different from the soils present in the immediately surrounding area (in BH 618–625) which are much more dark brown, clay-rich, fine sandy/silty clay loams. Figures A2.5 and A2.6 show photographs of this site.

OSL profiling and sampling was undertaken at two profiles in the 2016 Trench A test excavation, from the east and south section faces. From the east section, 15 small bulk samples were taken at about 10 cm intervals from *c.* 22–148 cm down-profile (Profile 4) In the south section, 6 small bulk samples were taken between 65 and 120 cm down-profile, again to target the buried soil and soil accumulation above and the possible Neolithic floor/surface between 75 and 78 cm down-profile (Profile 6). The luminescence-depth profiles (Fig. A2.12) were extremely informative (profile 4):

1. unit [2] contains re-deposited materials, that carry luminescence residuals from an earlier depositional cycle;
2. units [11], [20] and [24] show a progression in luminescence signals with depth, consistent with a normal age-depth progression and a gradual accumulation of sediment; moreover, the range in signal intensities through these units is consistent with an age progression over a temporal range of a multiple of 1.5–2;
3. the upper *c.* 20 cm of the buried soil was probably disturbed in prehistoric times; note, the inflexion in luminescence intensities at *c.* 138 cm, indicating modification of this unit at the time this soil represented a former land-surface (and thus, that it is material at this depth, which should provide a constraint on the age of this palaeo-surface);
4. there is a clear temporal break between deposition of the soil, and units [24], [20] and [11]; this temporal break represents a short interval, equivalent to a temporal range in the order of 1.2–1.5; (profile 6)
5. there is no clear progression in luminescence signals across the possible Neolithic floor/surface (in the position of this profile); this may indicate that this surface was not exposed for any length of time (further characterization of these units in the laboratory will test this hypothesis); and
6. again, the upper part of the buried soil shows signs of disturbance in the past; note, by now the obvious inflexion in luminescence intensities occurs at *c.* 115 cm.

Three OSL tube samples were taken at 118, 128 and 145 cm down-profile from the east section, to target the chronology of the buried soil and old land surface. In both cases, the buried soil/soil accumulation/floor zone was also sampled for micromorphological analysis as well as physical characterization and geo-chemical analysis.

A2.5.4. Tal-Istabal, Qormi

Dr Tony Pace and Nathaniel Cutajar accompanied us to a commercial development site in Qormi on the northwestern side of a former marine embayment where a large Punic-Roman area of terraces and irrigation features had been recently excavated. Although there was little in the way of soil survival on this site due to total excavation, one zone of better preservation was located on the western edge of the site (N 36 03.423/E 014 17.047). Here beneath *c.* 2.7 m of surviving Globigerina Limestone terrace wall construction was *c.* 30–40 cm of agricultural/buried soil survival (Figs. A2.7 & A2.8). This was sampled for micromorphological analysis as well as physical characterization and geo-chemical analysis, and OSL profiling (Profile 5), with laser scans made of large sections of the terrace walls, and cut irrigation and burial features (by J. Bennett). The luminescence profile (Fig. A2.13) shows an increasing net signal with depth. A single tube sample was taken for OSL dating from the base of this profile.

A2.6. Laboratory calibrated screening measurements

The laboratory screening data are shown in Figures A2.14 to A2.20, with the data tabulated in the Supplement A Tables SA.2–SA.5. In most cases, the IRSL sensitivity is significantly lower than the OSL sensitivity. IRSL and OSL apparent doses follow similar stratigraphic trends, with a general increase in apparent dose with increasing depth for all profiles, for the sections at Marsalforn, Ġgantija (Gozo) and Skorba (Malta) the two estimates are in good agreement with agreement to within a factor of two to three for the other sections.

Figure A2.7. *Tal-Istabal, Qormi, Malta.*

Figure A2.8. *Tal-Istabal, Qormi, Malta.*

For Profile 1 (Fig. A2.14) there is a gradual increase in apparent dose with depth, for both IRSL and OSL which are in good agreement, with P1/4 showing higher apparent doses than the neighbouring samples, and a slight inversion of the profile with smaller apparent doses for the bottom two samples. OSL sensitivity is approximately two orders of magnitude greater than IRSL sensitivity, with both sensitivities showing a slight increase down the top half of the profile, a slight decrease down the bottom half, and a higher sensitivity for the sample below the soil layer. This broadly explains the variation of intensities observed in the field profiles (Fig. A2.9), and supports the conclusion that this profile represents a gradual accumulation of sediment.

For Profile 2 (Fig. A2.15) the sensitivities of both OSL and IRSL are similar and generally unchanged down the profile. The apparent dose in the IRSL measurements is approximately twice that of the OSL, with values for both scattered without any obvious trend down profile. For the lower part of the profile, this pattern reflects the field profile measurements (Fig. A2.10) which showed approximately constant intensities for most of the profile. However, the larger intensities for the uppermost three samples in the field measurements are not explained by the laboratory measurements. The approximately constant apparent doses and intensities suggest that the material in this profile accumulated rapidly.

For Profile 3 (Fig. A2.16) the apparent dose measured by OSL and IRSL is in general agreement, with no apparent trend down profile for the top 60 cm and a rapid increase with depth below that. The OSL sensitivities are two to three orders of magnitude greater than the IRSL sensitivities, with neither showing any significant trend down profile. This broadly reflects the field profiles (Fig. A2.11), which showed approximately constant and relatively low net intensities for the top 60 cm increasing significantly below that. Both field and laboratory measurements suggest a slow accumulation of material in the lower part of the profile, with a rapid accumulation for the top 60 cm.

For Profiles 4 and 6 (Figs. A2.17 & A2.19) the apparent dose increases gradually with depth down profile, with the OSL measurements generally slightly greater than the IRSL for profile 4. The OSL sensitivities are two to three orders of magnitude greater than the IRSL, without any obvious trend down profile with the exception of a significant reduction in sensitivity for P6/6. This reflects the observed gradual increase in net intensities down profile observed in the field profiles (Fig. A2.12), supporting the suggestion that

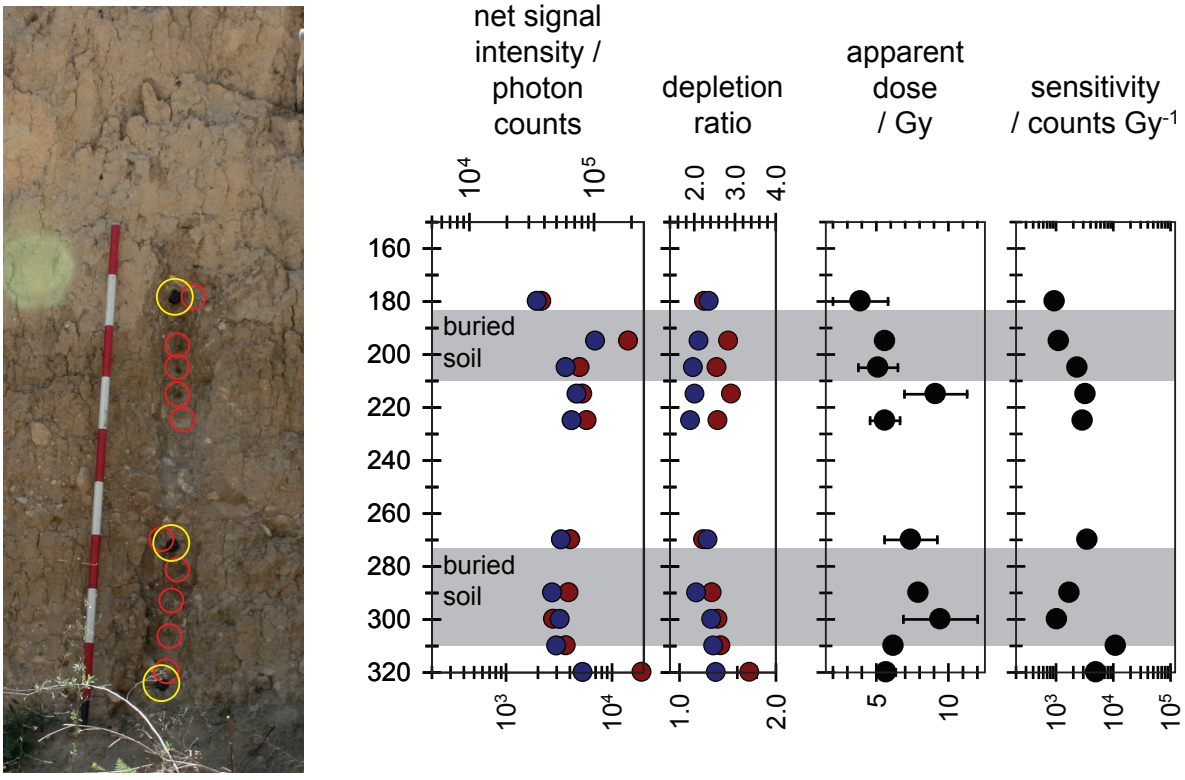

Figure A2.9. *Photograph, showing locations of profile sample (red circles) and OSL tubes (yellow circles), and luminescence-depth profile, for the sediment stratigraphy sampled in profile 1.*

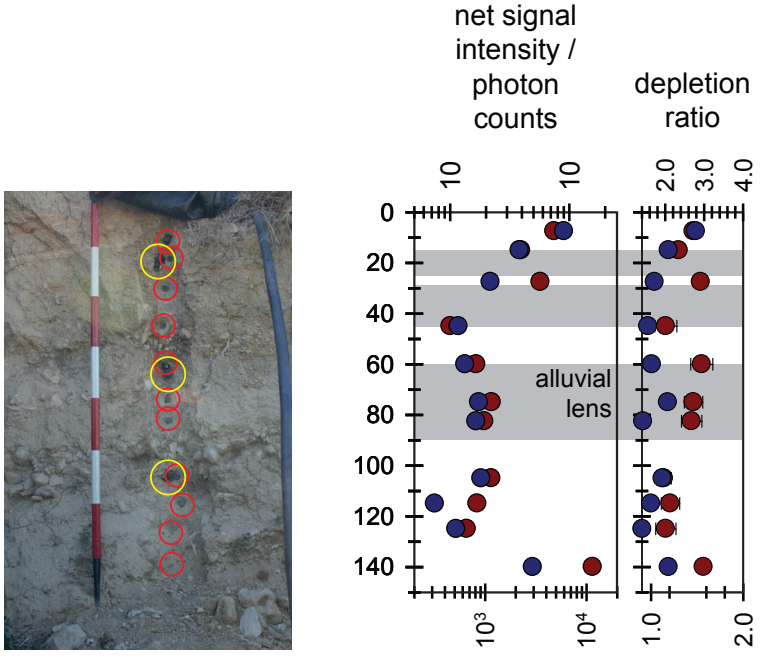

Figure A2.10. *Photograph, and luminescence-depth profile, for the sediment stratigraphy sampled in profile 3.*

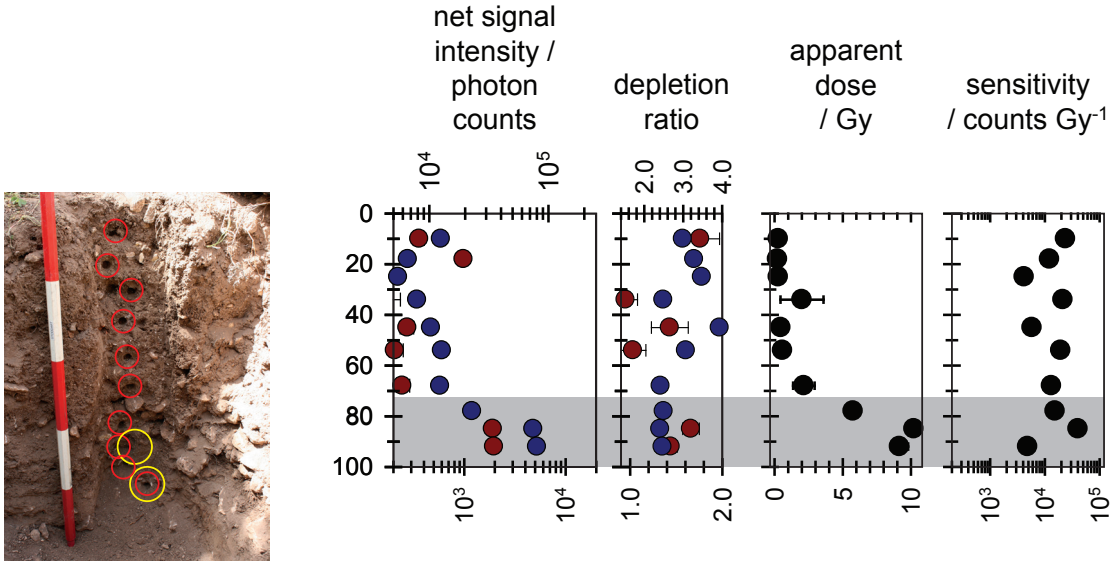

Figure A2.11. *Photograph, and luminescence-depth profile, for the sediment stratigraphy sampled in profile 2.*

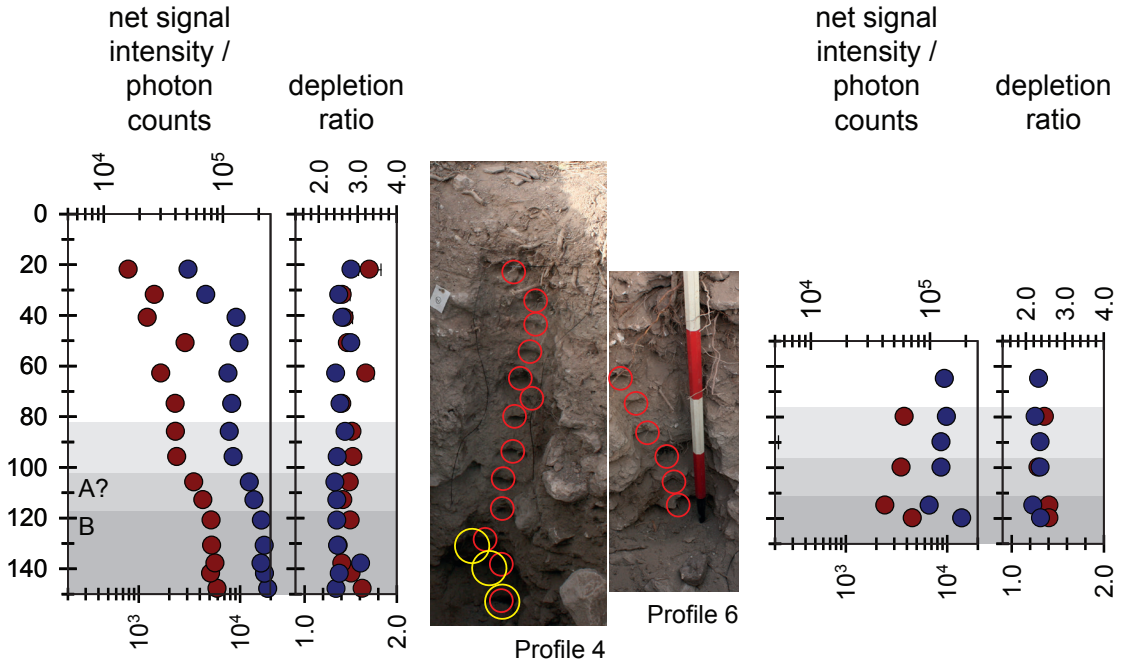

Figure A2.12. *Photograph, and luminescence-depth profile, for the sediment stratigraphy sampled in profiles 4 and 6.*

this represents a gradual accumulation of material over an extended period of time. The bottom sample of Profile 7 (Fig. A2.20) has similar apparent doses and sensitivities to the samples in profiles 4 and 6 that are identified as the same context, the upper samples within the backfill of the 1961 trench show a lower apparent dose and an inverted profile.

For Profile 5 (Fig. A2.18) the apparent dose measured by IRSL is 2–3 times that measured by OSL, with both increasing marginally down profile. The sensitivities for the two methods are similar, with differences less than an order of magnitude. This reflects the field profiles (Fig. A2.13) which showed a small increase in net intensities down profile.

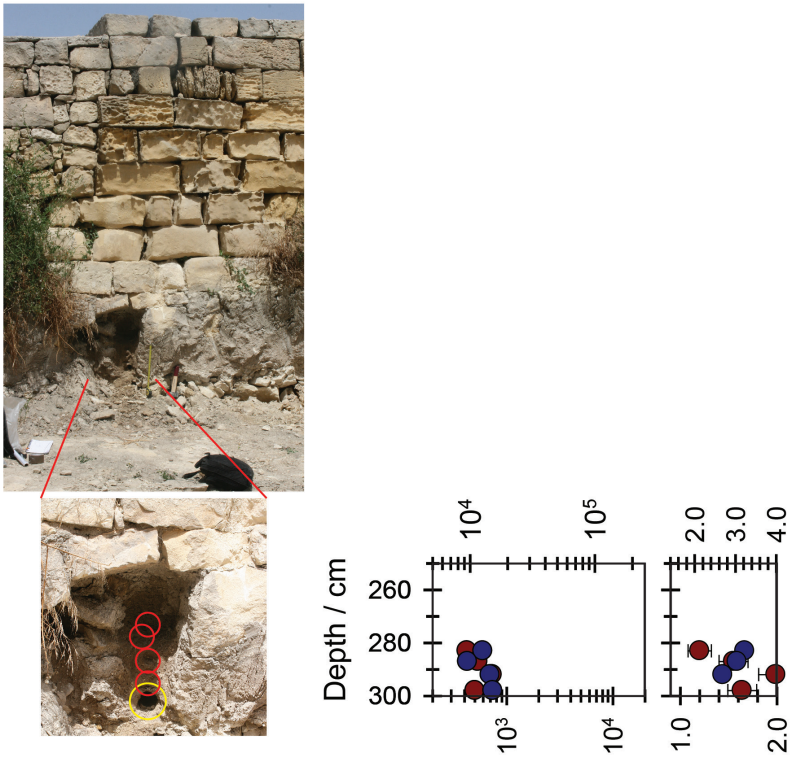

Figure A2.13. *Photograph, and luminescence-depth profile, for the sediment stratigraphy sampled in profile 5.*

A2.6.1. Dose rates

HRGS results are shown in Table A2.3, both as activity concentrations (i.e. disintegrations per second per kilogram) and as equivalent parent element concentrations (in per cent and ppm), based in the case of U and Th on combining nuclide specific data assuming decay series equilibrium.

Infinite matrix alpha, beta and gamma dose rates from HRGS are listed for all samples in Table A2.4, together with infinite matrix beta dose rates from TSBC and field gamma dose rates from FGS. Beta dose rates from HRGS are typically lower than those determined from TSBC by approximately 20 per cent. Wet gamma dose rates were measured in situ by FGS for each of the dating positions, and are typically lower than the HGRS gamma dose rates after water content corrections.

The water content measurements are given in Table A2.5, together with the assumed values for the average water content during burial. Field (ranging from 3–26 per cent of dry weight) and saturated (18–38 per cent of dry weight) water contents were determined from all samples in the laboratory, with working values for each site adopted for effective dose rate evaluation. Effective dose rates to the HF-etched 90–150 μm quartz grains are given in Table A2.5 (the mean of the TSBC and HRGS data, accounting for water content and grain size), together with the estimate of the gamma dose rate (the mean of the FGS and HRGS data, accounting for water content).

A2.6.2. Quartz single aliquot equivalent dose determinations

For equivalent dose determination, data from single aliquot regenerative dose measurements were analysed using the Risø TL/OSL Viewer programme to export integrated summary files that were analysed in MS Excel and SigmaPlot. The quality parameters for these analyses (sensitivity and sensitivity change, recycling ratio and response to zero dose) are given in Table A2.6. This shows considerable variation in sensitivity between samples, a small increase (5–15 per cent) in sensitivity for all samples, with all samples showing recycling ratios consistent with unity (with the exception of SUTL2923) and very low signals from the zero cycle and IRSL.

Composite dose response curves were constructed from selected discs and when possible, for each of the eight preheating groups from each sample, and used to estimate equivalent dose values for each individual

Table A2.3. *Activity and equivalent concentrations of K, U and Th determined by HRGS ([a]Shap granite reference, working values determined by David Sanderson in 1986, based on HRGS relative to CANMET and NBL standards; [b]Activity and equivalent concentrations for U, Th and K determined by HRGS (Conversion factors based on NEA (2000) decay constants): 40K: 309.3 Bq kg^{-1} %K^{-1}, 238U: 12.35 Bq kg^{-1} ppmU^{-1}, 232Th: 4.057 Bq kg^{-1} ppm Th^{-}).*

	Activity Concentration[a] / Bq kg^{-1}			Equivalent Concentration[b]		
SUTL no.	K	U	Th	K / %	U / ppm	Th / ppm
2914	264 ± 13	26.4 ± 1.6	26.6 ± 1.8	0.85 ± 0.04	2.14 ± 0.13	6.56 ± 0.45
(bulk)	260 ± 9	31.4 ± 1.2	25.2 ± 0.9	0.84 ± 0.03	2.54 ± 0.10	6.20 ± 0.22
2915	245 ± 9	19.9 ± 1.1	20.1 ± 0.9	0.79 ± 0.03	1.61 ± 0.09	4.95 ± 0.21
2917	294 ± 10	41.0 ± 1.5	24.2 ± 0.9	0.95 ± 0.03	3.32 ± 0.12	5.96 ± 0.22
(bulk)	225 ± 9	49.5 ± 1.6	22.0 ± 0.9	0.73 ± 0.03	4.01 ± 0.13	5.43 ± 0.22
2918	313 ± 9	42.1 ± 1.5	27.0 ± 0.9	1.01 ± 0.03	3.41 ± 0.12	6.65 ± 0.22
(bulk)	289 ± 9	61.3 ± 1.9	25.5 ± 0.9	0.93 ± 0.03	4.97 ± 0.15	6.28 ± 0.23
2919	240 ± 8	66.4 ± 1.9	20.8 ± 0.9	0.78 ± 0.03	5.37 ± 0.16	5.13 ± 0.22
(bulk)	268 ± 9	77.8 ± 2.2	25.0 ± 0.9	0.87 ± 0.03	6.30 ± 0.18	6.17 ± 0.23
2921	173 ± 7	31.4 ± 1.3	17.8 ± 0.8	0.56 ± 0.02	2.55 ± 0.10	4.38 ± 0.20
2922	164 ± 8	34.1 ± 1.3	17.4 ± 0.9	0.53 ± 0.02	2.76 ± 0.11	4.28 ± 0.21
2923	140 ± 9	42.0 ± 1.5	17.3 ± 0.9	0.45 ± 0.03	3.41 ± 0.12	4.25 ± 0.22
(bulk)	228 ± 10	41.5 ± 1.6	18.8 ± 0.9	0.74 ± 0.03	3.36 ± 0.13	4.63 ± 0.22
2925	304 ± 9	26.5 ± 1.2	23.0 ± 0.9	0.98 ± 0.03	2.14 ± 0.10	5.66 ± 0.21
2926	342 ± 9	27.7 ± 1.2	25.6 ± 0.9	1.11 ± 0.03	2.24 ± 0.09	6.31 ± 0.21
2927	338 ± 9	28.9 ± 1.2	26.0 ± 0.9	1.09 ± 0.03	2.34 ± 0.10	6.41 ± 0.22
(bulk)	360 ± 11	33.4 ± 1.3	26.8 ± 0.9	1.16 ± 0.04	2.71 ± 0.10	6.60 ± 0.22
2930	92 ± 8	84.4 ± 2.3	14.3 ± 0.8	0.30 ± 0.03	6.84 ± 0.18	3.53 ± 0.21

Table A2.4. *Infinite matrix dose rates determined by HRGS and TSBC ([a]based on dose rate conversion factors in Aikten (1983), Sanderson (1987) and Cresswell* et al. *(2018); [b]average of tube and bulk samples, where available).*

SUTL	HRGS, dry[a] / mGy a^{-1}				
no.	Alpha	Beta	Gamma[b]	TSBC, dry / mGy a^{-1}	FGS, wet / mGy a^{-1}
2914	10.8 ± 0.5	1.21 ± 0.04	0.80 ± 0.03	1.44 ± 0.09	0.31 ± 0.03
2915	8.1 ± 0.3	1.04 ± 0.03	0.63 ± 0.02	1.50 ± 0.09	0.25 ± 0.02
2917	13.6 ± 0.4	1.44 ± 0.03	0.91 ± 0.02	1.75 ± 0.10	0.57 ± 0.05
2918	14.4 ± 0.4	1.53 ± 0.03	1.05 ± 0.03	1.80 ± 0.10	0.48 ± 0.03
2919	16.7 ± 0.5	1.58 ± 0.03	1.16 ± 0.03	1.74 ± 0.10	0.51 ± 0.04
2921	10.3 ± 0.3	0.96 ± 0.03	0.65 ± 0.02	1.12 ± 0.08	0.32 ± 0.02
2922	10.8 ± 0.3	0.96 ± 0.03	0.66 ± 0.02	1.27 ± 0.09	0.39 ± 0.03
2923	12.6 ± 0.4	0.99 ± 0.03	0.76 ± 0.03	1.32 ± 0.09	0.37 ± 0.02
2925	10.1 ± 0.3	1.29 ± 0.03	0.77 ± 0.02	1.71 ± 0.10	0.35 ± 0.02
2926	10.9 ± 0.3	1.43 ± 0.03	0.85 ± 0.02	1.82 ± 0.10	0.36 ± 0.03
2927	11.2 ± 0.3	1.43 ± 0.03	0.90 ± 0.03	1.78 ± 0.10	0.30 ± 0.02
2930	21.6 ± 0.5	1.35 ± 0.03	1.04 ± 0.02	1.35 ± 0.09	0.40 ± 0.01

disc and their combined sets. Dose response curves (shown in Supplement B Figures SB.1–SB.12) for each of the preheating temperature groups and the combined data were determined using a fit to a saturating exponential function. There was no evidence of significant differences in normalized OSL ratios (both in natural and regenerated dose points) between subsets of discs pre-heated at temperatures from 200° to 270° C. Accordingly composite dose response curves from selected discs for each sample were constructed and used to estimate equivalent dose values for each individual discs and their combined sets.

Three average values were calculated from the dose estimates from individual aliquots for each

Table A2.5. *Effective beta and gamma dose rates following water correction ([a] Effective beta dose rate combining water content corrections with inverse grain size attenuation factors obtained by weighting the 90–150[b] µm attenuation factors of Mejdahl (1979) for K, U, and Th by the relative beta dose contributions for each source determined by Gamma Spectrometry; [d] includes a cosmic dose contribution).*

	Water contents / %			Effective Dose Rate[a] / mGy a^{-1}		
SUTL no.	Field	Sat	Assumed	Beta[b]	Gamma	Total[b,d]
2914	26	34	30 ± 5	0.89 ± 0.08	0.46 ± 0.05	1.51 ± 0.09
2915	16	38	30 ± 5	0.86 ± 0.07	0.36 ± 0.03	1.39 ± 0.08
2917	6	18	15 ± 5	1.24 ± 0.10	0.68 ± 0.07	2.09 ± 0.12
2918	6	20	15 ± 5	1.29 ± 0.11	0.69 ± 0.06	2.15 ± 0.12
2919	9	23	15 ± 5	1.28 ± 0.11	0.75 ± 0.07	2.20 ± 0.13
2921	3	21	10 ± 5	0.85 ± 0.08	0.45 ± 0.04	1.47 ± 0.09
2922	4	19	10 ± 5	0.91 ± 0.09	0.49 ± 0.05	1.57 ± 0.10
2923	4	27	10 ± 5	0.94 ± 0.09	0.53 ± 0.05	1.64 ± 0.10
2925	15	24	20 ± 5	1.11 ± 0.10	0.49 ± 0.04	1.78 ± 0.10
2926	16	24	20 ± 5	1.21 ± 0.10	0.53 ± 0.05	1.90 ± 0.11
2927	15	34	20 ± 5	1.19 ± 0.10	0.52 ± 0.04	1.88 ± 0.11
2930	14	20	17 ± 3	1.00 ± 0.08	0.64 ± 0.03	1.81 ± 0.09

Table A2.6. *SAR quality parameters.*

SUTL No.	Sensitivity (c Gy^{-1})	Sensitivity change (% per cycle)	Recycling ratio	Zero cycle	IRSL (%)
2914	5900 ± 750	15 ± 3	1.01 ± 0.01	0.04 ± 0.01	0.22 ± 0.18
2915	5240 ± 530	13 ± 2	1.05 ± 0.01	0.04 ± 0.01	0.00 ± 0.03
2917	188 ± 142	4.5 ± 4.1	0.90 ± 0.05†	0.07 ± 0.02†	0.02 ± 0.44
2918	1750 ± 250	5.0 ± 1.1	1.01 ± 0.05	0.09 ± 0.05	0.06 ± 0.21
2919	900 ± 175	9.2 ± 2.2	0.96 ± 0.06	0.06 ± 0.06	0.40 ± 0.57
2921	2540 ± 1050	8.8 ± 4.8	1.02 ± 0.05	0.10 ± 0.07	0.45 ± 0.23
2922	1700 ± 380	9.6 ± 3.1	1.06 ± 0.12	0.08 ± 0.04	0.42 ± 0.35
2923	470 ± 170	15 ± 8	1.25 ± 0.06†	0.00 ± 0.09	0.84 ± 1.70
2925	11600 ± 2500	8.1 ± 2.2	0.99 ± 0.01	0.04 ± 0.01	-0.02 ± 0.04
2926	7980 ± 940	14 ± 2	0.99 ± 0.01	0.03 ± 0.01	-0.02 ± 0.03
2927	12900 ± 1300	12 ± 2	1.02 ± 0.01	0.03 ± 0.01	-0.01 ± 0.06
2930	4420 ± 650	24 ± 4	0.95 ± 0.01	0.03 ± 0.01	0.12 ± 0.07

† Weighted mean used to reduce influence of low precision aliquots

sample, the mean, a weighted mean and the robust mean. These are given in Table 3.7. Probability density functions (pdfs) and abanico plots were generated to describe the dose distributions. The pdfs are shown in Figures A2.21–A2.25, grouping the samples from each site, with the abanico plots in Supplement C Figures SC.1–SC.12.

For the Ġgantija samples (SUTL2914–2915), Figure A2.21, it can be seen that the pdfs for both samples form approximately Gaussian peaks centred on the mean value, with evidence of a tail to higher doses. There is no significant difference between the different averages, and so the mean was taken as the preferred estimate for the stored dose.

Similarly, for the Skorba samples (SUTL2925–2927) (Fig. A2.24), two of the pdfs have approximately Gaussian shapes whereas SUTL2926 is bimodal. The three different averages are, again, very similar and the slightly higher precision weighted mean has been used as the preferred estimate for the stored dose.

For the samples from Marsalforn (SUTL2917–2919) and Ramla (SUTL2921–2923) (Figs. A2.22 & A2.23), the pdfs are generally complex with very broad distributions and multiple peaks. SUTL2918 and 2923 show approximately Gaussian shapes, with tails to high dose rates. In both cases the weighted mean approximates to the position of the peak with better precision, and has been used as the preferred estimate

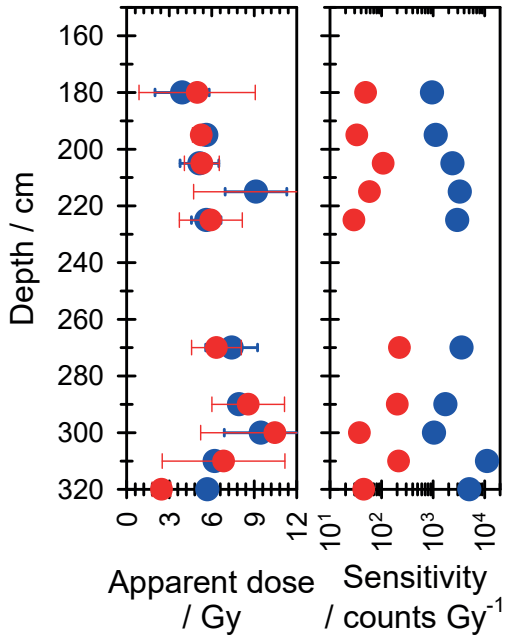

Figure A2.14. *Apparent dose and sensitivity for laboratory OSL (blue) and IRSL (red) profile measurements for SUTL2916 (P1).*

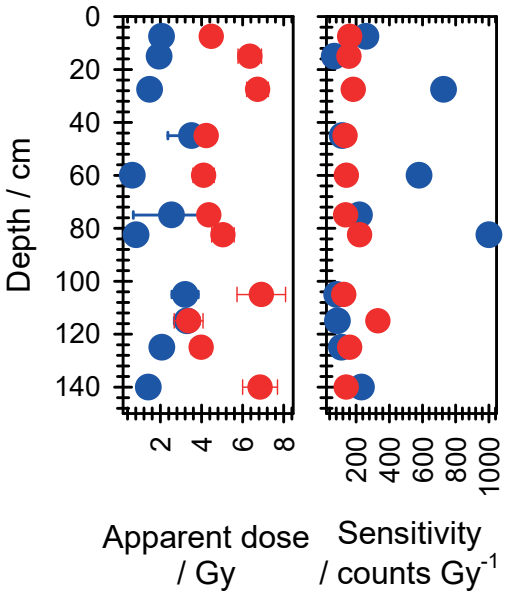

Figure A2.15. *Apparent dose and sensitivity for laboratory OSL (blue) and IRSL (red) profile measurements for SUTL2920 (P2).*

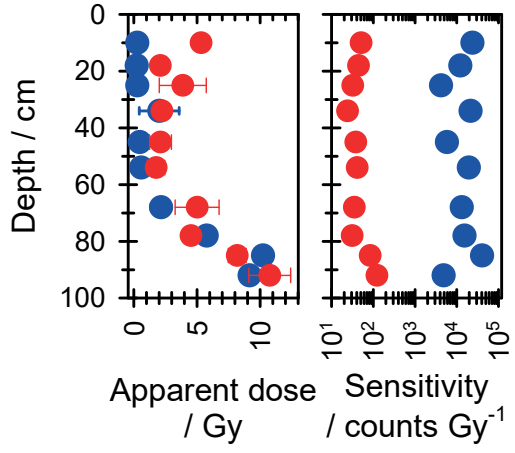

Figure A2.16. *Apparent dose and sensitivity for laboratory OSL (blue) and IRSL (red) profile measurements for SUTL2913 (P3).*

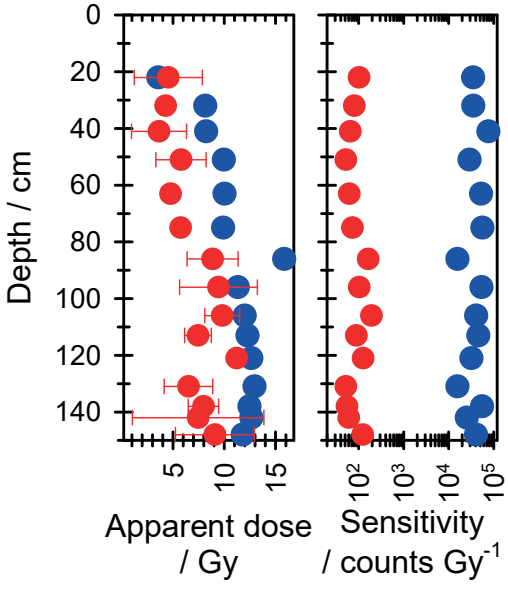

Figure A2.17. *Apparent dose and sensitivity for laboratory OSL (blue) and IRSL (red) profile measurements for SUTL2924 (P4).*

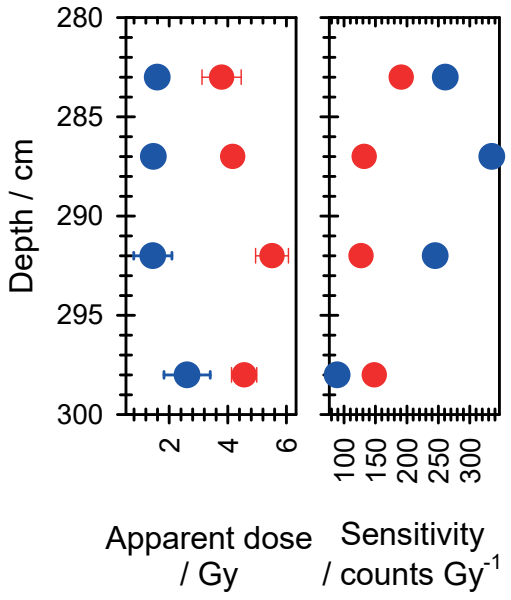

Figure A2.18. *Apparent dose and sensitivity for laboratory OSL (blue) and IRSL (red) profile measurements for SUTL2929 (P5).*

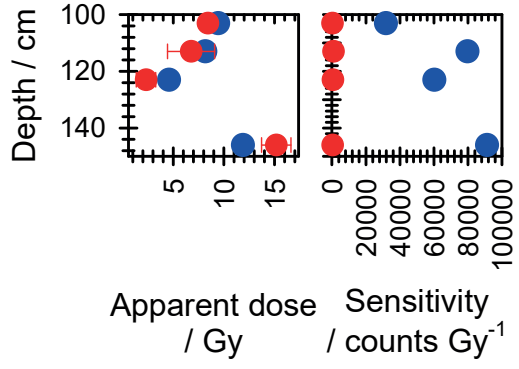

Figure A2.20. *Apparent dose and sensitivity for laboratory OSL (blue) and IRSL (red) profile measurements for SUTL2931 (P7).*

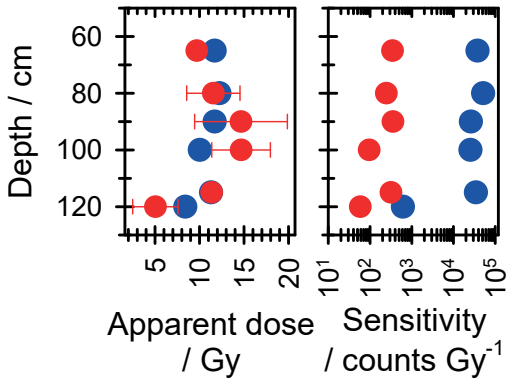

Figure A2.19. *Apparent dose and sensitivity for laboratory OSL (blue) and IRSL (red) profile measurements for SUTL2928 (P6).*

for the stored dose. SUTL2917 shows a very broad peak, with no readily defined preferred stored dose, and the weighted mean has been used since this is generally the preferred value in this project. SUTL2919 shows a lower peak at ~5 Gy which corresponds to a single aliquot, and the mean has been used as the preferred value as this best represents the remaining aliquots. SUTL2921 and 2922 both show multiple peaks, each supported by more than one aliquot. In both cases the weighted mean approximates to the lowest dose peak, and has been preferred.

The sample from Tal-Istabal, Qormi (SUTL2930) (Fig. A2.25), shows a large dominant peak, with two smaller peaks at higher doses. Both the weighted and robust means approximate to the position of this peak, and the slightly higher precision weighted mean has been preferred.

A2.6.3. Age determinations

The total dose rate is determined from the sum of the equivalent beta and gamma dose rates, and the cosmic dose rate. Age estimates are determined by dividing the equivalent stored dose by the dose rate (Table A2.8).

The dose rates for the laboratory profile samples can be estimated by interpolating and extrapolating from the dose rates measured from the OSL samples. This allows an apparent age for the profile samples to be estimated from the apparent doses estimated from the laboratory profile analyses. These are shown in Supplement D Figures SD.1–SD.6.

Table A2.7. *Comments on equivalent dose distributions of SUTL2914 to SUTL2930; preferred estimates in bold (errors stated: ± weighted standard deviation or weighted error).*

SUTL no.	n	Comments on apparent age distribution / individual samples	Mean	Weighted Mean	Robust Mean
2914	8		**4.77 ± 0.25**	4.61 ± 0.13	4.70 ± 0.23
2915	16		**15.0 ± 0.4**	14.7 ± 0.2	15.0 ± 0.4
2917	12	Generally very poor statistics throughout. Dispersed apparent ages	10.8 ± 4.9	**5.8 ± 1.9**	7.3 ± 2.1
2918	16	One significant outlier (67 ± 48 Gy) excluded from means	9.5 ± 1.0	**7.7 ± 0.3**	9.2 ± 0.9
2919	8	One aliquot with Ed = 4.9 ± 0.3 Gy. Remaining aliquots 6.7–10.4 Gy	**7.7 ± 0.6**	6.3 ± 0.2	7.8 ± 0.6
2921	8	Large dispersion of Ed values	1.3 ± 0.7	**0.20 ± 0.02**	0.83 ± 0.34
2922	8		0.48 ± 0.09	**0.26 ± 0.01**	0.52 ± 0.11
2923	8	Large dispersion of Ed values	0.12 ± 0.50	**0.17 ± 0.05**	0.39 ± 0.32
2925	16		17.6 ± 0.4	**17.4 ± 0.2**	17.5 ± 0.5
2926	16	12 aliquots with Ed 17.0–19.6 Gy. 4 aliquots with Ed 21.0–23.0 Gy.	19.6 ± 0.5	**19.2 ± 0.2**	19.6 ± 0.6
2927	16		20.8 ± 0.6	**20.3 ± 0.6**	20.5 ± 0.5
2930	12		0.81 ± 0.08	**0.72 ± 0.02**	0.74 ± 0.04

Table A2.8. *Quartz OSL sediment ages.*

SUTL no.	Dose (Gy)	Dose Rate (mGy a^{-1})	Years / ka	Calendar years
2914	4.77 ± 0.25	1.51 ± 0.09	3.16 ± 0.25	1140±250 BC
2915	15.0 ± 0.4	1.39 ± 0.08	10.79 ± 0.68	8770±680 BC
2917	5.8 ± 1.9	2.09 ± 0.12	2.78 ± 0.92	760±920 BC
2918	7.7 ± 0.3	2.15 ± 0.12	3.58 ± 0.24	1560±240 BC
2919	7.7 ± 0.6	2.20 ± 0.13	3.50 ± 0.34	1480±340 BC
2921	0.20 ± 0.02	1.47 ± 0.09	0.14 ± 0.02	AD 1880±16
2922	0.26 ± 0.01	1.57 ± 0.10	0.17 ± 0.01	AD 1850±12
2923	0.17 ± 0.05	1.64 ± 0.10	0.10 ± 0.03	AD 1910±30
2925	17.4 ± 0.2	1.78 ± 0.10	9.78 ± 0.56	7760±560 BC
2926	19.2 ± 0.2	1.90 ± 0.11	10.11 ± 0.59	8090±590 BC
2927	20.3 ± 0.6	1.88 ± 0.11	10.80 ± 0.71	8780±710 BC
2930	0.72 ± 0.02	1.81 ± 0.09	0.40 ± 0.02	AD 1620±23

A2.7. Discussion

The dates determined from the OSL measurements and their contexts are summarized in Tables A2.8 and A2.9.

A2.7.1. Ġgantija Temple (SUTL2914 and 2915)

The samples were taken from a reopened test pit, initially excavated in 2014, on the western edge of the platform south of Ġgantija temple, which showed agricultural soil build-up over an *in situ* buried soil. Profiling shows low apparent dose (approximately 1 Gy or less, in most cases corresponding to an apparent age of a few centuries) for the agricultural soil, with a significant increase in dose with depth for the buried soil. The samples for OSL dating were taken from immediately below the base of the agricultural soil and the base of the buried soil. For SUTL2914 immediately below the agricultural soil the estimated stored doses and corresponding ages are consistent, and confirms that the agricultural soil is modern, and that the buries soil is prehistoric (older than 1000 BC). The date determined for the onset of the soil accumulation from SUTL2915 (8770±680 BC) is older than the apparent age from the corresponding profile sample (~5000 BC) and both age estimates significantly pre-date Neolithic human activity on the islands, and the initial construction of the Ġgantija temples (3600 BC). The date for the final exposure of the soil (1140±250 BC) is in the Bronze Age,

Table A2.9. *Locations, dates and archaeological significance of sediment samples SUTL2914–2930 (Dates in italics are poorly constrained due to low precision and large dispersion of equivalent doses determined by OSL analysis).*

Sample ID	SUTL no.	Depth /cm	Date	Archaeological significance
Marsalforn valley				
OSL1	2917	175–180	*760±920 BC*	Constrains the final period that the upper incipient soil in hillwash was exposed, phase 2
OSL2	2918	265–270	1560±240 BC	Constrains the final period that the lower incipient soil in hillwash was exposed, phase 1
OSL3	2919	320–330	1480±340 BC	Constrains the onset of hillwash accumulation, phase 1
Ramla valley				
OSL4	2921	15–20	*AD 1880±16*	Provides a temporal constraint on degradation of upper slope
OSL5	2922	62–66	AD 1850±12	Provide temporal constraints on periods of colluviation
OSL6	2923	103–106	*AD 1910±30*	
Ġgantija Temple				
OSL7	2914	78	1140±250 BC	Constrains the final period that the buried soil was exposed
OSL8	2915	92	8770±680 BC	Constrains onset of soil formation
Tal-Istabal, Qormi				
OSL9	2930	295–298	AD 1620±23	Constrains the burial of soil
Skorba Neolithic site				
OSL10	2925	118	7760±560 BC	Constrains the final period that the buried soil was exposed
OSL11	2926	128	8090±590 BC	Constrains the age of the buried land surface
OSL12	2927	145	8780±710 BC	Constrains onset of soil formation

significantly later than the last stages of construction at the temples (2500 BC). However, there is evidence of Bronze Age activity at other Neolithic sites in the islands.

A2.7.2. Ramla and Marsalforn Valleys (SUTL2917–2923)

The Ramla valley, and the tributary Marsalforn valley, form the southern boundary of the Xagħra plateau, on which the Neolithic temple site of Ġgantija is located. It is known that the plateau is largely denuded of Holocene soils, which are concentrated in the valleys. The OSL investigations in these valleys were undertaken with the aim of generating a chronology for the sequences of buried palaeosols, hillwash and alluvial deposits preserved there. The OSL dates for these materials are generally poorly constrained due to poor signal and dispersed stored doses, suggesting considerable re-working of material.

For Marsalforn Valley, the upper-most sample (SUTL2917) could not be dated, with the ages for the lower two samples consistent with being the same age (SUTL2918 1560±240 BC, SUTL2919 1480±340 BC). These are also consistent with the apparent ages from the profile measurements, which suggest a gradual increase in age from approximately 2–3.5 ka over the 180 to 290 cm depth range, with a slight inversion to younger ages below that. The impressions from the field and laboratory profiles that this section represents gradual accumulation of material is not contradicted by the OSL dates for the upper samples given the poor precision of SUTL2917 and the general agreement between OSL ages and profile apparent ages for the lower samples, giving an accumulation rate for the upper part of the section of approximately 1 m ka^{-1}. However, the data suggest that the lower part of the section (290–320 cm depth) accumulated rapidly, with the inverted apparent age profile suggesting better zeroed material being deposited first.

The Ramla Valley dating samples (SUTL2921–2923) are all modern, with OSL dates in the nineteenth and early twentieth centuries AD, based on the youngest component in the dose distributions, although it is noted that these distributions also contain older components and that the apparent ages from the profile samples are significantly older (0.5–2.0 ka, with the best constrained apparent ages at 0.5–1.0 ka). This supports the inference from the field and laboratory profiling that this material was deposited over a short period of time.

A2.7.3. Skorba Neolithic site (SUTL2925–2927)

Excavations on the western edge of the Skorba temple/settlement revealed three curvilinear stone walls of the Neolithic period effectively sealing an accumulated soil. The profile samples indicate a gradual increase in

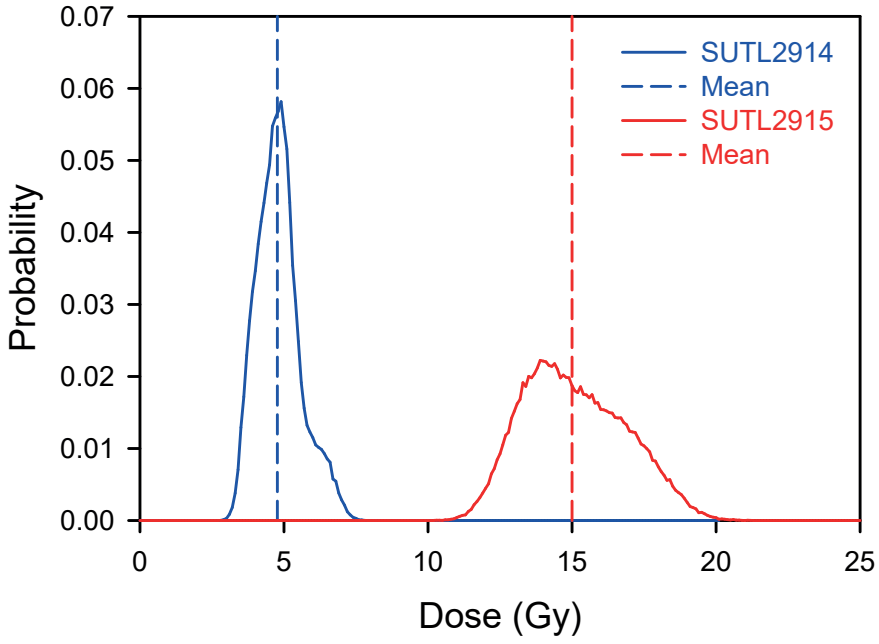

Figure A2.21. *Probability Distribution Functions for the stored dose on samples SUTL2914 and 2915.*

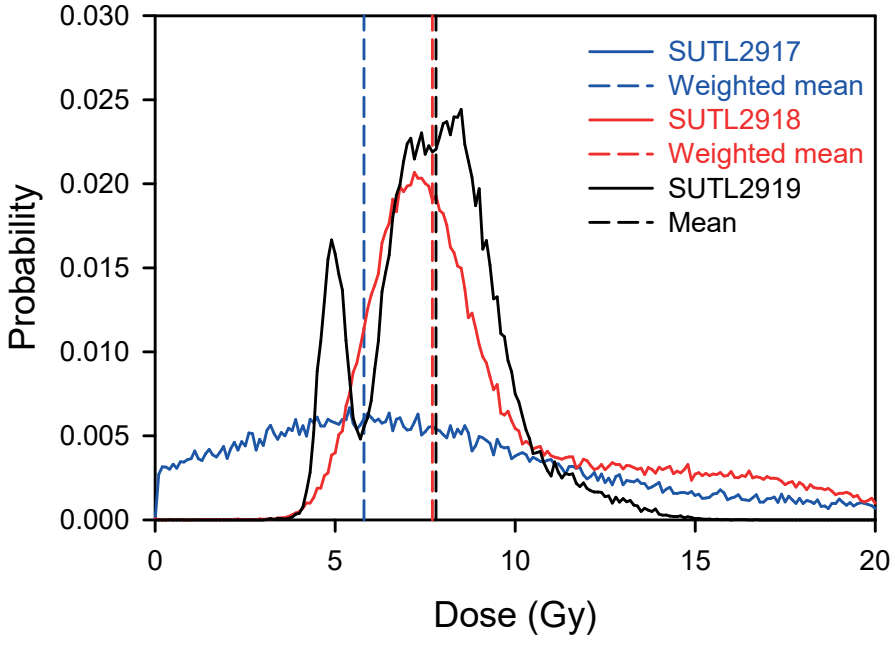

Figure A2.22. *Probability Distribution Functions for the stored dose on samples SUTL2917–2919. Note, SUTL2918 includes a single aliquot with a stored dose of 67 ± 48 Gy.*

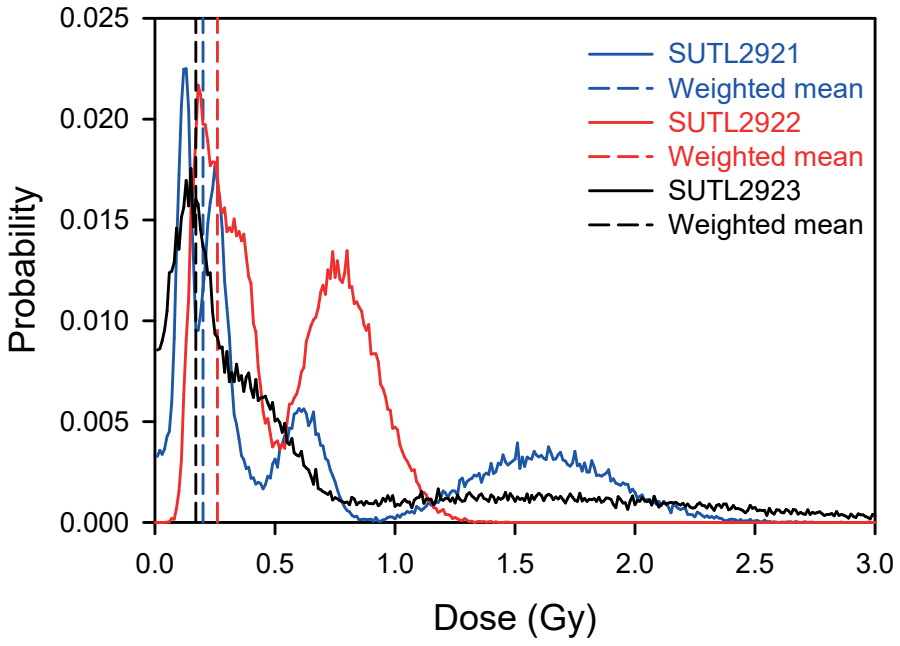

Figure A2.23. *Probability Distribution Functions for the stored dose on samples SUTL2921–2923. Note, SUTL2921 includes a single aliquot with a stored dose of 5.8 ± 0.9 Gy.*

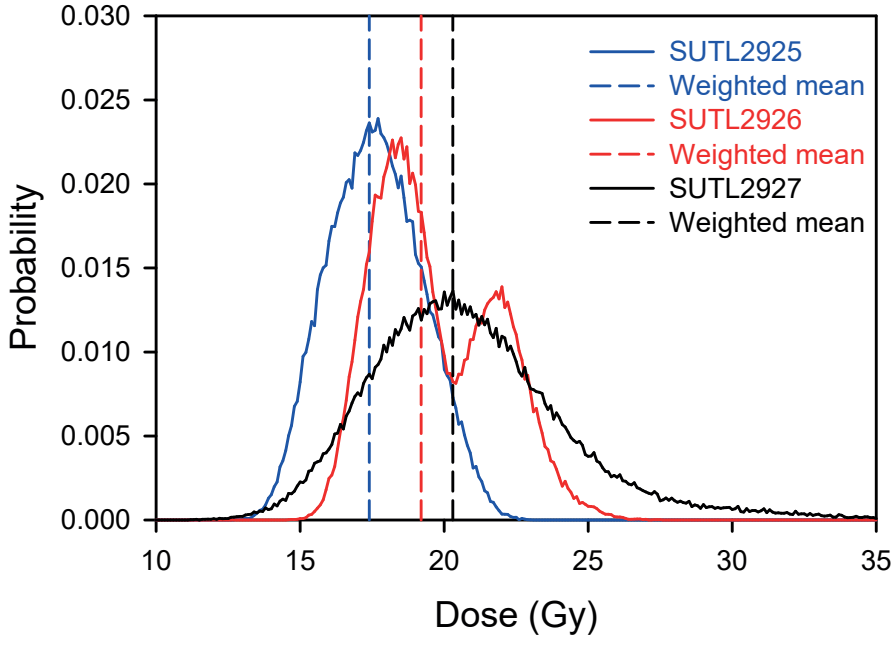

Figure A2.24. *Probability Distribution Functions for the stored dose on samples SUTL2925–2927.*

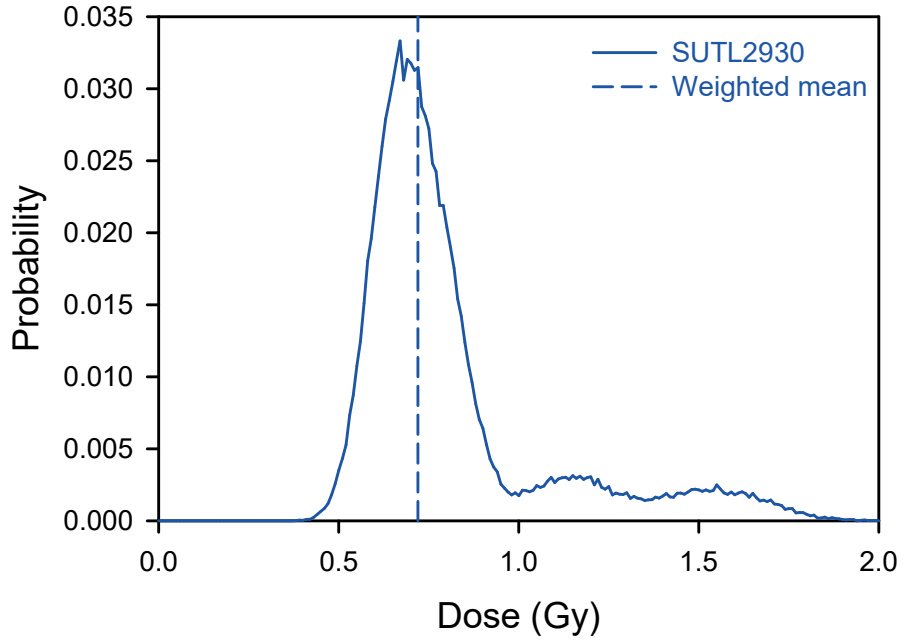

Figure A2.25. *Probability Distribution Function for the stored dose on sample SUTL2930.*

stored dose with depth, with no clear change in stored dose below the Neolithic structure. The profile apparent age estimates show generally very good agreement between equivalent contexts in profiles 4 and 6, with a couple of exceptions. The uppermost profile sample shows an apparent age of approximately 2.0 ka, with the remaining samples showing a gradual increase in apparent age from approximately 5.0 to 7.0 ka down the sections. These are lower than the ages obtained for the OSL dating samples, with a very similar pattern to the bottom sample of profile 3 at the Ġgantija site. The OSL dating samples were selected to constrain the period of accumulation of this soil. The onset of soil accumulation (8780±710 BC) is consistent with the onset of soil accumulation at the Ġgantija site (SUTL2915 8770±680 BC). The upper two samples produce consistent OSL dates (7760±560 BC and 8090±590 BC) which are significantly older than the earliest known human activity in the vicinity (5000 BC) (Trump 1966). These samples are located below the context that had been suggested corresponded to the context at the base of the Trump (1966) excavation.

A2.7.4. Tal-Istabal, Qormi (SUTL2930)

Within excavations of a large Punic-Roman area of terraces and irrigation features *c*. 30–40 cm of agricultural/buried soil was sampled beneath a surviving wall. The laboratory and field profile measurements indicated a slight increase in stored dose with depth below the wall, which is reflected in the apparent age estimates, which carry large uncertainties. The OSL date (AD 1620±23) significantly post-dates the Roman period, lower than the apparent ages from the profiling for the upper three samples (AD 1200±250), which would still result in a post-Roman date. These young ages for material from beneath a surviving Punic-Roman age wall are unexpected.

A2.8. Conclusions

Despite the local limestone geology not supplying abundant quantities of silicates to the soils and sediments at these sites, micromorphological studies had already shown the presence of small quantities of silicate minerals. Both field and laboratory profiling measurements had indicated that these minerals carry measurable luminescence signals, with the OSL signals associated with quartz the most promising for dating. Although the quartz yields from the samples collected for OSL dating were limited the signals from the quartz grains extracted were generally bright, in most cases providing sufficient signal to quantify the

ages of the sampled sediments and soils. It is known that dust from the Sahara has been transported across the Mediterranean, and beyond, for approximately five million years and that this has contributed to the soils on Malta and Gozo. The large signals observed from the quartz grains studied here are similar to those observed from Saharan sand, supporting that source for the silicates measured. This work has demonstrated that even in locations where the local geology is deficient in quartz OSL measurements can be conducted using aeolian quartz from more distant sources. In locations where this primary aeolian mineral input is preserved this should retain a palaeoclimatic signal combining aridity history in the Saharan source regions and wind patterns that move these minerals across the Mediterranean region.

For most of the samples collected from hillwash and alluvial deposits in valleys the equivalent doses showed variations of a factor of two to three between aliquots, reflecting inhomogeneous or partial bleaching of the quartz grains in these samples. This suggests that the erosion and sediment transport processes resulting in these deposits did not expose the minerals to sufficient light to remove all the residual signals from burial in earlier sediments. This could be the result of bulk movement of sediment or the rapid erosion, movement and re-burial of the minerals. Although reliable dates were not always quantifiable, the data do provide information about the processes of formation for these deposits.

For the soils directly associated with the temple sites the equivalent dose values did not show significant dispersion, suggesting that the quartz grains had been well zeroed prior to burial and that there has not been substantial disturbance since then. This allowed ages to be determined even from the small number of aliquots available. This has demonstrated that OSL dating provides valuable information, and should be applied in any further studies of these and similar monuments.

Appendix 2 – Supplement A

Table SA.1. *Field profiling data, as obtained using portable OSL equipment, for the sediment stratigraphies examined on Gozo and Malta.*

Sample no.	IRSL net signal intensities	IRSL depletion ratio	OSL net signal intensities	OSL depletion ratio	IRSL/OSL ratio
P1/1	2178 ± 66	1.26 ± 0.06	35102 ± 194	2.37 ± 0.03	0.0620 ± 0.0019
P1/2	14293 ± 129	1.51 ± 0.03	103206 ± 325	2.12 ± 0.01	0.1385 ± 0.0013
P1/3	4997 ± 86	1.39 ± 0.04	59909 ± 250	1.98 ± 0.02	0.0834 ± 0.0015
P1/4	5290 ± 86	1.54 ± 0.05	73218 ± 275	2.02 ± 0.02	0.0722 ± 0.0012
P1/5	5817 ± 89	1.40 ± 0.04	66796 ± 263	1.91 ± 0.02	0.0871 ± 0.0014
P1/6	4077 ± 80	1.25 ± 0.04	54936 ± 240	2.34 ± 0.02	0.0742 ± 0.0015
P1/7	3935 ± 80	1.34 ± 0.05	46536 ± 222	2.06 ± 0.02	0.0846 ± 0.0018
P1/8	2804 ± 74	1.40 ± 0.06	53609 ± 238	2.43 ± 0.02	0.0523 ± 0.0014
P1/9	3692 ± 77	1.43 ± 0.05	50362 ± 230	2.48 ± 0.02	0.0733 ± 0.0016
P1/10	19162 ± 148	1.73 ± 0.03	81874 ± 291	2.54 ± 0.02	0.2340 ± 0.0020
P2/1	4792 ± 81	1.46 ± 0.05	90499 ± 304	2.79 ± 0.02	0.0530 ± 0.0009
P2/2	2261 ± 66	1.30 ± 0.06	38257 ± 201	2.09 ± 0.02	0.0591 ± 0.0017
P2/3	3511 ± 76	1.54 ± 0.06	21854 ± 155	1.73 ± 0.02	0.1607 ± 0.0036
P2/4	454 ± 49	1.16 ± 0.12	11777 ± 118	1.56 ± 0.03	0.0385 ± 0.0042
P2/5	818 ± 54	1.55 ± 0.12	13389 ± 124	1.66 ± 0.03	0.0611 ± 0.0041
P2/6	1161 ± 55	1.46 ± 0.10	17459 ± 140	2.07 ± 0.03	0.0665 ± 0.0032
P2/7	980 ± 54	1.44 ± 0.11	16591 ± 137	1.43 ± 0.02	0.0591 ± 0.0033
P2/8	1151 ± 55	1.14 ± 0.08	18251 ± 142	1.93 ± 0.03	0.0631 ± 0.0030
P2/9	836 ± 51	1.21 ± 0.10	7448 ± 96	1.64 ± 0.04	0.1122 ± 0.0070
P2/10	659 ± 49	1.16 ± 0.11	11238 ± 115	1.41 ± 0.03	0.0586 ± 0.0044
P2/11	11480 ± 115	1.57 ± 0.03	49486 ± 228	2.09 ± 0.02	0.2320 ± 0.0026
P3/1	359 ± 45	1.76 ± 0.21	12511 ± 119	2.99 ± 0.06	0.0287 ± 0.0036
P3/2	-	-	6605 ± 93	3.28 ± 0.10	
P3/3	-	-	5468 ± 90	3.48 ± 0.12	
P3/4	-	-	7899 ± 98	2.49 ± 0.07	
P3/5	275 ± 42	1.43 ± 0.20	10350 ± 110	3.94 ± 0.10	0.0266 ± 0.0040
P3/6	207 ± 43	1.03 ± 0.14	12783 ± 120	3.07 ± 0.07	0.0162 ± 0.0034
P3/7	245 ± 44	2.89 ± 0.40	12328 ± 119	2.42 ± 0.05	0.0199 ± 0.0036
P3/8	-	-	22897 ± 164	2.50 ± 0.04	
P3/9	1912 ± 62	1.66 ± 0.09	74749 ± 277	2.41 ± 0.02	0.0256 ± 0.0008
P3/10	1967 ± 62	1.44 ± 0.07	80253 ± 287	2.47 ± 0.02	0.0245 ± 0.0008

Table SA.1 *(cont.).*

Sample no.	IRSL net signal intensities	IRSL depletion ratio	OSL net signal intensities	OSL depletion ratio	IRSL/OSL ratio
P4/15	5995 ± 88	1.63 ± 0.05	240349 ± 493	2.46 ± 0.01	0.0249 ± 0.0004
P4/14	5177 ± 87	1.51 ± 0.05	226018 ± 478	2.54 ± 0.01	0.0229 ± 0.0004
P4/13	5712 ± 90	1.41 ± 0.04	211440 ± 462	3.09 ± 0.02	0.0270 ± 0.0004
P4/12	5291 ± 87	1.37 ± 0.04	225233 ± 477	2.50 ± 0.01	0.0235 ± 0.0004
P4/11	5240 ± 88	1.50 ± 0.04	213038 ± 465	2.48 ± 0.01	0.0246 ± 0.0004
P4/10	4344 ± 82	1.42 ± 0.05	184363 ± 432	2.48 ± 0.01	0.0236 ± 0.0004
P4/9	3525 ± 77	1.49 ± 0.06	168705 ± 414	2.43 ± 0.01	0.0209 ± 0.0005
P4/8	2397 ± 73	1.53 ± 0.07	123329 ± 355	2.49 ± 0.02	0.0194 ± 0.0006
P4/7	2331 ± 73	1.52 ± 0.07	114334 ± 342	2.69 ± 0.02	0.0204 ± 0.0006
P4/6	2312 ± 70	1.41 ± 0.06	119908 ± 350	2.56 ± 0.02	0.0193 ± 0.0006
P4/5	1670 ± 70	1.67 ± 0.08	111527 ± 339	2.45 ± 0.02	0.0150 ± 0.0006
P4/4	2896 ± 80	1.47 ± 0.06	138249 ± 376	2.84 ± 0.02	0.0209 ± 0.0006
P4/3	1227 ± 64	1.43 ± 0.08	130444 ± 365	2.61 ± 0.02	0.0094 ± 0.0005
P4/2	1443 ± 65	1.41 ± 0.08	72598 ± 274	2.53 ± 0.02	0.0199 ± 0.0009
P4/1	796 ± 60	1.71 ± 0.12	51567 ± 233	2.84 ± 0.03	0.0154 ± 0.0012
P5/1	422 ± 62	1.20 ± 0.12	12643 ± 125	3.23 ± 0.07	0.0334 ± 0.0049
P5/2	535 ± 60	1.55 ± 0.15	9533 ± 113	3.04 ± 0.08	0.0561 ± 0.0064
P5/3	730 ± 62	1.99 ± 0.18	14463 ± 134	2.69 ± 0.05	0.0505 ± 0.0043
P5/4	502 ± 62	1.64 ± 0.15	15182 ± 135		0.0331 ± 0.0041
P6/1	-	-	133503 ± 377	2.34 ± 0.01	
P6/2	3808 ± 71	1.36 ± 0.05	139097 ± 375	2.25 ± 0.01	0.0274 ± 0.0005
P6/3	-	-	125277 ± 365	2.38 ± 0.01	
P6/4	3547 ± 71	1.29 ± 0.05	125270 ± 357	2.38 ± 0.01	0.0283 ± 0.0006
P6/5	2451 ± 64	1.41 ± 0.06	99668 ± 319	2.19 ± 0.02	0.0246 ± 0.0006
P6/6	4579 ± 79	1.41 ± 0.04	186586 ± 434	2.39 ± 0.01	0.0245 ± 0.0004

Table SA.2. *OSL screening measurements on paired aliquots of 90–250 μm 40% HF-etched 'quartz'.*

SUTL no.	Field ID	Stored dose / Gy		Sensitivity / photon counts Gy^{-1}		/ Gy	/ photon counts Gy^{-1}
		Aliquot 1	Aliquot 2	Aliquot 1	Aliquot 2	Mean	
2916A	P1/1	5.82 ± 0.24	2.00 ± 0.18	1506 ± 39	389 ± 20	3.91 ± 1.91	948 ± 559
2916B	P1/2	5.62 ± 0.25	28.35 ± 1.39	1222 ± 35	1017 ± 32	16.98 ± 11.37	1120 ± 103
2916C	P1/3	3.76 ± 0.47	6.49 ± 0.15	201 ± 14	4550 ± 67	5.13 ± 1.37	2376 ± 2174
2916D	P1/4	6.95 ± 0.25	11.30 ± 0.24	1516 ± 39	5046 ± 71	9.12 ± 2.17	3281 ± 1764
2916E	P1/5	4.57 ± 0.48	6.65 ± 0.13	220 ± 15	5627 ± 75	5.61 ± 1.04	2924 ± 2703
2916F	P1/6	5.58 ± 0.17	9.23 ± 0.21	2764 ± 53	4319 ± 66	7.40 ± 1.83	3541 ± 777
2916G	P1/7	7.83 ± 0.31	8.02 ± 0.26	1354 ± 37	2099 ± 46	7.92 ± 0.24	1726 ± 373
2916H	P1/8	12.02 ± 0.71	6.89 ± 0.31	843 ± 29	1240 ± 35	9.45 ± 2.57	1041 ± 199
2916I	P1/9	5.93 ± 0.11	6.48 ± 0.08	7038 ± 84	15101 ± 123	6.20 ± 0.27	11070 ± 4031
2916J	P1/10	6.35 ± 0.21	5.03 ± 0.09	2390 ± 49	7691 ± 88	5.69 ± 0.66	5040 ± 2650
2920A	P2/1	2.05 ± 0.24		259 ± 16		2.05 ± 0.24	259 ± 16
2920B	P2/2	1.93 ± 0.47		68 ± 8		1.93 ± 0.47	68 ± 8
2920C	P2/3	1.47 ± 0.10		727 ± 27		1.47 ± 0.10	727 ± 27
2920D	P2/4	4.66 ± 1.00	2.35 ± 0.45	85 ± 9	148 ± 12	3.51 ± 1.63	116 ± 45
2920E	P2/5	0.63 ± 0.07		579 ± 24		0.63 ± 0.07	579 ± 24

Table SA.2 *(cont.).*

SUTL no.	Field ID	Stored dose / Gy		Sensitivity / photon counts Gy^{-1}		/ Gy	/ photon counts Gy^{-1}
		Aliquot 1	Aliquot 2	Aliquot 1	Aliquot 2	Mean	
2920F	P2/6	0.68 ± 0.09	4.40 ± 1.11	381 ± 20	59 ± 8	2.54 ± 2.63	220 ± 228
2920G	P2/7	0.81 ± 0.06		1000 ± 32		0.81 ± 0.06	1000 ± 32
2920H	P2/8	3.20 ± 0.64		83 ± 9		3.20 ± 0.64	83 ± 9
2920I	P2/9	3.29 ± 0.61		87 ± 9		3.29 ± 0.61	87 ± 9
2920J	P2/10	2.07 ± 0.40		111 ± 11		2.07 ± 0.40	111 ± 11
2920K	P2/11	1.41 ± 0.22		232 ± 15		1.41 ± 0.22	232 ± 15
2913A	P3/1	0.33 ± 0.01	0.200 ± 0.003	6948 ± 83	40747 ± 202	0.27 ± 0.07	23848 ± 16900
2913B	P3/2	0.167 ± 0.004	0.27 ± 0.01	20089 ± 142	4222 ± 65	0.22 ± 0.05	12156 ± 7933
2913C	P3/3	0.25 ± 0.01	0.28 ± 0.01	4437 ± 67	3944 ± 63	0.27 ± 0.02	4190 ± 247
2913D	P3/4	0.43 ± 0.01	3.59 ± 0.04	24997 ± 158	17770 ± 133	2.01 ± 1.58	21384 ± 3614
2913E	P3/5	0.56 ± 0.02	0.35 ± 0.01	4973 ± 71	6688 ± 82	0.46 ± 0.10	5831 ± 857
2913F	P3/6	0.48 ± 0.01	0.67 ± 0.01	30097 ± 173	8899 ± 94	0.58 ± 0.09	19498 ± 10599
2913G	P3/7	2.94 ± 0.09	1.36 ± 0.02	2885 ± 54	23541 ± 153	2.15 ± 0.79	13213 ± 10328
2913H	P3/8	5.38 ± 0.06	6.13 ± 0.08	17333 ± 132	13410 ± 116	5.76 ± 0.38	15372 ± 1961
2913I	P3/9	10.12 ± 0.08	10.31 ± 0.07	37034 ± 192	43696 ± 209	10.22 ± 0.09	40365 ± 3331
2913J	P3/10	8.53 ± 0.17	9.79 ± 0.24	5952 ± 77	3745 ± 61	9.16 ± 0.63	4849 ± 1103
2929A	P5/1	1.70 ± 0.26	1.48 ± 0.18	236 ± 15	285 ± 17	1.59 ± 0.16	261 ± 35
2929B	P5/2	1.73 ± 0.27	1.19 ± 0.11	181 ± 13	489 ± 22	1.46 ± 0.38	335 ± 218
2929C	P5/3	0.80 ± 0.10	2.09 ± 0.38	369 ± 19	121 ± 11	1.44 ± 0.92	245 ± 176
2929D	P5/4	3.40 ± 0.72	1.82 ± 0.32	70 ± 8	108 ± 10	2.61 ± 1.12	89 ± 27
2928A	P6/1	11.39 ± 0.08	12.01 ± 0.10	41658 ± 204	33686 ± 184	11.70 ± 0.31	37672 ± 3986
2928B	P6/2	11.92 ± 0.11	12.55 ± 0.11	25557 ± 160	77647 ± 279	12.23 ± 0.31	51602 ± 26045
2928C	P6/3	11.52 ± 0.09	11.86 ± 0.15	38308 ± 196	13986 ± 118	11.69 ± 0.17	26147 ± 12161
2928D	P6/4	9.82 ± 0.09	10.24 ± 0.09	23824 ± 154	27373 ± 165	10.03 ± 0.21	25598 ± 1774
2928E	P6/5	11.78 ± 0.08	10.81 ± 0.10	42131 ± 205	26739 ± 164	11.30 ± 0.48	34435 ± 7969
2928F	P6/6	8.38 ± 0.58	8.43 ± 0.58	615 ± 25	612 ± 25	8.40 ± 0.48	613 ± 21
2931A	P7/1	9.14 ± 0.07	9.70 ± 0.10	42722 ± 207	20750 ± 144	9.42 ± 0.28	31736 ± 10986
2931B	P7/2	8.38 ± 0.04	7.93 ± 0.04	83074 ± 288	76168 ± 276	8.16 ± 0.23	79621 ± 3453
2931C	P7/3	4.93 ± 0.04	4.22 ± 0.02	34230 ± 185	86158 ± 294	4.58 ± 0.35	60194 ± 25964
2931D	P7/4	11.84 ± 0.06	11.89 ± 0.05	80656 ± 284	101688 ± 319	11.87 ± 0.05	91172 ± 10516

Table SA.3. *OSL screening measurements on three aliquots of 90–250 μm 40% HF-etched 'quartz' for SUTL2924.*

SUTL no.	Field ID	Stored dose / Gy			Sensitivity / photon counts Gy^{-1}			/ Gy	/ photon counts Gy^{-1}
		Aliquot 1	Aliquot 2	Aliquot 3	Aliquot 1	Aliquot 2	Aliquot 3	Mean	
2924A	P4/1	3.55 ± 0.03	3.59 ± 0.03	3.56 ± 0.03	27174 ± 165	40827 ± 202	36701 ± 192	3.57 ± 0.02	34901 ± 6827
2924B	P4/2	8.13 ± 0.08	8.38 ± 0.06	7.90 ± 0.06	23619 ± 154	46797 ± 216	35381 ± 188	8.14 ± 0.24	35266 ± 11589
2924C	P4/3	8.49 ± 0.04	7.81 ± 0.05	8.38 ± 0.05	111907 ± 335	57758 ± 240	58463 ± 242	8.23 ± 0.34	76042 ± 27074
2924D	P4/4	10.27 ± 0.09	10.23 ± 0.08	9.36 ± 0.09	25766 ± 161	39058 ± 198	22088 ± 149	9.96 ± 0.45	28971 ± 8485
2924E	P4/5	10.09 ± 0.08	9.74 ± 0.06	10.24 ± 0.06	30295 ± 174	55414 ± 235	70989 ± 266	10.02 ± 0.25	52233 ± 20347
2924F	P4/6	10.00 ± 0.06	9.26 ± 0.06	10.41 ± 0.06	58387 ± 242	47008 ± 217	62521 ± 250	9.89 ± 0.57	55972 ± 7756
2924G	P4/7	15.84 ± 0.19	5.04 ± 0.81	4.64 ± 0.74	15685 ± 125			8.51 ± 5.60	15685 ± 125
2924H	P4/8	11.14 ± 0.07	10.93 ± 0.07	11.91 ± 0.08	55414 ± 235	54789 ± 234	49922 ± 223	11.32 ± 0.49	53375 ± 2746
2924I	P4/9	12.42 ± 0.09	10.99 ± 0.11	12.56 ± 0.08	40395 ± 201	23165 ± 152	58415 ± 242	11.99 ± 0.79	40658 ± 17625
2924J	P4/10	11.78 ± 0.09	12.48 ± 0.09	12.50 ± 0.08	39231 ± 198	43100 ± 208	54282 ± 233	12.26 ± 0.36	45538 ± 7526
2924K	P4/11	12.24 ± 0.10	12.67 ± 0.08	12.99 ± 0.17	29496 ± 172	54219 ± 233	12411 ± 111	12.63 ± 0.38	32042 ± 20904
2924L	P4/12	12.72 ± 0.11	13.16 ± 0.31	4.72 ± 0.80	27041 ± 164	4188 ± 65		10.20 ± 4.22	15615 ± 11426
2924M	P4/13	13.28 ± 0.09	11.89 ± 0.06	12.19 ± 0.10	49639 ± 223	81273 ± 285	34906 ± 187	12.46 ± 0.69	55273 ± 23183
2924N	P4/14	13.05 ± 0.09	12.44 ± 0.17	12.41 ± 0.12	40900 ± 202	11550 ± 107	23300 ± 153	12.63 ± 0.32	25250 ± 14675
2924O	P4/15	12.02 ± 0.25	12.15 ± 0.06	11.25 ± 0.09	5366 ± 73	86947 ± 295	29330 ± 171	11.80 ± 0.45	40548 ± 40790

Table SA.4. *IRSL screening measurements on paired aliquots of 90–250 μm 15% HF-etched 'polymineral' for SUTL2924.*

SUTL no.	Field ID	Stored dose / Gy		Sensitivity / photon counts Gy^{-1}		/ Gy	/ photon counts Gy^{-1}
		Aliquot 1	Aliquot 2	Aliquot 1	Aliquot 2	Mean	
2916A	P1/1	0.87 ± 0.20	9.07 ± 2.99	72 ± 8	26 ± 5	4.97 ± 4.10	49 ± 23
2916B	P1/2	5.87 ± 1.77	4.64 ± 1.29	34 ± 6	32 ± 6	5.26 ± 0.62	33 ± 6
2916C	P1/3	6.53 ± 1.42	4.07 ± 0.63	67 ± 8	147 ± 12	5.30 ± 1.23	107 ± 40
2916D	P1/4	4.72 ± 0.80	99.38 ± 28.49	94 ± 10	23 ± 5	52.05 ± 47.33	58 ± 36
2916E	P1/5	8.15 ± 2.25	3.71 ± 1.12	31 ± 6	27 ± 5	5.93 ± 2.22	29 ± 4
2916F	P1/6	4.58 ± 1.65	8.08 ± 0.76	27 ± 5	416 ± 20	6.33 ± 1.75	222 ± 194
2916G	P1/7	11.14 ± 3.64	6.01 ± 0.56	25 ± 5	376 ± 19	8.57 ± 2.56	201 ± 176
2916H	P1/8	15.68 ± 3.60	5.21 ± 1.50	47 ± 7	27 ± 5	10.45 ± 5.23	37 ± 10
2916I	P1/9	11.16 ± 1.20	2.51 ± 0.50	348 ± 19	80 ± 9	6.83 ± 4.33	214 ± 134
2916J	P1/10	3.12 ± 1.06	1.79 ± 0.54	45 ± 7	44 ± 7	2.45 ± 0.66	45 ± 6
2920A	P2/1	4.32 ± 0.53	4.61 ± 0.61	171 ± 13	150 ± 12	4.47 ± 0.20	161 ± 14
2920B	P2/2	5.78 ± 0.65	6.92 ± 0.93	178 ± 13	133 ± 12	6.35 ± 0.80	156 ± 32
2920C	P2/3	7.26 ± 0.84	6.21 ± 0.70	181 ± 13	182 ± 13	6.73 ± 0.75	182 ± 9
2920D	P2/4	3.80 ± 0.50	4.66 ± 0.63	139 ± 12	127 ± 11	4.23 ± 0.60	133 ± 9
2920E	P2/5	3.58 ± 0.51	4.61 ± 0.67	145 ± 12	137 ± 12	4.10 ± 0.73	141 ± 6
2920F	P2/6	4.54 ± 0.59	4.15 ± 0.55	138 ± 12	134 ± 12	4.35 ± 0.28	136 ± 3
2920G	P2/7	5.04 ± 0.55		221 ± 15		5.04 ± 0.55	221 ± 15
2920H	P2/8	8.09 ± 1.12	5.74 ± 0.76	116 ± 11	134 ± 12	6.91 ± 1.67	125 ± 13
2920I	P2/9	2.67 ± 0.28	4.08 ± 0.34	227 ± 15	434 ± 21	3.37 ± 1.00	331 ± 146
2920J	P2/10	3.98 ± 0.48		161 ± 13		3.98 ± 0.48	161 ± 13
2920K	P2/11	6.85 ± 0.85		140 ± 12		6.85 ± 0.85	140 ± 12
2913A	P3/1	5.68 ± 1.68	4.96 ± 1.61	59 ± 8	43 ± 7	5.32 ± 0.36	51 ± 8
2913B	P3/2	2.49 ± 0.77	1.69 ± 0.55	43 ± 7	45 ± 7	2.09 ± 0.40	44 ± 1

Table SA.4 *(cont.).*

SUTL no.	Field ID	Stored dose / Gy		Sensitivity / photon counts Gy^{-1}		/ Gy	/ photon counts Gy^{-1}
		Aliquot 1	Aliquot 2	Aliquot 1	Aliquot 2	Mean	
2913C	P3/3	2.01 ± 0.66	5.74 ± 2.07	42 ± 6	22 ± 5	3.87 ± 1.86	32 ± 10
2913D	P3/4	1.88 ± 0.79	2.55 ± 0.90	23 ± 5	25 ± 5	2.22 ± 0.33	24 ± 1
2913E	P3/5	1.25 ± 0.45	2.97 ± 0.80	42 ± 6	35 ± 6	2.11 ± 0.86	38 ± 3
2913F	P3/6	1.07 ± 0.42	2.44 ± 0.58	41 ± 6	41 ± 6	1.76 ± 0.69	41 ± 5
2913G	P3/7	3.27 ± 0.99	6.75 ± 2.13	44 ± 7	26 ± 5	5.01 ± 1.74	35 ± 9
2913H	P3/8	4.40 ± 1.87	4.65 ± 1.16	19 ± 4	43 ± 7	4.52 ± 1.29	31 ± 12
2913I	P3/9	7.47 ± 1.36	8.89 ± 1.74	112 ± 11	55 ± 7	8.18 ± 0.71	84 ± 29
2913J	P3/10	12.41 ± 2.12	9.11 ± 1.74	183 ± 14	62 ± 8	10.76 ± 1.65	122 ± 60
2929A	P5/1	3.12 ± 0.38	4.47 ± 0.51	188 ± 14	195 ± 14	3.79 ± 0.95	191 ± 5
2929B	P5/2	4.05 ± 0.54	4.29 ± 0.59	136 ± 12	128 ± 11	4.17 ± 0.17	132 ± 6
2929C	P5/3	4.94 ± 0.70	6.07 ± 0.83	132 ± 12	122 ± 11	5.51 ± 0.80	127 ± 7
2929D	P5/4	4.13 ± 0.51	4.99 ± 0.70	162 ± 13	135 ± 12	4.56 ± 0.61	148 ± 19
2928A	P6/1	9.65 ± 1.19	9.72 ± 0.79	263 ± 16	427 ± 21	9.69 ± 0.87	345 ± 82
2928B	P6/2	8.55 ± 0.86	14.55 ± 0.86	340 ± 18	151 ± 12	11.55 ± 3.00	245 ± 94
2928C	P6/3	19.88 ± 1.56	9.45 ± 1.13	510 ± 23	199 ± 14	14.66 ± 5.21	355 ± 156
2928D	P6/4	17.96 ± 2.82	11.37 ± 3.94	145 ± 12	44 ± 7	14.67 ± 3.30	95 ± 50
2928E	P6/5	12.19 ± 1.35	10.50 ± 0.98	298 ± 17	339 ± 18	11.35 ± 0.85	318 ± 20
2928F	P6/6	2.49 ± 0.58	7.59 ± 1.64	44 ± 8	72 ± 8	5.04 ± 2.55	58 ± 14
2931A	P7/1	8.30 ± 0.91	8.54 ± 0.94	281 ± 17	310 ± 18	8.42 ± 0.77	296 ± 15
2931B	P7/2	9.08 ± 0.39	4.45 ± 0.43	1474 ± 38	356 ± 19	6.76 ± 2.32	915 ± 559
2931C	P7/3	3.27 ± 0.21	1.34 ± 0.18	805 ± 28	285 ± 17	2.31 ± 0.96	545 ± 260
2931D	P7/4	16.61 ± 1.04	13.72 ± 1.81	668 ± 26	159 ± 13	15.17 ± 1.45	413 ± 255

Table SA.5. *IRSL screening measurements on three aliquots of 90–250 μm 15% HF-etched 'polymineral' for SUTL2924.*

SUTL no.	Field ID	Stored dose / Gy			Sensitivity / photon counts Gy^{-1}			/ Gy	/ photon counts Gy^{-1}
		Aliquot 1	Aliquot 2	Aliquot 3	Aliquot 1	Aliquot 2	Aliquot 3	Mean	
2924A	P4/1	7.69 ± 0.88	1.04 ± 0.11	4.89 ± 0.54	60 ± 8	179 ± 13	66 ± 8	4.54 ± 3.32	102 ± 59
2924B	P4/2	4.69 ± 0.29	4.46 ± 0.36	3.70 ± 0.49	124 ± 11	74 ± 9	42 ± 7	4.28 ± 0.49	80 ± 41
2924C	P4/3	7.00 ± 0.35	2.28 ± 0.47	1.65 ± 0.31	141 ± 12	25 ± 5	29 ± 5	3.64 ± 2.68	65 ± 58
2924D	P4/4	7.76 ± 0.83	6.72 ± 0.60	2.85 ± 0.33	49 ± 7	60 ± 8	47 ± 7	5.78 ± 2.45	52 ± 6
2924E	P4/5	5.20 ± 0.39	4.66 ± 0.48	4.43 ± 0.47	78 ± 9	54 ± 7	54 ± 7	4.76 ± 0.39	62 ± 12
2924F	P4/6	6.38 ± 0.44	5.74 ± 0.67	5.10 ± 0.38	90 ± 10	46 ± 7	82 ± 9	5.74 ± 0.64	73 ± 22
2924G	P4/7	10.84 ± 0.49	9.87 ± 0.55	5.86 ± 0.68	163 ± 13	82 ± 9	163 ± 13	8.86 ± 2.49	136 ± 41
2924H	P4/8	12.01 ± 0.58	4.44 ± 1.02	11.84 ± 0.58	149 ± 12	21 ± 5	139 ± 12	9.43 ± 3.79	103 ± 64
2924I	P4/9	7.85 ± 0.52	10.28 ± 0.61	11.26 ± 0.31	92 ± 10	109 ± 10	379 ± 19	9.80 ± 1.70	193 ± 144
2924J	P4/10	6.16 ± 0.52	8.77 ± 0.42	7.40 ± 0.72	64 ± 8	149 ± 12	54 ± 7	7.44 ± 1.30	89 ± 47
2924K	P4/11	10.86 ± 0.57	12.04 ± 0.74	10.71 ± 0.53	132 ± 11	106 ± 10	140 ± 12	11.20 ± 0.67	126 ± 17
2924L	P4/12	8.98 ± 0.99	4.26 ± 0.40	6.29 ± 0.41	46 ± 7	59 ± 8	46 ± 7	6.51 ± 2.36	50 ± 6
2924M	P4/13	9.90 ± 0.80	7.08 ± 0.88	6.95 ± 0.66	67 ± 8	39 ± 6	58 ± 8	7.97 ± 1.48	55 ± 14
2924N	P4/14	14.74 ± 0.91	5.71 ± 0.54	1.91 ± 0.43	101 ± 10	58 ± 8	21 ± 5	7.45 ± 6.41	60 ± 40
2924O	P4/15	11.86 ± 0.97	4.17 ± 0.27	11.24 ± 0.43	68 ± 8	98 ± 10	204 ± 14	9.09 ± 3.85	123 ± 68

Appendix 2 – Supplement B

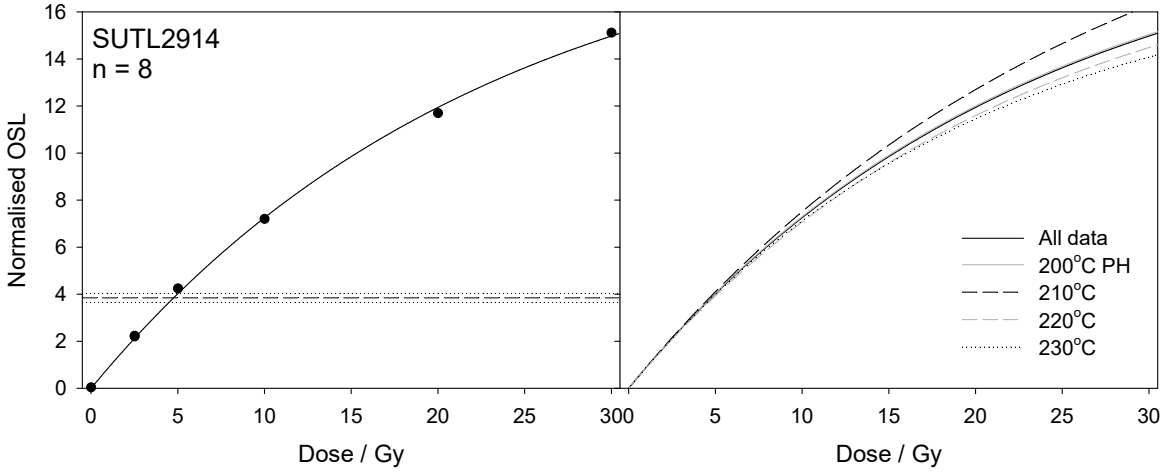

Figure SB.1. *Dose response curves for SUTL2914, showing the mean of all groups (left) with the fitted saturating exponential function and mean normalized natural signal, and the exponential functions for the different preheat groups (right).*

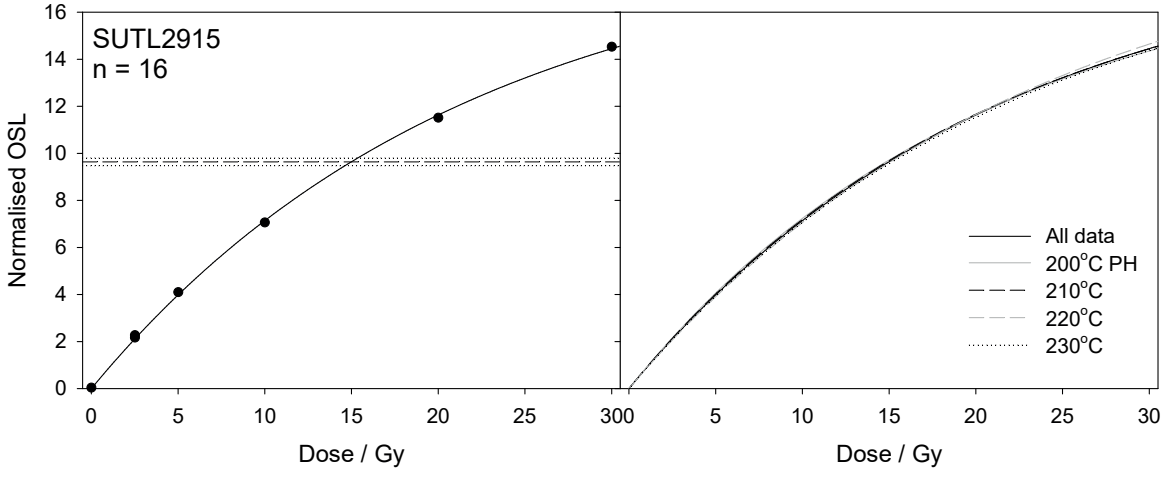

Figure SB.2. *Dose response curves for SUTL2915, showing the mean of all groups (left) with the fitted saturating exponential function and mean normalized natural signal, and the exponential functions for the different preheat groups (right).*

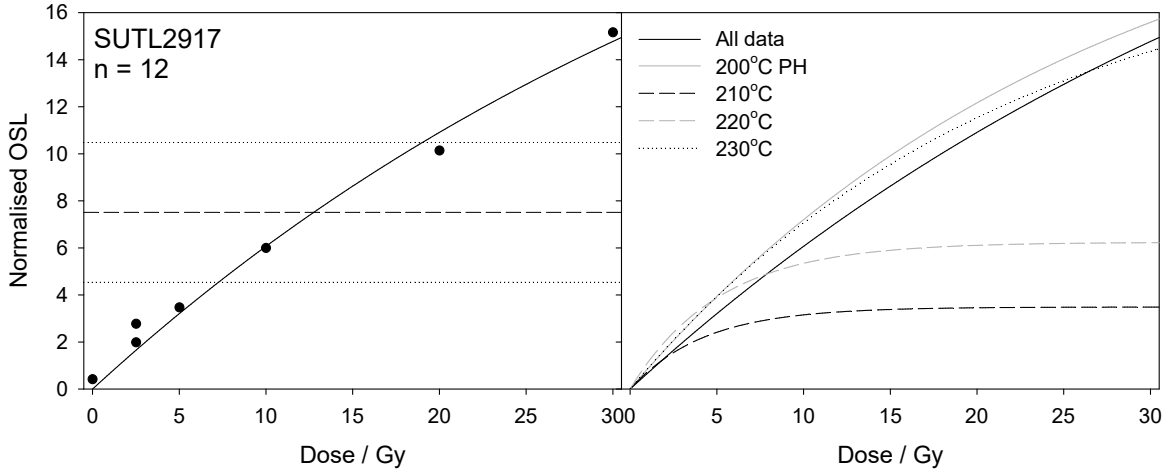

Figure SB.3. *Dose response curves for SUTL2917, showing the mean of all groups (left) with the fitted saturating exponential function and mean normalized natural signal, and the exponential functions for the different preheat groups (right).*

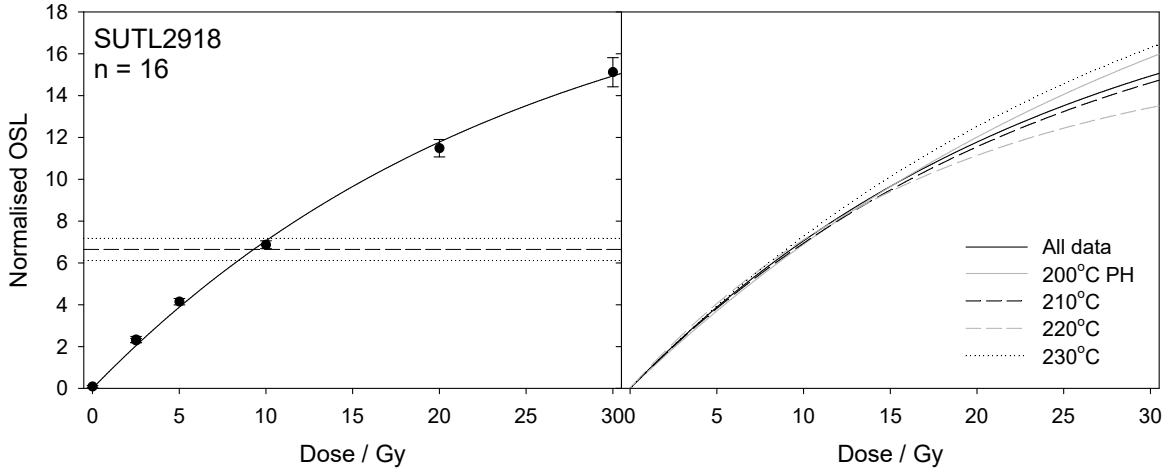

Figure SB.4. *Dose response curves for SUTL2918, showing the mean of all groups (left) with the fitted saturating exponential function and mean normalized natural signal, and the exponential functions for the different preheat groups (right).*

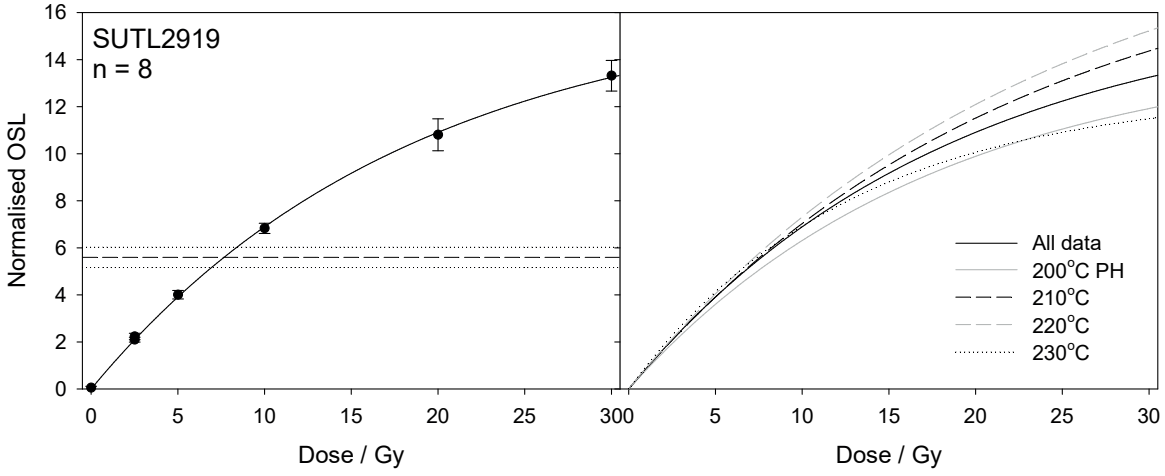

Figure SB.5. *Dose response curves for SUTL2919, showing the mean of all groups (left) with the fitted saturating exponential function and mean normalized natural signal, and the exponential functions for the different preheat groups (right).*

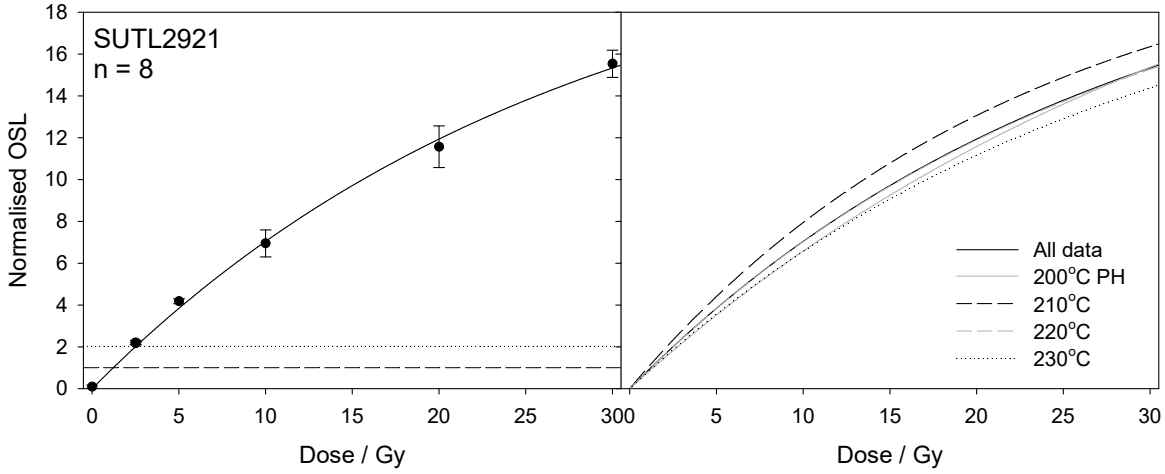

Figure SB.6. *Dose response curves for SUTL2921, showing the mean of all groups (left) with the fitted saturating exponential function and mean normalized natural signal, and the exponential functions for the different preheat groups (right).*

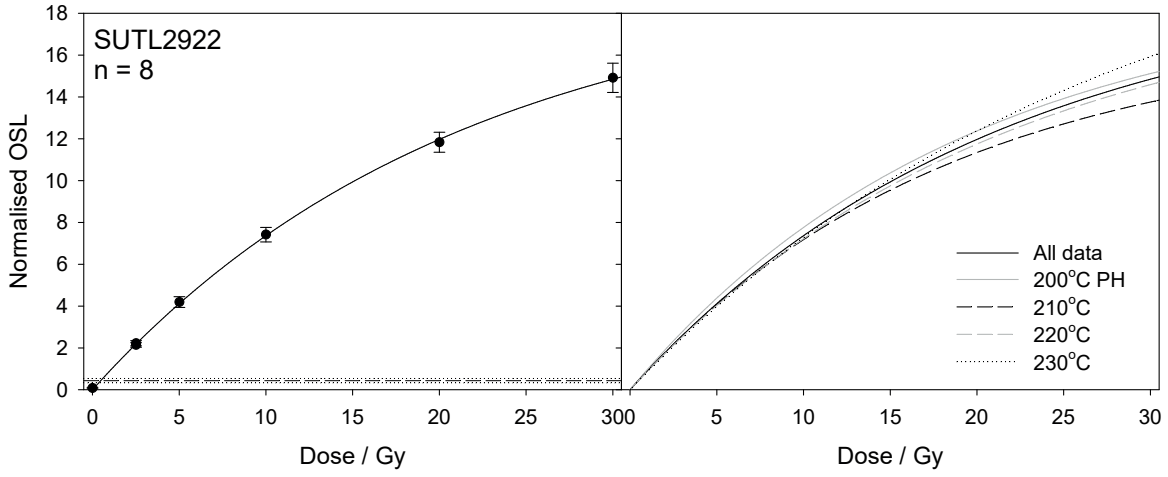

Figure SB.7. *Dose response curves for SUTL2922, showing the mean of all groups (left) with the fitted saturating exponential function and mean normalized natural signal, and the exponential functions for the different preheat groups (right).*

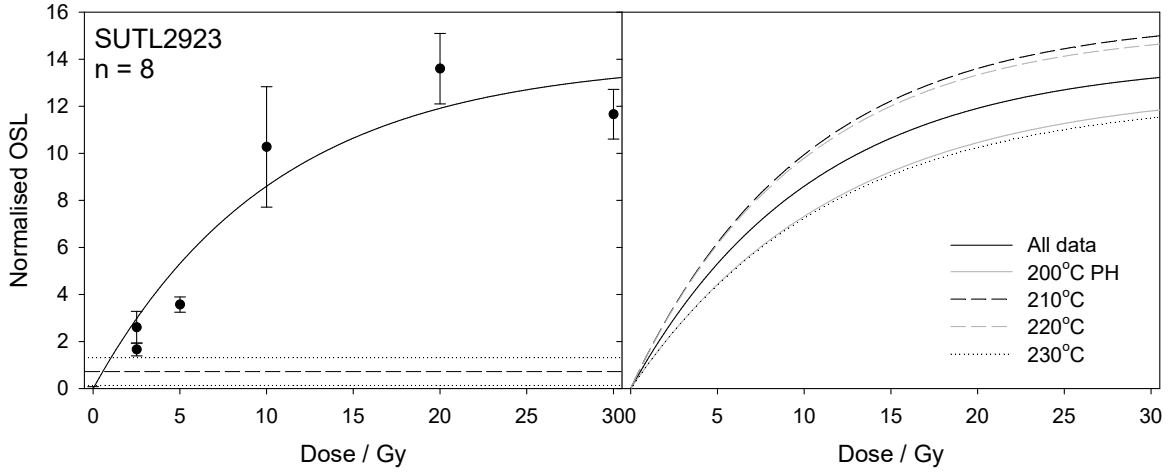

Figure SB.8. *Dose response curves for SUTL2923, showing the mean of all groups (left) with the fitted saturating exponential function and mean normalized natural signal, and the exponential functions for the different preheat groups (right).*

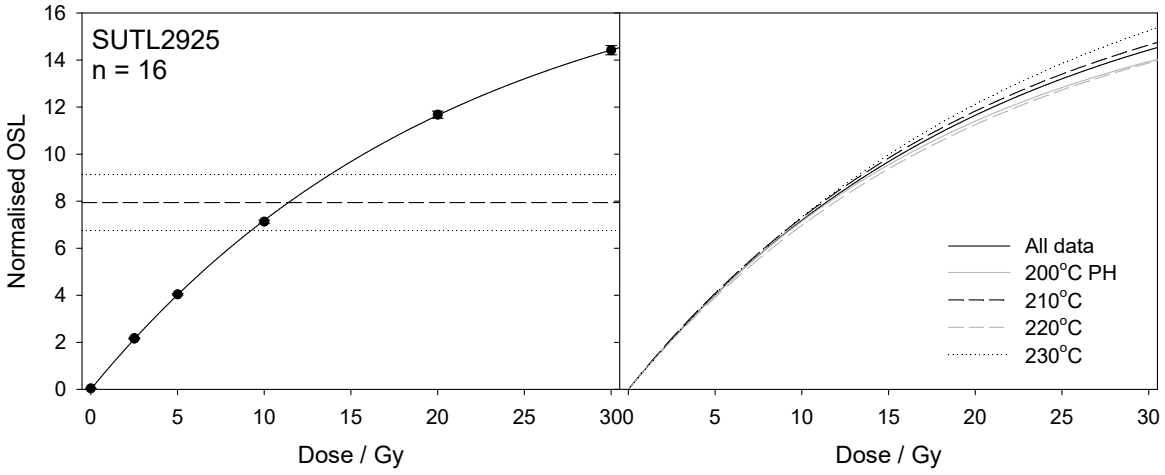

Figure SB.9. *Dose response curves for SUTL2925, showing the mean of all groups (left) with the fitted saturating exponential function and mean normalized natural signal, and the exponential functions for the different preheat groups (right).*

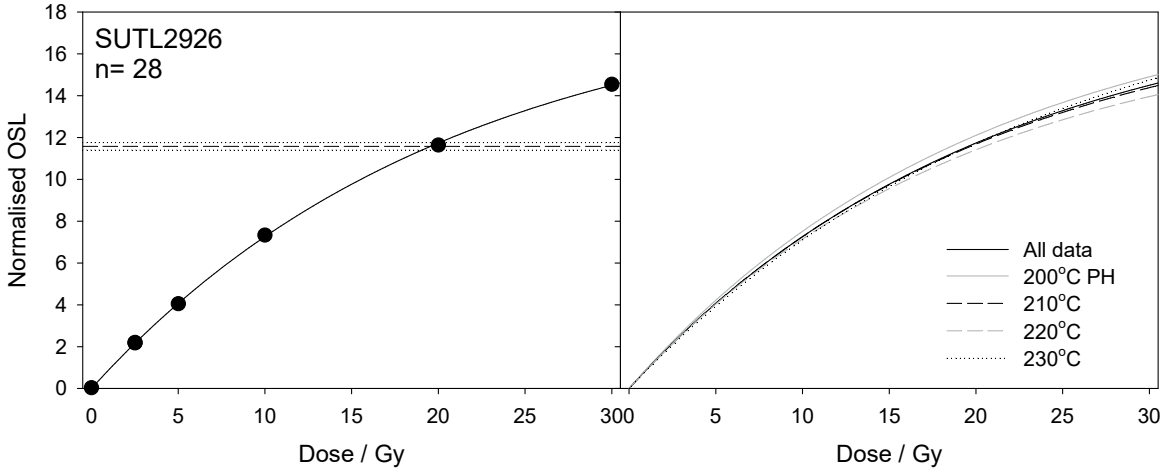

Figure SB.10. *Dose response curves for SUTL2926, showing the mean of all groups (left) with the fitted saturating exponential function and mean normalized natural signal, and the exponential functions for the different preheat groups (right).*

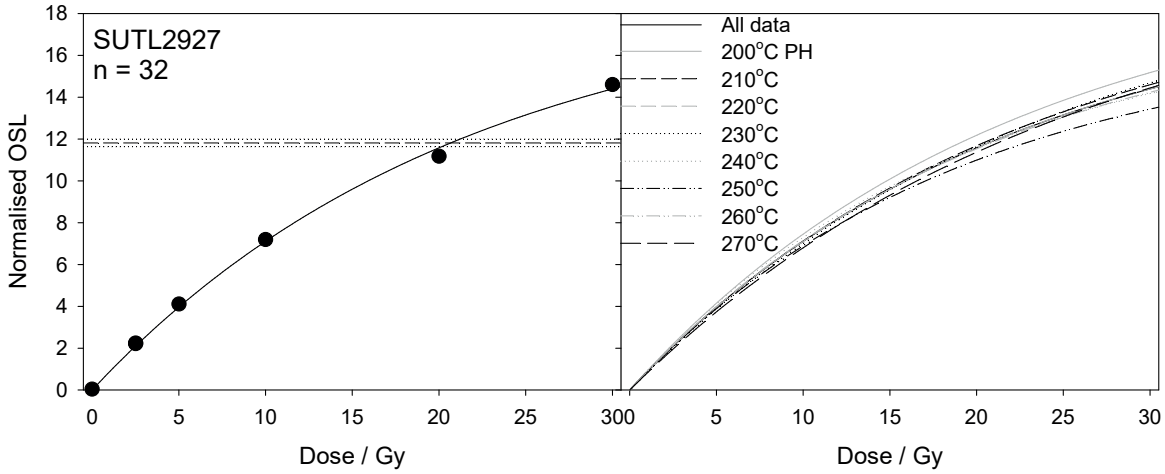

Figure SB.11. *Dose response curves for SUTL2927, showing the mean of all groups (left) with the fitted saturating exponential function and mean normalized natural signal, and the exponential functions for the different preheat groups (right).*

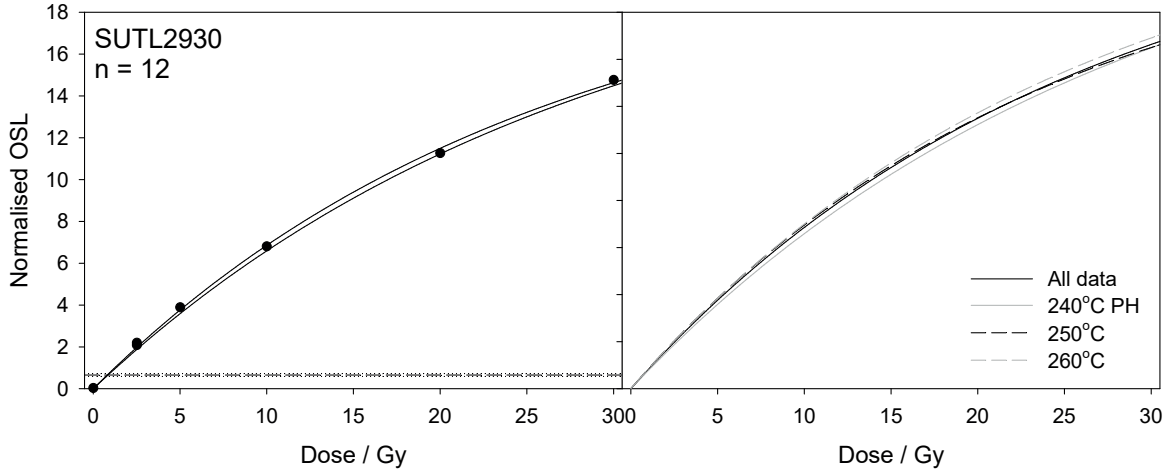

Figure SB.12. *Dose response curves for SUTL2930, showing the mean of all groups (left) with the fitted saturating exponential function and mean normalized natural signal, and the exponential functions for the different preheat groups (right).*

Appendix 2 – Supplement C

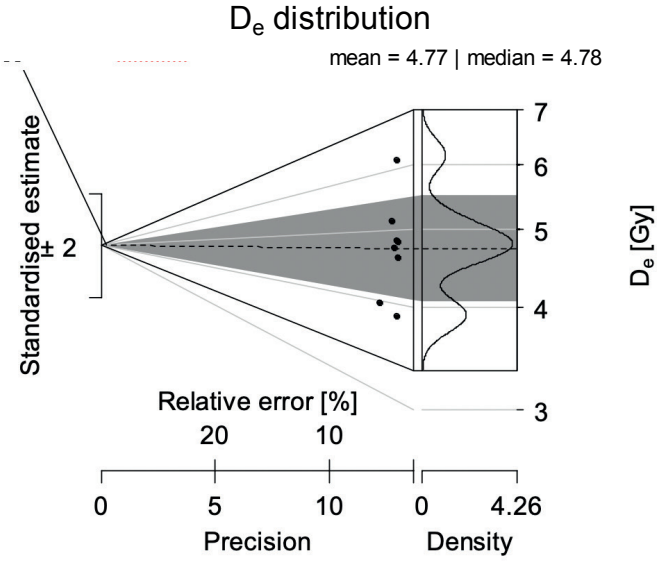

Figure SC.1. *Abanico plot for SUTL2914.*

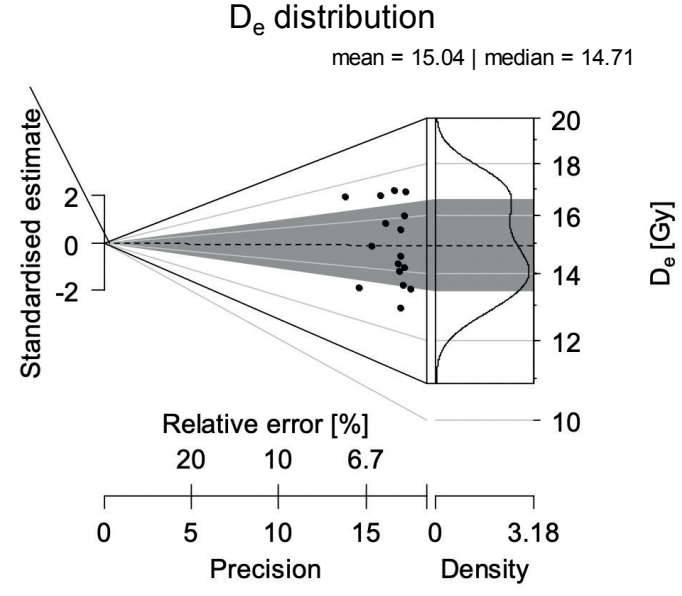

Figure SC.2. *Abanico plot for SUTL2915.*

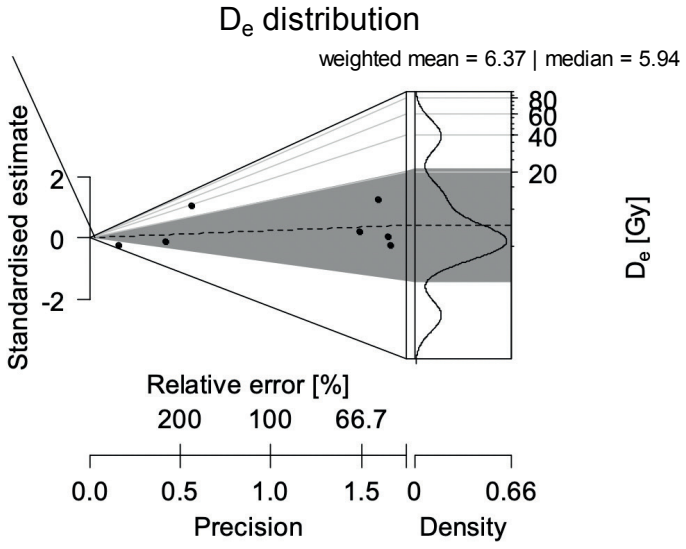

Figure SC.3. *Abanico plot for SUTL2917.*

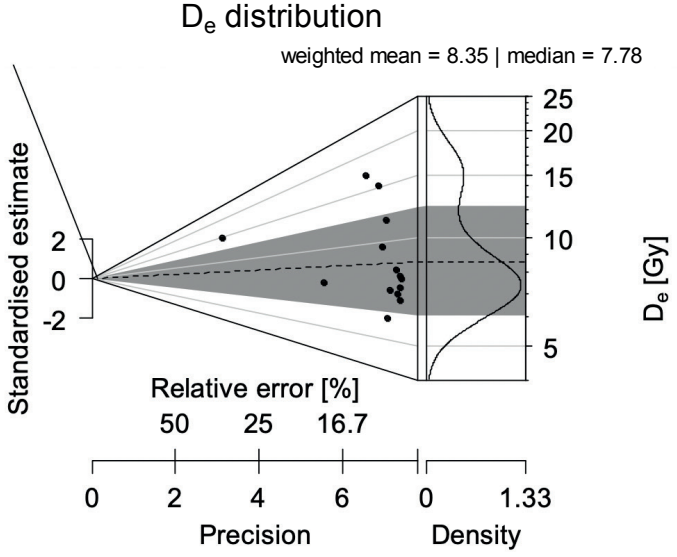

Figure SC.4. *Abanico plot for SUTL2918.*

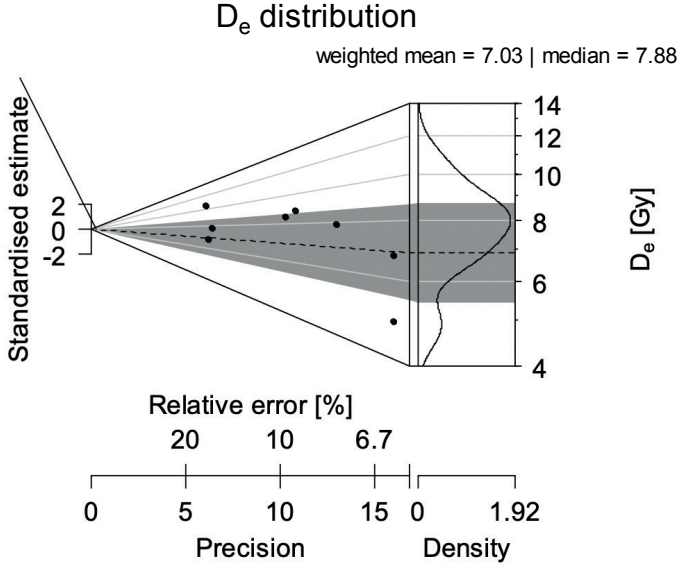

Figure SC.5. *Abanico plot for SUTL2919.*

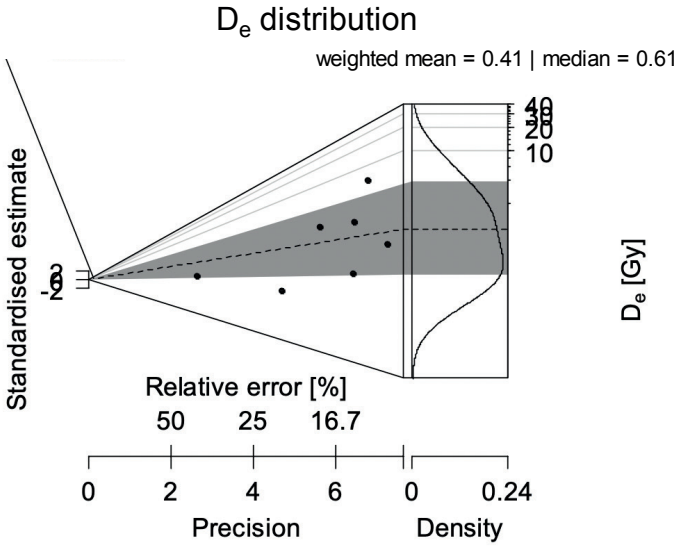

Figure SC.6. *Abanico plot for SUTL2921 (note: data point for -0.032 ± 0.136 Gy excluded).*

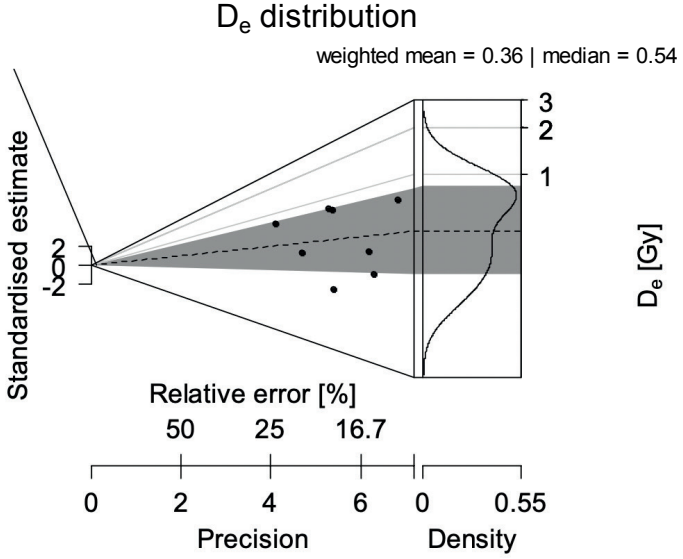

Figure SC.7. *Abanico plot for SUTL2922.*

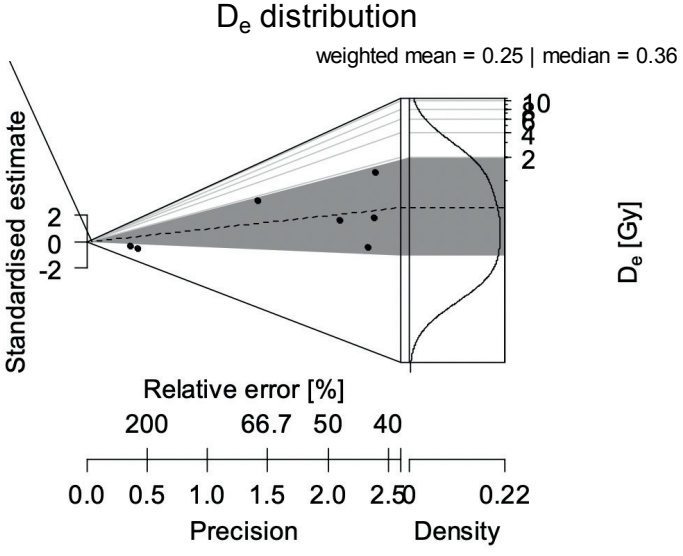

Figure SC.8. *Abanico plot for SUTL2923 (note: data point for -3.03 ± 3.53 Gy excluded).*

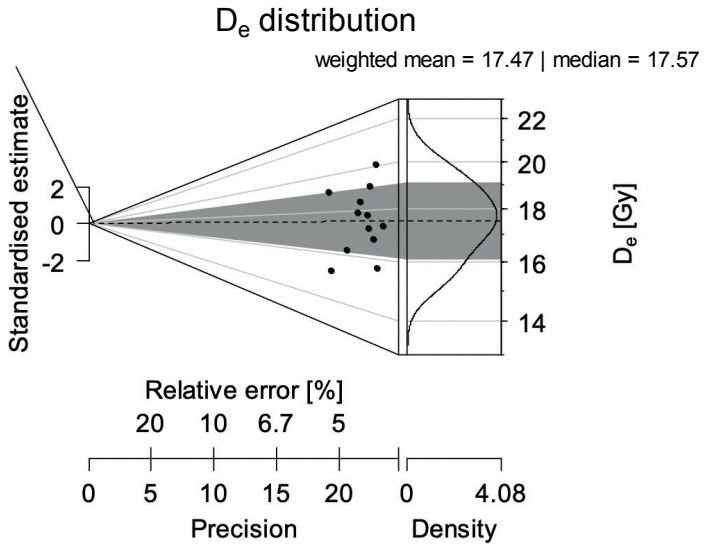

Figure SC.9. *Abanico plot for SUTL2925.*

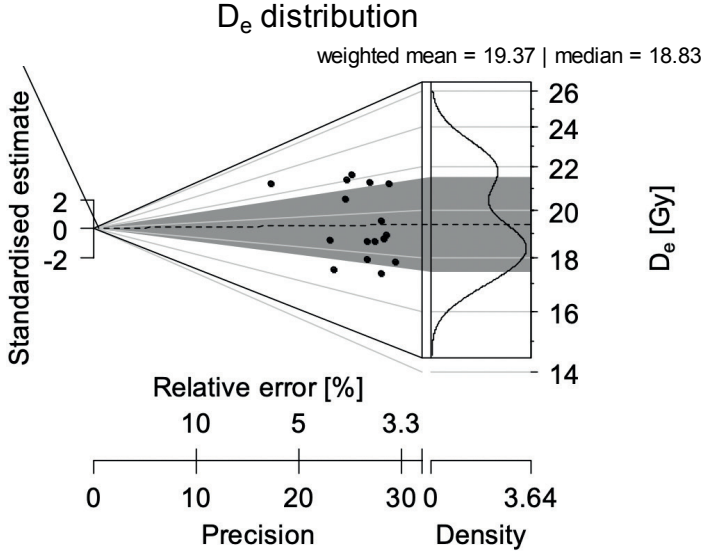

Figure SC.10. *Abanico plot for SUTL2926.*

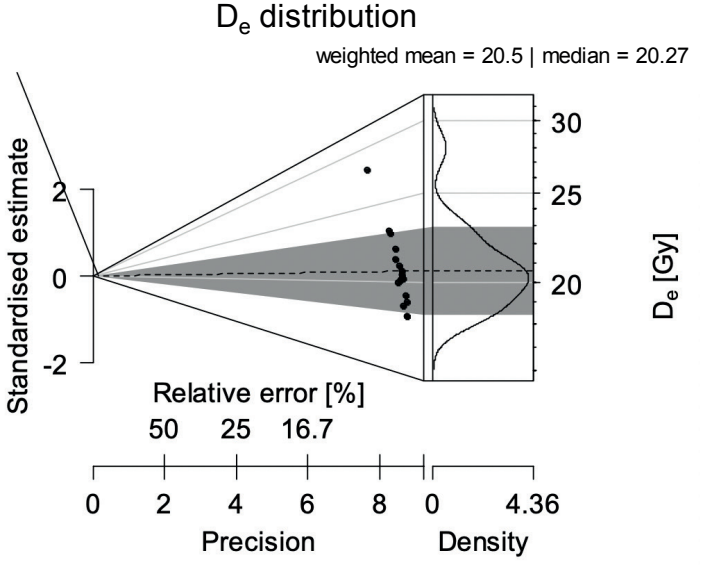

Figure SC.11. *Abanico plot for SUTL2927.*

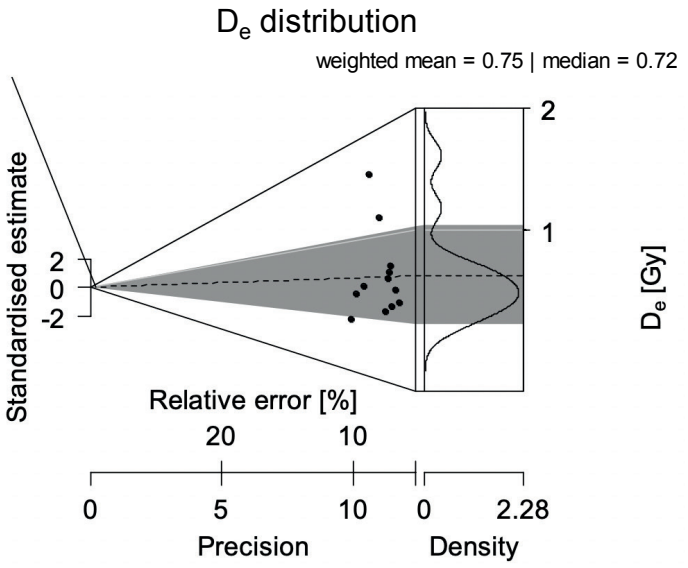

Figure SC.12. *Abanico plot for SUTL2930.*

Appendix 2 – Supplement D

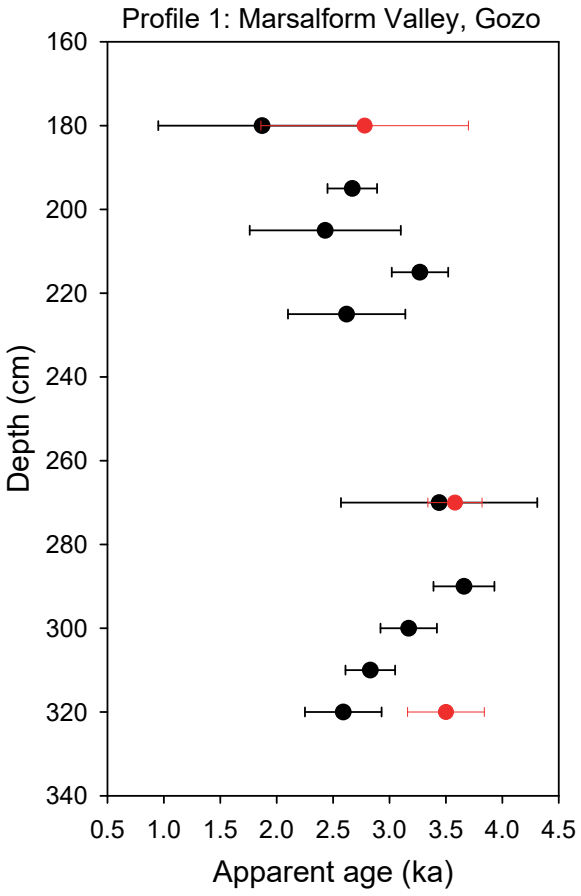

Figure SD.1. *Apparent ages for profile 1 (black) with OSL ages (red).*

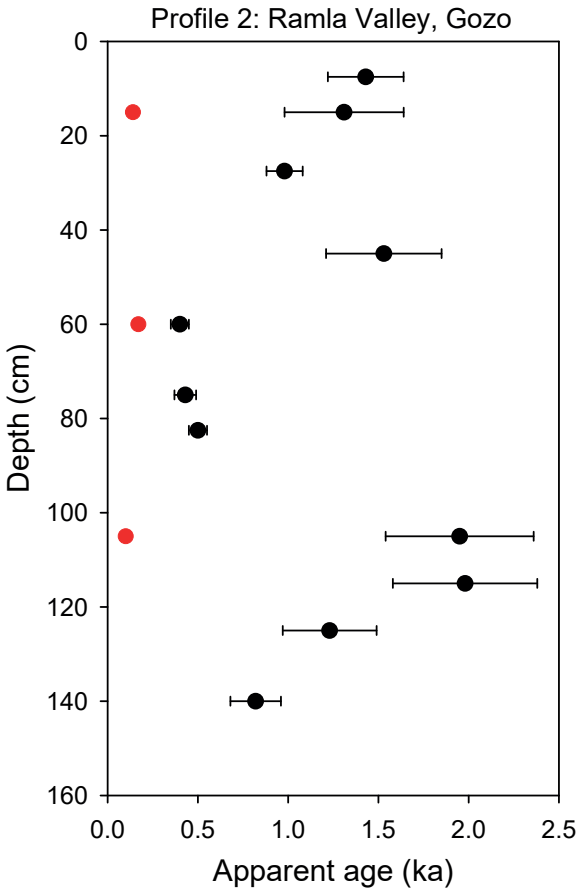

Figure SD.2. *Apparent ages for profile 2 (black) with OSL ages (red).*

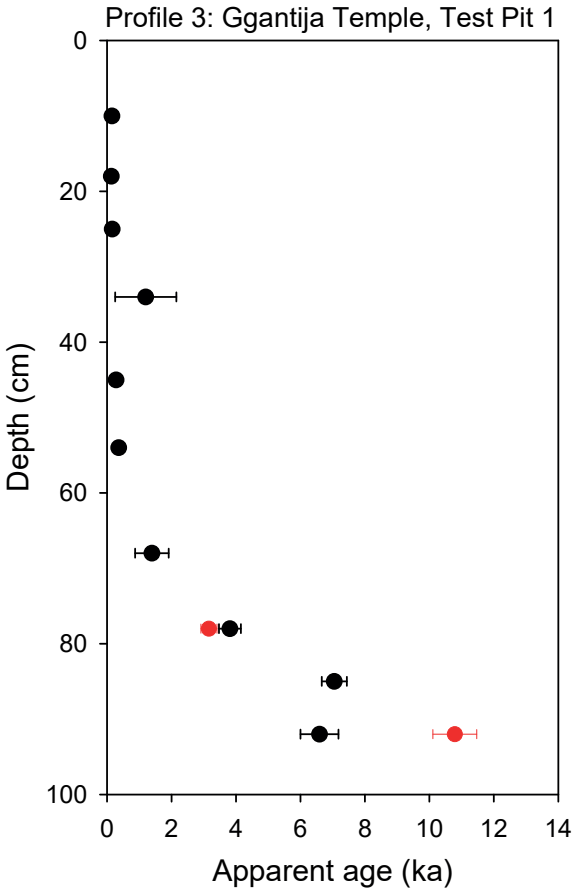

Figure SD.3. *Apparent ages for profile 3 (black) with OSL ages (red). Note that dose rates for 0–75 cm are extrapolated.*

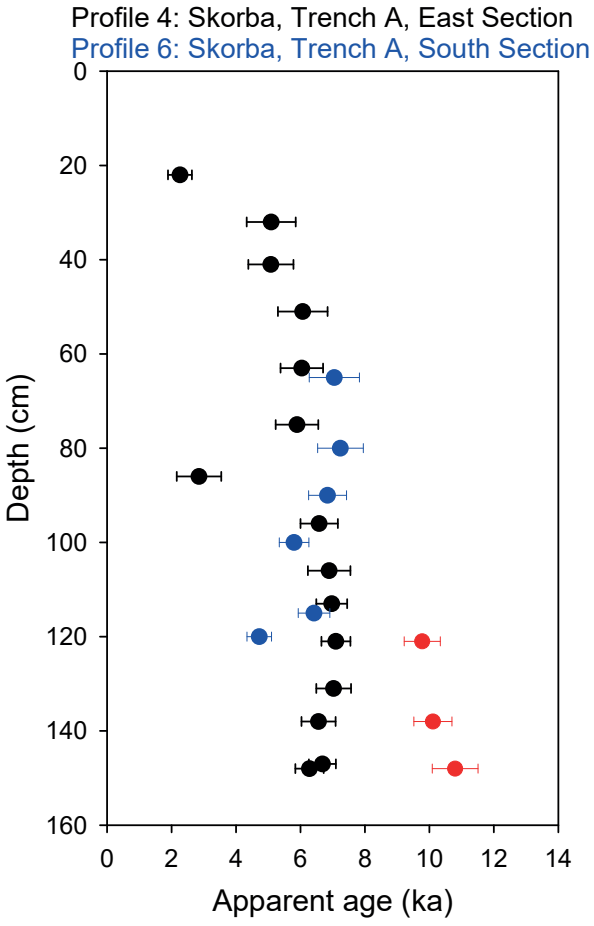

Figure SD.4. *Apparent ages for profiles 4 (black) and 6 (blue) with OSL ages (red). Note that dose rates for 0–120 cm are extrapolated, and for the south section assumed to be the same as the corresponding depth on the east section.*

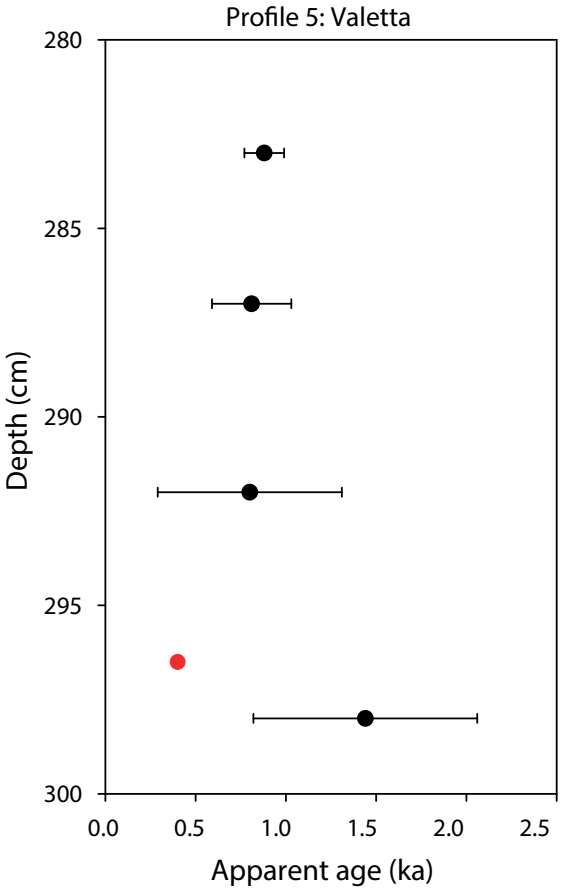

Figure SD.5. *Apparent ages for profile 5 (black) with OSL ages (red).*

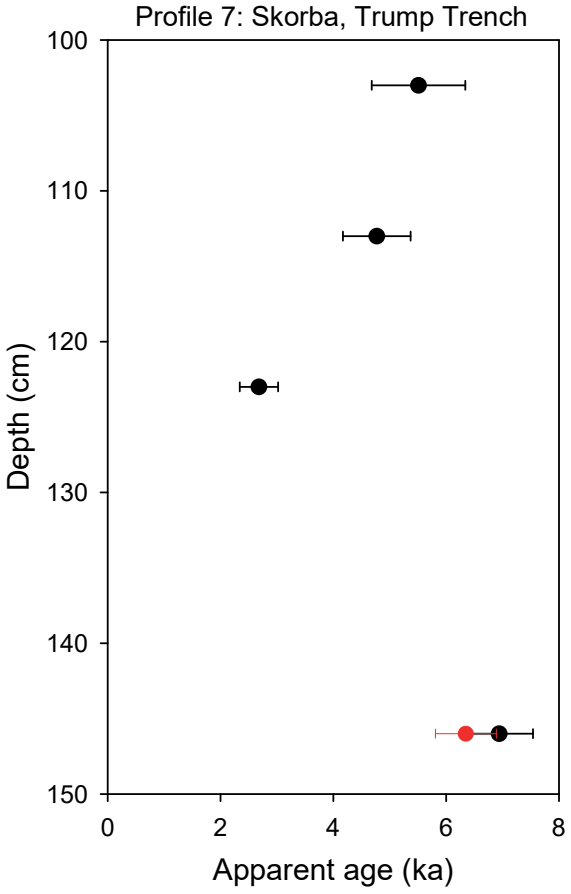

Figure SD.6. *Apparent ages for profile 7 (black). The dose rate for the bottom sample was assumed to equal the corresponding context in P4, the apparent age for that context in P4 is shown (red).*

Appendix 3

Deep core borehole logs

Chris O. Hunt, Katrin Fenech, Michelle Farrell & Rowan McLaughlin

Table A3.1. *Stratigraphy and interpretation of the Salina Deep Core.*

Core	Depth (m)	Sediments	Interpretation
22	29.50–29.47	Creamy micritic limestone	Rockhead: Globigerina Limestone
	29.47–29.30	Yellowish-brown (10 YR5/4) to greyish-brown (10YR 4/3) very compact silty clay with sub-angular to rounded clasts. Clay skins present beneath clasts, a few clay-lined rootlet casts, occasional rootlets and very occasional land snail and charcoal fragments	Palaeosol developed on colluvium (? Late Pleistocene interstadial)
	29.30–29.17	Grey (10YR 5/1) to greyish-brown (10YR 5/2) very muddy sandy gravel with occasional land snail and charcoal fragments	Fluvial gravel: poor sorting is consistent with deposition from muddy flow (? Late Pleistocene)
21A	28.50–28.32	Dark yellowish-brown (10YR 4/4) matrix-supported limestone gravel, clasts rounded to sub-rounded, micritic calcite skins under clasts, matrix showing some slickensiding	Fluvial gravels with pedogenic features (? Late Pleistocene)
	28.32–28.20	Very dark brown (10YR 8/2) clast-supported sandy to openwork gravel, clasts rounded to sub-rounded, micritic calcite skins under clasts	
	28.20–28.12	Very pale brown (10YR 7/3) mottled yellowish-brown matrix-supported cobbly gravel clasts rounded to sub-rounded, micritic calcite skins under clasts, matrix showing some slickensiding	
21B	28.12–28.04	Brown (7.5YR 4/3) silty sandy clay with rare small sub-rounded stones with blocky structure and hair-like micritic fills between peds, rare root pores	Fluvial deposits with pedogenic features (? Late Pleistocene)
	28.04–27.97	Yellowish-brown (10YR 5/4) clast-supported gritty sandy gravel	
	27.97–27.95	Dark greyish-brown (10YR 4/2) slightly sandy clayey silt with pronounced blocky structure and micritic fills between peds	
	27.95–27.78	Dark grey (10YR 4/1) and brown (10YR 4/3) slightly gritty silty clay, coarsening upward, crudely laminated and with occasional charcoal flecks	
21C	27.78–27.61	Brown (10YR 4/3) to dark brown (10YR 3/3) matrix-supported fine clayey gravel with small-scale trough cross-sets	Fluvial deposits with pedogenic features (? Late Pleistocene or Holocene)
	27.61–27.58	Dull brown (10YR 5/3) muddy clast-supported gravel, fining upward	
	27.58–27.56	Brown (10YR 4/3) clay	
	27.56–27.53	Dark brown (10YR 3/3) matrix-supported gravel, sandy clay matrix, odd charcoal and land snail fragments	
	27.53–27.42	Brown (10YR 4/3) sandy clay with very occasional stones, small scale trough cross-sets, blocky structure with micritic joint linings and clay skins beneath pebbles. Some land snail fragments	

Table A3.1 *(cont.).*

Core	Depth (m)	Sediments	Interpretation
20A	27.00–26.96	Very dark grey (2.5Y 3/1) stony silty clay	Shallow marine sediments, probably sub-littoral or upper delta-front (Holocene)
	26.96–26.93	Dull brown (10YR 5/4) muddy gravel	
	26.93–26.87	Very dark grey (2.5Y 3/1) slightly stony silty clay	
	26.87–26.70	Dark greyish brown (2.5Y 4/2) slightly muddy granules to fine gravel	
	26.70–26.65	Very dark grey (2.5Y 3/1) slightly stony clay	
20B	26.65–26.56	Bluish-grey (10BG 4/1) shelly clay	Shallow marine sediments, probably delta-front
	26.56–26.46	Dark grey (N 4/1) silty clay, crudely laminated with sand lenses	
	26.46–26.38	Dark grey (N 3.5/1) shelly clay	
	26.38–26.25	Dark grey (N 3/1) fine muddy gravel	
20C	26.25–26.13	Dark grey (N 3.5/1) medium muddy sand	
	26.13–26.00	Dark grey (N 4.5/1) coarse muddy sand	
	26.00–25.95	Greyish yellow-brown (10YR 4.5/2) coarse gritty sand	
20D	25.95–25.60	Dull yellowish-brown (10YR 4.5/3) slightly muddy gritty coarse sand	
19A	25.50–25.28	Brownish-grey (10YR 4/1) silty clay	Shallow marine delta front and proximal pro-deltaic sediments, deposited mostly from gravity flows, interbedded with quiet water laminated sediments
19B	25.28–24.85	Brownish-grey (10YR 4/1) silty clay, becoming slightly sandy upwards	
19C	24.85–24.48	Dark grey (2.5Y 3.5/1) silty sandy clay and fine muddy sand, indefinitely laminated	
19D	24.48–24.18	Dark grey (2.5Y 3.5/1) slightly sandy silty clay	
	24.18–24.12	Dark grey (2.5Y 3.5/1) gritty sandy silty clay	
18A	24.00–23.80	Grey (2.5Y 5/1) clay	
	23.80–23.68	Dark grey (2.5Y 4/1) silty clay, indistinctly laminated, some shells	
18B	23.68–23.62	Grey (2.5Y5/1) muddy sand, some shells	
	23.62–23.36	Dark grey (2.5Y4/1 to 2.5Y3/1) silty clay, thickly but indistinctly laminated, odd shells	
18C	23.36–23.33	Grey (2.5Y 5/1) muddy sand, some shells	
	23.33–23.32	Light brownish-grey (5YR 7/2) sandy clay	
	23.32–23.19	Grey (2.5Y 5/1) muddy sand, some shells	
	23.19–23.10	Dark grey (2.5Y4.5/1) sandy mud with very abundant, mostly angular, wood fragments	
	23.10–23.09	Grey (2.5Y 5/1) muddy sand, some shells	
	23.09–23.06	Dark grey (2.5 Y4/1) mud with lenses of fine sand	
	23.06–23.02	Grey (2.5Y 5/1) very muddy sand	
18D	23.02–22.70	Dark grey (2.5Y 4.5/1) clay, very plastic	
17A	22.50–22.22	Grey (2.5Y 5/1) silty clay, laminated, shelly	

Table A3.1 *(cont.).*

Core	Depth (m)	Sediments	Interpretation
17B	22.22–21.83	Grey (2.5Y 5/1) to dark greenish-grey (2.5YR 4/1) silty clay and silty sand in three coarsening-up laminated units	
17C	21.83–21.71	Dark grey (2.5Y 4/1) silty clay, indistinctly but finely laminated	
	21.71–21.63	Dark grey (2.5Y 4/1) sand and silty clay in fining-upward couplets 2–4 mm thick	
	21.63–21.52	Dark grey (2.5Y 4/1) silty clay, passing up into dark greenish-grey (2.5Y 4/1) silty and then sandy clay	
	21.52–21.43	Dark grey (2.5Y 4/1) fine sandy silty clay, indistinctly laminated	
17D	21.43–21.13	Very dark grey (2.5Y 3/1) to dark grey (2.5Y 4/1) sands, silty clays and clays, finely laminated	
	21.13–21.06	Very dark grey (2.5Y 3/1) silty clays interlaminated with olive-yellow (2.5Y 6/8) sands	
16A	21.00–20.66	Dark grey (2.5Y 4.5/1) clayey sand and sandy clay, laminated	Marine distal pro-deltaic sediments, mostly deposited by small-scale gravity flows, interbedded with lower-energy quiet-water sediments
16B	20.66–20.43	Dark grey (2.5Y 4.5/1 to 2.5Y 5/1) slightly silty fine sandy clay with partings covered in bivalve fragments	
16C	20.43–20.14	Dark grey (2.5Y 4/1 to 2.5Y 5/1) silty clay, thinly laminated	
16D	20.14–19.91	Dark grey (2.5Y 4/1 to 2.5Y 5/1) silty clay, thinly laminated	
16E	19.91–19.66	Dark grey (2.5Y 4/1 to 2.5Y 5/1) silty clay with a little fine sand, thinly laminated	
15A	19.50–19.36	Dark grey (2.5Y 4/1) silty clay	
	19.36–19.34	Very dark grey (2.5 Y3.5/1) sandy silty clay with abundant charcoal	
	19.34–19.10	Dark grey (2.5Y 4/1) silty clay, sandy silty clay and silty sand, in three coarsening-upward units	
15B	19.10–18.79	Dark grey (2.5Y 3/1 to 2.5Y 4/1) sandy silty clay and silty clay, laminated	
15C	18.79–18.51	Dark grey (2.5Y 3/1 to 2.5Y 4/1) sandy silty clay and silty clay, laminated	
15D	18.51–18.23	Dark grey (2.5Y 4/1) sandy silty clay, laminated	
14A	18.00–17.64	Dark grey (2.5Y 4/1) sandy silty clay, odd shells	
14B	17.64–17.39	Dark grey to grey (2.5Y 4/1 to 2.5Y 5/1) slightly sandy silty clay	
14C	17.39–17.01	Dark grey (2.5Y 4/1) clayey silty sands and grey (2.5Y 5/1) silty clays in four fining-upward units	
14D	17.01–16.70	Grey (2.5 Y5/1) sandy silty clay and silty clays in three fining-upward units	
13A	16.50–16.24	Grey (2.5Y 5/1) silty clay	
	16.24–16.20	Dark grey (2.5Y 4/1) fine sandy silty clay	

Table A3.1 *(cont.).*

Core	Depth (m)	Sediments	Interpretation
13B	16.20–15.85	Grey (2.5Y 5/1) fine sandy silty clay with occasional sandy partings	
13C	15.85–15.45	Dark grey (2.5Y 4/1) sandy silty clay and greyish-brown (2.5Y 5/2) silty clay in four fining-upward units	
12A	15.0–14.90	Dark grey (2.5Y 4/1) silty clay	
	14.90–14.68	Grey (2.5Y 5/1) sandy silty clay with shells	
12B	14.68–14.42	Dark grey (2.5Y 4/1) sandy silty clay	
12C	14.42–14.22	Grey (2.5Y 5/1) sandy silty clay	
	14.22–14.12	Grey (2.5Y 5/1) silty clay	
12D	14.12–13.98	Dark grey (5Y 4/1) silty clay	
	13.98–13.90	Dark grey (5Y 4/1) sandy silty clay with charcoal fragments	
	13.90–13.77	Dark grey (2.5Y 4/1) silty clay	
11A	13.20–12.77	Dark grey (5Y 5/1) muddy gravelly sand	Shallow sandy marine shoal sediments, often deposited within wave-base, possibly eel-grass meadows
11B	12.77–12.41	Dark grey (5Y 4/1) gritty muddy sand with shells	
11C	12.41–12.16	Dark grey (5Y 5/1) muddy sand with shells	
	12.16–12.11	Dark grey (5Y 4/1) muddy sand, very shelly	
11D	12.11–11.81	Dark grey (5Y 4/1) sandy mud and muddy sand with some shell	
10	11.60–11.31	Grey (10Y 4/1) silty sand with much shell	
	11.31–11.13	Grey (5Y 4/1) sandy mud with odd shells	
	11.13–11.05	Grey (5Y 4/1) sandy mud with abundant shell and eelgrass fibre, becoming more clayey upward	
	11.00–2.40	Shell gravel, hydro-collapsed and not sampled	Shallow marine, high energy shoal sediments deposited within wave-base
	2.40–0.00	Rubble and masonry	Salt pan roadway and wall foundation

Table A3.2. *Stratigraphy and interpretation of the Salina 4 core.*

Core	Depth (m)	Description	Interpretation
SA4-K	11.02–10.82	Dark greenish-grey (2.5GY 4/1) mud. Ag1, As3	Quiet-water estuarine, deposition mostly from suspension
	10.82–10.7	Dark grey (7.5Y 4/1) mud with few shells. Gs1, Ga1, As2	
	10.7–10.67	Dark grey (7.5Y 4/1) sandy silty mud. Ga1, As3	Estuarine sediments. Coarser layers reflect flood input of sediment from upstream, finer layers are suspension deposits between major floods
	10.67–10.47	Dark grey (7.5Y 4/1) shelly gravelly mud. Poorly sorted, no bedding. Lots of shells. Ggmin1, Ga1, As2	
	10.47–10.02	Olive-grey (7.5Y 4/2) sandy silty mud with shell fragments. No bedding. Lumps of humified material at 10.69–10.71 m. Ga1, As3	
SA4-J	10.02–9.48	Grey (7.5Y 4/1) shelly sandy mud. Gs1, Ag1, As2	
	9.48–9.34	Grey (7.5Y 4/1) Ag1, As3	
	9.34–9.02	Grey (7.5Y 4/1) shelly sandy mud. Gs1, Ag1, As2	
SA4-I	9.02–8.15	Dark greenish grey (5GY 4/1) muddy sand. Large shell at 8.86–8.875 m, stone at 8.34–8.37 m. Ag1, As3	
	8.15–8.02	Olive-grey (7.5Y 5/2) muddy sand. Ag1, Gs3	
SA4-H	8.02–7.88	Grey (7.5Y 4/1) sandy mud. Gs0.5, As3.5	
	7.88–7.87	Grey (7.5Y 4/1) very sandy mud. Gs2, As2	
	7.87–7.58	Grey (7.5Y 4/1) sand. Ag1, As3	
	7.58–7.56	Grey (7.5Y 4/1) shelly sand. As1, Ag1, Gs2	
	7.56–7.02	Greenish-grey (2.5GY 6/1) sandy mud. As3, Gs1	
SA4-G	7.02–6.86	Grey (7.5Y 5/1) poorly sorted sandy shelly silt with clay. Lots of broken shells, some herbaceous detritus. Gs3, Ga1, Dh 5–10%	
	6.86–6.38	Grey (7.5Y 5/1) silty clay. Trace amounts of sand, band of humified organic detritus at 6.785 m. No structures. Ag1, As3, Dh 5–10%	
	6.38–6.02	Olive grey (5Y 5/2) muddy sand. Slightly humified eelgrass at 6.32–6.29 m. Gs3, Ga1.	
SA4-F	6.02–5.84	Grey (7.5Y 5/1) silty clay. Ag1, As3	
	5.84–5.80	Grey (7.5Y 5/1) sandy silty mud. Ag1, Ga1, As1, Gs1	
	5.80–5.78	Grey (7.5Y 5/1) silty clay. Ag1, As3	
	5.78–5.70	Grey (7.5Y 5/1) sandy mud. Poorly sorted. Gs3, Ag1	
	5.70–5.63	Grey (7.5Y 5/1) silty clay. Ag1, As3	
	5.63–5.43	Grey (7.5Y 5/1) muddy sand. Poorly sorted, some Fe staining. Gs3, Ga1	
	5.43–5.39	Grey (2.5Y 6/1) sandy mud. Gs1, As3	
	5.39–5.02	Grey (2.5Y 6/1) well sorted medium to coarse sand. Gs4	
SA4-E	5.02–4.90	Olive-grey (7.5Y 5/2) silty clay with some organic detritus. Ag1, As3, Dh 5–10% Sharp upper boundary	
	4.90–4.38	Grey (7.5Y 5/1) sandy silt with some large shells at 4.76 m. Moderately sorted, traces of Dh detritus. Shell fragments present. Gs4	
	4.38–4.02	Missing/liquified	

Table A3.2 *(cont.).*

Core	Depth (m)	Description	Interpretation
SA 4-D	4.02–3.47	Greyish-olive (7.5Y 6/2) silty clay with lump of very humified organic material at 3.77 m. Eelgrass (humified) at 3.54 and (humified) at 3.72 m	
	3.47–3.38	Olive-grey (5Y 5/2) sandy silty clay	
	3.38–3.36	Olive-black (7.5Y 2/2) silty clay with moderately humified eelgrass at 3.37 m	
	3.36–3.26	Olive-grey (5Y 5/2) sandy silty clay	
	3.26–3.18	Olive-black (7.5Y 2/2) silty clay with slightly humified eelgrass at 3.18–3.25 m	
	3.18–3.02	Olive-grey (5Y 5/2) sandy silty clay	
SA4-C	3.02–2.70	Olive-grey (7.5Y 7/2) silty clay	Lagoonal sediments
	2.70–2.52	Olive-grey (7.5Y 7/2) silty clay	
	2.52–2.02	Olive-grey (7.5Y 7/2) silty clay	
SA4-B	2.02–1.89	Greenish-grey (2.5GY 6/1) silty clay. Some charcoal and shells (very minor traces). No structures. Diffuse upper boundary. Ag1, As3	Floodplain back-basin lagoonal sediments with coarse layers deposited during major floods
	1.89–1.23	Very pale brown (10YR 7/3) silty clay (fine to medium silt). Fine textural laminations detected with scalpel (not visible). Fe stained. At 1.8 m transition to olive grey (2.5GY 6/1) silty clay. Slightly sharp upper boundary. Ag1, As3	
	1.23–1.16	Very pale brown (10YR 7/3) poorly sorted silty sand with some clay. Shell fragments. Gs2, Ag1, As1	
	1.16–1.02	Brown 10YR 5/3 silty clay darkening to dark grey (10YR 4/ at 1.095 m. Textural laminations detected with scalpel (not visible). Fe stained. Ag1, As3	
SA4-A	1.01–0.89	Brownish-yellow (10YR 6/6) moderately well sorted clayey silt. Looks mottled, oxidized. Some broken shell fragments present throughout. Some coarse bedding. Silty-sand beds interdigitated throughout (at 0.99, 0.96, 0.94, 0.92 and possibly 0.90–0.89 m). Ag2, As1, Ga1	
	0.89–0.83	Light yellowish-brown (10YR 6/4) poorly sorted sandy silt with shell fragments. Massive, poorly structured. GS3, Ag1	
	0.83–0.58	Brownish-yellow (10YR 6/6) moderately well sorted clayey silt. Mottled, oxidized. Some broken shell fragments present throughout. Some coarse bedding (sedimentary structures). Ag2, As1, Ga1	
	0.58–0.51	Not recovered (made ground)	Made ground

Table A3.3. *Stratigraphy and interpretation of the Salina 2 core.*

Core	Depths in core	Lithology	Interpretation
SA2-7 (6.54-5.24 m)	6.54–6.47 m	Dark grey brown highly organic sandy silty clay.	Estuarine sediments. Mostly quiet-water suspension deposits
	6.47-6.36 m	Grey shelly coarse sand	High-energy shallow estuarine sediments
	6.36-6.24 m	Dark grey brown highly organic sandy silty clay becoming shelly upward. Burrowed upper surface with *in-situ* deep infaunal mollusc in burrow.	Estuarine sediments. Mostly quiet-water suspension deposits
	6.24-5.68 m	Grey shelly to very shelly very coarse sand with some organic fragments. Some bedding suggesting layers of about 5-8 cm thickness	High-energy shallow estuarine sediments
	5.68-5.24	Probably hydrocollapsed coarse shelly sand	High-energy estuarine shoal sediments, very rapidly deposited
SA2-6 (5.06-4.12 m)	5.06-4.36 m	Dark grey fine silty sand, gradually coarsening upward and with occasional shell, showing faint bedding 1-2 cm thick.	Estuarine sediments. Mostly quiet-water suspension deposits
	4.36-4.12 m	Grey, coarse, occasionally shelly sand with water-escape structures, possibly partly hydrocollapsed	High-energy shallow estuarine sediments
SA2-5 (4.04-3.26 m)	4.04-3.26 m	Grey very coarse sand with very abundant shell and occasional organic matter, hydrocollapsed	High-energy shallow estuarine sediments
SA2-4 (3.19-2.35 m)	3.19-2.82 m	Grey mottled strong-brown laminated sandy clayey silt with odd shell. Mottles probably mark the location of burrows.	Estuarine quiet-water sediments.
	2.82-2.78 m	Grey and light grey laminated slightly silty clay. Erosive upper boundary	Estuarine quiet-water sediments.
	2.78-2.72 m	Grey fine shell gravel, fining upward into	High-energy shallow estuarine sediments
	2.72-2.49 m	Grey very shelly slightly silty sand passing gradually upward into greyish-brown shell gravel. Sharp upper boundary	
	2.49-2.37 m	Grey brown coarse shelly sand, fining upward	
	2.37-2.35 m	Grey brown shelly sand	
SA2-3 (2.27-1.78 m)	2.27-1.78 m	Light greyish brown coarse to very coarse shelly sand, with indistinct layering. Layers 5-6 cm thick are marked by differences in grain size and porosity	High-energy shallow estuarine sediments
SA2-2 (1.63-0.94 m)	1.63-1.27 m	Light greyish brown coarse to very coarse shelly sand, but gradually fining upward to medium to coarse shelly sand, with indistinct layering. Layers 5-6 cm thick are marked by differences in grain size and porosity, Sharp but burrowed upper boundary	High-energy shallow estuarine sediments
	1.27-0.97 m	Pale yellowish brown to brownish yellow coarse to medium sand	High-energy littoral sediments
SA2-1 (0.73-0.03 m)	0.73-0.66 m	Light greyish brown coarse shelly sand, coarsening up into fine shelly gravel. Sharp upper boundary	High-energy shallow estuarine sediments
	0.66-0.45 m	Brownish-grey to dark brownish-grey organic fine shelly sand with indistinct layering 2-5 cm thick and occasional burrows picked out by colour variation, Occasional shallow infaunal bivalves *in-situ*. Sharp upper boundary	Estuarine sandflat
	0.45-0.19 m	Very light brownish yellow coarse to medium sand with abundant shell, showing indistinct layering 6-8 cm thick, picked out by grain size variation	High-energy littoral sediments

Table A3.4. *Stratigraphy and interpretation of the Xemxija 1 core.*

Core	Depth (m)	Description	Interpretation
XEM1-9	9.99–9.93	Brown (10YR 4/4) matrix-supported breccia of fairly uniform clasts of soil aggregates (mainly sub-angular) with occasional limestone grit. Slightly silty clay with grit and occasional shell fragments	Mass-flow deposits composed of aggregates derived from eroded soil
	9.93–9.81	Dark brown (7.5YR 3/3) coarse diamict with sub-rounded to sub-angular limestone clasts to 2 cm. Gritty clay matrix. Very gradual transition to	
	9.81–9.67	Dark brown (7.5YR 3.5/3.5) diamict with disordered sub-rounded to sub-angular limestone clasts in a matrix of sandy clay. Odd tiny mollusc fragments.	
	9.67–9.50	Brown (10YR 4.5/3) matrix-supported breccia of limestone fragments (mostly sub-angular) and soil aggregates. Gritty clay with particles all aligned in one direction.	
	9.50–9.39	Dark greyish-brown (10YR 4/2) breccia of clay soil aggregates (some sub-angular whereas in the rest of the core most are rounded). Mostly clast-supported but some matrix-supported. *c*. 20% limestone fragments at the bottom, *c*. 5% at the top	
	9.39–9.26	Brown (7.5YR 3/2) breccia of clay soil aggregates with occasional limestone fragments and charcoal. Relatively coarse at the bottom – appears to fine upwards. Transition to	
	9.26–9.21	Dark brown (7.5YR 3.5/2) breccia of soil aggregates up to 5 mm, and limestone grit (*c*. 30%, small, sub-rounded clasts). Mostly matrix-supported but odd voids around some clasts. Slightly silty clay. Transitional above and below	
	9.21–9.13	Very dark grey (10YR 3/1) matrix-/clast-supported breccia of soil aggregates, size 2–5 mm. Rather clayey, possibly some silt. Odd limestone chips, occasional very small charcoal fragments, little bit of sand-sized limestone	
	9.13–9.09	Dark grey (10YR 4/1) breccia of 2–3 mm soil aggregates with small voids between some. Occasional brownish red (2.5YR 4/8) mottling. Tiny limestone chips and possible shell fragments	A-B profile of a buried soil; very micritic indicating calcareous groundwater and seasonal drying, developed on mass-flow deposit of aggregates derived from eroded soil
	9.09–8.97	Very dark greyish-brown (10YR 2.5/1) matrix-supported fine breccia of soil aggregates. Nearly 100% clay with tiny charcoal fragments and very occasional very small limestone chips	Mass-flow deposit composed of aggregates derived from eroded soil
	8.97–8.88	Brown (10YR 3/2) slightly silty clay, slightly fining upwards with dark red (2.5YR 3/6) mottling. Breccia of soil aggregates. Abundant small limestone fragments	Truncated profile of a buried soil; developed on mass-flow deposit of aggregates derived from eroded soil
XEM1-8	8.90–8.83	Very dark grey (10YR 3/1) almost pure clay with odd shell fragments and little bits of wood	Freshwater marsh and shallow pool deposits, probably a lagoonal setting behind a bay-bar
	8.83–8.76	Black (2.5Y 2/1) to dark grey (2.5Y 4/1) clayey silt with clod of peaty organic matter (very highly humified with abundant ostracods). Occasional shell and wood fragments	
	8.76–8.56	Very dark grey (10YR 3/1) clayey silt / silty clay. Very organic, full of very small gastropod fragments. Occasional wood and charcoal	
	8.56–8.46	Very dark grey (10YR 3/1 silty clay / clayey silt. Fairly abundant lumps of tufa (root encrustations?) and odd bits of charcoal and wood. Abundant freshwater gastropods	
	8.46–8.25	Dark grey (10YR 4.5/1) clay with possible slight silt component. Odd tufa lumps (one has a core of organic material suggesting they are encrustations around organic matter). Odd shell fragments (mainly gastropods). Rootlets preserved as very rotten organic matter, mostly near the top	
	8.25–8.09	Very dark grey (7.5YR 3/1) slightly shelly, slightly silty clay with occasional tufa lumps, charcoal fragments and little bits of organic matter. Gradual transition over *c*. 2 cm to	
	8.09–8.00	Dark grey (2.5Y 4/1) clayey silt with very high organic content and very occasional shell fragments. *c*. 1 cm thick light brownish-grey (2.5Y 6/2) tufa layers and 0.5 cm thick layers of brown mud	

Table A3.4 *(cont.).*

Core	Depth (m)	Description	Interpretation
XEM1-7	7.80–7.67	Strong brown (7.5YR 5/6) becoming downwards brown 10YR 4/3 clayey silt/silty clay with occasional shells and large root casts from unit above. Perhaps more clayey with depth	Deposits of a seasonally drying marsh
	7.67–7.30	Dark greyish-brown (10YR 4/2) variably matrix-/clast-supported breccia of soil aggregates with occasional angular to sub-rounded limestone fragments, slightly silty clay. Occasional rootlets, a very little shell. Odd orange ironstone-like small pebbles. Potsherd present at 7.62 m	Mass-flow deposits of aggregates derived from eroded soil profiles, from a series of grain/mud flow events, interrupted by phases of weak pedogenesis (at 6.03–6.05 m and 6.7–6.85 m) indicating periods of some stabilization.
	7.30–6.73	Greyish-brown (10YR 4.5/2) matrix-supported breccia of soil aggregates. Slightly silty clay with odd small limestone clasts and large rootlets (longest = *c.* 12 cm)	
XEM1-6	6.68–6.57	Very dark grey (7.5YR 3/1.5) slightly silty clay. Very fine matrix-supported breccia	
	6.57–6.38	Dark grey (10YR 4/1) mottled brown (7.5YR 4/4) and strong brown (7.5YR 4/6) clayey silt. Clast-supported breccia of soil aggregates	
	6.38–6.32	Brown (10YR 4/4) to brownish-yellow (10YR 6/8) very slightly silty clay. Clast-supported breccia of soil aggregates	
	6.32–6.15	Dark greyish-yellow (10YR 4/2) slightly silty clay. Partly matrix-, partly clast-supported breccia of soil aggregates	
	6.15–6.05	Dark greyish-yellow (10YR 4/2) clay silty clay. Clast-supported breccia of soil aggregates with occasional sub-angular limestones	
	6.05–6.03	Dark greyish-brown (10YR 4/2) clay. Matrix-supported breccia of soil aggregates	
	6.03–5.89	Dark greyish-brown (10YR 4/2) clast-supported breccia of clay soil aggregates. Less dense with more air gaps than unit above. Some brighter mottles (10YR 5/6)	
	5.89–5.79	Brown (10YR 4/3) matrix-supported breccia of silty clays and fine soil aggregates	
XEM1-5	5.67–5.64	Very dark grey (2.5Y 3.5/1) shelly, slightly silty clay. Very distinct line of organic matter fragments at top of unit	Shallow freshwater lagoon, some clastic input
	5.64–5.36	Dark grey (10YR 4/1) to grey (10YR 6/1) slightly clayey silt containing organic matter. Contains tiny limestone and shell fragments. Patchy – contains little marly lumps	
	5.36–5.25	Very dark grey (10YR 3/1) highly organic clay with little pockets of very humified organic matter. Contains one piece of sub-rounded limestone and odd little bits of shell	
	5.25–5.17	Brownish-grey (10YR 4/1) organic marl passing up into greyish-yellow-brown (10YR 6/2) very organic marl. Silty clay with abundant chunks of organic matter and occasional shell fragments. Banded, darkening upwards	
	5.17–5.12	Black (10YR 2/1) dense organic matter, slightly fibrous. Much more solid than previous 'peat' units. No inorganic matter. Humification H3. Tiny fragments of shell at 5.17 m – erosion surface?	Shallow freshwater lagoon, probably with much dense vegetation and minimal clastic input
	5.12–4.98	Very dark grey (10YR 3/1) slightly shelly, highly organic, silty clay with very abundant plant fragments. Less humified than previous layer	
	4.98–4.89	Black (N 2/0) highly organic, very well humified, slightly fibrous peat. Humification H9–10	
	4.89–4.85	Very dark grey (10YR 3/1) slightly shelly silty clay, grades upwards into peat	
	4.85–4.79	Slightly shelly black (N 2/0) organic mud. Quite fibrous and very highly humified	

Table A3.4 *(cont.).*

Core	Depth (m)	Description	Interpretation
XEM1-4	4.60–4.53	Dark grey (2.5Y 4/1) shelly clay with odd bits of charcoal, no obvious roots. More shelly than other units	Shallow freshwater lagoon and paludal marsh. Near permanent waterlogged conditions, and only minimal input of very fine sediment
	4.53–3.62	Grey (2.5Y 5/1) clay to very slightly silty clay. Odd fragments of vegetable material, charcoal, rootlets and darker streaks. Occasional sub-angular rocks	
XEM1-3	3.55–3.40	Grey (5Y 5/1) slightly shelly clay with rootlets and odd charcoal flecks.	
	3.40–3.20	Grey (5Y 5/1) slightly shelly silty clay. Very vague laminations at 3.36–3.38 m. Slight transition to…	
	3.20–3.03	Reddish-grey (2.5 YR 5/1) shelly, very slightly silty clay with occasional irregular, weathered-looking limestone lumps.	
	3.03–2.92	Grey (2.5Y 5/1) slightly silty clay. Slightly shelly with occasional small stones. Mottles could be mud pellets again. Gradual transition to	
	2.92–2.65	Grey (2.5Y 6/1) slightly shelly clay with odd charcoal fragments and abundant iron mottling brown (10YR 5/3) and brownish-yellow (10YR 6/6). Mottles actually appear to be mud clasts from soil inwash	
XEM1-2	2.40–2.36	Grey (2.5Y 6/1) clayey fine to medium sand. Fines upwards slightly – sand coarser below 2.37 m. Estuarine shell fragments	Storm runoff input to lagoon
	2.36–2.25	Grey (2.5Y 6/1) sandy clay, slightly mottled with flecks of organic matter. Occasional rootlets and shell fragments	Lagoonal sediments
	2.25–1.99	Grey (2.5Y 5/1) silty clay with flecks of blackish organic matter. Some possible pieces of wood	
	1.99–1.92	Light brownish-grey (2.5Y 6/2) organic clay with *c*. 2 mm greyish-brown (2.5Y 5/2) laminations of more organic material showing current bedding. Occasional reed macrofossils and charcoal	
	1.92–1.80	'Transition zone' light brownish-grey (2.5Y 6/2) clay with odd shell fragments. Very small black mottles throughout.	Deposits of a seasonal marsh
	1.80–1.40	Light olive-brown (2.5Y 5/3) slightly clayey silt with *c*. 2 mm laminations in places and yellowish-brown mottles throughout. Black mottling along roots. Odd small shell fragments	
XEM1-1	1.42–1.33	Light reddish-brown (2.5YR 6/4) clay with light grey (10Y 7/1) mottles and occasional roots and sub-rounded small limestone clasts	Colluvium
	1.33–1.23	Reddish-brown (5YR 4.5/4) with mottles black (5YR 2.5/1) and yellowish-red (2.5YR 4/8) diamict with sub-angular to sub-rounded limestone clasts in a silty clay matrix with manganese and iron oxide staining	
	1.23–0.75	Breccia of sub rounded pale yellow (2.5Y 7/4) limestone fragments in a matrix of crushed limestone	Made ground
	0.75–0.54	Light yellowish-brown (2.5Y 6/4) with occasional mottles of brown (7.5YR 5/4) and light olive-grey (5Y 6/2) slightly clayey silt light	Overbank alluvium, gleyed

Table A3.5. *Stratigraphy and interpretation of the Xemxija 2 core.*

Core segment	Depth (m)	Description	Interpretation
XEM2-8	9.33–8.99	Brown (10YR 4/3) breccia of clay soil aggregates. Occasional charcoal and limestone chippings. Some voids	Mass-flow deposits of aggregates derived from eroded soil profiles, from a series of grain/mud flow events
	8.99–8.91	Very dark grey (2.5Y 3.5/1.5) clay with shell fragments and very finely comminuted charcoal	Paludal marsh sediments. Marsh was episodically in receipt of distal mudflows or muddy floods
	8.91–8.72	Grey (2.5Y 5/1) slightly gritty grey clay with limestone lumps, odd little tufaceous bits, very small shell fragments. Quite frequent charcoal	
	8.72–8.66	Black (10YR 2/1) highly organic slightly silty clay. Possible burrow, may also be soft sediment deformation structures	
	8.66–8.55	Dark grey (10YR 3.5/1) silty clay/clayey silt with shell fragments and odd tiny limestone particles. Lots of very waterlogged wood	
XEM2-7	8.22–7.89	Dark greyish-brown (10YR 4/2) breccia of soil aggregates up to 5–6 mm across. Quite a lot of void space. Very occasional shell fragments, occasional limestone chippings. Very slightly silty clay	Mass-flow deposits of aggregates derived from eroded soil profiles, from a series of grain/mud flow events
	7.89–7.63	Brown (10YR 4/3) breccia of soil aggregates, mostly matrix-supported but some slightly clast-supported. Slightly silty clay with possible dark soil mottles. Odd tiny charcoal flecks and limestone bits	
	7.63–7.38	Greyish-brown (10YR 4.5/2) diamict. Slightly silty clay matrix, mostly in the form of sub-rounded soil aggregates. Quite stony (up to 2 cm irregular limestone lumps). Occasional charcoal	
	7.38–7.26	Dark greyish-brown (10YR 4.5/2) clay with tiny black flecks (probably charcoal), odd limestone pebbles and charcoal/wood. Fairly dense, not much structure, occasional quite large voids	
XEM2-6	7.17–6.88	Dark grey (10YR 4.5/1.5) clay with occasional charcoal and limestone fragments. Very little shell compared with units above. Some quite large (*c.* 8 cm) rootlets, some containing very rotten organic matter. Mottling at top of unit. Small patches where pellets of soil (peds) are present – soil aggregates?	Marshy soil with input of aggregates from eroded soil profiles
	6.88–6.81	Very dark grey (10YR 3/1) slightly silty clay with odd shells, piece of charcoal, small mud pellet	Freshwater lagoon with declining clastic input through time
	6.81–6.69	Dark grey (10YR 4/1) slightly tufaceous clay with odd shell fragments and occasional vegetable matter	
	6.69–6.53	Black (10YR 2/1) highly organic slightly clayey silt. Contains mollusc fragments, at least one seed and rather decayed wood/charcoal	
	6.53–6.22	Very dark grey (10YR 3/1) highly organic slightly silty clay with occasional tufa lumps, some freshwater molluscs, tiny organic chunks (wood/charcoal). Vague layering in places, particularly at bottom	
XEM2-5	6.12–6.05	Very dark grey (10YR 3/1) silty clay with abundant tufa lumps. Also contains molluscs and black organic matter (wood/charcoal). Denser than layer above	
	6.05–5.72	Grey (10YR 4.5/1) clay with definite lumps of charcoal, wood fragments and tufa lumps	
	5.72–5.64	Grey (10YR 5/1) highly organic clay with plant fragments. Odd limestone fragments and shell, much comminuted organic matter	
	5.64–5.62	Grey (10YR 4.5/1) smooth clay with tiny shell fragments	
	5.62–5.59	Dark grey (5YR 4/1) silty clay with much finely divided organic matter. Little bits of charcoal/wood and shell	
	5.59–5.43	Yellowish-brown (10YR 5/5) clay with occasional tufaceous lumps and limestone pebbles, odd shell fragments and bits of charcoal/wood	
	5.43–5.28	Brownish-grey (10YR 4/1) very organic-rich clay with occasional shells, some plant fibres, lumps of tufa and wood/charcoal. Limestone pebble. Slightly gritty (sand-sized limestone)	
	5.28–5.23	Black (10YR 2/1) very rich silty clay. Drawn down in burrow-like structure to 5.33 m	

Table A3.5 *(cont.).*

Core segment	Depth (m)	Description	Interpretation
XEM2-4	5.03–4.26	Brownish-grey (10YR 5/1) highly organic slightly silty clay. Occasional slightly tufaceous lumps, little bits of shell and limestone chippings, small fragments of wood and/or charcoal, very occasional molluscs. Large rock at 4.63–4.58 m. Possibly was another at 4.40–4.36 m. A *c.* 5 mm thick blackish band at 4.71 m. Slightly tufaceous band at 4.88 m	
	4.26–4.24	Black (10YR 2/1) laminated fibrous organic matter, humification H7 interspersed with a very thin clay layer (5 mm). Very pasty macrofossils, small lump of tufa	
	4.24–4.18	Brownish-grey (10YR 4/1) slightly silty clay with shell fragments and organic matter fragments (possibly wood)	
	4.18–4.11	Black (10YR 2/1) organic matter, humification H7, with plant macrofossils. Very little structure	
XEM2-3	4.02–3.34	Grey (5Y 5.5/1) slightly shelly clay with occasional limestone fragments	Lagoon of variable salinity
	3.34–3.26	Brown (2.5Y 5/2) silty clay with occasional tiny limestone fragments and shell fragments. Gradual transition to	
	3.26–3.15	Grey (2.5Y 5/1) clay with odd limestone pebbles and some very finely divided charcoal. Gradual transition to	
XEM2-2	3.03–2.96	Grey (5Y 4.5/1) slightly shelly clay. Appears to have faint partings – may well be laminated	
	2.96–2.87	Grey (2.5Y 6/1) slightly shelly clay with yellowish (10YR 5/4) mottling and odd charcoal fragments. Indefinite transition over c. 2 cm to	
	2.87–2.85	Greyish-yellow-brown (10YR 5/2) very shelly clay	
	2.85–2.64	Black (2.5Y 5/1) silty clay with very abundant shells (freshwater snails?), charcoal and plant fragments	
	2.64–2.60	Grey (10YR 5/1) very shelly clay with odd charcoal fragments	
	2.60–2.52	Light brownish-grey (2.5Y 6/2) very shelly clay containing chunk of wood. Gradual transition to	
	2.52–2.46	Black (2.5Y 5/1) slightly clayey sand with abundant shell fragments (estuarine gastropods). Becomes siltier downwards	
	2.46–2.23	Black (2.5Y 5/1) slightly silty clay with some charcoal and plant fibres, very occasional wood and shell fragments	
	2.23–2.15	Brown (10YR 5/3) clay with odd bits of charcoal. More oxidized form of unit above	Seasonal lagoon passing upwards into pedogenically altered overbank floodplain
	2.15–2.10	Light brownish-grey (2.5Y 4/2) pure clay with occasional grassy fibres, small charcoal fragments and small piece of wood.	
	2.10–1.98	Olive-brown (2.5Y 4.5/3) mottled with brownish yellow (10YR 6/6) silty clay	
XEM2-1	2.03–1.87	Dull yellowish-brown (10YR 4.5/3) silty clay with odd smears of black (manganese or charcoal?) and some definite charcoal fragments	
	1.87–1.73	Dull yellowish-brown (10YR 5/4) fairly uniform clay with poorly developed pedogenic structures	
	1.73–1.52	Dull orange-brown (10YR 5.5/4) with mottles of yellowish-brown (10YR 5/8) silty clay with rusty mottles (probably alongside root voids). Occasional angular limestone particles and charcoal	Pedogenically altered colluvium
	1.52–1.36	Orange (2.5Y 6/6) clay with very occasional limestone clasts and black charcoal-like smears.	
	1.36–1.33	Yellowish-brown (10YR 5/6) slightly gritty slightly pebbly silty clay	
	1.33–1.17	Limestone rubble	Made ground

Table A3.6. *Stratigraphy and interpretation of the Wied Żembaq 1 core.*

Core	Depth (m)	Description	Interpretation
WZ1-5	5.48–5.23	Black (10YR 2/1) clay with minor sand component. Occasional shells and root channels. Core stopped by stone at 5.48 m	Salt marsh
	5.23–4.84	Dark grey (10YR 4/1) clay, less sandy than unit above. Dark-stained root channels, small shells and stones (*c.* 2–3 mm) present	
	4.84–4.54	Dark brown (10YR 3/3) slightly sandy orange clay with occasional shells and small stones. Particularly stony layer 4.69–4.74 m	
WZ1-4	4.51–3.71	Dark grey (10YR 4/1) clay, slightly organic. Occasional shells, small stones and root channels. Black (10YR 2/1) organic band 4.0–4.2 m	
	3.71–3.64	Dark brown (10YR 3/3) lightly sandy smooth brown clay.	Colluvium on the fringes of a floodplain
	3.64–3.51	Dark yellowish-brown (10YR 3/4) sandy clay with occasional shells, dark staining along root channels and small limestone fragments	
WZ1-3	3.49–2.51	Dark yellowish-brown (10YR 4/4) sandy clay with occasional shells, dark staining along root channels and small limestone fragments, darkening at base	
WZ1-2	2.42–2.36	Brown (10YR 4/3) slightly sandy orange clay containing small limestone fragments and shells	Salt marsh with input of colluvial sediments
	2.36–2.16	Weathered limestone	
WZ1-1	2.16–1.74	Dark brown (10YR 3/3) clay with black mottling along several root channels. More shelly than unit above	
	1.74–1.42	Yellowish-brown (10YR 5/4) slightly sandy orange clay containing small limestone fragments and shells. Large stone at 1.45–1.52 m	
	1.42–1.28	Yellowish-brown (10YR 5/4) sandy clay	Alluvial overbank
	1.28–1.16	Compact brown (7.5 YR 4/4) clay with occasional limestone grit	

Table A3.7. *Stratigraphy and interpretation of the Wied Żembaq 2 core.*

Core segment	Depth (m)	Description	Interpretation
WZ2-5	5.13–5.03	Very dark grey (10YR 3/1) clay. Large limestone boulder at 5.05–5.19 m, below this is almost pure clay	Salt marsh in receipt of occasional colluvial sediment
	5.03–4.89	Very dark greyish-brown (10YR 3/2) same as lowest unit in WZ2-4, but more brownish hue	
WZ2-4	4.90–4.82	Very dark grey (10YR 3/1) slightly sandier clay with occasional small shells and stones. Slightly organic? Transitional zone over 2 cm	
	4.82–4.74	Dark yellowish-brown (10YR 4/4) clay. Less sandy with occasional small stones. Sharp boundary	
	4.74–4.71	Dark yellowish-brown (10YR 4/4) sandy clay with small (2–3 mm) limestone fragments. Sharp boundary	
WZ2-3	3.95–3.85	Very dark grey (10YR 3/1) clay with higher sand content	
	3.85–3.18	Very slightly darker than unit above. More frequent dark staining along root channels	Shallow possibly seasonal saline lagoon with marine connection and input of colluvial sediment
	3.18–2.95	Sandy dark brown (10YR 3/3) clay with occasional small rotten limestone fragments (2–3 mm). Some dark staining along root channels	
WZ2-2	2.95–2.89	Dark brown (10YR 3/3) silty clay	
	2.89–2.65	Large pieces of rotten limestone	
	2.65–2.21	Brown (10YR 4/3) slightly sandy clay with occasional small shells and limestone fragments (2–3 mm)	
WZ2-1	1.95–1.35	Brown (10YR 5/3) varying to (10YR 4/3) slightly sandy clay with occasional small shells and limestone fragments (2–3 mm)	
	1.35–1.31	Brown (7.5YR 4/2) darker brownish-red clay	
	1.31–1.15	Compact brown (7.5 YR 4/4) clay. Large stone at base	

Table A3.8. *Stratigraphy and interpretation of the Mgarr ix-Xini core.*

Core segment	Depth (m)	Description	Interpretation
MGX1-K	7.43–7.21	Pale brown (2.5Y 7/4) gravel fining up to silt. From base to 7.375 m clasts are sub-angular to angular with a size range 42 x 33 mm to 20 x 19 mm; clast at 7.28–7.32 m is sub-rounded and 48 x 46 mm. Rest of unit consists of granules and fine gravels in a slightly clayey sandy silt matrix. Very compacted. Ggmax2, Ggmin1, Gs1, Ag 2%, As 5%	Estuary subjected to high-energy flood events delivering coarse clastics as gravity flows, interspersed with fine-grained sediments from fall-out
	7.21–7.12	Light greyish-brown (2.5Y 6/3) coarse and fine sands with some broken shell fragments. Gs4, Ggmin 2%	
	7.12–6.93	Grey (10Y 4/1) slightly silty clay. As3, Ag1	
	6.93–6.84	Breccia. Ggmax2, As1, Ag1	
MGX1-J	6.80–6.75	Light yellow (2.5Y 7/4) very consolidated slightly gravelly sand with coarse silt. Poorly sorted, no bedding. Clasts sub-angular to sub-rounded. Gs2, Ga1, Ggmin 1	
	6.75–6.60	One or two large gravel clasts, some mud but mostly missing. No Troels-Smith description possible. Probably openwork gravel.	
	6.60–6.45	Yellowish grey (2.5Y 5/1) poorly sorted muddy sand with gravel. Shell fragments throughout. Gs2, Ga1, Ggmin1	
	6.45–6.21	Not recovered	
MGX1-I	6.17–5.82	Very dark grey (2.5Y 3/1) slightly clayey fine sandy silt with some gravel. Cryptic plane bedding. Some plant remains. Ag2, Ga1, Gs1, As *c.* 5%	
	5.82–5.72	Very dark grey (2.5Y 3/1) slightly gravelly silt. As3, Gs1, Ggmin 2–5%	
	5.72–5.58	Olive-yellow (5Y 6/4) gravel with one very big clast (30 x 26 mm). Gs3, GGmin1, Ggmax *c.* 2%	
MGX1-H	5.38–5.33	Dull yellow (2.5Y 6/4) gravelly coarse sand with some shell fragments. Grains sub-rounded and poorly sorted. Gs3, Ggmin1	
	5.33–5.06	Grey (5Y 5/1) (at 5.295 m grading to yellowish-grey (2.5Y 4/1) shelly sand. Bedding shown by sharp colour changes. Ag2, Ga1, Gs1, Ggmax 2–5%, Ggmin 2–5%	
	5.06–4.95	Dull yellow (2.5Y 6/3) at 5.01 m grading to grey (5Y 5/1) gravelly sandy mud. Poorly sorted, no bedding. Ggmin1, Ag1, Gs2, Ggmax 1–2%	
MGX1-G	4.91–4.69	Bright yellowish-brown (2.5Y 7/6) coarse sand, fining upward into medium sand with a mud drape of sandy silty clay. Gs3, Ga1	
	4.69–4.65	Greyish-yellow (2.5Y 7/2) gravel, with large angular to sub-angular clasts with some sand and silt. Ggmax3, Gs1, Ga *c.* 5%	
	4.65–4.60	Grey (10Y 5/1) coarse to medium sandy clayey silt with a little gravel. Gs1, Ga1, Ag2	
	4.60–4.56	Greyish-yellow (2.5Y 7/2) poorly sorted coarse sand with some granules and a gravel clast. Gradual transition into overlying unit. Ggmax1, Ggmin1, Gs2	
	4.56–4.46	Grey (10Y 6/1) poorly sorted sandy silty mud. Gs1, Ga1, Ag1, Ggmin 2–5%	
	4.46–4.32	Light yellow (2.5Y 7/3) poorly sorted gravels. One large (c. 15 x 46 mm) gravel clast). Gs2, Ggmin1, Ggmax1	
MGX1-F	4.28–4.15	Greyish-olive (7.5Y 5/2) massive fine to medium silt with shell fragments and slightly humified plant remains throughout. Some complete shell tests. 4.24–4.25 m: poorly sorted silty gravelly sands. Ag3, Gs1, Ggmin *c.* 5%, shell fragments *c.* 10%	
	4.15–3.97	Pale yellow (2.5Y 8/4) fine to coarse gravel. Ggmin3, Ggmax1	
	3.97–3.78	Light yellow (2.5Y 7/4) silty gravelly coarse shelly sand. Lots of broken shell fragments. Clasts fairly angular. Ga1, Gs3	
	3.78–3.69	Not recovered	

Table A3.8 *(cont.).*

Core segment	Depth (m)	Description	Interpretation
MGX1-E	3.65–3.62	Grey (5Y 5/1) moderately well sorted sandy mud with some granules and gravel. Some shells. As1, Ag1, Ga1, Gs1	
	3.62–3.57	Grey (5Y 5/1) sandy gravelly mud/muddy sand with broken shell fragments. Sharp upper boundary; more diffuse lower boundary. Gs2, As1, Ag1	
	3.57–3.55	Grey (5Y 5/1) moderately well sorted sandy mud with some granules and gravel. Some shells. Sharp upper boundary. As1, Ag1, Ga1, Gs1	
	3.55–3.37	Light grey (10Y 7/1) very well lithified sandy muddy micrite with manganese nodules. Bedded, friable. No Troels-Smith description possible	Palaeosol with calcrete developed on estuarine sediments suggesting a strongly seasonal climate and several hundred years of emergence above sea level.
	3.37–3.33	Grey (5Y 5/1) sandy mud with some shell fragments and manganese nodules; fewer plant remains. As2, Ag1, Gs1, Dl 2–5%, Dh 2–5%, Ggmin 2–5%	
	3.33–3.30	Light olive-grey (5GY 7/1) almost pure massive clay with some roots present. As3, Ag1	
	3.30–3.09	Grey (5Y 5/1) gravelly sandy mud with some shell fragments. Woody (?) plant macrofossil at 3.24 m. As2, Ag1, Gs1, Dl 2–5%, Dh 2–5%, Ggmin 2–5%	Estuarine sediment
	3.09–3.06	Light greenish-grey (5GY 7/1) almost pure massive clay with a few roots. As3, Ag1	Short-lived palaeosol
MGX1-D	3.02–2.98	Not recovered	
	2.98–2.95	Grey (7.5Y 4/1) clayey silt with sand, trace of organic detritus. As1, Ag1, Gs2	Estuary with fine deposits from fall-out interspersed with coarse clastics deposited from gravity flows originating as catchment floods
	2.95–2.82	Grey (10Y 6/1) clayey, sandy silt. As1, Ag2, Gs1	
	2.82–2.69	Grey (10Y 4/1) clayey, sandy silt. As1, Ag2, Gs1	
	2.69–2.60	Grey (10Y 6/1) clayey, sandy silt, As1, Ag2, Gs1	
	2.60–2.43	Greyish-olive (5Y 5/2) gravelly sand, poorly sorted, well rounded clasts. Gs3, Gg(min)1, Lim. 3	
MGX1-C	2.39–2.14	Light olive grey (2.5GY 7/1) massive slightly gravelly silty clay. Some humified plant detritus and broken shells. Ag1, As3, Dl *c.* 10%, Dh c.5%, Ggmin *c.* 2–5%.	
	2.14–1.91	Greyish-olive (7.5Y 5/2) poorly sorted shelly gravelly sand. Shell mostly fragmentary. Gs3, Ggmin1	
	1.91–1.80	Not recovered	
MGX1-B	1.76–1.49	Greyish-olive (7.5Y 6/2) coarse slightly gravelly sand with some shell fragments and humified detritus Gs4, Dh 5%, Gg(min) 5%	
	1.49–1.39	Greyish-olive (5Y 4/2) sandy coarse gravel. Gs1, Gg(max)2, Gg(min)1, Lim. 3–4	
	1.39–1.26	Not recovered	
	1.26–1.17	Light yellow (2.5Y 7/4) very poorly sorted gravelly sand Gs3, Gg(min)1, Gg(max)10%, Lim. 4	
MGX1-A	1.13–0.93	Pale yellow (2.5Y 8/4) poorly sorted gravelly sand with some shell fragments. Ggmin1, Gs2, Ga1	
	0.93–0.54	Dull yellow (2.5Y 6/4) massive slightly stony sandy clayey silt. As1, Ag2, Gs2, Ggmin 5–10%	

Table A3.9. *Stratigraphy and interpretation of the Marsaxlokk core (a second core, MX2, was attempted but was blocked at 2 m).*

Core	Depth (m)	Description	Interpretation
MX1-4	3.86–3.53	Pale pinkish-brown (10YR 8/4) calcitic silt; dense amorphous calcium carbonate	Palaeosol: rather muddy plugged calcrete horizon
	3.53–3.32	Pinkish-brown (10YR 7/4), calcitic silty clay loam with common weathered limestone	Palaeosol: B horizon
	3.32–2.92	Brown to reddish-brown (5YR 4/4) silty clay loam	Palaeosol: *in situ terra rossa* topsoil; Early to mid-Holocene
	2.92–2.86	Light yellowish-brown (10YR 6/4) fine gravel and coarse sand with marine shell fragments	Probable ancient beach
MX1-3	2.86–2.45	Dark yellowish-brown (10YR 4/4) silty clay loam with frequent fine limestone pebbles	Lagoon with abundant terrestrial clastic input
	2.45–1.92	Yellowish-red (5YR 4/4) silty (clay) loam with occasional fine limestone pebbles	Salt marsh in receipt of abundant terrestrial clastic sediment
	1.92–1.86	Pale brown (10YR 6/3) fine gravel and coarse sand	
MX1-2	1.85–1.70	Light brownish-grey (10YR 6/2) very fine sandy/silt; possibly micro-laminated; laminar humified and amorphous sesquioxide replaced plant remains	
	1.70–1.65	Very dark grey (10YR 3/1) organic silt mud	
	1.65–1.55	Brownish-yellow (10YR 6/6) fine gravel and coarse sand	
	1.55–0.86	Light grey (10YR 7/1), calcitic, very fine sandy silt	
MX1-1	0.86–0.50	Light yellowish-brown (10YR 6/4) silt loam	
	0.50–0.12	Pale brown (10YR 6/3) fine sandy/silt loam with fine limestone fragments	

Table A3.10. *Stratigraphy and interpretation of the Marsa 2 core (after Carroll 2007).*

Core segments	Depth (m)	Munsell colour	Description	Interpretation
11	9.25–8.8	7.5YR5/6	Strong brown stony sandy silty clay, below 8.95 m sandy clayey gravel. Rockhead at 9.25 m	Riverine braidplain sediments
10	8.8–8.2	7.5YR5/6-5YR3/4	Strong brown stony sandy silty clay, then at 8.5 m dark reddish brown very stony sandy silty clay, with a large rock between 87.5 and 8.8 m	Riverine braidplain sediments
9	8.2–7.6	7.5YR6/6-7.5YR5/6-7.5YR4/6-5YR3/4	Reddish-yellow gravel, then at 7.85 m strong brown silty sand, then at 8.05 m dark reddish brown sandy silty clay	Riverine braidplain sediments
8	7.6–7.0	7.5YR6/8-7.5YR5/6-7.5YR6/6	Reddish-yellow gravel, then at 7.15 m strong brown stony silty sand, at 7.25 m strong brown clayey silty sand, at 7.50 m reddish yellow clayey silty sand	Riverine praidplain sediments
7	6.8–5.9	2.5YR4/1-7.5YR3/3-5YR3/2-10YR4/3-10YR5/4-10YR5/3	Dark grey silty clay with marine shell, with a sharp change at ~6.28 m to dark brown sandy clay, then at ~6.42 m brown and yellowish-brown silty sand, then at 6.5 m yellowish-brown stony silty sand grading into gravel, then at 6.75 m brown stony silty sand	Quiet-water estuarine sediments. Below 6.28 m riverine braidplain sediments, possibly of Late Pleistocene age
6	5.2–4.2	2.5YR4/1	Dark grey sandy silty clay with marine shell	Quiet-water estuarine sediments
5	4.2–3.2	2.5YR5/1-2.5YR4/1	Grey sandy silty clay with marine shell becoming dark grey below 3.85 m and increasingly sandy below 4.05 m	Quiet-water estuarine sediments, with some distal fluvial input below 4.05 m
4	3.2–2.55	7.5YR5/6-5YR3/4	Grey sandy silty clay with some marine shell, large rock and some stones between 2.55 and 2.7 m	Quiet-water estuarine sediments with a density-flow deposit between 2.55 and 2.7 m
3	2.2–1.7	2.5YR6/1-2.5YR5/1	Grey silty sand, passing into grey sandy silty clay below 1.85 m	Estuarine sediments
2	1.2–0.8	10YR5/4-10YR 5/2	Yellowish-brown sandy silt becoming greyish brown below 0.95 m	Overbank and colluvial sediments
1	0.3–0	10YR6/4	Yellowish-brown sandy silt	Overbank and colluvial sediments

Table A3.11. *Stratigraphy and interpretation of the Mellieha Bay core.*

Core	Depth (m)	Description	Interpretation
MB1-E	5.44–5.36	Not recovered	
	5.36–5.15	Light grey (2.5Y 7/2) silty clay, with pocket of relatively well-sorted sand at 5.26–5.28 m, grading to very dark greyish-brown (10YR 3/2) at bottom. Shell fragments present throughout. Sharp upper boundary. Ag1, As3	Offshore suspension deposits, below wave-base. Sand layer probably relates to storm sedimentation
	5.15–4.44	Medium to coarse grey (5Y 6/1) sand with traces of gravel at *c*. 5.38 m and granules at *c*. 5.27 m. Grains sub-rounded. Organic material and shell fragments present throughout. Gs3, Ga1, Ggmin 2%	Shallow marine sands, probably within wave-base
MB1-D	4.44–4.27	Coarse grey (10Y 6/1) slightly clayey well-sorted sand with shell fragments. Diffuse upper boundary. Gs3–4.	
	4.27–4.24	Light grey (10Y 7/1) slightly silty fine to medium sand with shell fragments. Sharp upper boundary. Gs3, Ga1	
	4.24–4.23	Light grey (10Y 7/1) poorly sorted fine gravel and very coarse sand with shell fragments. Sharp upper boundary; slightly diffuse lower boundary. Gs3, Ggmin1	
	4.23–3.44	Pale yellow (7.5Y 8/3) moderately sorted slightly gravelly medium to coarse sand. (*c*. 2–5% fine gravel). Grains sub-angular to sub-rounded. Eelgrass noted at 4.17–4.18 m; macroscopic charcoal at 4.08 m. Slight colour change and fining upwards towards top of unit – diffuse transition from *c*. 3.74 m. More shell fragments present from 30–36 cm. Gs3, Gg1 (whole unit)	
MB1-C	3.35–3.18	Grey (5Y 5/1), darkening to very dark grey (10YR 3/2) by 3.19 m, very shelly clay with some coarse sand. As3, Gs1	Suspension deposits below wave base
	3.18–3.14	Grey silty clay (5Y 5/1). Ag3, As1	
	3.14–2.44	Pale brown (2.5Y 7/3) slightly clayey slightly gritty silt (~90% silt) transitioning to grey (5Y 5/1) silt at 2.53 m. Gs4, Ggmin 5%, Lim. 2	
MB1-B	2.44–2.01	Grey (5Y 5/1) slightly gravelly, gritty coarse to medium sand with shell fragments. Grains sub-rounded to sub-angular. Some laminations apparent at 2.28–2.305 m. Some very faint possible structure below this. Diffuse upper boundary. Gs4, Ggmin 1–2%, also shell fragments	Shallow marine sands, probably within wave-base
	2.01–1.60	Pale brown (2.5Y 7/3) medium sand, well-sorted. Fewer shell fragments than previously. Grains mainly sub-rounded. Some fine silt content (*c*. 10%). Some structure visible – bedding at 1.81–1.92 m. Slightly diffuse upper boundary. Gs3, Ga1	Beach or shallow marine within wave-base
	1.60–1.48	Light yellow (5Y 7/3) fine sandy silt. Well-sorted. Gs2, Ga2	Lagoon
	1.48–1.44	Light yellow (5Y 7/3) well-rounded to sub-rounded medium to coarse sand with some shell fragments	Beach
MB1-A	1.44–1.42	Large clast of ~35 mm	
	1.44–1.24	Greyish-brown (2.5Y 5/2) sand becoming paler (2.5Y 7/3) at 1.265 m; medium to coarse, sub-rounded to rounded. Gs4	
	1.24–1.19	Greyish-brown (2.5Y 5/2) sand with clay and silt, noticeable root material present. Gs2, Ag1, As1, Dl5%	Paludal marsh or shallow lagoon
	1.19–1.08	Pale brown (2.5Y 7/3) coarse to very coarse sand with angular to sub-angular grains; 62–73	Beach
	1.08–0.66	Pale brown (2.5Y 7/3) medium sand with sub-angular to sub-rounded grains	Dune sand
	0.66–0.64	Black (N1) organic clay mud, ~ 6 mm thick layer	Dune slack
	0.64–0.44	Pale brown (2.5Y 7/3) medium to coarse sand with angular to sub-angular grains. Top 15 cm collapsed and unconsolidated. Gs4	Dune sands

Table A3.12. *Key to the scheme for the description of Quaternary sediments, modified to exclude categories of organic sediments not encountered (after Troels-Smith 1955).*

Class	Code	Element	Description
Detritus	Dl	*Detritus lignosus*	Fragments of woody plants > 2 mm
	Dh	*Detritus herbosus*	Fragments of herbaceous plants > 2 mm
	Dg	*Detritus granosus*	Woody and herbaceous plant remains < 2 mm and > 0.1 mm
Argilla	As	*Argilla steatodes*	Particles of clay < 0.002 mm
	Ag	*Argilla granosa*	Particles of silt 0.06 to 0.002 mm
Grana	Ga	*Grana arenosa*	Mineral particles 0.6 to 0.2 mm
	Gs	*Grana saburralia*	Mineral particles 2.0 to 0.6 mm
	Gg(min)	*Grana glareosa minora*	Mineral particles 6.0 to 2.0 mm
	Gg(max)	*Grana glareosa majora*	Mineral particles 20.0 to 6.0 mm

Appendix 4

Granulometry of the deep cores

Katrin Fenech

Table A4.1. *Marsa 2.*

Depth (cm)	3	8	13	18	23	28	33	38	43
>8 mm	0	13	0	0	0	0	0	0	0
>500 µ	7	12	15	21	15	17	0	0	0
>63 µ	59	53	56	48	56	87	100	100	100
<63 µ	146	123	145	156	135	132	0	0	0
Munsell	10 YR 6/4	10 YR 6/4	10 YR 6/4	10 YR 6/4	10 YR 6/4	10 YR 6/4			

Depth (cm)	48	53	58	63	68	73	78	83	88
>8 mm	0	0	0	0	0	0	0	0	0
>500 µ	0	0	0	0	0	0	0	15	58
>63 µ	100	100	100	100	100	100	100	65	13
<63 µ	0	0	0	0	0	0	0	191	144
Munsell								10 YR 5/4	10 YR 5/4

Depth (cm)	93	98	103	107	113	118	123	128	133
>8 mm	0	0	0	0	12	132	100	100	100
>500 µ	17	15	14	22	25	24	0	0	0
>63 µ	58	65	77	72	90	30	0	0	0
<63 µ	103	127	127	126	81	48	0	0	0
Munsell	10 YR 5/4	2.5 YR 5/2	2.5 YR 5/2	2.5 YR 5/2	2.5 YR 5/2	2.5 YR 5/2			

Depth (cm)	138	143	148	153	158	163	168	173	178
>8 mm	100	100	100	100	100	100	100	49	38
>500 µ	0	0	0	0	0	0	0	38	26
>63 µ	0	0	0	0	0	0	0	90	43
<63 µ	0	0	0	0	0	0	0	116	24
Munsell								2.5 YR 6/1	2.5 YR 6/1

Depth (cm)	183	188	193	198	203	208	213	218	223
>8 mm	8	8	0	0	0	0	0	0	100
>500 µ	57	55	23	10	12	8	10	8	0
>63 µ	54	57	51	28	18	38	36	33	0
<63 µ	45	53	105	136	140	89	98	141	0
Munsell	2.5 YR 6/1	2.5 YR 6/1	2.5 YR 6/1	2.5 YR 5/1	2.5 YR 5/1	2.5 YR 5/1	2.5 YR 5/1	2.5 YR 5/1	

Table A4.1 *(cont.).*

Depth (cm)	228	233	238	243	248	253	258	263	268
>8 mm	100	100	100	100	100	100	137	42	133
>500 µ	0	0	0	0	0	0	0	7	12
>63 µ	0	0	0	0	0	0	0	9	19
<63 µ	0	0	0	0	0	0	0	16	34
Munsell							2.5 YR 5/1	2.5 YR 5/1	2.5 YR 5/1

Depth (cm)	273	278	283	288	293	298	303	308	313
>8 mm	30	0	0	0	0	0	0	0	0
>500 µ	14	13	7	11	12	14	10	13	14
>63 µ	31	32	31	45	44	34	24	39	29
<63 µ	89	120	108	111	72	105	88	74	91
Munsell	2.5 YR 5/1	2.5 YR 5/1	2.5 YR 5/1	2.5 YR 5/1	2.5 YR 5/1	2.5 YR 5/1	2.5 YR 5/1	2.5 YR 5/1	2.5 YR 5/1

Depth (cm)	318	323	328	333	338	343	348	353	358
>8 mm	0	0	0	0	0	0	0	0	0
>500 µ	12	9	17	12	16	16	16	18	22
>63 µ	24	29	33	41	30	23	38	32	38
<63 µ	103	53	75	60	74	66	62	92	99
Munsell	2.5 YR 5/1	2.5 YR 5/1	2.5 YR 5/1	2.5 YR 5/1	2.5 YR 5/1	2.5 YR 5/1	2.5 YR 5/1	2.5 YR 5/1	2.5 YR 5/1

Depth (cm)	363	368	373	378	383	388	393	398	403
>8 mm	0	0	0	0	0	0	0	0	0
>500 µ	26	14	18	17	18	16	20	34	31
>63 µ	36	48	45	34	48	44	50	54	62
<63 µ	92	50	103	87	66	80	79	48	68
Munsell	2.5 YR 5/1	2.5 YR 5/1	2.5 YR 5/1	2.5 YR 5/1	2.5 YR 5/1	2.5 YR 4/1	2.5 YR 4/1	2.5 YR 4/1	2.5 YR 4/1

Depth (cm)	408	413	418	423	428	433	438	443	448
>8 mm	0	0	0	0	0	0	0	0	0
>500 µ	23	24	34	31	24	12	21	22	29
>63 µ	73	62	72	53	42	27	38	40	46
<63 µ	42	72	101	63	63	23	47	43	52
Munsell	2.5 YR 4/1	2.5 YR 4/1	2.5 YR 4/1	2.5 YR 4/1	2.5 YR 4/1	2.5 YR 4/1	2.5 YR 4/1	2.5 YR 4/1	2.5 YR 4/1

Depth (cm)	453	458	463	468	473	478	483	488	493
>8 mm	0	0	0	0	20	4	0	26	0
>500 µ	19	41	31	38	28	46	30	28	29
>63 µ	44	57	60	61	55	52	50	40	49
<63 µ	46	58	58	83	71	64	76	85	84
Munsell	2.5 YR 4/1	2.5 YR 4/1	2.5 YR 4/1	2.5 YR 4/1	2.5 YR 4/1	2.5 YR 4/1	2.5 YR 4/1	2.5 YR 4/1	2.5 YR 4/1

Depth (cm)	498	503	508	513	518	523	528	533	538
>8 mm	0	14	42	0	17	0	0	0	0
>500 µ	25	41	31	34	10	100	0	0	0
>63 µ	45	49	37	34	46	100	100	100	100
<63 µ	84	69	55	96	112	0	0	0	0
Munsell	2.5 YR 4/1	2.5 YR 4/1	2.5 YR 4/1	2.5 YR 4/1	2.5 YR 4/1				

Table A4.1 *(cont.).*

Depth (cm)	543	548	553	558	563	568	573	578	583
>8 mm	0	0	0	0	0	0	0	0	0
>500 µ	0	0	0	0	0	0	0	0	0
>63 µ	100	100	100	100	100	100	100	100	100
<63 µ	0	0	0	0	0	0	0	0	0
Munsell									

Depth (cm)	588	593	598	603	608	613	618	623	628
>8 mm	0	0	0	0	11	0	0	2	0
>500 µ	0	28	30	29	26	35	37	23	14
>63 µ	100	29	32	19	29	31	23	29	31
<63 µ	0	24	59	61	62	51	68	59	97
Munsell		2.5 YR 4/1	2.5 YR 4/1	2.5 YR 4/1	2.5 YR 4/1	2.5 YR 4/1	2.5 YR 4/1	2.5 YR 4/1	2.5 YR + 7.5 YR 3/2

Depth (cm)	633	638	643	648	653	658	663	668	673
>8 mm	0	0	8	12	36	16	73	46	55
>500 µ	30	13	22	42	50	45	33	62	65
>63 µ	42	52	30	47	24	29	29	21	16
<63 µ	82	110	106	99	136	91	85	106	85
Munsell	5 YR 3/2	5 YR 3/2	5 YR 3/2 + 10 YR 4/3	10 YR 4/3	10 YR 5/4	10 YR 5/4	10 YR 5/4	10 YR 5/4	10 YR 5/4

Depth (cm)	678	683	688	693	698	703	708	713	718
>8 mm	154	100	100	100	100	12	8	0	0
>500 µ	52	0	0	0	0	25	45	34	30
>63 µ	25	0	0	0	0	4	11	7	54
<63 µ	40	0	0	0	0	3	14	11	68
Munsell	10 YR 5/3					7.5 YR 6/8	7.5 YR 6/8	7.5 YR 6/8	7.5 YR 5/6

Depth (cm)	723	728	733	738	743	748	753	758	763
>8 mm	0	0	0	0	0	16	4	11	0
>500 µ	23	129	65	61	33	65	56	32	22
>63 µ	47	31	41	32	41	30	34	39	26
<63 µ	112	36	109	94	103	109	106	106	29
Munsell	7.5 YR 5/6	7.5 YR 5/6	7.5 YR 5/6	7.5 YR 5/6	7.5 YR 5/6	7.5 YR 5/6	7.5 YR 6/6	7.5 YR 6/6	7.5 YR 6/6

Depth (cm)	768	773	778	783	788	793	798	803	808
>8 mm	8	0	28	16	10	17	0	0	0
>500 µ	25	70	84	115	46	18	22	18	19
>63 µ	20	46	27	26	35	40	39	56	40
<63 µ	37	61	60	45	113	116	107	117	96
Munsell	7.5 YR 6/6	7.5 YR 6/6	7.5 YR 6/6	7.5 YR 6/6	7.5 YR 5/6	7.5 YR 5/6	7.5 YR 4/6	7.5 YR 4/6	5 YR 3/4

Depth (cm)	813	818	823	828	833	838	843	848	853
>8 mm	6	0	13	0	0	0	31	4	0
>500 µ	21	3	95	50	72	75	51	31	40
>63 µ	31	19	27	34	46	33	36	32	39
<63 µ	151	74	55	59	61	46	41	73	128
Munsell	5 YR 3/4	5 YR 3/4	7.5 YR 5/6	7.5 YR 5/6	7.5 YR 5/6	7.5 YR 5/6	7.5 YR 5/6	7.5 YR 5/6	7.5 YR 5/6

Table A4.1 *(cont.).*

Depth (cm)	858	863	868	873	878	883	888	893	898
>8 mm	0	10	183	47	371	0	5	69	186
>500 µ	19	46	31	47	12	23	41	51	31
>63 µ	21	19	14	14	6	31	42	17	9
<63 µ	128	127	27	30	14	46	46	43	12
Munsell	5 YR 3/4	5 YR 3/4	5 YR 3/4	7.5 YR 5/6		7.5 YR 5/6	7.5 YR 5/6	7.5 YR 5/6	7.5 YR 5/6

Depth (cm)	903	908	913	918	923	928	933	938
>8 mm	128	175	62	59	55	24	75	106
>500 µ	81	40	63	64	61	22	42	58
>63 µ	12	18	20	16	10	4	18	14
<63 µ	24	27	33	31	21	9	23	29
Munsell	7.5 YR 5/6	7.5 YR 5/6	7.5 YR 5/6	7.5 YR 5/6	7.5 YR 5/6	7.5 YR 5/6	7.5 YR 5/6	7.5 YR 5/6

Table A4.2. *Mgarr ix-Xini.*

Depth (cm)	56	60	64	67	71	75	79	82	86
>8mm	1	0	2	3	0	4	4	6	0
>500µ	5	5	6	2	7	8	3	5	8
>63µ	7	8	8	4	8	4	4	6	7
<63µ	33	26	33	20	33	13	13	24	25
Munsell	10YR 5/4	10YR 5/4	10YR 5/4	10YR 5/4	10YR 5/4	10YR 5/4	10YR 5/4	10YR 5/4	10YR 5/4

Depth (cm)	90	93	97	100	104	108	111	120	124
>8mm	10	4	8	0	7	2	9	4	15
>500µ	6	6	5	13	12	13	18	25	10
>63µ	7	8	8	9	8	14	7	9	6
<63µ	23	19	19	10	1	10	1	0	1
Munsell	10YR 5/4	10YR 5/4	10YR 5/4	10YR 5/4 + 7/3	10YR 7/3	10YR 7/3	10YR 7/3	10YR 8/2	10YR 8/2

Depth (cm)	132	142	147	152	157	162	167	172	175
>8mm	16	45	16	0	2	0	2	0	0
>500µ	5	7	11	30	20	13	17	11	5
>63µ	7	10	7	9	11	7	8	8	2
<63µ	2	1	1	1	2	1	0	0	0
Munsell	10YR 8/2	10YR 5/2	10YR 5/2	10YR 6/1	10YR 6/1	10YR 6/1	10YR 6/1	10YR 6/1	10YR 6/1

Depth (cm)	191	195	199	204	208	212	216	220	225
>8mm	0	9	5	10	3	3	0	0	0
>500µ	13	14	25	8	10	5	2	2	2
>63µ	10	11	10	3	5	6	5	4	5
<63µ	1	3	4	3	6	30	35	20	40
Munsell	10YR 7/1	10YR 7/1	10YR 7/1	10YR 7/1	10YR 7/1	10YR 5/1	10YR 5/1	10YR 5/1	10YR 6/1

Table A4.2 *(cont.).*

Depth (cm)	229	233	237	246	251	256	261	266	271
>8mm	0	0	0	10	7	11	2	0	4
>500µ	4	1	2	20	31	29	15	9	7
>63µ	5	2	3	9	12	9	6	12	12
<63µ	34	30	17	1	6	6	25	42	33
Munsell	10YR 6/1	10YR 6/1	10YR 6/1	10YR 5/2	10YR 5/2	10YR 5/2	10YR 5/2 + 6/1	10YR 6/1	10YR 6/1 + 4/1

Depth (cm)	276	281	286	291	296	300	309	314	319
>8mm	0	0	0	0	0	0	0	0	0
>500µ	2	1	1	1	1	1	8	9	8
>63µ	5	5	3	2	4	1	8	11	12
<63µ	30	44	55	58	46	0	38	29	34
Munsell	10YR 4/1	10YR 4/1 + 5/1 + 6/1	10YR 6/1	10YR 6/1	10YR 6/1 + 4/1	10YR 6/1	10YR 6/1	10YR 6/1 + 6/6	10YR 6/1

Depth (cm)	324	329	334	339	344	352	359	364	383
>8mm	0	0	0	36	108	132	0	0	0
>500µ	5	2	2	5	4	21	8	4	10
>63µ	6	5	4	6	4	20	14	7	8
<63µ	27	33	35	22	9	42	34	24	2
Munsell	10YR 6/1	10YR 6/1	10YR 6/1 + 3/1	10YR 6/1 + 3/1	10YR 6/1	10YR 3/1	10YR 3/1	10YR 3/1	10YR 7/2

Depth (cm)	387	391	395	399	403	407	411	415	419
>8mm	0	3	0	6	26	19	11	0	0
>500µ	22	21	30	12	18	12	25	31	21
>63µ	10	10	13	5	6	2	4	3	7
<63µ	3	4	5	5	14	4	6	5	21
Munsell	10YR 7/2	10YR 7/2	10YR 7/2	10YR 7/2 + 3/1	10YR 7/2 + 3/1	10YR 7/2 + 3/1	10YR 7/2 + 3/1	10YR 7/2	10YR 7/2 + 3/1

Depth (cm)	423	427	434	439	444	449	454	459	464
>8mm	0	0	94	26	27	19	7	11	6
>500µ	2	10	7	16	25	7	11	21	15
>63µ	9	9	4	8	10	6	7	10	9
<63µ	38	20	0	2	8	8	14	4	13
Munsell	10YR 4/1	10YR 4/1	10YR 7/2	10YR 7/2	10YR 7/2	10YR 6/1	10YR 6/1	110YR 6/2	10YR 4/1 + 6/2

Depth (cm)	469	474	479	484	489	499	502	506	510
>8mm	31	0	1	0	0	1	2	7	0
>500µ	7	8	17	28	46	7	15	7	6
>63µ	10	17	16	9	5	1	4	6	4
<63µ	7	7	6	2		0	3	4	2
Munsell	10YR 4/1 + 6/2	10YR 4/1 + 6/2	10YR 6/2	10YR 6/2	10YR 6/2	10YR 7/1	10YR 7/1	10YR 7/1	10YR 7/1

Table A4.2 *(cont.).*

Depth (cm)	513	517	520	524	528	531	535	538	542
>8mm	0	0	0	0	15	0	0	0	0
>500µ	3	2	2	3	8	11	23	22	12
>63µ	3	2	2	3	5	5	12	13	10
<63µ	2	2	2	1	4	6	7	9	8
Munsell	10YR 6/1	10YR 6/1	10YR 6/1	10YR 4/1	10YR 4/1	10YR 4/1	10YR 4/1 + 6/4	10YR 4/1 + 6/4	10YR 4/1 + 6/4

Depth (cm)	546	549	553	561	566	571	576	581	586
>8mm	0	0	0	10	24	8	3	1	1
>500µ	6	2	1	24	32	19	8	7	5
>63µ	11	12	8	14	12	8	15	16	14
<63µ	13	22	16	6	8	5	8	12	11
Munsell	10YR 4/1 + 6/4	10YR 5/2	10YR 5/2	10YR 7/2	10YR 7/3	10YR 7/3 + 6/1	10YR 6/1	10YR 6/1	10YR 6/1

Depth (cm)	591	596	601	606	611	615	641	644	648
>8mm	0	0	0	0	0	0	0	1	0
>500µ	2	4	3	2	1	1	7	7	8
>63µ	13	11	11	8	5	7	4	5	5
<63µ	11	16	31	26	25	24	1	0	2
Munsell	10YR 6/1	10YR 6/1	10YR 5/1	10YR 5/1	10YR 5/1	10YR 4/1	10YR 5/1	10YR 5/1	10YR 5/1

Depth (cm)	651	655	658	661	665	668	671	675	678
>8mm	0	0	6	2	7	3	5	7	10
>500µ	13	11	4	5	4	5	8	15	17
>63µ	8	8	7	8	6	4	4	5	6
<63µ	4	4	2	4	1	3	3	5	2
Munsell	10YR 5/1	10YR 5/2	10YR 5/2	10YR 5/2	10YR 5/2	10YR 5/2	10YR 5/2	10YR 7/2	10YR 7/2

Depth (cm)	687	692	697	702	707	712	717	722	727
>8mm	21	16	0	1	1	7	5	34	8
>500µ	15	8	2	7	6	14	14	15	28
>63µ	9	10	6	11	10	8	15	14	9
<63µ	11	10	20	21	24	12	10	13	9
Munsell	10YR 4/1 + 7/2	10YR 4/1	10YR 4/1	10YR 4/1	10YR 4/1	10YR 4/1 + 5/3	10YR 4/1 + 5/3	10YR 5/3	10YR 5/3

Depth (cm)	732	737	741
>8mm	62	40	85
>500µ	17	18	14
>63µ	6	7	10
<63µ	7	5	9
Munsell	10YR 5/3 + 8/2	10YR 5/3 + 8/2	10YR 8/2

Table A4.3. *Salina Deep Core.*

Depth (cm)	1113	1121	1131	1140	1150	1160	1191	1201	1211
>8mm	0	0	0	0	3	0	0	0	0
>500µ	8	26	48	40	70	47	11	62	36
>63µ	112	227	263	156	203	140	128	204	138
<63µ	274	365	384	325	447	374	599	554	589

Depth (cm)	1216	1221	1231	1241	1247	1257	1267	1277	1290
>8mm	0	0	5	3	0	0	0	0	0
>500µ	24	20	43	23	16	36	32	38	48
>63µ	165	127	377	180	135	302	320	305	150
<63µ	183	189	366	435	180	412	454	311	431

Depth (cm)	1300	1310	1384	1394	1404	1414	1425	1434	1444
>8mm	0	12	0	0	0	0	0	0	0
>500µ	121	48	15	9	9	9	6	11	13
>63µ	194	262	86	129	94	121	87	128	178
<63µ	370	435	350	646	466	537	655	507	641

Depth (cm)	1450	1459	1470	1479	1489	1630	1640	1650	1682
>8mm	0	0	0	0	0	0	0	4	0
>500µ	15	47	52	90	69	4	2	28	2
>63µ	70	185	191	257	223	103	87	144	75
<63µ	250	451	439	455	516	438	397	475	521

Depth (cm)	1692	1702	1710	1720	1730	1740	1745	1755	1765
>8mm	0	0	0	0	0	0	0	0	0
>500µ	1	1	1	1	1	1	3	2	1
>63µ	62	57	11	24	47	29	35	18	23
<63µ	391	536	387	701	551	515	193	579	449

Depth (cm)	1770	1780	1790	1841	1851	1861	1869	1879	1889
>8mm	0	0	1	0	0	0	0	0	0
>500µ	3	5	4	2	1	1	1	1	1
>63µ	54	42	62	45	12	15	8	12	6
<63µ	205	519	669	326	523	509	328	575	544

Depth (cm)	1890	1900	1910	1920	1930	1940	1971	1981	1991
>8mm	0	0	0	10	2	0	0	0	0
>500µ	1	1	1	5	4	4	2	2	2
>63µ	8	17	23	30	180	102	17	34	16
<63µ	657	593	669	553	489	529	377	564	462

Depth (cm)	1994	2004	2014	2023	2033	2043	2046	2056	2066
>8mm	0	0	0	0	0	13	0	0	0
>500µ	1	2	3	3	4	3	1	2	2
>63µ	1	13	8	13	17	16	6	6	22
<63µ	221	586	551	514	635	558	275	583	438

Table A4.3 *(cont.).*

Depth (cm)	2070	2080	2100	2101	2103	2105	2106	2113	2123
>8mm	13	0	0	0	0	0	0	1	0
>500µ	6	13	4	1	1	1	1	1	4
>63µ	4	13	12	2	4	7	2	50	12
<63µ	259	581	469	358	653	662	530	388	628

Depth (cm)	2133	2143	2153	2163	2183	2192	2202	2222	2240
>8mm	0	0	0	0	0	0	0	0	0
>500µ	7	1	1	1	1	1	1	1	2
>63µ	34	8	31	4	26	17	20	13	28
<63µ	523	456	411	337	576	487	502	430	554

Depth (cm)	2260	2285	2295	2305	2308	2318	2328	2338	2348
>8mm	0	0	0	0	0	0	0	0	0
>500µ	2	3	5	4	20	21	37	38	2
>63µ	7	8	19	9	70	88	171	164	2
<63µ	511	513	393	553	263	578	393	483	644

Depth (cm)	2358	2363	2368	2380	2390	2398	2408	2418	2428
>8mm	0	0	0	0	0	0	0	0	0
>500µ	2	5	10	2	1	229	130	160	226
>63µ	20	37	38	18	8	88	61	125	110
<63µ	646	378	244	598	674	238	492	506	298

Depth (cm)	2458	2468	2508	2528	2550	2570	2580	2590	2600
>8mm	0	0	0	0	0	0	0	0	0
>500µ	72	316	74	14	28	235	298	528	479
>63µ	140	178	207	54	106	54	89	147	91
<63µ	499	428	403	511	635	90	169	270	267

Depth (cm)	2613	2625	2638	2646	2656	2665	2670	2687	2693
>8mm	0	9	2	42	0	0	0	0	0
>500µ	399	134	336	288	314	305	159	712	316
>63µ	158	49	70	117	139	141	58	144	45
<63µ	333	132	197	293	317	447	186	434	163

Depth (cm)	2696	2700	2782	2786	2792	2797	2804	2807	2812
>8mm	0	0	0	0	0	6	16	0	0
>500µ	188	174	29	4	7	4	98	10	4
>63µ	37	47	30	13	50	21	26	19	22
<63µ	56	142	282	66	389	198	199	183	223

Depth (cm)	2820	2825	2832	2850
>8mm	393	230	209	1142
>500µ	209	74	171	310
>63µ	44	13	42	164
<63µ	171	44	123	505

Table A4.4. *Wied Żembaq 2.*

Depth (cm)	117	121	125	129	133	137	141	145	149
>8mm	0	0	1	81	10	12	24	11	0
>500µ	5	4	5	1	8	8	10	16	12
>63µ	8	8	8	2	6	6	7	7	11
<63µ	32	33	31	15	26	26	24	25	25
Munsell	10YR 4/6	10YR 4/6	10YR 4/6	10YR 4/6	10YR 4/6 + 10YR 3/3	10YR 4/4	10YR 4/4	10YR 4/4	10YR 4/4

Depth (cm)	153	157	161	165	169	173	177	181	185
>8mm	13	0	77	4	11	5	0	3	6
>500µ	9	9	5	12	12	13	10	9	8
>63µ	8	7	4	6	5	7	6	7	7
<63µ	25	25	19	24	31	36	36	42	42
Munsell	10YR 4/4	10YR 4/4	10YR 4/4	10YR 4/4	10YR 4/4	10YR 4/4	10YR 4/4	10YR 4/4	10YR 4/4

Depth (cm)	189	193	227	230	234	237	240	244	248
>8mm	0	6	0	0	0	1	0	0	0
>500µ	10	6	3	8	7	7	7	5	7
>63µ	9	7	6	8	8	7	7	5	5
<63µ	44	48	38	26	29	28	28	33	33
Munsell	10YR 4/4	10YR 4/4	10YR 5/8	10YR 5/8	10YR 5/8	10YR 5/8	10YR 5/8	10YR 5/8	10YR 5/6

Depth (cm)	251	254	258	262	265	269	272	276	279
>8mm	0	0	1	0	70	14	0	7	10
>500µ	5	3	6	3	2	8	4	3	7
>63µ	5	5	4	3	1	4	2	2	3
<63µ	39	36	33	21	12	23	18	10	16
Munsell	10YR 5/6	10YR 5/6	10YR 5/6	10YR 5/6	10YR 5/6	10YR 5/6	10YR 5/6	10YR 5/6	10YR 5/6

Depth (cm)	283	286	290	293	297	302	307	312	317
>8mm	32	19	22	0	40	5	9	2	2
>500µ	6	10	7	8	3	1	1	2	2
>63µ	2	3	5	8	6	5	6	4	6
<63µ	15	14	29	35	30	53	49	49	62
Munsell	10YR 5/6	10YR 4/2	10YR 4/2	10YR 4/2	10YR 4/2	10YR 4/2	10YR 4/2	10YR 4/2	10YR 4/2

Depth (cm)	322	327	332	337	342	347	352	357	362
>8mm	0	34	5	0	0	3	0	0	0
>500µ	2	1	1	1	2	2	2	2	2
>63µ	5	4	7	7	8	8	9	8	6
<63µ	59	42	56	50	49	61	55	53	56
Munsell	10YR 4/2	10YR 4/2	10YR 4/2	10YR 4/2	10YR 4/2	10YR 4/2	10YR 4/2	10YR 3/3	10YR 3/3

Depth (cm)	367	372	377	382	387	392	461	463	464
>8mm	0	0	0	0	0	0	0	0	2
>500µ	2	2	1	2	1	1	8	7	7
>63µ	6	5	7	8	5	5	4	2	2
<63µ	47	47	44	56	57	63	9	9	6
Munsell	10YR 3/3	10YR 3/3	10YR 3/3	10YR 3/3	10YR 3/2	10YR 3/2	10YR 5/4	10YR 5/4	10YR 5/4

Table A4.4 *(cont.).*

Depth (cm)	466	468	470	471	473	475	477	479	480
>8mm	0	3	0	0	0	0	0	0	0
>500µ	8	3	2	1	1	1	1	1	1
>63µ	3	2	2	3	3	3	3	3	3
<63µ	8	13	12	13	13	13	12	12	16
Munsell	10YR 5/4	10YR 5/4	10YR 5/4 + 1.7/1	10YR 5/4 + 1.7/1	7.5YR 4/2 + 1/71	7.5YR 4/2 + 1/71	7.5YR 4/2 + 1/71	7.5YR 4/2 + 1/71	7.5YR 4/2 + 1/71

Depth (cm)	481	483	485	487	489	490	492	494	503
>8mm	0	0	0	0	0	0	0	0	0
>500µ	2	4	2	1	1	1	1	1	2
>63µ	4	3	3	4	3	3	4	3	6
<63µ	14	12	15	13	14	14	16	17	37
Munsell	7.5YR 4/2 + 2/1	7.5YR 4/2 + 2/1	7.5YR 4/2 + 2/1	7.5YR 4/2 + 2/1	7.5YR 4/2 + 2/1	7.5YR 4/2 + 2/1	7.5YR 4/2 + 2/1	7.5YR 4/2 + 2/1	7.5YR 2/1 + 5/4

Depth (cm)	507	511	515	519	523
>8mm	0	5	0	0	0
>500µ	2	1	2	1	2
>63µ	6	5	5	3	3
<63µ	35	31	40	18	32
Munsell	7.5 YR 2/1 + 4/3	7.5 YR 2/1	7.5YR 1.7/1 + 4/3	7.5YR 1.7/1 + 4/3	7.5 YR 1.7/1

Table A4.5. *Wied Żembaq 1.*

Depth (cm)	126	131	136	141	145	150	154	159	163
>8mm	7	15	0	0	2	0	0	2	0
>500µ	7	6	14	11	6	11	8	6	11
>63µ	6	7	7	8	6	6	4	4	3
<63µ	22	18	20	19	17	23	13	12	2
Munsell	10YR 3/3	10YR 4/3	10YR 4/3	10YR 4/4	10YR 4/4	10YR 4/3	10YR 4/3	10YR 4/3	10YR 7/6

Depth (cm)	168	173	178	182	187	191	195	199	204
>8mm	8	4	0	2	0	11	0	0	0
>500µ	12	9	6	5	5	7	7	4	8
>63µ	5	6	5	6	5	4	5	5	9
<63µ	30	31	28	30	18	17	32	31	51
Munsell	10YR 4/3	10YR 4/3	10YR 4/3	10YR 4/3	10YR 2/3	10YR 2/3	10YR 2/3	10YR 2/3	10YR 3/2

Depth (cm)	208	213	227	232	237	242	247	253	258
>8mm	0	3	0	6	11	12	7	5	0
>500µ	6	9	8	10	8	8	8	6	4
>63µ	8	9	7	5	4	5	3	7	6
<63µ	44	49	19	9	4	5	2	40	24
Munsell	10YR 3/2	10YR 3/2	10YR 4/3	10YR 6/4	10YR 4/3 + 6/4	10YR 7/4	10YR 7/4	10YR 4/2	10YR 4/2

Table A4.5 *(cont.).*

Depth (cm)	263	268	273	278	283	288	293	298	303
>8mm	0	0	0	2	6	6	1	7	2
>500µ	6	7	7	6	10	6	3	5	5
>63µ	5	7	8	6	5	5	5	3	4
<63µ	30	33	42	47	27	39	47	42	45
Munsell	10YR 4/2	10YR 4/2	10YR 4/2	10YR 4/2	10YR 4/2	10YR 4/2	10YR 4/2	10YR 4/2	10YR 4/2

Depth (cm)	308	313	318	323	328	333	338	343	348
>8mm	4	7	9	0	0	0	0	0	0
>500µ	5	4	3	2	1	2	3	2	3
>63µ	5	6	4	4	4	6	7	6	5
<63µ	45	44	36	51	42	50	49	37	40
Munsell	10YR 4/2	10YR 3/2	10YR 3/2	10YR 3/2	10YR 3/2	10YR 3/2	10YR 3/2	10YR 3/2	10YR 3/1

Depth (cm)	353	358	363	368	373	378	383	388	393
>8mm	0	3	7	0	0	0	0	0	0
>500µ	6	8	2	1	1	1	1	1	2
>63µ	5	4	5	6	5	5	4	4	5
<63µ	16	21	45	44	50	58	51	48	38
Munsell	10YR 4/3	10YR 4/3	10YR 3/2	10YR 3/2	10YR 3/2	10YR 3/2	10YR 3/1	10YR 4/1 + 4/3	10YR 4/1 + 4/3

Depth (cm)	398	403	408	413	418	423	428	433	438
>8mm	0	0	0	0	0	0	0	0	0
>500µ	1	1	2	2	2	4	5	3	2
>63µ	5	4	5	9	5	7	8	6	6
<63µ	47	37	40	41	41	39	50	43	44
Munsell	10YR 2/1	10YR 2/1	10YR 2/1	10YR 2/1	10YR 2/1	10YR 4/1	10YR 4/1	10YR 4/1	10YR 4/1

Depth (cm)	443	448	456	468	480	492	504	516	528
>8mm	0	0	0	7	9	1	0	0	0
>500µ	3	2	11	26	6	6	3	3	2
>63µ	6	4	12	11	11	14	15	14	12
<63µ	33	25	90	72	109	111	124	104	79
Munsell	10YR 4/1	10YR 4/1	10YR 3/2	10YR 3/2	10YR 4/1	10YR 4/1	10YR 3/1	10YR 3/1	10YR 3/1

Depth (cm)	540
>8mm	7
>500µ	5
>63µ	12
<63µ	84
Munsell	10YR 3/1

Table A4.6. *Xemxija 1.*

Depth (cm)	49	54	59	64	69	72	76	81	86
>8mm	0	0	0	0	0	1	3	0	0
>500µ	1	1	1	1	3	9	7	6	6
>63µ	1	2	2	1	4	4	9	8	5
<63µ	44	41	37	51	54	8	36	47	51
Munsell	10YR 6/4 +4/3	10YR 7/4	10YR 7/3	10YR 7/3	10YR 6/4	10YR 7/3	10YR 7/3	10YR 7/4	10YR 7/4

Depth (cm)	91	96	101	106	111	116	121	126	131
>8mm	7	3	1	18	3	0	5	13	14
>500µ	10	19	17	14	25	18	17	9	10
>63µ	7	9	7	8	12	8	8	3	5
<63µ	32	18	13	20	27	17	23	25	46
Munsell	10YR 8/4	10YR 7/4	10YR 7/4	10YR 7/4	10YR 7/4	10YR 7/4	10YR 7/4	10YR 5/6	10YR 6/4

Depth (cm)	136	141	145	149	154	158	163	168	173
>8mm	6	0	0	0	0	0	0	0	0
>500µ	4	2	0	1	1	1	1	1	1
>63µ	4	3	3	3	2	3	2	2	3
<63µ	55	61	52	51	43	51	54	55	56
Munsell	10YR 6/4 + 7/4	10YR 6/4	10YR 5/4	10YR 5/4	7.5YR 5/3	10YR 5/4	10YR 5/4	10YR 5/3	10YR 5/3

Depth (cm)	178	183	188	193	198	203	208	213	218
>8mm	0	0	0	0	0	0	0	0	0
>500µ	1	1	1	1	1	1	1	1	1
>63µ	1	1	1	1	1	3	3	6	4
<63µ	53	52	53	52	60	49	51	48	53
Munsell	10YR 5/4	10YR 5/4	7.5YR 5/4	7.5YR 6/3	7.5 YR 7/3 + 6/4	7.5 YR 7/3 + 6/4	10YR 5/2	10YR 5/2	10YR 4/1

Depth (cm)	223	238	233	238	243	248	267	271	275
>8mm	0	0	0	0	0	0	0	0	0
>500µ	1	1	1	1	1	1	1	1	1
>63µ	7	4	7	10	11	11	2	2	3
<63µ	51	56	52	56	55	23	50	53	51
Munsell	10YR 4/1	10YR 4/1	7.5 YR 5/1	7.5YR 6/1	10YR 6/2	10YR 5/2	10YR 5/3 +5/2	10YR 6/2	10YR 5/3 +5/2

Depth (cm)	280	284	288	293	297	301	306	310	314
>8mm	0	0	0	2	0	0	0	4	6
>500µ	1	3	5	2	2	2	3	7	9
>63µ	2	2	2	2	3	2	2	1	1
<63µ	52	49	48	50	46	46	49	42	39
Munsell	10YR 6/3	10YR 5/3	10YR 5/3	10YR 5/2	10YR 5/2	10YR 5/2	10YR 6/2 +5/1	10YR 6/2 +5/1	10YR 5/2

Table A4.6 *(cont.).*

Depth (cm)	318	323	327	331	336	340	344	349	353
>8mm	1	1	1	0	0	0	0	0	0
>500µ	5	3	2	1	2	1	1	1	1
>63µ	2	1	2	2	2	2	2	1	2
<63µ	43	45	49	47	48	49	53	47	52
Munsell	10YR 4/1	10YR 5/2	10YR 6/2 +4/1	7.5YR 3/1 +10YR 6/2	10YR 4/1	10YR 5/1	10YR 5/1	10YR 5/1	10YR 6/1

Depth (cm)	366	370	375	380	384	389	393	398	403
>8mm	0	4	5	7	0	4	4	0	0
>500µ	3	6	9	6	4	5	4	2	2
>63µ	2	1	1	1	3	2	1	2	1
<63µ	51	50	46	44	47	47	48	51	49
Munsell	10YR 6/1	10YR 6/1	10YR 6/1	10YR 6/1	10YR 6/1	10YR 5/2	10YR 5/2	10YR 5/2	10YR 5/2

Depth (cm)	407	412	416	421	426	430	435	439	440
>8mm	0	2	0	0	0	0	0	0	0
>500µ	4	3	3	6	3	2	1	1	1
>63µ	2	2	1	2	3	2	2	2	2
<63µ	52	54	49	50	48	51	54	49	51
Munsell	10YR 5/2	10YR 5/2 +7/2	10YR 5/2	10YR 5/2	10YR 5/1	10YR 6/1	10YR 5/1	10YR 5/1	10YR 5/1

Depth (cm)	449	453	458	483	487	491	495	499	503
>8mm	0	0	0	0	0	0	0	0	0
>500µ	1	1	1	2	1	2	2	0.8	1
>63µ	2	2	2	5	3	6	5	3	3
<63µ	52	52	50	33	37	26	30	36.2	32
Munsell	10YR 5/1	10YR 5/1	10YR 5/1	10YR 1.7/1	10YR 1.7/1	10YR 1.7/1	10YR 1.7/1	10YR 2/2	10YR 1.7/1

Depth (cm)	507	511	515	519	523	527	531	535	539
>8mm	0	0	0	0	0	1	0	1	0
>500µ	1	3	2	0.8	2	4	0.8	2	0.8
>63µ	4	3	4	3	3	2	3	2	2
<63µ	32	28	30	36.2	36	34	34.2	36	39.2
Munsell	10YR 1.7/1	10YR 1.7/1	10YR 1.7/1 +2/1 +7/1	10YR 3/1 +4/1	10YR 2/1 + 5/2	10YR 2/1 +4/1 +5/2	10YR 1.7/1	10YR 2/2 +4/1	10YR 1.7/1

Depth (cm)	543	547	551	555	559	563	582	586	590
>8mm	0	0	0	0	0	0	0	0	0
>500µ	1	1	1	1	0.8	0.8	1	1	1
>63µ	3	2	2	1	2	1	2	4	5
<63µ	37	41	43	40	39.2	38.2	50	46	44
Munsell	10YR 2/1 +4/1	10YR 3/1 +4/1	10YR 3/1	10YR 3/1 +4/1	10YR 3/1	10YR 3/1 +2/1	10YR 2/1	10YR 1.7/1	10YR 1.7/1

Table A4.6 *(cont.).*

Depth (cm)	595	599	603	607	612	616	621	625	629
>8mm	0	0	0	0	0	0	0	0	0
>500µ	1	1	1	1	1	1	2	1	1
>63µ	4	4	6	6	4	5	5	3	3
<63µ	46	45	42	40	45	42	40	48	48
Munsell	10YR 1.7/1 +3/1	10YR 1.7/1	10YR 1.7/1	10YR 1.7/1	10YR 2/1	10YR 1.7/1	10YR 1.7/1	10YR 1.7/1 +2/2	10YR 2/2

Depth (cm)	633	638	642	646	651	655	659	634	668
>8mm	0	0	0	0	0	0	0	0	0
>500µ	1	2	5	2	2	3	3	6	1
>63µ	3	3	3	4	2	4	3	4	2
<63µ	48	51	39	49	46	42	45	40	36
Munsell	10YR 4/1	10YR 4/1	10YR 4/1	10YR 2/1	10YR 1.7/1 +2/2	10YR 2/2	10YR 1.7/1 +2/2	10YR 2/3	10YR 1.7/1

Depth (cm)	672	682	686	691	696	701	706	710	715
>8mm	0	0	0	0	0	0	0	0	0
>500µ	1	0	1	1	2	2	5	5	4
>63µ	4	1	5	7	8	10	6	6	6
<63µ	53	60	54	52	50	51	57	49	55
Munsell	10YR 2/3	10YR 3/2	10YR 2/3	10YR 3/1	10YR 4/2	10YR 4/2	10YR 4/2	10YR 3/2	10YR 4/2

Depth (cm)	720	725	730	734	739	744	749	754	758
>8mm	0	0	0	0	0	0	0	0	0
>500µ	4	8	6	5	9	8	15	19	19
>63µ	6	7	7	6	7	7	8	5	6
<63µ	51	49	57	49	54	48	57	48	46
Munsell	10YR 2/3	10YR 2/3	10YR 2/3	10YR 3/2	10YR 3/3	10YR 3/2	10YR 4/2	10YR 4/2	10YR 4/2

Depth (cm)	763	768	773	778	802	806	810	814	818
>8mm	0	0	0	0	0	0	0	0	0
>500µ	12	15	9	3	1	2	1	1	1
>63µ	8	8	8	8	10	9	9	10	10
<63µ	54	54	51	68	54	46	47	49	45
Munsell	10YR 4/2	10YR 3/3	10YR 4/2 +5/6	10YR 4/2 +5/6	10YR 4/2	10YR 2/3	10YR 2/3	10YR 2/3	10YR 2/3

Depth (cm)	822	826	831	835	839	843	847	851	855
>8mm	0	0	0	0	0	0	0	0	0
>500µ	1	1	1	2	1	1	1	1	1
>63µ	7	9	12	12	10	12	11	4	10
<63µ	50	43	45	45	44	44	45	51	44
Munsell	10YR 2/3	10YR 2/3	10YR 2/3	10YR 2/3	10YR 2/3	10YR 2/3	10YR 2/3	10YR 2/3	10YR 2/3

Table A4.6 *(cont.).*

Depth (cm)	859	863	867	871	876	880	884	887	888
>8mm	0	0	0	0	0	0	0	0	0
>500µ	5	8	7	5	6	2	1	1	3
>63µ	13	16	10	9	13	10	8	5	7
<63µ	40	37	37	42	42	48	46	49	61
Munsell	10YR 2/3 +6/8 +5/8	10YR 2/3	10YR 2/3	10YR 2/3	10YR 2/3	10YR 3/2	10YR 2/3	10YR 2/2	10YR 2/2

Depth (cm)	889	894	899	905	910	916	921	927	932
>8mm	0	0	0	0	0	0	0	0	0
>500µ	1	1	1	1	2	1	1	1	2
>63µ	5	4	7	5	8	8	5	7	8
<63µ	69	67	67	69	64	62	72	66	64
Munsell	10YR 2/3	10YR 3/2	10YR 2/3	10YR 3/2	10YR 3/3	10YR 2/3	10YR 2/3	10YR 2/2	10YR 2/2

Depth (cm)	938	943	949	954	960	965	971	976	982
>8mm	2	0	0	11	5	0	0	4	4
>500µ	5	16	18	16	12	11	7	8	7
>63µ	7	8	10	5	7	10	11	8	6
<63µ	51	49	49	21	29	57	47	55	45
Munsell	10YR 3/2	10YR 5/4 +3/2	10YR 5/3 +4/2	10YR 4/2	10YR 4/3	10YR 4/2	10YR 4/3	10YR 4/2	10YR 4/3

Depth (cm)	987
>8mm	0
>500µ	7
>63µ	9
<63µ	51
Munsell	10YR 4/3

Table A4.7. *Xemxija 2.*

Depth (cm)	120	124	129	133	137	141	146	150	154
>8mm	24	0	5	1	28	1	0	4	1
>500µ	6	10	12	6	5	5	2	2	1
>63µ	3	7	5	2	2	3	3	3	3
<63µ	7	34	22	17	18	48	49	48	57
Munsell	10YR 8/4	10YR 6/4	10YR 7/4	10YR 7/4 + 10YR 4/3	10YR 5/6	10YR 5/3	10YR 5/6	10YR 6/3	10YR 6/4

Depth (cm)	158	163	167	171	175	180	184	188	192
>8mm	0	0	0	0	0	0	0	0	0
>500µ	2	1	1	1	1	1	1	1	1
>63µ	3	3	3	3	2	2	2	2	2
<63µ	47	54	54	57	56	56	50	55	46
Munsell	10YR 5/3	10YR 4/3	10YR 4/3	10YR 4/2	10YR 4/3	10YR 4/3	10YR 4/2	10YR 4/3	10YR 4/4

Table A4.7 *(cont.).*

Depth (cm)	197	200	201	206	211	216	223	227	232
>8mm	0	0	0	0	0	0	0	0	0
>500µ	1	1	1	1	1	1	1	1	1
>63µ	2	2	5	2	2	1	2	2	4
<63µ	49	48	41	57	51	53	59	59	63
Munsell	10YR 4/3	10YR 4/2	10YR 6/3	10YR 5/3	10YR 5/2	10YR 5/2	10YR 6/2	10YR 5/1	10YR 5/1

Depth (cm)	237	242	248	253	258	264	269	274	279
>8mm	0	0	0	0	0	0	0	0	0
>500µ	1	2	1	1	1	1	1	1	3
>63µ	4	18	11	4	3	2	1	3	1
<63µ	61	43	52	58	63	60	65	57	61
Munsell	10YR 5/3	10YR 5/3	10YR 5/2	10YR 5/3	10YR 5/2	10YR 4/1	10YR 5/2	10YR 5/3	10YR 5/2

Depth (cm)	285	290	295	300	319	323	328	332	336
>8mm	0	0	0	0	2	0	0	0	0
>500µ	1	1	1	1	2	5	1	1	1
>63µ	1	1	1	2	1	1	1	1	1
<63µ	38	42	35	40	35	41	48	52	49
Munsell	10YR 5/3	10YR 5/2	10YR 5/1	10YR 5/1 + 10YR 5/3	10YR 6/1 + 10YR 4/1	10YR 5/1 + 10YR 4/1	10YR 4/1	10YR 2/1	10YR 4/1

Depth (cm)	340	345	349	353	358	362	366	371	375
>8mm	0	0	0	0	0	0	0	0	4
>500µ	1	1	2	1	2	1	3	4	6
>63µ	1	1	1	1	1	1	1	1	1
<63µ	48	44	45	45	44	47	49	44	44
Munsell	10YR 5/1	10YR 5/1	10YR 6/1	10YR 6/1	10YR 6/1	10YR 6/1 + 10YR 5/1	10YR 6/1 + 10YR 5/1	10YR 6/1	10YR 6/1

Depth (cm)	379	384	388	392	397	401	415	420	424
>8mm	9	0	0	0	0	0	0	0	0
>500µ	9	3	2	2	2	3	5	1	1
>63µ	1	1	1	1	1	1	2	3	3
<63µ	36	44	46	45	40	46	20	43	42
Munsell	10YR 6/1	10YR 6/1	10YR 6/1	10YR 6/1	10YR 5/1	10YR 5/1	10YR 5/2 + 10YR 2/1	10YR 4/1	10YR 4/1 + 10YR 2/1

Depth (cm)	429	433	438	442	447	451	456	460	465
>8mm	0	3	13	0	0	0	0	0	0
>500µ	1	1	1	2	3	1	3	1	2
>63µ	2	1	1	2	1	1	1	2	2
<63µ	35	29	23	37	34	26	15	40	44
Munsell	10YR 4/1	10YR 4/1	10YR 4/1	10YR 4/1	10YR 4/1	10YR 4/1	10YR 4/1	10YR 4/1	10YR 4/1

Table A4.7 *(cont.).*

Depth (cm)	470	474	478	483	488	492	496	501	526
>8mm	0	0	0	0	0	0	0	0	0
>500µ	1	1	1	1	1	1	1	1	2
>63µ	2	3	2	1	2	1	1	1	2
<63µ	41	46	45	45	43	44	47	47	32
Munsell	10YR 4/1	10YR 4/1	10YR 4/1	10YR 4/1	10YR 4/1	10YR 4/1	10YR 4/1	10YR 4/1	10YR 2/1 + 10YR 5/2

Depth (cm)	530	534	539	543	547	551	556	560	564
>8mm	0	0	0	0	0	0	0	0	0
>500µ	1	1	1	2	2	2	2	1	1
>63µ	3	2	2	2	2	2	2	1	1
<63µ	38	41	42	40	39	40	42	45	42
Munsell	10YR 5/2+ 10YR 2/1	10YR 4/2 + 10YR 2/1	10YR 4/2 + 10YR 2/1	10YR 3/1	10YR 4/1	10YR 4/1	10YR 4/1	10YR 4/1	10YR 4/1 + 10YR 5/1

Depth (cm)	568	573	577	581	585	590	594	598	602
>8mm	0	0	0	0	0	0	0	0	0
>500µ	1	1	1	1	2	1	1	1	1
>63µ	2	2	3	2	2	1	1	2	1
<63µ	42	37	44	44	40	41	47	46	42
Munsell	10YR 4/1	10YR 4/1	10YR 4/1	10YR 4/1	10YR 4/1	10YR 4/1	10YR 4/1	10YR 4/1	10YR 4/1

Depth (cm)	606	611	626	630	635	639	644	648	653
>8mm	0	0	0	0	0	0	0	0	0
>500µ	2	4	2	1	1	1	2	2	2
>63µ	2	3	3	4	4	4	5	5	4
<63µ	40	36	49	48	40	42	41	38	40
Munsell	10YR 4/1	10YR 4/3 + 1.7/1	10YR 1.7/1	10YR 1.7/1	10YR 1.7/1	10YR 1.7/1	10YR 1.7/1	10YR 1.7/1	10YR 1.7/1

Depth (cm)	657	662	666	671	675	680	684	689	693
>8mm	0	0	0	0	0	0	0	0	0
>500µ	1	1	1	1	1	1	1	1	2
>63µ	5	4	4	2	2	3	2	3	4
<63µ	40	41	43	52	51	51	49	55	50
Munsell	10YR 1.7/1	10YR 1.7/1	10YR 1.7/1	10YR 3/1	10YR 4/1	25YR 2/1	25YR 2/1	25YR 4/2	25YR 3/2

Depth (cm)	698	702	707	711	716	738	742	746	750
>8mm	0	0	0	0	0	5	1	0	0
>500µ	1	2	2	4	3	9	8	9	9
>63µ	3	4	5	5	4	8	5	4	6
<63µ	53	50	52	54	52	71	43	40	39
Munsell	25YR 4/2	10YR 3/1 + 10YR 4/2	10YR 3/1	10YR 4/2	10YR 4/2	10YR 4/2	10YR 4/2	10YR 4/2	10YR 4/2

Table A4.7 *(cont.).*

Depth (cm)	754	758	763	767	771	775	779	783	788
>8mm	7	4	0	10	1	0	0	0	0
>500µ	7	8	9	6	8	6	4	2	3
>63µ	4	5	5	5	8	8	8	7	7
<63µ	37	39	39	41	45	46	47	49	49
Munsell	10YR 4/2	10YR 4/2	10YR 5/3	10YR 5/3	10YR 5/3 + 10YR 4/2	10YR 5/3	10YR 5/3	10YR 5/3	10YR 4/3

Depth (cm)	792	796	800	804	808	813	817	821	858
>8mm	0	0	0	0	0	0	0	0	0
>500µ	2	2	1	1	1	3	1	1	1
>63µ	8	8	8	6	5	7	5	6	1
<63µ	49	49	52	53	52	49	52	53	23
Munsell	10YR 4/2 + 10YR 4/3	10YR 4/3	10YR 4/3	10YR 3/3	10YR 4/3	10YR 4/3	10YR 4/2 + 10YR 7/8	10YR 4/2	10YR 3/1 + 10YR 4/2

Depth (cm)	861	865	868	872	875	879	882	886	889
>8mm	0	0	0	0	0	0	0	0	0
>500µ	1	1	2	1	2	1	2	2	4
>63µ	2	2	2	2	2	2	2	2	2
<63µ	25	24	24	25	26	29	35	36	37
Munsell	10YR 5/2 + 10YR 3/1	10YR 5/2	10YR 1.7/1 + 10YR 4/1	10YR 1.7/1	10YR 1.7/1 + 10YR 4/2	10YR 4/1	10YR 4/1	10YR 4/1	10YR 4/1

Depth (cm)	893	896	900	903	907	910	914	917	921
>8mm	0	0	0	0	0	0	0	0	0
>500µ	1	1	1	1	1	1	1	1	1
>63µ	1	2	4	6	5	4	7	3	4
<63µ	33	29	35	37	34	33	35	35	38
Munsell	10YR 4/1	10YR 5/2	10YR 4/2 + 10YR 6/2	10YR 5/3 + 10YR 5/2	10YR 4/3	10YR 4/2	10YR 4/2 + 10YR 4/3	10YR 4/2	10YR 4/2

Depth (cm)	924	928	931
>8mm	0	0	0
>500µ	1	1	1
>63µ	4	4	4
<63µ	37	35	35
Munsell	10YR 4/2	10YR 4/3	10YR 4/2

Table A4.8. *Marsaxlokk 1.*

Depth (cm)	15	19	24	28	32	36	41	45	49
>8mm	3	0	1	0	3	0	5	11	12
>500µ	4	4	4	5	7	8	4	5	7
>63µ	9	9	10	10	11	8	8	8	9
<63µ	20	17	22	22	26	31	22	16	32
Munsell	10YR 5/4	10YR 5/4	10YR 5/4	10YR 5/4	10YR 5/4	10YR 5/4	10YR 5/4	10YR 5/4	10YR 5/4

Table A4.8 *(cont.).*

Depth (cm)	54	58	62	67	71	75	80	84	89
>8mm	0	0	0	0	0	0	0	2	0
>500µ	11	17	10	12	11	8	5	4	2
>63µ	12	9	12	13	12	12	12	11	10
<63µ	44	28	37	22	32	31	48	40	58
Munsell	10YR 5/6	10YR 5/6	10YR 5/6	10YR 5/6	10YR 5/6	10YR 6/4	10YR 6/4 + 10YR 4/3	10YR 4/3 + 10YR 6/4	10YR 6/3 + 10YR 6/2

Depth (cm)	94	99	104	109	114	119	124	129	134
>8mm	0	0	0	0	0	0	0	0	0
>500µ	1	1	1	1	1	1	2	2	1
>63µ	4	3	6	9	8	2	10	16	17
<63µ	60	61	63	55	59	67	56	44	52
Munsell	10YR 6/3 + 10YR 6/2	10YR 6/3	10YR 6/2 + 10YR 7/1	10YR 7/1	10YR 7/1	10YR 7/2	10YR 7/2	10YR 7/2	10YR 7/2

Depth (cm)	139	144	149	154	159	164	169	174	179
>8mm	2	1	0	0	3	1	0	0	0
>500µ	3	3	2	3	27	19	2	3	1
>63µ	16	18	15	14	14	8	6	8	6
<63µ	43	37	42	42	15	22	50	49	64
Munsell	10YR 7/2	10YR 7/2	10YR 7/2	10YR 7/2	10YR 7/2 + 10YR 6/4	10YR 6/4	10YR 3/1 + 10YR 7/2	10YR 7/1	10YR 7/2

Depth (cm)	184	189	194	199	204	209	214	219	224
>8mm	0	12	1	0	0	6	3	0	0
>500µ	3	19	17	8	10	9	9	12	13
>63µ	13	7	10	10	11	7	7	5	6
<63µ	63	7	31	39	38	34	34	40	42
Munsell	10YR 7/2	10YR 6/3	10YR 6/3 + 10YR 4/3	10YR 4/6	10YR 4/6	10YR 4/6	10YR 4/6	10YR 4/6	10YR 5/8

Depth (cm)	229	234	239	244	249	254	259	264	269
>8mm	11	3	6	0	7	0	6	3	2
>500µ	12	9	8	5	5	7	4	4	3
>63µ	2	4	5	5	4	5	3	3	3
<63µ	26	36	33	52	48	40	42	44	44
Munsell	10YR 5/3	10YR 5/8	10YR 4/6	10YR 5/8	10YR 4/4	10YR 4/6	10YR 4/6	10YR 3/4	10YR 3/4

Depth (cm)	274	279	284	289	294	299	304	309	314
>8mm	2	0	0	1	1	3	6	2	1
>500µ	2	3	2	10	19	11	3	5	5
>63µ	3	3	3	2	3	6	6	3	6
<63µ	36	40	53	1	12	34	43	42	50
Munsell	10YR 3/3	10YR 4/4	10YR 4/3	10YR 4/2	10YR 4/4	10YR 3/4	10YR 3/4	10YR 4/6	10YR 3/3

Table A4.8 *(cont.).*

Depth (cm)	419	324	329	334	339	344	349	354	359
>8mm	5	0	6	3	7	0	0	9	0
>500µ	3	1	4	30	24	31	3	18	6
>63µ	4	2	5	9	6	5	4	8	6
<63µ	49	50	44	35	19	14	61	23	54
Munsell	10YR 3/3	10YR 4/6	10YR 3/3	10YR 8/3 + 10YR 8/4	10YR 8/4 + 10YR 6/6	10YR 5/8	10YR 5/8 + 10YR 8/3	10YR 8/2	10YR 8/3

Depth (cm)	364	369	374	379	384
>8mm	0	1	0	7	0
>500µ	7	1	8	1	2
>63µ	8	2	2	6	10
<63µ	31	34	47	37	47
Munsell	10YR 8/3	10YR 8/3	10YR 8/3	10YR 8/3	10YR 8/3 + 10YR 7/6

Appendix 5

The molluscan counts for the deep cores

Katrin Fenech

Table A5.1. *Marsa 2.*

Species/Depth (cm)	**3**	**8**	**13**	**18**	**23**	**28**	**33**	**38**	**43**	**48**	**53**	**58**	**63**	**68**
Bittium reticulatum (Da Costa, 1778)	0	0	0	0	0	0	0	0	0	0	0	0	0	0
Cerithium spp.	0	0	0	0	0	0	0	0	0	0	0	0	0	0
Conus mediterraneus (Hwass, 1792)	0	0	0	0	0	0	0	0	0	0	0	0	0	0
Gibbula sp.	0	0	0	0	0	0	0	0	0	0	0	0	0	0
Haminoea sp.	0	0	0	0	0	0	0	0	0	0	0	0	0	0
Hexaplex trunculus (Linnaeus, 1758)	0	0	0	0	0	0	0	0	0	0	0	0	0	0
Pirenella conica (Blainville, 1826)	0	0	0	0	0	0	0	0	0	0	0	0	0	0
Retusa truncatula (Brugière, 1792)	0	0	0	0	0	0	0	0	0	0	0	0	0	0
Rissoa sp.	0	0	0	0	0	0	0	0	0	0	0	0	0	0
Turbonilla sp.	0	0	0	0	0	0	0	0	0	0	0	0	0	0
Acanthocardia sp.	0	0	0	0	0	0	0	0	0	0	0	0	0	0
Cardiidae	0	0	0	0	0	0	0	0	0	0	0	0	0	0
Cerastoderma sp.	0	1	0	0	0	0	0	0	0	0	0	0	0	0
Kelliidae	0	0	0	0	0	0	0	0	0	0	0	0	0	0
Loripes lucinalis (Lamarck, 1818)	0	0	0	0	0	0	0	0	0	0	0	0	0	0
Ostrea sp.	0	0	0	0	0	0	0	0	0	0	0	0	0	0
Paphia sp.	0	0	0	0	0	0	0	0	0	0	0	0	0	0
Parvicardium sp.	0	0	0	0	0	0	0	0	0	0	0	0	0	0
Pectinidae	0	0	0	0	0	0	0	0	0	0	0	0	0	0
Tapes decussatus (Linnaeus, 1758)	0	0	0	0	0	0	0	0	0	0	0	0	0	0
Tellina sp.	0	0	0	0	0	0	0	0	0	0	0	0	0	0
Veneridae	0	0	0	0	0	0	0	0	0	0	0	0	0	0
other/indeterminate	0	0	0	0	0	0	0	0	0	0	0	0	0	0
Hydrobia sp. Hartmann, 1821	0	0	0	0	0	0	0	0	0	0	0	0	0	0
Ovatella myosotis (Draparnaud, 1801)	0	0	0	0	0	0	0	0	0	0	0	0	0	0
Truncatella subcylindrica (Linnaeus, 1767)	0	0	0	0	0	0	0	0	0	0	0	0	0	0
Oxyloma elegans (Risso, 1826)	0	0	0	0	0	0	0	0	0	0	0	0	0	0
Pseudamnicola (s.str.) *moussonii* (Calcara, 1841)	0	0	0	0	0	0	0	0	0	0	0	0	0	0
Ancylus fluviatilis Müller, 1774	0	0	0	0	0	0	0	0	0	0	0	0	0	0
Bulinus cf. *truncatus* (Audouin, 1827)	0	0	0	0	0	0	0	0	0	0	0	0	0	0
Pisidium caesertanum (Poli, 1791)	0	0	0	0	0	0	0	0	0	0	0	0	0	0
Lymnaea (Galba) truncatula (Müller, 1774)	0	0	0	0	0	0	0	0	0	0	0	0	0	0
Planorbis moquini (Requien, 1848)	0	0	0	0	0	0	0	0	0	0	0	0	0	0
Planorbis planorbis (Linnaeus, 1758)	0	0	0	0	0	0	0	0	0	0	0	0	0	0
Carychium cf. *schlickumi* Strauch, 1977	0	0	0	0	0	0	0	0	0	0	0	0	0	0
Vertigo cf. *antivertigo* (Draparnaud, 1801)	0	0	0	0	0	0	0	0	0	0	0	0	0	0
Oxychilus (Mediterranea) *hydatinus* (Rossmässler, 1838)	0	0	0	0	0	0	0	0	0	0	0	0	0	0
Truncatellina callicratis (Scacchi, 1833)	0	0	0	0	0	0	0	0	0	0	0	0	0	0
Vitrea Fitzinger, 1833	0	0	1	0	0	0	0	0	0	0	0	0	0	0
Xerotricha Monterosato, 1892	0	0	0	0	0	0	0	0	0	0	0	0	0	0
Clausiliidae Mörch, 1864	0	0	0	0	0	0	0	0	0	0	0	0	0	0
Granopupa granum (Draparnaud, 1801)	0	0	0	0	0	0	0	0	0	0	0	0	0	0
Muticaria Lindholm, 1925	0	1	0	0	0	0	0	0	0	0	0	0	0	0
Papillifera papillaris (Müller, 1774)	0	0	0	0	0	0	0	0	0	0	0	0	0	0
Rumina decollata (Linnaeus, 1758)	0	0	0	0	0	0	0	0	0	0	0	0	0	0
Trochoidea spratti (Pfeiffer, 1846)	0	1	1	1	1	3	0	0	0	0	0	0	0	0
Cernuella caruanae (Kobelt, 1888)	1	0	0	1	5	4	0	0	0	0	0	0	0	0
Cochlicella acuta (Müller, 1774)	1	5	0	0	3	3	0	0	0	0	0	0	0	0
Pomatias sulcatus (Draparnaud, 1801)	0	0	0	0	0	0	0	0	0	0	0	0	0	0
Theba pisana (Müller, 1774)	0	3	0	0	0	1	0	0	0	0	0	0	0	0
Helicioidae	1	1	3	3	5	7	0	0	0	0	0	0	0	0
Cecilioides acicula (Müller, 1774)	3	1	0	3	4	2	0	0	0	0	0	0	0	0
Total amount of molluscs	**6**	**13**	**5**	**8**	**18**	**20**	**1**	**1**	**1**	**1**	**1**	**1**	**1**	**1**

Table A5.1 *(cont.).*

Species/Depth (cm)	73	78	83	88	93	98	103	107	113	118	123	128	133	138
Bittium reticulatum (Da Costa, 1778)	0	0	1	0	0	0	0	0	0	0	0	0	0	0
Cerithium spp.	0	0	0	0	0	0	0	0	0	0	0	0	0	0
Conus mediterraneus (Hwass, 1792)	0	0	0	0	0	0	0	0	0	0	0	0	0	0
Gibbula sp.	0	0	0	0	0	0	0	0	0	0	0	0	0	0
Haminoea sp.	0	0	0	0	0	0	0	0	0	0	0	0	0	0
Hexaplex trunculus (Linnaeus, 1758)	0	0	0	0	0	0	0	0	0	0	0	0	0	0
Pirenella conica (Blainville, 1826)	0	0	0	0	0	0	0	0	0	0	0	0	0	0
Retusa truncatula (Brugière, 1792)	0	0	0	0	0	0	0	0	0	0	0	0	0	0
Rissoa sp.	0	0	0	0	0	0	0	0	0	0	0	0	0	0
Turbonilla sp.	0	0	0	0	0	0	0	0	0	0	0	0	0	0
Acanthocardia sp.	0	0	0	0	0	0	0	0	0	0	0	0	0	0
Cardiidae	0	0	0	0	0	0	0	0	0	0	0	0	0	0
Cerastoderma sp.	0	0	0	0	1	0	0	0	0	0	0	0	0	0
Kelliidae	0	0	0	0	0	0	0	0	0	0	0	0	0	0
Loripes lucinalis (Lamarck, 1818)	0	0	0	0	0	0	0	0	0	0	0	0	0	0
Ostrea sp.	0	0	0	0	0	0	0	0	0	0	0	0	0	0
Paphia sp.	0	0	0	0	0	0	0	0	0	0	0	0	0	0
Parvicardium sp.	0	0	0	0	0	0	0	0	0	0	0	0	0	0
Pectinidae	0	0	0	0	0	0	0	0	0	0	0	0	0	0
Tapes decussatus (Linnaeus, 1758)	0	0	0	0	0	0	0	0	0	0	0	0	0	0
Tellina sp.	0	0	0	0	0	0	0	0	0	0	0	0	0	0
Veneridae	0	0	0	0	0	0	0	0	0	0	0	0	0	0
other/indeterminate	0	0	0	0	0	0	0	0	0	0	0	0	0	0
Hydrobia sp. Hartmann, 1821	0	0	0	0	0	0	0	0	0	0	0	0	0	0
Ovatella myosotis (Draparnaud, 1801)	0	0	0	0	0	0	0	0	0	0	0	0	0	0
Truncatella subcylindrica (Linnaeus, 1767)	0	0	0	0	0	0	0	0	0	0	0	0	0	0
Oxyloma elegans (Risso, 1826)	0	0	0	0	0	0	0	0	0	0	0	0	0	0
Pseudamnicola (s.str.) *moussonii* (Calcara, 1841)	0	0	0	0	1	1	1	0	0	0	0	0	0	0
Ancylus fluviatilis Müller, 1774	0	0	0	0	0	0	0	0	0	0	0	0	0	0
Bulinus cf. *truncatus* (Audouin, 1827)	0	0	0	0	0	0	0	0	0	0	0	0	0	0
Pisidium caesertanum (Poli, 1791)	0	0	0	0	0	0	0	0	0	0	0	0	0	0
Lymnaea (Galba) truncatula (Müller, 1774)	0	0	0	0	0	0	1	0	2	0	0	0	0	0
Planorbis moquini (Requien, 1848)	0	0	0	0	0	0	0	0	0	0	0	0	0	0
Planorbis planorbis (Linnaeus, 1758)	0	0	0	0	0	0	1	0	1	0	0	0	0	0
Carychium cf. *schlickumi* Strauch, 1977	0	0	0	0	0	0	0	0	0	0	0	0	0	0
Vertigo cf. *antivertigo* (Draparnaud, 1801)	0	0	0	0	0	0	0	0	0	0	0	0	0	0
Oxychilus (Mediterranea) *hydatinus* (Rossmässler, 1838)	0	0	0	0	0	0	0	0	0	0	0	0	0	0
Truncatellina callicratis (Scacchi, 1833)	0	0	0	0	0	0	0	0	0	0	0	0	0	0
Vitrea Fitzinger, 1833	0	0	0	0	0	0	0	0	0	0	0	0	0	0
Xerotricha Monterosato, 1892	0	0	0	0	0	0	0	0	2	0	0	0	0	0
Clausiliidae Mörch, 1864	0	0	0	0	0	0	0	0	0	0	0	0	0	0
Granopupa granum (Draparnaud, 1801)	0	0	0	0	0	1	0	0	0	0	0	0	0	0
Muticaria Lindholm, 1925	0	0	0	0	1	1	0	0	1	0	0	0	0	0
Papillifera papillaris (Müller, 1774)	0	0	0	0	1	0	0	0	1	0	0	0	0	0
Rumina decollata (Linnaeus, 1758)	0	0	0	0	0	0	0	0	0	0	0	0	0	0
Trochoidea spratti (Pfeiffer, 1846)	0	0	1	0	0	0	0	6	2	0	0	0	0	0
Cernuella caruanae (Kobelt, 1888)	0	0	7	0	4	0	8	0	1	0	0	0	0	0
Cochlicella acuta (Müller, 1774)	0	0	11	0	18	15	17	18	7	0	0	0	0	0
Pomatias sulcatus (Draparnaud, 1801)	0	0	0	0	0	0	0	0	0	0	0	0	0	0
Theba pisana (Müller, 1774)	0	0	4	0	4	0	1	0	2	0	0	0	0	0
Helicioidae	0	0	11	0	7	6	4	13	8	3	0	0	0	0
Cecilioides acicula (Müller, 1774)	0	0	0	0	2	4	1	0	0	0	0	0	0	0
Total amount of molluscs	**1**	**1**	**35**	**1**	**39**	**28**	**34**	**37**	**27**	**3**	**1**	**1**	**1**	**1**

Table A5.1 *(cont.).*

Species/Depth (cm)	143	148	153	158	163	168	173	178	183	188	193	198	203	208
Bittium reticulatum (Da Costa, 1778)	0	0	0	0	0	0	0	0	0	2	2	0	0	0
Cerithium spp.	0	0	0	0	0	0	0	0	0	0	0	0	0	0
Conus mediterraneus (Hwass, 1792)	0	0	0	0	0	0	0	0	0	0	0	0	0	0
Gibbula sp.	0	0	0	0	0	0	0	0	0	0	0	0	0	0
Haminoea sp.	0	0	0	0	0	0	0	0	0	0	0	0	0	0
Hexaplex trunculus (Linnaeus, 1758)	0	0	0	0	0	0	0	0	0	0	0	0	0	0
Pirenella conica (Blainville, 1826)	0	0	0	0	0	0	0	0	0	0	0	0	0	0
Retusa truncatula (Brugière, 1792)	0	0	0	0	0	0	0	0	0	0	0	0	0	0
Rissoa sp.	0	0	0	0	0	0	0	0	0	1	3	0	0	0
Turbonilla sp.	0	0	0	0	0	0	0	0	0	0	0	0	0	0
Acanthocardia sp.	0	0	0	0	0	0	0	0	0	0	0	0	0	0
Cardiidae	0	0	0	0	0	0	0	0	0	0	0	0	0	0
Cerastoderma sp.	0	0	0	0	0	0	0	1	0	0	0	0	0	0
Kelliidae	0	0	0	0	0	0	0	0	0	0	0	0	0	0
Loripes lucinalis (Lamarck, 1818)	0	0	0	0	0	0	0	0	0	0	0	0	0	0
Ostrea sp.	0	0	0	0	0	0	0	0	0	0	0	0	0	0
Paphia sp.	0	0	0	0	0	0	0	0	0	0	0	0	0	0
Parvicardium sp.	0	0	0	0	0	0	0	0	0	0	0	0	0	0
Pectinidae	0	0	0	0	0	0	0	0	0	0	0	0	0	0
Tapes decussatus (Linnaeus, 1758)	0	0	0	0	0	0	0	0	0	0	0	0	0	0
Tellina sp.	0	0	0	0	0	0	0	0	0	0	0	0	0	0
Veneridae	0	0	0	0	0	0	0	0	0	0	0	0	0	0
other/indeterminate	0	0	0	0	0	0	0	0	0	0	0	0	1	0
Hydrobia sp. Hartmann, 1821	0	0	0	0	0	0	77	40	71	42	6	0	2	0
Ovatella myosotis (Draparnaud, 1801)	0	0	0	0	0	0	0	2	0	4	1	2	4	0
Truncatella subcylindrica (Linnaeus, 1767)	0	0	0	0	0	0	0	0	0	0	0	0	0	0
Oxyloma elegans (Risso, 1826)	0	0	0	0	0	0	0	0	0	0	0	0	0	0
Pseudamnicola (s.str.) *moussonii* (Calcara, 1841)	0	0	0	0	0	0	5	6	5	5	0	0	0	0
Ancylus fluviatilis Müller, 1774	0	0	0	0	0	0	0	0	0	0	0	0	0	0
Bulinus cf. *truncatus* (Audouin, 1827)	0	0	0	0	0	0	0	0	0	0	0	0	0	0
Pisidium caesertanum (Poli, 1791)	0	0	0	0	0	0	0	0	0	0	0	0	0	0
Lymnaea (Galba) truncatula (Müller, 1774)	0	0	0	0	0	0	2	3	2	1	0	0	0	0
Planorbis moquini (Requien, 1848)	0	0	0	0	0	0	0	0	0	0	0	0	0	0
Planorbis planorbis (Linnaeus, 1758)	0	0	0	0	0	0	0	0	1	0	0	0	0	0
Carychium cf. *schlickumi* Strauch, 1977	0	0	0	0	0	0	0	0	0	0	0	0	0	0
Vertigo cf. *antivertigo* (Draparnaud, 1801)	0	0	0	0	0	0	0	0	0	0	0	0	0	0
Oxychilus (Mediterranea) *hydatinus* (Rossmässler, 1838)	0	0	0	0	0	0	0	0	0	0	0	0	0	0
Truncatellina callicratis (Scacchi, 1833)	0	0	0	0	0	0	0	0	0	0	0	0	0	0
Vitrea Fitzinger, 1833	0	0	0	0	0	0	0	1	0	0	0	0	0	0
Xerotricha Monterosato, 1892	0	0	0	0	0	0	0	0	0	0	0	0	0	0
Clausiliidae Mörch, 1864	0	0	0	0	0	0	0	2	6	2	1	0	0	0
Granopupa granum (Draparnaud, 1801)	0	0	0	0	0	0	0	0	0	0	0	0	0	0
Muticaria Lindholm, 1925	0	0	0	0	0	0	1	1	1	1	1	0	0	0
Papillifera papillaris (Müller, 1774)	0	0	0	0	0	0	2	1	2	0	0	0	0	0
Rumina decollata (Linnaeus, 1758)	0	0	0	0	0	0	0	1	0	1	0	0	0	0
Trochoidea spratti (Pfeiffer, 1846)	0	0	0	0	0	0	0	0	1	13	1	0	1	0
Cernuella caruanae (Kobelt, 1888)	0	0	0	0	0	0	8	1	3	4	0	0	0	0
Cochlicella acuta (Müller, 1774)	0	0	0	0	0	0	10	7	12	0	5	1	0	0
Pomatias sulcatus (Draparnaud, 1801)	0	0	0	0	0	0	1	0	0	1	1	0	0	0
Theba pisana (Müller, 1774)	0	0	0	0	0	0	0	1	4	1	2	0	0	0
Helicioidae	0	0	0	0	0	0	4	0	23	20	3	1	0	0
Cecilioides acicula (Müller, 1774)	0	0	0	0	0	0	2	0	2	0	0	1	0	0
Total amount of molluscs	**1**	**1**	**1**	**1**	**1**	**1**	**112**	**67**	**133**	**98**	**26**	**5**	**8**	**1**

Table A5.1 *(cont.).*

Species/Depth (cm)	213	218	223	228	233	238	243	248	253	258	263	268	273	278
Bittium reticulatum (Da Costa, 1778)	0	0	0	0	0	0	0	0	0	0	1	2	0	1
Cerithium spp.	0	0	0	0	0	0	0	0	0	0	0	4	0	0
Conus mediterraneus (Hwass, 1792)	0	0	0	0	0	0	0	0	0	0	0	0	0	0
Gibbula sp.	0	0	0	0	0	0	0	0	0	0	0	0	0	0
Haminoea sp.	0	0	0	0	0	0	0	0	0	0	0	0	0	0
Hexaplex trunculus (Linnaeus, 1758)	0	0	0	0	0	0	0	0	0	0	0	0	0	0
Pirenella conica (Blainville, 1826)	0	0	0	0	0	0	0	0	0	0	0	0	0	0
Retusa truncatula (Brugière, 1792)	0	0	0	0	0	0	0	0	0	0	0	0	0	0
Rissoa sp.	0	0	0	0	0	0	0	0	0	0	0	0	0	0
Turbonilla sp.	0	0	0	0	0	0	0	0	0	0	0	0	0	0
Acanthocardia sp.	0	0	0	0	0	0	0	0	0	0	0	0	0	0
Cardiidae	0	0	0	0	0	0	0	0	0	0	0	0	0	0
Cerastoderma sp.	0	0	0	0	0	0	0	0	0	0	2	1	0	5
Kelliidae	0	0	0	0	0	0	0	0	0	0	0	0	0	0
Loripes lucinalis (Lamarck, 1818)	0	0	0	0	0	0	0	0	0	0	0	0	0	0
Ostrea sp.	0	0	0	0	0	0	0	0	0	0	0	0	0	0
Paphia sp.	0	0	0	0	0	0	0	0	0	0	0	0	0	0
Parvicardium sp.	0	0	0	0	0	0	0	0	0	0	0	0	0	0
Pectinidae	0	0	0	0	0	0	0	0	0	0	0	2	0	2
Tapes decussatus (Linnaeus, 1758)	0	0	0	0	0	0	0	0	0	0	0	0	0	0
Tellina sp.	0	0	0	0	0	0	0	0	0	0	2	0	0	3
Veneridae	0	0	0	0	0	0	0	0	0	0	0	0	0	0
other/indeterminate	0	0	0	0	0	0	0	0	0	0	0	0	0	0
Hydrobia sp. Hartmann, 1821	0	0	0	0	0	0	0	0	0	0	0	4	1	1
Ovatella myosotis (Draparnaud, 1801)	0	0	0	0	0	0	0	0	0	0	0	0	0	0
Truncatella subcylindrica (Linnaeus, 1767)	0	0	0	0	0	0	0	0	0	0	0	0	0	0
Oxyloma elegans (Risso, 1826)	0	0	0	0	0	0	0	0	0	0	0	0	0	0
Pseudamnicola (s.str.) *moussonii* (Calcara, 1841)	0	0	0	0	0	0	0	0	0	0	0	0	0	0
Ancylus fluviatilis Müller, 1774	0	0	0	0	0	0	0	0	0	0	0	0	0	0
Bulinus cf. *truncatus* (Audouin, 1827)	0	0	0	0	0	0	0	0	0	0	0	0	0	0
Pisidium caesertanum (Poli, 1791)	0	0	0	0	0	0	0	0	0	0	0	0	0	0
Lymnaea (Galba) truncatula (Müller, 1774)	0	0	0	0	0	0	0	0	0	0	0	0	0	0
Planorbis moquini (Requien, 1848)	0	0	0	0	0	0	0	0	0	0	0	0	0	0
Planorbis planorbis (Linnaeus, 1758)	0	0	0	0	0	0	0	0	0	0	0	0	0	0
Carychium cf. *schlickumi* Strauch, 1977	0	0	0	0	0	0	0	0	0	0	0	0	0	0
Vertigo cf. *antivertigo* (Draparnaud, 1801)	0	0	0	0	0	0	0	0	0	0	0	0	0	0
Oxychilus (Mediterranea) *hydatinus* (Rossmässler, 1838)	0	0	0	0	0	0	0	0	0	0	0	0	0	0
Truncatellina callicratis (Scacchi, 1833)	0	0	0	0	0	0	0	0	0	0	0	0	0	0
Vitrea Fitzinger, 1833	0	0	0	0	0	0	0	0	0	0	0	0	0	0
Xerotricha Monterosato, 1892	0	0	0	0	0	0	0	0	0	0	0	0	0	0
Clausiliidae Mörch, 1864	0	0	0	0	0	0	0	0	0	0	0	0	0	0
Granopupa granum (Draparnaud, 1801)	0	0	0	0	0	0	0	0	0	0	0	0	0	0
Muticaria Lindholm, 1925	0	0	0	0	0	0	0	0	0	0	0	0	0	0
Papillifera papillaris (Müller, 1774)	0	0	0	0	0	0	0	0	0	0	0	0	0	0
Rumina decollata (Linnaeus, 1758)	0	0	0	0	0	0	0	0	0	0	0	0	0	0
Trochoidea spratti (Pfeiffer, 1846)	0	0	0	0	0	0	0	0	0	0	0	0	0	0
Cernuella caruanae (Kobelt, 1888)	0	0	0	0	0	0	0	0	0	0	0	0	0	0
Cochlicella acuta (Müller, 1774)	0	0	0	0	0	0	0	0	0	0	0	0	0	3
Pomatias sulcatus (Draparnaud, 1801)	0	0	0	0	0	0	0	0	0	0	0	0	0	0
Theba pisana (Müller, 1774)	0	0	0	0	0	0	0	0	0	0	0	0	0	0
Helicioidae	0	0	0	0	0	0	0	0	0	1	2	2	1	2
Cecilioides acicula (Müller, 1774)	0	0	0	0	0	0	0	0	0	0	0	0	0	1
Total amount of molluscs	**1**	**1**	**1**	**1**	**1**	**1**	**1**	**1**	**1**	**1**	**7**	**15**	**2**	**18**

Table A5.1 *(cont.).*

Species/Depth (cm)	283	288	293	298	303	308	313	318	323	328	333	338	343	348
Bittium reticulatum (Da Costa, 1778)	1	27	31	26	4	1	10	32	11	4	3	25	47	33
Cerithium spp.	2	0	4	0	1	1	2	4	1	0	0	2	7	4
Conus mediterraneus (Hwass, 1792)	0	0	0	0	0	0	0	0	0	0	0	0	0	0
Gibbula sp.	0	0	0	0	0	0	0	0	0	0	0	0	1	2
Haminoea sp.	0	0	0	0	0	0	0	0	0	0	0	0	0	0
Hexaplex trunculus (Linnaeus, 1758)	0	0	0	0	0	0	0	0	0	0	0	0	1	0
Pirenella conica (Blainville, 1826)	0	0	0	1	0	0	0	5	0	0	0	0	4	0
Retusa truncatula (Brugière, 1792)	0	0	0	1	0	1	0	0	0	0	0	0	0	0
Rissoa sp.	0	0	0	7	2	6	4	8	2	2	0	6	6	4
Turbonilla sp.	0	1	1	5	0	3	2	2	0	0	1	2	1	2
Acanthocardia sp.	0	0	0	0	0	0	0	0	0	0	0	0	0	0
Cardiidae	0	0	0	0	0	0	0	0	0	0	0	0	0	0
Cerastoderma sp.	0	4	19	14	5	6	9	6	10	8	6	15	14	12
Kelliidae	0	0	0	0	0	0	0	0	0	0	0	0	1	0
Loripes lucinalis (Lamarck, 1818)	0	0	0	0	0	0	0	0	0	0	0	0	0	0
Ostrea sp.	0	0	0	0	0	0	0	0	0	0	0	0	0	0
Paphia sp.	0	0	0	0	0	0	0	0	0	0	0	0	0	0
Parvicardium sp.	0	1	0	0	0	0	1	0	0	0	0	0	0	1
Pectinidae	2	1	2	10	0	0	0	1	1	0	1	1	2	2
Tapes decussatus (Linnaeus, 1758)	0	0	0	0	0	0	0	0	0	0	0	0	0	0
Tellina sp.	0	2	7	11	1	0	6	2	2	1	0	7	5	3
Veneridae	0	0	0	0	0	0	0	0	0	0	0	0	0	0
other/indeterminate	0	0	0	0	0	0	0	0	0	0	0	0	2	0
Hydrobia sp. Hartmann, 1821	0	32	310	232	50	21	108	56	45	26	32	161	113	141
Ovatella myosotis (Draparnaud, 1801)	0	0	1	3	0	0	0	0	1	1	2	1	0	0
Truncatella subcylindrica (Linnaeus, 1767)	0	0	3	3	0	0	2	0	1	0	0	1	0	0
Oxyloma elegans (Risso, 1826)	0	0	0	0	0	0	0	0	0	0	0	0	0	0
Pseudamnicola (s.str.) *moussonii* (Calcara, 1841)	0	0	1	0	0	1	1	0	1	2	1	0	0	1
Ancylus fluviatilis Müller, 1774	0	0	0	0	0	0	0	0	0	0	0	0	0	0
Bulinus cf. *truncatus* (Audouin, 1827)	0	0	0	0	0	0	0	0	0	0	0	0	0	0
Pisidium caesertanum (Poli, 1791)	0	0	0	0	0	0	0	0	0	0	0	0	0	0
Lymnaea (Galba) truncatula (Müller, 1774)	0	0	0	0	0	0	0	0	0	0	0	0	0	0
Planorbis moquini (Requien, 1848)	0	0	0	0	0	0	0	0	0	0	0	0	0	0
Planorbis planorbis (Linnaeus, 1758)	0	0	0	0	1	0	0	0	0	0	0	0	0	0
Carychium cf. *schlickumi* Strauch, 1977	0	0	0	0	0	0	0	0	0	0	0	0	0	0
Vertigo cf. *antivertigo* (Draparnaud, 1801)	0	0	0	0	0	0	0	0	0	0	0	0	0	0
Oxychilus (Mediterranea) *hydatinus* (Rossmässler, 1838)	0	0	0	0	0	0	0	0	0	0	0	0	0	0
Truncatellina callicratis (Scacchi, 1833)	0	0	0	0	0	0	0	0	0	0	0	0	0	0
Vitrea Fitzinger, 1833	0	0	0	0	0	0	0	0	0	0	0	0	0	0
Xerotricha Monterosato, 1892	0	0	0	0	0	0	0	0	0	0	0	0	0	0
Clausiliidae Mörch, 1864	0	0	1	0	0	0	0	0	0	0	0	0	0	0
Granopupa granum (Draparnaud, 1801)	0	0	0	0	0	0	1	0	0	0	0	0	0	0
Muticaria Lindholm, 1925	0	0	0	0	0	0	0	0	0	0	0	0	0	0
Papillifera papillaris (Müller, 1774)	0	0	0	0	0	0	0	0	0	0	0	0	0	0
Rumina decollata (Linnaeus, 1758)	0	0	0	0	0	0	0	0	0	0	0	0	0	0
Trochoidea spratti (Pfeiffer, 1846)	0	0	1	0	0	0	0	0	0	0	0	0	0	0
Cernuella caruanae (Kobelt, 1888)	0	0	0	0	0	0	0	1	0	0	0	0	0	0
Cochlicella acuta (Müller, 1774)	1	0	4	7	0	0	0	4	0	3	4	2	3	4
Pomatias sulcatus (Draparnaud, 1801)	0	0	0	0	0	0	0	0	0	0	0	0	0	0
Theba pisana (Müller, 1774)	0	0	0	1	0	0	0	0	0	0	0	1	2	0
Helicioidae	1	1	0	1	1	3	1	2	0	4	1	3	5	6
Cecilioides acicula (Müller, 1774)	0	1	2	0	0	0	0	0	2	0	0	0	0	1
Total amount of molluscs	**7**	**70**	**387**	**322**	**64**	**43**	**147**	**123**	**77**	**51**	**51**	**227**	**214**	**216**

Table A5.1 *(cont.).*

Species/Depth (cm)	353	358	363	368	373	378	383	388	393	398	403	408	413	418
Bittium reticulatum (Da Costa, 1778)	16	25	42	40	28	24	15	14	24	38	48	41	30	16
Cerithium spp.	3	2	11	12	10	15	16	34	37	36	33	23	7	5
Conus mediterraneus (Hwass, 1792)	0	0	0	0	1	1	0	0	0	0	0	0	0	0
Gibbula sp.	4	0	0	0	0	0	0	1	0	1	2	0	1	0
Haminoea sp.	0	0	0	0	0	2	0	0	0	0	0	1	0	0
Hexaplex trunculus (Linnaeus, 1758)	0	0	0	0	0	1	3	1	0	1	4	0	0	1
Pirenella conica (Blainville, 1826)	2	0	0	0	1	0	0	0	0	0	4	1	0	0
Retusa truncatula (Brugière, 1792)	0	0	2	0	0	2	0	0	0	0	1	1	1	0
Rissoa sp.	7	11	14	23	24	18	48	24	15	18	24	20	23	8
Turbonilla sp.	1	5	10	7	6	8	8	13	9	4	19	15	7	5
Acanthocardia sp.	0	0	0	1	0	0	0	0	1	0	2	0	0	0
Cardiidae	0	0	0	0	0	0	0	0	0	0	0	0	0	0
Cerastoderma sp.	9	92	113	44	35	28	24	52	56	88	104	110	85	25
Kelliidae	0	0	0	0	1	1	5	4	4	13	9	17	10	4
Loripes lucinalis (Lamarck, 1818)	0	0	0	1	2	0	0	1	4	2	17	8	10	2
Ostrea sp.	0	0	1	1	0	2	2	1	5	4	6	1	1	0
Paphia sp.	0	1	0	0	1	0	2	2	1	0	2	1	1	2
Parvicardium sp.	2	0	1	2	1	2	2	10	3	4	11	11	3	0
Pectinidae	1	11	22	17	7	6	3	16	21	19	44	14	5	3
Tapes decussatus (Linnaeus, 1758)	0	0	4	2	1	2	0	3	6	6	3	1	0	1
Tellina sp.	3	22	29	22	13	17	18	24	17	37	45	29	33	12
Veneridae	0	0	0	0	0	1	0	0	0	0	1	5	1	2
other/indeterminate	0	0	0	0	0	0	0	0	0	0	1	1	2	0
Hydrobia sp. Hartmann, 1821	154	224	251	159	101	60	105	183	172	212	268	320	162	57
Ovatella myosotis (Draparnaud, 1801)	0	0	0	0	0	0	0	0	0	0	0	0	0	0
Truncatella subcylindrica (Linnaeus, 1767)	0	0	2	2	0	0	2	4	3	5	10	18	8	2
Oxyloma elegans (Risso, 1826)	0	0	0	0	0	0	0	0	0	0	0	0	0	1
Pseudamnicola (s.str.) *moussonii* (Calcara, 1841)	0	1	2	0	0	0	0	2	5	14	12	21	19	11
Ancylus fluviatilis Müller, 1774	0	0	0	0	0	0	2	0	1	2	4	1	2	1
Bulinus cf. *truncatus* (Audouin, 1827)	0	0	0	0	0	0	0	0	0	2	5	3	0	1
Pisidium caesertanum (Poli, 1791)	0	4	0	0	0	0	0	0	0	1	1	0	0	0
Lymnaea (Galba) truncatula (Müller, 1774)	1	0	0	0	0	0	0	1	1	2	5	6	4	0
Planorbis moquini (Requien, 1848)	0	0	0	0	0	0	0	2	0	0	0	0	0	0
Planorbis planorbis (Linnaeus, 1758)	0	0	0	1	0	0	0	0	1	7	11	10	8	1
Carychium cf. *schlickumi* Strauch, 1977	0	0	0	0	0	0	0	0	0	1	1	0	0	1
Vertigo cf. *antivertigo* (Draparnaud, 1801)	0	0	0	0	0	0	0	0	0	0	0	0	0	1
Oxychilus (Mediterranea) *hydatinus* (Rossmässler, 1838)	0	0	0	0	0	0	0	0	0	0	0	0	0	0
Truncatellina callicratis (Scacchi, 1833)	0	0	0	0	0	1	2	2	1	5	0	3	3	1
Vitrea Fitzinger, 1833	0	0	1	0	0	0	1	1	1	2	5	5	5	2
Xerotricha Monterosato, 1892	0	0	0	0	0	0	0	0	0	0	3	0	0	0
Clausiliidae Mörch, 1864	0	0	0	0	0	0	0	1	0	1	1	3	0	0
Granopupa granum (Draparnaud, 1801)	0	0	0	0	0	0	0	0	0	0	6	1	0	1
Muticaria Lindholm, 1925	0	0	0	0	0	1	1	0	1	2	0	1	1	1
Papillifera papillaris (Müller, 1774)	0	0	0	0	0	0	0	0	0	0	3	1	2	0
Rumina decollata (Linnaeus, 1758)	0	0	0	0	0	0	0	0	0	0	2	0	0	0
Trochoidea spratti (Pfeiffer, 1846)	0	1	1	0	1	0	0	0	3	2	7	7	2	4
Cernuella caruanae (Kobelt, 1888)	0	0	0	0	1	0	0	1	0	2	3	1	1	1
Cochlicella acuta (Müller, 1774)	4	3	1	1	5	4	3	7	6	18	16	27	23	15
Pomatias sulcatus (Draparnaud, 1801)	0	0	0	0	0	0	0	0	1	0	0	0	0	0
Theba pisana (Müller, 1774)	1	0	0	0	1	0	0	0	0	0	2	0	0	2
Helicioidae	3	3	1	2	1	2	3	3	8	19	15	19	17	13
Cecilioides acicula (Müller, 1774)	2	1	1	0	0	0	0	1	2	9	17	11	13	5
Total amount of molluscs	**213**	**406**	**509**	**337**	**241**	**198**	**265**	**408**	**409**	**577**	**777**	**758**	**490**	**207**

Table A5.1 *(cont.).*

Species/Depth (cm)	423	428	433	438	443	448	453	458	463	468	473	478	483	488
Bittium reticulatum (Da Costa, 1778)	39	22	10	12	17	20	19	11	29	72	52	58	47	95
Cerithium spp.	4	11	2	11	7	6	20	15	26	66	101	113	83	127
Conus mediterraneus (Hwass, 1792)	0	0	0	0	0	0	0	0	0	0	0	0	0	0
Gibbula sp.	2	0	0	0	0	1	0	0	0	1	0	0	0	0
Haminoea sp.	0	0	0	0	0	1	1	2	0	2	0	0	0	0
Hexaplex trunculus (Linnaeus, 1758)	0	2	0	2	0	1	0	1	0	1	0	1	0	0
Pirenella conica (Blainville, 1826)	1	1	0	0	1	0	3	0	3	12	8	6	4	4
Retusa truncatula (Brugière, 1792)	0	1	0	0	0	0	1	0	1	0	0	0	0	1
Rissoa sp.	19	17	7	17	5	12	13	9	16	19	18	24	31	49
Turbonilla sp.	4	7	3	3	4	3	7	1	7	8	14	18	27	14
Acanthocardia sp.	0	0	0	0	0	0	1	0	0	1	0	0	0	9
Cardiidae	0	0	0	0	0	0	0	0	0	0	0	0	0	0
Cerastoderma sp.	122	46	26	43	45	31	54	32	102	118	118	97	129	118
Kelliidae	0	0	2	2	7	1	5	5	17	49	18	9	5	7
Loripes lucinalis (Lamarck, 1818)	2	0	0	0	0	3	4	2	1	16	3	12	7	15
Ostrea sp.	1	0	0	0	0	2	2	0	1	5	4	1	1	1
Paphia sp.	0	1	0	0	0	0	2	0	1	1	0	0	2	1
Parvicardium sp.	1	0	1	1	4	2	1	1	10	7	7	5	4	9
Pectinidae	14	5	1	2	7	4	2	9	6	1	5	2	6	5
Tapes decussatus (Linnaeus, 1758)	5	0	1	0	3	0	0	2	2	6	7	18	6	2
Tellina sp.	43	19	11	9	18	6	19	11	15	46	50	33	59	46
Veneridae	1	0	0	1	0	0	1	1	0	1	3	1	4	0
other/indeterminate	4	0	0	0	2	1	1	0	0	0	2	4	6	1
Hydrobia sp. Hartmann, 1821	272	96	38	77	118	115	106	63	247	583	509	524	445	344
Ovatella myosotis (Draparnaud, 1801)	0	0	0	0	0	0	0	0	0	0	0	0	0	0
Truncatella subcylindrica (Linnaeus, 1767)	2	2	0	0	0	5	4	3	5	4	9	1	0	0
Oxyloma elegans (Risso, 1826)	0	0	0	0	0	0	0	0	0	0	0	0	1	0
Pseudamnicola (s.str.) *moussonii* (Calcara, 1841)	2	0	1	2	8	2	8	2	2	9	2	0	3	1
Ancylus fluviatilis Müller, 1774	1	3	0	0	1	0	2	0	3	3	0	1	0	0
Bulinus cf. *truncatus* (Audouin, 1827)	0	0	0	0	0	1	2	0	0	1	1	0	0	0
Pisidium caesertanum (Poli, 1791)	0	0	0	0	0	1	1	0	0	0	0	0	0	0
Lymnaea (Galba) truncatula (Müller, 1774)	0	0	0	0	0	0	2	0	0	0	0	0	0	0
Planorbis moquini (Requien, 1848)	0	0	0	0	0	0	1	2	1	4	1	1	0	0
Planorbis planorbis (Linnaeus, 1758)	0	0	0	1	2	1	0	0	0	0	0	0	0	0
Carychium cf. *schlickumi* Strauch, 1977	0	0	0	0	0	0	0	0	1	0	0	0	0	0
Vertigo cf. *antivertigo* (Draparnaud, 1801)	0	0	0	0	0	0	0	0	0	0	0	0	0	0
Oxychilus (Mediterranea) *hydatinus* (Rossmässler, 1838)	0	0	0	0	0	0	0	0	0	0	0	0	1	0
Truncatellina callicratis (Scacchi, 1833)	0	0	0	1	0	0	2	0	0	1	3	0	0	1
Vitrea Fitzinger, 1833	0	0	0	2	1	1	2	1	1	0	0	2	2	0
Xerotricha Monterosato, 1892	0	0	0	0	0	0	0	0	0	0	0	0	0	0
Clausiliidae Mörch, 1864	0	0	0	0	0	0	0	0	0	2	0	0	0	2
Granopupa granum (Draparnaud, 1801)	0	0	0	0	0	0	0	0	0	0	0	1	0	0
Muticaria Lindholm, 1925	0	0	1	0	1	1	1	1	1	0	0	0	0	0
Papillifera papillaris (Müller, 1774)	0	0	0	0	0	0	2	1	0	0	0	0	0	0
Rumina decollata (Linnaeus, 1758)	0	0	0	0	0	0	0	0	0	0	0	0	0	0
Trochoidea spratti (Pfeiffer, 1846)	0	0	1	0	3	0	4	3	0	4	3	1	5	2
Cernuella caruanae (Kobelt, 1888)	0	0	0	0	3	1	2	0	1	2	4	3	0	0
Cochlicella acuta (Müller, 1774)	1	0	5	5	15	6	5	1	4	10	13	8	4	3
Pomatias sulcatus (Draparnaud, 1801)	0	0	0	0	0	0	0	0	0	0	0	0	0	0
Theba pisana (Müller, 1774)	0	0	0	0	0	1	0	0	1	0	1	0	0	0
Helicioidae	1	0	4	4	10	4	10	4	0	6	8	5	4	6
Cecilioides acicula (Müller, 1774)	0	0	1	3	2	0	2	3	0	2	2	2	1	2
Total amount of molluscs	**541**	**233**	**115**	**198**	**284**	**233**	**312**	**186**	**504**	**1063**	**966**	**951**	**887**	**865**

Table A5.1 *(cont.).*

Species/Depth (cm)	493	498	503	508	513	518	523	528	533	538	543	548	553	558
Bittium reticulatum (Da Costa, 1778)	219	161	27	9	4	5	0	0	0	0	0	0	0	0
Cerithium spp.	78	34	2	9	5	0	0	0	0	0	0	0	0	0
Conus mediterraneus (Hwass, 1792)	1	0	0	0	0	0	0	0	0	0	0	0	0	0
Gibbula sp.	0	0	0	0	0	0	0	0	0	0	0	0	0	0
Haminoea sp.	2	0	0	0	0	0	0	0	0	0	0	0	0	0
Hexaplex trunculus (Linnaeus, 1758)	4	4	0	0	0	0	0	0	0	0	0	0	0	0
Pirenella conica (Blainville, 1826)	10	1	0	1	1	0	0	0	0	0	0	0	0	0
Retusa truncatula (Brugière, 1792)	0	2	0	0	0	0	0	0	0	0	0	0	0	0
Rissoa sp.	56	46	6	10	2	0	0	0	0	0	0	0	0	0
Turbonilla sp.	34	9	3	2	2	0	0	0	0	0	0	0	0	0
Acanthocardia sp.	0	0	0	0	0	0	0	0	0	0	0	0	0	0
Cardiidae	0	0	0	0	0	0	0	0	0	0	0	0	0	0
Cerastoderma sp.	124	40	24	23	6	9	0	0	0	0	0	0	0	0
Kelliidae	5	1	0	0	2	0	0	0	0	0	0	0	0	0
Loripes lucinalis (Lamarck, 1818)	33	8	3	0	0	1	0	0	0	0	0	0	0	0
Ostrea sp.	4	3	0	2	1	1	0	0	0	0	0	0	0	0
Paphia sp.	1	0	0	0	0	0	0	0	0	0	0	0	0	0
Parvicardium sp.	14	6	3	2	0	0	0	0	0	0	0	0	0	0
Pectinidae	2	6	2	2	1	0	0	0	0	0	0	0	0	0
Tapes decussatus (Linnaeus, 1758)	8	2	2	2	1	0	0	0	0	0	0	0	0	0
Tellina sp.	97	30	14	7	4	1	0	0	0	0	0	0	0	0
Veneridae	3	4	2	0	0	1	0	0	0	0	0	0	0	0
other/indeterminate	1	0	1	0	0	1	0	0	0	0	0	0	0	0
Hydrobia sp. Hartmann, 1821	315	238	71	49	20	6	0	0	0	0	0	0	0	0
Ovatella myosotis (Draparnaud, 1801)	0	0	0	0	0	0	0	0	0	0	0	0	0	0
Truncatella subcylindrica (Linnaeus, 1767)	2	4	0	2	0	0	0	0	0	0	0	0	0	0
Oxyloma elegans (Risso, 1826)	0	0	0	0	0	0	0	0	0	0	0	0	0	0
Pseudamnicola (s.str.) *moussonii* (Calcara, 1841)	0	1	0	1	1	0	0	0	0	0	0	0	0	0
Ancylus fluviatilis Müller, 1774	0	1	0	1	0	0	0	0	0	0	0	0	0	0
Bulinus cf. *truncatus* (Audouin, 1827)	0	0	0	0	0	0	0	0	0	0	0	0	0	0
Pisidium caesertanum (Poli, 1791)	0	0	0	0	0	0	0	0	0	0	0	0	0	0
Lymnaea (Galba) truncatula (Müller, 1774)	0	0	0	0	0	0	0	0	0	0	0	0	0	0
Planorbis moquini (Requien, 1848)	0	0	1	0	0	0	0	0	0	0	0	0	0	0
Planorbis planorbis (Linnaeus, 1758)	0	0	0	0	0	0	0	0	0	0	0	0	0	0
Carychium cf. *schlickumi* Strauch, 1977	0	0	0	0	0	0	0	0	0	0	0	0	0	0
Vertigo cf. *antivertigo* (Draparnaud, 1801)	0	0	0	0	0	0	0	0	0	0	0	0	0	0
Oxychilus (Mediterranea) *hydatinus* (Rossmässler, 1838)	0	0	0	0	0	0	0	0	0	0	0	0	0	0
Truncatellina callicratis (Scacchi, 1833)	0	0	0	0	0	0	0	0	0	0	0	0	0	0
Vitrea Fitzinger, 1833	1	3	2	0	3	0	0	0	0	0	0	0	0	0
Xerotricha Monterosato, 1892	0	0	0	0	0	0	0	0	0	0	0	0	0	0
Clausiliidae Mörch, 1864	1	0	0	0	0	0	0	0	0	0	0	0	0	0
Granopupa granum (Draparnaud, 1801)	0	0	0	0	0	0	0	0	0	0	0	0	0	0
Muticaria Lindholm, 1925	1	0	1	0	0	0	0	0	0	0	0	0	0	0
Papillifera papillaris (Müller, 1774)	0	0	0	0	0	0	0	0	0	0	0	0	0	0
Rumina decollata (Linnaeus, 1758)	0	0	0	0	0	0	0	0	0	0	0	0	0	0
Trochoidea spratti (Pfeiffer, 1846)	1	3	1	6	0	2	0	0	0	0	0	0	0	0
Cernuella caruanae (Kobelt, 1888)	1	1	1	2	1	0	0	0	0	0	0	0	0	0
Cochlicella acuta (Müller, 1774)	6	5	9	22	3	0	0	0	0	0	0	0	0	0
Pomatias sulcatus (Draparnaud, 1801)	0	0	0	0	0	0	0	0	0	0	0	0	0	0
Theba pisana (Müller, 1774)	0	0	0	0	0	0	0	0	0	0	0	0	0	0
Helicioidae	4	1	5	2	1	0	0	0	0	0	0	0	0	0
Cecilioides acicula (Müller, 1774)	1	3	15	10	6	3	0	0	0	0	0	0	0	0
Total amount of molluscs	**1029**	**617**	**195**	**164**	**64**	**30**	**1**	**1**	**1**	**1**	**1**	**1**	**1**	**1**

Table A5.1 *(cont.).*

Species/Depth (cm)	563	568	573	578	583	588	593	598	603	608	613	618	623	628
Bittium reticulatum (Da Costa, 1778)	0	0	0	0	0	0	12	20	57	36	9	47	23	8
Cerithium spp.	0	0	0	0	0	0	9	20	45	12	14	36	8	9
Conus mediterraneus (Hwass, 1792)	0	0	0	0	0	0	0	0	0	0	0	1	1	0
Gibbula sp.	0	0	0	0	0	0	1	0	0	0	0	1	0	0
Haminoea sp.	0	0	0	0	0	0	0	1	0	0	0	1	0	0
Hexaplex trunculus (Linnaeus, 1758)	0	0	0	0	0	0	0	0	0	0	0	0	1	0
Pirenella conica (Blainville, 1826)	0	0	0	0	0	0	0	2	2	2	0	0	1	0
Retusa truncatula (Brugière, 1792)	0	0	0	0	0	0	0	0	1	0	0	0	0	0
Rissoa sp.	0	0	0	0	0	0	19	16	17	9	5	17	4	0
Turbonilla sp.	0	0	0	0	0	0	6	2	10	9	0	4	2	0
Acanthocardia sp.	0	0	0	0	0	0	0	0	0	0	0	0	0	0
Cardiidae	0	0	0	0	0	0	0	0	0	0	0	0	0	0
Cerastoderma sp.	0	0	0	0	0	0	41	65	60	43	24	47	25	11
Kelliidae	0	0	0	0	0	0	0	8	3	0	2	6	2	0
Loripes lucinalis (Lamarck, 1818)	0	0	0	0	0	0	1	4	5	5	1	0	1	0
Ostrea sp.	0	0	0	0	0	0	1	0	0	1	1	1	1	0
Paphia sp.	0	0	0	0	0	0	0	1	0	0	1	0	1	0
Parvicardium sp.	0	0	0	0	0	0	1	3	1	1	0	0	3	1
Pectinidae	0	0	0	0	0	0	1	1	2	0	3	4	3	1
Tapes decussatus (Linnaeus, 1758)	0	0	0	0	0	0	1	5	4	1	2	6	1	0
Tellina sp.	0	0	0	0	0	0	6	15	22	22	4	11	5	2
Veneridae	0	0	0	0	0	0	1	1	2	0	1	1	1	0
other/indeterminate	0	0	0	0	0	0	0	2	0	0	1	0	0	0
Hydrobia sp. Hartmann, 1821	0	0	0	0	0	0	49	171	216	57	65	198	62	31
Ovatella myosotis (Draparnaud, 1801)	0	0	0	0	0	0	0	0	0	0	0	0	0	0
Truncatella subcylindrica (Linnaeus, 1767)	0	0	0	0	0	0	1	3	2	1	0	3	2	0
Oxyloma elegans (Risso, 1826)	0	0	0	0	0	0	0	0	0	0	0	0	0	0
Pseudamnicola (s.str.) *moussonii* (Calcara, 1841)	0	0	0	0	0	0	4	5	3	3	0	1	1	0
Ancylus fluviatilis Müller, 1774	0	0	0	0	0	0	0	1	0	1	0	1	0	1
Bulinus cf. *truncatus* (Audouin, 1827)	0	0	0	0	0	0	0	1	1	0	0	0	0	0
Pisidium caesertanum (Poli, 1791)	0	0	0	0	0	0	0	0	0	0	0	0	0	0
Lymnaea (Galba) truncatula (Müller, 1774)	0	0	0	0	0	0	0	0	0	0	0	0	0	0
Planorbis moquini (Requien, 1848)	0	0	0	0	0	0	2	0	0	0	1	0	0	0
Planorbis planorbis (Linnaeus, 1758)	0	0	0	0	0	0	0	1	1	0	0	0	0	0
Carychium cf. *schlickumi* Strauch, 1977	0	0	0	0	0	0	0	0	0	0	0	0	0	0
Vertigo cf. *antivertigo* (Draparnaud, 1801)	0	0	0	0	0	0	0	0	0	0	0	0	0	0
Oxychilus (Mediterranea) *hydatinus* (Rossmässler, 1838)	0	0	0	0	0	0	0	0	1	0	0	0	0	0
Truncatellina callicratis (Scacchi, 1833)	0	0	0	0	0	0	1	1	0	0	0	1	0	1
Vitrea Fitzinger, 1833	0	0	0	0	0	0	0	0	0	5	1	1	2	0
Xerotricha Monterosato, 1892	0	0	0	0	0	0	0	0	0	0	0	0	0	0
Clausiliidae Mörch, 1864	0	0	0	0	0	0	0	0	0	0	0	0	0	0
Granopupa granum (Draparnaud, 1801)	0	0	0	0	0	0	0	0	0	0	0	0	0	0
Muticaria Lindholm, 1925	0	0	0	0	0	0	1	1	0	1	1	1	0	1
Papillifera papillaris (Müller, 1774)	0	0	0	0	0	0	0	1	0	0	0	0	0	0
Rumina decollata (Linnaeus, 1758)	0	0	0	0	0	0	0	0	0	0	0	0	0	0
Trochoidea spratti (Pfeiffer, 1846)	0	0	0	0	0	0	0	6	7	3	5	1	3	0
Cernuella caruanae (Kobelt, 1888)	0	0	0	0	0	0	3	7	0	0	3	0	2	0
Cochlicella acuta (Müller, 1774)	0	0	0	0	0	0	2	9	9	10	4	7	8	4
Pomatias sulcatus (Draparnaud, 1801)	0	0	0	0	0	0	0	0	0	0	0	0	0	0
Theba pisana (Müller, 1774)	0	0	0	0	0	0	1	1	2	1	0	4	0	0
Helicioidae	0	0	0	0	0	0	0	4	4	7	2	2	5	5
Cecilioides acicula (Müller, 1774)	0	0	0	0	0	0	0	2	2	4	6	2	3	10
Total amount of molluscs	**1**	**1**	**1**	**1**	**1**	**1**	**164**	**380**	**479**	**234**	**156**	**405**	**171**	**84**

Table A5.1 *(cont.).*

Species/Depth (cm)	633	638	643	648	653	658	663	668	673	678	683	688	693	698
Bittium reticulatum (Da Costa, 1778)	3	1	1	0	0	0	0	0	0	0	0	0	0	0
Cerithium spp.	0	0	1	0	0	0	0	0	0	1	0	0	0	0
Conus mediterraneus (Hwass, 1792)	0	0	0	0	0	0	0	0	0	0	0	0	0	0
Gibbula sp.	0	0	0	0	0	0	0	0	0	0	0	0	0	0
Haminoea sp.	0	0	0	0	0	0	0	0	0	0	0	0	0	0
Hexaplex trunculus (Linnaeus, 1758)	0	0	0	0	0	0	0	0	0	0	0	0	0	0
Pirenella conica (Blainville, 1826)	2	0	0	0	0	0	0	0	0	0	0	0	0	0
Retusa truncatula (Brugière, 1792)	0	0	0	0	0	0	0	0	0	0	0	0	0	0
Rissoa sp.	4	0	0	0	0	0	0	0	0	0	0	0	0	0
Turbonilla sp.	0	0	0	0	0	0	0	0	0	0	0	0	0	0
Acanthocardia sp.	0	0	0	0	0	0	0	0	0	0	0	0	0	0
Cardiidae	0	0	0	0	0	0	0	0	0	0	0	0	0	0
Cerastoderma sp.	8	1	0	0	0	0	0	0	0	0	0	0	0	0
Kelliidae	0	0	0	0	0	0	0	0	0	0	0	0	0	0
Loripes lucinalis (Lamarck, 1818)	0	0	0	0	0	0	0	0	0	0	0	0	0	0
Ostrea sp.	0	1	0	0	0	0	0	0	0	0	0	0	0	0
Paphia sp.	0	0	0	0	0	0	0	0	0	0	0	0	0	0
Parvicardium sp.	0	0	0	0	0	0	0	0	0	0	0	0	0	0
Pectinidae	0	0	0	0	0	0	0	0	0	0	0	0	0	0
Tapes decussatus (Linnaeus, 1758)	0	0	0	0	0	0	0	0	0	0	0	0	0	0
Tellina sp.	2	1	1	0	0	0	0	0	0	1	0	0	0	0
Veneridae	2	0	0	0	0	0	0	0	0	0	0	0	0	0
other/indeterminate	0	0	0	0	0	1	0	0	0	0	0	0	0	0
Hydrobia sp. Hartmann, 1821	7	1	2	0	0	0	0	0	0	0	0	0	0	0
Ovatella myosotis (Draparnaud, 1801)	0	0	0	0	0	0	0	0	0	0	0	0	0	0
Truncatella subcylindrica (Linnaeus, 1767)	0	0	0	0	0	0	0	0	0	0	0	0	0	0
Oxyloma elegans (Risso, 1826)	0	0	0	0	0	0	0	0	0	0	0	0	0	0
Pseudamnicola (s.str.) *moussonii* (Calcara, 1841)	0	0	0	0	0	0	0	0	0	0	0	0	0	0
Ancylus fluviatilis Müller, 1774	0	0	0	0	0	0	0	0	0	0	0	0	0	0
Bulinus cf. *truncatus* (Audouin, 1827)	0	0	0	0	0	0	0	0	0	0	0	0	0	0
Pisidium caesertanum (Poli, 1791)	0	0	0	0	0	0	0	0	0	0	0	0	0	0
Lymnaea (Galba) truncatula (Müller, 1774)	0	0	0	0	0	0	0	0	0	0	0	0	0	0
Planorbis moquini (Requien, 1848)	0	0	0	0	0	0	0	0	0	0	0	0	0	0
Planorbis planorbis (Linnaeus, 1758)	0	0	0	0	0	0	0	0	0	0	0	0	0	0
Carychium cf. *schlickumi* Strauch, 1977	0	0	0	0	0	0	0	0	0	0	0	0	0	0
Vertigo cf. *antivertigo* (Draparnaud, 1801)	0	0	0	0	0	0	0	0	0	0	0	0	0	0
Oxychilus (Mediterranea) *hydatinus* (Rossmässler, 1838)	0	0	0	0	0	0	0	0	0	0	0	0	0	0
Truncatellina callicratis (Scacchi, 1833)	0	0	0	0	0	0	0	0	0	0	0	0	0	0
Vitrea Fitzinger, 1833	0	0	0	0	0	0	0	0	0	0	0	0	0	0
Xerotricha Monterosato, 1892	0	0	0	0	0	0	0	0	0	0	0	0	0	0
Clausiliidae Mörch, 1864	0	0	0	0	0	0	0	0	0	0	0	0	0	0
Granopupa granum (Draparnaud, 1801)	0	0	0	0	0	0	0	0	0	0	0	0	0	0
Muticaria Lindholm, 1925	0	0	0	0	0	0	0	0	0	0	0	0	0	0
Papillifera papillaris (Müller, 1774)	0	0	0	0	0	0	0	0	0	0	0	0	0	0
Rumina decollata (Linnaeus, 1758)	0	0	0	0	0	0	0	0	0	0	0	0	0	0
Trochoidea spratti (Pfeiffer, 1846)	1	1	2	1	2	2	1	0	3	1	0	0	0	0
Cernuella caruanae (Kobelt, 1888)	0	0	0	0	0	1	0	0	0	0	0	0	0	0
Cochlicella acuta (Müller, 1774)	2	0	0	0	0	0	0	0	0	0	0	0	0	0
Pomatias sulcatus (Draparnaud, 1801)	0	0	0	0	0	0	0	0	0	0	0	0	0	0
Theba pisana (Müller, 1774)	0	0	0	0	0	0	0	0	0	0	0	0	0	0
Helicioidae	0	0	0	1	0	4	0	1	0	1	0	0	0	0
Cecilioides acicula (Müller, 1774)	3	0	0	1	0	0	0	0	0	0	0	0	0	0
Total amount of molluscs	**34**	**6**	**7**	**3**	**2**	**8**	**1**	**1**	**3**	**4**	**1**	**1**	**1**	**1**

Table A5.1 *(cont.).*

Species/Depth (cm)	703	708	713	718	723	728	733	738	743	748	753	758	763	768
Bittium reticulatum (Da Costa, 1778)	1	0	0	0	0	0	0	0	0	0	0	0	0	0
Cerithium spp.	0	3	1	0	0	0	0	0	0	0	0	0	0	0
Conus mediterraneus (Hwass, 1792)	0	0	0	0	0	0	0	0	0	0	0	0	0	0
Gibbula sp.	0	0	0	0	0	0	0	0	0	0	0	0	0	0
Haminoea sp.	0	0	0	0	0	0	0	0	0	0	0	0	0	0
Hexaplex trunculus (Linnaeus, 1758)	0	0	0	0	0	0	0	0	0	0	0	0	0	0
Pirenella conica (Blainville, 1826)	0	0	0	0	0	0	0	0	0	0	0	0	0	0
Retusa truncatula (Brugière, 1792)	0	0	0	0	0	0	0	0	0	0	0	0	0	0
Rissoa sp.	0	0	0	0	0	0	0	0	0	0	0	0	0	0
Turbonilla sp.	0	0	0	0	0	0	0	0	0	0	0	0	0	0
Acanthocardia sp.	0	0	0	0	0	0	0	0	0	0	0	0	0	0
Cardiidae	4	0	0	0	0	1	0	0	0	0	0	0	0	0
Cerastoderma sp.	0	2	0	0	0	0	0	1	0	0	0	1	1	3
Kelliidae	0	0	0	0	0	0	0	0	0	0	0	0	0	0
Loripes lucinalis (Lamarck, 1818)	0	0	0	0	0	0	0	0	0	0	0	0	0	0
Ostrea sp.	1	1	0	1	0	0	0	0	0	0	0	1	0	1
Paphia sp.	0	0	0	0	0	0	0	0	0	0	0	0	0	0
Parvicardium sp.	0	0	0	0	0	0	0	0	0	0	0	0	0	0
Pectinidae	0	0	0	0	0	0	0	0	0	0	0	0	0	0
Tapes decussatus (Linnaeus, 1758)	0	0	0	0	0	0	0	0	0	0	0	0	0	0
Tellina sp.	0	0	0	0	0	0	0	0	0	0	0	1	0	0
Veneridae	0	0	0	0	0	0	0	0	0	0	0	0	0	0
other/indeterminate	0	0	0	0	0	0	0	0	0	0	0	0	0	0
Hydrobia sp. Hartmann, 1821	0	1	0	0	0	0	0	0	0	0	0	2	0	0
Ovatella myosotis (Draparnaud, 1801)	0	0	0	0	0	0	0	0	0	0	0	0	0	0
Truncatella subcylindrica (Linnaeus, 1767)	0	0	0	0	0	0	0	0	0	0	0	0	0	0
Oxyloma elegans (Risso, 1826)	0	0	0	0	0	0	0	0	0	0	0	0	0	0
Pseudamnicola (s.str.) *moussonii* (Calcara, 1841)	0	0	0	0	0	0	0	0	0	0	0	0	0	0
Ancylus fluviatilis Müller, 1774	0	0	0	0	0	0	0	0	0	0	0	0	0	0
Bulinus cf. *truncatus* (Audouin, 1827)	0	0	0	0	0	0	0	0	0	0	0	0	0	0
Pisidium caesertanum (Poli, 1791)	0	0	0	0	0	0	0	0	0	0	0	0	0	0
Lymnaea (Galba) truncatula (Müller, 1774)	0	0	0	0	0	0	0	0	0	0	0	0	0	0
Planorbis moquini (Requien, 1848)	0	0	0	0	0	0	0	0	0	0	0	0	0	0
Planorbis planorbis (Linnaeus, 1758)	0	0	0	0	0	0	0	0	0	0	0	0	0	0
Carychium cf. *schlickumi* Strauch, 1977	0	0	0	0	0	0	0	0	0	0	0	0	0	0
Vertigo cf. *antivertigo* (Draparnaud, 1801)	0	0	0	0	0	0	0	0	0	0	0	0	0	0
Oxychilus (Mediterranea) *hydatinus* (Rossmässler, 1838)	0	0	0	0	0	0	0	0	0	0	0	0	0	0
Truncatellina callicratis (Scacchi, 1833)	0	0	0	0	0	0	0	0	0	0	0	0	0	0
Vitrea Fitzinger, 1833	0	0	0	0	0	0	0	0	0	0	0	0	0	0
Xerotricha Monterosato, 1892	0	0	0	0	0	0	0	0	0	0	0	0	0	0
Clausiliidae Mörch, 1864	0	0	0	0	0	0	0	0	0	0	0	0	0	0
Granopupa granum (Draparnaud, 1801)	0	0	0	0	0	0	0	0	0	0	0	0	0	0
Muticaria Lindholm, 1925	0	0	0	0	0	0	0	0	0	0	0	0	0	0
Papillifera papillaris (Müller, 1774)	0	0	0	0	0	0	0	0	0	0	0	0	0	0
Rumina decollata (Linnaeus, 1758)	0	0	0	0	0	0	0	0	0	0	0	0	0	0
Trochoidea spratti (Pfeiffer, 1846)	0	0	0	0	0	0	0	0	0	0	0	0	0	0
Cernuella caruanae (Kobelt, 1888)	0	0	0	0	0	0	0	0	0	0	0	0	0	0
Cochlicella acuta (Müller, 1774)	0	0	0	0	0	0	0	0	0	0	0	1	0	0
Pomatias sulcatus (Draparnaud, 1801)	0	0	0	0	0	0	0	0	0	0	0	0	0	0
Theba pisana (Müller, 1774)	0	0	0	0	0	0	0	0	0	0	0	0	0	0
Helicioidae	0	0	0	0	0	0	0	0	0	0	0	1	0	1
Cecilioides acicula (Müller, 1774)	0	0	0	0	0	0	0	0	0	0	0	0	0	0
Total amount of molluscs	**6**	**7**	**1**	**1**	**1**	**1**	**1**	**1**	**1**	**1**	**1**	**7**	**1**	**5**

Table A5.1 *(cont.).*

Species/Depth (cm)	773	778	783	788	793	798	803	808	813	818	823	828	833	838
Bittium reticulatum (Da Costa, 1778)	0	0	1	0	0	0	0	0	0	0	0	0	1	0
Cerithium spp.	1	2	1	1	0	0	0	0	0	0	0	1	0	0
Conus mediterraneus (Hwass, 1792)	0	0	0	0	0	0	0	0	0	0	0	0	0	0
Gibbula sp.	0	0	0	0	0	0	0	0	0	0	0	0	0	1
Haminoea sp.	0	0	0	0	0	0	0	0	0	0	0	0	0	0
Hexaplex trunculus (Linnaeus, 1758)	1	0	0	0	0	0	0	0	0	0	0	0	0	0
Pirenella conica (Blainville, 1826)	0	0	0	0	0	0	0	0	0	0	0	0	0	0
Retusa truncatula (Brugière, 1792)	0	0	0	0	0	0	0	0	0	0	0	0	0	0
Rissoa sp.	0	0	0	0	0	0	0	0	0	0	0	0	0	0
Turbonilla sp.	0	0	0	0	0	0	0	0	0	0	0	0	0	0
Acanthocardia sp.	0	0	0	0	0	0	0	0	0	0	0	0	0	0
Cardiidae	0	0	0	0	0	0	0	0	0	0	0	0	0	0
Cerastoderma sp.	2	6	3	0	0	0	1	0	0	0	0	0	0	0
Kelliidae	0	0	0	0	0	0	0	0	0	0	0	0	0	0
Loripes lucinalis (Lamarck, 1818)	0	0	0	0	0	0	0	0	0	0	0	0	0	0
Ostrea sp.	0	1	1	1	0	0	0	0	0	0	1	0	1	0
Paphia sp.	0	0	0	0	0	0	0	0	0	0	0	0	0	0
Parvicardium sp.	0	0	0	0	0	0	0	0	0	0	0	0	0	0
Pectinidae	0	0	0	1	0	0	0	0	0	0	0	0	0	0
Tapes decussatus (Linnaeus, 1758)	0	0	0	0	0	0	0	0	0	0	0	0	0	1
Tellina sp.	1	1	0	0	0	0	0	0	0	0	0	0	0	1
Veneridae	0	0	0	0	0	0	0	0	0	0	0	0	0	0
other/indeterminate	0	0	0	0	0	0	1	0	0	0	0	0	0	0
Hydrobia sp. Hartmann, 1821	0	0	1	1	0	0	0	0	0	0	0	1	0	0
Ovatella myosotis (Draparnaud, 1801)	0	0	0	0	0	0	0	0	0	0	0	0	0	0
Truncatella subcylindrica (Linnaeus, 1767)	0	0	0	0	0	0	0	0	0	0	0	0	0	0
Oxyloma elegans (Risso, 1826)	0	0	0	0	0	0	0	0	0	0	0	0	0	0
Pseudamnicola (s.str.) *moussonii* (Calcara, 1841)	0	0	0	0	0	0	0	0	0	0	0	0	0	0
Ancylus fluviatilis Müller, 1774	0	0	0	0	0	0	0	0	0	0	0	0	0	0
Bulinus cf. *truncatus* (Audouin, 1827)	0	0	0	0	0	0	0	0	0	0	0	0	0	0
Pisidium caesertanum (Poli, 1791)	0	0	0	0	0	0	0	0	0	0	0	0	0	0
Lymnaea (Galba) truncatula (Müller, 1774)	0	0	0	0	0	0	0	0	0	0	0	0	0	0
Planorbis moquini (Requien, 1848)	0	0	0	0	0	0	0	0	0	0	0	0	0	0
Planorbis planorbis (Linnaeus, 1758)	0	0	0	0	0	0	0	0	0	0	0	0	0	0
Carychium cf. *schlickumi* Strauch, 1977	0	0	0	0	0	0	0	0	0	0	0	0	0	0
Vertigo cf. *antivertigo* (Draparnaud, 1801)	0	0	0	0	0	0	0	0	0	0	0	0	0	0
Oxychilus (Mediterranea) *hydatinus* (Rossmässler, 1838)	0	0	0	0	0	0	0	0	0	0	0	0	0	0
Truncatellina callicratis (Scacchi, 1833)	0	0	0	0	0	0	0	0	0	0	0	0	0	0
Vitrea Fitzinger, 1833	0	0	0	0	0	0	0	0	0	0	0	0	0	0
Xerotricha Monterosato, 1892	0	0	0	0	0	0	0	0	0	0	0	0	0	0
Clausiliidae Mörch, 1864	0	0	0	0	0	0	0	0	0	0	0	0	0	0
Granopupa granum (Draparnaud, 1801)	0	0	0	0	0	0	0	0	0	0	0	0	0	0
Muticaria Lindholm, 1925	0	0	0	0	0	0	0	0	0	0	0	0	0	0
Papillifera papillaris (Müller, 1774)	0	0	0	0	0	0	0	0	0	0	0	0	0	0
Rumina decollata (Linnaeus, 1758)	0	0	0	0	0	0	0	0	0	0	0	0	0	0
Trochoidea spratti (Pfeiffer, 1846)	0	0	0	0	0	0	0	0	0	0	0	0	0	1
Cernuella caruanae (Kobelt, 1888)	0	0	0	0	0	0	0	0	0	0	0	0	0	0
Cochlicella acuta (Müller, 1774)	0	0	0	0	0	0	0	0	0	0	0	0	0	0
Pomatias sulcatus (Draparnaud, 1801)	0	0	0	0	0	0	0	0	0	0	0	0	0	0
Theba pisana (Müller, 1774)	0	0	0	0	0	0	0	0	0	0	0	0	0	0
Helicioidae	1	1	1	1	0	0	0	0	0	0	0	0	1	0
Cecilioides acicula (Müller, 1774)	0	0	0	0	0	0	0	2	0	0	0	0	0	0
Total amount of molluscs	**6**	**11**	**8**	**5**	**1**	**1**	**2**	**2**	**1**	**1**	**1**	**2**	**3**	**4**

Table A5.1 *(cont.).*

Species/Depth (cm)	843	848	853	858	863	868	873	878	883	888	893	898	903	908
Bittium reticulatum (Da Costa, 1778)	1	0	1	0	0	0	0	1	0	0	0	0	0	0
Cerithium spp.	0	0	0	0	0	0	0	0	1	0	0	0	0	0
Conus mediterraneus (Hwass, 1792)	0	0	0	0	0	0	0	0	0	0	0	0	0	0
Gibbula sp.	0	0	0	0	0	0	0	0	0	0	1	0	0	0
Haminoea sp.	0	0	0	0	0	0	0	0	0	0	0	0	0	0
Hexaplex trunculus (Linnaeus, 1758)	0	0	0	0	0	0	0	0	0	0	0	0	0	0
Pirenella conica (Blainville, 1826)	0	0	0	0	0	0	0	0	0	0	0	0	0	0
Retusa truncatula (Brugière, 1792)	0	0	0	0	0	0	0	0	0	0	0	0	0	0
Rissoa sp.	0	1	0	0	0	0	0	0	0	0	0	0	0	0
Turbonilla sp.	0	0	0	0	0	0	0	0	0	0	0	0	0	0
Acanthocardia sp.	0	0	0	0	0	0	0	0	0	0	0	0	0	0
Cardiidae	0	0	0	1	0	0	0	0	1	0	0	0	0	0
Cerastoderma sp.	0	1	0	0	0	0	0	0	0	1	0	1	0	0
Kelliidae	0	0	0	0	0	0	0	0	0	0	0	0	0	0
Loripes lucinalis (Lamarck, 1818)	0	0	0	0	0	0	0	0	0	0	0	0	0	0
Ostrea sp.	0	1	0	0	0	0	0	0	1	1	0	0	0	0
Paphia sp.	0	0	0	0	0	0	0	0	0	0	0	0	0	0
Parvicardium sp.	0	0	0	0	0	0	0	0	0	0	0	0	0	0
Pectinidae	0	0	0	0	0	0	0	0	0	0	0	0	0	0
Tapes decussatus (Linnaeus, 1758)	0	1	0	0	0	0	0	0	0	0	1	0	0	0
Tellina sp.	0	0	0	0	0	0	0	0	0	0	0	0	0	0
Veneridae	0	0	0	0	0	0	0	0	0	0	0	0	0	0
other/indeterminate	0	0	0	0	0	0	0	0	1	0	0	0	0	0
Hydrobia sp. Hartmann, 1821	0	2	0	0	0	0	0	0	0	0	1	0	0	0
Ovatella myosotis (Draparnaud, 1801)	0	0	0	0	0	0	0	0	0	0	0	0	0	0
Truncatella subcylindrica (Linnaeus, 1767)	0	0	0	0	0	0	0	0	0	0	0	0	0	0
Oxyloma elegans (Risso, 1826)	0	0	0	0	0	0	0	0	0	0	0	0	0	0
Pseudamnicola (s.str.) *moussonii* (Calcara, 1841)	0	0	0	0	0	0	0	0	0	0	0	0	0	0
Ancylus fluviatilis Müller, 1774	0	0	0	0	0	0	0	0	0	0	0	0	0	0
Bulinus cf. *truncatus* (Audouin, 1827)	0	0	0	0	0	0	0	0	0	0	0	0	0	0
Pisidium caesertanum (Poli, 1791)	0	0	0	0	0	0	0	0	0	0	0	0	0	0
Lymnaea (Galba) truncatula (Müller, 1774)	0	0	0	0	0	0	0	0	0	0	0	0	0	0
Planorbis moquini (Requien, 1848)	0	0	0	0	0	0	0	0	0	0	0	0	0	0
Planorbis planorbis (Linnaeus, 1758)	0	0	0	0	0	0	0	0	0	0	0	0	0	0
Carychium cf. *schlickumi* Strauch, 1977	0	0	0	0	0	0	0	0	0	0	0	0	0	0
Vertigo cf. *antivertigo* (Draparnaud, 1801)	0	0	0	0	0	0	0	0	0	0	0	0	0	0
Oxychilus (Mediterranea) *hydatinus* (Rossmässler, 1838)	0	0	0	0	0	0	0	0	0	0	0	0	0	0
Truncatellina callicratis (Scacchi, 1833)	0	0	0	0	0	0	0	0	0	0	0	0	0	0
Vitrea Fitzinger, 1833	0	0	0	0	0	0	0	0	0	0	0	0	0	0
Xerotricha Monterosato, 1892	0	0	0	0	0	0	0	0	0	0	0	0	0	0
Clausiliidae Mörch, 1864	0	0	0	0	0	0	0	0	0	0	0	0	0	0
Granopupa granum (Draparnaud, 1801)	0	0	0	0	0	0	0	0	0	0	0	0	0	0
Muticaria Lindholm, 1925	0	0	0	0	0	0	0	0	0	0	0	0	0	0
Papillifera papillaris (Müller, 1774)	0	0	0	0	0	0	0	0	0	0	0	0	0	0
Rumina decollata (Linnaeus, 1758)	0	0	0	0	0	0	0	0	0	0	0	0	0	0
Trochoidea spratti (Pfeiffer, 1846)	0	0	0	0	0	0	0	0	0	0	0	0	0	0
Cernuella caruanae (Kobelt, 1888)	0	0	0	0	0	0	0	0	1	0	0	0	0	0
Cochlicella acuta (Müller, 1774)	0	0	0	0	0	0	0	0	0	0	0	0	0	0
Pomatias sulcatus (Draparnaud, 1801)	0	0	0	0	0	0	0	0	0	0	0	0	0	0
Theba pisana (Müller, 1774)	0	0	0	0	0	0	0	0	0	0	0	0	0	0
Helicioidae	0	0	0	0	0	0	0	1	1	0	0	0	0	0
Cecilioides acicula (Müller, 1774)	0	0	0	0	0	0	0	0	0	0	0	0	0	0
Total amount of molluscs	**1**	**6**	**1**	**1**	**1**	**1**	**1**	**2**	**6**	**2**	**3**	**1**	**1**	**1**

Table A5.1 *(cont.).*

Species/Depth (cm)	913	918	923	928	933	938
Bittium reticulatum (Da Costa, 1778)	0	0	0	0	0	0
Cerithium spp.	0	0	0	0	0	0
Conus mediterraneus (Hwass, 1792)	0	0	0	0	0	0
Gibbula sp.	0	0	0	0	0	0
Haminoea sp.	0	0	0	0	0	0
Hexaplex trunculus (Linnaeus, 1758)	0	0	0	0	0	0
Pirenella conica (Blainville, 1826)	0	0	0	0	0	0
Retusa truncatula (Brugière, 1792)	0	0	0	0	0	0
Rissoa sp.	0	0	0	0	0	0
Turbonilla sp.	0	0	0	0	0	0
Acanthocardia sp.	0	0	0	0	0	0
Cardiidae	0	0	0	0	0	0
Cerastoderma sp.	0	0	0	0	0	0
Kelliidae	0	0	0	0	0	0
Loripes lucinalis (Lamarck, 1818)	0	0	0	0	0	0
Ostrea sp.	0	0	0	0	0	0
Paphia sp.	0	0	0	0	0	0
Parvicardium sp.	0	0	0	0	0	0
Pectinidae	0	0	0	0	0	0
Tapes decussatus (Linnaeus, 1758)	0	0	0	0	0	0
Tellina sp.	0	0	0	0	0	0
Veneridae	0	0	0	0	0	0
other/indeterminate	0	0	0	0	0	0
Hydrobia sp. Hartmann, 1821	0	0	0	0	0	0
Ovatella myosotis (Draparnaud, 1801)	0	0	0	0	0	0
Truncatella subcylindrica (Linnaeus, 1767)	0	0	0	0	0	0
Oxyloma elegans (Risso, 1826)	0	0	0	0	0	0
Pseudamnicola (s.str.) *moussonii* (Calcara, 1841)	0	0	0	0	0	0
Ancylus fluviatilis Müller, 1774	0	0	0	0	0	0
Bulinus cf. *truncatus* (Audouin, 1827)	0	0	0	0	0	0
Pisidium caesertanum (Poli, 1791)	0	0	0	0	0	0
Lymnaea (Galba) truncatula (Müller, 1774)	0	0	0	0	0	0
Planorbis moquini (Requien, 1848)	0	0	0	0	0	0
Planorbis planorbis (Linnaeus, 1758)	0	0	0	0	0	0
Carychium cf. *schlickumi* Strauch, 1977	0	0	0	0	0	0
Vertigo cf. *antivertigo* (Draparnaud, 1801)	0	0	0	0	0	0
Oxychilus (Mediterranea) *hydatinus* (Rossmässler, 1838)	0	0	0	0	0	0
Truncatellina callicratis (Scacchi, 1833)	0	0	0	0	0	0
Vitrea Fitzinger, 1833	0	0	0	0	0	0
Xerotricha Monterosato, 1892	0	0	0	0	0	0
Clausiliidae Mörch, 1864	0	0	0	0	0	0
Granopupa granum (Draparnaud, 1801)	0	0	0	0	0	0
Muticaria Lindholm, 1925	0	0	0	0	0	0
Papillifera papillaris (Müller, 1774)	0	0	0	0	0	0
Rumina decollata (Linnaeus, 1758)	0	0	0	0	0	0
Trochoidea spratti (Pfeiffer, 1846)	0	0	0	0	0	0
Cernuella caruanae (Kobelt, 1888)	0	0	0	0	0	0
Cochlicella acuta (Müller, 1774)	0	0	0	0	0	0
Pomatias sulcatus (Draparnaud, 1801)	0	0	0	0	0	0
Theba pisana (Müller, 1774)	0	0	0	0	0	0
Helicioidae	0	0	0	0	0	0
Cecilioides acicula (Müller, 1774)	0	0	0	0	0	0
Total amount of molluscs	**1**	**1**	**1**	**1**	**1**	**1**

Table A5.2. *Mgarr ix-Xini.*

Species/Depth (cm)	56	60	64	67	71	75	79	82	86	90	93	97	100	104
Alvania sp.	0	0	0	0	0	0	0	0	0	1	1	0	2	2
Bittium sp.	0	0	0	0	0	0	0	0	1	0	0	2	0	0
Calliostoma sp.	0	0	0	0	0	0	0	0	0	0	0	0	0	0
Cerithium sp.	0	0	0	0	0	0	0	0	1	0	3	0	2	1
Cylichnea sp.	0	0	0	0	0	0	0	0	0	0	0	0	0	0
Conus mediterraneus (Hwass, 1792)	0	0	0	0	0	0	0	0	0	0	0	0	0	0
Epitonium sp.	0	0	0	0	0	0	0	0	0	0	0	0	0	0
Gibberula sp.	0	0	0	0	0	0	0	0	0	0	0	0	0	0
Gibbula sp.	0	0	0	0	0	0	0	0	0	0	0	1	1	2
Hexaplex trunculus (Linnaeus, 1758)	0	0	0	0	0	0	0	0	0	0	0	0	0	0
Jujubinus sp.	0	0	0	0	0	0	0	0	0	0	0	0	0	0
Nassarius sp.	0	0	0	0	0	0	0	0	0	0	0	0	0	0
Pirenella conica (Blainville, 1826)	0	0	0	0	0	0	0	0	0	0	0	0	0	0
Pisania striata	0	0	0	0	0	0	0	0	0	0	0	0	0	0
Retusa truncatula (Brugière, 1792)	0	0	0	0	0	0	0	0	0	0	0	0	1	0
Rissoa sp.	0	0	0	0	0	0	0	1	1	1	0	0	0	2
Tricolia sp.	0	0	0	0	0	0	0	0	0	0	0	0	1	0
Turbonilla lactea	0	0	0	0	0	0	0	0	0	0	0	0	0	0
Cardium sp.	0	0	0	0	0	1	0	0	0	0	0	0	0	0
Ostrea sp.	0	0	0	0	0	0	0	0	0	0	0	0	0	0
Loripes lucinalis (Lamarck, 1818)	0	0	0	0	0	0	0	0	0	0	0	0	0	1
Abra sp.	0	0	0	0	0	0	0	0	0	0	0	0	0	0
other/unknown marine	1	0	0	0	0	0	0	0	0	0	1	1	0	0
Hydrobia Hartmann, 1821	1	0	2	1	5	1	1	3	2	1	1	3	8	10
Ovatella myosotis (Draparnaud, 1801)	0	0	0	0	0	0	1	0	0	0	0	0	0	0
Truncatella subcylindrica (Linnaeus, 1767)	0	0	0	0	0	0	0	0	0	0	0	0	0	0
Oxychilus (Mediterranea) *hydatinus* (Rossmässler, 1838)	0	0	0	0	0	0	0	0	0	0	0	0	0	0
Truncatellina callicratis (Scacchi, 1833)	0	0	0	0	0	0	0	0	0	0	0	0	0	0
Xerotricha conspurcata (Draparnaud, 1801)	0	0	0	0	0	0	0	0	0	0	0	0	1	0
Clausiliidae Mörch, 1864	0	0	0	0	1	0	0	0	0	0	0	1	0	0
Granopupa granum (Draparnaud, 1801)	0	0	0	0	0	0	0	0	0	0	0	0	0	0
Papillifera papillaris (Müller, 1774)	0	0	0	0	0	0	0	0	0	0	1	0	0	0
Muticaria Lindholm, 1925	0	1	1	1	1	1	1	1	1	0	1	1	1	1
Rumina decollata (Linnaeus, 1758)	0	0	0	0	0	0	0	0	0	0	0	0	0	0
Trochoidea spratti (Pfeiffer, 1846)	0	0	0	0	0	0	0	1	0	0	0	0	0	0
Cernuella caruanae	0	0	0	0	0	0	0	0	0	0	1	2	0	0
Cochlicella acuta (Müller, 1774)	0	0	0	0	0	0	1	2	0	0	0	0	2	0
Eobania vermiculata (Müller, 1774)	0	0	0	0	0	0	0	0	0	0	0	0	0	0
Pomatias sulcatus (Draparnaud, 1801)	1	1	0	0	1	1	0	1	1	1	1	0	1	1
Theba pisana (Müller, 1774)	0	0	0	0	0	0	0	0	0	0	0	1	0	1
Helicioid fragments	1	1	1	1	1	1	1	1	1	1	1	1	1	1
Cecilioides acicula (Müller, 1774)	0	0	0	0	0	0	1	0	0	0	0	3	0	0
Total amount of molluscs	**4**	**3**	**4**	**3**	**9**	**5**	**6**	**10**	**8**	**5**	**11**	**16**	**21**	**22**

Table A5.2 *(cont.).*

Species/Depth (cm)	108	111	120	124	132	142	147	152	157	162	167	172	175	191
Alvania sp.	0	2	2	0	1	2	0	18	5	3	0	1	0	2
Bittium sp.	0	0	2	0	0	2	2	7	0	6	5	5	2	5
Calliostoma sp.	0	1	0	0	0	0	0	1	1	0	0	0	0	0
Cerithium sp.	3	2	2	2	1	0	1	19	20	9	9	11	6	20
Cylichnea sp.	0	0	0	0	0	0	0	0	1	0	0	0	1	0
Conus mediterraneus (Hwass, 1792)	1	0	0	0	0	0	0	1	0	0	0	1	0	0
Epitonium sp.	0	0	0	0	0	0	0	0	0	0	0	0	0	0
Gibberula sp.	0	0	0	0	0	0	0	0	0	0	0	0	0	0
Gibbula sp.	0	1	3	2	0	1	2	5	2	5	5	2	3	1
Hexaplex trunculus (Linnaeus, 1758)	0	1	0	0	0	0	0	0	0	0	0	0	0	1
Jujubinus sp.	0	0	0	1	0	0	0	0	0	0	0	0	0	0
Nassarius sp.	0	0	0	0	0	0	0	0	0	0	0	0	0	0
Pirenella conica (Blainville, 1826)	0	0	0	0	0	0	0	0	0	2	2	4	0	0
Pisania striata	0	1	0	0	0	0	0	0	0	3	0	0	0	2
Retusa truncatula (Brugière, 1792)	0	0	0	0	0	0	0	0	0	0	0	0	0	1
Rissoa sp.	2	0	0	0	0	0	0	0	0	2	2	0	0	1
Tricolia sp.	0	0	0	0	0	0	0	1	0	0	0	0	1	1
Turbonilla lactea	0	0	0	0	0	0	0	0	2	1	0	1	0	1
Cardium sp.	0	1	0	0	0	1	1	1	2	1	1	1	2	1
Ostrea sp.	0	0	0	0	0	0	0	0	0	0	1	1	0	0
Loripes lucinalis (Lamarck, 1818)	0	1	1	0	0	1	0	5	5	0	3	1	1	3
Abra sp.	0	0	0	0	1	0	0	0	1	0	0	0	0	0
other/unknown marine	0	0	0	0	2	0	1	0	0	0	0	0	0	0
Hydrobia Hartmann, 1821	9	8	4	3	6	2	0	5	2	0	0	2	0	5
Ovatella myosotis (Draparnaud, 1801)	0	0	0	0	0	0	0	0	0	0	0	0	0	2
Truncatella subcylindrica (Linnaeus, 1767)	0	0	0	0	0	0	0	0	0	0	0	0	0	0
Oxychilus (Mediterranea) *hydatinus* (Rossmässler, 1838)	0	0	0	0	0	0	0	0	0	0	0	0	0	0
Truncatellina callicratis (Scacchi, 1833)	0	0	0	0	0	0	0	0	0	0	0	0	0	0
Xerotricha conspurcata (Draparnaud, 1801)	0	0	0	0	0	0	0	0	0	0	0	0	0	0
Clausiliidae Mörch, 1864	0	1	1	0	0	0	0	0	0	0	0	0	0	0
Granopupa granum (Draparnaud, 1801)	0	0	0	0	0	0	0	0	0	0	0	0	0	0
Papillifera papillaris (Müller, 1774)	1	0	0	1	0	0	0	0	0	0	0	0	1	0
Muticaria Lindholm, 1925	0	1	1	1	1	1	1	1	1	1	1	1	0	0
Rumina decollata (Linnaeus, 1758)	0	0	0	0	0	0	0	0	0	0	0	0	0	0
Trochoidea spratti (Pfeiffer, 1846)	1	0	0	0	1	0	0	0	1	1	0	0	0	0
Cernuella caruanae	0	0	0	0	0	0	0	0	1	0	0	0	0	0
Cochlicella acuta (Müller, 1774)	0	0	0	0	1	0	0	0	0	0	0	2	0	0
Eobania vermiculata (Müller, 1774)	0	0	0	0	0	0	0	0	0	0	0	0	0	0
Pomatias sulcatus (Draparnaud, 1801)	1	1	1	1	0	1	1	1	1	1	1	1	0	0
Theba pisana (Müller, 1774)	0	1	1	1	1	0	0	0	0	0	0	0	0	0
Helicioid fragments	1	1	1	1	1	1	1	1	1	1	1	1	1	1
Cecilioides acicula (Müller, 1774)	0	0	0	0	0	0	0	0	0	0	1	0	0	0
Total amount of molluscs	**19**	**23**	**19**	**13**	**16**	**12**	**10**	**66**	**46**	**36**	**32**	**35**	**18**	**47**

Table A5.2 *(cont.).*

Species/Depth (cm)	195	199	204	208	212	216	220	225	229	233	237	246	251	256
Alvania sp.	5	3	4	1	0	0	0	0	0	0	0	1	3	2
Bittium sp.	8	6	1	3	1	0	0	0	0	0	0	5	7	1
Calliostoma sp.	0	0	0	0	0	0	0	0	0	0	0	0	0	0
Cerithium sp.	5	4	0	4	0	0	0	0	0	0	0	9	16	7
Cylichnea sp.	0	0	0	1	0	0	0	0	0	0	0	0	0	0
Conus mediterraneus (Hwass, 1792)	0	0	0	0	0	0	0	0	0	0	0	0	0	0
Epitonium sp.	0	0	0	0	0	0	0	0	0	0	0	0	0	0
Gibberula sp.	0	0	0	0	0	0	0	0	0	0	0	0	0	0
Gibbula sp.	1	1	1	0	1	0	0	0	0	0	1	0	2	7
Hexaplex trunculus (Linnaeus, 1758)	0	0	0	0	0	0	0	0	0	0	0	0	0	0
Jujubinus sp.	0	0	0	0	0	0	0	0	0	0	0	0	1	0
Nassarius sp.	3	2	0	0	0	0	0	0	0	0	0	0	0	0
Pirenella conica (Blainville, 1826)	1	1	0	0	0	0	0	0	0	0	0	0	1	0
Pisania striata	0	0	0	0	0	0	0	0	0	0	0	0	0	2
Retusa truncatula (Brugière, 1792)	0	0	0	0	0	0	0	0	0	0	0	0	0	0
Rissoa sp.	7	7	3	2	0	0	0	0	0	0	1	2	1	0
Tricolia sp.	0	0	0	0	0	0	0	0	0	0	0	0	1	0
Turbonilla lactea	0	0	0	0	0	0	0	0	0	0	0	1	0	0
Cardium sp.	0	0	0	0	0	0	0	0	0	0	1	0	0	1
Ostrea sp.	0	0	0	0	0	0	0	0	0	0	0	0	0	0
Loripes lucinalis (Lamarck, 1818)	1	0	0	2	0	0	0	0	0	0	0	2	4	3
Abra sp.	0	0	0	0	0	0	0	0	0	0	0	0	0	0
other/unknown marine	0	0	0	0	1	2	1	1	1	0	0	0	0	1
Hydrobia Hartmann, 1821	0	2	0	1	0	0	0	0	0	0	0	3	0	0
Ovatella myosotis (Draparnaud, 1801)	0	0	0	0	0	0	0	0	0	0	0	0	0	0
Truncatella subcylindrica (Linnaeus, 1767)	0	0	0	0	0	0	0	0	0	0	0	0	0	0
Oxychilus (Mediterranea) *hydatinus* (Rossmässler, 1838)	0	0	0	0	0	0	0	0	0	0	0	0	0	0
Truncatellina callicratis (Scacchi, 1833)	0	0	0	0	0	0	0	0	0	0	0	0	0	0
Xerotricha conspurcata (Draparnaud, 1801)	0	0	0	0	0	0	0	0	0	0	0	0	0	0
Clausiliidae Mörch, 1864	0	0	0	0	0	0	0	0	0	0	0	0	1	0
Granopupa granum (Draparnaud, 1801)	0	0	0	0	0	0	0	0	0	0	0	0	0	0
Papillifera papillaris (Müller, 1774)	0	0	0	0	0	0	0	0	0	0	0	0	1	0
Muticaria Lindholm, 1925	0	1	0	0	0	0	0	0	0	0	0	1	1	1
Rumina decollata (Linnaeus, 1758)	0	0	0	0	0	0	0	0	0	0	0	0	0	0
Trochoidea spratti (Pfeiffer, 1846)	0	0	0	0	0	0	0	0	0	0	0	0	1	1
Cernuella caruanae	0	0	0	0	0	0	0	0	0	0	0	0	0	0
Cochlicella acuta (Müller, 1774)	0	0	0	0	0	0	0	0	0	0	0	1	0	0
Eobania vermiculata (Müller, 1774)	0	0	0	0	0	0	0	0	0	0	0	0	0	0
Pomatias sulcatus (Draparnaud, 1801)	0	0	0	1	0	0	0	0	0	0	1	1	0	1
Theba pisana (Müller, 1774)	3	0	0	0	0	0	0	0	0	0	0	0	0	0
Helicioid fragments	1	1	1	1	1	1	1	1	1	1	1	1	1	1
Cecilioides acicula (Müller, 1774)	0	0	0	0	0	0	0	0	0	0	0	0	0	0
Total amount of molluscs	**35**	**28**	**10**	**16**	**4**	**3**	**2**	**2**	**2**	**1**	**5**	**27**	**41**	**28**

Table A5.2 *(cont.).*

Species/Depth (cm)	261	266	271	276	281	286	291	296	300	309	314	319	324	329
Alvania sp.	0	1	1	0	0	0	0	0	0	0	1	0	1	0
Bittium sp.	1	0	3	0	0	0	0	0	0	1	10	8	0	0
Calliostoma sp.	0	0	0	0	0	0	0	0	0	0	0	0	0	0
Cerithium sp.	3	2	2	0	0	0	0	0	0	1	4	0	0	0
Cylichnea sp.	0	0	0	0	0	0	0	0	0	0	0	0	0	0
Conus mediterraneus (Hwass, 1792)	1	0	0	0	0	0	0	0	0	0	0	0	0	0
Epitonium sp.	0	0	0	0	0	0	0	0	0	0	0	0	0	0
Gibberula sp.	0	0	0	0	0	0	0	0	0	0	0	0	0	0
Gibbula sp.	3	2	0	0	0	1	0	0	1	0	0	1	1	1
Hexaplex trunculus (Linnaeus, 1758)	0	0	0	0	0	0	0	0	0	0	0	0	0	0
Jujubinus sp.	0	0	0	0	0	0	0	0	0	0	0	0	0	0
Nassarius sp.	0	0	0	0	0	0	0	0	0	0	0	0	0	0
Pirenella conica (Blainville, 1826)	0	0	0	0	0	0	0	0	0	0	0	0	1	0
Pisania striata	0	0	0	0	0	0	0	0	0	1	0	0	0	0
Retusa truncatula (Brugière, 1792)	0	0	0	0	0	0	0	0	0	0	0	0	0	0
Rissoa sp.	2	1	1	0	0	0	0	0	0	0	2	2	0	0
Tricolia sp.	0	0	1	0	0	0	0	0	0	0	0	0	0	0
Turbonilla lactea	0	0	0	0	0	0	0	0	0	0	0	0	0	0
Cardium sp.	1	0	0	0	0	0	0	0	1	1	0	0	0	0
Ostrea sp.	0	0	0	0	0	0	0	0	0	0	0	0	0	0
Loripes lucinalis (Lamarck, 1818)	0	0	0	0	0	0	0	0	0	0	0	0	0	0
Abra sp.	0	0	0	0	0	0	0	0	0	0	0	0	0	0
other/unknown marine	0	0	0	0	0	1	1	0	0	1	0	0	0	0
Hydrobia Hartmann, 1821	0	2	2	0	1	0	0	42	0	2	6	4	0	1
Ovatella myosotis (Draparnaud, 1801)	0	0	0	0	0	0	0	0	0	0	0	0	0	0
Truncatella subcylindrica (Linnaeus, 1767)	0	0	0	0	0	0	0	0	0	0	0	0	0	0
Oxychilus (Mediterranea) *hydatinus* (Rossmässler, 1838)	0	0	0	0	0	0	0	0	0	0	0	0	1	0
Truncatellina callicratis (Scacchi, 1833)	0	0	0	0	0	0	0	0	0	0	0	0	0	0
Xerotricha conspurcata (Draparnaud, 1801)	0	0	0	0	0	0	0	0	0	0	0	0	0	0
Clausiliidae Mörch, 1864	1	0	0	0	0	0	0	0	0	0	0	2	0	0
Granopupa granum (Draparnaud, 1801)	0	0	0	0	0	0	0	0	0	0	0	0	1	0
Papillifera papillaris (Müller, 1774)	1	0	1	0	0	0	0	0	0	0	0	1	0	0
Muticaria Lindholm, 1925	1	1	1	0	1	0	1	0	0	1	1	1	1	1
Rumina decollata (Linnaeus, 1758)	0	0	0	0	0	0	0	0	0	0	0	0	0	0
Trochoidea spratti (Pfeiffer, 1846)	0	0	1	0	0	0	0	0	0	0	0	0	0	1
Cernuella caruanae	0	1	0	0	0	0	0	0	0	1	0	0	2	0
Cochlicella acuta (Müller, 1774)	0	0	0	0	0	0	0	0	0	0	0	0	0	0
Eobania vermiculata (Müller, 1774)	0	0	0	0	0	0	0	0	0	0	0	0	1	0
Pomatias sulcatus (Draparnaud, 1801)	1	0	1	0	0	1	0	0	1	1	1	1	1	1
Theba pisana (Müller, 1774)	0	0	0	0	0	0	0	0	0	1	0	0	0	0
Helicioid fragments	1	1	1	0	1	1	1	1	0	1	1	0	0	1
Cecilioides acicula (Müller, 1774)	0	0	0	0	0	0	0	1	0	0	0	0	0	0
Total amount of molluscs	**16**	**11**	**15**	**1**	**3**	**4**	**3**	**44**	**3**	**12**	**26**	**20**	**10**	**6**

Table A5.2 *(cont.).*

Species/Depth (cm)	334	339	344	352	359	364	383	387	391	395	399	403	407	411
Alvania sp.	0	0	0	0	0	0	1	2	0	1	2	0	0	0
Bittium sp.	0	0	0	1	1	0	0	1	3	5	2	1	0	0
Calliostoma sp.	0	0	0	0	0	0	0	0	0	0	0	0	0	0
Cerithium sp.	0	0	0	0	0	0	1	3	3	2	6	0	1	0
Cylichnea sp.	0	0	0	0	0	0	0	1	0	1	0	0	0	0
Conus mediterraneus (Hwass, 1792)	0	0	0	0	0	0	0	0	0	0	0	0	0	0
Epitonium sp.	0	0	0	0	0	0	0	0	0	0	0	0	0	0
Gibberula sp.	0	0	0	0	0	0	0	2	0	0	3	0	0	0
Gibbula sp.	0	0	0	0	0	0	0	0	3	2	0	1	0	0
Hexaplex trunculus (Linnaeus, 1758)	0	0	0	0	0	0	0	0	0	0	0	0	0	0
Jujubinus sp.	0	0	0	0	0	0	0	1	0	0	0	0	0	0
Nassarius sp.	0	0	0	0	0	0	0	0	0	0	0	0	0	0
Pirenella conica (Blainville, 1826)	0	0	0	0	0	0	1	2	1	1	0	0	0	0
Pisania striata	0	0	0	0	0	0	0	0	1	0	0	0	0	0
Retusa truncatula (Brugière, 1792)	0	0	0	0	0	0	0	0	0	0	0	0	0	0
Rissoa sp.	0	0	0	0	0	0	1	0	2	2	0	0	0	0
Tricolia sp.	0	0	0	0	0	1	0	0	0	0	0	0	0	0
Turbonilla lactea	0	0	0	0	0	0	1	0	0	0	0	0	0	0
Cardium sp.	0	0	0	0	0	0	0	0	0	0	0	0	0	0
Ostrea sp.	0	0	0	0	0	0	0	0	0	0	0	0	0	0
Loripes lucinalis (Lamarck, 1818)	0	0	0	0	0	0	0	1	0	0	1	0	0	1
Abra sp.	0	0	0	0	0	0	0	0	0	0	0	0	0	0
other/unknown marine	0	0	1	0	0	0	0	0	0	1	1	1	0	0
Hydrobia Hartmann, 1821	60	114	4	76	120	148	8	8	13	12	8	24	1	1
Ovatella myosotis (Draparnaud, 1801)	0	0	0	0	0	0	0	0	0	0	0	0	0	0
Truncatella subcylindrica (Linnaeus, 1767)	0	0	0	0	0	0	0	0	0	0	0	0	0	0
Oxychilus (Mediterranea) *hydatinus* (Rossmässler, 1838)	0	0	0	0	0	0	0	0	0	0	0	0	0	0
Truncatellina callicratis (Scacchi, 1833)	0	0	0	0	0	1	0	0	0	0	0	0	0	0
Xerotricha conspurcata (Draparnaud, 1801)	0	0	0	0	0	0	0	0	0	0	0	0	0	0
Clausiliidae Mörch, 1864	0	0	0	0	0	0	0	0	0	0	0	0	0	0
Granopupa granum (Draparnaud, 1801)	0	0	0	1	1	0	0	0	0	0	0	0	0	0
Papillifera papillaris (Müller, 1774)	0	0	0	2	1	0	0	0	0	1	1	0	0	0
Muticaria Lindholm, 1925	1	1	1	1	1	1	1	1	1	1	0	1	0	0
Rumina decollata (Linnaeus, 1758)	0	0	0	0	0	0	0	0	0	0	0	0	0	0
Trochoidea spratti (Pfeiffer, 1846)	1	0	1	1	3	3	0	0	0	0	0	0	0	0
Cernuella caruanae	0	0	0	0	2	1	0	0	0	1	1	0	0	0
Cochlicella acuta (Müller, 1774)	0	0	0	0	2	0	0	0	1	1	0	0	0	0
Eobania vermiculata (Müller, 1774)	0	0	0	0	0	0	0	0	0	0	0	0	0	0
Pomatias sulcatus (Draparnaud, 1801)	1	1	0	1	2	1	1	1	1	1	1	1	0	1
Theba pisana (Müller, 1774)	0	0	0	0	2	0	0	0	0	1	0	0	0	0
Helicioid fragments	1	1	1	1	1	1	1	1	1	1	0	1	1	1
Cecilioides acicula (Müller, 1774)	0	0	0	1	1	1	0	0	0	0	0	1	0	0
Total amount of molluscs	**64**	**117**	**8**	**85**	**137**	**158**	**16**	**24**	**30**	**34**	**26**	**31**	**3**	**4**

Table A5.2 *(cont.).*

Species/Depth (cm)	415	419	423	427	434	439	444	449	454	459	464	469	474	479
Alvania sp.	0	1	0	0	2	3	0	0	2	2	3	2	2	6
Bittium sp.	0	1	1	0	0	0	3	1	1	2	0	3	0	0
Calliostoma sp.	0	0	0	0	0	0	0	0	0	0	0	0	0	0
Cerithium sp.	0	0	0	3	1	7	8	1	0	2	0	0	1	5
Cylichnea sp.	0	0	0	0	0	0	0	0	0	0	0	0	0	0
Conus mediterraneus (Hwass, 1792)	0	0	0	0	0	0	0	0	0	0	0	0	0	0
Epitonium sp.	0	0	0	0	0	1	0	0	0	0	0	0	0	1
Gibberula sp.	0	0	0	0	0	0	0	0	0	0	0	0	0	0
Gibbula sp.	0	0	0	2	2	1	2	2	0	2	1	1	1	0
Hexaplex trunculus (Linnaeus, 1758)	0	0	0	0	0	0	0	0	0	0	0	0	0	0
Jujubinus sp.	0	0	0	0	0	0	0	0	0	0	0	0	0	0
Nassarius sp.	0	0	0	0	0	0	0	0	0	0	0	0	0	0
Pirenella conica (Blainville, 1826)	0	0	0	1	0	0	1	0	0	0	0	0	0	0
Pisania striata	0	0	0	0	0	1	0	0	0	0	0	0	0	0
Retusa truncatula (Brugière, 1792)	0	0	0	0	0	0	0	0	0	0	0	0	0	0
Rissoa sp.	0	0	0	0	0	0	0	0	0	0	1	0	0	2
Tricolia sp.	0	0	0	0	0	0	0	0	0	2	0	0	0	1
Turbonilla lactea	0	0	0	0	0	0	0	0	0	0	0	0	0	0
Cardium sp.	0	0	1	0	1	0	1	0	0	0	0	0	0	0
Ostrea sp.	0	0	0	0	0	0	0	0	0	0	0	0	0	0
Loripes lucinalis (Lamarck, 1818)	0	0	0	0	0	0	1	0	0	1	1	1	0	0
Abra sp.	0	0	0	0	0	0	0	0	0	0	0	0	1	0
other/unknown marine	0	1	1	0	0	0	0	0	0	1	0	0	0	0
Hydrobia Hartmann, 1821	2	137	309	146	2	5	6	14	16	21	58	23	340	69
Ovatella myosotis (Draparnaud, 1801)	0	0	0	0	0	0	0	0	0	0	0	0	0	0
Truncatella subcylindrica (Linnaeus, 1767)	0	0	0	1	0	1	0	0	0	1	0	0	0	0
Oxychilus (Mediterranea) *hydatinus* (Rossmässler, 1838)	0	0	0	0	0	0	0	0	0	1	0	1	0	0
Truncatellina callicratis (Scacchi, 1833)	0	0	0	0	0	0	0	0	0	0	0	0	0	0
Xerotricha conspurcata (Draparnaud, 1801)	0	0	0	0	0	0	0	0	0	0	0	0	0	0
Clausiliidae Mörch, 1864	0	0	0	0	0	0	0	0	0	0	0	0	0	0
Granopupa granum (Draparnaud, 1801)	0	0	0	0	0	0	0	0	0	0	0	0	2	0
Papillifera papillaris (Müller, 1774)	0	0	0	0	0	0	0	0	0	1	1	0	1	0
Muticaria Lindholm, 1925	1	0	1	1	1	1	1	1	1	1	1	1	1	0
Rumina decollata (Linnaeus, 1758)	0	0	0	0	0	0	0	1	0	0	0	0	0	0
Trochoidea spratti (Pfeiffer, 1846)	0	0	0	0	0	0	0	0	0	2	0	0	2	0
Cernuella caruanae	0	0	0	0	0	0	0	0	0	3	0	1	0	0
Cochlicella acuta (Müller, 1774)	0	0	0	0	0	0	0	0	0	0	1	0	0	0
Eobania vermiculata (Müller, 1774)	0	0	0	0	0	0	0	0	0	0	0	0	0	0
Pomatias sulcatus (Draparnaud, 1801)	0	0	1	0	1	1	1	1	1	1	1	0	1	0
Theba pisana (Müller, 1774)	0	0	0	0	0	1	0	0	1	0	0	0	0	0
Helicioid fragments	1	0	1	1	1	1	1	1	1	1	1	1	1	1
Cecilioides acicula (Müller, 1774)	0	0	0	0	0	1	0	0	0	0	0	0	0	0
Total amount of molluscs	**4**	**140**	**315**	**155**	**11**	**24**	**25**	**22**	**23**	**44**	**69**	**34**	**353**	**85**

Table A5.2 *(cont.).*

Species/Depth (cm)	484	489	499	502	506	510	513	517	520	524	528	531	535	538
Alvania sp.	2	2	0	1	0	0	0	0	1	0	0	0	2	0
Bittium sp.	6	2	0	0	0	0	0	1	0	2	0	2	0	1
Calliostoma sp.	1	0	0	0	0	0	0	0	0	0	0	0	0	1
Cerithium sp.	8	7	0	0	2	2	1	0	0	1	2	1	2	3
Cylichnea sp.	0	1	0	0	0	0	0	0	0	0	0	0	0	2
Conus mediterraneus (Hwass, 1792)	0	0	0	0	0	0	0	0	0	0	0	0	0	0
Epitonium sp.	0	1	0	0	0	0	0	0	0	0	0	0	0	0
Gibberula sp.	0	0	0	0	0	0	0	0	0	0	0	0	0	0
Gibbula sp.	3	3	0	1	0	1	1	0	0	0	1	1	2	1
Hexaplex trunculus (Linnaeus, 1758)	0	1	0	0	0	0	0	0	0	0	0	0	0	0
Jujubinus sp.	0	0	0	0	0	0	0	0	0	0	0	0	0	0
Nassarius sp.	0	2	0	0	0	0	0	0	0	0	0	0	0	2
Pirenella conica (Blainville, 1826)	0	2	0	0	0	2	0	0	0	0	0	0	3	1
Pisania striata	0	0	0	0	0	0	0	0	1	0	0	0	0	2
Retusa truncatula (Brugière, 1792)	0	0	0	0	0	0	0	0	0	0	0	0	0	0
Rissoa sp.	0	0	0	0	0	0	1	0	1	0	0	0	0	3
Tricolia sp.	0	0	0	0	0	0	0	0	0	0	0	0	0	0
Turbonilla lactea	0	0	0	0	0	0	0	0	0	0	0	0	0	0
Cardium sp.	1	1	0	0	1	0	0	0	0	0	1	1	1	0
Ostrea sp.	0	0	0	0	0	0	0	0	0	0	0	0	0	0
Loripes lucinalis (Lamarck, 1818)	1	2	1	1	0	0	0	0	0	0	0	0	0	0
Abra sp.	0	0	0	0	0	0	0	0	0	0	0	0	0	0
other/unknown marine	0	0	0	1	1	0	0	0	0	1	1	0	0	0
Hydrobia Hartmann, 1821	21	7	6	7	2	4	1	3	9	12	19	23	37	39
Ovatella myosotis (Draparnaud, 1801)	0	0	0	0	0	0	0	0	0	0	0	1	0	0
Truncatella subcylindrica (Linnaeus, 1767)	0	0	0	0	0	0	0	0	0	0	0	0	0	1
Oxychilus (Mediterranea) *hydatinus* (Rossmässler, 1838)	0	0	0	0	0	0	0	0	0	0	0	0	2	0
Truncatellina callicratis (Scacchi, 1833)	0	0	0	0	0	0	0	0	0	0	0	0	0	0
Xerotricha conspurcata (Draparnaud, 1801)	0	0	0	0	0	0	0	0	0	0	0	0	0	0
Clausiliidae Mörch, 1864	0	0	0	0	0	0	0	0	0	0	0	0	0	0
Granopupa granum (Draparnaud, 1801)	0	0	0	0	0	0	0	0	0	0	0	0	0	0
Papillifera papillaris (Müller, 1774)	1	0	0	0	0	0	0	0	0	0	0	0	0	0
Muticaria Lindholm, 1925	1	1	0	0	1	0	1	0	0	1	1	1	1	1
Rumina decollata (Linnaeus, 1758)	0	0	0	0	0	0	0	0	0	0	0	0	0	0
Trochoidea spratti (Pfeiffer, 1846)	0	0	0	0	0	0	0	0	0	0	0	2	0	0
Cernuella caruanae	0	0	0	0	1	0	1	1	0	1	1	0	0	1
Cochlicella acuta (Müller, 1774)	1	0	0	0	0	0	0	0	0	0	0	1	1	0
Eobania vermiculata (Müller, 1774)	0	0	0	0	0	0	0	0	0	0	0	0	0	0
Pomatias sulcatus (Draparnaud, 1801)	1	0	0	0	1	0	1	0	0	1	1	0	1	0
Theba pisana (Müller, 1774)	2	5	0	0	0	0	0	0	0	0	0	0	0	1
Helicioid fragments	1	1	1	1	1	1	1	1	1	1	1	1	1	1
Cecilioides acicula (Müller, 1774)	0	0	1	1	0	0	0	0	0	0	1	0	0	0
Total amount of molluscs	**50**	**38**	**9**	**13**	**10**	**10**	**8**	**6**	**13**	**20**	**29**	**34**	**53**	**60**

Table A5.2 *(cont.).*

Species/Depth (cm)	542	546	549	553	561	566	571	576	581	586	591	596	601	606
Alvania sp.	0	2	0	0	2	3	5	0	0	0	1	0	0	0
Bittium sp.	0	0	0	0	3	2	0	1	0	0	0	0	0	0
Calliostoma sp.	0	0	0	0	0	0	0	0	0	0	0	0	0	0
Cerithium sp.	3	6	1	3	3	2	3	1	4	3	1	2	4	1
Cylichnea sp.	0	0	0	0	0	0	1	0	0	0	0	0	0	0
Conus mediterraneus (Hwass, 1792)	0	0	0	0	0	0	0	1	0	0	0	0	0	0
Epitonium sp.	0	0	0	0	0	0	0	0	0	0	0	0	0	0
Gibberula sp.	0	0	0	0	0	0	0	0	0	0	0	0	0	0
Gibbula sp.	2	0	1	0	1	3	0	1	0	1	0	0	0	0
Hexaplex trunculus (Linnaeus, 1758)	0	0	0	0	1	0	0	1	0	0	0	0	0	0
Jujubinus sp.	0	0	0	0	0	0	0	0	0	0	0	0	0	0
Nassarius sp.	0	0	0	0	0	0	0	0	0	0	0	0	0	0
Pirenella conica (Blainville, 1826)	0	0	0	0	0	1	0	0	0	0	0	0	0	0
Pisania striata	0	0	0	2	0	0	0	0	0	0	0	0	0	0
Retusa truncatula (Brugière, 1792)	0	0	0	0	0	0	0	0	0	0	0	0	0	0
Rissoa sp.	3	2	0	0	5	1	0	0	0	0	0	0	0	0
Tricolia sp.	0	0	0	0	0	0	0	0	0	0	0	0	0	0
Turbonilla lactea	0	0	0	0	0	0	0	0	0	0	0	0	0	0
Cardium sp.	0	0	1	0	0	0	0	0	0	0	0	0	0	0
Ostrea sp.	0	0	0	0	0	0	0	0	0	0	0	0	0	0
Loripes lucinalis (Lamarck, 1818)	0	0	0	0	0	1	0	0	1	1	0	0	0	0
Abra sp.	0	0	0	0	0	0	0	0	0	0	0	0	0	0
other/unknown marine	1	0	0	1	0	0	0	1	0	0	0	0	0	0
Hydrobia Hartmann, 1821	23	29	30	13	27	29	21	23	22	16	20	24	6	2
Ovatella myosotis (Draparnaud, 1801)	0	0	0	0	0	0	0	1	1	0	0	1	0	1
Truncatella subcylindrica (Linnaeus, 1767)	0	0	0	1	0	0	0	0	0	0	0	1	1	1
Oxychilus (Mediterranea) *hydatinus* (Rossmässler, 1838)	0	0	0	0	0	0	0	0	0	0	0	0	0	1
Truncatellina callicratis (Scacchi, 1833)	0	0	0	0	0	0	0	0	0	0	0	0	0	0
Xerotricha conspurcata (Draparnaud, 1801)	0	0	0	0	0	0	0	0	0	0	0	0	0	0
Clausiliidae Mörch, 1864	0	0	0	0	0	0	0	0	0	0	0	0	0	0
Granopupa granum (Draparnaud, 1801)	0	2	1	0	0	0	0	0	0	0	0	0	0	0
Papillifera papillaris (Müller, 1774)	0	0	0	0	1	1	0	0	1	0	0	0	0	0
Muticaria Lindholm, 1925	1	1	0	0	1	1	0	1	0	1	0	1	0	0
Rumina decollata (Linnaeus, 1758)	0	0	0	0	0	0	0	0	0	0	0	0	0	0
Trochoidea spratti (Pfeiffer, 1846)	0	0	0	0	0	0	0	1	1	0	0	0	0	3
Cernuella caruanae	0	0	0	0	2	0	0	0	0	0	0	0	0	0
Cochlicella acuta (Müller, 1774)	1	0	0	0	0	2	0	1	0	0	0	0	0	0
Eobania vermiculata (Müller, 1774)	0	0	0	0	0	0	0	0	0	0	0	0	0	0
Pomatias sulcatus (Draparnaud, 1801)	1	1	0	0	1	1	0	0	1	0	1	0	0	0
Theba pisana (Müller, 1774)	0	0	0	0	0	0	0	0	0	0	0	0	0	0
Helicioid fragments	1	1	0	0	1	1	1	1	1	1	1	1	0	0
Cecilioides acicula (Müller, 1774)	0	1	0	0	0	0	0	0	0	0	0	1	0	0
Total amount of molluscs	**36**	**45**	**34**	**20**	**48**	**48**	**31**	**34**	**32**	**23**	**24**	**31**	**11**	**9**

Table A5.2 *(cont.).*

Species/Depth (cm)	611	615	641	644	648	651	655	658	661	665	668	671	675	678
Alvania sp.	0	0	0	0	0	1	0	0	0	0	0	0	0	0
Bittium sp.	0	0	0	0	0	0	1	0	0	0	2	0	0	0
Calliostoma sp.	0	0	0	0	0	0	0	0	0	0	0	0	0	0
Cerithium sp.	0	1	1	2	1	0	2	2	1	1	0	1	1	0
Cylichnea sp.	0	0	0	0	0	0	0	0	0	0	0	0	0	0
Conus mediterraneus (Hwass, 1792)	0	0	0	0	0	0	0	0	0	0	0	0	0	0
Epitonium sp.	0	0	0	0	0	0	0	0	0	0	0	0	0	0
Gibberula sp.	0	0	0	0	0	0	0	0	0	0	0	0	0	0
Gibbula sp.	0	0	0	2	0	0	0	0	0	0	1	0	0	1
Hexaplex trunculus (Linnaeus, 1758)	0	0	0	0	0	0	0	0	0	0	0	0	0	0
Jujubinus sp.	0	0	0	0	0	0	0	0	0	0	0	0	0	0
Nassarius sp.	0	0	0	0	0	0	0	0	0	0	0	0	0	0
Pirenella conica (Blainville, 1826)	0	0	0	0	0	0	0	0	0	0	0	0	0	0
Pisania striata	0	0	0	0	0	0	0	0	0	0	0	0	0	0
Retusa truncatula (Brugière, 1792)	0	0	0	0	0	0	0	0	0	0	0	0	0	0
Rissoa sp.	0	0	0	1	0	0	1	2	0	2	0	1	0	0
Tricolia sp.	0	0	0	0	0	0	0	0	0	0	0	0	0	0
Turbonilla lactea	0	0	0	0	0	0	0	0	0	0	0	0	0	0
Cardium sp.	0	3	0	1	0	0	0	1	1	0	3	0	0	0
Ostrea sp.	0	0	0	0	0	0	0	0	0	0	0	0	0	0
Loripes lucinalis (Lamarck, 1818)	0	0	0	0	1	0	0	0	1	0	0	1	0	0
Abra sp.	0	0	0	0	0	0	1	0	0	0	0	0	0	0
other/unknown marine	0	0	1	0	0	0	0	0	0	1	1	1	1	0
Hydrobia Hartmann, 1821	4	35	11	16	32	54	41	32	10	5	3	6	5	1
Ovatella myosotis (Draparnaud, 1801)	0	0	0	0	0	0	0	0	0	0	0	0	0	0
Truncatella subcylindrica (Linnaeus, 1767)	0	0	0	0	0	0	0	0	0	0	0	0	0	0
Oxychilus (Mediterranea) *hydatinus* (Rossmässler, 1838)	0	0	0	0	0	0	0	0	0	0	0	0	0	0
Truncatellina callicratis (Scacchi, 1833)	0	0	0	0	0	0	0	0	0	0	0	0	0	0
Xerotricha conspurcata (Draparnaud, 1801)	0	0	0	0	0	0	0	0	0	0	0	0	0	0
Clausiliidae Mörch, 1864	0	0	0	0	0	0	0	1	0	0	0	0	0	0
Granopupa granum (Draparnaud, 1801)	0	0	0	0	0	0	0	0	0	0	0	0	0	0
Papillifera papillaris (Müller, 1774)	0	0	1	0	0	1	0	0	0	0	0	0	0	1
Muticaria Lindholm, 1925	0	0	1	1	0	1	1	1	1	1	0	1	0	0
Rumina decollata (Linnaeus, 1758)	0	0	0	0	0	0	0	0	0	0	0	0	0	0
Trochoidea spratti (Pfeiffer, 1846)	0	0	0	0	0	0	1	0	0	0	0	0	0	0
Cernuella caruanae	0	1	0	0	0	0	0	0	1	0	0	0	0	0
Cochlicella acuta (Müller, 1774)	0	0	0	0	1	0	3	1	0	0	0	0	0	0
Eobania vermiculata (Müller, 1774)	0	0	0	0	0	0	1	0	0	0	0	0	0	0
Pomatias sulcatus (Draparnaud, 1801)	0	0	0	1	1	0	0	0	0	0	1	0	0	0
Theba pisana (Müller, 1774)	0	0	0	1	0	0	0	0	0	0	0	0	0	0
Helicioid fragments	1	1	1	1	1	1	1	1	1	1	1	1	1	0
Cecilioides acicula (Müller, 1774)	0	0	0	0	0	0	0	1	0	0	0	0	0	0
Total amount of molluscs	**5**	**41**	**16**	**26**	**37**	**58**	**53**	**42**	**16**	**11**	**12**	**12**	**8**	**3**

Table A5.2 *(cont.).*

Species/Depth (cm)	687	692	697	702	707	712	717	722	727	732	737	741
Alvania sp.	0	0	0	0	0	0	1	0	2	0	0	0
Bittium sp.	0	0	0	0	0	0	1	2	3	0	0	2
Calliostoma sp.	0	0	0	0	0	0	0	0	0	0	0	0
Cerithium sp.	2	0	0	0	2	2	6	7	0	0	3	2
Cylichnea sp.	0	0	0	0	0	0	0	0	0	0	0	0
Conus mediterraneus (Hwass, 1792)	0	0	0	0	0	0	0	0	0	0	0	0
Epitonium sp.	0	0	0	0	0	0	0	0	0	0	0	0
Gibberula sp.	0	0	0	0	0	0	0	0	0	0	0	0
Gibbula sp.	0	0	0	0	0	0	0	0	1	0	2	1
Hexaplex trunculus (Linnaeus, 1758)	0	0	0	0	0	0	0	0	0	0	0	0
Jujubinus sp.	0	0	0	0	0	0	0	0	0	0	0	0
Nassarius sp.	0	0	0	0	0	0	0	0	0	0	0	0
Pirenella conica (Blainville, 1826)	0	0	0	0	0	0	0	0	0	0	0	0
Pisania striata	0	0	0	0	0	0	0	0	0	0	0	0
Retusa truncatula (Brugière, 1792)	0	0	0	0	0	0	1	0	0	0	0	0
Rissoa sp.	0	1	0	0	0	1	0	1	1	0	0	1
Tricolia sp.	0	1	0	0	0	0	1	0	0	0	0	0
Turbonilla lactea	0	0	0	0	0	0	0	1	0	0	0	0
Cardium sp.	0	0	0	0	0	0	1	3	0	0	0	0
Ostrea sp.	0	0	0	0	0	0	0	0	0	0	0	0
Loripes lucinalis (Lamarck, 1818)	0	0	0	0	0	0	0	0	0	0	0	0
Abra sp.	0	0	0	0	0	0	0	0	0	0	1	0
other/unknown marine	1	0	0	0	0	0	1	0	0	1	0	0
Hydrobia Hartmann, 1821	68	53	81	73	154	25	24	27	11	1	0	1
Ovatella myosotis (Draparnaud, 1801)	0	0	0	0	0	0	0	0	0	0	0	0
Truncatella subcylindrica (Linnaeus, 1767)	0	0	0	0	1	0	0	0	0	0	0	0
Oxychilus (Mediterranea) *hydatinus* (Rossmässler, 1838)	0	0	0	0	0	0	0	0	0	0	0	0
Truncatellina callicratis (Scacchi, 1833)	0	0	0	0	0	0	0	0	0	0	0	0
Xerotricha conspurcata (Draparnaud, 1801)	0	0	0	0	0	0	0	0	0	0	0	0
Clausiliidae Mörch, 1864	0	0	2	0	0	0	0	0	0	0	0	0
Granopupa granum (Draparnaud, 1801)	0	0	0	1	0	0	0	0	0	0	0	0
Papillifera papillaris (Müller, 1774)	0	1	0	2	1	1	1	0	0	0	0	0
Muticaria Lindholm, 1925	1	1	1	1	1	1	1	1	0	1	0	1
Rumina decollata (Linnaeus, 1758)	0	0	0	0	0	0	0	0	0	0	0	0
Trochoidea spratti (Pfeiffer, 1846)	0	2	0	1	0	0	0	0	0	0	0	0
Cernuella caruanae	0	0	0	1	0	0	1	0	0	0	0	0
Cochlicella acuta (Müller, 1774)	0	1	0	0	1	0	0	1	1	0	0	0
Eobania vermiculata (Müller, 1774)	0	0	0	0	0	0	0	0	1	0	0	0
Pomatias sulcatus (Draparnaud, 1801)	1	1	1	1	2	1	1	1	1	1	1	1
Theba pisana (Müller, 1774)	0	0	0	0	0	0	1	0	0	0	0	0
Helicioid fragments	1	1	1	1	1	1	1	1	1	1	1	1
Cecilioides acicula (Müller, 1774)	0	1	0	0	1	0	0	0	1	0	0	0
Total amount of molluscs	**74**	**63**	**86**	**81**	**164**	**32**	**42**	**45**	**23**	**5**	**8**	**10**

Table A5.3. *Salina Deep Core non-marine.*

Species/Depth (cm)	1113	1121	1131	1140	1150	1160	1191	1201	1211	1216	1221	1231
Pseudamnicola (s.str.) *moussonii* (Calcara, 1841)	4	5	6	0	8	6	2	3	4	0	0	2
Ancylus fluviatilis Müller, 1774	0	0	0	0	0	0	0	0	0	1	0	0
Bulinus cf. *truncatus* (Audouin, 1827)	0	0	0	0	0	0	1	1	9	0	0	1
Oxyloma elegans (Risso, 1826)	0	0	0	0	0	0	0	0	0	0	0	0
Gyraulus (Armiger) crista (Linnaeus, 1758)	0	0	0	0	0	0	0	0	1	0	0	0
Lymnaea sp. (Feilden, 1879)	3	3	7	0	2	0	2	0	3	1	1	1
Vallonia pulchella (Müller, 1774)	0	0	0	0	0	0	0	0	0	0	0	0
Carychium cf. *schlickumi* Strauch, 1977	0	0	1	0	0	0	0	0	0	0	0	0
Planorbis moquini (Requien, 1848)	0	0	0	0	0	0	0	0	0	1	0	0
Vertigo cf. *antivertigo* (Draparnaud, 1801)	0	0	0	0	0	0	0	0	0	0	0	0
Pisidium Pfeiffer, 1821	0	0	0	0	0	0	2	0	0	1	0	0
Oxychilus (Mediterranea) *hydatinus* (Rossmässler, 1838)	0	1	1	0	1	1	0	0	0	1	1	1
Vitrea Fitzinger, 1833	4	6	8	0	0	0	0	0	2	2	0	2
Ferussacia (s.str.) *folliculus* (Gmelin, 1791)	0	0	0	0	0	0	0	0	0	0	0	0
Clausiliidae Mörch, 1864	0	0	0	0	0	0	0	0	0	0	0	0
Muticaria Lindholm, 1925	0	0	0	0	0	0	0	0	1	0	0	1
Papillifera papillaris (Müller, 1774)	0	0	0	1	1	0	0	1	0	0	1	0
Rumina decollata (Linnaeus, 1758)	0	1	0	1	0	0	0	0	0	0	0	0
Trochoidea spratti (Pfeiffer, 1846)	3	1	1	7	6	3	0	5	2	3	0	2
Truncatellina callicratis (Scacchi, 1833)	0	0	0	0	0	0	1	0	0	0	0	1
Granopupa granum (Draparnaud, 1801)	2	0	0	0	0	0	0	0	0	0	0	0
Pomatias sulcatus (Draparnaud, 1801)	0	0	0	0	0	0	0	0	0	0	0	0
Xerotricha Monterosato, 1892	0	0	0	0	0	0	0	0	1	1	0	0
Cernuella caruanae (Kobelt, 1888)	8	5	13	0	3	2	2	6	10	4	5	4
Chondrula (Mastus) pupa (Linnaeus, 1758)	0	0	0	0	0	0	0	0	0	0	0	0
Cochlicella acuta (Müller, 1774)	7	4	10	6	7	6	1	2	0	7	9	7
Eobania vermiculata (Müller, 1774)	0	0	0	0	0	0	0	0	0	0	0	0
Helicioidae	1	0	2	3	0	0	1	1	3	0	0	2
Cecilioides acicula (Müller, 1774)	9	2	5	0	6	2	6	2	7	8	2	2
Total amount of molluscs	**41**	**28**	**54**	**18**	**34**	**20**	**18**	**21**	**43**	**30**	**19**	**26**

Table A5.3 *(cont.).*

Species/Depth (cm)	1241	1247	1257	1267	1277	1290	1300	1310	1384	1394	1404	1414
Pseudamnicola (s.str.) *moussonii* (Calcara, 1841)	1	2	3	4	0	7	17	8	0	1	1	2
Ancylus fluviatilis Müller, 1774	1	0	0	0	0	0	0	1	0	0	0	0
Bulinus cf. *truncatus* (Audouin, 1827)	0	2	0	4	1	0	3	3	1	2	0	0
Oxyloma elegans (Risso, 1826)	0	0	0	2	0	0	0	0	0	0	0	0
Gyraulus (Armiger) crista (Linnaeus, 1758)	0	1	1	2	0	0	1	3	0	1	2	1
Lymnaea sp. (Feilden, 1879)	1	1	2	2	2	3	4	7	1	1	0	0
Vallonia pulchella (Müller, 1774)	0	0	0	0	0	0	0	0	0	0	0	0
Carychium cf. *schlickumi* Strauch, 1977	0	0	0	0	0	0	0	0	0	0	0	0
Planorbis moquini (Requien, 1848)	0	0	0	0	0	0	1	0	0	0	0	0
Vertigo cf. *antivertigo* (Draparnaud, 1801)	0	0	0	0	0	0	0	0	0	0	0	0
Pisidium Pfeiffer, 1821	0	0	0	0	1	0	0	0	0	0	1	0
Oxychilus (Mediterranea) *hydatinus* (Rossmässler, 1838)	2	0	0	0	0	0	0	2	0	1	1	1
Vitrea Fitzinger, 1833	1	0	0	4	1	1	8	1	0	0	0	1
Ferussacia (s.str.) *folliculus* (Gmelin, 1791)	0	0	0	0	0	0	0	0	0	0	0	0
Clausiliidae Mörch, 1864	0	0	0	0	0	3	0	0	0	0	0	0
Muticaria Lindholm, 1925	0	0	0	1	1	0	0	0	1	0	1	0
Papillifera papillaris (Müller, 1774)	0	1	0	1	1	0	0	1	0	0	0	0
Rumina decollata (Linnaeus, 1758)	0	0	0	0	0	0	0	0	0	0	0	0
Trochoidea spratti (Pfeiffer, 1846)	2	0	2	7	0	2	1	0	1	0	0	0
Truncatellina callicratis (Scacchi, 1833)	0	0	1	0	0	0	1	0	0	0	0	0
Granopupa granum (Draparnaud, 1801)	0	0	0	0	0	0	1	0	0	0	0	0
Pomatias sulcatus (Draparnaud, 1801)	0	0	0	0	0	0	0	0	0	0	0	0
Xerotricha Monterosato, 1892	0	0	0	0	0	0	0	0	0	0	0	0
Cernuella caruanae (Kobelt, 1888)	1	3	6	14	5	8	0	10	3	5	4	5
Chondrula (Mastus) pupa (Linnaeus, 1758)	0	0	0	0	0	0	0	0	0	0	0	0
Cochlicella acuta (Müller, 1774)	7	9	9	17	16	13	23	26	1	0	0	0
Eobania vermiculata (Müller, 1774)	0	0	0	0	0	0	0	0	0	0	0	0
Helicioidae	1	0	3	7	1	0	0	1	1	2	0	1
Cecilioides acicula (Müller, 1774)	2	6	5	13	1	4	12	8	3	2	4	6
Total amount of molluscs	**19**	**25**	**32**	**78**	**30**	**41**	**72**	**71**	**12**	**15**	**14**	**17**

Table A5.3 *(cont.).*

Species/Depth (cm)	1425	1434	1444	1450	1459	1470	1479	1489	1630	1640	1650	1682
Pseudamnicola (s.str.) *moussonii* (Calcara, 1841)	0	5	2	0	3	3	9	2	2	0	3	0
Ancylus fluviatilis Müller, 1774	0	0	0	0	1	0	1	0	0	0	0	0
Bulinus cf. *truncatus* (Audouin, 1827)	1	0	0	0	2	0	1	3	0	1	1	0
Oxyloma elegans (Risso, 1826)	0	0	0	0	0	0	0	1	0	0	0	0
Gyraulus (Armiger) crista (Linnaeus, 1758)	0	0	1	0	1	0	0	3	0	0	0	0
Lymnaea sp. (Feilden, 1879)	0	3	5	1	0	3	9	3	1	0	1	0
Vallonia pulchella (Müller, 1774)	1	0	0	0	0	0	0	0	0	0	0	0
Carychium cf. *schlickumi* Strauch, 1977	0	0	0	0	0	0	0	1	0	0	0	0
Planorbis moquini (Requien, 1848)	0	0	0	0	0	0	0	0	0	0	0	0
Vertigo cf. *antivertigo* (Draparnaud, 1801)	0	0	0	0	0	0	0	0	0	0	0	0
Pisidium Pfeiffer, 1821	1	1	1	0	0	0	0	0	0	0	0	0
Oxychilus (Mediterranea) *hydatinus* (Rossmässler, 1838)	0	1	5	2	2	0	2	2	1	1	0	6
Vitrea Fitzinger, 1833	0	2	0	0	0	0	2	0	1	0	1	0
Ferussacia (s.str.) *folliculus* (Gmelin, 1791)	0	0	0	0	0	0	0	0	0	0	0	0
Clausiliidae Mörch, 1864	0	0	0	0	1	0	0	0	0	0	0	0
Muticaria Lindholm, 1925	0	1	1	0	1	0	0	0	1	0	0	0
Papillifera papillaris (Müller, 1774)	1	0	0	0	0	1	0	0	0	0	0	0
Rumina decollata (Linnaeus, 1758)	0	0	0	0	0	0	3	1	0	0	1	0
Trochoidea spratti (Pfeiffer, 1846)	2	0	0	0	0	1	5	0	0	0	0	0
Truncatellina callicratis (Scacchi, 1833)	0	0	1	1	0	0	2	1	0	0	1	0
Granopupa granum (Draparnaud, 1801)	0	0	0	0	0	0	0	0	0	0	0	0
Pomatias sulcatus (Draparnaud, 1801)	0	0	0	0	0	0	0	0	0	0	0	0
Xerotricha Monterosato, 1892	0	0	0	0	0	0	0	0	0	0	0	0
Cernuella caruanae (Kobelt, 1888)	2	7	6	7	7	5	8	1	0	0	9	0
Chondrula (Mastus) pupa (Linnaeus, 1758)	0	0	0	0	0	0	0	0	0	0	0	0
Cochlicella acuta (Müller, 1774)	0	0	0	2	4	5	19	13	0	0	0	0
Eobania vermiculata (Müller, 1774)	0	0	0	0	0	0	0	0	0	0	0	0
Helicioidae	3	0	2	0	2	2	3	6	1	1	0	0
Cecilioides acicula (Müller, 1774)	1	6	6	0	10	5	9	8	6	1	6	2
Total amount of molluscs	**12**	**26**	**30**	**13**	**34**	**25**	**73**	**45**	**13**	**4**	**23**	**8**

Table A5.3 *(cont.).*

Species/Depth (cm)	1692	1702	1710	1720	1730	1740	1745	1755	1765	1770	1780	1790
Pseudamnicola (s.str.) *moussonii* (Calcara, 1841)	0	0	0	0	0	0	1	0	0	1	0	0
Ancylus fluviatilis Müller, 1774	0	0	0	0	0	0	0	0	0	0	0	0
Bulinus cf. *truncatus* (Audouin, 1827)	0	0	0	0	0	0	0	0	0	0	2	0
Oxyloma elegans (Risso, 1826)	0	0	0	0	0	0	0	0	0	0	0	0
Gyraulus (Armiger) crista (Linnaeus, 1758)	0	0	0	0	0	0	0	0	0	2	1	0
Lymnaea sp. (Feilden, 1879)	0	0	0	0	0	0	0	0	0	0	0	2
Vallonia pulchella (Müller, 1774)	0	0	0	0	0	0	0	0	0	0	0	0
Carychium cf. *schlickumi* Strauch, 1977	0	0	0	0	0	0	0	0	0	0	0	0
Planorbis moquini (Requien, 1848)	0	0	0	0	0	0	0	0	0	0	0	0
Vertigo cf. *antivertigo* (Draparnaud, 1801)	0	0	0	0	0	0	0	0	0	0	0	0
Pisidium Pfeiffer, 1821	0	0	0	0	0	0	0	0	0	0	0	0
Oxychilus (Mediterranea) *hydatinus* (Rossmässler, 1838)	0	0	0	0	0	0	0	1	0	0	0	2
Vitrea Fitzinger, 1833	0	0	0	0	0	0	0	0	0	0	0	0
Ferussacia (s.str.) *folliculus* (Gmelin, 1791)	0	0	0	0	0	0	0	0	0	0	0	0
Clausiliidae Mörch, 1864	0	0	0	0	0	0	0	0	0	0	0	0
Muticaria Lindholm, 1925	0	0	0	0	0	0	0	0	0	0	0	0
Papillifera papillaris (Müller, 1774)	0	0	0	0	0	0	0	0	0	0	1	0
Rumina decollata (Linnaeus, 1758)	0	0	0	0	0	0	0	0	0	0	0	0
Trochoidea spratti (Pfeiffer, 1846)	0	0	0	0	0	0	0	0	0	1	0	0
Truncatellina callicratis (Scacchi, 1833)	0	0	0	0	0	0	0	0	0	0	0	0
Granopupa granum (Draparnaud, 1801)	0	0	0	0	0	0	0	0	0	0	0	0
Pomatias sulcatus (Draparnaud, 1801)	0	0	0	0	0	0	0	0	0	0	0	0
Xerotricha Monterosato, 1892	0	0	0	0	0	0	0	0	0	0	0	0
Cernuella caruanae (Kobelt, 1888)	0	0	0	0	0	0	0	0	0	0	1	1
Chondrula (Mastus) pupa (Linnaeus, 1758)	0	0	0	0	0	0	0	0	0	0	0	0
Cochlicella acuta (Müller, 1774)	0	0	0	0	0	0	0	0	1	0	0	0
Eobania vermiculata (Müller, 1774)	0	0	0	0	0	0	0	0	0	0	0	0
Helicioidae	1	0	0	0	1	1	0	1	1	0	0	0
Cecilioides acicula (Müller, 1774)	1	3	0	0	0	0	0	0	0	0	0	2
Total amount of molluscs	**2**	**3**	**1**	**1**	**1**	**1**	**1**	**2**	**2**	**4**	**5**	**7**

Table A5.3 *(cont.).*

Species/Depth (cm)	1841	1851	1861	1869	1879	1889	1890	1900	1910	1920	1930	1940
Pseudamnicola (s.str.) *moussonii* (Calcara, 1841)	0	0	0	0	0	0	0	0	0	0	2	1
Ancylus fluviatilis Müller, 1774	0	0	0	0	0	0	0	0	0	0	0	0
Bulinus cf. *truncatus* (Audouin, 1827)	0	0	0	0	0	0	0	0	0	1	0	0
Oxyloma elegans (Risso, 1826)	0	0	0	0	0	0	0	0	0	0	0	0
Gyraulus (Armiger) crista (Linnaeus, 1758)	0	0	0	0	0	0	0	0	0	0	0	0
Lymnaea sp. (Feilden, 1879)	0	0	0	0	0	0	0	0	0	0	1	1
Vallonia pulchella (Müller, 1774)	0	0	0	0	0	0	0	0	0	0	0	0
Carychium cf. *schlickumi* Strauch, 1977	0	0	0	0	0	0	0	0	0	0	0	0
Planorbis moquini (Requien, 1848)	0	0	0	0	0	0	0	0	0	0	0	0
Vertigo cf. *antivertigo* (Draparnaud, 1801)	0	0	0	0	0	0	0	0	0	0	0	0
Pisidium Pfeiffer, 1821	0	0	0	0	0	0	0	0	0	0	0	0
Oxychilus (Mediterranea) *hydatinus* (Rossmässler, 1838)	1	0	0	0	0	0	0	0	0	0	4	3
Vitrea Fitzinger, 1833	0	0	0	0	0	0	0	0	0	0	0	0
Ferussacia (s.str.) *folliculus* (Gmelin, 1791)	0	0	0	0	0	0	0	0	1	0	0	0
Clausiliidae Mörch, 1864	0	0	0	0	0	0	0	0	0	0	0	0
Muticaria Lindholm, 1925	0	0	0	0	0	0	0	0	0	0	0	0
Papillifera papillaris (Müller, 1774)	0	0	0	0	0	0	0	0	0	0	0	0
Rumina decollata (Linnaeus, 1758)	0	0	0	0	0	0	0	0	0	0	0	0
Trochoidea spratti (Pfeiffer, 1846)	0	0	0	0	0	0	0	0	0	0	0	0
Truncatellina callicratis (Scacchi, 1833)	0	0	0	0	0	0	0	0	0	0	0	0
Granopupa granum (Draparnaud, 1801)	0	0	0	0	0	0	0	0	0	0	0	0
Pomatias sulcatus (Draparnaud, 1801)	0	0	0	0	0	0	0	0	0	0	0	0
Xerotricha Monterosato, 1892	0	0	0	0	0	0	0	0	0	0	0	0
Cernuella caruanae (Kobelt, 1888)	0	0	0	0	0	0	0	0	0	1	0	6
Chondrula (Mastus) pupa (Linnaeus, 1758)	0	0	0	0	0	0	0	0	0	0	0	0
Cochlicella acuta (Müller, 1774)	0	0	0	0	0	0	0	0	0	0	0	0
Eobania vermiculata (Müller, 1774)	0	0	0	0	0	0	0	0	0	0	0	0
Helicioidae	0	0	0	0	0	0	0	0	0	0	1	0
Cecilioides acicula (Müller, 1774)	4	0	0	0	0	0	0	0	0	0	1	2
Total amount of molluscs	**5**	**1**	**1**	**1**	**1**	**1**	**1**	**1**	**1**	**2**	**9**	**13**

Table A5.3 *(cont.).*

Species/Depth (cm)	1971	1981	1991	1994	2004	2014	2023	2033	2043	2046	2056	2066
Pseudamnicola (s.str.) *moussonii* (Calcara, 1841)	0	0	0	0	0	0	0	0	0	0	0	0
Ancylus fluviatilis Müller, 1774	0	0	0	0	0	0	0	0	0	0	0	0
Bulinus cf. *truncatus* (Audouin, 1827)	0	0	0	0	0	0	0	0	0	0	0	0
Oxyloma elegans (Risso, 1826)	0	0	0	0	0	0	0	0	0	0	0	0
Gyraulus (Armiger) crista (Linnaeus, 1758)	0	0	0	0	0	0	0	0	0	0	0	0
Lymnaea sp. (Feilden, 1879)	0	0	0	0	0	0	0	0	0	0	0	0
Vallonia pulchella (Müller, 1774)	0	0	0	0	0	0	0	0	0	0	0	0
Carychium cf. *schlickumi* Strauch, 1977	0	0	0	0	0	0	0	0	0	0	0	0
Planorbis moquini (Requien, 1848)	0	0	0	0	0	0	0	0	0	0	0	0
Vertigo cf. *antivertigo* (Draparnaud, 1801)	0	0	0	0	0	0	0	0	0	0	0	0
Pisidium Pfeiffer, 1821	0	0	0	0	0	0	0	0	0	0	0	0
Oxychilus (Mediterranea) *hydatinus* (Rossmässler, 1838)	0	0	0	0	0	0	0	0	0	0	0	0
Vitrea Fitzinger, 1833	0	0	0	0	0	0	0	0	0	0	0	0
Ferussacia (s.str.) *folliculus* (Gmelin, 1791)	0	0	0	0	0	0	0	0	0	0	0	0
Clausiliidae Mörch, 1864	0	0	0	0	0	0	0	0	0	0	0	0
Muticaria Lindholm, 1925	0	0	0	0	0	0	0	0	0	0	0	0
Papillifera papillaris (Müller, 1774)	0	0	0	0	0	0	0	0	0	0	0	0
Rumina decollata (Linnaeus, 1758)	0	0	0	0	0	0	0	0	0	0	0	0
Trochoidea spratti (Pfeiffer, 1846)	0	0	0	0	0	0	0	0	1	0	0	0
Truncatellina callicratis (Scacchi, 1833)	0	0	0	0	0	0	0	0	0	0	0	0
Granopupa granum (Draparnaud, 1801)	0	0	0	0	0	0	0	0	0	0	0	0
Pomatias sulcatus (Draparnaud, 1801)	0	0	0	0	0	0	0	0	0	0	0	0
Xerotricha Monterosato, 1892	0	0	0	0	0	0	0	0	0	0	0	0
Cernuella caruanae (Kobelt, 1888)	0	0	1	0	0	0	0	0	0	0	0	0
Chondrula (Mastus) pupa (Linnaeus, 1758)	0	0	0	0	0	0	0	0	0	0	0	0
Cochlicella acuta (Müller, 1774)	0	0	1	0	0	0	0	0	0	0	0	0
Eobania vermiculata (Müller, 1774)	0	0	0	0	0	0	0	0	0	0	0	0
Helicioidae	0	0	0	0	0	0	0	0	0	0	0	0
Cecilioides acicula (Müller, 1774)	0	0	0	0	0	0	0	0	0	0	0	0
Total amount of molluscs	**1**	**1**	**2**	**1**	**1**	**1**	**1**	**1**	**1**	**1**	**1**	**1**

Table A5.3 *(cont.).*

Species/Depth (cm)	2070	2080	2100	2106	2113	2123	2133	2143	2153	2163	2183	2192
Pseudamnicola (s.str.) *moussonii* (Calcara, 1841)	0	1	0	0	0	1	0	0	0	0	0	0
Ancylus fluviatilis Müller, 1774	0	0	0	0	0	0	0	0	0	0	0	0
Bulinus cf. *truncatus* (Audouin, 1827)	0	0	0	0	0	0	0	0	0	0	0	0
Oxyloma elegans (Risso, 1826)	0	0	0	0	0	0	0	0	0	0	0	0
Gyraulus (Armiger) crista (Linnaeus, 1758)	0	0	0	0	0	0	0	0	0	0	0	0
Lymnaea sp. (Feilden, 1879)	0	0	0	0	0	0	0	0	0	0	0	0
Vallonia pulchella (Müller, 1774)	0	0	0	0	0	0	0	0	0	0	0	0
Carychium cf. *schlickumi* Strauch, 1977	0	0	0	0	0	0	0	0	0	0	0	0
Planorbis moquini (Requien, 1848)	0	0	0	0	0	0	0	0	0	0	0	0
Vertigo cf. *antivertigo* (Draparnaud, 1801)	0	0	0	0	0	0	0	0	0	0	0	0
Pisidium Pfeiffer, 1821	0	0	0	0	0	0	0	0	0	0	0	0
Oxychilus (Mediterranea) *hydatinus* (Rossmässler, 1838)	0	0	1	0	0	0	0	0	0	0	1	0
Vitrea Fitzinger, 1833	0	0	0	0	0	1	0	0	0	0	0	0
Ferussacia (s.str.) *folliculus* (Gmelin, 1791)	0	0	0	0	0	0	0	0	0	0	0	0
Clausiliidae Mörch, 1864	0	0	0	0	0	0	0	0	0	0	0	0
Muticaria Lindholm, 1925	0	0	0	0	0	0	0	0	0	0	0	0
Papillifera papillaris (Müller, 1774)	0	0	0	0	0	0	0	0	0	0	0	0
Rumina decollata (Linnaeus, 1758)	0	0	0	0	0	0	0	0	0	0	0	0
Trochoidea spratti (Pfeiffer, 1846)	0	1	0	0	0	0	0	0	0	0	0	0
Truncatellina callicratis (Scacchi, 1833)	0	1	0	0	0	0	0	0	0	0	0	0
Granopupa granum (Draparnaud, 1801)	0	0	0	0	0	0	0	0	0	0	0	0
Pomatias sulcatus (Draparnaud, 1801)	0	0	0	0	0	0	0	0	0	0	0	0
Xerotricha Monterosato, 1892	0	0	0	0	0	0	0	0	0	0	0	0
Cernuella caruanae (Kobelt, 1888)	0	0	1	0	0	0	0	0	1	0	0	0
Chondrula (Mastus) pupa (Linnaeus, 1758)	0	0	0	0	0	0	0	0	0	0	0	0
Cochlicella acuta (Müller, 1774)	0	1	0	0	0	0	0	0	0	0	0	0
Eobania vermiculata (Müller, 1774)	0	1	0	0	0	0	0	0	0	0	0	0
Helicioidae	0	0	0	0	0	0	1	1	1	0	0	0
Cecilioides acicula (Müller, 1774)	0	0	0	0	0	0	0	0	0	0	1	0
Total amount of molluscs	**1**	**5**	**2**	**1**	**1**	**2**	**1**	**1**	**2**	**1**	**2**	**1**

Table A5.3 *(cont.).*

Species/Depth (cm)	2202	2222	2240	2260	2285	2295	2305	2308	2318	2328	2338	2348
Pseudamnicola (s.str.) *moussonii* (Calcara, 1841)	0	0	0	0	0	0	0	0	2	5	1	0
Ancylus fluviatilis Müller, 1774	0	0	0	0	0	0	0	0	0	0	0	0
Bulinus cf. *truncatus* (Audouin, 1827)	0	0	0	0	0	0	0	0	0	0	0	0
Oxyloma elegans (Risso, 1826)	0	0	0	0	0	0	0	0	0	0	0	0
Gyraulus (Armiger) crista (Linnaeus, 1758)	1	0	0	0	0	0	0	0	1	2	1	0
Lymnaea sp. (Feilden, 1879)	0	0	0	0	0	0	0	0	0	7	2	0
Vallonia pulchella (Müller, 1774)	0	0	0	0	0	0	0	0	0	0	0	0
Carychium cf. *schlickumi* Strauch, 1977	0	0	0	0	0	0	0	0	0	0	0	0
Planorbis moquini (Requien, 1848)	0	0	0	0	0	0	0	0	0	0	0	0
Vertigo cf. *antivertigo* (Draparnaud, 1801)	0	0	0	0	0	0	0	0	0	0	0	0
Pisidium Pfeiffer, 1821	0	0	0	0	0	0	0	0	0	0	0	0
Oxychilus (Mediterranea) *hydatinus* (Rossmässler, 1838)	1	1	0	0	0	0	0	2	6	0	0	0
Vitrea Fitzinger, 1833	0	0	0	0	0	0	0	1	0	13	0	0
Ferussacia (s.str.) *folliculus* (Gmelin, 1791)	0	0	0	0	0	0	0	0	0	0	0	0
Clausiliidae Mörch, 1864	0	0	0	0	0	0	0	0	0	0	0	0
Muticaria Lindholm, 1925	0	0	0	0	0	0	0	0	0	1	0	0
Papillifera papillaris (Müller, 1774)	0	0	0	0	0	0	0	0	1	0	1	0
Rumina decollata (Linnaeus, 1758)	0	0	0	0	0	0	0	0	0	0	0	0
Trochoidea spratti (Pfeiffer, 1846)	0	0	0	0	0	0	0	0	0	0	0	0
Truncatellina callicratis (Scacchi, 1833)	0	0	0	0	0	0	0	0	1	1	0	0
Granopupa granum (Draparnaud, 1801)	0	0	0	0	0	0	0	0	0	0	0	0
Pomatias sulcatus (Draparnaud, 1801)	0	0	0	0	0	0	0	0	0	0	0	0
Xerotricha Monterosato, 1892	0	0	0	0	0	0	0	0	0	0	0	0
Cernuella caruanae (Kobelt, 1888)	0	0	0	0	1	0	0	0	1	5	2	0
Chondrula (Mastus) pupa (Linnaeus, 1758)	0	0	0	0	0	0	0	0	0	0	0	0
Cochlicella acuta (Müller, 1774)	0	0	0	0	0	1	0	0	0	0	1	0
Eobania vermiculata (Müller, 1774)	0	0	0	0	0	0	0	0	0	0	0	0
Helicioidae	0	0	0	1	0	1	1	0	1	0	0	1
Cecilioides acicula (Müller, 1774)	1	0	0	0	0	0	0	0	2	3	0	0
Total amount of molluscs	**3**	**1**	**1**	**1**	**1**	**2**	**1**	**3**	**15**	**37**	**8**	**1**

Table A5.3 *(cont.).*

Species/Depth (cm)	2358	2363	2368	2380	2390	2398	2408	2418	2428	2458	2468	2508
Pseudamnicola (s.str.) *moussonii* (Calcara, 1841)	0	0	0	0	0	0	1	3	1	3	1	10
Ancylus fluviatilis Müller, 1774	0	0	0	0	0	0	0	0	0	0	0	4
Bulinus cf. *truncatus* (Audouin, 1827)	0	0	0	0	0	0	0	0	0	0	0	0
Oxyloma elegans (Risso, 1826)	0	0	0	0	0	0	0	0	0	0	0	0
Gyraulus (Armiger) crista (Linnaeus, 1758)	0	0	1	0	0	0	0	0	0	1	0	8
Lymnaea sp. (Feilden, 1879)	0	1	1	0	0	2	0	1	0	2	0	8
Vallonia pulchella (Müller, 1774)	0	0	0	0	0	0	0	0	0	0	0	0
Carychium cf. *schlickumi* Strauch, 1977	0	0	0	0	0	0	0	0	0	0	0	0
Planorbis moquini (Requien, 1848)	0	0	0	0	0	0	0	0	0	0	0	0
Vertigo cf. *antivertigo* (Draparnaud, 1801)	0	0	0	0	0	0	0	0	0	0	0	0
Pisidium Pfeiffer, 1821	0	0	0	0	0	0	0	0	0	0	0	0
Oxychilus (Mediterranea) *hydatinus* (Rossmässler, 1838)	0	1	0	0	0	0	0	0	2	1	0	0
Vitrea Fitzinger, 1833	0	0	2	0	0	0	0	1	0	0	1	14
Ferussacia (s.str.) *folliculus* (Gmelin, 1791)	0	0	0	0	0	0	0	0	0	0	0	0
Clausiliidae Mörch, 1864	0	0	0	0	0	0	0	0	0	0	0	0
Muticaria Lindholm, 1925	0	0	0	0	0	1	0	0	1	0	0	0
Papillifera papillaris (Müller, 1774)	0	0	0	0	0	1	0	0	0	0	0	1
Rumina decollata (Linnaeus, 1758)	0	0	0	0	0	0	0	0	0	1	0	0
Trochoidea spratti (Pfeiffer, 1846)	0	0	0	0	0	0	1	0	2	0	0	0
Truncatellina callicratis (Scacchi, 1833)	1	0	0	0	0	0	0	3	1	2	0	5
Granopupa granum (Draparnaud, 1801)	0	0	0	0	0	0	0	0	0	0	0	0
Pomatias sulcatus (Draparnaud, 1801)	0	0	0	0	0	0	1	0	0	0	0	0
Xerotricha Monterosato, 1892	0	0	0	0	0	0	0	0	0	0	0	0
Cernuella caruanae (Kobelt, 1888)	0	0	0	0	0	0	0	1	1	0	3	4
Chondrula (Mastus) pupa (Linnaeus, 1758)	0	0	0	0	0	0	0	0	0	0	0	0
Cochlicella acuta (Müller, 1774)	0	0	0	0	0	0	0	0	0	2	0	0
Eobania vermiculata (Müller, 1774)	0	0	0	0	0	0	0	0	0	0	0	1
Helicioidae	0	0	0	1	0	3	1	2	2	0	1	0
Cecilioides acicula (Müller, 1774)	0	0	0	0	0	0	0	0	0	2	1	8
Total amount of molluscs	**1**	**2**	**4**	**1**	**1**	**7**	**4**	**11**	**10**	**14**	**7**	**63**

Table A5.3 *(cont.).*

Species/Depth (cm)	2528	2550	2570	2580	2590	2600	2613	2625	2638	2646	2656	2665
Pseudamnicola (s.str.) *moussonii* (Calcara, 1841)	0	1	0	0	0	0	0	0	1	3	2	4
Ancylus fluviatilis Müller, 1774	0	0	0	0	0	0	0	0	0	0	0	1
Bulinus cf. *truncatus* (Audouin, 1827)	0	0	0	0	0	0	0	0	0	0	0	0
Oxyloma elegans (Risso, 1826)	0	0	0	0	0	0	0	0	0	0	0	0
Gyraulus (Armiger) crista (Linnaeus, 1758)	0	0	0	0	0	0	0	0	0	0	0	0
Lymnaea sp. (Feilden, 1879)	0	0	0	0	0	0	0	1	0	2	2	1
Vallonia pulchella (Müller, 1774)	0	0	0	0	0	0	0	0	0	0	0	0
Carychium cf. *schlickumi* Strauch, 1977	0	0	0	0	0	0	0	0	0	0	0	0
Planorbis moquini (Requien, 1848)	0	0	0	0	0	0	0	0	0	0	0	1
Vertigo cf. *antivertigo* (Draparnaud, 1801)	0	0	0	0	0	0	0	0	0	0	0	1
Pisidium Pfeiffer, 1821	0	0	0	0	0	0	0	0	0	0	0	0
Oxychilus (Mediterranea) *hydatinus* (Rossmässler, 1838)	0	0	0	0	0	0	0	0	0	0	0	0
Vitrea Fitzinger, 1833	0	3	0	0	0	0	0	0	0	0	1	0
Ferussacia (s.str.) *folliculus* (Gmelin, 1791)	0	0	0	0	0	0	0	0	0	0	0	0
Clausiliidae Mörch, 1864	0	0	1	0	0	0	0	0	0	0	1	0
Muticaria Lindholm, 1925	0	0	0	0	0	0	0	1	0	1	0	1
Papillifera papillaris (Müller, 1774)	0	0	0	0	0	0	0	1	0	0	0	1
Rumina decollata (Linnaeus, 1758)	0	0	0	0	0	0	0	0	1	1	1	0
Trochoidea spratti (Pfeiffer, 1846)	0	0	0	0	0	0	0	0	0	1	3	0
Truncatellina callicratis (Scacchi, 1833)	1	0	0	0	0	0	0	0	0	1	0	0
Granopupa granum (Draparnaud, 1801)	0	0	0	0	0	0	0	0	0	0	0	0
Pomatias sulcatus (Draparnaud, 1801)	0	0	0	0	0	0	0	0	0	0	0	0
Xerotricha Monterosato, 1892	0	0	0	0	0	0	0	0	0	0	0	0
Cernuella caruanae (Kobelt, 1888)	0	1	0	0	0	0	0	0	0	1	2	1
Chondrula (Mastus) pupa (Linnaeus, 1758)	0	0	0	0	0	0	0	0	0	0	1	0
Cochlicella acuta (Müller, 1774)	1	0	0	0	0	0	0	0	0	0	3	0
Eobania vermiculata (Müller, 1774)	0	0	0	0	0	0	0	0	0	0	0	0
Helicioidae	0	0	1	0	0	0	1	1	1	0	0	0
Cecilioides acicula (Müller, 1774)	0	1	0	0	0	0	0	0	0	0	0	0
Total amount of molluscs	**2**	**6**	**2**	**1**	**1**	**1**	**1**	**4**	**3**	**10**	**16**	**11**

Table A5.3 *(cont.).*

Species/Depth (cm)	2670	2687	2693	2696	2700	2782	2786	2792	2797	2804	2807	2812
Pseudamnicola (s.str.) *moussonii* (Calcara, 1841)	0	1	0	0	0	0	0	0	0	0	0	0
Ancylus fluviatilis Müller, 1774	0	0	0	0	0	0	0	0	0	0	0	0
Bulinus cf. *truncatus* (Audouin, 1827)	0	0	0	0	0	0	0	0	0	0	0	0
Oxyloma elegans (Risso, 1826)	0	0	0	0	0	0	0	0	0	0	0	0
Gyraulus (Armiger) crista (Linnaeus, 1758)	0	0	0	0	0	0	0	0	0	0	0	0
Lymnaea sp. (Feilden, 1879)	1	0	0	0	0	0	0	0	0	0	0	0
Vallonia pulchella (Müller, 1774)	0	0	0	0	0	0	0	0	0	0	0	0
Carychium cf. *schlickumi* Strauch, 1977	0	0	0	0	0	0	0	0	0	0	0	0
Planorbis moquini (Requien, 1848)	0	0	0	0	0	0	0	0	0	0	0	0
Vertigo cf. *antivertigo* (Draparnaud, 1801)	0	0	0	0	0	0	0	0	0	0	0	0
Pisidium Pfeiffer, 1821	0	0	0	0	0	0	0	0	0	0	0	0
Oxychilus (Mediterranea) *hydatinus* (Rossmässler, 1838)	1	0	0	0	0	0	0	0	0	0	0	0
Vitrea Fitzinger, 1833	0	0	0	0	0	0	0	0	0	0	0	0
Ferussacia (s.str.) *folliculus* (Gmelin, 1791)	0	0	0	0	0	0	0	0	0	0	0	0
Clausiliidae Mörch, 1864	0	2	0	0	0	0	0	0	0	0	0	0
Muticaria Lindholm, 1925	0	0	0	0	0	1	0	1	0	1	0	0
Papillifera papillaris (Müller, 1774)	0	1	0	0	0	0	0	0	0	0	0	0
Rumina decollata (Linnaeus, 1758)	0	0	0	0	0	1	0	0	0	0	0	0
Trochoidea spratti (Pfeiffer, 1846)	0	0	0	0	0	0	0	0	0	0	0	0
Truncatellina callicratis (Scacchi, 1833)	0	0	0	0	0	0	0	0	0	0	0	0
Granopupa granum (Draparnaud, 1801)	0	0	0	0	0	0	0	0	0	0	0	0
Pomatias sulcatus (Draparnaud, 1801)	0	0	0	0	0	1	0	1	0	0	0	0
Xerotricha Monterosato, 1892	0	0	0	0	0	0	0	0	0	0	0	0
Cernuella caruanae (Kobelt, 1888)	0	0	0	0	0	0	0	0	0	0	0	0
Chondrula (Mastus) pupa (Linnaeus, 1758)	0	0	0	0	0	0	0	0	0	0	0	0
Cochlicella acuta (Müller, 1774)	0	0	0	0	0	0	0	0	0	0	0	0
Eobania vermiculata (Müller, 1774)	0	0	0	0	0	0	0	0	0	0	0	0
Helicioidae	0	2	0	1	0	1	1	1	0	1	1	1
Cecilioides acicula (Müller, 1774)	0	0	0	0	0	0	0	0	0	0	0	0
Total amount of molluscs	**2**	**6**	**1**	**1**	**1**	**4**	**2**	**3**	**1**	**2**	**1**	**1**

Table A5.3 *(cont.).*

Species/Depth (cm)	2820	2825	2832	2850
Pseudamnicola (s.str.) *moussonii* (Calcara, 1841)	0	0	0	0
Ancylus fluviatilis Müller, 1774	0	0	0	0
Bulinus cf. *truncatus* (Audouin, 1827)	0	0	0	0
Oxyloma elegans (Risso, 1826)	0	0	0	0
Gyraulus (Armiger) crista (Linnaeus, 1758)	0	0	0	0
Lymnaea sp. (Feilden, 1879)	0	0	0	0
Vallonia pulchella (Müller, 1774)	0	0	0	0
Carychium cf. *schlickumi* Strauch, 1977	0	0	0	0
Planorbis moquini (Requien, 1848)	0	0	0	0
Vertigo cf. *antivertigo* (Draparnaud, 1801)	0	0	0	0
Pisidium Pfeiffer, 1821	0	0	0	0
Oxychilus (Mediterranea) *hydatinus* (Rossmässler, 1838)	0	0	0	0
Vitrea Fitzinger, 1833	0	0	0	0
Ferussacia (s.str.) *folliculus* (Gmelin, 1791)	0	0	0	0
Clausiliidae Mörch, 1864	0	0	0	0
Muticaria Lindholm, 1925	0	0	0	1
Papillifera papillaris (Müller, 1774)	0	0	0	1
Rumina decollata (Linnaeus, 1758)	0	0	0	1
Trochoidea spratti (Pfeiffer, 1846)	0	0	0	0
Truncatellina callicratis (Scacchi, 1833)	0	0	0	0
Granopupa granum (Draparnaud, 1801)	0	0	0	0
Pomatias sulcatus (Draparnaud, 1801)	0	0	0	1
Xerotricha Monterosato, 1892	0	0	0	0
Cernuella caruanae (Kobelt, 1888)	0	0	0	0
Chondrula (Mastus) pupa (Linnaeus, 1758)	0	0	0	0
Cochlicella acuta (Müller, 1774)	0	0	0	0
Eobania vermiculata (Müller, 1774)	0	0	0	0
Helicioidae	1	0	0	1
Cecilioides acicula (Müller, 1774)	0	0	0	0
Total amount of molluscs	**1**	**1**	**1**	**5**

Table A5.4. *Salina Deep Core marine.*

Species/Depth (cm)	1113	1121	1131	1140	1150	1160	1191	1201	1211	1216	1221	1231
Cardiidae	0	0	30	4	48	0	0	0	0	50	0	9
Cerastoderma sp.	54	49	20	19	32	77	26	42	119	45	21	45
Loripes lucinalis (Lamarck, 1818)	108	140	380	157	602	363	3	1	0	40	14	9
Parvicardium sp.	210	133	110	49	176	286	0	0	7	85	12	9
Pectinidae	0	0	0	0	0	0	0	0	0	5	0	0
Tapes decussatus (Linnaeus, 1758)	0	0	0	0	0	0	0	0	0	5	1	0
Tellina sp.	210	182	180	48	288	151	6	49	7	60	34	72
Abra sp.	0	0	0	0	0	0	0	0	0	0	0	0
Mactra sp.	0	0	0	0	0	0	0	0	0	0	0	0
Nucula sp.	0	0	0	4	0	0	0	0	0	0	0	0
Donax sp.	0	14	0	0	0	11	0	0	0	0	0	18
Veneridae	0	0	0	0	0	0	0	0	0	10	0	0
Alvania sp.	24	21	20	5	32	0	0	0	0	0	0	9
Bulla striata (Brugière, 1792)	0	0	0	0	0	0	0	0	0	0	0	0
Gibberula sp.	6	21	0	1	0	0	0	0	0	0	0	0
Nassarius sp.	6	21	0	2	0	22	0	0	0	5	0	0
Pirenella conica (Blainville, 1826)	0	7	0	13	0	0	0	1	0	0	0	0
Retusa truncatula (Brugière, 1792)	48	70	50	0	80	99	0	1	0	20	1	9
Turridiidae	0	0	0	0	0	0	0	0	0	5	0	0
Turritella communis (Risso, 1826)	0	0	0	0	0	0	0	0	0	0	0	0
Acanthocardia sp.	0	0	5	1	7	0	0	2	0	5	1	0
Corbula gibba (Olivi, 1792)	0	0	0	0	0	0	0	0	21	0	8	0
Dentalium sp.	0	0	0	0	0	0	0	0	0	0	0	0
Rissoa sp.	450	70	330	308	528	660	5	24	35	260	93	225
Lithophaga lithophaga (Linnaeus, 1758)	0	0	0	0	0	0	0	0	0	0	0	0
Conus mediterraneus (Hwass, 1792)	0	0	5	0	8	0	0	0	0	5	0	0
Gibbula sp.	54	3	10	17	16	77	0	0	0	0	0	0
Ostrea sp.	0	0	0	0	0	0	0	0	0	0	1	0
Tricolia sp.	18	49	40	22	64	11	0	0	0	0	1	0
Bittium reticulatum (Da Costa, 1778)	1110	354	1160	611	1856	1353	38	3	350	1180	339	630
Cerithium sp.	54	28	30	80	48	110	0	0	0	20	3	18
Cerithiopsis sp.	0	0	0	0	0	0	0	0	0	0	0	0
Columbella rustica (Linnaeus, 1758)	0	0	0	1	0	1	0	0	0	0	0	0
Hexaplex trunculus (Linnaeus, 1758)	0	0	0	4	0	0	0	0	0	0	0	0
Natica sp.	0	0	0	0	0	0	0	0	0	0	0	0
Kelliidae	0	49	70	38	102	33	0	0	0	0	5	0
Melanella sp.	0	7	10	0	16	0	0	2	0	0	0	0
Turbonilla sp.	72	28	30	12	48	66	0	1	0	30	7	0
Azorinus sp.	0	0	0	0	0	0	0	0	0	0	0	0
Glycimeris sp.	0	0	0	5	0	0	0	3	0	0	0	0
Mytilidae	0	0	0	0	0	0	0	0	0	0	0	0
Arca noae (Linnaeus, 1758)	0	0	0	0	0	0	0	0	0	0	0	0
unknown	0	7	0	9	0	0	0	1	0	0	3	18
Hydrobia Hartmann, 1821	576	546	400	583	640	759	4	0	7	50	6	18
Truncatella subcylindrica (Linnaeus, 1767)	0	0	0	2	0	0	0	0	0	0	0	0
Paracentrotus lividus	0	1	1	1	1	1	0	0	0	0	0	1
Total amount of molluscs	**3000**	**1800**	**2881**	**1996**	**4592**	**4080**	**82**	**130**	**546**	**1880**	**550**	**1090**

Table A5.4 *(cont.).*

Species/Depth (cm)	1241	1247	1257	1267	1277	1290	1310	1384	1394	1404	1414	1425
Cardiidae	28	10	0	0	27	78	361	0	0	3	9	1
Cerastoderma sp.	12	60	80	18	108	221	0	20	24	10	13	8
Loripes lucinalis (Lamarck, 1818)	16	115	230	63	81	351	456	1	3	5	3	4
Parvicardium sp.	8	85	110	72	108	520	152	3	9	6	5	2
Pectinidae	0	0	0	0	0	0	0	1	2	0	0	0
Tapes decussatus (Linnaeus, 1758)	0	0	0	0	9	0	0	0	0	0	0	0
Tellina sp.	12	90	220	211	108	429	361	6	16	16	7	9
Abra sp.	0	0	0	0	0	0	0	0	0	0	0	0
Mactra sp.	0	0	0	0	0	0	0	0	0	0	0	0
Nucula sp.	0	0	10	0	0	0	0	0	0	0	0	0
Donax sp.	0	0	20	0	2	13	38	0	0	0	0	0
Veneridae	0	0	0	9	0	0	38	0	0	0	0	0
Alvania sp.	0	0	0	0	0	13	0	0	0	0	0	0
Bulla striata (Brugière, 1792)	0	0	0	0	0	0	0	1	0	0	0	0
Gibberula sp.	0	0	0	0	0	0	0	0	0	0	0	0
Nassarius sp.	0	0	0	0	36	13	0	0	0	0	0	0
Pirenella conica (Blainville, 1826)	0	0	0	0	0	13	38	0	0	0	0	0
Retusa truncatula (Brugière, 1792)	0	15	10	9	9	156	76	0	4	1	0	0
Turridiidae	0	0	0	0	9	13	19	0	0	0	0	0
Turritella communis (Risso, 1826)	0	0	0	0	0	0	0	0	0	0	0	0
Acanthocardia sp.	0	0	0	18	0	0	0	0	0	1	0	0
Corbula gibba (Olivi, 1792)	0	0	0	0	0	0	0	1	11	1	5	3
Dentalium sp.	0	0	10	0	0	13	0	0	0	0	0	0
Rissoa sp.	40	230	370	216	234	1443	399	9	14	6	6	3
Lithophaga lithophaga (Linnaeus, 1758)	0	0	0	0	0	0	0	0	0	0	0	0
Conus mediterraneus (Hwass, 1792)	0	5	0	4	9	0	19	0	0	0	0	0
Gibbula sp.	0	5	0	9	9	13	19	0	0	0	0	0
Ostrea sp.	2	0	5	9	0	13	19	0	0	0	0	0
Tricolia sp.	0	15	10	0	0	0	19	0	0	0	0	0
Bittium reticulatum (Da Costa, 1778)	196	1420	2882	1719	2088	2860	6555	31	28	10	5	20
Cerithium sp.	0	35	30	9	27	169	85	0	0	0	0	0
Cerithiopsis sp.	0	0	0	0	0	0	0	0	0	0	0	0
Columbella rustica (Linnaeus, 1758)	0	0	0	0	0	0	19	0	0	0	0	0
Hexaplex trunculus (Linnaeus, 1758)	0	0	0	0	0	0	19	0	0	0	0	0
Natica sp.	0	0	0	0	0	0	0	0	0	0	0	0
Kelliidae	0	45	0	27	0	39	152	0	4	5	3	3
Melanella sp.	0	0	10	0	9	26	0	0	0	0	0	0
Turbonilla sp.	4	0	100	72	81	169	114	0	3	1	0	1
Azorinus sp.	0	0	0	0	0	0	0	0	0	0	0	0
Glycimeris sp.	0	0	0	0	0	0	0	0	0	0	0	0
Mytilidae	0	0	0	0	0	0	0	0	0	0	0	0
Arca noae (Linnaeus, 1758)	0	0	0	0	0	0	0	0	0	0	0	0
unknown	12	0	20	9	27	0	76	0	0	0	0	0
Hydrobia Hartmann, 1821	0	25	140	45	0	507	209	0	7	3	0	0
Truncatella subcylindrica (Linnaeus, 1767)	0	5	0	0	0	39	0	0	2	0	0	1
Paracentrotus lividus	0	1	1	0	0	0	1	0	0	0	0	0
Total amount of molluscs	**330**	**2161**	**4258**	**2519**	**2981**	**7111**	**9244**	**73**	**127**	**68**	**56**	**55**

Table A5.4 *(cont.).*

Species/Depth (cm)	1434	1444	1450	1459	1470	1479	1489	1630	1640	1650	1682	1692
Cardiidae	16	0	0	0	0	159	51	0	1	14	0	2
Cerastoderma sp.	14	15	32	49	56	371	102	4	3	60	2	1
Loripes lucinalis (Lamarck, 1818)	3	9	3	35	70	424	374	1	2	30	0	0
Parvicardium sp.	4	7	4	49	73	212	459	5	1	35	0	0
Pectinidae	1	0	0	0	0	0	0	0	0	5	0	1
Tapes decussatus (Linnaeus, 1758)	0	0	1	0	0	0	0	0	0	0	0	0
Tellina sp.	22	22	12	70	66	212	255	4	3	35	0	0
Abra sp.	0	0	0	0	0	0	0	0	0	0	0	0
Mactra sp.	0	0	0	0	0	0	0	0	0	0	0	0
Nucula sp.	0	0	0	0	0	0	0	0	0	0	0	0
Donax sp.	0	0	0	0	0	0	0	0	0	0	0	0
Veneridae	0	0	0	0	0	0	0	0	0	0	0	0
Alvania sp.	0	0	0	0	0	0	0	0	0	0	0	0
Bulla striata (Brugière, 1792)	1	0	0	0	7	0	0	0	0	0	0	0
Gibberula sp.	0	0	0	0	0	0	0	0	0	0	0	0
Nassarius sp.	0	0	1	0	0	159	34	0	0	0	0	0
Pirenella conica (Blainville, 1826)	0	0	0	0	0	0	0	0	0	0	1	0
Retusa truncatula (Brugière, 1792)	1	0	0	0	14	212	51	1	1	0	0	0
Turridiidae	0	0	1	0	0	106	0	0	0	0	0	0
Turritella communis (Risso, 1826)	0	0	0	0	0	0	0	0	0	0	0	0
Acanthocardia sp.	0	1	0	0	4	106	17	0	0	0	0	1
Corbula gibba (Olivi, 1792)	5	1	0	28	7	106	68	1	4	5	1	0
Dentalium sp.	0	0	0	0	0	0	0	0	0	0	0	0
Rissoa sp.	4	28	13	154	165	2704	1088	8	3	115	0	0
Lithophaga lithophaga (Linnaeus, 1758)	0	0	0	0	0	0	0	0	0	0	0	0
Conus mediterraneus (Hwass, 1792)	0	0	0	0	0	53	0	0	0	0	0	0
Gibbula sp.	0	1	0	0	0	0	17	0	0	10	0	0
Ostrea sp.	1	0	0	0	3	1	17	0	0	5	0	0
Tricolia sp.	0	1	0	0	0	0	0	0	0	0	0	0
Bittium reticulatum (Da Costa, 1778)	97	132	50	336	630	6344	3230	19	10	349	1	1
Cerithium sp.	1	0	1	0	7	371	34	0	0	5	0	0
Cerithiopsis sp.	0	0	0	0	0	0	0	0	0	0	0	0
Columbella rustica (Linnaeus, 1758)	0	0	0	0	0	0	0	0	0	0	0	0
Hexaplex trunculus (Linnaeus, 1758)	0	0	0	0	0	0	0	0	0	0	0	0
Natica sp.	0	0	0	0	0	0	0	0	0	0	0	0
Kelliidae	3	8	2	7	0	159	51	0	3	5	0	0
Melanella sp.	0	0	0	0	0	0	17	0	0	0	0	0
Turbonilla sp.	0	0	1	28	35	212	153	0	0	10	0	0
Azorinus sp.	0	0	0	0	0	0	0	0	0	0	0	0
Glycimeris sp.	0	0	0	0	0	0	0	0	0	0	0	0
Mytilidae	0	0	0	0	0	0	0	0	0	0	0	0
Arca noae (Linnaeus, 1758)	0	0	0	0	0	0	0	0	0	0	0	0
unknown	0	0	0	0	0	0	0	0	0	0	0	0
Hydrobia Hartmann, 1821	7	2	1	0	7	159	119	0	0	30	0	0
Truncatella subcylindrica (Linnaeus, 1767)	2	1	0	7	0	0	0	0	3	0	0	0
Paracentrotus lividus	0	0	0	0	1	1	0	0	0	0	1	0
Total amount of molluscs	**182**	**228**	**122**	**763**	**1145**	**12071**	**6137**	**43**	**34**	**713**	**6**	**6**

Table A5.4 *(cont.).*

Species/Depth (cm)	1702	1710	1720	1730	1740	1745	1755	1765	1770	1780	1790	1841
Cardiidae	0	0	0	0	0	0	0	1	0	0	0	0
Cerastoderma sp.	0	1	1	1	0	0	1	0	1	3	4	0
Loripes lucinalis (Lamarck, 1818)	0	1	1	0	0	0	1	1	0	2	5	0
Parvicardium sp.	0	0	0	1	0	2	1	0	1	7	10	0
Pectinidae	0	0	0	0	0	0	0	0	0	1	0	0
Tapes decussatus (Linnaeus, 1758)	0	0	1	0	0	0	0	0	0	0	1	0
Tellina sp.	1	2	0	1	1	1	3	1	1	3	7	0
Abra sp.	0	0	0	0	0	0	0	1	0	0	0	5
Mactra sp.	0	0	0	1	0	0	0	0	0	0	0	0
Nucula sp.	0	0	0	0	0	0	0	0	0	0	0	0
Donax sp.	0	0	0	0	0	0	0	0	0	0	0	0
Veneridae	0	0	0	0	0	0	0	0	0	0	0	0
Alvania sp.	0	0	0	0	0	0	0	0	0	0	0	0
Bulla striata (Brugière, 1792)	0	0	0	0	0	0	0	0	0	0	0	0
Gibberula sp.	0	0	0	0	0	0	0	0	0	0	0	0
Nassarius sp.	0	1	0	0	0	0	0	0	0	0	0	0
Pirenella conica (Blainville, 1826)	0	0	0	0	0	0	0	0	0	0	0	0
Retusa truncatula (Brugière, 1792)	0	0	0	0	0	0	0	0	0	0	0	0
Turridiidae	0	0	0	0	0	0	0	0	0	0	0	0
Turritella communis (Risso, 1826)	0	0	0	0	0	0	0	0	0	0	0	0
Acanthocardia sp.	1	0	0	0	0	1	0	1	0	1	2	0
Corbula gibba (Olivi, 1792)	0	1	2	1	0	1	1	0	0	3	4	1
Dentalium sp.	0	0	0	0	0	0	0	0	0	0	0	0
Rissoa sp.	1	1	1	1	1	6	5	0	3	13	29	0
Lithophaga lithophaga (Linnaeus, 1758)	0	0	0	0	0	0	0	0	0	0	0	0
Conus mediterraneus (Hwass, 1792)	0	0	0	0	0	1	0	0	0	1	0	0
Gibbula sp.	0	0	0	0	0	1	0	0	0	0	1	0
Ostrea sp.	0	0	0	1	0	0	0	0	0	0	1	0
Tricolia sp.	0	0	0	0	0	0	0	0	0	1	0	0
Bittium reticulatum (Da Costa, 1778)	0	0	0	2	3	12	8	1	20	54	64	5
Cerithium sp.	0	0	0	0	0	0	0	0	1	2	4	0
Cerithiopsis sp.	0	0	0	0	0	0	0	0	0	0	0	0
Columbella rustica (Linnaeus, 1758)	0	0	0	0	0	0	0	0	0	0	0	0
Hexaplex trunculus (Linnaeus, 1758)	0	0	0	0	0	0	0	0	0	0	0	0
Natica sp.	0	0	0	0	0	0	0	0	0	0	0	0
Kelliidae	0	0	0	0	0	1	0	1	0	0	0	0
Melanella sp.	0	0	0	0	0	0	0	0	0	0	0	0
Turbonilla sp.	0	0	0	0	0	2	0	1	1	2	1	4
Azorinus sp.	0	0	0	0	0	0	0	0	0	0	0	0
Glycimeris sp.	0	0	0	0	0	0	0	0	0	0	0	0
Mytilidae	0	0	0	0	0	0	0	0	0	0	0	0
Arca noae (Linnaeus, 1758)	0	0	0	0	0	0	0	0	0	0	0	0
unknown	0	0	0	0	0	0	1	0	0	0	0	0
Hydrobia Hartmann, 1821	0	0	0	0	0	1	0	0	0	0	0	0
Truncatella subcylindrica (Linnaeus, 1767)	0	0	0	0	0	0	0	0	0	0	0	0
Paracentrotus lividus	0	0	0	0	0	0	1	0	0	0	0	1
Total amount of molluscs	**3**	**7**	**6**	**9**	**5**	**29**	**22**	**8**	**28**	**93**	**133**	**16**

Table A5.4 *(cont.).*

Species/Depth (cm)	1851	1861	1869	1879	1889	1890	1900	1910	1920	1930	1940	1971
Cardiidae	0	0	0	0	1	3	0	0	1	0	0	0
Cerastoderma sp.	1	1	1	1	0	0	0	0	5	2	1	3
Loripes lucinalis (Lamarck, 1818)	0	0	1	1	0	0	0	1	5	1	1	2
Parvicardium sp.	1	0	1	0	0	1	0	0	3	5	5	0
Pectinidae	0	0	1	0	0	0	0	0	0	0	0	0
Tapes decussatus (Linnaeus, 1758)	0	0	0	0	0	0	0	0	0	0	0	0
Tellina sp.	0	1	1	1	1	3	0	2	5	1	3	1
Abra sp.	0	0	0	0	0	12	0	0	0	0	0	0
Mactra sp.	0	0	0	0	0	0	0	0	0	0	0	0
Nucula sp.	0	0	0	0	0	0	0	0	0	0	0	0
Donax sp.	0	0	0	0	0	0	0	0	0	0	0	0
Veneridae	0	0	0	0	0	0	0	0	0	0	0	0
Alvania sp.	0	0	0	0	0	0	0	0	0	1	0	0
Bulla striata (Brugière, 1792)	0	0	0	0	0	0	0	0	0	0	0	0
Gibberula sp.	0	0	0	0	0	0	0	0	0	0	0	0
Nassarius sp.	0	0	0	0	0	0	0	0	0	0	0	0
Pirenella conica (Blainville, 1826)	0	0	0	0	0	0	0	0	0	0	0	0
Retusa truncatula (Brugière, 1792)	0	0	0	0	1	3	1	0	0	0	0	0
Turridiidae	0	0	0	0	0	0	0	0	0	0	0	0
Turritella communis (Risso, 1826)	0	0	0	0	0	0	0	0	0	0	0	0
Acanthocardia sp.	0	0	1	1	0	4	1	2	1	0	1	0
Corbula gibba (Olivi, 1792)	1	1	3	1	0	15	5	10	3	1	5	3
Dentalium sp.	0	0	0	0	0	0	0	0	0	0	0	0
Rissoa sp.	3	1	1	1	1	3	1	0	19	8	16	8
Lithophaga lithophaga (Linnaeus, 1758)	0	0	0	0	0	0	0	0	0	0	0	0
Conus mediterraneus (Hwass, 1792)	0	0	0	0	0	0	0	0	2	0	0	0
Gibbula sp.	0	0	0	0	0	0	0	0	0	1	1	0
Ostrea sp.	0	0	0	0	0	0	0	0	3	1	0	2
Tricolia sp.	0	0	0	0	0	0	0	0	0	0	0	0
Bittium reticulatum (Da Costa, 1778)	2	1	2	2	1	3	6	9	69	38	43	19
Cerithium sp.	0	0	0	0	0	0	0	0	4	1	1	1
Cerithiopsis sp.	0	0	0	0	0	0	0	0	0	0	1	0
Columbella rustica (Linnaeus, 1758)	0	0	0	0	0	0	0	0	0	0	0	0
Hexaplex trunculus (Linnaeus, 1758)	0	0	0	0	0	0	0	0	1	1	0	0
Natica sp.	0	0	0	0	0	0	0	0	0	0	0	0
Kelliidae	0	0	0	0	0	0	0	0	3	0	0	0
Melanella sp.	0	0	0	0	0	0	0	0	0	0	0	0
Turbonilla sp.	0	0	1	0	0	4	3	7	0	1	1	1
Azorinus sp.	0	0	0	0	0	0	0	0	0	0	0	0
Glycimeris sp.	0	0	0	0	0	0	0	0	0	0	0	0
Mytilidae	0	0	0	0	0	0	0	0	0	0	0	0
Arca noae (Linnaeus, 1758)	0	0	0	0	0	0	0	0	0	0	0	0
unknown	1	0	0	0	0	0	0	0	0	0	0	0
Hydrobia Hartmann, 1821	0	0	1	0	0	0	0	1	12	5	5	2
Truncatella subcylindrica (Linnaeus, 1767)	0	0	0	0	0	0	0	0	0	1	0	0
Paracentrotus lividus	0	1	0	0	0	0	0	0	1	0	0	0
Total amount of molluscs	**9**	**6**	**14**	**8**	**5**	**51**	**17**	**32**	**137**	**68**	**84**	**42**

Table A5.4 *(cont.).*

Species/Depth (cm)	1981	1991	1994	2004	2014	2023	2033	2043	2046	2056	2066	2070
Cardiidae	0	0	0	0	2	0	0	0	0	0	1	0
Cerastoderma sp.	2	1	1	2	0	3	1	1	2	2	1	4
Loripes lucinalis (Lamarck, 1818)	2	2	0	1	0	3	1	2	0	0	0	5
Parvicardium sp.	1	4	0	1	1	0	1	1	2	1	1	1
Pectinidae	1	0	0	0	0	0	0	0	0	0	0	0
Tapes decussatus (Linnaeus, 1758)	0	0	0	0	0	0	0	0	0	0	0	0
Tellina sp.	2	1	3	2	0	0	1	1	2	5	0	1
Abra sp.	0	0	0	0	0	0	0	0	0	0	0	0
Mactra sp.	0	0	0	0	0	0	0	0	0	0	0	0
Nucula sp.	0	0	0	0	0	0	0	0	0	0	0	0
Donax sp.	0	0	0	0	0	0	0	0	0	0	0	0
Veneridae	0	0	0	0	0	0	0	0	0	0	0	0
Alvania sp.	0	0	0	0	0	0	0	0	0	0	0	0
Bulla striata (Brugière, 1792)	0	0	0	0	0	0	0	0	0	0	0	0
Gibberula sp.	0	0	0	0	0	0	0	0	0	0	0	0
Nassarius sp.	0	0	1	1	1	0	0	0	0	1	0	1
Pirenella conica (Blainville, 1826)	0	0	0	0	0	0	0	0	0	0	0	0
Retusa truncatula (Brugière, 1792)	0	0	1	0	2	0	0	1	1	0	1	1
Turridiidae	0	0	0	0	0	0	0	0	0	0	0	0
Turritella communis (Risso, 1826)	0	0	0	0	1	0	0	2	0	0	0	0
Acanthocardia sp.	1	0	0	0	1	0	1	0	0	1	0	0
Corbula gibba (Olivi, 1792)	3	2	0	4	7	2	1	4	1	3	4	1
Dentalium sp.	0	0	0	1	0	0	0	0	0	0	0	0
Rissoa sp.	6	4	4	2	3	6	3	5	1	2	2	4
Lithophaga lithophaga (Linnaeus, 1758)	0	0	0	0	0	0	0	0	0	0	0	0
Conus mediterraneus (Hwass, 1792)	0	0	0	0	0	0	0	0	0	0	0	0
Gibbula sp.	0	0	0	0	0	0	1	0	0	0	0	1
Ostrea sp.	0	0	1	0	0	0	0	0	0	0	1	1
Tricolia sp.	0	0	0	0	0	0	0	0	0	0	0	0
Bittium reticulatum (Da Costa, 1778)	34	19	3	19	16	27	17	27	9	20	11	33
Cerithium sp.	1	0	1	0	0	3	1	2	0	0	1	1
Cerithiopsis sp.	0	0	0	0	0	0	0	0	0	0	0	0
Columbella rustica (Linnaeus, 1758)	0	0	0	0	0	0	0	0	0	0	0	0
Hexaplex trunculus (Linnaeus, 1758)	0	0	0	0	0	0	0	0	0	0	0	0
Natica sp.	0	0	0	0	0	0	0	0	0	0	0	0
Kelliidae	0	1	0	2	1	0	0	0	0	3	0	1
Melanella sp.	0	0	0	0	0	0	0	0	0	0	0	1
Turbonilla sp.	4	0	0	1	1	0	1	0	2	2	1	0
Azorinus sp.	0	0	0	0	0	0	0	0	0	0	0	0
Glycimeris sp.	0	0	0	0	0	0	0	0	0	0	0	0
Mytilidae	0	0	0	0	0	0	0	0	0	0	0	0
Arca noae (Linnaeus, 1758)	0	0	0	0	0	0	0	0	0	0	0	0
unknown	0	0	0	0	0	0	0	0	0	0	0	0
Hydrobia Hartmann, 1821	2	1	0	3	2	6	1	2	1	5	0	7
Truncatella subcylindrica (Linnaeus, 1767)	0	0	0	0	0	0	0	0	0	0	0	0
Paracentrotus lividus	0	0	0	0	1	0	0	0	0	0	0	1
Total amount of molluscs	**59**	**35**	**15**	**39**	**39**	**50**	**30**	**48**	**21**	**45**	**24**	**64**

Table A5.4 *(cont.).*

Species/Depth (cm)	2080	2100	2113	2123	2133	2143	2153	2163	2183	2192	2202	2222
Cardiidae	0	5	1	1	0	2	1	0	1	2	1	1
Cerastoderma sp.	2	0	0	0	0	0	0	0	0	0	0	0
Loripes lucinalis (Lamarck, 1818)	3	9	0	0	0	0	0	0	0	0	0	0
Parvicardium sp.	9	3	0	0	0	0	0	0	0	0	0	0
Pectinidae	1	0	0	0	0	0	0	0	0	0	0	0
Tapes decussatus (Linnaeus, 1758)	0	0	0	0	0	0	0	0	0	0	0	0
Tellina sp.	5	3	0	0	0	0	0	0	0	3	1	0
Abra sp.	0	0	0	0	0	0	0	0	0	0	0	0
Mactra sp.	0	0	0	0	0	0	0	0	0	0	0	0
Nucula sp.	0	0	0	0	0	0	0	0	0	0	0	0
Donax sp.	0	0	0	0	0	0	0	0	0	0	0	0
Veneridae	0	0	0	0	0	0	0	0	0	0	0	0
Alvania sp.	0	0	0	0	0	0	0	0	0	0	0	0
Bulla striata (Brugière, 1792)	0	0	0	0	0	0	0	0	0	0	0	0
Gibberula sp.	1	0	0	0	0	0	0	0	0	0	0	0
Nassarius sp.	0	0	0	1	3	0	0	0	0	0	0	0
Pirenella conica (Blainville, 1826)	0	0	0	0	0	0	0	0	0	0	0	0
Retusa truncatula (Brugière, 1792)	1	0	0	1	0	0	0	0	0	1	1	0
Turridiidae	1	0	0	0	0	0	0	0	0	0	0	0
Turritella communis (Risso, 1826)	3	0	0	0	0	0	0	1	0	1	0	0
Acanthocardia sp.	1	0	0	2	2	0	1	0	1	1	0	1
Corbula gibba (Olivi, 1792)	0	4	8	9	16	6	4	6	5	6	3	3
Dentalium sp.	0	0	0	0	0	0	0	0	0	0	0	0
Rissoa sp.	26	9	0	1	2	1	0	0	0	0	0	2
Lithophaga lithophaga (Linnaeus, 1758)	0	0	0	0	0	0	0	0	0	0	0	0
Conus mediterraneus (Hwass, 1792)	0	0	0	0	0	0	0	0	0	0	0	0
Gibbula sp.	2	1	0	1	0	1	0	0	0	1	0	1
Ostrea sp.	0	0	0	0	0	0	0	0	0	0	0	0
Tricolia sp.	0	0	0	0	0	0	0	0	0	0	0	0
Bittium reticulatum (Da Costa, 1778)	65	34	1	5	9	4	2	1	1	7	5	2
Cerithium sp.	3	1	0	0	1	0	0	1	0	0	0	0
Cerithiopsis sp.	0	0	0	0	0	0	0	0	0	0	0	0
Columbella rustica (Linnaeus, 1758)	0	0	0	0	0	0	0	0	0	0	0	0
Hexaplex trunculus (Linnaeus, 1758)	0	0	0	0	0	0	0	0	0	0	0	0
Natica sp.	0	0	0	0	0	0	0	0	0	0	0	0
Kelliidae	2	0	0	0	0	0	0	0	0	0	0	1
Melanella sp.	0	0	0	0	0	0	0	0	0	0	0	0
Turbonilla sp.	1	4	3	1	1	1	0	0	0	1	0	0
Azorinus sp.	0	0	0	0	0	0	0	0	0	0	0	0
Glycimeris sp.	0	0	0	0	0	0	0	0	0	0	0	0
Mytilidae	0	0	0	0	0	0	0	0	0	0	0	0
Arca noae (Linnaeus, 1758)	0	0	0	0	0	0	0	0	0	0	0	0
unknown	0	0	0	0	0	0	0	0	0	0	0	0
Hydrobia Hartmann, 1821	24	3	1	8	13	4	2	0	1	0	0	2
Truncatella subcylindrica (Linnaeus, 1767)	0	0	0	0	0	0	0	0	0	0	0	0
Paracentrotus lividus	1	1	0	0	1	0	0	0	0	0	0	1
Total amount of molluscs	**151**	**77**	**14**	**30**	**48**	**19**	**10**	**9**	**9**	**23**	**11**	**14**

Table A5.4 *(cont.).*

Species/Depth (cm)	2230	2240	2275	2285	2295	2298	2308	2318	2328	2338	2348	2353
Cardiidae	0	2	2	3	1	16	22	27	55	2	0	8
Cerastoderma sp.	0	0	0	0	0	0	0	0	0	0	0	0
Loripes lucinalis (Lamarck, 1818)	2	1	1	3	1	16	8	0	44	0	0	10
Parvicardium sp.	0	0	0	0	0	4	0	36	0	2	3	6
Pectinidae	0	0	0	0	0	0	0	0	5	0	0	0
Tapes decussatus (Linnaeus, 1758)	0	0	0	0	0	0	0	0	0	0	0	0
Tellina sp.	0	0	0	3	1	110	92	81	191	6	4	122
Abra sp.	0	0	0	0	0	0	0	0	0	0	0	0
Mactra sp.	0	0	0	0	0	0	0	0	0	0	0	0
Nucula sp.	0	0	0	0	0	0	0	0	0	0	1	0
Donax sp.	0	0	0	0	0	0	0	0	0	0	0	0
Veneridae	0	0	0	0	0	0	0	0	0	0	0	0
Alvania sp.	0	0	0	0	0	0	0	0	0	0	0	0
Bulla striata (Brugière, 1792)	0	0	0	0	0	0	0	0	0	0	0	0
Gibberula sp.	0	0	0	0	0	0	0	0	0	0	0	0
Nassarius sp.	0	0	0	1	0	24	12	9	11	2	3	12
Pirenella conica (Blainville, 1826)	0	0	0	0	0	0	3	5	5	0	0	0
Retusa truncatula (Brugière, 1792)	1	1	0	0	0	24	27	45	198	5	4	18
Turridiidae	0	0	0	0	0	4	2	0	11	0	1	6
Turritella communis (Risso, 1826)	0	0	1	0	0	0	0	0	0	0	0	0
Acanthocardia sp.	1	2	1	0	1	20	34	54	131	8	6	10
Corbula gibba (Olivi, 1792)	4	10	1	1	10	256	384	477	968	67	78	114
Dentalium sp.	0	0	0	0	0	8	8	9	33	3	3	0
Rissoa sp.	3	4	3	11	5	12	5	0	110	0	8	10
Lithophaga lithophaga (Linnaeus, 1758)	0	0	0	0	0	0	0	0	0	0	0	0
Conus mediterraneus (Hwass, 1792)	0	0	0	0	0	0	2	5	0	0	0	0
Gibbula sp.	0	1	0	0	1	0	0	0	0	0	0	2
Ostrea sp.	0	1	0	0	0	4	2	9	11	0	0	0
Tricolia sp.	0	0	0	0	0	0	0	0	0	0	0	0
Bittium reticulatum (Da Costa, 1778)	4	11	17	22	25	192	310	405	720	12	20	92
Cerithium sp.	0	0	1	3	0	0	0	0	5	1	1	0
Cerithiopsis sp.	0	0	0	0	0	0	0	0	0	0	0	0
Columbella rustica (Linnaeus, 1758)	0	0	0	0	0	0	0	0	0	0	0	0
Hexaplex trunculus (Linnaeus, 1758)	0	0	0	0	0	2	0	0	0	0	0	0
Natica sp.	0	0	0	0	0	0	0	0	0	0	0	0
Kelliidae	0	0	0	0	0	12	152	207	396	4	3	12
Melanella sp.	0	0	0	0	0	0	2	9	0	0	0	0
Turbonilla sp.	2	0	1	1	3	20	23	27	18	11	12	8
Azorinus sp.	0	0	0	0	0	0	0	0	0	0	0	0
Glycimeris sp.	0	0	0	0	0	0	0	0	0	0	0	0
Mytilidae	0	0	0	0	0	0	0	0	0	0	0	0
Arca noae (Linnaeus, 1758)	0	0	0	0	0	0	0	0	0	0	0	0
unknown	0	0	0	0	0	0	0	0	0	0	0	0
Hydrobia Hartmann, 1821	2	5	2	10	1	68	24	9	110	5	5	20
Truncatella subcylindrica (Linnaeus, 1767)	0	0	0	0	0	0	2	5	5	2	0	4
Paracentrotus lividus	0	1	0	1	1	1	1	1	1	0	0	0
Total amount of molluscs	**19**	**39**	**30**	**59**	**50**	**793**	**1115**	**1420**	**3028**	**130**	**152**	**454**

Table A5.4 *(cont.).*

Species/Depth (cm)	2358	2370	2380	2398	2408	2418	2428	2458	2468	2508	2528	2550
Cardiidae	20	0	2	0	0	30	0	0	0	16	4	15
Cerastoderma sp.	0	0	0	36	60	36	105	88	226	5	21	32
Loripes lucinalis (Lamarck, 1818)	25	2	1	6	8	14	18	0	16	20	14	35
Parvicardium sp.	0	7	0	24	36	22	19	22	170	31	3	23
Pectinidae	0	0	0	18	4	4	0	5	0	0	0	12
Tapes decussatus (Linnaeus, 1758)	0	0	0	6	0	0	12	0	0	0	0	0
Tellina sp.	298	2	0	30	32	27	12	44	113	55	38	53
Abra sp.	0	0	0	0	0	0	0	0	0	0	0	0
Mactra sp.	0	0	0	0	0	0	0	0	0	0	0	0
Nucula sp.	0	0	0	0	0	0	0	0	0	0	0	0
Donax sp.	0	0	0	0	0	0	0	0	0	0	0	0
Veneridae	0	0	0	0	0	0	0	0	0	0	0	0
Alvania sp.	0	0	0	0	0	0	0	0	0	2	0	0
Bulla striata (Brugière, 1792)	0	0	0	0	0	0	0	0	0	0	0	0
Gibberula sp.	0	0	0	0	0	0	0	0	0	0	0	0
Nassarius sp.	30	0	0	0	12	4	0	11	8	5	22	60
Pirenella conica (Blainville, 1826)	0	0	0	0	0	4	6	5	0	0	0	0
Retusa truncatula (Brugière, 1792)	45	2	0	6	4	0	0	11	45	45	25	60
Turridiidae	15	1	0	0	0	0	2	5	8	5	4	0
Turritella communis (Risso, 1826)	0	0	2	0	0	0	0	0	0	0	0	0
Acanthocardia sp.	25	1	0	12	4	9	12	44	16	30	21	38
Corbula gibba (Olivi, 1792)	276	15	0	54	40	27	56	77	0	140	211	102
Dentalium sp.	3	0	1	0	0	0	12	22	0	11	21	38
Rissoa sp.	25	12	3	24	60	36	31	88	130	31	21	45
Lithophaga lithophaga (Linnaeus, 1758)	0	0	0	0	0	0	2	0	0	0	0	0
Conus mediterraneus (Hwass, 1792)	0	0	0	0	0	0	0	0	0	0	0	0
Gibbula sp.	5	0	0	0	0	4	0	0	0	0	0	0
Ostrea sp.	0	0	0	18	16	9	31	11	16	15	7	0
Tricolia sp.	0	0	0	0	0	0	0	0	0	0	0	0
Bittium reticulatum (Da Costa, 1778)	235	30	16	312	560	616	512	436	930	165	172	352
Cerithium sp.	0	0	0	12	12	0	6	0	16	5	4	60
Cerithiopsis sp.	0	0	0	0	0	0	0	0	0	0	0	0
Columbella rustica (Linnaeus, 1758)	0	0	0	0	0	0	0	0	0	0	0	0
Hexaplex trunculus (Linnaeus, 1758)	0	0	0	0	0	0	0	0	0	2	0	0
Natica sp.	0	0	0	0	0	0	0	0	0	0	0	0
Kelliidae	30	0	0	0	8	0	6	110	60	45	137	150
Melanella sp.	0	0	0	0	0	0	0	11	8	0	0	15
Turbonilla sp.	20	7	1	18	8	36	6	5	16	16	11	0
Azorinus sp.	0	0	0	0	0	0	0	0	0	0	0	0
Glycimeris sp.	0	0	0	0	0	0	2	0	0	0	0	0
Mytilidae	0	0	0	0	4	4	12	0	0	0	0	0
Arca noae (Linnaeus, 1758)	0	0	0	0	0	0	0	0	0	1	0	0
unknown	0	0	0	0	0	0	0	0	0	0	0	0
Hydrobia Hartmann, 1821	50	8	4	0	0	4	2	5	16	16	35	38
Truncatella subcylindrica (Linnaeus, 1767)	10	0	0	0	0	0	0	5	0	2	0	0
Paracentrotus lividus	0	0	0	1	1	0	1	1	1	1	0	0
Total amount of molluscs	**1112**	**87**	**30**	**577**	**869**	**886**	**865**	**1006**	**1795**	**664**	**771**	**1128**

Table A5.4 *(cont.).*

Species/Depth (cm)	2570	2580	2590	2600	2613	2625	2638	2646	2656	2665	2670	2687
Cardiidae	0	3	0	0	17	18	0	36	3	0	0	0
Cerastoderma sp.	18	15	14	13	18	0	22	0	24	4	17	120
Loripes lucinalis (Lamarck, 1818)	0	0	0	0	28	4	0	4	45	0	0	9
Parvicardium sp.	0	0	0	0	9	5	8	9	9	1	4	0
Pectinidae	0	0	0	0	24	2	4	0	4	0	0	9
Tapes decussatus (Linnaeus, 1758)	0	3	2	0	0	2	0	2	0	0	4	0
Tellina sp.	0	3	0	0	4	22	4	90	45	3	34	18
Abra sp.	0	0	0	0	0	0	0	0	0	0	0	0
Mactra sp.	0	0	0	0	0	0	0	0	0	0	0	0
Nucula sp.	0	0	0	0	0	0	0	0	0	0	0	0
Donax sp.	0	0	0	0	0	0	0	0	0	0	0	0
Veneridae	0	0	0	0	0	0	0	0	0	0	0	0
Alvania sp.	0	0	0	0	0	0	0	0	4	0	0	32
Bulla striata (Brugière, 1792)	0	0	0	0	0	0	0	0	0	0	0	0
Gibberula sp.	0	0	0	0	0	0	0	0	0	0	0	0
Nassarius sp.	3	0	0	6	17	2	8	18	16	1	0	18
Pirenella conica (Blainville, 1826)	0	0	0	0	0	0	4	0	10	1	4	18
Retusa truncatula (Brugière, 1792)	0	0	0	0	9	7	4	18	21	1	4	54
Turridiidae	0	0	0	0	4	2	0	9	4	1	4	0
Turritella communis (Risso, 1826)	0	0	0	0	0	0	0	0	0	0	0	0
Acanthocardia sp.	3	3	14	0	9	14	8	18	11	3	4	90
Corbula gibba (Olivi, 1792)	6	15	0	13	86	52	22	263	273	11	150	270
Dentalium sp.	0	0	0	0	4	2	4	18	0	0	4	54
Rissoa sp.	0	3	0	0	28	7	8	63	141	7	21	54
Lithophaga lithophaga (Linnaeus, 1758)	0	0	0	0	2	2	0	2	0	0	2	0
Conus mediterraneus (Hwass, 1792)	0	0	0	0	0	0	0	0	0	0	0	9
Gibbula sp.	0	0	0	0	0	0	0	0	6	0	0	0
Ostrea sp.	6	5	2	6	0	4	4	4	4	1	4	18
Tricolia sp.	0	0	0	0	0	0	0	0	10	0	0	0
Bittium reticulatum (Da Costa, 1778)	48	45	68	28	270	352	78	459	583	27	198	486
Cerithium sp.	0	7	0	0	38	10	8	18	51	1	8	18
Cerithiopsis sp.	0	0	0	0	0	0	0	0	0	0	0	0
Columbella rustica (Linnaeus, 1758)	0	0	0	0	0	0	0	0	0	0	0	0
Hexaplex trunculus (Linnaeus, 1758)	0	0	0	0	0	0	2	0	4	0	0	4
Natica sp.	0	0	0	0	0	0	0	0	0	0	2	0
Kelliidae	0	0	0	0	24	23	24	108	65	6	12	36
Melanella sp.	0	0	0	0	0	0	7	9	0	0	0	0
Turbonilla sp.	0	0	0	0	4	3	0	9	21	2	9	75
Azorinus sp.	0	0	0	0	0	0	2	0	0	0	0	0
Glycimeris sp.	0	0	0	0	0	0	0	1	0	0	0	0
Mytilidae	0	0	0	0	0	0	0	0	0	0	0	0
Arca noae (Linnaeus, 1758)	0	0	0	0	0	0	0	0	0	0	0	0
unknown	0	0	0	0	24	3	0	0	21	0	0	8
Hydrobia Hartmann, 1821	0	0	0	6	5	7	4	4	65	1	4	9
Truncatella subcylindrica (Linnaeus, 1767)	0	0	0	0	4	0	4	0	1	1	4	9
Paracentrotus lividus	1	0	1	1	1	1	0	1	1	0	1	1
Total amount of molluscs	**85**	**102**	**101**	**73**	**629**	**544**	**229**	**1163**	**1442**	**72**	**494**	**1419**

Table A5.4 *(cont.).*

Species/Depth (cm)	2693	2696	2700	2782	2786	2792	2797	2804	2807	2812	2820	2825
Cardiidae	5	3	0	0	0	1	1	0	0	0	0	0
Cerastoderma sp.	0	0	4	2	0	0	0	1	0	0	0	0
Loripes lucinalis (Lamarck, 1818)	2	0	0	0	0	0	0	0	0	0	0	0
Parvicardium sp.	0	0	0	0	0	0	0	0	0	0	0	0
Pectinidae	0	2	0	0	0	0	0	0	0	0	0	0
Tapes decussatus (Linnaeus, 1758)	2	3	0	0	0	0	0	0	0	0	0	0
Tellina sp.	2	0	1	0	0	0	0	0	0	0	1	0
Abra sp.	0	0	0	0	0	0	0	0	0	0	0	0
Mactra sp.	0	0	0	0	0	0	0	0	0	0	0	0
Nucula sp.	0	0	0	0	0	0	0	0	0	0	0	0
Donax sp.	0	0	0	0	0	0	0	0	0	0	0	0
Veneridae	0	0	0	0	0	0	0	0	0	0	0	0
Alvania sp.	2	3	0	0	0	0	0	0	0	0	0	0
Bulla striata (Brugière, 1792)	0	0	0	0	0	0	0	0	0	0	0	0
Gibberula sp.	0	0	0	0	0	0	0	0	0	0	0	0
Nassarius sp.	3	0	0	0	0	0	0	0	0	0	0	0
Pirenella conica (Blainville, 1826)	0	0	1	0	0	0	0	0	0	0	0	0
Retusa truncatula (Brugière, 1792)	0	0	1	0	0	0	0	0	0	0	0	0
Turridiidae	0	0	1	0	0	0	0	0	0	0	0	0
Turritella communis (Risso, 1826)	0	0	0	0	0	0	0	0	0	0	0	0
Acanthocardia sp.	5	4	1	2	1	1	0	0	0	0	0	0
Corbula gibba (Olivi, 1792)	21	3	9	0	0	0	1	0	0	0	0	0
Dentalium sp.	0	0	0	0	0	0	0	0	0	0	0	0
Rissoa sp.	0	0	2	0	0	0	0	0	0	0	0	0
Lithophaga lithophaga (Linnaeus, 1758)	0	0	0	0	0	0	0	0	0	0	0	0
Conus mediterraneus (Hwass, 1792)	0	0	0	0	0	0	0	0	0	0	0	0
Gibbula sp.	0	2	0	0	0	0	0	0	0	0	0	0
Ostrea sp.	2	2	1	0	0	0	0	0	0	0	0	0
Tricolia sp.	0	0	0	0	0	0	0	0	0	0	0	0
Bittium reticulatum (Da Costa, 1778)	7	11	57	0	1	0	1	0	0	0	1	0
Cerithium sp.	2	3	1	0	0	0	0	0	0	0	0	0
Cerithiopsis sp.	0	0	0	0	0	0	0	0	0	0	0	0
Columbella rustica (Linnaeus, 1758)	0	0	0	0	0	0	0	0	0	0	0	0
Hexaplex trunculus (Linnaeus, 1758)	0	0	0	0	0	0	0	0	0	0	0	0
Natica sp.	0	0	0	0	0	0	0	0	0	0	0	0
Kelliidae	0	3	1	0	0	0	0	0	0	0	0	0
Melanella sp.	0	0	0	0	0	0	0	0	0	0	0	0
Turbonilla sp.	2	0	1	0	0	0	1	0	0	0	0	0
Azorinus sp.	0	0	0	0	0	0	0	0	0	0	0	0
Glycimeris sp.	0	0	0	0	0	0	0	0	0	0	0	0
Mytilidae	0	0	0	0	0	0	0	0	0	0	0	0
Arca noae (Linnaeus, 1758)	0	0	0	0	0	0	0	0	0	0	0	0
unknown	0	0	0	0	0	0	0	0	0	0	0	0
Hydrobia Hartmann, 1821	0	0	1	0	0	0	0	0	0	0	0	0
Truncatella subcylindrica (Linnaeus, 1767)	0	0	0	0	0	0	0	0	0	0	0	0
Paracentrotus lividus	1	0	1	0	0	1	0	0	0	0	0	0
Total amount of molluscs	**56**	**39**	**83**	**4**	**2**	**3**	**4**	**1**	**1**	**1**	**2**	**1**

Table A5.4 *(cont.).*

Species/Depth (cm)	2832	2850
Cardiidae	0	0
Cerastoderma sp.	0	0
Loripes lucinalis (Lamarck, 1818)	0	0
Parvicardium sp.	0	0
Pectinidae	0	0
Tapes decussatus (Linnaeus, 1758)	0	0
Tellina sp.	0	0
Abra sp.	0	0
Mactra sp.	0	0
Nucula sp.	0	0
Donax sp.	0	0
Veneridae	0	0
Alvania sp.	0	0
Bulla striata (Brugière, 1792)	0	0
Gibberula sp.	0	0
Nassarius sp.	0	0
Pirenella conica (Blainville, 1826)	0	0
Retusa truncatula (Brugière, 1792)	0	0
Turridiidae	0	0
Turritella communis (Risso, 1826)	0	0
Acanthocardia sp.	0	0
Corbula gibba (Olivi, 1792)	1	0
Dentalium sp.	0	0
Rissoa sp.	0	0
Lithophaga lithophaga (Linnaeus, 1758)	0	0
Conus mediterraneus (Hwass, 1792)	0	0
Gibbula sp.	0	0
Ostrea sp.	0	0
Tricolia sp.	0	0
Bittium reticulatum (Da Costa, 1778)	1	2
Cerithium sp.	0	0
Cerithiopsis sp.	0	0
Columbella rustica (Linnaeus, 1758)	0	0
Hexaplex trunculus (Linnaeus, 1758)	0	0
Natica sp.	0	0
Kelliidae	0	0
Melanella sp.	0	0
Turbonilla sp.	0	0
Azorinus sp.	0	0
Glycimeris sp.	0	0
Mytilidae	0	0
Arca noae (Linnaeus, 1758)	0	0
unknown	0	0
Hydrobia Hartmann, 1821	0	0
Truncatella subcylindrica (Linnaeus, 1767)	0	0
Paracentrotus lividus	0	0
Total amount of molluscs	**2**	**2**

Table A5.5. *Wied Żembaq 2.*

Species/Depth (cm)	117	121	125	129	133	137	141	145	149	153	157	161	165	169
Alvania sp.	1	1	0	0	3	1	3	3	2	7	2	0	0	1
Bittium reticulatum (Da Costa, 1778)	7	3	3	1	9	14	26	21	42	48	27	11	1	0
Cerithium sp.	0	0	0	0	1	0	2	2	3	5	5	0	0	0
Cylichnea sp.	0	1	1	0	0	0	1	1	1	2	2	0	0	0
Gibbula sp.	0	0	0	0	0	2	0	1	2	2	0	2	0	0
Hexaplex trunculus (Linnaeus, 1758)	0	0	1	0	0	0	1	1	1	0	1	0	0	0
Nassarius sp.	0	0	0	0	0	0	0	0	0	0	0	0	0	0
Pirenella conica (Blainville, 1826)	0	0	1	0	0	1	1	0	0	0	0	0	0	0
Rissoa sp.	2	0	2	0	0	0	0	3	8	8	7	1	0	0
Tricolia sp.	0	0	0	0	0	0	0	0	0	0	0	0	0	0
Turbonilla sp.	0	1	0	0	1	0	1	0	0	2	0	0	0	0
Cardium sp.	0	1	1	0	2	0	0	1	1	1	0	0	0	1
Loripes lucinalis (Lamarck, 1818)	0	0	1	0	0	1	0	0	2	0	5	2	0	0
other/unknown marine	2	3	1	0	1	0	3	0	0	2	0	0	0	0
Hydrobia Hartmann, 1821	0	0	0	0	2	3	1	4	6	4	8	2	1	1
Ovatella myosotis (Draparnaud, 1801)	0	0	0	0	1	0	1	0	0	0	0	0	0	0
Truncatella subcylindrica (Linnaeus, 1767)	0	1	1	0	0	3	0	0	0	2	0	0	0	0
Pseudamnicola (s.str.) *moussonii* (Calcara, 1841)	0	0	0	0	0	0	0	0	0	0	0	0	0	0
Ferussacia (s.str.) *folliculus* (Gmelin, 1791)	0	0	0	0	0	0	0	0	0	0	0	0	0	0
Oxychilus (Mediterranea) *hydatinus* (Rossmässler, 1838)	1	0	0	0	0	0	0	0	0	0	0	0	0	0
Pleurodiscus balmei (Potiez & Michaud, 1838)	0	0	0	0	0	0	0	0	0	0	0	0	0	0
Truncatellina callicratis (Scacchi, 1833)	0	0	0	0	0	0	0	0	0	0	0	0	0	0
Vitrea Fitzinger, 1833	0	0	0	0	0	0	0	0	0	0	0	0	0	0
Clausiliidae Mörch, 1864	0	0	0	0	0	0	0	0	2	1	0	0	0	0
Granopupa granum (Draparnaud, 1801)	0	0	0	0	0	0	0	0	0	0	0	0	0	0
Muticaria Lindholm, 1925	1	1	1	1	1	1	1	1	1	1	1	1	0	1
Papillifera papillaris (Müller, 1774)	0	0	0	0	0	0	2	1	0	0	0	0	0	0
Rumina decollata (Linnaeus, 1758)	0	0	0	0	0	0	0	0	0	0	0	0	0	0
Trochoidea spratti (Pfeiffer, 1846)	1	0	0	0	0	0	1	0	0	1	0	0	0	0
Caracollina lenticula (Michaud, 1831)	0	0	0	0	0	0	0	0	0	0	0	0	0	0
Cernuella caruanae (Kobelt, 1888)	1	0	1	1	0	0	0	0	0	1	0	0	0	0
Cochlicella acuta (Müller, 1774)	0	0	0	0	0	0	5	0	1	0	0	0	0	0
Eobania vermiculata (Müller, 1774)	0	0	0	0	0	0	0	0	0	0	0	0	0	0
Pomatias sulcatus (Draparnaud, 1801)	1	1	0	0	1	1	0	0	0	1	1	1	1	0
Theba pisana (Müller, 1774)	0	0	0	0	0	0	0	0	0	0	0	0	0	0
Cecilioides acicula (Müller, 1774)	1	0	1	0	0	0	0	0	1	0	0	0	0	0
Helicioid fragments	1	1	1	1	1	1	1	1	1	1	1	1	1	1
Total amount of molluscs	**19**	**14**	**16**	**4**	**23**	**28**	**50**	**40**	**74**	**89**	**60**	**21**	**4**	**5**

Table A5.5 *(cont.).*

Species/Depth (cm)	173	177	181	185	189	193	227	230	234	237	240	244	248	251
Alvania sp.	1	4	0	0	0	0	0	1	1	0	0	0	0	0
Bittium reticulatum (Da Costa, 1778)	6	0	1	2	13	0	1	20	6	3	5	2	1	1
Cerithium sp.	1	2	0	1	0	0	0	1	3	1	1	0	0	0
Cylichnea sp.	0	0	0	0	0	0	0	0	0	0	0	0	0	0
Gibbula sp.	0	2	0	0	0	0	0	2	0	0	0	0	0	0
Hexaplex trunculus (Linnaeus, 1758)	0	0	0	0	0	0	0	1	0	0	0	0	0	0
Nassarius sp.	0	0	0	0	0	0	0	0	0	0	0	0	0	0
Pirenella conica (Blainville, 1826)	0	0	0	0	0	0	0	1	0	0	1	0	0	0
Rissoa sp.	2	3	0	0	1	0	0	2	0	2	3	0	0	0
Tricolia sp.	0	1	1	0	0	0	0	0	0	0	0	0	0	0
Turbonilla sp.	0	1	0	0	1	0	0	0	0	0	1	0	0	0
Cardium sp.	1	0	0	0	0	0	0	0	1	0	0	0	0	0
Loripes lucinalis (Lamarck, 1818)	0	2	0	0	0	0	0	3	1	0	1	0	0	0
other/unknown marine	2	1	0	0	1	0	0	0	2	0	0	0	0	0
Hydrobia Hartmann, 1821	0	10	1	1	2	0	1	2	2	0	1	1	1	0
Ovatella myosotis (Draparnaud, 1801)	0	0	0	1	0	0	10	0	0	0	1	1	0	0
Truncatella subcylindrica (Linnaeus, 1767)	0	1	0	0	0	0	0	0	1	0	0	0	0	0
Pseudamnicola (s.str.) *moussonii* (Calcara, 1841)	0	0	0	0	0	0	0	0	0	0	0	0	0	0
Ferussacia (s.str.) *folliculus* (Gmelin, 1791)	0	0	0	0	0	0	0	0	0	0	0	0	0	0
Oxychilus (Mediterranea) *hydatinus* (Rossmässler, 1838)	0	0	0	0	0	0	0	0	0	0	0	0	0	0
Pleurodiscus balmei (Potiez & Michaud, 1838)	0	0	0	0	0	0	0	0	0	0	0	0	0	0
Truncatellina callicratis (Scacchi, 1833)	0	0	0	0	0	0	2	0	0	0	0	0	0	0
Vitrea Fitzinger, 1833	0	0	0	0	0	0	1	0	0	0	0	0	0	0
Clausiliidae Mörch, 1864	0	0	1	0	2	1	0	0	0	0	0	0	0	0
Granopupa granum (Draparnaud, 1801)	0	0	0	0	0	0	0	0	0	0	0	1	0	0
Muticaria Lindholm, 1925	1	0	1	1	0	1	1	0	1	1	1	0	1	1
Papillifera papillaris (Müller, 1774)	0	0	0	0	0	0	2	0	0	0	0	0	1	2
Rumina decollata (Linnaeus, 1758)	0	0	0	0	0	0	0	0	0	0	0	0	0	0
Trochoidea spratti (Pfeiffer, 1846)	1	0	0	1	0	1	0	0	1	0	1	1	0	0
Caracollina lenticula (Michaud, 1831)	0	0	0	0	0	0	0	0	0	0	0	0	0	1
Cernuella caruanae (Kobelt, 1888)	0	0	0	0	0	0	1	1	0	0	0	0	0	0
Cochlicella acuta (Müller, 1774)	1	0	0	0	0	0	0	1	0	0	0	0	0	1
Eobania vermiculata (Müller, 1774)	0	0	0	0	0	0	0	0	0	1	0	0	0	0
Pomatias sulcatus (Draparnaud, 1801)	0	0	1	1	0	0	1	0	1	1	1	2	2	0
Theba pisana (Müller, 1774)	1	0	0	0	0	0	0	0	0	0	0	0	0	0
Cecilioides acicula (Müller, 1774)	0	0	0	0	0	0	0	0	0	0	0	1	0	1
Helicioid fragments	1	1	1	1	1	1	1	1	1	1	1	1	1	1
Total amount of molluscs	**18**	**28**	**7**	**9**	**21**	**4**	**21**	**36**	**21**	**10**	**18**	**10**	**7**	**8**

Table A5.5 *(cont.).*

Species/Depth (cm)	254	258	262	265	269	272	276	279	283	286	290	293	297	302
Alvania sp.	0	1	0	0	0	0	0	0	0	0	0	1	0	0
Bittium reticulatum (Da Costa, 1778)	4	3	1	1	0	0	0	0	0	0	0	23	5	1
Cerithium sp.	0	0	0	0	0	0	0	0	0	0	0	0	0	0
Cylichnea sp.	0	0	0	0	0	0	0	0	0	0	0	1	0	0
Gibbula sp.	0	0	0	0	0	0	0	0	0	0	0	2	0	0
Hexaplex trunculus (Linnaeus, 1758)	0	0	0	0	0	0	0	0	0	0	0	0	0	0
Nassarius sp.	0	0	0	0	0	0	0	0	0	0	0	0	0	0
Pirenella conica (Blainville, 1826)	0	0	0	0	0	0	0	0	0	0	0	4	0	0
Rissoa sp.	0	0	0	0	0	0	0	0	0	0	0	6	1	0
Tricolia sp.	0	0	0	0	0	0	0	0	0	0	0	0	0	0
Turbonilla sp.	1	0	0	0	0	0	0	0	0	0	0	0	0	0
Cardium sp.	1	0	0	0	0	0	0	0	0	0	0	0	1	0
Loripes lucinalis (Lamarck, 1818)	0	1	0	0	0	0	0	0	0	0	0	2	0	0
other/unknown marine	0	0	0	0	0	0	0	0	0	0	0	0	0	0
Hydrobia Hartmann, 1821	2	3	0	0	0	1	1	2	1	0	0	1	5	0
Ovatella myosotis (Draparnaud, 1801)	2	1	0	0	1	0	0	0	0	0	4	0	0	0
Truncatella subcylindrica (Linnaeus, 1767)	0	0	0	0	0	0	0	0	0	0	0	0	0	0
Pseudamnicola (s.str.) *moussonii* (Calcara, 1841)	0	0	0	0	0	0	0	0	0	0	0	0	0	0
Ferussacia (s.str.) *folliculus* (Gmelin, 1791)	0	0	0	0	0	0	0	0	0	0	0	0	0	0
Oxychilus (Mediterranea) *hydatinus* (Rossmässler, 1838)	0	1	0	0	0	0	0	0	0	0	0	0	0	1
Pleurodiscus balmei (Potiez & Michaud, 1838)	0	0	0	0	0	0	0	0	0	0	0	0	0	0
Truncatellina callicratis (Scacchi, 1833)	0	0	0	0	0	0	0	0	0	1	0	0	0	0
Vitrea Fitzinger, 1833	0	0	0	0	0	0	0	0	0	0	0	0	0	0
Clausiliidae Mörch, 1864	0	0	0	0	0	0	0	0	0	0	1	0	0	0
Granopupa granum (Draparnaud, 1801)	0	0	0	0	0	0	0	0	0	0	0	0	0	0
Muticaria Lindholm, 1925	1	1	1	0	1	0	0	0	0	0	1	1	1	0
Papillifera papillaris (Müller, 1774)	1	0	1	0	0	0	0	0	0	0	0	0	0	1
Rumina decollata (Linnaeus, 1758)	0	0	0	0	0	0	0	0	0	0	0	0	0	1
Trochoidea spratti (Pfeiffer, 1846)	0	1	1	0	0	0	0	0	0	0	1	0	0	0
Caracollina lenticula (Michaud, 1831)	0	0	0	0	0	0	0	0	0	0	0	0	0	0
Cernuella caruanae (Kobelt, 1888)	0	0	0	0	1	0	2	0	0	0	1	0	0	1
Cochlicella acuta (Müller, 1774)	0	0	0	0	1	0	0	0	0	1	0	1	0	0
Eobania vermiculata (Müller, 1774)	0	0	1	0	1	0	0	0	0	0	1	0	0	0
Pomatias sulcatus (Draparnaud, 1801)	0	1	0	0	0	1	0	0	1	0	0	1	0	0
Theba pisana (Müller, 1774)	0	0	0	0	0	0	0	0	0	0	0	0	0	0
Cecilioides acicula (Müller, 1774)	0	0	1	0	0	0	0	0	0	0	0	1	0	3
Helicioid fragments	1	1	1	1	1	1	1	1	1	1	1	1	1	1
Total amount of molluscs	**13**	**14**	**7**	**2**	**6**	**3**	**4**	**3**	**3**	**3**	**10**	**45**	**14**	**9**

Table A5.5 *(cont.).*

Species/Depth (cm)	307	312	317	322	327	332	337	342	347	352	357	362	367	372
Alvania sp.	0	0	0	0	0	0	0	0	0	0	0	0	0	0
Bittium reticulatum (Da Costa, 1778)	0	0	0	0	0	0	0	0	0	0	0	0	0	0
Cerithium sp.	0	0	0	0	0	0	0	0	0	0	0	0	0	0
Cylichnea sp.	0	0	0	0	0	0	0	0	0	0	0	0	0	0
Gibbula sp.	0	0	0	0	0	0	0	0	0	0	0	0	0	0
Hexaplex trunculus (Linnaeus, 1758)	0	0	0	0	0	0	0	0	0	0	0	0	0	0
Nassarius sp.	0	0	0	0	0	0	0	0	0	0	0	0	0	0
Pirenella conica (Blainville, 1826)	0	0	0	0	0	0	0	0	0	0	0	0	0	0
Rissoa sp.	0	0	0	0	0	0	0	0	0	0	0	0	0	0
Tricolia sp.	0	0	0	0	0	0	0	0	0	0	0	0	0	0
Turbonilla sp.	0	0	0	0	0	0	0	0	0	0	0	0	0	0
Cardium sp.	0	0	0	0	0	0	0	0	0	0	0	0	0	0
Loripes lucinalis (Lamarck, 1818)	0	0	0	0	0	0	0	0	0	0	0	0	0	0
other/unknown marine	0	0	0	0	0	0	0	0	0	0	0	0	0	0
Hydrobia Hartmann, 1821	0	0	0	0	0	0	0	0	1	0	0	0	0	0
Ovatella myosotis (Draparnaud, 1801)	0	0	0	0	0	0	3	0	0	0	0	1	0	0
Truncatella subcylindrica (Linnaeus, 1767)	0	0	0	0	0	0	0	0	0	0	0	0	0	0
Pseudamnicola (s.str.) *moussonii* (Calcara, 1841)	0	0	0	0	0	0	0	0	0	0	0	0	0	0
Ferussacia (s.str.) *folliculus* (Gmelin, 1791)	0	0	0	0	0	0	0	0	0	0	0	1	0	0
Oxychilus (Mediterranea) *hydatinus* (Rossmässler, 1838)	0	1	0	0	1	1	0	0	1	0	0	1	0	1
Pleurodiscus balmei (Potiez & Michaud, 1838)	0	0	0	0	0	0	0	0	0	1	0	0	0	0
Truncatellina callicratis (Scacchi, 1833)	0	0	0	0	0	0	0	0	0	0	0	0	0	0
Vitrea Fitzinger, 1833	0	0	0	0	0	0	0	0	0	0	0	0	0	0
Clausiliidae Mörch, 1864	0	0	1	0	0	0	0	0	0	0	3	0	0	1
Granopupa granum (Draparnaud, 1801)	1	0	0	1	0	0	0	0	0	0	0	0	0	0
Muticaria Lindholm, 1925	0	0	1	1	0	1	1	1	1	1	1	1	1	1
Papillifera papillaris (Müller, 1774)	0	0	0	1	0	1	1	0	0	0	0	0	4	0
Rumina decollata (Linnaeus, 1758)	0	0	0	0	0	0	1	0	0	0	0	0	0	0
Trochoidea spratti (Pfeiffer, 1846)	0	0	0	1	0	0	1	0	0	0	0	0	0	0
Caracollina lenticula (Michaud, 1831)	0	0	0	0	0	0	0	0	0	0	0	0	0	0
Cernuella caruanae (Kobelt, 1888)	0	0	0	1	0	0	0	0	1	0	1	0	1	0
Cochlicella acuta (Müller, 1774)	0	1	0	0	0	1	0	0	0	0	0	0	1	1
Eobania vermiculata (Müller, 1774)	0	0	0	0	0	0	1	0	0	0	0	0	0	0
Pomatias sulcatus (Draparnaud, 1801)	0	0	0	0	0	0	0	1	0	1	0	1	1	1
Theba pisana (Müller, 1774)	0	0	0	0	0	0	0	0	0	0	0	0	0	0
Cecilioides acicula (Müller, 1774)	0	0	0	6	0	4	0	0	0	0	1	0	0	1
Helicioid fragments	1	1	1	1	1	1	1	1	1	1	1	1	1	1
Total amount of molluscs	**2**	**3**	**3**	**12**	**2**	**9**	**9**	**3**	**5**	**4**	**7**	**6**	**9**	**7**

Table A5.5 *(cont.).*

Species/Depth (cm)	377	382	387	392	463	468	473	479	483	489	494	503	507	511
Alvania sp.	0	0	0	0	0	0	0	0	0	0	0	0	0	0
Bittium reticulatum (Da Costa, 1778)	0	0	0	0	1	1	0	0	0	0	0	2	0	0
Cerithium sp.	0	0	0	0	0	0	0	0	0	0	0	0	0	0
Cylichnea sp.	0	0	0	0	0	0	0	0	0	0	0	0	0	0
Gibbula sp.	0	0	0	0	0	0	0	0	0	0	0	0	0	0
Hexaplex trunculus (Linnaeus, 1758)	0	0	0	0	0	0	0	0	0	0	0	0	0	0
Nassarius sp.	0	0	0	0	0	0	0	0	0	0	0	1	0	0
Pirenella conica (Blainville, 1826)	0	0	0	0	0	0	0	0	0	0	0	0	0	0
Rissoa sp.	0	0	0	0	0	1	0	0	0	0	0	0	0	0
Tricolia sp.	0	0	0	0	0	0	0	0	0	0	0	0	0	0
Turbonilla sp.	0	0	0	0	0	0	0	0	0	0	0	0	0	0
Cardium sp.	0	0	0	0	0	0	0	0	0	0	0	0	0	0
Loripes lucinalis (Lamarck, 1818)	0	0	0	0	0	0	0	0	0	0	0	0	0	0
other/unknown marine	0	0	0	0	0	0	0	0	0	0	0	0	0	0
Hydrobia Hartmann, 1821	0	0	0	0	0	0	13	18	3	0	0	5	3	2
Ovatella myosotis (Draparnaud, 1801)	0	12	21	29	15	6	51	62	1	2	1	23	14	7
Truncatella subcylindrica (Linnaeus, 1767)	0	0	0	0	1	0	0	0	0	0	0	0	0	0
Pseudamnicola (s.str.) *moussonii* (Calcara, 1841)	0	0	0	0	0	0	0	0	0	0	0	1	0	0
Ferussacia (s.str.) *folliculus* (Gmelin, 1791)	0	0	0	0	0	0	0	0	0	0	0	0	0	0
Oxychilus (Mediterranea) *hydatinus* (Rossmässler, 1838)	0	0	1	0	0	0	0	0	0	0	0	0	0	0
Pleurodiscus balmei (Potiez & Michaud, 1838)	0	0	1	1	0	0	2	0	0	0	0	1	2	0
Truncatellina callicratis (Scacchi, 1833)	0	0	0	0	0	1	0	0	0	0	0	0	0	0
Vitrea Fitzinger, 1833	0	0	0	0	0	0	0	0	0	0	0	0	0	0
Clausiliidae Mörch, 1864	0	0	0	1	0	0	2	0	0	0	0	0	1	0
Granopupa granum (Draparnaud, 1801)	0	0	0	0	0	0	0	0	0	0	0	0	0	0
Muticaria Lindholm, 1925	1	1	1	1	2	2	3	3	3	3	2	1	1	1
Papillifera papillaris (Müller, 1774)	1	0	2	0	1	0	1	2	0	0	0	1	1	0
Rumina decollata (Linnaeus, 1758)	0	0	0	0	0	0	0	0	0	0	1	1	0	1
Trochoidea spratti (Pfeiffer, 1846)	0	0	0	0	2	0	1	0	1	0	0	0	0	0
Caracollina lenticula (Michaud, 1831)	0	0	0	0	0	0	0	0	0	0	0	0	0	0
Cernuella caruanae (Kobelt, 1888)	0	0	0	0	0	0	0	0	0	0	0	2	0	0
Cochlicella acuta (Müller, 1774)	0	0	0	0	0	0	0	0	0	0	0	0	1	0
Eobania vermiculata (Müller, 1774)	0	0	0	0	0	0	0	0	0	1	0	0	0	0
Pomatias sulcatus (Draparnaud, 1801)	1	0	1	0	2	1	0	1	1	0	2	0	1	1
Theba pisana (Müller, 1774)	0	0	0	0	0	0	0	0	0	0	0	0	0	0
Cecilioides acicula (Müller, 1774)	0	0	0	0	0	0	0	0	0	0	0	0	0	0
Helicioid fragments	1	1	1	1	2	3	3	3	3	3	2	1	1	1
Total amount of molluscs	**4**	**14**	**28**	**33**	**26**	**15**	**76**	**89**	**12**	**9**	**8**	**39**	**25**	**13**

Table A5.5 *(cont.).*

Species/Depth (cm)	515	519	523
Alvania sp.	0	0	0
Bittium reticulatum (Da Costa, 1778)	1	0	1
Cerithium sp.	0	0	0
Cylichnea sp.	0	0	0
Gibbula sp.	0	0	0
Hexaplex trunculus (Linnaeus, 1758)	0	0	0
Nassarius sp.	0	0	1
Pirenella conica (Blainville, 1826)	0	0	0
Rissoa sp.	0	0	0
Tricolia sp.	0	0	0
Turbonilla sp.	0	0	0
Cardium sp.	0	0	0
Loripes lucinalis (Lamarck, 1818)	0	0	0
other/unknown marine	0	0	0
Hydrobia Hartmann, 1821	3	1	0
Ovatella myosotis (Draparnaud, 1801)	2	0	0
Truncatella subcylindrica (Linnaeus, 1767)	0	0	0
Pseudamnicola (s.str.) *moussonii* (Calcara, 1841)	0	0	0
Ferussacia (s.str.) *folliculus* (Gmelin, 1791)	0	0	0
Oxychilus (Mediterranea) *hydatinus* (Rossmässler, 1838)	0	0	0
Pleurodiscus balmei (Potiez & Michaud, 1838)	0	0	0
Truncatellina callicratis (Scacchi, 1833)	0	0	0
Vitrea Fitzinger, 1833	0	0	0
Clausiliidae Mörch, 1864	0	1	0
Granopupa granum (Draparnaud, 1801)	0	0	0
Muticaria Lindholm, 1925	1	1	0
Papillifera papillaris (Müller, 1774)	0	0	0
Rumina decollata (Linnaeus, 1758)	0	0	0
Trochoidea spratti (Pfeiffer, 1846)	0	0	1
Caracollina lenticula (Michaud, 1831)	0	0	0
Cernuella caruanae (Kobelt, 1888)	0	0	0
Cochlicella acuta (Müller, 1774)	0	0	0
Eobania vermiculata (Müller, 1774)	0	0	0
Pomatias sulcatus (Draparnaud, 1801)	1	0	0
Theba pisana (Müller, 1774)	0	0	0
Cecilioides acicula (Müller, 1774)	0	0	0
Helicioid fragments	1	1	1
Total amount of molluscs	**9**	**4**	**4**

Table A5.6. *Wied Żembaq 1.*

Species/Depth (cm)	**126**	**131**	**136**	**141**	**145**	**150**	**154**	**159**	**163**	**168**	**173**	**178**	**182**	**187**
Alvania sp.	1	2	0	6	2	0	0	0	1	0	0	0	0	0
Bittium sp.	16	28	28	51	26	8	1	2	1	0	1	0	0	1
Cerithium sp.	0	2	2	4	0	0	0	0	0	0	0	0	0	0
Cylichnea sp.	0	1	1	0	1	0	0	0	0	1	0	0	0	0
Gibbula sp.	0	1	0	2	1	0	0	0	0	0	0	0	0	0
Pirenella conica (Blainville, 1826)	0	0	1	2	0	0	0	0	0	0	0	0	0	0
Rissoa sp.	2	2	2	2	4	3	0	2	0	0	1	0	1	0
Cardium sp.	0	1	0	0	0	0	0	0	0	0	0	0	1	0
Loripes lucinalis (Lamarck, 1818)	0	1	0	2	0	0	0	0	0	0	0	0	0	0
other/unknown	1	3	2	0	1	0	0	2	0	0	0	1	0	0
Hydrobia Hartmann, 1821	0	2	1	7	2	1	0	1	0	0	0	1	2	0
Ovatella myosotis (Draparnaud, 1801)	0	0	0	1	0	0	0	0	0	0	0	0	0	0
Truncatella subcylindrica (Linnaeus, 1767)	0	1	0	1	0	0	0	0	0	0	0	0	0	0
Pseudamnicola (s.str.) *moussonii* (Calcara, 1841)	0	0	0	0	0	0	0	0	0	0	0	0	0	0
Ferussacia (s.str.) *folliculus* (Gmelin, 1791)	0	0	0	0	0	0	0	0	0	0	0	0	0	0
Oxychilus (Mediterranea) *hydatinus* (Rossmässler, 1838)	0	0	0	1	0	0	0	0	0	0	1	0	0	0
Pleurodiscus balmei (Potiez & Michaud, 1838)	0	0	0	0	0	0	0	0	0	0	0	0	0	0
Truncatellina callicratis (Scacchi, 1833)	0	0	0	0	0	0	0	0	0	0	0	0	0	0
Cantareus Risso, 1826	0	0	0	0	0	0	0	0	0	0	1	0	0	0
Clausiliidae Mörch, 1864	1	0	0	1	0	0	0	0	1	0	0	0	0	0
Granopupa granum (Draparnaud, 1801)	0	0	0	0	0	0	0	0	0	0	0	0	0	0
Papillifera papillaris (Müller, 1774)	1	0	0	0	1	0	0	0	0	1	1	0	1	0
Muticaria Lindholm, 1925	1	1	0	1	1	1	1	1	1	1	1	1	1	1
Rumina decollata (Linnaeus, 1758)	0	0	0	0	0	0	0	0	0	0	0	0	0	0
Trochoidea spratti (Pfeiffer, 1846)	0	0	0	2	0	2	1	1	0	0	0	0	0	0
Cernuella Schlüter, 1838	0	0	0	0	0	0	0	0	0	0	1	1	0	0
Chondrula (Mastus) pupa (Linnaeus, 1758)	0	0	0	0	0	0	0	0	0	0	0	0	0	0
Cochlicella acuta (Müller, 1774)	0	3	2	4	0	2	0	2	2	0	0	0	0	0
Eobania vermiculata (Müller, 1774)	0	0	0	0	0	0	0	0	0	0	0	0	0	0
Pomatias sulcatus (Draparnaud, 1801)	0	1	1	1	1	0	1	1	0	1	0	1	1	0
Theba pisana (Müller, 1774)	0	0	0	0	0	0	0	0	0	0	0	0	0	0
Cecilioides acicula (Müller, 1774)	0	0	0	0	0	0	0	0	0	0	0	0	0	0
Helicioid	1	1	1	1	1	1	1	1	1	1	1	1	1	1
Total amount of molluscs	**24**	**50**	**41**	**89**	**41**	**18**	**5**	**13**	**7**	**5**	**8**	**6**	**8**	**3**

Table A5.6 *(cont.).*

Species/Depth (cm)	191	195	199	204	208	213	227	232	237	242	247	253	258	263
Alvania sp.	0	0	1	0	0	0	0	0	0	0	0	0	0	0
Bittium sp.	0	3	0	2	2	1	3	0	0	0	0	0	1	0
Cerithium sp.	0	0	0	0	0	0	0	0	0	0	0	0	0	0
Cylichnea sp.	0	0	0	0	0	0	0	0	0	0	0	0	0	0
Gibbula sp.	0	0	0	0	0	0	0	0	0	0	0	0	0	0
Pirenella conica (Blainville, 1826)	0	0	0	0	0	0	0	0	0	0	0	0	0	0
Rissoa sp.	0	1	0	1	5	0	1	1	0	0	0	0	0	0
Cardium sp.	0	0	0	0	0	0	0	0	0	0	0	0	0	0
Loripes lucinalis (Lamarck, 1818)	0	0	1	0	0	0	0	0	0	0	0	0	0	0
other/unknown	0	0	0	0	0	0	0	0	1	0	0	0	0	0
Hydrobia Hartmann, 1821	0	0	0	0	1	4	1	0	0	1	0	0	1	4
Ovatella myosotis (Draparnaud, 1801)	0	0	0	3	0	0	3	0	1	2	0	27	8	2
Truncatella subcylindrica (Linnaeus, 1767)	0	0	0	0	0	0	0	0	0	0	0	0	0	0
Pseudamnicola (s.str.) *moussonii* (Calcara, 1841)	0	0	0	0	0	0	0	0	0	0	0	0	0	0
Ferussacia (s.str.) *folliculus* (Gmelin, 1791)	1	0	0	0	0	0	0	0	0	0	0	0	0	0
Oxychilus (Mediterranea) *hydatinus* (Rossmässler, 1838)	0	0	0	0	0	0	0	0	0	0	0	1	0	1
Pleurodiscus balmei (Potiez & Michaud, 1838)	0	0	0	0	0	0	0	0	0	0	0	0	0	0
Truncatellina callicratis (Scacchi, 1833)	0	0	0	0	0	0	0	0	0	0	0	1	0	0
Cantareus Risso, 1826	0	0	0	0	0	0	0	0	0	0	0	0	0	0
Clausiliidae Mörch, 1864	0	0	0	0	0	0	0	0	0	0	0	0	0	0
Granopupa granum (Draparnaud, 1801)	0	0	0	0	0	0	0	0	0	0	0	0	0	0
Papillifera papillaris (Müller, 1774)	0	0	0	2	0	2	1	1	0	0	0	0	0	0
Muticaria Lindholm, 1925	1	1	1	1	1	1	4	2	0	1	0	1	1	1
Rumina decollata (Linnaeus, 1758)	0	0	0	0	0	1	0	0	0	0	0	0	0	0
Trochoidea spratti (Pfeiffer, 1846)	0	1	2	0	0	2	0	1	0	0	0	0	0	0
Cernuella Schlüter, 1838	0	0	2	2	2	0	1	0	0	0	0	0	0	0
Chondrula (Mastus) pupa (Linnaeus, 1758)	0	0	0	0	0	0	0	0	0	0	0	0	0	0
Cochlicella acuta (Müller, 1774)	0	1	0	0	0	1	0	1	0	0	0	1	1	0
Eobania vermiculata (Müller, 1774)	0	0	0	0	0	0	0	0	0	0	0	0	0	0
Pomatias sulcatus (Draparnaud, 1801)	0	1	1	2	1	0	1	0	0	0	0	1	1	0
Theba pisana (Müller, 1774)	0	0	0	0	0	0	0	0	0	0	0	0	0	0
Cecilioides acicula (Müller, 1774)	0	0	1	0	0	0	1	0	0	0	0	0	0	0
Helicioid	1	1	1	1	1	1	1	1	1	1	1	1	1	1
Total amount of molluscs	**3**	**9**	**10**	**14**	**13**	**13**	**17**	**7**	**3**	**5**	**1**	**33**	**14**	**9**

Table A5.6 *(cont.).*

Species/Depth (cm)	**268**	**273**	**278**	**283**	**288**	**293**	**298**	**303**	**308**	**313**	**318**	**323**	**328**	**333**
Alvania sp.	0	1	0	0	0	0	0	0	0	0	0	0	0	0
Bittium sp.	0	0	1	3	0	0	0	0	0	0	0	1	0	0
Cerithium sp.	0	0	0	0	0	0	0	0	0	0	0	0	0	0
Cylichnea sp.	0	0	0	0	0	0	0	0	0	0	0	0	0	0
Gibbula sp.	0	0	0	0	0	0	0	0	0	0	0	0	0	0
Pirenella conica (Blainville, 1826)	0	0	0	0	0	0	0	0	0	0	0	0	0	0
Rissoa sp.	0	0	0	0	0	0	0	0	0	0	0	0	0	0
Cardium sp.	0	0	0	1	0	0	0	0	0	0	0	0	0	0
Loripes lucinalis (Lamarck, 1818)	0	0	1	2	0	0	0	0	0	0	0	0	0	0
other/unknown	0	0	0	0	0	0	0	0	0	0	0	0	0	0
Hydrobia Hartmann, 1821	0	6	0	1	0	0	0	0	0	0	0	0	1	0
Ovatella myosotis (Draparnaud, 1801)	4	0	0	0	0	0	0	0	0	0	0	0	2	0
Truncatella subcylindrica (Linnaeus, 1767)	0	0	1	0	0	0	0	0	0	0	0	0	0	0
Pseudamnicola (s.str.) *moussonii* (Calcara, 1841)	0	0	0	0	0	0	0	0	0	0	0	0	0	0
Ferussacia (s.str.) *folliculus* (Gmelin, 1791)	0	0	0	0	0	0	0	0	0	0	0	0	0	0
Oxychilus (Mediterranea) *hydatinus* (Rossmässler, 1838)	0	0	0	0	0	1	1	0	2	1	0	0	0	1
Pleurodiscus balmei (Potiez & Michaud, 1838)	0	0	0	0	0	0	0	0	0	0	0	0	1	0
Truncatellina callicratis (Scacchi, 1833)	0	0	0	0	0	0	0	0	0	0	0	0	0	1
Cantareus Risso, 1826	0	0	0	0	0	0	0	0	0	0	0	0	0	0
Clausiliidae Mörch, 1864	0	0	1	0	0	0	0	0	1	0	0	1	0	0
Granopupa granum (Draparnaud, 1801)	0	0	0	0	0	0	2	0	0	2	0	0	0	0
Papillifera papillaris (Müller, 1774)	0	0	0	0	0	0	1	0	0	0	0	0	0	0
Muticaria Lindholm, 1925	1	1	1	1	0	1	1	0	1	1	1	1	1	1
Rumina decollata (Linnaeus, 1758)	0	0	0	0	0	0	0	1	0	0	0	0	0	0
Trochoidea spratti (Pfeiffer, 1846)	0	0	0	0	0	0	0	0	0	1	0	0	1	0
Cernuella Schlüter, 1838	0	1	0	0	0	1	0	1	0	1	0	0	1	0
Chondrula (Mastus) pupa (Linnaeus, 1758)	0	0	0	0	0	1	0	0	0	0	0	0	0	0
Cochlicella acuta (Müller, 1774)	0	1	0	0	0	1	0	1	0	1	0	1	0	1
Eobania vermiculata (Müller, 1774)	0	0	0	0	0	0	0	0	0	0	0	0	0	0
Pomatias sulcatus (Draparnaud, 1801)	0	1	1	0	0	1	0	0	0	0	0	0	0	0
Theba pisana (Müller, 1774)	0	0	0	0	0	0	0	0	0	0	0	0	0	0
Cecilioides acicula (Müller, 1774)	0	0	0	0	2	8	1	4	2	4	1	0	1	0
Helicioid	1	1	1	1	1	1	1	1	1	1	1	1	1	1
Total amount of molluscs	**6**	**12**	**7**	**9**	**3**	**15**	**7**	**8**	**7**	**12**	**3**	**5**	**9**	**5**

Table A5.6 *(cont.).*

Species/Depth (cm)	338	343	348	353	358	363	368	373	378	383	388	393	398	403
Alvania sp.	0	0	0	0	0	0	0	0	0	0	0	0	0	0
Bittium sp.	0	0	0	0	0	0	0	0	0	0	0	0	0	0
Cerithium sp.	0	0	0	0	0	0	0	0	0	0	0	0	0	0
Cylichnea sp.	0	0	0	0	0	0	0	0	0	0	0	0	0	0
Gibbula sp.	0	0	0	0	0	0	0	0	0	0	0	0	0	0
Pirenella conica (Blainville, 1826)	0	0	0	0	0	0	0	0	0	0	0	0	0	0
Rissoa sp.	0	0	0	0	0	0	0	0	0	0	0	0	0	0
Cardium sp.	0	0	0	0	0	0	0	0	0	0	0	0	0	0
Loripes lucinalis (Lamarck, 1818)	0	0	0	0	0	0	0	0	0	0	0	0	0	0
other/unknown	0	0	0	0	0	0	0	0	0	0	0	0	0	0
Hydrobia Hartmann, 1821	0	0	0	2	0	0	0	0	0	0	23	32	29	27
Ovatella myosotis (Draparnaud, 1801)	0	0	0	1	0	1	8	28	9	6	8	18	27	27
Truncatella subcylindrica (Linnaeus, 1767)	0	0	0	0	0	0	0	0	0	0	0	0	0	0
Pseudamnicola (s.str.) *moussonii* (Calcara, 1841)	0	0	0	0	0	0	0	0	0	0	14	13	5	3
Ferussacia (s.str.) *folliculus* (Gmelin, 1791)	0	0	0	0	0	0	0	0	0	0	0	0	0	0
Oxychilus (Mediterranea) *hydatinus* (Rossmässler, 1838)	0	0	0	0	1	0	1	0	0	0	0	0	0	1
Pleurodiscus balmei (Potiez & Michaud, 1838)	0	0	0	0	0	0	2	8	0	1	0	0	0	0
Truncatellina callicratis (Scacchi, 1833)	0	0	0	0	0	0	0	1	0	0	0	0	0	0
Cantareus Risso, 1826	0	0	0	0	0	0	0	0	0	0	0	0	0	0
Clausiliidae Mörch, 1864	0	0	1	0	0	0	2	0	0	2	0	0	0	0
Granopupa granum (Draparnaud, 1801)	0	0	0	0	0	0	0	0	0	0	0	0	0	0
Papillifera papillaris (Müller, 1774)	0	0	1	0	2	1	1	1	0	1	0	0	0	1
Muticaria Lindholm, 1925	1	1	1	1	1	1	1	1	1	0	0	1	1	1
Rumina decollata (Linnaeus, 1758)	0	0	0	0	0	0	0	0	0	0	0	0	0	0
Trochoidea spratti (Pfeiffer, 1846)	0	0	0	0	0	0	0	1	0	0	0	0	0	0
Cernuella Schlüter, 1838	0	0	0	0	0	0	1	0	0	0	1	0	0	0
Chondrula (Mastus) pupa (Linnaeus, 1758)	0	0	0	0	0	0	0	0	0	0	0	0	0	0
Cochlicella acuta (Müller, 1774)	0	0	0	0	0	1	0	0	0	0	0	0	0	0
Eobania vermiculata (Müller, 1774)	0	0	0	0	0	0	0	0	0	0	0	0	0	0
Pomatias sulcatus (Draparnaud, 1801)	1	0	1	1	1	0	0	0	0	0	0	0	1	1
Theba pisana (Müller, 1774)	0	0	0	0	0	0	0	0	0	0	0	0	0	0
Cecilioides acicula (Müller, 1774)	0	0	0	1	0	0	0	0	0	0	0	0	0	0
Helicioid	1	1	1	1	1	1	1	1	1	1	1	1	1	1
Total amount of molluscs	**3**	**2**	**5**	**7**	**6**	**5**	**17**	**41**	**11**	**11**	**47**	**65**	**64**	**62**

Table A5.6 *(cont.).*

Species/Depth (cm)	**408**	**413**	**418**	**423**	**428**	**433**	**438**	**443**	**448**	**456**	**468**	**480**	**492**	**504**
Alvania sp.	0	0	0	0	0	0	0	0	0	0	0	1	0	0
Bittium sp.	0	0	0	0	0	0	0	0	0	2	1	0	0	0
Cerithium sp.	0	0	0	0	0	0	0	0	0	0	0	0	0	0
Cylichnea sp.	0	0	0	0	0	0	0	0	0	0	0	0	0	0
Gibbula sp.	0	0	0	0	0	0	0	0	0	0	0	0	0	0
Pirenella conica (Blainville, 1826)	0	0	0	0	0	0	0	0	0	0	0	0	0	0
Rissoa sp.	0	0	0	0	0	0	0	0	0	1	0	1	0	0
Cardium sp.	0	0	0	0	0	0	0	0	0	0	1	0	0	0
Loripes lucinalis (Lamarck, 1818)	0	0	0	0	0	0	0	0	0	0	0	0	0	0
other/unknown	0	0	0	0	0	0	0	0	0	0	0	0	0	0
Hydrobia Hartmann, 1821	21	29	27	33	3	1	0	0	0	0	0	13	17	0
Ovatella myosotis (Draparnaud, 1801)	29	45	43	33	6	0	1	0	2	1	1	11	13	3
Truncatella subcylindrica (Linnaeus, 1767)	0	0	0	0	0	0	0	0	0	0	0	0	0	0
Pseudamnicola (s.str.) *moussonii* (Calcara, 1841)	7	1	0	1	0	0	0	0	0	0	0	2	0	0
Ferussacia (s.str.) *folliculus* (Gmelin, 1791)	0	0	0	0	0	0	0	0	0	0	0	0	0	0
Oxychilus (Mediterranea) *hydatinus* (Rossmässler, 1838)	0	1	0	0	0	0	0	0	0	0	0	0	0	0
Pleurodiscus balmei (Potiez & Michaud, 1838)	0	0	0	0	0	0	0	0	0	0	0	0	0	0
Truncatellina callicratis (Scacchi, 1833)	0	0	0	0	0	0	0	0	0	0	0	0	0	0
Cantareus Risso, 1826	0	0	0	0	0	0	0	0	0	0	0	0	0	0
Clausiliidae Mörch, 1864	1	0	0	0	0	0	0	0	0	0	1	2	0	0
Granopupa granum (Draparnaud, 1801)	0	0	0	0	0	0	0	0	0	0	0	0	0	0
Papillifera papillaris (Müller, 1774)	0	0	0	0	0	0	0	1	0	0	1	1	1	1
Muticaria Lindholm, 1925	1	1	1	1	1	1	1	1	1	1	2	1	1	1
Rumina decollata (Linnaeus, 1758)	0	0	0	0	0	0	0	0	0	0	0	0	0	0
Trochoidea spratti (Pfeiffer, 1846)	0	0	0	0	0	0	0	1	0	0	2	0	0	0
Cernuella Schlüter, 1838	0	0	0	0	0	0	1	0	0	0	0	1	0	0
Chondrula (Mastus) pupa (Linnaeus, 1758)	0	0	0	0	0	0	0	0	0	0	0	0	0	0
Cochlicella acuta (Müller, 1774)	0	0	0	0	0	0	0	1	0	0	0	0	1	0
Eobania vermiculata (Müller, 1774)	0	0	0	0	0	0	0	0	0	0	0	0	0	0
Pomatias sulcatus (Draparnaud, 1801)	0	0	1	0	1	1	0	1	1	0	0	1	1	0
Theba pisana (Müller, 1774)	0	0	0	0	0	0	0	0	0	0	0	0	0	0
Cecilioides acicula (Müller, 1774)	0	1	0	0	0	0	0	0	0	2	0	0	0	0
Helicioid	1	1	1	1	1	1	1	1	1	1	1	1	1	1
Total amount of molluscs	**60**	**79**	**73**	**69**	**12**	**4**	**4**	**6**	**5**	**8**	**10**	**35**	**35**	**6**

Table A5.6 *(cont.).*

Species/Depth (cm)	516	528	540
Alvania sp.	0	0	0
Bittium sp.	0	1	0
Cerithium sp.	0	0	0
Cylichnea sp.	0	0	0
Gibbula sp.	0	0	0
Pirenella conica (Blainville, 1826)	0	0	0
Rissoa sp.	0	0	0
Cardium sp.	0	0	0
Loripes lucinalis (Lamarck, 1818)	0	0	0
other/unknown	0	0	0
Hydrobia Hartmann, 1821	1	10	16
Ovatella myosotis (Draparnaud, 1801)	1	1	0
Truncatella subcylindrica (Linnaeus, 1767)	0	0	0
Pseudamnicola (s.str.) *moussonii* (Calcara, 1841)	0	4	0
Ferussacia (s.str.) *folliculus* (Gmelin, 1791)	0	0	0
Oxychilus (Mediterranea) *hydatinus* (Rossmässler, 1838)	0	0	0
Pleurodiscus balmei (Potiez & Michaud, 1838)	0	0	0
Truncatellina callicratis (Scacchi, 1833)	0	0	0
Cantareus Risso, 1826	0	0	0
Clausiliidae Mörch, 1864	1	0	0
Granopupa granum (Draparnaud, 1801)	0	0	0
Papillifera papillaris (Müller, 1774)	0	0	0
Muticaria Lindholm, 1925	1	1	1
Rumina decollata (Linnaeus, 1758)	0	0	0
Trochoidea spratti (Pfeiffer, 1846)	0	0	0
Cernuella Schlüter, 1838	0	0	0
Chondrula (Mastus) pupa (Linnaeus, 1758)	0	0	0
Cochlicella acuta (Müller, 1774)	2	1	1
Eobania vermiculata (Müller, 1774)	0	0	0
Pomatias sulcatus (Draparnaud, 1801)	1	1	1
Theba pisana (Müller, 1774)	0	0	0
Cecilioides acicula (Müller, 1774)	0	0	0
Helicioid	1	1	1
Total amount of molluscs	**8**	**20**	**20**

Table A5.7. *Xemxija 1.*

Species/Depth (cm)	**49**	**54**	**59**	**64**	**69**	**72**	**76**	**81**	**86**	**91**	**96**	**101**	**106**	**111**
Bittium reticulatum (Da Costa, 1778)	0	0	0	0	0	0	0	0	0	0	0	0	0	0
Cardium sp.	0	0	0	0	0	0	0	0	0	0	0	0	0	0
Hydrobia Hartmann, 1821	0	0	0	0	0	0	0	0	0	1	0	0	0	0
Ovatella myosotis (Draparnaud, 1801)	0	0	0	0	0	0	0	0	0	0	0	0	0	0
Paludinella cf. *littorina* (Delle Chiaje, 1828)	0	0	0	0	0	0	0	0	0	0	0	0	0	0
Truncatella subcylindrica (Linnaeus, 1767)	0	0	0	0	0	0	0	0	0	0	0	0	0	0
Oxyloma elegans (Risso, 1826)	0	0	0	0	0	0	0	0	0	0	0	0	0	0
Pseudamnicola (s.str.) *moussonii* (Calcara, 1841)	0	0	0	0	0	0	0	0	0	0	0	0	0	0
Ancylus fluviatilis Müller, 1774	0	0	0	0	0	0	0	0	0	0	0	0	0	0
Bulinus cf. *truncatus* (Audouin, 1827)	0	0	0	0	0	0	0	0	0	0	0	0	0	0
Lymnaea (Feilden, 1879)	0	0	0	0	0	0	0	0	0	0	0	0	0	0
Planorbis Müller, 1774	0	0	0	0	0	0	0	0	0	0	0	0	0	0
Carychium cf. *schlickumi* Strauch, 1977	0	0	0	0	0	0	0	0	0	0	0	0	0	0
Vallonia pulchella (Müller, 1774)	0	0	0	0	0	0	0	0	0	0	0	0	0	0
Vertigo cf. *antivertigo* (Draparnaud, 1801)	0	0	0	0	0	0	0	0	0	0	0	0	0	0
Oxychilus Fitzinger, 1833	0	0	0	0	0	0	0	0	0	0	0	0	0	0
Truncatellina callicratis (Scacchi, 1833)	0	0	0	0	0	0	0	0	0	0	0	0	0	0
Papillifera papillaris (Müller, 1774)	0	0	0	0	0	0	0	0	0	0	0	0	0	0
Rumina decollata (Linnaeus, 1758)	0	0	0	0	0	0	0	0	0	0	0	0	0	0
Trochoidea spratti (Pfeiffer, 1846)	0	0	0	0	0	0	0	0	0	0	0	0	0	0
Cernuella caruanae (Kobelt, 1888)	0	0	0	0	0	0	0	0	0	0	0	0	0	0
Cochlicella acuta (Müller, 1774)	0	0	0	0	0	0	0	0	0	0	0	0	0	0
Pomatias sulcatus (Draparnaud, 1801)	0	0	0	0	0	0	0	0	0	0	0	0	0	0
Helicioid juveniles	0	0	1	0	0	0	0	0	0	0	0	0	0	0
Cecilioides acicula (Müller, 1774)	0	0	0	0	0	0	0	0	0	0	0	0	0	0
Total amount of molluscs	**1**	**1**	**1**	**1**	**1**	**1**	**1**	**1**	**1**	**1**	**1**	**1**	**1**	**1**

Table A5.7 *(cont.).*

Species/Depth (cm)	116	121	126	131	136	141	145	149	154	158	163	168	173	178
Bittium reticulatum (Da Costa, 1778)	0	0	1	0	0	0	0	0	0	0	0	0	0	0
Cardium sp.	0	0	0	1	0	0	0	0	0	0	0	0	0	0
Hydrobia Hartmann, 1821	0	0	0	0	0	0	0	0	0	0	0	0	1	0
Ovatella myosotis (Draparnaud, 1801)	0	0	0	0	0	0	0	0	0	1	2	1	1	2
Paludinella cf. *littorina* (Delle Chiaje, 1828)	0	0	0	0	0	0	0	0	0	0	0	0	0	0
Truncatella subcylindrica (Linnaeus, 1767)	0	0	1	0	0	0	0	0	0	0	0	0	0	0
Oxyloma elegans (Risso, 1826)	0	0	0	0	0	0	0	0	0	0	0	0	0	0
Pseudamnicola (s.str.) *moussonii* (Calcara, 1841)	0	0	0	0	0	0	0	0	0	0	0	0	4	6
Ancylus fluviatilis Müller, 1774	0	0	0	0	0	0	0	0	0	0	0	0	0	0
Bulinus cf. *truncatus* (Audouin, 1827)	0	0	0	0	0	0	0	0	0	0	0	0	0	0
Lymnaea (Feilden, 1879)	0	0	0	0	0	0	0	0	0	0	0	0	0	0
Planorbis Müller, 1774	0	0	0	0	0	0	0	0	0	0	0	0	0	0
Carychium cf. *schlickumi* Strauch, 1977	0	0	0	0	0	0	0	0	0	0	0	0	0	0
Vallonia pulchella (Müller, 1774)	0	0	0	0	0	0	0	0	0	0	0	0	0	0
Vertigo cf. *antivertigo* (Draparnaud, 1801)	0	0	0	0	0	0	0	0	0	0	0	0	0	0
Oxychilus Fitzinger, 1833	0	0	0	0	0	0	0	0	0	0	0	0	0	0
Truncatellina callicratis (Scacchi, 1833)	0	0	0	0	0	0	0	0	0	0	0	0	0	0
Papillifera papillaris (Müller, 1774)	0	0	0	0	0	0	0	0	0	0	0	0	0	0
Rumina decollata (Linnaeus, 1758)	0	0	0	0	0	0	0	0	0	0	0	0	0	0
Trochoidea spratti (Pfeiffer, 1846)	0	0	0	0	0	0	0	0	0	0	0	0	0	0
Cernuella caruanae (Kobelt, 1888)	0	0	1	0	0	0	0	0	0	0	0	0	0	0
Cochlicella acuta (Müller, 1774)	0	0	0	0	0	0	0	0	0	0	0	2	0	0
Pomatias sulcatus (Draparnaud, 1801)	0	0	0	0	0	0	1	0	0	0	0	0	0	0
Helicioid juveniles	0	1	0	0	0	1	0	0	0	0	0	0	0	0
Cecilioides acicula (Müller, 1774)	0	0	1	0	0	0	0	0	0	0	0	0	0	0
Total amount of molluscs	**1**	**1**	**4**	**1**	**1**	**1**	**1**	**1**	**1**	**1**	**2**	**3**	**6**	**8**

Table A5.7 *(cont.).*

Species/Depth (cm)	**183**	**188**	**193**	**198**	**203**	**208**	**213**	**218**	**223**	**228**	**233**	**238**	**243**	**248**
Bittium reticulatum (Da Costa, 1778)	0	2	0	0	1	1	2	0	0	0	0	0	0	0
Cardium sp.	0	0	0	0	0	0	0	0	0	0	0	0	1	0
Hydrobia Hartmann, 1821	4	0	1	0	17	249	8	3	0	0	0	0	0	1
Ovatella myosotis (Draparnaud, 1801)	1	0	12	10	23	3	1	1	1	2	12	25	8	13
Paludinella cf. *littorina* (Delle Chiaje, 1828)	0	0	0	0	0	0	0	0	0	0	0	0	0	0
Truncatella subcylindrica (Linnaeus, 1767)	0	0	0	1	0	0	1	0	1	0	2	1	0	0
Oxyloma elegans (Risso, 1826)	0	0	0	0	0	0	0	0	0	0	0	0	0	0
Pseudamnicola (s.str.) *moussonii* (Calcara, 1841)	0	0	0	0	13	0	0	0	0	0	0	0	0	0
Ancylus fluviatilis Müller, 1774	0	0	0	0	0	0	0	0	0	0	0	0	0	0
Bulinus cf. *truncatus* (Audouin, 1827)	0	0	0	0	0	0	0	0	0	0	0	0	0	0
Lymnaea (Feilden, 1879)	0	0	0	0	0	0	0	0	0	0	0	0	0	0
Planorbis Müller, 1774	0	0	0	0	0	0	0	0	0	0	0	0	0	0
Carychium cf. *schlickumi* Strauch, 1977	0	0	0	0	0	0	0	0	0	0	0	0	0	0
Vallonia pulchella (Müller, 1774)	0	0	0	0	0	0	0	0	0	0	0	0	0	0
Vertigo cf. *antivertigo* (Draparnaud, 1801)	0	0	0	0	0	0	0	0	0	0	0	0	0	0
Oxychilus Fitzinger, 1833	0	0	0	0	0	0	0	0	0	0	0	0	0	0
Truncatellina callicratis (Scacchi, 1833)	0	0	0	0	0	0	0	0	0	0	0	0	0	0
Papillifera papillaris (Müller, 1774)	0	0	1	0	0	0	0	0	0	0	0	0	0	1
Rumina decollata (Linnaeus, 1758)	0	0	0	0	0	0	0	0	0	0	0	0	0	0
Trochoidea spratti (Pfeiffer, 1846)	0	0	0	0	0	0	0	0	0	0	0	0	0	0
Cernuella caruanae (Kobelt, 1888)	0	0	0	0	0	0	0	0	0	0	0	0	0	0
Cochlicella acuta (Müller, 1774)	0	0	0	0	0	0	0	0	0	0	0	0	0	1
Pomatias sulcatus (Draparnaud, 1801)	0	0	0	0	0	0	0	0	0	0	0	0	0	0
Helicioid juveniles	0	0	0	0	0	0	0	0	0	0	0	0	0	0
Cecilioides acicula (Müller, 1774)	0	0	0	0	0	0	0	0	0	0	0	0	0	0
Total amount of molluscs	**5**	**2**	**14**	**11**	**54**	**253**	**12**	**4**	**2**	**2**	**14**	**26**	**9**	**16**

Table A5.7 *(cont.).*

Species/Depth (cm)	267	271	275	280	284	288	293	297	301	306	310	314	318	323
Bittium reticulatum (Da Costa, 1778)	0	0	0	0	0	0	0	0	0	0	0	0	0	0
Cardium sp.	0	0	0	0	0	0	0	0	0	0	0	0	0	0
Hydrobia Hartmann, 1821	0	0	0	0	0	0	0	0	0	0	0	0	0	0
Ovatella myosotis (Draparnaud, 1801)	49	38	46	107	93	71	37	48	60	17	2	1	28	59
Paludinella cf. *littorina* (Delle Chiaje, 1828)	0	0	0	0	0	0	0	0	0	0	0	0	0	0
Truncatella subcylindrica (Linnaeus, 1767)	0	0	0	0	0	0	0	0	0	0	0	0	0	0
Oxyloma elegans (Risso, 1826)	0	0	0	0	0	0	0	0	0	0	0	0	0	0
Pseudamnicola (s.str.) *moussonii* (Calcara, 1841)	0	0	0	0	0	0	0	0	0	0	0	0	0	0
Ancylus fluviatilis Müller, 1774	0	0	0	0	0	0	0	0	0	0	0	0	0	0
Bulinus cf. *truncatus* (Audouin, 1827)	0	0	0	0	0	0	0	0	0	0	0	0	0	0
Lymnaea (Feilden, 1879)	0	0	0	0	0	0	0	0	0	0	0	0	0	0
Planorbis Müller, 1774	0	0	0	0	0	0	0	0	0	0	0	0	0	0
Carychium cf. *schlickumi* Strauch, 1977	0	0	0	0	0	0	0	0	0	0	0	0	0	0
Vallonia pulchella (Müller, 1774)	0	0	0	0	0	0	0	0	0	0	0	0	0	0
Vertigo cf. *antivertigo* (Draparnaud, 1801)	0	0	0	0	0	0	0	0	0	0	0	0	0	0
Oxychilus Fitzinger, 1833	0	0	0	0	0	0	0	0	0	0	0	0	0	0
Truncatellina callicratis (Scacchi, 1833)	0	0	0	0	0	0	0	0	0	0	0	0	0	0
Papillifera papillaris (Müller, 1774)	0	0	0	0	0	0	0	0	0	0	1	0	0	1
Rumina decollata (Linnaeus, 1758)	0	0	0	0	0	0	0	0	0	0	0	0	0	0
Trochoidea spratti (Pfeiffer, 1846)	0	0	0	0	0	0	0	0	0	0	0	0	0	0
Cernuella caruanae (Kobelt, 1888)	0	0	0	0	0	0	0	0	0	0	0	0	0	0
Cochlicella acuta (Müller, 1774)	2	0	1	2	0	1	0	0	0	0	0	0	0	0
Pomatias sulcatus (Draparnaud, 1801)	0	0	0	0	0	0	0	0	0	0	0	0	0	0
Helicioid juveniles	0	0	0	0	0	0	0	0	0	0	0	0	0	0
Cecilioides acicula (Müller, 1774)	0	0	0	0	0	0	0	0	0	0	0	0	0	0
Total amount of molluscs	**51**	**38**	**47**	**109**	**93**	**72**	**37**	**48**	**60**	**17**	**3**	**1**	**28**	**60**

Table A5.7 *(cont.).*

Species/Depth (cm)	327	331	336	340	344	349	353	366	370	375	380	384	389	393
Bittium reticulatum (Da Costa, 1778)	1	0	0	0	0	0	0	0	0	0	0	0	0	2
Cardium sp.	0	0	0	0	0	0	0	0	0	0	0	0	0	0
Hydrobia Hartmann, 1821	0	0	0	0	0	0	0	0	0	0	0	0	0	0
Ovatella myosotis (Draparnaud, 1801)	42	20	6	6	4	0	2	0	0	0	0	0	0	0
Paludinella cf. *littorina* (Delle Chiaje, 1828)	0	0	0	0	0	0	0	0	0	0	0	0	0	0
Truncatella subcylindrica (Linnaeus, 1767)	0	1	0	0	0	0	0	0	0	0	0	0	0	0
Oxyloma elegans (Risso, 1826)	0	0	0	0	0	0	0	0	0	0	0	0	0	0
Pseudamnicola (s.str.) *moussonii* (Calcara, 1841)	0	0	0	0	0	0	0	0	0	0	0	0	0	0
Ancylus fluviatilis Müller, 1774	0	0	0	0	0	0	0	0	0	0	0	0	0	0
Bulinus cf. *truncatus* (Audouin, 1827)	0	0	0	0	0	0	0	0	0	0	0	0	0	0
Lymnaea (Feilden, 1879)	0	0	0	0	0	0	0	1	0	0	0	0	0	0
Planorbis Müller, 1774	0	0	0	0	0	2	0	0	0	0	0	0	0	0
Carychium cf. *schlickumi* Strauch, 1977	0	0	0	0	0	0	0	0	0	0	0	0	0	0
Vallonia pulchella (Müller, 1774)	0	0	0	0	2	1	0	0	0	0	0	0	0	0
Vertigo cf. *antivertigo* (Draparnaud, 1801)	0	0	0	1	3	1	0	0	0	0	0	0	0	1
Oxychilus Fitzinger, 1833	0	0	0	0	0	1	0	0	0	0	0	0	0	0
Truncatellina callicratis (Scacchi, 1833)	1	0	0	0	0	0	0	0	0	0	0	0	0	0
Papillifera papillaris (Müller, 1774)	1	0	0	0	0	0	0	0	0	0	0	0	0	0
Rumina decollata (Linnaeus, 1758)	0	0	0	0	0	0	0	0	0	0	0	0	0	0
Trochoidea spratti (Pfeiffer, 1846)	0	0	0	0	0	0	0	0	0	0	0	0	0	0
Cernuella caruanae (Kobelt, 1888)	0	0	0	0	0	0	0	0	0	0	0	0	0	0
Cochlicella acuta (Müller, 1774)	0	3	3	0	1	0	0	0	0	0	0	0	0	0
Pomatias sulcatus (Draparnaud, 1801)	0	0	0	0	0	0	0	0	0	0	0	0	0	0
Helicioid juveniles	3	0	0	2	0	0	0	0	0	0	0	0	0	0
Cecilioides acicula (Müller, 1774)	0	0	0	0	1	0	1	0	0	0	0	0	0	0
Total amount of molluscs	**48**	**24**	**9**	**9**	**11**	**5**	**3**	**1**	**1**	**1**	**1**	**1**	**1**	**3**

Table A5.7 *(cont.).*

Species/Depth (cm)	398	403	407	412	416	421	426	430	435	439	440	449	453	458
Bittium reticulatum (Da Costa, 1778)	0	0	1	1	2	2	0	0	0	0	0	0	0	0
Cardium sp.	0	0	0	0	0	0	0	0	0	0	0	0	0	0
Hydrobia Hartmann, 1821	0	0	0	0	0	0	0	0	0	0	0	0	0	0
Ovatella myosotis (Draparnaud, 1801)	0	0	0	0	0	1	0	0	1	9	9	9	32	16
Paludinella cf. *littorina* (Delle Chiaje, 1828)	0	0	0	0	0	0	0	0	0	0	1	0	0	0
Truncatella subcylindrica (Linnaeus, 1767)	0	0	0	0	0	0	0	0	0	0	0	0	0	0
Oxyloma elegans (Risso, 1826)	0	1	0	0	1	0	3	2	0	2	2	2	1	0
Pseudamnicola (s.str.) *moussonii* (Calcara, 1841)	0	0	0	0	0	0	0	0	0	0	0	0	0	0
Ancylus fluviatilis Müller, 1774	0	0	0	0	0	0	0	0	0	0	0	0	0	0
Bulinus cf. *truncatus* (Audouin, 1827)	0	0	0	0	0	0	0	0	0	0	0	0	0	0
Lymnaea (Feilden, 1879)	0	1	0	0	1	0	0	0	0	1	0	1	0	0
Planorbis Müller, 1774	0	0	0	0	0	0	0	0	0	0	0	0	0	0
Carychium cf. *schlickumi* Strauch, 1977	0	0	0	0	5	2	1	6	0	0	1	2	0	0
Vallonia pulchella (Müller, 1774)	0	0	0	0	0	0	0	0	0	0	0	0	0	0
Vertigo cf. *antivertigo* (Draparnaud, 1801)	1	0	0	0	11	2	0	3	2	0	0	0	0	2
Oxychilus Fitzinger, 1833	0	0	0	0	0	0	0	0	0	0	0	0	0	1
Truncatellina callicratis (Scacchi, 1833)	0	0	0	0	0	0	0	0	0	0	0	0	0	1
Papillifera papillaris (Müller, 1774)	0	0	0	0	0	0	0	0	0	0	0	0	0	1
Rumina decollata (Linnaeus, 1758)	0	0	0	0	0	0	0	0	0	0	0	0	0	0
Trochoidea spratti (Pfeiffer, 1846)	0	0	0	0	0	0	0	0	0	0	0	0	0	1
Cernuella caruanae (Kobelt, 1888)	0	0	0	0	0	0	0	0	0	0	0	0	0	0
Cochlicella acuta (Müller, 1774)	0	0	0	1	0	0	2	1	2	2	1	0	0	1
Pomatias sulcatus (Draparnaud, 1801)	0	0	0	0	0	0	0	0	0	0	0	0	0	0
Helicioid juveniles	0	0	0	0	0	0	0	0	0	0	0	0	0	1
Cecilioides acicula (Müller, 1774)	0	0	0	0	0	0	0	0	0	0	0	0	0	0
Total amount of molluscs	**1**	**2**	**1**	**2**	**20**	**7**	**6**	**12**	**5**	**14**	**14**	**14**	**33**	**24**

Table A5.7 *(cont.).*

Species/Depth (cm)	483	487	491	495	499	503	507	511	515	519	523	527	531	535
Bittium reticulatum (Da Costa, 1778)	0	0	0	0	0	0	0	0	0	0	0	0	0	0
Cardium sp.	0	0	0	0	0	0	0	0	0	0	0	0	0	0
Hydrobia Hartmann, 1821	2	1	0	0	0	0	0	0	0	0	0	0	0	0
Ovatella myosotis (Draparnaud, 1801)	26	117	270	367	40	16	9	0	16	16	18	8	0	32
Paludinella cf. *littorina* (Delle Chiaje, 1828)	0	0	0	0	0	0	0	0	0	0	0	0	0	0
Truncatella subcylindrica (Linnaeus, 1767)	0	0	0	0	0	0	0	0	0	0	0	0	0	0
Oxyloma elegans (Risso, 1826)	3	0	3	9	2	1	0	0	1	0	0	1	0	2
Pseudamnicola (s.str.) *moussonii* (Calcara, 1841)	29	25	19	78	44	11	3	0	1	2	5	0	2	11
Ancylus fluviatilis Müller, 1774	0	0	0	0	0	0	0	0	0	0	0	0	0	0
Bulinus cf. *truncatus* (Audouin, 1827)	0	0	0	0	0	0	0	0	0	0	0	0	0	0
Lymnaea (Feilden, 1879)	3	0	2	14	5	1	1	0	0	2	0	1	0	2
Planorbis Müller, 1774	2	12	35	38	2	2	0	0	0	0	0	0	0	1
Carychium cf. *schlickumi* Strauch, 1977	0	0	0	2	4	2	0	0	0	1	1	2	0	1
Vallonia pulchella (Müller, 1774)	0	0	0	0	2	0	2	0	1	1	1	1	0	0
Vertigo cf. *antivertigo* (Draparnaud, 1801)	0	0	0	0	1	0	0	0	0	0	0	0	0	1
Oxychilus Fitzinger, 1833	0	0	0	0	0	0	0	0	0	0	0	0	0	0
Truncatellina callicratis (Scacchi, 1833)	0	0	0	0	0	0	0	0	0	0	0	0	0	0
Papillifera papillaris (Müller, 1774)	0	0	0	0	0	0	0	0	0	0	0	0	0	0
Rumina decollata (Linnaeus, 1758)	0	0	0	0	0	0	1	0	0	0	0	0	0	0
Trochoidea spratti (Pfeiffer, 1846)	0	0	0	0	0	0	0	0	0	0	0	0	0	0
Cernuella caruanae (Kobelt, 1888)	0	0	0	0	0	0	0	0	0	0	0	0	0	0
Cochlicella acuta (Müller, 1774)	0	0	0	0	0	0	2	0	0	0	0	0	0	0
Pomatias sulcatus (Draparnaud, 1801)	0	0	0	0	0	0	0	0	0	0	0	0	0	0
Helicioid juveniles	0	0	0	0	0	0	0	0	0	0	0	0	0	0
Cecilioides acicula (Müller, 1774)	0	0	0	0	0	0	0	0	0	0	0	0	0	0
Total amount of molluscs	**65**	**155**	**329**	**508**	**100**	**33**	**18**	**1**	**19**	**22**	**25**	**13**	**2**	**50**

Table A5.7 *(cont.).*

Species/Depth (cm)	539	543	547	551	555	559	563	582	586	590	595	599	603	607
Bittium reticulatum (Da Costa, 1778)	0	0	0	0	0	0	0	0	0	0	0	0	0	0
Cardium sp.	0	0	0	0	0	0	0	0	0	0	0	0	0	0
Hydrobia Hartmann, 1821	0	0	0	0	0	0	0	0	0	0	0	0	0	0
Ovatella myosotis (Draparnaud, 1801)	46	32	15	18	12	8	0	0	0	3	3	0	2	1
Paludinella cf. *littorina* (Delle Chiaje, 1828)	0	0	0	0	0	0	0	0	0	0	0	0	0	0
Truncatella subcylindrica (Linnaeus, 1767)	0	0	0	0	0	0	0	0	0	0	0	0	0	0
Oxyloma elegans (Risso, 1826)	1	11	1	0	0	1	0	7	4	4	4	0	2	1
Pseudamnicola (s.str.) *moussonii* (Calcara, 1841)	15	126	0	13	2	8	0	10	13	26	15	1	7	3
Ancylus fluviatilis Müller, 1774	0	0	0	0	0	0	0	0	0	0	0	1	0	1
Bulinus cf. *truncatus* (Audouin, 1827)	0	0	0	0	0	0	0	0	0	0	0	0	0	0
Lymnaea (Feilden, 1879)	0	10	3	4	4	9	0	5	2	3	4	0	1	0
Planorbis Müller, 1774	4	16	12	19	3	3	0	5	30	28	34	10	24	8
Carychium cf. *schlickumi* Strauch, 1977	0	7	0	0	0	0	0	14	2	3	2	2	0	1
Vallonia pulchella (Müller, 1774)	0	0	0	0	1	3	0	2	0	0	0	1	0	0
Vertigo cf. *antivertigo* (Draparnaud, 1801)	2	0	0	0	1	0	0	0	1	2	1	0	0	0
Oxychilus Fitzinger, 1833	0	0	0	0	0	0	0	0	0	0	0	0	0	0
Truncatellina callicratis (Scacchi, 1833)	0	0	0	0	0	0	0	0	0	0	0	0	0	0
Papillifera papillaris (Müller, 1774)	0	0	0	0	0	0	0	0	0	0	0	0	0	0
Rumina decollata (Linnaeus, 1758)	0	0	0	0	0	0	0	0	0	0	0	0	0	0
Trochoidea spratti (Pfeiffer, 1846)	0	0	0	0	0	0	0	0	0	0	0	0	0	0
Cernuella caruanae (Kobelt, 1888)	0	0	0	0	0	0	0	0	0	0	0	0	0	0
Cochlicella acuta (Müller, 1774)	0	0	0	0	0	0	0	0	0	0	0	0	0	0
Pomatias sulcatus (Draparnaud, 1801)	0	0	0	0	0	0	0	0	0	0	0	0	0	0
Helicioid juveniles	1	0	0	0	0	0	0	0	0	0	0	0	0	0
Cecilioides acicula (Müller, 1774)	0	0	1	0	0	0	0	0	0	0	0	0	0	0
Total amount of molluscs	**69**	**202**	**32**	**54**	**23**	**32**	**1**	**43**	**52**	**69**	**63**	**15**	**36**	**15**

Table A5.7 *(cont.).*

Species/Depth (cm)	612	616	621	625	629	633	638	642	646	651	655	659	663	668
Bittium reticulatum (Da Costa, 1778)	0	0	0	0	0	0	0	0	0	0	0	0	0	0
Cardium sp.	0	0	0	0	0	0	0	0	0	0	0	0	0	0
Hydrobia Hartmann, 1821	0	0	0	0	0	0	0	0	0	0	0	0	0	0
Ovatella myosotis (Draparnaud, 1801)	0	1	0	0	0	0	0	0	2	0	1	0	0	2
Paludinella cf. *littorina* (Delle Chiaje, 1828)	0	0	0	0	0	0	0	0	0	0	0	0	0	0
Truncatella subcylindrica (Linnaeus, 1767)	0	0	0	0	0	0	0	0	0	0	0	0	0	0
Oxyloma elegans (Risso, 1826)	1	0	0	0	0	0	0	0	0	0	0	0	0	2
Pseudamnicola (s.str.) *moussonii* (Calcara, 1841)	7	9	2	3	1	2	8	2	9	8	15	6	7	4
Ancylus fluviatilis Müller, 1774	2	0	0	1	0	0	1	3	0	0	1	2	2	0
Bulinus cf. *truncatus* (Audouin, 1827)	1	0	0	0	0	1	0	0	0	0	0	0	0	0
Lymnaea (Feilden, 1879)	0	0	1	0	0	0	0	0	0	0	0	0	0	0
Planorbis Müller, 1774	19	24	22	12	11	4	9	2	22	14	11	6	1	5
Carychium cf. *schlickumi* Strauch, 1977	0	1	0	0	0	0	0	0	0	0	0	0	0	0
Vallonia pulchella (Müller, 1774)	0	0	0	0	0	0	0	0	0	0	0	0	0	0
Vertigo cf. *antivertigo* (Draparnaud, 1801)	1	0	0	0	0	0	0	0	0	0	0	0	0	0
Oxychilus Fitzinger, 1833	0	0	0	0	0	0	0	0	0	0	0	0	0	0
Truncatellina callicratis (Scacchi, 1833)	0	0	0	0	0	0	0	0	0	0	0	0	0	0
Papillifera papillaris (Müller, 1774)	0	0	0	0	0	0	0	0	0	0	0	0	0	0
Rumina decollata (Linnaeus, 1758)	0	0	0	0	0	0	0	0	0	0	0	0	0	0
Trochoidea spratti (Pfeiffer, 1846)	0	0	0	0	0	0	0	0	0	0	0	0	0	0
Cernuella caruanae (Kobelt, 1888)	0	0	0	0	0	0	0	0	0	0	0	0	0	0
Cochlicella acuta (Müller, 1774)	0	0	0	0	0	0	0	0	0	0	0	0	0	0
Pomatias sulcatus (Draparnaud, 1801)	0	0	0	0	0	0	0	0	0	0	0	0	0	0
Helicioid juveniles	0	0	0	0	0	0	0	0	0	0	0	0	0	0
Cecilioides acicula (Müller, 1774)	0	0	0	0	0	0	0	0	0	0	0	0	0	0
Total amount of molluscs	**31**	**35**	**25**	**16**	**12**	**7**	**18**	**7**	**33**	**22**	**28**	**14**	**10**	**13**

Table A5.7 *(cont.).*

Species/Depth (cm)	672	682	686	691	696	701	706	710	715	720	725	730	734	739
Bittium reticulatum (Da Costa, 1778)	0	0	0	0	0	0	0	0	0	0	0	0	0	0
Cardium sp.	0	0	0	0	0	0	0	1	0	0	0	0	0	0
Hydrobia Hartmann, 1821	0	0	1	0	0	0	0	0	0	0	0	0	0	0
Ovatella myosotis (Draparnaud, 1801)	0	0	0	0	0	0	0	0	0	0	0	0	0	0
Paludinella cf. *littorina* (Delle Chiaje, 1828)	0	0	0	0	0	0	0	0	0	0	0	0	0	0
Truncatella subcylindrica (Linnaeus, 1767)	0	0	0	0	0	0	0	0	0	0	0	0	0	0
Oxyloma elegans (Risso, 1826)	0	0	0	0	0	0	0	0	0	0	0	0	0	0
Pseudamnicola (s.str.) *moussonii* (Calcara, 1841)	0	0	0	0	0	0	0	0	0	0	0	0	0	0
Ancylus fluviatilis Müller, 1774	0	0	0	0	0	0	0	0	0	0	0	0	0	0
Bulinus cf. *truncatus* (Audouin, 1827)	0	0	0	0	0	0	0	0	0	0	0	0	0	0
Lymnaea (Feilden, 1879)	0	0	0	0	0	0	0	0	0	0	0	0	0	0
Planorbis Müller, 1774	0	0	0	0	0	0	0	0	0	0	0	0	0	0
Carychium cf. *schlickumi* Strauch, 1977	0	0	0	0	0	0	0	0	0	0	0	0	0	0
Vallonia pulchella (Müller, 1774)	0	0	0	0	3	0	0	0	2	3	0	0	0	0
Vertigo cf. *antivertigo* (Draparnaud, 1801)	0	0	0	0	0	0	0	0	0	4	2	1	0	0
Oxychilus Fitzinger, 1833	0	0	0	0	0	0	0	0	0	0	0	0	0	0
Truncatellina callicratis (Scacchi, 1833)	0	0	0	0	0	0	0	0	0	0	0	0	0	0
Papillifera papillaris (Müller, 1774)	0	0	0	0	0	0	0	0	0	0	0	0	0	0
Rumina decollata (Linnaeus, 1758)	0	0	0	0	0	0	0	0	0	0	0	0	0	0
Trochoidea spratti (Pfeiffer, 1846)	0	0	0	0	0	0	0	0	0	0	1	1	0	0
Cernuella caruanae (Kobelt, 1888)	0	0	0	0	0	0	0	0	0	0	0	0	0	0
Cochlicella acuta (Müller, 1774)	4	3	8	5	5	3	4	1	6	2	6	3	0	1
Pomatias sulcatus (Draparnaud, 1801)	0	0	0	0	0	0	0	0	0	0	0	0	1	0
Helicioid juveniles	0	0	0	1	0	0	0	0	1	0	1	0	0	0
Cecilioides acicula (Müller, 1774)	0	0	0	0	0	0	0	0	0	0	0	1	0	1
Total amount of molluscs	**4**	**3**	**9**	**6**	**8**	**3**	**4**	**2**	**9**	**9**	**10**	**6**	**1**	**2**

Table A5.7 *(cont.).*

Species/Depth (cm)	**744**	**749**	**754**	**758**	**763**	**768**	**773**	**778**	**802**	**806**	**810**	**814**	**818**	**822**
Bittium reticulatum (Da Costa, 1778)	0	0	0	0	0	0	0	0	0	0	0	0	0	0
Cardium sp.	0	0	0	0	0	0	0	0	0	0	0	0	0	0
Hydrobia Hartmann, 1821	0	0	0	0	0	0	0	0	0	0	0	0	0	0
Ovatella myosotis (Draparnaud, 1801)	0	0	0	0	0	0	0	0	0	0	0	0	0	0
Paludinella cf. *littorina* (Delle Chiaje, 1828)	0	0	0	0	0	0	0	0	0	0	0	0	0	0
Truncatella subcylindrica (Linnaeus, 1767)	0	0	0	0	0	0	0	0	0	0	0	0	0	0
Oxyloma elegans (Risso, 1826)	0	0	0	0	0	0	0	0	0	0	0	0	0	0
Pseudamnicola (s.str.) *moussonii* (Calcara, 1841)	0	0	0	0	0	0	0	0	0	0	0	0	0	0
Ancylus fluviatilis Müller, 1774	0	0	0	0	0	0	0	0	0	0	0	0	0	0
Bulinus cf. *truncatus* (Audouin, 1827)	0	0	0	0	0	0	0	0	0	0	0	0	0	0
Lymnaea (Feilden, 1879)	0	0	0	0	0	0	0	0	0	0	0	0	0	0
Planorbis Müller, 1774	0	0	0	0	0	0	0	0	0	0	0	0	0	0
Carychium cf. *schlickumi* Strauch, 1977	0	0	0	0	0	0	0	0	0	0	0	0	0	0
Vallonia pulchella (Müller, 1774)	0	0	0	0	0	0	0	0	0	0	0	0	0	0
Vertigo cf. *antivertigo* (Draparnaud, 1801)	0	0	0	0	0	0	0	0	0	0	0	0	0	0
Oxychilus Fitzinger, 1833	0	0	0	0	0	1	1	0	0	0	0	0	0	0
Truncatellina callicratis (Scacchi, 1833)	0	0	0	0	0	0	0	0	0	0	0	0	0	0
Papillifera papillaris (Müller, 1774)	0	0	0	0	0	0	0	0	0	0	0	0	0	0
Rumina decollata (Linnaeus, 1758)	0	0	0	0	0	0	0	0	0	0	0	0	0	0
Trochoidea spratti (Pfeiffer, 1846)	0	0	0	0	0	0	0	0	0	0	0	0	0	0
Cernuella caruanae (Kobelt, 1888)	0	0	0	0	0	0	0	0	0	0	0	0	0	0
Cochlicella acuta (Müller, 1774)	2	0	0	0	0	0	0	0	0	0	0	0	0	0
Pomatias sulcatus (Draparnaud, 1801)	0	0	0	0	0	0	0	0	0	0	0	0	0	0
Helicioid juveniles	0	0	0	0	1	0	0	0	0	0	0	0	0	0
Cecilioides acicula (Müller, 1774)	1	4	1	3	4	6	3	2	0	0	0	3	0	0
Total amount of molluscs	**3**	**4**	**1**	**3**	**5**	**7**	**4**	**2**	**1**	**1**	**1**	**3**	**1**	**1**

Table A5.7 *(cont.).*

Species/Depth (cm)	826	831	835	839	843	847	851	855	859	863	867	871	876	880
Bittium reticulatum (Da Costa, 1778)	0	0	0	0	0	0	0	0	0	0	0	0	0	0
Cardium sp.	0	0	0	0	0	0	0	0	0	0	0	0	0	0
Hydrobia Hartmann, 1821	0	0	0	0	0	0	0	0	0	0	0	0	0	0
Ovatella myosotis (Draparnaud, 1801)	0	0	0	0	0	0	0	0	0	0	0	0	0	0
Paludinella cf. *littorina* (Delle Chiaje, 1828)	0	0	0	0	0	0	0	0	0	0	0	0	0	0
Truncatella subcylindrica (Linnaeus, 1767)	0	0	0	0	0	0	0	0	0	0	0	0	0	0
Oxyloma elegans (Risso, 1826)	0	0	0	0	0	0	0	0	0	0	0	0	0	0
Pseudamnicola (s.str.) *moussonii* (Calcara, 1841)	0	0	1	0	0	0	0	0	0	0	3	1	0	0
Ancylus fluviatilis Müller, 1774	0	0	0	0	0	0	0	0	0	0	0	0	0	0
Bulinus cf. *truncatus* (Audouin, 1827)	0	0	0	0	0	0	0	0	0	0	0	0	0	0
Lymnaea (Feilden, 1879)	0	0	0	0	0	0	0	0	0	0	0	0	0	0
Planorbis Müller, 1774	0	0	1	0	0	0	0	0	0	0	0	0	0	0
Carychium cf. *schlickumi* Strauch, 1977	0	0	0	0	0	0	0	0	0	0	0	0	0	0
Vallonia pulchella (Müller, 1774)	0	0	0	0	0	0	0	0	0	0	0	0	0	0
Vertigo cf. *antivertigo* (Draparnaud, 1801)	0	0	0	0	0	0	0	0	0	0	0	0	0	0
Oxychilus Fitzinger, 1833	0	0	0	0	0	0	0	0	0	0	0	0	0	0
Truncatellina callicratis (Scacchi, 1833)	0	0	0	0	0	0	0	0	0	0	0	0	0	0
Papillifera papillaris (Müller, 1774)	0	0	0	0	0	0	0	0	1	0	0	0	0	0
Rumina decollata (Linnaeus, 1758)	0	0	0	0	0	0	0	0	0	0	0	0	0	0
Trochoidea spratti (Pfeiffer, 1846)	0	0	0	0	0	0	0	0	0	0	0	0	0	0
Cernuella caruanae (Kobelt, 1888)	0	0	0	0	0	0	0	0	0	0	0	0	0	0
Cochlicella acuta (Müller, 1774)	0	0	0	0	0	0	0	0	0	0	0	0	0	0
Pomatias sulcatus (Draparnaud, 1801)	0	0	0	0	0	0	0	0	0	0	0	0	0	0
Helicioid juveniles	0	0	0	0	0	0	0	0	0	0	0	0	0	0
Cecilioides acicula (Müller, 1774)	0	0	0	0	0	1	0	0	0	1	0	0	0	0
Total amount of molluscs	**1**	**1**	**2**	**1**	**1**	**2**	**1**	**1**	**1**	**1**	**3**	**1**	**1**	**1**

Table A5.7 *(cont.).*

Species/Depth (cm)	**884**	**887**	**888**	**889**	**894**	**899**	**905**	**910**	**916**	**921**	**927**	**932**	**938**	**943**
Bittium reticulatum (Da Costa, 1778)	0	0	0	0	0	0	0	0	0	0	0	0	0	0
Cardium sp.	0	0	0	0	0	0	0	0	0	0	0	0	0	0
Hydrobia Hartmann, 1821	0	0	0	0	0	0	0	0	0	0	0	0	0	0
Ovatella myosotis (Draparnaud, 1801)	0	0	1	1	1	1	0	0	0	0	0	0	0	0
Paludinella cf. *littorina* (Delle Chiaje, 1828)	0	0	0	0	0	0	0	0	0	0	0	0	0	0
Truncatella subcylindrica (Linnaeus, 1767)	0	0	0	0	0	0	0	0	0	0	0	0	0	0
Oxyloma elegans (Risso, 1826)	0	0	0	0	0	0	0	0	0	0	0	0	0	0
Pseudamnicola (s.str.) *moussonii* (Calcara, 1841)	0	0	2	9	3	14	5	11	9	3	2	1	2	6
Ancylus fluviatilis Müller, 1774	0	0	0	0	1	0	0	0	0	0	0	0	0	0
Bulinus cf. *truncatus* (Audouin, 1827)	0	0	1	0	0	0	1	0	0	0	0	0	0	0
Lymnaea (Feilden, 1879)	0	0	0	0	0	0	0	0	0	0	0	0	0	0
Planorbis Müller, 1774	0	0	0	0	1	0	1	0	0	0	0	0	1	0
Carychium cf. *schlickumi* Strauch, 1977	0	0	0	0	0	0	0	0	0	0	0	0	0	0
Vallonia pulchella (Müller, 1774)	0	0	2	2	2	1	1	0	1	0	2	1	2	1
Vertigo cf. *antivertigo* (Draparnaud, 1801)	0	0	0	0	0	0	0	1	0	0	0	0	0	0
Oxychilus Fitzinger, 1833	0	0	0	0	0	0	0	0	1	1	0	1	1	0
Truncatellina callicratis (Scacchi, 1833)	0	0	0	0	0	0	0	0	0	2	0	0	0	0
Papillifera papillaris (Müller, 1774)	0	0	0	0	0	0	0	0	0	0	0	0	0	0
Rumina decollata (Linnaeus, 1758)	0	0	0	0	0	0	0	0	0	0	0	0	0	0
Trochoidea spratti (Pfeiffer, 1846)	0	0	0	0	0	0	0	0	0	0	0	0	0	0
Cernuella caruanae (Kobelt, 1888)	0	0	0	0	0	0	0	0	0	0	0	0	0	0
Cochlicella acuta (Müller, 1774)	0	0	0	0	0	0	0	0	0	0	0	0	0	0
Pomatias sulcatus (Draparnaud, 1801)	0	0	0	0	0	0	0	0	0	0	0	0	0	0
Helicioid juveniles	0	0	0	0	0	0	0	1	0	0	0	0	0	0
Cecilioides acicula (Müller, 1774)	0	0	0	1	1	1	0	0	0	0	0	0	0	1
Total amount of molluscs	**1**	**1**	**6**	**13**	**9**	**17**	**8**	**13**	**11**	**6**	**4**	**3**	**6**	**8**

Table A5.7 *(cont.).*

Species/Depth (cm)	949	954	960	965	971	976	982	987
Bittium reticulatum (Da Costa, 1778)	0	0	0	0	0	0	0	0
Cardium sp.	0	0	0	1	0	0	0	0
Hydrobia Hartmann, 1821	0	0	0	0	0	0	0	0
Ovatella myosotis (Draparnaud, 1801)	0	0	1	0	0	0	0	0
Paludinella cf. *littorina* (Delle Chiaje, 1828)	0	0	0	0	0	0	0	0
Truncatella subcylindrica (Linnaeus, 1767)	0	0	0	0	0	0	0	0
Oxyloma elegans (Risso, 1826)	0	0	0	0	0	0	0	0
Pseudamnicola (s.str.) *moussonii* (Calcara, 1841)	9	1	4	24	12	4	0	0
Ancylus fluviatilis Müller, 1774	0	0	0	1	0	0	0	0
Bulinus cf. *truncatus* (Audouin, 1827)	0	0	1	0	0	0	0	0
Lymnaea (Feilden, 1879)	0	0	0	0	0	0	0	0
Planorbis Müller, 1774	0	0	0	0	0	0	0	0
Carychium cf. *schlickumi* Strauch, 1977	0	0	0	0	0	0	0	0
Vallonia pulchella (Müller, 1774)	1	1	0	1	0	0	0	0
Vertigo cf. *antivertigo* (Draparnaud, 1801)	0	0	0	0	0	0	0	0
Oxychilus Fitzinger, 1833	0	0	0	0	0	0	0	0
Truncatellina callicratis (Scacchi, 1833)	0	0	0	0	0	0	0	0
Papillifera papillaris (Müller, 1774)	0	0	0	0	0	0	0	0
Rumina decollata (Linnaeus, 1758)	0	0	0	0	0	0	0	0
Trochoidea spratti (Pfeiffer, 1846)	0	0	0	0	0	0	0	0
Cernuella caruanae (Kobelt, 1888)	0	0	0	0	0	0	0	0
Cochlicella acuta (Müller, 1774)	0	0	0	0	0	0	1	0
Pomatias sulcatus (Draparnaud, 1801)	0	0	0	0	0	0	0	0
Helicioid juveniles	0	0	0	0	0	0	0	0
Cecilioides acicula (Müller, 1774)	1	0	0	0	0	0	0	0
Total amount of molluscs	**11**	**2**	**6**	**27**	**12**	**4**	**1**	**1**

Table A5.8. *Xemxija 2.*

Species/Depth (cm)	120	124	129	133	137	141	146	150	154	158	163	167	171	175
Bittium reticulatum (Da Costa, 1778)	0	0	0	0	0	0	0	0	0	0	1	2	3	0
Cardium sp.	0	0	0	0	0	0	0	0	0	0	0	0	0	0
Cerithium sp.	0	0	0	0	0	0	0	0	0	0	0	0	0	0
Gibbula sp.	0	0	0	0	0	0	0	0	0	0	0	0	0	0
Rissoa sp.	0	0	0	0	0	0	0	0	0	0	1	0	0	0
Hydrobia Hartmann, 1821	0	0	0	0	0	0	0	0	0	0	0	0	0	0
Ovatella myosotis (Draparnaud, 1801)	0	0	0	0	0	0	0	1	1	3	1	2	1	2
Truncatella subcylindrica (Linnaeus, 1767)	0	0	0	0	0	0	0	0	0	0	0	0	0	0
Oxyloma elegans (Risso, 1826)	0	0	0	0	0	0	0	0	0	0	0	0	0	0
Pisidium caesertanum (Poli, 1791)	0	0	0	0	0	0	0	0	0	0	0	0	0	0
Pseudamnicola (s.str.) *moussonii* (Calcara, 1841)	0	0	0	0	0	0	0	0	0	0	0	0	0	0
Ancylus fluviatilis Müller, 1774	0	0	0	0	0	0	0	0	0	0	0	0	0	0
Lymnaea (Galba) truncatula (Müller, 1774)	0	0	0	0	0	0	0	0	0	0	0	0	0	0
Planorbis Müller, 1774	0	0	0	0	0	0	0	0	0	0	0	0	0	0
Carychium cf. *schlickumi* Strauch, 1977	0	0	0	0	0	0	0	0	0	0	0	0	0	0
Vallonia pulchella (Müller, 1774)	0	0	0	0	0	0	0	0	0	0	0	0	0	0
Vertigo cf. *antivertigo* (Draparnaud, 1801)	0	0	0	0	0	0	0	0	0	0	0	0	0	0
Lauria cylindracea (Da Costa, 1778)	0	0	0	0	0	0	0	0	0	0	0	0	0	0
Oxychilus Fitzinger, 1833	0	0	0	0	0	0	0	0	0	0	0	0	0	0
Truncatellina callicratis (Scacchi, 1833)	0	0	0	0	0	0	0	0	0	0	0	0	0	0
Papillifera papillaris (Müller, 1774)	0	0	0	0	0	0	0	0	0	0	0	0	0	0
Muticaria macrostoma (Cantraine, 1835)	0	0	0	0	0	0	0	0	0	0	0	0	0	0
Rumina decollata (Linnaeus, 1758)	0	0	0	0	0	0	0	0	0	0	0	0	0	0
Trochoidea spratti (Pfeiffer, 1846)	0	0	0	0	0	0	0	0	0	0	0	0	0	0
Cernuella caruanae (Kobelt, 1888)	0	0	0	0	0	0	2	0	0	0	0	0	0	0
Chondrula (Mastus) pupa (Linnaeus, 1758)	0	0	0	0	0	0	0	0	0	0	0	0	0	0
Cochlicella acuta (Müller, 1774)	0	0	0	0	0	0	0	1	0	0	0	0	0	0
Pomatias sulcatus (Draparnaud, 1801)	0	0	0	0	0	0	0	0	0	0	0	0	0	0
Helicioid juveniles	0	0	0	2	1	0	0	0	1	0	0	1	0	0
Cecilioides acicula (Müller, 1774)	0	0	0	0	0	0	0	0	0	0	0	0	0	0
Total amount of molluscs	**1**	**1**	**1**	**2**	**1**	**1**	**2**	**2**	**2**	**3**	**3**	**5**	**4**	**2**

Table A5.8. *Xemxija 2.*

Species/Depth (cm)	180	184	188	192	197	200	201	206	211	216	223	227	232	237
Bittium reticulatum (Da Costa, 1778)	1	0	0	0	0	0	2	0	0	0	0	0	0	1
Cardium sp.	0	0	0	0	0	0	0	0	0	0	0	0	0	0
Cerithium sp.	0	0	0	0	0	0	0	0	0	0	0	0	0	0
Gibbula sp.	0	0	0	0	0	0	0	0	0	0	0	0	0	0
Rissoa sp.	0	0	0	0	0	0	0	0	0	0	0	0	0	0
Hydrobia Hartmann, 1821	1	0	2	1	0	3	6	17	18	8	70	59	28	21
Ovatella myosotis (Draparnaud, 1801)	3	5	3	3	0	2	10	1	1	0	0	1	2	6
Truncatella subcylindrica (Linnaeus, 1767)	1	0	0	0	0	0	1	1	0	0	0	1	0	0
Oxyloma elegans (Risso, 1826)	0	0	0	0	0	0	0	0	0	0	0	0	0	0
Pisidium caesertanum (Poli, 1791)	0	0	0	0	0	0	0	0	0	0	0	0	0	0
Pseudamnicola (s.str.) *moussonii* (Calcara, 1841)	0	0	1	1	0	0	7	12	24	6	7	11	10	10
Ancylus fluviatilis Müller, 1774	0	0	0	0	0	0	0	0	0	0	0	0	0	0
Lymnaea (Galba) truncatula (Müller, 1774)	0	0	0	0	0	0	0	0	0	0	0	0	0	0
Planorbis Müller, 1774	0	0	0	0	0	0	0	0	0	0	0	0	0	0
Carychium cf. *schlickumi* Strauch, 1977	0	0	0	0	0	0	0	0	0	0	0	0	0	0
Vallonia pulchella (Müller, 1774)	0	0	0	0	0	0	0	0	0	0	0	0	0	0
Vertigo cf. *antivertigo* (Draparnaud, 1801)	0	0	0	0	0	0	0	0	0	0	0	0	0	0
Lauria cylindracea (Da Costa, 1778)	0	0	0	0	0	0	0	0	0	0	0	0	0	0
Oxychilus Fitzinger, 1833	0	0	0	0	0	0	0	0	0	0	0	0	0	0
Truncatellina callicratis (Scacchi, 1833)	0	0	0	0	0	0	0	0	0	0	0	0	0	0
Papillifera papillaris (Müller, 1774)	0	0	0	0	0	0	0	0	0	0	0	0	0	0
Muticaria macrostoma (Cantraine, 1835)	0	0	0	0	0	0	0	0	0	0	0	0	0	0
Rumina decollata (Linnaeus, 1758)	0	0	0	0	0	0	0	0	0	0	0	0	0	0
Trochoidea spratti (Pfeiffer, 1846)	0	0	0	0	0	0	1	0	0	0	0	0	1	0
Cernuella caruanae (Kobelt, 1888)	0	0	0	0	0	0	0	0	0	0	0	0	0	0
Chondrula (Mastus) pupa (Linnaeus, 1758)	0	0	0	0	0	0	0	0	0	0	0	0	0	0
Cochlicella acuta (Müller, 1774)	0	0	0	2	0	0	0	0	0	0	0	0	0	0
Pomatias sulcatus (Draparnaud, 1801)	0	0	0	0	0	0	0	0	0	0	0	0	0	0
Helicioid juveniles	0	1	0	1	0	1	1	0	1	0	0	0	0	0
Cecilioides acicula (Müller, 1774)	0	0	0	0	0	0	0	0	0	0	0	0	0	0
Total amount of molluscs	**6**	**6**	**6**	**8**	**1**	**6**	**28**	**31**	**44**	**14**	**77**	**72**	**41**	**38**

Table A5.8. *Xemxija 2.*

Species/Depth (cm)	242	248	253	258	264	269	274	279	285	290	295	300	319	323
Bittium reticulatum (Da Costa, 1778)	4	1	0	0	0	0	0	0	0	0	0	0	0	0
Cardium sp.	0	0	0	0	0	0	0	0	0	0	0	0	0	0
Cerithium sp.	0	1	0	0	0	0	0	0	0	0	0	0	0	0
Gibbula sp.	1	0	0	0	0	0	0	0	0	0	0	0	0	0
Rissoa sp.	0	1	0	0	0	0	0	0	0	0	0	0	0	0
Hydrobia Hartmann, 1821	2	2	0	1	1	0	0	0	0	0	0	0	0	0
Ovatella myosotis (Draparnaud, 1801)	22	55	42	45	43	78	18	84	58	89	77	75	18	39
Truncatella subcylindrica (Linnaeus, 1767)	0	0	0	0	0	0	0	0	0	0	0	0	0	0
Oxyloma elegans (Risso, 1826)	0	0	0	0	0	0	0	0	0	0	0	0	0	0
Pisidium caesertanum (Poli, 1791)	0	0	0	0	0	0	0	0	0	0	0	0	0	0
Pseudamnicola (s.str.) *moussonii* (Calcara, 1841)	0	1	0	0	0	0	0	0	0	0	0	0	0	0
Ancylus fluviatilis Müller, 1774	0	0	0	0	0	0	0	0	0	0	0	0	0	0
Lymnaea (Galba) truncatula (Müller, 1774)	0	0	0	0	0	0	0	0	0	0	0	0	0	1
Planorbis Müller, 1774	0	0	0	0	0	0	0	0	0	0	0	0	0	0
Carychium cf. *schlickumi* Strauch, 1977	0	0	0	0	0	0	0	0	0	0	0	0	0	0
Vallonia pulchella (Müller, 1774)	0	0	0	0	0	0	0	0	0	0	0	0	0	0
Vertigo cf. *antivertigo* (Draparnaud, 1801)	0	0	0	0	0	0	0	0	0	0	0	0	0	0
Lauria cylindracea (Da Costa, 1778)	0	0	0	0	0	0	0	0	0	0	0	0	0	0
Oxychilus Fitzinger, 1833	0	0	0	0	0	0	0	0	0	0	0	0	0	0
Truncatellina callicratis (Scacchi, 1833)	0	0	0	0	0	0	0	0	0	0	0	0	0	0
Papillifera papillaris (Müller, 1774)	0	0	0	0	0	0	0	0	0	0	0	0	0	1
Muticaria macrostoma (Cantraine, 1835)	0	0	0	0	0	0	0	0	0	0	0	0	0	0
Rumina decollata (Linnaeus, 1758)	0	0	0	0	0	0	0	0	0	0	0	0	0	0
Trochoidea spratti (Pfeiffer, 1846)	0	0	0	0	0	0	0	0	0	0	0	0	0	0
Cernuella caruanae (Kobelt, 1888)	0	0	0	0	0	0	0	0	0	0	0	0	0	0
Chondrula (Mastus) pupa (Linnaeus, 1758)	0	0	0	0	0	0	0	0	0	0	0	0	0	0
Cochlicella acuta (Müller, 1774)	2	1	2	0	0	0	0	2	0	0	2	0	1	1
Pomatias sulcatus (Draparnaud, 1801)	0	0	0	0	0	0	0	0	0	0	0	0	0	0
Helicioid juveniles	0	0	0	1	0	0	0	0	0	1	0	0	0	0
Cecilioides acicula (Müller, 1774)	0	0	0	0	0	0	0	0	0	0	0	0	0	0
Total amount of molluscs	**31**	**62**	**44**	**47**	**44**	**78**	**18**	**86**	**58**	**90**	**79**	**75**	**19**	**42**

Table A5.8 *(cont.).*

Species/Depth (cm)	328	332	336	340	345	349	353	358	362	366	371	375	379	384
Bittium reticulatum (Da Costa, 1778)	0	0	0	0	0	0	0	0	0	0	0	0	0	0
Cardium sp.	0	0	0	0	0	0	0	0	0	0	0	0	0	0
Cerithium sp.	0	0	0	0	0	0	0	0	0	0	0	0	0	0
Gibbula sp.	0	0	0	0	0	0	0	0	0	0	0	0	0	0
Rissoa sp.	0	0	0	0	0	0	0	0	0	0	0	0	0	0
Hydrobia Hartmann, 1821	0	0	0	0	0	0	0	0	0	0	0	0	0	0
Ovatella myosotis (Draparnaud, 1801)	49	5	3	4	4	1	0	3	0	0	0	0	0	0
Truncatella subcylindrica (Linnaeus, 1767)	0	0	0	0	0	0	0	0	0	0	0	0	0	0
Oxyloma elegans (Risso, 1826)	0	0	0	0	0	0	0	0	0	0	0	0	0	1
Pisidium caesertanum (Poli, 1791)	0	0	0	0	0	0	0	0	0	0	0	0	0	0
Pseudamnicola (s.str.) *moussonii* (Calcara, 1841)	0	0	0	0	0	0	0	0	0	0	0	0	0	0
Ancylus fluviatilis Müller, 1774	0	0	0	0	0	0	0	0	0	0	0	0	0	0
Lymnaea (Galba) truncatula (Müller, 1774)	0	0	0	0	0	0	0	0	1	2	1	0	0	1
Planorbis Müller, 1774	0	0	0	0	0	0	0	0	0	0	0	0	0	0
Carychium cf. *schlickumi* Strauch, 1977	0	0	0	0	0	1	0	0	0	0	0	0	0	0
Vallonia pulchella (Müller, 1774)	0	0	0	0	0	0	0	0	0	0	0	0	0	0
Vertigo cf. *antivertigo* (Draparnaud, 1801)	0	0	0	0	1	0	0	0	0	5	1	0	2	0
Lauria cylindracea (Da Costa, 1778)	0	0	0	0	0	0	0	0	0	0	1	0	0	0
Oxychilus Fitzinger, 1833	0	0	0	0	0	0	0	0	0	0	0	0	0	0
Truncatellina callicratis (Scacchi, 1833)	0	0	0	0	0	0	0	0	0	0	0	0	0	0
Papillifera papillaris (Müller, 1774)	0	0	0	0	0	0	0	0	0	0	0	0	0	0
Muticaria macrostoma (Cantraine, 1835)	0	0	0	0	0	0	0	0	0	0	0	0	0	0
Rumina decollata (Linnaeus, 1758)	0	0	0	0	0	0	0	0	0	0	0	0	0	0
Trochoidea spratti (Pfeiffer, 1846)	0	0	0	0	0	0	0	0	0	0	0	0	0	0
Cernuella caruanae (Kobelt, 1888)	0	0	0	0	0	0	0	0	0	0	0	0	0	0
Chondrula (Mastus) pupa (Linnaeus, 1758)	0	0	0	0	0	0	0	0	0	0	0	0	0	0
Cochlicella acuta (Müller, 1774)	1	9	6	5	4	0	0	0	0	0	0	0	2	0
Pomatias sulcatus (Draparnaud, 1801)	0	0	0	0	0	0	0	0	0	0	0	0	0	0
Helicioid juveniles	0	0	0	0	0	0	0	0	0	0	0	0	0	0
Cecilioides acicula (Müller, 1774)	0	0	0	0	0	0	0	0	0	0	0	0	0	0
Total amount of molluscs	**50**	**14**	**9**	**9**	**9**	**2**	**1**	**3**	**1**	**7**	**3**	**1**	**4**	**2**

Table A5.8 *(cont.).*

Species/Depth (cm)	388	392	397	401	415	420	424	429	433	438	442	447	451	456
Bittium reticulatum (Da Costa, 1778)	0	0	0	0	0	0	0	0	0	0	0	0	0	0
Cardium sp.	0	0	0	0	0	0	0	0	0	0	0	0	0	0
Cerithium sp.	0	0	0	0	0	0	0	0	0	0	0	0	0	0
Gibbula sp.	0	0	0	0	0	0	0	0	0	0	0	0	0	0
Rissoa sp.	0	0	0	0	0	0	0	0	0	0	0	0	0	0
Hydrobia Hartmann, 1821	0	0	0	0	0	0	0	0	0	0	0	0	0	0
Ovatella myosotis (Draparnaud, 1801)	0	1	0	0	1	2	15	57	20	64	50	24	11	8
Truncatella subcylindrica (Linnaeus, 1767)	0	0	0	0	0	0	0	0	0	0	0	0	0	0
Oxyloma elegans (Risso, 1826)	0	0	1	1	0	0	0	2	3	2	3	2	2	1
Pisidium caesertanum (Poli, 1791)	0	0	0	0	0	0	0	0	0	0	0	0	0	0
Pseudamnicola (s.str.) *moussonii* (Calcara, 1841)	0	0	0	0	4	1	4	4	2	13	55	34	24	4
Ancylus fluviatilis Müller, 1774	0	0	0	0	0	0	0	0	0	0	0	0	0	0
Lymnaea (Galba) truncatula (Müller, 1774)	2	0	2	1	0	1	1	1	2	7	9	5	3	1
Planorbis Müller, 1774	0	0	0	0	0	0	0	2	0	3	5	9	14	4
Carychium cf. *schlickumi* Strauch, 1977	1	0	0	0	0	0	0	2	0	1	0	2	4	0
Vallonia pulchella (Müller, 1774)	0	0	0	0	0	0	0	0	0	0	0	0	0	0
Vertigo cf. *antivertigo* (Draparnaud, 1801)	1	1	0	0	0	0	0	1	0	2	1	1	0	0
Lauria cylindracea (Da Costa, 1778)	0	0	0	1	0	0	0	0	0	0	1	0	0	0
Oxychilus Fitzinger, 1833	0	0	0	0	0	0	0	0	0	0	0	0	0	0
Truncatellina callicratis (Scacchi, 1833)	0	0	0	0	0	0	0	0	0	0	0	0	0	0
Papillifera papillaris (Müller, 1774)	0	0	0	0	0	0	0	0	0	0	0	0	0	0
Muticaria macrostoma (Cantraine, 1835)	0	0	0	0	0	0	0	0	0	0	0	0	0	0
Rumina decollata (Linnaeus, 1758)	0	0	0	0	0	0	0	0	0	0	0	0	0	0
Trochoidea spratti (Pfeiffer, 1846)	0	0	0	0	0	0	0	1	0	0	0	0	0	0
Cernuella caruanae (Kobelt, 1888)	0	0	0	0	0	0	0	0	0	0	0	0	0	0
Chondrula (Mastus) pupa (Linnaeus, 1758)	0	0	0	0	0	0	0	0	0	0	0	0	0	0
Cochlicella acuta (Müller, 1774)	0	0	0	0	0	0	0	1	1	0	0	0	0	0
Pomatias sulcatus (Draparnaud, 1801)	0	0	0	0	0	0	0	0	0	0	0	0	0	0
Helicioid juveniles	0	0	0	0	0	0	0	0	1	0	0	0	0	0
Cecilioides acicula (Müller, 1774)	0	0	0	1	0	0	0	0	0	0	0	0	0	0
Total amount of molluscs	**4**	**2**	**3**	**4**	**5**	**4**	**20**	**71**	**29**	**92**	**124**	**77**	**58**	**18**

Table A5.8 *(cont.).*

Species/Depth (cm)	460	465	470	474	478	483	488	492	496	501	526	530	534	539
Bittium reticulatum (Da Costa, 1778)	0	0	0	0	0	0	0	0	0	0	0	0	0	0
Cardium sp.	0	0	0	0	0	0	0	0	0	0	0	0	0	0
Cerithium sp.	0	0	0	0	0	0	0	0	0	0	0	0	0	0
Gibbula sp.	0	0	0	0	0	0	0	0	0	0	0	0	0	0
Rissoa sp.	0	0	0	0	0	0	0	0	0	0	0	0	0	0
Hydrobia Hartmann, 1821	0	0	0	0	0	0	0	0	0	0	1	2	0	1
Ovatella myosotis (Draparnaud, 1801)	38	9	33	39	21	20	8	5	7	2	33	43	14	33
Truncatella subcylindrica (Linnaeus, 1767)	0	0	0	0	0	0	0	0	0	0	0	0	0	0
Oxyloma elegans (Risso, 1826)	0	1	0	4	1	4	2	2	3	0	2	0	4	2
Pisidium caesertanum (Poli, 1791)	0	0	0	0	0	0	0	0	0	0	0	0	0	0
Pseudamnicola (s.str.) *moussonii* (Calcara, 1841)	10	7	51	12	12	0	4	4	11	9	14	13	6	2
Ancylus fluviatilis Müller, 1774	0	0	0	0	0	0	0	0	0	1	0	0	0	0
Lymnaea (Galba) truncatula (Müller, 1774)	7	2	1	14	14	1	0	2	3	1	10	1	1	1
Planorbis Müller, 1774	8	8	18	4	8	0	1	1	4	3	1	0	2	3
Carychium cf. *schlickumi* Strauch, 1977	0	0	1	2	5	10	2	0	4	0	0	0	1	1
Vallonia pulchella (Müller, 1774)	0	0	0	0	0	0	0	0	0	0	1	0	0	0
Vertigo cf. *antivertigo* (Draparnaud, 1801)	1	0	0	0	0	0	5	1	0	0	1	2	7	1
Lauria cylindracea (Da Costa, 1778)	0	0	0	0	0	1	0	0	0	0	0	0	0	0
Oxychilus Fitzinger, 1833	0	0	0	0	0	0	0	0	0	0	0	0	0	0
Truncatellina callicratis (Scacchi, 1833)	0	0	0	0	0	0	0	0	0	0	0	0	0	0
Papillifera papillaris (Müller, 1774)	0	0	0	0	0	0	0	0	0	0	0	0	0	0
Muticaria macrostoma (Cantraine, 1835)	0	0	0	0	0	0	0	0	0	0	0	0	0	0
Rumina decollata (Linnaeus, 1758)	0	0	0	0	0	0	0	0	0	0	0	0	0	0
Trochoidea spratti (Pfeiffer, 1846)	0	0	0	0	0	0	0	0	0	0	0	0	0	0
Cernuella caruanae (Kobelt, 1888)	0	0	0	0	0	0	0	0	0	0	0	0	0	0
Chondrula (Mastus) pupa (Linnaeus, 1758)	0	0	0	0	0	0	0	0	0	0	1	0	0	0
Cochlicella acuta (Müller, 1774)	0	0	0	0	0	0	0	0	0	0	0	1	0	0
Pomatias sulcatus (Draparnaud, 1801)	0	0	0	0	0	0	0	0	0	0	0	0	0	0
Helicioid juveniles	0	0	0	0	0	0	0	0	0	0	0	0	0	1
Cecilioides acicula (Müller, 1774)	0	0	0	0	0	0	0	0	0	0	0	1	0	1
Total amount of molluscs	**64**	**27**	**104**	**75**	**61**	**36**	**22**	**15**	**32**	**16**	**64**	**63**	**35**	**46**

Table A5.8 *(cont.).*

Species/Depth (cm)	543	547	551	556	560	564	568	573	577	581	585	590	594	598
Bittium reticulatum (Da Costa, 1778)	0	0	0	0	0	0	0	0	0	0	0	0	0	0
Cardium sp.	0	0	0	0	0	0	0	0	0	0	0	0	0	0
Cerithium sp.	0	0	0	0	0	0	0	0	0	0	0	0	0	0
Gibbula sp.	0	0	0	0	0	0	0	0	0	0	0	0	0	0
Rissoa sp.	0	0	0	0	0	0	0	0	0	0	0	0	0	0
Hydrobia Hartmann, 1821	0	1	0	0	0	0	0	0	0	0	0	0	0	0
Ovatella myosotis (Draparnaud, 1801)	34	18	21	28	29	17	27	28	30	17	5	8	3	1
Truncatella subcylindrica (Linnaeus, 1767)	0	0	0	0	0	0	0	0	0	0	0	0	0	0
Oxyloma elegans (Risso, 1826)	4	2	2	5	2	0	2	2	2	4	1	0	0	1
Pisidium caesertanum (Poli, 1791)	0	0	0	0	0	0	0	0	0	0	0	0	0	0
Pseudamnicola (s.str.) *moussonii* (Calcara, 1841)	13	24	23	21	28	6	21	37	11	5	0	2	10	10
Ancylus fluviatilis Müller, 1774	0	0	0	0	0	0	0	0	0	0	0	1	0	0
Lymnaea (Galba) truncatula (Müller, 1774)	4	12	3	5	3	4	3	3	14	2	0	4	1	1
Planorbis Müller, 1774	0	9	13	9	16	6	3	11	7	2	1	9	3	7
Carychium cf. *schlickumi* Strauch, 1977	2	1	0	6	0	0	1	2	0	4	2	4	0	1
Vallonia pulchella (Müller, 1774)	0	0	0	0	0	0	0	0	0	0	0	0	0	0
Vertigo cf. *antivertigo* (Draparnaud, 1801)	2	0	0	0	1	1	0	0	0	0	3	0	0	0
Lauria cylindracea (Da Costa, 1778)	0	0	0	0	0	0	0	0	0	1	1	0	0	0
Oxychilus Fitzinger, 1833	0	0	0	0	0	0	0	0	0	0	0	0	0	0
Truncatellina callicratis (Scacchi, 1833)	0	0	0	0	0	0	0	0	0	0	0	0	0	0
Papillifera papillaris (Müller, 1774)	0	0	0	0	0	0	0	0	0	0	0	0	0	0
Muticaria macrostoma (Cantraine, 1835)	0	0	0	0	0	0	0	0	0	0	0	0	0	0
Rumina decollata (Linnaeus, 1758)	0	0	0	0	0	0	0	0	0	0	0	0	0	0
Trochoidea spratti (Pfeiffer, 1846)	0	0	0	0	0	0	0	0	0	0	0	0	0	0
Cernuella caruanae (Kobelt, 1888)	0	0	0	0	0	0	0	0	0	0	0	0	0	0
Chondrula (Mastus) pupa (Linnaeus, 1758)	0	0	0	0	0	0	0	0	0	0	0	0	0	0
Cochlicella acuta (Müller, 1774)	0	0	0	0	0	0	0	0	0	0	0	0	0	0
Pomatias sulcatus (Draparnaud, 1801)	0	0	0	0	0	0	0	0	0	0	0	0	0	0
Helicioid juveniles	0	0	0	0	0	0	0	0	0	0	0	0	0	0
Cecilioides acicula (Müller, 1774)	2	0	0	0	0	0	0	0	0	0	0	0	0	0
Total amount of molluscs	**61**	**67**	**62**	**74**	**79**	**34**	**57**	**83**	**64**	**35**	**13**	**28**	**17**	**21**

Table A5.8 *(cont.).*

Species/Depth (cm)	602	606	611	626	630	635	639	644	648	653	657	662	666	671
Bittium reticulatum (Da Costa, 1778)	0	0	0	0	0	0	0	0	0	0	0	0	0	0
Cardium sp.	0	0	0	0	0	0	0	0	0	0	0	0	0	0
Cerithium sp.	0	0	0	0	0	0	0	0	0	0	0	0	0	0
Gibbula sp.	0	0	0	0	0	0	0	0	0	0	0	0	0	0
Rissoa sp.	0	0	0	0	0	0	0	0	0	0	0	0	0	0
Hydrobia Hartmann, 1821	0	0	0	0	0	0	0	0	0	0	0	0	0	0
Ovatella myosotis (Draparnaud, 1801)	5	4	2	1	1	1	1	0	0	0	1	1	4	0
Truncatella subcylindrica (Linnaeus, 1767)	0	0	0	0	0	0	0	0	0	0	0	0	0	0
Oxyloma elegans (Risso, 1826)	2	0	0	0	0	0	1	1	0	3	2	2	4	0
Pisidium caesertanum (Poli, 1791)	0	0	0	0	0	0	0	0	0	0	0	0	0	0
Pseudamnicola (s.str.) *moussonii* (Calcara, 1841)	11	6	3	1	4	2	3	4	6	8	4	5	9	0
Ancylus fluviatilis Müller, 1774	2	0	0	0	1	0	2	0	0	1	0	0	0	0
Lymnaea (Galba) truncatula (Müller, 1774)	3	0	1	1	0	0	0	1	2	2	3	0	0	3
Planorbis Müller, 1774	5	1	6	18	24	34	14	12	6	24	23	25	19	0
Carychium cf. *schlickumi* Strauch, 1977	0	0	0	0	0	0	0	0	0	1	0	1	2	9
Vallonia pulchella (Müller, 1774)	0	0	0	0	0	0	0	0	0	0	0	0	1	0
Vertigo cf. *antivertigo* (Draparnaud, 1801)	0	0	0	1	1	0	0	0	0	1	0	0	1	4
Lauria cylindracea (Da Costa, 1778)	0	0	0	0	0	0	0	0	0	0	0	0	0	0
Oxychilus Fitzinger, 1833	0	0	0	0	0	0	0	0	0	0	0	0	1	0
Truncatellina callicratis (Scacchi, 1833)	0	0	0	0	0	0	0	0	0	0	0	0	0	0
Papillifera papillaris (Müller, 1774)	0	0	0	0	0	0	0	0	0	0	0	0	0	0
Muticaria macrostoma (Cantraine, 1835)	0	0	0	0	0	0	0	0	0	0	0	0	0	0
Rumina decollata (Linnaeus, 1758)	0	0	0	0	0	0	0	0	0	0	0	0	0	0
Trochoidea spratti (Pfeiffer, 1846)	0	0	0	0	0	0	0	0	0	0	0	0	0	0
Cernuella caruanae (Kobelt, 1888)	0	0	0	0	0	0	0	0	0	0	0	0	0	0
Chondrula (Mastus) pupa (Linnaeus, 1758)	0	0	0	0	0	0	0	0	0	0	0	0	0	0
Cochlicella acuta (Müller, 1774)	0	0	0	0	0	0	0	0	0	0	0	0	0	0
Pomatias sulcatus (Draparnaud, 1801)	0	0	0	0	0	0	0	0	0	0	0	0	0	0
Helicioid juveniles	0	0	0	0	0	0	0	0	0	0	0	0	0	0
Cecilioides acicula (Müller, 1774)	0	0	0	0	0	0	0	0	0	0	0	0	0	0
Total amount of molluscs	**28**	**11**	**12**	**22**	**31**	**37**	**21**	**18**	**14**	**40**	**33**	**34**	**41**	**16**

Table A5.8 *(cont.).*

Species/Depth (cm)	675	680	684	689	693	698	702	707	711	716	738	742	746	750
Bittium reticulatum (Da Costa, 1778)	0	0	0	0	0	0	0	0	0	0	0	0	0	0
Cardium sp.	0	0	0	0	0	0	0	0	0	0	0	0	0	0
Cerithium sp.	0	0	0	0	0	0	0	0	0	0	0	0	0	0
Gibbula sp.	0	0	0	0	0	0	0	0	0	0	0	0	0	0
Rissoa sp.	0	0	0	0	0	0	0	0	0	0	0	0	0	0
Hydrobia Hartmann, 1821	0	0	0	0	0	0	0	0	0	0	0	0	0	0
Ovatella myosotis (Draparnaud, 1801)	0	0	0	0	0	0	0	0	0	0	0	0	0	0
Truncatella subcylindrica (Linnaeus, 1767)	0	0	0	0	0	0	0	0	0	0	0	0	0	0
Oxyloma elegans (Risso, 1826)	0	0	0	0	0	0	0	0	0	0	0	0	0	0
Pisidium caesertanum (Poli, 1791)	0	0	0	0	0	0	0	0	0	0	0	0	0	0
Pseudamnicola (s.str.) *moussonii* (Calcara, 1841)	0	0	0	0	0	0	0	0	0	0	0	0	0	0
Ancylus fluviatilis Müller, 1774	0	0	0	0	0	0	0	0	0	0	0	0	0	0
Lymnaea (Galba) truncatula (Müller, 1774)	1	6	4	8	4	0	0	0	0	0	0	0	0	0
Planorbis Müller, 1774	0	0	0	0	0	0	0	0	0	0	0	0	0	0
Carychium cf. *schlickumi* Strauch, 1977	3	4	0	0	0	0	0	0	0	0	0	0	0	0
Vallonia pulchella (Müller, 1774)	0	0	0	0	0	0	0	0	0	0	0	0	0	0
Vertigo cf. *antivertigo* (Draparnaud, 1801)	5	4	2	0	0	0	0	0	0	0	0	0	0	0
Lauria cylindracea (Da Costa, 1778)	0	0	0	0	0	0	0	0	0	0	0	0	0	0
Oxychilus Fitzinger, 1833	1	0	5	0	0	0	0	0	0	0	0	0	1	0
Truncatellina callicratis (Scacchi, 1833)	0	0	0	0	0	0	0	0	0	0	0	0	0	0
Papillifera papillaris (Müller, 1774)	0	0	0	0	0	0	0	0	0	0	0	0	0	0
Muticaria macrostoma (Cantraine, 1835)	0	0	0	0	0	0	0	0	0	0	0	0	0	0
Rumina decollata (Linnaeus, 1758)	0	0	0	0	0	0	0	0	0	0	0	0	0	0
Trochoidea spratti (Pfeiffer, 1846)	0	0	0	0	0	0	0	0	0	0	0	0	0	0
Cernuella caruanae (Kobelt, 1888)	0	0	0	0	0	0	0	0	0	0	0	0	0	2
Chondrula (Mastus) pupa (Linnaeus, 1758)	0	0	0	0	0	0	0	0	0	0	0	0	0	0
Cochlicella acuta (Müller, 1774)	0	0	15	5	4	3	0	6	5	7	3	0	0	0
Pomatias sulcatus (Draparnaud, 1801)	0	0	0	0	0	0	0	0	0	0	0	0	0	0
Helicioid juveniles	0	1	0	0	1	0	3	0	0	2	0	0	2	0
Cecilioides acicula (Müller, 1774)	2	0	0	0	0	0	0	0	0	0	0	0	0	1
Total amount of molluscs	**12**	**15**	**26**	**13**	**9**	**3**	**3**	**6**	**5**	**9**	**3**	**1**	**3**	**3**

Table A5.8 *(cont.).*

Species/Depth (cm)	754	758	763	767	771	775	779	783	788	792	796	800	804	808
Bittium reticulatum (Da Costa, 1778)	0	0	0	0	0	0	0	0	0	0	0	0	0	0
Cardium sp.	0	0	0	0	0	0	0	0	0	0	0	0	0	0
Cerithium sp.	0	0	0	0	0	0	0	0	0	0	0	0	0	0
Gibbula sp.	0	0	0	0	0	0	0	0	0	0	0	0	0	0
Rissoa sp.	0	0	0	0	0	0	0	0	0	0	0	0	0	0
Hydrobia Hartmann, 1821	0	0	0	0	0	0	0	0	0	0	0	0	0	0
Ovatella myosotis (Draparnaud, 1801)	0	0	0	0	0	0	0	0	0	0	0	0	0	0
Truncatella subcylindrica (Linnaeus, 1767)	0	0	0	0	0	0	0	0	0	0	0	0	0	0
Oxyloma elegans (Risso, 1826)	0	0	0	0	0	0	0	0	0	0	0	0	0	0
Pisidium caesertanum (Poli, 1791)	0	0	0	0	0	0	0	0	0	0	0	0	0	0
Pseudamnicola (s.str.) *moussonii* (Calcara, 1841)	0	0	0	0	0	0	0	0	0	0	0	0	1	0
Ancylus fluviatilis Müller, 1774	0	0	0	0	0	0	0	0	0	0	0	0	0	0
Lymnaea (Galba) truncatula (Müller, 1774)	0	0	0	0	0	0	0	0	0	0	0	0	0	0
Planorbis Müller, 1774	0	0	0	0	0	0	0	0	0	0	0	0	0	0
Carychium cf. *schlickumi* Strauch, 1977	0	0	0	0	0	0	0	0	0	0	0	0	0	0
Vallonia pulchella (Müller, 1774)	0	0	0	0	0	0	0	0	0	0	0	0	0	0
Vertigo cf. *antivertigo* (Draparnaud, 1801)	0	0	0	0	0	0	0	0	0	0	0	0	0	0
Lauria cylindracea (Da Costa, 1778)	0	0	0	0	0	0	0	0	0	0	0	0	0	0
Oxychilus Fitzinger, 1833	0	0	0	1	0	0	0	0	1	0	0	0	0	0
Truncatellina callicratis (Scacchi, 1833)	0	0	0	0	0	0	0	0	0	0	0	0	0	0
Papillifera papillaris (Müller, 1774)	0	0	0	0	0	0	0	0	0	0	0	0	0	0
Muticaria macrostoma (Cantraine, 1835)	0	0	0	0	0	1	0	0	0	0	0	0	0	0
Rumina decollata (Linnaeus, 1758)	0	0	0	0	0	0	0	0	0	0	0	0	0	0
Trochoidea spratti (Pfeiffer, 1846)	0	0	0	0	0	0	0	0	0	0	0	0	0	0
Cernuella caruanae (Kobelt, 1888)	0	0	0	0	0	0	0	0	0	0	0	0	0	0
Chondrula (Mastus) pupa (Linnaeus, 1758)	0	0	0	0	0	0	0	0	0	0	0	0	0	0
Cochlicella acuta (Müller, 1774)	0	0	0	0	0	0	0	0	0	0	0	0	0	0
Pomatias sulcatus (Draparnaud, 1801)	0	0	0	0	0	0	0	0	0	0	0	0	0	0
Helicioid juveniles	0	0	0	1	0	1	2	1	0	0	0	0	0	0
Cecilioides acicula (Müller, 1774)	0	0	0	1	1	0	0	0	0	0	1	0	0	0
Total amount of molluscs	**1**	**1**	**1**	**3**	**1**	**2**	**2**	**1**	**1**	**1**	**1**	**1**	**1**	**1**

Table A5.8 *(cont.).*

Species/Depth (cm)	813	817	821	858	861	865	868	872	875	879	882	886	889	893
Bittium reticulatum (Da Costa, 1778)	0	0	0	0	0	0	0	0	0	0	0	0	0	0
Cardium sp.	0	0	0	0	0	0	0	0	0	0	0	0	0	0
Cerithium sp.	0	0	0	0	0	0	0	0	0	0	0	0	0	0
Gibbula sp.	0	0	0	0	0	0	0	0	0	0	0	0	0	0
Rissoa sp.	0	0	0	0	0	0	0	0	0	0	0	0	0	0
Hydrobia Hartmann, 1821	0	0	0	0	0	0	0	0	0	0	0	0	0	0
Ovatella myosotis (Draparnaud, 1801)	0	0	0	0	0	0	0	0	0	0	0	0	4	5
Truncatella subcylindrica (Linnaeus, 1767)	0	0	0	0	0	0	0	0	0	0	0	0	0	0
Oxyloma elegans (Risso, 1826)	0	0	0	0	0	0	0	0	0	0	0	0	0	0
Pisidium caesertanum (Poli, 1791)	0	0	0	0	0	0	0	0	0	0	0	0	0	0
Pseudamnicola (s.str.) *moussonii* (Calcara, 1841)	0	1	0	0	0	0	0	1	0	0	0	0	1	0
Ancylus fluviatilis Müller, 1774	0	0	0	0	0	0	0	0	0	0	0	0	0	0
Lymnaea (Galba) truncatula (Müller, 1774)	0	0	0	0	0	0	1	0	0	0	0	0	0	0
Planorbis Müller, 1774	0	0	0	0	0	0	0	0	0	0	0	0	0	0
Carychium cf. *schlickumi* Strauch, 1977	0	0	0	0	0	0	0	0	0	0	0	0	0	0
Vallonia pulchella (Müller, 1774)	0	0	0	0	0	0	0	0	0	0	0	0	0	0
Vertigo cf. *antivertigo* (Draparnaud, 1801)	0	0	0	0	0	0	0	0	0	0	0	0	0	0
Lauria cylindracea (Da Costa, 1778)	0	0	0	0	0	0	0	0	0	0	0	0	0	0
Oxychilus Fitzinger, 1833	0	0	0	0	0	0	0	0	1	0	0	0	0	0
Truncatellina callicratis (Scacchi, 1833)	0	0	0	0	0	0	0	0	0	0	0	0	0	0
Papillifera papillaris (Müller, 1774)	0	0	0	0	0	0	0	0	0	0	0	0	0	0
Muticaria macrostoma (Cantraine, 1835)	0	0	0	0	0	0	0	0	0	0	0	0	0	0
Rumina decollata (Linnaeus, 1758)	0	0	0	0	0	0	0	0	0	0	0	0	0	0
Trochoidea spratti (Pfeiffer, 1846)	0	0	0	0	0	0	0	0	0	0	0	0	0	0
Cernuella caruanae (Kobelt, 1888)	0	0	0	0	0	0	0	0	0	0	0	0	0	0
Chondrula (Mastus) pupa (Linnaeus, 1758)	0	0	0	0	0	0	0	0	0	0	0	0	0	0
Cochlicella acuta (Müller, 1774)	0	0	0	0	0	0	0	0	0	0	0	0	0	0
Pomatias sulcatus (Draparnaud, 1801)	0	0	0	0	0	0	0	0	0	0	0	0	0	0
Helicioid juveniles	0	0	0	0	0	1	0	0	0	0	0	0	0	0
Cecilioides acicula (Müller, 1774)	1	0	0	0	0	1	0	1	0	0	0	0	1	0
Total amount of molluscs	**1**	**1**	**1**	**1**	**1**	**2**	**1**	**2**	**1**	**1**	**1**	**1**	**6**	**5**

Table A5.8 *(cont.).*

Species/Depth (cm)	896	900	903	907	910	914	917	921	924	928	931
Bittium reticulatum (Da Costa, 1778)	0	0	0	0	0	0	0	0	0	0	0
Cardium sp.	0	0	0	0	0	0	0	0	0	0	0
Cerithium sp.	0	0	0	0	0	0	0	0	0	0	0
Gibbula sp.	0	0	0	0	0	0	0	0	0	0	0
Rissoa sp.	0	0	0	0	0	0	0	0	0	0	0
Hydrobia Hartmann, 1821	0	0	0	1	0	1	1	1	0	0	2
Ovatella myosotis (Draparnaud, 1801)	6	9	13	25	18	18	20	58	41	22	7
Truncatella subcylindrica (Linnaeus, 1767)	0	0	0	0	0	0	0	0	0	0	0
Oxyloma elegans (Risso, 1826)	0	1	0	2	3	2	0	2	1	1	1
Pisidium caesertanum (Poli, 1791)	0	0	0	0	0	0	0	1	0	0	0
Pseudamnicola (s.str.) *moussonii* (Calcara, 1841)	0	0	0	1	2	3	7	14	12	7	1
Ancylus fluviatilis Müller, 1774	0	0	0	1	0	0	0	0	0	0	0
Lymnaea (Galba) truncatula (Müller, 1774)	0	0	0	0	0	4	3	2	2	3	1
Planorbis Müller, 1774	0	0	0	2	0	0	0	3	2	3	0
Carychium cf. *schlickumi* Strauch, 1977	0	0	0	1	0	1	0	0	0	0	0
Vallonia pulchella (Müller, 1774)	0	0	0	0	0	0	0	0	0	0	0
Vertigo cf. *antivertigo* (Draparnaud, 1801)	0	0	0	0	1	0	2	0	1	1	0
Lauria cylindracea (Da Costa, 1778)	0	0	0	0	0	0	0	0	0	0	0
Oxychilus Fitzinger, 1833	0	0	0	0	0	0	0	0	0	0	0
Truncatellina callicratis (Scacchi, 1833)	0	0	0	0	0	0	0	0	0	0	0
Papillifera papillaris (Müller, 1774)	0	0	0	0	0	0	0	0	0	0	0
Muticaria macrostoma (Cantraine, 1835)	0	0	0	0	0	0	0	0	0	0	0
Rumina decollata (Linnaeus, 1758)	0	0	0	0	0	0	0	0	0	0	0
Trochoidea spratti (Pfeiffer, 1846)	0	0	0	0	0	0	0	0	0	0	0
Cernuella caruanae (Kobelt, 1888)	0	0	0	0	0	0	0	0	0	0	0
Chondrula (Mastus) pupa (Linnaeus, 1758)	0	0	0	0	0	0	0	0	0	0	0
Cochlicella acuta (Müller, 1774)	1	0	0	0	0	2	0	0	0	0	0
Pomatias sulcatus (Draparnaud, 1801)	0	0	0	0	0	0	0	0	0	0	0
Helicioid juveniles	0	0	1	0	0	0	0	0	0	0	0
Cecilioides acicula (Müller, 1774)	0	0	0	0	0	1	0	0	0	0	0
Total amount of molluscs	**7**	**10**	**14**	**33**	**24**	**32**	**33**	**81**	**59**	**37**	**12**

Table A5.9. *Marsaxlokk 1.*

Species/Depth (cm)	15	19	24	28	32	36	41	45	49	54	58	62	67	71
Alvania sp.	0	0	0	0	0	0	0	0	0	1	3	0	3	1
Bittium sp.	1	1	0	2	3	6	2	2	7	8	12	6	14	8
Bolma rugosa (Linnaeus, 1767)	0	0	0	0	0	0	0	0	0	0	0	0	0	0
Calliostoma sp.	0	1	0	0	0	0	0	0	0	0	0	1	0	1
Cerithium sp.	1	0	6	2	4	7	2	3	3	17	18	8	27	9
Conus mediterraneus (Hwass, 1792)	0	0	0	0	0	1	0	0	0	0	0	0	0	0
Cylichnia sp.	0	0	0	1	0	0	0	0	2	0	0	0	1	1
Gibberula sp.	0	0	0	0	0	0	0	0	0	0	0	0	0	0
Gibbula sp.	0	1	1	1	0	1	1	0	0	3	6	2	2	1
Hexaplex trunculus (Linnaeus, 1758)	0	0	0	0	0	0	1	0	0	0	0	0	0	0
Pirenella conica (Blainville, 1826)	0	1	0	1	0	0	0	0	1	5	2	2	3	6
Retusa truncatula (Brugière, 1792)	0	0	0	0	0	0	0	0	0	0	0	0	2	0
Rissoa sp.	0	3	2	3	4	3	0	2	4	5	10	4	10	2
Tricolia sp.	0	0	0	1	0	0	0	0	0	0	1	0	1	0
Turrida sp.	0	0	0	0	0	0	0	0	0	0	1	3	0	0
Cardium sp.	0	0	0	0	0	0	0	0	0	0	0	0	0	0
Cerastoderma sp.	0	0	0	2	1	0	0	0	0	0	3	0	1	0
Loripes lucinalis (Lamarck, 1818)	0	1	0	0	0	0	0	0	1	1	3	2	3	2
Ostrea sp.	0	0	0	0	0	0	0	0	0	0	0	0	0	0
Spondylus gaedaeropus (Linnaeus, 1758)	0	0	0	0	0	0	0	0	0	0	0	0	0	0
Tellina planata (Linnaeus, 1767)	0	0	0	0	0	0	0	0	0	0	0	0	0	0
other/unknown	0	0	0	0	0	0	0	0	0	0	1	0	0	0
Hydrobia Hartmann, 1821	5	6	10	18	9	12	13	7	14	30	28	18	62	27
Ovatella myosotis (Draparnaud, 1801)	0	0	0	0	0	0	0	0	0	0	0	0	0	0
Truncatella subcylindrica (Linnaeus, 1767)	2	1	1	2	0	0	3	1	0	9	8	3	18	10
Xerotricha Monterosato, 1892	0	1	0	0	0	0	0	0	0	0	0	0	0	0
Granopupa granum (Draparnaud, 1801)	0	0	0	0	0	0	0	0	0	0	0	0	0	0
Papillifera papillaris (Müller, 1774)	0	0	0	0	0	0	0	0	0	0	0	0	0	0
Muticaria Lindholm, 1925	0	0	0	0	0	0	0	0	0	0	0	0	0	0
Trochoidea Brown, 1827	0	0	0	0	0	0	0	0	0	0	0	0	0	0
Cernuella caruanae (Kobelt, 1888)	0	0	0	0	0	0	0	0	0	0	0	0	0	0
Cochlicella acuta (Müller, 1774)	3	2	0	1	0	0	0	0	0	1	0	0	0	0
Eobania vermiculata (Müller, 1774)	0	0	0	0	0	0	0	0	0	0	0	0	0	0
Pomatias sulcatus (Draparnaud, 1801)	0	0	0	0	0	0	0	0	0	0	0	0	0	0
Cecilioides acicula (Müller, 1774)	0	0	0	0	0	0	0	0	0	0	0	1	0	0
Helicioid juveniles	1	0	1	2	0	1	2	1	2	0	0	0	0	0
Total amount of molluscs	**13**	**18**	**21**	**36**	**21**	**31**	**24**	**16**	**34**	**80**	**96**	**50**	**147**	**68**

Table A5.9 *(cont.).*

Species/Depth (cm)	75	80	84	89	94	99	104	109	114	119	124	129	134	139
Alvania sp.	0	0	0	0	0	0	0	0	0	0	0	0	1	0
Bittium sp.	2	0	0	0	0	0	0	0	0	0	0	0	2	18
Bolma rugosa (Linnaeus, 1767)	0	0	0	0	0	0	0	0	0	0	0	0	0	0
Calliostoma sp.	0	1	1	0	0	0	0	0	0	0	0	0	0	0
Cerithium sp.	1	3	1	0	0	0	0	1	1	0	0	13	28	49
Conus mediterraneus (Hwass, 1792)	0	0	0	0	0	0	0	0	0	0	0	0	0	1
Cylichnia sp.	0	0	0	0	0	0	0	0	0	0	0	0	0	0
Gibberula sp.	0	0	0	1	0	0	0	0	0	0	0	0	1	0
Gibbula sp.	0	0	1	0	0	0	0	0	0	0	0	2	4	8
Hexaplex trunculus (Linnaeus, 1758)	0	0	0	0	0	0	0	0	0	0	0	1	0	1
Pirenella conica (Blainville, 1826)	1	0	0	0	0	1	0	0	0	0	3	10	16	40
Retusa truncatula (Brugière, 1792)	0	0	0	0	0	0	0	0	0	0	0	0	0	0
Rissoa sp.	2	0	0	0	1	0	0	1	0	0	2	2	1	3
Tricolia sp.	0	0	0	0	0	0	0	0	0	0	0	0	0	0
Turrida sp.	0	0	0	0	0	0	0	0	0	0	0	0	0	0
Cardium sp.	0	0	0	0	0	0	1	0	0	0	0	0	0	0
Cerastoderma sp.	0	0	1	0	1	0	0	0	0	0	0	0	0	4
Loripes lucinalis (Lamarck, 1818)	0	0	0	0	0	0	0	1	0	2	1	0	3	2
Ostrea sp.	0	0	0	0	0	0	0	0	0	0	0	0	0	0
Spondylus gaedaeropus (Linnaeus, 1758)	0	0	0	0	0	0	0	0	0	0	0	0	0	0
Tellina planata (Linnaeus, 1767)	0	1	1	0	0	0	0	0	1	0	0	0	0	1
other/unknown	0	0	0	0	0	0	0	0	0	0	0	1	0	0
Hydrobia Hartmann, 1821	17	9	10	1	1	1	3	15	24	22	59	47	46	109
Ovatella myosotis (Draparnaud, 1801)	3	1	0	1	14	0	0	0	10	17	21	0	0	0
Truncatella subcylindrica (Linnaeus, 1767)	4	5	6	1	1	0	0	0	3	5	32	23	10	29
Xerotricha Monterosato, 1892	0	0	0	0	0	0	0	0	0	0	0	0	0	0
Granopupa granum (Draparnaud, 1801)	0	0	0	0	0	0	0	0	0	0	0	0	0	0
Papillifera papillaris (Müller, 1774)	1	1	0	0	0	0	0	0	0	0	0	0	0	0
Muticaria Lindholm, 1925	0	0	0	0	0	0	0	0	0	0	0	0	0	0
Trochoidea Brown, 1827	0	0	0	0	0	0	0	0	0	0	0	0	0	0
Cernuella caruanae (Kobelt, 1888)	0	0	0	0	0	0	0	0	0	0	0	0	1	0
Cochlicella acuta (Müller, 1774)	0	1	0	1	0	0	0	0	0	0	0	0	2	0
Eobania vermiculata (Müller, 1774)	0	0	0	0	0	0	0	0	0	0	0	0	0	0
Pomatias sulcatus (Draparnaud, 1801)	0	0	0	0	0	0	0	0	0	0	0	0	1	0
Cecilioides acicula (Müller, 1774)	0	0	0	0	2	1	0	0	0	0	0	0	0	0
Helicioid juveniles	0	0	0	0	0	0	0	0	0	0	0	0	2	1
Total amount of molluscs	**31**	**22**	**21**	**5**	**20**	**3**	**4**	**18**	**39**	**46**	**118**	**99**	**118**	**266**

Table A5.9 *(cont.).*

Species/Depth (cm)	144	149	154	159	164	169	174	179	184	189	194	199	204	209
Alvania sp.	0	3	0	5	3	0	0	0	0	5	0	0	0	0
Bittium sp.	7	2	7	21	34	0	2	2	3	21	21	1	2	2
Bolma rugosa (Linnaeus, 1767)	0	0	0	0	0	0	0	0	0	0	0	0	0	0
Calliostoma sp.	0	0	0	0	0	0	0	0	0	0	0	0	0	0
Cerithium sp.	23	28	15	16	38	3	5	2	15	30	19	2	1	0
Conus mediterraneus (Hwass, 1792)	0	0	0	0	0	0	0	0	0	0	1	0	0	0
Cylichnia sp.	0	0	0	0	1	0	0	0	0	0	0	0	0	0
Gibberula sp.	0	0	0	1	0	0	0	0	0	0	1	0	0	0
Gibbula sp.	5	5	2	8	4	0	0	1	2	5	4	0	0	0
Hexaplex trunculus (Linnaeus, 1758)	0	0	0	2	1	0	0	0	0	0	1	0	0	0
Pirenella conica (Blainville, 1826)	10	7	4	6	9	10	15	3	10	16	13	0	0	0
Retusa truncatula (Brugière, 1792)	0	0	0	0	0	0	0	0	0	0	0	0	0	0
Rissoa sp.	1	4	1	4	11	0	2	0	1	3	3	0	0	0
Tricolia sp.	0	0	0	0	1	0	0	0	0	0	0	0	0	0
Turrida sp.	0	0	0	0	0	0	0	0	0	0	0	0	0	0
Cardium sp.	0	0	0	0	0	0	0	0	0	0	0	1	0	0
Cerastoderma sp.	0	0	0	1	2	1	0	0	1	0	1	0	0	0
Loripes lucinalis (Lamarck, 1818)	0	3	5	4	5	2	3	0	2	3	3	0	0	0
Ostrea sp.	0	0	0	0	0	0	0	0	0	0	1	0	0	0
Spondylus gaedaeropus (Linnaeus, 1758)	0	0	0	0	0	0	0	0	0	0	0	0	0	0
Tellina planata (Linnaeus, 1767)	2	0	0	0	0	0	0	0	0	0	0	0	0	0
other/unknown	0	0	0	0	0	0	0	0	0	0	0	0	0	0
Hydrobia Hartmann, 1821	91	48	37	10	35	59	249	103	26	15	12	1	0	0
Ovatella myosotis (Draparnaud, 1801)	1	0	0	0	0	7	0	1	1	2	4	3	8	1
Truncatella subcylindrica (Linnaeus, 1767)	40	103	42	9	6	62	35	10	18	3	4	1	1	0
Xerotricha Monterosato, 1892	0	0	1	0	0	0	0	0	0	0	0	0	0	0
Granopupa granum (Draparnaud, 1801)	0	0	0	0	0	0	0	0	0	0	0	0	1	0
Papillifera papillaris (Müller, 1774)	0	0	1	0	0	0	0	0	0	0	0	1	0	0
Muticaria Lindholm, 1925	0	0	0	0	0	0	0	0	0	0	0	0	0	0
Trochoidea Brown, 1827	0	0	0	0	0	0	0	0	0	0	0	3	1	1
Cernuella caruanae (Kobelt, 1888)	0	0	0	0	0	0	0	0	0	0	1	3	2	2
Cochlicella acuta (Müller, 1774)	1	0	1	1	0	0	1	0	2	1	0	1	16	1
Eobania vermiculata (Müller, 1774)	0	0	0	0	0	0	0	0	0	0	0	0	0	0
Pomatias sulcatus (Draparnaud, 1801)	0	0	0	0	0	0	0	0	0	0	2	0	0	0
Cecilioides acicula (Müller, 1774)	1	0	0	0	0	0	0	0	0	0	0	0	0	2
Helicioid juveniles	0	0	0	0	0	0	0	0	0	1	1	0	0	0
Total amount of molluscs	**182**	**203**	**116**	**88**	**150**	**144**	**312**	**122**	**81**	**105**	**92**	**17**	**32**	**9**

Table A5.9 *(cont.).*

Species/Depth (cm)	214	219	224	229	234	239	244	249	254	259	264	269	274	279
Alvania sp.	0	0	0	0	0	0	0	0	0	0	0	0	0	0
Bittium sp.	0	1	0	1	0	0	1	0	0	1	0	1	0	1
Bolma rugosa (Linnaeus, 1767)	0	0	0	0	0	0	0	0	0	0	0	0	0	0
Calliostoma sp.	0	0	0	0	0	0	0	0	0	0	0	0	0	0
Cerithium sp.	0	0	0	0	0	0	0	0	0	0	0	0	0	0
Conus mediterraneus (Hwass, 1792)	0	0	0	0	0	0	0	0	0	0	0	0	0	0
Cylichnia sp.	0	0	0	0	0	0	0	0	0	0	0	0	0	0
Gibberula sp.	0	0	0	0	0	0	0	0	0	0	0	0	0	0
Gibbula sp.	0	0	0	0	0	0	0	0	0	0	0	0	0	0
Hexaplex trunculus (Linnaeus, 1758)	0	0	0	0	0	0	0	0	0	0	0	0	0	0
Pirenella conica (Blainville, 1826)	0	1	0	0	0	0	0	0	0	0	0	0	0	0
Retusa truncatula (Brugière, 1792)	0	0	0	0	0	0	0	0	0	0	0	0	0	0
Rissoa sp.	0	0	0	0	0	0	0	0	0	0	0	0	0	0
Tricolia sp.	0	0	0	0	0	0	0	0	0	0	0	0	0	0
Turrida sp.	0	0	0	0	0	0	0	0	0	0	0	0	0	0
Cardium sp.	0	0	0	0	0	0	0	0	0	0	0	0	0	0
Cerastoderma sp.	0	0	0	0	0	0	0	0	0	0	0	0	0	0
Loripes lucinalis (Lamarck, 1818)	0	0	0	0	0	0	0	0	0	0	0	0	0	0
Ostrea sp.	0	0	0	0	0	0	0	0	0	0	0	1	0	0
Spondylus gaedaeropus (Linnaeus, 1758)	0	0	0	0	0	0	0	0	0	0	0	0	0	0
Tellina planata (Linnaeus, 1767)	0	0	0	0	0	0	0	0	0	0	0	0	0	0
other/unknown	0	0	0	0	0	0	0	0	0	0	0	0	0	0
Hydrobia Hartmann, 1821	0	1	0	0	1	0	0	2	0	0	2	0	0	0
Ovatella myosotis (Draparnaud, 1801)	0	0	0	0	0	0	0	0	0	0	0	0	0	0
Truncatella subcylindrica (Linnaeus, 1767)	0	0	0	0	0	0	0	0	0	0	0	0	0	0
Xerotricha Monterosato, 1892	0	0	0	0	0	0	0	0	0	0	0	0	0	0
Granopupa granum (Draparnaud, 1801)	0	0	0	0	0	0	0	0	0	0	0	0	0	0
Papillifera papillaris (Müller, 1774)	0	0	0	0	1	0	0	0	0	2	0	0	0	0
Muticaria Lindholm, 1925	0	0	0	0	0	0	0	0	0	0	1	0	0	1
Trochoidea Brown, 1827	1	0	2	2	0	1	0	0	1	0	0	2	3	0
Cernuella caruanae (Kobelt, 1888)	1	1	2	1	2	1	1	0	1	0	1	2	0	0
Cochlicella acuta (Müller, 1774)	0	0	2	0	2	0	1	1	2	0	0	1	0	0
Eobania vermiculata (Müller, 1774)	0	0	0	0	0	0	0	0	0	0	0	0	3	0
Pomatias sulcatus (Draparnaud, 1801)	0	0	0	0	0	0	0	0	0	0	1	0	0	1
Cecilioides acicula (Müller, 1774)	0	0	0	0	0	0	0	1	0	0	0	0	0	0
Helicioid juveniles	0	0	0	0	0	0	1	0	1	1	2	0	3	0
Total amount of molluscs	**2**	**4**	**6**	**4**	**6**	**2**	**4**	**4**	**5**	**4**	**7**	**7**	**9**	**3**

Table A5.9 *(cont.).*

Species/Depth (cm)	284	289	294	299	304	309	314	319	324	329	334	339	344	349
Alvania sp.	0	0	4	2	2	0	0	0	0	0	0	0	0	0
Bittium sp.	0	5	15	6	2	2	0	0	0	0	0	0	0	0
Bolma rugosa (Linnaeus, 1767)	0	0	0	1	1	0	0	0	0	0	0	0	0	0
Calliostoma sp.	0	0	0	0	0	0	0	0	0	0	0	0	0	0
Cerithium sp.	0	5	31	9	3	2	0	0	0	0	0	0	0	0
Conus mediterraneus (Hwass, 1792)	0	0	0	0	0	0	0	0	0	0	0	0	0	0
Cylichnia sp.	0	2	0	0	0	0	0	0	0	0	0	0	0	0
Gibberula sp.	0	0	0	0	0	0	0	0	0	0	0	0	0	0
Gibbula sp.	0	5	8	3	1	1	0	1	1	0	0	0	0	0
Hexaplex trunculus (Linnaeus, 1758)	0	0	0	0	0	0	0	0	0	0	0	0	0	0
Pirenella conica (Blainville, 1826)	0	9	8	5	0	0	0	0	0	0	0	0	0	0
Retusa truncatula (Brugière, 1792)	0	0	0	0	0	0	0	0	0	0	0	0	0	0
Rissoa sp.	0	10	6	2	1	1	0	0	0	0	0	0	0	0
Tricolia sp.	0	1	0	0	1	0	0	0	0	0	0	0	0	0
Turrida sp.	0	0	1	0	0	0	0	0	0	0	0	0	0	0
Cardium sp.	0	0	0	0	0	0	0	0	0	0	0	0	0	0
Cerastoderma sp.	0	1	3	1	0	0	0	0	0	0	0	0	0	0
Loripes lucinalis (Lamarck, 1818)	0	3	3	1	1	0	0	0	1	0	0	0	0	0
Ostrea sp.	0	0	0	0	1	0	0	0	0	0	0	0	0	0
Spondylus gaedaeropus (Linnaeus, 1758)	0	1	0	0	0	0	0	0	0	0	0	0	0	0
Tellina planata (Linnaeus, 1767)	0	0	0	0	0	0	0	0	0	0	0	0	0	0
other/unknown	0	0	0	0	0	0	2	0	0	0	0	0	0	0
Hydrobia Hartmann, 1821	0	4	4	4	0	0	0	0	0	0	0	0	0	0
Ovatella myosotis (Draparnaud, 1801)	0	0	0	0	0	0	0	0	0	0	0	0	0	0
Truncatella subcylindrica (Linnaeus, 1767)	0	0	3	3	0	0	0	0	0	0	0	0	0	0
Xerotricha Monterosato, 1892	0	0	0	0	0	0	0	0	0	0	0	0	0	0
Granopupa granum (Draparnaud, 1801)	0	0	0	0	0	0	0	0	0	0	0	0	0	0
Papillifera papillaris (Müller, 1774)	0	0	0	0	0	0	0	0	0	0	0	0	0	0
Muticaria Lindholm, 1925	0	0	0	0	0	0	0	0	0	0	0	0	0	0
Trochoidea Brown, 1827	1	0	0	0	0	0	0	0	0	0	0	0	0	0
Cernuella caruanae (Kobelt, 1888)	0	0	0	0	0	0	0	0	0	0	0	0	0	0
Cochlicella acuta (Müller, 1774)	0	0	1	0	0	0	0	0	0	0	0	0	0	0
Eobania vermiculata (Müller, 1774)	0	0	1	0	0	0	0	0	0	0	0	0	0	0
Pomatias sulcatus (Draparnaud, 1801)	0	0	0	0	0	0	0	0	0	0	0	0	0	0
Cecilioides acicula (Müller, 1774)	0	0	0	0	0	0	0	0	0	0	0	0	0	0
Helicioid juveniles	0	1	0	0	0	0	0	0	0	0	0	0	0	0
Total amount of molluscs	**1**	**47**	**88**	**37**	**13**	**6**	**1**	**1**	**2**	**1**	**1**	**1**	**1**	**1**

Table A5.9 *(cont.).*

Species/Depth (cm)	354	359	364	369	374	379	384
Alvania sp.	0	0	0	0	0	0	0
Bittium sp.	0	0	0	0	0	0	0
Bolma rugosa (Linnaeus, 1767)	0	0	0	0	0	0	0
Calliostoma sp.	0	0	0	0	0	0	0
Cerithium sp.	0	0	0	0	0	0	0
Conus mediterraneus (Hwass, 1792)	0	0	0	0	0	0	0
Cylichnia sp.	0	0	0	0	0	0	0
Gibberula sp.	0	0	0	0	0	0	0
Gibbula sp.	0	0	0	0	0	0	0
Hexaplex trunculus (Linnaeus, 1758)	0	0	0	0	0	0	0
Pirenella conica (Blainville, 1826)	0	0	0	0	0	0	0
Retusa truncatula (Brugière, 1792)	0	0	0	0	0	0	0
Rissoa sp.	0	0	0	0	0	0	0
Tricolia sp.	0	0	0	0	0	0	0
Turrida sp.	0	0	0	0	0	0	0
Cardium sp.	0	0	0	0	0	0	0
Cerastoderma sp.	0	0	0	0	0	0	0
Loripes lucinalis (Lamarck, 1818)	0	0	0	0	0	0	0
Ostrea sp.	0	0	0	0	0	0	0
Spondylus gaedaeropus (Linnaeus, 1758)	0	0	0	0	0	0	0
Tellina planata (Linnaeus, 1767)	0	0	0	0	0	0	0
other/unknown	0	0	0	0	0	0	0
Hydrobia Hartmann, 1821	0	0	0	0	0	0	0
Ovatella myosotis (Draparnaud, 1801)	0	0	0	0	0	0	0
Truncatella subcylindrica (Linnaeus, 1767)	0	0	0	0	0	0	0
Xerotricha Monterosato, 1892	0	0	0	0	0	0	0
Granopupa granum (Draparnaud, 1801)	0	0	0	0	0	0	0
Papillifera papillaris (Müller, 1774)	0	0	0	0	0	0	0
Muticaria Lindholm, 1925	0	0	0	0	0	0	0
Trochoidea Brown, 1827	0	0	0	0	0	0	0
Cernuella caruanae (Kobelt, 1888)	0	0	0	0	0	0	0
Cochlicella acuta (Müller, 1774)	0	0	0	0	0	0	0
Eobania vermiculata (Müller, 1774)	0	0	0	0	0	0	0
Pomatias sulcatus (Draparnaud, 1801)	0	0	0	0	0	0	0
Cecilioides acicula (Müller, 1774)	0	0	0	0	0	0	0
Helicioid juveniles	0	0	0	0	0	0	0
Total amount of molluscs	**1**	**1**	**1**	**1**	**1**	**1**	**1**

Appendix 6

The borehole and test excavation profile log descriptions

Charles French & Sean Taylor

Ġgantija and Ramla Valley

Transect A: Ġgantija to In-Nuffara across Ramla valley

BH 1 (N 36° 02.812/E 014° 16.100)
0–45 dark greyish brown silty clay loam with few fine stone fragments; Ap
45–55 dark brown silty clay loam with few charcoal fragments; B
55+cm weathered Coralline Limestone; C

BH2 (N 36° 02.807/E 014° 16.185)
0–55 dark greyish brown silty clay loam with few fine stone fragments; Ap
55–95 dark brown silty clay loam with few charcoal fragments; B
95+cm weathered Coralline Limestone; C

BH3 (N 36° 02.798/E 014° 16.189)
0–35 dark greyish brown silty clay loam with few fine stone fragments; Ap
35–45+cm weathered Coralline Limestone; C

BH4 (N 36° 02.798/E 014° 16.193)
0–35 dark greyish brown silty clay loam with few fine stone fragments; Ap
35–45+cm weathered Coralline Limestone; C

BH5 (N 36° 02.792/E 014° 16.193)
0–35 dark greyish brown silty clay loam with few fine stone fragments; Ap
35–40+cm weathered Coralline Limestone; C

BH6 (N 36° 02.777/E 014° 16.207)
0–40 grey silty clay; Ap
40+cm weathered, mottled grey/orange silty clay; B/C (change to Blue Clay geology)

BH7 (N 36° 02.770/E 014° 16.210)
0–40 grey silty clay; Ap
40+cm weathered, mottled grey/orange silty clay; B/C

BH8 (N 36° 02.764/E 014° 16.215)
0–40 grey silty clay loam; Ap
40+cm weathered, mottled grey/orange silty clay; B/C

BH9 (N 36° 02.760/E 014° 16.216)
0–40 grey silty clay loam; Ap
40+cm weathered, mottled grey/orange silty clay; B/C

BH10 (N 36° 02.753/E 014° 16.224)
0–40 grey silty clay loam; Ap
40+cm weathered, mottled grey/orange silty clay; B/C

BH11 (N 36° 02.745/E 014° 14.229)
0–40 grey silty clay loam; Ap
40+cm weathered, mottled grey/orange silty clay; B/C

BH12 (N 36° 02.734/E 014° 16.245)
0–40 grey silty clay loam; Ap
40+cm weathered, mottled grey/orange silty clay; B/C

BH13 (N 36° 02.723/E 014° 16.245)
0–70 grey silty clay loam; Ap
70+cm weathered, mottled grey/orange silty clay; B/C

BH14 (N 36° 02.715/E 014° 16.251)
0–50 grey silty clay loam; Ap
50+cm weathered, mottled grey/orange silty clay; B/C

BH15 (N 36° 02.704/E 014° 16.266)
0–50 grey silty clay loam; Ap
50+cm weathered, mottled grey/orange silty clay; B/C

BH16 (N 36° 02.693/E 014° 16.280)
0–50 grey silty clay loam; Ap
50–70 yellowish/orangey brown gravelly silt; stream bed
70–80 weathered, mottled grey/orange silty clay and stones (<5 cm); B/C and stream bed
80+cm limestone pebbles and Blue Clay; C

BH17 (N 36° 02.696/E 014° 16.294)
0–70 grey silty clay loam; Ap
70+cm weathered, mottled grey/orange silty clay; B/C (on Blue Clay geology)

BH18 (N 36° 02.677/E 014° 16.313)
0–70 grey silty clay loam; Ap
70+cm weathered, mottled grey/orange silty clay; B/C

BH19 (N 36° 02.661/E 014° 16.332)
0–70 grey silty clay loam; Ap
70+cm weathered, mottled grey/orange silty clay; Blue Clay B/C

BH20 (N 36° 02.642/E 014° 16.341)
0–70 grey silty clay loam; Ap
70+cm weathered, mottled grey/orange silty clay; B/C

BH21 (N 36° 02.634/E 014° 16.339)
0–70 grey silty clay loam; Ap
70+cm weathered, mottled grey/orange silty clay; B/C

BH22 (N 36° 02.624/E 014° 16.359)
0–70 grey silty clay loam; Ap
70+cm weathered, mottled grey/orange silty clay; B/C

BH23 (N 36° 02.610/E 014° 16.360)
0–70 grey/orangey brown silty clay loam with occasional quartz gravel (<1 cm); Ap
70+cm weathered, yellowish brown silt; B/C

BH24 (N 36° 02.603/E 014° 16.383)
0–60 brown/yellowish/orangey brown silty clay loam with mix of limestone gravel (<1 cm); Ap
60+cm weathered Coralline Limestone; B/C

BH25 (N 36° 02.592/E 014° 16.374)
0–85 orangey brown loam; Ap
85+cm stone boulders (<20 cm); C

BH26 (N 36° 02.540/E 014° 16.412)
0–30 brown sandy loam with even mix of limtestone pebbles (<1 cm); Ap
35+cm weathered Coralline Limestone of In-Nuffara plateau; C

Transect B: downstream along southern side of Ramla valley to the coast

BH27 (N 36° 02.769/E 014° 16.745)
0–35 reddish brown loam with few fragments of limestone rubble
35+cm grey silty clay; B/C

BH28 (N 36° 02.745/E 014° 16.726)
0–10 yellowish brown silt loam with mix of limestone fragments
10–30 grey clay
30+cm reddish brown sandy loam; ? made ground

BH 29 (N 36° 02.830/E 014° 16.809)
0–60 mix of greyish brown silty clay loam with common fine gravel (<3 cm)
60+cm mottled brown silty clay; B/C

BH 30 (N 36° 02.907/E 014° 16.905)
0–50 mix of greyish brown silty clay loam with common fine gravel (<3 cm)
50+cm mottled greyish brown clay; B/C

BH 600 (N 36° 02.921/E 014° 16.923
0–80 very pale brown, calcareous, very fine sandy/silt loam, becoming mottled from *c.* 50 cm
80+cm weathered Globigerina Limestone

BH 601 (N 36° 02.915/E 014° 16.961)
0–100 yellowish brown silty clay loam and limestone rubble
100+cm weathered Globigerina Limestone

Transect C: from Ramla Bay up-valley

4 sets of terraces visible up-valley from sea on low Globigerina/ Upper Coralline mesa-like spines

BH31 (N 36° 03.140/E 014° 17.097; 3rd terrace)
0–80 pale brown very fine sandy silt loam; loessic like Ap
80–100 orangey/pale brown fine sandy silt loam; loessic B
100+cm orangey brown fine sand; ? loessic B/C

BH32 (N 36° 03.135/E 014° 17.087; 2nd terrace)
0–90 pale brown very fine sandy silt loam; loessic like Ap
90+cm orangey brown fine sand; ? loessic B/C

BH33 (N 36° 03.110/E 014° 17.083; 2nd terrace)
0–70 pale brown very fine sandy silty clay loam; loessic like Ap
70+cm grey/orange mottled sandy/silty clay; Blue Clay B/C

BH34 (N 36° 03.034/E 014° 17.165; 1st terrace)
0–80 pale brown very fine sandy silt loam; loessic like Ap
80–100 orangey/pale brown fine sandy silt; loessic B
100+cm orangey brown fine sand; ? loessic B/C

Transect D: from platform infront of Ġgantija temple to west

BH35 (N 36° 02.810/E 014° 16.156)
0–45 brown silty clay loam with common small limestone pebbles (<2 cm); Ap
45+cm iron-rich weathered Coralline Limestone; C

BH36 (N 36° 02.800/E 014° 16.141)
0–15 brown silty clay loam with common small limestone pebbles (<2 cm); Ap
15+cm iron-rich weathered Coralline Limestone; C

BH37 (N 36° 02.79/E 014° 16.120)
0+cm weathered Coralline Limestone at surface; C

BH38 (N 36° 02.807/E 014° 16.124)
0–25 reddish brown silty clay loam; Ap
15+cm iron-rich weathered Coralline Limestone; C

BH39 (N 36° 02.806/E 014° 16.100)
0–10 reddish brown silty clay loam; Ap
10+cm iron-rich weathered Coralline Limestone; C

BH40 (N 36° 02.797/E 014° 16.090)
0–30 reddish brown silty clay loam with limestone pebbles (<2 cm); Ap
30+cm iron-rich weathered Coralline Limestone; C

BH41 (N 36° 02.789/E 014° 16.155)
0–70 dark reddish brown silty clay loam with even mix of limestone pebbles (<2 cm); Ap
70+cm iron-rich weathered Coralline Limestone; C

BH59 (N 36° 02.855/E 014° 16.199)
0–130 greyish brown/grey mottled silty clay loam; Ap and ? imported soil/made ground
130–135 dark reddish brown silty clay loam; ? buried B
135+cm weathered Coralline limestone; C

Transect E: to east and northeast of Ġgantija temple, east of Tr A

BH42 (N 36° 02.830/E 014° 16.198)
0–30 reddish brown silty clay loam with common stone rubble; Ap
30+cm Coralline Limestone bedrock; C

BH43 (N 36° 02.837/E 014° 16.211)
0–30 reddish brown silty clay loam with common stone rubble; Ap
30+cm Coralline Limestone bedrock; C

BH44 (N 36° 02.869/E 014° 16.173)
0–30 pale brown fine sandy silt loam; Ap
30–40 dark brown silt loam with few fine charcoal and pottery fragments; anthropogenic buried Ah
40+cm Coralline Limestone bedrock; C

BH45 (N 36° 02.872/E 014° 16.179)
0–55 pale greyish brown silt loam; Ap
55–75 reddish brown silty clay loam with fine pea-grit gravel
75+cm weathered Coralline Limestone; C

BH46 (N 36° 02.875/E 014° 16.182)
0–35 pale brown silt loam; Ap
35–120 pale brown to brown mixture of silt and silty clay with few fine charcoal fragments; imported soil ? (tenant farmer said soil imported in 1961 when olive grove planted) as a B mixed with anthropogenic buried soil ?
120+cm reddish brown silty clay loam with mollusc shell fragments; buried *terra rossa* B horizon ?

BH47 (N 36° 02.880/E 014° 16.186)
0–45 pale brown silt loam; Ap
45–120 mottled grey/orangey/yellowish brown, fine sandy/silty clay loam; imported soil ?
120–140 grey/yellow very fine sand and silt; B/C
140+cm weathered Coralline Limestone; C

BH48 (N 36° 02.886/E 014° 16.196)
0–45 pale brown silt loam; Ap
45–110 yellowish brown fine sandy/silty clay; imported soil ? as a B
110+cm reddish brown silty clay loam with fine limestone fragments; buried *terra rossa* B horizon ?

BH49 (N 36° 02.889/E 014° 16.207)
0–50 pale brown silt loam; Ap
50–65 brown silty clay with limestone fragments; imported soil ?
65–120 mottled yellow/grey silt loam; imported soil ?
120–130 yellow/grey silty clay; imported soil ?
130+cm pale yellow silt and very fine sand; B/C

BH50 (N 36° 02.895/E 014° 16.177)
0–110 reddish brown silty clay loam with pea-grit gravel and limestone pebbles (<5 cm); imported soil ?
110+ weathered Coralline limestone; C

BH51 (N 36° 02.908/E 014° 16.174)
0–110 reddish brown silty clay loam with pea-grit gravel and limestone pebbles (<5 cm); imported soil ?
110+ weathered Coralline Limestone; C
Samples taken: spot small bulk at 10–20 cm

BH52 (N 36° 02.913/E 014° 16.165)
0–10 brown silty clay loam with common limestone rubble; Ap
10+ cm weathered Coralline Limestone: C

BH53 (N 36° 02.904/E 014° 16.149)
0–60 brown to greyish brown silty clay loam; Ap
60+cm weathered Coralline Limestone; C

Transect F: parallel and to east of Tr E

BH54 (N 36° 02.863/E 014° 16.184)
0–70 greyish brown silt loam with even mix of small limestone fragments (<10 cm); Ap
70–115 dark brown silty clay loam with few pottery and charcoal fragments; anthropogenic buried Ah
115–130 brown silty clay loam with minor pottery/charcoal fragments; buried B horizon
130+cm weathered Coralline Limestone; C
Samples taken: spot micromorphology block at *c.* 80–85 cm; spot small bulks at 10–20 and 70–80 cm

BH55 (N 36° 02.870/E 014° 16.195)
0–35 greyish brown/grey mottled silt loam; Ap
35–50 dark reddish brown silty clay loam with fine pea-grit limestone
50+cm weathered Coralline Limestone; C

BH56 (N 36° 02.876/E 014° 16.200)
0–65 greyish brown/grey mottled silt loam; Ap
65–80 dark reddish brown silty clay loam with fine pea-grit limestone
80+cm weathered Coralline Limestone; C

BH57 (N 36° 02.894/E 014° 16.2111)
0–50 greyish brown/grey mottled silt loam; Ap
50–60 dark reddish brown silty clay loam with fine pea-grit limestone
60+cm weathered Coralline Limestone; C

BH58 (N 36° 02.907/E 014° 16.204)
0–100 greyish brown/grey mottled silt loam; Ap
100–110 dark reddish brown silty clay loam wit fine pea-grit limestone
110+cm weathered Coralline Limestone; C

Transect G: Ramla valley

BH60 (N 36° 03.318/E 014° 16.023)
0–150 yellowish brown very fine sand silt loam; Ap and hillwash
150+cm bedded Coralline Limestone; C

BH61 (N 36° 03.314/E 014° 16.039)
0–80 pale brown fine sandy silt loam with small irregular blocky structure; alluvial valley fill
80–140 grey clay and limestone blocks (<15 cm); C

BH62 (N 36° 03.313/E 014° 16.039)
0–200 pale brown very fine sand silt loam with common very fine gravel (<1 cm) with columnar blocky structure; colluvial valley fill
200+cm Coralline limestone bedrock; C

BH63 (N 36° 03.397/E 014° 16.975)

0–50	pale brown fine sandy/silty clay loam; Ap
50–80	mix of pale brown fine sandy/silty clay loam and limestone pebbles; colluvial valley fill
80–160	weathered, crumbly limestone; B/C
160+cm	Coralline Limestone bedrock; C

BH64 (N 36° 03.424/E 014° 17.047)

0–175	banded, grey to pale brown, calcareous fine sandy silts; episodes of eroded soil deposition
175–190	bedded rounded pebbles, <5 cm; riverbed/outwash
190–220	bedded brown silt; episodes of eroded soil deposition
220+cm	riverbed cobbles (<20 cm)

BH65 (N 36° 03.479/E 014° 17.058)

0–50	brown sandy silty clay loam; eroded soil deposition
50–125	brown sandy silty clay with even mix of pebbles; eroded colluvial soil/bedload
125–250	partly bedded river cobbles (<20 cm) and stones (5 cm); high velocity mixture of erosion and riverbed deposits

BH 66 (N 36° 03.522/E 014° 17.031)

0–150	bedded sand and sandy silts interrupted by few lenses of pebbles; episodes of eroded soil deposition
150–250	coarse bedded cobbles in a greyish brown silt loam soil matrix interrupted by lenses of sand/silt; episodic high/low velocity erosion; contains a few pieces of included Roman pottery
250–310	grey silty clay; eroded clay substrate from up-valley
310–350	reddish brown silt loam; eroded soil from up-valley
350–365	fine pebbles (<10 cm)
365+cm	bedded cobbles; riverbed

Profile 627 (N36° 03.442/E 014° 17.045): for OSL, micromorphology and small bulk sampling

+100	modern made ground and water pipes
0–4	(= top of modern stone wall adjacent); pinkish-grey (5YR7/3) fine gravel and coarse sand; waterborne/ colluvial coarse material
4–13	pale grey (5YR7/1), calcareous silt loam; fine alluvium with drying and secondary calcification
13–15	fine rounded pebbles (<1 cm); colluvial wash
15–26	pale grey (5YR7/1), calcareous silt loam; fine alluvium with secondary calcification
26–28	fine rounded pebbles (<1 cm); colluvial wash
28–46	pale grey (5YR7/1), calcareous silt loam; fine alluvium with secondary calcification
46–60	pale grey (5YR7/1) calcareous silt loam; fine alluvium
90–100	greyish brown (10YR5/2) silt loam with abundant horizontally bedded fine to medium pebbles (<5 cm); mixed soil/limestone rubble erosion as possible small alluvial outwash fans
100–140	greyish brown (10YR5/2) fine and silt; becoming more a loamy sand with depth; fine alluvium
140+cm	Globigerina Limestone; bedrock

Samples taken: Micromorphology blocks and small bulk samples at 4–14, 75–85 and 103–110 cm; OSL profiling samples at 7.5, 15, 27.5, 45, 60, 75, 82.5, 105, 115, 125 and 140 cm; OSL dating tubes at 15–20, 62–66 and 103–106 cm

Transect H: Ta Marziena

BH67 (N 36° 02.005/E 014° 14.400; inside temple)

0–10	brown silt loam with occasional fine limestone pebbles (<5 mm); Ah
10+cm	Coralline Limestone bedrock; C

BH68 (N 36° 01.978/E 014° 14.407)

0–50	grey silty clay loam with common calcium carbonate aggregates and few limestone fragments (<1 cm)
50+cm	grey/yellowish grey mottled clay loam; B/C

BH69 (N 36° 01.983/E 014° 14.382)

0–45	brown fine sandy silt loam with few fine limestone pebbles (<5 mm); Ap
45+cm	Coralline Limestone bedrock; C

BH70 (N 36° 01.964/E 014° 14.391)

0–50	brown fine sandy silt loam with few fine limestone pebbles (<5 mm); Ap
50–75	pale grey/yellowish grey silty clay loam; B
75+cm	grey/yellowish grey mottled clay loam; B/C

BH71 (N 36° 01.926/E 014° 14.400)

0–50	brown fine sandy silt loam with few fine limestone pebbles (<5 mm); Ap
50–75	pale grey/yellowish grey silty clay loam; B
75+cm	grey/yellowish grey mottled clay loam; B/C

BH72 (N 36° 01.891/E 014° 14.391)

0–50	brown fine sandy silt loam with few fine limestone pebbles (<5 mm); Ap
50–75	pale grey/yellowish grey silty clay loam; B
75+cm	grey/yellowish grey mottled clay loam; B/C

BH73 (N 36° 01.827/E 014° 14.391)

0–80	brown silty clay loam with common fine limestone pebbles (<5 mm); Ap
80–90	pale reddish/yellowish brown silty clay loam with common fine limestone fragments (<5 mm); buried B of palaeosol
90–120	dark reddish brown silty clay loam with common fine limestone fragments (<5 mm); probably buried clay-enriched Bt of palaeosol
120+cm	weathered Coralline Limestone bedrock; C

BH74 (N 36° 01.792/E 014° 14.331)

0–50	reddish brown silty clay loam with common fine limestone pebbles (<5 mm); Ap
50–80	pale reddish brown silty clay loam with common fine limestone pebbles and fragments (<5 cm); B
80+cm	weathered Coralline Limestone bedrock; C

BH75 (N 36°01.744/E 014° 14.299)

0–50	pale reddish brown silt loam with common fine limestone pebbles (<2 cm); Ap
50+cm	weathered Coralline Limestone bedrock; C

BH 602 (N 36° 01.987/E 014° 14.387)

0–50	brown sandy/silt loam with even mix of limestone
50+cm	weathered Coralline Limestone

BH 603 (N 36° 01.979/E 014° 14.380)

0–40	brown sandy/silt loam with even mix of limestone
40+cm	weathered Coralline Limestone

BH 604 (N 36° 01.972/E 014° 14.382)
0–30 greyish brown silty clay loam
30–100 mottled greyish/yellowish brown silty clay with calcium carbonate aggregates
100+cm grey clay B/C

BH 605 (N 36° 01.969/E 014° 14.385)
0–30 yellowish brown silty clay loam
30–100 mottled greyish/yellowish brown silty clay with calcium carbonate aggregates
100+cm grey clay B/C

Transect I: southwest side of Ramla valley, starting between Tal Hamrija and It Tafilija)

BH76 (N 36° 03.428/E 014° 16.532)
0–45 yellowish brown fine to coarse sandy silt loam; Ap
45–60 yellow sand/silt; B
60+cm weathered Coralline Limestone; C

BH77 (N 36° 03.425/E 014° 16.545)
0–50 aggregated pale yellowish brown silty clay loam with few limestone pebbles; Ap
50+cm grey/yellowish brown silty clay with limestone fragments; B/C

BH78 (N 36° 03.425/E 014° 16.557)
0–60 yellowish brown to pale reddish brown coarse-fine sandy/silt loam with few limestone pebbles; Ap
60–70 orangey brown silty clay loam
70+cm grey/yellow silt; B/C

BH79 (N 36° 03.429/E 014° 16.567)
0–35 grey silty clay loam; Ap
35–60+cm pale grey/yellow silt with orange mottles; B/C

BH80 (N 36° 03.430/E 014° 16.570)
0–35 greyish brown silty clay loam; Ap
35–70+cm pale grey/yellow silt with orange mottles; B/C

BH81 (N 36° 03.430/E 014° 16.570)
0–30 greyish brown silty clay loam; Ap
30+cm Coralline Limestone pebbles; C

BH82 (N 36° 03.419/E 014° 16.620)
0–50 grey silty clay loam; Ap
50+cm grey silty clay; B/C

BH83 (N 36° 03.487/E 014° 16.694)
0–60 pale brown silt loam; Ap
60+cm grey silty clay; B/C

BH84 (N 36° 03.479/E 014° 16.761)
0–50 greyish brown silty clay loam; Ap
50+cm grey silty clay; B/C

BH85 (N 36° 03.473/E 014° 16.797)
0–30 greyish brown silty clay loam with few limestone pebbles
30+cm Coralline Limestone pebbles; C

BH86 (N 36° 03.487/E 014° 16.890)
0–50 pale greyish brown fine sandy clay loam; Ap
50+cm laminar pale grey Globigerina Limestone; C

Transect J: from southern end of In-Nuffara downslope to east

BH87 (N 36° 02.401/E 014° 16.430)
0–5 pale brown fine sandy silt loam; Ah
5+cm Coralline Limestone bedrock; C

BH88 (N 36° 02.410/E 014° 16.446)
0–50 greyish yellow silt loam; Ap
50+cm Coralline Limestone bedrock; C

BH89 (N 36° 02.406/E 014° 16.523)
0–60 greyish yellow silt loam; Ap
60+cm Coralline Limestone bedrock; C

BH90 (N 36° 02.406/E 014° 16.523)
0–60 greyish yellow silt loam; Ap
60+cm Coralline Limestone bedrock; C

BH91 (N 36° 02.395/E 014° 15.545)
0–60 grey silty clay loam; Ap
60+cm Coralline Limestone bedrock; C

BH92 (N 36° 02.389/E 014° 16.590)
0–60 grey silty clay loam; Ap
60+cm Coralline Limestone bedrock; C
Samples taken: spot small bulk sample at 10–20 cm

BH93 (N 36° 02.377/E 014° 16.646)
0–50 yellowish brown to grey silt loam; Ap
50+cm Coralline Limestone bedrock; C

BH94 (N 36° 02.392/E 014° 16.646)
0–60 greyish brown fine sandy/silt loam with even mix of limestone pebbles; Ap
60+cm Globigerina Limestone bedrock; C

BH95 (N 36° 02.358/E 014° 16.659)
0–60 greyish brown fine sandy/silt loam with even mix of limestone pebbles; Ap
60+cm Globigerina Limestone bedrock; C

Transect M: from Tar-Rumiena round-about southwards to Xewkija

BH104 (N 36° 02.860/E 014° 16.200)
0–50 pal brown fine sandy silt loam; Ap
50–110+cm pale yellowish/greyish brown silt loam; gleyed B/C

BH105 (N 36° 02.287/E 014° 15.864)
0–50 pal brown fine sandy silt loam; Ap
50–90+cm pale yellowish/greyish brown silt loam with small weathered limestone fragments (<1 cm); gleyed B/C

BH106 (N 36° 02.266/E 014° 15.052)
0–50 pal brown fine sandy silt loam; Ap
50–70+cm yellowish/greyish brown fine sandy silt loam with small weathered limestone fragments (<1 cm); gleyed B/C

BH107 (N 36° 02.235/E 014° 15.854)
0–40 brown fine sandy silt loam; Ap
40+cm weathered Coralline Limestone bedrock; C

BH108 (N 36° 02.222/E 014° 15.846)
0–50 orangey brown fine sandy silt loam; Ap
50+cm weathered Coralline limestone bedrock; C

BH109 (N 36° 02.214/E 014° 15.839)
0–20 orangey brown fine sandy silt loam; Ap
20+cm weathered Coralline Limestone bedrock; C

Transect K: from north end of In-Nuffara to east-north-east

BH96 (N 36° 02.350/E 014° 16.658)
0–30 grey silt loam with fine limestone pebbles (<5 cm); Ap
30–60 grey/orange mottled silt; B
60+cm Coralline Limestone bedrock; C

BH97 (N 36° 02.559/E 014° 16.496)
0–30 grey silty clay loam with fine limestone pebbles (<5 cm); Ap
30–60 grey/orange mottled silt; B
60+cm Coralline Limestone bedrock; C

BH98 (N 36° 02.562/E 014° 16.496)
0–30 grey silty clay loam with fine limestone pebbles (<5 cm); Ap
30–60 grey/orange mottled silt; B
60+cm Coralline Limestone bedrock; C

BH99 (N 36° 02.545/E 014° 16.510)
0–20 grey silty clay loam with fine limestone pebbles (<5 cm); Ap
20+cm grey/yellow silty clay; B/C

BH100 (N 36° 02.550/E 014° 16.526)
0–80 grey silty clay loam with fine limestone pebbles (<5 cm); Ap
80+cm grey/yellow silt; B/C

BH101 (N 36° 02.554/E 014° 16.598)
0–30 grey silt loam with fine limestone pebbles (<5 cm); Ap
30+cm grey/orange silty clay; B/C

BH102 (N 36° 02.521/E 014° 16.619
0–70 grey silty clay loam with fine limestone pebbles (<5 cm); Ap
70+cm grey/yellow silty clay; B/C

Transect N: in small walled field between TP1 and west side of Ġgantija temple platform

BH124 (N 36° 02.813/E 014° 16.141)
0–60 brown to reddish brown silt loam with even mix of limestone; Ap on terrace
60+cm limestone, not necessarily bedrock
BH125 (N 36° 02.817/E 014° 16.137)
0–70 brown to reddish brown silt loam with even mix of limestone; Ap on terrace
70+cm limestone, not necessarily bedrock

BH126 (N 36° 02.814/E 014° 16.139)
0–70 brown to reddish brown silt loam with even mix of limestone; Ap on terrace
70–80 reddish brown silt with abundant limestone fragments; remnant of buried B ?
70+cm limestone, not necessarily bedrock

BH127 (N 36° 02.815/E 014° 16.135)
0–20 brown to reddish brown silt loam with even mix of limestone; Ap
20–30 reddish brown silt with abundant limestone fragments; remnant of buried B ?
30+cm limestone, not necessarily bedrock

Transect P (2015): southeast side of Ramla valley across abandoned terraces

BH500 (grid)
0–10 grey silty clay loam; Ap
10–70 grey with orange mottles silty clay loam; B
70–100 yellowish grey silty clay with common limestone fragments
100+cm grey silt; B/C

BH501 (grid)
0–10 grey silty clay) loam; Ap
10–65 grey silty clay loam; B
65–100 grey silty clay with few limestone fragments and some orange mottles; gleyed B
100–150 grey silty clay with few limestone fragments; gleyed B
150–200 grey silt, limestone fragments and calcium carbonate mottles; Bgk
200–230 yellowish grey silty clay with calcium carbonate mottles; Bgk2
230+cm grey silt; B/C
Samples taken: Small bulk samples at 0–10, 50–60, 90–100, 160–170 and 230–240 cm

BH502 (grid)
0–10 grey silty clay loam; Ap
10–40 grey silty clay with calcium carbonate mottling; Bgk1
40–90 grey silty clay; Bg1
90–127 grey silty clay with calcium carbonate mottling; Bgk2
127–140 grey silty clay loam; Bg2
140–150+cm grey/greyish brown clay; C of Blue Clay

BH503 (grid)
0–10 grey silty clay loam; Ap
10–40 grey silty clay; B
40–95 grey/orange mottled silty clay; Bg
95–134 grey silty clay with calcium carbonate mottling; Bgk
134+cm grey silty clay; C of Blue Clay

BH504 (grid)
0–10 grey silty clay loam; Ap
10–30 greyish brown silty clay; B
30–65 greyish brown silty clay with few stone fragments (<1 cm); Bg with colluvial input
65–170 greyish brown silt clay; Bg
170–200 grey silty clay with calcium carbonate mottling; Bgk
200+cm greyish blue silty clay; C of Blue Clay

BH505 (grid)
0–10 grey silty clay loam; Ap
10–50 greyish brown silty clay with few stone fragments (<1 cm); B with colluvial input
50–220 greyish brown silty clay; Bg
220–285 greyish brown silty clay with orange mottles and abundant calcium carbonate nodules and gypsum concretions; Bgk
285–310 grey/yellowish brown silty clay; B/C
310+cm grey silty clay; C of Blue Clay

BH506 (grid)
0–10 grey silty clay loam; Ap
10–160 greyish brown silty clay; Bg
160–300+cm greyish brown silty clay with orange mottles and abundant calcium carbonate nodules; Bgk

BH507 (grid)
0–10 grey silty clay loam; Ap
10–150 pale greyish brown with orange mottles silty clay and occasional limestone pebbles (<1 cm); Bg
150–215 greyish brown silty clay with orange mottles and abundant calcium carbonate nodules; Bgk
215+cm grey silty clay; C of Blue Clay

BH508 (grid)
0–10 grey silty clay loam; Ap
10–300 pale greyish brown with orange mottles silty clay and occasional limestone pebbles (<1 cm); with more very fine sand and silt with depth; Bg
300+cm grey fine sandy/silty clay with weathered limestone; B/C

BH509 (grid)
0–10 grey silty clay loam; Ap
10–230 pale greyish brown fine sandy silty clay with occasional limestone pebbles; Bg
230+cm bluish green silty clay; C of Blue Clay

Transect R: northwest side of Ramla valley across terraces

BH510 (grid)
0–30 pale greyish brown silt loam; Ap
30–160 pale greyish/yellowish brown mottled silt loam; Bg
160–195 pale greyish/yellowish brown mottled silt loam with calcium carbonate nodules; Bgk
195+cm bluish grey silty clay; C of Blue Clay

BH511 (grid)
0–35 pale greyish brown silt loam; Ap
30–115 yellowish brown silty clay with few limestone pebbles (<2 cm); Bw
115–210 pale grey silty clay with calcium carbonate nodules and gypsum concretions; Bgk
210+cm grey/orangey brown mottled silty clay; C of Blue Clay

BH512 (grid)
0–42 pale greyish brown silty clay loam; Ap
42–115 yellowish brown silt loam with few gravel pebbles (<2 cm); Bg1
115–132 greyish brown fine sandy silt loam with minor clay; Bg2
132+cm grey/orangey brown mottled silty clay; C of Blue Clay

BH513 (grid)
0–35 pale greyish brown silty clay loam; Ap
35–98 yellowish brown silt loam with few limestone pebbles (<2 cm); Bg1
98–100 lens of brown fine sandy silt loam; hillwash epsisode
100–118 greyish brown fine sandy silt loam with minor clay with calcium carbonate nodules and gypsum concretions; Bg2
210+cm grey/yellowish brown mottled silty clay; C of Blue Clay

BH514 (grid)
0–30 pale greyish brown silty clay loam; Ap
30–90 greyish brown silty clay loam with few limestone pebbles (<2 cm); Bw
90–130 greyish brown silty clay loam; Bg
130–190 greyish brown silty clay loam with calcium carbonate nodules and gypsum concretions; Bg
190+cm greyish blue silty clay; C of Blue Clay

BH515 (grid)
0–30 pale greyish brown silty clay loam; Ap
30–45 yellowish brown silt loam with few limestone pebbles (<2 cm); Bg1
45–120 pale greyish brown silt; Bg
120–130 pale greyish brown silt with weathered limestone fragments; colluvial input
130–220 greyish brown silt loam with occasional weathered limestone fragments; Bg with colluvial input
220–260 grey/yellow/blue silt with Globigerina fragments; B/C
260+cm Globigerina Limestone bedrock; C

Mgarr ix-Xini

BH 606 (N 36° 01.259/E 014° 16.133)
0+cm beach pebbles

BH 607 (N 36° 01.303/E 014° 16.097)
0–60 reddish brown sandy loam with fine limestone pebbles
60–100+cm limestone pebbles

BH 608 (N 36° 01.536/E 014° 15.737)
0–50 greyish brown silt loam
50–128 pale greyish/yellowish brown silty clay loam
128–180 pale greyish white calcareous silt with 25% coarse-fine gravel content
180+cm limestone gravel

Transect S: Xagħra to Rabat

BH 609 (N 36° 02.718/E 014° 15.330)
0–30 yellowish brown fine sandy/silt loam with limestone pebbles
30–60 greyish brown fine sandy/silty clay loam with fine limestone pebbles nodules
60–110 greenish-grey silt loam with limestone pebbles and iron nodules
110+cm pale greyish/reddish brown silty clay; B/C

BH 610 (N 36° 02.684/E 014° 15.296)
0–40 yellowish brown fine sandy/silt loam
40+cm greyish brown fine sandy/silty clay loam with fine limestone pebbles and calcium carbonate nodules

BH 611 (N 36° 02.638/E 014° 15.257)
0–55 greyish brown silty clay loam
55+cm Globigerina limestone

BH 612 (N 36° 02.615/E 014° 15.205)
0–55 greyish brown silty clay loam
55+cm Globigerina Limestone

BH 613 (N 36° 02.615/E 014° 15.205)
0–55 greyish brown silty clay loam
55+cm Globigerina Limestone

BH 614 (N 36° 02.571/E 014° 15.152)
0–50 pale greyish brown fine sandy clay loam
50–90 greyish brown fine sandy clay loam with fine Globigerina pebbles
90–120 yellow fine sandy/silty/clay weathered bedrock; B/C
120+cm Globigerina Limestone rubble and pale greyish brown silt loam; B/C

BH 615 (N 36° 02.554/E 014° 15.121)
0–70 greyish brown fine sandy/silt loam
70–120 pale yellowish brown sandy/silt loam with 5% calcium carbonate aggregates; hillwash
120–150+cm yellowish brown fine sandy/silt with fine limestone mix; weathered B/C

Dweija Valley

BH 616 (N 36° 02.572/E 014° 11.526)
0–100 pale greyish white calcitic silt with fine limestone pebbles
100–120 stone terrace wall
120–220 pale greyish white calcitic silt with large limestone fragments
220–250 brown calcitic loam with large irregular blocky structure; buried soil
250+cm Globigerina Limestone bedrock; C
Samples taken: spot micromorphology and small bulk sample from 225–235 cm

BH 617 (N 36° 02.549/E 014° 11.793)
0–80 pale greyish brown calcitic silt loam; terrace make-up
80+cm weathered Globigerina Limestone bedrock; C

Transect T: Skorba environs

BH 618 (N 35° 55.254/E 014° 22.606)
0–55 mid-brown fine sandy/silt loam with common fine gravel size limestone pebbles
55+cm Coralline Limestone bedrock; C

BH 619 (N 35° 55.239/E 014° 22.629)
0–60 brown silty clay loam with common fine gravel size limestone pebbles
60+cm Coralline Limestone bedrock; C

BH 620 (N 35° 55.233/E 014° 22.660)
0–50 brown silty clay loam with common fine gravel size limestone pebbles
50+cm Coralline Limestone bedrock; C
Samples taken: small bulks from 0–10, 35–40 and 40–50 cm

BH 621 (N 35° 55.220/E 014° 22.695)
0–55 brown fine sandy/silty clay loam with common fine gravel size limestone pebbles
55+cm Coralline limestone bedrock; C

BH 622 (N 35° 55.220/E 014° 22.670)
0–40 brown fine sandy/silty clay loam with common fine gravel size limestone pebbles
40+cm Coralline Limestone bedrock; C

BH 623 (N 35° 55.203/E 014° 22.671)
0–45 dark brown silty clay loam with common fine gravel size limestone pebbles
45+cm Coralline Limestone bedrock; C

BH 624 (N 35° 55.187/E 014° 22.677)
0–48 dark brown silty clay loam with common fine gravel size limestone pebbles
48+cm Coralline Limestone bedrock; C

BH 625 (N 35° 55.172/E 014° 22.660)
0–40 dark brown silty clay loam with common fine gravel size limestone pebbles
40+cm Coralline limestone bedrock; C

Ġgantija Test Pits

Test Pit 1 (2014 and 2015): composite section

Southwest facing section
0–152 Modern stone retaining wall of the visitor's platform; contains two vertical megaliths, one of *c*. 100 cm and the other of *c*. 142 cm in height

---

Northeast facing section (N 36° 02.818/E 014° 16.149)

Modern ground surface outside platform
0–80 greyish brown silt loam with common limestone fragments (<5 cm); Ap and terrace soil
80–90 brown silt loam with abundant Neolithic artefacts (pot, bone, lithics); *in situ* Ah of palaeosol
90–120 mid-brown silt loam with abundant Neolithic artefacts (pot, bone, lithics); buried lower A
120–130 reddish brown fine sandy silt loam; buried Bw
130+cm undulating Upper Coralline Limestone bedrock; C
Samples taken: Micromorphology blocks at 40–47, 50–60, 60–77, 87–100, 100–111 and 111–125 cm; small bulk samples at 10–20, 70–80, 80–90, 90–100, 100–110, 110–120 and 120–130 cm; pollen spots at 5 cm intervals from 80–130 cm; 2 large bulk samples for wet sieving/macro-botanical remains at 40–70 and 90–120 cm

Test Pits for moving palm trees on east side of platform (2014):

Test Pit 2 (N 36° 02.818/E 014° 16.149)
0–70 grey silty clay loam with even mix of limestone fragments; Ap; imported soil from 1982
70–130 pale grey/yellowish brown silty clay with even mix of limestone fragments; imported soil from 1961; anthropogenic B
130–137 dark grey silty clay loam; buried Ah
137–142 pale grey silt; ? introduced/truncation zone?
142–148 reddish brown fine sandy silt loam; buried B
148+cm Coralline Limestone bedrock; C
Samples taken: Spot small bulk sample at 142–148 cm

Test Pit 3 (N 36° 02.873/E 014° 16.188)
0–50 grey silty clay loam with even mix of limestone fragments; Ap; imported soil from 1982
50–105 pale grey/yellowish brown silty clay with even mix of limestone fragments; imported soil from 1961; anthropogenic B
105–112 limestone rubble
112–135 reddish brown fine sandy silt loam
135+cm Coralline Limestone bedrock; C
Samples taken: Spot small bulk sample at 120–130 cm

Test Pit 4 (N 36° 02.854/E 014° 16.201)
0–50 grey silty clay loam with even mix of limestone fragments; Ap; imported soil from 1982
50–150 pale grey/yellowish brown silty clay with even mix of limestone fragments; imported soil from 1961; anthropogenic B
150–160 reddish brown fine sandy silt loam; buried upper B
160–180 brown sandy silt loam with fine limestone pebbles; buried lower B-B/C
180+cm Coralline Limestone bedrock; C
Samples taken: Spot small bulk samples at 150–160 and 165–175 cm

Test Pit 5 (N 36° 02.861/E 014° 16.201)
0–54 grey silty clay loam with even mix of limestone fragments; Ap; imported soil from 1982
54–75 pale grey silty clay with even mix of limestone fragments; imported soil from 1961; anthropogenic B
75–98 reddish brown fine sandy silt loam; buried upper B
98+cm Coralline limestone bedrock; C
Samples taken: Spot micromorphology block sample at 78–88 cm; spot small bulk sample at 80–90 cm

Ġgantija WC Trench (2015)

South section 2015:
c. 0–110 greyish brown silt loam and limestone rubble; made ground for 1970s toilet block
April excavations starting surface
0–35/40 large limestone blocks
35/40–60 dark brown silt loam with abundant pottery and bone, and the occasional fragment of calcitic plaster; 10YR4/3; context 1015; midden and soil accumulation
60–80 dark brown silt loam with abundant pottery and bone, and the occasional fragment of fired clay; 10YR5/2; context 1016; midden and soil accumulation
80–83 discontinuous lens of black humic and very fine charcoal 'soot'; context 1040; hearth dumped material
80–82 discontinuous, slightly undulating lens of pale yellowish brown pea-grit gravel; context 1041; ground surface
82/83–90 greyish brown silt loam with abundant pottery and bone; 10YR4/2; context 1004; buried Ah of palaeosol with abundant anthropogenic inclusions
90–105/125 reddish brown silty clay loam with common pottery and bone; 5YR3/3; context 1019; buried B of palaeosol with common anthropogenic inclusions
110/125+cm weathered Upper Coralline Limestone bedrock; C; rising in height northwards
Samples taken: Micromorphology blocks at *c*. 60, 68–86, 84–94 and *c*. 78–83 cm, and a further four samples taken continuously through the buried soil from the same sequence (as at *c*. 85–105 cm), but at *c*. 50 cm in/to north of section described above; and a further two spot micromorphology blocks from contexts 1015 and 1016; 13 small bulk samples taken to match each of these micromorphology samples

Xagħra town/plateau construction site profiles

House construction site 1 (N 36° 03.058/E 014° 16.601):

Profile 1: back wall
0–20 stone rubble wall
20–60 reddish brown silty clay loam; buried B of *terra rossa* palaeosol
60+cm fissured Upper Coralline limestone bedrock; C

Profile 2: near front gate
0–15 brown silt loam with tree rooting; modern topsoil
15–25 red silt loam; redeposited soil ?
25–80 pale reddish brown calcareous silt loam with common limestone pebbles; terrace soil
80–85 pockets of reddish brown silt loam; buried Bw of palaeosol
85+cm undulating Upper Coralline limestone bedrock; C

House construction site 2 (N 36° 03.004/E 014° 16.549):
0–15 modern concrete yard surface
15–35 pockets of reddish brown silt loam; buried Bw of palaeosol
35+cm undulating Upper Coralline limestone bedrock; C
Samples taken: Micromorphology blocks at 15–25 and 25–35 cm; small bulk samples at 15–25 and 25–35 cm

House construction site 3 (N 36° 03.536/E 014° 16.221):
0–50/80 dark brown silt loam with even mix of limestone fragments (<3 cm)
50/80–100/160 red silt loam; buried Bw of palaeosol
100/160+cm undulating Upper Coralline limestone bedrock; C
Samples taken: Micromorphology blocks at 50–60 and 60–70 cm; small bulk samples at 50–60 and 60–70 cm

Ta Marziena temple site and environs

Transect H:

BH67 (N 36° 02.005/E 014° 14.400; inside temple)
0–10 brown silt loam with occasional fine limestone pebbles (<5 mm); Ah
10+cm Coralline Limestone bedrock; C

BH68 (N 36° 01.978/E 014° 14.407)
0–50 grey silty clay loam with common calcium carbonate aggregates and few limestone fragments (<1 cm)
50+cm grey/yellowish grey mottled clay loam; B/C

BH69 (N 36° 01.983/E 014° 14.382)
0–45 brown fine sandy silt loam with few fine limestone pebbles (<5 mm); Ap
45+cm Coralline Limestone bedrock; C

BH70 (N 36° 01.964/E 014° 14.391)
0–50 brown fine sandy silt loam with few fine limestone pebbles (<5 mm); Ap
50–75 pale grey/yellowish grey silty clay loam; B
75+cm grey/yellowish grey mottled clay loam; B/C

BH71 (N 36° 01.926/E 014° 14.400)
0–50 brown fine sandy silt loam with few fine limestone pebbles (<5 mm); Ap
50–75 pale grey/yellowish grey silty clay loam; B
75+cm grey/yellowish grey mottled clay loam; B/C

BH72 (N 36° 01.891/E 014° 14.391)
0–50 brown fine sandy silt loam with few fine limestone pebbles (<5 mm); Ap
50–75 pale grey/yellowish grey silty clay loam; B
75+cm grey/yellowish grey mottled clay loam; B/C

BH73 (N 36° 01.827/E 014° 14.391)
0–80 brown silty clay loam with common fine limestone pebbles (<5 mm); Ap
80–90 pale reddish/yellowish brown silty clay loam with common fine limestone fragments (<5 mm); buried B of palaeosol
90–120 dark reddish brown silty clay loam with common fine limestone fragments (<5 mm); probably buried clay-enriched Bt of palaeosol
120+cm weathered Coralline Limestone bedrock; C

BH74 (N 36° 01.792/E 014° 14.331)
0–50 reddish brown silty clay loam with common fine limestone pebbles (<5 mm); Ap
50–80 pale reddish brown silty clay loam with common fine limestone pebbles and fragments (<5 cm); B
80+cm weathered Coralline Limestone bedrock; C

BH75 (N 36° 01.744/E 014° 14.299)
0–50 pale reddish brown silt loam with common fine limestone pebbles (<2 cm); Ap
50+cm weathered Coralline Limestone bedrock; C

Ortine land-fill site

Area of possible prehistoric, small rectilinear stone demarcated fields, mainly of bedrock at or near surface; very denuded

Marsalforn Valley

BH110 (N 36° 03.485/E 014° 14.946)
0–150 pale yellowish grey silty clay loam; hillwash
150–180 pale yellowish brown silty clay loam with columnar blocky ped structure; buried old land surface in colluvium
180–220 rounded stone pebbles (<5 cm); stream bed
220–340 greyish brown fine-medium sand and silt
340–350 rounded stone pebbles (<10 cm); stream bed
350+cm modern road surface, with Globigerina Limestone bedrock beneath

Profile 626 (N 36° 03.485/E 014° 14.946): OSL, micromorphology and small bulk sampling profile
0–10 turf/topsoil; modern ploughsoil and land surface
10–175 pale yellowish grey silty clay loam with weakly developed blocky ped structure; hillwash
175–210 pale yellowish brown silty clay loam with well developed columnar blocky ped structure; incipient soil in stabilized hillwash
210–270 rounded stone pebbles (<5 cm) in grey silty clay loam; hillwash
270–310 very pale brown (10YR7/4) very fine sandy/silt loam with even mix of fine limestone pebbles (<2 cm); mix of colluvial soil and pebbles
310–370 grey (10YR5/1) silty clay loam with <10% fine to coarse stone pebbles (<10 cm); coarser mix of colluvial soil and pebbles
370–400 grey clay; weathered B/C
400+cm Globigerina Limestone; bedrock
Samples taken: Micromorphology blocks and small bulks at 175–185, 200–210 and 275–285 cm; OSL profiling samples at 180, 195, 205, 215, 225, 270, 290, 300, 310 and 320 cm; OSL dating tubes at 175–180, 265–270 and 320–325 cm

Ta' Kulijat

Messa plateau above Marsalforn valley:
0–25/35 brown coarse sandy loam; Ap
25/35+cm weathered Coralline Limestone bedrock; C; sometimes exposed at surface

Ghajn Abdul and Wied il-Kibr valley, northwest of Xlendi

Terraces on limestone ridges:
0–25/35 brown coarse fine sandy silt loam; Ap, with common prehistoric pottery
25/35+cm weathered Coralline Limestone bedrock; C, sometimes exposed at surface
Sample taken: spot small bulk sample at 0–10 cm

Santa Verna and environs

Transect L:

BH111 (N 36° 02.743/E 014° 15.520)
0–20 pale brown fine sandy silt loam; Ap
20+cm Coralline Limestone bedrock; C

BH112 (N 36° 02.755/E 014° 15.527)
0–45 brown to reddish brown fine sandy silt loam with few fine limestone fragments (<2 cm) and rare pottery fragments; Ap
45+cm weathered Coralline Limestone bedrock; C

BH113 (N 36° 02.762/E 014° 15.530)
0–60 brown to reddish brown fine sandy silt loam with few fine limestone fragments; Ap
60–65 reddish brown silt loam with few fine limestone fragments (<1 cm); B
65+cm weathered Coralline Limestone bedrock; C

BH114 (N 36° 02.775/E 014° 15.544)
0–60 brown fine sandy silt loam with few fine limestone fragments; Ap
60+cm weathered Coralline Limestone bedrock; C
Sample taken: spot small bulk sample at 0–10 cm

BH115 (N 36° 02.784/E 014° 15.565)
0–30 dark brown fine sandy silt loam with few fine limestone fragments; Ap
30–50 reddish brown fine sandy clay loam with few fine limestone fragments; B
50+cm weathered Coralline Limestone bedrock; C
Samples taken: Spot micromorphology blocks at 20–30 and 30–40 cm

BH116 (N 36° 02.789/E 014° 15.587)
0–60 brown silt loam with few fine limestone fragments; Ap
60+cm weathered Coralline Limestone bedrock; C

BH117 (N 36° 02.797/E 014° 15.591)
0–50 brown silt loam; Ap
50–90 brown with orange mottles silt loam with few fine limestone fragments; B
90+cm weathered Coralline Limestone bedrock; C

BH118 (N 36° 02.807/E 014° 15.614)
0–30 brown silt loam; Ap
30–40 orangey brown silty clay loam; B
40+cm weathered Coralline Limestone bedrock; C

BH119 (N 36° 02.845/E 014° 15.634)
0–25 brown silty clay loam with few fine limestone fragments (<2 cm); Ap
25–35 orangey brown silty clay loam with few fine limestone fragments; B
35+cm weathered Coralline Limestone bedrock; C

BH120 (N 36° 02.838/E 014° 15.650)
0–45 reddish brown silty clay loam; Ap
45–80 yellowish brown coarse sandy loam with few fine limestone fragments; B
80+cm weathered Coralline Limestone bedrock; C

BH121 (N 36 02.717/E 014 15.566)
0–10 grey silt loam; Ap
10+cm weathered Coralline Limestone bedrock; C

BH122 (N 36° 02.743/E 014° 15.499)
0–45 brown silty clay loam with abundant limestone pebbles (<2 cm); Ap
45+cm weathered Coralline Limestone bedrock; C

BH123 (N 36° 02.743/E 014° 15.499)
0–20 grey silt loam with common limestone pebbles (<2 cm); Ap
20+cm weathered Coralline Limestone bedrock; C
Note: remainder of plateau to northwest is very denuded with limestone bedrock near or at the surface

Santa Verna Excavations (2015)

Off-site trench, Profile SV15/1:
0–40 greyish brown fine sandy silt loam with few fine gravel pebbles (<1 cm); Ap
40–58 brown silt loam; buried Ah of palaeosol
58–90 reddish brown silt loam; buried Bw of *terra rossa* palaeosol
90+cm weathered Upper Coralline Limestone bedrock; C
Samples taken: Micromorphology blocks at 42–52, 53–66, 66–73 and 74–88 cm; small bulk samples at 10–20, 50–58, 60–70, 80–90 and 90–95 cm

Profile SV15/2: Ashby sondage
0–20 modern topsoil and limestone rubble
20–22 compacted brown silt; torba floor
22–65 limestone rubble
65–70 compacted brown silt; torba floor
70–80 limestone rubble
80–95 brown silt loam; buried Ah of palaeosol
95–115 reddish brown silt loam; buried Bw1 of *terra rossa* palaeosol
115–125 dark reddish brown silt loam; buried Bw2 of *terra rossa* palaeosol
125+cm weathered Upper Coralline Limestone bedrock; C
Samples taken: Micromorphology blocks at 95–105, 105–115 and 115–125 cm; micromorphology spot samples of torba floor contexts 28 and 78; small bulks at 95–105, 105–115 and 115–125 cm

Profile SV15/3: Trump Sondage, Cut 55 (contexts 28/29/30/51):
0–10 greyish brown silt loam; Ah topsoil
10–100 limestone rubble
100–120 dark brown silt loam; buried Ah of palaeosol; (note: adjacent feature cut defines from *c*. 110 cm down-profile)
120–165 reddish brown silt loam; buried Bw of palaeosol
165+cm weathered Upper Coralline Limestone bedrock; C
Samples taken: Micromorphology blocks at 100–120 and 120–140 cm from buried soil, and 110–130 and 130–160 cm from feature fill; small bulk samples at 100–110 and 130–140 cm, from buried soil, and 110–120 and 140–150 cm from feature fill

Profile SV15/4: Trench E, A section:
0–10 greyish brown silt loam; Ah topsoil
10–40 limestone rubble
40–43 compacted brown silt; torba floor
43–71 limestone rubble
71–75 compacted brown silt; torba floor
75–83 limestone rubble
83–100/105 dark brown silt loam; buried Ah of palaeosol
100/105+cm weathered Upper Coralline Limestone bedrock; C
Samples taken: Micromorphology blocks at 40–44, 68–75, 83–93 and *c*. 65–70 cm; small bulks at 40–43, 66–74, 83–93 and *c*. 65–70 cm

Taċ-Ċawla (TCC/14) Neolithic settlement site excavations (2014)

Section 1:

0–50	made ground and Horton 1985 excavation trench backfill
50–54	brown silt loam; remnant of post-site B horizon ?
54–57	compacted brown silt with fine charcoal; possible floor surface
57–63	brown silt loam; soil aggradation ?
63–72	compacted mixture of brown silt, fine charcoal and pale grey calcitic ash; possible floor surface accumulation
72–74	reddish brown silt loam; possible upper surface of buried Bw of palaeosol

Samples taken: Micromorphology blocks at 50–59 and 59–73 cm; small bulk samples at 54–57, 57–63, 63–72 and 72–74 cm

Section 2:

Excavated surface

0–28	greyish brown fine sandy silt loam; trench backfill or old terrace soil
28–29	lens of fine charcoal and humic matter; anthropogenic accumulation
29–32	laminar pale grey silt or calcitic ash with fine limestone fragments (<1 cm); possible floor deposits
32–41	greyish brown fine sandy silt loam; soil aggradation
41+cm	excavation surface of Horton 1985

Samples taken: Micromorphology blocks at 16–31, 22–37 and 26–42 cm; small bulks at 20–25, 28–32 and 32–40 cm

Deep valley cores: sample depths of small bulk and micromorphology samples

Xemxija 1 valley core

Sample depth (cm)	Description	Micromorphology block sample at cm	Small bulk sample at cm
47–70	yellowish brown silty clay; 5Y6/4		
70–85	yellowish brown calcitic silt with fine stone; 5Y8/3		
85–112	calcitic silt with orange mottles; 5Y8/3		
112–122	reddish brown silty clay; 10YR5/6		
122–151	light reddish brown silt; 5YR6/4		
165–206	yellowish brown silt; 10YR5/4	199-201	205
206–250	pale grey silt; 10YR5/1 to 6/1	220-3	
250–265	pale grey fine sand; 2.5YR6/2	250-3	255
265–295	grey/orange sine sandy/silt loam; 10YR6/4	273-5	275
295–317	mid-grey silt; 5Y4/1	302-4	300
317–319	dark grey silt with fine sand; 5Y3/1		
319–335	black silt with fine sand; 5Y2/1		330
335–355	grey silt; 7.5Y1	335-9	
355–405	grey silt with common humified organic matter; 7.5Y4/1	403-5	365
405–425	black organic silt mud; 10YR2/1		405
425–450	grey silt with common humified organic matter; 7.5Y4/1		435
460–528	black organic silt mud; 10YR2/1; C-14 date of 2198–1985 cal. BC at 460 cm	495-7	490, 513
528–543	greyish black silt; 10YR4/1		535
543–565	dark grey silt with common humic/organic fragments; 10YR4/1	545-7	555
565–600	dark grey silt; 10YR4/1; C-14 date of 4326–4053 cal BC at 570 cm	578-80	570
600–630	black organic silt; 10YR2/1	610-2	600
630–635	mottled grey/black organic silt; 10YR4/1 and 2/1		630
635–655	dark grey silt; 5Y4/1	645-7	638
670–685	brown to dark brown silt loam with few fine stones, manganese flecks, few plant remains fragments; 10YR4/3		680
685–815	brown silt loam with orange oxidation mottling; 10YR4/4	685-7, 725-7, 772-5, 785-7	710, 740, 775, 787, 800
815–832	brown to dark brown silt loam with few fine stones, manganese flecks, few plant remains fragments; 10YR4/3	823-5	818
832–855	brown to dark brown silt loam with few fine stones; 10YR4/3	833-5	835
855–870	brown silt loam with orange oxidation mottling; 7.5YR4/2	868-70	865
870–890	brown silt loam with orange oxidation mottling and limestone fragments; 7.5YR4/2		875
890–910	dark greyish brown organic silt; 7.5YR2/2		890
910–922	brown organic silt with limestone fragments; 7.5YR4/4	913-5	913
922–943	dark brown silt loam; 7.5YR3/2	025-7	922
943–960	pale brown fine sandy/silt loam with abundant limestone pebbles; 10YR6/3	945-7	945
960–990	dark yellowish brown fine sandy/silty clay loam with abundant limestone pebbles; 10YR64/4; C-14 date of 7000 cal BC at 990 cm	965-7, 975-7	970
990+	Limestone bedrock		

Wied Żembaq 1 valley core

Sample depth (cm)	Description	Micromorphology block sample	Small bulk sample
0–119	dark brown silt loam; 10YR4/3	7-9, 45-7, 80-2	9, 47, 82
119–161	yellowish brown coarse sandy silt loam with occasional limestone pebbles; 10YR4/2		
161–213	dark greyish brown sandy silt loam with occasional limestone pebbles and common organic fragments; 10YR4/2		
215–217	yellowish brown silt loam; 10YR5/4	215-7	217
217–315	weathered limestone pebbles		
250–260	greyish brown silt loam; 10YR5/2	253-5	255
260–350	dark brown silt loam; 10YR4/3	300-02	302
350–362	limestone pebbles		
362–380	dark greyish brown silt loam; 10YR4/2	365-7	367
380–400	dark grey silt loam; 10YR4/1	396-8	398
400–420	very dark grey organic silt mud; 10YR3/1	410-12	412
420–450	dark grey organic silt mud with occasional humified plant remains and iron mottling; 10YR4/1	433-5	435
450–480	dark yellowish brown silt loam with orange oxidation mottling; 10YR4/4	460-2	461
480–518	dark grey organic silt mud with orange oxidation mottling; 10YR4/1	496-8	498
518–558	very dark grey organic silt mud with pebbles at base; 10YR3/1	528-30	530

Marsaxlokk valley core

Sample depth (cm)	Description	Micromorphology block sample	Small bulk sample
0–40	pale brown fine sandy/silt loam with fine limestone fragments; 10YR6/3	5-7	6
40–76	light yellowish brown silt loam; 10YR6/4	62-66	66
86–155	light grey, calcitic, very fine sandy/silt; possibly micro-laminated; 10YR7/1	110-112	112
155–165	brownish yellow fine gravel and coarse sand; 10YR6/6		
165–170	very dark grey organic silt mud; 10YR3/1		
170–185	light brownish grey very fine sandy/silt; possibly micro-laminated; 10YR6/2	170-2	172
186–192	pale brown fine gravel and coarse sand; 10YR6/3		
192–245	yellowish red silty (clay) loam with occasional fine limestone pebbles; 5YR4/4	215-7	217
245–286	dark yellowish brown silty clay loam with frequent fine limestone pebbles; 10YR4/4	255-7	257
286–292	light yellowish brown fine gravel and coarse sand with marine shell fragments; 10YR6/4		
292–332	brown to reddish brown silty clay loam; 5YR4/4	296-9, 320-2	299, 322
332–353	pinkish brown, calcitic silty clay loam with common weathered limestone; 10YR7/4		
353–386	pale pinkish brown calcitic silt; 10YR8/4	365-7	367

Appendix 7

The detailed soil micromorphological descriptions from the buried soils and Ramla and Marsalforn valleys

Charles French

A7.1. Santa Verna

Transect L:

Sample 39, BH115, 30–40 cm

Structure: weak small columnar blocky peds, <3 cm, with pellety, <250 μm, to aggregated, sub-rounded to irregular, <5 mm, microstructure; *Porosity*: <5% vughs, sub-rounded, <200 μm; <5% fine channels, <3 cm long, <250 μm wide, vertical, accommodated, weakly serrated; *Mineral components*: <2% fine limestone pebbles, 2–5 mm; c/f ratio: 25/75; coarse fraction: 5% coarse sand-size limestone, 1–2 mm, sub-rounded; 10% medium and 10% fine quartz sand, sub-rounded, 200–750 μm; fine fraction: 10% very fine quartz sand, 50–100 μm, sub-rounded; 30% micro-sparite; 35% dusty clay; reddish brown (CPL/PPL); *Organic components*: 5–10% organic punctuations, <50 μm; *Pedofeatures*: *Amorphous*: very strong amorphous sesquioxide impregnation of whole groundmass; abundant (40%) aggregates of strongly amorphous sesquioxide impregnated clay, sub-rounded, <2 mm, no birefringence.

Trench B:

Sample 1/1, 42–52 cm

Structure: pellety, <500 μm, to aggregated, <1.5 cm, sub-rounded to irregular; *Porosity*: 10% vughs, sub-rounded to irregular to interconnected, <1 mm; <2% fine channels, <3 cm long, <1.5 mm wide, accommodated, smooth to weakly serrated; <1% cracks, <1 cm long, <50 μm wide; *Mineral components*: 10–20% fine limestone pebbles, <1.5 and 2–5 cm, sub-rounded to sub-angular, unsorted; c/f ratio: 5/95; coarse fraction: 5% fine quartz sand, sub-rounded, 100–500 μm; fine fraction: 10% very fine quartz sand, 50–100 μm, sub-rounded; 10–20% micro-sparite; 65% dusty clay, non-birefringent, gold to golden brown (CPL/PPL); reddish/orangey brown (CPL/PPL); *Organic components*: 10–20% organic/charred punctuations, <50 μm; 2% fine charcoal, <75 μm; *Pedofeatures*: *Amorphous*: common to abundant (10–20%) impregnative sesquioxide nodules, sub-rounded, sometimes with soil fabric coatings around them, <2 mm, no birefringence, strong red/orangey-red (CPL), reddish brown to dark brown (PPL).

Sample 1/2, 53–66 cm

Two fabric units: Upper fabric unit 1: as for sample 1/1 above; irregular but distinct boundary with Lower fabric unit 2: *Structure*: pellety, <500 μm; *Porosity*: 10–20% vughs, sub-rounded to irregular to interconnected, <2 mm; *Mineral components*: 5% fine limestone pebbles, 2–5 mm and <3 cm, sub-rounded to sub-angular, unsorted; 70% micro-sparite; 5% fine-medium quartz sand, sub-rounded, 100–500 μm; 10% very fine quartz sand, 50–100 μm, sub-rounded; 15% aggregates of silty clay, speckled to short striated, moderate birefringence, golden brown (CPL), orange (PPL); pale grey/brown (CPL), pale brown/orangey brown (PPL); *Organic components*: 10–20% organic/charred punctuations throughout groundmass, <50 μm; *Pedofeatures*: *Amorphous*: strong amorphous sesquioxide impregnation of silty clay aggregates, strong red/orangey-red (CPL), reddish brown to dark brown (PPL).

Sample 1/3, 66–73 cm

Structure: weakly to moderately well developed small blocky, <1.5 cm, with pellety fabric in some voids, <500 μm; *Porosity*: 5–10% vughs, sub-rounded to elongated, <750 μm; 2% fine channels, <1.5 cm long, <500 μm wide, accommodated, smooth to weakly serrated; *Mineral components*: all fine fraction: 5% very fine quartz sand, 50–100 μm, sub-rounded; 95% silty clay, pure to dusty in groundmass, moderate birefringence, orangey red (CPL); reddish brown (PPL); *Organic components*: <1% organic/charred punctuations, <50 μm; *Pedofeatures*: *Amorphous*: few discontinuous linings/infills of voids/channels with micro-sparite.

Sample 1/4, 74–87 cm

Structure: well developed small blocky, <2 cm, with pellety microstructure, <1 mm, sub-rounded to irregular; *Porosity*: <5% vughs, sub-rounded, <250 μm; 2% fine channels, <2 cm long, <250 μm wide, accommodated, smooth to weakly serrated; *Mineral components*: all fine fraction: 10% very fine quartz sand, 50–100 μm, sub-rounded; 90% silty clay, pure to dusty in groundmass, short striated to weakly reticulate, moderate to strong birefringence, gold (CPL); strong to moderate reddish orange (CPL/PPL); *Organic components*: 5% organic/charred punctuations, <50 μm; *Pedofeatures*: *Amorphous*: all strongly reddened with amorphous sesquioxides; towards base of slide, few to common (up to 25% of groundmass), discontinuous linings/infills of voids/channels with micro-sparite and as irregular aggregates/zones in groundmass.

Ashby Sondage:

Sample 28, 65–70 cm

Structure: dense, sub-angular blocky, <4 cm; *Porosity*: <1% fine cracks, <4 cm long, <200 μm wide, accommodated, smooth to weakly serrated; *Mineral Components*: 25% fine gravel, <1 cm, sub-rounded to sub-angular, mainly limestone; 75% micro-sparitic silt;

grey/yellowish brown (CPL), pale brown (PPL); *c*. 2% aggregates of clay, <1 mm, sub-rounded, reddish brown to reddish orange (CPL); *Organic components*: 25% very fine organic punctuations, <50 μm.

Sample 2/1, 95–105 cm (context 30)

Structure: two, heterogeneous mixed fabrics; pellety, <2 mm, to aggregates, <2 cm; all sub-rounded; *Porosity*: *c*. 5–10% interconnected vughy; *Mineral components*: Main fabric 1: 50–80% of groundmass; pellety, <2 mm; 10% very fine quartz, 50–100 μm, sub-rounded; 90% silty clay, with weak birefringence, dark golden brown (CPL), orangey brown (PPL); Secondary fabric 2: 20–50% of groundmass; pellety to irregular zones, 100 μm to 4 mm; 5% very fine to fine quartz sand, 100–250 μm, sub-rounded; 10% medium quartz sand, 500–750 μm; 85% micro-sparite; pale grey/yellowish grey (CPL/PPL); *Organic components*: in both fabrics: common to abundant (10–20%) fine charcoal, 100–500 μm; abundant (10–20%) organic punctuations, <50 μm; rare (<1%) bone fragments, <500 μm; rare (<1%) pottery fragment, <1 cm.

Sample 2/2, 105–115 cm (context 51)

Structure: two, heterogeneous mixed fabrics; pellety, <2 mm, to aggregates, <2 cm, to small blocky, <3 cm; sub-rounded to irregular; *Porosity*: 10–20% interconnected vughy; <5% fine channels, <3 cm long, <1 mm wide, accommodated, serrated; *Mineral components*: 5% limestone gravel, 2–4 mm; sub-rounded; Main fabric 1: 90% of groundmass; pellety, <2 mm, to blocky peds; 5% very fine quartz, 50–100 μm, sub-rounded; 95% silty clay, striated, with weak to moderate birefringence, gold to dark golden brown (CPL), orangey brown (PPL); Secondary fabric 2: <10% of groundmass; pellety to irregular zones, 100um to 4 mm; 5% very fine to fine quartz sand, 100–250 μm, sub-rounded; 10% medium quartz sand, 500–750 μm; 85% micro-sparite; pale grey/yellowish grey (CPL/PPL); *Organic components*: in both fabrics: common to abundant (10–20%) fine charcoal, 100–500 μm; abundant (10–20%) organic punctuations, <50 μm; *Amorphous*: all strongly reddened with amorphous sesquioxides.

Sample 2/3, 115–125 cm (context 51 continued)

As for Sample 2/2 above

Trump Cut 55:

Sample 78, 'torba' floor

Structure: small blocky to aggregated to pellety, 2 cm to <500 μm; *Porosity*: 10% interconnected vughy; 10–15% large channels, <2 cm long, <4 mm wide, smooth, accommodated; *Mineral components*: 10% coarse sand-size limestone pebbles, 1–2 mm, sub-rounded to sub-angular, unsorted; 10% medium and 10% fine quartz sand, 100–750 μm, sub-rounded to sub-angular; 30% micro-sparite; 30% silty clay, speckled to short striated, weak birefringence; golden brown (CPL), brown (PPL); *Organic components*: 10–20% organic/charred punctuations throughout groundmass, <50 μm; 5% fine charcoal, <75 μm; few (2%) bone fragments, <1 mm; rare (1%) dung aggregate, <1.5 mm, black (CPL/PPL); *Pedofeatures*: *Amorphous*: strong amorphous sesquioxide impregnation of silty clay aggregates, strong red/orangey-red (CPL), reddish brown to dark brown (PPL); *Fabric*: few (2%) clay aggregates, <1 mm, sub-rounded, orangey red (CPL).

Sample 3/1, 100–120 cm

Structure: well developed columnar blocky, <6 cm, with some pellety fabric within, <500 μm; *Porosity*: 5% vughs, sub-rounded to elongated, <750 μm; 10% large channels, <6 cm long, <2.5 mm wide, accommodated, smooth to weakly serrated; *Mineral components*: 5% fine quartz sand, 100–250 μm, sub-rounded; 10% very fine quartz sand, 50–100 μm, sub-rounded; 10% micrite; 75% silty clay, dusty clay as groundmass, weak birefringence; golden reddish brown (CPL/PPL); *Organic components*: 10% organic/charred punctuations, <50 μm; *Pedofeatures*: *Amorphous*: 10% amorphous sesquioxide nodules, <750 μm, sub-rounded.

Sample 3/2, 120–140 cm

Structure: weakly developed columnar blocky, <10 cm, with pellety microstructure, <500 μm, sub-rounded; *Porosity*: 5% vughs, sub-rounded, <750 μm; 5% channels, <8 cm long, <1 mm wide, accommodated, smooth to weakly serrated; *Mineral components*: 10% fine quartz sand, 100–250 μm, sub-rounded; 5% very fine quartz sand, 50–100 μm, sub-rounded; 85% silty clay, dusty clay as groundmass, speckled, weak to moderate birefringence; reddish/orangey brown (CPL), orangey brown (PPL); *Organic components*: <2% organic/charred punctuations, <50 μm; *Pedofeatures*: *Amorphous*: 10% amorphous sesquioxide nodules, <750 μm, sub-rounded.

Sample 3/3, *c*. 114–127 cm

Three fabric units: Upper and lower fabric units: *Structure*: pellety, <500 μm, to aggregated, <1 cm, sub-rounded; *Porosity*: 10% vughs, sub-rounded to irregular to interconnected, <1 mm; <2% fine channels, <5 mm long, <500 μm wide, accommodated, smooth to weakly serrated; *Mineral components*: <5% fine limestone pebbles, <5 mm, sub-rounded to sub-angular, unsorted; c/f ratio: 5/95; coarse fraction: 5% fine quartz sand, sub-rounded, 100–500 μm; fine fraction: 10% very fine quartz sand, 50–100 μm, sub-rounded; 10–20% micro-sparite; 65% dusty clay, non-birefringent, gold to golden brown (CPL/PPL); reddish/orangey brown (CPL/PPL); *Organic components*: 10–20% organic/charred punctuations, <50 μm; 2% fine charcoal, <75 μm; rare (<1%) burnt bone fragment, <500 μm; *Pedofeatures*: *Amorphous*: common to abundant (10–20%) impregnative sesquioxide nodules, sub-rounded, <2 mm, no birefringence, strong red/orangey-red (CPL), reddish brown to dark brown (PPL); distinct upper/lower boundaries with Middle fabric unit 2: repeated/alternating fine (*c*. 15) and coarser (*c*. 14) crust laminae over 7 cm horizon, composed of silt (80–90%) and very fine charcoal/organic punctuations, <50 μm (10–20%); planar voids inbetween crusts and vertical cracks within crust laminae; fine crust components: 45% micro-sparite, 55% silt, 5% clay, 10% organic dust; coarser crust components: 10% very fine quartz sand, 45% micro-sparite, 40% silt, 5% clay, 5–10% very fine charcoal, <75 μm, 10% organic punctuations, <50 μm; generally laminae/crusts fining up-profile.

Sample 3/4, 130–160 cm

Structure: pellety, <500 μm, to aggregated, <600 mm, sub-rounded; *Porosity*: up to 40% open vughy; <2% fine channels, <2 cm long, <500 μm wide, short, irregular, smooth to weakly serrated; *Mineral components*: 10% fine limestone pebbles, <8 mm, sub-rounded to sub-angular, unsorted; c/f ratio: 5/95; coarse fraction: 5% fine quartz sand, sub-rounded, 100–500 μm; fine fraction: 10% very fine quartz sand, 50–100 μm, sub-rounded; 35% micro-sparite; 50% dusty clay, non-birefringent; golden brown (CPL), brown (PPL); *Organic components*: 30% organic/charred punctuations, <50 μm; 2% fine charcoal, <75 μm; rare (<1%) bone fragment, <500 μm; rare (1%) shell fragments; rare (1%) plant tissue fragments.

Trench E:

Sample 4/1, 40–44 cm

Structure: dense, apedal; *Porosity*: <2% vughs, sub-rounded to elongated, <500 μm; <2% short horizontal channels, <1 cm long, <750 μm

wide, accommodated, smooth to weakly serrated; *Mineral components*: 5% fine quartz sand, 100–250 μm, sub-rounded; 10% very fine quartz sand, 50–100 μm, sub-rounded; 10% micro-sparite; 75% silty clay, dusty clay as groundmass, weak birefringence; brown (CPL/PPL); *Organic components*: <5% organic/charred punctuations, <50 μm; 2% shell fragments; 2% bone fragments, <4 mm.

Sample 4/2, 68–75 cm

Two fabric units: Upper fabric unit 1: 95% limestone, <5 mm, sub-rounded to irregular, with <5% as pellety aggregates of fabric unit 2 material as below, <2 mm; irregular but distinct contact with Lower fabric unit 2: *Structure*: dense, apedal; *Porosity*: <2% vughs, sub-rounded to elongated, <500 μm; <2% short horizontal channels, <1 cm long, <750 μm wide, accommodated, smooth to weakly serrated; *Mineral components*: 5% fine quartz sand, 100–250 μm, sub-rounded; 10% very fine quartz sand, 50–100 μm, sub-rounded; 10% micro-sparite; 75% silty clay, dusty clay as groundmass, weak birefringence; brown (CPL/PPL); *Organic components*: <5% organic/charred punctuations, <50 μm; 2% shell fragments; 2% bone fragments, <4 mm.

Sample 4/3, 83–93 cm

Structure: pellety, <500 μm, to aggregated, <1 cm, sub-rounded; *Porosity*: 10% vughs, sub-rounded to irregular to interconnected, <1 mm; <2% fine channels, <5 mm long, <500 μm wide, accommodated, smooth to weakly serrated; *Mineral components*: <5% fine limestone pebbles, <5 mm, sub-rounded to sub-angular, unsorted; c/f ratio: 5/95; coarse fraction: 5% fine quartz sand, sub-rounded, 100–500 μm; fine fraction: 10% very fine quartz sand, 50–100 μm, sub-rounded; 10–20% micro-sparite; 65% dusty clay, non-birefringent, gold to golden brown (CPL/PPL); reddish/orangey brown (CPL/PPL); *Organic components*: 10–20% organic/charred punctuations, <50 μm; 2% fine charcoal, <75 μm; rare (<1%) burnt bone fragment, <500 μm; *Pedofeatures*: *Amorphous*: common to abundant (10–20%) impregnative sesquioxide nodules, sub-rounded, <2 mm, no birefringence, strong red/orangey-red (CPL), reddish brown to dark brown (PPL).

Sample 4/4, 65–70 cm context 80 (wall plaster?)

Structure: dense, apedal; *Porosity*: <2% vughs, sub-rounded to elongated, <500 μm; *Mineral components*: 40–50% fine limestone, 2–5 mm, sub-rounded, evenly distributed; 10% very fine quartz sand, 50–100 μm, sub-rounded; 50% micro-sparitic silt; greyish/yellowish brown (CPL), pale brown (PPL); *Organic components*: 25% organic/charred punctuations, <50 μm; 1% bone fragments, <2 mm; 2% degraded plant tissue remains.

A7.2. Ġgantija Test Pit 1

Sample 28, 40–47 cm

Structure: pellety, <250 μm, to irregular/sub-rounded aggregated, 500 μm to 4 mm; well sorted; *Porosity*: 20–25% open vughy; <5% fine channels, <1 cm long, <100 μm wide, partly accommodated, weakly serrated; *Mineral components*: 20% small limestone/carbonate gravel, <1 cm, sub-rounded to sub-angular; coarse/fine ratio: 42/58; coarse fraction: 2% coarse, 10% medium and 30% fine quartz sand, 100–1000 μm, sub-rounded; fine fraction: 20% very fine quartz sand, 50–100 μm, sub-rounded; 5% micro-sparite; *c*. 32% dusty clay in groundmass, weak to non-birefringent, gold/golden brown (CPL); brown (CPL), reddish brown to very dark brown (PPL); *Organic component*: very strong brown staining of whole groundmass; 5% shell fragments, <2 mm; <2% bone fragments, burnt and unburnt, <1.5 mm; <1% very fine charcoal fragments, <500 μm; *Pedofeatures*: *Textural*: see above; *Fabric*: few (5%) aggregates of silty clay and clay (Bt material), strong birefringence, sub-rounded, <750 μm, gold (CPL); *Amorphous*: weak to moderate amorphous sesquioxide impregnation of whole groundmass; few (5%) sesquioxide nodules, <750 μm, sub-rounded.

Sample 27, 50–67 cm

As for Sample 28 above, except for:
Pedofeatures: *Excrements*: rare (<1%) dung fragment, sub-rounded, <1 mm; *Amorphous*: rare (<1%) rolled clay (Bt material) aggregate, sub-rounded, gold (CPL), strong birefringence, <1 mm.

Sample 26, 60–77 cm

Structure: weak irregular small blocky, <2 cm; pellety, <500 μm, to sub-rounded aggregated micro-structure, 1–5 mm; *Porosity*: 10–20% interconnected vughy; <5% fine channels, <2 cm long, <500 μm wide, accommodated, smooth; *Mineral components*: <5% small limestone gravel, <1 cm, sub-rounded to sub-angular; coarse/fine ratio: 15/85; coarse fraction: 5% medium and 10% fine quartz sand, 100–500 μm, sub-rounded; fine fraction: 20% very fine quartz sand, 50–100 μm, sub-rounded; 10% micro-sparite; 45% dusty clay in groundmass, weak to non-birefringent, gold/golden brown (CPL); dark brown (CPL), brown to reddish brown (PPL); *Organic component*: very strong brown staining of whole groundmass; <5% shell fragments, <2 mm; 10% bone fragments, burnt and unburnt, <500 μm; <5% very fine charcoal/organic punctuations, <50 μm; *Pedofeatures*: *Textural*: see above; *Fabric*: few (5%) aggregates of silty clay (Bt material), strong birefringence, sub-rounded, <750 μm, gold (CPL); *Amorphous*: moderate amorphous sesquioxide impregnation of whole groundmass.

Sample 25, 88–100 cm

Structure: finely aggregated micro-structure, <2 mm; close porphyric; *Porosity*: 5% vughs, sub-rounded to irregular, <500 μm; 5–10% fine channels, <1 cm long, <250 μm wide, accommodated, smooth; *Mineral components*: <5% small limestone/carbonate gravel, <1 cm, sub-rounded to sub-angular; coarse/fine ratio: 20/80; coarse fraction: 10% medium to coarse sand size limestone, 500–1000 μm, sub-rounded; 10% fine quartz sand, 100–250 μm, sub-rounded; fine fraction: 10% very fine quartz sand, 50–10 μm, sub-rounded; 40% micro-sparite; 30% dusty clay in groundmass, weak to non-birefringent, gold (CPL); gold (CPL), golden brown (PPL); *Organic component*: 5% bone fragments, <1000 μm; <5% very fine charcoal, <50 μm; 2% coarse charcoal, 1–2 mm; 10% organic punctuations, <50 μm; *Pedofeatures*: *Textural*: see above; *Fabric*: few (2%) clay aggregates (Bt material), <500 μm, strong birefringence, sub-rounded, reddish brown (CPL/PPL); *Amorphous*: few to common (<10%) calcitic hypo-coatings.

Sample 24, 100–111 cm

Structure: weakly developed sub-angular blocky, <2 cm; pellety, <500 μm, to sub-rounded aggregated, 2–4 mm, micro-structure in zones; *Porosity*: 10–15% open interconnected vughy and sub-rounded, <1 mm; 10% fine channels, <5 cm long, <2 mm wide, accommodated, weakly serrated; *Mineral components*: <5% small limestone/carbonate gavel, <5 mm, sub-rounded to sub-angular; coarse/fine ratio: 15/85; coarse fraction: 5% coarse, 5% medium and 5% fine quartz sand, 100–500 μm, sub-rounded; fine fraction: 20% very fine quartz sand, 50–100 μm, sub-rounded; 25% micro-sparite; 40% dusty clay in groundmass, weak birefringence, gold to yellowish brown (CPL); brown to reddish/yellowish brown (CPL), brown to reddish brown (PPL); *Organic component*: 10% organic/charred punctuations in groundmass; <10% shell fragments, <2 mm; <2% bone fragments, <1 mm; *Pedofeatures*: *Textural*: see above; *Fabric*: one large aggregate, <1 cm, sub-rounded, of organic fabric of Sample 26 incorporated from above; common (5–10%) aggregates of silty

clay (Bt material), strong birefringence, sub-rounded, <750 μm, gold (CPL); *Amorphous*: *c*. 40–60% of groundmass with stronger staining with amorphous sesquioxides in irregular zones; common (*c*. 20% of groundmass) partial void infills with amorphous to micro-sparitic calcium carbonate.

Sample 23, 111–125 cm

Structure: weakly developed sub-angular blocky, <2 cm; pellety, <500 μm, to sub-rounded aggregated, 2–4 mm, micro-structure in zones; *Porosity*: 10–15% open interconnected vughy and sub-rounded, <1 mm; 10% fine channels, <5 cm long, <2 mm wide, accommodated, weakly serrated; *Mineral components*: <5% small limestone gavel, <5 mm, sub-rounded to sub-angular; coarse/fine ratio: 15/85; coarse fraction: 5% coarse, 5% medium and 5% fine quartz sand, 100–500 μm, sub-rounded; fine fraction: 20% very fine quartz sand, 50–100 μm, sub-rounded; 25% micro-sparite; 40% dusty clay in groundmass, weak birefringence, gold to yellowish brown (CPL); brown to reddish/yellowish brown (CPL), brown to reddish brown (PPL); *Organic component*: 10% organic/charred punctuations in groundmass; <10% shell fragments, <2 mm; <2% bone fragments, <1 mm; *Pedofeatures*: *Textural*: see above; few (2%) aggregates of clay (Bt material), strong birefringence, sub-rounded, <750 μm, gold (CPL); *Amorphous*: up to 20% of groundmass with irregular/sub-rounded aggregates of strongly amorphous sesquioxide impregnated silty clay, <1 mm; *c*. 40–60% of groundmass with stronger staining with amorphous sesquioxides in irregular zones.

A7.3. Ġgantija WC Trench 1

Sample 3/2, 60–63 cm

Structure: apedal, homogeneous; *Porosity*: <10% vughs, <250 μm, sub-rounded to irregular; <2% channels, <1 cm long, <750 μm wide, accommodated, smooth to weakly serrated; *Mineral components*: 100% silt-sized calcium carbonate; greyish yellow (CPL), pale greyish brown (PPL).

Sample 3/9, context 1015, 45–56 cm

Structure: fine aggregated, <2 mm to weak to moderately well developed small blocky, <1.5 cm, with pellety micro-structure, <500 μm; *Porosity*: 10% open vughy; <10% channels, <1.5 cm long, <750 μm wide, partly accommodated, weakly serrated; *Mineral components*: 10–20% small limestone gravel towards base of slide, <1.5 cm, sub-rounded to sub-angular; coarse/fine ratio: 40–50/50–60; coarse fraction: 10% coarse sand size limestone, 1–2 mm, sub-rounded; 20% medium and 10–20% fine quartz sand, 100–1000 μm, sub-rounded; fine fraction: 5–10% very fine quartz sand, 50–100 μm, sub-rounded; 20–25% micro-sparite; 20–25% dusty clay in groundmass, weak to non-birefringent, gold/golden brown (CPL); brown (CPL), pale brown to brown (PPL); *Organic component*: <10% organic punctuations, <50 μm; <1% very fine charcoal fragments, <500 μm; *Pedofeatures*: *Textural*: see above; *Amorphous*: weak to moderate amorphous sesquioxide impregnation of whole groundmass.

Sample 3/10, context 1016, 70–80 cm

Structure: fine aggregated, <2 mm to weak to moderately well developed small to columnar blocky, <3 cm, with pellety micro-structure, <500 μm; *Porosity*: 10% open vughy; <10% channels, <1.5 cm long, <750 μm wide, partly accommodated, weakly serrated; *Mineral components*: 20–30% small limestone gravel towards base of slide, 2–4 cm, sub-rounded to sub-angular; coarse/fine ratio: 40/60; coarse fraction: 10% coarse sand size limestone, 1–2 mm, sub-rounded; 20% medium and 10% fine quartz sand, 100–1000 μm, sub-rounded; fine fraction: 10% very fine quartz sand, 50–100 μm, sub-rounded; 25% micro-sparite; 25% dusty clay in groundmass, weak to non-birefringent, gold/golden brown (CPL); brown (CPL), pale brown to brown (PPL); *Organic component*: 10–20% organic punctuations, <50 μm; <1% very fine charcoal fragments, <500 μm; <2% fine bone fragments, <1 mm, sub-rounded; *Pedofeatures*: *Textural*: see above; *Amorphous*: weak to moderate amorphous sesquioxide impregnation of whole groundmass; common strong humic/amorphous sesquioxide staining of groundmass around void spaces.

Sample 3/1/1, context 1016, 68–77.5 cm

Lower fabric unit: *Structure*: fine aggregated to pellety, <500 μm; *Porosity*: 10–15% open vughy, <1 mm; two fabric units: *Mineral components*: 20% small limestone gravel, <2 cm, sub-rounded to sub-angular; coarse/fine ratio: 50/50; coarse fraction: 20% coarse sand size limestone, 1–2 mm, sub-rounded; 10% medium and 20% fine quartz sand, 100–1000 μm, sub-rounded; fine fraction: 10% very fine quartz sand, 50–100 μm, sub-rounded; 30–40% micro-sparite; 20–25% dusty clay in groundmass, weak to non-birefringent, gold/golden brown (CPL); brown (CPL), pale brown to brown (PPL); *Organic component*: 10–50% of groundmass as humified organic/charred fragments and punctuations, <250 μm and <50 μm; few (<2%) bone fragments, <500 μm; few (2%) fine charcoal, 250–500 μm; *Amorphous*: weak to moderate amorphous sesquioxide impregnation of whole groundmass; merging over <1 mm with Upper fabric unit: same as below, except 20% fine limestone gravel, <8 mm, sub-rounded; and <10% humified organics/punctuations.

Sample 3/1/2, context 1016, 78–85 cm

As for the lower fabric unit of Sample 3/1/1 above, except for: *Mineral components*: up to 40% fine limestone gravel, <1 cm, sub-rounded; *Fabric*: rare (<1%) silty clay soil aggregate, sub-rounded, <500 μm, with short clay striae, orange (CPL), moderate birefringence.

Sample 3/3, context transition of 1004/1019, 84–94 cm

Structure: well developed small blocky, <2.5 cm, to columnar blocky, <5 cm, with fine aggregated to pellety microstructure, <1 mm; *Porosity*: 10% channels, <7 cm long, <2 mm wide, accommodated, smooth to weakly serrated; 10% open vughy, <1 mm; two fabric units: *Mineral components*: 20% small limestone gravel, <2 cm, sub-rounded to sub-angular; coarse/fine ratio: 50/50; coarse fraction: 20% coarse sand size limestone, 1–2 mm, sub-rounded; 10% medium and 20% fine quartz sand, 100–1000 μm, sub-rounded; fine fraction: 10% very fine quartz sand, 50–100 μm, sub-rounded; 30–40% micro-sparite; 20–25% dusty clay in groundmass, weak to non-birefringent, gold/golden brown (CPL); brown (CPL), pale brown to brown (PPL); one large pottery fragment, <1.5 cm, sub-angular; *Organic component*: 10% of groundmass as humified organic/charred fragments and punctuations, <250 μm and <50 μm; few (<2%) bone fragments, <500 μm; few (2%) fine charcoal, 250–500 μm; *Amorphous*: weak to moderate amorphous sesquioxide impregnation of whole groundmass.

Sample 3/4, contexts 1016/1040 transition, 80–85 cm

Lower fabric unit: *Structure*: fine aggregated to pellety, <500 μm; *Porosity*: 10–15% open vughy, <1 mm; two fabric units: *Mineral components*: 75–80% small limestone gravel, <1 cm, sub-rounded to sub-angular; with 20–25% soil fabric inbetween: coarse/fine ratio: 50/50; coarse fraction: 20% coarse sand size limestone, 1–2 mm, sub-rounded; 10% medium and 20% fine quartz sand, 100–1000 μm, sub-rounded; fine fraction: 10% very fine quartz sand, 50–100 μm, sub-rounded; 30–40% micro-sparite; 20–25% dusty clay in groundmass, weak to non-birefringent, gold/golden brown (CPL); brown (CPL), pale brown to brown (PPL); *Organic component*: 10–30% organic/charred punctuations, <50 μm; few (<2%) bone fragments, <500 μm; few (2%) fine charcoal, 250–500 μm; *Amorphous*: weak to

moderate amorphous sesquioxide impregnation of whole groundmass; with dispersed horizontal zone of red soil aggregates above, sub-rounded, <4 mm, with strong amorphous sesquioxide reddening; same as lower B horizon of Santa Verna Trench B; associated with *c.* 1.5–2 cm thick zone of fine limestone gravel above; then Upper fabric unit: as for lower unit.

Sample 3/5, context 1004, 85–96 cm

As for Sample 3/1/1 above

Sample 3/6, context 1016, 96–104 cm

As for Sample 3/1/1 above, except:
Upper fabric unit: *Structure*: fine aggregated to pellety, <500 μm; *Porosity*: 10–15% open vughy, <1 mm; two fabric units: *Mineral components*: 20% small limestone gravel, <2 cm, sub-rounded to sub-angular; coarse/fine ratio: 50/50; coarse fraction: 20% coarse sand size limestone, 1–2 mm, sub-rounded; 10% medium and 20% fine quartz sand, 100–1000 μm, sub-rounded; fine fraction: 10% very fine quartz sand, 50–100 μm, sub-rounded; 30–40% micro-sparite; 20–25% dusty clay in groundmass, weak to non-birefringent, gold/golden brown (CPL); brown (CPL), pale brown to brown (PPL); *Organic component*: 20% organic/charred punctuations, <250 μm and <50 μm; few (<2%) bone fragments, <500 μm; common (10%) fine charcoal, <75 μm; *Amorphous*: weak amorphous sesquioxide impregnation of whole groundmass; merging/undulating boundary with Lower fabric unit: as above except for: *Amorphous*: strongly reddened with amorphous sesquioxides.

Sample 3/7, context 1019, 104–113 cm

As for Sample 3/6, lower fabric unit (above).

Sample 3/8, context 1019, 113–124 cm

Structure: fine aggregated, 1–2 mm, to pellety, <100 μm; *Porosity*: 25% open, interconnected vughy, <1 mm; *Mineral components*: 30% small limestone gravel, <2.5 cm, sub-rounded to sub-angular, all orientations; coarse/fine ratio: 10/90; coarse fraction: 20% coarse sand size limestone, 1–2 mm, sub-rounded; 5% coarse and 5% medium quartz sand, 500–1000 μm, sub-rounded; fine fraction: 15% very fine quartz sand, 50–100 μm, sub-rounded; 10% micro-sparite; 40% dusty clay in groundmass, weak to non-birefringent, golden brown (CPL); brown to golden brown (CPL), orangey/reddish brown (PPL); *Organic component*: 10–15% organic/charred punctuations, <50 μm; *Fabric*: rare (1%) fine sandy/silty clay soil aggregate, <1 mm, sub-rounded, dark orangey red (CPL/PPL); *Amorphous*: moderate amorphous sesquioxide impregnation of whole groundmass.

A7.4. Ġgantija olive grove and environs

Sample 35, Test Pit 5, 75–80 cm

Structure: pellety to fine aggregated, <2 mm; *Porosity*: 10–20% interconnected vughy; *Mineral components*: 50–75% fine limestone gravel, <1 cm, sub-rounded; c/f ratio: 50/50; coarse fraction: 15% coarse sand size limestone, 1–2 mm; 20% medium and 15% fine quartz, 100–750 μm, sub-rounded to sub-angular; fine fraction: 15% fine quartz sand, 50–100 μm; 25% dusty clay, non-birefringent, orangey brown (CPL); greyish brown (CPL/PPL); *Organic component*: few charcoal, <1 mm; <5% organic punctuations.

Sample 41, BH54, 70–80 cm

Structure: pellety to fine aggregated, <5 mm; *Porosity*: 10–20% interconnected vughy; *Mineral components*: 20% fine limestone gravel, <1 cm, sub-rounded; c/f ratio: 30/70; coarse fraction: 10% coarse, 10% medium and 10% fine quartz, 100–750 μm, sub-rounded to sub-angular; fine fraction: 20% fine quartz sand, 50–100 μm; 20% micro-sparite; 30% dusty clay, non-birefringent, orangey brown (CPL); golden brown (CPL), pale reddish brown (PPL); *Organic component*: few charcoal, <1 mm; <5% organic punctuations; *c.* 2 cm thick zone of plant cell tissue at base of slide, with abundant excrements within; *Amorphous*: weak to moderate sesquioxide impregnation of groundmass.

A7.5. Skorba

Trench A, section 1:

Sample 11, 70–82 cm

Two fabric units: Upper fabric unit 1: *Structure*: pellety, <2 mm; *Mineral components*: as for lower fabric 2 below; Lower fabric unit 2: *Structure*: well developed sub-angular blocky, <4 cm; pellety micro-structure, <500 μm; *Porosity*: 10% channels, <4 cm, <1 mm wide, accommodated, weakly serrated, vertical/horizontal, all lined with micro-sparite and with up to 50% discontinuous infills of same fabric; 5–10% vughs, <250 μm, irregular to sub-rounded; both contain discontinuous pellety fabric within; *Mineral components*: 10% fine limestone, <2 cm, sub-rounded; coarse/fine ratio: 25/75; coarse fraction: 5% coarse and 10% medium sand-size limestone, 250–1500 μm, sub-rounded; 10% fine quartz sand, 100–250 μm, sub-rounded; fine fraction: 10% very fine quartz sand, 50–100 μm, sub-rounded; 20–40% micro-sparite; 25–45% dusty clay, weak to moderate birefringence; golden/reddish brown (CPL/PPL); *Organic components*: 5–10% fine charcoal, <250 μm; 5% organic/charred punctuations, <50 μm; rare (<1%) amorphous sesquioxide replaced plant tissue fragment; rare (<1%) shell fragments; *Amorphous*: rare (<1%) sesquioxide nodule, sub-rounded, <500 μm.

Sample 20, 85–97 cm

Mixture of two fabric units as for Sample 28: Fabric 1: 60% of groundmass; Fabric 2: 40% of groundmass; *Amorphous*: moderate amorphous sesquioxide staining of whole fabric.

Sample 24, 105–114 cm

Structure: aggregated micro-structure, <5 mm; *Porosity*: up to 20% interconnected vughy; *Mineral components*: coarse/fine ratio: 40/60; coarse fraction: 20% medium sand-size limestone, 500–1000 μm, sub-rounded; 20% fine quartz sand, 250–750 μm, sub-rounded; fine fraction: 10% very fine quartz, 100–250 μm, sub-rounded; 20% micro-sparite; 30% dusty clay, weak birefringence; towards base of slide are rare aggregates of dusty cay, <500 μm, sub-rounded, weak birefringence, golden brown (CPL); golden brown (CPL), brown (PPL); *Organic components*: 2–5% fine charcoal, <250 μm; 2% shell fragments; 2% bone fragments, <50 μm; rare (<1%) plant tissue fragments.

Sample 28, 120–131 cm

Main fabric 1: >90% of total groundmass; *Structure:* pellety, <250 μm; *Porosity*: up to 20% vughs, interconnected, irregular to sub-rounded, <3 mm; *Mineral components*: 3% of total groundmass; *Structure*: pellety micro-structure, <500 μm; 30–40% fine limestone pebbles, <5 cm, sub-rounded; slight horizontal orientation; coarse/fine ratio: 25/75; coarse fraction: 10% coarse and 10% medium sand-size limestone, 250–1500 μm, sub-rounded; 5% fine quartz sand, 100–250 μm, sub-rounded; fine fraction: 10% very fine quartz sand, 50–100 μm, sub-rounded; 25% micro-sparite; 40% dusty clay, pellety, weak to moderate birefringence, golden brown (CPL); whitish/golden brown

(CPL), pale grey/golden brown (PPL); *Organic components*: 2% very fine charcoal, <250 μm; 5% organic/charred punctuations, <50 μm; *Anthropogenic inclusions*: rare (<1%) bone fragments, <250 μm; Minor fabric 2: <10% of total groundmass; *Structure*: aggregated micro-structure, <1 cm; *Porosity*: <2% vughs, <200 μm; *Mineral components*: coarse/fine ratio: 40/60; coarse fraction: 20% medium sand-size limestone, 500–1000 μm, sub-rounded; 20% fine quartz sand, 250–750 μm, sub-rounded; fine fraction: 10% very fine quartz, 100–250 μm, sub-rounded; 20% micro-sparite; 30% dusty clay, weak birefringence; dark golden brown (CPL), golden brown (PPL); *Organic components*: 2–5% fine charcoal, <250 μm.

Trench A, section 2:

Sample 26, 70–80 cm

Two fabric units: Upper fabric unit 1: *Structure:* pellety, <250 μm; *Porosity*: up to 20% vughs, interconnected, irregular to sub-rounded, <3 mm; *Mineral components*: 3% of total groundmass; *Structure*: pellety micro-structure, <500 μm; 30–40% fine limestone pebbles, <5 cm, sub-rounded; slight horizontal orientation; coarse/fine ratio: 25/75; coarse fraction: 10% coarse and 10% medium sand-size limestone, 250–1500 μm, sub-rounded; 5% fine quartz sand, 100–250 μm, sub-rounded; fine fraction: 10% very fine quartz sand, 50–100 μm, sub-rounded; 25% micro-sparite; 40% dusty clay, pellety, weak to moderate birefringence, golden brown (CPL); whitish/golden brown (CPL), pale grey/golden brown (PPL); *Organic components*: 2% very fine charcoal, <250 μm; 5% organic/charred punctuations, <50 μm; *Anthropogenic inclusions*: rare (<1%) bone fragments, <250 μm; distinct horizontal boundary with Lower fabric unit 2: *Structure*: dense, apedal; *Porosity*: none; *Mineral components*: <2% fine limestone fragments, <1 cm, sub-rounded; 98% calcitic amorphous 'slurry'; 10% calcitic soil fabric aggregates, <1 cm, irregular, same fabric as for Sample 78; *Organic components*: 5–10% charred organic punctuations, <50 μm; 5% fine charcoal, <3 mm, sub-rounded; 5% burnt and amorphous sesquioxide replaced plant fragments, <3 mm.

'Floor' spot sample, upper sample 26, 75–82 cm

Two well mixed fabrics: Main fabric 1: 60% of groundmass; *Structure*: dense, apedal; *Porosity*: none; *Mineral components*: <2% fine limestone fragments, <1 cm, sub-rounded; 98% calcitic amorphous 'slurry'; 10% micritic soil fabric aggregates, <1 cm, irregular, same fabric as for Sample 78; *Organic components*: 5–10% charred organic punctuations, <50 μm; 5% fine charcoal, <3 mm, sub-rounded; 5% burnt and amorphous sesquioxide replaced plant fragments, <3 mm; *Fabric*: rare (<1%) burnt soil aggregate, reddish/crimson brown (CPL), <2 mm; Minor fabric 2: 40% of groundmass; *Structure*: pellety, <2 mm; *Porosity*: 15% interconnected vughy; *Mineral components*: same as Sample 20.

Sample 75, 91–100 cm

Structure: pellety, <5 mm; *Porosity*: 20% interconnected vughy; *Mineral components*: mixture of three main components: 1) 40–50% of groundmass: 40% fine sand-size limestone, 100–200 μm, sub-rounded; 10% fine quartz, 100–200 μm, sub-rounded; fine fraction: 50% micro-sparite; 2) 10–20% aggregates of calcitic ash, <1 mm, sub-rounded, grey (CPL/PPL); 3) 20–30% aggregates of dusty clay, non- to weak birefringence, <5 mm, sub-rounded to sub-angular, golden brown (CPL), sometimes coated with birefringent dusty clay; *Organic components*: 5% charred organic punctuations, <50 μm.

Sample 78, 107–120 cm

Structure: weakly developed columnar blocky, <5 cm; pellety micro-structure, <500 μm; *Porosity*: 5% channels, <5 cm, <1 mm wide, accommodated, smooth to weakly serrated, mainly vertical; 10% vughs, <2 mm, irregular to sub-rounded; both contain discontinuous pellety fabric within; *Mineral components*: 5% fine limestone, <5 mm, sub-rounded; coarse/fine ratio: 25/75; coarse fraction: 10% coarse and 10% medium sand-size limestone, 250–1500 μm, sub-rounded; 5% fine quartz sand, 100–250 μm, sub-rounded; fine fraction: 10% very fine quartz sand, 50–100 μm, sub-rounded; 25% micro-sparite; 40% dusty clay, pellety, weak to moderate birefringence, golden brown (CPL); golden brown (CPL), pale grey/golden brown/brown (PPL); *Organic components*: 2–5% fine charcoal, <500 μm; 5% organic/charred punctuations, <50 μm; *Anthropogenic inclusions*: few (<2%) pot and burnt/unburnt bone fragments, <8 mm; rare (<1%) calcitic ash fragment, <1 mm, sub-rounded; *Amorphous*: rare (<1%) sesquioxide nodule, <500 μm, rounded.

Plaster spot sample

Structure: dense, apedal; *Mineral components*: <1% fine limestone fragments, <1 cm, sub-rounded; 70–80% calcitic amorphous 'slurry'; 10% calcitic soil fabric aggregates, <1 cm, irregular, same fabric as for Sample 78; *Organic components*: 5% charred organic punctuations, <50 μm; 2% very fine charcoal, <200 μm.

A7.6. Xagħra town

Sample 5: Abandoned stone quarry on northeast side of town on road to Ramla Bay

Structure: very well developed sub-angular blocky, <6 cm; *Porosity*: 10% channels, <5 cm long, <750 μm wide, accommodated, smooth; 5% vughs, sub-rounded, <500 μm; *Mineral components*: all fine fraction: 15–20% very fine quartz, 50–100 μm, sub-rounded; 80–85% dusty clay in groundmass, speckled to striated to reticulate striated in places, gold to orange (CPL), moderate to strong birefringence; orangey brown (CPL), reddish orange (PPL); *Organic components*: <1% fine charcoal, <100 μm; 5% organic punctuations in groundmass; rare (<1%) silicified/clay replaced plant tissue fragments; *Amorphous*: 90% of the groundmass strongly impregnated with amorphous sesquioxides.

Sample 11: Modern house construction site 2

Structure: very well developed sub-angular blocky; *Porosity*: <5% vughs, sub-rounded, <500 μm; *Mineral components*: c/f ratio: 5/95; coarse fraction: 5% fine quartz, 100–250 μm; fine fraction: 15% very fine quartz, 50–100 μm, sub-rounded; 80% dusty clay in groundmass, striated to weakly reticulate striated in places, gold to orange (CPL), moderate to strong birefringence; orangey brown (CPL), reddish orange (PPL); *Organic components*: <1% fine charcoal, <100 μm; 5% organic punctuations in groundmass, <50 μm; *Amorphous*: 90% of the groundmass strongly impregnated with amorphous sesquioxides; *Fabric*: occasional aggregate of humic, fine sandy/silty clay loam, sub-rounded, <2 mm.

Sample 12: Modern house construction site 3: upper red soil

Structure: pellety, <500 μm, to sub-rounded aggregated, 2–4 mm; *Porosity*: 15–20% open interconnected vughy, sub-rounded to elongate, <3 mm; *Mineral components*: <5% small limestone gavel, <5 mm, sub-rounded to sub-angular; coarse/fine ratio: 15/85; coarse fraction: 5% coarse, 5% medium and 5% fine quartz sand, 100–500 μm, sub-rounded; fine fraction: 20% very fine quartz sand, 50–100 μm, sub-rounded; 25% micro-sparite; 40% dusty clay in groundmass, weak birefringence, gold to yellowish brown (CPL); dark brown to reddish brown (CPL/PPL); *Organic component*: brown to dark brown humic staining of whole groundmass; rare (<2%) charcoal fragments, <500 μm; 10% organic/charred punctuations in groundmass; rare (1%) bone fragments, <1 mm; *Pedofeatures*: *Textural*: see above; *Fabric*:

one aggregate of humic silt Ah material, <5 mm, sub-rounded, dark brown to black (CPL/PPL); *Amorphous*: strong to very strong staining with amorphous sesquioxides throughout groundmass.

Sample 14: Modern house construction site 3: lower red soil

Structure: very well developed, small irregular/sub-angular blocky, <3 cm; *Porosity*: 10% channels, <5 cm long, <750 μm wide, accommodated, smooth; 5% vughs, sub-rounded, <500 μm; *Mineral components*: 20% fine limestone gravel, <1.5 cm, sub-rounded; c/f ratio: 20/80; coarse fraction: 10% medium and 10% fine quartz sand, 100–500 μm, sub-rounded; fine fraction: 20% very fine quartz, 50–100 μm, sub-rounded; 60% dusty clay in groundmass, mainly speckled, gold to orange to reddish brown (CPL), moderate to strong birefringence; brown (CPL), reddish brown (PPL); *Organic components*: <1% fine charcoal, <100 μm; 5% organic punctuations in groundmass; *Amorphous*: groundmass moderately impregnated with amorphous sesquioxides.

A7.7. Taċ-Ċawla

Sample 9

Structure: dense, well developed small blocky, <3 cm; irregular aggregated to pellety micro-structure, <2 mm; *Porosity*: 5% vughs <250 μm, sub-rounded to irregular; 2% fine channels, <3 cm long, <750 μm wide, accommodated, smooth to weakly serrated; *Mineral components*: 25% very fine quartz sand, 50–100 μm, sub-rounded; 75% silty clay, stipple speckled and short striae, moderate to strong birefringence, red/reddish orange (CPL); very strong red (CPL/PPL); *Amorphous*: very severe amorphous sesquioxide impregnation of whole groundmass.

Sample 14

Structure: dense, moderately well developed blocky, <6 cm; irregular aggregated to pellety micro-structure, <2 mm; *Porosity*: 5% vughs, <500 μm, sub-rounded to irregular; 5% fine channels, <3 cm long, <500 μm wide, accommodated, smooth to weakly serrated; *Mineral components*: <2% fine limestone gravel, 2–4 mm, sub-angular; 20–25% very fine quartz sand, 50–100 μm, sub-rounded; 75–80% silty clay, striated to weakly reticulate striated, moderate to strong birefringence, red/reddish orange (CPL); very strong red (CPL/PPL); *Amorphous*: very severe amorphous sesquioxide impregnation of whole groundmass; 5–15% amorphous sesquioxide nodules, <250 μm, sub-rounded, orangey red (CPL/PPL).

Sample 139

Structure: aggregated, sub-rounded to irregular, <4 mm; *Porosity*: 5% channels, <5 mm long, <250 μm wide; 5% vughs, sub-rounded to irregular, <500 μm; *Mineral components*: 5% fine stone, <2 cm, sub-rounded to sub-angular; c/f ratio: 15/85; coarse fraction: 10% medium and 5% fine quartz sand, sub-rounded, 200–750 μm; fine fraction: 20% very fine quartz sand, 50–100 μm, sub-rounded; 20% micro-sparite; 10% silt; 25% dusty clay; golden brown (CPL), yellowish brown (PPL); *Organic components*: very few (1%) charcoal fragments, <5 mm; few (2%) micro-charcoal, <75 μm; 5–10% organic punctuations, <50 μm; *Pedofeatures*: *Amorphous*: weak to moderate amorphous sesquioxide impregnation of whole groundmass with few zones of greater impregnation; common partial infills and linings of voids with micritic to amorphous calcium carbonate.

Sample 261

Structure: aggregated, 100 μm to <2 mm; *Porosity*: up to 20% vughs, sub-rounded to irregular, <1 mm; most with calcitic coatings; *Mineral components*: c/f ratio: 15/85; coarse fraction: 10% medium and 5% fine quartz sand, sub-rounded, 200–750 μm; fine fraction: 5% very fine quartz sand, 50–100 μm, sub-rounded; 75% micro-sparite; 20% dusty clay; pale golden/greyish brown (CPL), pale yellowish brown (PPL); *Excremental*: few (<5%) dung aggregates, <4 mm, sub-rounded; *Organic components*: 5–10% organic/charred fragments, <500 μm.

Sample 301

Two fabric units; Upper fabric unit 1: *Structure*: dense, aggregated, <5 mm; *Porosity*: 10% vughs, <500 μm, sub-rounded; <5% channels, <5 cm long, <500 μm wide, partly accommodated; *Mineral components*: <10% very fine quartz sand, 50–100 μm, sub-rounded; 80–90% dusty clay, weak to non-birefringent; aggregate of silt crust in upper right hand corner of slide, <1 cm; reddish brown (CPL), golden brown (PPL); *Organic components*: 10–20% organic/charcoal dust, <50 μm; Lower fabric unit 2: 50–75% limestone pebbles, <1.5 cm, sub-rounded in matrix of fabric as above; orangey red (CPL/PPL); very strong amorphous sesquioxide impregnation.

A7.8. In-Nuffara

Sample 17

Structure: aggregated, 500 μm to 4 mm, sub-rounded to irregular; *Porosity*: 20–50% interconnected vughy; 10% horizontal channels, <2 mm wide, weakly serrated, partly accommodated; *Mineral components*: 10% large limestone pebbles, <3 cm, sub-rounded to sub-angular; 10% fine limestone gravel, <5 mm, sub-rounded to sub-angular; c/f ratio = 10–20/80–90; coarse fraction: 10–20% fine sand-size limestone, sub-rounded to sub-angular, 100–250 μm; fine fraction: 10% very fine sand-size limestone, sub-rounded to sub-angular, 50–100 μm; 10% micro-sparite; 40% silty clay, in groundmass, weak birefringence; golden brown to brown (CPL); dark greyish brown (PPL); *Organic components*: <1% charcoal, <5 mm; 5–10% charred 'dust' in groundmass, <50 μm; <1% shell fragments.

Sample 40

As for Sample 17, except for:
Mineral components: 20% micro-sparite; occasional zone of amorphous calcium carbonate; *Organic components*: <1% bone fragments, <2 cm; <1% pot fragments, <1 cm; <1% fired clay fragments, <6 mm; *Fabric pedofeatures*: few silt crust fragments, with micro-lamination, <4 mm.

Sample 503

Structure: weakly developed sub-angular blocky, <3 cm; *Porosity*: 10–20% vughs, sub-rounded to irregular, <2 mm; 5% channels, irregular, <3 mm long, <500 μm wide, weakly serrated to smooth, partly accommodated; *Mineral components*: c/f ratio = 10/90; coarse fraction: 10% fine quartz sand, sub-rounded to sub-angular, 100–250 μm; fine fraction: 20% very fine quartz sand, sub-rounded to sub-angular, 50–100 μm; 70% silty clay, in groundmass and coating grains and voids, weak birefringence; golden brown (CPL); brown (PPL); *Organic components*: <1% charcoal, <500 μm; 5% charred 'dust' in groundmass, <50 μm; <1% bone fragments, <2 mm; <1% pot fragments, <4 mm; *Amorphous pedofeatures*: 10% of groundmass with irregular zones of sesquioxide formation.

Sample 509

As for Sample 503, except for:
Structure: very weakly developed sub-angular blocky, <5 cm; *Organic components*: whole groundmass is stained dark brown to brown.

A7.9. Marsalforn Valley Profile 626

Sample 626/1, 175–185 cm

Structure: weakly developed, sub-angular to columnar blocky, <1.5 cm; *Porosity*: <5% vughs, sub-rounded to irregular, <1 mm; 5% channels, <1.5 cm long, <500 μm wide, smooth to weakly serrated, accommodated; *Mineral components*: 5–10% fine limestone, sub-rounded, <5 mm; c/f ratio: 50/50; coarse fraction: 10% shell fragments; 2–5% coarse, 5% medium and 20% fine sand-size limestone, sub-rounded, 100–1000 μm; fine fraction: 10% very fine quartz sand, 50–100 μm, sub-rounded; 20% micro-sparite; 20% dusty clay; golden brown (CPL), greyish/yellowish brown (PPL); *Organic components*: rare (<1%) fragments of amorphous iron replaced humified organic matter and/or vegetal voids; *Fabric*: rare void infill of weakly reticulate, very fine sandy clay loam, golden brown/yellow (CPL), moderate birefringence, with 5% charred punctuations; *Amorphous*: rare (<1%) sesquioxide nodule, sub-rounded, <750 μm.

Sample 627/2, 200–210 cm

Structure: moderately well developed, sub-angular blocky, <4 cm; *Porosity*: <5% vughs, sub-rounded to irregular, <750 μm; 5% channels, <4 cm long, <750 μm wide, smooth to weakly serrated, accommodated; *Mineral components*: 5–10% fine limestone, sub-rounded, <5 mm; c/f ratio: 50/50; coarse fraction: 10% shell fragments; 2–5% coarse, 5% medium and 20% fine sand-size limestone, sub-rounded, 100–1000 μm; fine fraction: 10% very fine quartz sand, 50–100 μm, sub-rounded; 20% micro-sparite; 20% dusty clay; golden brown (CPL), greyish/yellowish brown (PPL); *Organic components*: rare (<1%) fragments of amorphous iron replaced humified organic matter and/or vegetal voids; *Amorphous*: rare (<1%) sesquioxide nodule, sub-rounded, <750 μm.

Sample 627/3, 275–285 cm

Structure: weakly developed, sub-angular blocky, <4 cm; *Porosity*: <5% vughs, sub-rounded to irregular, <750 μm; 5% channels, <4 cm long, <750 μm wide, smooth to weakly serrated, accommodated; *Mineral components*: 5–10% fine limestone, sub-rounded, <5 mm; c/f ratio: 50/50; coarse fraction: 10% shell fragments; 2–5% coarse, 5% medium and 20% fine sand-size limestone, sub-rounded, 100–1000 μm; fine fraction: 10% very fine quartz sand, 50–100 μm, sub-rounded; 20% micro-sparite; 20% dusty clay; golden brown (CPL), greyish/yellowish brown (PPL); *Organic components*: rare (<1%) fragments of amorphous iron replaced humified organic matter and/or vegetal voids; *Fabric*: few (<5%) silt and silty clay crust fragments, <2 mm; *Amorphous*: rare (<1%) sesquioxide nodule, sub-rounded, <750 μm.

A7.10. Ramla Valley Profile 627

Sample 627/1, 4–14 cm

Structure: moderately well developed, large sub-angular to columnar blocky, <5 cm; *Porosity*: <5% vughs, sub-rounded, <500 μm; 5% channels, <5 cm long, <1 mm wide, smooth to weakly serrated, accommodated; *Mineral components*: 10–15% fine limestone, sub-rounded, <6 mm; c/f ratio: 40/60; coarse fraction: 10–15% shell fragments; 10% coarse, <5% medium and 10% fine sand-size limestone, sub-rounded, 100–1000 μm; fine fraction: 20% very fine quartz sand, 50–100 μm, sub-rounded; 40% micro-sparite; 20% dusty clay; yellowish brown (CPL), pale yellowish brown (PPL); *Organic components*: rare (<1%) bone fragment, <500 μm; few (<2%) irregular zones of humified organic matter.

Sample 627/2, 75–85 cm

Structure: 50% of groundmass is small, irregular, sub-angular blocky, <1 cm; 50% of groundmass is granular to small aggregated, <500 μm; *Porosity*: 50–75% open vughy in latter fabric; usually infilled with micrite; *Mineral components*: up to 50% fine limestone, sub-rounded, <1 cm, all orientations, occasionally weakly laminar; c/f ratio: 60/40; coarse fraction: 20% shell fragments; 10% coarse, 20% medium and 10% fine sand-size limestone, sub-rounded, 100–1000 μm; fine fraction: 5% very fine quartz sand, 50–100 μm, sub-rounded; 25% micro-sparite; 10% dusty clay; greyish brown (CPL/PPL); *Organic components*: rare (<1%) bone fragment, <250 μm.

Sample 626/3, 103–113 cm

Two fabric units: Upper fabric unit (0–3/4 cm): as for Pr 626/2 above; undulating, merging boundary over 1 mm with Lower fabric unit (3/4–8.5 cm): *Structure*: aggregated, <500 μm; *Porosity*: <5% vughs, sub-rounded, <500 μm; 5% channels, <5 cm long, <1 mm wide, smooth to weakly serrated, accommodated; *Mineral components*: <5% fine limestone, <4 mm; c/f ratio: 30/70; coarse fraction: 10% shell fragments; 5% coarse, <5% medium and 10% fine sand-size limestone, sub-rounded, 100–1000 μm; fine fraction: 15% very fine quartz sand, 50–100 μm, sub-rounded; 50% micro-sparite; 20–25% dusty clay, aggregated, <500 μm; brown (CPL/PPL); *Organic components*: few (<2%) irregular zones of humified organic matter; *Fabric*: occasional (2%) silty clay aggregate, <1 mm, sub-rounded, yellowish brown (CPL).

A7.11. Dwerja

Sample 616: 2.25–2.35 m

Structure: weakly developed, small irregular to sub-angular blocky, <5 cm; *Porosity*: <5% vughs, sub-rounded, <250 μm; 2% channels, <1 cm long, <500 μm wide, weakly serrated, partly accommodated; *Mineral components*: <5% fine limestone, sub-rounded, <8 mm; c/f ratio: 35/65; coarse fraction: 10% shell fragments; 5% coarse, 10% medium and 10% fine sand-size limestone, sub-rounded, 100–1000 μm; fine fraction: 10% very fine quartz sand, 50–100 μm, sub-rounded; 35% micro-sparite; 10% coarse calcitic, <50 μm; 10% dusty clay; brown (CPL), yellowish brown (PPL).

(Note: PPL = plane polarized light; CPL = cross polarized light; μm = microns; mm = millimetres; cm = centimeters)

Appendix 8

The micromorphological descriptions for the Malta deep cores of Xemxija 1, Wied Żembaq 1, Marsaxlokk and the base of the Salina Deep Core (21B)

Charles French & Sean Taylor

Table A8.1. *Xemxija 1 core micromorphology sample descriptions.*

Sample no.	Depth (m)	Description
1	1.99–2.01	fine gravelly, calcitic sandy clay loam; *Structure*: massive to incipient, sub-angular small blocky, <1 cm, porphyric; *Porosity*: <5% vughs, <200 μm; <2% channels/planes, <100 μm wide, <1 cm long, weakly serrated, accommodated; *Mineral components*: 15% limestone gravel, <5 mm, sub-rounded to sub-angular; c/f ratio = 25/75; coarse fraction: 10% coarse sand & limestone fragments, sub-rounded; 5% medium & 10% fine quartz sand; fine fraction: 10–15% very fine quartz sand; 10–15% micro-sparite; few (<2%) coarse silt-sized glauconite grains, 25–50 μm; few (<2%) haematite crystals, 25–50 μm; 35% dusty clay, weak to non-birefringent, stipple-speckled; golden brown (CPL) to brown (PPL); *Organic components*: 10% organic/charcoal punctuations, <50 μm; *Amorphous*: common thin calcitic coatings of voids; weak to moderate amorphous sesquioxide staining of dusty clay and few zones of more strongly sesquioxide staining; few (5%) amorphous sesquioxide nodules, <100 μm, sub-rounded
2	2.20–2.23	sub-angular blocky, fine gravelly, calcitic sandy clay loam; as for sample 1, but well developed sub-angular blocky ped structure, <2 cm
3	2.50–2.53	mix of fine gravel, sand-size limestone and crumb structured minor micritic silty clay; *Structure*: massive to large crumb, <4 mm, sub-rounded; *Porosity*: 10% vughs, <200 um; 10% channels, <1 cm long, <200 μm wide, weakly serrated, accommodated; *Mineral components*: <40% limestone gravel, <6 mm, sub-rounded to sub-angular; c/f ratio = 60/40; coarse fraction: 30% coarse, 15% medium and 15% fine sand-sized limestone fragments, sub-rounded; fine fraction: 5% very fine quartz sand; 15% micro-sparite; few (2–5%) coarse silt/very fine sand-sized glauconite grains, 50–60 μm; 20% dusty clay, weak to moderate birefringence, stipple-speckled to striated; golden brown (CPL) to brown (PPL); *Organic components*: 20% organic/charcoal punctuations, <50 μm; few (<2%) charcoal fragments, <300 μm; *Amorphous*: weakly calcitic groundmass; weak to moderate amorphous sesquioxide staining of dusty clay; few (5%) amorphous sesquioxide nodules, <100 μm, sub-rounded
4	2.73–2.75	very fine sandy silty clay loam with 10% very fine limestone gravel; *Structure*: small aggregated to weakly pellety, <5 mm; *Porosity*: <1% channels, <2 cm long, <200 μm wide, weakly serrated, accommodated; <20% vughs, <400 μm; *Mineral components*: 10% limestone gravel, <6 mm, sub-rounded to sub-angular; c/f ratio = 5/95; coarse fraction: 5% fine sand and limestone, sub-rounded; fine fraction: 20% very fine quartz sand; few (2–5%) coarse silt/very fine sand-sized glauconite grains, 50–100 μm; <5% micro-sparite; up to 65% dusty clay, weak to moderate birefringence, stipple-speckled to striated; gold (CPL); reddish to brown (CPL/PPL); *Organic components*: general humic staining of groundmass; rare fine charcoal, 50–400 μm; *Amorphous*: 50% of groundmass with moderate to strong amorphous sesquioxide staining
5	3.02–3.04	mix of very fine sandy clay loam and 25–50% very fine limestone gravel; few (2–5%) coarse silt/very fine sand-sized glauconite, 50–100 μm; as for sample 6 below
6	3.35–3.39	finely aggregated very fine sandy clay loam with up to 50% amorphous sesquioxide staining; *Structure*: small aggregated to weakly pellety, <5 mm; porphyric; *Porosity*: <5% planar channels, <2 cm long, <200 μm wide, weakly serrated, accommodated; <5% vughs, <300 μm; *Mineral components*: <5% limestone gravel, <6 mm, sub-rounded to sub-angular; c/f ratio = 10/90; coarse fraction: 5% fine sand, sub-rounded; few (2–5%) very fine sand-sized glauconite grains, 50–60 μm; fine fraction: 25% very fine quartz sand; <5% micr-sparite; up to 65% dusty clay, weak to moderate birefringence, stipple-speckled to striated; gold (CPL); reddish to brown (CPL/PPL); *Amorphous*: 50% of groundmass with strong amorphous sesquioxide staining

Table A8.1 *(cont.).*

Sample no.	Depth (m)	Description
7	4.03–4.05	micro-laminar very fine quartz and silt, strongly reddened with amorphous sesquioxides; *Structure*: single grain to finely laminar in places, <100 μm and <1 mm; *Mineral components*: <5% fine sand-sized limestone, 100–250 μm; 45% very fine quartz sand, 50–100 μm, sub-rounded; 50% silt; 1 zone, *c*. 10% of groundmass, with micro-laminar silt crusts; golden to reddish brown (CPL/PPL); *Amorphous*: <75% of groundmass strongly reddened with amorphous sesquioxides
	4.60–5.43	black organic silt mud to highly humified peat
8	4.95–4.97	heterogeneous mix of very fine quartz sand and silt with greater/lesser zones of amorphous sesquioxides and humic staining; Main fabric: >90% as for sample 7 (above), but stone-free and without laminae; few (2–5%) very fine/fine sand-sized glauconite grains, 50–250 μm; dark brown to dark reddish brown (CPL), golden to dark reddish brown (PPL); Minor fabric: <10% of soil fabric similar to sample 1;
9	5.15–5.17	very fine sand silt with strong amorphous sesquioxide staining; *Structure*: single grain to sub-angular blocky, <2 cm; porphyric; *Porosity*: 5% planar voids, <4 cm long, <200 μm wide, smooth, accommodated; *Mineral components*: 50% very fine quartz sand, 50–100 μm, sub-rounded; 5% micro-sparite; 40% silt; 5% dusty clay aggregates with rare to few dusty clay coatings with strong birefringence, 50–750 μm; golden to reddish brown (CPL/PPL); *Amorphous*: <60% of groundmass strongly reddened with amorphous sesquioxides
10	5.45–5.47	as for samples 9 and 11; very fine sand silt with strong sesquioxide staining throughout; few (2–5%) coarse silt/very fine sand-sized glauconite grains, 50–100 μm
	5.43–6.75	dark grey to black highly organic silt mud with common organic matter fragments; 10YR4/1; 10YR2/1
11	5.78–5.80	as for samples 9 and 10; very fine sand silt with moderate sesquioxide staining; few (2–5%) coarse silt/very fine sand-sized glauconite grains, 50–100 μm
12	6.10–6.12	heterogeneous mix of shell-rich, calcitic, very fine sand silt (as in samples 9–11) and 10% charred plant matter
13	6.45–6.47	calcitic, very fine sandy/silty clay loam; *Structure*: dense, massive to very weakly sub-angular blocky, <1 cm; *Porosity*: 20% vughs, <100 μm; 10% channels, <1.5 cm long, <1 mm wide, partly accommodated, weakly serrated; *Mineral components*: 15% very fine quartz sand, 50–100 μm; few (<2%) gypsum crystals, in clusters, <50 μm; 40% micro-sparite; 30% silt; 10% clay, weak birefringence, pale golden brown (CPL); yellowish brown to grey (CPL), reddish brown (PPL); *Organic components*: 10–15% charred organic punctuations, <50 μm; *Excremental*: few (<5%) calcitic aggregates as discontinuous infills in voids, <50 μm; *Amorphous*: >50% of groundmass strongly reddened with sesquioxide staining
14	6.85–6.87	as for sample 13; calcitic very fine sandy/silty clay loam with >50% strong amorphous sesquioxide staining; except for: 40% porosity; few (5%) humified plant tissue fragments, <50 μm; few (5%) shell fragments, <50 μm; and few (5%) amorphous sesquioxide nodules, <250 μm
15	7.25–7.27	as for samples 13 and 14; calcitic very fine to fine sandy/silty clay loam with *c*. 50% strong amorphous sesquioxide staining; few (<2%) gypsum crystals, in clusters, <50 μm; common shell fragments, <50 μm
16	7.72–7.74	as for samples 17, 18 and 20; reddish brown humic, calcitic silt with very strong amorphous sesquioxide staining and 5% shell fragments, <50 μm
17	7.85–7.87	as for sample 20; dark reddish brown, calcitic, very fine sandy silt with strong amorphous sesquioxide staining throughout; few (2–5%) very fine/fine sand-sized glauconite grains, 50–250 μm; few (<2%) gypsum crystals, in clusters, <50 μm
18	8.23–8.26	as for sample 20; yellowish brown, calcitic, very fine sandy silt with strong amorphous sesquioxide replaced organic matter fragments, 10–15% organic punctuations and 5% shell fragments
19	8.33–8.35	as for sample 23; pale yellowish brown, calcitic, very fine sandy silt
20	8.68–8.70	yellowish brown/grey, calcitic, very fine sandy silt with small, very weakly developed sub-angular blocky peds; *Structure*: dense, massive to very weakly sub-angular blocky, <1 cm; *Porosity*: <1% vughs, <100 μm; <1% channels, <1.5 cm long, <200 μm wide, accommodated; *Mineral components*: 15% very fine quartz sand, 50–100 μm; few (<5%) gypsum crystals; few (2–5%) very fine sand-sized glauconite grains, 50–100 μm; 40% micro-sparite; 30% silt; 10% clay, weak birefringence, pale golden brown (CPL); yellowish brown to grey (CPL), reddish brown (PPL); *Organic components*: 5% shell fragments; 10% organic punctuations, <50 μm; *Amorphous*: weak to moderate sesquioxide staining of whole groundmass
21	9.13–9.15	as for sample 20

Table A8.1 *(cont.).*

Sample no.	Depth (m)	Description
22	9.25–9.27	weak sub-angular blocky, pale brown, calcitic silty clay; *Structure*: dense, massive to very weakly sub-angular blocky, <5 mm; *Porosity*: <2% vughs, <100 μm; 5–8% channels, discontinuous, <1.5 cm long, <500 μm wide, accommodated; *Mineral components*: 10% very fine quartz sand, 50–100 μm; 40% micro-sparite; 40% dusty clay, weak birefringence, pale golden brown (CPL); pale golden brown (CPL/PPL); *Organic components*: 10% organic punctuations, <50 um; *Amorphous*: <20% of groundmass with weak sesquioxide staining
23	9.45–9.47	as above with minor charcoal and amorphous sesquioxide replaced organic matter; *Structure*: dense, massive to very weakly sub-angular blocky, <5 mm; porphyric; *Porosity*: 2% vughs, irregular, <2 mm; 5% channels, discontinuous, <1.5 cm long, <500 μm wide, accommodated; *Mineral components*: 5% very fine quartz sand, 50–10 μm; rare (<1%) gypsum crystals, <50 μm; 44% micro-sparite; 40% dusty clay, weak birefringence, pale golden brown (CPL); pale brown to pale yellowish brown (PPL); *Organic components*: rare (<1%) wood charcoal, <1 mm; 5% sesquioxide replaced plant tissue fragments; 10% organic punctuations, <50 μm; <5% shell fragments; common root holes infilled with same fabric; *Amorphous*: few channels with amorphous sesquioxide hypo-coatings; very weak sesquioxide staining of whole groundmass
24	9.65–9.67	as for sample 23, with 5–10% shell fragments
25	9.75–9.77	dense, homogeneous, pale golden brown, calcitic silty clay; *Structure*: dense, massive, apedal; *Porosity*: <1% vughs, <250 μm; <2% planar voids, <1 cm long, <500 μm wide, weakly serrated; *Mineral components*: 5–10% very fine quartz sand, 50–100 μm; 70% micro-sparite; 10% sparite, as dense infills in some voids; 10% dusty clay, weak birefringence, pale golden brown (CPL); pale brown to pale golden brown (CPL/PPL); *Organic components*: <2% organic punctuations, <50 μm; *Amorphous*: 20% of groundmass with weak, irregular staining with amorphous sesquioxides; <2% amorphous sesquioxide nodules, <10 μm

Table A8.2. *Wied Żembaq 1 core micromorphology sample descriptions.*

Sample no.	Depth (m)	Description
26	0.07–0.09	reddish brown coarse-very fine sandy/silty clay with minor very fine charcoal; *Structure*: dense, massive; *Porosity*: <2% vughs, <250 μm; <2% channels, <500 μm long, <100 μm wide, vertical, accommodated, weakly serrated; *Mineral components*: c/f ratio: 22/78; coarse fraction: 2% coarse sand-size limestone; 10% fine quartz sand, 100–250 μm, sub-rounded; fine fraction: 20% very fine quartz sand, 50–100 μm, sub-rounded; 10% micro-sparite; 48% dusty clay, in groundmass, non-birefringent, with moderate to strong amorphous sesquioxide staining; reddish brown (CPL), brown (PPL); *Organic components*: 5% shell fragments, <1 mm; 5% very fine charcoal, <100 μm; 5% charred organic punctuations, <50 μm; *Amorphous*: few zones (<10% of groundmass) of very strong staining with amorphous sesquioxides
27	0.45–0.70	as for sample 26
28	0.80–0.82	golden brown, calcitic, coarse-very fine sandy/silty clay with illuvial silty clay infills; *Structure*: dense, massive; *Porosity*: <2% vughs, <250 μm; <2% channels, <500 μm long, <100 μm wide, vertical, accommodated, weakly serrated; *Mineral components*: c/f ratio: 25/75; coarse fraction: 5% coarse sand-size limestone; 10% medium and 10% fine quartz sand, 100–500 μm, sub-rounded; fine fraction: 10% very fine quartz sand, 50–100 μm, sub-rounded; 20% micro-sparite; 45% dusty clay, in groundmass and as void coatings/infills, weak birefringence; golden brown (CPL/PPL); *Organic components*: 5% very fine charcoal, <100 μm; 5% charred organic punctuations, <50 μm
29	2.15–2.17	as for sample 26, with 20% fine limestone gravel content
30	2.53–2.55	as for sample 28, with 10–15% fine limestone gravel content and up to 50% of groundmass strongly stained with amorphous sesquioxides
31	3.00–3.02	small blocky, golden/reddish brown, calcitic, very fine sandy/silty clay, with weakly laminar micro-structure; *Structure*: moderately well developed small sub-angular blocky, <2 cm; *Porosity*: <2% vughs, <250 μm; <5% channels, <2 cm long, <500 μm wide, vertical/horizontal, partly accommodated, weakly serrated; *Mineral components*: 30% very fine quartz sand, 50–100 μm, sub-rounded; 5–10% micro-sparite; 10% irregular zones of amorphous calcium carbonate; 50–55% dusty clay, in groundmass, non-birefringent, with strong amorphous sesquioxide staining; golden/reddish brown (CPL/PPL); *Organic components*: 2% very fine charcoal, <100 μm; 5% organic punctuations, <50 μm; part charred/part replaced with amorphous sesquioxides wood fragment; *Amorphous*: much of groundmass very strongly stained with amorphous sesquioxides

Table A8.2 *(cont.).*

Sample no.	Depth (m)	Description
32	3.65–3.67	four thin fabric units: Upper fabric unit 1: as for sample 31; Fabric unit 2: mix of very fine quartz sand and micro-sparite; Fabric unit 3: as for sample 31; Lower fabric unit 4: very fine quartz sand
33	3.96–3.98	as for sample 28, except a few glauconite grains, 50–100 μm
34	4.10–4.12	humified and amorphous sesquioxide replaced organic matter with <5% shell fragments
35	4.33–4.35	small blocky, golden/reddish brown, coarse-very fine sandy/silty clay; *Structure*: weakly developed small sub-angular blocky, <2 cm; *Porosity*: <2% vughs, <250 μm; <5% channels, <2 cm long, <500 μm wide, vertical/horizontal, partly accommodated, weakly serrated; *Mineral components*: c/f ratio: 40/60; 2% coarse, 8% medium and 30% very fine quartz sand and limestone, 50–1000 μm, sub-rounded; few gypsum crystals, <50 μm, lenticular; 20% very fine quartz sand, 50–100 μm, sub-rounded; 40% dusty clay, in groundmass, non-birefringent, with strong amorphous sesquioxide staining; golden/reddish brown (CPL/PPL); *Organic components*: 5% charred organic punctuations, <50 μm; part charred/part replaced with amorphous sesquioxides wood fragment; *Amorphous*: *c*. 50% of groundmass strongly stained with amorphous sesquioxides
36	4.60–4.61	porous (15% irregular vughs), humified and amorphous sesquioxide replaced organic matter with 20% coarse-fine limestone/quartz, few gypsum crystals, <50 μm, and 2% shell fragments
37	4.96–4.98	fine gravelly, brown, calcitic, coarse-very fine sandy/silty clay with minor very fine charcoal; *Structure*: dense, massive; *Porosity*: <2% vughs, <250 μm; <2% channels, <500 μm long, <100 μm wide, vertical, accommodated, weakly serrated; *Mineral components*: c/f ratio: 40/60; coarse fraction: 5% coarse and 15%medium sand-size limestone, 500–1000 μm, sub-angular to sub-rounded; 10% fine quartz sand, 100–250 μm, sub-rounded; fine fraction: 20% very fine quartz sand, 50–100 μm, sub-rounded; 15% micro-sparite; 45% dusty clay, in groundmass, weak birefringence, golden brown (CPL); golden brown (CPL), brown (PPL); *Organic components*: 2% shell fragments, <1 mm; 5% very fine charcoal, <100 μm; 5% charred organic punctuations, <50 μm; 5–10% part charred/part humified plant tissue; *Amorphous*: few (<2%) amorphous sesquioxide nodules, <100 μm
38	5.28–5.30	as for sample 37, except fabric moderately to strongly reddened with amorphous sesquioxides, and few very fine sand-sized glauconite grains, 50–100 μm

Table A8.3. *Marsaxlokk core micromorphology sample descriptions.*

Sample	Depth (m)	Description
39	0.05–0.06	finely aggregated, vughy, pale brown calcitic silt; *Structure*: pellety to aggregated, <1 mm; *Porosity*: 10–20% interconnected vughy; *Mineral components*: 5% fine limestone gravel, <4 mm, sub-rounded; 10% fine and 5% very fine limestone, 50–250 μm, sub-rounded; 80% micro-sparite; pale brown (CPL), pale golden brown (PPL); *Organic components*: <2% amorphous sesquioxide replaced plant tissue
40	0.62–0.66	dense, pale grey weathered limestone and calcium carbonate; *Structure*: dense, aggregated, <5 mm; *Porosity*: <2% interconnected vughy; *Mineral components*: 15% fine limestone gravel, <4 mm, sub-rounded; 80% fine and 5% very fine limestone, 50–250 μm, sub-rounded;<5% dusty clay; pale grey brown (CPL/PPL); *Organic components*: <2% shell fragments; <2% charred organic punctuations, <50 μm
41	1.10–1.12	dense, pale grey weathered limestone and calcium carbonate and silt/micro-sparite; *Structure*: dense, homogeneous; *Porosity*: <1% interconnected vughy; *Mineral components*: < 5% very fine quart sand, 50–100 μm, sub-rounded; 95% micro-sparite; pale grey (CPL/PPL)
42	1.70–1.72	two units of micro-laminar humified and amorphous sesquioxide replaced plant remains; Upper fabric unit: finely laminar amorphous sesquioxide replaced plant tissue over weathered limestone (as in sample 40); over Fabric unit 2: dense humified/sesquioxide replaced plant tissue interleaved with 10–20% very fine quartz sand and 10% micro-sparite
43	2.15–2.17	reddish brown, coarse to very fine sandy/silty clay loam; *Structure*: weakly developed small sub-angular blocky, <1 cm; *Porosity*: <2% vughs, <250 μm; <5% short channels, <5 mm long, <100 μm wide, partly accommodated, weakly serrated; *Mineral components*: 5% limestone gravel, <1 cm, sub-rounded; c/f ratio: 25/75; coarse fraction: 10% coarse, 10% medium and 5% fine quartz sand, 100–1000 μm, sub-rounded; fine fraction: 10% very fine quartz sand, 50–100 μm, sub-rounded; 5–10% micro-sparite; 55–60% dusty clay, in groundmass, non-birefringent; dark reddish brown (CPL/PPL); *Organic components*: 5% charred organic punctuations, <50 μm

Table A8.3 *(cont.).*

Sample	Depth (m)	Description
44	2.55–2.57	as for sample 43, except 20% micro-sparite content
45	2.96–2.99	as for sample 44, with well developed, small sub-angular blocky structure
46	3.20–3.22	as above
47	3.65–3.67	very dense, massive, amorphous calcium carbonate

Table A8.4. *Salina Deep Core (21B; base of) micromorphology sample descriptions.*

Sample	Depth (m)	Description
Spot 1	27.83–27.88	well developed, small, sub-angular blocky, calcitic fine sandy clay loam over basal lens of fine limestone gravel; *Structure*: well developed small sub-angular blocky, <2.5 cm; *Porosity*: <2% vughs, <500 μm, sub-rounded; 10% channels, <3 cm long, <500 μm wide, accommodated, smooth to weakly serrated; *Mineral components*: in base of slide, 20–25% limestone gravel, <1 cm, sub-rounded to sub-angular; c/f ratio: 50/50; coarse fraction: 20% medium and 30% fine quartz sand, 100–500 μm, sub-rounded; fine fraction: 10% very fine quartz sand, 50–100 μm, sub-rounded; 10–20% micro-sparite; 20–30% dusty clay, in groundmass, weak birefringence; golden brown (CPL), brown (PPL); *Organic components*: rare (<1%) humified plant tissue; rare (<1%) shell fragments; *Amorphous*: few vughs with up to 50% micro-sparitic/amorphous calcium carbonate infillings; rare (<1%) amorphous sesquioxide nodule, <250 μm
Spot 2	27.91–27.96	as for spot sample 1, except no limestone gravel, fabric all weakly developed sub-angular blocky to massive, all voids filled with micro-sparite/amorphous calcium carbonate, and 30% amorphous humic/sesquioxide staining of groundmass
Spot 3	28.08–28.12	as for spot sample 1, except well developed, small, sub-angular blocky, minor limestone gravel, a few very fine sand-sized glauconite grains, 50–100 μm, and with micro-sparitic/amorphous calcium carbonate linings of all channels

Appendix 9

The charcoal data

Nathan Wright

Table A9.1. *The charcoal data from the Skorba (SV15), Kordin (KRD15), In-Nuffara (NUF15) and Salina Deep Core SDC.*

Taxon/Site	SV15 (95)	SV15 (95)	SV15 (90)	SV15 (90)	KRD15 (77)	KRD15 (77)	KRD15 (99)	KRD15 (99)	NUF15 (41)	NUF15 (41)	SDC	SDC	Total*	
	Af	*%f*	*Af*	*%f*	*Af*	*%f*	*Af*	*%f*	*Af*	*%f*	*Af*	*%f*	*Af*	*%f*
Quercus deciduous spp.	11	10.6	10	23.3	4	3.6			14	9.0			59	13.5
Quercus evergreen cf. *ilex*	16	15.4	6	14.0	20	17.9			33	21.3			55	15.2
↑ Woodland Total	**27**	**26.0**	**16**	**37.2**	**24**	**21.4**			**47**	**30.3**			**114**	**28.7**
Pistacia cf. *lentiscus*	31	29.8	4	9.3	21	18.8			39	25.2			95	20.8
Olea cf. *europea*	21	20.2	5	11.6	19	17.0	2	100.0	32	20.6			77	17.4
Rosaceae family	1	1.0			11	9.8			20	12.9			32	5.9
Ceratonia siliqua					2	1.8							2	0.4
Cistus sp.	3	2.9							4	2.6			7	1.4
Rhamnus cf. *oleioides*	12	11.5	3	7.0	3	2.7			4	2.6			22	5.9
Crataegus sp.	3	2.9	1	2.3	5	4.5			2	1.3			11	2.7
Cercis cf. siliquastrum	1	1.0							1	0.6			2	0.4
Ostrya carpinifolia					2	1.8							2	0.4
Carpinus spp.			1	2.3	1	0.9			1	0.6			3	1.0
↑ Woodland sub-dominant and marquis	**72**	**69.2**	**14**	**32.6**	**64**	**57.1**	**2**	**100.0**	**103**	**66.5**			**253**	**56.3**
Tetraclinus articularta	2	1.9			1	0.9							3	0.7
Abies sp.					2	1.8			1	0.6	5	100.0	3	0.6
↑ Conifers Total	**2**	**1.9**			**3**	**2.7**			**1**	**0.6**	**5**	**100**	**6**	**1.3**
Salix/Populus	3	2.9	9	20.9	14	12.5			3	1.9			29	9.6
Ulmus cf. *canescens*			1	2.3	4	3.6							5	1.5
Fraxinus angustifolia			1	2.3									1	0.6
Myrtus cf. *communis*					1	0.9							1	0.2
Tamarix sp.			1	2.3									1	0.6
Betula spp.					2	1.8			1	0.6			3	0.4
*Laurus nobilus***			1	2.3									1	0.6
↑ Riparian Total	**3**	**2.9**	**13**	**30.2**	**21**	**18.8**			**4**	**1.9**			**41**	**13.5**
NTAXA	**11**		**12**		**16**		**2**		**13**		**5**		**21**	

Taxonomic identifications from four sites in Malta. (*Totals exclude KRD15 (99) and SDC data. ***Laurus nobilus* can also be considered a marquis taxa.

Index

M

N

O

P

Q

R

S

T

U

V

W

X

Z

Temple landscapes

The ERC-funded *FRAGSUS Project* (*Fragility and sustainability in small island environments: adaptation, cultural change and collapse in prehistory, 2013–18*), led by Caroline Malone (Queens University Belfast) has explored issues of environmental fragility and Neolithic social resilience and sustainability during the Holocene period in the Maltese Islands. This, the first volume of three, presents the palaeo-environmental story of early Maltese landscapes.

The project employed a programme of high-resolution chronological and stratigraphic investigations of the valley systems on Malta and Gozo. Buried deposits extracted through coring and geoarchaeological study yielded rich and chronologically controlled data that allow an important new understanding of environmental change in the islands. The study combined AMS radiocarbon and OSL chronologies with detailed palynological, molluscan and geoarchaeological analyses. These enable environmental reconstruction of prehistoric landscapes and the changing resources exploited by the islanders between the seventh and second millennia BC. The interdisciplinary studies combined with excavated economic and environmental materials from archaeological sites allows Temple landscapes to examine the dramatic and damaging impacts made by the first farming communities on the islands' soil and resources. The project reveals the remarkable resilience of the soil-vegetational system of the island landscapes, as well as the adaptations made by Neolithic communities to harness their productivity, in the face of climatic change and inexorable soil erosion. Neolithic people evidently understood how to maintain soil fertility and cope with the inherently unstable changing landscapes of Malta. In contrast, second millennium BC Bronze Age societies failed to adapt effectively to the long-term aridifying trend so clearly highlighted in the soil and vegetation record. This failure led to severe and irreversible erosion and very different and short-lived socio-economic systems across the Maltese islands.

Editors:
Charles French is Professor of Geoarchaeology in the Department of Archaeology, University of Cambridge.
Chris O. Hunt is a Professor in the School of Biological and Environmental Sciences, Liverpool John Moores University, Liverpool.
Reuben Grima is a Senior Lecturer in the Department of Conservation and Built Heritage, University of Malta.
Rowan McLaughlin is Senior Researcher in the Department of Scientific Research at the British Museum and honorary research scholar at Queen's University Belfast.
Caroline Malone is a Professor in the School of Natural and Built Environment, Queen's University Belfast.
Simon Stoddart is Reader in Prehistory in the Department of Archaeology, University of Cambridge.

Published by the McDonald Institute for Archaeological Research,
University of Cambridge, Downing Street, Cambridge, CB2 3ER, UK.

Cover design by Dora Kemp and Ben Plumridge.

ISBN: 978-1-902937-99-1

UNIVERSITY OF CAMBRIDGE